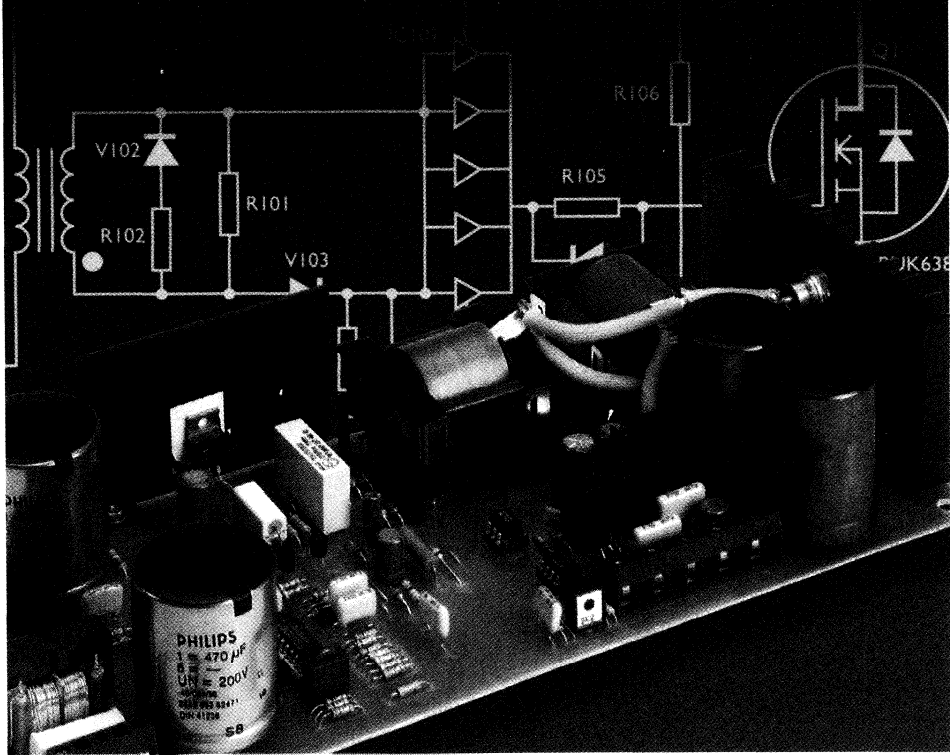


Power Semiconductors



APPLICATIONS HANDBOOK 1995

Philips
Semiconductors



PHILIPS

Acknowledgments

We are grateful for all the contributions from our colleagues within Philips and to the Application Laboratories in Eindhoven and Hamburg.

We would also like to thank Dr.P.H.Mellor of the University of Sheffield for contributing the application note of section 3.1.5.

The authors thank Mrs.R.Hayes for her considerable help in the preparation of this book.

The authors also thank Mr.D.F.Haslam for his assistance in the formatting and printing of the manuscripts.

Contributing Authors

N.Bennett	D.J.Harper	J.Oosterling
M.Bennion	W.Hettersheid	N.Pichowicz
D.Brown	J.v.d.Hooff	W.B.Rosink
C.Buethker	J.Houldsworth	D.C. de Ruiter
L.Burley	M.J.Humphreys	D.Sharples
G.M.Fry	P.H.Mellor	H.Simons
R.P.Gant	R.Miller	T.Stork
J.Gilliam	H.Misdorn	D.Tebb
D.Grant	P.Moody	H.Verhees
N.J.Ham	S.A.Mulder	F.A.Woodworth
C.J.Hammerton	E.B.G. Nijhof	T.van de Wouw

This book was originally prepared by the Power Semiconductor Applications Laboratory, of the Philips Semiconductors product division, Hazel Grove:

M.J.Humphreys	D.Brown	L.Burley
C.J.Hammerton	R.Miller	

It was revised and updated, in 1994, by:

N.J.Ham	C.J.Hammerton	D.Sharples
---------	---------------	------------

Preface

This book was prepared by the Power Semiconductor Applications Laboratory of the Philips Semiconductors product division, Hazel Grove. The book is intended as a guide to using power semiconductors both efficiently and reliably in power conversion applications. It is made up of eight main chapters each of which contains a number of application notes aimed at making it easier to select and use power semiconductors.

CHAPTER 1 forms an introduction to power semiconductors concentrating particularly on the two major power transistor technologies, Power MOSFETs and High Voltage Bipolar Transistors.

CHAPTER 2 is devoted to Switched Mode Power Supplies. It begins with a basic description of the most commonly used topologies and discusses the major issues surrounding the use of power semiconductors including rectifiers. Specific design examples are given as well as a look at designing the magnetic components. The end of this chapter describes resonant power supply technology.

CHAPTER 3 describes motion control in terms of ac, dc and stepper motor operation and control. This chapter looks only at transistor controls, phase control using thyristors and triacs is discussed separately in chapter 6.

CHAPTER 4 looks at television and monitor applications. A description of the operation of horizontal deflection circuits is given followed by transistor selection guides for both deflection and power supply applications. Deflection and power supply circuit examples are also given based on circuits designed by the Product Concept and Application Laboratories (Eindhoven).

CHAPTER 5 concentrates on automotive electronics looking in detail at the requirements for the electronic switches taking into consideration the harsh environment in which they must operate.

CHAPTER 6 reviews thyristor and triac applications from the basics of device technology and operation to the simple design rules which should be followed to achieve maximum reliability. Specific examples are given in this chapter for a number of the common applications.

CHAPTER 7 looks at the thermal considerations for power semiconductors in terms of power dissipation and junction temperature limits. Part of this chapter is devoted to worked examples showing how junction temperatures can be calculated to ensure the limits are not exceeded. Heatsink requirements and designs are also discussed in the second half of this chapter.

CHAPTER 8 is an introduction to the use of high voltage bipolar transistors in electronic lighting ballasts. Many of the possible topologies are described.

Table of Contents

CHAPTER 1 Introduction to Power Semiconductors	1
<i>General</i>	3
1.1.1 An Introduction To Power Devices	5
<i>Power MOSFET</i>	17
1.2.1 PowerMOS Introduction	19
1.2.2 Understanding Power MOSFET Switching Behaviour	29
1.2.3 Power MOSFET Drive Circuits	39
1.2.4 Parallel Operation of Power MOSFETs	49
1.2.5 Series Operation of Power MOSFETs	53
1.2.6 Logic Level FETS	57
1.2.7 Avalanche Ruggedness	61
1.2.8 Electrostatic Discharge (ESD) Considerations	67
1.2.9 Understanding the Data Sheet: PowerMOS	69
<i>High Voltage Bipolar Transistor</i>	77
1.3.1 Introduction To High Voltage Bipolar Transistors	79
1.3.2 Effects of Base Drive on Switching Times	83
1.3.3 Using High Voltage Bipolar Transistors	91
1.3.4 Understanding The Data Sheet: High Voltage Transistors	97
CHAPTER 2 Switched Mode Power Supplies	103
<i>Using Power Semiconductors in Switched Mode Topologies</i>	105
2.1.1 An Introduction to Switched Mode Power Supply Topologies	107
2.1.2 The Power Supply Designer's Guide to High Voltage Transistors	129
2.1.3 Base Circuit Design for High Voltage Bipolar Transistors in Power Converters	141
2.1.4 Isolated Power Semiconductors for High Frequency Power Supply Applications	153
<i>Output Rectification</i>	159
2.2.1 Fast Recovery Epitaxial Diodes for use in High Frequency Rectification	161
2.2.2 Schottky Diodes from Philips Semiconductors	173
2.2.3 An Introduction to Synchronous Rectifier Circuits using PowerMOS Transistors	179

<i>Design Examples</i>	185
2.3.1 Mains Input 100 W Forward Converter SMPS: MOSFET and Bipolar Transistor Solutions featuring ETD Cores	187
2.3.2 Flexible, Low Cost, Self-Oscillating Power Supply using an ETD34 Two-Part Coil Former and 3C85 Ferrite	199
<i>Magnetics Design</i>	205
2.4.1 Improved Ferrite Materials and Core Outlines for High Frequency Power Supplies	207
<i>Resonant Power Supplies</i>	217
2.5.1. An Introduction To Resonant Power Supplies	219
2.5.2. Resonant Power Supply Converters - The Solution For Mains Pollution Problems	225
CHAPTER 3 Motor Control	241
<i>AC Motor Control</i>	243
3.1.1 Noiseless A.C. Motor Control: Introduction to a 20 kHz System	245
3.1.2 The Effect of a MOSFET's Peak to Average Current Rating on Inverter Efficiency	251
3.1.3 MOSFETs and FREDFETs for Motor Drive Equipment	253
3.1.4 A Designers Guide to PowerMOS Devices for Motor Control	259
3.1.5 A 300V, 40A High Frequency Inverter Pole Using Paralleled FREDFET Modules	273
<i>DC Motor Control</i>	283
3.2.1 Chopper circuits for DC motor control	285
3.2.2 A switched-mode controller for DC motors	293
3.2.3 Brushless DC Motor Systems	301
<i>Stepper Motor Control</i>	307
3.3.1 Stepper Motor Control	309
CHAPTER 4 Televisions and Monitors	317
<i>Power Devices in TV & Monitor Applications (including selection guides)</i>	319
4.1.1 An Introduction to Horizontal Deflection	321
4.1.2 The BU25XXA/D Range of Deflection Transistors	331



4.1.3 Philips HVT's for TV & Monitor Applications 339
 4.1.4 TV and Monitor Damper Diodes 345

TV Deflection Circuit Examples 349

4.2.1 Application Information for the 16 kHz Black Line Picture Tubes 351
 4.2.2 32 kHz / 100 Hz Deflection Circuits for the 66FS Black Line Picture Tube 361

SMPS Circuit Examples 377

4.3.1 A 70W Full Performance TV SMPS Using The TDA8380 379
 4.3.2 A Synchronous 200W SMPS for 16 and 32 kHz TV 389

Monitor Deflection Circuit Example 397

4.4.1 A Versatile 30 - 64 kHz Autosync Monitor 399

CHAPTER 5 Automotive Power Electronics 421

Automotive Motor Control (including selection guides) 423

5.1.1 Automotive Motor Control With Philips MOSFETS 425

Automotive Lamp Control (including selection guides) 433

5.2.1 Automotive Lamp Control With Philips MOSFETS 435

The TOPFET 443

5.3.1 An Introduction to the 3 pin TOPFET 445
 5.3.2 An Introduction to the 5 pin TOPFET 447
 5.3.3 BUK101-50DL - a Microcontroller compatible TOPFET 449
 5.3.4 Protection with 5 pin TOPFETs 451
 5.3.5 Driving TOPFETs 453
 5.3.6 High Side PWM Lamp Dimmer using TOPFET 455
 5.3.7 Linear Control with TOPFET 457
 5.3.8 PWM Control with TOPFET 459
 5.3.9 Isolated Drive for TOPFET 461
 5.3.10 3 pin and 5 pin TOPFET Leadforms 463
 5.3.11 TOPFET Input Voltage 465
 5.3.12 Negative Input and TOPFET 467
 5.3.13 Switching Inductive Loads with TOPFET 469
 5.3.14 Driving DC Motors with TOPFET 471
 5.3.15 An Introduction to the High Side TOPFET 473
 5.3.16 High Side Linear Drive with TOPFET 475

<i>Automotive Ignition</i>	477
5.4.1 An Introduction to Electronic Automotive Ignition	479
5.4.2 IGBTs for Automotive Ignition	481
5.4.3 Electronic Switches for Automotive Ignition	483
 CHAPTER 6 Power Control with Thyristors and Triacs	 485
<i>Using Thyristors and Triacs</i>	487
6.1.1 Introduction to Thyristors and Triacs	489
6.1.2 Using Thyristors and Triacs	497
6.1.3 The Peak Current Handling Capability of Thyristors	505
6.1.4 Understanding Thyristor and Triac Data	509
<i>Thyristor and Triac Applications</i>	521
6.2.1 Triac Control of DC Inductive Loads	523
6.2.2 Domestic Power Control with Triacs and Thyristors	527
6.2.3 Design of a Time Proportional Temperature Controller	537
<i>Hi-Com Triacs</i>	547
6.3.1 Understanding Hi-Com Triacs	549
6.3.2 Using Hi-Com Triacs	551
 CHAPTER 7 Thermal Management	 553
<i>Thermal Considerations</i>	555
7.1.1 Thermal Considerations for Power Semiconductors	557
7.1.2 Heat Dissipation	567
 CHAPTER 8 Lighting	 575
<i>Fluorescent Lamp Control</i>	577
8.1.1 Efficient Fluorescent Lighting using Electronic Ballasts	579
8.1.2 Electronic Ballasts - Philips Transistor Selection Guide	587
8.1.3 An Electronic Ballast - Base Drive Optimisation	589

Index

- Airgap, transformer core, 111, 113
- Anti saturation diode, 590
- Asynchronous, 497
- Automotive
 - fans
 - see motor control
 - IGBT, 481, 483
 - ignition, 479, 481, 483
 - lamps, 435, 455
 - motor control, 425, 457, 459, 471, 475
 - resistive loads, 442
 - reverse battery, 452, 473, 479
 - screen heater, 442
 - seat heater, 442
 - solenoids, 469
 - TOPFET, 473
- Avalanche, 61
- Avalanche breakdown
 - thyristor, 490
- Avalanche multiplication, 134
- Baker clamp, 138, 187, 190
- Ballast
 - electronic, 580
 - fluorescent lamp, 579
 - switchstart, 579
- Base drive, 136
 - base inductor, 147
 - base inductor, diode assisted, 148
 - base resistor, 146
 - drive transformer, 145
 - drive transformer leakage inductance, 149
 - electronic ballast, 589
 - forward converter, 187
 - power converters, 141
 - speed-up capacitor, 143
- Base inductor, 144, 147
- Base inductor, diode assisted, 148
- Boost converter, 109
 - continuous mode, 109
 - discontinuous mode, 109
 - output ripple, 109
- Bootstrap, 303
- Breakback voltage
 - diac, 492
- Breakdown voltage, 70
- Breakover current
 - diac, 492
- Breakover voltage
 - diac, 492, 592
 - thyristor, 490
- Bridge circuits
 - see Motor Control - AC
- Brushless motor, 301, 303
- Buck-boost converter, 110
- Buck converter, 108 - 109
- Burst firing, 537
- Burst pulses, 564
- Capacitance
 - junction, 29
- Capacitor
 - mains dropper, 544
- CENELEC, 537
- Charge carriers, 133
 - triac commutation, 549
- Choke
 - fluorescent lamp, 580
- Choppers, 285
- Clamp diode, 117
- Clamp winding, 113
- Commutation
 - diode, 164
 - Hi-Com triac, 551
 - thyristor, 492
 - triac, 494, 523, 529
- Compact fluorescent lamp, 585
- Continuous mode
 - see Switched Mode Power Supplies
- Continuous operation, 557
- Converter (dc-dc)
 - switched mode power supply, 107
- Cookers, 537
- Cooling
 - forced, 572
 - natural, 570
- Crest factor, 529
- Critical electric field, 134
- Cross regulation, 114, 117
- Current fed resonant inverter, 589
- Current Mode Control, 120
- Current tail, 138, 143
- Damper Diodes, 345, 367
 - forward recovery, 328, 348
 - losses, 347
 - outlines, 345
 - picture distortion, 328, 348
 - selection guide, 345
- Darlington, 13
- Data Sheets
 - High Voltage Bipolar Transistor, 92,97,331
 - MOSFET, 69

- dc-dc converter, 119
- Depletion region, 133
- Desaturation networks, 86
 - Baker clamp, 91, 138
- di/dt
 - triac, 531
- Diac, 492, 500, 527, 530, 591
- Diode, 6
 - double diffused, 162
 - epitaxial, 161
 - schottky, 173
 - structure, 161
- Diode Modulator, 327, 367
- Disc drives, 302
- Discontinuous mode
 - see Switched Mode Power Supplies
- Domestic Appliances, 527
- Dropper
 - capacitive, 544
 - resistive, 544, 545
- Duty cycle, 561

- EFD core
 - see magnetics
- Efficiency Diodes
 - see Damper Diodes
- Electric drill, 531
- Electronic ballast, 580
 - base drive optimisation, 589
 - current fed half bridge, 584, 587, 589
 - current fed push pull, 583, 587
 - flyback, 582
 - transistor selection guide, 587
 - voltage fed half bridge, 584, 588
 - voltage fed push pull, 583, 587
- EMC, 260, 455
 - see RFI, ESD
 - TOPFET, 473
- Emitter shorting
 - triac, 549
- Epitaxial diode, 161
 - characteristics, 163
 - di/dt, 164
 - forward recovery, 168
 - lifetime control, 162
 - operating frequency, 165
 - passivation, 162
 - reverse leakage, 169
 - reverse recovery, 162, 164
 - reverse recovery softness, 167
 - selection guide, 171
 - snap-off, 167
 - softness factor, 167
 - stored charge, 162
 - technology, 162
- ESD, 67
 - see Protection, ESD
 - precautions, 67
- ETD core
 - see magnetics

- F-pack
 - see isolated package
- Fall time, 143, 144
- Fast Recovery Epitaxial Diode (FRED)
 - see epitaxial diode
- FBSOA, 134
- Ferrites
 - see magnetics
- Flicker
 - fluorescent lamp, 580
- Fluorescent lamp, 579
 - colour rendering, 579
 - colour temperature, 579
 - efficacy, 579, 580
 - triphosphor, 579
- Flyback converter, 110, 111, 113
 - advantages, 114
 - clamp winding, 113
 - continuous mode, 114
 - coupled inductor, 113
 - cross regulation, 114
 - diodes, 115
 - disadvantages, 114
 - discontinuous mode, 114
 - electronic ballast, 582
 - leakage inductance, 113
 - magnetics, 213
 - operation, 113
 - rectifier circuit, 180
 - self oscillating power supply, 199
 - synchronous rectifier, 156, 181
 - transformer core airgap, 111, 113
 - transistors, 115
- Flyback converter (two transistor), 111, 114
- Food mixer, 531
- Forward converter, 111, 116
 - advantages, 116
 - clamp diode, 117
 - conduction loss, 197
 - continuous mode, 116
 - core loss, 116
 - core saturation, 117
 - cross regulation, 117
 - diodes, 118
 - disadvantages, 117
 - duty ratio, 117
 - ferrite cores, 116
 - magnetics, 213
 - magnetisation energy, 116, 117

- operation, 116
- output diodes, 117
- output ripple, 116
- rectifier circuit, 180
- reset winding, 117
- switched mode power supply, 187
- switching frequency, 195
- switching losses, 196
- synchronous rectifier, 157, 181
- transistors, 118
- Forward converter (two transistor), 111, 117
- Forward recovery, 168
- FREDFET, 250, 253, 305
 - bridge circuit, 255
 - charge, 254
 - diode, 254
 - drive, 262
 - loss, 256
 - reverse recovery, 254
- FREDFETs
 - motor control, 259
- Full bridge converter, 111, 125
 - advantages, 125
 - diodes, 126
 - disadvantages, 125
 - operation, 125
 - transistors, 126
- Gate
 - triac, 538
- Gate drive
 - forward converter, 195
- Gold doping, 162, 169
- GTO, 11
- Guard ring
 - schottky diode, 174
- Half bridge, 253
- Half bridge circuits
 - see also Motor Control - AC
- Half bridge converter, 111, 122
 - advantages, 122
 - clamp diodes, 122
 - cross conduction, 122
 - diodes, 124
 - disadvantages, 122
 - electronic ballast, 584, 587, 589
 - flux symmetry, 122
 - magnetics, 214
 - operation, 122
 - synchronous rectifier, 157
 - transistor voltage, 122
 - transistors, 124
 - voltage doubling, 122
- Heat dissipation, 567
- Heat sink compound, 567
- Heater controller, 544
- Heaters, 537
- Heatsink, 569
- Heatsink compound, 514
- Hi-Com triac, 519, 549, 551
 - commutation, 551
 - di/dt , 552
 - gate trigger current, 552
 - inductive load control, 551
- High side switch
 - MOSFET, 44, 436
 - TOPFET, 430, 473
- High Voltage Bipolar Transistor, 8, 79, 91, 141, 341
 - 'bathtub' curves, 333
 - avalanche breakdown, 131
 - avalanche multiplication, 134
 - Baker clamp, 91, 138
 - base-emitter breakdown, 144
 - base drive, 83, 92, 96, 136, 336, 385
 - base drive circuit, 145
 - base inductor, 138, 144, 147
 - base inductor, diode assisted, 148
 - base resistor, 146
 - breakdown voltage, 79, 86, 92
 - carrier concentration, 151
 - carrier injection, 150
 - conductivity modulation, 135, 150
 - critical electric field, 134
 - current crowding, 135, 136
 - current limiting values, 132
 - current tail, 138, 143
 - current tails, 86, 91
 - d-type, 346
 - data sheet, 92, 97, 331
 - depletion region, 133
 - desaturation, 86, 88, 91
 - device construction, 79
 - di/dt , 139
 - drive transformer, 145
 - drive transformer leakage inductance, 149
 - dV/dt , 139
 - electric field, 133
 - electronic ballast, 581, 585, 587, 589
 - Fact Sheets, 334
 - fall time, 86, 99, 143, 144
 - FBSOA, 92, 99, 134
 - hard turn-off, 86
 - horizontal deflection, 321, 331, 341
 - leakage current, 98
 - limiting values, 97
 - losses, 92, 333, 342
 - Miller capacitance, 139
 - operation, 150

- optimum drive, 88
- outlines, 332, 346
- over current, 92, 98
- over voltage, 92, 97
- overdrive, 85, 88, 137, 138
- passivation, 131
- power limiting value, 132
- process technology, 80
- ratings, 97
- RBSOA, 93, 99, 135, 138, 139
- RC network, 148
- reverse recovery, 143, 151
- safe operating area, 99, 134
- saturation, 150
- saturation current, 79, 98, 341
- secondary breakdown, 92, 133
- smooth turn-off, 86
- SMPS, 94, 339, 383
- snubber, 139
- space charge, 133
- speed-up capacitor, 143
- storage time, 86, 91, 92, 99, 138, 144, 342
- sub emitter resistance, 135
- switching, 80, 83, 86, 91, 98, 342
- technology, 129, 149
- thermal breakdown, 134
- thermal runaway, 152
- turn-off, 91, 92, 138, 142, 146, 151
- turn-on, 91, 136, 141, 149, 150
- underdrive, 85, 88
- voltage limiting values, 130
- Horizontal Deflection, 321, 367
 - base drive, 336
 - control ic, 401
 - d-type transistors, 346
 - damper diodes, 345, 367
 - diode modulator, 327, 347, 352, 367
 - drive circuit, 352, 365, 406
 - east-west correction, 325, 352, 367
 - line output transformer, 354
 - linearity correction, 323
 - operating cycle, 321, 332, 347
 - s-correction, 323, 352, 404
 - TDA2595, 364, 368
 - TDA4851, 400
 - TDA8433, 363, 369
 - test circuit, 321
 - transistors, 331, 341, 408
 - waveforms, 322
- IGBT, 11, 305
 - automotive, 481, 483
 - clamped, 482, 484
 - ignition, 481, 483
- Ignition
 - automotive, 479, 481, 483
 - darlington, 483
- Induction heating, 53
- Induction motor
 - see Motor Control - AC
- Inductive load
 - see Solenoid
- Inrush current, 528, 530
- Intrinsic silicon, 133
- Inverter, 260, 273
 - see motor control ac
 - current fed, 52, 53
 - switched mode power supply, 107
- Irons, electric, 537
- Isolated package, 154
 - stray capacitance, 154, 155
 - thermal resistance, 154
- Isolation, 153
- J-FET, 9
- Junction temperature, 470, 557, 561
 - burst pulses, 564
 - non-rectangular pulse, 565
 - rectangular pulse, composite, 562
 - rectangular pulse, periodic, 561
 - rectangular pulse, single shot, 561
- Lamp dimmer, 530
- Lamps, 435
 - di/dt, 438
 - inrush current, 438
 - MOSFET, 435
 - PWM control, 455
 - switch rate, 438
 - TOPFET, 455
- Latching current
 - thyristor, 490
- Leakage inductance, 113, 200, 523
- Lifetime control, 162
- Lighting
 - fluorescent, 579
 - phase control, 530
- Logic Level FET
 - motor control, 432
- Logic level MOSFET, 436
- Magnetics, 207
 - 100W 100kHz forward converter, 197
 - 100W 50kHz forward converter, 191
 - 50W flyback converter, 199
 - core losses, 208
 - core materials, 207
 - EFD core, 210
 - ETD core, 199, 207

- flyback converter, 213
- forward converter, 213
- half bridge converter, 214
- power density, 211
- push-pull converter, 213
- switched mode power supply, 187
- switching frequency, 215
- transformer construction, 215
- Mains Flicker, 537
- Mains pollution, 225
 - pre-converter, 225
- Mains transient, 544
- Mesa glass, 162
- Metal Oxide Varistor (MOV), 503
- Miller capacitance, 139
- Modelling, 236, 265
- MOS Controlled Thyristor, 13
- MOSFET, 9, 19, 153, 253
 - bootstrap, 303
 - breakdown voltage, 22, 70
 - capacitance, 30, 57, 72, 155, 156
 - capacitances, 24
 - characteristics, 23, 70 - 72
 - charge, 32, 57
 - data sheet, 69
 - di/dt, 36
 - diode, 253
 - drive, 262, 264
 - drive circuit loss, 156
 - driving, 39, 250
 - dV/dt, 36, 39, 264
 - ESD, 67
 - gate-source protection, 264
 - gate charge, 195
 - gate drive, 195
 - gate resistor, 156
 - high side, 436
 - high side drive, 44
 - inductive load, 62
 - lamps, 435
 - leakage current, 71
 - linear mode, parallelling, 52
 - logic level, 37, 57, 305
 - loss, 26, 34
 - maximum current, 69
 - motor control, 259, 429
 - modelling, 265
 - on-resistance, 21, 71
 - package inductance, 49, 73
 - parallel operation, 26, 47, 49, 265
 - parasitic oscillations, 51
 - peak current rating, 251
 - Resonant supply, 53
 - reverse diode, 73
 - ruggedness, 61, 73
 - safe operating area, 25, 74
 - series operation, 53
 - SMPS, 339, 384
 - solenoid, 62
 - structure, 19
 - switching, 24, 29, 58, 73, 194, 262
 - switching loss, 196
 - synchronous rectifier, 179
 - thermal impedance, 74
 - thermal resistance, 70
 - threshold voltage, 21, 70
 - transconductance, 57, 72
 - turn-off, 34, 36
 - turn-on, 32, 34, 35, 155, 256
- Motor, universal
 - back EMF, 531
 - starting, 528
- Motor Control - AC, 245, 273
 - anti-parallel diode, 253
 - antiparallel diode, 250
 - carrier frequency, 245
 - control, 248
 - current rating, 262
 - dc link, 249
 - diode, 261
 - diode recovery, 250
 - duty ratio, 246
 - efficiency, 262
 - EMC, 260
 - filter, 250
 - FREDFET, 250, 259, 276
 - gate drives, 249
 - half bridge, 245
 - inverter, 250, 260, 273
 - line voltage, 262
 - loss, 267
 - MOSFET, 259
 - Parallel MOSFETs, 276
 - peak current, 251
 - phase voltage, 262
 - power factor, 262
 - pulse width modulation, 245, 260
 - ripple, 246
 - short circuit, 251
 - signal isolation, 250
 - snubber, 276
 - speed control, 248
 - switching frequency, 246
 - three phase bridge, 246
 - underlap, 248
- Motor Control - DC, 285, 293, 425
 - braking, 285, 299
 - brushless, 301
 - control, 290, 295, 303
 - current rating, 288

- drive, 303
- duty cycle, 286
- efficiency, 293
- FREDFET, 287
- freewheel diode, 286
- full bridge, 287
- half bridge, 287
- high side switch, 429
- IGBT, 305
- inrush, 430
- inverter, 302
- linear, 457, 475
- logic level FET, 432
- loss, 288
- MOSFET, 287, 429
- motor current, 295
- overload, 430
- permanent magnet, 293, 301
- permanent magnet motor, 285
- PWM, 286, 293, 459, 471
- servo, 298
- short circuit, 431
- stall, 431
- TOPFET, 430, 457, 459, 475
- topologies, 286
- torque, 285, 294
- triac, 525
- voltage rating, 288
- Motor Control - Stepper, 309
 - bipolar, 310
 - chopper, 314
 - drive, 313
 - hybrid, 312
 - permanent magnet, 309
 - reluctance, 311
 - step angle, 309
 - unipolar, 310
- Mounting, transistor, 154
- Mounting base temperature, 557
- Mounting torque, 514

- Parasitic oscillation, 149
- Passivation, 131, 162
- PCB Design, 368, 419
- Phase angle, 500
- Phase control, 546
 - thyristors and triacs, 498
 - triac, 523
- Phase voltage
 - see motor control - ac
- Power dissipation, 557
 - see High Voltage Bipolar Transistor loss, MOSFET loss
- Power factor correction, 580
 - active, boost converted, 581

- Power MOSFET
 - see MOSFET
- Proportional control, 537
- Protection
 - ESD, 446, 448, 482
 - overvoltage, 446, 448, 469
 - reverse battery, 452, 473, 479
 - short circuit, 251, 446, 448
 - temperature, 446, 447, 471
 - TOPFET, 445, 447, 451
- Pulse operation, 558
- Pulse Width Modulation (PWM), 108
- Push-pull converter, 111, 119
 - advantages, 119
 - clamp diodes, 119
 - cross conduction, 119
 - current mode control, 120
 - diodes, 121
 - disadvantages, 119
 - duty ratio, 119
 - electronic ballast, 582, 587
 - flux symmetry, 119, 120
 - magnetics, 213
 - multiple outputs, 119
 - operation, 119
 - output filter, 119
 - output ripple, 119
 - rectifier circuit, 180
 - switching frequency, 119
 - transformer, 119
 - transistor voltage, 119
 - transistors, 121

- Qs (stored charge), 162

- RBSOA, 93, 99, 135, 138, 139
- Rectification, synchronous, 179
- Reset winding, 117
- Resistor
 - mains dropper, 544, 545
- Resonant power supply, 219, 225
 - modelling, 236
 - MOSFET, 52, 53
 - pre-converter, 225
- Reverse leakage, 169
- Reverse recovery, 143, 162
- RFI, 154, 158, 167, 393, 396, 497, 529, 530, 537
- Ruggedness
 - MOSFET, 62, 73
 - schottky diode, 173

- Safe Operating Area (SOA), 25, 74, 134, 557
 - forward biased, 92, 99, 134
 - reverse biased, 93, 99, 135, 138, 139

- Saturable choke
 - triac, 523
- Schottky diode, 173
 - bulk leakage, 174
 - edge leakage, 174
 - guard ring, 174
 - reverse leakage, 174
 - ruggedness, 173
 - selection guide, 176
 - technology, 173
- SCR
 - see Thyristor
- Secondary breakdown, 133
- Selection Guides
 - BU25XXA, 331
 - BU25XXD, 331
 - damper diodes, 345
 - EPI diodes, 171
 - horizontal deflection, 343
 - MOSFETs driving heaters, 442
 - MOSFETs driving lamps, 441
 - MOSFETs driving motors, 426
 - Schottky diodes, 176
 - SMPS, 339
- Self Oscillating Power Supply (SOPS)
 - 50W microcomputer flyback converter, 199
 - ETD transformer, 199
- Servo, 298
- Single ended push-pull
 - see half bridge converter
- Snap-off, 167
- Snubber, 93, 139, 495, 502, 523, 529, 549
 - active, 279
- Softness factor, 167
- Solenoid
 - TOPFET, 469, 473
 - turn off, 469, 473
- Solid state relay, 501
- SOT186, 154
- SOT186A, 154
- SOT199, 154
- Space charge, 133
- Speed-up capacitor, 143
- Speed control
 - thyristor, 531
 - triac, 527
- Starter
 - fluorescent lamp, 580
- Startup circuit
 - electronic ballast, 591
 - self oscillating power supply, 201
- Static Induction Thyristor, 11
- Stepdown converter, 109
- Stepper motor, 309
- Stepup converter, 109
- Storage time, 144
- Stored charge, 162
- Suppression
 - mains transient, 544
- Switched Mode Power Supply (SMPS)
 - see also self oscillating power supply
 - 100W 100kHz MOSFET forward converter, 192
 - 100W 500kHz half bridge converter, 153
 - 100W 50kHz bipolar forward converter, 187
 - 16 & 32 kHz TV, 389
 - asymmetrical, 111, 113
 - base circuit design, 149
 - boost converter, 109
 - buck-boost converter, 110
 - buck converter, 108
 - ceramic output filter, 153
 - continuous mode, 109, 379
 - control ic, 391
 - control loop, 108
 - core excitation, 113
 - core loss, 167
 - current mode control, 120
 - dc-dc converter, 119
 - diode loss, 166
 - diode reverse recovery effects, 166
 - diode reverse recovery softness, 167
 - diodes, 115, 118, 121, 124, 126
 - discontinuous mode, 109, 379
 - epitaxial diodes, 112, 161
 - flux swing, 111
 - flyback converter, 92, 111, 113, 123
 - forward converter, 111, 116, 379
 - full bridge converter, 111, 125
 - half bridge converter, 111, 122
 - high voltage bipolar transistor, 94, 112, 115, 118, 121, 124, 126, 129, 339, 383, 392
 - isolated, 113
 - isolated packages, 153
 - isolation, 108, 111
 - magnetics design, 191, 197
 - magnetisation energy, 113
 - mains filter, 380
 - mains input, 390
 - MOSFET, 112, 153, 33, 384
 - multiple output, 111, 156
 - non-isolated, 108
 - opto-coupler, 392
 - output rectifiers, 163
 - parasitic oscillation, 149
 - power-down, 136
 - power-up, 136, 137, 139
 - power MOSFET, 153, 339, 384
 - pulse width modulation, 108
 - push-pull converter, 111, 119

- RBSOA failure, 139
- rectification, 381, 392
- rectification efficiency, 163
- rectifier selection, 112
- regulation, 108
- reliability, 139
- resonant
 - see resonant power supply
- RFI, 154, 158, 167
- schottky diode, 112, 154, 173
- snubber, 93, 139, 383
- soft start, 138
- standby, 382
- standby supply, 392
- start-up, 391
- stepdown, 109
- stepup, 109
- symmetrical, 111, 119, 122
- synchronisation, 382
- synchronous rectification, 156, 179
- TDA8380, 381, 391
- topologies, 107
- topology output powers, 111
- transformer, 111
- transformer saturation, 138
- transformers, 391
- transistor current limiting value, 112
- transistor mounting, 154
- transistor selection, 112
- transistor turn-off, 138
- transistor turn-on, 136
- transistor voltage limiting value, 112
- transistors, 115, 118, 121, 124, 126
- turns ratio, 111
- TV & Monitors, 339, 379, 399
- two transistor flyback, 111, 114
- two transistor forward, 111, 117
- Switching loss, 230
- Synchronous, 497
- Synchronous rectification, 156, 179
 - self driven, 181
 - transformer driven, 180
- Temperature control, 537
- Thermal
 - continuous operation, 557, 568
 - intermittent operation, 568
 - non-rectangular pulse, 565
 - pulse operation, 558
 - rectangular pulse, composite, 562
 - rectangular pulse, periodic, 561
 - rectangular pulse, single shot, 561
 - single shot operation, 561
- Thermal capacity, 558, 568
- Thermal characteristics
 - power semiconductors, 557
- Thermal impedance, 74, 568
- Thermal resistance, 70, 154, 557
- Thermal time constant, 568
- Thyristor, 10, 497, 509
 - 'two transistor' model, 490
 - applications, 527
 - asynchronous control, 497
 - avalanche breakdown, 490
 - breakover voltage, 490, 509
 - cascading, 501
 - commutation, 492
 - control, 497
 - current rating, 511
 - di/dt , 490
 - dI/dt , 491
 - dV/dt , 490
 - energy handling, 505
 - external commutation, 493
 - full wave control, 499
 - fusing I^2t , 503, 512
 - gate cathode resistor, 500
 - gate circuits, 500
 - gate current, 490
 - gate power, 492
 - gate requirements, 492
 - gate specifications, 512
 - gate triggering, 490
 - half wave control, 499
 - holding current, 490, 509
 - inductive loads, 500
 - inrush current, 503
 - latching current, 490, 509
 - leakage current, 490
 - load line, 492
 - mounting, 514
 - operation, 490
 - overcurrent, 503
 - peak current, 505
 - phase angle, 500
 - phase control, 498, 527
 - pulsed gate, 500
 - resistive loads, 498
 - resonant circuit, 493
 - reverse characteristic, 489
 - reverse recovery, 493
 - RFI, 497
 - self commutation, 493
 - series choke, 502
 - snubber, 502
 - speed controller, 531
 - static switching, 497
 - structure, 489
 - switching, 489

- switching characteristics, 517
- synchronous control, 497
- temperature rating, 512
- thermal specifications, 512
- time proportional control, 497
- transient protection, 502
- trigger angle, 500
- turn-off time, 494
- turn-on, 490, 509
- turn-on di/dt , 502
- varistor, 503
- voltage rating, 510
- Thyristor data, 509
- Time proportional control, 537
- TOPFET
 - 3 pin, 445, 449, 461
 - 5 pin, 447, 451, 457, 459, 463
 - driving, 449, 453, 461, 465, 467, 475
 - high side, 473, 475
 - lamps, 455
 - leadforms, 463
 - linear control, 451, 457
 - motor control, 430, 457, 459
 - negative input, 456, 465, 467
 - protection, 445, 447, 451, 469, 473
 - PWM control, 451, 455, 459
 - solenoids, 469
- Transformer
 - triac controlled, 523
- Transformer core airgap, 111, 113
- Transformers
 - see magnetics
- Transient thermal impedance, 559
- Transient thermal response, 154
- Triac, 497, 510, 518
 - 400Hz operation, 489, 518
 - applications, 527, 537
 - asynchronous control, 497
 - breakover voltage, 510
 - charge carriers, 549
 - commutating di/dt , 494
 - commutating dV/dt , 494
 - commutation, 494, 518, 523, 529, 549
 - control, 497
 - dc inductive load, 523
 - dc motor control, 525
 - di/dt , 531, 549
 - $dIcom/dt$, 523
 - dV/dt , 523, 549
 - emitter shorting, 549
 - full wave control, 499
 - fusing I^2t , 503, 512
 - gate cathode resistor, 500
 - gate circuits, 500
 - gate current, 491
 - gate requirements, 492
 - gate resistor, 540, 545
 - gate sensitivity, 491
 - gate triggering, 538
 - holding current, 491, 510
 - Hi-Com, 549, 551
 - inductive loads, 500
 - inrush current, 503
 - isolated trigger, 501
 - latching current, 491, 510
 - operation, 491
 - overcurrent, 503
 - phase angle, 500
 - phase control, 498, 527, 546
 - protection, 544
 - pulse triggering, 492
 - pulsed gate, 500
 - quadrants, 491, 510
 - resistive loads, 498
 - RFI, 497
 - saturable choke, 523
 - series choke, 502
 - snubber, 495, 502, 523, 529, 549
 - speed controller, 527
 - static switching, 497
 - structure, 489
 - switching, 489
 - synchronous control, 497
 - transformer load, 523
 - transient protection, 502
 - trigger angle, 492, 500
 - triggering, 550
 - turn-on di/dt , 502
 - varistor, 503
 - zero crossing, 537
- Trigger angle, 500
- TV & Monitors
 - 16 kHz black line, 351
 - 30-64 kHz autosync, 399
 - 32 kHz black line, 361
 - damper diodes, 345, 367
 - diode modulator, 327, 367
 - EHT, 352 - 354, 368, 409, 410
 - high voltage bipolar transistor, 339, 341
 - horizontal deflection, 341
 - picture distortion, 348
 - power MOSFET, 339
 - SMPS, 339, 354, 379, 389, 399
 - vertical deflection, 358, 364, 402
- Two transistor flyback converter, 111, 114
- Two transistor forward converter, 111, 117
- Universal motor
 - back EMF, 531

starting, 528

Vacuum cleaner, 527

Varistor, 503

Vertical Deflection, 358, 364, 402

Voltage doubling, 122

Water heaters, 537

Zero crossing, 537

Zero voltage switching, 537

CHAPTER 1

Introduction to Power Semiconductors

1.1 General

1.2 Power MOSFETS

1.3 High Voltage Bipolar Transistors

General



1.1.1 An Introduction To Power Devices

Today's mains-fed switching applications make use of a wide variety of active power semiconductor switches. This chapter considers the range of power devices on the market today, making comparisons both in terms of their operation and their general areas of application. The P-N diode will be considered first since this is the basis of all active switches. This will be followed by a look at both 3 layer and 4 layer switches.

Before looking at the switches let's briefly consider the various applications in which they are used. Virtually all mains fed power applications switch a current through an inductive load. This is the case even for resonant systems where the operating point is usually on the "inductive" side of the resonance curve. The voltage that the switch is normally required to block is, in the majority of cases, one or two times the maximum rectified input voltage depending on the configuration used. Resonant applications are the exception to this rule with higher voltages being generated by the circuit. For 110-240 V mains, the required voltage ratings for the switch can vary from 200 V to 1600 V.

Under normal operating conditions the off-state losses in the switch are practically zero. For square wave systems, the on-state losses (occurring during the on-time), are primarily determined by the on-state resistance which gives rise to an on-state voltage drop, V_{ON} . The (static) on-state losses may be calculated from:

$$P_{STATIC} = \delta \cdot V_{ON} \cdot I_{ON} \quad (1)$$

At the end of the "ON" time the switch is turned off. The turn-off current is normally high which gives rise to a loss dependent on the turn-off properties of the switch. The process of turn-on will also involve a degree of power loss so it is important not to neglect the turn-on properties either. Most applications either involve a high turn-on current or the current reaching its final value very quickly (high di/dt). The total dynamic power loss is proportional to both the frequency and to the turn-on and turn-off energies.

$$P_{DYNAMIC} = f \cdot (E_{ON} + E_{OFF}) \quad (2)$$

The total losses are the sum of the on-state and dynamic losses.

$$P_{TOT} = \delta \cdot V_{ON} \cdot I_{ON} + f \cdot (E_{ON} + E_{OFF}) \quad (3)$$

The balance of these losses is primarily determined by the switch used. If the on-state loss dominates, operating frequency will have little influence and the maximum frequency of the device is limited only by its total delay time (the sum of all its switching times). At the other extreme a device whose on-state loss is negligible compared with the switching loss, will be limited in frequency due to the increasing dynamic losses.

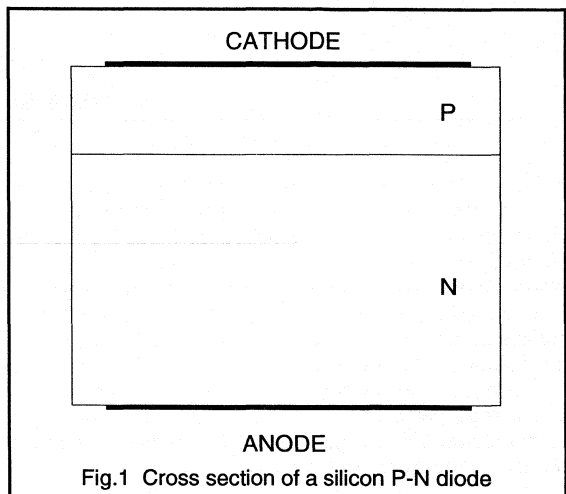
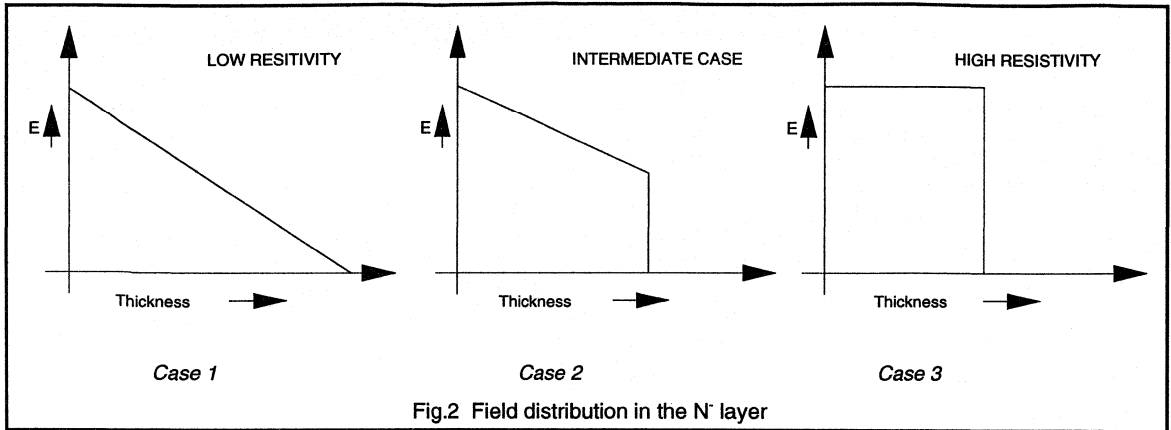


Fig.1 Cross section of a silicon P-N diode

High frequency switching When considering frequency limitation it is important to realise that the real issue is not just the frequency, but also the minimum on-time required. For example, an SMPS working at 100 kHz with an almost constant output power, will have a pulse on-time t_p of about 2-5 μ s. This can be compared with a high performance UPS working at 10 kHz with low distortion which also requires a minimum on-time of 2 μ s. Since the 10 kHz and 100 kHz applications considered here, require similar short on-times, both may be considered high frequency applications.

Resonant systems have the advantage of relaxing turn-on or turn-off or both. This however tends to be at the expense of V-A product of the switch. The relaxed switching conditions imply that in resonant systems switches can be used at higher frequencies than in non resonant systems. When evaluating switches this should be taken into account.

Fig.2 Field distribution in the N⁺ layer

At higher values of *throughput power*, the physical size of circuits increases and as a consequence, the stray inductances will also tend to increase. Since the required currents are higher, the energy stored in the stray inductances rises significantly, which in turn means the induced peak voltages also rise. As a result such applications force the use of longer pulse times, to keep losses down, and protection networks to limit overshoot or networks to slow down switching speeds. In addition the use of larger switches will also have consequences in terms of increasing the energy required to turn them on and off and drive energy is very important.

So, apart from the voltage and current capabilities of devices, it is necessary to consider static and dynamic losses, drive energy, dV/dt , dI/dt and Safe Operating Areas.

The silicon diode

Silicon is the semiconductor material used for all power switching devices. Lightly doped N⁻ silicon is usually taken as the starting material. The resistance of this material depends upon its resistivity, thickness and total area.

$$R = \rho \cdot \frac{l}{A} \quad (4)$$

A resistor as such does not constitute an active switch, this requires an extra step which is the addition of a P-layer. The result is a diode of which a cross section is drawn in Fig.1

The blocking diode

Since all active devices contain a diode it is worth considering its structure in a little more detail. To achieve the high blocking voltages required for active power switches necessitates the presence of a thick N⁻ layer. To withstand a given voltage the N⁻ layer must have the right

combination of thickness and resistivity. Some flexibility exists as to what that combination is allowed to be, the effects of varying the combination are described below.

Case 1: Wide N⁻ layer and low resistivity

Figure 2 gives the field profile in the N⁻ layer, assuming the junction formed with the P layer is at the left. The maximum field at the P-N junction is limited to 22 kV/cm by the breakdown properties of the silicon. The field at the other end is zero. The slope of the line is determined by the resistivity. The total voltage across the N⁻ layer is equal to the area underneath the curve. Please note that increasing the thickness of the device would not contribute to its voltage capability in this instance. This is the normal field profile when there is another P-layer at the back as in 4 layer devices (described later).

Case 2: Intermediate balance

In this case the higher resistivity material reduces the slope of the profile. The field at the junction is the same so the same blocking voltage capability (area under the profile) can be achieved with a thinner device.

The very steep profile at the right hand side of the profile indicates the presence of an N⁺ layer which often required to ensure a good electrical contact

Case 3: High resistivity material

With sufficiently high resistivity material a near horizontal slope to the electric field is obtained. It is this scenario which will give rise to the thinnest possible devices for the same required breakdown voltage. Again an N⁺ layer is required at the back.

An optimum thickness and resistivity exists which will give the lowest possible resistance for a given voltage capability. Both case 1 (very thick device) and case 3 (high resistivity) give high resistances, the table below shows the thickness and resistivity combinations possible for a 1000 V diode.

The column named RA gives the resistance area product. (A device thickness of less than 50 μm will never yield 1000 V and the same goes for a resistivity of less than 26 Ωcm .) The first specification is for the thinnest device possible and the last one is for the thickest device, (required when a P layer is present at the back). It can be seen that the lowest resistance is obtained with an intermediate value of resistivity and material thickness.

Thickness (μm)	Resistivity (Ωcm)	RA Ωcm^2	Comments
50	80	0.400	case 3
60	34	0.204	
65	30	0.195	
70	27	0.189	min. R
75	26	0.195	
80	26	0.208	
90	26	0.234	
100	26	0.260	case 1

To summarise, a designer of high voltage devices has only a limited choice of material resistivity and thickness with which to work. The lowest series resistance is obtained for a material thickness and resistivity intermediate between the possible extremes. This solution is the optimum for all majority carrier devices such as the PowerMOSFET and the J-FET where the on-resistance is uniquely defined by the series resistance. Other devices make use of charge storage effects to lower their on-state voltage. Consequently to optimise switching performance in these devices the best choice will be the thinnest layer such that the volume of stored charge is kept to a minimum. Finally as mentioned earlier, the design of a 4 layer device requires the thickest, low resistivity solution.

The forward biased diode

When a diode is forward biased, a forward current will flow. Internally this current will have two components: an electron current which flows from the N layer to the P layer and a hole current in the other direction. Both currents will generate a charge in the opposite layer (indicated with Q_p and Q_n in Fig.3). The highest doped region will deliver most of the current and generate most of the charge. Thus in a P^+N diode the current will primarily be made up of holes flowing from P to N and there will be a significant volume of hole charge in the N layer. This point is important when discussing active devices: whenever a diode is forward biased (such as a base-emitter diode) there will be a charge stored in the lowest doped region.

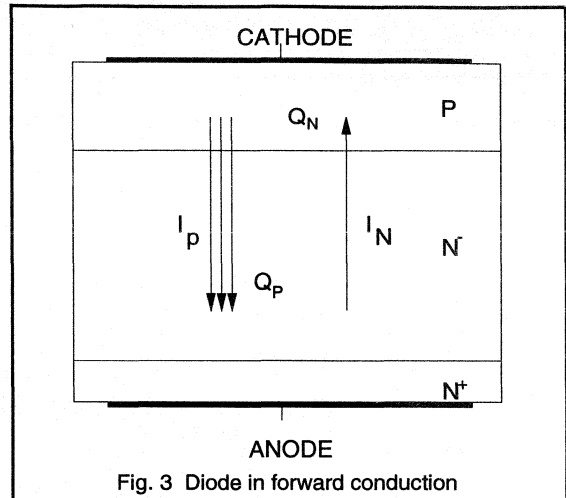


Fig. 3 Diode in forward conduction

The exact volume of charge that will result is dependent amongst other things on the minority carrier lifetime, τ . Using platinum or gold doping or by irradiation techniques the value of τ can be decreased. This has the effect of reducing the volume of stored charge and causing it to disappear more quickly at turn-off. A side effect is that the resistivity will increase slightly.

Three layer devices

The three basic designs, which form the basis for all derived 3 layer devices, are given in Fig.4. It should be emphasised here that the discussion is restricted to high voltage devices only as indicated in the first section. This means that all relevant devices will have a *vertical structure*, characterised by a wide N⁻ layer.

The figure shows how a three layer device can be formed by adding an N type layer to the P-N diode structure. Two back to back P-N diodes thus form the basis of the device, where the P layer provides a means to control the current when the device is in the on-state.

There are three ways to use this P-layer as a control terminal. The first is to feed current into the terminal itself. The current through the main terminals is now proportional to the drive current. This device is called a *High Voltage Transistor* or *HVT*.

The second one is to have openings in the P-layer and permit the main current to flow between them. When reverse biasing the gate-source, a field is generated which blocks the opening and pinches off the main current. This device is known as the *J-FET* (junction FET) or *SIT* (Static Induction Transistor).

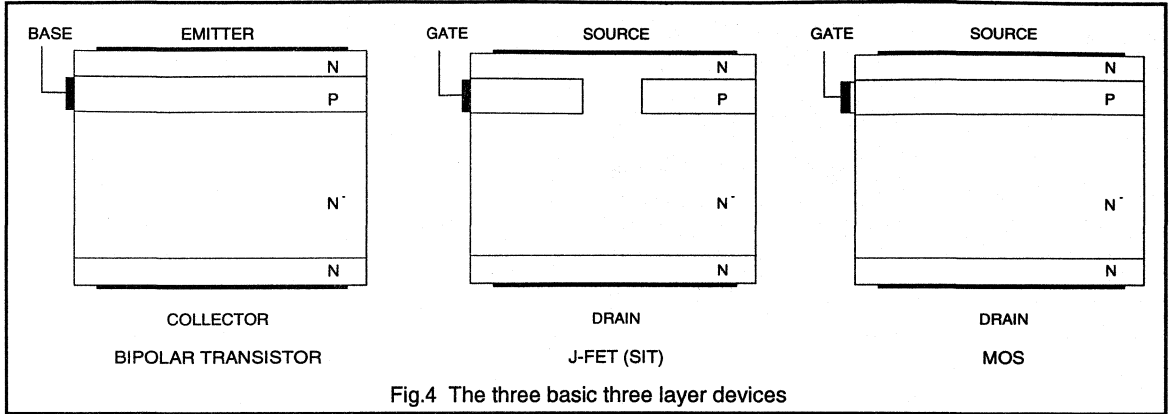


Fig.4 The three basic three layer devices

The third version has an electrode (gate) placed very close to the P-layer. The voltage on this gate pushes away the holes in the P-area and attracts electrons to the surface beneath the gate. A channel is thus formed between the main terminals so current can flow. The well known name for this device is *MOS transistor*.

In practice however, devices bear little resemblance to the constructions of Fig.4. In virtually all cases a planar construction is chosen i.e. the construction is such that one main terminal (emitter or source) and the drive contact are on the surface of the device. Each of the devices will now be considered in some more detail.

The High Voltage Transistor (HVT)

The *High Voltage Transistor* uses a positive base current to control the main collector current. The relation is: $I_C = H_{FE} \cdot I_B$. The base drive forward biases the base emitter P-N junction and charge (holes and electrons) will pass through it. Now the base of a transistor is so thin that the most of the electrons do not flow to the base but into the collector - giving rise to a collector current. As explained previously, the ratio between the holes and electrons depend on the doping. So by correctly doping the base emitter junction, the electron current can be made much larger than the hole current, which means that I_C can be much larger than I_B .

When enough base drive is provided it is possible to forward bias the base-collector P-N junction also. This has a significant impact on the resistance of the N' layer; holes now injected from the P type base constitute stored charge causing a substantial reduction in on-state resistance, much lower than predicted by equation 4. Under these conditions the collector is an effective extension of the base. Unfortunately the base current required to maintain this

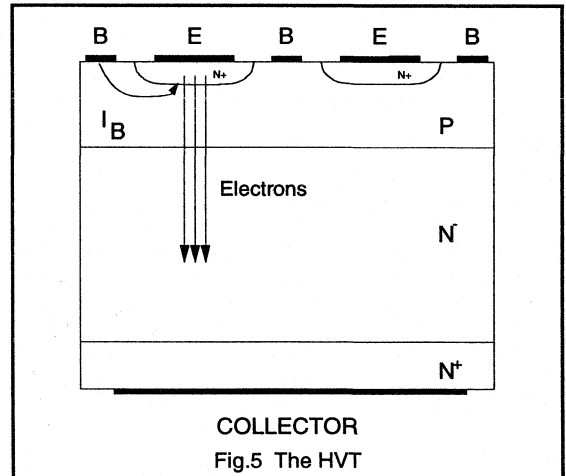


Fig.5 The HVT

condition causes the current gain to drop. For this reason one cannot use a HVT at a very high current density because then the gain would become impractically low.

The on-state voltage of an HVT will be considerably lower than for a MOS or J-FET. This is its main advantage, but the resulting charge stored in the N' layer has to be delivered and also to be removed. This takes time and the speed of a bipolar transistor is therefore not optimal. To improve speed requires optimisation of a fine emitter structure in the form of fingers or cells.

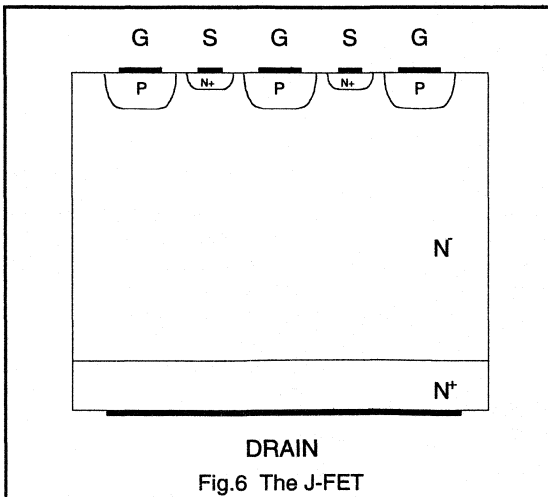
Both at turn-on and turn-off considerable losses may occur unless care is taken to optimise drive conditions. At turn-on a short peak base current is normally required. At turn-off a negative base current is required and negative drive has to be provided.

A serious limitation of the HVT is the occurrence of *second breakdown* during switch off. The current contracts towards the middle of the emitter fingers and the current density can become very high. The RBSOAR (Reverse Bias Safe Operating Area) graph specifies where the device can be used safely. Device damage may result if the device is not properly used and one normally needs a snubber (dV/dt network) to protect the device. The price of such a snubber is normally in the order of the price of the transistor itself. In resonant applications it is possible to use the resonant properties of the circuit to have a slow dV/dt .

So, the bipolar transistor has the advantage of a very low forward voltage drop, at the cost of lower speed, a considerable energy is required to drive it and there are also limitations in the RBSOAR.

The J-FET.

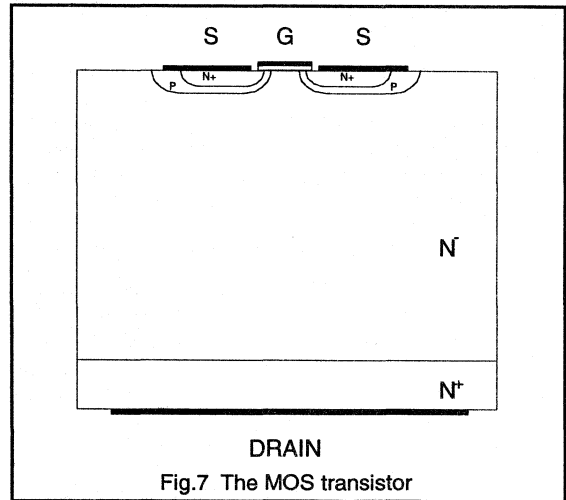
The *J-FET* (Junction Field Effect Transistor) has a direct resistance between the Source and the Drain via the opening in the P-layer. When the gate-source voltage is zero the device is on. Its on-resistance is determined by the resistance of the silicon and no charge is present to make the resistance lower as in the case of the bipolar transistor. When a negative voltage is applied between Gate and Source, a depletion layer is formed which pinches off the current path. So, the current through the switch is determined by the voltage on the gate. The drive energy is low, it consists mainly of the charging and discharging of the gate-source diode capacitance. This sort of device is normally very fast.



Its main difficulty is the opening in the P-layer. In order to speed up performance and increase current density, it is necessary to make a number of openings and this implies fine geometries which are difficult to manufacture. A solution exists in having the P-layer effectively on the surface, basically a diffused grid as shown in Fig.6. Unfortunately the voltages now required to turn the device off may be very large: it is not uncommon that a voltage of 25 V negative is needed. This is a major disadvantage which, when combined with its "normally-on" property and the difficulty to manufacture, means that this type of device is not in mass production.

The MOS transistor.

The *MOS* (Metal Oxide Semiconductor) transistor is normally off: a positive voltage is required to induce a channel in the P-layer. When a positive voltage is applied to the gate, electrons are attracted to the surface beneath the gate area. In this way an "inverted" N-type layer is forced in the P-material providing a current path between drain and source.



Modern technology allows a planar structure with very narrow cells as shown in Fig.7. The properties are quite like the J-FET with the exception that the charge is now across the (normally very thin) gate oxide. Charging and discharging the gate oxide capacitance requires drive currents when turning on and off. Switching speeds can be controlled by controlling the amount of drive charge during the switching interval. Unlike the J-FET it does not require a negative voltage although a negative voltage may help switch the device off quicker.

The MOSFET is the preferred device for higher frequency switching since it combines fast speed, easy drive and wide commercial availability.

Refinements to the basic structure

A number of techniques are possible to improve upon behaviour of the basic device.

First, the use of *finer geometries* can give lower on-state voltages, speed up devices and extend their energy handling capabilities. This has led to improved "Generation 3" devices for bipolars and to lower $R_{DS(ON)}$ for PowerMOS. Secondly, *killing the lifetime* τ in the device can also yield improvements. For bipolar devices, this positively affects the switching times. The gain, however, will drop, and this sets a maximum to the amount of lifetime killing. For MOS a lower value for τ yields the so-called FREDFETs, with an intrinsic diode fast enough for many half bridge applications such as in AC Motor Controllers. The penalty here is that $R_{DS(ON)}$ is adversely effected (slightly). Total losses, however, are decreased considerably.

Four layer devices

The three basic designs from the previous section can be extended with a P^+ -layer at the back, thereby generating three basic Four Layer Devices. The addition of this extra layer creates a PNP transistor from the P^+ -N'-P-layers. In all cases the 3 layer NPN device will now deliver an electron current into the back P^+ -layer which acts as an emitter. The PNP transistor will thus become active which results in a hole current flowing from the P^+ -layer into the high resistive region. This in its turn will lead to a *hole charge* in the high resistive region which lowers the on-state voltage considerably, as outlined above for High Voltage Transistors. Again, the penalty is in the switching times which will increase.

All the devices with an added P^+ -layer at the back will inject holes into the N'-layer. Since the P^+ -layer is much heavier doped than the N'-layer, this hole current will be the major contributor to the main current. This means that the charge in the N'-layer, especially near the N'- P^+ -junction, will be large. Under normal operation the hole current will be large enough to influence the injection of electrons from the top N^+ -layer. This results in extra electron current being injected from the top, leading to extra hole current from the back etc. This situation is represented in the schematic of Fig.8.

An important point is *latching*. This happens when the internal currents are such that we are not able to turn off the device using the control electrode. The only way to turn it off is by externally removing the current from the device.

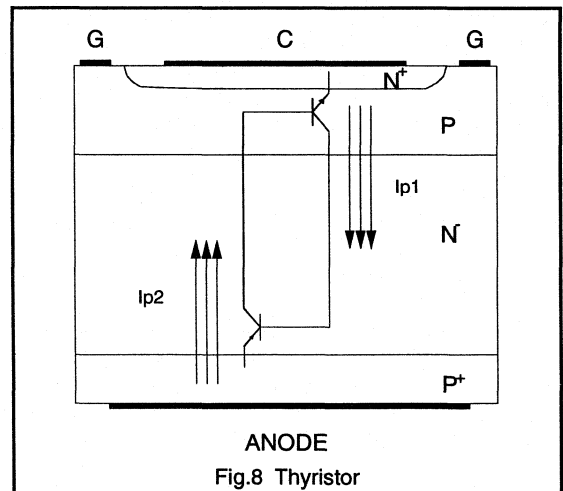
The switching behaviour of all these devices is affected by the behaviour of the PNP: as long as a current is flowing through the device, the back will inject holes into the N'-layer. This leads to switching tails which contribute heavily to switching losses. The tail is strongly affected by the lifetime τ and by the application of negative drive current

when possible. As previously explained, adjustment of the lifetime affects the on-state voltage. Carefully adjusting the lifetime τ will balance the on-state losses with the switching losses.

All four layer devices show this trade-off between switching losses and on-state losses. When minimising switching losses, the devices are optimised for high frequency applications. When the on-state losses are lowest the current density is normally highest, but the device is only useful at low frequencies. So two variants of the four layer device generally exist. In some cases intermediate speeds are also useful as in the case of very high power GTOs.

The Thyristor

A *thyristor* (or SCR, Silicon Controlled Rectifier) is essentially an HVT with an added P^+ -layer. The resulting P^+ -N'- P^+ transistor is on when the whole device is on and provides enough base current to the N^+ -P-N' transistor to stay on. So after an initial kick-on, no further drive energy is required.

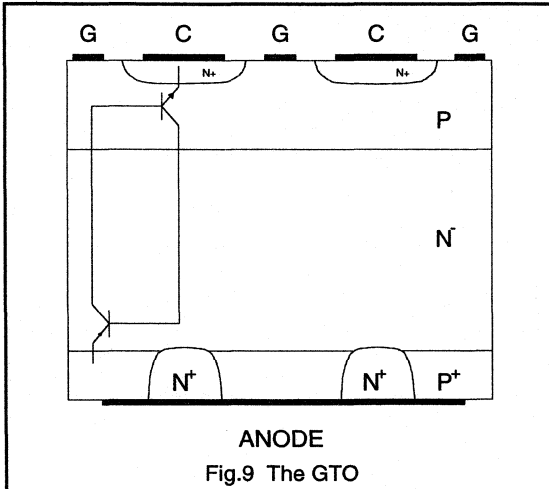


The classical thyristor is thus a latching device. Its construction is normally not very fine and as a result the gate contact is too far away from the centre of the active area to be able to switch it off. Also the current density is much higher than in a bipolar transistor. The switching times however are very long. Its turn-on is hampered by its structure since it takes quite a while for the whole crystal to become active. This seriously limits its di/dt .

Once a thyristor is on it will only turn-off after having zero current for a few microseconds. This is done by temporarily forcing the current via a so-called commutation circuit.

The charge in the device originates from two sources: The standard NPN transistor structure injects holes in the N-layer (I_{P1} in Fig.8) and the PNP transistor injects a charge from the back (I_{P2} in Fig.8). Therefore the total charge is big and switching performance is very poor. Due to its slow switching a normal thyristor is only suitable up to a few kHz.

A major variation on the thyristor is the *GTO* (Gate Turn Off Thyristor). This is a thyristor where the structure has been tailored to give better speed by techniques such as accurate lifetime killing, fine finger or cell structures and "anode shorts" (short circuiting P⁺ and N⁻ at the back in order to decrease the current gain of the PNP transistor). As a result, the product of the gain of both NPN and PNP is just sufficient to keep the GTO conductive. A negative gate current is enough to sink the hole current from the PNP and turn the device off.

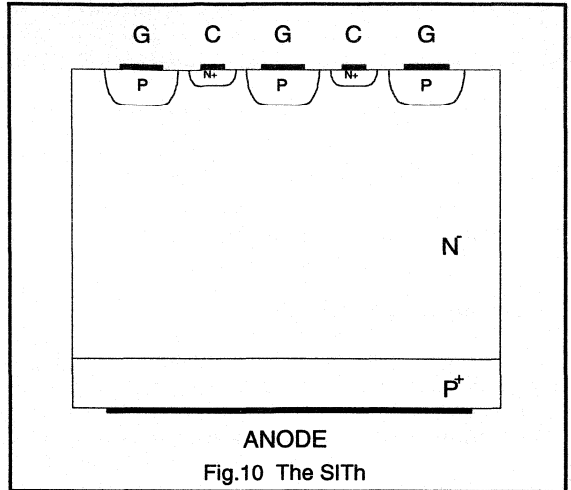


A GTO shows much improved switching behaviour but still has the tail as described above. Lower power applications, especially resonant systems, are particularly attractive for the GTO because the turn-off losses are virtually zero.

The SITH

The *SITH* (Static Induction Thyristor) sometimes also referred to as *FCT* (Field Controlled Thyristor) is essentially a J-FET with an added P⁺ back layer. In contrast to the standard thyristor, charge is normally only injected from the back, so the total amount of charge is limited. However, a positive gate drive is possible which will reduce on-state resistance.

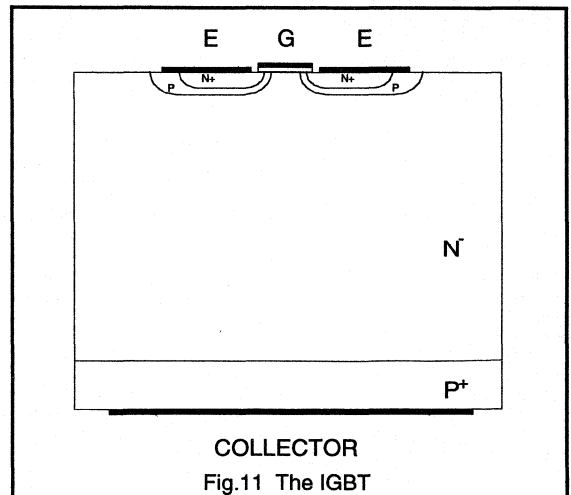
Active extraction of charge via the gate contact is possible and switching speeds may be reduced considerably by applying an appropriate negative drive as in the case of an HVT. As for the SIT the technological complexity is a severe



drawback, as is its negative drive requirements. Consequently mass production of this device is not available yet.

The IGBT

An *IGBT* (Insulated Gate Bipolar Transistor) is an MOS transistor with P⁺ at the back. Charge is injected from the back only, which limits the total amount of charge. Active charge extraction is not possible, so the carrier lifetime τ should be chosen carefully, since that determines the switching losses. Again two ranges are available with both fast and slow IGBTs.



The speed of the fast IGBT is somewhat better than that of a GTO because a similar technology is used to optimise the IGBT but only the back P⁺-layer is responsible for the charge.

The IGBT is gaining rapidly in popularity since its manufacturing is similar to producing PowerMOS and an increasing market availability exists. Although the latching of IGBTs was seen as a problem, modern optimised devices don't suffer from latch-up in practical conditions.

Refinements to the basic structure

The refinements outlined for 3 layer devices also apply to 4 layer structures. In addition to these, an N⁺-layer may be inserted between the P⁺ and N⁻-layer. Without such a layer the designer is limited in choice of starting material to Case 3 as explained in the diode section. Adding the extra N⁺-layer allows another combination of resistivity and thickness to be used, improving device performance. An example of this is the ASCR, the Asymmetric SCR, which is much faster than normal thyristors. The reverse blocking capability, however, is now reduced to a value of 10-20 V.

Comparison of the Basic Devices.

It is important to consider the properties of devices mentioned when choosing the optimum switch for a particular application. Table 2 gives a survey of the essential device properties of devices capable of withstanding 1000 V. IGBTs have been classed in terms of fast and slow devices, however only the fast GTO and slow thyristor are represented. The fast devices are optimised for speed, the slow devices are optimised for On voltage.

Comments

This table is valid for 1000 V devices. Lower voltage devices will always perform better, higher voltage devices are worse.

A dot means an average value in between "+" and "-"

The "(--)" for a thyristor means a "--" in cases where forced commutation is used; in case of natural commutation it is "+"

Most figures are for reference only: in exceptional cases better performance has been achieved, but the figures quoted represent the state of the art.

	HVT	J-FET	MOS	THY	GTO	IGBT slow	IGBT fast	Unit
V(ON)	1	10	5	1.5	3	2	4	V
Positive Drive Requirement	-	+	+	+	+	+	+	+ = Simple to implement
Turn-Off requirement	-	-	+	(--)	-	+	+	+ = Simple to implement
Drive circuit complexity	-	.	+	(-)	.	+	+	- = complex
Technology Complexity	+	.	.	+	-	-	-	- = complex
Device Protection	-	.	+	+	-	-	-	+ = Simple to implement
Delay time (ts, tq)	2	0.1	0.1	5	1	2	0.5	µs
Switching Losses	.	++	++	--	-	-	.	+ = good
Current Density	50	12	20	200	100	50	50	A/cm ²
Max dv/dt (Vin = 0)	3	20	10	0.5	1.5	3	10	V/ns
di/dt	1	10	10	1	0.3	10	10	A/ns
Vmax	1500	1000	1000	5000	4000	1000	1000	V
I _{max}	1000	10	100	5000	3000	400	400	A
Over Current factor	5	3	5	15	10	3	3	

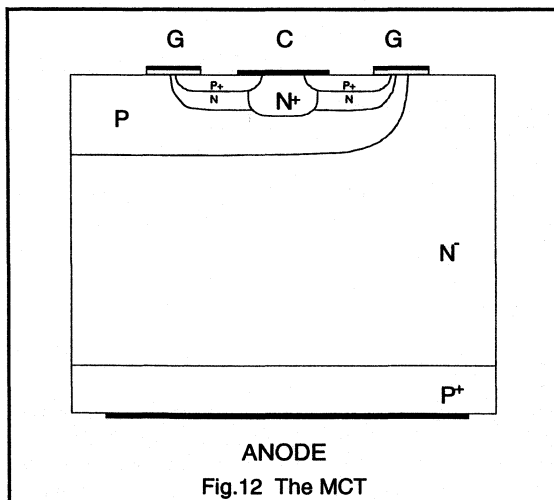
Merged devices

Merged devices are the class of devices composed of two or more of the above mentioned basic types. They don't offer any breakthrough in device performance. This is understandable since the basic properties of the discussed devices are not or are hardly effected. They may be beneficial for the user though, primarily because they may result in lower positive and/or negative drive requirements.

Darlington and BiMOS

A darlington consists of two bipolar transistors. The emitter current of the first (the driver) forms the base current of the output transistor. The advantages of darlington may be summarised as follows. A darlington has a higher gain than a single transistor. It also switches faster because the input transistor desaturates the output transistor and lower switching losses are the result. However, the resulting $V_{CE(sat)}$ is higher. The main issue, especially for higher powers is the savings in drive energy. This means that darlington can be used at considerably higher output powers than standard transistors. Modern darlington in high power packages can be used in 20 kHz motor drives and power supplies.

A BiMOS consists of a MOS driver and a bipolar output transistor. The positive drive is the same as MOS but turn-off is generally not so good. Adding a "speed-up" diode coupled with some negative drive improves things.



MCT

MCT stands for *MOS Controlled Thyristor*. This device is effectively a GTO with narrow tolerances, plus a P-MOS transistor between gate and source (P⁺-N-P MOS, the left hand gate in Fig.12) and an extra N-MOS to turn it on, the N-P-N-MOS shown underneath the right hand gate.

Where the GTO would like to be switched off with a negative gate, the internal GTO in an MCT can turn off by short circuiting its gate-cathode, due to its fine structure. Its drive therefore is like a MOS transistor and its behaviour similar to a GTO. Looking closely at the device it is obvious that a GTO using similar fine geometries with a suitable external drive can always perform better, at the cost of some drive circuitry. The only plus point seems to be its ease of drive.

Application areas of the various devices

The following section gives an *indication* of where the various devices are best placed in terms of applications. It is possible for circuit designers to use various tricks to integrate devices and systems in innovative manners, applying devices far outside their 'normal' operating conditions. As an example, it is generally agreed that above 100 kHz bipolars are too difficult to use. However, a 450 kHz converter using bipolars has been already described in the literature.

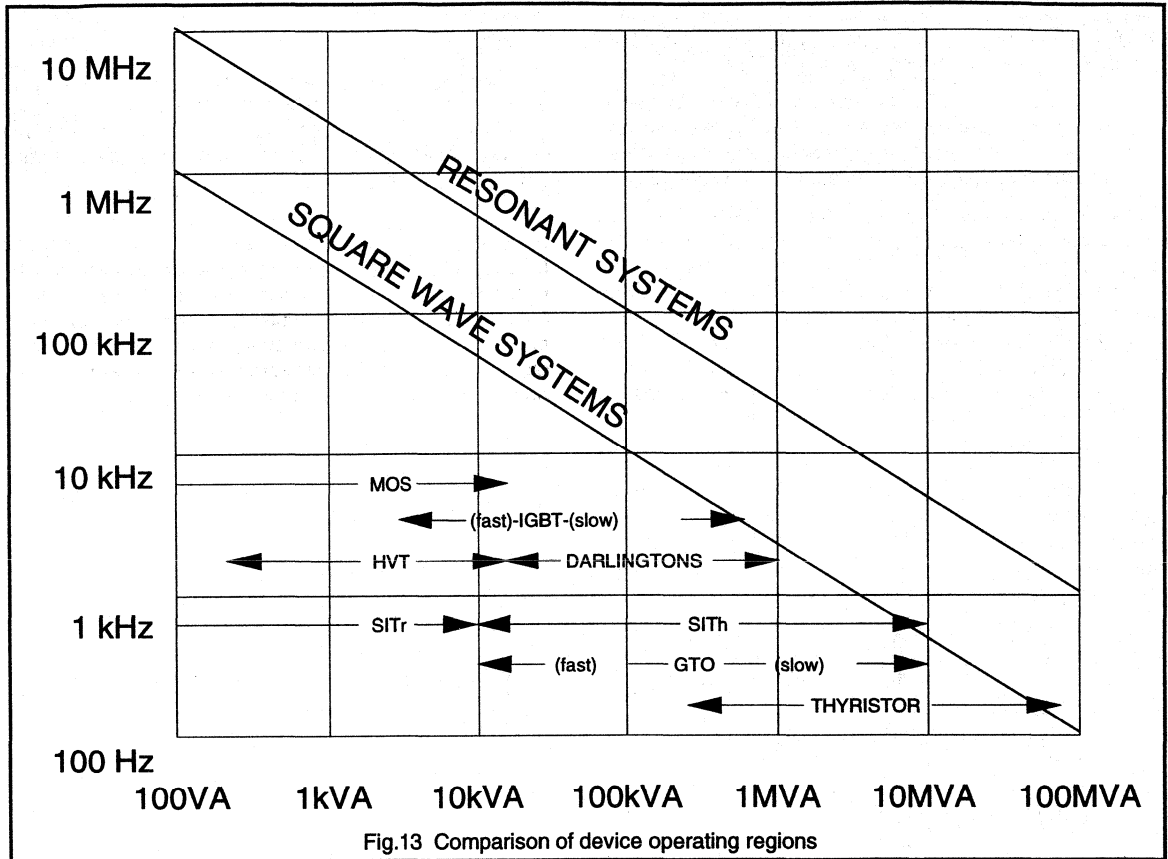
As far as the maximum frequency is concerned a number of arguments must be taken into account.

First the *delay times*, either occurring at turn-on or at turn-off, will limit the maximum operating frequency. A reasonable rule of thumb for this is $f_{MAX} = 3 / t_{DELAY}$. (There is a danger here for confusion: switching times tend to depend heavily on circuit conditions, drive of the device and on current density. This may lead to a very optimistic or pessimistic expectation and care should be taken to consider reasonable conditions.)

Another factor is the *switching losses* which are proportional to the frequency. These power losses may be influenced by optimising the drive or by the addition of external circuits such as dV/dt or dI/dt networks. Alternatively the heatsink size may be increased or one may choose to operate devices at a lower current density in order to decrease power losses. It is clear that this argument is very subjective.

A third point is *manufacturability*. The use of fine structures for example, which improves switching performance, is possible only for small silicon chip sizes: larger chips with very fine MOS-like structures will suffer from unacceptable low factory yields. Therefore high power systems requiring large chip areas are bound to be made with less fine structures and will consequently be slower.

The *operating current density* of the device will influence its physical size. A low current density device aimed at high power systems would need a large outline which tends to be expensive. Large outlines also increase the physical size of the circuit, which leads to bigger parasitic inductances and associated problems.



High power systems will, because of the mechanical size, be restricted in speed as explained earlier in the text. This coincides well with the previously mentioned slower character of higher power devices.

Last but not least it is necessary to take the *application topology* into account. Resonant systems allow the use of considerably higher frequencies, since switching losses are minimised. Square wave systems cause more losses in the devices and thus restrict the maximum frequency. To make a comparison of devices and provide insight into which powers are realistic for which devices we have to take all the above mentioned criteria into account.

Figure 13 shows the optimum working areas of the various switching devices as a function of switchable power and frequency. The *switchable power* is defined as I_{AV} times V_{MAX} as seen by the device.

As an example, darlington's will work at powers up to 1 MVA i.e. 1000 V devices will switch 1000 A. The frequency is then limited to 2.5 kHz. At lower powers higher frequencies

can be achieved however above 50 kHz, darlington's are not expected to be used. One should use this table only as guidance; using special circuit techniques, darlington's have actually been used at higher frequencies. Clearly operation at lower powers and frequencies is always possible.

Conclusions

The starting material for active devices aimed at high voltage switching are made on silicon of which the minimum resistivity and thickness are limited. This essentially determines device performance, since all active switches incorporate such a layer. Optimisation can be performed for either minimum thickness, as required in the case of HVTs, or for minimum resistance, as required for MOS and J-FETs. The thickest variation (lowest resistivity) is required in the case of some 4 layer devices.

Basically three ways exist to control current through the devices: feeding a base current into a P-layer (transistor),

using a voltage to pinch-off the current through openings in the P-layer (J-FET) and by applying a voltage onto a gate which inverts the underlying P-layer (MOS).

The HVT is severely limited in operating frequency due to its stored hole charge, but this at the same time allows a greater current density and a lower on-state voltage. It also requires more drive energy than both MOS and J-FET.

When we add a P⁺-layer at the back of the three basic three layer devices we make three basic four layer devices. The P⁺-layer produces a PNP transistor at the back which exhibits hole storage. This leads to much improved current densities and lower on-state losses, at the cost of switching speed. The four layer devices can be optimised for low on-state losses, in which case the switching will be poor, or for fast switching, in which case the on-state voltage will

be high.

The properties of all six derived basic devices are determined to a large extent by the design of the high resistive area and can be optimised by applying technological features in the devices such as lifetime killing and fine geometries.

Resonant systems allow devices to be used at much higher frequencies due to the lower switching losses and the minimum on-times which may be longer, compared to square wave switching systems. Figure 13 gives the expected maximum frequency and switching power for the discussed devices. The difference for square wave systems and resonant systems is about a factor of 10.

Power MOSFET



1.2.1 PowerMOS Introduction

Device structure and fabrication

The idea of a vertical channel MOSFET has been known since the 1930s but it was not until the mid 1970s that the technology of diffusion, ion implantation and material treatment had reached the level necessary to produce DMOS on a commercial scale. The vertical diffusion technique uses technology more commonly associated with the manufacture of large scale integrated circuits than with traditional power devices. Figure 1(a) shows the vertical double implanted (DIMOS) channel structure which is the basis for all Philips power MOSFET devices.

An N-channel PowerMOS transistor is fabricated on an N⁺ substrate with a drain metallization applied to its underside. Above the N⁺ substrate is an N⁻ epi layer, the thickness and resistivity of which depends on the required drain-source breakdown voltage. The channel structure, formed from a double implant in to the surface epi material, is laid down in a cellular pattern such that many thousands of cells go to make a single transistor. The N⁺ polysilicon gate which is embedded in an isolating silicon dioxide layer, is a single structure which runs between the cells across the entire active region of the device. The source metallization also covers the entire structure and thus

parallels all the individual transistor cells on the chip. The layout of a typical low voltage chip is shown in Fig.1(b). The polysilicon gate is contacted by bonding to the defined pad area while the source wires are bonded directly to the aluminium over the cell array. The back of the chip is metallized with a triple layer of titanium/nickel/silver and this enables the drain connection to be formed using a standard alloy bond process.

The active part of the device consists of many cells connected in parallel to give a high current handling capability where the current flow is vertical through the chip. Cell density is determined by photolithographic tolerance requirements in defining windows in the polysilicon and gate-source oxide and also by the width of the polysilicon track between adjacent cells. The optimum value for polysilicon track width and hence cell density varies as a function of device drain-source voltage rating, this is explained in more detail further in the section. Typical cell densities are 1.6 million cells per square inch for low voltage types and 350,000 cells per square inch for high voltage types. The cell array is surrounded by an edge termination structure to control the surface electric field distribution in the device off-state.

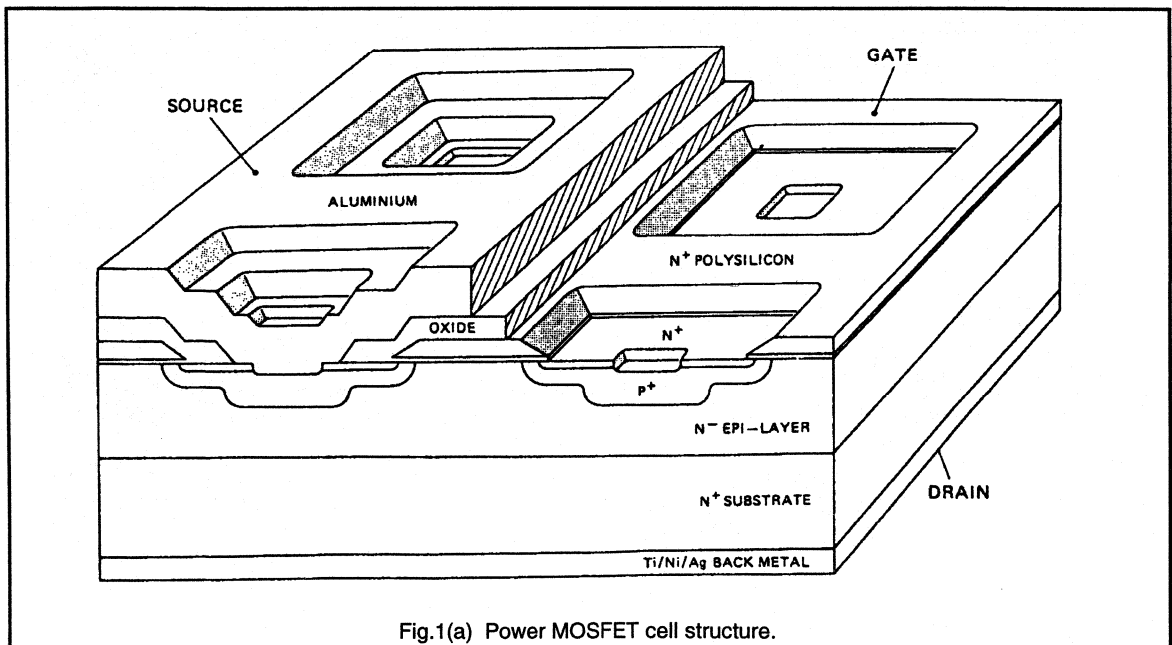


Fig.1(a) Power MOSFET cell structure.

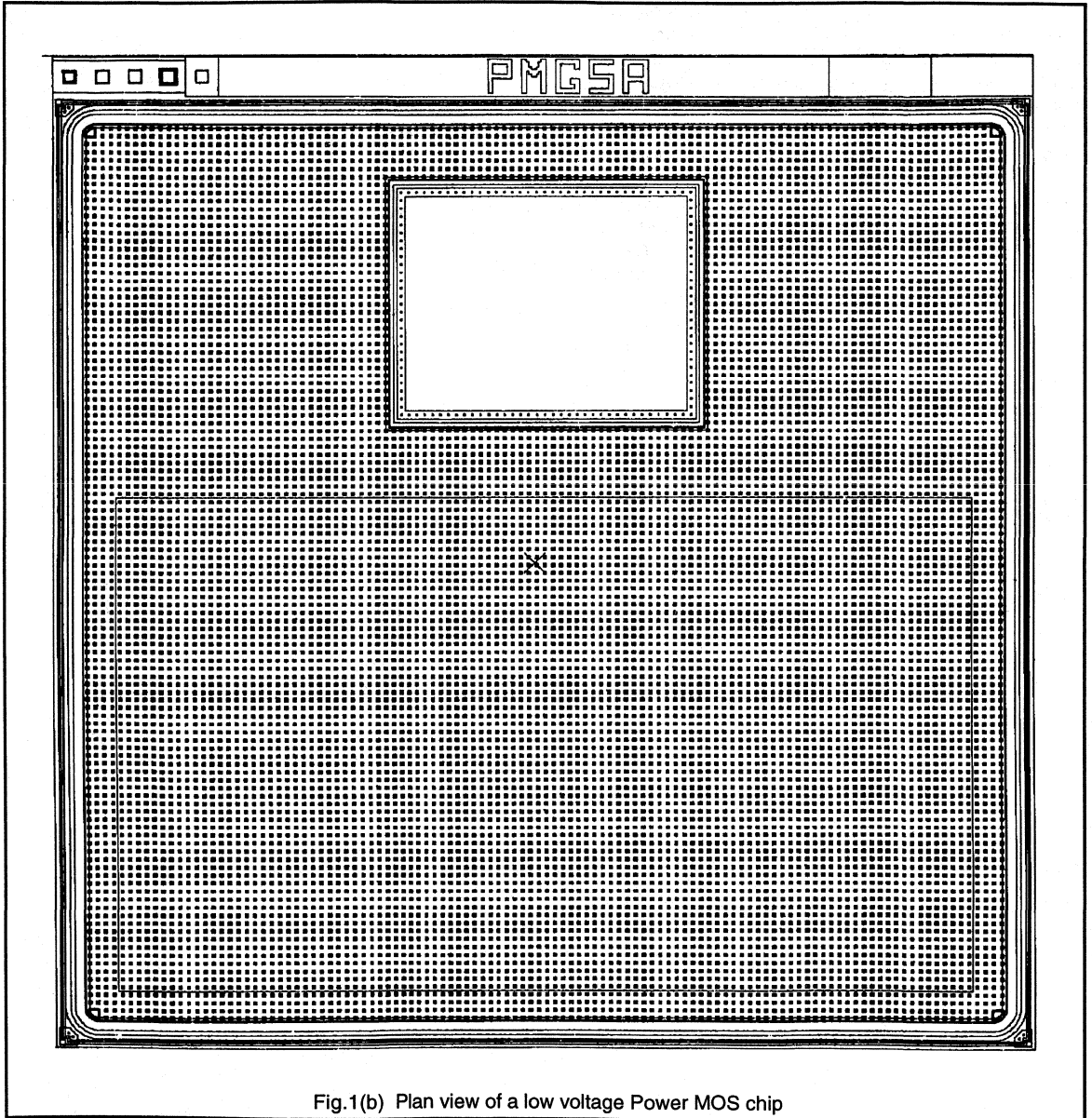


Fig.1(b) Plan view of a low voltage Power MOS chip

A cross-section through a single cell of the array is shown in Fig.2. The channel length is approximately 1.5 microns and is defined by the difference in the sideways diffusion of the N⁺ source and the P-body. Both these diffusions are auto-aligned to the edge of the polysilicon gate during the fabrication process. All diffusions are formed by ion implantation followed by high temperature anneal/drive-in to give good parameter reproducibility. The gate is electrically isolated from the silicon by an 800 Angstrom layer of gate oxide (for standard types, 500 Angstrom for Logic level and from the overlying aluminium by a thick layer of phosphorus doped oxide. Windows are defined in the latter oxide layer to enable the aluminium layer to contact the N⁺ source and the P⁺ diffusion in the centre of each cell. The P⁺ diffusion provides a low resistance connection between the P⁻ body and ground potential, thus inhibiting turn-on of the inherent parasitic NPN bipolar structure.

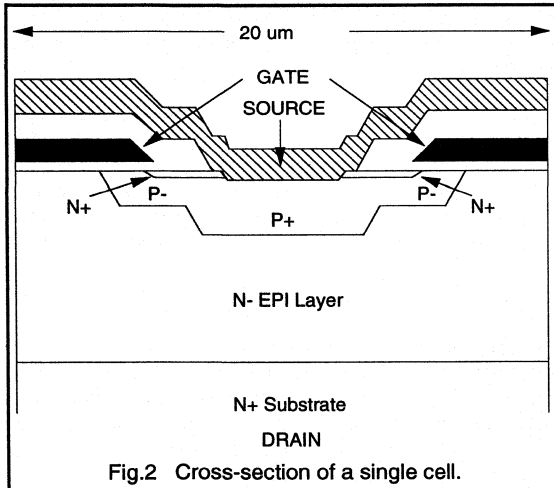


Fig.2 Cross-section of a single cell.

Device operation

Current flow in an enhancement mode power MOSFET is controlled by the voltage applied between the gate and source terminals. The P⁻ body isolates the source and drain regions and forms two P-N junctions connected back-to-back. With both the gate and source at zero volts there is no source-drain current flow and the drain sits at the positive supply voltage. The only current which can flow from source to drain is the reverse leakage current.

As the gate voltage is gradually made more positive with respect to the source, holes are repelled and a depleted region of silicon is formed in the P⁻ body below the silicon-gate oxide interface. The silicon is now in a 'depleted' state, but there is still no significant current flow between the source and drain.

When the gate voltage is further increased a very thin layer of electrons is formed at the interface between the P⁻ body and the gate oxide. This conductive N-type channel enhanced by the positive gate-source voltage, now permits current to flow from drain to source. The silicon in the P⁻ body is referred to as being in an 'inverted' state. A slight increase in gate voltage will result in a very significant increase in drain current and a corresponding rapid decrease in drain voltage, assuming a normal resistive load is present.

Eventually the drain current will be limited by the combined resistances of the load resistor and the $R_{DS(ON)}$ of the MOSFET. The MOSFET resistance reaches a minimum when $V_{GS} = +10$ volts (assuming a standard type). Subsequently reducing the gate voltage to zero volts reverses the above sequence of events. There are no stored charge effects since power MOSFETs are majority carrier devices.

Power MOSFET parameters

Threshold voltage

The threshold voltage is normally measured by connecting the gate to the drain and then determining the voltage which must be applied across the devices to achieve a drain current of 1.0 mA. This method is simple to implement and provides a ready indication of the point at which channel inversion occurs in the device.

The P⁻ body is formed by the implantation of boron through the tapered edge of the polysilicon followed by an anneal and drive-in. The main factors controlling threshold voltage are gate oxide thickness and peak surface concentration in the channel, which is determined by the P-body implant dose. To allow for slight process variation a window is usually defined which is 2.1 to 4.0 volts for standard types and 1.0 to 2.0 volts for logic level types.

Positive charges in the gate oxide, for example due to sodium, can cause the threshold voltage to drift. To minimise this effect it is essential that the gate oxide is grown under ultra clean conditions. In addition the polysilicon gate and phosphorus doped oxide layer provide a good barrier to mobile ions such as sodium and thus help to ensure good threshold voltage stability.

Drain-source on-state resistance

The overall drain-source resistance, $R_{DS(ON)}$, of a power MOSFET is composed of several elements, as shown in Fig.3.

The relative contribution from each of the elements varies with the drain-source voltage rating. For low voltage devices the channel resistance is very important while for

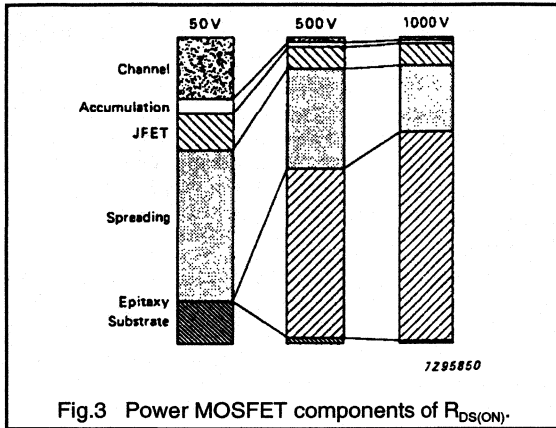


Fig.3 Power MOSFET components of $R_{DS(ON)}$.

the high voltage devices the resistivity and thickness of the epitaxial layer dominates. The properties of the various resistive components will now be discussed:

Channel. The unit channel resistance is determined by the channel length, gate oxide thickness, carrier mobility, threshold voltage, and the actual gate voltage applied to the device. The channel resistance for a given gate voltage can be significantly reduced by lowering the thickness of the gate oxide. This approach is used to fabricate the Logic Level MOSFET transistors and enables a similar value $R_{DS(ON)}$ to be achieved with only 5 volts applied to the gate. Of course, the gate-source voltage rating must be reduced to allow for the lower dielectric breakdown of the thinner oxide layer.

The overall channel resistance of a device is inversely proportional to channel width, determined by the total periphery of the cell windows. Channel width is over 200 μm for a 20 mm^2 low voltage chip. The overall channel resistance can be significantly reduced by going to higher cell densities, since the cell periphery per unit area is reduced.

Accumulation layer. The silicon interface under the centre of the gate track is 'accumulated' when the gate is biased above the threshold voltage. This provides a low resistance path for the electrons when they leave the channel, prior to entering the bulk silicon. This effect makes a significant contribution towards reducing the overall $R_{DS(ON)}$.

Parasitic JFET. After leaving the accumulation layer the electrons flow vertically down between the cells into the bulk of the silicon. Associated with each P-N junction there is a depletion region which, in the case of the high voltage devices, extends several microns into the N epitaxial region, even under zero bias conditions. Consequently the current path for the electrons is restricted by this parasitic JFET structure. The resistance of the JFET structure can be reduced by increasing the polysilicon track width. However this reduces the cell density. The need for compromise

leads to an optimum value for the polysilicon track width for a given drain-source voltage rating. Since the zero-bias depletion width is greater for low doped material, then a wider polysilicon track width is used for high voltage chip designs.

Spreading resistance. As the electrons move further into the bulk of the silicon they are able to spread sideways and flow under the cells. Eventually paths overlap under the centre of each cell.

Epitaxial layer. The drain-source voltage rating requirements determine the resistivity and thickness of the epitaxial layer. For high voltage devices the resistance of the epitaxial layer dominates the overall value of $R_{DS(ON)}$.

Substrate. The resistance of the N^+ substrate is only significant in the case of 50 V devices.

Wires and leads. In a completed device the wire and lead resistances contribute a few milli-ohms to the overall resistance.

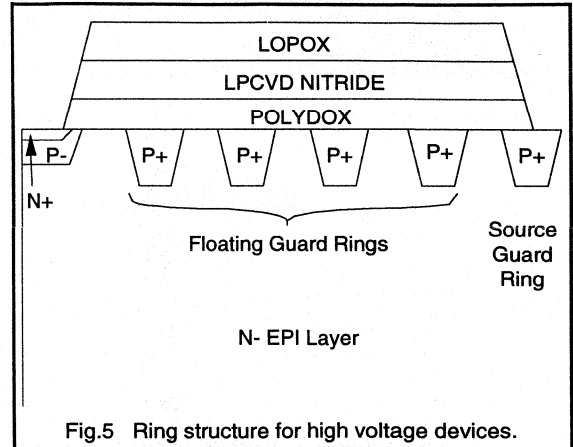
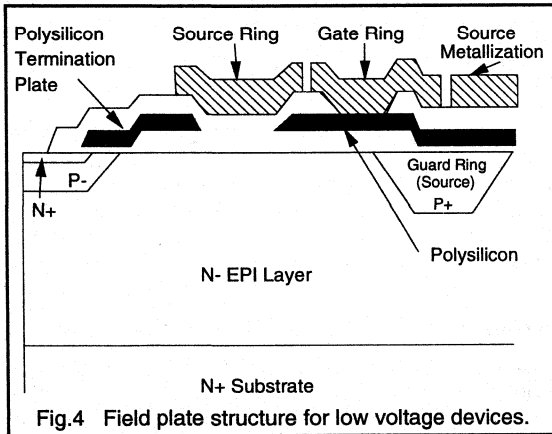
For all the above components the actual level of resistance is a function of the mobility of the current carrier. Since the mobility of holes is much lower than that of electrons the resistance of P-Channel MOSFETs is significantly higher than that of N-Channel devices. For this reason P-Channel types tend to be unattractive for most applications.

Drain-source breakdown voltage

The voltage blocking junction in the PowerMOS transistor is formed between the P-body diffusion and the N^+ epi layer. For any P-N junction there exists a maximum theoretical breakdown voltage, which is dependent on doping profiles and material thickness. For the case of the N-channel PowerMOS transistor nearly all the blocking voltage is supported by the N^+ epi layer. The ability of the N^+ epi layer to support voltage is a function of its resistivity and thickness where both must increase to accommodate a higher breakdown voltage. This has obvious consequences in terms of drain-source resistance with $R_{DS(ON)}$ being approximately proportional to $B_{VDSS}^{2.5}$. It is therefore important to design PowerMOS devices such that the breakdown voltage is as close as possible to the theoretical maximum otherwise thicker, higher resistivity material has to be used. Computer models are used to investigate the influence of cell design and layout on breakdown voltage. Since these factors also influence the 'on-state' and switching performances a degree of compromise is necessary.

To achieve a high percentage of the theoretical breakdown maximum it is necessary to build edge structures around the active area of the device. These are designed to reduce the electric fields which would otherwise be higher in these regions and cause premature breakdown.

For low voltage devices this structure consists of a field plate design, Fig.4. The plates reduce the electric field intensity at the corner of the P⁺ guard ring which surrounds the active cell area, and spread the field laterally along the surface of the device. The polysilicon gate is extended to form the first field plate, whilst the aluminium source metallization forms the second plate. The polysilicon termination plate which is shorted to the drain in the corners of the chip (not shown on the diagram) operates as a channel stopper. This prevents any accumulation of positive charge at the surface of the epi layer and thus improves stability. Aluminium overlaps the termination plate and provides a complete electrostatic screen against any external ionic charges, hence ensuring good stability of blocking performance.



Electrical characteristics

The DC characteristic

If a dc voltage source is connected across the drain and source terminals of an N channel enhancement mode MOSFET, with the positive terminal connected to the drain, the following characteristics can be observed. With the gate to source voltage held below the threshold level negligible current will flow when sweeping the drain source voltage positive from zero. If the gate to source voltage is taken above the threshold level, increasing the drain to source voltage will cause current to flow in the drain. This current will increase as the drain-source voltage is increased up to a point known as the pinch off voltage. Increasing the drain-source terminal voltage above this value will not produce any significant increase in drain current.

The pinch off voltage arises from a rapid increase in resistance which for any particular MOSFET will depend on the combination of gate voltage and drain current. In its simplest form, pinch off will occur when the ohmic drop across the channel region directly beneath the gate becomes comparable to the gate to source voltage. Any further increase in drain current would now reduce the net voltage across the gate oxide to a level which is no longer sufficient to induce a channel. The channel is thus pinched off at its edge furthest from the source N⁺ (see Fig.6).

A typical set of output characteristics is shown in Fig.7. The two regions of operation either side of the pinch off voltage can be seen clearly. The region at voltages lower than the pinch off value is usually known as the ohmic region. Saturation region is the term used to describe that part of the characteristic above the pinch-off voltage. (NB This definition of saturation is different to that used for bipolar devices.)

All types have a final passivation layer of plasma nitride, which acts as a further barrier to mobile charge and also gives anti-scratch protection to the top surface.

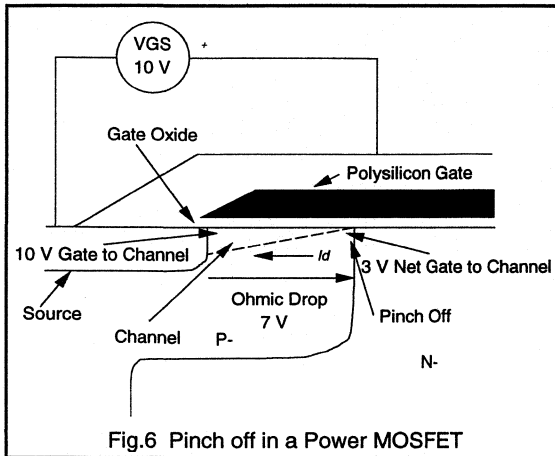


Fig.6 Pinch off in a Power MOSFET

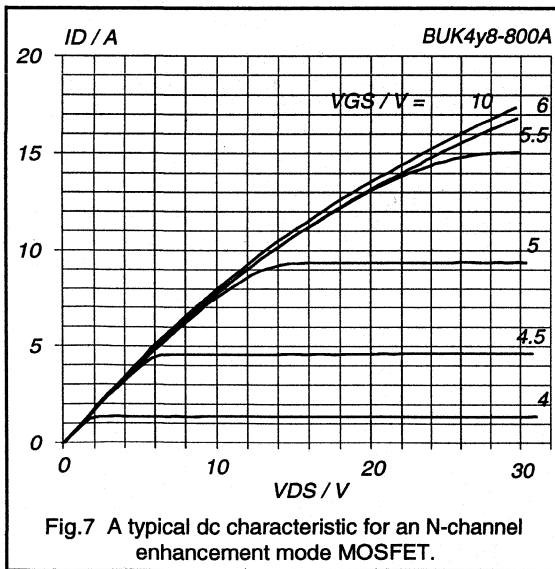


Fig.7 A typical dc characteristic for an N-channel enhancement mode MOSFET.

The switching characteristics

The switching characteristics of a Power MOSFET are determined largely by the various capacitances inherent in its' structure. These are shown in Fig.8.

To turn the device on and off the capacitances have to be charged and discharged, the rate at which this can be achieved is dependent on the impedance and the current sinking/sourcing capability of the drive circuit. Since it is only the majority carriers that are involved in the conduction process, MOSFETs do not suffer from the same storage time problems which limit bipolar devices where minority carriers have to be removed during turn-off. For most applications therefore the switching times of the Power

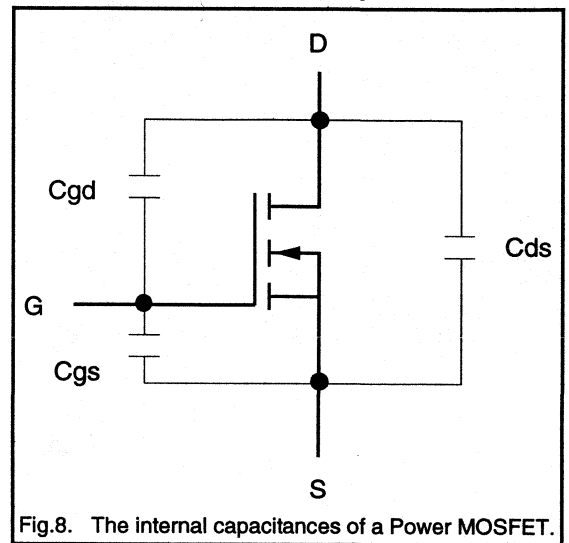


Fig.8. The internal capacitances of a Power MOSFET.

MOSFET are limited only by the drive circuit and can be very fast. Temperature has only a small effect on device capacitances therefore switching times are independent of temperature.

In Fig.9 typical gate-source and drain-source voltages for a MOSFET switching current through a resistive load are shown. The gate source capacitance needs to be charged up to a threshold voltage of about 3 V before the MOSFET begins to turn on. The time constant for this is $C_{GS}(R_{DR}+R_G)$ and the time taken is called the turn-on delay time ($t_{D(ON)}$). As V_{GS} starts to exceed the threshold voltage the MOSFET begins to turn on and V_{DS} begins to fall. C_{GD} now needs to be discharged as well as C_{GS} being charged so the time constant is increased and the gradient of V_{GS} is reduced. As V_{DS} becomes less than V_{GS} the value of C_{GD} increases sharply since it is depletion dependent. A plateau thus occurs in the V_{GS} characteristic as the drive current goes into the charging of C_{GD} .

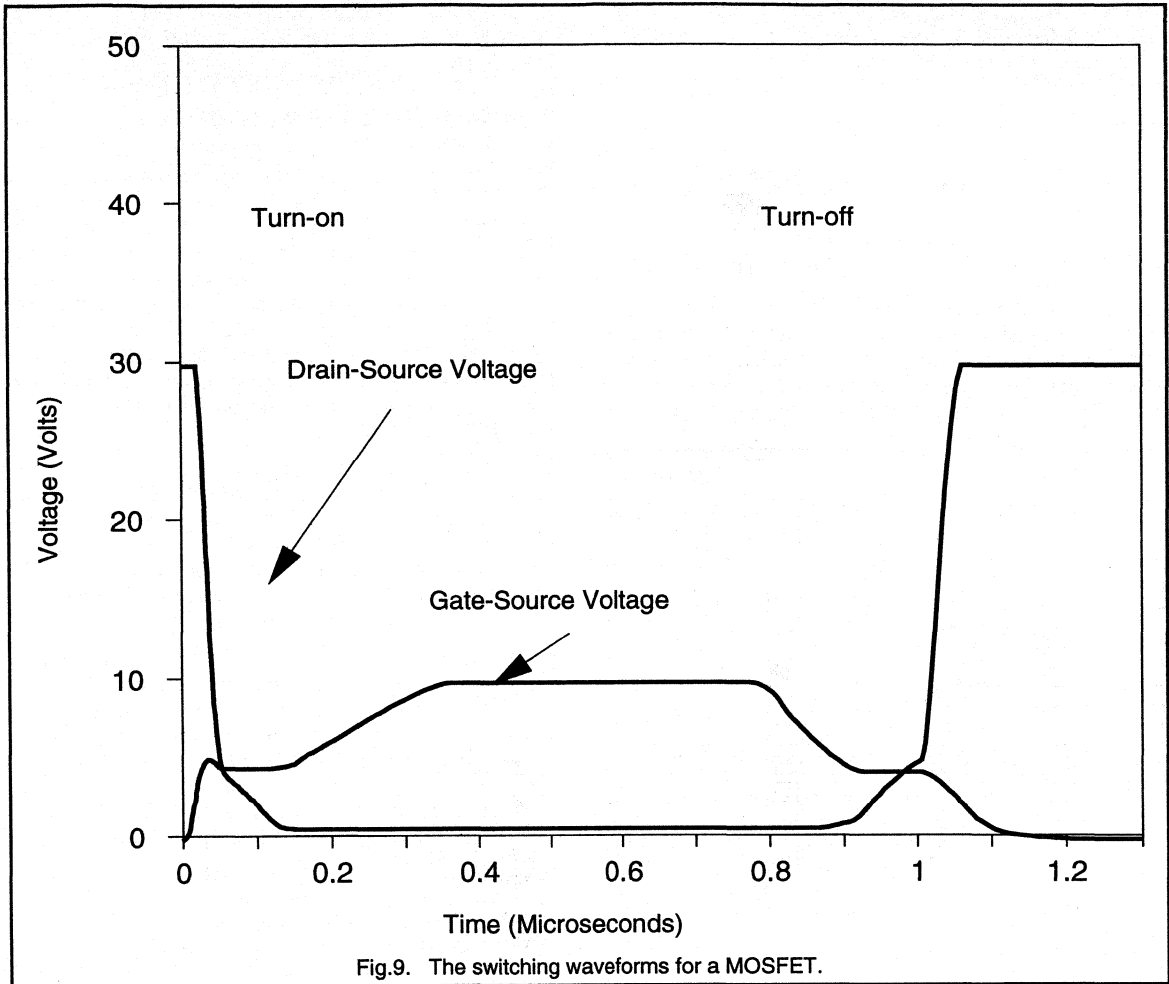


Fig.9. The switching waveforms for a MOSFET.

When V_{DS} has collapsed V_{GS} continues to rise as overdrive is applied. Gate overdrive is necessary to reduce the on-resistance of the MOSFET and thereby keep power loss to a minimum.

To turn the MOSFET off the overdrive has first to be removed. The charging path for C_{GD} and C_{DS} now contains the load resistor (R_L) and so the turn-off time will be generally longer than the turn-on time.

The Safe Operating Area

Unlike bipolar devices Power MOSFETs do not suffer from second breakdown phenomena when operated within their voltage rating. Essentially therefore the safe operating area of a Power MOSFET is determined only by the power

necessary to raise its junction temperature to the rated maximum of 150 °C or 175 °C (which T_{JMAX} depends on package and voltage rating). Whether a MOSFET is being operated safely with respect to thermal stress can thus be determined directly from knowledge of the power function applied and the thermal impedance characteristics.

A safe operating area calculated assuming a mounting base temperature of 25 °C is shown in Fig.10 for a BUK438-800 device. This plot shows the constant power curves for a variety of pulse durations ranging from dc to 10 μs. These curves represent the power levels which will raise T_J up to the maximum rating. Clearly for mounting base temperatures higher than 25 °C the safe operating area is smaller. In addition it is not usually desirable to operate the

device at its T_{JMAX} rating. These factors can be taken into account quite simply where maximum power capability for a particular application is calculated from:

$$P_{max} = \frac{(T_j - T_{mb})}{Z_{th}}$$

T_j is the desired operating junction temperature (must be less than T_{jmax})

T_{mb} is the mounting base temperature

Z_{th} is the thermal impedance taken from the data curves

The safe operating area is bounded by a peak pulse current limit and a maximum voltage. The peak pulse current is based on a current above which internal connections may be damaged. The maximum voltage is an upper limit above which the device may go into avalanche breakdown.

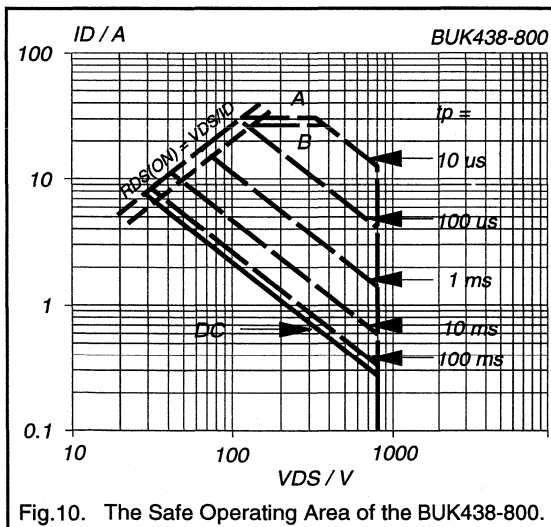


Fig.10. The Safe Operating Area of the BUK438-800.

In a real application the case temperature will be greater than 25 °C because of the finite thermal impedance of practical heatsinks. Also a junction temperature of between 80 °C and 125 °C would be preferable since this improves reliability. If a nominal junction temperature of 80 °C instead of 150 °C is used then the ability of the MOSFET to withstand current spikes is improved.

Causes of Power Loss

There are four main causes of power dissipation in MOSFETs.

Conduction losses - The conduction losses (P_C) are given by equation (1).

$$P_C = I_D^2 \cdot R_{DS(ON)} \quad (1)$$

It is important to note that the on-resistance of the MOSFET when it is operated in the Ohmic region is dependent on the junction temperature. On-resistance roughly doubles between 25 °C and 150 °C, the exact characteristics are shown in the data sheets for each device.

Switching losses - When a MOSFET is turned on or off it carries a large current and sustains a large voltage at the same time. There is therefore a large power dissipation during the switching interval. Switching losses are negligible at low frequencies but are dominant at high frequencies. The cross-over frequency depends on the circuit configuration. For reasons explained in the section on switching characteristics, a MOSFET usually turns off more slowly than it turns on so the losses at turn-off will be larger than at turn-on. Switching losses are very dependent on circuit configuration since the turn-off time is affected by the load impedance.

Turn-off losses may be reduced by the use of snubber components connected across the MOSFET which limit the rate of rise of voltage. Inductors can be connected in series with the MOSFET to limit the rate of rise of current at turn-on and reduce turn-on losses. With resonant loads switching can take place at zero crossing of voltage or current so switching losses are very much reduced.

Diode losses - These losses only occur in circuits which make use of the antiparallel diode inherent in the MOSFET structure. A good approximation to the dissipation in the diode is the product of the diode voltage drop which is typically less than 1.5 V and the average current carried by the diode. Diode conduction can be useful in such circuits as pulse width modulated circuits used for motor control, in some stepper motor drive circuits and in voltage fed circuits feeding a series resonant load.

Gate losses - The losses in the gate are given in equation 2 where R_G is the internal gate resistance, R_{DR} is the external drive resistance, V_{GSD} is the gate drive voltage and C_{IP} is the capacitance seen at the input to the gate of the MOSFET.

$$P_G = \frac{C_{IP} \cdot V_{GSD}^2 \cdot f \cdot R_G}{(R_G + R_{DR})} \quad (2)$$

The input capacitance varies greatly with the gate drain voltage so the expression in equation 3 is more useful.

$$P_G = \frac{Q_G \cdot V_{GSD} \cdot f \cdot R_G}{(R_G + R_{DR})} \quad (3)$$

(3)

Where Q_G is the peak gate charge.

Parallel Operation

If power requirements exceed those of available devices then increased power levels can be achieved by paralleling devices. Paralleling of devices is made easier using

MOSFETs because they have a positive temperature coefficient of resistance. If one paralleled MOSFET carries more current than the others it becomes hotter. This causes the on-resistance of that particular device to become greater than that of the others and so the current in it reduces. This mechanism opposes thermal runaway in one of the devices. The positive temperature coefficient also helps to prevent hot spots within the MOSFET itself.

Applications of Power MOSFETs

Power MOSFETs are ideally suited for use in many applications, some of which are listed below. Further information on the major applications is presented in

subsequent chapters.

Chapter 2: Switched mode power supplies (SMPS)

Chapter 3: Variable speed motor control.

Chapter 5: Automotive switching applications.

Conclusions

It can be seen that the operation of the Power MOSFET is relatively easy to understand. The advantages of fast switching times, ease of parallelling and low drive power requirements make the device attractive for use in many applications.

1.2.2 Understanding Power MOSFET Switching Behaviour

Power MOSFETs are well known for their ease of drive and fast switching behaviour. Being majority carrier devices means they are free of the charge storage effects which inhibit the switching performance of bipolar products. How fast a Power MOSFET will switch is determined by the speed at which its internal capacitances can be charged and discharged by the drive circuit. MOSFET switching times are often quoted as part of the device data however as an indication as to the true switching capability of the device, these figures are largely irrelevant. The quoted values are only a snapshot showing what will be achieved under the stated conditions.

This report sets out to explain the switching characteristics of Power MOSFETs. It will consider the main features of the switching cycle distinguishing between what is device determinant and what can be controlled by the drive circuit. The requirements for the drive circuit are discussed in terms of the energy that it must supply as well as the currents it is required to deliver. Finally, how the drive circuit influences switching performance, in terms of switching times, dV/dt and dI/dt will be reviewed.

Voltage dependent capacitance

The switching characteristics of the Power MOSFET are determined by its capacitances. These capacitances are not fixed but are a function of the relative voltages between each of the terminals. To fully appreciate Power MOSFET switching, it is necessary to understand what gives rise to this voltage dependency.

Parallel plate capacitance is expressed by the well known equation

$$C = E \frac{a}{d} \quad 1$$

where 'a' is the area of the plates, d is the separating distance and E is the permittivity of the insulating material between them. For a parallel plate capacitor, the plates are surfaces on which charge accumulation / depletion occurs in response to a change in the voltage applied across them. In a semiconductor, static charge accumulation / depletion can occur either across a PN junction or at semiconductor interfaces either side of a separating oxide layer.

i) P-N junction capacitance

The voltage supporting capability of most power semiconductors is provided by a reverse biased P-N junction. The voltage is supported either side of the junction by a region of charge which is exposed by the applied voltage. (Usually referred to as the depletion region because it is depleted of majority carriers.) Fig.1 shows how the electric field varies across a typical P-N junction

for a fixed dc voltage. The shaded area beneath the curve must be equal to the applied voltage. The electric field gradient is fixed, independent of the applied voltage, according to the concentration of exposed charge. (This is equal to the background doping concentration used during device manufacture.) A slight increase in voltage above this dc level will require an extension of the depletion region, and hence more charge to be exposed at its edges, this is illustrated in Fig.1. Conversely a slight reduction in voltage will cause the depletion region to contract with a removal of exposed charge at its edge. Superimposing a small ac signal on the dc voltage thus causes charge to be added and subtracted at either side of the depletion region of width $d1$. The effective capacitance per unit area is

$$C1 = \frac{E}{d1} \quad 2$$

Since the depletion region width is voltage dependent it can be seen from Fig.1 that if the dc bias is raised to say $V2$, the junction capacitance becomes

$$C2 = \frac{E}{d2} \quad 3$$

Junction capacitance is thus dependent on applied voltage with an inverse relationship.

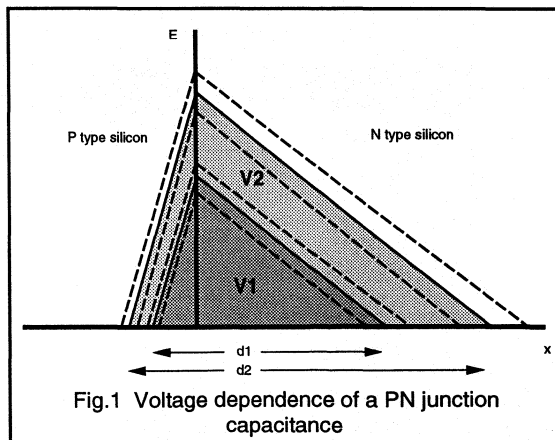


Fig.1 Voltage dependence of a PN junction capacitance

ii) Oxide capacitance

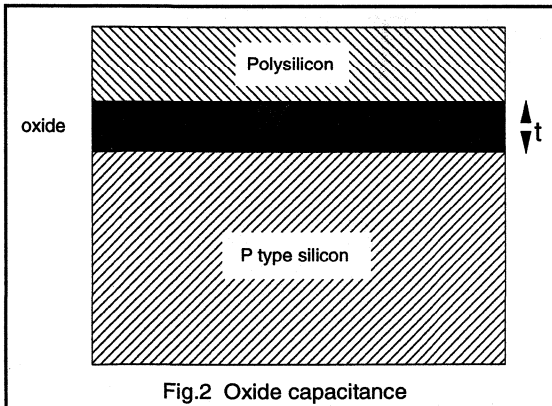
Fig.2 shows two semiconductor layers separated by an insulating oxide. In this case the surface layer is polysilicon (representative of the PowerMOS gate structure) and the lower layer is a P-type substrate. Applying a negative voltage to the upper layer with respect to the lower will cause positive charge accumulation at the surface of the P-doped

material (positively charged holes of the P material are attracted by the negative voltage). Any changes in this applied voltage will cause a corresponding change in the accumulation layer charge. The capacitance per unit area is thus

$$C_{ox} = \frac{E}{t} \quad 4$$

where t = oxide thickness

Applying a positive voltage to the gate will cause a depletion layer to form beneath the oxide, (ie the positively charged holes of the P-material are repelled by the positive voltage). The capacitance will now decrease with increasing positive gate voltage as a result of widening of the depletion layer. Increasing the voltage beyond a certain point results in a process known as inversion; electrons pulled into the conduction band by the electric field accumulate at the surface of the P-type semiconductor. (The voltage at which this occurs is the threshold voltage of the power MOSFET.) Once the inversion layer forms, the depletion layer width will not increase with additional dc bias and the capacitance is thus at its minimum value. (NB the electron charge accumulation at the inversion layer cannot follow a high frequency ac signal in the structure of Fig.2, so high frequency capacitance is still determined by the depletion layer width.) The solid line of Fig.3 represents the capacitance-voltage characteristic of an MOS capacitor.



In a power MOSFET the solid line is not actually observed; the formation of the inversion layer in the P-type material allows electrons to move from the neighbouring N⁺-source, the inversion layer can therefore respond to a high frequency gate signal and the capacitance returns to its maximum value, dashed line of Fig.3.

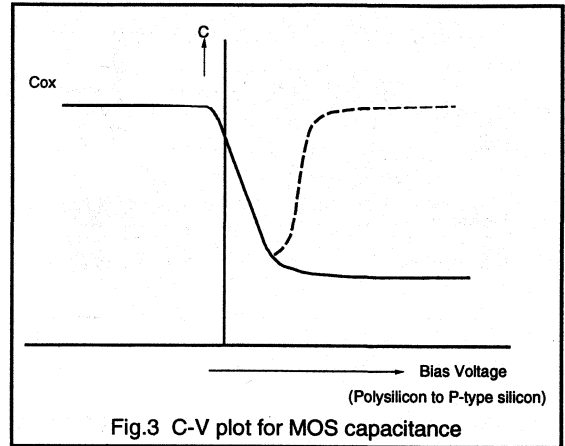


Fig.3 C-V plot for MOS capacitance

Power MOSFET capacitances

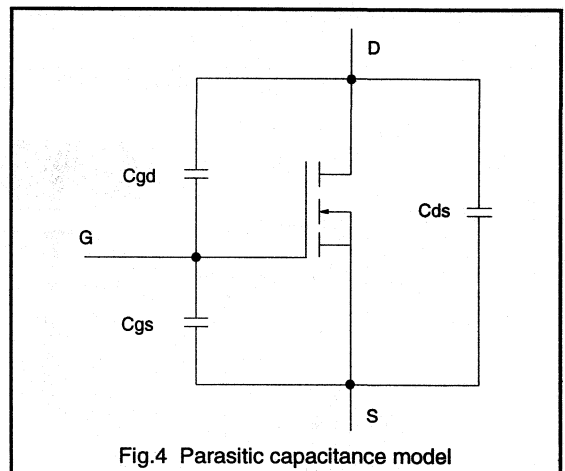
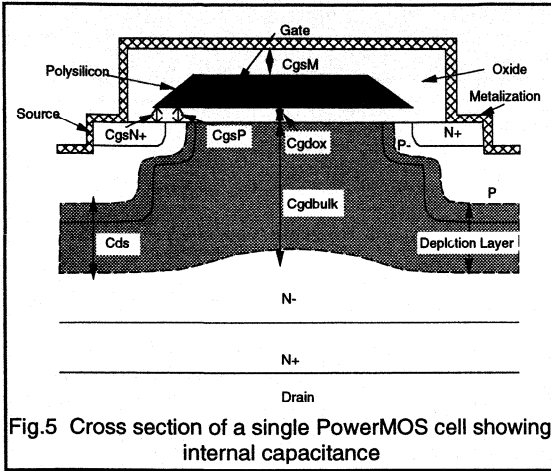


Fig.4 Parasitic capacitance model

The circuit model of Fig.4 illustrates the parasitic capacitances of the Power MOSFET. Most PowerMOS data sheets do not refer to these components but to input capacitance C_{iss}, output capacitance C_{oss} and feedback capacitance C_{rss}. The data sheet capacitances relate to the primary parasitic capacitances of Fig.4 as follows:

- C_{iss}: Parallel combination of C_{gs} and C_{gd}
- C_{oss}: Parallel combination of C_{ds} and C_{gd}
- C_{rss}: Equivalent to C_{gd}

Fig.5 shows the cross section of a power MOSFET cell indicating where the parasitic capacitances occur internally.



The capacitance between drain and source is a P-N junction capacitance, varying in accordance with the width of the depletion layer, which in turn depends on the voltage being supported by the device. The gate source capacitance consists of the three components, CgsN⁺, CgsP and CgsM. Of these CgsP is across the oxide which will vary according to the applied gate source voltage as described above.

Of particular interest is the feedback capacitance Cgd. It is this capacitance which plays a dominant role during switching and which is also the most voltage dependent. Cgd is essentially two capacitors in series such that

$$\frac{1}{C_{gd}} = \frac{1}{C_{gdox}} + \frac{1}{C_{gdbulk}} \quad 5$$

Fig.5 Cross section of a single PowerMOS cell showing internal capacitance

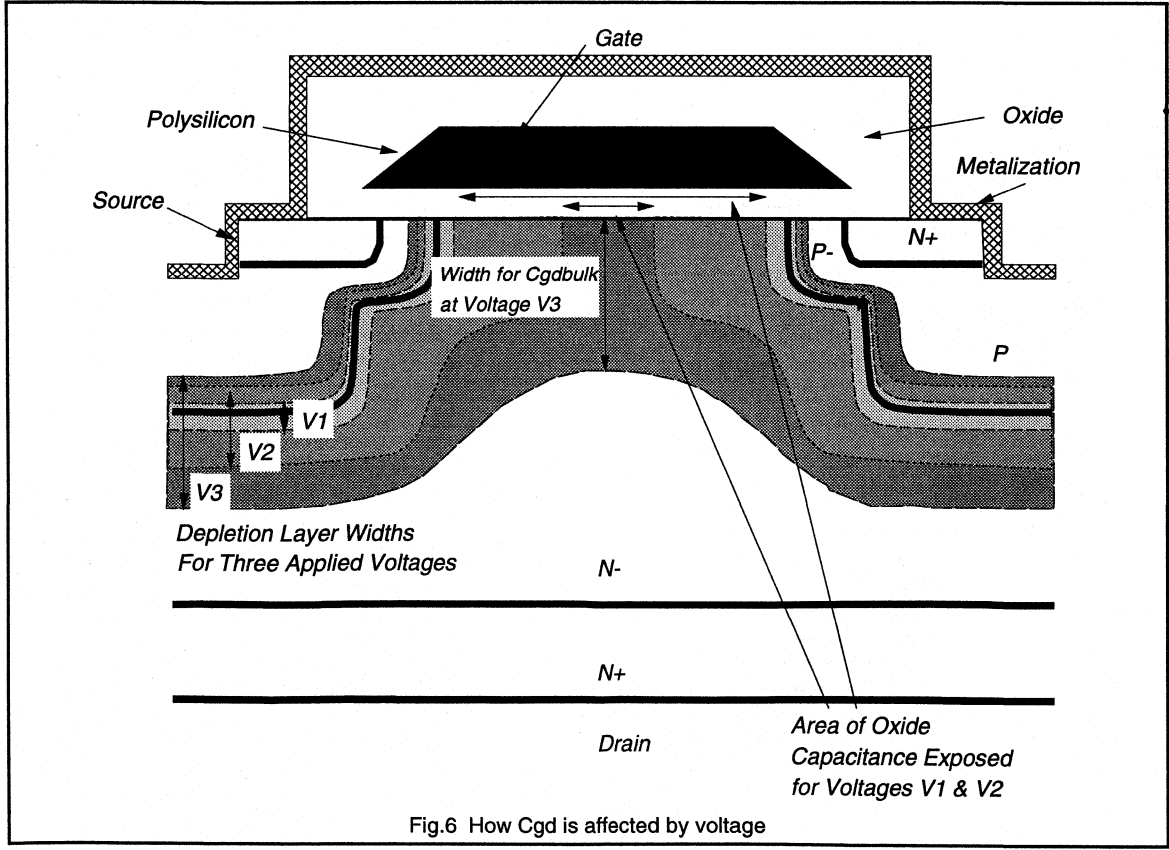


Fig.6 How Cgd is affected by voltage

Fig.6 illustrates how this capacitance is affected by the drain to gate voltage. With a large voltage drain to gate, C_{gd} is very small due to the wide depletion region and thus maintains C_{gd} at a low value. As the voltage is reduced the depletion region shrinks until eventually the oxide semiconductor interface is exposed. This occurs as V_{dg} approaches 0 V. C_{gd} now dominates C_{gd} . As V_{dg} is further reduced the drain will become negative with respect to the gate (normal on-state condition) an increasing area of the oxide-semiconductor interface is exposed and an accumulation layer forms at the semiconductor surface. The now large area of exposed oxide results in a large value for C_{gd} and hence C_{gd} . Fig.7 shows C_{gd} plotted as a function of drain to gate voltage. This illustrates the almost step increase in capacitance at the point where $V_{gs} = V_{dg}$.

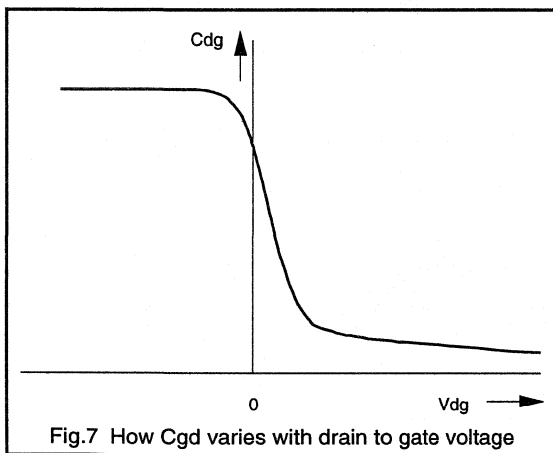


Fig.7 How C_{gd} varies with drain to gate voltage

Charging cycle - The Gate Charge Oscillogram

The switching cycle of a power MOSFET can be clearly observed by applying a constant current to the gate and using a constant current source as the load, Fig.8. In this circuit the MOSFET is turned on by feeding a constant current of 1 mA on to the gate, conversely the device is turned off by extracting a constant current of 1 mA from the gate. The gate and drain voltages with respect to source can be monitored on an oscilloscope as a function of time. Since $Q = it$, a 1 μ sec period equates to 1 nc of charge applied to the gate. The gate source voltage can thus be plotted as a function of charge on the gate. Fig.9 shows such a plot for the turn-on of a BUK555-100A, also shown is the drain to source voltage. This gate voltage plot shows the characteristic shape which results from charging of the power MOSFET's input capacitance. This shape arises as follows: (NB the following analysis uses the two circuit models of Fig.10 to represent a MOSFET operating in the active region (a) and the ohmic region (b). In the active

region the MOSFET is a constant current source where the current is a function of the gate-source voltage. In the ohmic region the MOSFET is in effect just a resistance.)

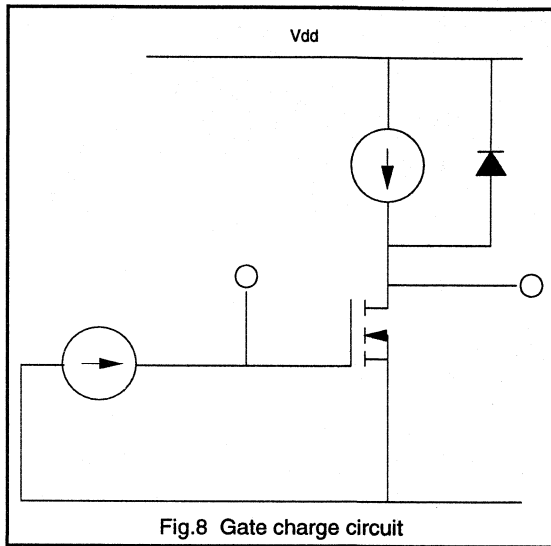


Fig.8 Gate charge circuit

At time, t_0 (Fig.9), the gate drive is activated. Current flows into the gate as indicated in Fig.11(a), charging both C_{gs} and C_{gd} . After a short period the threshold voltage is reached and current begins to rise in the MOSFET. The equivalent circuit is now as shown in Fig.11(b). The drain source voltage remains at the supply level as long as $i_d < I_0$ and the free wheeling diode D is conducting.

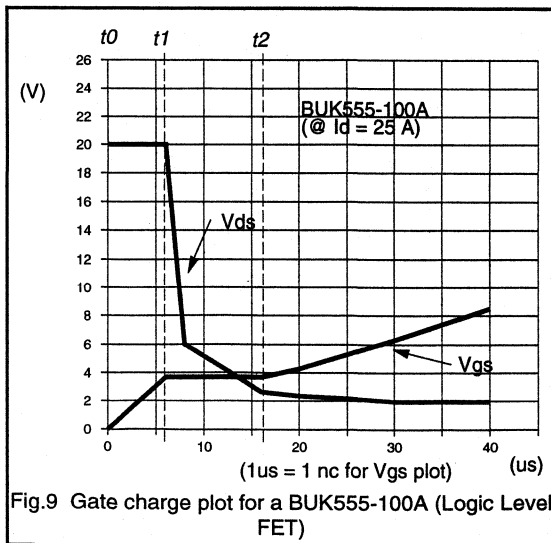


Fig.9 Gate charge plot for a BUK555-100A (Logic Level FET)

The current in the MOSFET continues to rise until $i_d = I_0$, since the device is still in its active region, the gate voltage becomes clamped at this point, (t1). The entire gate current now flows through C_{gd} causing the drain-source voltage to drop as C_{gd} is discharged, Fig.11(c). The rate at which V_{ds} falls is given by:

$$\frac{dV_{ds}}{dt} = \frac{dV_{dg}}{dt} = \frac{i_g}{C_{gd}} \quad 6$$

As V_{dg} approaches zero, C_{gd} starts to increase dramatically, reaching its maximum as V_{dg} becomes negative. dV_{ds}/dt is now greatly reduced giving rise to the voltage tail.

Once the drain-source voltage has completed its drop to the on-state value of $I_0 \cdot R_{DS(ON)}$, (point t2), the gate source voltage becomes unclamped and continues to rise, Fig.11(d). (NB dV_{gs}/dQ in regions 1 and 3 indicates the input capacitance values.)

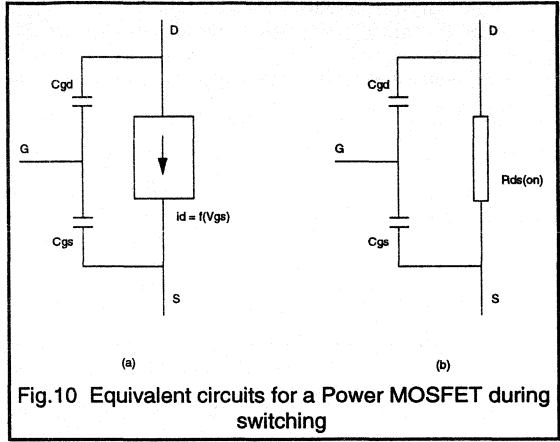


Fig.10 Equivalent circuits for a Power MOSFET during switching

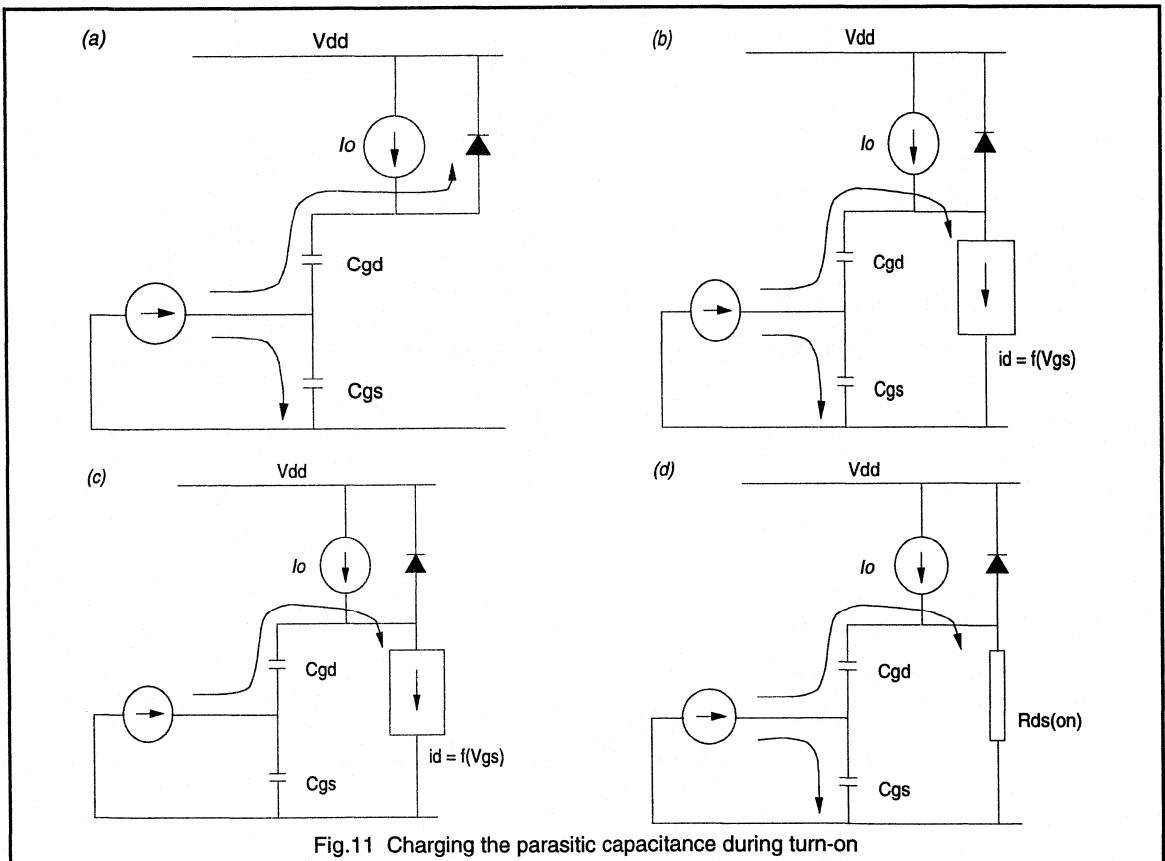


Fig.11 Charging the parasitic capacitance during turn-on

The gate charge oscillogram can be found in the data for all Philips PowerMOS devices. This plot can be used to determine the required average gate drive current for a particular switching speed. The speed is set by how fast the charge is supplied to the MOSFET.

Energy consumed by the switching event

In the majority of applications the power MOSFET will be driven not from a constant current source but via a fixed

gate drive impedance from a voltage source. Fig.13 shows the voltage on a voltage independent capacitor as a function of charge. The area beneath the charge vs voltage curve equals the stored energy ($E = Q.V/2$). The area above the charge vs voltage curve (bounded by the supply voltage) is the amount of energy dissipated during the charging cycle from a fixed voltage source. The total energy delivered by the supply is therefore $Q.V$, where $1/2 Q.V$ is stored on the capacitor to be dissipated during the discharge phase.

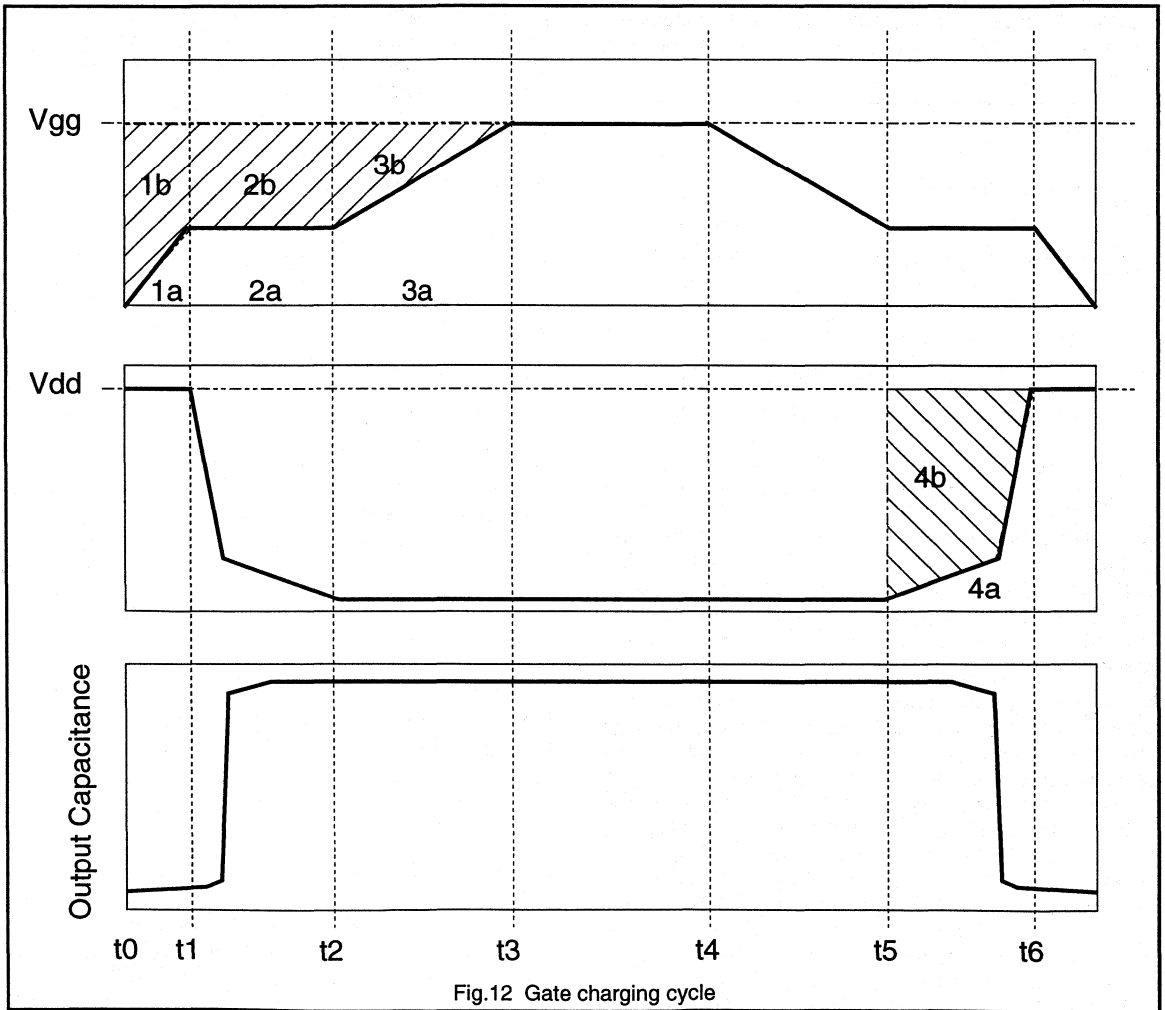


Fig.12 Gate charging cycle

Although the voltage vs charge relationship for the MOSFET's gate is not linear, energy loss is easily identified. The following discussion assumes a simple drive circuit consisting of a voltage source and drive resistance.

From t_0 to t_1 energy is stored in the gate capacitance which is equal to the area of region 1a. Since this charge has fallen through a voltage $V_{gg} - V_{gs}(t)$, the area of region 1b represents the energy dissipated in the drive resistance during its delivery. Between t_1 and t_2 all charge enters C_{gd} , the area of region 2a represents the energy stored in C_{gd} while 2b again corresponds with the energy dissipation in the drive resistor. Finally, between t_2 and t_3 additional energy is stored by the input capacitance equal to the area of region 3a.

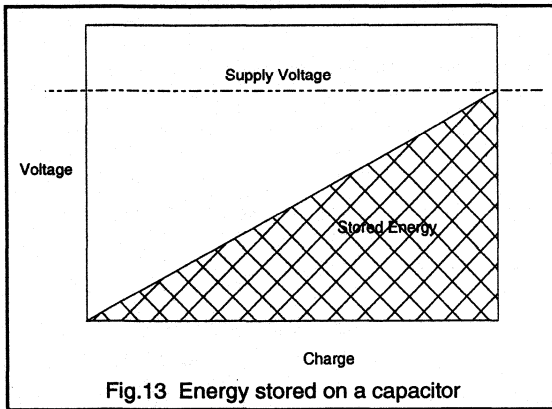


Fig.13 Energy stored on a capacitor

The total energy dissipated in the drive resistance at turn-on is therefore equal to the area $1b + 2b + 3b$. The corresponding energy stored on the input capacitance is $1a + 2a + 3a$, this energy will be dissipated in the drive resistance at turn-off. The total energy expended by the gate drive for the switching cycle is $Q \cdot V_{gg}$.

As well as energy expended by the drive circuit, a switching cycle will also require energy to be expended by the drain circuit due to the charging and discharging of C_{gd} and C_{ds} between the supply rail and $V_{DS(ON)}$. Moving from t_5 to t_6 the drain side of C_{gd} is charged from $I_o \cdot R_{DS(ON)}$ to V_{DD} . The drain circuit must therefore supply sufficient current for this charging event. The total charge requirement is given by the plateau region, $Q_6 - Q_5$. The area 4a (Fig.12) under the drain-source voltage curve represents the energy stored by the drain circuit on C_{gd} during turn-on. Region 4b represents the corresponding energy delivered to the load during this period. The energy consumed from the drain supply to charge and discharge C_{gd} over one switching cycle is thus given by:

$$W_{DD} = (Q_6 - Q_5) \cdot (V_{DD} - V_{DS(ON)}) \quad 7$$

(The energy stored on C_{gd} during turn-off is dissipated internally in the MOSFET during turn-on.) Additional energy is also stored on C_{ds} during turn-off which again is dissipated in the MOSFET at turn-on.

The energy lost by both the gate and drain supplies in the charging and discharging of the capacitances is very small over 1 cycle; Fig.9 indicates 40 nc is required to raise the gate voltage to 10 V, delivered from a 10 V supply this equates to 400 nJ; to charge C_{gd} to 80 V from an 80 V supply will consume 12 nc x 80 V = 1.4 μ J. Only as switching frequencies approach 1 MHz will this energy loss start to become significant. (NB these losses only apply to square wave switching, the case for resonant switching is some-what different.)

Switching performance

1) Turn-on

The parameters likely to be of most importance during the turn-on phase are,

turn-on time
turn-on loss
peak dV/dt
peak dI/dt .

Turn-on time is simply a matter of how quickly the specified charge can be applied to the gate. The average current that must be supplied over the turn-on period is

$$I_{on} = \frac{Q}{t_{on}} \quad 8$$

For repetitive switching the average current requirement of the drive is

$$I = Q \cdot f \quad 9$$

where f = frequency of the input signal

Turn-on loss occurs during the initial phase when current flows in the MOSFET while the drain source voltage is still high. To minimise this loss, a necessary requirement of high frequency circuits, requires the turn-on time to be as small as possible. To achieve fast switching the drive circuit must be able to supply the initial peak current, given by equation 10.

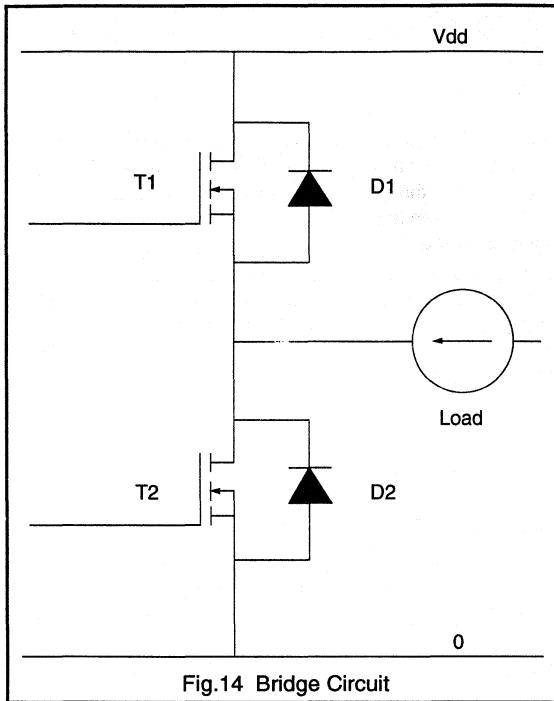


Fig.14 Bridge Circuit

$$I_{pk} = \frac{V_{GG}}{R_g} \quad 10$$

One of the main problems associated with very fast switching MOSFETs is the high rates of change in voltage and current. High values of dV/dt can couple through parasitic capacitances to give unwanted noise on signal lines. Similarly a high dI/dt may react with circuit inductance to give problematic transients and overshoot voltages in the power circuit. dI/dt is controlled by the time taken to charge the input capacitance up to the plateau voltage, while dV/dt is governed by the rate at which the plateau region is moved through.

$$\frac{dV_{ds}}{dt} = \frac{i_g}{C_{gd}} = \frac{V_{GG} - V_{GS}}{R_G \cdot C_{gd}} \quad 11$$

Particular care is required regarding dV/dt when switching in bridge circuits, (Fig.14). The free wheeling diode will have associated with it a reverse recovery current. When the opposing MOSFET switches on, the drain current rises beyond the load current value I_o to a value $I_o + I_{rr}$. Consequently V_{GS} increases beyond $V_{gt}(I_o)$ to $V_{gt}(I_o + I_{rr})$ as shown in Fig.15. Once the diode has recovered there is a rapid decrease in V_{GS} to $V_{gt}(I_o)$ and this rapid decrease provides additional current to C_{gd} on top of that being supplied by the gate drive. This in turn causes V_{dg} and V_{ds} to decrease very rapidly during this recovery period.

The dV/dt in this period is determined by the recovery properties of the diode in relation to the dI/dt imposed upon it by the turn-on of the MOSFET, (reducing dI/dt will reduce this dV/dt , however it is best to use soft recovery diodes).

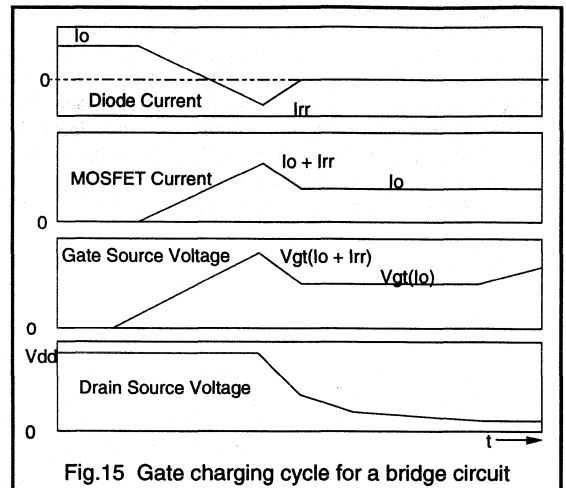


Fig.15 Gate charging cycle for a bridge circuit

ii) Turn-off

The parameters of most importance during the turn-off phase are,

- turn-off time
- turn-off loss
- peak dV_{ds}/dt
- peak dI/dt .

Turn-off of a power MOSFET is more or less the inverse of the turn-on process. The main difference is that the charging current for C_{gd} during turn-off must flow through both the gate circuit impedance and the load impedance. A high load impedance will thus slow down the turn-off speed.

The speed at which the plateau region is moved through determines the voltage rise time. In most applications the charging current for C_{gd} will be limited by the gate drive circuitry. The charging current, assuming no negative drive, is simply

$$i = \frac{V_{gt}}{R_G} \quad 12$$

and the length of the plateau region will be

$$t_p = \frac{Q \cdot R_G}{V_{gt}} \quad 13$$

The implications for low threshold (Logic Level) MOSFETs are clear from the above equations. The lower value of V_{gt} will mean a slower turn-off for a given gate impedance when compared to an equivalent standard threshold device. Equivalent switching therefore requires a lower drive impedance to be used.

Conclusions

In theory the speed of a power MOSFET is limited only by the parasitic inductances of its internal bond wires. The

speed is essentially determined by how fast the internal capacitances can be charged and discharged by the drive circuit. Switching speeds quoted in data should be treated with caution since they only reflect performance for one particular drive condition. The gate charge plot is a more useful way of looking at switching capability since it indicates how much charge needs to be supplied by the drive to turn the device on. How fast that charge should be applied depends on the application and circuit performance requirements.



1.2.3 Power MOSFET Drive Circuits

MOSFETs are being increasingly used in many switching applications because of their fast switching times and low drive power requirements. The fast switching times can easily be realised by driving MOSFETs with relatively simple drive circuits. The following paragraphs outline the requirements of MOSFET drive circuits and present various circuit examples. A look at the special requirements of very fast switching circuits is also presented, this can be found in the latter part of this article.

The requirements of the drive circuit

The switching of a MOSFET involves the charging and discharging of the capacitance between the gate and source terminals. This capacitance is related to the size of the MOSFET chip used typically about 1-2 nF. A gate-source voltage of 6V is usually sufficient to turn a standard MOSFET fully on. However further increases in gate-to-source voltage are usually employed to reduce the MOSFETs on-resistance. Therefore for switching times of about 50 ns, applying a 10 V gate drive voltage to a MOSFET with a 2 nF gate-source capacitance would require the drive circuit to sink and source peak currents of about 0.5 A. However it is only necessary to carry this current during the switching intervals.

The gate drive power requirements are given in equation (1)

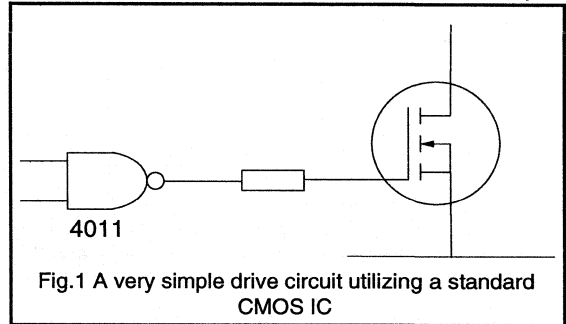
$$P_G = Q_G \cdot V_{GS} \cdot f \quad 1$$

where Q_G is the peak gate charge, V_{GS} is the peak gate source voltage and f is the switching frequency.

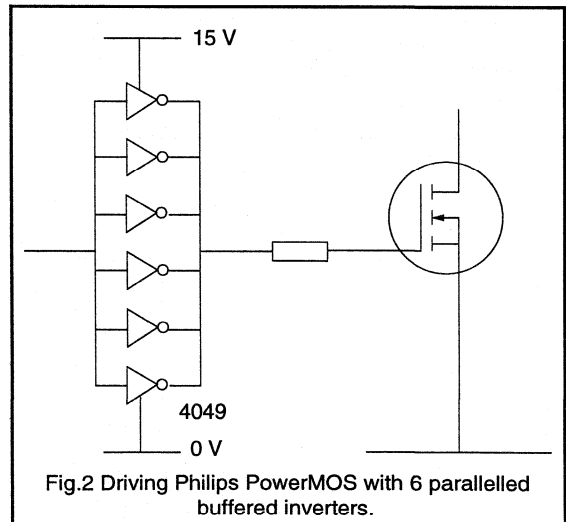
In circuits which use a bridge configuration, the gate terminals of the MOSFETs in the circuit need to float relative to each other. The gate drive circuitry then needs to incorporate some isolation. The impedance of the gate drive circuit should not be so large that there is a possibility of dV/dt turn on. dV/dt turn on can be caused by rapid changes of drain to source voltage. The charging current for the gate-drain capacitance C_{GD} flows through the gate drive circuit. This charging current can cause a voltage drop across the gate drive impedance large enough to turn the MOSFET on.

Non-isolated drive circuits

MOSFETs can be driven directly from a CMOS logic IC as shown in Fig.1.



Faster switching speeds can be achieved by parallelling CMOS hex inverting (4049) or non-inverting (4050) buffers as shown in Fig.2.



A push pull circuit can also be used as shown in Fig.3.

The connections between the drive circuit and the MOSFET should be kept as short as possible and twisted together if the shortest switching times are required. If both the drive circuit and the terminals of the MOSFET are on the same PCB, then the inductance of tracks, between the drive transistors and the terminals of the MOSFETs, should be kept as small as possible. This is necessary to reduce the impedance of the drive circuit in order to reduce the switching times and lessen the susceptibility of the circuit

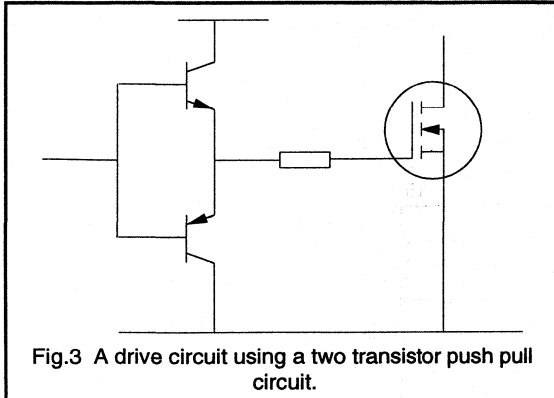


Fig.3 A drive circuit using a two transistor push pull circuit.

to dV/dt turn-on of the MOSFET. Attention to layout also improves the immunity to spurious switching by interference.

One of the advantages of MOSFETs is that their switching times can be easily controlled. For example it may be required to limit the rate of change of drain current to reduce overshoot on the drain source voltage waveform. The overshoot may be caused by switching current in parasitic lead or transformer leakage inductance. The slower switching can be achieved by increasing the value of the gate drive resistor.

The supply rails should be decoupled near to fast switching elements such as the push-pull transistors in Fig.3. An electrolytic capacitor in parallel with a ceramic capacitor are recommended since the electrolytic capacitor will not be a low enough impedance to the fast edges of the MOSFET drive pulse.

Isolated drive circuits

Some circuits demand that the gate and source terminals of MOSFETs are floating with respect to those of other MOSFETs in the circuit. Isolated drive to these MOSFETs can be provided in the following way:

(a) Opto-isolators.

A drive circuit using an opto-isolator is shown in Fig.4.

A diode in the primary side of the opto-isolator emits photons when it is forward biased. These photons impinge on the base region of a transistor in the secondary side. This causes photogeneration of carriers sufficient to satisfy the base requirement for turn-on. In this way the opto-isolator provides isolation between the primary and secondary of the opto-isolator. An isolated supply is required for the circuitry on the secondary side of the opto-isolator. This supply can be derived, in some cases, from the drain-to-source voltage across the MOSFET being driven as shown in Fig.5. This is made possible by the low drive power requirements of MOSFETs.

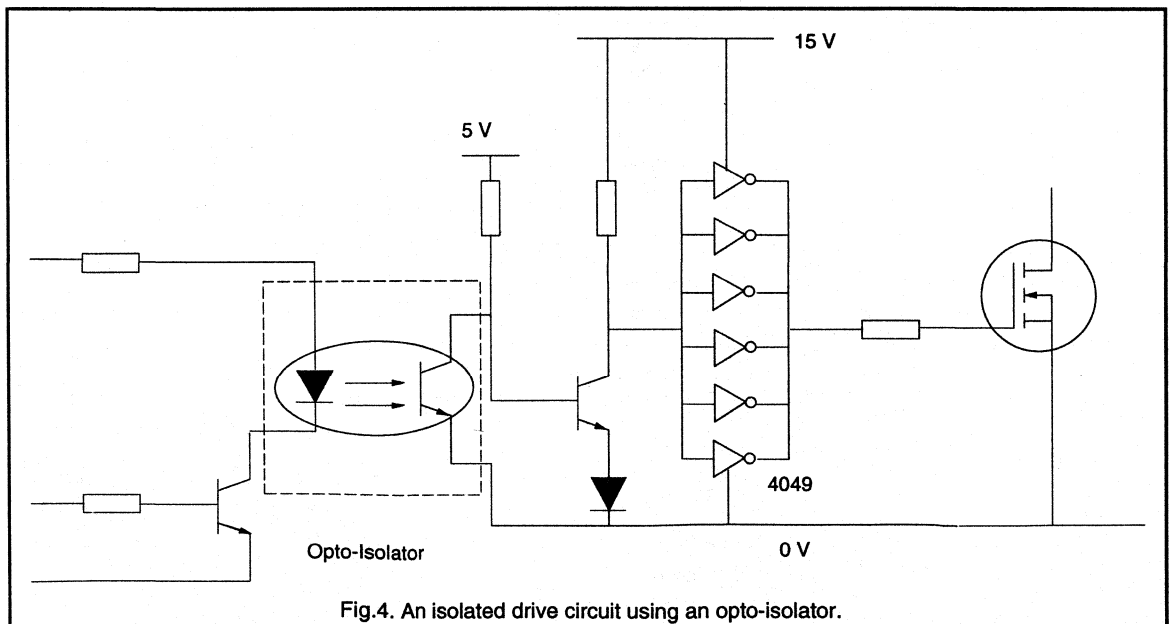
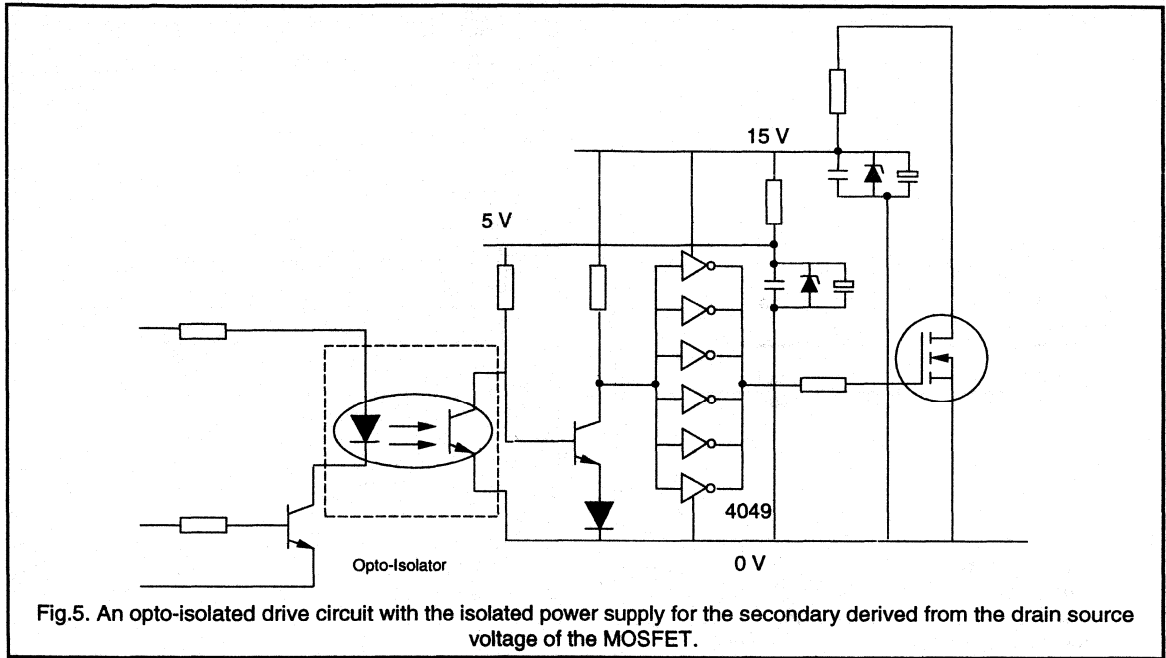


Fig.4. An isolated drive circuit using an opto-isolator.



Some opto-isolators incorporate an internal screen to improve the common mode transient immunity. Values as high as 1000 V/ μ s are quoted for common mode rejection which is equivalent to rejecting a 300V peak-to-peak sine wave.

The faster opto-isolators work off a maximum collector voltage on the secondary side of 5V so some form of level shifting may be required.

(b) Pulse transformers.

A circuit using a pulse transformer for isolation is shown in Fig.6(a).

When T2 switches on, voltage is applied across the primary of the pulse transformer. The current through T2 consists of the sum of the gate drive current for T1 and the magnetising current of the pulse transformer. From the waveforms of current and voltage around the circuit shown in Fig.6(b), it can be seen that after the turn off of T2 the voltage across it rises to $V_D + V_Z$, where V_Z is the voltage across the zener diode Z_D . The zener voltage V_Z applied across the pulse transformer causes the flux in the core to be reset. Thus the net volt second area across the pulse transformer is zero over a switching cycle. The minimum number of turns on the primary is given by equation (2).

$$N = \frac{V \cdot t}{B \cdot A_e}$$

2

where B is the maximum flux density, A_e is the effective cross sectional area of the core and t is the time that T2 is on for.

The circuit in Fig.6(a) is best suited for fixed duty cycle operation. The zener diode has to be large enough so that the flux in the core will be reset during operation with the maximum duty cycle. For any duty cycle less than the maximum there will be a period when the voltage across the secondary is zero as shown in Fig.7.

In Fig.8 a capacitor is used to block the dc components of the drive signal.

Drive circuits using pulse transformers have problems if a widely varying duty cycle is required. This causes widely varying gate drive voltages when the MOSFET is off. In consequence there are variable switching times and varying levels of immunity to dV/dt turn on and interference. There are several possible solutions to this problem, some examples are given in Figs.9 - 12.

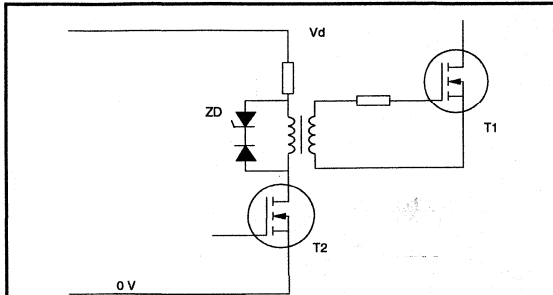


Fig.6(a) A circuit using a pulse transformer for isolation.

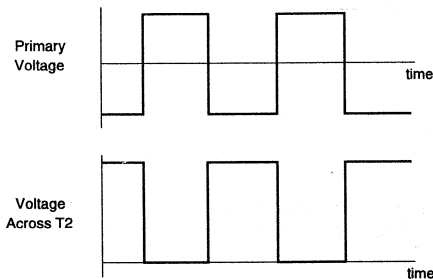


Fig.6(b) Waveforms associated with pulse transformer.

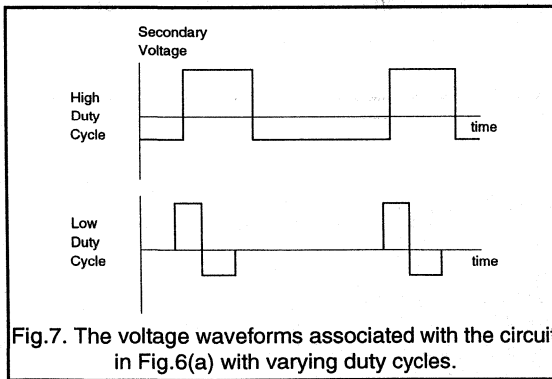


Fig.7. The voltage waveforms associated with the circuit in Fig.6(a) with varying duty cycles.

In the circuit shown in Fig.9 when A is positive with respect to B the input capacitance of T1 is charged through the parasitic diode of T2. The voltage across the secondary of the pulse transformer can then fall to zero and the input capacitance of T1 will remain charged. (It is sometimes necessary to raise the effective input capacitance with an external capacitor as indicated by the dashed lines.) When B becomes positive with respect to A T2 will turn on and the input capacitance of T2 will be discharged. The noise immunity of the circuit can be increased by using another MOSFET as shown in Fig.10.

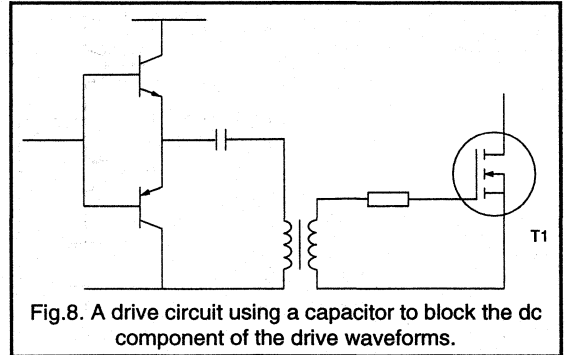


Fig.8. A drive circuit using a capacitor to block the dc component of the drive waveforms.

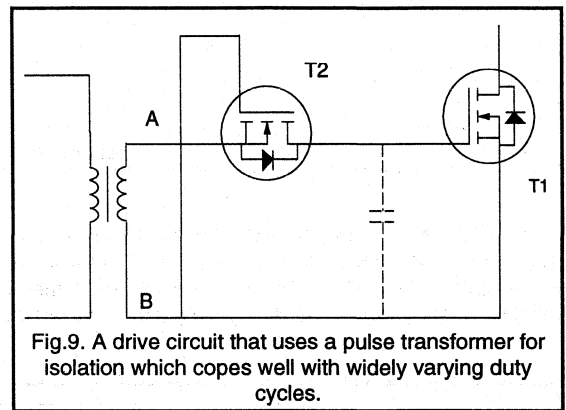


Fig.9. A drive circuit that uses a pulse transformer for isolation which copes well with widely varying duty cycles.

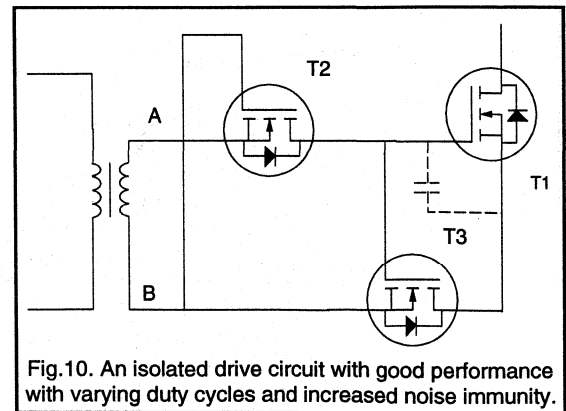
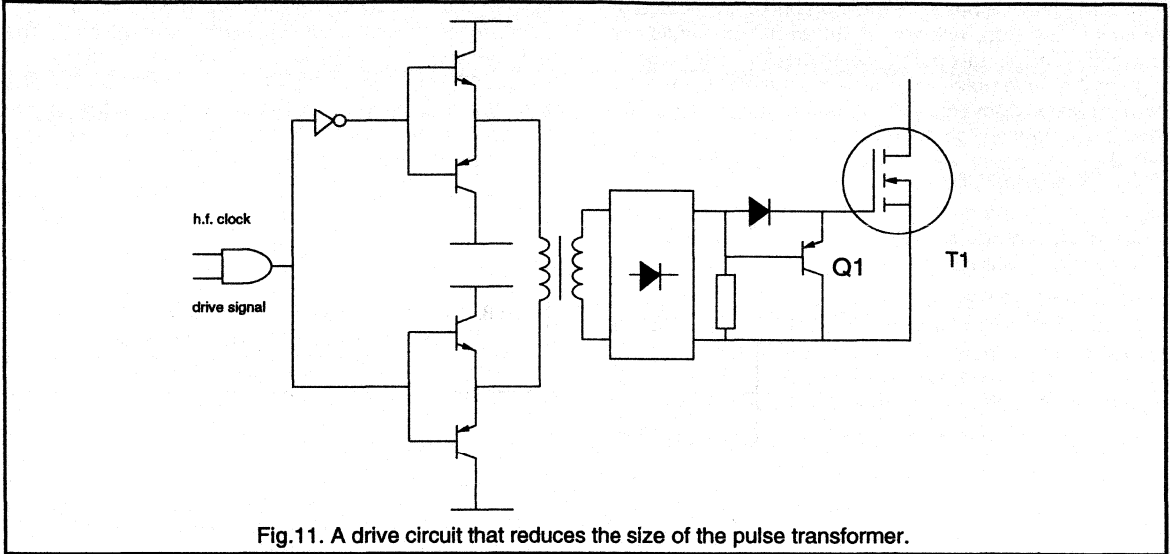


Fig.10. An isolated drive circuit with good performance with varying duty cycles and increased noise immunity.

In Fig.10 the potential at A relative to B has to be sufficient to charge the input capacitance of T3 and so turn T3 on before T1 can begin to turn on.



In Fig.11 the drive signal is ANDed with a hf clock. If the clock has a frequency much higher than the switching frequency of T1 then the size of the pulse transformer is reduced. The hf signal on the secondary of the pulse

transformer is rectified. Q1 provides a low impedance path for discharging the input capacitance of T1 when the hf signal on the secondary of the pulse transformer is absent.

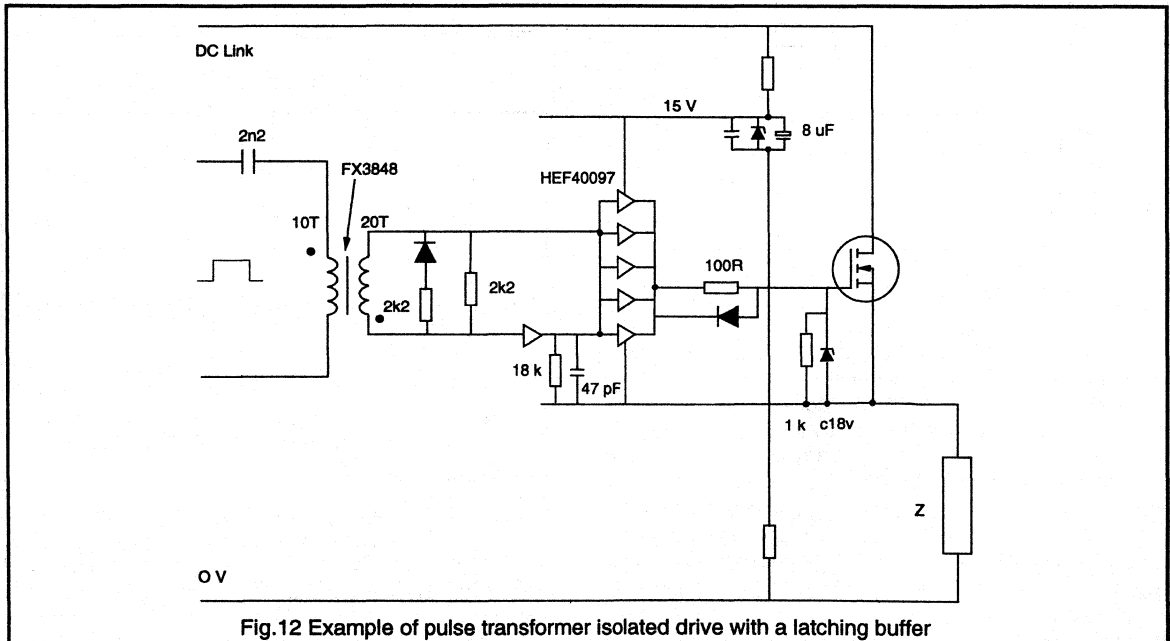


Figure 12 shows a hex non-inverting buffer connected on the secondary side, with one of the six buffers configured as a latch. The circuit operates such that the positive going edge of the drive pulse will cause the buffers to latch into the high state. Conversely the negative going edge of the drive pulse causes the buffers to latch into the low state. With the component values indicated on the diagram this circuit can operate with pulse on-times as low as 1 μ s. The impedance Z represents either the low side switch in a bridge circuit (which can be a MOSFET configured with identical drive) or a low side load.

The impedance of the gate drive circuit may be used to control the switching times of the MOSFET. Increasing gate drive impedance however can increase the risk of dV/dt turn-on. To try and overcome this problem it may be necessary to configure the drive as outlined in Fig.13.

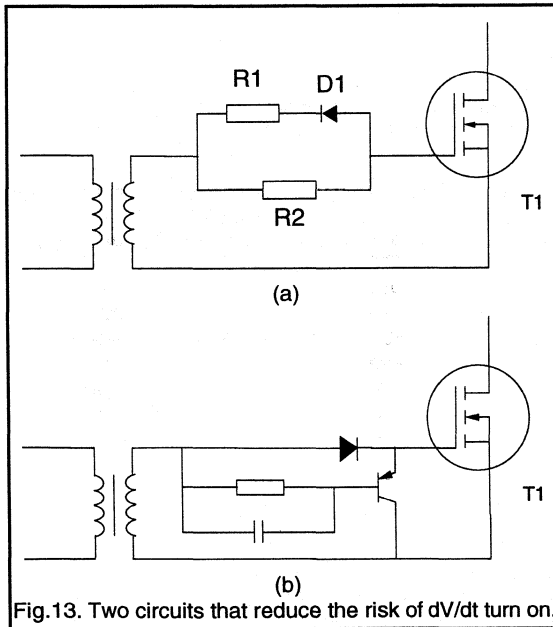


Fig.13. Two circuits that reduce the risk of dV/dt turn-on.

The diode in Fig.13(a) reduces the gate drive impedance when the MOSFET is turned off. In Fig.13(b) when the drive pulse is taken away, the pnp transistor is turned on. When the pnp transistor is on it short-circuits the gate to the source and so reduces the gate drive impedance.

High side drive circuits

The isolated drive circuits in the previous section can be used for either high or low side applications. Not all high side applications however require an isolated drive. Two examples showing how a high side drive can be achieved simply with a boot strap capacitor are shown in Fig.14. Both these circuits depend upon the topping up of the charge on

the boot strap capacitor while the MOSFET is off. For this reason these circuits cannot be used for dc switching. The minimum operating frequency is determined by the size of the boot strap capacitor (and R1 in circuit (a)), as the operating frequency is increased so the value of the capacitor can be reduced. The circuit example in Fig. 14(a) has a minimum operating frequency of 500 Hz.

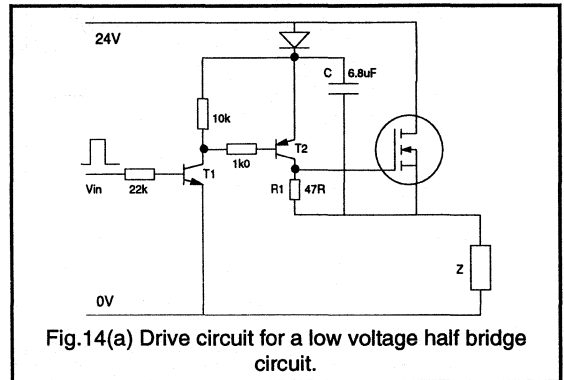


Fig.14(a) Drive circuit for a low voltage half bridge circuit.

At high frequencies it may be necessary to replace R1 with the transistor T3 as shown in Fig.14(b). This enables very fast turn-off times which would be difficult to achieve with circuit (a) since reducing R1 to a low value would cause the boot strap capacitor to discharge during the on-period. The impedance Z represents either the low side switch part of the bridge or the load.

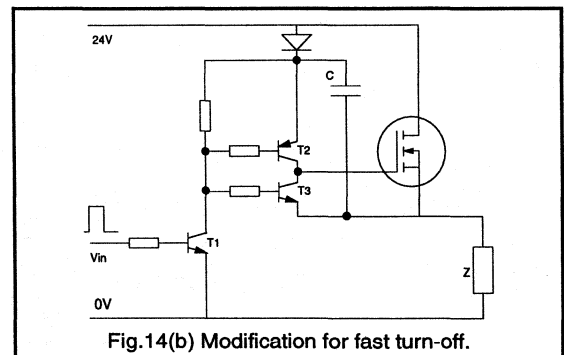


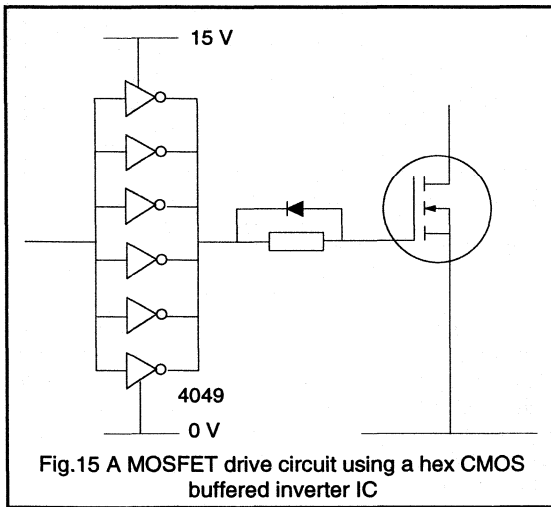
Fig.14(b) Modification for fast turn-off.

Very fast drive circuits for frequencies up to 1 MHz

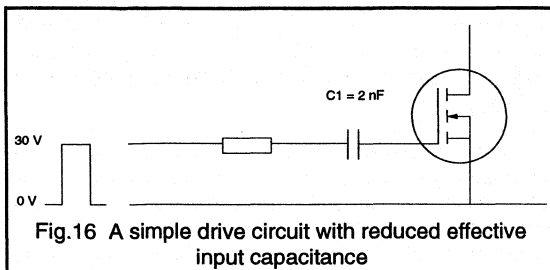
The following drive circuits can charge the gate source capacitance particularly fast and so realise extremely short switching times. These fast transition times are necessary to reduce the switching losses. Switching losses are directly proportional to the switching frequency and are greater than conduction losses above a frequency of about 500 kHz,

although this crossover frequency is dependent on circuit configuration. Thus for operation above 500 kHz it is important to have fast transition times.

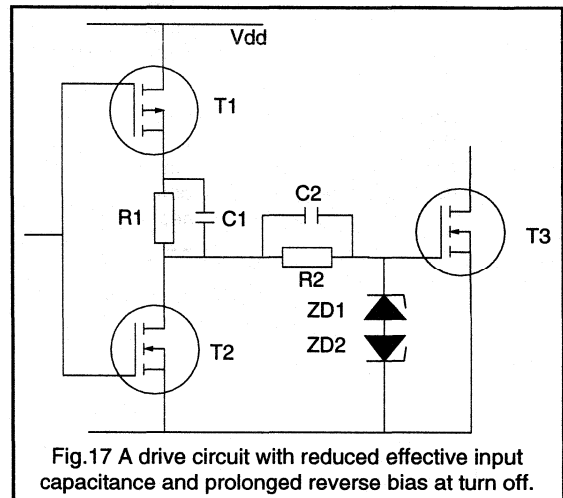
At frequencies below 500 kHz the circuit in Fig.15 is often used. Above 500 kHz the use of the DS0026 instead of the 4049 is recommended. The DS0026 has a high current sinking and sourcing capability of 2.5 A. It is a National Semiconductor device and is capable of charging a capacitance of 100 pF in as short a time as 25 ns.



In Fig.16 the value of capacitor C1 is made approximately equal to the input capacitance of the driven MOSFET. Thus the RC time constant for the charging circuit is approximately halved. The disadvantage of this arrangement is that a drive voltage of 30V instead of 15V is needed because of the potential divider action of C1 and the input capacitance of the driven MOSFET. A small value of C1 would be ideal for a fast turn on time and a large value of C1 would produce a fast turn off. The circuit in Fig.17 replaces C1 by two capacitors and enables fast turn on and fast turn off.



For the circuit in Fig.17 when MOSFET T1 is turned on the driven MOSFET T3 is driven initially by a voltage V_{DD} feeding three capacitors in series, namely C1, C2 and the input capacitance of T3. Since the capacitors are in series their equivalent capacitance will be low and so the RC time constant of the charging circuit will be low. C1 is made low to make the turn on time very fast.

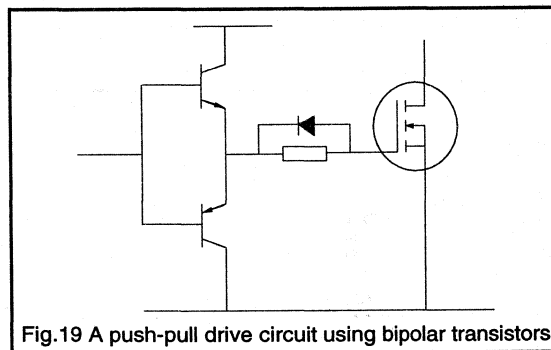
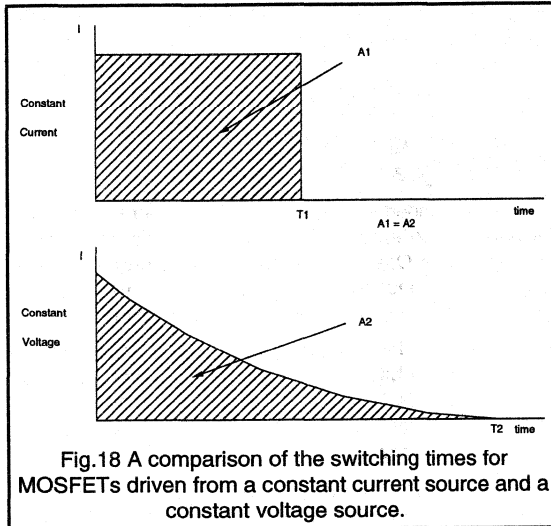


The voltage across C2 will then settle down to $(V_{DD} - V_{ZD1}) R2 / (R1 + R2)$. Therefore the inclusion of resistors R1 and R2 means that C2 can be made larger than C1 and still have a large voltage across it before the turn off of T3. Thus C2 can sustain a reverse voltage across the gate source of T3 for the whole of the turn off time. The initial discharging current will be given by Equation 3,

$$I = \frac{V_{ZD1} + \frac{R_2(V_{DD} - V_{ZD1})}{(R_1 + R_2)}}{R_{STRAY} + R_{DS(ON)T2}} \quad 3$$

Making V_{DD} large will make turn on and turn off times very small.

Fast switching speeds can be achieved with the push pull circuit of Fig.19. A further improvement can be made by replacing the bipolar devices by MOSFETs as shown in Fig.20. The positions of the P and N channel MOSFETs may be interchanged and connected in the alternative arrangement of Fig.21. However it is likely that one MOSFET will turn on faster than the other turns off and so the circuit in Fig.21 may cause a current spike during the switching interval. The peak to average current rating of MOSFETs is excellent so this current spike is not usually a problem. In the circuit of Fig.20 the input capacitance of the driven MOSFET is charged up to $V_{DD} - V_T$, where V_T is the threshold voltage, at which point the MOSFET T1 turns off. Therefore when T2 turns on there is no current spike.

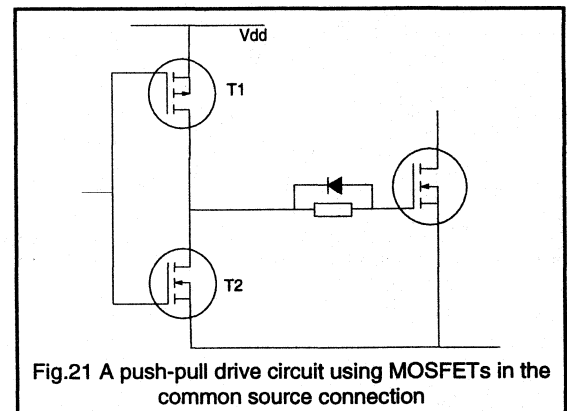
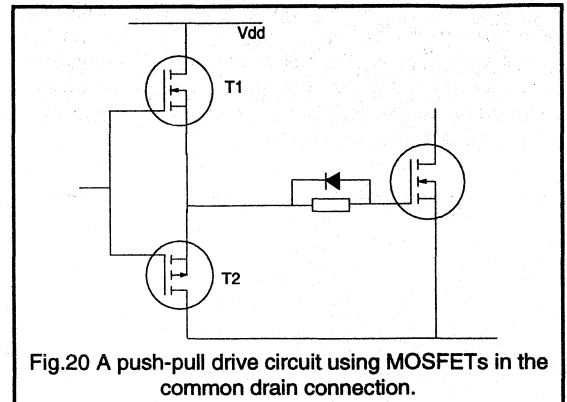


There may well be some advantages in charging the input capacitance of the MOSFET from a constant current source rather than a constant voltage source. For a given drain source voltage a fixed amount of charge has to be transferred to the input capacitance of a MOSFET to turn it on. As illustrated in Fig. 18 this charge can be transferred more quickly with a constant current of magnitude equal to the peak current from a constant voltage source.

A few other points are worthy of note when discussing very fast drive circuits.

(1) SMPS working in the 1 - 15 MHz range sometimes use resonant drive circuits. These SMPS are typically QRC (Quasi Resonant Circuits). The resonant drive circuits do not achieve faster switching by the fact that they are resonant. But by being resonant, they recoup some of the drive energy and reduce the gate drive power. There are two main types of QRC - zero voltage and zero current switching circuits. In one of these types, fall times are not critical and in the other, rise times are not critical. On the

critical switching edge, a normal, fast switching edge is provided by using a circuit similar to those given above. For the non-critical edge there is a resonant transfer of energy. Thus drive losses of $Q_G \cdot V_{GS} \cdot f$ become $0.5 \cdot Q_G \cdot V_{GS} \cdot f$.



(2) It is usual to provide overdrive of the gate source voltage. This means charging the input capacitance to a voltage which is more than sufficient to turn the MOSFET fully on. This has advantages in achieving lower on-resistance and increasing noise immunity. The gate power requirements are however increased when overdrive is applied. It may well be a good idea therefore to drive the gate with only 12 V say instead of 15 V.

(3) It is recommended that a zener diode be connected across the gate source terminals of a MOSFET to protect against over voltage. This zener can have a capacitance which is not insignificant compared to the input capacitance of small MOSFETs. The zener can thus affect switching times.

Parallel operation

Power MOSFETs lend themselves readily to operation in parallel since their positive temperature coefficient of resistance opposes thermal runaway. Since MOSFETs have low gate drive power requirements it is not normally necessary to increase the rating of drive circuit components if more MOSFETs are connected in parallel. It is however recommended that differential resistors are used in the drive circuits as shown in Fig.22.

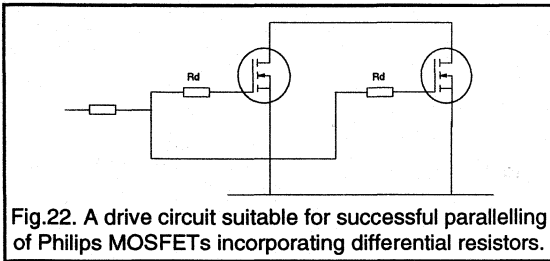


Fig.22. A drive circuit suitable for successful parallelling of Philips MOSFETs incorporating differential resistors.

These differential resistors (R_D) damp down possible oscillations between reactive components in the device and in connections around the MOSFETs, with the MOSFETs themselves, which have a high gain even up to 200 MHz.

Protection against gate-source overvoltages

It is recommended that zener diodes are connected across the gate-source terminals of the MOSFET to protect against voltage spikes. One zener diode or two back-to-back zener diodes are necessary dependent on whether the gate-source is unipolar or bipolar, as shown in Fig.23.

The zener diodes should be connected close to the terminals of the MOSFET to reduce the inductance of the connecting leads. If the inductance of the connecting leads is too large it can support sufficient voltage to cause an overvoltage across the gate-source oxide.

In conclusion the low drive power requirement of Philips PowerMOS make provision of gate drive circuitry a relatively straightforward process as long as the few guide-lines outlined in this note are heeded.

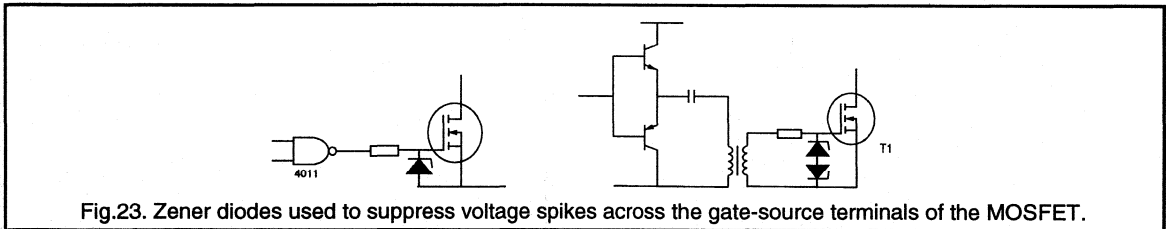


Fig.23. Zener diodes used to suppress voltage spikes across the gate-source terminals of the MOSFET.

1.2.4 Parallel Operation of Power MOSFETs

This section is intended as a guide to the successful parallelling of Power MOSFETs in switching circuits.

Advantages of operating devices in parallel

Increased power handling capability

If power requirements exceed those of available devices then increased power levels can be achieved by parallelling devices. The alternative means of meeting the power requirements would be to increase the area of die. The processing of the larger die would have a lower yield and so the relative cost of the die would be increased. The larger die may also require a more expensive package.

Standardisation

Parallelling devices can mean that only one package, say the TO220 package, needs to be used. This can result in reduced production costs.

Increased operating frequency

Packages are commercially available which contain upto five die connected in parallel. The switching capabilities of these packages are typically greater than 10 kVA. The parasitic inductances of connections to the parallellled dies are different for each die. This means that the current rating of the package has to be derated at high frequencies to allow for unequal current sharing. The voltage rating of the multiple die package has to be derated for higher switching speeds. This is because the relatively large inductances of connections within the package sustain appreciable voltages during the switching intervals. This means that the voltages at the drain connections to the dice will be appreciably greater than voltages at the terminals of the package. By parallelling discrete devices these problems can be overcome.

Faster switching speeds are achieved using parallellled devices than using a multiple die package. This is because switching times are adversely affected by the impedance of the gate drive circuit. When devices are parallellled these impedances are parallellled and so their effect is reduced. Hence faster switching times and so reduced switching losses can be achieved.

Faster switching speeds improve parallelling. During switching intervals one MOSFET may carry more current than other MOSFETs in parallel with it. This is caused by differences in electrical parameters between the parallellled MOSFETs themselves or between their drive circuits. The increased power dissipation in the MOSFET which carries more current will be minimised if switching speeds are

increased. The inevitable inductance in the source connection, caused by leads within the package, causes a negative feedback effect during switching. If the rate of rise of current in one parallellled MOSFET is greater than in the others then the voltage drop across inductances in its drain and source terminals will be greater. This will oppose the build up of current in this MOSFET and so have a balancing effect. This balancing effect will be greater if switching speeds are faster. This negative feedback effect reduces the deleterious effect of unequal impedances of drive circuit connections to parallellled MOSFETs. The faster the switching speeds then the greater will be the balancing effect of the negative feedback. Parallelling devices enables higher operating frequencies to be achieved than using multiple die packages. The faster switching speeds possible by parallelling at the device level promote better current sharing during switching intervals.

Increased power dissipation capability

If two devices, each rated for half the total required current, are parallellled then the sum of their individual power dissipation capabilities will be more than the possible power dissipation in a single device rated for the total required current. This is especially useful for circuits operating above 100 kHz where switching losses predominate.

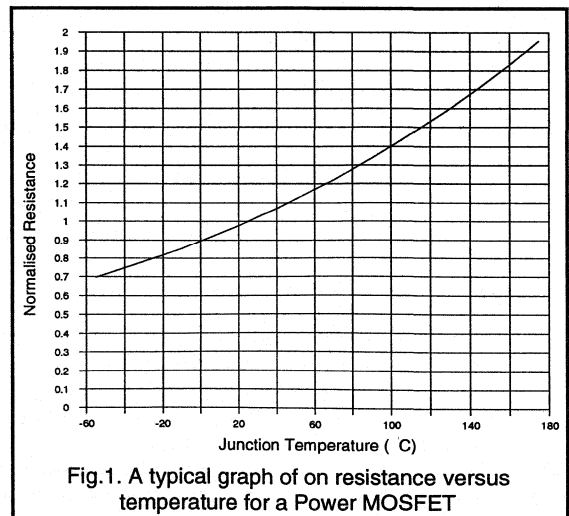


Fig. 1. A typical graph of on resistance versus temperature for a Power MOSFET

Advantages of power MOSFETs for parallel operation

Reduced likelihood of thermal runaway

If one of the paralleled devices carries more current than the power dissipation in this device will be greater and its junction temperature will increase. The temperature coefficient of $R_{DS(ON)}$ for Power MOSFETs is positive as shown in Fig.1. Therefore there will be a rise in $R_{DS(ON)}$ for the device carrying more current. This mechanism will oppose thermal runaway in paralleled devices and also in paralleled cells in the device.

Low Drive Power Requirements

The low drive power requirements of power MOSFETs mean that many devices can be driven from the same gate drive that would be used for one MOSFET.

Very good tolerance of dynamic unbalance

The peak to average current carrying capability of power MOSFETs is very good. A device rated at 8A continuous drain current can typically withstand a peak current of about 30A. Therefore, for the case of three 8A devices in parallel, if one of the devices switches on slightly before the others no damage will result since it will be able to carry the full load current for a short time.

Design points

Derating

Since there is a spread in on-resistance between devices from different batches it is necessary to derate the continuous current rating of paralleled devices by about 20%.

Layout

There are two aspects to successful parallelling which are static and dynamic balance. Static balance refers to equal sharing of current between paralleled devices when they have been turned on. Dynamic balance means equal sharing of current between paralleled transistors during switching intervals.

Unsymmetrical layout of the circuit causes static imbalance. If the connections between individual MOSFETs and the rest of the power circuit have different impedances then there will be static imbalance. The connections need to be kept as short as possible to keep their inductance as small as possible. Symmetrical layout is particularly important in resonant circuits where MOSFETs carry a sinusoidal current e.g. in a voltage fed inverter feeding a series resonant circuit. In a current fed inverter, where switching in the inversion stage causes a rectangular wave of current

to be passed through a parallel resonant tank circuit, the voltage sustained by MOSFETs when they are off will be half sinusoid. A component of the current carried by MOSFETs will be a charging current for snubber capacitors which will be sinusoidal so again symmetrical layout will be important.

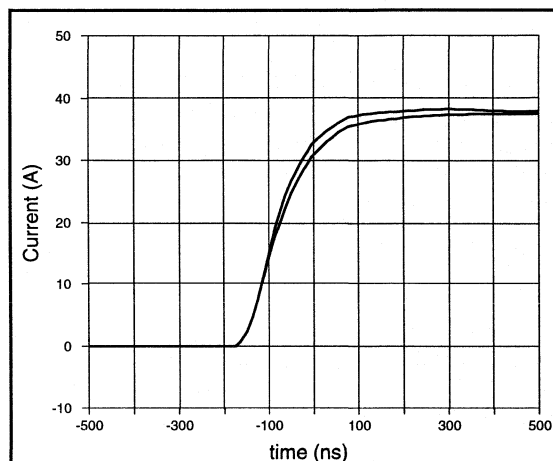


Fig.2. The waveforms of current through two paralleled BUK453-50A MOSFETs with symmetrical layout.

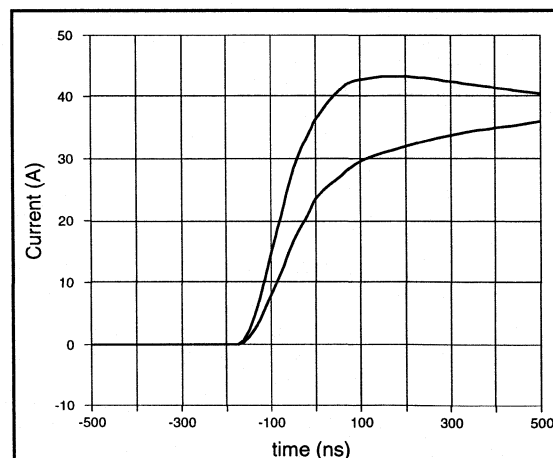


Fig.3. The waveforms of current through two paralleled BUK453-50A MOSFETs with 50 nH connected in the source connection on one MOSFET.

Unsymmetrical layout of the gate drive circuitry causes dynamic imbalance. Connections between the gate drive circuitry and the MOSFETs need to be kept short and twisted together to reduce their inductance. Further to this

the connections between the gate drive circuit and paralleled MOSFETs need to be approximately the same length.

Figures 2 and 3 illustrate the effect of unsymmetrical layout on the current sharing of two paralleled MOSFETs. The presence of 50 nH in the source connection of one of the two paralleled BUK453-50A MOSFETs causes noticeable imbalance. A square shaped loop of 1 mm diameter wire and side dimension only 25 mm is sufficient to produce an inductance of 50 nH.

Symmetrical layout becomes more important if more MOSFETs are paralleled, e.g. if a MOSFET with an $R_{DS(ON)}$ of 0.7 Ohm was connected in parallel with a MOSFET with an $R_{DS(ON)}$ of 1 Ohm then the MOSFET with the lower $R_{DS(ON)}$ would carry 18% more current than if both MOSFETs had an $R_{DS(ON)}$ of 1 ohm. If the MOSFET with an $R_{DS(ON)}$ of 0.7 ohm was connected in parallel with a hundred MOSFETs with $R_{DS(ON)}$ of 1 ohm it would carry 42% more current than if all the MOSFETs had an $R_{DS(ON)}$ 1 Ohm.

Good Thermal Coupling

There should be good thermal coupling between paralleled MOSFETs. This is achieved by mounting paralleled MOSFETs on the same heatsink or on separate heatsinks which are in good thermal contact with each other.

If poor thermal coupling existed between paralleled MOSFETs and the positive temperature coefficient of resistance was relied on to promote static balance, then the total current carried by the MOSFETs would be less than with good thermal coupling. Some MOSFETs would also have relatively high junction temperatures and so their reliability would be reduced. The temperature coefficient of MOSFETs is not large enough to make poor thermal coupling tolerable.

The Suppression of Parasitic Oscillations

Parasitic oscillations can occur. MOSFETs have transition frequencies typically in excess of 200 MHz and parasitic reactances are present both in the MOSFET package and circuit connections, so the necessary feedback conditions for parasitic oscillations exist. These oscillations typically occur at frequencies above 100 MHz so a high bandwidth oscilloscope is necessary to investigate them. The likelihood of these parasitic oscillations occurring is very much reduced if small differential resistors are connected in the leads to each paralleled MOSFET. A common gate drive resistor of between 10 and 100 Ohms with differential resistors of about 10 Ohm are recommended as shown in Fig.4.

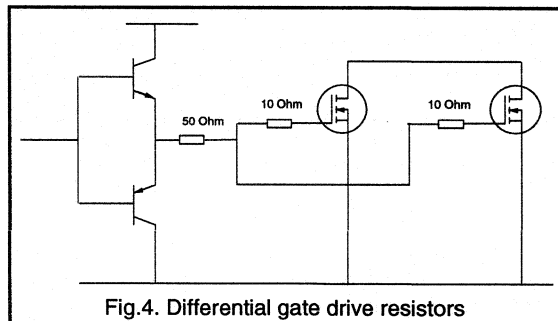


Fig.4. Differential gate drive resistors

The suppression of parasitic oscillations between paralleled MOSFETs can also be aided by passing the connections from the gate drive circuit through ferrite beads. The effect of these beads below 1 MHz is negligible. The ferrite beads however damp the parasitic oscillations which occur at frequencies typically above 100 MHz. An example of parasitic oscillations is shown in Fig.5.

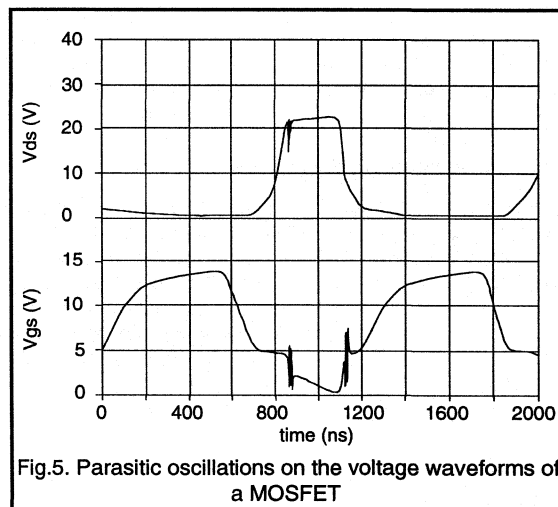


Fig.5. Parasitic oscillations on the voltage waveforms of a MOSFET

If separate drive circuits with closely decoupled power supplies are used for each paralleled device then parasitic oscillations will be prevented. This condition could be satisfied by driving each paralleled MOSFET from 3 buffers in a CMOS Hex buffer ic.

To take this one stage further, separate push pull transistor drivers could be used for each MOSFET. (A separate base resistor is needed for each push-pull driver to avoid a MOSFET with a low threshold voltage clamping the drive voltage to all the push pull drivers). This arrangement also has the advantage that the drive circuits can be positioned very close to the terminals of each MOSFET. The impedance of connections from the drive circuits to the MOSFETs will be minimised and so there will be a reduced

likelihood of spurious turn on. Spurious turn on can occur when there is a fast change in the drain to source voltage. The charging current for the gate drain capacitance inherent in the MOSFET structure can cause a voltage drop across the gate drive impedance large enough to turn the MOSFET on. The gate drive impedance needs to be kept as low as possible to reduce the likelihood of spurious turn on.

Resonant power supplies

If a resonant circuit is used then there will be reduced interference and switching losses. The reduced interference is achieved because sinusoidal waveforms are present in resonant circuits rather than rectangular waveforms. Rectangular waveforms have large high frequency harmonic components.

MOSFETs are able to switch at a zero crossing of either the voltage or the current waveform and so switching losses are ideally zero. For example, in the case of a current fed inverter feeding a parallel resonant load switching can take place at a zero crossing of voltage so switching losses are negligible. In this case the sinusoidal drain source voltage sustained by MOSFETs reduces the likelihood of spurious dv/dt turn on. This is because the peak charging current for the internal gate to drain capacitance of the MOSFET is reduced.

The current fed approach

Switch mode power supplies using the current fed topology have a d.c. link which contains a choke to smooth the current in the link. Thus a high impedance supply is presented to the inversion stage. Switching in the inversion stage causes a rectangular wave of current to be passed through the load. The current fed approach has many advantages for switch mode power supplies. It causes reduced stress on devices caused by the slow reverse recovery time of the parasitic diode inherent in the structure of MOSFETs.

The current fed approach can also reduce problems caused by dynamic imbalance. If more than three MOSFETs are paralleled then it is advantageous to use more than one choke in the d.c. link rather than wind a single choke out of thicker gauge wire. One of the connections to each choke

is connected to the output of the rectification stage. The other connection of each choke is connected to a group of three MOSFETs. This means that if one MOSFET switches on before the others it will carry a current less than its peak pulse value even when many MOSFETs are paralleled.

The parallel operation of MOSFETs in the linear mode

The problems of paralleling MOSFETs which are being used in the linear mode are listed below.

(a) The paralleled devices have different threshold voltages and transconductances. This leads to poor sharing.

(b) MOSFETs have a positive temperature coefficient of gain at low values of gate to source voltage. This can lead to thermal runaway.

The imbalance caused by differences in threshold voltage and transconductance can be reduced by connecting resistors (R_s) in the source connections. These resistors are in the gate drive circuit and so provide negative feedback. The negative feedback reduces the effect of different values of V_T and g_m . The effective transconductance g_m of the MOSFET is given in Equation 1.

$$g_m = \frac{1}{R_s + \frac{1}{g_m}} \quad 1$$

R_s must be large compared to $1/g_m$ to reduce the effects of differences in g_m . Values of $1/g_m$ typically vary between 0.1 and 1.0 Ohm. Therefore values of R_s between 1 ohm and 10 ohm are recommended.

Differential heating usually has a detrimental effect on sharing and so good thermal coupling is advisable.

Conclusions

Power MOSFETs can successfully be paralleled to realise higher power handling capability if a few guidelines are followed.

1.2.5 Series Operation of Power MOSFETs

The need for high voltage switches can be well illustrated by considering the following examples. In flyback converters the leakage inductance of an isolating transformer can cause a large voltage spike across the switch when it switches off. If high voltage MOSFETs are used the snubber components can be reduced in size and in some cases dispensed with altogether.

For industrial equipment operation from a supply of 415 V, 550 V or 660 V is required. Rectification of these supply voltages produces d.c. rails of approximately 550 V, 700 V and 800 V. The need for high voltage switches in these cases is clear.

Resonant topologies are being increasingly used in switching circuits. These circuits have advantages of reduced RFI and reduced switching losses. To reduce the size of magnetic components and capacitors the switching frequency of power supplies is increased. RFI and switching losses become more important at high frequencies so resonant topologies are more attractive. Resonant circuits have the disadvantage that the ratio of peak to average voltage can be large. For example a Parallel Resonant Power Supply for a microwave oven operating off a 240 V supply can be designed most easily using a switch with a voltage rating of over 1000 V.

In high frequency induction heating power supplies capacitors are used to resonate the heating coil. The use of high voltage switches in the inversion bridge can result in better utilisation of the kVAr capability of these capacitors. This is advantageous since capacitors rated at tens of kVAr above 100 kHz are very expensive.

In most TV deflection and monitor circuits peak voltages of up to 1300 V have to be sustained by the switch during the flyback period. This high voltage is necessary to reset the current in the horizontal deflection coil. If the EHT flashes over, the switch will have to sustain a higher voltage so 1500 V devices are typically required.

The Philips range of PowerMOS includes devices rated at voltages up to 1000 V to cater for these requirements. However in circuits, particularly in resonant applications where voltages higher than this are required, it may be necessary to operate devices in series.

Series operation can be attractive for the following reasons:

Firstly, the voltage rating of a PowerMOS transistor cannot be exceeded. A limited amount of energy can be absorbed by a device specified with a ruggedness rating

(eg device can survive some overvoltage transients), but a 1000 V device cannot block voltages in excess of 1000 V.

Secondly, series operation allows flexibility as regards on-resistance and so conduction losses.

The following are problems that have to be overcome for successful operation of MOSFETs in series. If one device turns off before another it may be asked to block a voltage greater than its breakdown voltage. This will cause a reduction in the lifetime of the MOSFET. Also there is a requirement for twice as many isolated gate drive circuits in many circuits.

The low drive power requirements of Philips PowerMOS mean that the provision of more isolated gate drive circuits is made easier. Resonant circuits can have advantages in reducing the problems encountered if one MOSFET turns off before another. The current fed full bridge inverter is one such circuit.

To illustrate how devices can be operated in series, a current fed full bridge inverter is described where the peak voltage requirement is greater than 1200 V.

The current fed inverter

A circuit diagram of the full bridge current fed inverter is shown in Fig.1. A choke in the d.c. link smooths the link current. Switching in the inversion bridge causes a rectangular wave of current to be passed through the load. The load is a parallel resonant tank circuit. Since the Q of the tank circuit is relatively high the voltage across the load is a sinewave. MOSFETs sustain a half sinusoid of voltage when they are off. Thus series operation of MOSFETs is made easier because if one MOSFET turns off before another it only has to sustain a small voltage. To achieve the best sharing, the gate drive to MOSFETs connected in series should be as similar as possible. In particular the zero crossings should be synchronised. The MOSFET drive circuit shown in Fig.2 has been found to be excellent in this respect. For current fed resonant circuits in which the duty cycle varies over large ranges the circuit in Fig.3 will perform well. A short pulse applied to the primary of the pulse transformer is sufficient to turn MOSFET M4 on. This short pulse can be achieved by designing the pulse transformer so that it saturates during the time that M1 is on. The gate source capacitance of M4 will remain charged until M2 is turned on. M3 will then be turned on and the gate source capacitance of M4 will be discharged and so

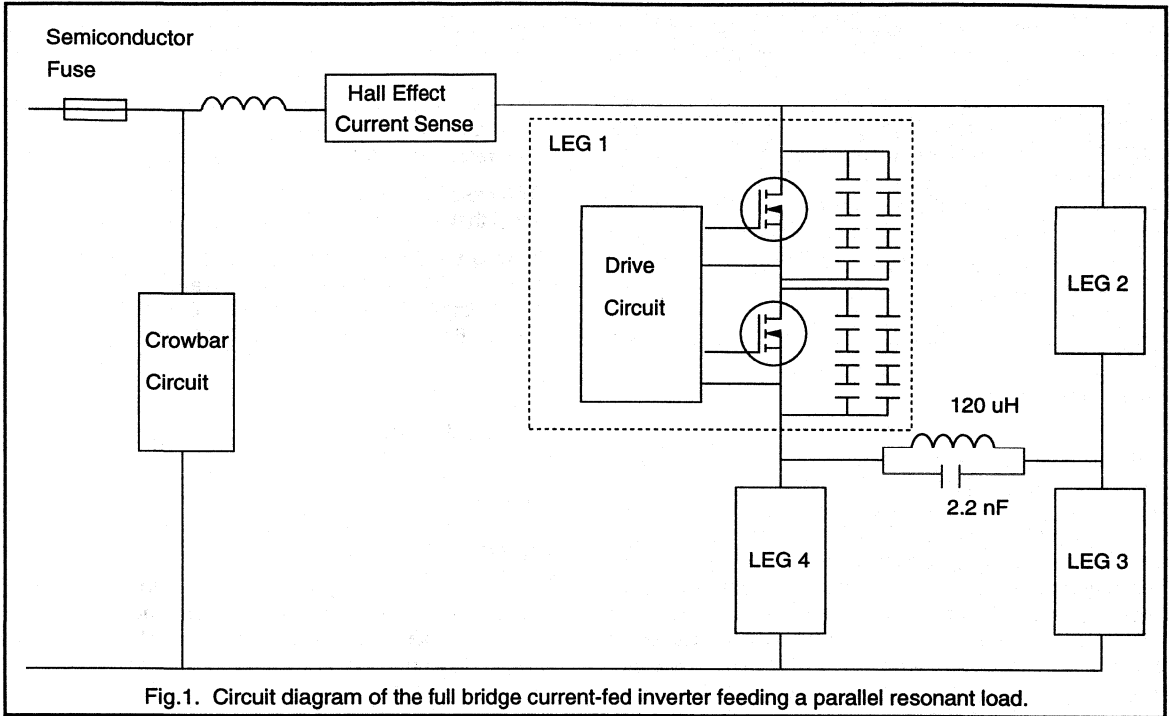


Fig.1. Circuit diagram of the full bridge current-fed inverter feeding a parallel resonant load.

M4 is turned off. Thus this circuit overcomes problems of resetting the flux in the core of the pulse transformer for large duty cycles.

Each leg of the inverter consists of two MOSFETs, type BUK456-800B, connected in series. The ideal rating of the two switches in each leg is therefore 1600 V and 3.5 A. The inverter is fed into a parallel resonant circuit with values of $L = 120 \mu\text{H}$ ($Q = 24$ at 150 kHz) and $C = 2.2 \text{ nF}$.

Capacitors are shown connected across the drain source terminals of MOSFETs. The value of the capacitor across the drain to source of each MOSFET is 6.6 nF. (Six 10 nF polypropylene capacitors, type 2222 376 92103.) This gives a peak voltage rating of about 850 V at 150 kHz for the capacitor combination across each MOSFET. (This voltage rating takes into account that the capacitors will only have to sustain voltage when the MOSFET is off). The function of these capacitors is twofold. Firstly they suppress spikes caused by switching off current in parasitic lead inductance. Secondly they improve the sharing of voltage between the MOSFETs connected in series. These capacitors are effectively in parallel with the tank circuit capacitor. However only half of the capacitors across MOSFETs are in circuit at any one time. This is because half of the capacitors are shorted out by MOSFETs which have been turned on. The resonant frequency of the tank circuit and drain source capacitors is given by Equation 1.

$$f = \frac{1}{2\pi\sqrt{L \cdot C_{tot}}} \quad 1$$

Where C_{tot} is the equivalent capacitance of the tank circuit capacitor and the drain source capacitors and is given by Equation 2.

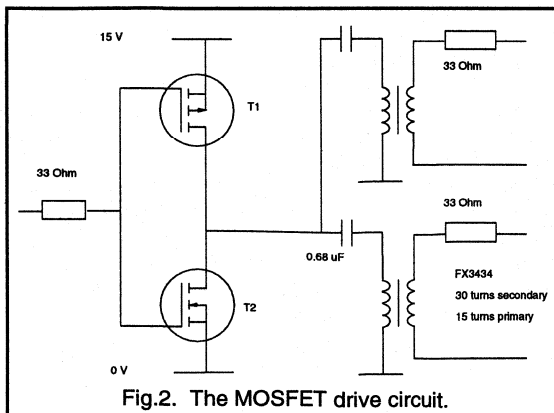


Fig.2. The MOSFET drive circuit.

$$C_{tot} = C_i + C_{DS} \quad 2$$

Therefore the resonant frequency of the tank circuit is 155 kHz.

An expression for the impedance at resonance of the parallel resonant circuit (Z_D) is given in Equation 3.

$$Z_D = \frac{L}{C_{tot} \cdot R} \quad 3$$

The Q of the circuit is given by Equation 4.

$$Q = \frac{1}{R} \cdot \sqrt{\frac{L}{C_{tot}}} \quad 4$$

Substituting Equation 3.

$$Z_D = Q \cdot \sqrt{\frac{L}{C_{tot}}} \quad 5$$

Thus Z_D for the parallel resonant load was 2.7 kOhms.

In a conventional rectangular switching circuit the connection of capacitors across MOSFETs will cause additional losses. These losses are caused because when a MOSFET turns on, the energy stored in the drain source capacitance is dissipated in the MOSFET and in a series resistor. This series resistor is necessary to limit the current

spike in the MOSFET at turn on. These losses are appreciable at 150 kHz, e.g. the connection of 1 nF across a MOSFET switching 600 V would cause losses of more than 25 W at 150 kHz. In the current fed inverter described in this article the MOSFETs turn on when the voltage across the capacitor is ideally zero. Thus there is no need for a series resistor and the turn on losses are ideally zero.

In this case the supply to the inverter was 470 V rms. This means that the peak voltage in the d.c. link was 650 V.

Equating the power flowing in the d.c. link to the power dissipated in the tank circuit produces an expression for the peak voltage across the tank circuit (V_T) as given in Equation 6.

$$V_T = 2 \times \sqrt{2} \times 1.11 \times V_{dlink} \quad 6$$

Therefore the peak to peak voltage across the tank circuit was ideally 2050 V

The voltage across each MOSFET should be 512 V.

Circuit performance

The switching frequency of this circuit is 120 kHz. Thus the load is fed slightly below its resonant frequency. This means that the load looks inductive and ensures that the MOSFETs do not switch on when the capacitors connected across their drain source terminals are charged.

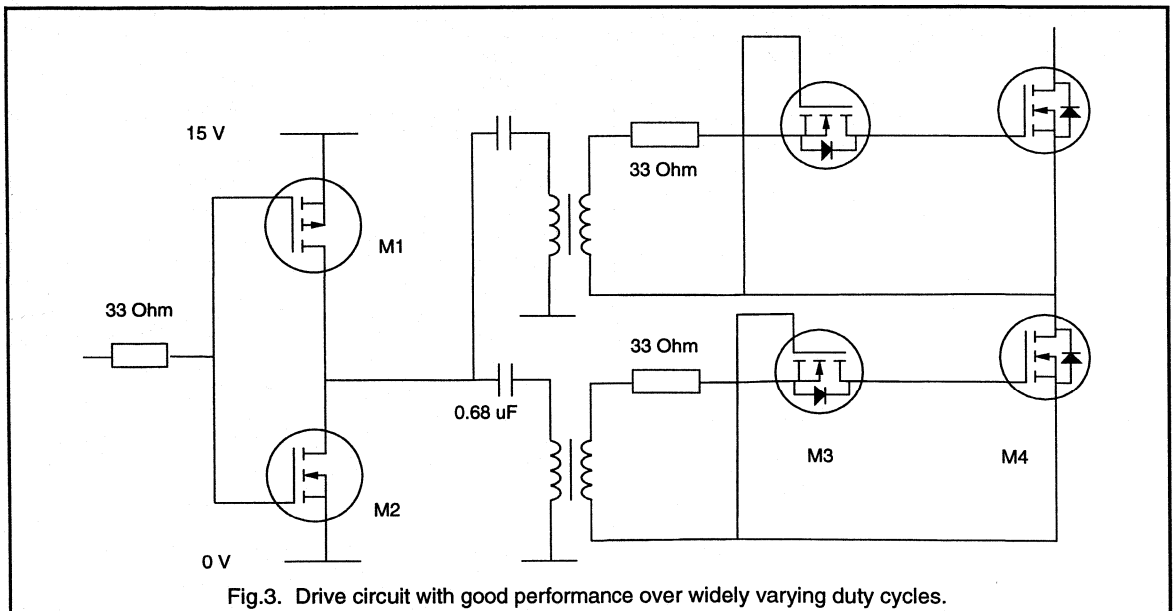


Fig.3. Drive circuit with good performance over widely varying duty cycles.

The waveforms of the voltage across two MOSFETs in series in a leg of the inversion bridge are shown in Fig.4. It can be seen that the sharing is excellent. The peak voltage across each MOSFET is 600 V. This is higher than 512 V because of ringing between parasitic lead inductance and the drain source capacitance of MOSFETs when they switch off.

The MOSFETs carry two components of current. The first component is the d.c. link current. The second component is a fraction of the circulating current of the tank circuit. The size of the second component is dependent on the relative sizes of the drain source capacitance connected across MOSFETs and the tank circuit capacitor.

In this circuit the peak value of charging current for drain source capacitors, which is carried by the MOSFET, is 4 A. The on-resistance of the BUK456-800B is about 5 Ohms at 80 °C. This explains the rise in $V_{DS(ON)}$ of about 20 V seen in Fig.4 just above the turn off of the MOSFETs.

The sharing of Philips PowerMOS in this configuration is so good that the value of drain source capacitance is not determined by its beneficial effect on sharing. Therefore, the value can be selected solely on the need to control ringing which in turn is dependent on power output and layout. (The increased current level associated with increased power output makes the ringing worse).

In any given configuration there is a maximum output power that single MOSFETs can handle and there will be a value of drain source capacitance associated with it. This value

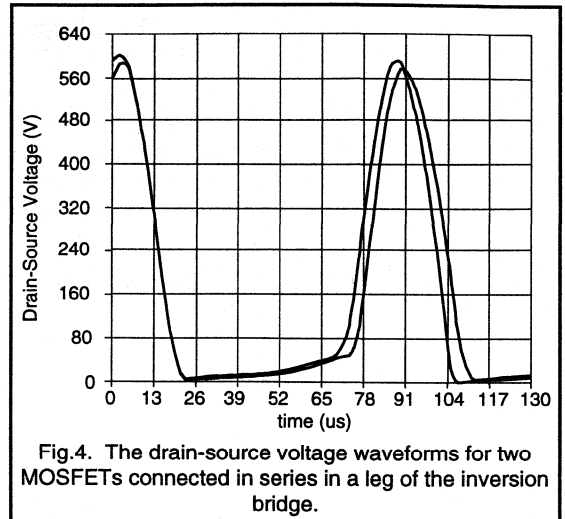


Fig.4. The drain-source voltage waveforms for two MOSFETs connected in series in a leg of the inversion bridge.

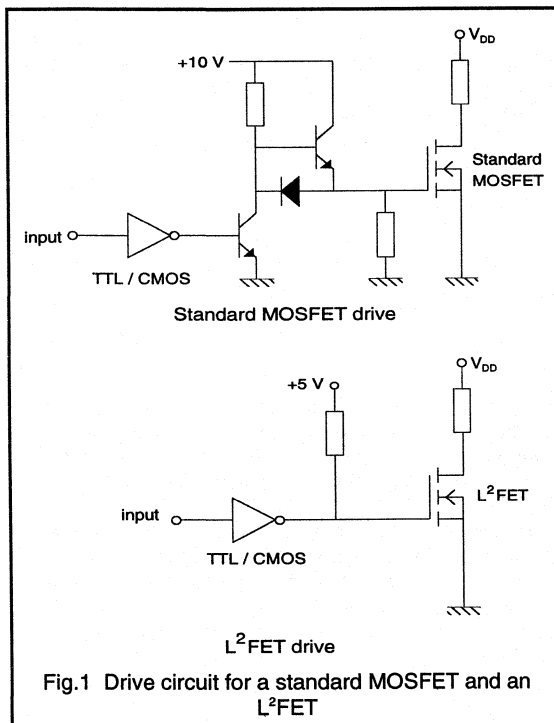
can be used as the 'capacitance per MOSFET' in higher power circuits where it becomes necessary to use MOSFETs connected in parallel. A value of between 5 and 10 nF is probably sufficient given a sensible layout.

Conclusions

It has been shown that MOSFETs can be connected in series to realise a switch that is as high as 90% of the sum of the voltage sustaining capabilities of the individual transistors.

1.2.6 Logic Level FETS

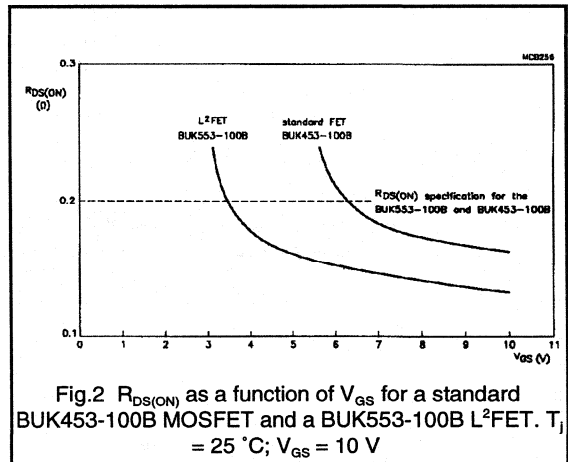
Standard Power MOSFETs require a gate-source voltage of 10 V to be fully ON. With Logic Level FETs (L²FETs) however, the same level of conduction is possible with a gate-source voltage of only 5 V. They can, therefore, be driven directly from 5 V TTL/CMOS ICs without the need for the level shifting stages required for standard MOSFETs, see Fig.1. This makes them ideal for today's sophisticated electrical systems, where microprocessors are used to drive switching circuits.



This characteristic of L²FETs is achieved by reducing the gate oxide thickness from - 800 Angstroms to - 500 Angstroms, which reduces the threshold voltage of the device from the standard 2.1-4.0 V to 1.0-2.0 V. However the result is a reduction in gate-source voltage ratings, from ± 30 V for a standard MOSFET to ± 15 V for the L²FET. The ± 15 V rating is an improvement over the 'industry standard' of ± 10 V, and permits Philips L²FETs to be used in demanding applications such as automotive.

Although a 5 V gate-drive is ideal for L²FETs, they can be used in circuits with gate-drive voltages of up to 10 V. Using

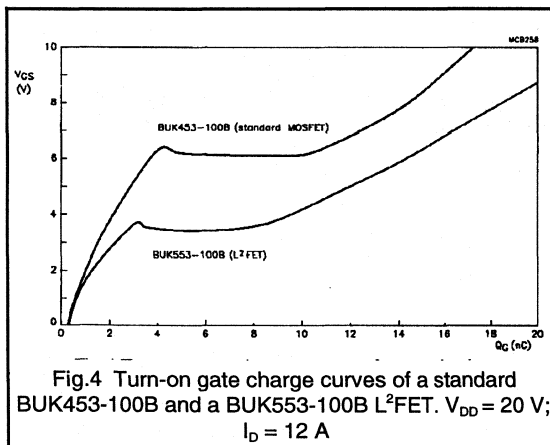
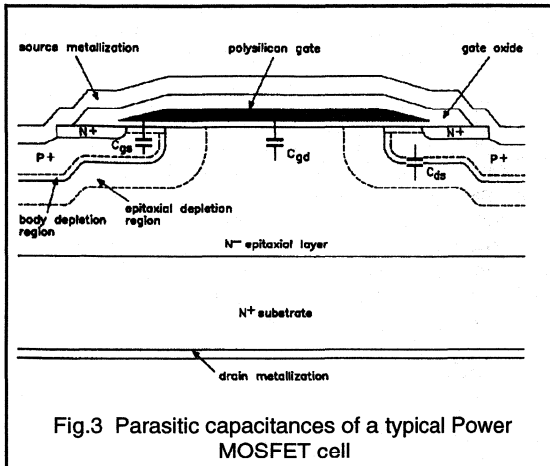
a 10 V gate-drive results in a reduced $R_{DS(ON)}$ (see Fig.2) but the turn-off delay time is increased. This is due to excessive charging of the L²FET's input capacitance.



Capacitances, Transconductance and Gate Charge

Figure 3 shows the parasitic capacitance areas of a typical Power MOSFET cell. Both the gate-source capacitance C_{gs} and the gate-drain capacitance C_{gd} increase due to the reduction in gate oxide thickness, although the increase in C_{gd} is only significant at low values of V_{DS} , when the depletion layer is narrow. Increases of the order of 25% in input capacitance C_{is} , output capacitance C_{oss} and reverse transfer capacitance C_{rss} result for the L²FET, compared with a similar standard type, at $V_{DS} = 0\text{ V}$. However at the standard measurement condition of $V_{DS} = 25\text{ V}$ the differences are virtually negligible.

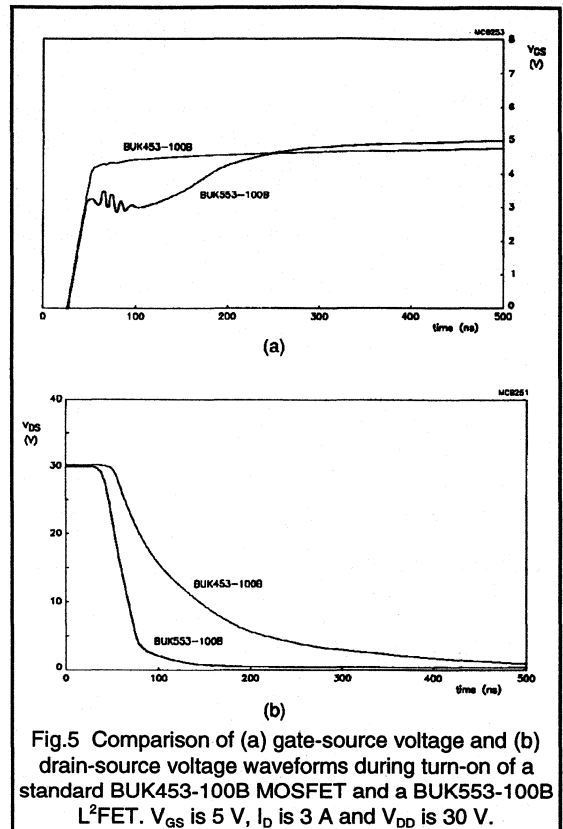
Forward transconductance g_{fs} is a function of the oxide thickness so the g_{fs} of an L²FET is typically 40% - 50% higher than a standard MOSFET. This increase in g_{fs} more than offsets the increase in capacitance of an L²FET, so the turn on charge requirement of the L²FET is lower than the standard type see Fig.4. For example, the standard BUK453-100B MOSFET requires about 17 nC to be fully switched on (at a gate voltage of 10 V) while the BUK553-100B L²FET only needs about 12 nC (at a gate source voltage of 5 V).



Switching speed.

Figure 5 compares the turn-on performance of the standard BUK453-100B MOSFET and the BUK553-100B L²FET, under identical drive conditions of 5 V from a 50 Ω generator using identical loads. Thanks to its lower gate threshold voltage $V_{GS,th}$, the L²FET can be seen to turn on in a much shorter time from the low level drive.

Figure 6 shows the turn-off performance of the standard BUK453-100B MOSFET and the BUK553-100B L²FET, again with the same drive. This time the L²FET is slower to switch. The turn-off times are determined mainly by the time required for C_{gd} to discharge. The C_{gd} is higher for the L²FET at low V_{DS} , and the lower value of $V_{GS,th}$ leads to a lower discharging current. The net result is an increase in turn off time.



Fast switching in many applications, for example automotive circuits, is not important. In areas where it is important however the drive conditions should be examined. For example, for a given drive power, a 10 V drive with a 50 Ω source impedance is equivalent to a 5 V drive with a source impedance of only 12 Ω . This results in faster switching for the L²FET compared with standard MOSFETs.

Ruggedness and reliability

MOSFETs are frequently required to be able to withstand the energy of an unclamped inductive load turn-off. Since this energy is dissipated in the bulk of the silicon, stress is avoided in the gate oxide. This means that the ruggedness performance of L²FETs is comparable with that of standard MOSFETs. The use of thinner gate oxide in no way compromises reliability. Good control of key process parameters such as pinhole density, mobile ion content, interface state density ensures good oxide quality. The projected MTBF is 2070 years at 90°C, at a 60% confidence level.

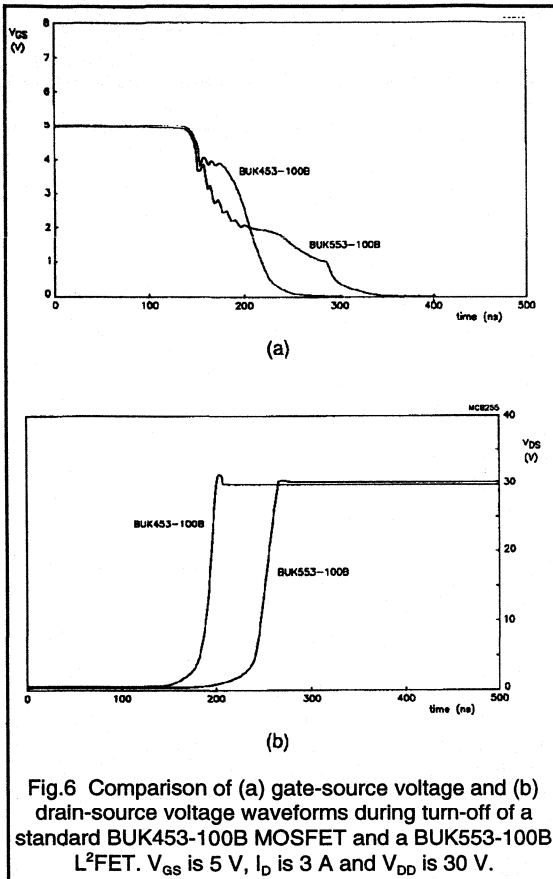


Fig.6 Comparison of (a) gate-source voltage and (b) drain-source voltage waveforms during turn-off of a standard BUK453-100B MOSFET and a BUK553-100B L²FET. V_{GS} is 5 V, I_D is 3 A and V_{DD} is 30 V.

The V_{GS} rating of an L²FET is about half that of a standard MOSFET, but this does not affect the V_{DS} rating. In principle, an L²FET version of any standard MOSFET is feasible.

Temperature stability

In general threshold voltage decreases with increasing temperature. Although the threshold voltage of L²FETs is lower than that of standard MOSFETs, so is their temperature coefficient of threshold voltage (about half in fact), so their temperature stability compares favourably with standard MOSFETs. Philips low voltage L²FETs (≤ 200 v) in TO220 all feature T_{jmax} of 175°C, rather than the industry standard of 150°C.

Applications

The Philips Components range of rugged Logic Level MOSFETs enable cost effective drive circuit design without compromising ruggedness or reliability. Since they enable power loads to be driven directly from ICs they may be considered to be the first step towards intelligent power switching. Thanks to their good reliability and 175°C T_{jmax} temperature rating, they are displacing mechanical relays in automotive body electrical functions and are being designed in to such safety critical areas as ABS.

1.2.7 Avalanche Ruggedness

Recent advances in power MOS processing technology now enables power MOS transistors to dissipate energy while operating in the avalanche mode. This feature results in transistors able to survive in-circuit momentary overvoltage conditions, presenting circuit designers with increased flexibility when choosing device voltage grade against required safety margins.

This paper considers the avalanche characteristics of 'rugged' power MOSFETs and presents results from investigations into the physical constraints which ultimately limit avalanche energy dissipation in the VDMOS structure. Results suggest that the maximum sustainable energy is a function of the applied power density waveform, independent of device voltage grade and chip size.

The ability of a rugged device to operate reliably in a circuit subject to extreme interference is also demonstrated.

Introduction.

Susceptibility to secondary breakdown is a phenomenon which limits the power handling capability of a bipolar transistor to below its full potential. For a power MOSFET, power handling capability is a simple function of thermal resistance and operating temperature since the device is not vulnerable to a second breakdown mechanism. The previous statement holds true provided the device is operated at or below its breakdown voltage rating (B_{VDSS}) and not subject to overvoltage. Should the transistor be forced into avalanche by a voltage surge the structure of the device permits possible activation of a parasitic bipolar transistor which may then suffer the consequences of second breakdown. In the past this mechanism was typical of failure in circuits where the device became exposed to overvoltage. To reduce the risk of device failure during momentary overloads improvements have been introduced to the Power MOS design which enable it to dissipate energy while operating in the avalanche condition. The term commonly used to describe this ability is 'Ruggedness', however before discussing in further detail the merits of a rugged Power MOSFET it is worth considering the failure mechanism of non-rugged devices.

Failure mechanism of a non-rugged Power MOS.

A power MOS transistor is made up of many thousands of cells, identical in structure. The cross section of a typical cell is shown in Fig. 1. When in the off-state or operating in saturation, voltage is supported across the p-n junction as shown by the shaded region. If the device is subjected to over-voltage (greater than the avalanche value of the

device), the peak electric field, located at the p-n junction, rises to the critical value (approx. 200 kV / cm) at which avalanche multiplication commences.

Computer modelling has shown that the maximum electric field occurs at the corners of the P diffusions. The electron-hole plasma generated by the avalanche process in these regions gives rise to a source of electrons, which are swept across the drain, and a source of holes, which flow through the P- and P regions towards the source metal contact.

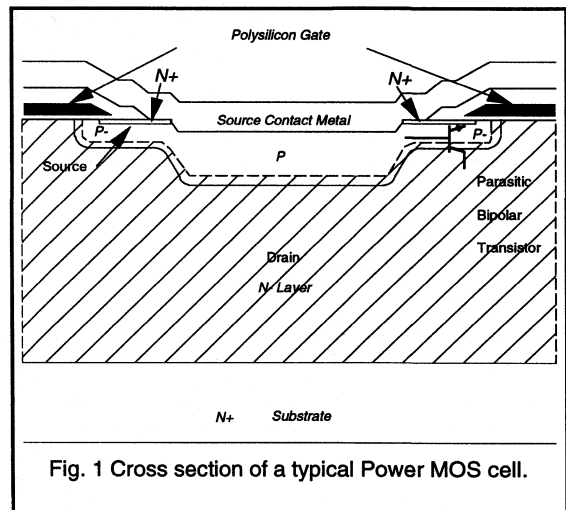


Fig. 1 Cross section of a typical Power MOS cell.

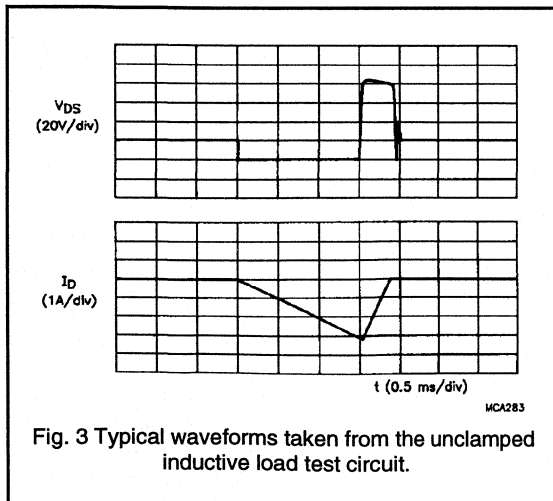
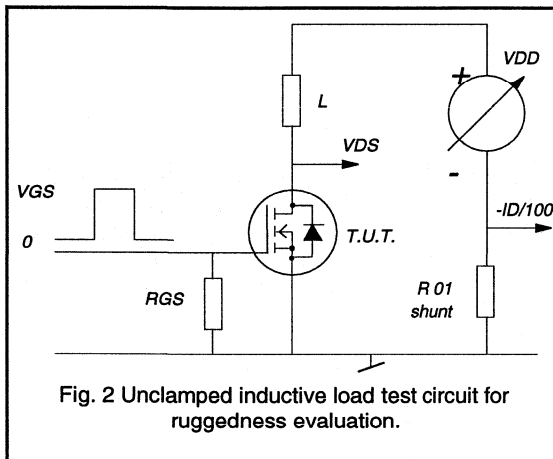
Clearly the P- region constitutes a resistance which will give rise to a potential drop beneath the n+. If this resistance is too large the p-n junction may become forward biased for relatively low avalanche currents.

Also if the manufacturing process does not yield a uniform cell structure across the device or if defects are present in the silicon then multiplication may be a local event within the crystal. This would give rise to a high avalanche current density flowing beneath the source n+ and cause a relatively large potential drop sufficient to forward bias the p-n junction and hence activate the parasitic npn bipolar transistor inherent in the MOSFET structure. Due to the positive temperature coefficient associated with a forward biased p-n junction, current crowding will rapidly ensue with the likely result of second breakdown and eventual device destruction.

In order that a power MOS transistor may survive transitory excursions into avalanche it is necessary to manufacture a device with uniform cell structure, free from defects throughout the crystal and that within the cell the resistance beneath the n+ should be kept to a minimum. In this way a forward biasing potential across the p-n junction is avoided.

Definition of ruggedness.

The term 'Ruggedness' when applied to a power MOS transistor, describes the ability of that device to dissipate energy while operating in the avalanche condition. To test ruggedness of a device it is usual to use the method of unclamped inductive load turn-off using the circuit drawn in Fig. 2.



Circuit operation:-

A pulse is applied to the gate such that the transistor turns on and load current ramps up according to the inductor value, L and drain supply voltage, V_{DD} . At the end of the gate pulse, channel current in the power MOS begins to fall while voltage on the drain terminal rises rapidly in accordance with equation 1.

$$\frac{dv}{dt} = L \frac{d^2I}{dt^2} \quad (1)$$

The voltage on the drain terminal is clamped by the avalanche voltage of the Power MOS for a duration equal to that necessary for dissipation of all energy stored in the inductor. Typical waveforms showing drain voltage and source current for a device undergoing successful test are shown in Fig. 3.

The energy stored in the inductor is given by equation 2 where I_D is the peak load current at the point of turn-off of the transistor.

$$W_{DSS} = 0.5LI_D^2 \quad (2)$$

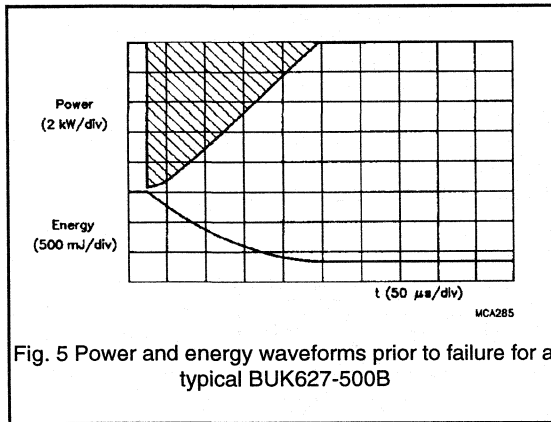
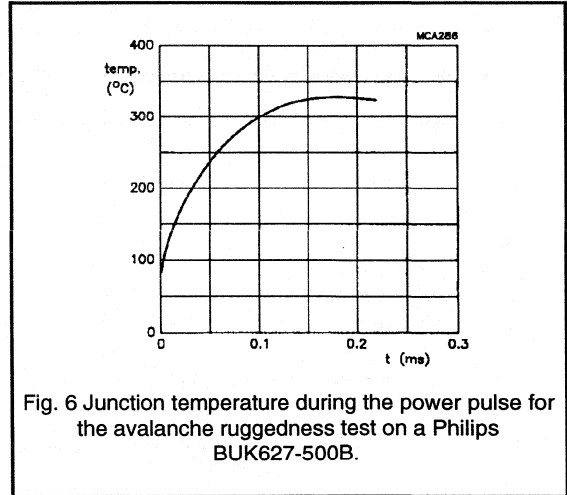
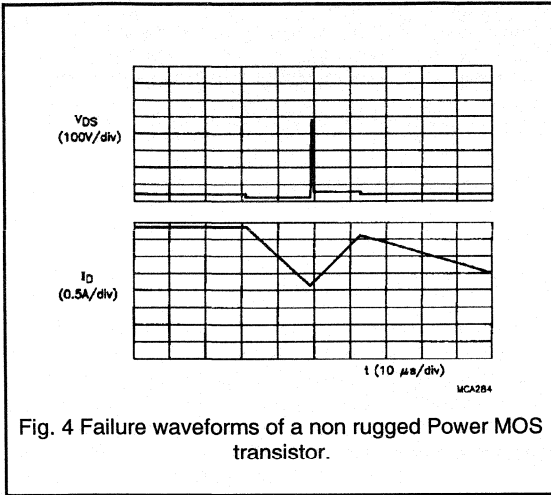
All this energy is dissipated by the Power MOS while the device is in avalanche.

Provided the supply rail is kept below 50 % of the avalanche voltage, equation 2 approximates closely to the total energy dissipation by the device during turn-off. However a more exact expression which takes account of additional energy delivered from the power supply is given by equation 3.

$$W_{DSS} = \frac{BV_{DSS}}{BV_{DSS} - V_{DD}} 0.5LI_D^2 \quad (3)$$

Clearly the energy dissipated is a function of both the inductor value and the load current I_D , the latter being set by the duration of the gate pulse. The 50 Ohm resistor between gate and source is necessary to ensure a fast turn-off such that the device is forced into avalanche.

The performance of a non-rugged device in response to the avalanche test is shown in Fig. 4. The drain voltage rises to the avalanche value followed by an immediate collapse to approximately 30 V. This voltage is typical of the sustaining voltage during Second Breakdown of a bipolar transistor, [1]. The subsequent collapse to zero volts after 12 μ S signifies failure of the device. The transistor shown here was only able to dissipate a few micro joules at a very low current if a failure of this type was to be avoided.



Equation 4 predicts that the junction temperature will pass through a maximum of 325 °C during the test. The calculation of $Z_{th}(t)$ assumes that the power dissipation is uniform across the active area of the device. When the device operates in the avalanche mode the power will be dissipated more locally in the region of the p-n junction where the multiplication takes place. Consequently a local temperature above that predicted by equation 4 is likely to be present within the device.

Work on bipolar transistors [2] has shown that at a temperature of the order of 400 °C, the voltage supporting p-n region becomes effectively intrinsic as a result of thermal multiplication, resulting in a rapid collapse in the terminal voltage. It is probable that a similar mechanism is responsible for failure of the Power MOS with a local temperature approaching 400 °C resulting in a device short circuit. A subsequent rapid rise in internal temperature will result in eventual device destruction.

Clearly the rise in T_j is a function of the applied power waveform which is in turn related to circuit current, avalanche voltage of the device and duration of the energy pulse. Thus the energy required to bring about device failure will vary as a function of each of these parameters. The ruggedness of Power MOSFETS of varying crystal size and voltage specification together with dependence on circuit current is considered below.

ii) Sustainable avalanche energy as a function of current.

The typical avalanche energy required to cause device failure is plotted as a function of peak current in Fig. 7 for a BUK553-60A (60 V, 0.085 Ohm Logic Level device). This result was obtained through destructive device testing using the circuit of Fig. 2 and a variety of inductor values.

Characteristics of a rugged Power MOS.

i) The energy limitation of a rugged device

The power waveform for a BUK627-500B (500 V, 0.8 Ohm) tested at a peak current of 15 A is presented in Fig. 5.

The area within the triangle represents the maximum energy that this particular device type may sustain without failure at the above current. Figure 6 shows the junction temperature variation in response to the power pulse, calculated from the convolution integral as shown in equation 4.

$$T_j(t) = \int_{\tau=0}^{\tau=t} P(t-\tau)Z_{th}(\tau)d\tau \quad (4)$$

where $Z_{th}(\tau)$ = transient thermal impedance.

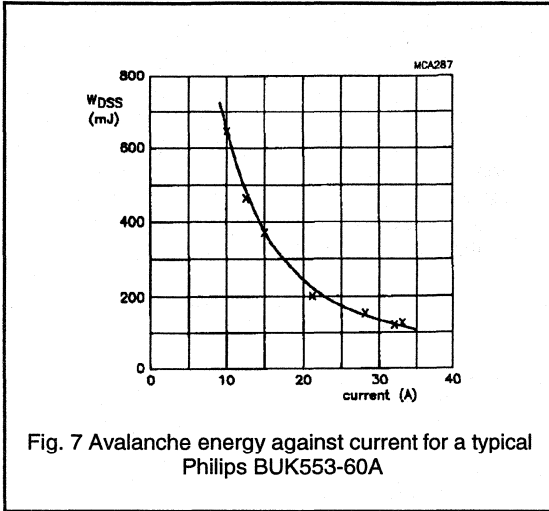


Fig. 7 Avalanche energy against current for a typical Philips BUK553-60A

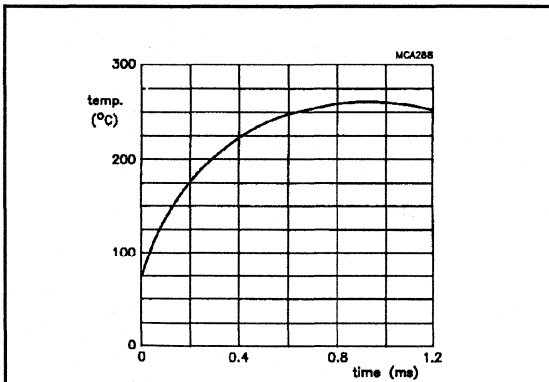


Fig. 8(a) Temperature during avalanche test for BUK553-60A; ID = 10 A

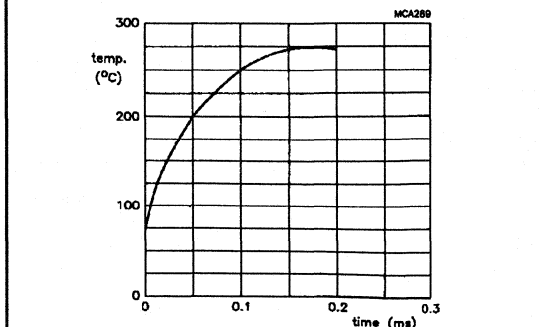


Fig. 8(b) Temperature during avalanche test for BUK553-60A; ID = 22 A

The plot shows that the effect of reducing current is to permit greater energy dissipation during avalanche prior to failure. This is an expected result since lower currents result in reduced power dissipation enabling avalanche to be sustained over a longer period. Temperature plots (Fig. 8) calculated for the 10 A and 22 A failure points confirm that the maximum junction temperature reached in each case is the same despite the different energy values. (N.B. The critical temperature is again underestimated as previously stated.)

iii) Effect of crystal size.

To enable a fair comparison of ruggedness between devices of various chip size it is necessary to normalise the results. Therefore instead of plotting avalanche energy against current, avalanche energy density and current density become more appropriate axes. Figure 9 shows the avalanche energy density against current density failure locus for two 100 V Philips Power MOS types which are different only in silicon area. Also shown on this plot are two competitor devices of different chip areas ($B_{VDSS} = 100$ V). This result demonstrates two points:

- a) the rise in T_j to the critical value for failure is dependent on the power density dissipated within the device as a function of time,
- b) the sustainable avalanche energy scales proportional to chip size.

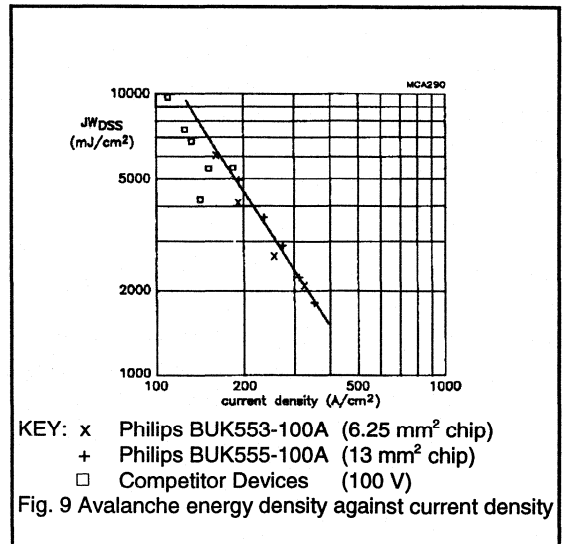


Fig. 9 Avalanche energy density against current density

iv) Dependence on the drain source breakdown voltage rating.

Energy density against current density failure loci are shown for devices of several different breakdown voltages in Fig. 10.

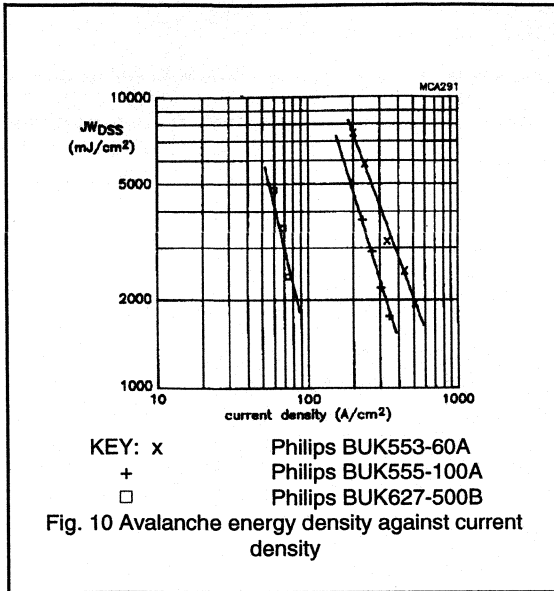


Fig. 10 Avalanche energy density against current density

Presented in this form it is difficult to assess the relative ruggedness of each device since the current density is reduced for increasing voltage. If instead of peak current density, peak power density is used for the x-axis then comparison is made very simple. The data of Fig. 10 has been replotted in Fig. 11 in the above manner. Represented in this fashion the ruggedness of each chip appears very similar highlighting that the maximum energy dissipation of a device while in avalanche is dependent only on the power density function.

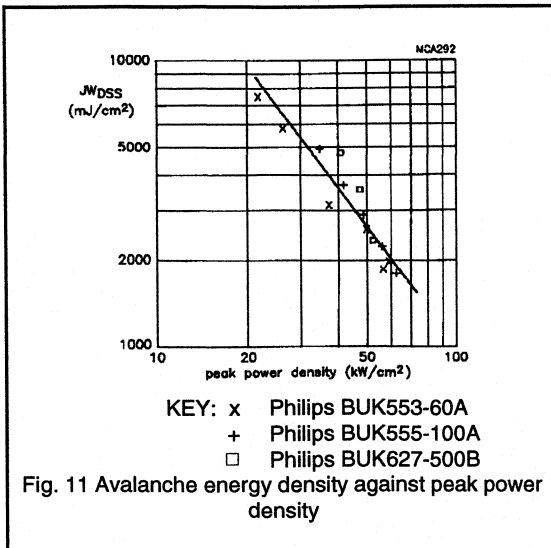


Fig. 11 Avalanche energy density against peak power density

Ruggedness ratings.

It should be stressed that the avalanche energies presented in the previous section result in a rise of the junction temperature far in excess of the device rating and in practice energies should be kept within the specification. Ruggedness is specified in data for each device in terms of an unclamped inductive load test maximum condition; recommended energy dissipation at a particular current (usually the rated current of the device).

DEVICE	R_{DSON}	V_{DS}	I_D	W_{DSS}
TYPE	(Ω)	(V)	(A)	(mJ)
BUK552-60A	0.15	60	14	30
BUK552-100A	0.28	100	10	30
BUK553-60A	0.085	60	20	45
BUK553-100A	0.18	100	13	70

Table 1 Ruggedness Ratings

The ruggedness rating is chosen to protect against a rise in T_j above the maximum rating. Examples of ruggedness ratings for a small selection of devices are shown in Table 1.

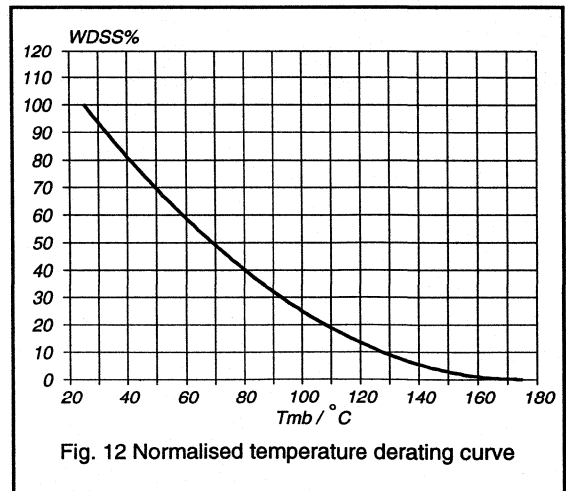
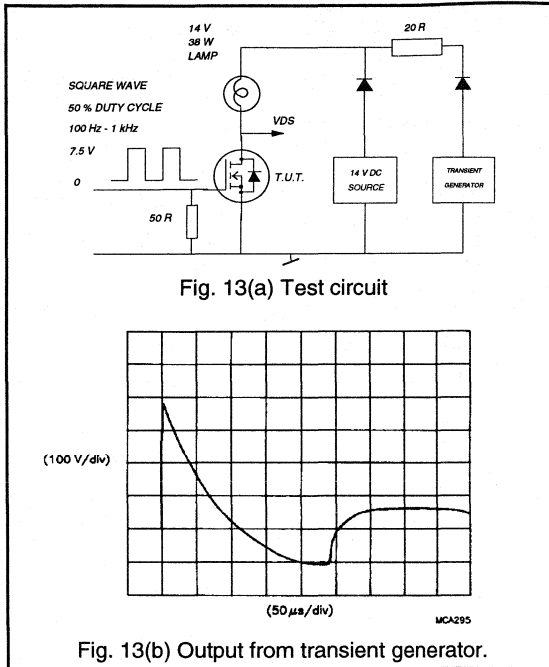


Fig. 12 Normalised temperature derating curve

This data is applicable for $T_j = 25$ °C. For higher operating temperatures the permissible rise in junction temperature during the energy test is reduced. Consequently ruggedness needs to be derated with increasing operating temperature. A normalised derating curve for devices with T_j max 175 °C is presented in Fig. 12.



Performance of a rugged Power MOS device.

The ability of a rugged Power MOS transistor to survive momentary power surges results in excellent device reliability. The response of a BUK553-60A to interference spikes while switching a load is presented below. The test

circuit is shown in Fig. 13(a) together with the profile of the interference spike in Fig. 13(b).

The interference generator produces pulses asynchronous to the switching frequency of the Power MOS. Figure 14 shows the drain voltage and load current response at four instances in the switching cycle. Devices were subjected to 5000 interference spikes at a frequency of 5 Hz. No degradation in device performance was recorded.

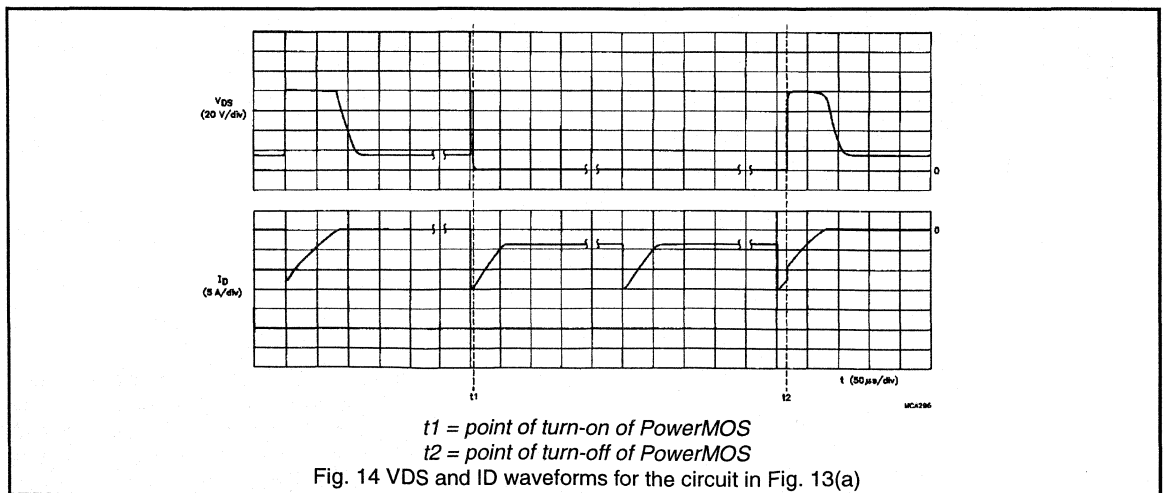
Conclusions.

The ability of power MOS devices to dissipate energy in the avalanche mode has been made possible by process optimisation to remove the possibility of turn-on of the parasitic bipolar structure. The failure mechanism of a rugged device is one of excessive junction temperature initiating a collapse in the terminal voltage as the junction area becomes intrinsic. The rise in junction temperature is dictated by the power density dissipation which is a function of crystal size, breakdown voltage and circuit current.

Ruggedness ratings for Philips PowerMOS are chosen to ensure that the specified maximum junction temperature of the device is not exceeded.

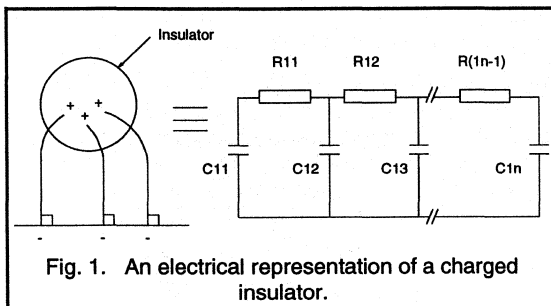
References.

1. DUNN and NUTTALL, An investigation of the voltage sustained by epitaxial bipolar transistors in current mode second breakdown. *Int.J.Electronics*, 1978, vol.45, no.4, 353-372
2. DOW and NUTTALL, A study of the current distribution established in npn epitaxial transistors during current mode second breakdown. *Int.J.Electronics*, 1981, vol.50, no.2, 93-108



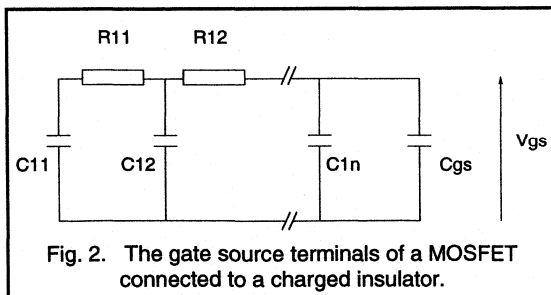
1.2.8 Electrostatic Discharge (ESD) Considerations

Charge accumulates on insulating bodies and voltages as high as 20,000 V can be developed by, for example, walking across a nylon carpet. Electrically the insulator can be represented by many capacitors and resistors connected as shown in Fig. 1. The value of the resistors is large and as a consequence it is not possible to discharge an insulator by connecting it straight to ground. An ion source is necessary to discharge an insulator.



Since MOSFETs have a very high input impedance, typically $> 10^9$ Ohms at dc, there is a danger of static electricity building up on the gate source capacitance of the MOSFET. This can lead to damage of the thin gate oxide. There are two ways in which the voltage across the gate source terminals of a MOSFET can be increased to its breakdown voltage by static electricity.

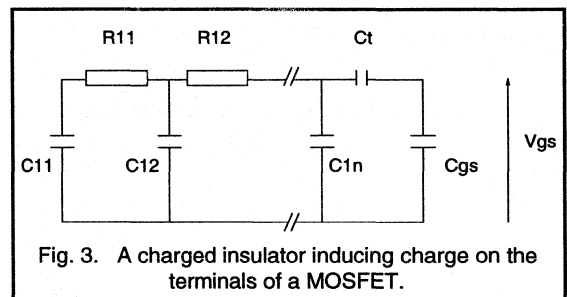
Firstly a charged object can be brought into contact with the MOSFET terminals or with tracks electrically connected to the terminals. This is represented electrically by Fig. 2. Secondly charge can be induced onto the terminals of the MOSFET. Electrically this can be represented by the circuit in Fig. 3.



From Figs. 2 and 3, it can be seen that, as the total area of the gate source region increases then the sensitivity of the devices to ESD will decrease. Hence power MOSFETs are less prone to ESD than CMOS ICs. Also, for a given

voltage rating, MOSFETs with a larger die area (i.e. the devices with lower on-resistance) are less prone to ESD than smaller dice.

To prevent the destruction of MOSFETs through ESD a two pronged approach is necessary. Firstly it is important to minimise the build up of static electricity. Secondly measures need to be taken to prevent the charging up of the input capacitance of MOSFETs by static electric charges.



In the Philips manufacturing facilities many precautions are taken to prevent ESD damage and these are summarised below.

Precautions taken to prevent the build up of static electricity

1. It is important to ensure that personnel working with MOSFETs are aware of the problems and procedures that have to be followed. This involves the training of staff. Areas in which MOSFETs are handled are designated Special Handling Areas (SHA) and are clearly marked as such. Checks are made every month that anti-static rules are being rigorously implemented.
2. Some materials are more prone to the build up of static electricity than others (e.g. polyester is worse than cotton). Therefore it is important to minimise the use of materials that enhance the likelihood of build up of static electricity. Materials best avoided are acetate, rayon and polyester. The wearing of overclothing made from polycotton with 1% stainless steel fibre is one solution. In clean rooms nylon overalls which have been antistatically treated are worn. The use of insulating materials is avoided.
3. Work benches and floors are covered in a static dissipative material and connected to a common earth. A high conductive material is not used since it would create an electric shock hazard and cause too rapid a discharge of charged material. From the point of view of ESD materials can be classified according to their conductivity as shown below.

- insulator ($>10^{14}$ ohm/square)
- antistatic ($10^9 - 10^{14}$ Ohm/square)
- static dissipative ($10^5 - 10^9$ Ohm/square)
- conductor ($<10^5$ Ohm/square).

4. Conducting straps are used to electrically connect personnel to the point of common earthing. This prevents the build up of static charge on staff. The connection is static dissipative to prevent an electric shock hazard.

5. Air plays an important part in the build up of static electricity.

This is particularly troublesome in a dry atmosphere.

Many of the techniques mentioned above are referred to in BS5783.

Precautions taken to prevent damage to MOSFETs by electrostatic build up of charge

1. When MOSFETs are being transported or stored they

should be in antistatic containers. These containers should be totally enclosed to prevent charges being induced onto the terminals of devices.

2. If MOSFETs have to be left out on the bench, e.g. during a test sequence, they should be in sockets which have the gate and source pins electrically connected together.

The precautions that should be taken at the customers' premises are the same as above. It should be remembered that whenever a MOSFET is touched by someone there is a danger of damage. The precautions should be taken in every area in which MOSFETs are tested or handled. In addition where devices are soldered into circuits with a soldering iron an earthed bit should always be used.

The probability of device destruction caused by ESD is low even if only the most rudimentary precautions are taken. However without such precautions and with large numbers of PowerMOS devices now being designed into equipment a few failures would be inevitable. The adoption of the precautions outlined will mean that ESD will no longer be a problem.

1.2.9 Understanding the Data Sheet: PowerMOS

All manufacturers of power MOSFETs provide a data sheet for every type produced. The purpose of the data sheet is primarily to give an indication as to the capabilities of a particular product. It is also useful for the purpose of selecting device equivalents between different manufacturers. In some cases however data on a number of parameters may be quoted under subtly different conditions by different manufacturers, particularly on second order parameters such as switching times. In addition the information contained within the data sheet does not always appear relevant for the application. Using data sheets and selecting device equivalents therefore requires caution and an understanding of exactly what the data means and how it can be interpreted. Throughout this chapter the BUK553-100A is used as an example, this device is a 100 V logic level MOSFET.

Information contained in the Philips data sheet

The data sheet is divided into 8 sections as follows:

- * Quick reference data
- * Limiting values
- * Thermal resistances
- * Static characteristics
- * Dynamic characteristics
- * Reverse diode limiting values and characteristics
- * Avalanche limiting value
- * Graphical data

The information contained within each of these sections is now described.

Quick reference data

This data is presented for the purpose of quick selection. It lists what is considered to be the key parameters of the device such that a designer can decide at a glance whether the device is likely to be the correct one for the application or not. Five parameters are listed, the two most important are the drain-source voltage V_{DS} and drain-source on-state resistance, $R_{DS(ON)}$. V_{DS} is the maximum voltage the device will support between drain and source terminals in the off-state. $R_{DS(ON)}$ is the maximum on-state resistance at the quoted gate voltage, V_{GS} , and a junction temperature of 25 °C. (NB $R_{DS(ON)}$ is temperature dependent, see static characteristics). It is these two parameters which provide a first order indication of the devices capability.

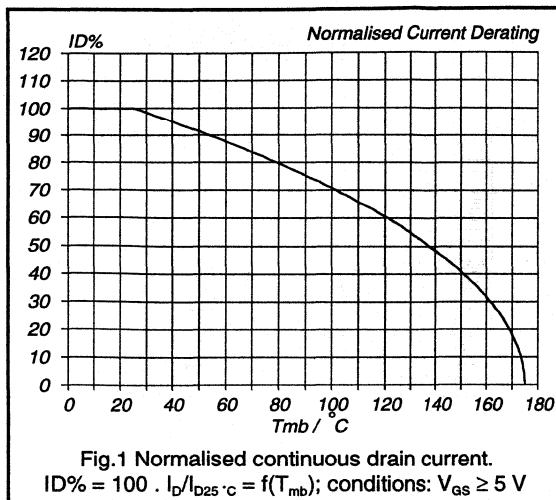
A drain current value (I_D) and a figure for total power dissipation are also given in this section. These figures should be treated with caution since they are quoted for conditions that are rarely attainable in real applications. (See limiting values.) For most applications the usable dc current will be less than the quoted figure in the quick reference data. Typical power dissipations that can be tolerated by the majority of designers are less than 20 W (for discrete devices), depending on the heatsinking arrangement used. The junction temperature (T_J) is usually given as either 150 °C or 175 °C. It is not recommended that the internal device temperature be allowed to exceed this figure.

Limiting values

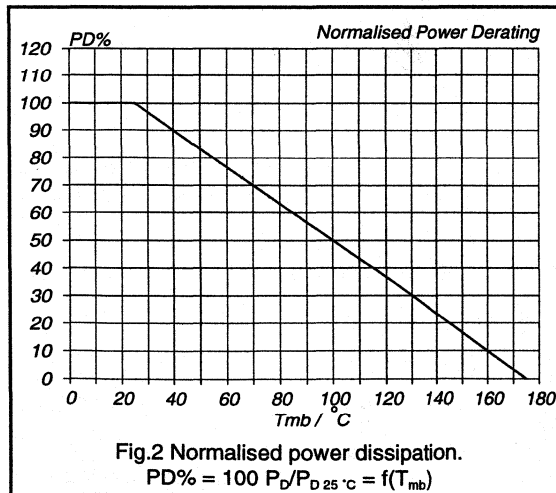
This table lists the absolute maximum values of six parameters. The device may be operated right up to these maximum levels however they must not be exceeded, to do so may incur damage to the device.

Drain-source voltage and drain-gate voltage have the same value. The figure given is the maximum voltage that may be applied between the respective terminals. Gate-source voltage, $\pm V_{GS}$, gives the maximum value that may be allowed between the gate and source terminals. To exceed this voltage, even for the shortest period can cause permanent damage to the gate oxide. Two values for the dc drain current, I_D , are quoted, one at a mounting base temperature of 25 °C and one at a mounting base temperature of 100 °C. Again these currents do not represent attainable operating levels. These currents are the values that will cause the junction temperature to reach its maximum value when the mounting base is held at the quoted value. The maximum current rating is therefore a function of the mounting base temperature and the quoted figures are just two points on the derating curve, see Fig. 1.

The third current level quoted is the pulse peak value, I_{DM} . PowerMOS devices generally speaking have a very high peak current handling capability. It is the internal bond wires which connect to the chip that provide the final limitation. The pulse width for which I_{DM} can be applied depends upon the thermal considerations (see section on calculating currents.) The total power dissipation, P_{tot} , and maximum junction temperature are also stated as for the quick reference data. The P_{tot} figure is calculated from the simple quotient given in equation 1 (see section on safe operating area). It is quoted for the condition where the mounting base temperature is maintained at 25 °C. As an example, for the BUK553-100A the P_{tot} figure is 75 W, dissipating this amount of power while maintaining the mounting base at 25 °C would be a challenge! For higher mounting base temperatures the total power that can be dissipated is less.



Obviously if the mounting base temperature was made equal to the max permitted junction temperature, then no power could be dissipated internally. A derating curve is given as part of the graphical data, an example is shown in Fig.2 for a device with a limiting T_J of 175 °C.



Storage temperature limits are also quoted, usually between -40 /-55 °C and +150 /+175 °C. Both the storage temperature limits and the junction temperature limit are figures at which extensive reliability work is performed by our Quality department. To exceed these figures will cause a reduction in long-term reliability.

Thermal resistance.

For non-isolated packages two thermal resistance values are given. The value from junction to mounting base (R_{thj-mb}) indicates how much the junction temperature will be raised above the temperature of the mounting base when dissipating a given power. Eg a BUK553-100A has a R_{thj-mb} of 2 K/W, dissipating 10 W, the junction temperature will be 20 °C above the temperature of its mounting base. The other figure quoted is from junction to ambient. This is a much larger figure and indicates how the junction temperature will rise if the device is NOT mounted on a heatsink but operated in free air. Eg for a BUK553-100A, $R_{thj-a} = 60 K/W$, dissipating 1 W while mounted in free air will produce a junction temperature 60 °C above the ambient air temperature.

For isolated packages, (F-packs) the mounting base (the metal plate upon which the silicon chip is mounted) is fully encapsulated in plastic. Therefore it is not possible to give a thermal resistance figure junction to mounting base. Instead a figure is quoted from junction to heatsink, R_{thj-hs} , which assumes the use of heatsink compound. Care should be taken when comparing thermal resistances of isolated and non-isolated types. Consider the following example:

The non-isolated BUK553-100A has a R_{thj-mb} of 2 K/W. The isolated BUK543-100A has a R_{thj-hs} of 5 K/W. These devices have identical crystals but mounted in different packages. At first glance the non-isolated type might be expected to offer much higher power (and hence current) handling capability. However for the BUK553-100A the thermal resistance junction to heatsink has to be calculated, this involves adding the extra thermal resistance between mounting base and heatsink. For most applications some isolation is used, such as a mica washer. The thermal resistance mounting base to heatsink is then of the order 2 K/W. The total thermal resistance junction to heatsink is therefore

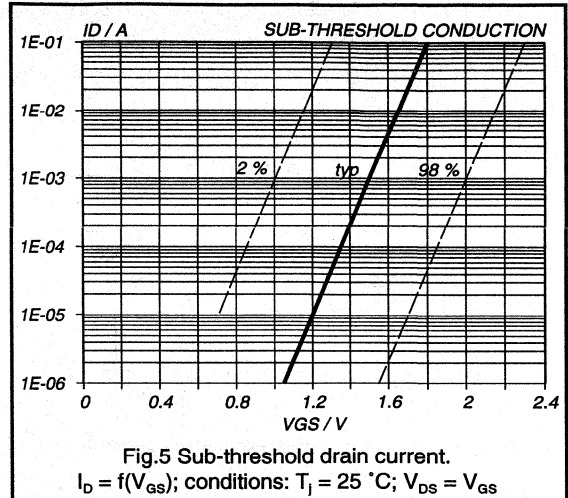
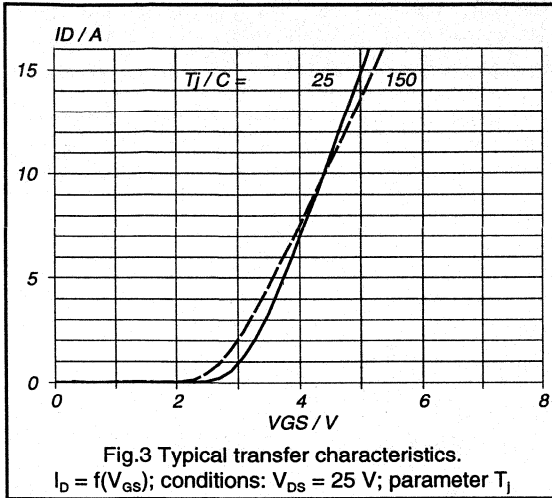
$$R_{thj-hs} (\text{non isolated type}) = R_{thj-mb} + R_{thmb-hs} = 4 K/W$$

It can be seen that the real performance difference between the isolated and non isolated types will not be significant.

Static Characteristics

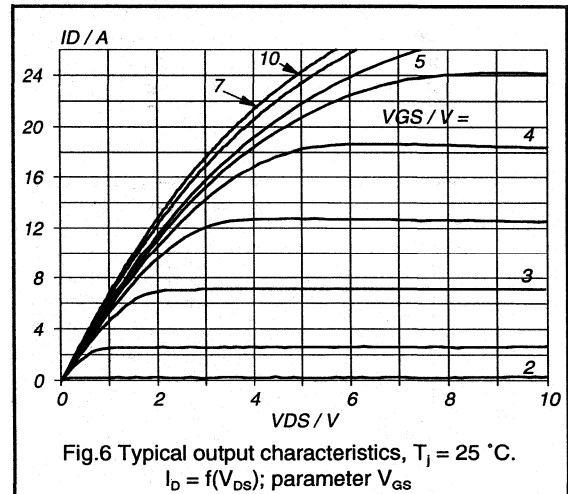
The parameters in this section characterise breakdown voltage, threshold voltage, leakage currents and on-resistance.

A drain-source breakdown voltage is specified as greater than the limiting value of drain-source voltage. It can be measured on a curve tracer, with gate terminal shorted to the source terminal, it is the voltage at which a drain current of 250 μA is observed. Gate threshold voltage, $V_{GS(TH)}$, indicates the voltage required on the gate (with respect to the source) to bring the device into its conducting state. For logic level devices this is usually between 1.0 and 2.0 V and for standard devices between 2.1 and 4 V.

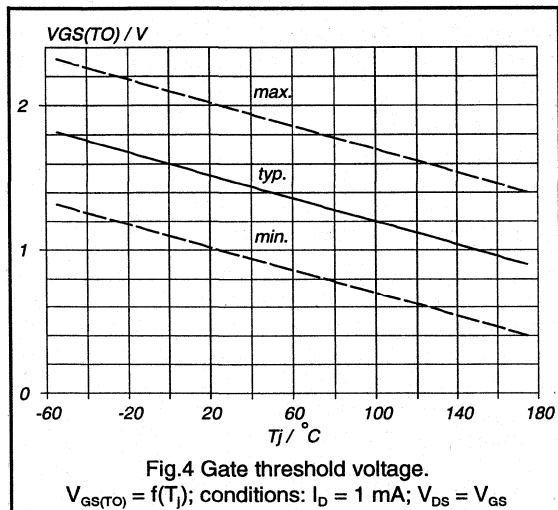


Useful plots in the graphical data are the typical transfer characteristics (Fig.3) showing drain current as a function of V_{GS} and the gate threshold voltage variation with junction temperature (Fig.4). An additional plot also provided is the sub-threshold conduction, showing how the drain current varies with gate-source voltage below the threshold level (Fig.5).

Off-state leakage currents are specified for both the drain-source and gate-source under their respective maximum voltage conditions. Note, although gate-source leakage current is specified in nano-amps, values are typically of the order of a few pico-amps.



The drain-source on-resistance is very important. It is specified at a gate-source voltage of 5 V for logic level FETs and 10 V for a standard device. The on-resistance for a standard MOSFET cannot be reduced significantly by increasing the gate source voltage above 10 V. Reducing the gate voltage will however increase the on-resistance. For the logic level FET, the on-resistance is given for a gate voltage of 5 V, a further reduction is possible however at gate voltages up to 10 V, this is demonstrated by the output characteristics, Fig.6 and on-resistance characteristics, Fig.7 for a BUK553-100A.



The on-resistance is a temperature sensitive parameter, between 25 °C and 150 °C it approximately doubles in value. A plot of normalised $R_{DS(ON)}$ versus temperature (Fig.8) is included in each data sheet. Since the MOSFET will normally operate at a T_j higher than 25 °C, when making estimates of power dissipation in the MOSFET, it is important to take into account the higher $R_{DS(ON)}$.

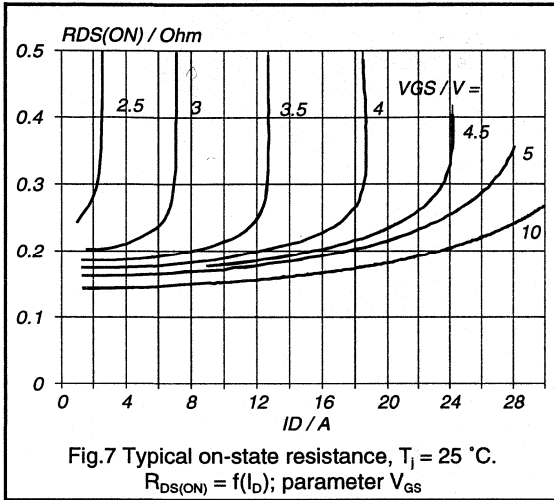


Fig.7 Typical on-state resistance, $T_j = 25\text{ °C}$.
 $R_{DS(ON)} = f(I_D)$; parameter V_{GS}

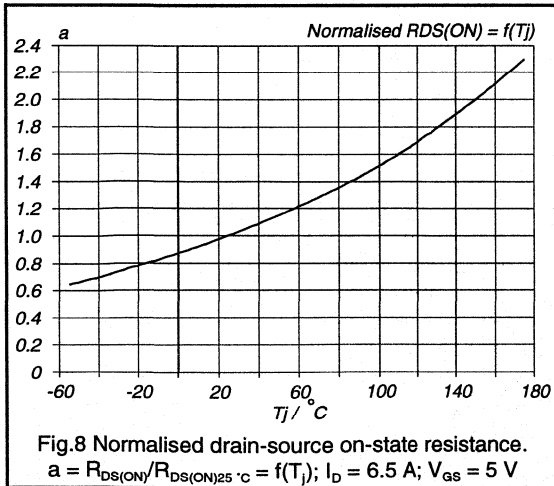


Fig.8 Normalised drain-source on-state resistance.
 $a = R_{DS(ON)} / R_{DS(ON)25\text{ °C}} = f(T_j)$; $I_D = 6.5\text{ A}$; $V_{GS} = 5\text{ V}$

Dynamic Characteristics

These include transconductance, capacitance and switching times. Forward transconductance, g_{fs} , is essentially the gain parameter which indicates the change in drain current that will result from a fluctuation in gate voltage when the device is saturated. (NB saturation of a

MOSFET refers to the flat portion of the output characteristics.) Fig.9 shows how g_{fs} varies as a function of the drain current for a BUK553-100A.

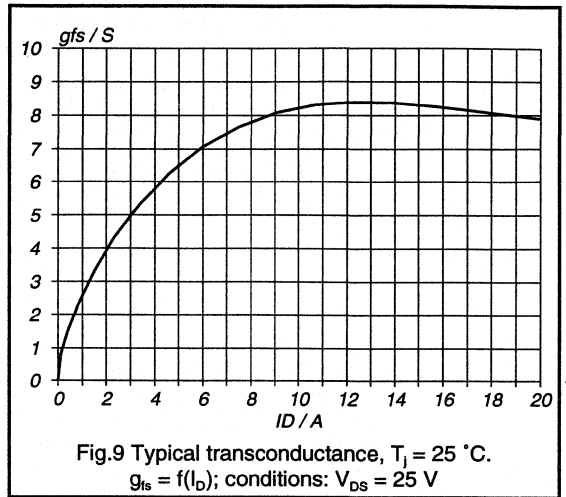


Fig.9 Typical transconductance, $T_j = 25\text{ °C}$.
 $g_{fs} = f(I_D)$; conditions: $V_{DS} = 25\text{ V}$

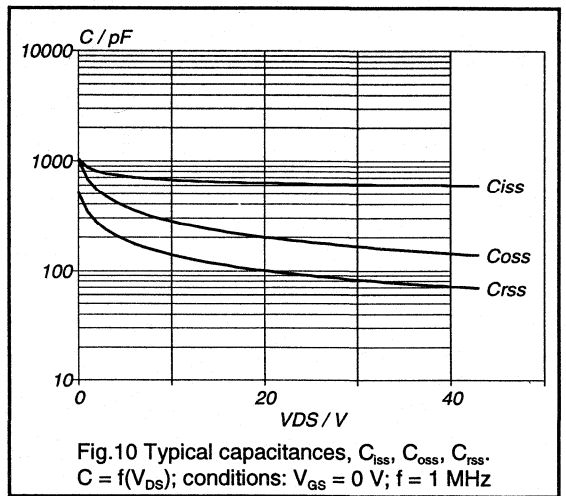
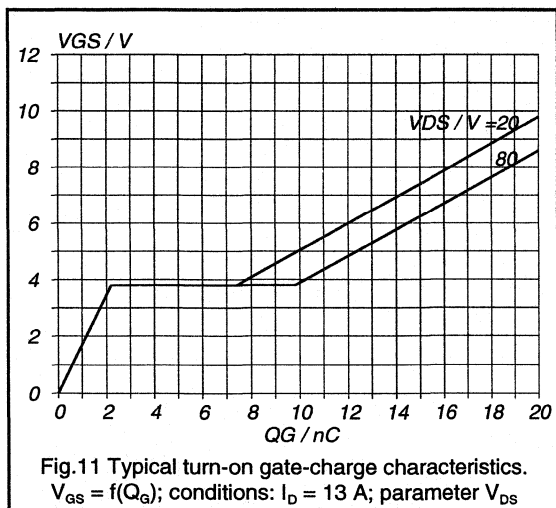


Fig.10 Typical capacitances, C_{iss} , C_{oss} , C_{rss} .
 $C = f(V_{DS})$; conditions: $V_{GS} = 0\text{ V}$; $f = 1\text{ MHz}$

Capacitances are specified by most manufacturers, usually in terms of input, output and feedback capacitance. The values quoted are for a drain-source voltage of 25 V. However this is only part of the story as the MOSFET capacitances are strongly voltage dependent, increasing as drain-source voltage is reduced. Fig.10 shows how these capacitances vary with voltage. The usefulness of the capacitance figures is limited. The input capacitance value gives only a rough indication of the charging required by the drive circuit. Perhaps more useful is the gate charge information an example of which is shown in Fig.11. This plot shows how much charge has to be input to the gate to

reach a particular gate-source voltage. Eg. to charge a BUK553-100A to $V_{GS} = 5$ V, starting from a drain-source voltage of 80 V, requires 12.4 nc. The speed at which this charge is to be applied will give the gate circuit current requirements. More information on MOSFET capacitance is given in chapter 1.2.2.

Resistive load switching times are also quoted by most manufacturers, however extreme care should be taken when making comparisons between different manufacturers data. The speed at which a power MOSFET can be switched is essentially limited only by circuit and package inductances. The actual speed in a circuit is determined by how fast the internal capacitances of the MOSFET are charged and discharged by the drive circuit. The switching times are therefore extremely dependent on the circuit conditions employed; a low gate drive resistance will provide for faster switching and vice-versa. The Philips data sheet presents the switching times for all PowerMOS with a resistor between gate and source of 50 Ω . The device is switched from a pulse generator with a source impedance also of 50 Ω . The overall impedance of the gate drive circuit is therefore 25 Ω .

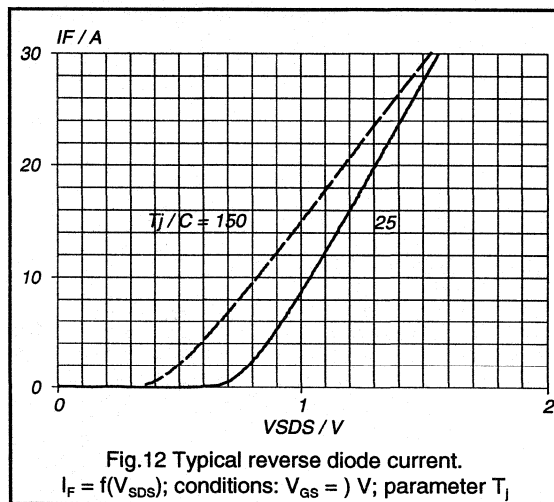


Also presented under dynamic characteristics are the typical inductances of the package. These inductances become important when very high switching speeds are employed such that large di/dt values exist in the circuit. Eg. turning-on 30 A within 60 ns gives a di/dt of 0.5 A/ns. The typical inductance of the source lead is 7.5 nH, from $V = -L \cdot di/dt$ the potential drop from the source bond pad (point where the source bond wire connects to the chip internally) to the bottom of the source lead would be 3.75 V. Normally a standard device will be driven with a gate-source voltage of 10 V applied across the gate and source terminals, the actual voltage gate to source on the

semiconductor however would only be 6.25 V during the turn-on period! The switching speed is therefore ultimately limited by package inductance.

Reverse diode limiting values and characteristics

The reverse diode is inherent in the vertical structure of the power MOSFET. In some circuits this diode is required to perform a useful function. For this reason the characteristics of the diode are specified. The forward currents permissible in the diode are specified as 'continuous reverse drain current' and 'pulsed reverse drain current'. The forward voltage drop of the diode is also provided together with a plot of the diode characteristic, Fig.12. The switching capability of the diode is given in terms of the reverse recovery parameters, t_{rr} and Q_{rr} .

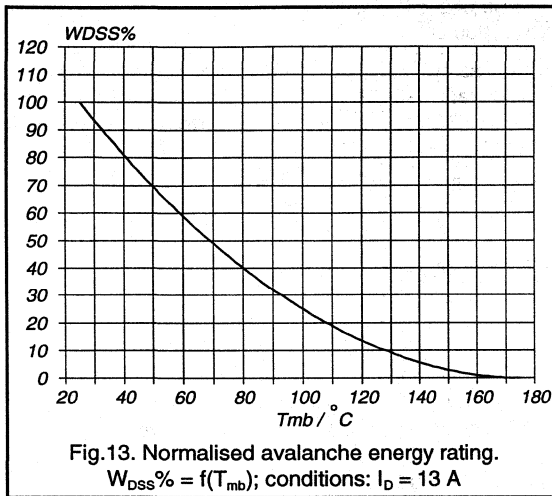


Because the diode operates as a bipolar device it is subject to charge storage effects. This charge must be removed for the diode to turn-off. The amount of charge stored is given by Q_{rr} , the reverse recovery charge, the time taken to extract the charge is given by t_{rr} , the reverse recovery time. NB. t_{rr} depends very much on the $-di/dt$ in the circuit, t_{rr} is specified in data at 100 A/ μ s.

Avalanche limiting value

This parameter is an indication as to the ruggedness of the product in terms of its ability to handle a transient overvoltage, ie the voltage exceeds the drain-source voltage limiting value and causes the device to operate in an avalanche condition. The ruggedness is specified in terms of a drain-source non-repetitive unclamped inductive turn-off energy at a mounting base temperature of 25 $^{\circ}$ C. This energy level must be derated at higher mounting base temperatures as shown in Fig.13. NB. this rating is

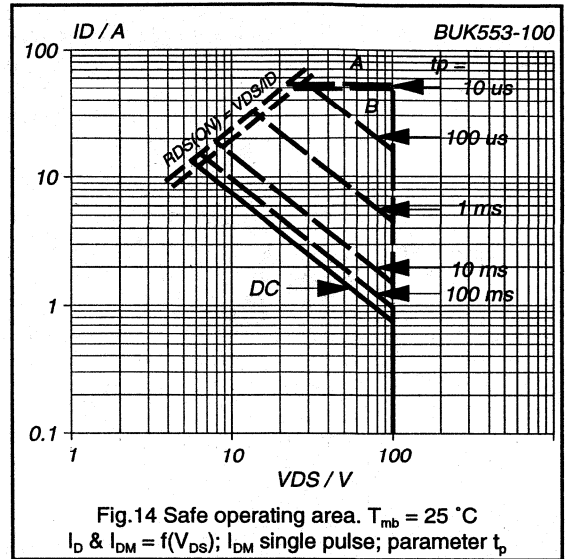
non-repetitive which means the circuit should not be designed to force the PowerMOS repeatedly into avalanche. This rating is only to permit the device to survive if exceptional circuit conditions arise such that a transient overvoltage occurs. (A more detailed explanation of Ruggedness is given in chapter 1.2.7.)



Safe Operating Area

A plot of the safe operating area is presented for every PowerMOS type. Unlike bipolar transistors a PowerMOS exhibits no second breakdown mechanism. The safe operating area is therefore simply defined from the power dissipation that will cause the junction temperature to reach the maximum permitted value.

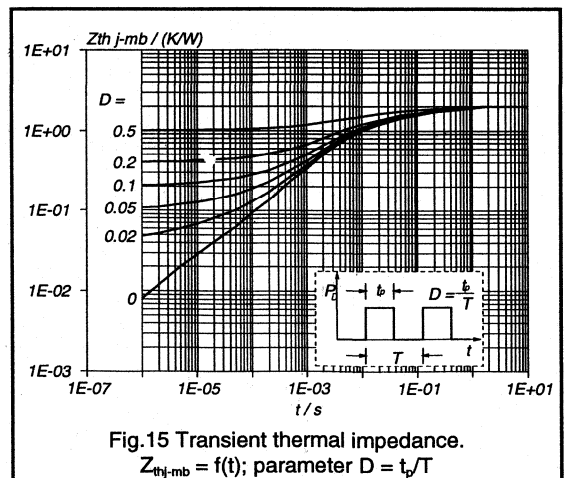
Fig.14 shows the SOA for a BUK553-100. The area is bounded by the limiting drain source voltage, limiting current values and a set of constant power curves for various pulse durations. The plots in data are all for a mounting base temperature of 25 °C. The constant power curves therefore represent the power that raises the junction temperature by an amount $T_{jmax} - T_{mb}$, ie. 150 °C for a device with a limiting T_j of 175 °C and 125 °C for a device with a limiting T_j of 150 °C. Clearly in most applications the mounting base temperature will be higher than 25 °C, the SOA would therefore need to be reduced. The maximum power curves are calculated very simply. The dc curve is based upon the thermal resistance junction to mounting base (junction to heatsink in the case of isolated packages), which is substituted into equation 1. The curves for pulsed operation assume a single shot pulse and instead of thermal resistance, a value for transient thermal impedance is used. Transient thermal impedance is supplied as graphical data for each type, an example is shown in Fig.15. For calculation of the single shot power dissipation capability, a value at the required pulse width is



read from the $D = 0$ curve and substituted in to equation 2. (A more detailed explanation of transient thermal impedance and how to use the curves can be found in chapter 7.)

$$P_{tot(dc)} = \frac{T_{jmax} - T_{mb}}{R_{thj-mb}} \quad 1$$

$$P_{tot(pulse)} = \frac{T_{jmax} - T_{mb}}{Z_{thj-mb}} \quad 2$$



Examples of how to calculate the maximum power dissipation for a 1 ms pulse are shown below. Example 1 calculates the maximum power assuming a T_j of 175 °C and T_{mb} of 25 °C. This power equates to the 1 ms curve on the SOA plot of Fig.14. Example 2 illustrates how the power capability is reduced if T_{mb} is greater than 25 °C.

Example 1: 1 ms pulse at 25 °C for a BUK553-100A

$Z_{th} = 0.32 \text{ K/W}$, $T_{jmax} = 175 \text{ °C}$, $T_{mb} = 25 \text{ °C}$

$$P_{\max(1 \text{ ms pulse})} = \frac{175 - 25}{0.32} = 469 \text{ W}$$

The 469 W line is observed on Fig.13, (4.69 A @ 100 V and 15.6 A @ 30 V etc)

Example 2: 1 ms pulse at 75 °C for a BUK553-100A

$Z_{th} = 0.32 \text{ K/W}$, $T_{jmax} = 175 \text{ °C}$, $T_{mb} = 75 \text{ °C}$

$$P_{\max(1 \text{ ms pulse})} = \frac{175 - 75}{0.32} = 312 \text{ W}$$

Therefore with a mounting base temperature of 75 °C the maximum permissible power dissipation is reduced by one third compared with the 25 °C value on the SOA plot.

Calculating Currents

The current ratings quoted in the data sheet are derived directly from the maximum power dissipation.

$$I_D(@T_{mb})^2 \cdot R_{DS(ON)}(@T_{jmax}) = P_{tot} \quad 3$$

substituting for P_{tot} from equation 1

$$I_D(@T_{mb}) = \left\{ \frac{T_{jmax} - T_{mb}}{R_{thj-mb} \cdot R_{DS(ON)}(@T_{jmax})} \right\}^{\frac{1}{2}} \quad 4$$

To calculate a more realistic current it is necessary to replace T_{jmax} in equation 4 with the desired operating junction temperature and T_{mb} with a realistic working value. It is generally recommended that devices are not operated continuously at T_{jmax} . For reasons of long term reliability, 125 °C is a more suitable junction operating temperature. A value of T_{mb} between 75 °C and 110 °C is also a more typical figure.

As an example a BUK553-100A is quoted as having a dc current rating of 13 A. Assuming a T_{mb} of 100 °C and operating T_j of 125 °C the device current is calculated as follows:

From Fig.8

$$R_{DS(ON)}(@125^\circ\text{C}) = 1.75 \cdot R_{DS(ON)}(@25^\circ\text{C}) = 1.75 \cdot 0.18 = 0.315 \Omega$$

$R_{thj-mb} = 2 \text{ K/W}$, using equation 4

$$I_D = \left\{ \frac{25}{2 \cdot 0.315} \right\}^{\frac{1}{2}} = 6.3 \text{ A}$$

The device could therefore conduct 6.3 A under these conditions which equates to a 12.5 W power dissipation.

Conclusions

The most important information presented in the data sheet is the on-resistance and the maximum voltage drain-source. Current values and maximum power dissipation values should be viewed carefully since they are only achievable if the mounting base temperature is held to 25 °C. Switching times are applicable only for the specific conditions described in the data sheet, when making comparisons between devices from different manufacturers, particular attention should be paid to these conditions.

High Voltage Bipolar Transistor



1.3.1 Introduction To High Voltage Bipolar Transistors

This section introduces the high voltage bipolar transistor and discusses its construction and technology. Specific transistor properties will be analysed in more detail in subsequent sections and in Chapter 2, section 2.1.2.

Basic Characteristics

High voltage transistors are almost exclusively used as electronic switches. Therefore, the characteristics of these devices are given for the on state, the off state and the transition between the two i.e. turn-on and turn-off.

The relative importance of the V_{CES} and V_{CEO} ratings usually depends on the application. In a half bridge converter, for instance, the rated V_{CEO} is the dominant factor, whilst in a forward converter V_{CES} is important. Which rating is most applicable may also depend on whether a slow rise network or snubber is applied (see section 1.3.3).

The saturation properties in the on state and the switching times are given at a specific collector current called the collector saturation current, I_{CSat} . It is this current which is normally considered to be the practical working current of the device. If this device is used at higher currents the total dissipation may be too high, while at low currents the storage time is long. At I_{CSat} the best compromise is present for the total spread of products. The value of the base current used to specify the saturation and switching properties of the device is called I_{BSat} which is also an important design parameter. As the device requirements can differ per application a universal I_{BSat} cannot be quoted.

Device Construction

A drawing of a high voltage transistor, in this case a fully isolated SOT186 F-pack, is shown in Fig. 1 with the plastic encapsulation stripped away. This figure shows the three leads, two of which are connected with wires to the transistor chip. The third lead makes contact with the mounting base on which the crystal is soldered, enabling good thermal contact with a heatsink. It is the transistor package which basically determines the thermal properties of the device. The electrical properties are mainly determined by the design of the chip inside.

A cross-section of a transistor chip is given in Fig. 2. Here the transistor structure can be recognised with the emitter and the base contacts at the top surface and the collector connected to the mounting base. The thickest part in the drawing is the collector n- region across which the high voltage will be supported in the off state. This layer is of

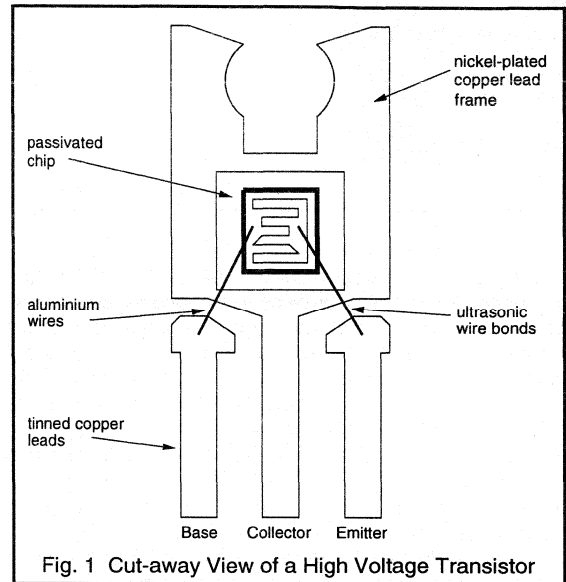


Fig. 1 Cut-away View of a High Voltage Transistor

prime importance in the determination of the characteristics of the device. Below the n- region is an extra n+ layer, needed for a good electrical contact to the heatsink.

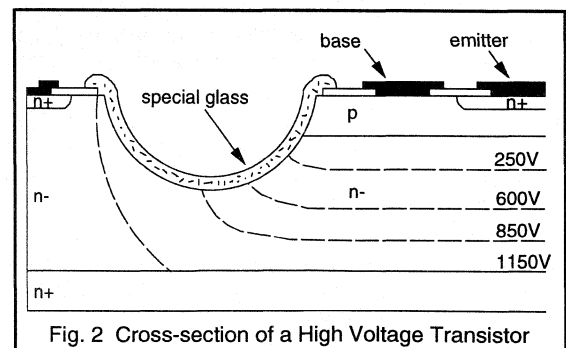


Fig. 2 Cross-section of a High Voltage Transistor

Above the collector is the base p layer, and the emitter n+ layer with their respective metallic contacts on top. It is important to realise that the characteristics of the device are determined by the active area, this is the area underneath the emitter where the collector current flows and the high voltage can be developed. The active area of two devices with the same chip size may not be the same.

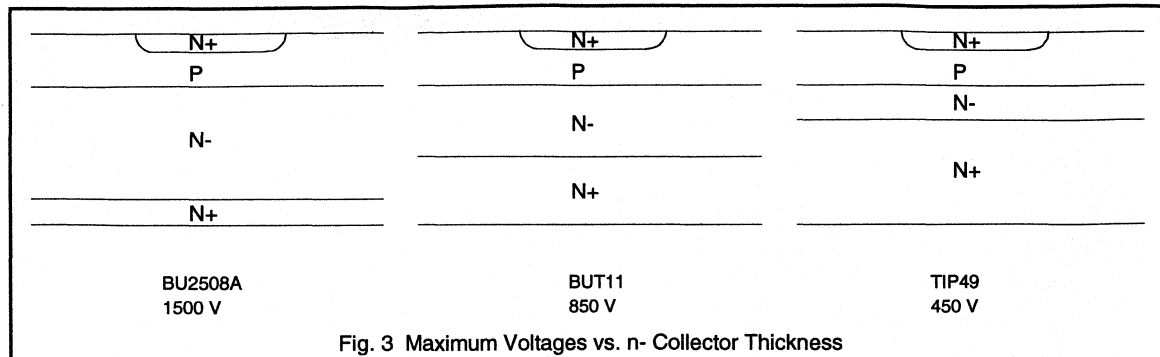


Fig. 3 Maximum Voltages vs. n- Collector Thickness

In addition to the basic collector-base-emitter structure manufacturers have to add electrical contacts, and special measures are needed at the edges of the crystal to sustain the design voltage. This introduces another very important feature, the high voltage passivation. The function of the passivation, (the example shown here is referred to as glass passivation), is to ensure that the breakdown voltage of the device is determined by the collector-base structure and not by the construction at the edges. If no special passivation was used the breakdown voltage might be as low as 50% of the maximum value. Manufacturers optimise the high voltage passivation and much work has also been done to ensure that its properties do not change in time.

Process Technology

There are several ways to make the above structure. The starting material can be an n- wafer where first an n+ diffusion is made in the back, followed by the base (p) and emitter (n+) diffusions. This is the well known triple diffused process.

Another way is to start with an n+ wafer onto which an n- layer is deposited using epitaxial growth techniques. A further two diffusions (base and emitter) forms the basic transistor structure. This is called a double diffused epitaxial process.

Another little used technology is to grow, epitaxially, the base p-type layer onto an n-/n+ wafer and then diffuse an n+ emitter. This is referred to as a single diffused epi-base transistor.

The question often asked is which is the best technology for high voltage bipolar transistors? The basic difference in the technologies is the concentration profile at the n-/n+ junction. For epitaxial wafers the concentration gradient is much more steeper from n- to n+ than it is for back diffused wafers. There are more applications where a smoother concentration gradient gives the better performance. Manufacturers utilising epitaxial techniques tend to use buffer layers between the n- and n+ to give smoother

concentration gradients. Another disadvantage of epitaxial processing is cost: back diffused wafers are much cheaper than equivalent high voltage epitaxial wafers.

The process technology used to create the edge passivation is also diverse. The expression "planar" is used to indicate the passivation technique which is most commonly used in semiconductors. This involves the diffusion of additional n-type rings around the active area of the device which give an even electric field distribution at the edge. However, for high voltage bipolar transistors planar passivation is relatively new and the long term reliability has yet to be completely optimised. For high voltage bipolar transistors the most common passivation systems employ a deep trough etched, or cut, into the device with a special glass coating. Like the planar passivation, the glass passivation ensures an even distribution of the electric field around the active area.

Maximum Voltage and Characteristics

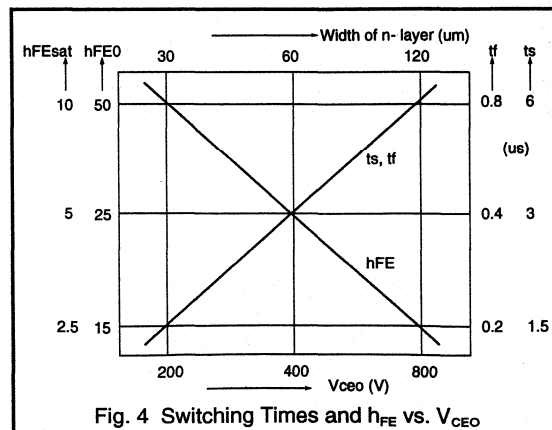


Fig. 4 Switching Times and h_{FE} vs. V_{CE0}

High voltage and low voltage transistors differ primarily in the thickness and resistivity of the n-layer. As the thickness and resistivity of this layer is increased, the breakdown voltage goes up. The difference over the range of Philips high voltage transistors of different voltages is illustrated in Fig. 3. The TIP49 has a $V_{CB0} = 450$ V, the BUT11 has a $V_{CES} = 850$ V, while the BU2508A can be used up to voltages of 1500 V.

The penalty for increasing the n-layer is a decrease in high current h_{FE} and an increase in switching times. The graph in Fig. 4 points this out by giving both switching times and h_{FE} as a function of the breakdown voltage. The values given should be used as a guide to illustrate the effect. The effect can be compensated for by having a bigger chip.

Applications of High Voltage Transistors

High voltage transistors are mainly used as the power switch in energy conversion systems. What is common to

all these systems, is that a current flows through an inductor, thus storing energy in its core. When the current is interrupted by turning off the power switch, the energy must be transferred one way or another. Very often the energy is converted into an electrical output e.g. in switched mode power supplies and battery chargers.

Two special applications are electronic fluorescent lamp ballasts and horizontal deflection of the electron beam in TV's and monitors. In the ballast, an ac voltage is generated to deliver energy to a fluorescent lamp. In the TV and monitor a sawtooth current in the deflection coil sweeps the beam across the screen from left to right and back again in a much shorter blanking, or flyback, period

Other ways to transfer the energy are ac and dc motor control where the output is delivered as movement, or induction heating where the output is delivered in the form of heat.

1.3.2 Effects of Base Drive on Switching Times

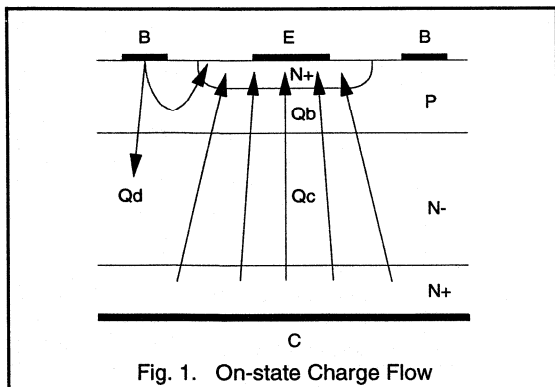
Introduction

The switching processes that take place within a high voltage transistor are quite different from those in a small signal transistor. This section describes, figuratively, what happens within high voltage transistors under various base drive conditions. After an analysis of the charges that are present in a high voltage transistor, the switch-off process is described. Then comparisons are made of switching for various forward and reverse base drive conditions. A fundamental knowledge of basic semiconductor physics is assumed.

Charge distribution within a transistor

An off-state transistor has no excess charge, but to enable transistor conduction in the on-state excess charge build up within the device takes place. There are three distinct charge distributions to consider that control the current through the device, see Fig. 1. These charge distributions are influenced by the level of collector-emitter bias, V_{CE} , and collector current, I_C , as shown in Fig. 2.

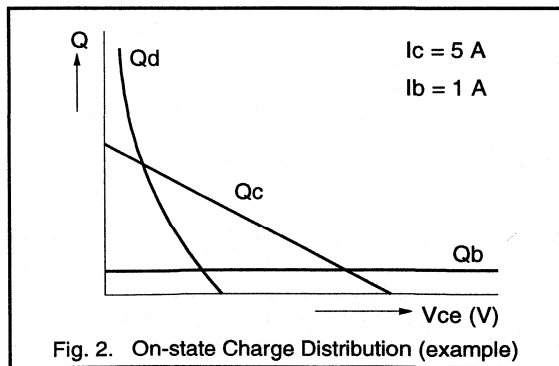
Forward biasing the base-emitter (BE) junction causes a depletion layer to form across the junction. As the bias exceeds the potential energy barrier (work function) for that junction, current will flow. Electrons will flow out of the emitter into the base and out of the base contact. For high voltage transistors the level of BE bias is much in excess of the forward bias for a small signal transistor. The bias generates free electron-hole pairs in the base-emitter leading to a concentration of electrons in the base in excess of the residual hole concentration. This produces an excess charge in the base, Q_b , concentrated underneath the emitter.



Not only is there an excess charge in the base near the emitter junction but the injection and base width ensure that this excess charge is also present at the collector junction. Applying a load in series with the collector and a dc supply between load and emitter will trigger some sort of collector current, I_C . The level of I_C is dependent on the base current, I_B , the load and supply voltage. For a certain I_B , low voltage supply and high impedance load there will be a small I_C . As the supply voltage rises and/or the load impedance falls so I_C will rise. As I_C rises so the collector-emitter voltage, V_{CE} , falls. The I_C is composed mainly of the excess emitter electrons that reach the base-collector junction (BC). This electron concentration will continue into the collector inducing an excess charge in the collector, Q_c .

The concentration of electrons decreases only slightly from the emitter-base junction to some way into the collector. In effect, the base width extends into the collector. Decreasing V_{CE} below V_{BE} causes the BC junction to become forward biased throughout. This creates a path for electrons from the collector to be driven back into the base and out of the base contact. This electron flow is in direct opposition to the established I_C . With no change in base drive, the ultimate effect is a reduction in I_C . This is the classical 'saturation' region of transistor operation. As V_{CE} falls so the BC forward bias increases leading to an excess of electrons at the depletion layer edge in the collector beneath the base contact. This concentration of electrons leads to an excess charge, Q_d .

The charge flows and excess charges Q_b , Q_c and Q_d are shown in Fig. 1. An example of the excess charge distributions for fixed I_C and I_B are shown in Fig. 2.



The switching process of a transistor

Removing the bias voltage, V_{BE} , will cause the electron-hole pairs to recombine and the excess charge regions to disappear. Allowing this to happen just by removing V_{BE}

takes a long time so usually turn-off is assisted in some way. It is common practice to apply a negative bias (typically 5V) to the base, via a resistor and/or inductor, inducing a negative current that draws the charge out of the transistor. In the sequence that follows, four phases of turn-off can be distinguished (see Fig. 3).

1. First the applied negative bias tries to force a negative bias across the BC junction. The BC electron flow now stops and the charge Q_d dissipates as the bias now causes the base holes out through the base contact and the collector electrons back into the bulk collector. When the BC was forward biased this current had the effect of reducing the total collector current, so now the negative V_{BE} can cause the total collector current to increase (this also depends on the load). Although the base has been switched off the load current is maintained by the stored charge effects; this is called the transistor storage time, t_s .

During this stage the applied negative bias appears as a positive V_{BE} at the device terminals as the internal charge distributions create an effective battery voltage. Depleting the charge, of course, lowers this effective battery voltage.

2. The next phase produces a reduction in both Q_b , Q_c and, consequently, I_C . The BC junction is no longer forward biased and Q_d has dissipated to provide the negative base current. The inductance in series in the base path requires a continuation in the base current. The injection of electrons into the base opposes the established electron flow from emitter to collector via the base. At first the opposing electron flows cancel at the edge of the emitter nearest the base contacts. This reduces both Q_b and Q_c in this region. Q_b and Q_c become concentrated in the centre of the emitter area. The decrease in I_C is called the fall time, t_f .

3. Now there is an extra resistance to the negative base current as the electrons flow through the base under the emitter area. This increase in resistance limits the increase in amplitude of the negative base current. As Q_b and Q_c reduce further so the resistance increases and the negative base current reaches its maximum value.

As Q_b and Q_c tend to zero the series inductance ensures that negative base current must be continued by other means. The actual mechanism is by avalanche breakdown of the base-emitter junction. This now induces a negative V_{BE} which is larger than the bias resulting in a reverse in polarity of the voltage across the inductance. This in turn triggers a positive rate of change in base current. The negative base current now quickly rises to zero while the base-emitter junction is in avalanche breakdown. Avalanche breakdown ceases when the base current tends to zero and the V_{BE} becomes equal to the bias voltage.

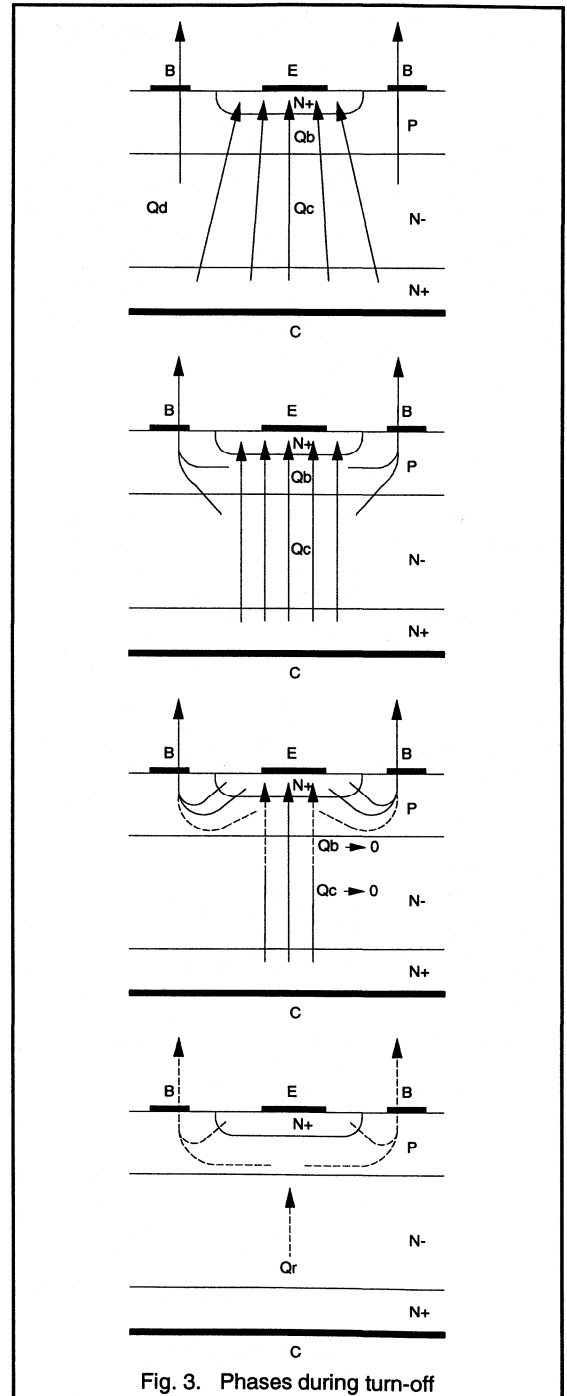


Fig. 3. Phases during turn-off

4. If a very small series base inductor is used with the 5V reverse bias then the base current will have a very fast rate of change. This will speed up the phases 1 to 3 and, therefore, the switching times of the transistor. However, there is a point when reducing the inductor further introduces another phase to the turn-off process. High reverse base currents will draw the charges out closest to the base contact and leave a residual charge trapped deep in the collector regions furthest away from the base. This charge, Q_r , must be removed before the transistor returns fully to the off-state. This is detected as a tail to I_c at the end of turn-off with a corresponding tail to the base current as it tends to zero.

The switching waveforms for a BUT11 in a forward converter are given in Fig. 4 where the four phases can easily be recognised. (Because of the small base coil used both phases in the fall time appear clearly!).

- | | |
|---|----|
| 1 - Removal of Q_d until $t \approx 0.7 \mu s$ | ts |
| 2 - Q_c and Q_b decrease until $t \approx 1.7 \mu s$ | ts |
| 3 - Removal of Q_b and Q_c until $t \approx 1.75 \mu s$ | tf |
| 4 - Removal of Q_r until $t \approx 1.85 \mu s$ | tf |

Note the course of V_{BE} : first the decrease in voltage due to the base resistance during current contraction and second (because a base coil has been used) the value of V_{BE} is clamped by the emitter-base breakdown voltage of the transistor. It should be remembered that because breakdown takes place near the surface and not in the active region no harm comes to the transistor.

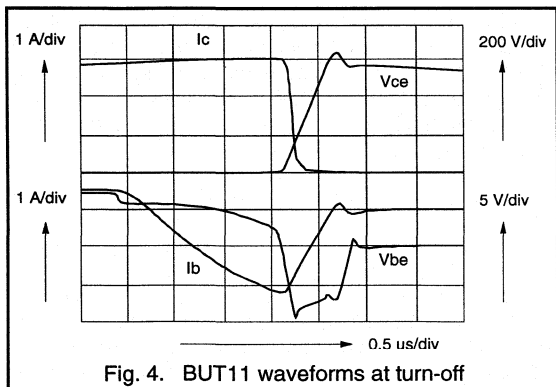


Fig. 4. BUT11 waveforms at turn-off

The influence of forward drive on stored charge

Fig. 5 shows how, for a transistor in the on-state, at a fixed value of I_c and I_b the three charges Q_b , Q_c and Q_d depend upon V_{CE} . The base charge, Q_b , is independent of V_{CE} , it primarily depends upon V_{BE} . For normal base drive

conditions, a satisfactory value for V_{CEsat} is obtained, indicated by N in Fig. 5, and moderate values for Q_c and Q_d result.

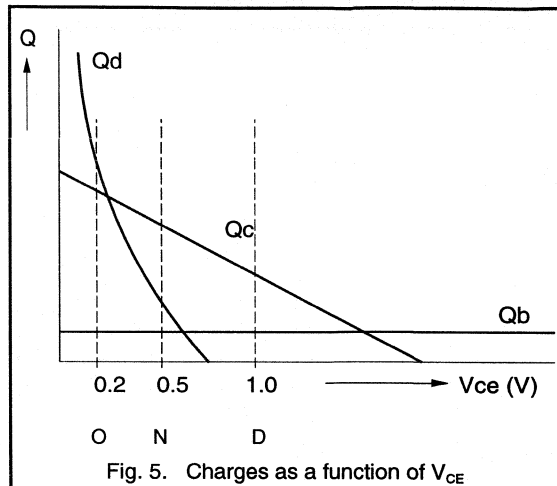


Fig. 5. Charges as a function of V_{CE}

With the transistor operating in the active region, for $V_{CE} \geq 1V$, there will be a charge Q_c but no charge Q_d . This is indicated by D in Fig. 5. At the other extreme, with the transistor operating in the saturation region Q_c will be higher and Q_d will be higher than Q_c . This is indicated by O in Fig. 5. In this condition there are more excess electron-hole pairs to recombine at switch off.

Increasing I_b causes Q_b to increase. Also, for a given I_c , Q_c and Q_d will be higher as V_{CE} reduces. Therefore, for a given I_c , the stored charge in the transistor can be controlled by the level of I_b . If the I_b is too low the V_{CE} will be high with low Q_c and zero Q_d , as D in Fig. 5. This condition is called **underdrive**. If the I_b is too high the V_{CE} will be low with high Q_c and Q_d , as O in Fig. 5. This condition is called **overdrive**. The overdrive condition (high forward drive) gives high stored charge and the underdrive condition (low forward drive) gives low stored charge.

Deep-hole storage

As the high free electron concentration extends into the base and collector regions there must be an equivalent hole concentration. Fig. 6 shows results obtained from a computer model which illustrates charge storage as a function of V_{CE} . Here the hole density, $p(x)$, is given as a function of depth inside the active area; the doping profile is also indicated. It can be seen that overdrive, O, causes holes to be stored deep in the collector at the collector-substrate junction known as "deep-hole storage", this is the main reason for the increase in residual charge, Q_r .

During overdrive not only Q_d becomes very big but also holes are stored far away from the junction: this thus leads not only to a longer storage time, but also to a large Q_c resulting in tails in the turn-off current.

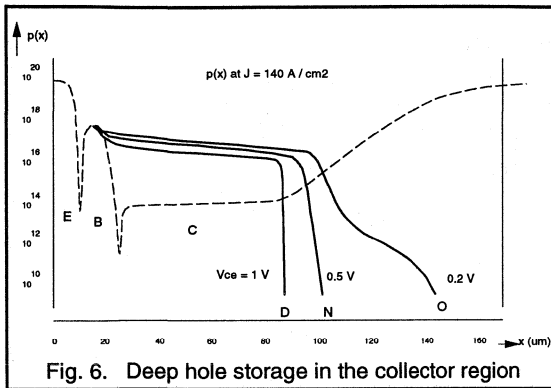


Fig. 6. Deep hole storage in the collector region

Desaturation networks

A desaturation network, as shown in Fig. 7, limits the stored charge in the transistor and, hence, aids switching. The series base diode, D1 means that the applied drive voltage now has to be V_{BE} plus the V_F of D1. The anti-parallel diode, D2 is necessary for the negative I_B at turn-off. As V_{CE} reduces below $V_{BE} + V_F$ so the external BC diode, D3, becomes forward biased. D3 now conducts any further increase in drive current away from the base and into the collector. Transistor saturation is avoided.

With a desaturation network the charge Q_d equals zero and the charge Q_c is minimised. When examining the distribution of the charge in the collector region (see Fig. 6) it can be seen that deep hole storage does not appear. Desaturation networks are a common technique for reducing switching times.

It should be realised that there is a drawback attached to operating out of saturation: increased dissipation during the on-state. Base drive design often requires a trade-off between switching and on-state losses.

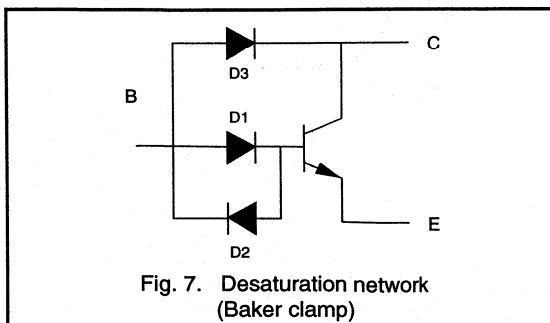


Fig. 7. Desaturation network (Baker clamp)

Breakdown voltage vs. switching times

For a higher breakdown voltage transistor the n-layer (see Fig. 1) will be thicker and of higher resistivity (ie a lower donor atom concentration). This means that when comparing identical devices the values for Q_d and Q_c will be higher, for a given I_C , in the device with the higher breakdown voltage.

In general:

- the higher BV_{CEO} the larger Q_d and Q_c will be;
- during overdrive Q_d is very high and there is a charge located deep in the collector region (deep hole storage);
- when desaturated Q_d equals zero and there is no deep hole storage: Q_c is minimised for the I_C .

Turn-off conditions

Various ways of turning off a high voltage transistor are used but the base should always be switched to a negative supply via an appropriate impedance. If this is not done, (ie turn-off is attempted by simply interrupting the base current), very long storage times result and the collector voltage increases, while the collector current falls only slowly. A very high dissipation and thus a short lifetime of the transistor are the result. The charges must be removed using a negative base current.

a) Hard turn-off

The technique widely used, especially for low voltage transistors, is to switch directly to a negative voltage, (see Fig. 8a). In the absence of a negative supply, this can be achieved with an appropriate R-C network (Fig. 8b). Also applying an "emitter-drive" (Fig. 8c) with a large base capacitor in fact is identical to hard-turn-off.

The main drawback for high voltage transistors is that the base charge Q_b is removed too quickly, leaving a high residual charge. This leads to current tails (long fall times) and high dissipation. It depends upon what state the transistor is in (overdriven or desaturated), whether this way of turn-off is best. It also depends upon the kind of transistor that must be switched off. If it is a lower voltage transistor ($BV_{CEO} \leq 200V$) then this will work very well because the charges Q_c and Q_d will be rather low. For transistors with a higher breakdown voltage, hard turn-off will yield the shortest storage time at the cost, however, of higher turn-off dissipation (longer t_f).

b) Smooth turn-off

To properly turn-off a high voltage transistor a storage time to minimise Q_d and Q_c is required, and then a large negative base current to give a short fall time.

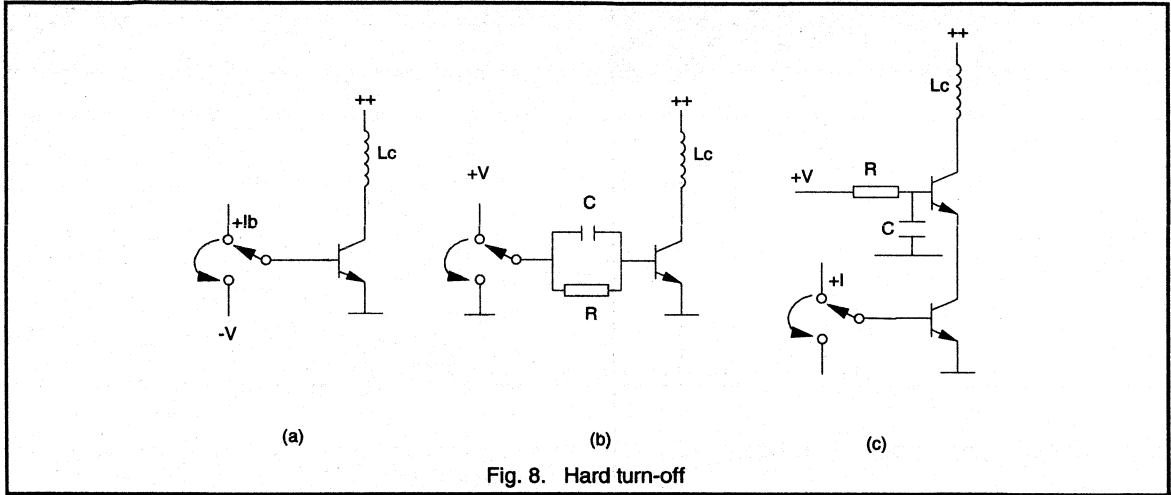


Fig. 8. Hard turn-off

The easiest way to obtain these turn-off requirements is to switch the base to a negative supply via a base coil, see Fig. 9.

The base coil gives a constant di_B/dt (approx.) during the storage time. When the fall time begins the negative base current reaches its maximum and the L_b induces the BE junction into breakdown (see Fig. 4).

An optimum value exists for the base coil: if $L_b = 0$ we have the hard turn-off condition which is not optimum for standard high voltage transistors. If the value of L_b is too high it slows the switching process so that the transistor desaturates. The V_{CE} increases too much during the storage time and so higher losses result (see Fig. 10).

For high voltage transistors in typical applications ($f = 15$ to 40 kHz, standard base drive, not overdriven, not desaturated) the following equations give a good indication for the value of L_b .

$$L_b = \frac{(-V_{dr} + V_{BEsat})}{\left(\frac{di_B}{dt}\right)}$$

with $\frac{di_B}{dt} \approx 0.5 \cdot I_C$ (A/ μ s) for $BV_{CEO} = 400V$, $BV_{CES} = 800V$

and $\frac{di_B}{dt} \approx 0.15 \cdot I_C$ (A/ μ s) for $BV_{CEO} = 700V$, $BV_{CES} = 1500V$

Using $-V_{dr} = 5V$, $V_{BEsat} = 1V$ and transistors having $BV_{CEO} = 400V$ it follows that:

$$L_b = \frac{12}{I_C} \text{ H } (I_C \text{ in Amps})$$

c) Other ways of turn-off

Of course, other ways of turn-off are applicable but in general these can be reduced to one of the methods described above, or something in between. The BV_{CEO} has a strong influence on the method used: the higher BV_{CEO} the longer the storage time required to achieve proper turn-off. For transistors having a BV_{CEO} of 200V or less hard turn-off and the use of a base coil yield comparable losses, so hard turn-off works well. For transistors having BV_{CEO} more than 400V hard turn-off is unacceptable because of the resulting tails.

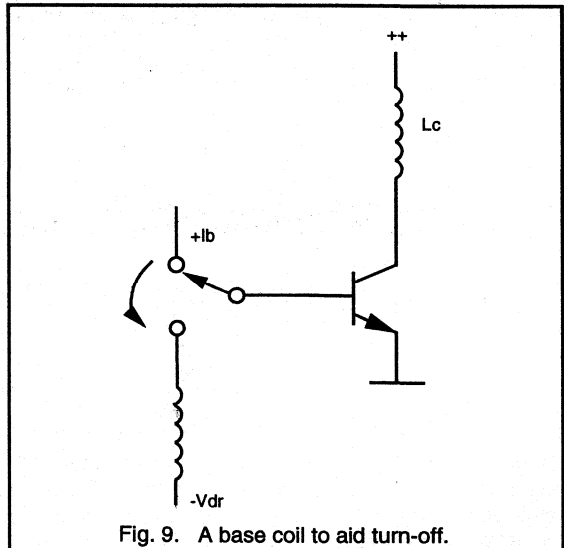
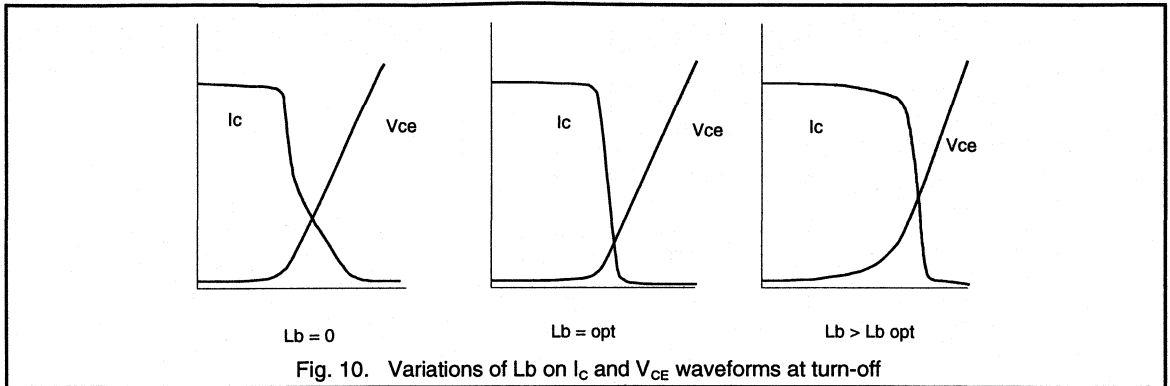


Fig. 9. A base coil to aid turn-off.

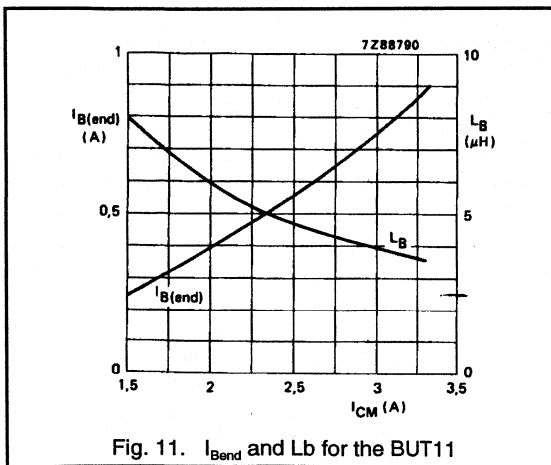


Turn-off for various forward drive conditions

Using the BUT11 as an example, turn-off characteristics are discussed for optimum drive, underdrive and overdrive with hard and smooth turn-off.

a) Optimum drive

The optimum I_B and L_b for a range of I_C is given in Fig. 11 for the BUT11. The I_B referred to is I_{Bend} which is the value of I_B at the end of the on-state of the applied base drive signal. In most applications during the on-state the I_B will not be constant, hence the term I_{Bend} rather than I_{Bon} . For optimum drive the level of I_{Bend} increases with I_C . For smooth turn-off the level of L_b decreases with increasing I_C .



Deviations from Fig. 11 will generally lead to higher power dissipation. If a short storage time is a must in a certain application then L_b can be reduced but this will lead to longer fall times and current tails.

With hard turn-off I_B reaches its peak negative value as all the charge is removed from the base. For continuity this current must be sourced from elsewhere. It has been shown that the BE junction now avalanches, giving instantaneous continuity followed by a positive dI_B/dt . However, for hard turn-off the current is sourced by the residual collector charge without BE avalanche, see Fig. 12. The small negative V_{BE} ensures a long tail to I_C and I_B .

b) Underdrive (Desaturated drive)

As has been indicated previously, desaturating, or underdriving, a transistor results in less internal charge. Q_d will be zero and Q_c is low and located near the junction.

If the application requires such a drive then steps should be taken to optimise the characteristics. One simple way of obtaining underdrive is to increase the series base resistance with smooth turn-off. The same effect can be achieved with optimum I_{Bend} and a base coil having half the value used for optimum drive, ie hard turn-off. Both methods give shorter t_s and t_f . For 400V V_{CE0} devices (like the Philips BUT range) such a harder turn-off can lead to reasonable results.

Fig. 13 compares the use of the optimum base coil with hard turn-off for an undriven BUT11. For underdrive the final I_C is less and hence the collector charge is less. Therefore, underdrive and hard turn-off gives less of a tail than for a higher I_{Bend} . Underdrive with smooth turn-off gives longer t_s but reduced losses.

c) Overdrive

When a transistor is severely overdriven the BC charge, Q_d , becomes so large that a considerable tail will result even with smooth turn-off. In general, deliberately designing a drive circuit to overdrive a transistor is not done: it has no real value. However, most circuits do have variable collector loads which can result in extreme conditions when the circuit is required to operate with the transistor in overdrive.

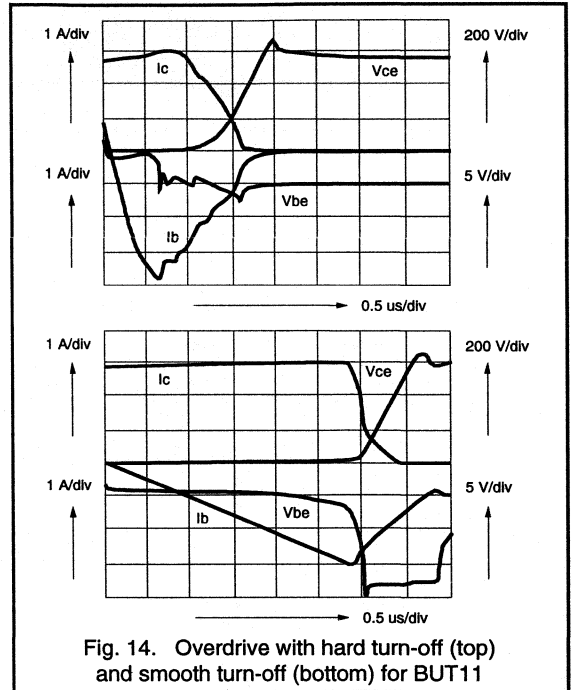
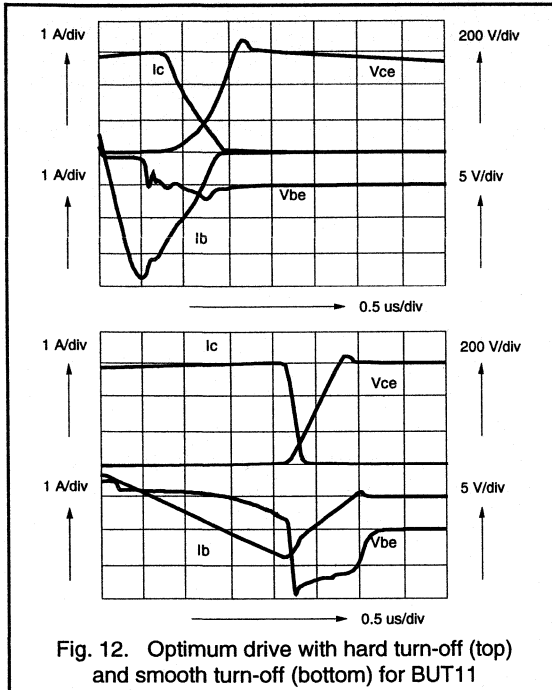


Fig. 14 compares the use of the optimum base coil with hard turn-off for an overdriven BUT11. For overdrive there is more base charge, also the final collector current will be higher and, hence, there will be more collector charge. The overdriven transistor is then certain to have longer switching times as there are more electron-hole pairs in the device that need to recombine before the off-state is reached.

Conclusions

Two ways of turning off a high voltage transistor, hard turn-off and the use of a base coil, were examined in three conditions of the on-state: optimum drive, overdrive and underdrive.

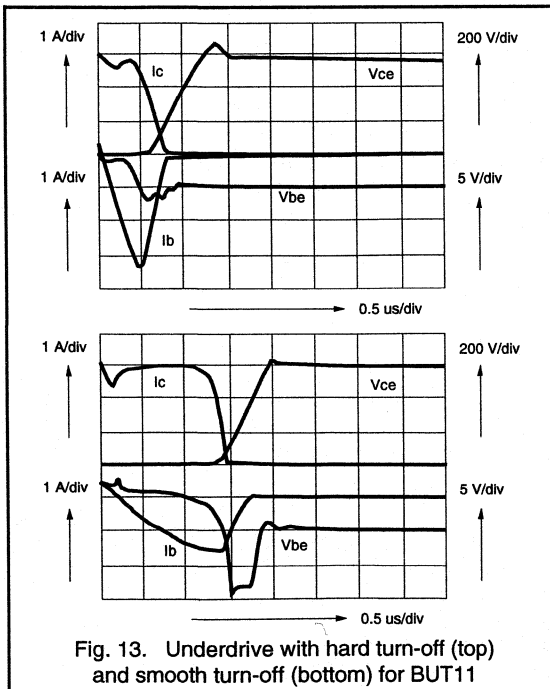
For transistors having $BV_{CEO} \sim 400$ V the use of a base coil yields low losses compared to hard turn-off. As a good approximation the base coil should have the value:

$$L_B = \frac{12}{I_C} \mu H$$

for optimum drive.

When using a desaturation circuit the value for L_B can be halved with acceptable results.

Overdrive should be prevented as much as possible because considerable tails in the collector current cause unacceptable losses.



1.3.3 Using High Voltage Bipolar Transistors

This section looks at some aspects of using high voltage bipolar transistors in switching circuits. It highlights points such as switching, both turn-on and turn-off, Safe Operating Areas and the need for snubber circuits. Base drive design curves for the BUT11, BUW12 and BUW13 are discussed under 'Application Information' at the end of this section.

Transistor switching: turn-on

To make optimum use of today's high voltage transistors, one should carefully choose the correct value for both the positive base current when the transistor is on and the negative base current when the device is switched off (see Application Information section).

When a transistor is in the off-state, there are no carriers in the thick n- collector, effectively there is a resistor with a relatively high value in the collector. To obtain a low on-state voltage, a base current is applied such that the collector area is quickly filled with electron - hole pairs causing the collector resistance to decrease. In the transition time, the so called turn-on time, the voltage and current may both be high, especially in forward converters, and high turn-on losses may result. Initially, all the carriers in the collector will be delivered via the base contact and, therefore, the base current waveform should have a peak at the beginning. In this way the carriers quickly fill the collector area so the voltage is lower and the losses decrease.

In flyback converters the current to be turned on is normally low, but in forward converters this current is normally high. The collector current, I_C , reaches its on-state value in a short time which is normally determined by the leakage inductance of the transformer.

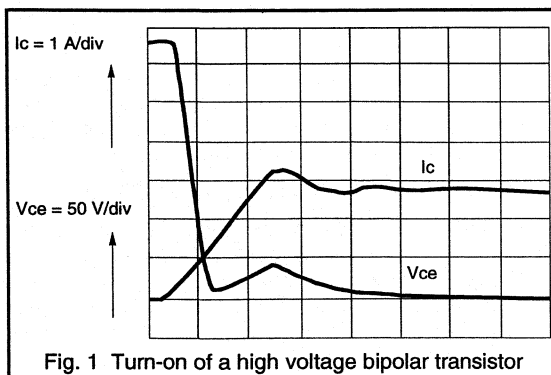


Fig. 1 Turn-on of a high voltage bipolar transistor

In Fig. 1 the characteristic 'hump' which often occurs at turn-on in forward converters due to the effect of the collector series resistance is observed.

The turn-on losses are strongly dependent on the value of the leakage inductance and the applied base drive. It is generally advised to apply a high initial $+I_B$ for a short time in order to minimise turn on losses.

A deeper analysis can be found in sections 1.3.2, 2.1.2 and 2.1.3. Turn on losses are generally low for flyback converters but are the most important factor in forward converter types.

Turn-off of high voltage transistors

All charge stored in the collector when the transistor is on should be removed again at turn-off. To ensure a quick turn-off a negative base current is applied. The time needed to remove the base - collector charge is called the storage time. A short storage time is needed to minimise problems within the control loop in SMPS and deflection applications.

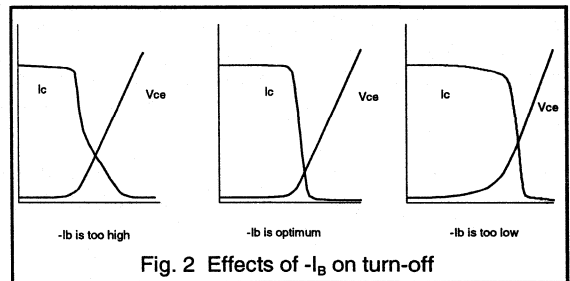


Fig. 2 Effects of $-I_B$ on turn-off

Care is needed to implement the optimum drive. First overdrive should be prevented by keeping $+I_B$ to a minimum. Overdrive results in current tails and long storage times. But, decreasing I_B too much results in high on-state losses.

Second, the negative base current should be chosen carefully. A small negative base current ($-I_B$) will give a long storage time and a high V_{CEsat} at the end of the storage time, while the current is still high. As a consequence, the turn-off losses will be high. If, however, a large negative base current is used, the danger exists that tails will occur in the collector current, again resulting in high losses. There is an optimum as shown in Fig. 2.

A circuit which is worth considering, especially for higher frequencies, is the Baker Clamp or desaturation circuit. This circuit prevents saturation of the transistor and, hence, faster switching times are achieved.

The total losses depend on the base drive and the collector current. In Fig.3 the total losses are shown for a BUW133 as a function of the positive base current, for both the saturated and the desaturated case. Note that when different conditions are being used the picture will change. The application defines the acceptable storage time which then determines the base drive requirements.

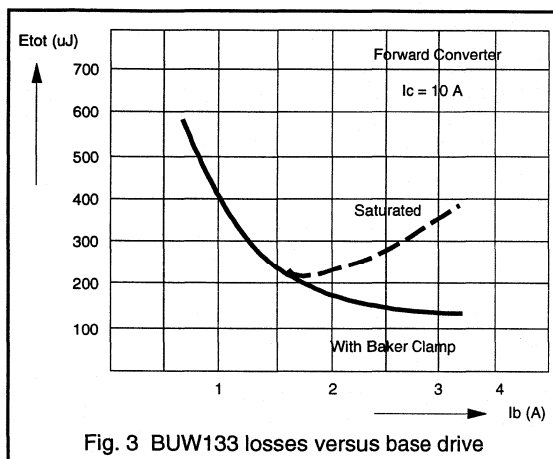


Fig. 3 BUW133 losses versus base drive

The total number of variables is too large to give unique base drive advice for each application. As a first hint the device data sheets give I_C and I_B values for V_{CEsat} , V_{BEsat} and switching. However, it is more important to appreciate the ways to influence base drive and the consequences of a non-optimised circuit.

For a flyback converter the best value of I_{Bend} to start with is about 2/3 of the I_B value given in data for V_{CEsat} and V_{BEsat} . In this application the forward base current is proportional to the collector current (triangular shaped waveforms) and this I_{Bend} value will give low on-state losses and fast switching.

The best turn-off base current depends on the breakdown voltage of the transistor. As a guide, Table 1 gives reasonable values for the target storage time and may be used to begin optimising the base drive:

f (kHz)	tp (μs)	target ts (μs)
25	20	2.0
150	10	1.5
100	5	1.0

Table 1 Target ts for varying frequency and pulse width

The above table holds for transistors with a V_{CE0max} rating of 400-450V and V_{CESmax} between 850-1000V. Transistors with higher voltages require longer storage times, eg.

transistors with $V_{CE0max} = 700V$ and $V_{CESmax} = 1500V$ need a storage time which is approximately double the value in the table.

A recommended way to control the storage time is by switching the base to a negative voltage rail via a base coil. The leakage inductance of a driver transformer may serve as an excellent base coil. As a guide, the base coil should be chosen such that the peak value of the negative base current equals half the value of the collector current.

Specific problems and solutions

A high voltage transistor needs protection circuits to ensure that the device will survive all the currents and voltages it will see during its life in an application.

a) Over Current

Exceeding current ratings normally does not lead to immediate transistor failure. In the case of a short circuit, the protection is normally fast enough for problems to be avoided. Most devices are capable of carrying very high currents for short periods of time. High currents will raise the junction temperature and if T_{jmax} is exceeded the reliability of the device may be weakened.

b) Over Voltage

In contrast with over current, it is NOT allowed to exceed the published voltage ratings for V_{CEO} and V_{CES} (or V_{CBO}). In switching applications it is common for the base - emitter junction to be taken into avalanche, this does not harm the device. For this reason V_{EBO} limits are not given in data.

Exceeding V_{CEO} and V_{CES} causes high currents to flow in very small areas of the device. These currents may cause immediate damage to the device in very short times (nanoseconds). So, even for very short times it is not allowed to have voltages above data for the device.

In reality V_{CEO} and V_{CES} are unlikely to occur in a circuit. If $V_{BE} = 0V$ there will probably still be a path between the base and the emitter. In fact the situation is V_{CEX} where X is the impedance of this path. To cover for all values of X, the limit is $X = \infty$, ie V_{CEO} . For all $V_{BE} < 0V$, ie V_{CEV} , the limit case is $V_{BE} = 0V$, ie V_{CES} .

If voltage transients that exceed the voltage limits are detected then a snubber circuit may limit the voltage to a safe value. If the over voltage states last greater than a few μs a higher voltage device is required.

c) Forward Bias Safe Operating Areas (FBSOA)

The FBSOA is valid for positive values of V_{BE} . There is a time limit to $V_{CE} - I_C$ operating points beyond which device failure becomes a risk. At certain values of V_{CE} and I_C there is a risk of secondary breakdown; this is likely to lead to the immediate failure of the device. The FBSOA curve should only be considered during drastic change sequences; for example, start-up, s/c or o/c load.

d) Reverse Bias Safe Operating Area (RBSOA)

The RBSOA is valid for negative values of V_{BE} . During turn-off with an inductive load the V_{CE} will rise as the I_C falls. For each device type there is a $V_{CE} - I_C$ boundary which, if exceeded, will lead to the immediate failure of the device. To limit the $V_{CE} - I_C$ path at turn-off snubber circuits are used, see Fig. 4.

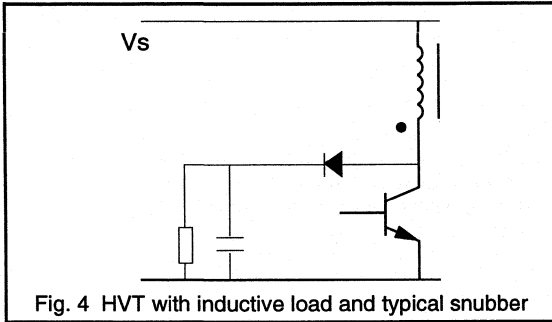


Fig. 4 HVT with inductive load and typical snubber

At turn-off, as the V_{CE} rises the diode starts conducting charging the capacitor. The additional diode current means that the total load current does not decrease so fast at turn-off. This slower current tail in turn ensures a slower V_{CE} rise. The slower V_{CE} rise takes the transistor through a safer $V_{CE} - I_C$ path away from the limit, see Fig. 5.

As a handy guide, the snubber capacitor in a 20-40 kHz converter is about 1nF for each 100W of throughput power (this is the power which is being transferred via the transformer). This value may be reduced empirically as required.

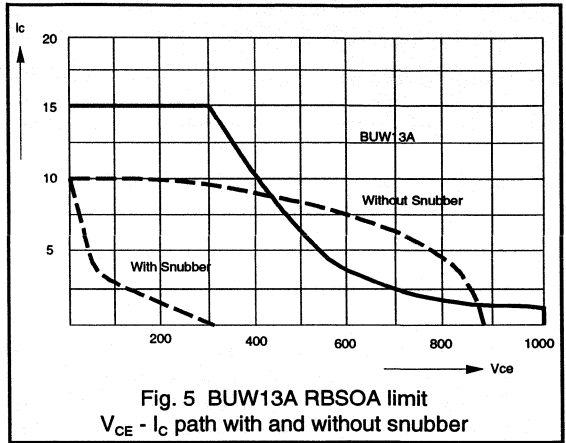


Fig. 5 BUW13A RBSOA limit
 $V_{CE} - I_C$ path with and without snubber

The following table may serve as a guide to the value of dV_{CE}/dt for some switching frequencies

f (kHz)	25	50	100
dV_{CE}/dt (kV/ μ s)	1	2	4

The snubber resistor should be chosen so that the capacitor will be discharged in the shortest occurring on-time of the switch.

In some cases the losses in the snubber may be considerable. Clever designs exist to feed the energy stored in the capacitor back into the supply capacitor, but this is beyond the scope of this report.

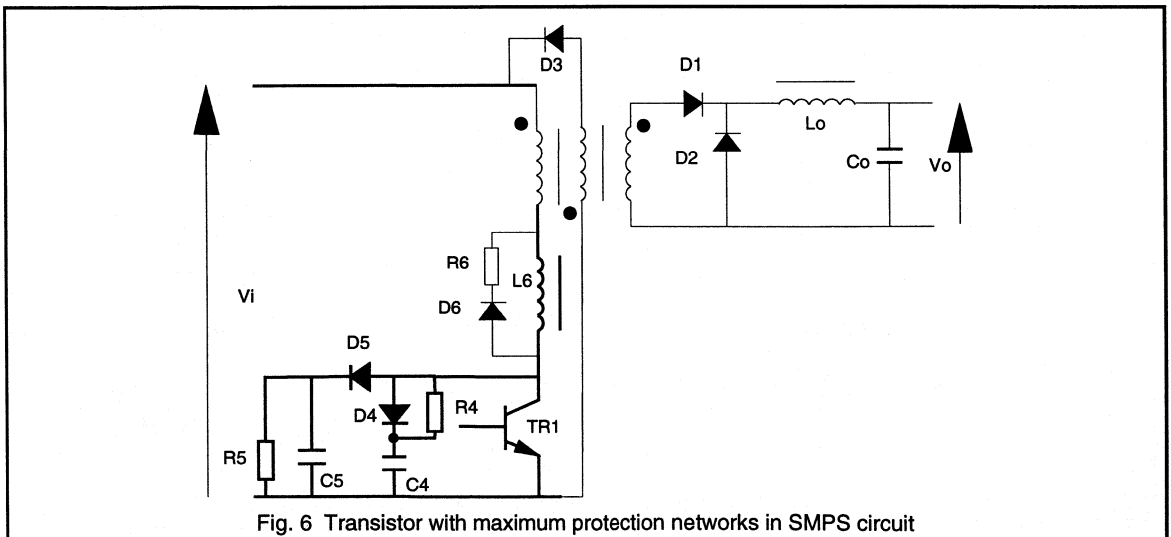


Fig. 6 Transistor with maximum protection networks in SMPS circuit

d) Other protection networks

In Fig. 6 a "maximum protection" diagram is shown with various networks connected. R4, C4, and D4 form the snubber to limit the rate of rise of V_{CE} . The network with D5, R5 and C5 forms a "peak detector" to limit the peak V_{CE} .

The inductor L6 serves to limit the rate of rise of I_C which may be very high for some transformer designs. The slower di_C/dt leads to considerably lower turn-on losses. Added to L6 is a diode D6 and resistor R6, with values chosen so that L6 loses its energy during the off-time of the power switch.

While the snubber is present in almost all SMPS circuits where transistors are used above V_{CE0max} , the di_C/dt limiter is only needed when the transformer leakage inductance is extremely low. The peak detector is applied in circuits which have bad coupling between primary and secondary windings.

Application Information

Important design factors of SMPS circuits are the maximum power losses, heatsink requirements and base drive conditions of the switching transistor. The power losses are very dependent on the operating frequency, the

maximum collector current amplitude and shape.

The operating frequency is usually between 15 and 50 kHz. The collector current shape varies from rectangular in a forward converter to sawtooth in a flyback converter.

Examples of base drive and losses are given in Appendix 1 for the BUT11, BUW12 and BUW13. In these figures I_{CM} represents the maximum repetitive peak collector current, which occurs during overload. The information is derived from limit-case transistors at a mounting base temperature of 100 °C under the following conditions (see also Fig. 7):

- collector current shape $I_{C1} / I_{CM} = 0.9$
- duty factor $(t_p / T) = 0.45$
- rate of rise of I_C during turn-on = 4 A/ μ s
- rate of rise V_{CE} during turn-off = 1 kV/ μ s
- reverse drive voltage during turn-off = 5 V
- base current shape $I_{B1} / I_{Be} = 1.5$

The required thermal resistance of the heatsink can be calculated from

$$R_{th(mb-amb)} < \frac{100 - T_{amb}}{P_{tot}} \text{ K/W}$$

To ensure thermal stability a maximum value of the ambient temperature, T_{amb} , is assumed: $T_{amb} \leq 40^\circ\text{C}$.

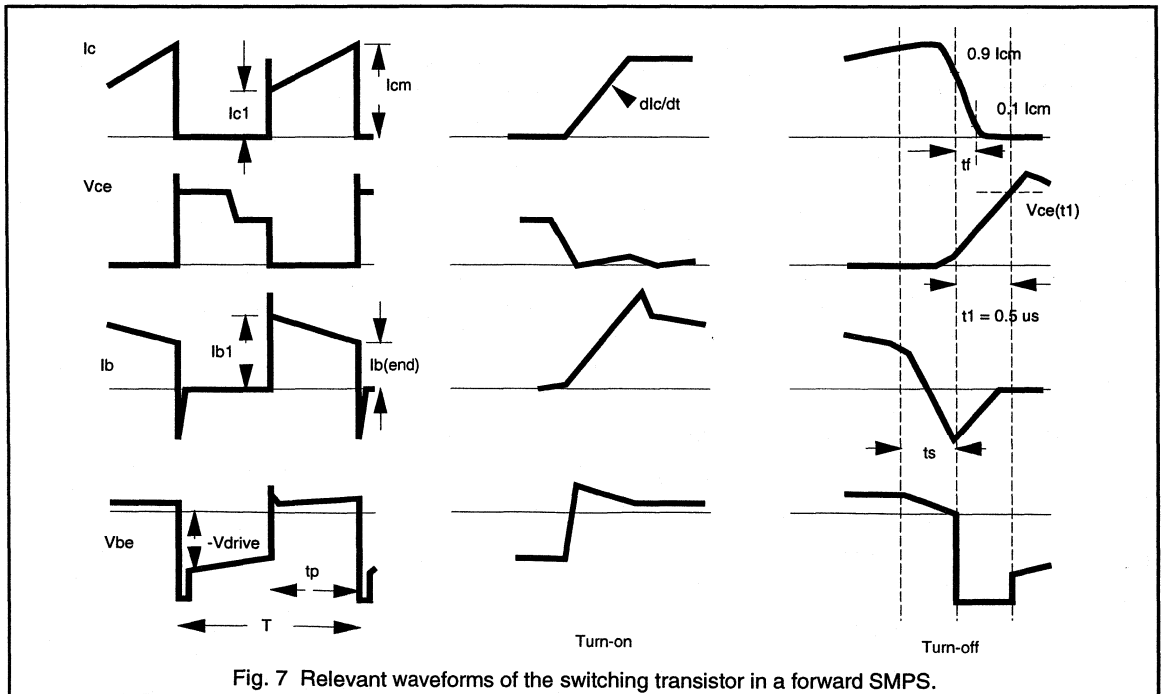


Fig. 7 Relevant waveforms of the switching transistor in a forward SMPS.

As a base coil is normally advised and a negative drive voltage of -5V is rather common, the value for the base coil, L_B , is given for these conditions. For other values of $-V_{drive}$ (-3 to -7 volt) the base coil follows from:

$$L_B = L_{Bnom} \cdot \frac{(-V_{drive} + 1)}{6}$$

Where L_{Bnom} is the value given in Appendix 1.

It should be noted, that this advice yields acceptable power losses for the whole spread in the product. It is not just for typical products as is sometimes thought ! This is demonstrated in Fig. 8, where limit and typical devices are compared (worst-case saturation and worst-case switching).

It appears that the worst-case fall time devices have losses P0 for $I_{Bend} = (I_B \text{ adv}) + 20\%$, while the saturation worst-case devices have the same losses at $(I_B \text{ adv}) - 20\%$. A typical device now has losses P1 at $I_B \text{ adv}$, while the optimum I_{Bend} for the typical case might yield losses P2 at an approximately 15% lower I_{Bend} (NB: this is not a rule, it is an example).

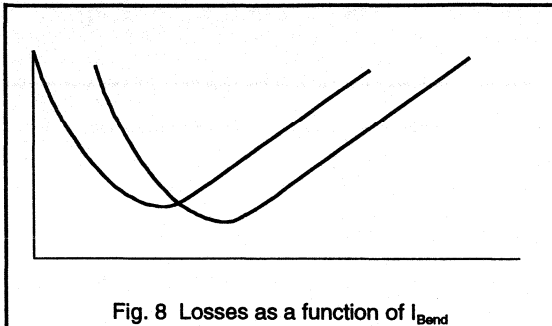
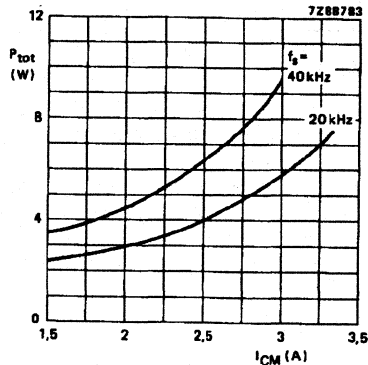
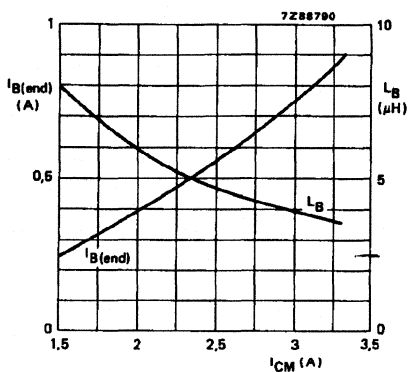


Fig. 8 Losses as a function of I_{Bend}

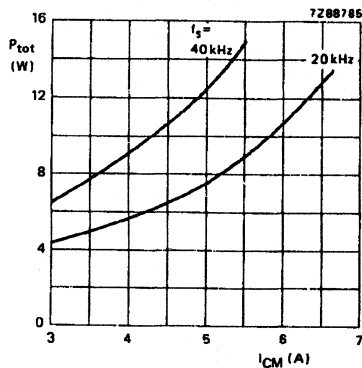
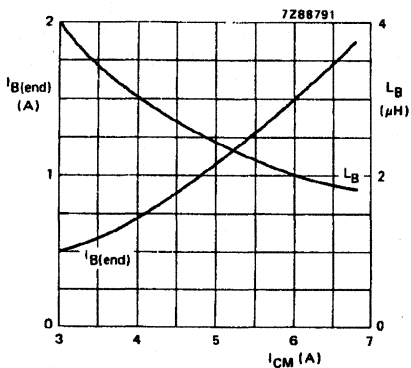
Conclusion

To avoid exceeding the RBSOA of an HVT, snubbers are a requirement for most circuits. To minimise both switching and on-state losses, particular attention should be given to the design of the base drive circuit. It is generally advised that a high initial base current is applied for a short time to minimise turn-on loss. As a guide-line for turn-off, a base coil should be chosen such that the peak value of the negative base current equals half the value of the collector current.

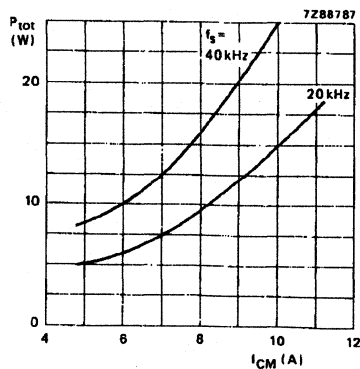
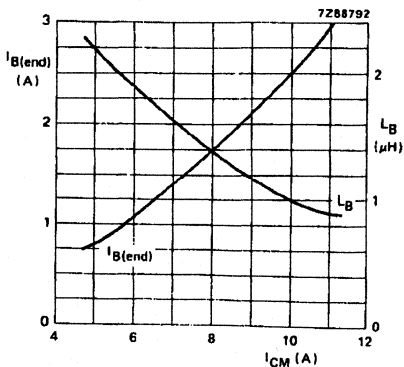
Appendix 1 Base Drive Design Graphs



BUT11 Base Drive Design Information



BUW12 Base Drive Design Information



BUW13 Base Drive Design Information

1.3.4 Understanding The Data Sheet: High Voltage Transistors

Introduction

Being one of the most important switching devices in present day switched mode power supplies and other fast switching applications, the high voltage transistor is a component with many aspects that designers do not always fully understand. In spite of its "age" and the variety of papers and publications by manufacturers and users of high voltage transistors, data sheets are somewhat limited in the information they give. This section deals with the data sheets of high voltage transistors and the background to their properties. A more detailed look at the background to transistor specifications can be found in chapter 2.1.2.

Fig. 1 shows the cross section of a high voltage transistor. The active part of the transistor is highlighted (the area underneath the emitter) and it is this part of the silicon that determines the primary properties of the device: breakdown voltages, h_{FE} , switching times. All the added parts can only make these properties worse: a bad passivation scheme can yield a much lower collector-base breakdown voltage, too thin wires may seriously decrease the current capability, a bad die bond (solder layer) leads to a high thermal resistance leading to poor thermal fatigue behaviour.

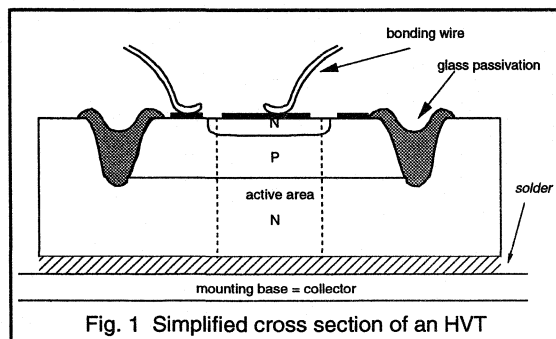


Fig. 1 Simplified cross section of an HVT

The Data Sheet

The data sheet of a high voltage transistor can specify -

* **Limiting Values / Ratings:** the maximum allowable currents through and voltages across terminals, as well as temperatures that must not be exceeded.

* **Characteristics:** describing properties in the on and off state (static) as well as dynamic, both in words and in figures.

* **SOA:** Safe Operating Area both in forward and reverse biased conditions.

Data sheets are intended to be a means of presenting the essentials of a device and, at the same time, to give an overview of the guaranteed specification points. This data is checked as a final measurement of the device and customers may wish to use it for their incoming inspection. For this reason the data is such that it can be inspected rather easily in relatively simple test circuits. This somewhat application unfriendly way of presenting data is unavoidable if cheap devices are a must, and they are!

Each of the above mentioned items will now be discussed in more detail, in some instances parts of the data for a BUT11 will be used as an example. The BUT11 is intended for 3A applications and has a maximum V_{CES} of 850V.

Limiting Values / Maximum Ratings

There is a significant difference between current and voltage ratings. Exceeding voltage ratings can lead to breakdown phenomena which are possibly destructive within fractions of a second. The avalanche effects normally take place within a very small volume and, therefore, only a little energy can be absorbed. Surge voltages, that are sometimes allowed for other components, are out of the question for high voltage transistors.

There is, however, no reason to have a derating on voltages: using the device up to its full voltage ratings - in worst case situations - is allowed. The life tests, carried out in Philips quality laboratories, clearly show that no voltage degradation takes place and excellent reliability is maintained.

From the above, it should be clear that the habit of derating is not a good one. If, in a particular application, the collector-emitter voltage never exceeds, say 800V, the required device should be an 850V device not a 1500V device. Higher voltage devices not only have lower h_{FE} , but also slower switching speeds and higher dissipation.

The rating for the emitter-base voltage is a special case: to allow a base coil to be used, the base-emitter diode may be brought into breakdown; in some cases a $-I_{Bav}$ is given to prevent excessive base-emitter dissipation. The only effect of long term repetitive base-emitter avalanche breakdown that has been observed is a slight decrease in h_{FE} at very low values of collector current (approximately 10% at $\leq 5mA$); at higher currents the effects can be neglected completely.

The maximum value for V_{CE0} is important if no snubber is applied; it sets a firm boundary in applications with a very fast rising collector voltage and a normal base drive (see also section on SOA).

Currents above a certain value may be destructive if they last long enough: bonding wires fuse due to excessive heating. Therefore, short peak currents are allowed well above the rated I_{CSat} with values up to five times this value being published for I_{CM} . Exceeding the published maximum temperatures is not immediately destructive, but may seriously affect the useful life of the device. It is well known, that the useful life of a semiconductor device doubles for each 10K decrease in working junction temperature. Another factor that should be kept in mind is the thermal fatigue behaviour, which strongly depends on the die-bonding technology used. Philips high voltage devices are capable of 10,000 cycles with a temperature rise of 90K without any degradation in performance.

This kind of consideration leads to the following advice: under worst case conditions the maximum case-temperature should not exceed 115 °C for reliable operation. This advice is valid regardless of the maximum temperature being specified. Of course, for storage the published values remain valid.

The maximum total power dissipation P_{tot} is an industry standard, but not very useful, parameter. It is the quotient of $T_{jmax} - T_{mb}$ and $R_{th(j-mb)}$ ($R_{th(j-mb)}$ is the thermal resistance from junction to mounting base and T_{mb} is assumed to be 25°C). This implies a rather impractical infinite heatsink, kept at 25°C !

Electrical Characteristics

Static parameters characterise leakage currents, h_{FE} , saturation voltages; dynamic parameters and switching times, but also include transition frequency and collector capacitance.

To start: I_{CSat} , the collector saturation current, is that value of the collector current where both saturation and switching properties of the devices are specified. I_{CSat} is not a characteristic that can be measured, but it is used as an indication of the of the peak working current allowed through a device.

In the off-state various leakage currents are specified, however, these are of little use as they indicate the low level of dissipation in the off state. Also a V_{CE0sus} is specified, usually being equal to the max. V_{CE0} . For switching purposes it is the RBSOA that is important (see next section).

In the on state the saturation voltages V_{CEsat} and, to a lesser extent, V_{BEsat} are important. V_{CEsat} is an indication of the saturation losses and V_{BEsat} normally influences base drive. Sometimes worst case V_{CEsat} is given as a function of both I_C and I_B . It is not possible to precisely relate these curves

to a real circuit; in practice, currents and voltages will vary over the switching cycle. The dynamic performance is different to the static performance. However, a reasonable indication can be obtained from these curves.

Both the transition frequency (f_T) and the collector capacitance (C_c or C_{ob}) are minor parameters relating to the design and processing technology used.

Switching times may be given in circuits with an inductive or a resistive collector load. See Figs. 2a-b for simplified test circuits and Figs. 3a-b for waveforms.

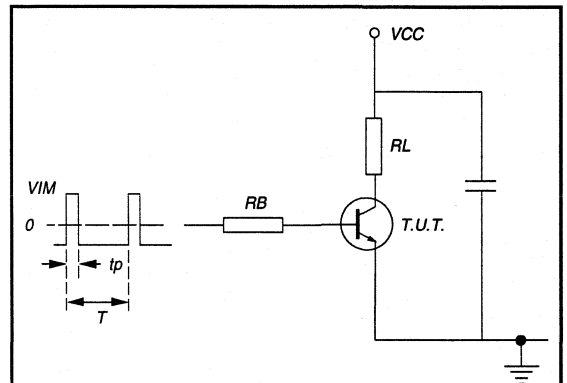


Fig. 2a Test circuit for resistive load

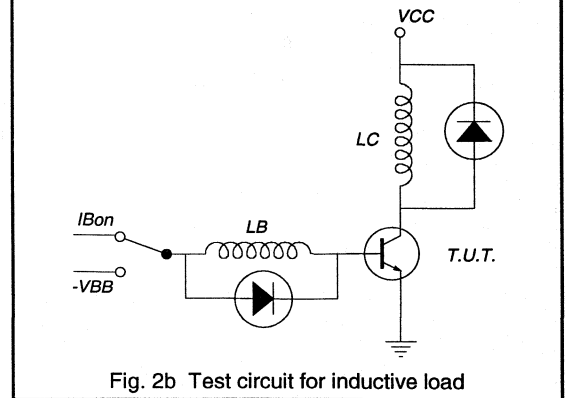


Fig. 2b Test circuit for inductive load

When comparing similar devices from different manufacturers one is confronted with a great variety of base drive conditions. The positive base current ($+I_B$) may be the same as the one used in the V_{CEsat} spec. but also lower values (up to 40% lower) or desaturation networks may be used, yielding better t_s and t_f values. The negative base drive, $-I_B$, may equal $+I_B$ or it may be twice this value, yielding a shorter t_s , and sometimes it is determined by switching the base to a negative voltage, possibly via a base coil. Altogether it is quite confusing and when comparing switching times one should be well aware of all the differences!

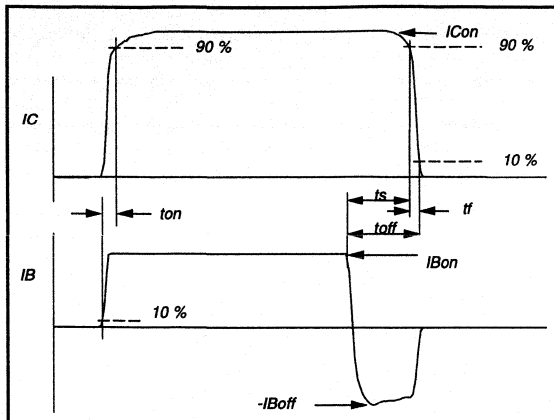


Fig. 3a Waveforms for Resistive Switching.

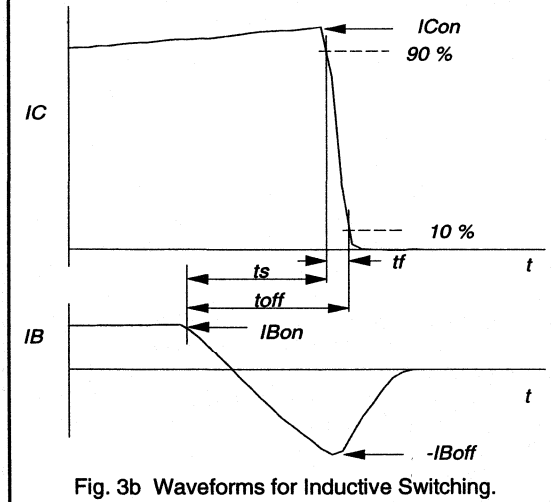


Fig. 3b Waveforms for Inductive Switching.

As an example a BUT11 has been measured at $I_C = 3A$ in a resistive test circuit varying both $+I_B$ and $-I_B$. The results in Table 1 show that it is possible to turn a normal transistor into a super device by simple specmanship!

$I_C = 3A$	$t_s (\mu s)$	$t_f (ns)$
$+I_B = 0.6A; -I_B = 0.6A$ (normal case)	2.5	260
$+I_B = 0.36A; -I_B = 0.72A$ (underdriven)	1.6	210
$+I_B = 0.36A; -V_{BE} = -5V$ (underdriven, hard turn-off)	0.8	50

Table 1 Switching times and base drive for the BUT11

The effect of base drive variations on storage and fall times is given in Table 2. The reference is the condition that both $+I_B$ as well as $-I_B$ equals the value for I_B given for the V_{CEsat} specification in the data sheet.

	t_s	t_f	comments
$+I_B = \text{ref.}$	normal	normal	reference
$+I_B = 40\% \text{ less}$	↓	↓	
Desaturated	↓	↓	
$-I_B = \text{ref.}$	normal	normal	reference
$-I_B = 2x +I_B$	↓	↓	
Directly to -5 V	↓	↑	with normal base drive!
Directly to -5 V	↓	↓	if underdriven
Via L to -5 V	↓	↓	

Table 2 Switching times and base drive variations.

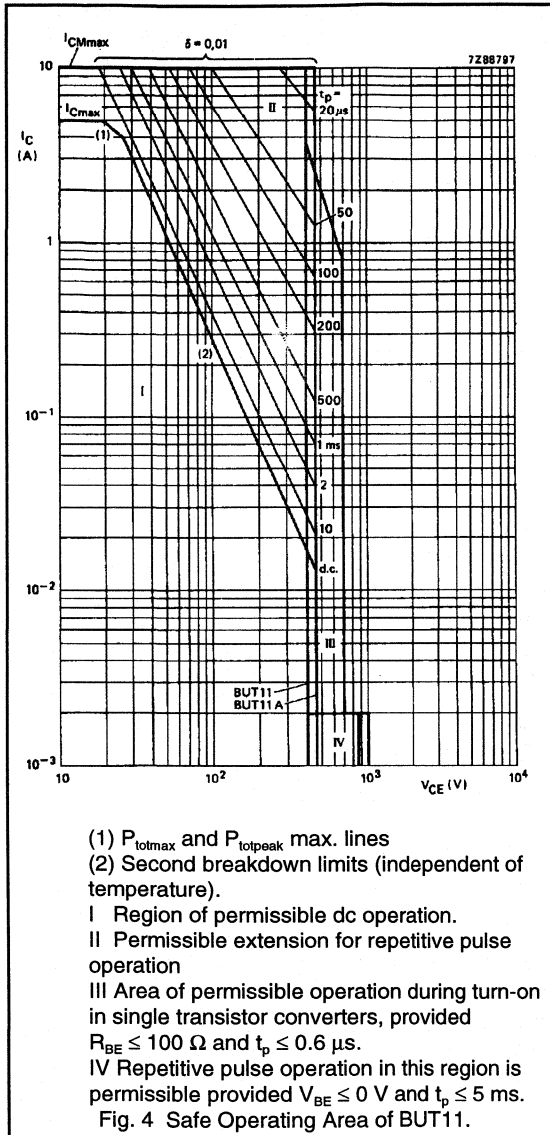
The turn-on time is a parameter which only partially correlates with dissipation as it is usually the behaviour directly after the turn-on time which appears to be most significant. Both inductive and resistive load test circuits are only partially useful, as resistive loads are seldom used and very often some form of slow-rise network is used with inductive loads. Both circuits provide easy lab. measurements and the results can be guaranteed. The alternative of testing the devices in a real switched mode power supply would be too costly!

Safe Operating Area

The difference between forward bias safe operating area (FBSOA) and reverse bias safe operating area (RBSOA) is in the device V_{BE} : if $V_{BE} > 0V$ it is FBSOA and if $V_{BE} < 0V$ it is RBSOA. Chapter 2.1.3 deals with both subjects in more detail, a few of the main points are covered below.

FBSOA gives boundaries for dc or pulsed operation. In switching applications, where the transistor is "on" or "off", normally the excursion in the $I_C - V_{CE}$ plane is fast enough to allow the designer to use the whole plane, with the boundaries I_{Cmax} and V_{CE0} , as given in the ratings. This is useful for snubberless applications and for overload, fault conditions or at switch-on of the power supply

Fig. 4 gives the FBSOA of the BUT11 with the boundaries of I_{Cmax} , I_{CMmax} and V_{CE0} , all as given in the ratings. There is a P_{totmax} (1) and I_{SB} boundary (2), that both shift at higher levels of I_C when shorter pulses are used. Note that in the upper right hand corner pulse times of $20\mu s$ are permitted leading to a square switching SOA. For overload, fault condition or power supply switch-on an extra area is added (area III). All these conditions are for $V_{BE} \geq 0V$.

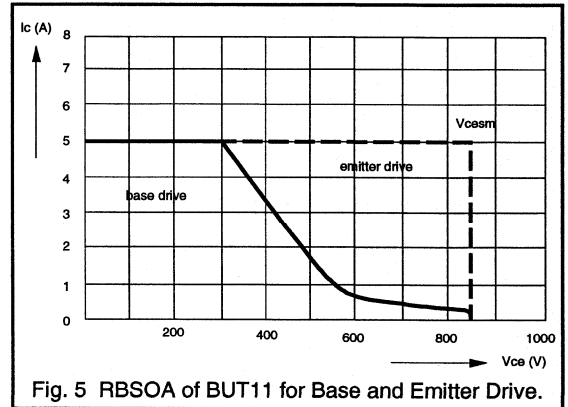


Area IV is only valid for $V_{BE} \leq 0V$, so this is an RBSOA extension to the SOA curve. This is not the full picture for RBSOA, area IV is only for continuous pulsed operation. For single cycle and short burst fault conditions see the separate RBSOA curve.

The RBSOA curve is valid when a negative voltage is applied to the base-emitter terminals during turn-off. This curve should be used for fault condition analysis only; continuous operation close to the limit will result in 100's W of dissipation! Due to localised current contraction within

the chip at turn-off, damage will occur if the limit is exceeded. In nearly all cases, the damage will result in the immediate failure of the device to short circuit.

Emitter switching applications force different mechanisms for carrier recombination in the device which allow a 'square' RBSOA. A typical example is shown in Fig. 5, where for both base and emitter drive the RBSOA of the BUT11 is given.



It is striking that for emitter drive the whole I_C - V_{CES} plane may be used so no snubber is necessary, however, a small snubber may prevent overshoot. The base drive RBSOA normally depends on base drive conditions, but unfortunately there is no uniform trend in this behaviour. Therefore, the RBSOA curve in the data gives the worst case behaviour of the worst case devices. Other data sheets may give RBSOA curves that at first sight look better than the Philips equivalent, but beware, these curves might hold for only a limited base drive range.

Summary

Voltage limiting values / ratings as given in the data must never be exceeded, as they may lead to immediate device failure. Surge voltages, as sometimes given for other components, are not allowed for high voltage transistors. Current limiting values / ratings are less strict as they are time-dependent and should be used in conjunction with the FBSOA.

Static characteristics are useful for comparisons but offer little in describing the performance in an application. The dynamic characteristics may be defined for a simple test circuit but the values give a good indication of the switching performance in an application.

RBSOA is, for all switching applications, of prime importance. Philips give in their data sheets a curve for worst case devices under worst case conditions. For snubber design a value of 1 nF per 100W of throughput

power is advised as a starter value; afterwards, the I_C - V_{CE} locus must be checked to see if it stays within the published RBSOA curve.

For characteristics both saturation and switching properties are given at I_{Csat} . Most figures are of limited use as they give static conditions, where in a practical situation properties are time-dependent. Switching times are given

in relatively simple circuits that may be replicated rather easily e.g. for incoming inspection.

Switching times depend strongly on drive conditions. By altering them a normal device can be turned into a super device. Beware of specmanship, this may disguise poor tolerance to variations in base drive.



Introduction

Introduction

Introduction

CHAPTER 2

Switched Mode Power Supplies

- 2.1 Using Power Semiconductors in Switched Mode Topologies
(including transistor selection guides)*
- 2.2 Output Rectification*
- 2.3 Design Examples*
- 2.4 Magnetics Design*
- 2.5 Resonant Power Supplies*

Using Power Semiconductors in Switched Mode Topologies



2.1.1 An Introduction to Switched Mode Power Supply Topologies

For many years the world of power supply design has seen a gradual movement away from the use of linear power supplies to the more practical switched mode power supply (S.M.P.S.). The linear power supply contains a mains transformer and a dissipative series regulator. This means the supply has extremely large and heavy 50/60 Hz transformers, and also very poor power conversion efficiencies, both serious drawbacks. Typical efficiencies of 30% are standard for a linear. This compares with efficiencies of between 70 and 80%, currently available using S.M.P.S. designs.

Furthermore, by employing high switching frequencies, the sizes of the power transformer and associated filtering components in the S.M.P.S. are dramatically reduced in comparison to the linear. For example, an S.M.P.S. operating at 20kHz produces a 4 times reduction in component size, and this increases to about 8 times at 100kHz and above. This means an S.M.P.S. design can produce very compact and lightweight supplies. This is now an essential requirement for the majority of electronic systems. The supply must slot into an ever shrinking space left for it by electronic system designers.

Outline

At the heart of the converter is the high frequency inverter section, where the input supply is chopped at very high frequencies (20 to 200kHz using present technologies) then filtered and smoothed to produce dc outputs. The circuit configuration which determines how the power is

transferred is called the TOPOLOGY of the S.M.P.S., and is an extremely important part of the design process. The topology consists of an arrangement of transformer, inductors, capacitors and power semiconductors (bipolar or MOSFET power transistors and power rectifiers).

Presently, there is a very wide choice of topologies available, each one having its own particular advantages and disadvantages, making it suitable for specific power supply applications. Basic operation, advantages, drawbacks and most common areas of use for the most common topologies are discussed in the following sections. A selection guide to the Philips range of power semiconductors (including bipolars, MOSFETs and rectifiers) suitable for use in S.M.P.S. applications is given at the end of each section.

(1) Basic switched mode supply circuit.

An S.M.P.S. can be a fairly complicated circuit, as can be seen from the block diagram shown in Fig. 1. (This configuration assumes a 50/60Hz mains input supply is used.) The ac supply is first rectified, and then filtered by the input reservoir capacitor to produce a rough dc input supply. This level can fluctuate widely due to variations in the mains. In addition the capacitance on the input has to be fairly large to hold up the supply in case of a severe drop in the mains. (The S.M.P.S. can also be configured to operate from any suitable dc input, in this case the supply is called a dc to dc converter.)

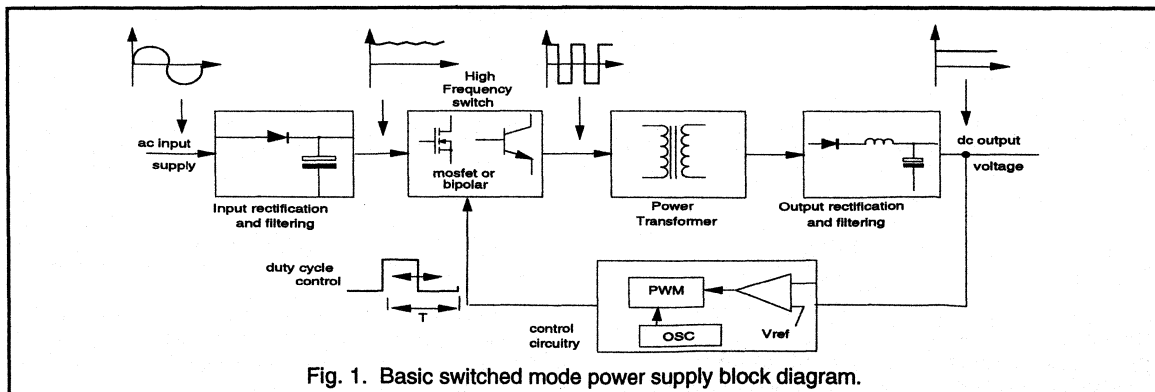


Fig. 1. Basic switched mode power supply block diagram.

The unregulated dc is fed directly to the central block of the supply, the high frequency power switching section. Fast switching power semiconductor devices such as MOSFETs and Bipolars are driven on and off, and switch the input voltage across the primary of the power transformer. The drive pulses are normally fixed frequency (20 to 200kHz) and variable duty cycle. Hence, a voltage pulse train of suitable magnitude and duty ratio appears on the transformer secondaries. This voltage pulse train is appropriately rectified, and then smoothed by the output filter, which is either a capacitor or capacitor / inductor arrangement, depending upon the topology used. This transfer of power has to be carried out with the lowest losses possible, to maintain efficiency. Thus, optimum design of the passive and magnetic components, and selection of the correct power semiconductors is critical.

Regulation of the output to provide a stabilised dc supply is carried out by the control / feedback block. Generally, most S.M.P.S. systems operate on a fixed frequency pulse width modulation basis, where the duration of the on time of the drive to the power switch is varied on a cycle by cycle basis. This compensates for changes in the input supply and output load. The output voltage is compared to an accurate reference supply, and the error voltage produced by the comparator is used by dedicated control logic to terminate the drive pulse to the main power switch/switches at the correct instance. Correctly designed, this will provide a very stable dc output supply.

It is essential that delays in the control loop are kept to a minimum, otherwise stability problems would occur. Hence, very high speed components must be selected for the loop. In transformer-coupled supplies, in order to keep the isolation barrier intact, some type of electronic isolation is required in the feedback. This is usually achieved by using a small pulse transformer or an opto-isolator, hence adding to the component count.

In most applications, the S.M.P.S. topology contains a power transformer. This provides isolation, voltage scaling through the turns ratio, and the ability to provide multiple outputs. However, there are non-isolated topologies (without transformers) such as the buck and the boost converters, where the power processing is achieved by inductive energy transfer alone. All of the more complex arrangements are based on these non-isolated types.

(2) Non-Isolated converters.

The majority of the topologies used in today's converters are all derived from the following three non-isolated versions called the buck, the boost and the buck-boost. These are the simplest configurations possible, and have the lowest component count, requiring only one inductor, capacitor, transistor and diode to generate their single output. If isolation between the input and output is required, a transformer must be included before the converter.

(a) The Buck converter.

The forward converter family which includes the push-pull and bridge types, are all based on the buck converter, shown in Fig. 2. Its operation is straightforward. When switch TR1 is turned on, the input voltage is applied to inductor L1 and power is delivered to the output. Inductor current also builds up according to Faraday's law shown below:-

$$V = L \frac{di}{dt}$$

When the switch is turned off, the voltage across the inductor reverses and freewheel diode D1 becomes forward biased. This allows the energy stored in the inductor to be delivered to the output. This continuous current is then smoothed by output capacitor Co. Typical buck waveforms are also shown in Fig. 2.

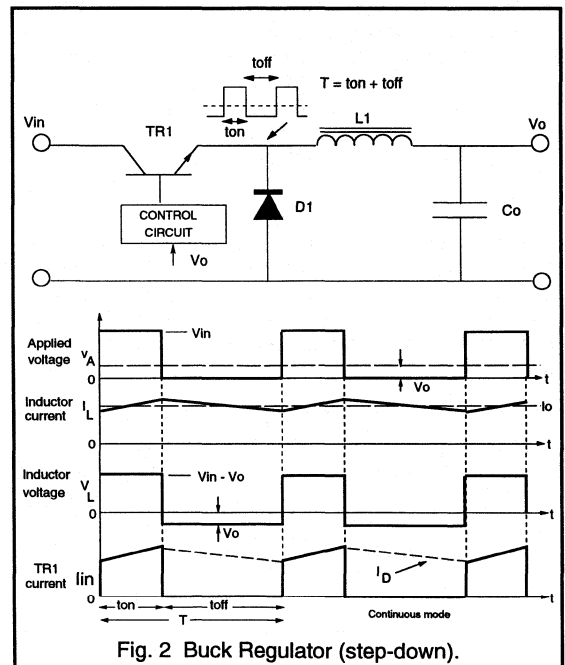


Fig. 2 Buck Regulator (step-down).

The LC filter has an averaging effect on the applied pulsating input, producing a smooth dc output voltage and current, with very small ripple components superimposed. The average voltage/sec across the inductor over a complete switching cycle must equal zero in the steady state. (The same applies to all of the regulators that will be discussed.)

Neglecting circuit losses, the average voltage at the input side of the inductor is $V_{in}D$, while V_o is the output side voltage. Thus, in the steady state, for the average voltage across the inductor to be zero, the basic dc equation of the buck is simply:-

$$\frac{V_o}{V_i} = D$$

D is the transistor switch duty cycle, defined as the conduction time divided by one switching period, usually expressed in the form shown below:-

$$D = \frac{t_{on}}{T}; \text{ where } T = t_{on} + t_{off}$$

Thus, the buck is a stepdown type, where the output voltage is always lower than the input. (Since D never reaches one.) Output voltage regulation is provided by varying the duty cycle of the switch. The LC arrangement provides very effective filtering of the inductor current. Hence, the buck and its derivatives all have very low output ripple characteristics. The buck is normally always operated in continuous mode (inductor current never falls to zero) where peak currents are lower, and the smoothing capacitor requirements are smaller. There are no major control problems with the continuous mode buck.

(b) The Boost Converter.

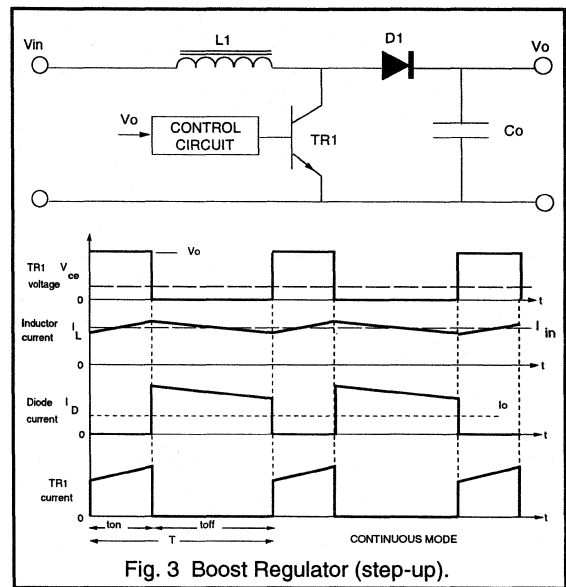
Operation of another fundamental regulator, the boost, shown in Fig. 3 is more complex than the buck. When the switch is on, diode $D1$ is reverse biased, and V_{in} is applied across inductor, $L1$. Current builds up in the inductor to a peak value, either from zero current in a discontinuous mode, or an initial value in the continuous mode. When the switch turns off, the voltage across $L1$ reverses, causing the voltage at the diode to rise above the input voltage. The diode then conducts the energy stored in the inductor, plus energy direct from the supply to the smoothing capacitor and load. Hence, V_o is always greater than V_{in} , making this a stepup converter. For continuous mode operation, the boost dc equation is obtained by a similar process as for the buck, and is given below:-

$$\frac{V_o}{V_i} = \frac{1}{1-D}$$

Again, the output only depends upon the input and duty cycle. Thus, by controlling the duty cycle, output regulation is achieved.

From the boost waveforms shown in Fig. 3, it is clear that the current supplied to the output smoothing capacitor from the converter is the diode current, which will always be discontinuous. This means that the output capacitor must be large, with a low equivalent series resistance (e.s.r) to

produce a relatively acceptable output ripple. This is in contrast to the buck output capacitor requirements described earlier. On the other hand, the boost input current is the continuous inductor current, and this provides low input ripple characteristics. The boost is very popular for capacitive load applications such as photo-flashers and battery chargers. Furthermore, the continuous input current makes the boost a popular choice as a pre-regulator, placed before the main converter. The main functions being to regulate the input supply, and to greatly improve the line power factor. This requirement has become very important in recent years, in a concerted effort to improve the power factor of the mains supplies.

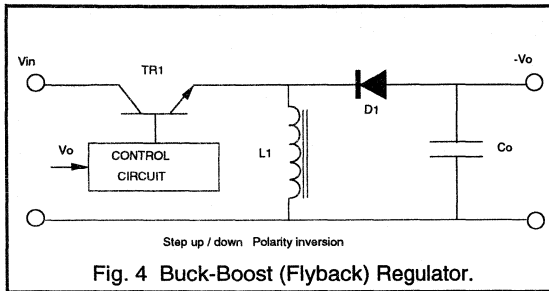


If the boost is used in discontinuous mode, the peak transistor and diode currents will be higher, and the output capacitor will need to be doubled in size to achieve the same output ripple as in continuous mode. Furthermore, in discontinuous operation, the output voltage also becomes dependent on the load, resulting in poorer load regulation.

Unfortunately, there are major control and regulation problems with the boost when operated in continuous mode. The pseudo LC filter effectively causes a complex second order characteristic in the small signal (control) response. In the discontinuous mode, the energy in the inductor at the start of each cycle is zero. This removes the inductance from the small signal response, leaving only the output capacitance effect. This produces a much simpler response, which is far easier to compensate and control.

(c) The Buck-Boost Regulator (Non-isolated Flyback).

The very popular flyback converter (see section 5(a)) is not actually derived solely from the boost. The flyback only delivers stored inductor energy during the switch off-time. The boost, however, also delivers energy from the input. The flyback is actually based on a combined topology of the previous two, called the buck-boost or non isolated flyback regulator. This topology is shown in Fig. 4.



When the switch is on, the diode is reverse biased and the input is connected across the inductor, which stores energy as previously explained. At turn-off, the inductor voltage reverses and the stored energy is then passed to the capacitor and load through the forward biased rectifier diode.

The waveforms are similar to the boost except that the transistor switch now has to support the sum of V_{in} and V_o across it. Clearly, both the input and output currents must be discontinuous. There is also a polarity inversion, the output voltage generated is negative with respect to the input. Close inspection reveals that the continuous mode dc transfer function is as shown below:-

$$\frac{V_o}{V_i} = \frac{D}{1-D}$$

Observation shows that the value of the switch duty ratio, D can be selected such that the output voltage can either be higher or lower than the input voltage. This gives the converter the flexibility to either step up or step down the supply.

This regulator also suffers from the same continuous mode control problems as the boost, and discontinuous mode is usually favoured.

Since both input and output currents are pulsating, low ripple levels are very difficult to achieve using the buck-boost. Very large output filter capacitors are needed, typically up to 8 times that of a buck regulator.

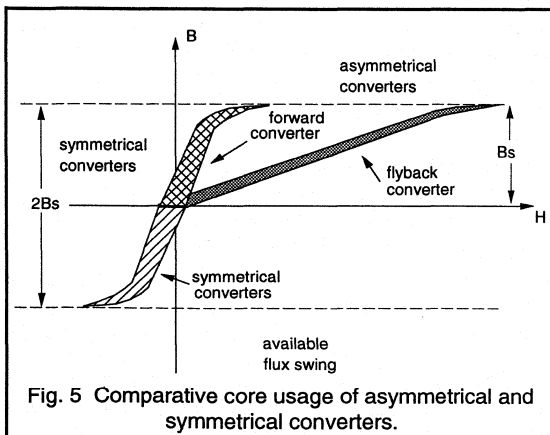
The transistor switch also needs to be able to conduct the high peak current, as well as supporting the higher summed voltage. The flyback regulator (buck-boost) topology places the most stress on the transistor. The rectifier diode also has to carry high peak currents and so the r.m.s conduction losses will be higher than those of the buck.

(3) Transformers in S.M.P.S. converters.

The non-isolated versions have very limited use, such as dc-dc regulators only capable of producing a single output. The output range is also limited by the input and duty cycle. The addition of a transformer removes most of these constraints and provides a converter with the following advantages:-

- 1) Input to output isolation is provided. This is normally always necessary for 220/110 V mains applications, where a degree of safety is provided for the outputs.
- 2) The transformer turns ratio can be selected to provide outputs widely different from the input; non-isolated versions are limited to a range of approximately 5 times. By selecting the correct turns ratio, the duty cycle of the converter can also be optimised and the peak currents flowing minimised. The polarity of each output is also selectable, dependent upon the polarity of the secondary w.r.t the primary.
- 3) Multiple outputs are very easily obtained, simply by adding more secondary windings to the transformer. There are some disadvantages with transformers, such as their additional size, weight and power loss. The generation of voltage spikes due to leakage inductance may also be a problem.

The isolated converters to be covered are split into two main categories, called asymmetrical and symmetrical converters, depending upon how the transformer is operated.



In asymmetrical converters the magnetic operating point of the transformer is always in one quadrant i.e the flux and the magnetic field never changes sign. The core has to be reset each cycle to avoid saturation, meaning that only half of the usable flux is ever exploited. This can be seen in Fig. 5, which shows the operating mode of each converter. The flyback and forward converter are both asymmetrical types. The diagram also indicates that the flyback converter is operated at a lower permeability (B/H) and lower inductance than the others. This is because the flyback transformer actually stores all of the energy before dumping into the load, hence an air gap is required to store this energy and avoid core saturation. The air gap has the effect of reducing the overall permeability of the core. All of the other converters have true transformer action and ideally store no energy, hence, no air gap is needed.

In the symmetrical converters which always require an even number of transistor switches, the full available flux swing in both quadrants of the B / H loop is used, thus utilising the core much more effectively. Symmetrical converters can therefore produce more power than their asymmetrical cousins. The 3 major symmetrical topologies used in practice are the push-pull, the half-bridge and the full bridge types.

Table 1 outlines the typical maximum output power available from each topology using present day technologies:-

Converter Topology	Typical max output power
Flyback	200W
Forward	300W
Two transistor forward / flyback	400W
Push-pull	500W
Half-Bridge	1000W
Full-Bridge	>1000W

Table 1. Converter output power range.

Many other topologies exist, but the types outlined in Table 1 are by far the most commonly used in present S.M.P.S. designs. Each is now looked at in more detail, with a selection guide for the most suitable Philips power semiconductors included.

(4) Selection of the power semiconductors.

The Power Transistor.

The two most common power semiconductors used in the S.M.P.S. are the Bipolar transistor and the power MOSFET. The Bipolar transistor is normally limited to use at frequencies up to 30kHz, due to switching loss. However, it has very low on-state losses and is a relatively cheap device, making it the most suitable for lower frequency applications. The MOSFET is selected for higher frequency operation because of its very fast switching speeds, resulting in low (frequency dependent) switching losses. The driving of the MOSFET is also far simpler and less expensive than that required for the Bipolar. However, the on-state losses of the MOSFET are far higher than the Bipolar, and they are also usually more expensive. The selection of which particular device to use is normally a compromise between the cost, and the performance required.

(i) Voltage limiting value:-

After deciding upon whether to use a Bipolar or MOSFET, the next step in deciding upon a suitable type is by the correct selection of the transistor voltage. For transformer coupled topologies, the maximum voltage developed across the device is normally at turn-off. This will be either half, full or double the magnitude of the input supply voltage, dependent upon the topology used. There may also be a significant voltage spike due to transformer leakage inductance that must be included. The transistor must safely withstand these worst case values without breaking down. Hence, for a bipolar device, a suitably high $V_{ces(max)}$ must be selected, and for a MOSFET, a suitably high $V_{BR(DSS)}$. At present 1750V is the maximum blocking voltage available for power Bipolars, and a maximum of 1000V for power MOSFETs.

The selection guides assume that a rectified 220V or 110V mains input is used. The maximum dc link voltages that will be produced for these conditions are 385V and 190V respectively. These values are the input voltage levels used to select the correct device voltage rating.

(ii) Current limiting value:-

The Bipolar device has a very low voltage drop across it during conduction, which is relatively constant within the rated current range. Hence, for maximum utilisation of a bipolar transistor, it should be run close to its I_{Csat} value. This gives a good compromise between cost, drive requirements and switching. The maximum current for a particular throughput power is calculated for each topology

using simple equations. These equations are listed in the appropriate sections, and the levels obtained used to select a suitable Bipolar device.

The MOSFET device operates differently from the bipolar in that the voltage developed across it (hence, transistor dissipation) is dependent upon the current flowing and the device "on-resistance" which is variable with temperature. Hence, the optimum MOSFET for a given converter can only be chosen on the basis that the device must not exceed a certain percentage of throughput (output) power. (In this selection a 5% loss in the MOSFET was assumed). A set of equations used to estimate the correct MOSFET $R_{DS(on)}$ value for a particular power level has been derived for each topology. These equations are included in Appendix A at the end of the paper. The value of $R_{DS(on)}$ obtained was then used to select a suitable MOSFET device for each requirement.

NOTE! This method assumes negligible switching losses in the MOSFET. However for frequencies above 50kHz, switching losses become increasingly significant.

Rectifiers

Two types of output rectifier are specified from the Philips range. For very low output voltages below 10V it is necessary to have an extremely low rectifier forward voltage drop, V_F , in order to keep converter efficiency high. Schottky types are specified here, since they have very low V_F values (typically 0.5V). The Schottky also has negligible switching losses and can be used at very high frequencies. Unfortunately, the very low V_F of the Schottky is lost at higher reverse blocking voltages (typically above 100V) and other diode types become more suitable. This means that the Schottky is normally reserved for use on outputs up to 20V or so.

Note. A suitable guideline in selecting the correct rectifier reverse voltage is to ensure the device will block 4 to 6 times the output voltage it is used to provide (depends on topology and whether rugged devices are being used).

For higher voltage outputs the most suitable rectifier is the fast recovery epitaxial diode (FRED). This device has been optimised for use in high frequency rectification. Its characteristics include low V_F (approx. 1V) with very fast and efficient switching characteristics. The FRED has reverse voltage blocking capabilities up to 800V. They are therefore suitable for use in outputs from 10 to 200V.

The rectifier devices specified in each selection guide were chosen as having the correct voltage limiting value and high enough current handling capability for the particular output power specified. (A single output is assumed).

(5) Standard isolated topologies.

(a) The Flyback converter.

Operation

Of all the isolated converters, by far the simplest is the single-ended flyback converter shown in Fig. 6. The use of a single transistor switch means that the transformer can only be driven unipolar (asymmetrical). This results in a large core size. The flyback, which is an isolated version of the buck-boost, does not in truth contain a transformer but a coupled inductor arrangement. When the transistor is turned on, current builds up in the primary and energy is stored in the core, this energy is then released to the output circuit through the secondary when the switch is turned off. (A normal transformer such as the types used in the buck derived topologies couples the energy directly during transistor on-time, ideally storing no energy).

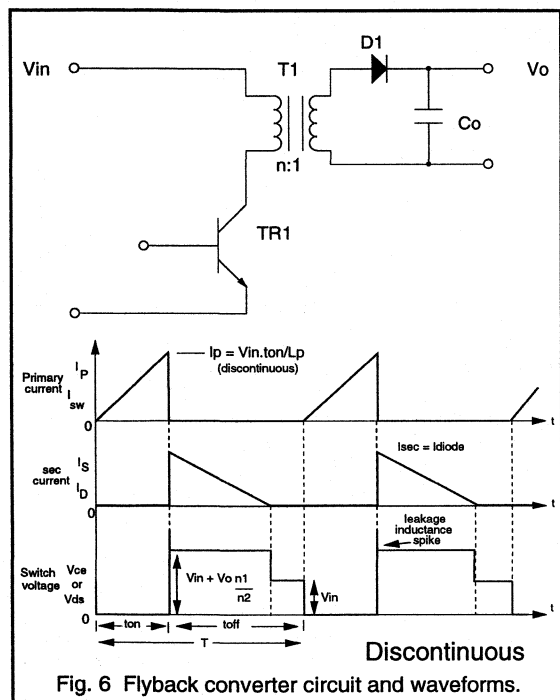


Fig. 6 Flyback converter circuit and waveforms.

The polarity of the windings is such that the output diode blocks during the transistor on time. When the transistor turns off, the secondary voltage reverses, maintaining a constant flux in the core and forcing secondary current to flow through the diode to the output load. The magnitude

of the peak secondary current is the peak primary current reached at transistor turn-off reflected through the turns ratio, thus maintaining a constant Ampere-turn balance.

The fact that all of the output power of the flyback has to be stored in the core as $1/2LI^2$ energy means that the core size and cost will be much greater than in the other topologies, where only the core excitation (magnetisation) energy, which is normally small, is stored. This, in addition to the initial poor unipolar core utilisation, means that the transformer bulk is one of the major drawbacks of the flyback converter.

In order to obtain sufficiently high stored energy, the flyback primary inductance has to be significantly lower than required for a true transformer, since high peak currents are needed. This is normally achieved by gapping the core. The gap reduces the inductance, and most of the high peak energy is then stored in the gap, thus avoiding transformer saturation.

When the transistor turns off, the output voltage is back reflected through the transformer to the primary and in many cases this can be nearly as high as the supply voltage. There is also a voltage spike at turn-off due to the stored energy in the transformer leakage inductance. This means that the transistor must be capable of blocking approximately twice the supply voltage plus the leakage spike. Hence, for a 220V ac application where the dc link can be up to 385V, the transistor voltage limiting value must lie between 800 and 1000V.

Using a 1000V Bipolar transistor such as the BUT11A or BUW13A allows a switching frequency of 30kHz to be used at output powers up to 200Watts.

MOSFETs with 800V and 1000V limiting values can also be used, such as the BUK456-800A which can supply 100W at switching frequencies anywhere up to 300kHz. Although the MOSFET can be switched much faster and has lower switching losses, it does suffer from significant on-state losses, especially in the higher voltage devices when compared to the bipolars. An outline of suitable transistors and output rectifiers for different input and power levels using the flyback is given in Table 2.

One way of removing the transformer leakage voltage spike is to add a clamp winding as shown in Fig. 8. This allows the leakage energy to be returned to the input instead of stressing the transistor. The diode is always placed at the high voltage end so that the clamp winding capacitance does not interfere with the transistor turn-on current spike, which would happen if the diode was connected to ground. This clamp is optional and depends on the designer's particular requirements.

Advantages.

The action of the flyback means that the secondary inductance is in series with the output diode when current is delivered to the load; i.e. driven from a current source. This means that no filter inductor is needed in the output circuit. Hence, each output requires only one diode and output filter capacitor. This means the flyback is the ideal choice for generating low cost, multiple output supplies. The cross regulation obtained using multiple outputs is also very good (load changes on one output have little effect on the others) because of the absence of the output choke, which degrades this dynamic performance.

The flyback is also ideally suited for generating high voltage outputs. If a buck type LC filter was used to generate a high voltage, a very large inductance value would be needed to reduce the ripple current levels sufficiently to achieve the continuous mode operation required. This restriction does not apply to the flyback, since it does not require an output inductance for successful operation.

Disadvantages.

From the flyback waveforms in Fig. 6 it is clear that the output capacitor is only supplied during the transistor off time. This means that the capacitor has to smooth a pulsating output current which has higher peak values than the continuous output current that would be produced in a forward converter, for example. In order to achieve low output ripple, very large output capacitors are needed, with very low equivalent series resistance (e.s.r.). It can be shown that at the same frequency, an LC filter is approximately 8 times more effective at ripple reduction than a capacitor alone. Hence, flybacks have inherently much higher output ripples than other topologies. This, together with the higher peak currents, large capacitors and transformers, limits the flyback to lower output power applications in the 20 to 200W range. (It should be noted that at higher voltages, the required output voltage ripple magnitudes are not normally as stringent, and this means that the e.s.r. requirement and hence capacitor size will not be as large as expected.)

Two transistor flyback.

One possible solution to the 1000V transistor requirement is the two transistor flyback version shown in Fig. 7. Both transistors are switched simultaneously, and all waveforms are exactly the same, except that the voltage across each transistor never exceeds the input voltage. The clamp winding is now redundant, since the two clamp diodes act to return leakage energy to the input. Two 400 or 500V devices can now be selected, which will have faster switching and lower conduction losses. The output power and switching frequencies can thus be significantly increased. The drawbacks of the two transistor version are the extra cost and more complex isolated base drive needed for the top floating transistor.

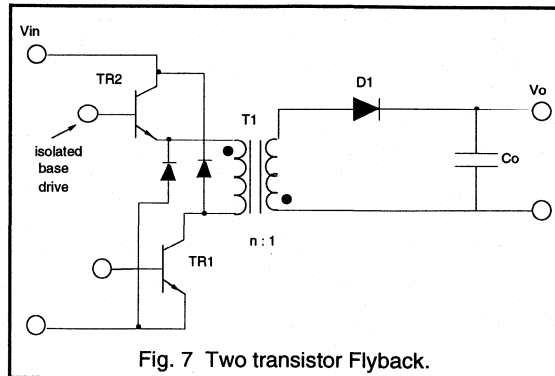


Fig. 7 Two transistor Flyback.

Continuous Vs Discontinuous operation.

As with the buck-boost, the flyback can operate in both continuous and discontinuous modes. The waveforms in Fig. 6 show discontinuous mode operation. In discontinuous mode, the secondary current falls to zero in each switching period, and all of the energy is removed from the transformer. In continuous mode there is current flowing in the coupled inductor at all times, resulting in trapezoidal current waveforms.

The main plus of continuous mode is that the peak currents flowing are only half that of the discontinuous for the same output power, hence, lower output ripple is possible. However, the core size is about 2 to 4 times larger in continuous mode to achieve the increased inductance needed to reduce the peak currents to achieve continuity.

A further disadvantage of continuous mode is that the closed loop is far more difficult to control than the discontinuous mode flyback. (Continuous mode contains a right hand plane zero in its open loop frequency response, the discontinuous flyback does not. See Ref[2] for further explanation.) This means that much more time and effort is required for continuous mode to design the much more complicated compensation components needed to achieve stability.

There is negligible turn-on dissipation in the transistor in discontinuous mode, whereas this dissipation can be fairly high in continuous mode, especially when the additional effects of the output diode reverse recovery current, which only occurs in the continuous case, is included. This normally means that a snubber must be added to protect the transistor against switch-on stresses.

One advantage of the continuous mode is that its open loop gain is independent of the output load i.e. V_o only depends upon D and V_{in} , as shown in the dc gain equation at the end of the section. Continuous mode has excellent open loop load regulation, i.e. varying the output load will not affect V_o . Discontinuous mode, on the other-hand, does have a dependency on the output, expressed as R_L in the dc gain equation. Hence, discontinuous mode has a much poorer

open loop load regulation, i.e changing the output will affect V_o . This problem disappears, however, when the control loop is closed, and the load regulation problem is usually completely overcome.

The use of current mode control with discontinuous flyback (where both the primary current and output voltage are sensed and combined to control the duty cycle) produces

a much improved overall loop regulation, requiring less closed loop gain.

Although the discontinuous mode has the major disadvantage of very high peak currents and a large output capacitor requirement, it is much easier to implement, and is by far the more common of the two methods used in present day designs.

Output power	50W		100W		200W	
	110V ac	220V ac	110V ac	220V ac	110V ac	220V ac
Line voltage, V_{in}						
Transistor requirements						
Max current	2.25A	1.2A	4A	2.5A	8A	4.4A
Max voltage	400V	800V	400V	800V	400V	800V
Bipolar transistors.						
TO-220	BUT11	BUX85	BUT12	BUT11A	---	BUT12A
Isolated SOT-186	BUT11F	BUX85F	BUT12F	BUT11AF	---	BUT12AF
SOT-93	---	---	---	---	BUW13	---
Isolated SOT-199	---	---	---	---	BUW13F	---
Power MOSFET						
TO-220	BUK454-400B	BUK454-800A	BUK455-400B	BUK456-800A	---	---
Isolated SOT-186	BUK444-400B	BUK444-800A	BUK445-400B	BUK446-800A	---	---
SOT-93	---	---	---	---	BUK437-400B	BUK438-800A
Output Rectifiers						
O/P voltage						
5V	PBYR1635		PBYR2535CT		---	
10V	PBYR10100		PBYR20100CT		PBYR30100PT	
	BYW29E-100/150/200		BYV79E-100/150/200		BYV42E-100/150/200	
					BYV72E-100/150/200	
20V	PBYR10100		PBYR10100		PBYR20100CT	
	BYW29E-100/150/200		BYW29E-100/150/200		BYV32E-100/150/200	
	BYV29-300		BYV29-300		BYV29-300	
50V	BYV29-500		BYV29-500		BYV29-500	
100V						

Table 2. Recommended Power Semiconductors for single-ended flyback.

Note! The above values are for discontinuous mode. In continuous mode the peak transistor currents are approximately halved and the output power available is thus increased.

Flyback

Converter efficiency, $\eta = 80\%$; Max duty cycle, $D_{max} = 0.45$

Max transistor voltage, V_{ce} or $V_{ds} = 2V_{in(max)} + \text{leakage spike}$

$$\text{Max transistor current, } I_C ; I_D = 2 \frac{P_{out}}{\eta D_{max} V_{min}}$$

$$\text{dc voltage gain:- (a) continuous } \frac{V_o}{V_{in}} = n \frac{D}{1-D}$$

$$\text{(b) Discontinuous } \frac{V_o}{V_{in}} = D \sqrt{\frac{R_L T}{2 L_p}}$$

Applications:- Lowest cost, multiple output supplies in the 20 to 200W range. E.g. mains input T.V. supplies, small computer supplies, E.H.T. supplies.

(b) The Forward converter.

Operation.

The forward converter is also a single switch isolated topology, and is shown in Fig. 8. This is based on the buck converter described earlier, with the addition of a transformer and another diode in the output circuit. The characteristic LC output filter is clearly present.

In contrast to the flyback, the forward converter has a true transformer action, where energy is transferred directly to the output through the inductor during the transistor on-time. It can be seen that the polarity of the secondary winding is opposite to that of the flyback, hence allowing direct current flow through blocking diode D1. During the on-time, the current flowing causes energy to be built up in the output inductor L1. When the transistor turns off, the secondary voltage reverses, D1 goes from conducting to blocking mode and the freewheel diode D2 then becomes forward biased and provides a path for the inductor current to continue to flow. This allows the energy stored in L1 to be released into the load during the transistor off time.

The forward converter is always operated in continuous mode (in this case the output inductor current), since this produces very low peak input and output currents and small ripple components. Going into discontinuous mode would greatly increase these values, as well as increasing the amount of switching noise generated. No destabilising right hand plane zero occurs in the frequency response of the forward in continuous mode (as with the buck). See Ref[2]. This means that the control problems that existed with the continuous flyback are not present here. So there are no real advantages to be gained by using discontinuous mode operation for the forward converter.

Advantages.

As can be seen from the waveforms in Fig. 8, the inductor current I_L , which is also the output current, is always continuous. The magnitude of the ripple component, and hence the peak secondary current, depends upon the size of the output inductor. Therefore, the ripple can be made relatively small compared to the output current, with the peak current minimised. This low ripple, continuous output current is very easy to smooth, and so the requirements for the output capacitor size, e.s.r and peak current handling are far smaller than they are for the flyback.

Since the transformer in this topology transfers energy directly there is negligible stored energy in the core compared to the flyback. However, there is a small magnetisation energy required to excite the core, allowing it to become an energy transfer medium. This energy is very small and only a very small primary magnetisation current is needed. This means that a high primary

inductance is usually suitable, with no need for the core air gap required in the flyback. Standard un-gapped ferrite cores with high permeabilities (2000-3000) are ideal for providing the high inductance required. Negligible energy storage means that the forward converter transformer is considerably smaller than the flyback, and core loss is also much smaller for the same throughput power. However, the transformer is still operated asymmetrically, which means that power is only transferred during the switch on-time, and this poor utilisation means the transformer is still far bigger than in the symmetrical types.

The transistors have the same voltage rating as the discontinuous flyback (see disadvantages), but the peak current required for the same output power is halved, and this can be seen in the equations given for the forward converter. This, coupled with the smaller transformer and output filter capacitor requirements means that the forward converter is suitable for use at higher output powers than the flyback can attain, and is normally designed to operate in the 100 to 400W range. Suitable bipolars and MOSFETs for the forward converter are listed in Table 3.

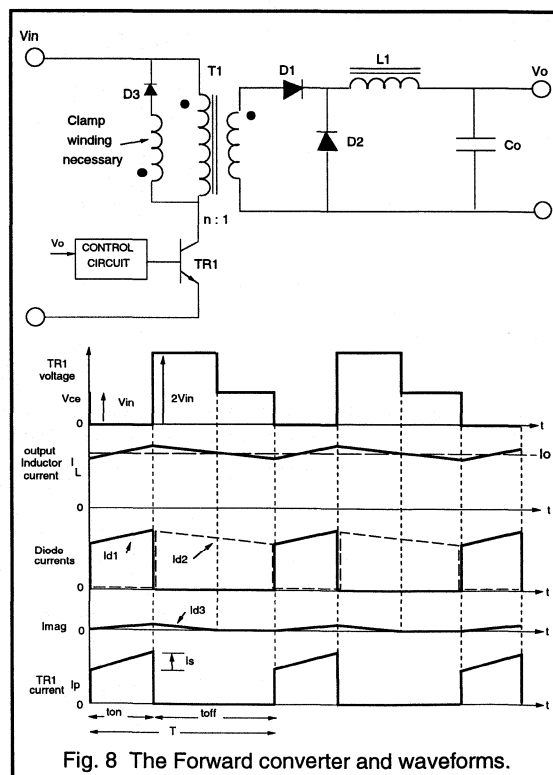


Fig. 8 The Forward converter and waveforms.

Disadvantages.

Because of the unipolar switching action of the forward converter, there is a major problem in how to remove the core magnetisation energy by the end of each switching cycle. If this did not happen, there would be a net dc flux build-up, leading to core saturation, and possible transistor destruction. This magnetisation energy is removed automatically by the push-pull action of the symmetrical types. In the flyback this energy is dumped into the load at transistor turn-off. However, there is no such path in the forward circuit.

This path is provided by adding an additional reset winding of opposite polarity to the primary. A clamp diode is added, such that the magnetisation energy is returned to the input supply during the transistor off time. The reset winding is wound bifilar with the primary to ensure good coupling, and is normally made to have the same number of turns as the primary. (The reset winding wire gauge can be very small, since it only has to conduct the small magnetisation current.) The time for the magnetisation energy to fall to zero is thus the same duration as the transistor on-time. This means that the maximum theoretical duty ratio of the forward converter is 0.5 and after taking into account switching delays, this falls to 0.45. This limited control range is one of the drawbacks of using the forward converter. The waveform of the magnetisation current is also shown in Fig. 8. The clamp winding in the flyback is optional, but is always needed in the forward for correct operation.

Due to the presence of the reset winding, in order to maintain volt-sec balance within the transformer, the input voltage is back reflected to the primary from the clamp winding at transistor turn-off for the duration of the flow of the magnetisation reset current through D3. (There is also a voltage reversal across the secondary winding, and this is why diode D1 is added to block this voltage from the output circuit.) This means that the transistor must block two times V_{in} during switch-off. The voltage returns to V_{in} after reset has finished, which means transistor turn-on losses will be smaller. The transistors must have the same added burden of the voltage rating of the flyback, i.e. 400V for 110V mains and 800V for 220V mains applications.

Output diode selection.

The diodes in the output circuit both have to conduct the full magnitude of the output current. They are also subject to abrupt changes in current, causing a reverse recovery spike, particularly in the freewheel diode, D2. This spike can cause additional turn-on switching loss in the transistor, possibly causing device failure in the absence of snubbing. Thus, very high efficiency, fast trr diodes are required to minimise conduction losses and to reduce the reverse recovery spike. These requirements are met with Schottky diodes for outputs up to 20V, and fast recovery epitaxial diodes for higher voltage outputs. It is not normal for forward converter outputs to exceed 100V because of the need for

a very large output choke, and flybacks are normally used. Usually, both rectifiers are included in a single package i.e. a dual centre-tap arrangement. The Philips range of Schottkies and FREDs which meet these requirements are also included in Table 3.

Two transistor forward.

In order to avoid the use of higher voltage transistors, the two transistor version of the forward can be used. This circuit, shown in Fig. 9, is very similar to the two transistor flyback and has the same advantages. The voltage across the transistor is again clamped to V_{in} , allowing the use of faster more efficient 400 or 500V devices for 220V mains applications. The magnetisation reset is achieved through the two clamp diodes, permitting the removal of the clamp winding.

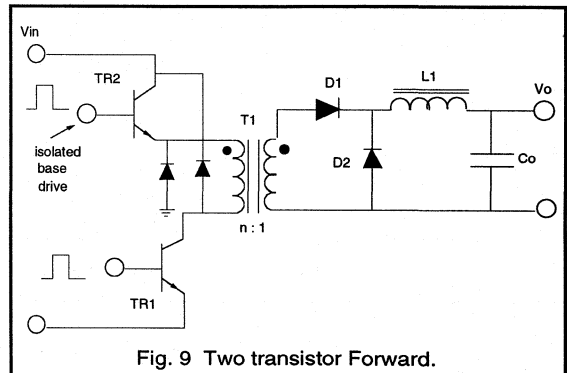


Fig. 9 Two transistor Forward.

The two transistor version is popular for off-line applications. It provides higher output powers and faster switching frequencies. The disadvantages are again the extra cost of the higher component count, and the need for an isolated drive for the top transistor.

Although this converter has some drawbacks, and utilises the transformer poorly, it is a very popular selection for the power range mentioned above, and offers simple drive for the single switch and cheap component costs. Multiple output types are very common. The output inductors are normally wound on a single core, which has the effect of improving dynamic cross regulation, and if designed correctly also reduces the output ripple magnitudes even further. The major advantage of the forward converter is the very low output ripple that can be achieved for relatively small sized LC components. This means that forward converters are normally used to generate lower voltage, high current multiple outputs such as 5, 12, 15, 28V from mains off-line applications, where lower ripple specifications are normally specified for the outputs. The high peak currents that would occur if a flyback was used would place an impossible burden on the smoothing capacitor.

Output power	100W		200W		300W	
Line voltage, V_{in}	110V ac	220V ac	110V ac	220V ac	110V ac	220V ac
Transistor requirements Max current Max voltage	2.25A 400V	1.2A 800V	4A 400V	2.5A 800V	6A 400V	3.3A 800V
Bipolar transistors. TO-220 Isolated SOT-186 SOT-93 Isolated SOT-199	BUT11 BUT11F --- ---	BUX85 BUX85F --- ---	BUT12 BUT12F --- ---	BUT11A BUT11AF --- ---	--- --- BUW13 BUW13F	BUT12A BUT12AF --- ---
Power MOSFET TO-220 Isolated SOT-186 SOT-93	BUK454-400B BUK444-400B ---	BUK454-800A BUK444-800A ---	BUK455-400B BUK445-400B ---	BUK456-800A BUK446-800A ---	--- --- BUK437-400B	--- --- BUK438-800A
Output Rectifiers (dual) O/P voltage 5V 10V 20V 50V	PBYR2535CT PBYR20100CT BYV32E-100/150/200 PBYR20100CT BYQ28E-100/150/200 BYT28-300		--- PBYR30100PT BYV42E-100/150/200 BYV72E100/150/200 PBYR20100CT BYV32E-100/150/200 BYT28-300		--- PBYR30100PT BYV72E-100/150/200 PBYR20100CT BYV32E-100/150/200 BYT28-300	

Table 3. Recommended Power Semiconductors for single-ended forward.

<p>Forward</p> <p>Converter efficiency, $\eta = 80\%$; Max duty cycle, $D_{max} = 0.45$</p> <p>Max transistor voltage, V_{ce} or $V_{ds} = 2V_{in(max)}$</p> <p>Max transistor current, I_C ; $I_D = \frac{P_{out}}{\eta D_{max} V_{min}}$</p> <p>dc voltage gain:- $\frac{V_o}{V_{in}} = n D$</p> <p>Applications:- Low cost, low output ripple, multiple output supplies in the 50 to 400W range. E.g. small computer supplies, DC/DC converters.</p>
--

(c) The Push-pull converter.

Operation.

To utilise the transformer flux swing fully, it is necessary to operate the core symmetrically as described earlier. This permits much smaller transformer sizes and provides higher output powers than possible with the single ended types. The symmetrical types always require an even number of transistor switches. One of the best known of the symmetrical types is the push-pull converter shown in Fig. 10.

The primary is a centre-tapped arrangement and each transistor switch is driven alternately, driving the transformer in both directions. The push-pull transformer is typically half the size of that for the single ended types, resulting in a more compact design. This push-pull action produces natural core resetting during each half cycle, hence no clamp winding is required. Power is transferred to the buck type output circuit during each transistor conduction period. The duty ratio of each switch is usually less than 0.45. This provides enough dead time to avoid transistor cross conduction. The power can now be transferred to the output for up to 90% of the switching period, hence allowing greater throughput power than with the single-ended types. The push-pull configuration is normally used for output powers in the 100 to 500W range.

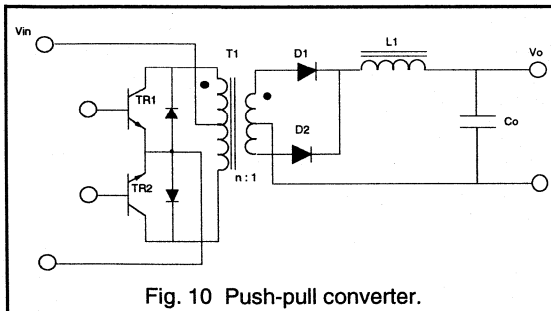


Fig. 10 Push-pull converter.

The bipolar switching action also means that the output circuit is actually operated at twice the switching frequency of the power transistors, as can be seen from the waveforms in Fig. 11. Therefore, the output inductor and capacitor can be even smaller for similar output ripple levels. Push-pull converters are thus excellent for high power density, low ripple outputs.

Advantages.

As stated, the push-pull offers very compact design of the transformer and output filter, while producing very low output ripple. So if space is a premium issue, the push-pull could be suitable. The control of the push-pull is similar to the forward, in that it is again based on the continuous mode

buck. When closing the feedback control loop, compensation is relatively easy. For multiple outputs, the same recommendations given for the forward converter apply.

Clamp diodes are fitted across the transistors, as shown. This allows leakage and magnetisation energy to be simply channelled back to the supply, reducing stress on the switches and slightly improving efficiency.

The emitter or source of the power transistors are both at the same potential in the push-pull configuration, and are normally referenced to ground. This means that simple base drive can be used for both, and no costly isolating drive transformer is required. (This is not so for the bridge types which are discussed later.)

Disadvantages.

One of the main drawbacks of the push-pull converter is the fact that each transistor must block twice the input voltage due to the doubling effect of the centre-tapped primary, even though two transistors are used. This occurs when one transistor is off and the other is conducting. When both are off, each then blocks the supply voltage, this is shown in the waveforms in Fig. 11. This means that TWO expensive, less efficient 800 to 1000V transistors would be required for a 220V off-line application. A selection of transistors and rectifiers suitable for the push-pull used in off-line applications is given in Table 4.

A further major problem with the push-pull is that it is prone to flux symmetry imbalance. If the flux swing in each half cycle is not exactly symmetrical, the volt-sec will not balance and this will result in transformer saturation, particularly for high input voltages. Symmetry imbalance can be caused by different characteristics in the two transistors such as storage time in a bipolar and different on-state losses.

The centre-tap arrangement also means that extra copper is needed for the primary, and very good coupling between the two halves is necessary to minimise possible leakage spikes. It should also be noted that if snubbers are used to protect the transistors, the design must be very precise since each tends to interact with the other. This is true for all symmetrically driven converters.

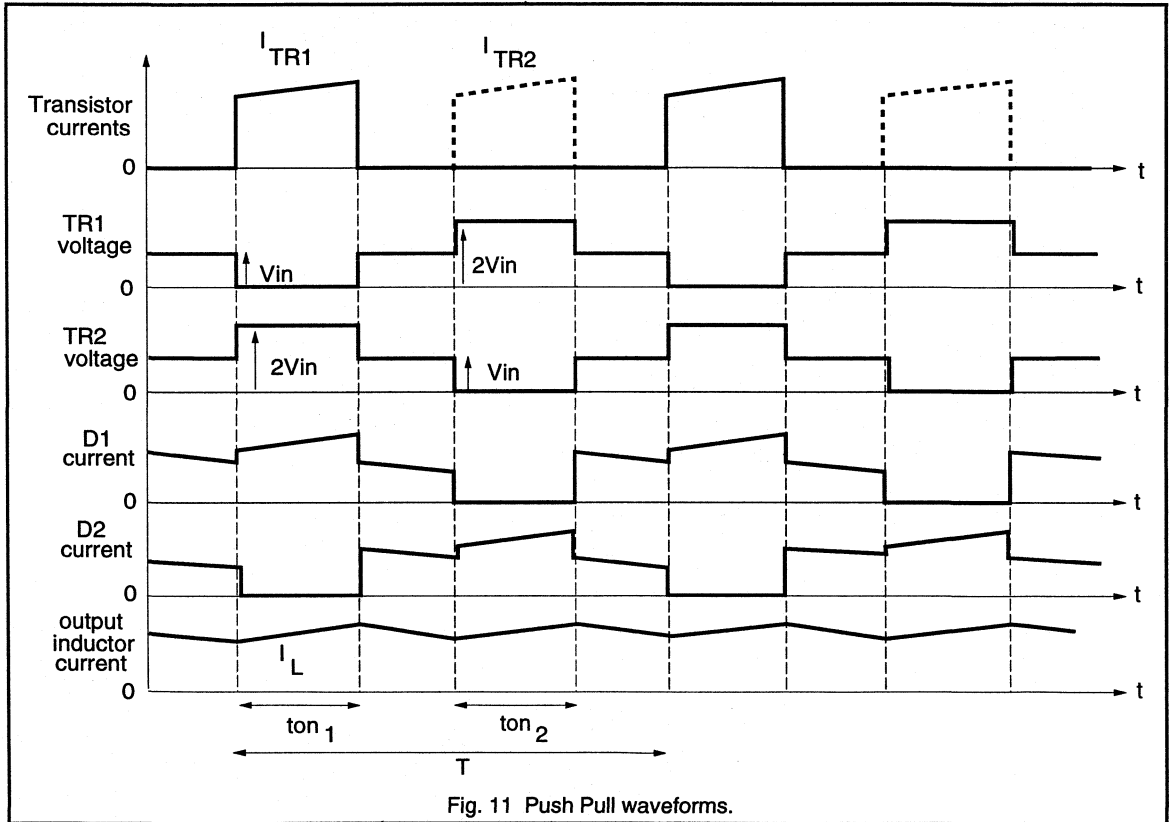
These disadvantages usually dictate that the push-pull is normally operated at lower voltage inputs such as 12, 28 or 48V. DC-DC converters found in the automotive and telecommunication industries are often push-pull designs. At these voltage levels, transformer saturation is easier to avoid.

Since the push-pull is commonly operated with low dc voltages, a selection guide for suitable power MOSFETs is also included for 48 and 96V applications, seen in Table 5.

Current mode control.

The introduction of current mode control circuits has also benefited the push-pull type. In this type of control, the primary current is monitored, and any imbalance which occurs is corrected on a cycle by cycle basis by varying the duty cycle immediately. Current mode control completely

removes the symmetry imbalance problem, and the possibilities of saturation are minimised. This has meant that push-pull designs have become more popular in recent years, with some designers even using them in off-line applications.



Output power	100W		300W		500W	
Line voltage, V_{in}	110V ac	220V ac	110V ac	220V ac	110V ac	220V ac
Transistor requirements						
Max current	1.2A	0.6A	4.8A	3.0A	5.8A	3.1A
Max voltage	400V	800V	400V	800V	400V	800V
Bipolar transistors.						
TO-220	BUT11	BUX85	BUT12	BUT11A	---	BUT12A
Isolated SOT-186	BUT11F	BUX85F	BUT12F	BUT11AF	---	BUT12AF
SOT-93	---	---	---	---	BUW13	---
Isolated SOT-199	---	---	---	---	BUW13F	---
Power MOSFET						
TO-220	BUK454-400B	BUK454-800A	BUK455-400B	BUK456-800A	---	---
Isolated SOT-186	BUK444-400B	BUK444-800A	BUK445-400B	BUK446-800A	---	---
SOT-93	---	---	---	---	BUK437-400B	BUK438-800A
Output Rectifiers (dual)						
O/P voltage						
5V	PBYR2535CT		---		---	
10V	PBYR20100CT		PBYR30100PT		---	
20V	BYV32E-100/150/200		BYV72E-100/150/200		BYT230PI-200	
50V	PBYR20100CT		PBYR20100CT		PBYR30100PT	
	BYQ28E-100/150/200		BYV32E-100/150/200		BYV42E-100/150/200	
					BYV72E-100/150/200	
					BYV34-300	

Table 4. Recommended Power Semiconductors for off-line Push-pull converter.

Output power	100W		200W		300W	
Line voltage, V_{in}	96V dc	48V dc	96V dc	48V dc	96V dc	48V dc
Power MOSFET						
TO-220	BUK455-400B	BUK454-200A	BUK457-400B	BUK456-200B	---	---
Isolated SOT-186	BUK445-400B	BUK444-200A	BUK437-400B	BUK436-200B	---	---
SOT-93	---	---	---	---	BUK437-400B	---

Table 5. Recommended power MOSFETs for lower input voltage push-pull.

Push-Pull converter.Converter efficiency, $\eta = 80\%$; Max duty cycle, $D_{max} = 0.9$ Max transistor voltage, V_{ce} or $V_{ds} = 2V_{in(max)} + \text{leakage spike}$.

$$\text{Max transistor current, } I_C ; I_D = \frac{P_{out}}{\eta D_{max} V_{min}}$$

$$\text{dc voltage gain:- } \frac{V_o}{V_{in}} = 2 n D$$

Applications:- Compact design, very low output ripple supplies in the 100 to 500W range. More suited to low input applications. E.g. battery, 28, 40V inputs, high current outputs. Telecommunication supplies.

(d) The Half-Bridge.

Of all the symmetrical high power converters, the half-bridge converter shown in Fig. 12 is the most popular. It is also referred to as the single ended push-pull, and in principle is a balanced version of the forward converter. Again it is a derivative of the buck. The Half-Bridge has some key advantages over the push-pull, which usually makes it first choice for higher power applications in the 500 to 1000W range.

Operation.

The two mains bulk capacitors C1 and C2 are connected in series, and an artificial input voltage mid-point is provided, shown as point A in the diagram. The two transistor switches are driven alternately, and this connects each capacitor across the single primary winding each half cycle. $V_{in}/2$ is superimposed symmetrically across the primary in a push-pull manner. Power is transferred directly to the output on each transistor conduction time and a maximum duty cycle of 90% is available (Some dead time is required to prevent transistor cross-conduction.) Since the primary is driven in both directions, (natural reset) a full wave buck output filter (operating at twice the switching frequency) rather than a half wave filter is implemented. This again results in very efficient core utilisation. As can be seen in Fig. 13, the waveforms are identical to the push-pull, except that the voltage across the transistors is halved. (The device current would be higher for the same output power.)

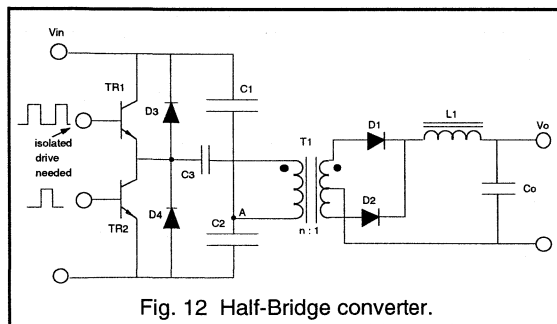


Fig. 12 Half-Bridge converter.

Advantages.

Since both transistors are effectively in series, they never see greater than the supply voltage, V_{in} . When both are off, their voltages reach an equilibrium point of $V_{in}/2$. This is half the voltage rating of the push-pull (although double the

current). This means that the half-bridge is particularly suited to high voltage inputs, such as off-line applications. For example, a 220V mains application can use two higher speed, higher efficiency 450V transistors instead of the 800V types needed for a push-pull. This allows higher frequency operation.

Another major advantage over the push-pull is that the transformer saturation problems due to flux symmetry imbalance are not a problem. By using a small capacitor (less than $10\mu\text{F}$) any dc build-up of flux in the transformer is blocked, and only symmetrical ac is drawn from the input.

The configuration of the half-bridge allows clamp diodes to be added across the transistors, shown as D3 and D4 in Fig. 12. The leakage inductance and magnetisation energies are dumped straight back into the two input capacitors, protecting the transistors from dangerous transients and improving overall efficiency.

A less obvious exclusive advantage of the half-bridge is that the two series reservoir capacitors already exist, and this makes it ideal for implementing a voltage doubling circuit. This permits the use of either 110V /220V mains as selectable inputs to the supply.

The bridge circuits also have the same advantages over the single-ended types that the push-pull possesses, including excellent transformer utilisation, very low output ripple, and high output power capabilities. The limiting factor in the maximum output power available from the half-bridge is the peak current handling capabilities of present day transistors. 1000W is typically the upper power limit. For higher output powers the four switch full bridge is normally used.

Disadvantages.

The need for two 50/60 Hz input capacitors is a drawback because of their large size. The top transistor must also have isolated drive, since the gate / base is at a floating potential. Furthermore, if snubbers are used across the power transistors, great care must be taken in their design, since the symmetrical action means that they will interact with one another. The circuit cost and complexity have clearly increased, and this must be weighed up against the advantages gained. In many cases, this normally excludes the use of the half-bridge at output power levels below 500W.

Suitable transistors and rectifiers for the half-bridge are given in Table 6.

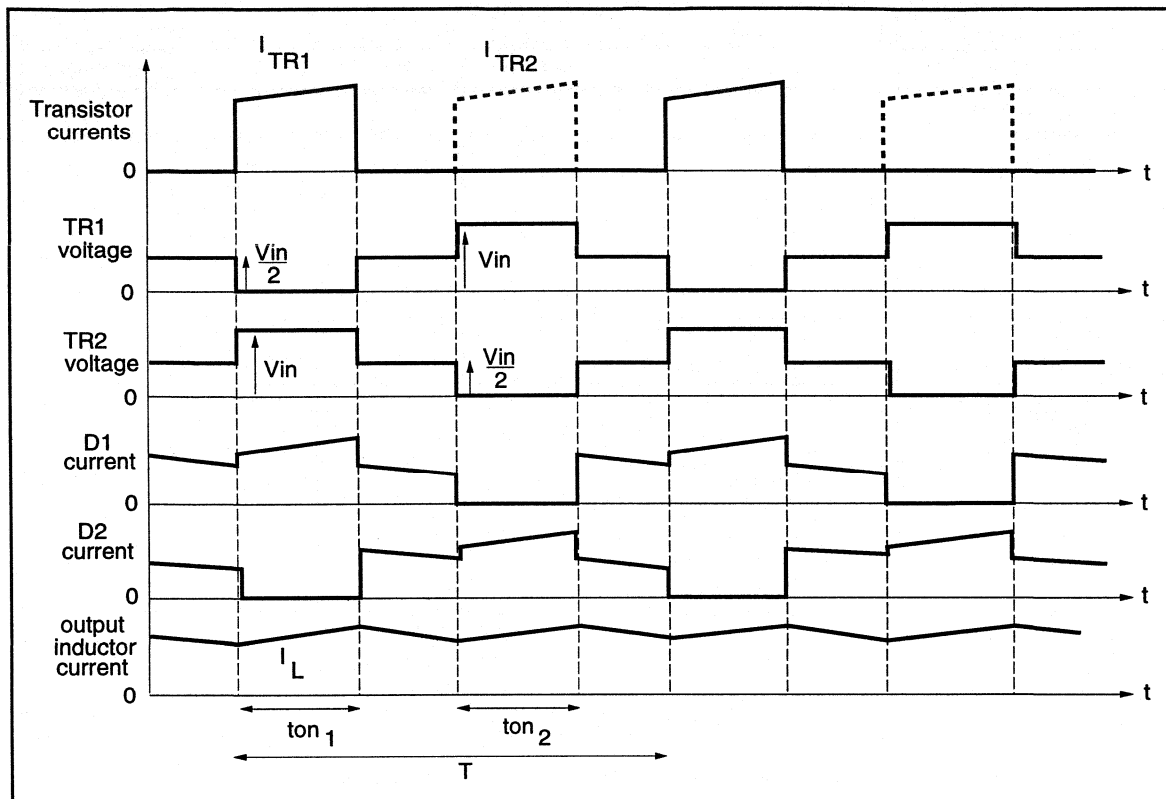


Fig. 13 Half-Bridge waveforms.

Output power	300W		500W		750W	
	110V ac	220V ac	110V ac	220V ac	110V ac	220V ac
Line voltage, Vin	110V ac	220V ac	110V ac	220V ac	110V ac	220V ac
Transistor requirements						
Max current	4.9A	2.66A	11.7A	6.25A	17.5A	9.4A
Max voltage	250V	450V	250V	450V	250V	450V
Bipolar transistors.						
TO-220	BUT12	BUT11	---	---	---	---
Isolated SOT-186	BUT12F	BUT11F	---	---	---	---
SOT-93	---	---	BUW13	BUW13	---	BUW13
Isolated SOT-199	---	---	BUW13F	BUW13F	---	BUW13F
Power MOSFET						
SOT-93	---	BUK437-500B	---	---	---	---
Output Rectifiers (dual)						
O/P voltage						
5V	---	---	---	---	---	---
10V	PBYR30100PT	---	---	---	---	---
20V	BYV72E-100/150/200	---	---	---	---	---
50V	PBYR20100CT	---	PBYR30100PT	---	---	---
	BYV32E-100/150/200	---	BYV42E-100/150/200	---	---	---
	BYT28-300	---	BYV72E-100/150/200	---	---	---
			BYV34-300	---	---	---
					BYV34-300	---

Table 6. Recommended Power Semiconductors for off-line Half-Bridge converter.

Half-Bridge converter.

Converter efficiency, $\eta = 80\%$; Max duty cycle, $D_{max} = 0.9$

Max transistor voltage, V_{ce} or $V_{ds} = V_{in(max)} + \text{leakage spike.}$

Max transistor current, I_C ; $I_D = 2 \frac{P_{out}}{\eta D_{max} V_{min}}$

dc voltage gain:- $\frac{V_o}{V_{in}} = n D$

Applications:- High power, up to 1000W. High current, very low output ripple outputs. Well suited for high input voltage applications. E.g. 110, 220, 440V mains. E.g. Large computer supplies, Lab equipment supplies.

(e) The Full-Bridge.Outline.

The Full-Bridge converter shown in Fig. 14 is a higher power version of the Half-Bridge, and provides the highest output power level of any of the converters discussed. The maximum current ratings of the power transistors will eventually determine the upper limit of the output power of the half-bridge. These levels can be doubled by using the Full-Bridge, which is obtained by adding another two transistors and clamp diodes to the Half-Bridge arrangement. The transistors are driven alternately in pairs, T1 and T3, then T2 and T4. The transformer primary is now subjected to the full input voltage. The current levels flowing are halved compared to the half-bridge for a given power level. Hence, the Full-Bridge will double the output power of the Half-Bridge using the same transistor types.

The secondary circuit operates in exactly the same manner as the push-pull and half-bridge, also producing very low ripple outputs at very high current levels. Therefore, the waveforms for the Full-Bridge are identical to the Half-Bridge waveforms shown in Fig. 13, except for the voltage across the primary, which is effectively doubled (and switch currents halved). This is expressed in the dc gain and peak current equations, where the factor of two comes in, compared with the Half-Bridge.

Advantages.

As stated, the Full-Bridge is ideal for the generation of very high output power levels. The increased circuit complexity normally means that the Full-Bridge is reserved for applications with power output levels of 1kW and above. For such high power requirements, designers often select power Darlington's, since their superior current ratings and switching characteristics provide additional performance and in many cases a more cost effective design.

The Full-Bridge also has the advantage of only requiring one mains smoothing capacitor compared to two for the Half-Bridge, hence, saving space. Its other major advantages are the same as for the Half-Bridge.

Disadvantages.

Four transistors and clamp diodes are needed instead of two for the other symmetrical types. Isolated drive for two floating potential transistors is now required. The Full-Bridge has the most complex and costly design of any of the converters discussed, and should only be used where other types do not meet the requirements. Again, the four transistor snubbers (if required) must be implemented carefully to prevent interactions occurring between them.

Table 7 gives an outline of the Philips power semiconductors suitable for use with the Full-Bridge.

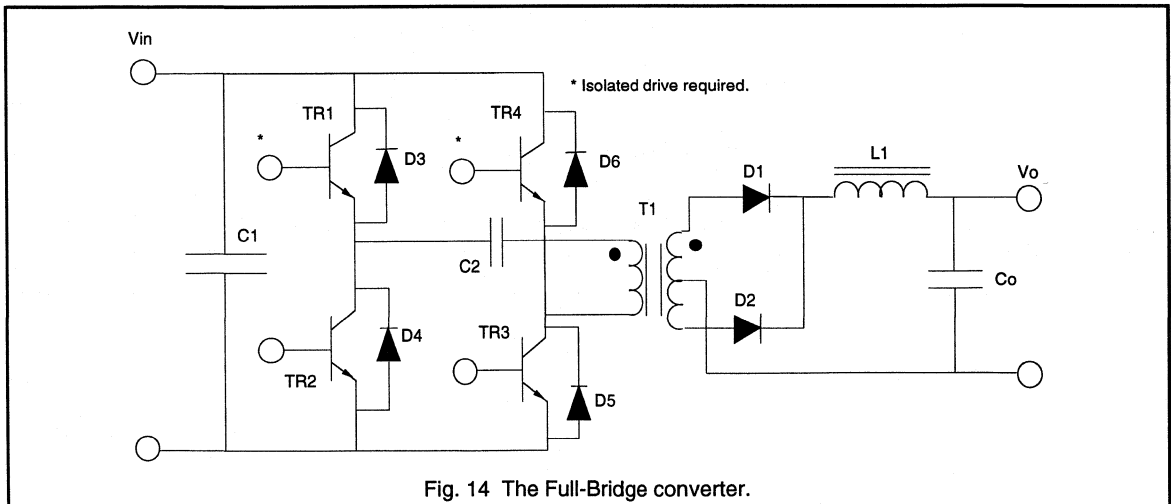


Fig. 14 The Full-Bridge converter.

Output power	500W		1000W		2000W	
	110V ac	220V ac	110V ac	220V ac	110V ac	220V ac
Transistor requirements						
Max current	5.7A	3.1A	11.5A	6.25A	23.0A	12.5A
Max voltage	250V	450V	250V	450V	250V	450V
Bipolar transistors.						
TO-220	BUT12	BUT18	---	---	---	---
Isolated SOT-186	BUT12F	BUT18F	---	---	---	---
SOT-93	---	---	BUW13	BUW13	---	BUW13
Isolated SOT-199	---	---	BUW13F	BUW13F	---	BUW13F
Power MOSFET						
SOT-93	---	BUK438-500B	---	---	---	---
Output Rectifiers (dual)						
O/P voltage						
5V	---		---		---	
10V	---		---		---	
20V	PBYR30100PT		---		---	
	BYV42E-100/150/200					
	BYV72E-100/150/200					
50V	BYV34-300		BYV44-300		---	

Table 7. Recommended Power Semiconductors for the Full-Bridge converter.

Full-Bridge converter.Converter efficiency, $\eta = 80\%$; Max duty cycle, $D_{\max} = 0.9$ Max transistor voltage, V_{ce} or $V_{ds} = V_{in(\max)} + \text{leakage spike}$.

$$\text{Max transistor current, } I_C ; I_D = \frac{P_{out}}{\eta D_{\max} V_{min}}$$

$$\text{dc voltage gain:- } \frac{V_o}{V_{in}} = 2 n D$$

Applications:- Very high power, normally above 1000W. Very high current, very low ripple outputs. Well suited for high input voltage applications. E.g. 110, 220, 440V mains. E.g. Computer Mainframe supplies, Large lab equipment supplies, Telecomm systems.

Conclusion.

The 5 most common S.M.P.S. converter topologies, the flyback, forward, push-pull, half-bridge and full-bridge types have been outlined. Each has its own particular operating characteristics and advantages, which makes it suited to particular applications.

The converter topology also defines the voltage and current requirements of the power transistors (either MOSFET or Bipolar). Simple equations and calculations used to outline the requirements of the transistors for each topology have been presented.

The selection guide for transistors and rectifiers at the end of each topology section shows some of the Philips devices which are ideal for use in S.M.P.S. applications.

References.

- (1) Philips MOSFET Selection Guide For S.M.P.S. by M.J.Humphreys. Philips Power Semiconductor Applications group, Hazel Grove.
- (2) Switch Mode Power Conversion - Basic theory and design by K.Kit.Sum. (Published by Marcel Dekker inc.1984)

Appendix A.

MOSFET throughput power calculations.

Assumptions made:-

The power loss (Watts) in the transistor due to on-state losses is 5% of the total throughput (output) power.

Switching losses in the transistor are negligible. N.B. At frequencies significantly higher than 50kHz the switching losses may become important.

The device junction temperature, T_j is taken to be 125°C. The ratio $R_{ds(125°C)}/R_{ds(25°C)}$ is dependent on the voltage of the MOSFET device. Table A1 gives the ratio for the relevant voltage limiting values.

The value of $V_{s(min)}$ for each input value is given in Table A2.

Device voltage limiting value.	$\frac{R_{ds(125°C)}}{R_{ds(25°C)}}$
100	1.74
200	1.91
400	1.98
500	2.01
800	2.11
1000	2.15

Table A1. On resistance ratio.

Main input voltage	Maximum dc link voltage	Minimum dc link voltage
220 / 240V ac	385V	200V
110 / 120V ac	190V	110V

Table A2. Max and Min dc link voltages for mains inputs.

Using the following equations, for a given device with a known $R_{ds(125°C)}$, the maximum throughput power in each topology can be calculated.

Where:-

- $P_{th(max)}$ = Maximum throughput power.
- D_{max} = maximum duty cycle.
- τ = required transistor efficiency (0.05 ± 0.005)
- $R_{ds(125°C)} = R_{ds(25°C)} \times \text{ratio.}$
- $V_{s(min)}$ = minimum dc link voltage.

Forward converter.

$$P_{th(max)} = \frac{\tau \times V_{s(min)}^2 \times D_{max}}{R_{ds(125°C)}}$$

$$D_{max} = 0.45$$

Flyback Converter.

$$P_{th(max)} = \frac{3 \times \tau \times V_{s(min)}^2 \times D_{max}}{4 \times R_{ds(125°C)}}$$

$$D_{max} = 0.45$$

Push Pull Converter.

$$P_{th(max)} = \frac{\tau \times V_{s(min)}^2 \times D_{max}}{R_{ds(125°C)}}$$

$$D_{max} = 0.9$$

Half Bridge Converter.

$$P_{th(max)} = \frac{\tau \times V_{s(min)}^2 \times D_{max}}{4 \times R_{ds(125°C)}}$$

$$D_{max} = 0.9$$

Full Bridge Converter.

$$P_{th(max)} = \frac{\tau \times V_{s(min)}^2 \times D_{max}}{2 \times R_{ds(125°C)}}$$

$$D_{max} = 0.9$$

2.1.2 The Power Supply Designer's Guide to High Voltage Transistors

One of the most critical components in power switching converters is the high voltage transistor. Despite its wide usage, feedback from power supply designers suggests that there are several features of high voltage transistors which are generally not well understood.

This section begins with a straightforward explanation of the key properties of high voltage transistors. This is done by showing how the basic technology of the transistor leads to its voltage, current, power and second breakdown limits. It is also made clear how deviations from conditions specified in the data book will affect the performance of the transistor. The final section of the paper gives practical advice for designers on how circuits might be optimised and transistor failures avoided.

Introduction

A large amount of useful information about the characteristics of a given component is provided in the relevant data book. By using this information, a designer can usually be sure of choosing the optimum component for a particular application.

However, if a problem arises with the completed circuit, and a more detailed analysis of the most critical components becomes necessary, the data book can become a source of frustration rather than practical assistance. In the data book, a component is often measured under a very specific set of conditions. Very little is said about how the component performance is affected if these conditions are not reproduced exactly when the component is used in a circuit.

There are as many different sets of requirements for high voltage transistors as there are circuits which make use of them. Covering every possible drive and load condition in the device specification is an impossible task. There is therefore a real need for any designer using high voltage transistors to have an understanding of how deviations from the conditions specified in the transistor data book will affect the electrical performance of the device, in particular its limiting values.

Feedback from designers implies that this information is not readily available. The intention of this report is therefore to provide designers with the information they need in order to optimise the reliability of their circuits. The characteristics of high voltage transistors stem from their basic technology and so it is important to begin with an overview of this.

HVT technology

Stripping away the encapsulation of the transistor reveals how the electrical connections are made (see Fig. 1). The collector is contacted through the back surface of the transistor chip, which is soldered to the nickel-plated copper lead frame. For Philips power transistors the lead frame and the centre leg are formed from a single piece of copper, and so the collector can be accessed through either the centre leg or any exposed part of the lead frame (eg the mounting base for TO-220 and SOT-93).

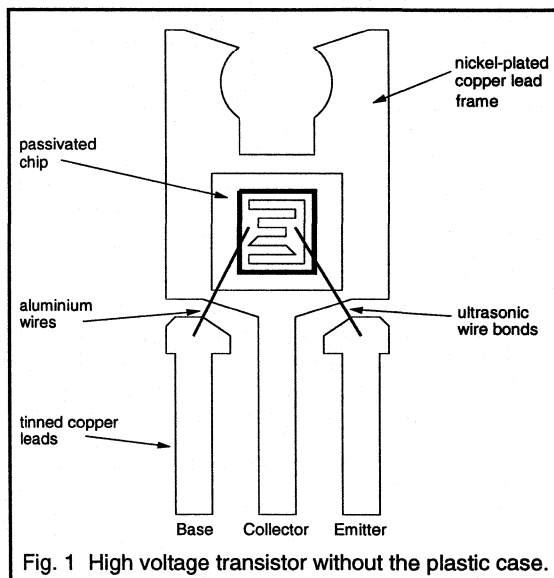


Fig. 1 High voltage transistor without the plastic case.

The emitter area of the transistor is contacted from the top surface of the chip. A thin layer of aluminium joins all of the emitter area to a large bond pad. This bond pad is aluminium wire bonded to the emitter leg of the transistor when the transistor is assembled. The same method is used to contact the base area of the chip. Fig. 2 shows the top view of a high voltage transistor chip in more detail.

Viewing the top surface of the transistor chip, the base and emitter fingers are clearly visible. Around the periphery of the chip is the high voltage glass passivation. The purpose of this is explained later.

Taking a cross section through the transistor chip reveals its npn structure. A cross section which cuts one of the emitter fingers and two of the base fingers is shown in Fig. 3.

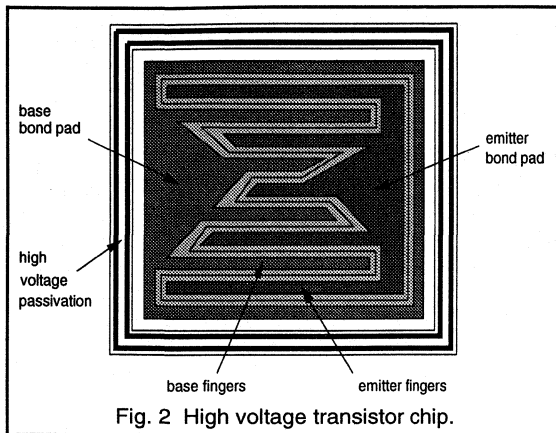


Fig. 2 High voltage transistor chip.

On the top surface of the transistor are the aluminium tracks which contact the base and emitter areas. The emitter finger is shown connected to an n+ region. This is the emitter area. The n+ denotes that this is very highly doped n type silicon. Surrounding the n+ emitter is the base, and as shown in Fig. 3 this is contacted by the base fingers, one on either side of the emitter. The p denotes that this is highly doped p type silicon.

On the other side of the base is the thick collector n- region. The n- denotes that this is lightly doped n type silicon. The collector region supports the transistor blocking voltage, and its thickness and resistivity must increase with the voltage rating of the device.

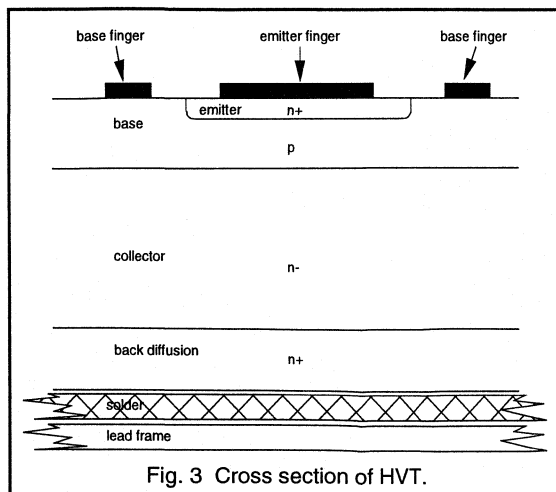


Fig. 3 Cross section of HVT.

Following the collector region is the n+ back diffusion. The n+ back diffusion ensures a good electrical contact is made between the collector region and the lead frame/collector leg, whilst also allowing the crystal to be thick enough to prevent it from cracking during processing and assembly. The bottom surface of the chip is soldered to the lead frame.

Voltage limiting values

Part 1: Base shorted to emitter.

When the transistor is in its off state with a high voltage applied to the collector, the base collector junction is reverse biased by a very high voltage. The voltage supporting depletion region extends deep into the collector, right up to the back diffusion, as shown in Fig. 4.

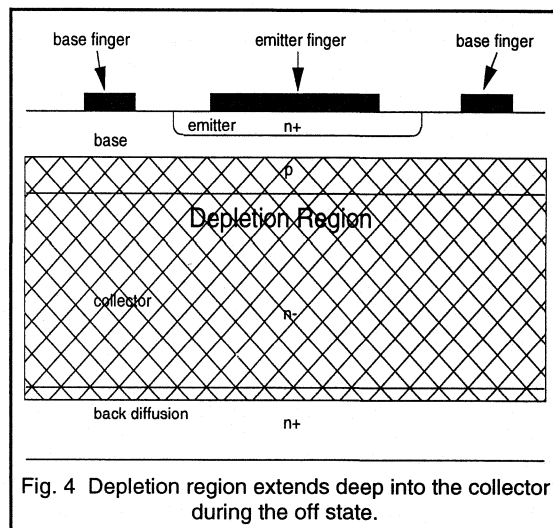
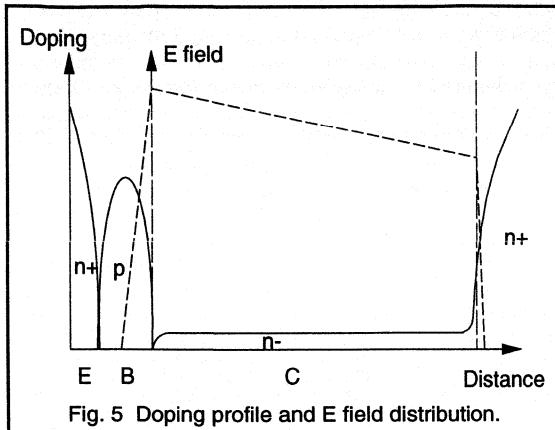


Fig. 4 Depletion region extends deep into the collector during the off state.

With the base of the transistor short circuited to the emitter, or at a lower potential than the emitter, the voltage rating is governed by the voltage supporting capability of the reverse biased base collector junction. This is the transistor $V_{CESMmax}$. The breakdown voltage of the reverse biased base collector junction is determined mainly by the collector width and resistivity as follows:

Figure 5 shows the doping profile of the transistor. Note the very high doping of the emitter and the back diffusion, the high doping of the base and the low doping of the collector. Also shown in Fig. 5 is the electric field concentration throughout the depletion region for the case where the transistor is supporting its off state voltage. The electric field, E, is given by the equation, $E = -dV/dx$, where -dV is the voltage drop in a distance dx. Rewriting this equation gives the voltage supported by the depletion region:

$$V = - \int E dx$$



This is the area under the dotted line in Fig.5.

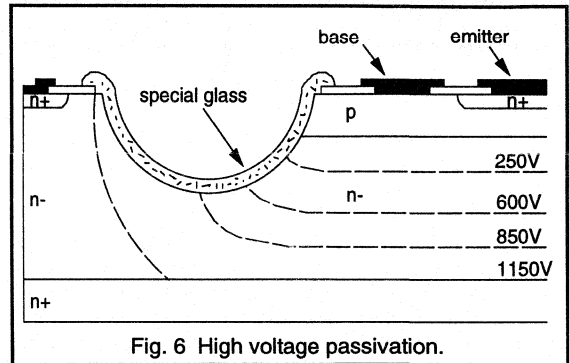
During the off state, the peak electric field occurs at the base collector junction as shown in Fig. 5. If the electric field anywhere in the transistor exceeds 200 kVolts per cm then avalanche breakdown occurs and the current which flows in the transistor is limited only by the surrounding circuitry. If the avalanche current is not limited to a very low value then the power rating of the transistor can easily be exceeded and the transistor destroyed as a result of thermal breakdown. Thus the maximum allowable value of electric field is 200 kV/cm.

The gradient of the electric field, dE/dx , is proportional to charge density which is in turn proportional to the level of doping. In the base, the gradient of the electric field is high because of the high level of doping, and positive because the base is p type silicon. In the collector, the gradient of the electric field is low because of the low level of doping, and negative because the collector is n type silicon. In the back diffused region, the gradient of the electric field is very highly negative because this is very highly doped n type silicon.

Increasing the voltage capability of the transistor can therefore be done by either increasing the resistivity (lowering the level of doping) of the collector region in order to maintain a high electric field for the entire collector width, or increasing the collector width itself. Both of these measures can be seen to work in principle because they increase the area under the dotted line in Fig. 5.

The breakdown voltage of the transistor, $V_{CESMmax}$, is limited by the need to keep the peak electric field, E , below 200 kV/cm. Without special measures, the electric field would crowd at the edges of the transistor chip because of the surface irregularities. This would limit breakdown voltages to considerably less than the full capability of the silicon. Crowding of the equipotential lines at the chip edges is

avoided by the use of a glass passivation (see Fig. 6). The glass passivation therefore allows the full voltage capability of the transistor to be realised.



The glass used is negatively charged to induce a p-channel underneath it. This ensures that the applied voltage is supported evenly over the width of the glass and does not crowd at any one point. High voltage breakdown therefore occurs in the bulk of the transistor, at the base collector junction, and not at the edges of the crystal.

Exceeding the voltage rating of the transistor, even for a fraction of a second, must be avoided. High voltage breakdown effects can be concentrated in a very small area of the transistor, and only a small amount of energy may damage the device. However, there is no danger in using the full voltage capability of the transistor as the limit under worst case conditions because the high voltage passivation is extremely stable.

Part 2: Open circuit base.

With the base of the transistor open circuit the voltage capability is much lower. This is the V_{CE0max} of the device and it is typically just less than half of the $V_{CESMmax}$ rating. The reason for the lower voltage capability under open circuit base conditions is as follows:

As the collector emitter voltage of the transistor rises, the peak electric field located at the base collector junction rises too. Above a peak E field value of 100 kV/cm there is an appreciable leakage current being generated.

In the previous case, with the base contact short circuited to the emitter, or held at a lower potential than the emitter, any holes which are generated drift from the edge of the depletion region towards the base contact where they are extracted. However, with the base contact open circuit, the holes generated diffuse from the edge of the depletion region towards the emitter where they effectively act as base current. This causes the emitter to inject electrons into the base, which diffuse towards the collector. Thus there is a flow of electrons from the emitter to the collector.

The high electric field in the collector accelerates the electrons to the level where some have sufficient energy to produce more hole electron pairs through their collisions with the lattice. The current generated in this way adds to the leakage current. Thus with the base contact open circuit the emitter becomes active and provides the system with *gain*, multiplying the leakage current and consequently reducing the breakdown voltage.

For a given transistor the gain of the system is dependant on two things. Firstly it is dependant on the probability that a hole leaving the depletion region will reach the emitter. If the base is open circuit and no recombination occurs then this probability is 1. If the base is not open circuit, and instead a potential below V_{BEon} is applied, then there is a chance that a hole leaving the depletion region will be extracted at the base contact. As the voltage on the base contact is made less positive the probability of holes reaching the emitter is reduced.

Secondly, the gain is dependant on the probability of electrons leaving the emitter, diffusing across the base and being accelerated by the high field in the collector to the level where they are able to produce a hole electron pair in one of their collisions with the lattice. This depends on the electric field strength which is in turn dependant on the collector voltage.

Thus for a given voltage at the base there is a corresponding maximum collector voltage before breakdown will occur. With the base contact shorted to the emitter, or at a lower potential than the emitter, the full breakdown voltage of the transistor is achieved ($V_{CESMmax}$). With the base contact open circuit, or at a *higher* potential than the emitter, the breakdown voltage is lower (V_{CEOmax}) because in this case the emitter is active and it provides the breakdown mechanism with gain.

With the base connected to the emitter by a non zero impedance, the breakdown voltage will be somewhere between the $V_{CESMmax}$ and the V_{CEOmax} . A low impedance approximates to the shorted base, 'zero gain', case and a high impedance approximates to the open base, 'high gain', case. With a base emitter impedance of 47 Ω and no externally applied base voltage, the breakdown voltage is typically 10% higher than the V_{CEOmax} .

Current limiting values

The maximum allowed DC current is limited by the size of the bond wires to the base and emitter. Exceeding the DC limiting values I_{Cmax} and I_{Bmax} , for any significant length of time, may blow these bond wires. If the current pulses are short and of a low duty cycle then values greatly in excess of the DC values are allowed. The I_{CMmax} and I_{BMmax} ratings are recommendations for peak current values. For a duty cycle of 0.01 and a pulse width of 10ms these values will typically be double the DC values.

If the pulses are shorter than 10ms then even the recommended peak values can be exceeded under worst case conditions. However, it should be noted that combinations of high collector current and high collector voltage can lead to failure by second breakdown (discussed later). As the collector current is increased, the collector voltage required to trigger second breakdown drops, and so allowing large collector current spikes increases the risk of failure by second breakdown. It is therefore advised that the peak values given in the data book are used as design limits in order to maximise the component reliability.

In emitter drive circuits, the peak reverse base current is equal to the peak collector current. The pulse widths and duty cycles involved are small, and this mode of operation is within the capability of all Philips high voltage transistors.

Power limiting value

The P_{totmax} given in device data is not generally an achievable parameter because in practice it is obtainable only if the mounting base temperature can be held to 25 °C. In practice, the maximum power dissipation capability of a given device is limited by the heatsink size and the ambient temperature. The maximum power dissipation capability for a particular circuit can be calculated as follows;

T_{jmax} is the maximum junction temperature given in the data sheet. The value normally quoted is 150 °C. T_{amb} is the ambient temperature around the device heatsink. A typical value in practice could be 65 °C. R_{thj-mb} is the device thermal resistance given in the data sheet, but to obtain a value of junction to *ambient* thermal resistance, R_{thj-a} , the thermal resistance of the mica spacer (if used), heatsink and heatsink compound should be added to this.

The maximum power which can be dissipated under a given set of circuit conditions is calculated using;

$$P_{max} = (T_{jmax} - T_{amb}) / R_{thj-a}$$

For a BUT11AF, an ambient temperature of 65 °C, mounted on a 10 K/W heatsink with heatsink compound, this gives;

$$R_{thj-a} = 3.95 \text{ K/W} + 10 \text{ K/W} = 13.95 \text{ K/W}$$

and hence the maximum power capable of being dissipated under these conditions is;

$$P_{max} = (150 - 65) / 13.95 = 6 \text{ W}$$

Exceeding the maximum junction temperature, T_{jmax} , is not recommended. All of the quality and reliability work carried out on the device is based on the maximum junction temperature quoted in data. If T_{jmax} is exceeded in the circuit then the reliability of the device is no longer guaranteed.

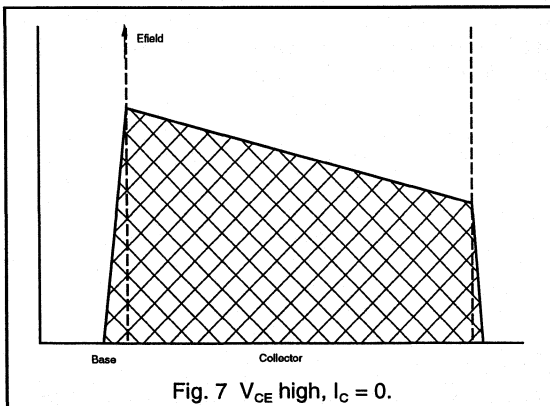
Secondary breakdown

Pure silicon, also known as 'intrinsic' silicon, contains few mobile charge carriers at room temperature and so its conductivity is low. By doping the silicon (ie introducing atoms of elements other than silicon) the number of mobile charge carriers, and hence the conductivity, can be increased. Silicon doped in such a way as to increase the number of mobile electrons (negative charge) is called n type silicon. Silicon doped in such a way as to increase the number of mobile holes (positive charge) is called p type silicon. Thus the base region of an npn transistor contains an excess of mobile holes and the collector and emitter regions contain an excess of mobile electrons.

When a high voltage is applied to the transistor, and the collector base junction is reverse biased, a depletion region is developed. This was shown in Fig. 4. The depletion region supports the applied voltage. The electric field distribution within the depletion region was shown in Fig. 5.

The term *depletion region* refers to a region depleted of mobile charge carriers. Therefore, within the depletion region, the base will have lost some holes and hence it is left with a net negative charge. Similarly the collector will have lost some electrons and hence it is left with a net positive charge. The collector is said to have a 'positive space charge' (and the base a 'negative space charge'.)

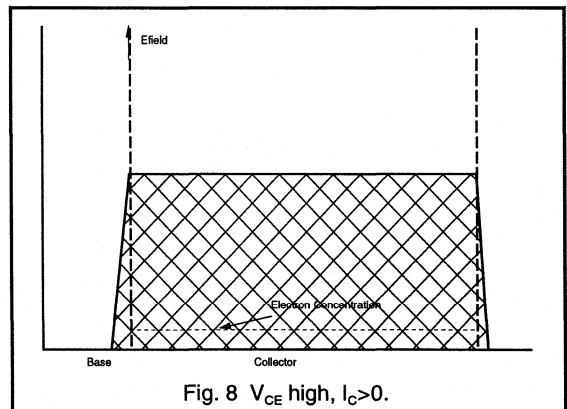
Consider the case where a transistor is in its off state supporting a high voltage which is within its voltage capability. The resulting electric field distribution is shown in Fig. 7.



If the collector voltage is held constant, and the collector current increased so that there is now some collector current flowing, this current will modify the charge distribution within the depletion region. The effect this has on the base is negligible because the base is very highly doped. The effect this has on the collector is significant because the collector is only lightly doped.

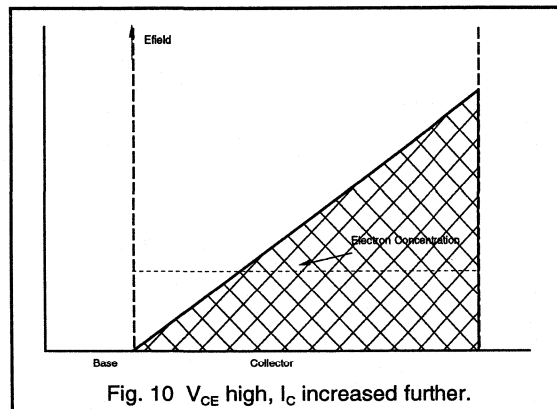
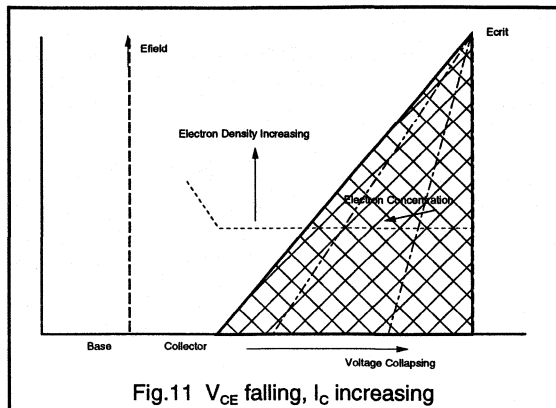
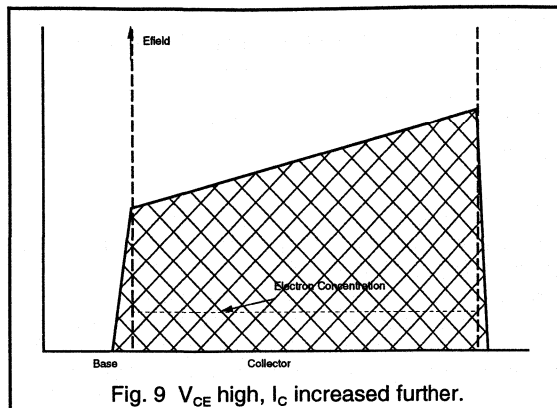
The collector current is due to the flow of electrons from the emitter to the collector. As the collector current increases, the collector current density increases. This increase in collector current density is reflected in Fig. 8 by an increase in the electron concentration in the collector.

At a certain collector current density, the negative charge of the electrons neutralises the positive space charge of the collector. The gradient of the electric field, dE/dx , is proportional to charge density. If the space charge is neutralised then the gradient of the electric field becomes zero. This is the situation illustrated in Fig. 8. Note that the shaded area remains constant because the applied voltage remains constant. Therefore the peak value of electric field drops slightly.



Keeping the collector-emitter voltage constant, and pushing up the collector current density another step, increases the concentration of electrons in the collector still further. Thus the collector charge density is now negative, the gradient of electric field in the collector is now positive, and the peak electric field has shifted from the collector-base junction to the collector-back diffusion interface. This is shown in Fig. 9.

Increasing the collector current density another step will further increase the positive gradient of electric field. The collector voltage is unchanged and so the shaded area must remain unchanged. Therefore the peak electric field is forced upwards. This is shown in Fig. 10.



Safe Operating Area

It has been shown that the electric field profile, and hence the peak electric field, is dependent on the combination of collector current density and applied collector voltage. The peak electric field increases with increasing collector voltage (increase in shaded area in Figs. 7 to 11). It also increases with increasing collector current density (increase in gradient of electric field). At all times the peak electric field must remain below the critical value. If the collector voltage is lowered then a higher collector current density is permitted. If the collector current density is lowered then a higher collector voltage is permitted.

Potentially destructive combinations of collector current density and collector voltage are most likely to occur during switching and during fault conditions in the circuit (eg a short circuited load). The safe operating areas give information about the capability of a given device under these conditions.

The collector current density is dependent on the collector current and the degree of current crowding in certain areas of the collector. The degree of current crowding is different for turn-on (positive base voltage) and turn-off (negative base voltage). Therefore the allowed combinations of collector current and collector voltage, collectively known as the safe operating area (SOA) of the transistor, will be different for turn-on of the transistor and turn-off.

Forward SOA

With a positive voltage applied to the base, the shape of the safe operating area for DC operation is that shown in Fig. 12. Operation outside the safe operating area is not allowed.

For pulsed operation the forward SOA increases, and for small, low duty cycle pulses it becomes square. The forward SOA provides useful information about the capabilities of the transistor under fault conditions in the circuit (eg. a short circuited load).

At a certain critical value of peak electric field, E_{crit} , a regenerative breakdown mechanism takes place which causes the electron concentration in the collector to increase uncontrollably by a process known as *avalanche multiplication*. As the electron concentration increases, the gradient of electric field increases (because the gradient of electric field is proportional to charge density). The peak electric field is clamped by the breakdown and so the collector voltage drops. In most circuits the collapsing collector voltage will result in a further rise in collector current density, causing a further rise in electron concentration (ie positive feedback). This is shown in Fig. 11.

At approximately 30 V, the holes produced by the avalanche multiplication build up sufficiently to temporarily stabilize the system. However, with 30 V across the device and a high collector current flowing through it, a considerable amount of heat will be generated. Within less than one microsecond thermal breakdown will take place, followed by device destruction.

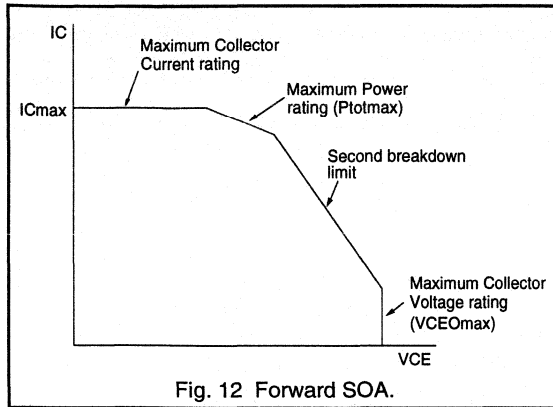


Fig. 12 Forward SOA.

The safe operating area is designed to protect the current, power, voltage and second breakdown limits of the transistor. The current, power and voltage limits of the transistor have already been discussed. Note that the peak voltage rating is the V_{CE0max} rating and not the $V_{CESMmax}$ rating. The $V_{CESMmax}$ rating only applies if the base-emitter voltage is not greater than zero volts.

Sometimes shown on forward SOA curves is an extension allowing higher voltages than V_{CE0max} to be tolerated for short periods (of the order of 0.5 μ s). This allows turn-on of the transistor from a higher voltage than V_{CE0max} . However, the pulses allowed are very short, and unless it can be guaranteed that the rated maximum pulse time will never be exceeded, transistor failures will occur. If the circuit conditions can be guaranteed then there is no danger in making use of this capability.

As mentioned in the previous section, second breakdown is triggered by combinations of high collector voltage and high collector current density. With a positive voltage applied to the base, the region of highest current density is at the edges of the emitter as shown in Fig. 13.

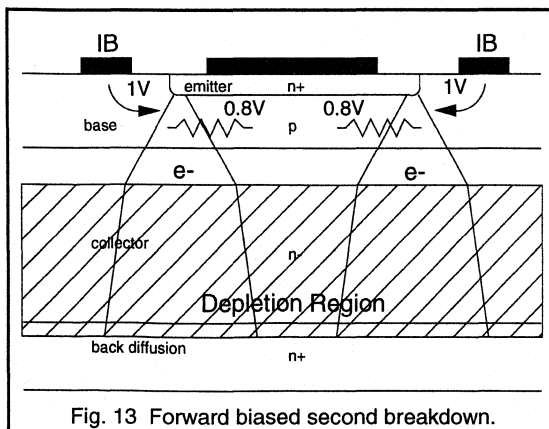


Fig. 13 Forward biased second breakdown.

The base region under the emitter constitutes a resistance (known as the *sub emitter resistance*). With a positive voltage applied to the base, the sub emitter resistance will mean that the areas of the emitter which are nearest to the base have a higher forward bias voltage than the areas furthest from the base. Therefore the *edges* of the emitter have a higher forward bias voltage than the centre and so they receive a higher base current.

As a result of this the edges of the emitter conduct a substantial proportion of the collector current when the base is forward biased. If the collector current is high then the current density at the edges of the emitter is also high. There will be some spreading out of this current as it traverses the base. When the edge of the depletion region is reached, the current is sucked across by the electric field.

If the transistor is conducting a high current and also supporting a high voltage, then the current density will be high when the current reaches the edge of the depletion region. If the current density is beyond that allowed at the applied voltage, then the second breakdown mechanism is triggered (as explained in the previous section) and the device will be destroyed.

With a positive base current flowing, the region of highest current density is at the edges of the emitter. A forward SOA failure will therefore produce burns which originate from the edge of one of the emitter fingers.

Forward SOA failure becomes more likely as pulse width and/or duty cycle is increased. Because the edges of the emitter are conducting more current than the centre, they will get hotter. The temperature of the emitter edges at the end of each current pulse is a function of the pulse width and the emitter current. Longer pulse widths will increase the temperature of the emitter edges at the end of each current pulse. Higher duty cycles will leave insufficient time for this heat to spread. In this manner, combinations of long pulse width and high duty cycle can give rise to cumulative heating effects. Current will crowd towards the hottest part of the emitter. There is therefore a tendency for current to become concentrated in very narrow regions at the edges of the emitter fingers, and as pulse width and/or duty cycle is increased the degree of current crowding increases. This is the reason why the forward SOA for DC operation is as shown in Fig. 12, but for pulsed operation it is enlarged and for small, low duty cycle pulses it becomes square.

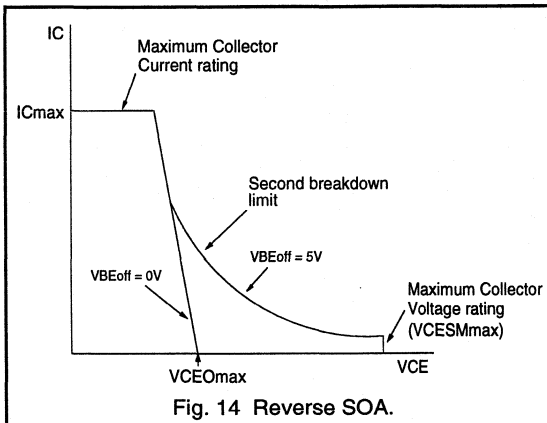
Reverse SOA

During turn-on of the transistor, the high resistance of the collector region is reduced by the introduction of holes (from the base) and electrons (from the emitter). This process, known as *conductivity modulation*, is the reason why bipolar transistors are able to achieve such a low collector voltage during the on state, typically 0.2 V. However, during turn-off

of the transistor, these extra holes and electrons constitute a stored charge which must be removed from the collector before the voltage supporting depletion region can develop.

To turn off the transistor, a negative voltage is applied to the base and a reverse base current flows. During turn-off of the transistor, it is essential that the device stays within its reverse bias safe operating area (RBSOA). The shape of a typical RBSOA curve is as shown in Fig. 14.

With no negative voltage applied to the base, the RBSOA is very much reduced, as shown in Fig. 14. This is particularly important to note at power up and power down of power supplies, when rail voltages are not well defined (see section on improving reliability).



On applying a negative voltage to the base, the charge stored in the collector areas nearest to the base contacts will be extracted, followed by the charge stored in the remaining collector area. Holes not extracted through the base contact are free to diffuse into the emitter where they constitute a base current which keeps the emitter active. During the transistor storage time, the collector charge is being extracted through the base, but the emitter is still active and so the collector current continues to flow.

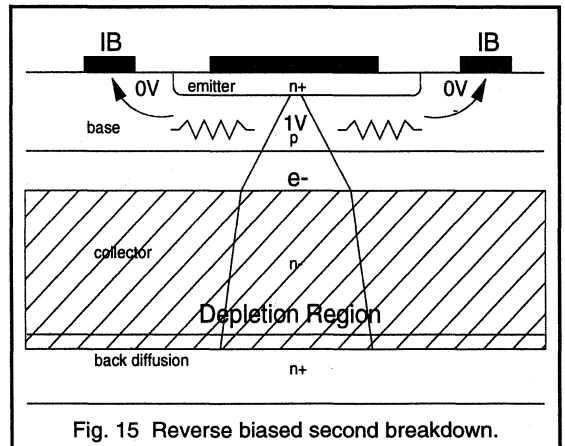
During the transistor fall time, the voltage supporting depletion region is being developed and therefore the collector voltage is rising. In addition to this, the negative voltage on the base is causing holes to drift towards the base contact where they are neutralised, thus preventing holes from diffusing towards the emitter.

This has two effects on the collector current. Firstly, the rising collector voltage results in a reduction in the voltage across the collector load, and so the collector current starts to drop. Secondly, the extraction of holes through the base will be most efficient nearest to the base contacts (due to the sub emitter resistance), and so the collector current becomes concentrated into narrow regions under the centre of the emitter fingers (furthest from the base). This

is shown in Fig. 15. This current crowding effect leads to an increase in the collector current density during turn off, even though the collector current itself is falling.

Thus for a portion of the fall time, the collector voltage is rising and the collector current density is also rising. This is a critical period in the turn-off phase. If the turn-off is not carefully controlled, the transistor may be destroyed during this period due to the onset of the second breakdown mechanism described earlier.

During this critical period, the collector current is concentrated into a narrow region under the centre of the emitter. RBSOA failure will therefore produce burns which originate from the centre of one of the emitter fingers.

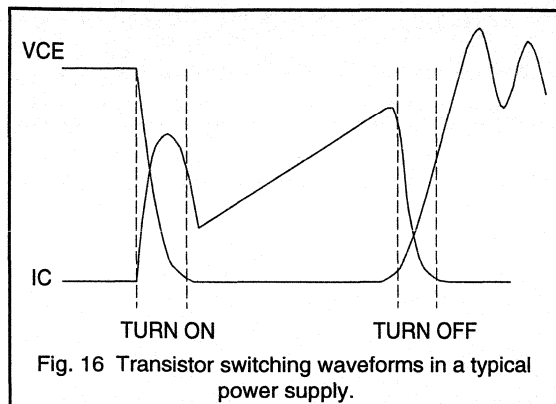


Useful tips as an aid to circuit design

In recent years, the Philips Components Power Semiconductor Applications Laboratory (P.S.A.L.) has worked closely with a number of HVT users. It has become apparent that there are some important circuit design features which, if overlooked, invariably give rise to circuit reliability problems. This section addresses each of these areas and offers guidelines which, if followed, will enhance the overall performance and reliability of any power supply.

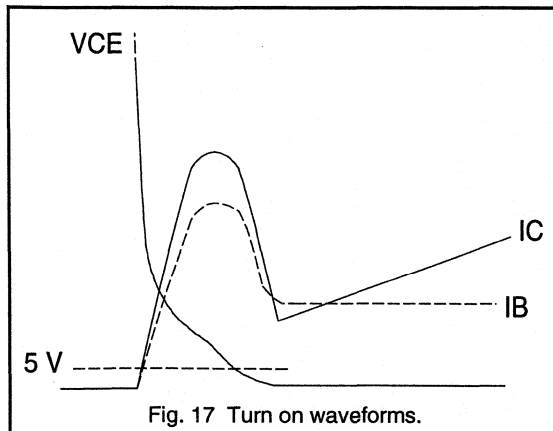
Improving turn-on

There is more to turning on a high voltage transistor than simply applying a positive base drive. The positive base drive must be at least sufficient to keep the transistor saturated at the current it is required to conduct. However, transistor gain as specified in data sheets tends to be assessed under static conditions and therefore assumes the device is already on.



Note 1. *The base current requirements at turn-on of the transistor are higher than the static gain would suggest.*

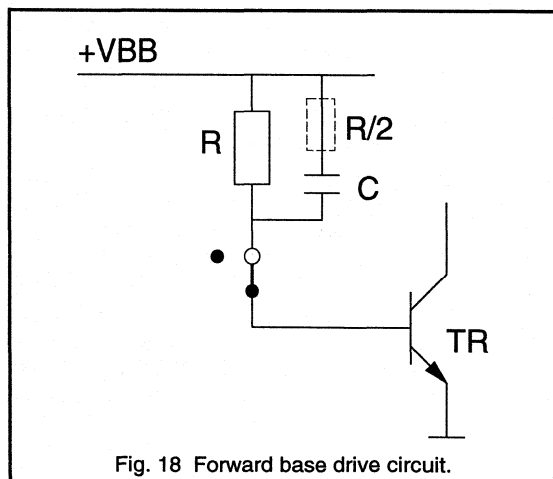
The conductivity modulation process, described at the beginning of the previous section, occurs every time the transistor is turned on. The faster the charges are introduced into the collector, the faster the collector resistance will drop, allowing the collector voltage to drop to its saturation level. The rate at which the collector charge is built up is dependent on the applied base current and the applied collector current. In order to turn the transistor on quickly, and hence minimise the turn-on dissipation, the transistor needs to be overdriven until the collector voltage has dropped to its saturation level. This is achieved by having a period of overshoot at the start of the base current pulse. The turn-on waveforms are shown in Fig. 17.



Note 2. *A fast rising base current pulse with an initial period of overshoot is a desirable design feature in order to keep the turn-on dissipation low.*

The base current overshoot is achieved by having a capacitor in parallel with the forward base drive resistor (see Fig. 18). The RC time constant determines the overshoot period and as a first approximation it should be comparable to the transistor storage time. The capacitor value is then adjusted until the overshoot period is almost over by the time the transistor is saturated. This is the optimum drive condition. A resistor in series with the capacitor (typically $R/2$) can be used to limit the peak base current overshoot and remove any undesirable oscillations.

The initial period of overshoot is especially necessary in circuits where the collector current rises quickly (ie square wave switching circuits and circuits with a high snubber discharge current). In these circuits the transistor would otherwise be conducting a high collector current during the early stages of the turn-on period where the collector voltage can still be high. This would lead to an unacceptable level of turn-on dissipation.



Note 3. *Square wave switching circuits, and circuits with a high snubber discharge current, are very susceptible to high turn-on dissipation. Using an RC network in series with the forward base current path increases the turn-on speed and therefore overcomes this problem.*

It should also be noted that during power up of power supply units, when all the output capacitors of the supply are discharged, the collector current waveform is often very different to that seen under normal running conditions. The rising edge of the collector current waveform is often faster, the collector current pulse width is often wider and the peak collector current value is often higher.

In order to prevent excessive collector current levels (and transformer saturation) a 'soft start' could be used to limit the collector current pulse width during power up. Alternatively, since many power supply designs are now using current mode control, excessive collector current can be avoided simply by setting the overcurrent threshold at an acceptable level.

Note 4. *Using the 'soft start' and/or the overcurrent protection capability of the SMPS control IC prevents excessive collector current levels at power up.*

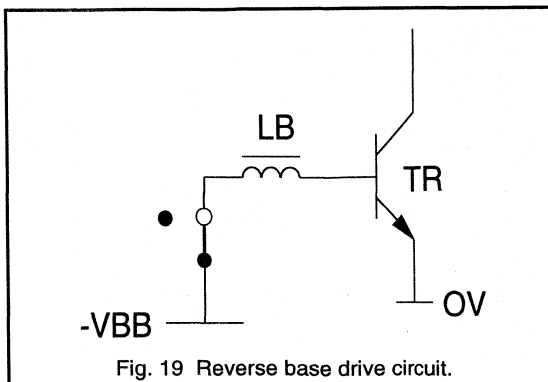
Improving turn-off

As far as the collector current is concerned, optimum turn-off for a particular device is determined by how quickly the structure of the device will allow the stored charge to be extracted. If the device is turned off too quickly, charge gets trapped in the collector when the collector base junction recovers. Trapped charge takes time to recombine leading to a long collector current tail at turn-off and hence high turn-off losses. On the other hand, if the device is turned off too slowly, the collector voltage starts to rise prematurely (ie while the collector current is at its peak). This would also lead to high turn-off losses.

Note 1. *Turning the transistor off either too quickly or too slowly leads to high turn-off losses.*

Optimum turn-off is achieved by using the correct combination of reverse base drive and storage time control. Reverse base drive is necessary to prevent storage times from being too long (and also to give the maximum RBSOA). Storage time control is necessary to prevent storage times from being too short.

Storage time control is achieved by the use of a small inductor in series with the reverse base current path (see Fig. 19). This controls the slope of the reverse base current (as shown in Fig. 20) and hence the rate at which charge is extracted from the collector. The inductor, or 'base coil', is typically between 1 and 6 μH , depending on the reverse base voltage and the required storage time.



Note 2. *Applying a base coil in series with the reverse base current path increases the transistor storage time but reduces both the fall time and the turn-off losses.*

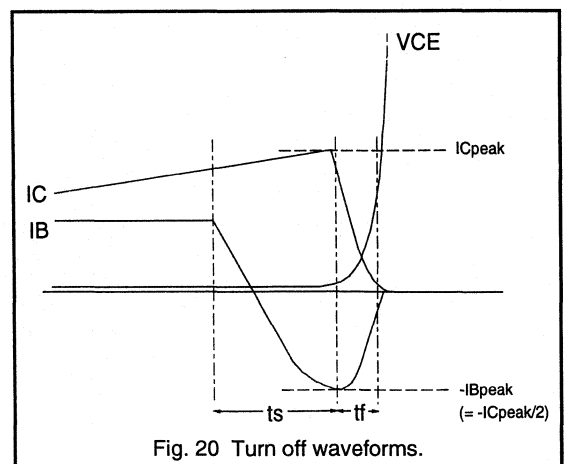
Applying this small base inductor will usually mean that the base emitter junction of the transistor is brought into breakdown during part of the turn-off cycle. This is not a problem for the device because the current is controlled by the coil and the duty cycle is low.

If the transistor being used is replaced by a transistor of the same technology but having either a higher current rating or a higher voltage rating, then the volume of the collector increases. If the collector volume increases then the volume of charge in the collector, measured at the same saturation voltage, also increases. Therefore the required storage time for optimum turn-off increases and also the required negative drive energy increases.

Overdriving the transistor (ie. driving it well into saturation) also increases the volume of stored charge and hence the required storage time for optimum turn-off. Conversely, the required storage time for a particular device can be reduced by using a desaturation network such as a Baker clamp. The Baker clamp reduces the volume of stored charge by holding the transistor out of heavy saturation.

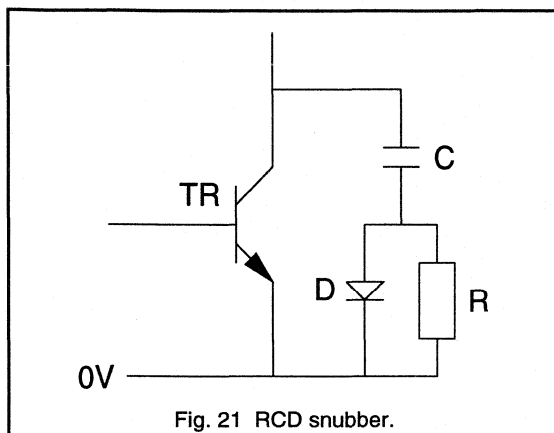
Note 3. *The required storage time for optimum turn-off and the required negative drive energy will both increase as the volume of stored charge in the collector is increased.*

The reverse base current reaches its peak value at about the same time as the collector current reaches its peak value. The turn-off waveforms are shown in Fig. 20.



Note 4. *For optimum turn-off of any transistor, the peak reverse base current should be half of the peak collector current and the negative drive voltage should be between 2 and 5 volts.*

As far as the collector voltage is concerned, the slower the dV/dt the lower the turn-off dissipation. Control of the collector dV/dt is achieved by the use of a snubber network (see Fig. 21). The snubber capacitor also controls the collector voltage overshoot and thus prevents overvoltage of the transistor.

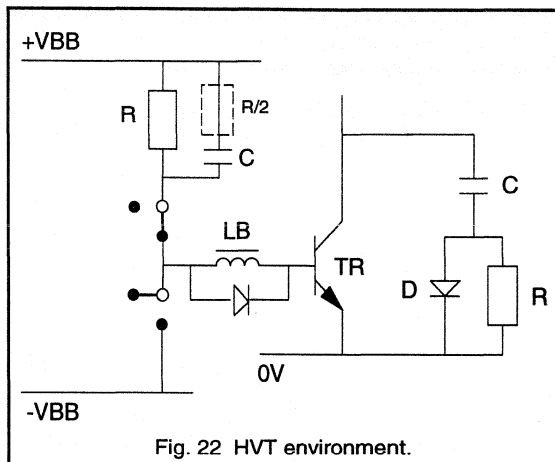


High collector dV/dt at turn-off can bring an additional problem for the transistor. A charging current flows through the collector-base (Miller) capacitance of the device, and according to the law, $I = C \times dV/dt$, this charging current increases in magnitude with increasing dV/dt . If this current enters the base then the transistor can begin to turn back on. Control of the collector dV/dt is usually enough to prevent this from happening. If this is insufficient then the base-emitter impedance must be reduced by applying a resistor and/or capacitor between base and emitter to shunt some of this current.

Note 5. High collector dV/dt at turn-off leads to parasitic turn-on if the charging current of the transistor Miller capacitance is not shunted away from the base.

High collector dI/dt at turn-off can also bring problems if the inductance between the emitter and the base ground reference is too high. The falling collector current will induce a voltage across this inductance which takes the emitter more negative. If the voltage on the emitter falls below the voltage on the base then the transistor can begin to turn back on. This problem is more rare but if it does arise then adding a resistor and/or capacitor between base and emitter helps to keep the base and emitter more closely coupled. At all times it is important to keep the length of the snubber wiring to an absolute minimum.

Note 6. High collector dI/dt at turn-off leads to parasitic turn-on if the inductance between the emitter and the base ground reference is too high.



Improving reliability

In the majority of cases, the most stressful circuit conditions occur during power up of the SMPS, when the base drive is least well defined and the collector current is often at its highest value. However, the electrical environment at power up is very often hardly considered, and potentially destructive operating conditions go unnoticed.

A very common circuit reliability problem is RBSOA failure occurring on the very first switching cycle, because the reverse drive to the base needs several cycles to become established. With no negative drive voltage on the base of the transistor, the RBSOA is reduced (as discussed earlier). To avoid RBSOA failure, the collector voltage must be kept below V_{CE0max} until there is sufficient reverse drive energy available to hold the base voltage negative during the turn-off phase.

Even with the full RBSOA available, control of the rate of rising collector voltage through the use of a snubber is often essential in order to keep the device within the specified operating limits.

Note 1. The conditions at power up often come close to the safe operating limits. Until the negative drive voltage supply is fully established, the transistor must be kept below its V_{CE0max} .

Another factor which increases the stress on many components is increased ambient temperature. It is essential that the transistor performance is assessed at the full operating temperature of the circuit. As the temperature of the transistor chip is increased, both turn-on and turn-off losses may also increase. In addition to this, the quantity of stored charge in the device rises with temperature, leading to higher reverse base drive energy requirements.

Note 2. *Transistor performance should be assessed under all operating conditions of the circuit, in particular the maximum ambient temperature.*

A significant proportion of power supply reliability problems could be avoided by applying these two guidelines alone. By making use of the information on how to improve turn-on

and turn-off, small design changes can be made to the circuit which will enhance the electrical performance and reliability of the transistor, leading to a considerable improvement in the performance and reliability of the power supply as a whole.

2.1.3 Base Circuit Design for High Voltage Bipolar Transistors in Power Converters

Fast, high voltage switching transistors such as the BUT211, BUT11, BUT12, BUT18, BUW13, BU1508, BU2508, BU1706 and BU1708 have all helped to simplify the design of converter circuits for power supply applications. Because the breakdown voltage of these transistors is high (from 850 to 1750V), they are suitable for operation direct from the rectified 110V or 230V mains supply. Furthermore, their fast switching properties allow the use of converter operating frequencies up to 30kHz (with emitter switching techniques pushing this figure past 100kHz).

The design of converter circuits using high-voltage switching transistors requires a careful approach. This is because the construction of these transistors and their behaviour in practical circuits is different from those of their low-voltage counterparts. In this article, solutions to base circuit design for transistor converters and comparable circuits are developed from a consideration of the construction and the inherent circuit behaviour of high voltage switching transistors.

Switching behaviour

Figure 1 shows a complete period of typical collector voltage and current waveforms for a power transistor in a switching converter. The turn-on and turn-off intervals are indicated. The switching behaviour of the transistor during these two intervals, and the way it is influenced by the transistor base drive, will now be examined.

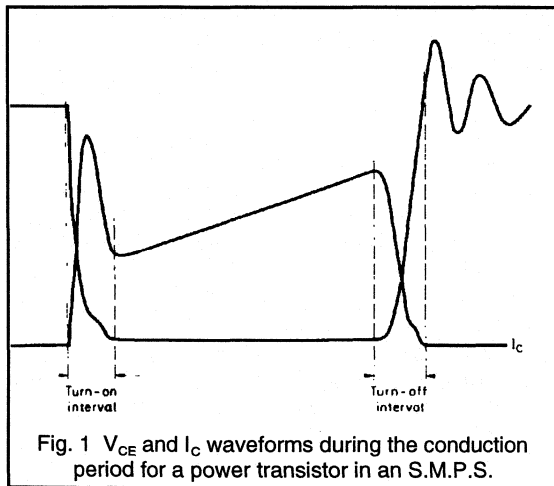


Fig. 1 V_{CE} and I_C waveforms during the conduction period for a power transistor in an S.M.P.S.

Turn-on behaviour

A particular set of voltage and current waveforms at the collector and base of a converter transistor during the turn-on interval is shown in Fig. 2(a). Such waveforms are found in a power converter circuit in which a (parasitic) capacitance is discharged by a collector current pulse at transistor turn-on. The current pulse due to this discharge can be considered to be superimposed on the trapezoidal current waveform found in basic converter operation.

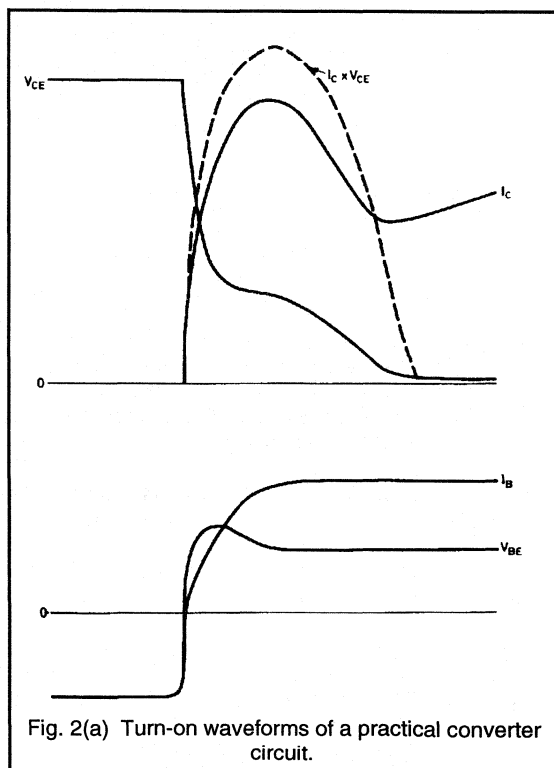


Fig. 2(a) Turn-on waveforms of a practical converter circuit.

A positive base current pulse I_B turns on the transistor. The collector-emitter voltage V_{CE} starts to decrease rapidly and the collector current I_C starts to increase. After some time, the rate of decrease of V_{CE} reduces considerably and V_{CE} remains relatively high because of the large collector current due to the discharge of the capacitance. Thus, the turn-on transient dissipation (shown by a broken line) reaches a high value.

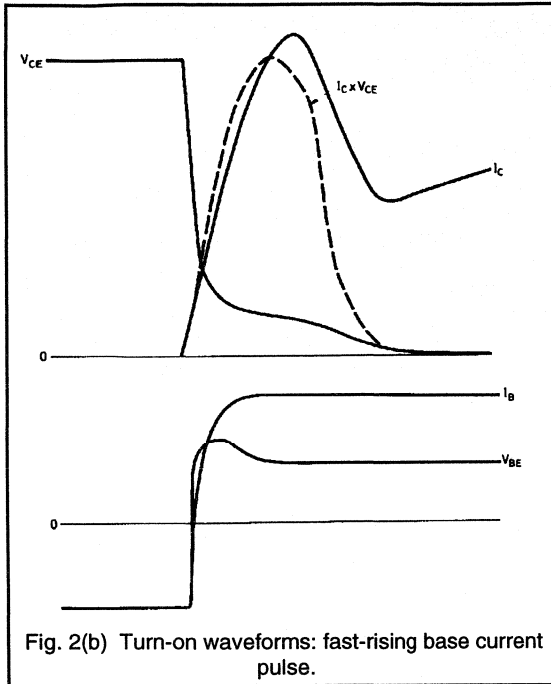


Fig. 2(b) Turn-on waveforms: fast-rising base current pulse.

The collector current then decreases to a trough before assuming the normal trapezoidal waveform. This is again followed by a rapid decrease in V_{CE} , which reaches the saturation value defined by the collector current and base current of the particular transistor.

Figure 2(b) depicts a similar situation but for a greater rate of rise of the base current. The initial rapid decrease in V_{CE} is maintained until a lower value is reached, and it can be seen that the peak and average values of turn-on dissipation are smaller than they are in Fig. 2(a).

Figure 2(c) shows the effect on the transistor turn-on behaviour of a very fast rising base current pulse which initially overshoots the final value. The collector-emitter voltage decreases rapidly to very nearly the transistor saturation voltage. The turn-on dissipation pulse is now lower and much narrower than those of Figs. 2(a) and 2(b).

From the situations depicted in Figs. 2(a), 2(b) and 2(c), it follows that for the power transistor of a converter circuit the turn-on conditions are most favourable when the driving base current pulse has a fast leading edge and overshoots the final value of I_B .

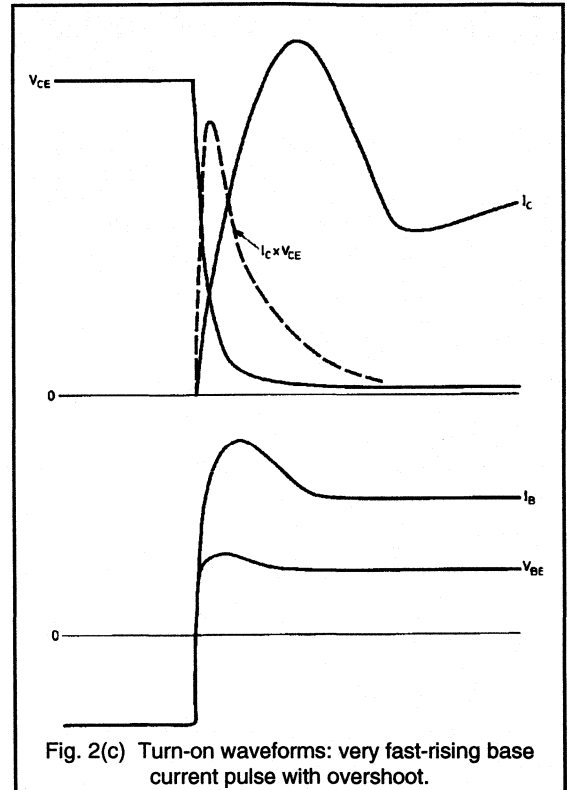
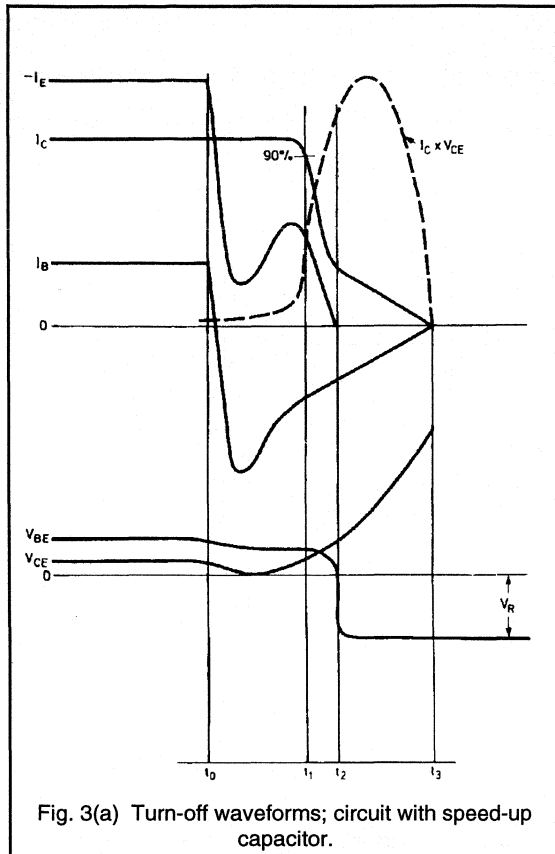


Fig. 2(c) Turn-on waveforms: very fast-rising base current pulse with overshoot.

Turn-off behaviour

The waveforms which occur during the turn-off interval indicated in Fig. 1 are shown on an expanded timescale and with four different base drive arrangements in Figs. 3(a) to 3(d). These waveforms can be provided by base drive circuits as shown in Figs. 4(a) to 4(c). The circuit of Fig. 4(a) provides the waveforms of Fig. 3(a); the circuit of Fig. 4(b) those of Fig. 3(b) and, with an increased reverse drive voltage, Fig. 3(c). The circuit of Fig. 4(c) provides the waveforms of Fig. 3(d). The waveforms shown are typical of those found in the power switching stages of S.M.P.S. and television horizontal deflection circuits, using high-voltage transistors.

In practical circuits, the waveform of the collector-emitter voltage is mainly determined by the arrangement of the collector circuit. The damping effect of the transistor on the base circuit is negligible except during the initial part of the turn-off period, when it only causes some delay in the rise of the V_{CE} pulse.

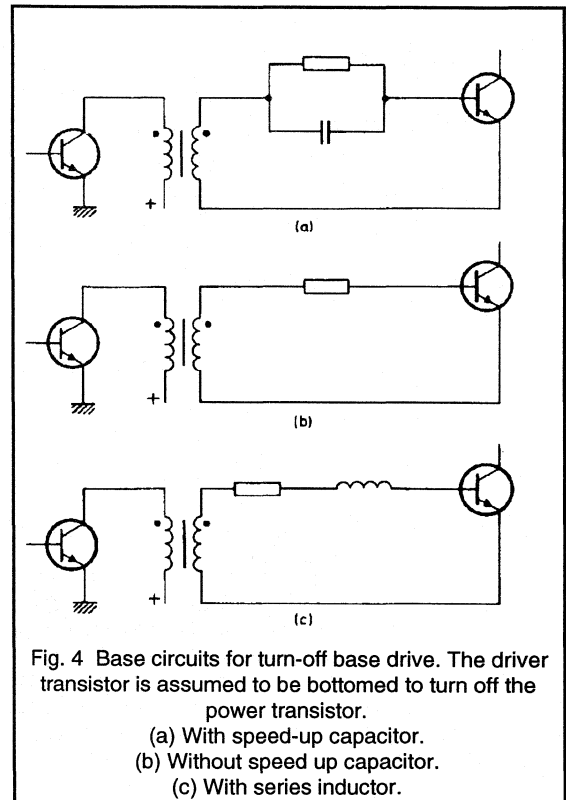


The $I_C \times V_{CE}$ (turn-off dissipation) pulse is dependent on both the transistor turn-off time and the collector current waveshape during turn-off. Turn-off dissipation pulses are indicated in Figs. 3(a) to 3(d) by the dashed lines.

The circuit of Fig. 4(a) incorporates a speed-up capacitor, an arrangement often used with low-voltage transistors. The effect of this is as shown in Fig. 3(a), a very rapid decrease in the base current I_B , which passes through a negative peak value, and becomes zero at t_3 . The collector current I_C remains virtually constant until the end of the storage time, at t_1 , and then decreases, reaching zero at t_2 . The waveform of the emitter current, I_E , is determined by I_C and I_B , until it reaches zero at t_2 , when the polarity of the base-emitter voltage V_{BE} is reversed.

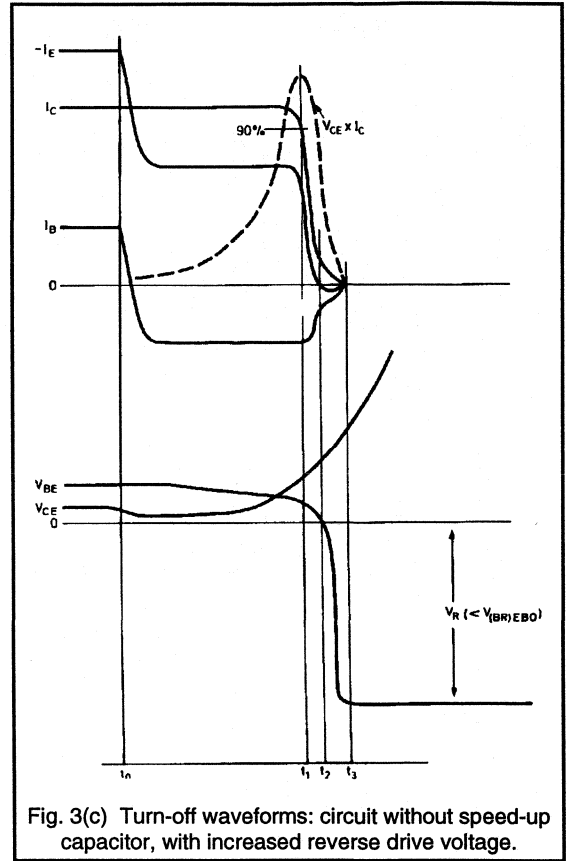
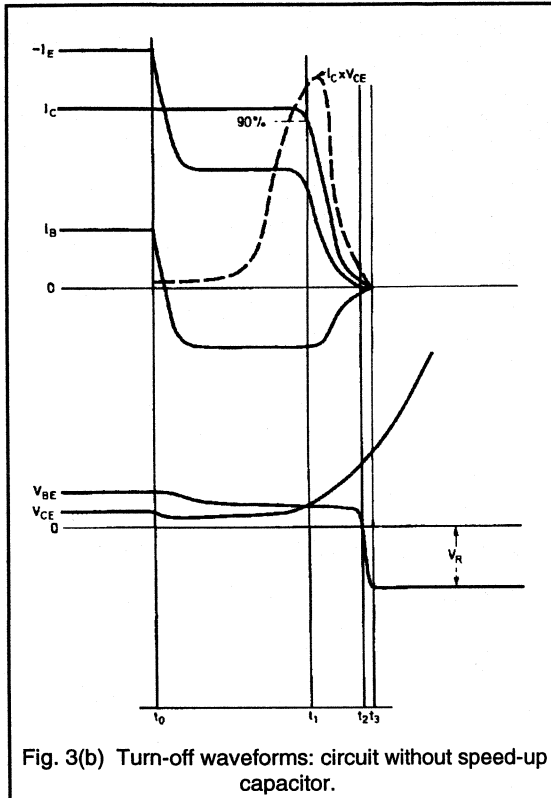
After time t_2 , when V_{BE} is negative and I_E is zero, the collector base currents are equal and opposite, and the emitter is no longer effective. Thus, the further decrease of collector current is governed by the reverse recovery process of the transistor collector-base diode. The reverse recovery 'tail' of I_C (from t_2 to t_3) is relatively long, and it is clear the turn-off dissipation is high.

In the circuit of Fig. 4(b) the capacitor is omitted. Fig. 3(b) shows that the negative base current is limited to a considerably lower value than in the previous case. All the currents I_B , I_C and I_E reach zero at time t_3 . The transistor emitter base junction becomes reverse biased at t_2 , so that during the short interval from t_2 to t_3 a small negative emitter current flows.



The emitter current, determined by the collector current and by the (driven) base current, therefore maintains control over the collector until it reaches zero. Furthermore, the collector current has a less pronounced tail and so the fall time is considerably shorter than that of Fig. 3(a). The turn-off dissipation is also lower than in the previous case.

Increasing the reverse base drive voltage in the circuit of Fig. 4(b), with the base series resistance adjusted so that the same maximum reverse base current flows, gives rise to the waveforms shown in Fig. 3(c). The collector current tail is even less pronounced, and the fall time shorter than in Fig. 3(b).



A further improvement in turn-off behaviour can be seen in the waveforms of Fig. 3(d), which are obtained by including an inductor in the base circuit as in Fig. 4(c). The rate of change of the negative base current is smaller than in the preceding cases, and the negative peak value of the base current is smaller than in Fig. 3(a). The collector current I_C reaches zero at t_3 , and from t_3 to t_4 the emitter and base currents are equal. At time t_2 the polarity of V_{BE} is reversed and the base-emitter junction breaks down. At time t_4 the negative base-emitter voltage decreases from the breakdown value $V_{(BR)EBO}$ to the voltage V_R produced by the drive circuit.

The collector current fall time in Fig. 3(d) is shorter than in any of the previous cases. The emitter current maintains control of the collector current throughout its decay. The large negative value of V_{BE} during the final part of the collector current decay drives the base-emitter junction into breakdown, and the junction breakdown voltage determines the largest possible reverse voltage. The turn-off of the transistor is considerably accelerated by the application (correctly timed) of this large base emitter-voltage, and the circuit gives the lowest turn-off dissipation of those considered.

The operation of the base-emitter junction in breakdown during transistor turn-off, as shown in Fig. 3(d), has no detrimental effect on the behaviour of transistors such as the BUT11 or BU2508 types. Published data on these transistors allow operation in breakdown as a method of achieving reliable turn-off, provided that the $-I_{B(AV)}$ and $-I_{BM}$ ratings are not exceeded.

It is evident from Figs. 3(a) to 3(d) that the respective turn-off dissipation values are related by:-

$$P_{off(a)} > P_{off(b)} > P_{off(c)} > P_{off(d)}$$

The fall times (related in each case to the interval from t_1 to t_3) are given by:-

$$t_{f(a)} > t_{f(b)} > t_{f(c)} > t_{f(d)}$$

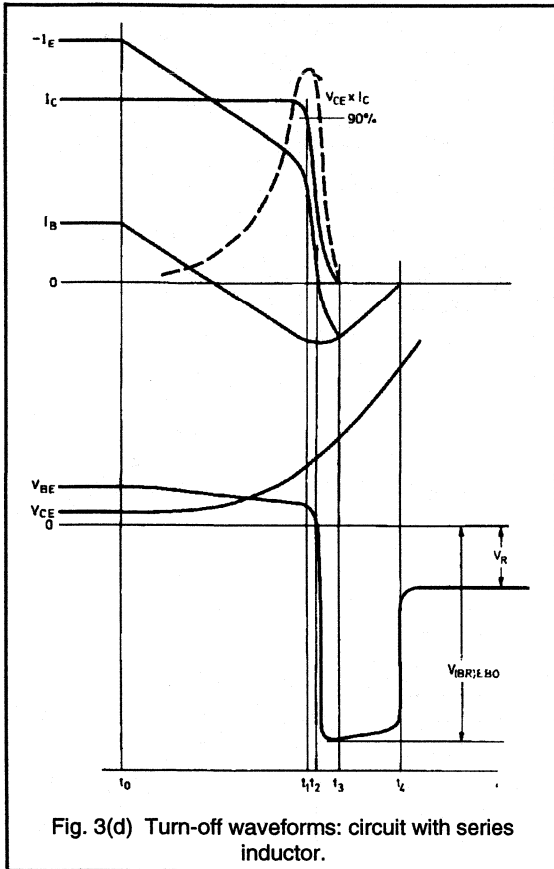
The storage times (equal to the interval from t_0 to t_1) are:-

$$t_{s(a)} < t_{s(b)} < t_{s(d)}$$

where the subscripts (a), (b), (c) and (d) refer to the waveforms of Figs. 3(a), 3(b), 3(c) and 3(d) respectively. It follows that the circuit of Fig. 4(c), which provides the waveforms of Fig. 3(d), gives the most favourable turn-off power dissipation. It has, however, the longest storage time.

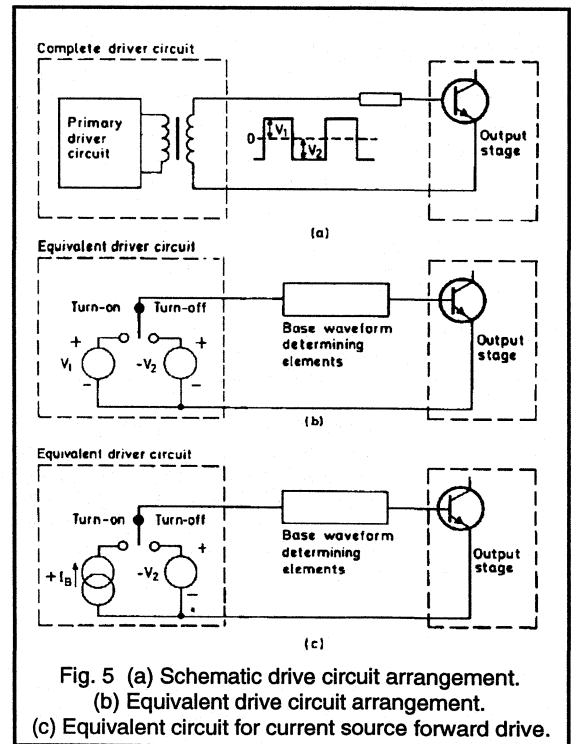
Optimum base drive circuitry

From the foregoing study of the required base current and base-emitter voltage waveforms, a fundamental base circuit arrangement to give optimum turn-on and turn-off of high voltage switching transistors will now be determined. It will be assumed that the driver stage is transformer-coupled to the base, as in Fig. 5(a), and that the driver transformer primary circuit is such that a low impedance is seen, looking into the secondary, during both the forward and reverse drive pulses. The complete driver circuit can then be represented as an equivalent voltage source of $+V_1$ volts during the forward drive period and $-V_2$ volts during the reverse drive/bias period. This is shown in Fig. 5(b).



From consideration of the waveforms in Figs. 3(a) to 3(d), it can be concluded that optimum turn-off of a high voltage transistor requires a sufficiently long storage time determined by the turn-off base current and a sufficiently large negative base-emitter voltage correctly timed with respect to the collector current waveform.

The phenomena which have been described in this section become more pronounced when the temperature of the operating junction of the transistor is increased: in particular, the fall times and storage times are increased. The design of a base drive circuit should therefore be checked by observing the waveforms obtained at elevated temperatures.



Forward base drive can also be obtained from a circuit which acts as a current source rather than a voltage source. This situation, where the reverse drive is still obtained from a voltage source, is represented in Fig. 5(c). The basic circuit arrangements of Figs. 5(b) and 5(c) differ only with respect to forward drive, and will where necessary be considered separately.

Comparable base drive waveforms can, of course, be obtained from circuits differing from those shown in Figs. 5(b) and 5(c). For such alternative circuit configurations the following discussion is equally valid.

Base series resistor

Most drive circuits incorporate a resistor R_B in series with the base. The influence of the value of this resistor on the drive characteristic will be briefly discussed.

Voltage source forward drive.

In circuits with a voltage source for forward drive, shown in a simplified form in Fig. 6(a), the following parameters determine the base current:-

The transistor base characteristic ;

The value of the base resistor R_B ;

The forward drive voltage V_1 .

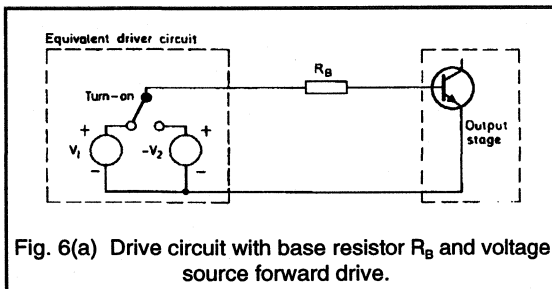


Fig. 6(a) Drive circuit with base resistor R_B and voltage source forward drive.

Figure 6(b) shows how the tolerances in these parameters affect the base current. It is clear that to avoid large variations in I_B , the tolerances in R_B and V_1 should be minimised. The voltage drop across R_B reduces the dependence of I_B on the spreads and variations of the transistor $V_{BE(on)}$. For good results the voltage drop across R_B must not be less than $V_{BE(on)}$.

Current source forward drive

In circuits where a current source is used for forward drive, the forward base current is independent of spreads and variations of $V_{BE(on)}$. The base current level and tolerances are governed entirely by the level and tolerances of the drive. A separate base series resistor is therefore unnecessary, but is nevertheless included in many practical current-source-driven circuits, to simplify the drive circuit design. The following discussions will assume that a series base resistor R_B always forms part of the base drive network.

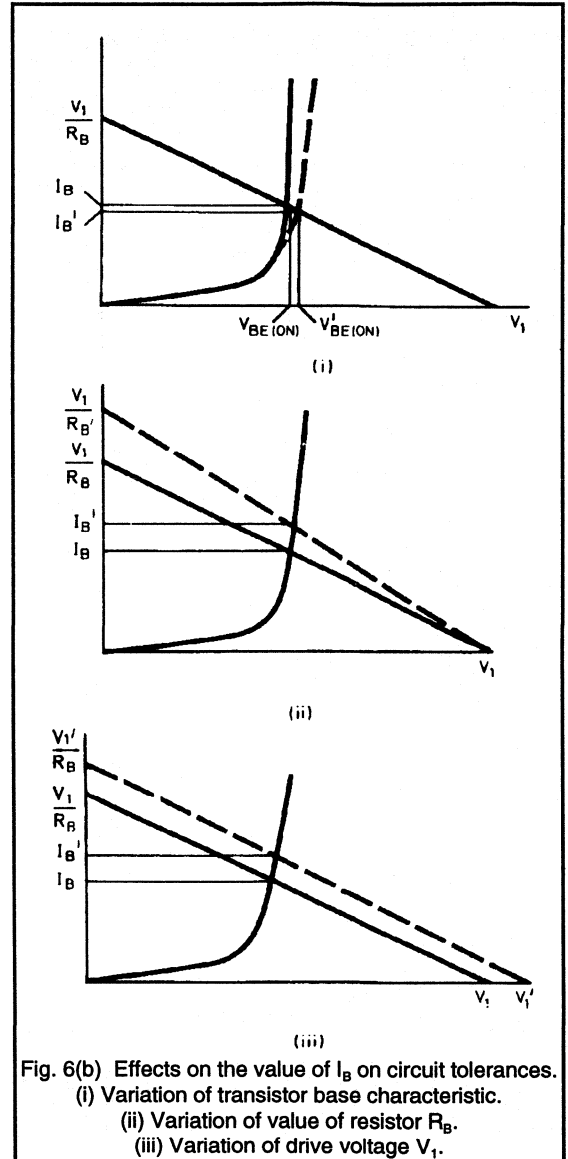


Fig. 6(b) Effects on the value of I_B on circuit tolerances.
(i) Variation of transistor base characteristic.
(ii) Variation of value of resistor R_B .
(iii) Variation of drive voltage V_1 .

Turn-off arrangement

To initiate collector current turn-off, the drive voltage is switched at time t_0 from the forward value $+V_1$ to the reverse value $-V_2$.

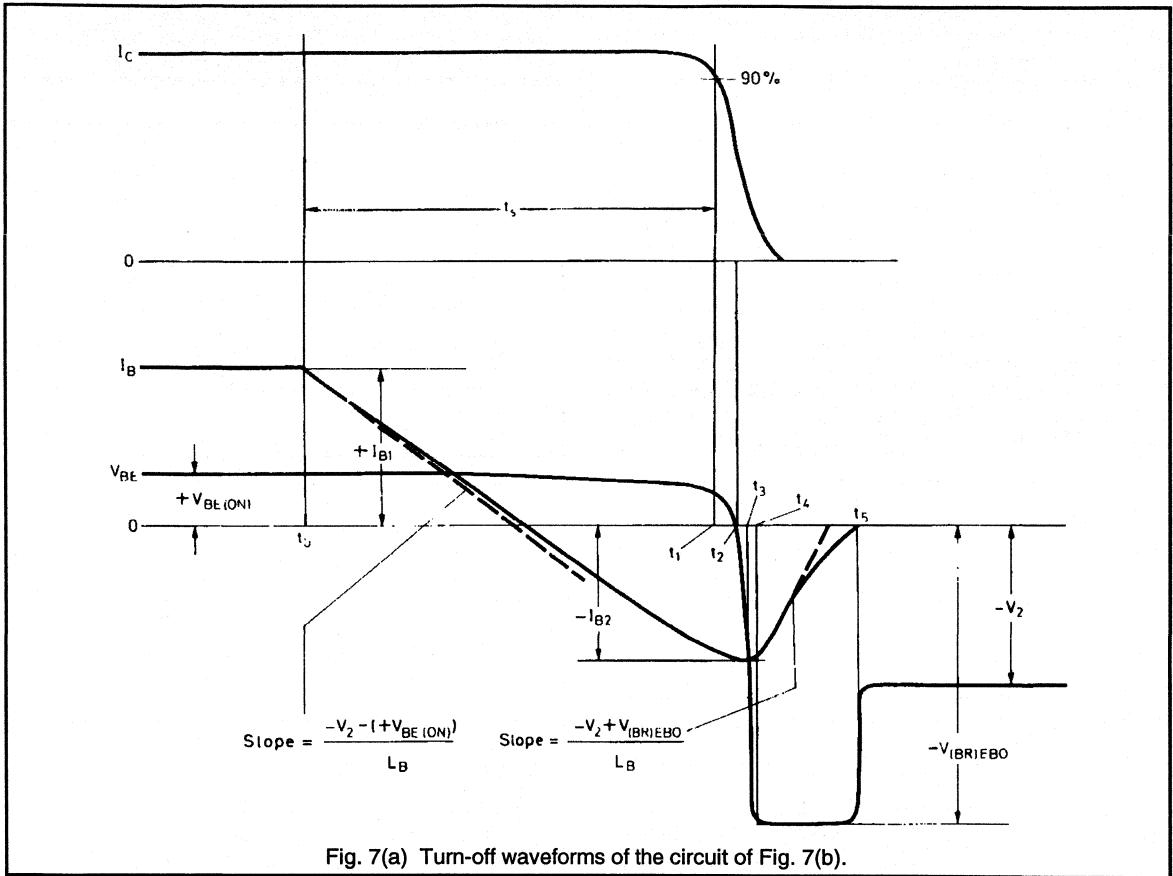


Fig. 7(a) Turn-off waveforms of the circuit of Fig. 7(b).

The desired turn-off voltage and current waveforms are obtained by adding various circuit elements to the basic resistive circuit of Fig. 6(a). A convenient method of achieving the desired slowly-decreasing base current is to use a series inductor L_B as shown in Fig. 7(b). The turn-off waveforms obtained by this method are shown in Fig. 7(a).

Base series inductor

At time t_0 the base current starts to decrease from the forward drive value I_{B1} with a slope equal to:-

$$\frac{-V_2 - (+V_{BE(on)})}{L_B}$$

For a considerable time after t_0 , the (decreasing) input capacitance of the transistor maintains a charge such that there is no perceptible change in V_{BE} . At time t_2 the amount of charge removed by the negative base current ($-I_B$) is insufficient to maintain this current, and its slope decreases.

At time t_3 , when:-

$$\frac{dI_B}{dt} = 0 \quad \text{where } I_B = I_{B2}$$

$$V_{BE} = -V_2 - R_B I_{B2}$$

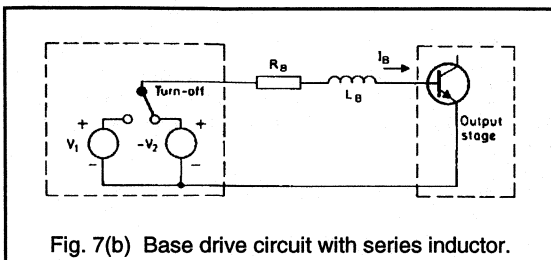


Fig. 7(b) Base drive circuit with series inductor.

Immediately after t_3 , the stored energy in L_B gives rise to a voltage peak tending to increase the reverse bias of the transistor. The voltage is clamped by the base-emitter breakdown voltage, so that:-

$$V_{BE} = -V_{(BR)EBO}$$

At time t_4 the negative base current starts to decrease with an initial slope equal to:-

$$\frac{-V_2 + V_{(BR)EBO}}{L_B}$$

At t_5 the base current reaches zero. The base-emitter voltage then changes from $-V_{(BR)EBO}$ to the value $-V_2$, the level of the drive voltage. As has been demonstrated, the collector storage time, t_s , is an important parameter of the drive circuit turn-off behaviour. Fig. 7(a) shows that the value of t_s can be calculated approximately from:-

$$\frac{-V_2 + V_{(BR)EBO}}{L_B} \cdot t_s = I_{B1} - I_{B2}$$

and this expression is sufficiently accurate in practice. In most cases the base current values are related by:-

$$\left(\frac{I_{B2}}{I_{B1}} \right) \approx 1 \text{ to } 3$$

In the case where $(-I_{B2} / I_{B1}) = 2$, the collector storage time is given by:-

$$t_s = \frac{3 I_{B1} L_B}{-V_2 - (+V_{BE(on)})}$$

In practical circuits, design considerations frequently indicate a relatively small value for V_2 . The required value of t_s is then obtained with a small value of L_B , and consequently the energy stored in the inductor ($1/2 L_B I_{B2}^2$) is insufficient to maintain the base-emitter junction in the breakdown condition. Figure 7(a) shows that breakdown should continue at least until the collector current is completely turned off. The higher the transistor junction temperature, the more stored energy is necessary to maintain breakdown throughout the increased turn-off time.

These phenomena are more serious in applications where the storage time must be short, as is the case for the BUT12 or BUW13 transistors, for example. For horizontal deflection output transistors such as the BU508 and BU2508, which require a much longer storage time, the base inductance usually stores sufficient energy for correct turn-off behaviour.

Diode assisted base inductor

It is possible to ensure the storage of sufficient turn-off energy by choosing a relatively large value for V_2 . Where a driver transformer is employed, there is then a corresponding increase in V_1 . To obtain the desired value

of forward base current, the base resistance R_B must also be large. A large value of R_B , however, diminishes the effect of L_B on the transistor turn-off behaviour, unless R_B is bypassed by a diode as in Fig. 8.

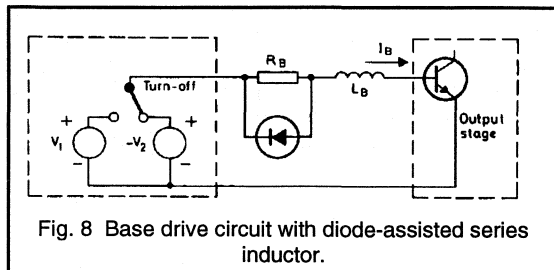


Fig. 8 Base drive circuit with diode-assisted series inductor.

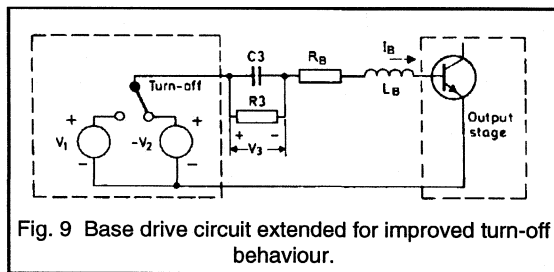


Fig. 9 Base drive circuit extended for improved turn-off behaviour.

Turn-off RC network

Improved turn-off behaviour can be obtained without increasing V_2 , if additional circuit elements are used. An arrangement used in practice is shown in Fig. 9, and consists of network $R_3 C_3$ which is connected in series with R_B and L_B .

A voltage V_3 is developed across C_3 because of the forward base current. (This voltage drop must be compensated by a higher value of V_1 .) When reverse current flows at turn-off, the polarity of V_3 is such that it assists the turn-off drive voltage V_2 . Using the same approximation as before, the storage time is given by:-

$$t_s = \frac{3 I_{B1} L_B}{-(V_2 + V_3) - (+V_{BE(on)})}$$

The same value of t_s now requires a larger value of L_B . The energy stored in L_B is therefore greater and the transistor can more reliably be driven into breakdown for the time required.

The waveforms of Fig. 7(a) are equally applicable to the circuit of Fig. 9, if V_2 is replaced by $(V_2 + V_3)$. In practice V_3 will not remain constant throughout the storage time, and replacing V_3 by its instantaneous value will make a slight difference to the waveforms.

Turn-on arrangements

It has been shown that for optimum turn-on of a high voltage switching transistor, the turn-on base current pulse must have a large amplitude and a fast leading edge with overshoot. However, the inductance L_B included in the circuits derived for optimum turn-off (Figs. 7 to 9) makes it difficult to produce such a turn-on pulse. The additional components (R_1 , C_1 , D_1) in the circuit of Fig. 10(a) help to solve this problem as shown by the waveforms of Fig. 10(b).

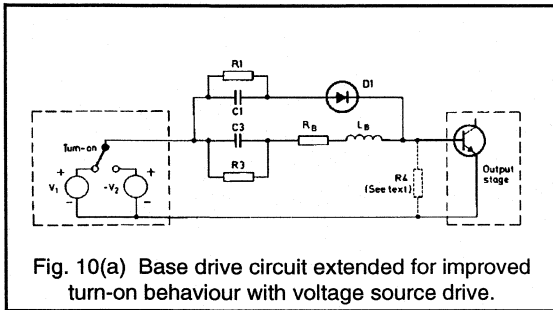


Fig. 10(a) Base drive circuit extended for improved turn-on behaviour with voltage source drive.

At the instant of turn-on, network R_1C_1 in series with D_1 provides a steep forward base current pulse. The turn-off network is effectively by-passed during the turn-on period by C_1 and D_1 . The time-constant R_1C_1 of the turn-on network should be chosen so that the forward current pulse amplitude is reduced virtually to zero by the time the transistor is turned on.

The turn-on network of Fig. 10(a) can also be added to the diode-assisted turn-off circuit of Fig. 8. In circuits which are forward driven by a current source, the overshoot required on the turn-on base current pulse must be achieved by appropriate current source design.

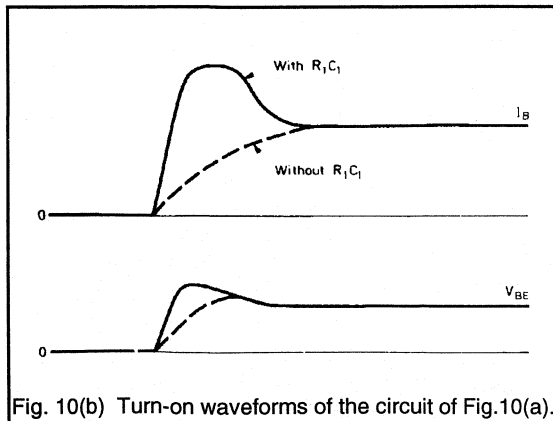


Fig. 10(b) Turn-on waveforms of the circuit of Fig.10(a).

Practical circuit design

The base drive circuit of Fig. 10(a) combines the drive voltage sources $+V_1$ and $-V_2$ with circuit elements R_B , L_B , R_3C_3 and $R_1C_1D_1$ which, if correctly dimensioned, allow optimum transient behaviour of the switching transistor. Not all these elements, however, will be necessary in every case for good results.

In circuits where the collector current rate of rise is limited by collector circuit inductance, the turn-on network $R_1C_1D_1$ can be omitted without danger of excessive collector dissipation at turn-on. In circuits where the base series inductance L_B is sufficiently large to give complete turn-off, network R_3C_3 can be omitted. Networks $R_1C_1D_1$ and R_3C_3 are superfluous in horizontal deflection circuits which use BU508, BU2508 transistors or similar types.

A discrete component for inductance L_B need not always be included, because the leakage inductance of the driver transformer is sometimes sufficient.

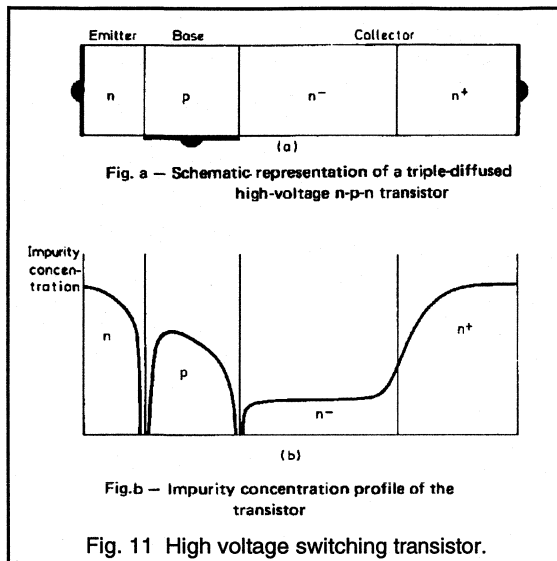
The omission of R_B from circuits which are forward driven by a voltage source should generally be considered bad design practice. It is, however, possible to select component values such that the functions of R_1C_1 and R_3C_3 are combined in a single network.

In some cases, the circuits of Figs. 7 to 10 may generate parasitic oscillations (ringing). These can usually be eliminated by connecting a damping resistor R_4 between the transistor base and emitter, as shown in broken lines in Fig. 10(a).

Physical behaviour of high-voltage switching transistors

Base circuit design for high-voltage switching transistors will now be considered with respect to the physical construction of the devices. To achieve a high breakdown voltage, the collector includes a thick region of high resistivity material. This is the major difference in the construction of high and low voltage transistors.

The construction of a triple-diffused high voltage transistor is represented schematically in Fig. 11(a). The collector region of an n-p-n transistor comprises a high resistivity n-region and a low resistivity n+ region. Most of the collector voltage is dropped across the n-region. For semiconductor material of a chosen resistivity, the thickness of the n-region is determined by the desired collector breakdown voltage. The thickness of the n+ region is determined by technological considerations, in particular the mechanical construction of the device. Fig. 11(b) shows the impurity concentration profile of the transistor of Fig. 11(a).

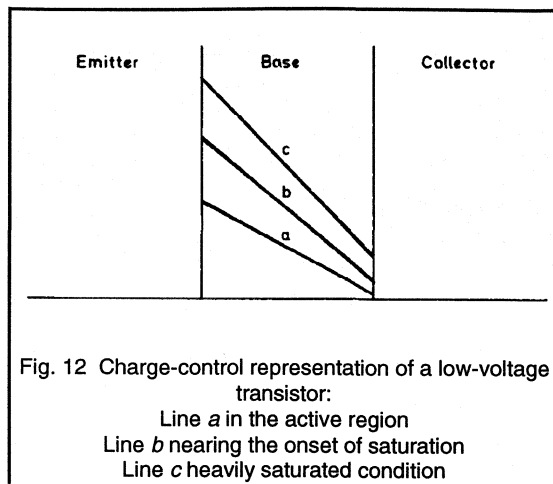


For good switching performance, the high voltage blocking characteristic of the transistor structure must be modified at transistor turn-on, so that a low forward voltage condition is exhibited. One method of achieving this is to inject a large number of carriers through the base to the collector region. The high resistivity of the n- region is then "swamped" by excess carriers. This effect is often referred to as a collector-width modulation.

The following discussion of the physical changes which occur at transistor turn-on and turn-off is based on a much simplified transistor model; that is, the one dimensional charge control model. Fig. 12 shows such a model of a low-voltage transistor, and assumes a large free carrier-to-doping concentration ratio in the base due to the carriers injected from the emitter. Line *a* represents the free carrier concentration in the base for transistor operation in the active region ($V_{CB} > 0$), and line *c* that for the saturated condition ($V_{CB} < 0$). Line *b* represents the concentration at the onset of saturation, where $V_{CB} = 0$. The slope of the free carrier concentration line at the collector junction is proportional to the collector current density, and therefore, to the collector current.

Turn-on behaviour

The carrier concentration profile of a high-voltage transistor during turn-on is shown in Fig. 13(a). Line 1 represents a condition where relatively few carriers are injected into the base from the emitter. Let line 1 be defined as representing the onset of saturation for the metallurgic collector junction; that is, point 1(C'). In this case, $V_{CB} = 0$, whereas the externally measured collector voltage is very high because of the voltage drop across the high-resistivity collector region.



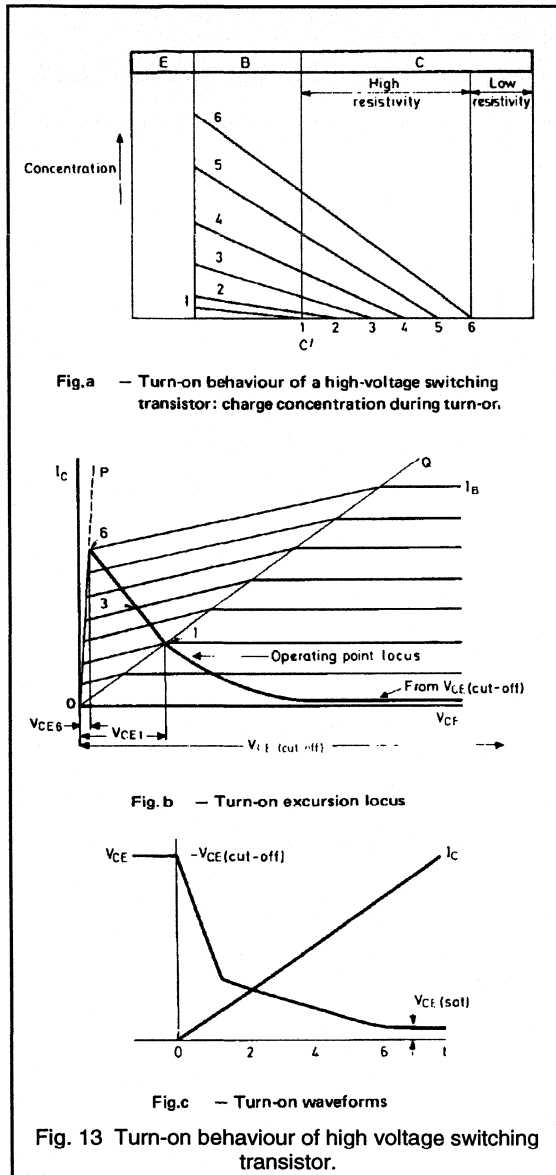
Line 2 in Fig. 13(a) represents a high level of carrier injection into the base from the emitter. Carriers have also penetrated the high-resistivity collector region as far as point 2(C'), and so the base region is now, in effect, extended to this point and the effective width of the collector region is reduced. The voltage drop across the collector region, caused by the collector current which is proportional to the concentration gradient at point 2(C'), is therefore less than the voltage drop which occurred with the level of carrier injection on line 1.

Lines 3, 4 and 5 represent still higher carrier injection levels, and hence decreasing effective collector widths. The voltage drop across the effective collector also decreases.

In the situation represented by line 6, the entire high resistivity collector region has been flooded with excess carriers. The collector-base voltage is therefore so low that the transistor is effectively saturated. The low saturation voltage has been obtained at the expense of a large base current, and this explains why a high-voltage transistor has a low current gain, especially at large collector currents.

Figure 13(b) shows simplified collector current/voltage characteristics for a typical high voltage transistor. Between lines OQ and OP, voltage V_{CE} progressively decreases as excess carriers swamp the high-resistivity collector region. Line OP can be regarded as the 'saturation' line.

When the transistor is turned on, the carrier injection level increases from the very small cut-off level (not shown in Fig. 13(a)) to the level represented by line 6 in Fig. 13(a). The transistor operating point therefore moves from the cut-off position along the locus shown in Fig. 13(b) to position 6, which corresponds to line 6 in Fig. 13(a). The effect of this process on I_C and V_{CE} is shown in Fig. 13(c), where the time axis is labelled 0 to 6 to correspond to the



numbered positions on the operating point locus of Fig. 13(b) and the numbered lines on the carrier concentration diagram of Fig. 13(a).

The time taken to reach the emitter injection level 6 is directly proportional to the turn-on time of the transistor. The rate of build-up of emitter injection depends on the peak amplitude and rise time of the turn-on base current pulse. The shortest turn-on time is obtained from a large amplitude

base current pulse with a fast leading edge. Thus, physical considerations support the conclusion already drawn from a study of the circuit behaviour of the transistor.

Turn-off behaviour

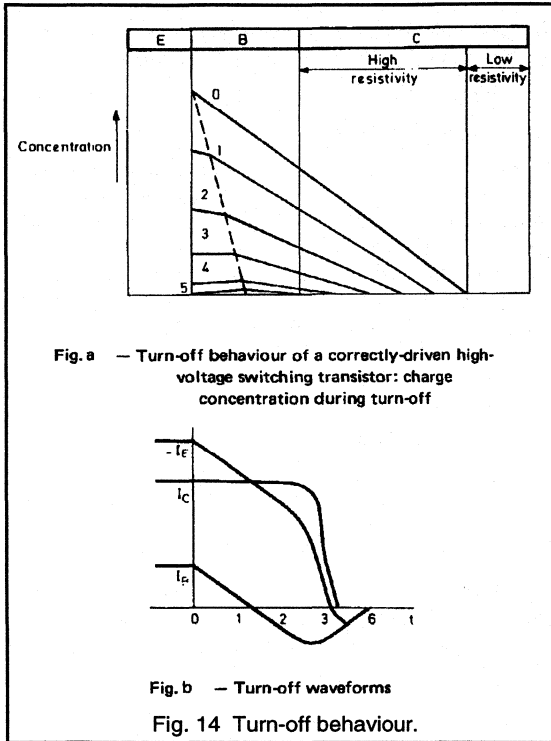
The carrier concentration in the saturated transistor at the beginning of the turn-off period is represented by line 0 in Fig. 14(a), corresponding to line 6 in Fig. 13(a). As shown in Fig. 14(b), the base current I_B gradually decreases, but I_C remains almost constant for some time, and $-I_E$ therefore decreases to match I_B . The resulting carrier concentration patterns are shown as lines 1 and 2 in Fig. 14(a). This process is plotted against time in Fig. 14(b) where, again, the graduation of the horizontal axis corresponds to that of the lines in Fig. 14(a).

At time point 3 the emitter current has reduced to zero, and is slightly negative until point 6. Thus the carrier concentration lines 4 and 5 have negative slope. Complete collector current cut-off is reached before point 6. (This situation is not represented in Fig. 14).

Excess carriers present in the collector region are gradually removed from point 0 onwards. This results in increasing collector voltage because of the increasing effective width of the high-resistivity collector region.

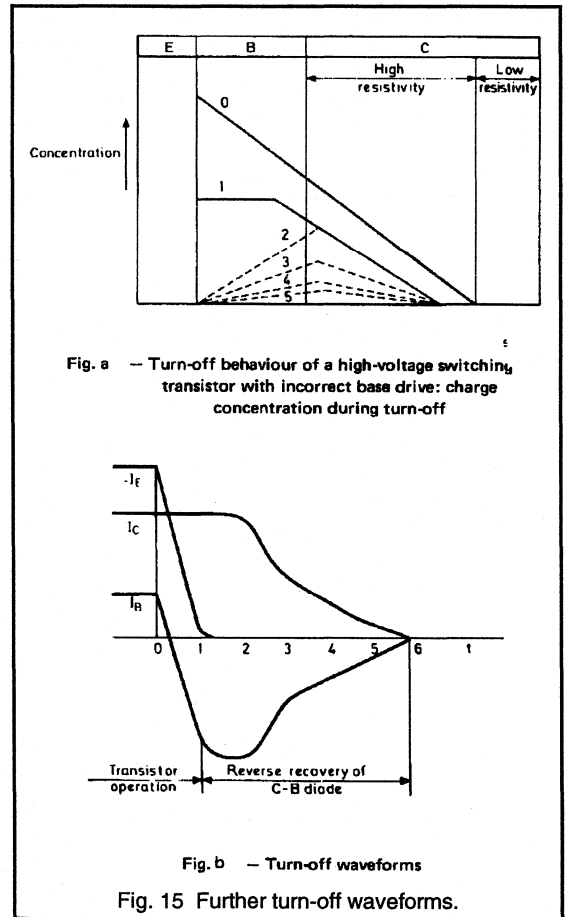
Figures 14(a) and 14(b) depict a typical turn-off process giving good results with high voltage transistors; the waveforms of Fig. 14(b) should be compared with those of Figs. 3(d) and 7(a). A different process is shown in Figs. 15(a) and 15(b). The initial situation is similar (line 0, Fig. 15(a)) but the base current has a steep negative slope. At time point 1 of Fig. 15(b), the emitter current $-I_E$ has reached zero, and so the carrier concentration line 1 has zero slope at the emitter junction. The emitter-base junction is effectively cut off and only the relatively small leakage current (not shown in Fig. 15(b)) is flowing. From point 1 onwards, therefore, the emitter has no influence on the behaviour of the transistor. The switching process is no longer 'transistor action', but the reverse recovery process of a diode. The carrier concentration pattern during this process is shown in Fig. 15(a) in broken lines, with zero slope at the emitter junction because the emitter is inoperative.

The reverse recovery process is slow because of the high resistivity of the collector region and the consequent slow decrease of collector current. (Collector and base currents are, of course, equal and opposite when the emitter is cut off). The turn-off dissipation increases progressively as the transition time from collector saturation to cut-off increases. Furthermore, at higher junction temperatures the reverse recovery charge, and hence the duration of the recovery process, is greater.



The longer the turn-off time, the greater the turn-off dissipation and, hence, the higher the device temperature which itself causes a further increase in turn-off time and dissipation. To avoid the risk of thermal runaway and subsequent transistor destruction which arises under these conditions, the turn-off drive must be such that no part of the turn-off is governed by the reverse recovery process of the collector base diode. Actual transistor action should be maintained throughout the time when an appreciable amount of charge is present in the transistor collector and base regions, and therefore the emitter should continue to operate to remove the excess charge.

There are many conditions of transistor turn-off which lie between the extreme cases of Figs. 14(a) and 15(a). Circuits in which the operating conditions tend towards those shown in Fig. 15(a) must be regarded as a potential source of unreliability, and so the performance of such circuits at elevated temperatures should be carefully assessed.



2.1.4 Isolated Power Semiconductors for High Frequency Power Supply Applications

This section describes a 100 W off-line switcher using the latest component and application technology for cost-effective miniaturisation (see Ref.1). The power supply has a switching frequency of 500kHz with 1MHz output ripple. The section focuses on new power semiconductor components and, in particular, the need for good thermal management and electrical isolation. The isolated F-pack - SOT-186, SOT-199 and the new SOT-186A - are introduced. Philips has developed these packages for applications in S.M.P.S. The importance of screening to minimise conducted R.F.I. is covered and supported with experimental results.

Introduction

There is an ever-growing interest in high frequency power supplies and examples are now appearing in the market place. The strong motivation for miniaturisation is well founded and a comprehensive range of high frequency components is evolving to meet this important new application area, including:-

The output filter capacitor, which was traditionally an electrolytic type, can be replaced by the lower impedance multi-layer ceramic type.

The output filter choke may be reduced in size and complexity to a simple U-core with only a few turns.

The benefits of reduced transformer size can be realised at high frequency by using core materials such as 3F3. However, transformer size is ultimately limited by creepage and clearance distances defined by international safety standards.

Power MOSFETs provide the almost ideal switch, since they are majority carrier devices with very low switching losses. Similarly, Schottky diodes are the best choice for the output rectifiers.

This paper concentrates on the semiconductors and introduces three isolated encapsulations:- the 'F-packs' - SOT-186, SOT-186A and SOT-199 - and applies them to high frequency S.M.P.S.

Power MOSFETs in isolated packages

Making power supplies smaller requires devices such as MOSFETs to be used as the power switch at high frequency. At this high frequency the size and efficiency of the output filter can be dramatically improved. Present abstract perception of acceptable inefficiency in power semiconductors remains constant i.e. 5 to 10% overall semiconductor loss at 500kHz is just as acceptable as at 50kHz. So throughout the trend to higher frequencies, the heatsink size has remained constant.

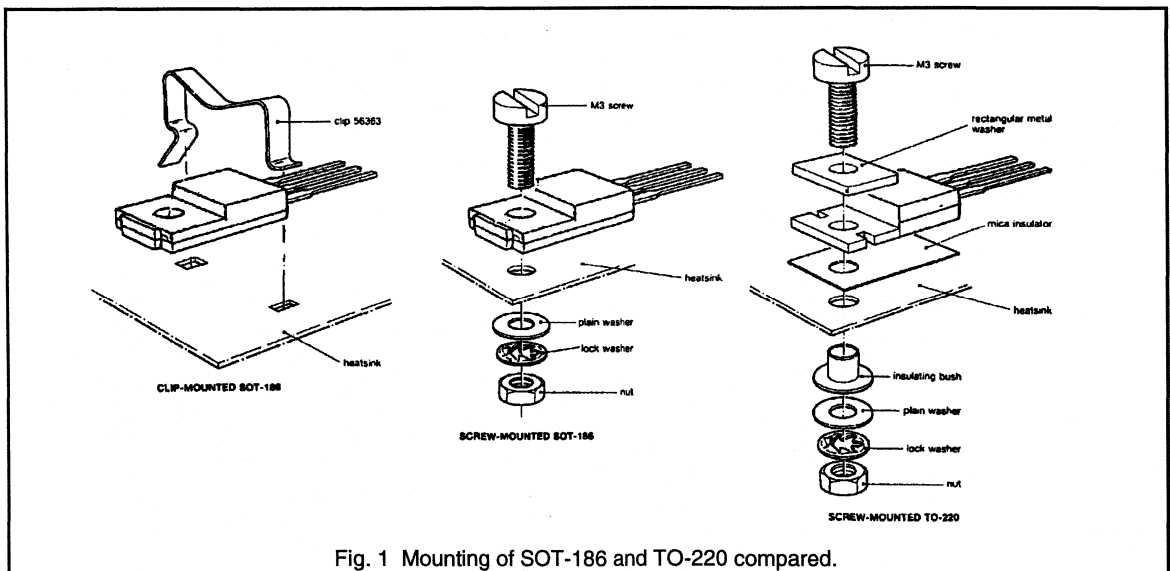


Fig. 1 Mounting of SOT-186 and TO-220 compared.

At 50kHz it is possible to use the earthed open frame of the power supply as the heatsink. Then all semiconductors are laid out around the periphery of the p.c.b. and mounted with isolation onto the heatsink. To gain the minimum overall size from high frequency operation, this technique must become standard practice to avoid having to leave clearance distances between primary and secondary side heatsinks. The component manufacturers are responding to the need for transistors with isolation by making them with a fully isolated package - the F-pack.

F-pack, SOT-186, is an encapsulation with a functionally isolating epoxy layer moulded onto its header; see Fig. 1. This allows a common heatsink to be used with no further isolation components. With just a spring clip, an insulated mounting (up to 1000V) of virtually all existing TO-220 components is possible without degrading performance. Screw mounted, the SOT-186 is still simplicity itself; there is no need for metal spacers, insulation bushes and mica insulators. Mounted either way, the F-pack reduces mounting hardware compared with that required for a standard TO-220.

The insulating layer of a SOT-186 can withstand more than 1000V, but the maximum voltage between adjacent leads is limited to 1000V. This is slightly less than the breakdown voltage between TO-220 legs due to the distance between the legs being reduced from 1.6mm to 1.05mm. However, the 375 μm thick epoxy gives more creepage and clearance between transistor legs and heatsink than a traditional mica washer of 50 μm . The capacitive coupling to an earthed heatsink is therefore reduced from 40pF to 13pF. This can be of significant help with the control of R.F.I.

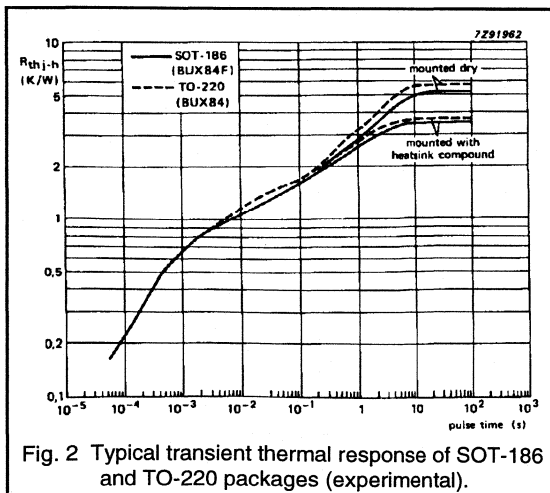


Fig. 2 Typical transient thermal response of SOT-186 and TO-220 packages (experimental).

The latest isolated package introduced by Philips is the SOT-186A. This is a fully encapsulated TO-220 replacement which provides true isolation from the heatsink of 2500V RMS. It is fully pin-compatible with the TO-220 package since it possesses the same distance between the leads and the back of the tab where thermal contact is made with the heatsink.

The transient thermal response of the SOT-186 and TO-220 encapsulations is shown in Fig. 2. A BUX84F (SOT-186) and a BUX84 (TO-220) were used for the test. Each transistor was mounted on a heatsink at 25°C. The BUX84 was mounted on a mica washer. The test conditions were given by: Mounting force = 30N; $I_E = 1\text{A}$; $V_{CB} = 10\text{V}$.

The thermal resistance of the F-pack is better than the standard package in free air because it is all black and slightly larger. The difference is quite small, 55K/W for the SOT-186 and 70K/W for the TO-220. Mounted on a heatsink, the typical thermal resistance of the SOT-186 is slightly better than the standard TO-220, see Fig. 2. However, the exact value of $R_{th(mb-hs)}$ depends on the following:

- Whether heatsink compound is used.
- The screw's torque or pressure on the encapsulation.
- The flatness of the heatsink.

The flatness of the TO-220 metal heatsink is more controllable than the moulded epoxy on the back of the SOT-186. Therefore, the use of a heatsink compound with SOT-186 is of great importance. Once this is done the thermal characteristics of the two approaches are similar.

Schottky diodes in isolated packages

To be consistent with the small, single heatsink approach, the output rectifying diodes must be isolated from the heatsink too. Schottky diodes in SOT-186 are available, and encapsulations accommodating larger crystal sizes are available for higher powers. The F-pack version of the larger SOT-93 package is the SOT-199. Two Schottky diodes can be mounted in SOT-199 for power outputs up to a maximum of $I_{F(AV)}$ equal to 30 A. The SOT-199 package is similar to, but larger than, the SOT-186 shown in Fig. 1, and can be mounted similarly.

The epoxy isolation is thicker at 475 μm . This further reduces the capacitive coupling to heatsink when compared to a Schottky diode isolated with either 50 μm mica or 250 μm alumina. Equally important is the increase in the breakdown voltage, from a guaranteed 1000V to 1500V. As with SOT-186, the use of heatsink compound is advised to give good thermal contact.

In conclusion, the combination of isolated packages allows an S.M.P.S. to be designed with many devices thermally connected to, but electrically isolated from, a single common heatsink.

Transistor characteristics affecting choice of high frequency converter

In this exercise only MOSFETs were considered practical for the target operating frequency of 500kHz. The range of converters to choose from is enormous if all the resonant circuits are included. The choice in this case is reduced by considering only the square wave types because:-

- The p.w.m technique is well understood.
- The main output is easily controlled over a wide range of input voltages and output loads.
- A resonant tank circuit, which may increase size, is not needed.

It is recognised that there are many situations and components which equally affect the choice of converter. The transformer component has been studied in Ref. 1. For maximum power through the transformer in a mains input, 500kHz, 100W power supply, a half-bridge converter configuration was chosen. The influence of the transistor is now examined.

The relationship of on-resistance $R_{DS(on)}$, with drain-source breakdown voltage, $V_{(BR)DSS}$, has been examined in Ref. 2. It was shown that $R_{DS(on)}$ is proportional to $V_{(BR)DSS}$ raised to the power 2. This implies equal losses for equal total silicon area. The advantage is therefore with the forward / flyback circuits because they have easier drive arrangements and often only require one encapsulation. Particular attention is paid to the frequency dependent losses, which are now considered.

C_{OSS} and the loss during turn-on

No matter how fast the transistor is switched in an attempt to avoid switching losses, there are always capacitances associated with the structure of the transistor which will dissipate energy each time the transistor is turned on and off. For a BUK456-800A, 800V MOSFET of 20mm² chip area, the turn-off waveform is shown in Fig. 3.

All loads have been reduced to nearly zero to highlight the turn-on current spike due to the capacitance of the circuit. The discharge of the output capacitance of the device will be similar but is unseen by the oscilloscope because it is completely internal to the device. The discharge of the energy is done in two different stages:-

Stage 1 - From the flyback voltage to the D.C link voltage.

This energy is mainly either returned to the supply or clamped in the inductance of the transformer by the secondary diodes, which release it to supply the load when the primary switch turns on. This energy is not dissipated in the power supply.

Stage 2 - From the link voltage to the on-state voltage.

This energy is dissipated in the transistor when it turns on. The calculation of the effective output capacitance at this voltage involves integration to take into account the varying nature of the capacitance with the applied drain voltage. The general expression for energy stored in the output capacitance of a MOSFET is:-

$$E = 3.3 C_{oss(25V)} V_d^{1.5}$$

For a BUK456-800A switching on with $V_{DS} = 325V$, the energy is 1.6 μJ . Gate to drain capacitance is not taken into account but would probably add about 20% extra dissipation to take it to 1.9 μJ . This is for a transistor operating in a fixed frequency flyback, forward, or push-pull converter. A transistor in the half bridge circuit switches on from half the line voltage and so the losses in each transistor would be approximately a quarter of those in the previous converters. In self-oscillating power supplies the transistor switches on from 750 V. This would dissipate all of the stage (1) energy as well and so that could make approximately four times the loss in the transistor in this configuration. This example of a BUK456-800A operating at 500kHz, in a fixed frequency forward, flyback, or push pull system would dissipate 0.95 W internal to the device.

Stray capacitance around the circuit includes mounting base to heatsink capacitance, which for a ceramic isolator is 18pF. The energy for this is simply calculated by using $0.5 CV^2$, and is 1 μJ when charged to 325 V. F-pack reduces this by about a factor of two.

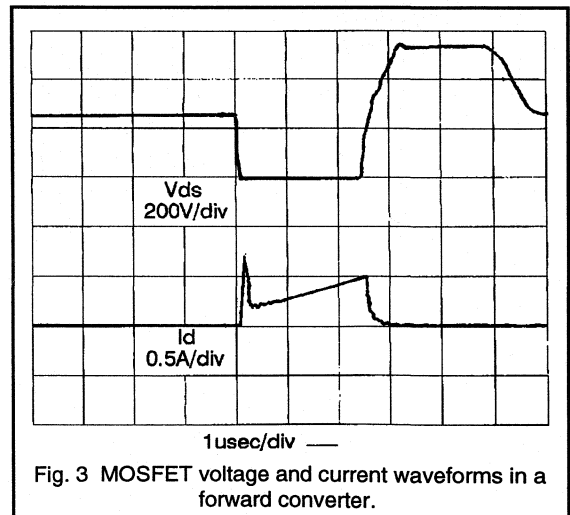


Fig. 3 MOSFET voltage and current waveforms in a forward converter.

In conclusion, the fixed frequency half-bridge system benefits from discharging from only half the d.c. link voltage and is the best choice to minimise these effects. There are two switches, so the overall benefit is only half, but the thermal resistance is also half, so the temperature rise of

each transistor is actually four times less than in a forward converter. This makes this internal loss at 500kHz, 0.25 W in each transistor.

C_{ISS} and drive circuit losses

It is common to drive MOSFETs from a voltage source, through a series gate resistor. This gate resistor is seen usually to dampen stray inductance ringing with the gate capacitance during turn-on and turn-off of the transistor. This effectively prevents spurious turn-on. The resistor has another function when operating at a frequency of 500kHz, and that is to remove the dissipation of the energy of the gate capacitance from inside to outside the transistor. This is important because at frequencies in the MHz region the dissipation becomes the order of 1 W. A graph of charging the gate with a constant 1mA current source is shown in Fig. 4. The area under the curve was measured as 220 μ Vs.

Therefore, at 10kHz, the power dissipation is 2mW and at 10MHz, 2W.

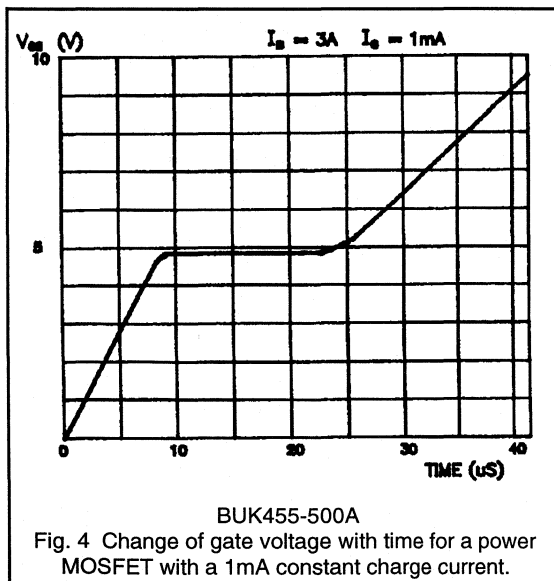


Fig. 4 Change of gate voltage with time for a power MOSFET with a 1mA constant charge current.

If the system chosen has two transistors, as in the half-bridge, then the dissipation will be doubled. Therefore, a single transistor solution is the most efficient to minimise these losses.

Concluding this section on the significant transistor characteristics, the power loss due to discharging internal MOSFET capacitances is seen to become significant around 500kHz to 1MHz, affecting the efficiency of a 100W converter. The predominant loss is output capacitance, which is discharged by, and dissipated in $R_{DS(on)}$. Converters which reduce this loss are those which switch from a lower V_{DS} , i.e.:-

- Resonant converters which switch at zero voltage.
- Converters designed for rectified 110V a.c. mains rather than 230V a.c. mains.
- Square-wave converters which use a half-bridge configuration rather than forward, flyback, or push-pull circuits.

Self oscillating power supplies give higher losses because they discharge from the flyback voltage of 750V at turn-on.

SMPS design considerations

There are two major areas which influence the choice of converter to be considered here:-

- multiple outputs
- R.F.I.

The influence of multiple outputs on the choice of converter.

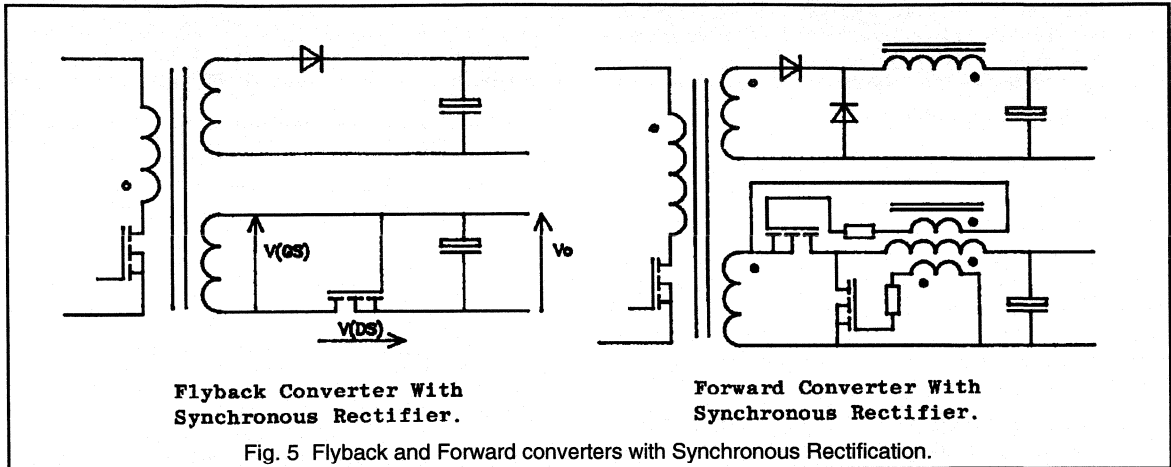
If only one output is required then the half-bridge would be selected to minimise the loss due to output capacitance, as described above.

If multiple outputs are specified, and some of these require rectifying diodes other than Schottky diodes, then the switching loss of power epitaxial diodes has to be considered. Before the arrival of 100V Schottky diodes, epitaxial diodes would have been a natural first choice for outputs higher than 5V. However, a 12V auxiliary output often has less current than a 5V output, so MOSFETs can compete better on forward volt drop. Then there is switching loss: a MOSFET can have less loss than an epitaxial diode, but the actual frequency at which it becomes effective is debatable.

Synchronous MOSFET rectifiers were first seen as a threat to Schottky diodes for use in low voltage outputs. They could rectify with less forward volt drop, albeit sometimes at a cost. MOSFET rectifiers are now more of a threat to epitaxial diodes in higher voltage outputs above 15 to 20V. Applying these transistors is not as straightforward as it may first appear. Looking at flyback, forward and bridge outputs in turn:-

Flyback converter

A diode rectified output is replaced by a MOSFET, with no extra components added, (Fig. 5). Putting the transistor in the negative line and orientating it with the cathode of the parasitic diode connected to the transformer allows it to be driven well and does not threaten the gate oxide isolation. If the drive is slowed down by the addition of a gate resistor, the voltage across R_{DS} during transient switching can be large enough such that, when added to the output voltage, gives V_{GS} greater than that recommended in data. Fast turn-on is therefore essential for the good health of the transistor.



Forward converter

Normal diode rectifiers are replaced by MOSFETs in a forward output, as shown in Fig. 5, with no extra components added. However, there is a problem at maximum input voltage. At minimum volts, the transformer winding supplies $V_{out} + V_{choke}$, where:-

$$V_{out} = V_{choke} = 12V \quad (\text{for a } 12V \text{ output}) \\ \text{at } 50\% \text{ mark/space ratio.}$$

$$V_{trans} = 24V$$

At maximum input volts, the choke may have 2 or 3 times the voltage across it, which makes the total 36V or 48V. With the gate rated at 20V, the choke is necessary for the forward transistor, as shown in Fig. 5, to supply the correct voltage. It may also be necessary for the freewheel diode, but this may be marginal depending on the input voltage range specified. This costs even more money, but may be considered good value if the loss in an epitaxial diode costs too much in efficiency.

Bridge converters

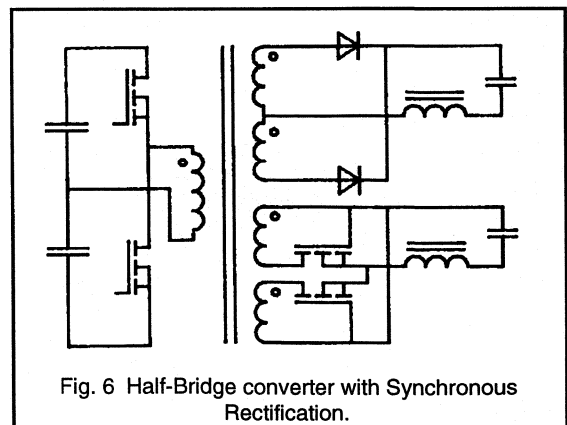
The circuit shown in Fig. 6 at first glance looks attractive. Parasitic diodes are arranged never to come on, and thus do not cause switching losses themselves. Also, the choke voltage drop is less than in the forward case, which may indicate that the MOSFETs can be used without extra overwinds to protect the gate voltage.

However, the simple drive waveforms used here, which are naturally synchronised to the primary switches, do not bias the rectifying transistors on when both the switches are off. During this time the transformer magnetising currents need a path to freewheel around. Normally this path is provided by the diodes. When the drive has been removed in the circuit example of Fig. 6, this path no longer exists. To turn

the transistor around so that their body diode can conduct during this freewheel time would only give diode turn-off loss, which is what the technique is intended to avoid. Any bypass diode has the same drawback. The correct drive waveforms are not even available from the choke. They can be generated most easily in conjunction with the primary switch waveforms, but involves expensive isolating drive toroids.

The conclusions on which converters are most suitable, and how to connect the MOSFETs in the most cost-effective manner for a 12V output are:-

- A flyback MOSFET rectifier can be connected with no extra components.
- A forward MOSFET needs one overwind, maybe two.
- A bridge output requires drive toroids whose signal is not easily derivable from the secondary side waveforms.



Even though MOSFETs may have less switching loss than epitaxial diodes, they do have capacitance discharged each cycle. The only consolation is that it has a built-in 'anti-snap-off' feature. If the rectifiers are switching at low V_{DS} then this loss is indeed very low.

Influence of R.F.I. on the choice of converter

This section deals with R.F.I. considerations of primary switches and secondary rectifying diodes only. The techniques will be applied to a power supply operating at 500kHz that has been developed to deliver a single 5V output at 15A, from 250V a.c. mains input. The converter choice is a half bridge circuit to minimise the loss in the circuit due to C_{OSS} .

A single heatsink arrangement is required to minimise size, so primary and secondary semiconductors need to be thermally cooled on the same heatsink. R.F.I. currents need to be prevented from coupling primary to secondary through the heatsink. Connection of R.F.I. screens underneath all components attached to the metal is not necessary when the structure of the semiconductors is understood.

Taking the rectifiers first:-

The arrangement of the output bridge is shown in Fig. 7. The cathodes of the diodes are connected to the substrate within their encapsulation. Thus, as long as the cathodes are connected as close as possible to the ceramic capacitor, C3, of the output filter, the common cathode/capacitor junction is a solid a.c. earth point. Therefore, no R.F.I. currents are connected into the common heatsink. An isolated encapsulation for an electrical arrangement such as this is all that is needed to minimise R.F.I. from diodes to heatsink.

Considering next the primary power transistors:-

The arrangement of power transistors is also shown in Fig. 7. The drains of the transistors are connected to the substrates of their encapsulations. Thus, as long as TR1 is connected as close as possible to the film-foil bridge capacitors, C1 and C2, the common drain/capacitor junction is a solid a.c. earth point. A SOT-186, SOT-186A, SOT-199 or TO-220 with mica washers may be suitable for TR1, the final selection being dependent on the isolation requirements. For TR2, the drain and therefore the substrate is modulated by the action of the circuit. Thus, without preventive action, R.F.I. currents will be coupled to the heatsink.

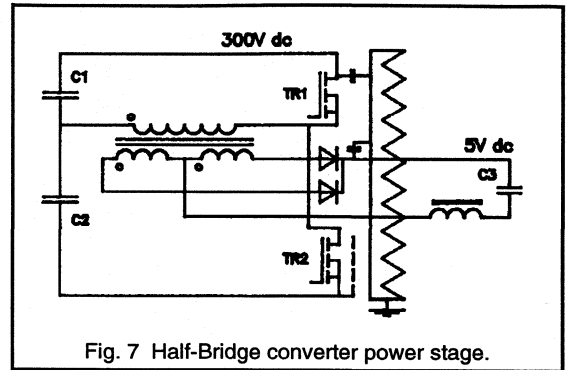


Fig. 7 Half-Bridge converter power stage.

The transistor TR2 is in a similar situation to one in a flyback or forward configuration. A simple solution is to use a SOT-186 (F-pack), plus copper screen connected to the transistor source lead and the film-foil capacitor, C2, plus whatever degree of isolation is required to the heatsink. This assembly was tested, and the result was that the screen reduced the line R.F.I. peaks by an average of 10dB over the range 500kHz to 10MHz. A small percentage of this can be attributed to the distance that the copper screen moves the substrate away from the heatsink. Nevertheless, the majority is due to the inclusion of the 0.1mm thick copper screen.

The conclusion is that a variety of encapsulations is necessary to allow R.F.I. to be minimised when the power supply is constructed.

Conclusions

This paper shows how to calculate some of the limiting parameters in the application of semiconductors to high frequency SMPS. It also highlights new encapsulations developed for high frequency power conversion applications. Some of the range of encapsulations were demonstrated in a 500kHz half-bridge off-line switcher.

References

1. Improved ferrite materials and core outlines for high frequency power supplies. Chapter 2.4.1
2. PowerMOS introduction. Chapter 1.2.1

Output Rectification



2.2.1 Fast Recovery Epitaxial Diodes for use in High Frequency Rectification

In the world of switched-mode power supply (S.M.P.S.) design, one of the most pronounced advances in recent years has been the implementation of ever increasing switching frequencies. The advantages include improved efficiency and an overall reduction in size, obtained by the shrinking volume of the magnetics and filtering components when operated at higher frequencies.

Developments in switching speeds and efficiency of the active switching power devices such as bipolars, Darlingtons and especially power MOSFETs, have meant that switching frequencies of 100kHz are now typical. Some manufacturers are presently designing p.w.m. versions at up to 500kHz, with resonant mode topologies (currently an area of intensive academic research) allowing frequencies of 1MHz and above to be achievable.

These changes have further increased demands on the other fundamental power semiconductor device within the S.M.P.S. - the power rectification diode.

Key Rectifier Characteristics.

In the requirements for efficient high frequency S.M.P.S. rectification, the diode has to meet the following critical requirements:-

- Short reverse recovery time, t_{rr} , for compatibility with high frequency use.
- Low forward voltage drop, V_F , to maximise overall converter efficiency.
- Low loss switching characteristics, which reduce the major frequency dependent loss in the diode.
- A soft reverse recovery waveform, with a low di_F/dt rate, reduces the generation of unwanted R.F.I. within the supply.

The Philips range of fast recovery epitaxial diodes (FREDs) has been developed to meet the requirements of high frequency, high power rectification. With many years' experience in the development of epitaxial device technology, Philips offers a comprehensive range of FREDs. Some of their standard characteristics include:-

- A reverse blocking voltage range from 100V to 800V, and forward current handling capability from 1A to 30A. Thus, they are compatible for use in a wide range of S.M.P.S. applications, from low voltage dc/dc converters right through to off-line ac/dc supplies. Philips epitaxial diodes are compatible with a range of output voltages from 10V to 200V, with the capability of supplying a large range of output powers. Several different package outlines are also available, offering the engineer flexibility in design.
- Very fast reverse recovery time, t_{rr} , as low as 20ns, coupled with inherent low switching losses permits the diode to be switched at frequencies up to 1MHz.
- Low V_F values, typically 0.8V, produce smaller on-state diode loss and increased S.M.P.S. efficiency. This is particularly important for low output voltage requirements.
- Soft recovery is assured with the whole range of FREDs, resulting in minimal R.F.I. generation.

Structure of the power diode

All silicon power diodes consist of some type of P-I-N structure, made up of a highly doped P type region on one side, and a highly doped N+ type on the other, both separated by a near intrinsic middle region called the base. The properties of this base region such as width, doping levels and recombination lifetime determine the most important diode characteristics, such as reverse blocking voltage capability, on-state voltage drop V_F , and switching speed, all critical for efficient high frequency rectification.

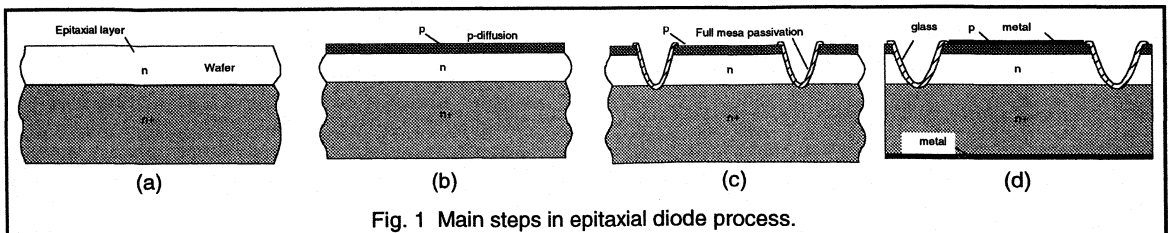


Fig. 1 Main steps in epitaxial diode process.

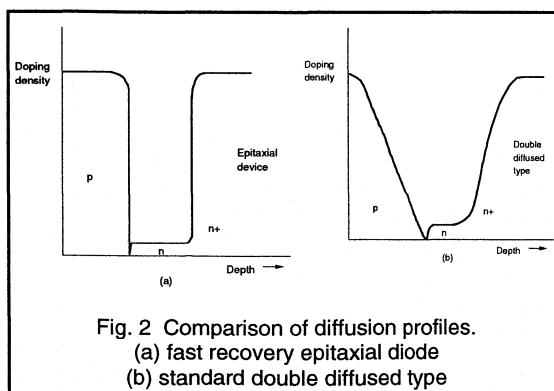
A high blocking voltage requires a wide lightly doped base, whereas a low V_F needs a narrow base. Using a short base recombination lifetime produces faster recovery times, but this also increases V_F . Furthermore, in any P-N junction rectifier operating at high currents, carrier injection into the base takes place from both the P and N+ regions, helping to maintain a low V_F .

Technology

High voltage power diodes are usually manufactured using either double-diffused or an epitaxial technology. High injection efficiency into the base coupled with a narrow base width are essential for achieving a low V_F . High injection efficiency requires the slope of the diffusion profile at the P+N and N+N junctions to be very steep. Achieving a minimum base width requires very tight control of the lightly doped base layer. Both these criteria can be met using epitaxial technology.

Epitaxial process

The epitaxial method involves growing a very lightly doped layer of silicon onto a highly doped N+ type wafer; see Fig. 1(a). A very shallow P type diffusion into the epi layer is then made to produce the required P-I-N structure (Fig. 1(b)). This gives accurate control of the base thickness such that very narrow widths may be produced. Abrupt junction transitions are also obtained, thus providing for the required high carrier injection efficiency. The tighter control of width and junction profile also provides a tighter control of Q_s , hence, the switching recovery times are typically ten times faster than double diffused types.



Double-diffused process

Double diffusion requires deep diffusions of the P+ and N+ regions into a slice of lightly doped silicon, to produce the required base width. This method is fraught with tolerance problems, resulting in poor control of the base region. The junction transitions are also very gentle, producing a poor carrier injection efficiency. The combination of the two

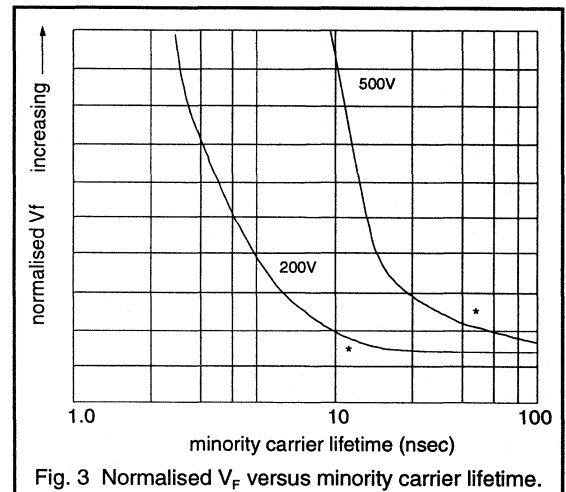
produces a higher V_F value, and also a poor control of stored charge Q_s in the base, leading to a relatively slow switching speed.

Figure 2 gives a comparison of the diffusion profiles for the two methods.

Lifetime control

To achieve the very fast recovery time and low stored charge, Q_s , required for high frequency rectification, it is necessary to introduce lifetime killing (gold doping) into the base of the diode. This produces a lower Q_s and faster reverse recovery time, t_{rr} . Unfortunately, doping also has the effect of increasing V_F . Fig. 3 shows a graph of normalised V_F versus the minority carrier lifetime for a 200V and 500V device. It can be seen that there is an optimum lifetime for each voltage grade, below which the V_F increases dramatically.

Philips has been using gold-killing techniques for well over twenty years, and combining this with epitaxial technology results in the excellent low V_F , t_{rr} and Q_s combinations found in the FRED range.



Passivation

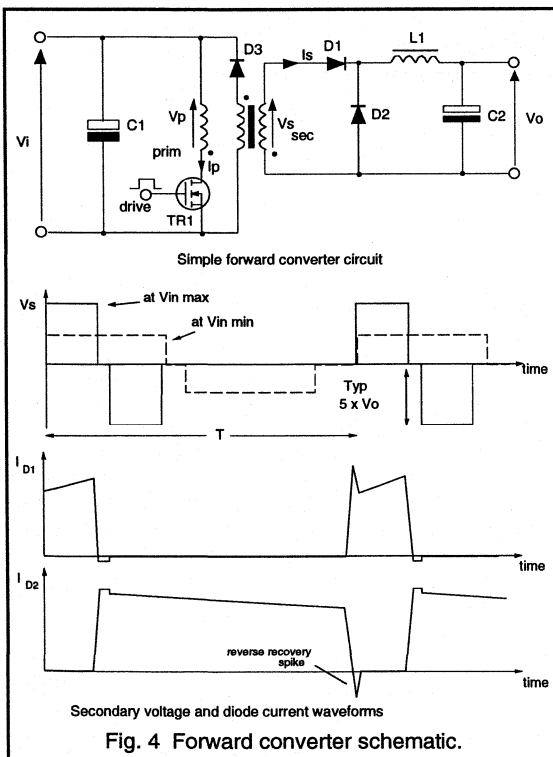
To ensure that the maximum reverse blocking potential of the diode is achieved, it is necessary to ensure that high fields do not occur around the edges of the chip. This is achieved by etching a trough in the epitaxial layer and depositing a special glass into it (Fig. 1(c)). Known as full mesa glass passivation, it achieves stable reverse blocking characteristics at high voltages by reducing charge build-up, and produces a strong chip edge, reducing the risk of assembly damage. This means that the diodes are rugged and reliable, and also allows all devices to be fully tested on-slice.

Finally, Fig. 1 (d) shows the chip after it has been diced and metallised. The rectifier is then assembled into a wide selection of different power packages, the standard TO-220 outline being one example.

Characteristics

Forward conduction loss

Forward conduction loss is normally the major component of power loss in the output rectification diodes of an S.M.P.S. For all buck derived output stages, for example the forward converter shown in Fig. 4, the choke current always flows in one or other of the output diodes (D1 and D2).



The output voltage is always lowered by the diode forward voltage drop V_F such that:-

$$V_o + V_f = V_s D \quad (1)$$

Where D is the transistor duty cycle. Thus, the resulting power loss due to V_F of the output rectifiers is:-

$$P_{on, loss} = V_f I_o \quad (2)$$

where I_o is the output load current of the converter. The loss as a percentage of the output power is thus:-

$$\frac{V_f I_o}{V_o I_o} = \frac{V_f}{V_o} \quad (3)$$

This loss in efficiency for a range of standard S.M.P.S. outputs is shown in Fig. 5. It is clear that V_f needs to be kept to an absolute minimum particularly for low output voltages if reasonable efficiency is to be achieved.

To accommodate variations in the input voltage, the output rectifiers are usually chosen such that their blocking voltage capability is between 4 and 8 times the output voltage. For the lowest output voltages, Schottky diodes should be the first choice. Unfortunately, the characteristically low V_f of the Schottky cannot be maintained at voltages much higher than 100V. For outputs above 24V, fast recovery epitaxial diodes are the most suitable rectifiers.

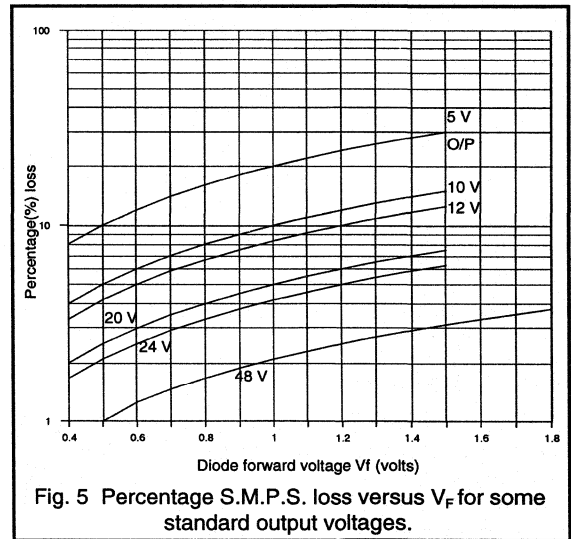
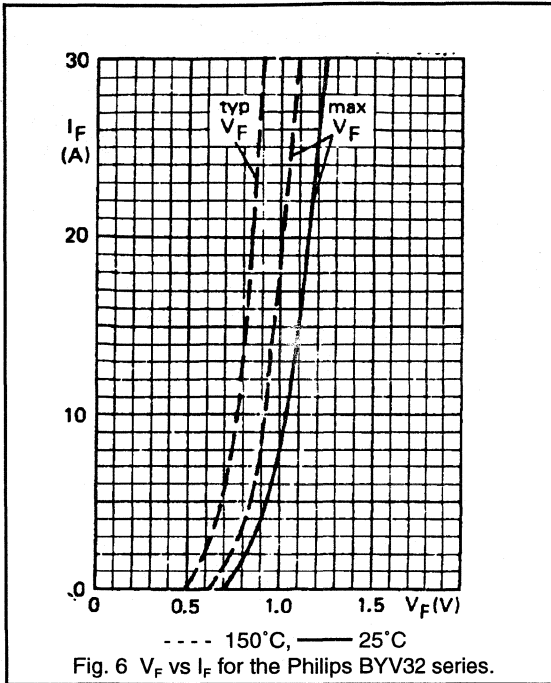


Figure 6 shows an example of V_F versus forward current I_F for the Philips BYV32 series, rated from 50V to 200V and with a maximum output current of 20A. This reveals the low V_F values typical of the epitaxial technique.

From Fig. 6 and equation 2, it is possible to estimate the loss due to the output rectifiers in an S.M.P.S. For example, for a 12V, 20A output, a conduction loss of 17W typical and 20W maximum is obtained. This corresponds to a worst case loss of 8% of total output power, normally an acceptable figure.

Philips devices offer some of the lowest V_F values on the market. Maximum as well as typical values are always quoted at full rated currents in the datasheets. However this is not the case with all manufacturers, and care should be taken when comparing Philips devices with those of other manufacturers.



Reverse recovery

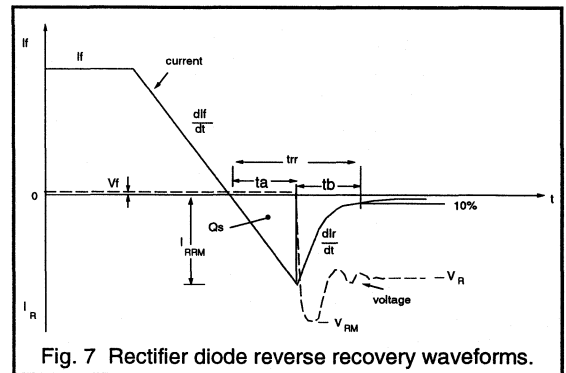
a) Q_s , t_{rr} and I_{rrm}

Following V_F , the most important feature of a high frequency rectifier is the reverse recovery characteristic. This affects S.M.P.S. performance in several ways. These include increased diode switching loss, higher peak turn-on current and dissipation in the power transistors, and increased generation of electro-magnetic interference (e.m.i.) and voltage transient oscillations in the outputs. Clearly, the rectifier must have optimum reverse recovery characteristics to keep this catalogue of effects to a minimum.

When the P-N diode is conducting forward current, a charge is built up in the base region, consisting of both electrons and holes. It is the presence of this charge which is the key to achieving low V_f . The higher the forward current, the greater is this stored charge. In order to commutate the diode (i.e switch the device from forward conduction into reverse blocking mode) this charge has to be removed from the diode before the base can sustain any reverse blocking voltage. The removal of this charge manifests itself as a substantial transient reverse current spike, which can also generate a reverse voltage overshoot oscillation across the diode.

The waveforms of the reverse recovery for a fast rectifier are shown in Fig. 7. The rectifier is switched from its forward conduction at a particular rate, called dI_F/dt . Stored charge begins to be extracted after the current passes through zero, and an excess reverse current flows. At this point the charge is being removed by both the forcing action of the circuit, and recombination within the device (dependent upon the base characteristics and doping levels).

At some point the charge has fallen to a low enough level for a depletion region to be supported across the base, thus allowing the diode to support reverse voltage. The peak of reverse current, I_{rrm} occurs just after this point. The time for the current to pass through zero to its peak reverse value is called t_a . From then on, the rectifier is in blocking mode, and the reverse current then falls back to zero, as the remainder of the stored charge is removed mostly by recombination. The time for the peak reverse current to fall from its maximum to 10% of this value is called t_b .



The stored charge, Q_s , is the area under the current-time curve and is normally quoted in nano-Coulombs. The sum of t_a and t_b is called the rectifier reverse recovery time, t_{rr} and gives a measure of the switching speed of the rectifier.

Factors influencing reverse recovery

In practice, the three major parameters t_{rr} , Q_s and I_{rrm} are all dependent upon the operating condition of the rectifier. This is summarised as follows:-

- Increasing the forward current, I_F , increases t_{rr} , Q_s and I_{rrm} .
- Increasing the dI_F/dt rate by using a faster transistor and reducing stray inductance, significantly decreases t_{rr} , but increases Q_s and I_{rrm} . High dI_F/dt rates occur in the high frequency square wave switching found in S.M.P.S. applications. (MOSFETs can produce very small fall times, resulting in very fast dI_F/dt).
- Increasing diode junction temperature, T_j increases all three.
- Reducing the reverse voltage across the diode, V_r , also slightly increases all three.

Specifying reverse recovery

Presently, all manufacturers universally quote the t_{rr} figure as a guide. This figure is obtained using fixed test procedures. There are two standard test methods normally used:-

Method 1

Referring to the waveform of Fig. 7:

$I_F = 1A$; $di_F/dt = 50A/\mu\text{sec}$; $V_r > 30V$; $T_j = 25^\circ\text{C}$.
 t_{rr} is measured to 10% of I_{RM} .

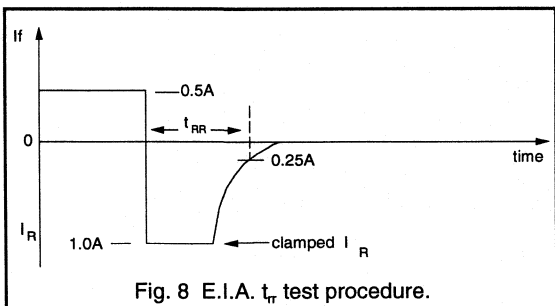


Fig. 8 E.I.A. t_{rr} test procedure.

Method 2

$I_F = 0.5A$, the reverse current is clamped to 1A and t_{rr} is measured to 0.25A.

This is the Electronics Industries Association (E.I.A.) test procedure, and is outlined in Fig. 8.

The first and more stringent test is the one used by Philips. The second method, used by the majority of competitors will give a t_{rr} figure typically 30% lower than the first, i.e. will make the devices look faster. Even so, Philips have the best t_{rr} / Q_s devices available on the market. For example,

the Philips BYW29 200V, 8A device has a t_{rr} of 25ns, the competitor devices quote 35ns using the easier second test. This figure would be even higher using test method 1.

Reverse recovery is specified in data by Philips in terms of all three parameters t_{rr} , Q_s and I_{RM} . Each of these parameters however is dependent on exact circuit conditions. A set of characteristics is therefore provided showing how each varies as a function of di/dt , forward current and temperature, Fig. 9. These curves enable engineers to realise what the precise reverse recovery performance will be under circuit operating conditions. This performance will normally be worse than indicated by the quoted figures, which generally speaking do not reflect circuit conditions. For example, a BYW29 is quoted as having a t_{rr} of 25 ns but from the curves it may be as high as 90 ns when operated at full current and high di/dt . Similarly a quoted Q_s of 11 nC compares with the full current worst case of 170 nC.

In the higher voltage devices (500V and 800V types) t_{rr} and Q_s are much higher, and will probably be the most critical parameters in the rectification process. Care must be taken to ensure that actual operating conditions are used when estimating more realistic values.

Frequency range

Figure 10 compares the recovery of a Philips 200V FRED with a double diffused type. The FRED may be switched approximately 10 times faster than the double diffused type. This allows frequencies of up to 1MHz to be achieved with the 200V range.

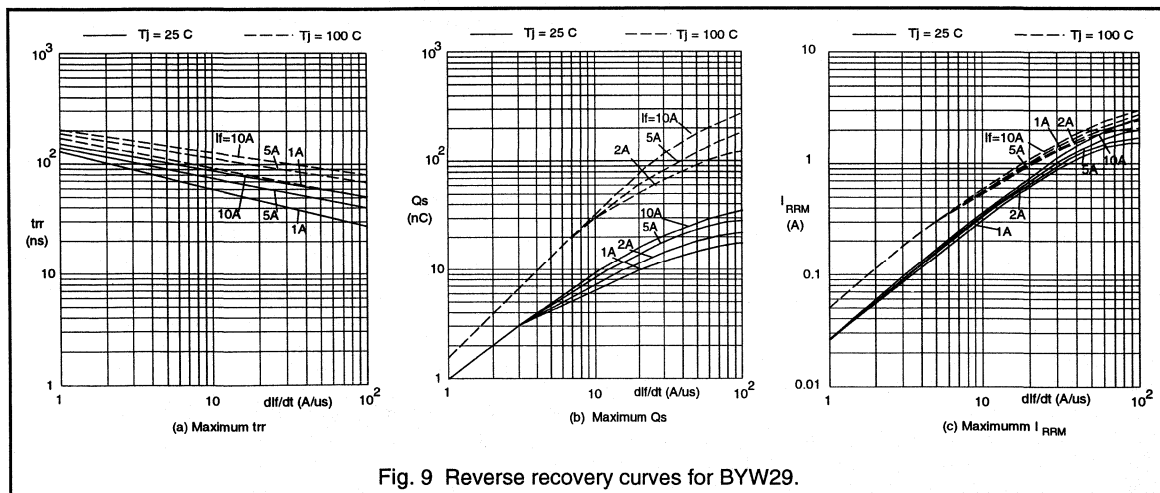
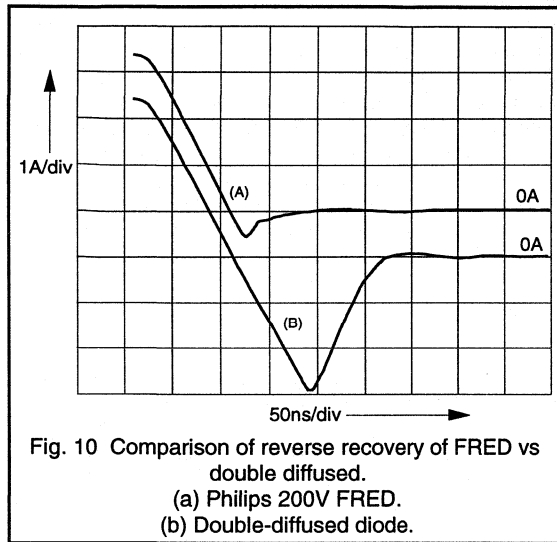


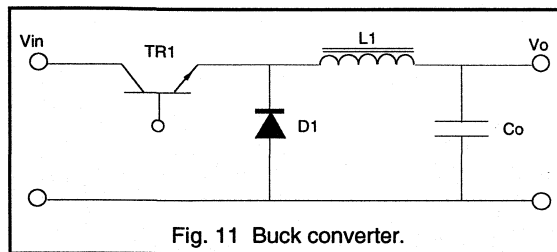
Fig. 9 Reverse recovery curves for BYW29.

In the higher voltage devices where the base width is increased to sustain the reverse voltage, the amount of stored charge increases, as does the t_{rr} . For a 500V device, 500kHz operation is possible, and for 800V typically 200kHz is realistic.



Effects on S.M.P.S operation

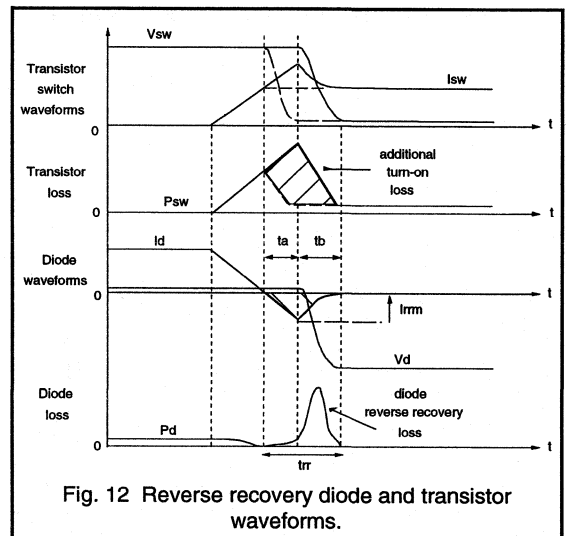
In order to analyse the effects of reverse recovery on the power supply, a simple non-isolated buck converter shown in Fig. 11 is considered. The rectifier D1 in this application is used in freewheel mode, and conducts forward current during the transistor off-time.



The waveforms for the diode and transistor switch during the reverse recovery of the diode when the transistor turns on again are given in Fig. 12.

As the transistor turns on, the current ramps up in the transistor as it decays and reverses in the diode. The di_F/dt is mainly dependent on the transistor fall time and, to some extent, the circuit parasitic inductances. During the period t_a the diode has no blocking capability and therefore the transistor must support the supply voltage. The transistor thus simultaneously supports a high voltage and conducts

both the load current and the reverse recovery current, implying a high internal power dissipation. After time t_a the diode blocking capability is restored and the voltage across the transistor begins to fall. It is clear that a diode with an I_{rm} half the value of I_F will effectively double the peak power dissipation in the transistor at turn-on. In severe cases where a high I_{rm} / t_{rr} rectifier is used, transistor failure could occur by exceeding the peak current or power dissipation rating of the device.



There is also an additional loss in the diode to be considered. This is a product of the peak I_{rm} and the diode reverse voltage, V_r . The duration of current recovery to zero will affect the magnitude of the diode loss. However, in most cases the additional transistor loss is much greater than the diode loss.

Diode loss calculation

As an example of the typical loss in the diode, consider the BYW29, 8A, 200V device as the buck freewheel diode, for the following conditions:-

$$I_F = 8A; V_r = 100V; di_F/dt = 50A/\mu s; T_1 = 25^\circ C; \text{duty ratio } D = 0.5; f = 100KHz.$$

The diode reverse recovery loss is given by:-

$$P_{rr} = \frac{1}{2} \cdot V_r \cdot I_{rm} \cdot t_b \cdot f$$

From the curves of Fig. 7, $t_{rr} = 35ns$, $I_{rm} = 1.5A$. Assuming $t_b = t_{rr}/2$ gives:

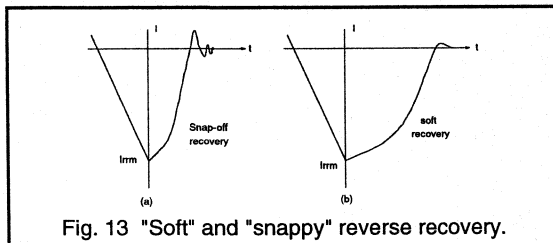
$$P_{rr} = \frac{1}{2} \cdot 100 \cdot 1.5 \cdot 17.5 \cdot 100k = 132mW$$

This is still small compared to the diode V_F conduction loss of approximately 3.6 W. However, at $T_J=100^\circ\text{C}$, $di_F/dt=100\text{A}/\mu\text{s}$ and $f=200\text{kHz}$, the loss becomes 1.05W, which is fairly significant. In the higher voltage devices where t_{rr} and I_{rrm} are significantly worse, then the frequency dependent switching loss will tend to dominate, and can be higher than the conduction loss. This will limit the upper frequency of operation of the diode.

The turn-on current spike generated in the primary circuits due to diode reverse recovery can also seriously affect the control of the S.M.P.S. when current mode control is used (where the peak current is sensed). An RC snubber is usually required to remove the spike from the sense inputs. Good reverse recovery removes the need for these additional components.

b) Softness and di_F/dt

When considering the reverse recovery characteristics, it is not just the magnitude (t_{rr} and I_{rrm}) which is important, but also the shape of the recovery waveform. The rate at which the peak reverse current I_{rrm} falls to zero during time t_b is also important. The maximum rate of this slope is called di_F/dt and is especially significant. If this slope is very fast, it will generate significant radiated and conducted electrical noise in the supply, causing R.F.I. problems. It will also generate high transient voltages across circuit inductances in series with the diode, which in severe cases may cause damage to the diode or the transistor switch by exceeding breakdown limits.



A diode which exhibits an extremely fast di_F/dt is said to have a "snap-off" or "abrupt" recovery, and one which returns at a relatively smooth, gentle rate to zero is said to have a soft recovery. These two cases are shown in the waveforms in Fig. 13. The softness is dependent upon whether there is enough charge left in the base, after the full spread of the depletion region in blocking mode, to allow the current to return to zero smoothly. It is mainly by the recombination mechanism that this remaining charge is removed during t_b .

Maintaining t_b at a minimum would obviously give some reduction to the diode internal loss. However, a snappy rectifier will produce far more R.F.I. and transient voltages. The power saving must therefore be weighed against the

additional cost of the snubbers and filtering which would otherwise be required if the rectifier had a snappy characteristic.

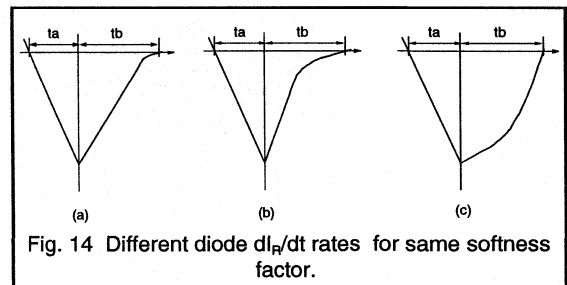
The frequency range of R.F.I. generated by di_F/dt typically lies in the range of 1MHz to 30MHz, the magnitude being dependent upon how abrupt the device is. One secondary effect that is rarely mentioned is the additional transformer losses that will occur due to the extremely high frequencies generated inside it by the diode recovery waveform. For example, core loss at 10MHz for a material designed to operate at 100kHz can be significant. There will also be additional high frequency loss in the windings due to the skin effect. In this case the use of a soft device which generates a lower frequency noise range will reduce these losses.

Characterising softness

A method currently used by some manufacturers to characterise the softness of a device is called the softness factor, S . This is defined as the ratio of t_b over t_a .

$$\text{softness factor, } S = \frac{t_b}{t_a}$$

An abrupt device would have S much less than 1, and a soft device would have S greater than 1. A compromise between R.F.I. and diode loss is usually required, and a softness factor equal to 1 would be the most suitable value for a fast epitaxial diode.



Although the softness factor does give a rough guide to the type of recovery and helps in the calculation of the diode switching loss, it does not give the designer any real idea of the di_F/dt that the rectifier will produce. Hence, levels of R.F.I. and overvoltages could be different for devices with the same softness factor. This is shown in Fig. 14, where the three characteristics have the same softness factor but completely different di_F/dt rates.

In practice, a suitable level for di_F/dt would be to have it very similar in magnitude to di_F/dt . This would keep the noise generated to a minimum.

At present there is no universal procedure used by manufacturers to characterise softness, and so any figures quoted must be viewed closely to check the conditions of the test.

Comparison with competitor devices

Figure 15 compares a BYV32 with an equivalent competitor device. This test was carried out using an L.E.M. Q_s test unit.

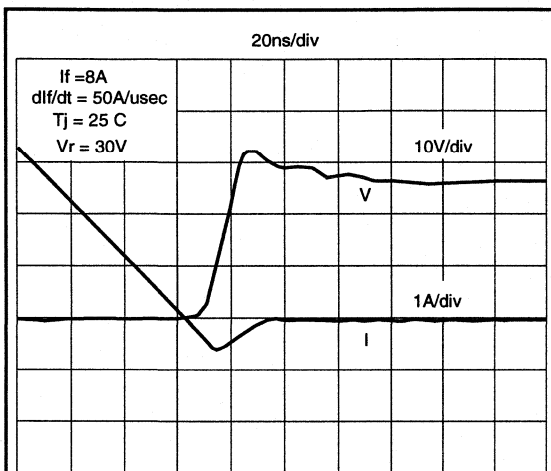
The conditions for each diode were identical. The results were as follows:-

BYV32:- $S = 1.2$, $di_R/dt = 40A/\mu s$,
Voltage overshoot = 5V

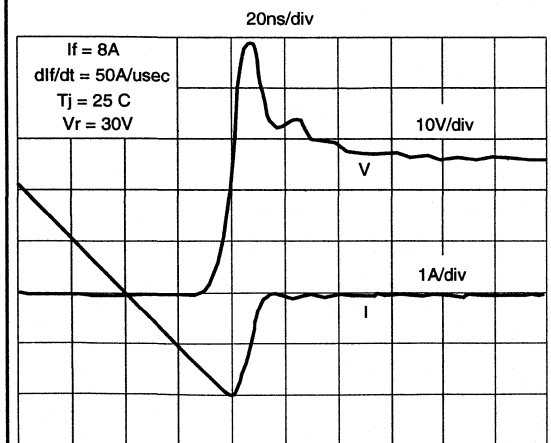
Competitor:- $S = 0.34$, $di_R/dt = 200A/\mu s$,
Voltage overshoot = 22V

For the Philips device, apart from the very low Q_s and I_{rm} values obtained, the S factor was near 1 and the di_R/dt rate was less than the original di_F/dt of $50A/\mu s$. These excellent parameters produce minimal noise and the very small overshoot voltage shown. The competitor device was much snappier, the di_R/dt was 4 times the original di_F/dt , and caused a much more severe overshoot voltage with the associated greater R.F.I. The diode loss is also higher in the competitor device even though it is more abrupt, since Q_s and I_{rm} are larger.

The low Q_s of the Philips FRED range thus maintains diode loss to a minimum while providing very soft recovery. This means using a Philips type will significantly reduce R.F.I. and dangerous voltage transients, and in many cases reduce the power supply component count by removing the need for diode snubbers.



(a)



(b)

Fig. 15 Comparison of softness of reverse recovery.
(a) Philips BYV32 200V 8A device
(b) Equivalent competitor device

Forward recovery

A further diode characteristic which can affect S.M.P.S. operation is the forward recovery voltage V_{fr} . Although this is not normally as important as the reverse recovery effects in rectification, it can be particularly critical in some special applications.

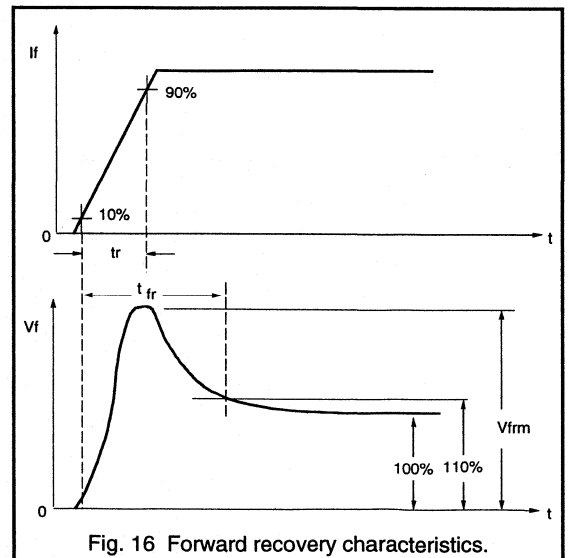


Fig. 16 Forward recovery characteristics.

Forward recovery is caused by the lack of minority carriers in the rectifier p-n junction during diode turn-on. At the instant a forward bias is applied, there are no carriers present at the junction. This means that at the start of conduction, the diode impedance is high, and an initial forward voltage overshoot will occur. As the current flows and charge builds up, conductivity modulation (minority carrier injection) takes place. The impedance of the rectifier falls and hence, the forward voltage drop falls rapidly back to the steady state value.

The peak value of the forward voltage is known as the forward recovery voltage, V_{fm} . The time from the forward current reaching 10% of the steady state value to the time the forward voltage falls to within 10% of the final steady state value is known as the forward recovery time (Fig. 16).

The magnitude and duration of the forward recovery is normally dependent upon the device and the way it is commutated in the circuit. High voltage devices will produce larger V_{fm} values, since the base width and resistivity (impedance) is greater.

The main operating conditions which affect V_{fr} are:-

- I_f ; high forward current, which produces higher V_{fr} .
- Current rise time, t_r ; a fast rise time produces higher V_{fr} .

Effects on s.m.p.s.

The rate of rise in forward current in the diode is normally controlled by the switching speed of the power transistor. When the transistor is turned off, the voltage across it rises, and the reverse voltage bias across the associated rectifier falls. Once the diode becomes forward biased there is a delay before conduction is observed. During this time, the transistor voltage overshoots the d.c supply voltage while it is still conducting a high current. This can result in the failure of the transistor in extreme cases if the voltage limiting value is exceeded. If not, it will simply add to the transistor and diode dissipation. Waveforms showing this effect are given in Fig. 17.

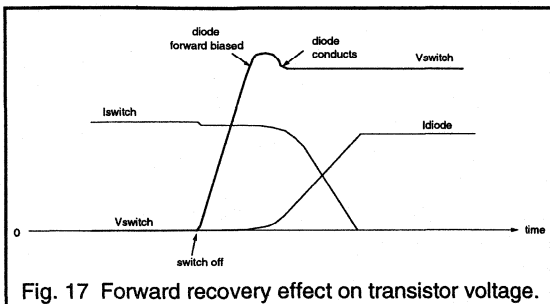


Fig. 17 Forward recovery effect on transistor voltage.

Table 1 outlines typical V_{fm} values specified for rectifiers of different voltage rating. This shows the relatively low values obtained. No comparable data for any of the competitor devices could be found in their datasheets. It should be noted that in most S.M.P.S. rectifier applications, forward recovery can be considered the least important factor in the selection of the rectifier.

Device type	V_{BR} (Volts)	I_f (Amps)	di/dt (A/ μ s)	typ V_{fm} (Volts)
BYW29	200	1.0	10	0.9
BYV29	500	10	10	2.5
BYR29	800	10	10	5.0

Table 1. V_{fm} values for different Philips devices.

Reverse leakage current

When a P-N junction is reverse biased, there is always an inherent reverse leakage current that flows. In any piece of undoped semiconductor material there is a thermally generated background level of electron and hole pairs. These pairs also naturally recombine, such that an equilibrium is established. In a p-n junction under reverse voltage conditions, the electric field generated will sweep some of the free carriers generated out of the device before they can recombine, hence causing a leakage current. This phenomenon is shown in Fig. 18.

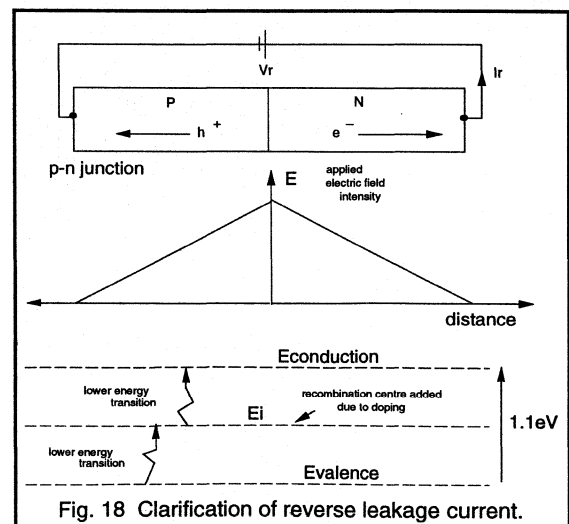


Fig. 18 Clarification of reverse leakage current.

When the rectifier base is gold doped to decrease Q_s and t_{rr} , a new energy level is introduced very close to the centre of the semiconductor energy band gap. This provides lower energy transition paths as shown, and thermal generation

(and recombination) of hole-electron pairs is more frequent. Thus, the reverse leakage current is greater still in the killed, fast rectifier.

Since the pairs are generated thermally, it is obvious that raising the junction temperature will increase the leakage significantly. For example, the leakage current of a FRED can increase by up to 20 times by raising the junction temperature, T_j from 25°C to 100°C. This increase can be far greater in other diode technologies.

Many S.M.P.S. designers have a misconception about leakage current, and believe that it renders the rectifier poor quality, giving high losses, and is unreliable. This is not so. Leakage is a naturally occurring effect, and is present in all rectifiers. The leakage in an S.M.P.S. diode is normally extremely small and stable, with very little effect on the rectification process. Some manufacturers have over-emphasised the benefits of very low leakage devices, claiming that they have great advantages. However, this will be shown to be groundless, since any reduction in the overall diode power loss will be minimal.

In practice, the reverse leakage current only becomes significant at high operating temperatures (above 75°C) and for high reverse blocking voltages (above 500V), where the product of reverse voltage and leakage current (hence, power loss) is higher. Even then, the leakage current is still usually lower than 1mA.

Table 2 lists the maximum leakage currents for some of the devices from the Philips range (gold killed), revealing low levels, even in the higher voltage devices, achieved through optimised doping.

Device type	$V_{BR(max)}$ (Volts)	max I_r (mA) $T_j = 100^\circ\text{C}$ full V_{rm}	max I_r (μA) $T_j = 25^\circ\text{C}$ full V_{rm}
BYW29	200	0.6	10
BYV29	500	0.35	10
BYR29	800	0.2	10

Table 2. Maximum reverse leakage currents for Philips devices.

The power dissipation due to leakage is a static loss and depends on the product of the reverse voltage and the leakage current over a switching cycle. A worst case example is given below where the data sheet leakage current maximum is used at maximum reverse blocking voltage of the diode.

S.M.P.S example:-Flyback converter

Consider first the BYV29-500 as the output rectifier in the discontinuous flyback converter (Note: the reverse blocking occurs during the transistor on time, and a minimum duty of 0.25 has been assumed.) The BYV29-500 could generate a possible maximum output voltage of 125V. The maximum leakage power loss is:-

$$P_L = 500\text{V} \cdot 0.35\text{mA} \cdot 0.25 = 43.75\text{mW}$$

Alternatively, for the BYR29-800, maximum rectified output is approximately 200V, and by similar calculations, its maximum loss is 40mW. Lower output voltages would give leakage losses lower than this figure.

These types of calculation can be carried out for other topologies, when similar low values are obtained.

Conclusion

Philips produces a comprehensive range of Fast Recovery Epitaxial Diodes. The devices have been designed to exhibit the lowest possible V_f while minimising the major reverse recovery parameters, Q_s , t_r and I_{rm} . Because of the low Q_s , switching losses within the circuit are minimised, allowing use up to very high frequencies. The soft recovery characteristic engineered into all devices makes them suitable for use in today's applications where low R.F.I. is an important consideration. Soft recovery also provides additional benefits such as reduced high frequency losses in the transformer core and, in some cases, the removal of snubbing components.

FRED Selection Guide

Single Diodes

Type Number	Outline	$I_{F(AV)}$ max Amps	Voltage Grades								
			100	150	200	300	400	500	600	700	800
BYW29E	TO-220AC	8	*	*	*						
BYV29	TO-220AC	9				*	*	*			
BYR29	TO-220AC	8						*	*	*	*
BYV79E	TO-220AC	14	*	*	*						
BYT79	TO-220AC	14				*	*	*			

Dual Diodes (Common cathode)

Type Number	Outline	I_o max Amps	Voltage Grades								
			100	150	200	300	400	500	600	700	800
BYV40	SOT-223	1.5	*	*	*						
BYQ27	SOT-82	10	*	*	*						
BYQ28E	TO-220AB	10	*	*	*						
BYT28	TO-220AB	10				*	*	*			
BYV32E	TO-220AB	20	*	*	*						
BYV34	TO-220AB	20				*	*	*			
BYV42E	TO-220AB	30	*	*	*						
BYV72E	SOT-93	30	*	*	*						
BYV44	TO-220AB	30				*	*	*			
BYV74	SOT-93	30				*	*	*			

'E' denotes rugged device.

Single Diodes (Electrically isolated Package)

Type Number	Outline	$I_{F(AV)}$ max Amps	Voltage Grades								
			100	150	200	300	400	500	600	700	800
BYW29F	SOT-186	8	*	*	*						
BYV29F	SOT-186	9				*	*	*			
BYR29F	SOT-186	8							*	*	*

Dual Diodes (Electrically Isolated Package)

Type Number	Outline	I_o max	Voltage Grades								
			100	150	200	300	400	500	600	700	800
BYQ28F	SOT-186	10	*	*	*						
BYV32F	SOT-186	12	*	*	*						
BYV72F	SOT-199	20	*	*	*						
BYV74F	SOT-199	20				*	*	*			

2.2.2 Schottky Diodes from Philips Semiconductors

The Schottky diodes from Philips have always had good forward characteristics and excellent switching performance. With this new, more extensive range of Schottky diodes come the additional benefits of stable, low leakage reverse characteristics and unsurpassed levels of guaranteed ruggedness.

The performance improvements have been achieved by changing both the design and the processing of Schottky diode wafers. The changes are the products of the continuing programme of research in the field of Schottky barrier technology being carried out at Stockport.

This report will look at the new range, the improvements that have been made and the changes that have produced them.

New process

The manufacturing process for all the devices in the new range includes several changes which have significantly improved the quality and performance of the product.

Perhaps the most significant change is moving the production of the Schottky wafers from the bipolar processing facility into the PowerMOS clean room. The Schottky diode is a 'surface' device - its active region is right at the conductor / semiconductor interface, not deep within the silicon crystal lattice. This means that it can usefully exploit the high precision equipments and extremely clean conditions needed to produce MOS transistors. In some respects Schottkies have more in common with MOS transistors than they do with traditional bipolar products. In one respect they are identical - their quality can be dramatically improved by:-

- growing purer oxide layers,
- depositing metal onto cleaner silicon,
- more precise control of ion implantation.

Another change has been in the method of producing the Schottky barrier. The original method was to 'evaporate' molybdenum onto the surface of the silicon. In the new process a Pt/Ni layer is 'sputtered' onto the surface and then a heat treatment is used to produce a Pt/Ni silicide. This has the effect of moving the actual conductor / semiconductor interface a small distance away from the surface and into the silicon.

The advantage of this change is that it puts the barrier in an environment where the conditions are more homogeneous, resulting in a more consistent barrier. This consistency produces devices in which every part of the active area has the same reverse characteristic.

Ruggedness

The RUGGEDNESS of a Schottky diode is a measure of its ability to withstand the surge of power generated by the reverse current which flows through it when the applied reverse voltage exceeds its breakdown voltage. Operation in this mode is, of course, outside the boundaries of normal operation - it always exceeds the V_{RRM} rating of the device. However, situations can arise where the voltages present in the circuit far exceed the expectations of the designer. If devices are damaged by these conditions then the equipment they are in may fail. Such failures often result in equipments being condemned as unreliable. In recognition of this, Philips will now supply devices which operate reliably during both normal and abnormal operation.

All the Schottky diodes supplied by Philips now have two guaranteed reverse surge current ratings:-

I_{RRM} - guarantees that devices can withstand repetitive reverse current pulses ($t_p = 2\mu s$; $\Delta = 0.001$) of greater than the quoted value,

I_{RSM} - guarantees that single, $100\mu s$ pulses of the rated value can be applied without damage.

At the moment these ratings are quoted as either 1A or 2A, depending on device size. It should be understood that these figures do not represent the limit of device capability. They do, however, represent the limit of what, experience suggests, might be needed in most abnormal operational situations.

In an attempt to determine the actual ruggedness of the new devices, a series of destructive tests was carried out. The results shown in Fig. 1 give the measured reverse ruggedness of different sizes of device. It clearly shows that even small devices easily survive the $1A I_{RRM} / I_{RSM}$ limit and that the larger devices can withstand reverse currents greater than the 85A that the test gear was designed to deliver.

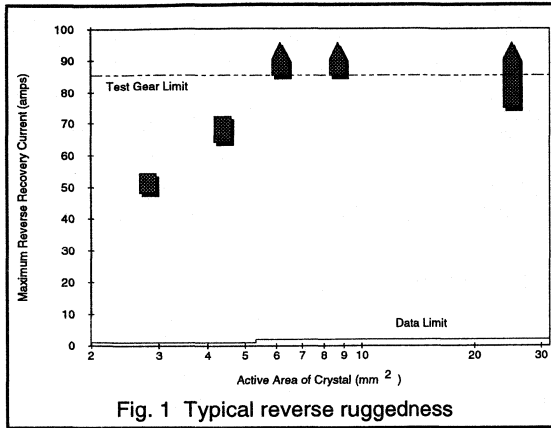


Fig. 1 Typical reverse ruggedness

Reverse leakage

The reverse characteristic of any diode depends upon two factors - 'bulk' and 'edge' leakage. The first is the current which leaks through the reverse biased junction in the main active area of the device. The second is the leakage through the junction around its periphery - where the junction meets the outside world. Attention must be paid to both of these factors if a high performance diode is to be produced. During the development of the new range of Philips Schottky diodes both of these factors received particular attention.

Bulk leakage

To achieve low forward voltage drop and very fast switching, Schottky diodes use the rectifying properties of a conductor / semiconductor interface. The 'height' of the potential barrier has a significant effect upon both the forward voltage drop and the reverse leakage. High barriers raise the V_F and lower the general reverse leakage level. Conversely low barrier devices have a lower V_F but higher leakage. So the choice of barrier height must result in the best compromise between leakage and V_F to produce devices with the best allround performance.

The height of a Schottky barrier depends, to a large extent, upon the composition of the materials at the interface. So the selection of the barrier metal and the process used for its deposition is very important. The final decision was made with the help of the extensive research and device modelling facilities available within the Philips organisation. The materials and processes that were selected have significantly reduced the bulk leakage of the new range of Schottky diodes. It is believed that this present design gives the optimum balance between leakage and V_F that is currently achievable.

Edge leakage

The other component influencing the reverse characteristic is edge leakage. In a diffused diode the mechanisms which operate at the edge of the active area - where the junction meets the outside world - are different from those which operate in the centre. The Schottky barrier is the same as a diffused junction in this respect. The field at the edge of a simple (untreated in any way) Schottky barrier is very high and as a consequence the leakage through the junction at the periphery can also be very high.

In diffused diodes the edge of the junction is treated by 'passivating' it. In a Schottky diode the edge of the barrier is treated by implanting a shallow, very low dose, p region around the periphery of the active area. This region, called a 'guard ring', effectively replaces the high field periphery of the barrier. It is now the characteristics of the guard ring which determine the edge leakage and not those of the Schottky barrier.

In this way the mechanisms controlling the two elements of leakage are now independent and can be adjusted separately, eliminating the need for compromises. This freedom, and a combination of good design and the close tolerance control - achievable with ion implantation - ensures that the characteristics are excellent, having both good stability and very low leakage.

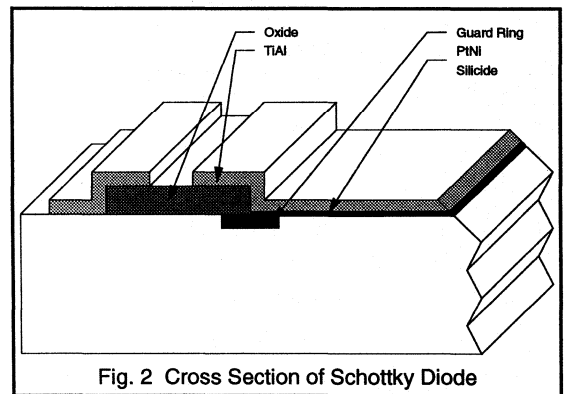


Fig. 2 Cross Section of Schottky Diode

Overall leakage

As mentioned earlier, good reverse characteristics rely upon both the edge and bulk leakages being good. By eliminating the interactions between the mechanisms and by concentrating on optimising each, it has been possible to improve both edge and bulk leakage characteristics. This has allowed Philips to produce Schottky diodes with typical room temperature reverse currents as low as 20 μ A, or 100 μ A max (PBYR645CT) - considerably lower than was ever achieved with molybdenum barrier devices.

Range

The Schottky diode was originally designed to be used as the rectifier and freewheel diode in the 5V output of high frequency SMPS. The arrival of the new 100V Schottkies has now extended this up to 24V outputs. These supplies are fitted into equipments whose power requirements vary widely. Satisfying these needs efficiently means that an equally wide range of supplies has to be produced. In recognition of this, Philips has produced a range of diode packages with current ratings from 6A to 30A. With this range it is possible to produce power supplies of 20W to 500W output - higher powers are achievable with parallelling.

The full range of Philips Schottky diodes is shown in Table 1. At the heart of the range are the 'PBYR' devices. The numbers and letters following the PBYR prefix are compatible with industry standards. These figures give an indication of a device's structure (single or dual) and its current and voltage rating. An explanation of the numbers is given in Table 2. Care has been taken to ensure compatibility between Philips devices and those from other suppliers, which share number/letter suffices. It is hoped that this will ease the process of equivalent type selection.

Included in the range is a group of devices with 'BYV1xx' numbers. These devices are a selection of the most popular types from the previous Philips Schottky range. They have proved to be conveniently sized devices which have a mix of ratings and characteristics not matched by other

manufacturers. Although these are 'old' numbers, delivered devices will have been manufactured by the new process and will therefore be better. However, changing the production process of established types can often cause concern amongst customers. Philips has recognised this and, during the development, took particular care to ensure that all the new devices would be as closely comparable as possible with previously delivered product. Clarification is given in the cross reference guide given in Table 3.

Summary

This range of Schottky diodes enhances the ability of Philips Components to meet all the requirements and needs of the SMPS designer. The well established range of epitaxial diodes, bipolar and PowerMOS transistors, ICs and passive components is now complemented by a range of Schottky diodes with:-

- very low forward voltage drop,
- extremely fast reverse recovery,
- low leakage reverse characteristics, achieved WITHOUT compromising overall system efficiency
- stable characteristics at both high and low temperatures
- guaranteed ruggedness, giving reliability under both normal and abnormal operating conditions.

Table 1 Range of Schottky Diodes
Single Diode

Type Number	Outline	$I_{F(AV)}$ (A) per diode	I_o (A) per device	Voltage Grades (V)					
				35	40	45	60	80	100
PBYR7**	TO-220AC	7.5	7.5	*	*	*			
PBYR10**	TO-220AC	10	10	*	*	*	*	*	*
PBYR16**	TO-220AC	16	16	*	*	*			

Dual Diodes - Common Cathode

Type Number	Outline	$I_{F(AV)}$ (A) per diode	I_o (A) per device	Voltage Grades (V)					
				35	40	45	60	80	100
PBYR2**CT	SOT-223	1	2	*	*	*			
PBYR6**CT	SOT-82	3	6	*	*	*			
BYV118**	TO-220AB	5	10	*	*	*			
PBYR15**CT	TO-220AB	7.5	15	*	*	*			
BYV133**	TO-220AB	10	20	*	*	*			
PBYR20**CT	TO-220AB	10	20	*	*	*	*	*	*
BYV143**	TO-220AB	15	30	*	*	*			
PBYR25**CT	TO-220AB	15	30	*	*	*			
PBYR30**PT	SOT-93	15	30	*	*	*	*	*	*

Dual Diodes - Common Cathode (Electrically Isolated Package)

Type Number	Outline	$I_{F(AV)}$ (A) per diode	I_o (A) per device	Voltage Grades (V)					
				35	40	45	60	80	100
BYV118F**	SOT-186 (3 leg)	5	10	*	*	*			
PBYR15**CTF	SOT-186 (3 leg)	7.5	15	*	*	*			
BYV133F**	SOT-186 (3 leg)	10	20	*	*	*			
PBYR20**CTF	SOT-186 (3 leg)	10	20	*	*	*			
BYV143F**	SOT-186 (3 leg)	15	30	*	*	*			
PBYR25**CTF	SOT-186 (3 leg)	15	30	*	*	*			
PBYR30**PTF	SOT-199	15	30	*	*	*			

Single Diodes (Electrically Isolated Package)

Type Number	Outline	$I_{F(AV)}$ (A) per diode	I_o (A) per device	Voltage Grades (V)					
				35	40	45	60	80	100
PBYR7**F	SOT-186 (2 leg)	7.5	7.5	*	*	*			
PBYR10**F	SOT-186 (2 leg)	10	10	*	*	*			
PBYR16**F	SOT-186 (2 leg)	16	16	*	*	*			

Table 2 'PBYR' Types - explanation of the numbering system.

The numerical part of the type number gives information about the current and voltage rating of the devices. The final two digits are the voltage grade. The number(s) preceding these give an indication of the current rating. This figure must be used with care. Single and dual devices derive this number in different ways so the data sheet should be consulted before final selection is made.

Letters after the type number indicate that the device is NOT a single diode package. The codes used by Philips can be interpreted as follows:-

CT - means that the device is dual and the cathodes of the two diodes are connected together.

PT - means the device is a dual with common cathode but for compatibility reasons 'CT' cannot be used.

For example

PBYR1645 a device consisting of a single diode with an average current rating ($I_{F(AV)}$) of 16 A and a reverse voltage capability of 45 V.

Table 3 Cross Reference Guide**Single Diodes**

Old Type	Intermediate Type	New Type
BYV19-**	none	PBYR7**
none	none	PBYR10**
BYV39-**	none	PBYR16**
BYV20-**	BYV120-**	none
BYV21-**	BYV121-**	none
BYV22-**	withdrawn	none
BYV23-**	withdrawn	none

Dual Diodes - Common Cathode

Old Type	Intermediate Type	New Type
none	none	PBYR6**CT
BYV18-**	BYV118-**	none
BYV33-**	BYV133-**	PBYR15**CT
none	none	PBYR20**CT
BYV43-**	BYV143-**	PBYR25**CT
BYV73-**	none	PBYR30**PT

FULL PACK Dual Diodes - Common Cathode

Old Type	Intermediate Type	New Type
none	BYV118F-**	none
BYV33F-**	BYV133F-**	PBYR15**CTF
none	none	PBYR20**CTF
BYV43F-**	BYV143F-**	PBYR25**CTF

2.2.3 An Introduction to Synchronous Rectifier Circuits using PowerMOS Transistors

Replacing diodes with very low $R_{DS(on)}$ POWERMOS transistors as the output rectifiers in Switch Mode Power Supplies operating at high operating frequencies can lead to significant increases in overall efficiency. However, this is at the expense of the extra circuitry required for transistor drive and protection. In applications where efficiency is of overriding importance (such as high current outputs below 5V) then synchronous rectification becomes viable.

This paper investigates two methods of driving synchronous rectifiers:-

- (i) Using extra transformer windings.
- (ii) Self-driven without extra windings.

Multi-output power supplies do not easily lend themselves to extra transformer windings (although there is usually only one very low output voltage required in each supply). Therefore, the self-driven approach is of more interest. If the additional circuitry and power devices were integrated, an easy to use, highly efficient rectifier could result.

Introduction.

The voltage drop across the output diode rectifiers during forward conduction in an SMPS absorbs a high percentage of the watts lost in the power supply. This is a major problem for low output voltage applications below 5V (See section 2.2.1). The conduction loss of this component can be reduced and hence, overall supply efficiency increased by using very low $R_{DS(on)}$ POWERMOS transistors as synchronous rectifiers (for example, the BUK456-60A).

The cost penalties involved with the additional circuitry required are usually only justified in the area of high frequency, low volume supplies with very low output voltages. The methods used to provide these drive waveforms have been investigated for various circuit configurations, in order to assess the suitability of the POWERMOS as a rectifier.

The main part of the paper describes these circuit configurations which include flyback, forward and push-pull topologies. To control the synchronous rectifiers they either use extra windings taken from the power transformer or self-driven techniques.

The PowerMOS as a synchronous rectifier.

POWERMOS transistors have become more suitable for low voltage synchronisation for the following reasons:-

- (1) The cost of the POWERMOS transistor has fallen sharply in recent years.

- (2) Very low $R_{DS(on)}$ versions which yield very low conduction losses have been developed.

- (3) The excellent POWERMOS switching characteristics and low gate drive requirements make them ideal for high frequency applications.

- (4) Paralleling the POWERMOS devices (which is normally straightforward) will significantly reduce the $R_{DS(on)}$, thus providing further increases in efficiency. This process is not possible with rectifier diodes since they have inherent forward voltage offset levels.

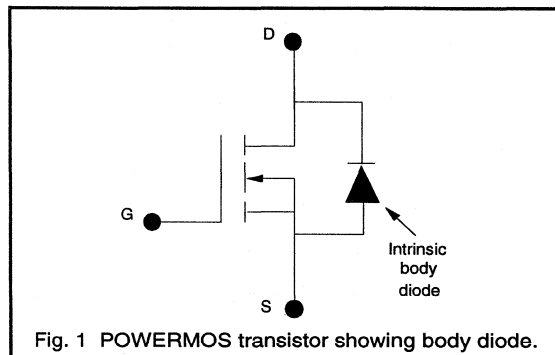


Fig. 1 POWERMOS transistor showing body diode.

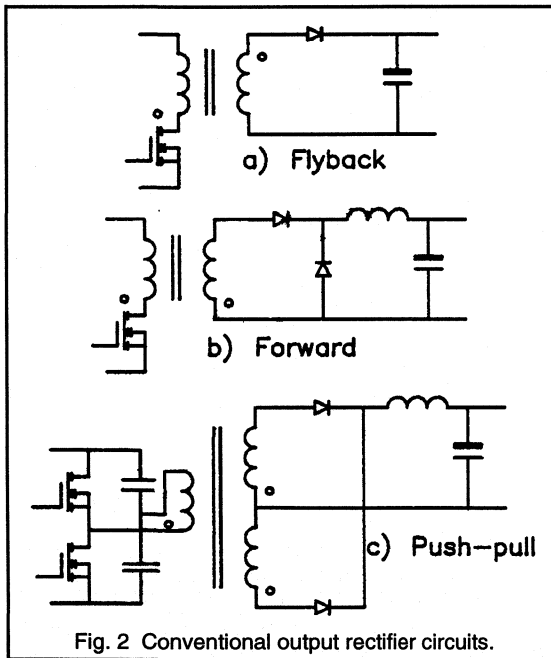
Design constraints.

When the POWERMOS transistor shown in Fig. 1 is used as a synchronous rectifier, the device is configured such that the current flow is opposite to that for normal operation i.e. from source to drain. This is to ensure reverse voltage blocking capability when the transistor is turned off, since there will be no current path through the parasitic body diode. This orientation also gives a degree of safety. If the gate drive is lost, the body diode will then perform the rectification, albeit at a much reduced efficiency.

Unfortunately, this configuration has limitations in the way in which it can be driven. The device gate voltage must always be kept below $\pm 30V$. The on-resistance ($R_{DS(on)}$) of the device must be low enough to ensure that the on-state voltage drop is always lower than the V_f of the POWERMOS intrinsic body diode. The gate drive waveforms have to be derived from the circuit in such a way as to ensure that the body diode remains off over the full switching period. For some configurations this will be costly since it can involve discrete driver I.C.s and isolation techniques.

If the body diode were to turn on at any point, it would result in a significant increase in the POWERMOS conduction loss. It would also introduce the reverse recovery characteristic of the body diode, which could seriously degrade switching performance and limit the maximum allowable frequency of operation.

It is well known that the $R_{DS(on)}$ of the POWERMOS is temperature dependent and will rise as the device junction temperature increases during operation. This means that the transistor conduction loss will also increase, hence, lowering the rectification efficiency. Therefore, to achieve optimum efficiency with the synchronous rectifier it is important that careful design considerations are taken (for example good heat-sinking) to ensure that the devices will operate at as low a junction temperature as possible.



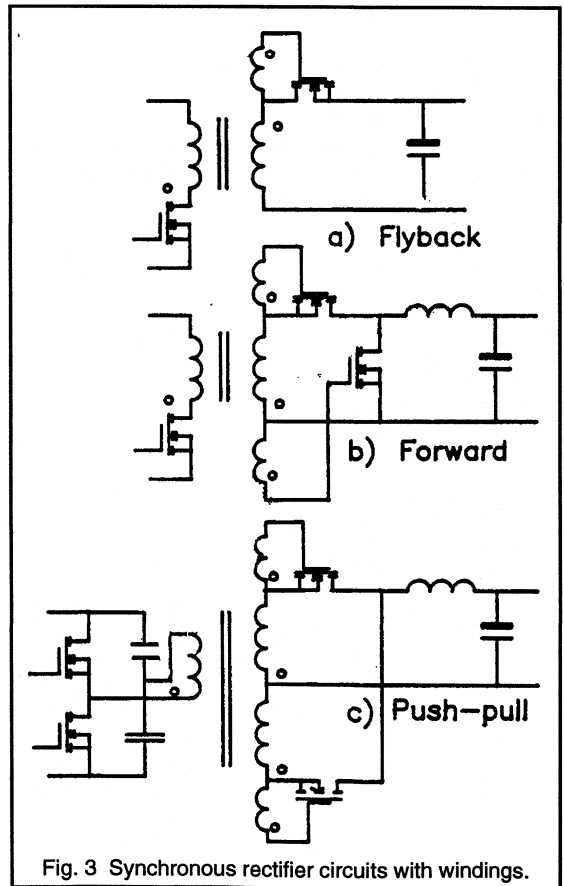
Transformer Driven Synchronous Rectifiers.

The conventional output rectifier circuits for the flyback, forward and push-pull converters are shown in Fig. 2. These diodes can be replaced by POWERMOS transistors which are driven off the transformer as shown in Fig. 3. These configurations can be summarised as follows:-

(a) Flyback converter - this is very straightforward; the gate voltage can be maintained at below 30V and the body diode will not come on.

(b) Forward converter - the gate drives for the two transistors can be maintained below 30V. However, due to the shape of the transformer waveforms, the freewheel rectifier will not have a square wave signal and the body diode could come on.

(c) Push-pull converter - deriving the gate drives for the two synchronous rectifiers from the transformer means that during the dead time which occurs in each switching cycle, both transistors are off. There is nowhere for the circulating current to go and body diodes will come on to conduct this current. This is not permissible because of the slow characteristics of the less than ideal body diode. Therefore, the push-pull configuration cannot be used for synchronous rectification without the costly derivation of complex drive waveforms.



One significant advantage of using this topology is that the r.m.s. current of the rectifiers and, hence, overall conduction loss is significantly lower in the push-pull than it is in the forward or flyback versions.

Self-Driven Synchronous Rectifiers.

The disadvantage of the transformer driven POWERMOS is the requirement for extra windings and extra pins on the power transformer. This may cause problems, especially for multi-output supplies. A method of driving the transistors without the extra transformer windings would probably be more practical. For this reason basic self-driven synchronous rectifier circuits were investigated.

It should be noted that the following circuits were based upon an output of 5V at 10A. In practice, applications requiring lower voltages such as 3 or 3.3 volts at output currents above 20A will benefit to a far greater extent by using synchronous rectification. For these conditions the efficiency gains will be far more significant. However, the 5V output was considered useful as a starting point for an introductory investigation.

(a) The Flyback converter.

An experimental circuit featuring the flyback converter self-oscillating power supply was developed. This was designed to operate at a switching frequency of 40kHz and delivered 50W (5V at 10A).

Directly substituting the single rectifier diode with the POWERMOS transistor as is shown in Fig. 4(a) does not work because the gate will always be held on. The gate is V_o above the source so the device will not switch.

Therefore, some additional circuitry is required to perform the switching, and the circuitry used is shown in Fig. 4(b). The BUK456-60A POWERMOS transistor which features a typical $R_{DS(on)}$ of 24m Ω (at 25°C) was used as the synchronous rectifier for these basic configurations.

The drive circuit operates as follows: the pnp transistor switches on the POWERMOS and the npn switches it off. Good control of the POWERMOS transistor is possible and the body diode does not come on. The waveforms obtained are also shown in Fig. 4.

If the small bipolar transistors were replaced by small POWERMOS devices, then this drive circuit would be a good candidate for miniaturisation in a Power Integrated Circuit. This could provide good control with low drive power requirements.

Unfortunately, the single rectifier in a flyback converter must conduct a much higher r.m.s. current than the two output diodes of the buck derived versions (for the same output power levels). Since the conduction loss in a POWERMOS is given by $I_{D(RMS)}^2 \cdot R_{DS(on)}$, it is clear that the flyback, although simple, does not lend itself as well to achieving large increases in efficiency when compared to other topologies that utilise POWERMOS synchronous rectifiers.

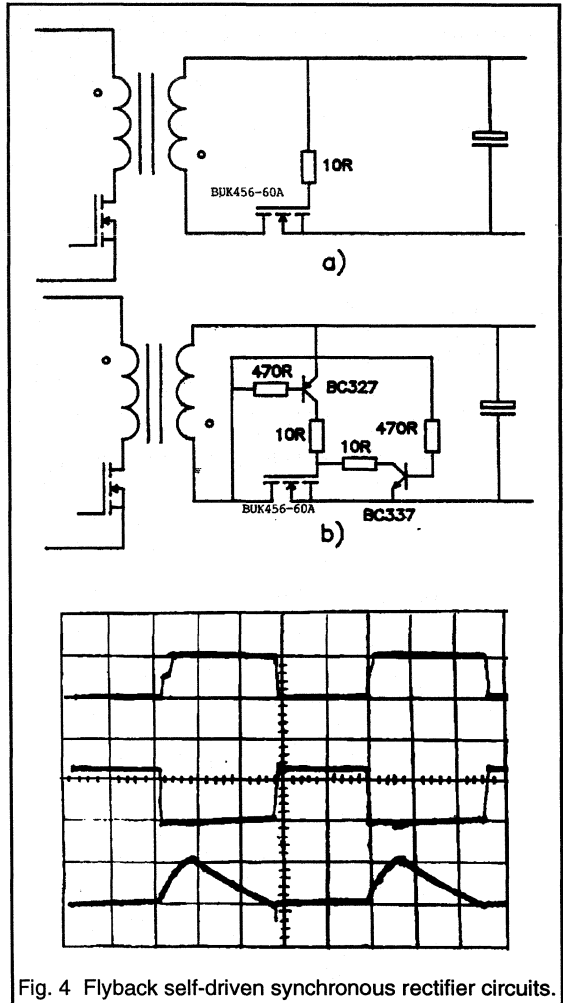


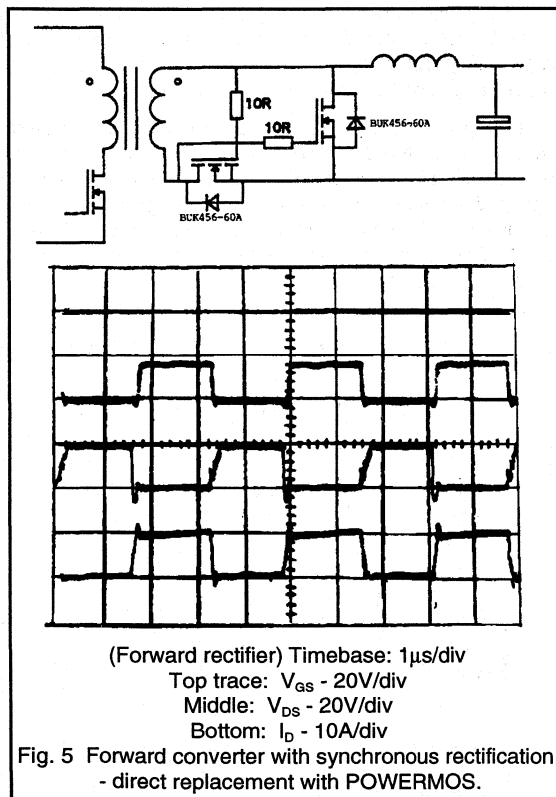
Fig. 4 Flyback self-driven synchronous rectifier circuits.

(b) The Forward converter.

An experimental self-driven circuit based on the forward converter was then investigated. In this version the frequency of operation was raised to 300kHz with the supply again delivering 5V at 10A.

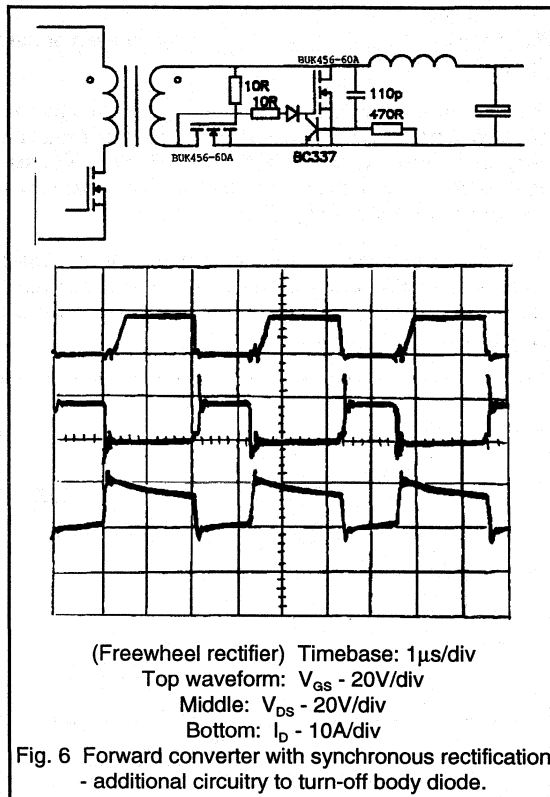
The direct replacement of the output diodes with POWERMOS transistors is shown in Fig. 5. In this arrangement, the gate sees the full voltage across the transformer winding. Therefore, the supply input voltage range must be restricted to ensure the gate of the POWERMOS is not driven by excessively high voltages. This would occur during low primary transistor duty cycle

conditions. The waveforms obtained for the forward synchronous rectifier in this configuration are also shown in Fig. 5.



In this case the method of control is such that the gate is referenced to the source via the drain-source body diode. This clamps the gate, enabling it to rise to a voltage which will turn the POWERMOS on. If the body diode was not present, the gate would always remain negative with respect to the source and an additional diode would have to be added to provide the same function.

Additional circuitry is required to turn off the freewheel synchronous rectifier. This is due to the fact that when the freewheel POWERMOS conducts, the body diode will take the current first before the gate drive turns the device on. An additional transistor can be used to turn off the POWERMOS in order to keep conduction out of the body diode. This additional transistor will short the gate to ground and ensures the proper turn-off of the POWERMOS. The circuit with this additional circuitry and the resulting freewheel rectifier waveforms are given in Fig. 6.



A very simple circuit configuration can be used in which body diode conduction in the freewheel synchronous rectifier does not occur. By driving the freewheel rectifier from the output choke via a closely coupled winding, a much faster turn-on can be achieved because the body diode does not come on. This circuit configuration and associated waveforms are shown in Fig. 7.

To avoid gate over-voltage problems a toroid can be added which will provide the safe drive levels. This toroid effectively simulates extra transformer windings without complicating the main power transformer design. The limitations of this approach are that there will be extra leakage inductance and that an additional wound component is required. The applicable circuit and waveforms for this arrangement are given in Fig. 8.

Conclusions

The main advantage of POWERMOS synchronous rectifiers over existing epitaxial and Schottky diode rectifiers is the increase in efficiency. This is especially true for applications below 5V, since the development of very low $R_{DS(on)}$ POWERMOS transistors allows very significant

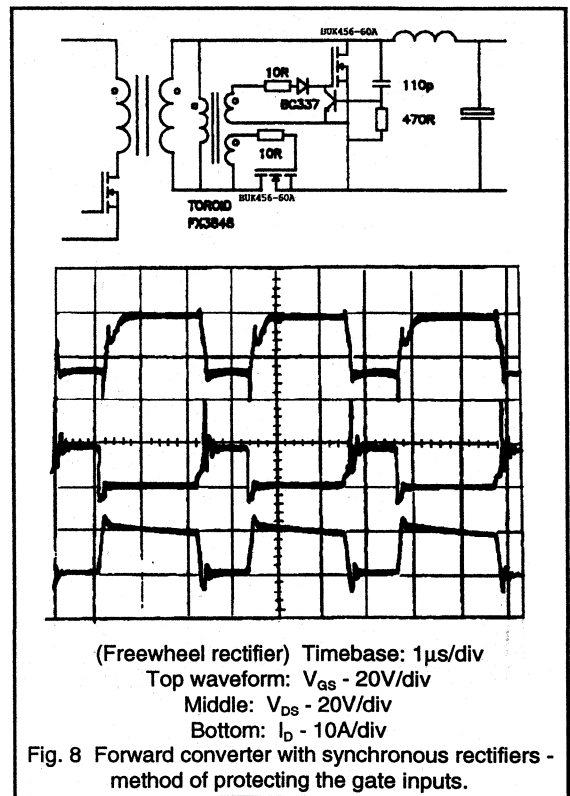
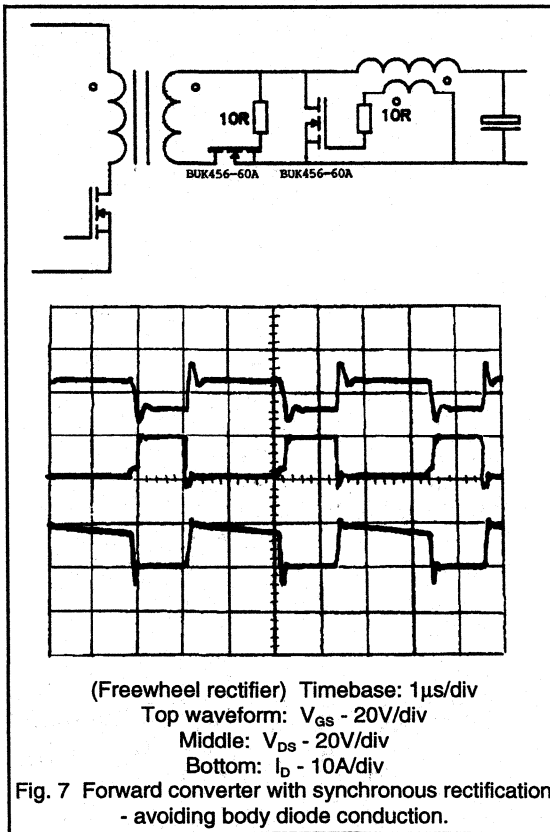
efficiency increases. It is also very easy to parallel the POWERMOS transistors in order to achieve even greater efficiency levels.

The difficulties involved with generating suitable drives for the POWERMOS synchronous rectifiers tend to restrict the number of circuits for which they are suitable. It will also significantly increase the cost of the supply compared with standard rectifier technology.

The circuit examples outlined in this paper were very basic. However, they did show what can be achieved. The flyback configuration was the simplest, and there were various possibilities for the forward converters.

Recent work has shown that there are topologies more suited to using MOSFET synchronous rectifiers (featuring low rectifier r.m.s. current levels) such as the push-pull. These can achieve overall power supply efficiency levels of up to 90% for outputs of 5V and below. However, the discrete control circuitry required is quite complex and requires optical/magnetic isolation, since the waveforms must be derived from the primary-side control.

The true advantage of synchronous rectifiers may only be reached when the drive circuit and POWERMOS devices are hybridised into Power Integrated Circuits. However, in applications where the efficiency performance is of more importance than the additional costs incurred, then POWERMOS synchronous rectification is presently the most suitable technique to use.



Design Examples

2.3.1 Mains Input 100 W Forward Converter SMPS: MOSFET and Bipolar Transistor Solutions featuring ETD Cores

The following two switched-mode power supplies described are low cost easy to assemble units, intended primarily for the large number of equipment manufacturers who wish to build power supplies in-house.

The designs are based upon recent technologies and both feature ETD (Economic Transformer Design) ferrite cores. The first design features a high voltage Bipolar transistor, the BUT11 at a switching frequency of 50kHz. The second design is based around a power MOSFET transistor, the BUK456-800A whose superior switching characteristics allow higher switching frequencies to be implemented. In this case 100kHz was selected for the MOSFET version allowing the use of smaller and cheaper magnetic components compared with the lower frequency version.

Both supplies operate from either 110/120 or 220/240 V mains input, and supply 100W of regulated output power up to 20A at 5V, with low power auxiliary outputs at $\pm 12V$. The PowerMOS solution provides an increase in efficiency of 5% compared with the Bipolar version, and both have been designed to meet stringent R.F.I. specifications.

ETD ferrite cores have round centre poles and constant cross-sectional area, making them ideally suited for the windings required in high-frequency S.M.P.S. converters. The cores are available with clips for rapid assembly, and the coil formers are suitable for direct mounting onto printed circuit boards.

The ETD cores, power transistors and power rectifiers featured are part of a comprehensive range of up-to-date components available from Philips from which cost effective and efficient S.M.P.S. designs can be produced.

50kHz Bipolar version

Circuit description

The circuit design which utilises the Bipolar transistor is shown in Fig. 1. This is based upon the forward converter topology, which has the advantage that only one power switching transistor is required.

An operating frequency of 50kHz was implemented using a BUT11 transistor (available in TO-220 package or isolated SOT-186 version). This was achieved by optimising the switching performance of the BUT11 Bipolar power transistor TR5, by careful design of the base drive circuitry and by the use of a Baker clamp. The 50kHz operating

frequency allows the size and the cost of the transformer and choke to be reduced compared with older Bipolar based systems which worked around 20kHz.

The base drive waveform generated by IC1 is buffered through TR3 and TR4 to the switching transistor TR5. Although operating from a single auxiliary supply line, the drive circuit provides optimum waveforms. At turn-off, inductor L3 controls the rate of change of reverse bias current ($-di_b/dt$). The reverse base-emitter voltage is provided by capacitor C16 (charged during the on-time). The resulting collector current and voltage waveforms are profiled by a snubber network to ensure that the transistor SOA limits are not exceeded.

Voltage regulation of the 5V output is effected by means of an error signal which is fed back, via the CNX82A opto-coupler, to IC1 which adjusts the transistor duty cycle. Over-current protection of this output is provided by monitoring the voltage developed across the 1 Ω resistor, R28 and comparing this with an internal reference in IC1. Voltage regulation and overcurrent protection for the 12V outputs are provided by the linear regulating integrated circuits IC4 and IC5.

Specification and performance (Bipolar version)

Input

220/240 V a.c. nominal (range 187 to 264 V a.c.)
110/120 V a.c. nominal (range 94 to 132 V a.c.)

Output

Total output power = 100 W.

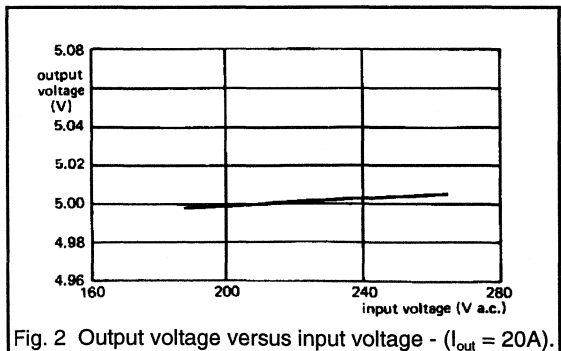


Fig. 2 Output voltage versus input voltage - ($I_{out} = 20A$).

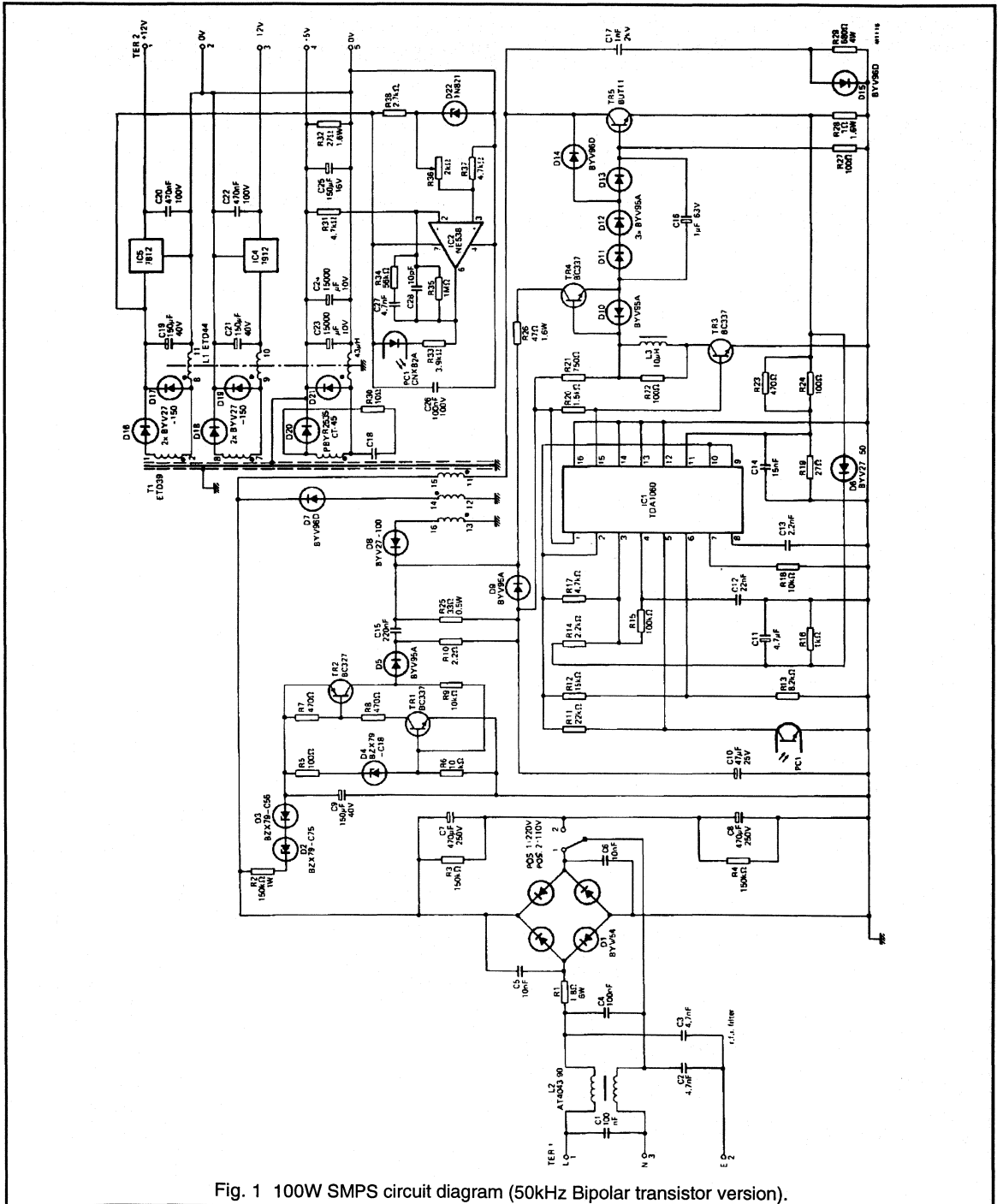


Fig. 1 100W SMPS circuit diagram (50kHz Bipolar transistor version).

Main output

5V at 20A max output power - Adjustment range $\pm 5\%$.

Line regulation

The change in output voltage over the full input voltage range of 187 to 264 V is typically 0.2%; see Fig. 2.

Load regulation

The change in output voltage over the full load range of zero to 100 W is typically 0.4%; see Fig. 3.

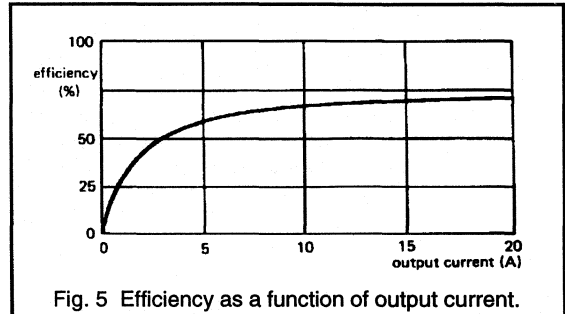
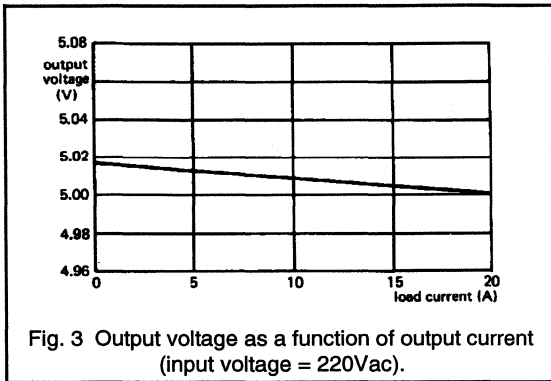
Both the main and auxiliary outputs will remain within specification for a missing half-cycle (18ms) at full load and minimum input voltage; see Fig. 4.

Isolation

Input to output ground 2kV r.m.s.
Output to ground 500V r.m.s.

Efficiency

The ratio of the d.c output power to the a.c input power is typically 71% at full load; See Fig. 5.



Auxiliary outputs

$\pm 12V$ at 0.1A.
Regulation (worst-case condition of max change in input voltage and output load) < 0.4%.

Radio frequency interference

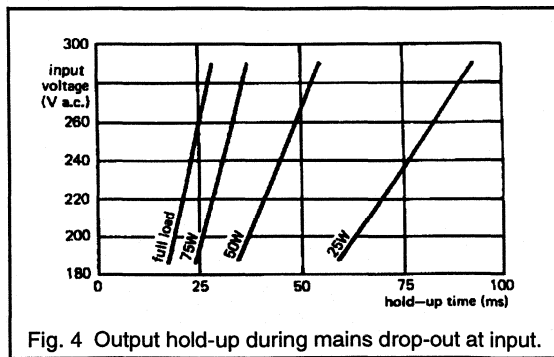
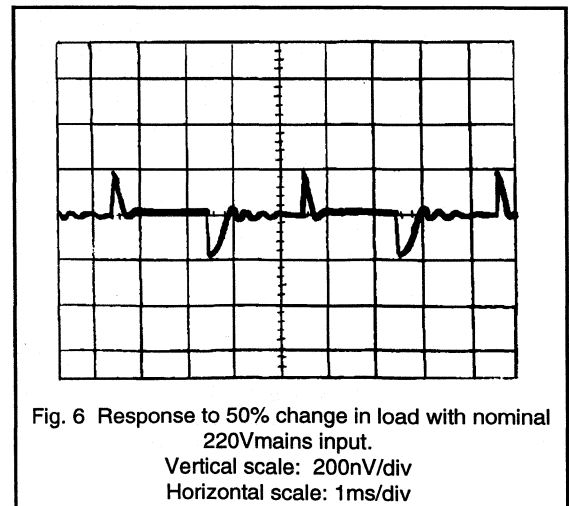
R.F.I. fed back to the mains meets VDE0875N and BS800.

Transient response

The response to a 50% change in load is less than 200mV and the output returns to the regulation band within 400 μ s: See Fig. 6.

Ripple and Noise

0.2% r.m.s. 1.0% pk-pk (d.c. to 100MHz).



Output hold-up

Optimum drive of high voltage Bipolar transistor (H.V.T.)

A feature of the high voltage Bipolar transistor is the very low conduction loss that can be obtained. This is made possible by the "conductivity modulation" process that takes place due to the influence of minority carriers in the collector region of the device. However, the presence of these carriers means that a stored charge will exist within the collector region (especially in high voltage types) which has the effect of producing relatively slow switching speeds. This leads to significant switching losses, limiting the maximum frequency of operation to around 50kHz.

To effectively utilise the power switching H.V.T. the base drive must be optimised to produce the lowest switching losses possible. This is achieved by accurate control of the injection and more importantly the removal of the stored charge during the switching periods. This is fulfilled by controlling the transistor base drive current. (The Bipolar transistor is a current-controlled device). The simple steps taken to achieve this are summarised as follows:-

- (1) A fast turn-on "kick-up" pulse in the base current should be provided to minimise the turn-on time and associated switching loss.
- (2) Provide the correct level of forward base current during conduction, based upon the high current gain of the transistor. This ensures the device is neither over-driven (which will cause a long turn-off current tail) nor under-driven (coming out of saturation causing higher conduction loss). The Baker clamp arrangement used (see Fig. 1) prevents transistor over-drive (hard saturation).
- (3) The correct level of negative base drive current must be produced to remove the stored charge from the transistor at turn-off. The majority of this charge is removed during the transistor storage time t_s . This cannot be swept out too quickly, otherwise a "crowding effect" will take place causing a turn-off current tail with very high switching loss. This accurate control of the charge is provided by a series inductor placed in the path of the negative base drive circuit. (For further information see sections 1.3.2. and 2.1.3).

BUT11 waveforms

These techniques have been applied in the BUT11 drive circuit shown in Fig. 1, and the resulting base drive waveforms are given in Fig. 7.

Optimised base drive minimises both turn-on and turn-off switching loss, limiting the power dissipation in both the transistor and snubber resistor allowing acceptable

operation at 50kHz. This is outlined in Fig. 8 which gives the BUT11 collector current (I_C) and collector-emitter voltage (V_{CE}) waveforms.

The transistor $V_{CE(sat)}$ would normally be as low as 0.3V. However, the use of the Baker clamp limits it to about 1V. Even so this still yields a transistor conduction loss of only 0.76W for the full output load condition.

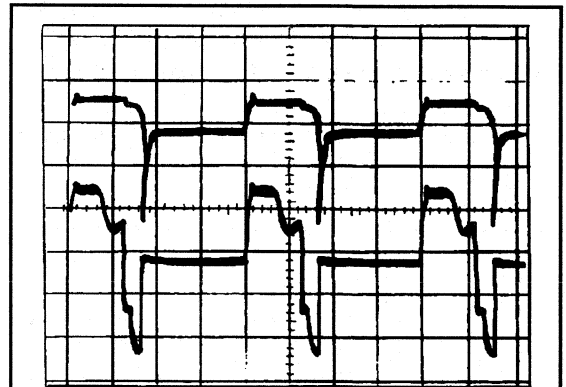


Fig. 7 Base voltage V_B and base current I_B of BUT11 with nominal 220V input and full 5V, 20A output.
Upper trace V_B : 5V/div
Lower trace I_B : 0.2A/div
Horizontal scale: 5 μ s/div

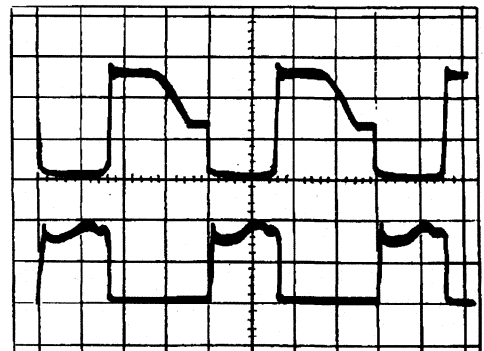


Fig. 8 Collector-emitter voltage V_{CE} and collector current I_C for the BUT11 with nominal 220V mains input and full 5V, 20A output.
Upper trace V_{CE} : 200V/div
Lower trace I_C : 1A/div
Horizontal scale: 5 μ s/div

50kHz Magnetics design

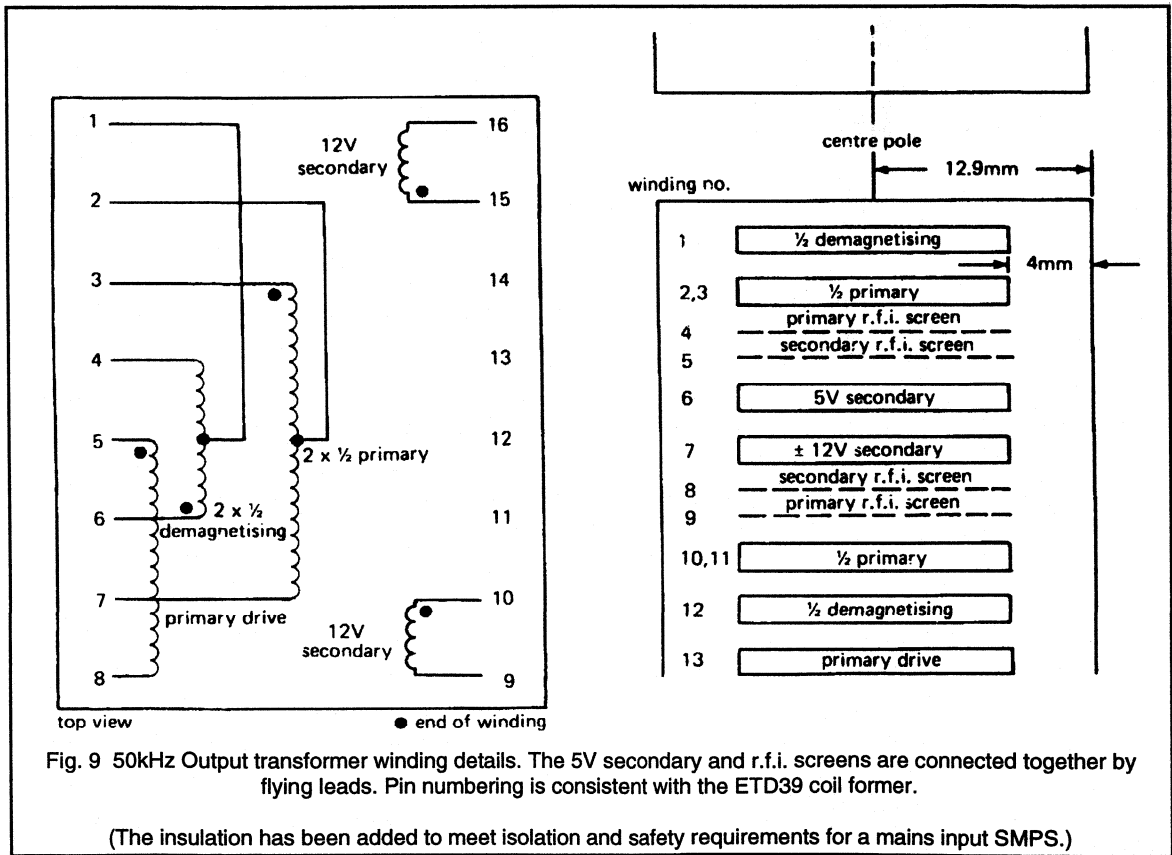
Output Transformer

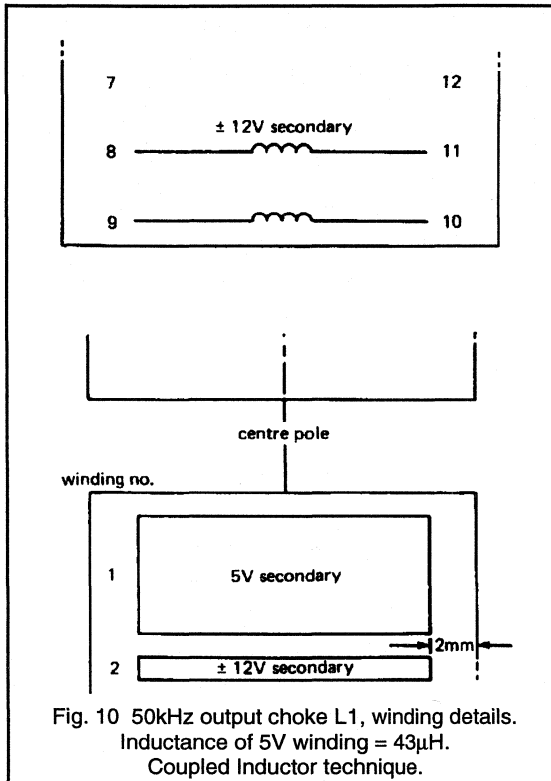
For 50kHz operation the transformer was designed using an ETD39 core. The winding details are given in Fig. 9 and listed as follows:-

Winding

1. 1/2 demag 42 turns 0.315mm dia. enamelled copper wire (e.c.w.) (single layer).
- 2, 3 1/2 primary 42 turns 0.315mm e.c.w.(2 layers in parallel).
- 4, 5 r.f.i. screens each 1 turn 0.05 x 16.5mm copper strip.

6. 5V sec 6 turns 0.2 x 16.5mm copper strip.
 7. $\pm 12V$ sec 18 turns 0.355mm e.c.w. bifilar wound (1 wire each output).
 - 8, 9 r.f.i. screens each 1 turn 0.05 x 16.55mm copper strip.
 - 10, 11 1/2 prim 42 turns 0.315mm e.c.w. (2 layers in parallel).
 12. 1/2 demag 42 turns 0.315 e.c.w (single layer).
 13. primary drive 7 turns 0.2mm e.c.w.
- interleaving 0.04mm film insulation.
- Airgap 0.1mm total in centre pole.





50kHz output chokes

All of the output chokes have been wound on a single core; i.e. using the coupled inductor approach. This reduces overall volume of the supply and provides better dynamic cross-regulation between the outputs. The design of this choke, L1, is based upon $43\mu\text{H}$ for the main 5V output, using an ETD44 core which was suitable for 100W, 50kHz operation.

The winding details are shown in Fig. 10 and are specified as follows :-

Windings

- 19 turns 0.25 x 25mm copper strip.
- 57 turns 0.4mm e.c.w. bifilar wound.

Airgap 2.5mm total in centre pole.

Note. Choke L3 was wound with 1 turn 0.4mm e.c.w.

100kHz MOSFET version

The circuit version of the 100W forward converter based around the high voltage power MOSFET is shown in Fig. 11. The operating frequency in this case has been doubled to 100kHz.

Feedback is again via opto-coupler IC1, the CNX83A which controls the output by changing the duty cycle of the drive waveform to the power MOSFET transistor, TR3 which is the BUK456-800A (available in TO-220 package or the fully isolated SOT-186 version). The transistor is driven by IC4 via R16 and operates within its SOA without a snubber: see the waveforms of Fig. 15. There is low auxiliary supply voltage protection and primary cycle by cycle current limiting which inhibit output drive pulses and protect the supply.

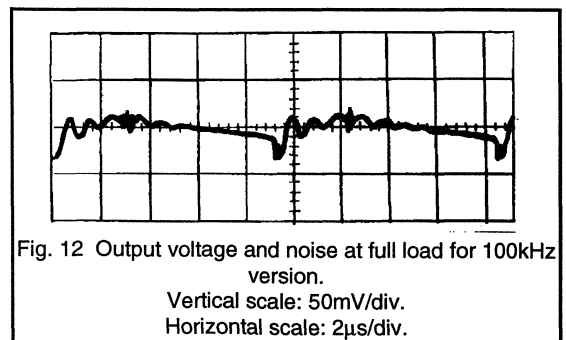
The power supply control and transistor drive circuitry (enclosed within the broken lines in Fig. 11) have low current requirements (5mA). This allows dropper resistors R2 and R3 to provide the supply for these circuits directly from the d.c. link thereby removing the supply winding requirement from the transformer.

Specification and performance (MOSFET version)

The specification and performance of the 100kHz MOSFET version is the same as the earlier 50kHz Bipolar version with the exception of the following parameters:-

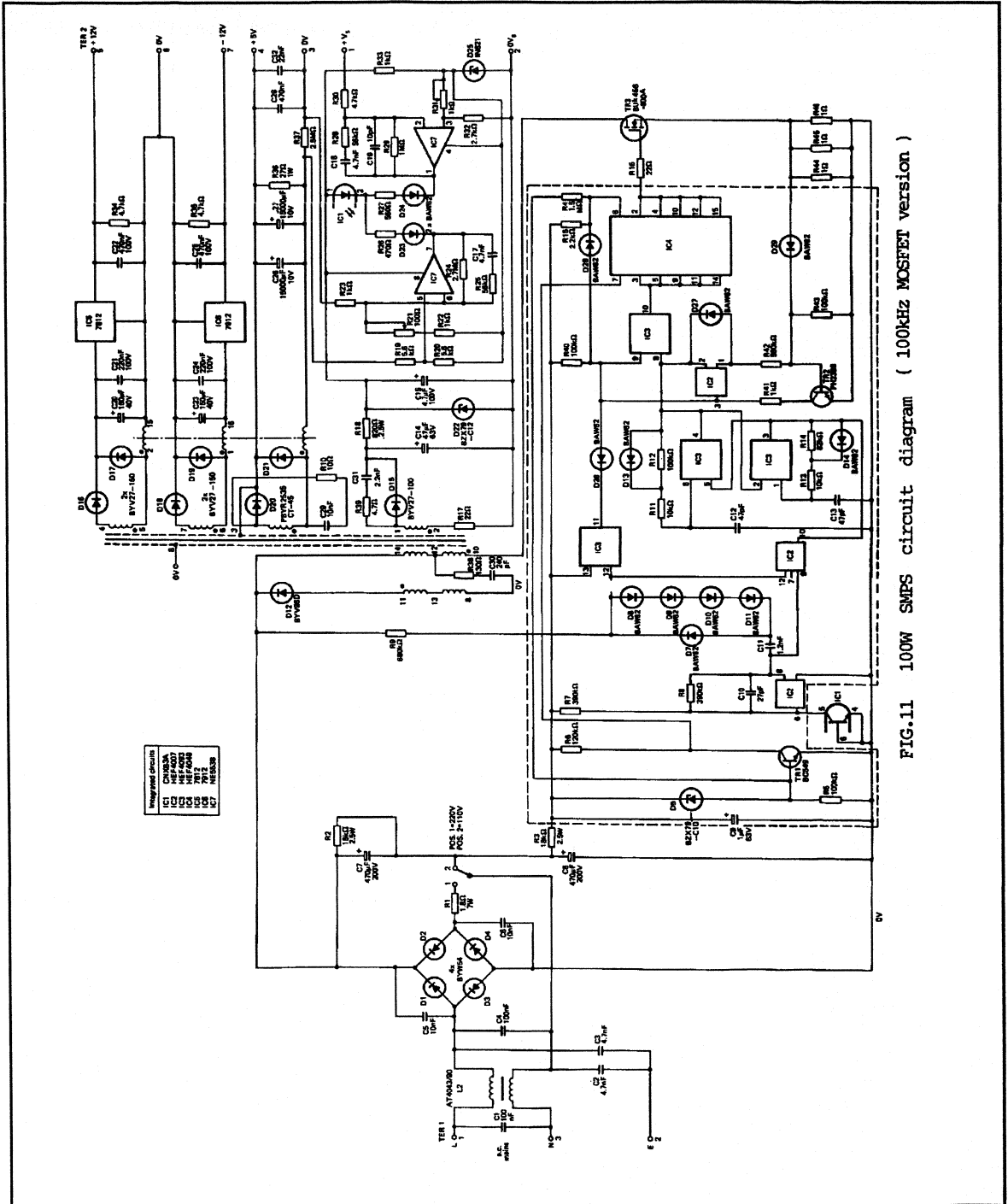
Output ripple and noise

- < 10 mV r.m.s.
- < 40mV pk-pk (100MHz bandwidth) See Fig. 12.



Transient response

The transient response has been improved to a 100mV line deviation returning to normal regulation limits within $100\mu\text{s}$ for a 10A change in load current.



Radio frequency interference

The 100kHz version meets BS800 and CISPR recommendations; see Fig. 13.

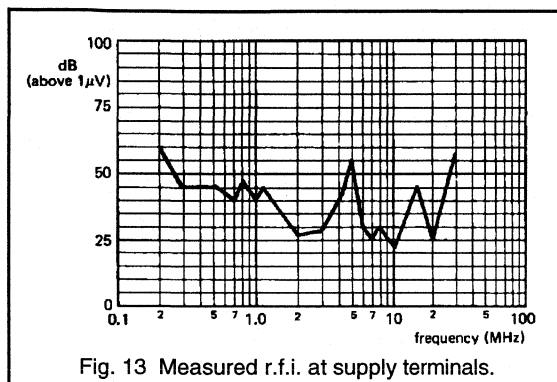


Fig. 13 Measured r.f.i. at supply terminals.

Efficiency

The overall efficiency has been improved by up to 5% compared to the Bipolar version, achieving 76% at full output load. This is mainly due to the more efficient switching characteristics of the MOSFET allowing the removal of the lossy snubber, reduced transistor drive power requirements and lower control circuit power requirements. Fig. 14 shows the overall efficiency of the power supply against load current.

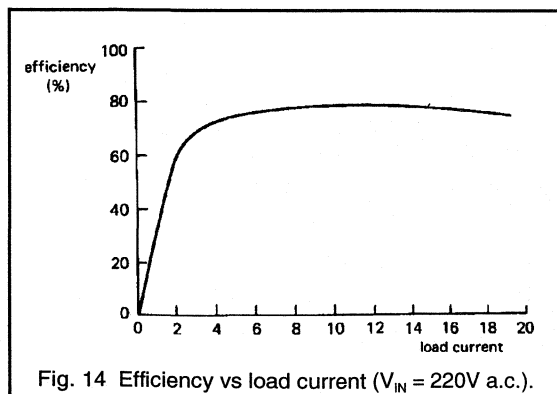


Fig. 14 Efficiency vs load current ($V_{IN} = 220V$ a.c.).

It should be noted that for the high current and low voltage (5V) main output, a large portion of the efficiency loss will be due solely to the output rectifiers' forward voltage drop V_F . Therefore, these two output rectifiers are required to be low loss, very low V_F power Schottky diodes in order to keep overall converter efficiency as high as possible. In this case the Dual PBYR2535CT device was selected for the 5V output. This is available in the TO-220 package and will

comfortably rectify an average output current well above the 20A required, providing a suitably sized heat-sink is added.

Mains isolation

The mains isolation conforms to IEC435.

The power MOSFET as a high frequency switch

Power MOSFET transistors are well known for their ease of drive and very fast switching characteristics. Since these are majority carrier devices, they are free from the charge storage effects which lessen the switching performance of the Bipolar products. Driving the MOSFET is far simpler and requires much less drive power than the equivalent Bipolar version.

The speed at which a MOSFET can be switched is determined by the rate at which its internal capacitances can be charged and discharged by the drive circuit. In practice these capacitances are very small (e.g the input capacitance C_{iss} for the BUK456-800A is quoted as 1000pF) allowing MOSFET rise and fall times in the tens of nano-seconds region. The MOSFET can conduct full current when the gate-source voltage V_{GS} , is typically 4V to 6V. However, further increases in V_{GS} are usually employed to reduce the device on-resistance and 8V to 10V is normally the final level applied to ensure a lower conduction loss.

With such fast switching times, the associated switching losses will be very low, giving the MOSFET the ability to operate as an extremely high frequency switch. Power switching in the MHz region can be obtained by using a MOSFET.

One major disadvantage of the MOSFET is that it has a relatively high conduction loss in comparison with bipolar types. This is due to the absence of the minority carriers meaning no "conductivity modulation" takes place.

MOSFET on-resistance

The conduction loss is normally calculated by using the MOSFET "on-resistance", $R_{DS(on)}$, expressed in Ohms. The voltage developed across the device during conduction is an Ohmic drop and will rise as the drain current increases. Therefore, the conduction loss is strongly dependent upon the operating current. Furthermore, the value of the MOSFET $R_{DS(on)}$ is strongly dependent upon temperature, and increases as the junction temperature of the device rises during operation. Clearly, the MOSFET does not compare well to the Bipolar which has a stable low saturation voltage drop $V_{CE(sat)}$, and is relatively independent of operating current or temperature.

It should be noted that the $R_{DS(on)}$ of the MOSFET also increases as the breakdown voltage capability of the device is increased.

How fast should the MOSFET be switched?

Although very fast switching times are achievable with the power MOSFET, it is not always suitable or necessary to use the highest frequency possible. A major limiting factor in S.M.P.S. design is the magnetics. Present high frequency core loss for high grade ferrite core materials such as 3C85 limits the maximum operating frequency to about 200kHz, although new types such as 3F3 are now suitable for use at 500kHz.

There has always been a drive to use ever higher operating frequencies with the aim of reducing magnetics and filter component sizes. However, most S.M.P.S. designs still operate below 300kHz, since these frequencies are quite adequate for most applications. There is no reason to go to higher frequencies unnecessarily, since very high frequency design is fraught with extra technical difficulties.

Furthermore, although the very fast MOSFET switching times reduce switching loss, the increased di/dt and dV/dt rates will generate far worse oscillations in the circuit parasitics requiring lossy snubbers. The R.F.I. levels generated will also be far more severe, requiring additional filtering to bring the supply within specification. The golden rule in S.M.P.S. square wave switching design is to use the lowest operating frequency and switching times that the application will tolerate.

Estimating required switching times

In the 100kHz example presented here, the typical conduction time of the transistor will be approximately $3\mu s$. A rule of thumb is to keep the sum of the turn-on and turn-off times below 10% of the conduction time. This ensures a wide duty cycle control range with acceptable levels of switching loss. Hence, the target here was to produce switching times of the order of 100ns to 150ns.

Gate drive requirements

The capacitances of the power MOSFET are related to the overall chip size with the gate-source capacitance typically in the range 1nF to 2nF. However, these capacitances are very voltage dependent and are not suitable for estimating the amount of drive current required to obtain the desired switching times. A more accurate method is to use the information contained in the turn-on gate charge (Q_g) characteristic given in the data-sheets. The graph of Q_g for the BUK456-800A for a maximum d.c. rated drain current of 4A is shown in Fig. 15.

The shape of this characteristic needs explaining. The initial slope shows the rise of V_{GS} to the device 4A threshold voltage V_{th} . This requires very little charge, and at the top point of this slope the MOSFET can then conduct full current. However, further gate charge is required while V_{DS} falls from its off-state high voltage to its low on-state level. This is the flat part of the characteristic and at the end of this region the MOSFET is fully switched on. (This is shown

for a range of initial off state voltages). The second slope characterises any further increase in Q_g and V_{GS} that may be employed to minimise the device on-resistance.

Note. Since the turn-off mechanism involving the removal of gate charge is almost identical to the turn-on mechanism, the required turn-off gate charge can also be estimated from the turn-on gate charge plot.

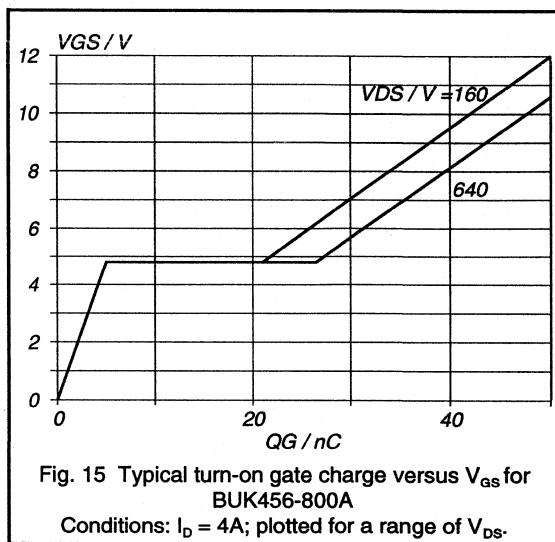


Fig. 15 Typical turn-on gate charge versus V_{GS} for BUK456-800A
Conditions: $I_D = 4A$; plotted for a range of V_{DS} .

In this topology the typical d.c. link voltage is 280V, hence the MOSFET V_{DS} prior to turn-on will be 280V, doubling to 560V at turn-off. From Fig. 14, for these two V_{DS} levels it can be estimated that the BUK456-800A will require 23nC to fully turn on and 27nC to turn off. It should be noted that this estimation of gate charge is for the 4A condition. In this present application the peak current is under 2A and in practice the actual Q_g required will be slightly less.

To a first approximation the gate current required can be estimated as follows:-

$$Q_G = I_G t_{sw}$$

where t_{sw} is the applicable switching time. If an initial value of the turn-on and turn-off time is taken to be 125ns then the required gate current is given by:-

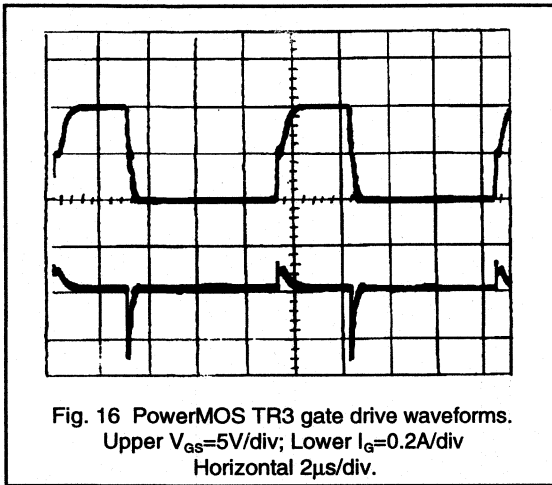
$$I_{G(on)} = \frac{23nC}{125ns} = 0.184A; \quad I_{G(off)} = \frac{27nC}{125ns} = 0.216A$$

In the majority of MOSFET drive circuits the peak currents and resulting switching times are controlled by using a series gate resistor R_G . An initial estimation of the value of this resistor can be found as follows:-

$$R_G = \frac{V_{drive} - V_{th}}{I_{G(ave)}}$$

where $I_{G(ave)}$ is the average value of the turn-on and turn-off peak gate current. In this example the gate driver I.C.4. consists of 5 parallel T.T.L. gates in order to provide high enough current sink and source capability. The driver supply voltage was approximately 10V, the MOSFET threshold voltage was 5V and the average peak gate current was 0.2A.

This gives a value for R_G of 25Ω. A value of 22Ω was selected, and the resulting gate drive waveforms for TR3 under these conditions at the full 100W output power are given in Fig. 16.



This shows a peak I_G of 0.17A at turn-on and 0.28A at turn-off. The magnitudes of the turn-on and turn-off peak gate currents in operation are slightly different to the calculated values. This is due to the effect of the internal impedance of the driver, where the impedance while sinking current is much lower than while sourcing, hence the discrepancy.

These drive conditions correspond to a turn-on time of 143ns and turn-off time of 97ns, which are reasonably close to the initial target values.

In this application, and for the majority of simple gate drive arrangements which contain a series gate resistor (see section 1.1.3) the total power dissipation of the gate drive circuit can be expressed by:-

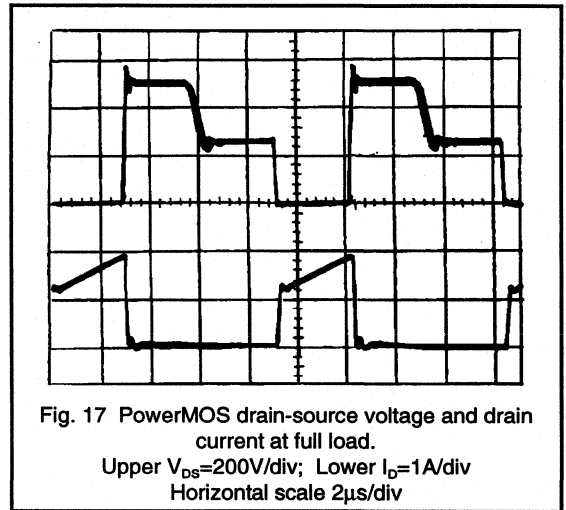
$$P_G = Q_G \cdot V_{GS} \cdot f$$

where Q_G is the peak gate charge and V_{GS} is the operating gate-source voltage. From Fig. 15, taking Q_G to be 43nC for a V_{GS} of 10V gives a maximum gate drive power dissipation of only 43mW, which is very small and can be neglected.

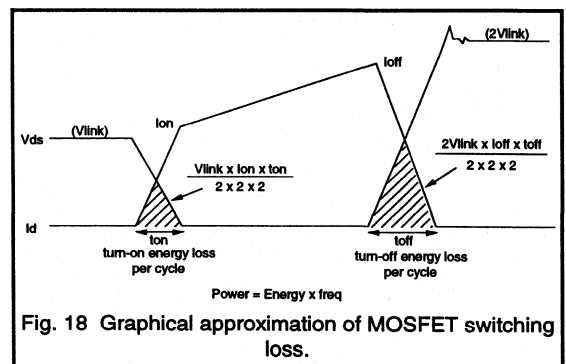
MOSFET losses

Switching losses

The waveforms for the drain current and drain-source voltage at full output load for the drive conditions specified are given in Fig. 17. In this case no transistor snubbing was required.



The waveforms of I_D and V_{DS} were found to cross at approximately half their maximum values for both turn on and turn-off. The switching loss can therefore be approximated to two triangular cross-conduction pulses shown in Fig. 18.



Hence, the total switching loss can be expressed by the following simplified equation:-

$$P_{sw} = \frac{1}{8} f (I_{Don} V_{link} t_{on} + I_{Doff} 2V_{link} t_{off})$$

Inserting the correct values for this example gives:-

$$P_{sw} = 0.125 \times 100k(1.3 \times 280 \times 147n + 1.95 \times 560 \times 97n)$$

$$= 0.67W + 1.06W = 1.73W$$

The MOSFET switching loss in this application is a very respectable 1.73W. It should be noted that a direct comparison with the switching loss of the earlier Bipolar version is not practical. It was necessary to use a snubber with the Bipolar in order to remove a large amount of the excessive switching loss generated by the device. Furthermore, the MOSFET switching frequency implemented was double that of the Bipolar version.

If a direct comparison were to be made under the same circuit conditions, the Bipolar switching loss would always be far in excess of the low values achievable with the MOSFET.

Conduction loss

The conduction loss for a power MOSFET is calculated by estimating $(I_{D(rms)})^2 R_{DS(on)}$. The drain current at full output load is as shown in Fig. 17 and the r.m.s. value of the trapezoidal current waveforms found in the forward converter is given by:-

$$I_{rms} = \sqrt{D \left(\frac{I_{min}^2 + I_{min} I_{max} + I_{max}^2}{3} \right)} \quad D = \frac{t_{ON}}{T}$$

At full load, these values can be seen to be $I_{min}=1.25A$; $I_{max}=1.95A$; $D=0.346$. Substituting these values into the above equation gives an $I_{D(rms)} = 0.95A$.

The typical $R_{DS(on)}$ value for the BUK456-800A is quoted as 2.7Ω . However, this is for a junction temperature of $25^\circ C$. The value at higher operating junction temperatures can be calculated from the normalisation curve given in the data-sheets. If a more realistic operating temperature of $100^\circ C$ is assumed, the weighting factor is 1.75. Hence, the correct $R_{DS(on)}$ to use is 4.725Ω . Therefore, the conduction loss is given by:-

$$P_{cond} = (0.95)^2 4.723 = 4.26W$$

The conduction loss of 4.26W is over double the switching loss. However, this is typical for a high voltage MOSFET operated around this frequency. The MOSFET conduction loss is much higher than was previously obtained using the Bipolar transistor at 50kHz, as expected.

The total loss for the MOSFET device thus comes to 6W i.e. 6% of the total output power.

It should be remembered that this figure has been calculated for the full output load condition which will be a transient worst case condition. A more realistic typical dissipation of approximately 4W has been estimated for the half load condition, where the conduction loss is approximately halved. This 4W figure should be used when

estimating the heatsink requirement. In this case a relatively small heatsink with a thermal co-efficient of around $10^\circ C/W$ would be adequate.

For more information on MOSFET switching refer to chapters 1.2.2. and 1.2.3. of this handbook.

100kHz magnetics design

Output transformer

Doubling the switching frequency to 100kHz has allowed the use of the smaller sized ETD34 core for the transformer. This transformer has been designed with a 0.1mm centre pole air gap. The winding details are shown in Fig. 19 and listed as follows:-

Winding

2 to 1	Regln supply	
5 to 4	+12V sec	3 x 12 turns 0.4mm e.c.w. in 1 layer.
6 to 7	-12V sec	3 x 12 turns 0.4mm e.c.w. in 1 layer.
8	r.f.i. screen	1 turn 0.1 x 13mm copper strip.
10 to 12	1/2 prim	28 turns 0.355mm e.c.w. bifilar in two layers.
11 to 13	1/2 demagn	28 turns 0.355mm e.c.w. in 1 layer.
12 to 14	1/2 prim	28 turns 0.355mm e.c.w. bifilar in 2 layers.
13 to 8	1/2 demagn	28 turns 0.355mm e.c.w. in 1 layer.

Interleaving:- 1turn 0.04mm insulation between each layer except 3 turns between r.f.i. screens.

Output choke

Again the implementation of the higher frequency has allowed the use of the smaller sized ETD39 core for the coupled output inductor. A centre pole air-gap of 2mm was utilised. The winding details are shown in Fig. 20 and are listed as follows:-

Winding

Copper strip	+5V	15 turns 0.3 x 21mm copper strip.
2 to 15	-12V	45 turns 0.4mm e.c.w. in 1 layer.
1 to 16	+12V	45 turns 0.4mm e.c.w. in 1 layer.

Interleave:- 1 layer 0.04mm insulation between each strip and winding.

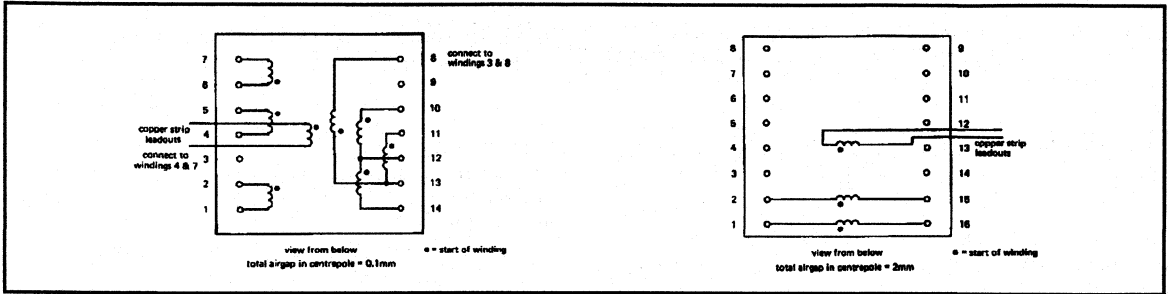


Fig. 19 100kHz transformer construction.

Fig. 20 100kHz inductor construction.

2.3.2 Flexible, Low Cost, Self-Oscillating Power Supply using an ETD34 Two-Part Coil Former and 3C85 Ferrite

This section describes a low-cost, flexible, full performance, Self Oscillating Power Supply (SOPS) using the flyback principle.

The circuit is based around an ETD34 transformer using a two-part coil former and 3C85 ferrite material. The feedback regulation is controlled from the secondary side by means of a small U10 transformer.

The circuit is described and the details of the magnetic design using the two-part coil former is given. The advantages of the two-part coil former are highlighted together with 3C85 material properties. Power supply performance of a 50W SMPS design example is given.

Introduction.

A recently developed low-cost full-performance switched-mode power supply design is presented, highlighting a new transformer concept using a novel ETD34 two-part coil former and 3C85 low-loss material. The SMPS is of the Self Oscillating Power Supply (SOPS) type and uses the flyback principle for minimum component count and ultra-low cost/watt.

Compliance with safety and isolation specifications has always been a headache for magnetics designers. Now, the introduction of the ETD34 two-part coil former solves the problem of the 4+4mm creepage and clearance distances by increasing the available winding area and consequently decreasing copper losses. It also offers the advantage of a more flexible approach with the possibility of using a standard 'plug-in' primary and a customised secondary to meet any set of output requirements.

3C85 is a recently developed material superseding 3C8 and offers lower core loss, better quality control and higher frequency operation at no extra cost.

These products are illustrated in the following 50W SMPS design example, which is suitable for microcomputer applications.

SOPS

The principle of the Self-Oscillating Power Supply is shown in Fig. 1 and is based on the flyback converter principle. Stabilisation of the output voltage against mains and load variation is achieved by varying the duty cycle of the powerMOS switching transistor. The on-time varies mainly with input voltage, whereas the off-time varies only with the load. This means that both the duty cycle and the frequency vary due to the control circuit. The switching frequency is

therefore at a maximum for maximum input voltage and minimum load. Regulation is achieved by varying the point at which the POWERMOS transistor is switched off. A.C. magnetic coupling is used in preference to opto-couplers for long-term life stability and guaranteed creepage and clearance. This circuit has the inherent property of self limiting energy transfer, since the maximum energy $1/2LI^2$, is defined by the bipolar transistor V_{BE} threshold and the source resistance value.

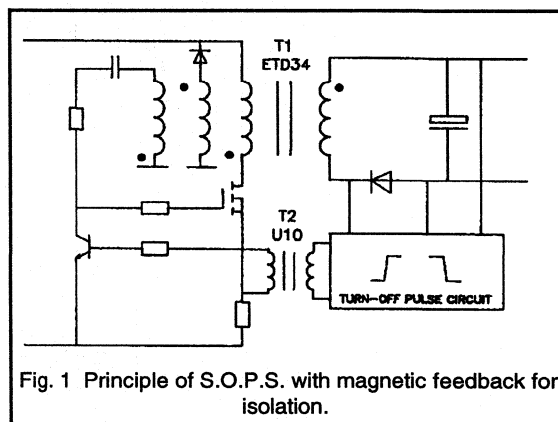


Fig. 1 Principle of S.O.P.S. with magnetic feedback for isolation.

The Transformer

The transformer uses the versatile ETD system. This is the range of four IEC standardised cores based on an E-core shape with a round centre pole. This permits easy winding especially for copper foil and standard wire. The ETD system includes coil formers into which the cores are clip assembled. The coil formers are designed for automatic winding and comply with all the standard safety specifications.

The two-part coil former was especially designed for the ETD34, and is shown in Fig. 2. There is 25% more winding area compared to the standard coil former yet full safety isolation is provided so that the creepage and clearance specifications are fully met. The inner part is a "click" fit into the outer part, such that the former is mechanically stable even with the cores removed. This two-part construction leads to a very versatile winding approach where standard primaries can be wound and assembled, yet still retaining the flexibility for various secondaries to be added for different requirements.

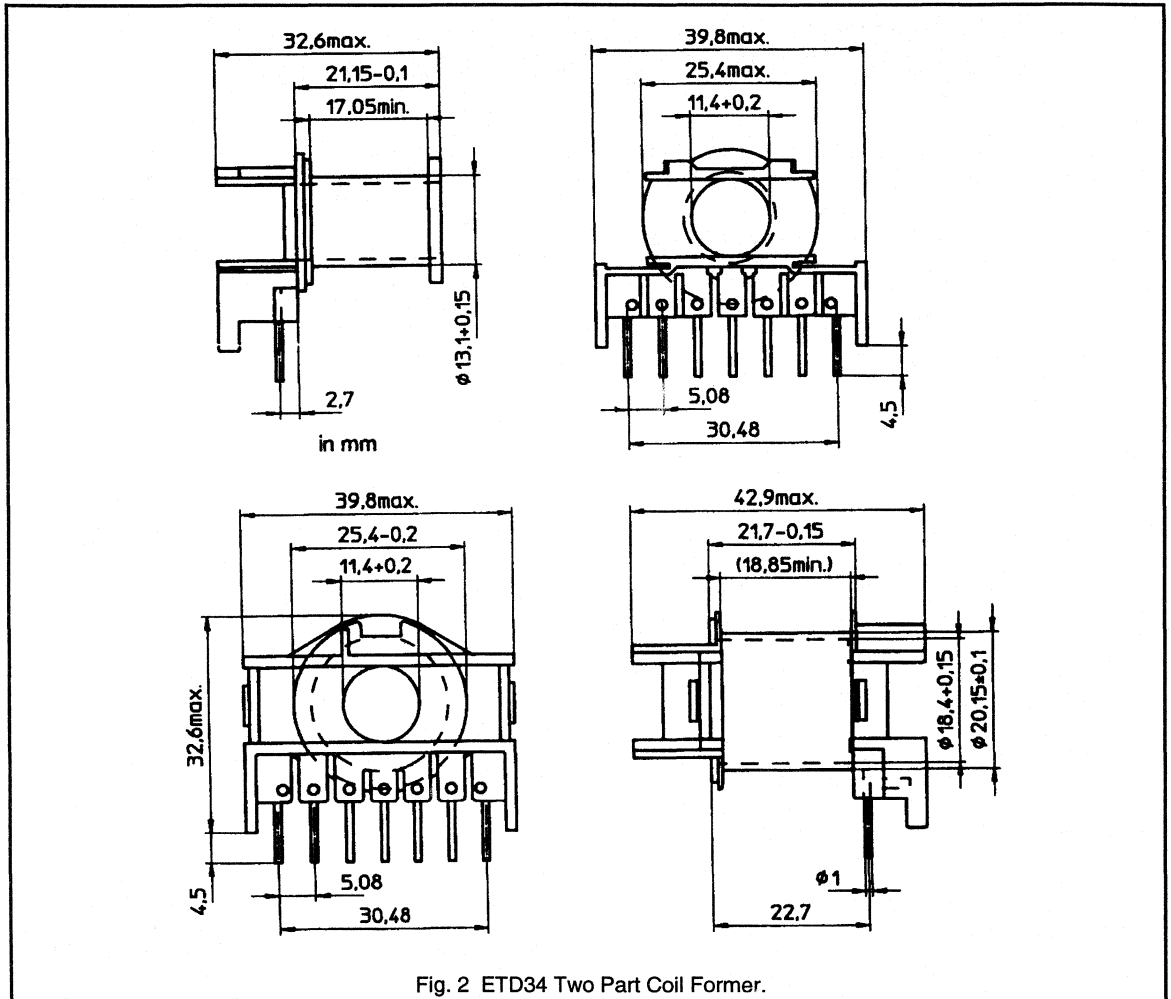


Fig. 2 ETD34 Two Part Coil Former.

Leakage inductance is always a problem with flyback transformers, but using this special construction the increase in leakage can be almost offset by the greater winding area of the two-part coil former when compared to the standard product with 4 + 4mm creepage and clearance. Fig. 3 shows standard and two part transformer cross-sections, where the leakage inductance is not more than 20% greater for the two-part coil former for this 50W design.

The transformer details for the 50W microcomputer power supply design example are shown in Fig. 4. The primary side consists of three windings:- a feedback winding of 5 turns, the main primary winding and a bifilar voltage clamp

winding of 92 turns. This is achieved with 4 layers to fill the inner coil space area. The secondaries consist of a 5V winding of 3 turns and the $\pm 12V$ windings of 7 turns each. As there are so few turns, the winding area is most effectively filled with stranded wire, copper strip or parallel windings, and these are therefore all possible choices.

In addition to the improved windings possibilities with the two-part coil former, the ETD core material has been enhanced. The quality of the 3C85 material is much improved compared to the older 3C8 type. Fig. 5 compares curves of core loss versus frequency for 3C85 against 3C8. The 30% improvement in 3C85 has been due to refining the material composition and tighter process quality control.

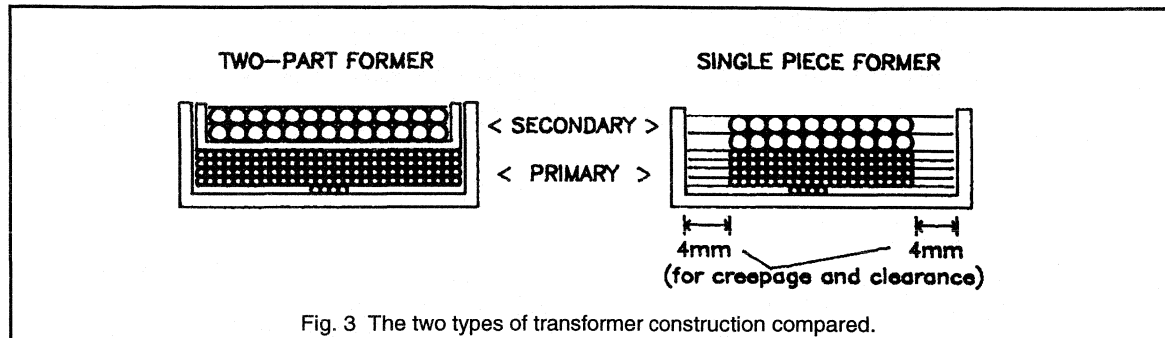


Fig. 3 The two types of transformer construction compared.

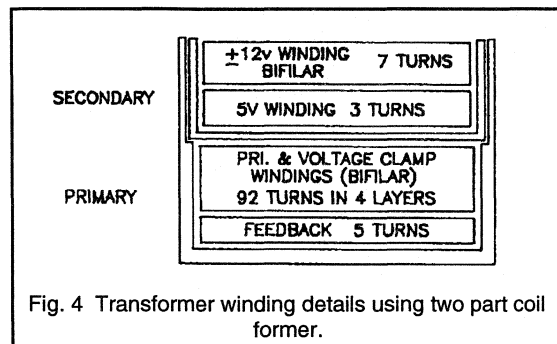


Fig. 4 Transformer winding details using two part coil former.

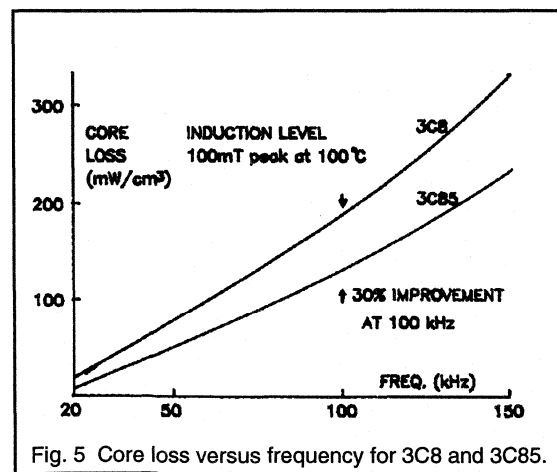


Fig. 5 Core loss versus frequency for 3C8 and 3C85.

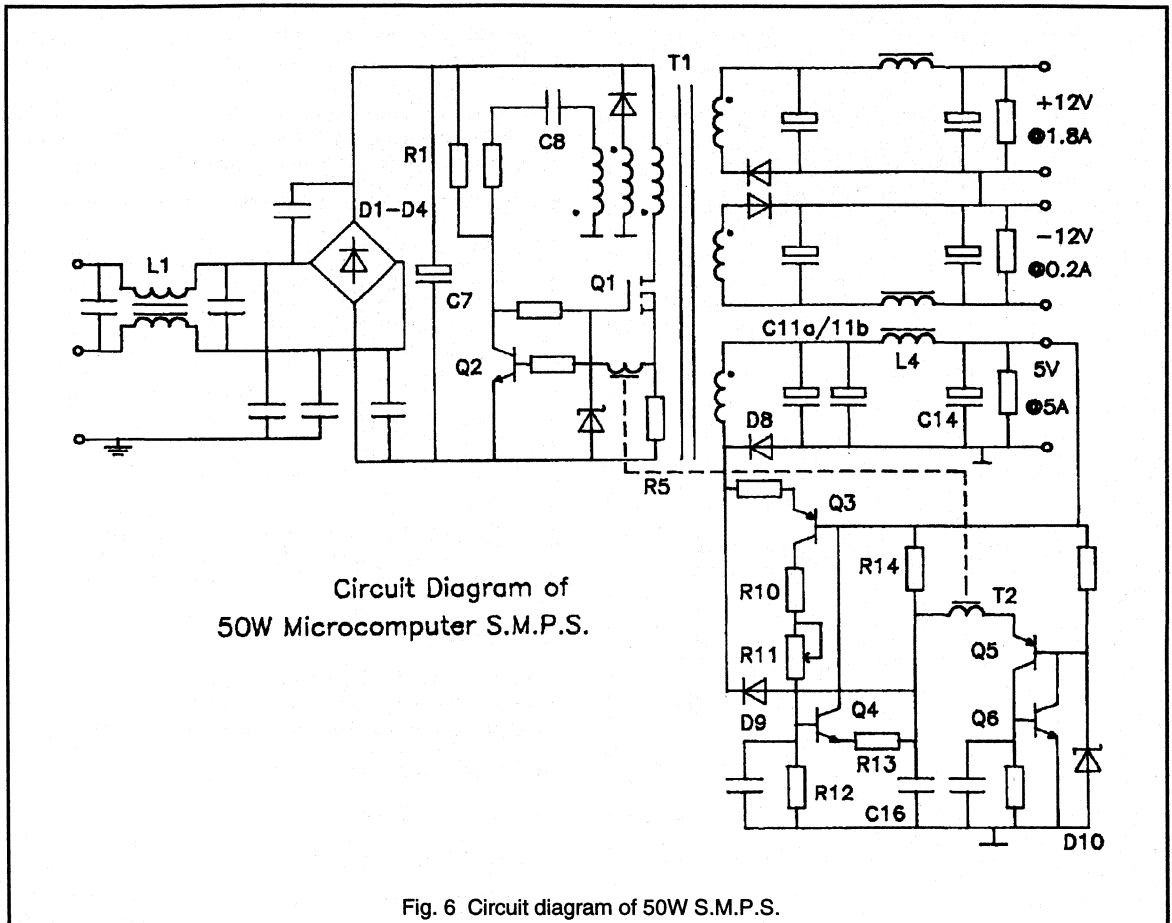
Application and Operation of SOPS

The SOPS circuit is ideally suited for microcomputer systems, where full performance at low cost is required. The 50W output power is split between a regulated 5V output at 5A for the logic, a +12V output at 1.8A and a -12V output at 0.2A for the peripherals. The circuit diagram of the power supply is shown in Fig. 6. The operating frequency varies from 250kHz at open circuit to 35kHz at full load. The circuit works as follows:-

The mains input is filtered (L1), rectified (D1-D4) and smoothed (C7) to provide a d.c. rail. This supply rail utilises a single electrolytic capacitor which is a low profile, low cost, snap-fit 055 type.

The main switching transistor, Q1, is a TO-220 powerMOS device, the BUK456-800A. Starting current is provided via R1 to Q1 to start the self-oscillating operation. Feedback current is provided by a small winding on the transformer (T1), via C8 to maintain bias. Duty cycle control is via R5 and T2, with final control being achieved with R5, T2 and Q2. The triangular transformer magnetising current is seen across R5 as a voltage ramp, (see Fig. 7). This is fed to the base of Q2, via a small U10 transformer, T2. When the voltage becomes greater than the V_{BE} of the transistor, Q2 is turned on, causing the gate of Q1 to be taken to the negative rail, so terminating the magnetisation of the transformer T1. The output voltage is controlled by feeding back a turn-off pulse by means of T2, thus causing Q2 to turn on earlier.

A voltage clamp winding is bifilar wound with the primary to limit voltage overshoots on the drain of Q1 at turn-off, thus ensuring that the transistor operates within its voltage rating.

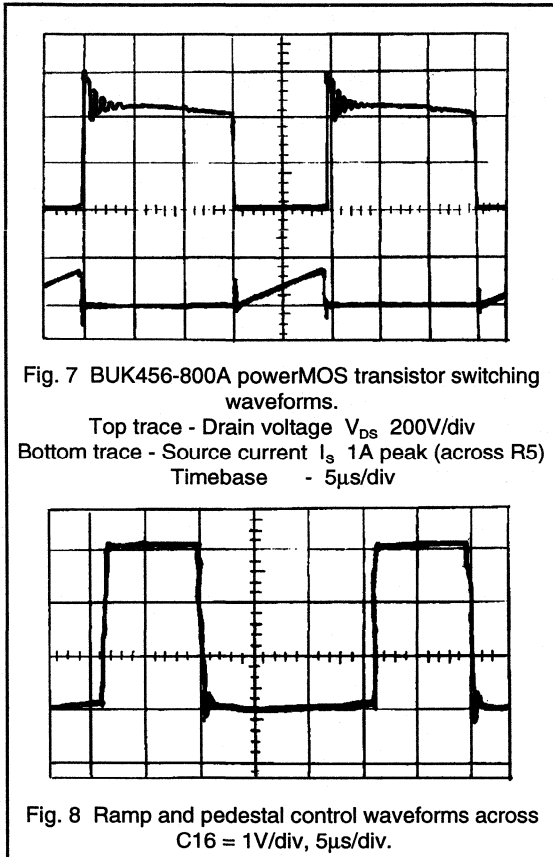


Maximum throughput power is determined by the value of R5: the higher its resistance value, the lower the maximum power. The same drive and control circuit can be used for different throughput powers, ETD core sizes and powerMOS transistors.

The 5V secondary uses a single plastic TO-220 Schottky diode, the PBYR1635 shown as D8. The output filter is a pi type giving acceptable output ripple voltage together with good transient response. Two electrolytic capacitors are used in parallel, C11a/C11b (to accommodate the ripple current inherent in flyback systems), together with a small inductor wound on a mushroom core, L4, and a second capacitor, C14.

The turn-off pulse is created, cycle-by-cycle, by charging a capacitor from the output and comparing it with a reference, D10 and by using the transition signal to feed back a turn-off pulse via transformer T2. A potential divider is present

across the output 5V rail, consisting of R10, R11 and R12, via Q3. The potential divider controls the base voltage of the transistor Q4, which charges capacitor C16 via R13. The voltage on C16 ramps up to a voltage equal to that on the base of the transistor less the V_{BE} , causing Q4 to switch off. The capacitor continues to charge more slowly via resistor R14, i.e. a ramp and pedestal (see Fig. 8), until the voltage on the emitter of Q5 is equal to the voltage determined by the band-gap reference D10 (2.45V) plus the V_{BE} drop of Q5. When this voltage is reached, Q5 switches on, causing Q6 to switch on, pulling Q5 on harder. The edge produced is transmitted across T2 and adds to the voltage on the base of Q2. Transistor Q3 is there to maintain the voltage level at the end of the 'on' period of the waveform to prevent premature switching. Capacitor C16 is reset by diode D9 on the edge of the switching waveform of the schottky diode, D8.

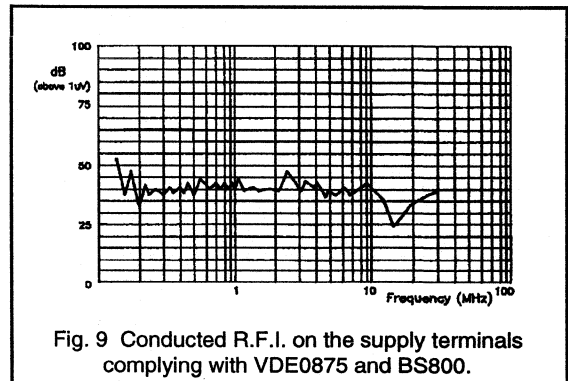


Performance

The performance of the supply is as follows:- the 5V output has load regulation of 1.2% from 0.5A to 5A load current. The line regulation is 0.5% for 187V to 264V a.c. mains input voltage.

The 12V secondaries are unregulated, and therefore have an inferior regulation compared to the 5V output. Each rail has a load regulation of 6% from open-circuit to full load. This is adequate for typical microcomputer peripheral requirements.

The efficiency of the power supply is typically 80%. The ripple and noise on all outputs is less than 75mV peak to peak. The radio frequency interference is less than 50dB (above 1 μ V) from 150kHz to 30MHz and complies with VDE0875 and BS800, based on a 150 Ω V network. See Fig. 9. The transient response of the 5V output due to a 2A to 5A step load change gives a deviation of 100mV.



Conclusion

A novel Self Oscillating Power Supply has been introduced featuring two recently developed products, increasing the cost effectiveness and efficiency of low-power SMPS:-

The new ETD34 two-part coil transformer featuring:

- * solving of isolation problems
- * standard 'plug-in' primaries
- * suitable for automatic winding
- * ETD system compatible.

The 3C85 ferrite material offers:

- * 30% lower loss than 3C8
- * comparable price with 3C8
- * high frequency operation, up to 150kHz
- * improved quality

Magnetics Design



2.4.1 Improved Ferrite Materials and Core Outlines for High Frequency Power Supplies

Increasing switching frequency reduces the size of magnetic components. The current trend is to promote SMPS miniaturisation by using this method. The maximum switching frequency used to be limited by the performance of available semiconductors. Nowadays however, Power MOSFETs are capable of square-wave switching at 1MHz and beyond. The ESL of the output capacitor had until recently limited any major size reduction in output filter above 100kHz. The advent of multi-layer ceramic capacitor stacks of up to 100 μ F removed this obstacle. This allowed the operating frequency to be raised significantly, providing a dramatic reduction in the size of the output filter (by an order of magnitude). The transformer has now become the largest single component in the power stage, and reducing its size is very important. The transformer frequency dependent core losses are now found to be a major contributing factor in limiting the operating frequency of the supply.

Part 1 of this section highlights the improvements in ferrite material properties for higher frequency operation. The standard 3C8 with its much improved version the 3C85 are discussed. However, the section concentrates on the new high frequency power ferrite, 3F3. This material features very low switching losses at higher frequencies, allowing the process of miniaturisation to be advanced yet further.

The popular ETD system shown in Fig. 1 is also outlined, and used as an example to compare the losses obtained with the above three materials.

In Part 2, the new EFD (Efficient Flat Design) core shape is introduced. These cores have been specifically designed for applications where a very low build height is important, such as the on-card d.c. - d.c. converters used in distributed power systems.

Circuit topologies suitable for high frequency applications are considered in the final part. Optimum winding designs for the high frequency transformer, which maximise the throughput power of the material are described.

PART 1: Improved magnetic materials

The ETD core system

The very widely used ETD core shape is shown in Fig. 1, which also outlines the method of coil-former assembly. The ETD range meets IEC standardisation, and is based on an E-core shape with a round centre pole. This permits easy winding especially for copper foil and stranded wire. The ETD system includes coil-formers into which the cores are clipped for quick, simple and reliable assembly. The

coil-formers are designed for automatic winding and enable conformance with all standard safety specifications including UL.

ETD cores are suitable for a wide range of transformer and inductor designs, and are very commonly featured in off-line power supply transformers because the ease of winding allows insulation and creepage specifications to be met.

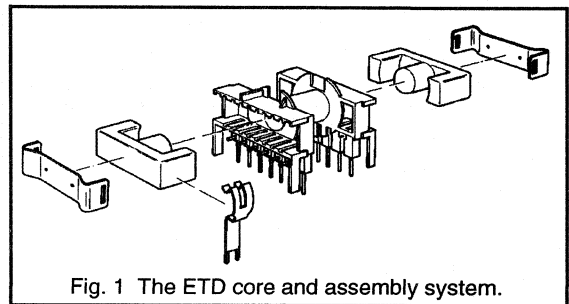


Fig. 1 The ETD core and assembly system.

Core materials

Three types of ferrite core material are compared. The standard 3C8 which is applicable for 50kHz use, the popular 3C85 which is usable at up to 200kHz, and the new high frequency core material 3F3, which has been optimised for use from 200kHz upwards.

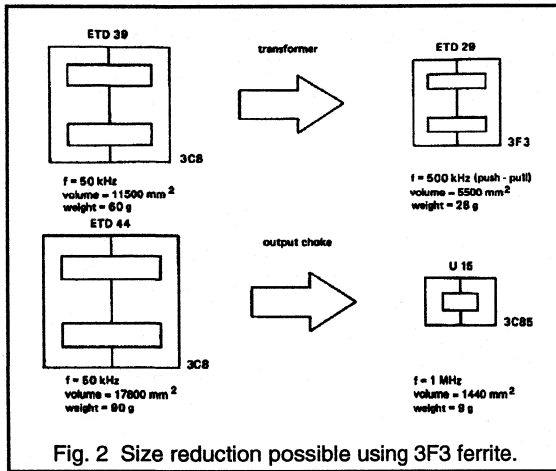
The throughput power of a ferrite transformer is, neglecting core losses, directly proportional to (amongst other things) the operating frequency and the cross-sectional area of the core. Hence for a given core, an increase in the operating frequency raises the throughput power, or for a given power requirement, raising the frequency allows smaller cores and higher power densities. This is expressed by the following equation:-

$$P_{th} = W_d \times C_d \times f \times B$$

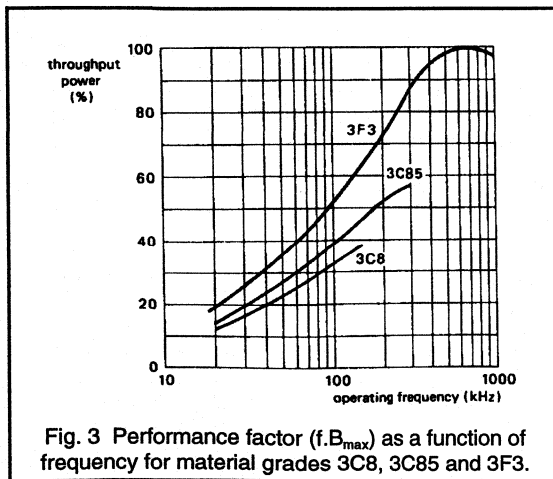
where W_d is the winding parameter, C_d is the core design parameter, f is the switching frequency and B is the induction (flux density) in Tesla.

Unfortunately, the core losses are also frequency dependent, and increasing frequency can substantially increase the core losses. Thus an increase in the core volume is required to maintain the desired power throughput without overheating the core. This means the transformer bulk in a higher frequency supply could limit the size reduction target.

The new 3F3 material with low-loss characteristics at high frequencies will reduce this problem, allowing new levels of miniaturisation to be obtained. An example of the practical size (and weight) reduction possible by moving to higher operating frequencies is given in Fig.2. In comparison with the 50kHz examples, there is a significant reduction in transformer size when switched at 500kHz, and an even more impressive shrinking of the output inductor when operated at 1MHz.



Note. The size of the output capacitor and inductor required to filter the high frequency output ripple components is greatly reduced - up to 90% smaller, resulting in excellent volume savings and very low ripple outputs.



The performance factor ($f \cdot B_{max}$) is a measure of the power throughput that a ferrite core can handle at a loss of 200 mW/cm^3 . This level is considered acceptable for a well designed medium size transformer. The performance factors for the three different material grades 3C8, 3C85 and 3F3 are shown in Fig. 3. For frequencies below 100kHz (the approximate transition frequency, f_t) the power throughput is limited by core saturation and there is not much difference between the grades. However for frequencies above 100kHz, core loss is the limitation, which reduces the allowable throughput power level by overheating the core. Therefore, in order to utilise higher frequencies to increase throughput power or reduce core size, it is important that the core losses must first be minimised.

Reducing the losses

There are three main identifiable types of ferrite material losses: namely, hysteresis, eddy current and residual.

Hysteresis loss

This occurs because the induced flux, B , lags the driving field H . The B/H graph is a closed loop and hysteresis loss per cycle is proportional to the area of the loop. This loss is expressed as:-

$$P_{hyst} = C_a \times f^x \times B_{pk}^y$$

where C_a is a constant, B_{pk} is the peak flux density, f is the frequency with x and y experimentally derived values.

Eddy current loss

This loss is caused by energy from the magnetic flux, B , setting up small currents in the ferrite which causes heat dissipation. The energy lost is represented by:-

$$P_{ec} = \frac{C_b \times f^2 \times B_{pk}^2 \times A_c}{\sigma}$$

C_b is a constant, A_c is the effective cross-sectional core area and σ is the material resistivity.

Residual/Resonant loss

Residual losses are due to the reversal of the orientation of magnetic domains in the material at high frequencies. When the driving frequency is in resonance with the natural frequency at which the magnetic domains flip, there is a large peak in the power absorption. This gives:-

$$P_{res} = C_c \times f \times B_{pk}^2 \times \frac{\tan \delta}{\delta}$$

where

$$\tan \delta = \text{loss angle} = \frac{\mu''}{\mu'} \quad \mu = \mu' + j\mu''$$

Comparison of different materials

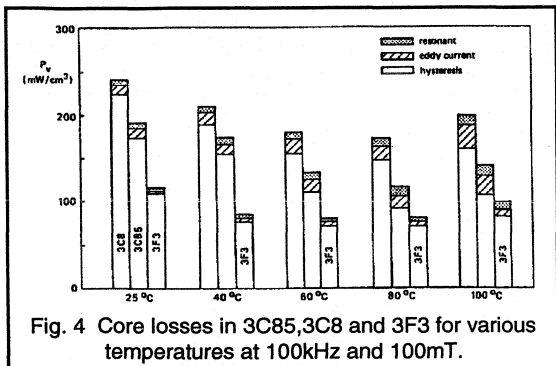


Fig. 4 Core losses in 3C85,3C8 and 3F3 for various temperatures at 100kHz and 100mT.

These losses (in mW/cm^3) are now presented for the three material grades in a partitioned form. These are given for various operating temperatures under two different operating conditions. Fig. 4 shows performance at 100kHz and a peak flux density of 100mT, which is typical for the 3C8 and 3C85 materials. The hysteresis loss is clearly dominant at this frequency. Inspection reveals a reasonable loss reduction when comparing 3C85 to the cheaper 3C8 grade. More significantly however, even at this lower frequency the new 3F3 grade can be seen to offer substantial loss reduction compared to 3C85 (especially at lower operating temperatures).

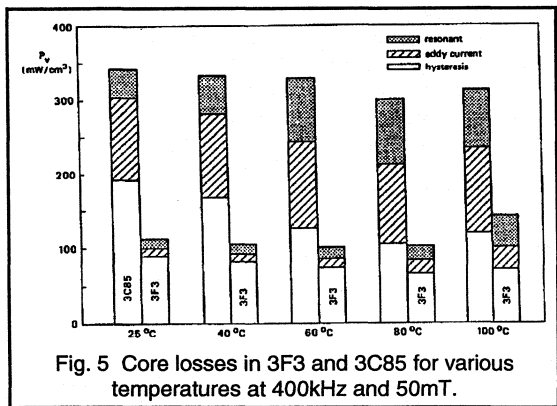


Fig. 5 Core losses in 3F3 and 3C85 for various temperatures at 400kHz and 50mT.

At higher operating frequencies well above 100kHz, eddy currents and residual losses are far more dominant. Fig. 5 gives the values for 400kHz and 50mT high frequency operation. This shows the superiority of the 3F3 material, offering significant reductions (60% vs 3C85) in all magnitudes, particularly in the eddy currents and residual losses.

Figure 6 gives a comparison of the peak operating flux density versus frequency at a core loss of $200mW/cm^3$ for each grade. This shows that the maximum allowable operating frequency for 3F3 is always higher than for the other two types, hence, making it much more suitable for miniaturisation purposes. For example, at 100mT, 3F3 can operate at 280kHz, compared to 170kHz for 3C85 and 100kHz for 3C8.

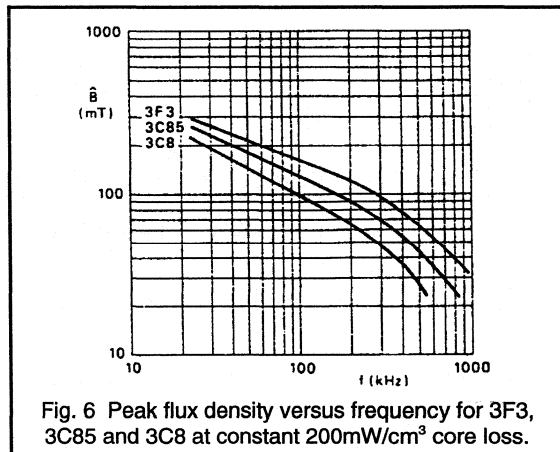


Fig. 6 Peak flux density versus frequency for 3F3, 3C85 and 3C8 at constant $200mW/cm^3$ core loss.

Figure 7 compares the three types of core material in terms of complex permeabilities μ' and μ'' over the frequency range 1 to 10 MHz, at very low flux density levels of < 0.1 mT. It can be seen that the resonant loss peaks at a higher frequency for 3F3, producing much lower high frequency residual losses right up to 1MHz.

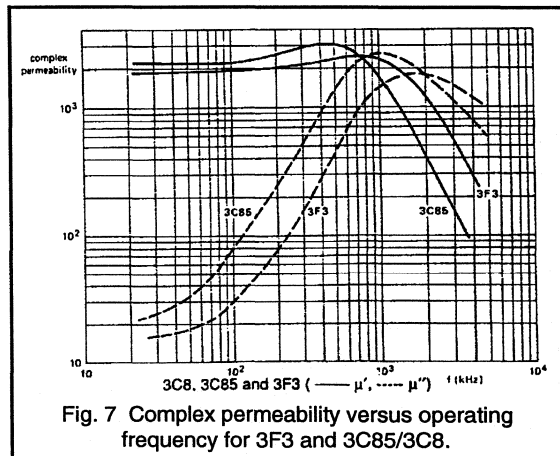


Fig. 7 Complex permeability versus operating frequency for 3F3 and 3C85/3C8.

Material	3C8		3C85			3F3		
B_{sat} (mT) at $f = 25\text{kHz}$ $H = 250\text{A/m}$	≥ 320		≥ 320			≥ 320		
Core type	A_L $\pm 25\%$ nH/N^2	P_V Watts	A_L $\pm 25\%$ nH/N^2	P_V Watts	P_V Watts	A_L $\pm 25\%$ nH/N^2	P_V Watts	P_V Watts
f	10kHz	25kHz	10kHz	25kHz	100kHz	10kHz	100kHz	400kHz
B	0.1mT	200mT	0.1mT	200mT	100mT	0.1mT	100mT	50mT
ETD29	-	-	2100	≤ 0.8	≤ 1.0	1900	≤ 0.6	≤ 1.0
ETD34	2500	≤ 1.6	2500	≤ 1.1	≤ 1.3	2300	≤ 0.85	≤ 1.5
ETD39	2800	≤ 2.2	2800	≤ 1.6	≤ 1.9	2600	≤ 1.3	≤ 2.3
ETD44	3500	≤ 3.6	3500	≤ 2.5	≤ 3.0	3200	≤ 2.0	≤ 3.7
ETD49	4000	≤ 4.6	4000	≤ 3.4	≤ 4.0	3600	≤ 2.6	≤ 5.2

Table 1. Comparison of material properties for the ETD range

Comparison of material grade properties for the ETD range

The values shown in Table 1 are for a core set under power conditions at an operating temperature of 100°C.

3F3 offers a major improvement over existing ferrites for SMPS transformers. With reduced losses across the entire frequency range (but most markedly at 400kHz and higher) 3F3 enables significant reductions in core volume while still maintaining the desired power throughput.

As well as the ETD range, 3F3 is also available in the following shapes:-

- RM core
- P core
- EP core
- EF core
- E core
- ring core
- new EFD core

The new EFD core system which also offers size reduction capabilities shall now be described.

PART 2: The EFD core (Economic flat design)

The newly developed EFD power transformer core system shown in Fig. 8 offers a further significant advance in circuit

miniaturisation. Their low build height and high throughput power density make them ideally suited to applications where space is at a premium.

One such application is with distributed power systems, which is becoming an increasingly popular method of power conversion, especially in the telecommunication and EDP market. Such power-systems convert a mains voltage into an unregulated voltage of about 44 to 80V d.c. This is then fed to individual sub-units, where d.c. - d.c. converters produce the required stabilised voltages. These converters are usually mounted on PCBs which in modern systems, are stacked close together to save space. The d.c. - d.c. converter, therefore, has to be designed with a very low build height.

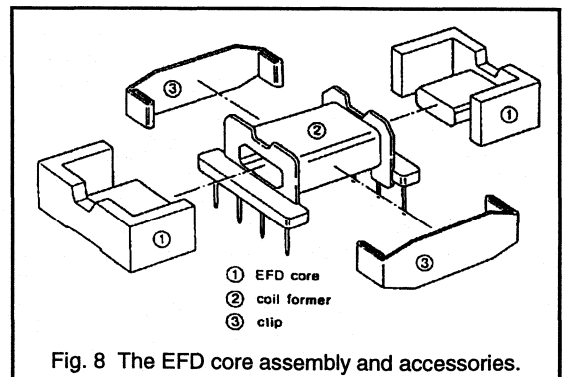


Fig. 8 The EFD core assembly and accessories.

The low-profile design

The EFD core offers a significant reduction in transformer core height. The ETD core combines extreme flatness with a very high throughput power-density. The range consists of four core assemblies complemented by a complete range of accessories. It is planned that the EFD outline will become a new European standard in d.c. - d.c. power transformer design.

The four core assemblies have a maximum finished height of 8mm, 10mm or 12.5mm. The type numbers are:-

- 8mm height - EFD 15/8/5
- 10mm height - EFD 20/10/7
- 12.5mm height - EFD 25/13/9 and EFD 30/15/9

Figure 9 shows that the EFD range has a lower build height than any other existing low profile design with the same magnetic volume.

Integrated product design

Because there is no room in a closely packed PCB for heavily built coil formers, they must be as small and light as possible. For this reason high quality thermo-setting plastics are used. This ensures that the connecting pins in the base remain positioned correctly.

To ensure suitability for winding equipment the connecting pins have been designed with a square base, saving time in wire terminating. To allow thick wire or copper foil windings to be easily led out, both core and coil former have a cut-out at the top (see Fig. 8).

To increase efficiency and reduce size, the ferrite core has been designed with the centre pole symmetrically positioned within the wound coil former. This is clearly shown in the cross-sectional view in Fig. 10.

Because of this, the full winding area can be used, resulting in an extremely flat design which is ideally suited for surface-mounting technology (SMT). SMT designs are already under consideration.

Maximising throughput power-density

Besides their extreme flatness, the most important feature of the EFD transformer is the very high throughput power density. This is especially true when the core is manufactured from the high-frequency low loss 3F3 material, which was described in the previous section. Combining EFD with 3F3 can provide throughput power densities (in terms of transformer volume) between 10 and 20 W/cm³. Furthermore, with a usable frequency range from 100kHz to 1MHz, the EFD transformer will cover most applications.

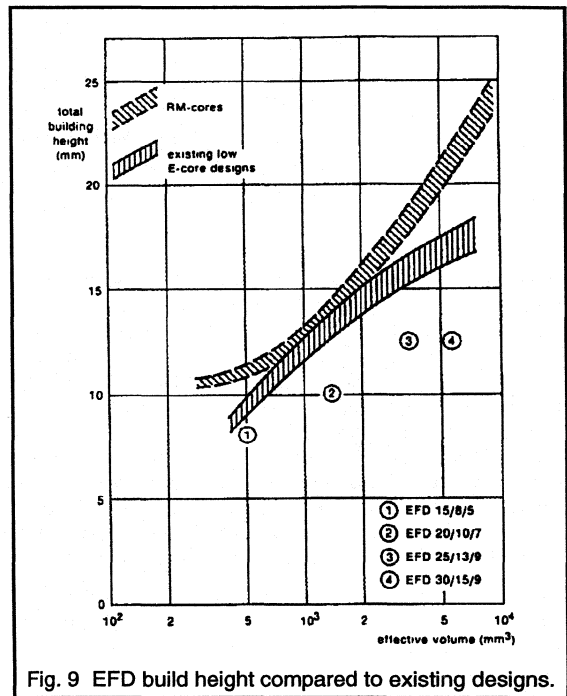


Fig. 9 EFD build height compared to existing designs.

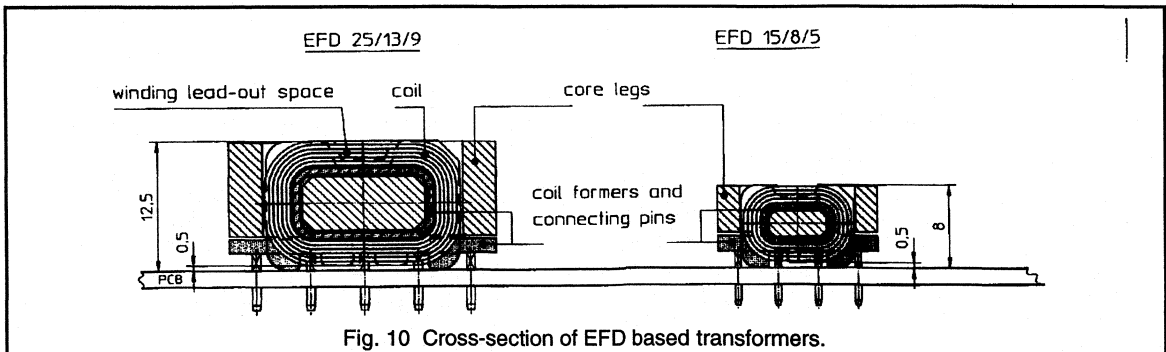


Fig. 10 Cross-section of EFD based transformers.

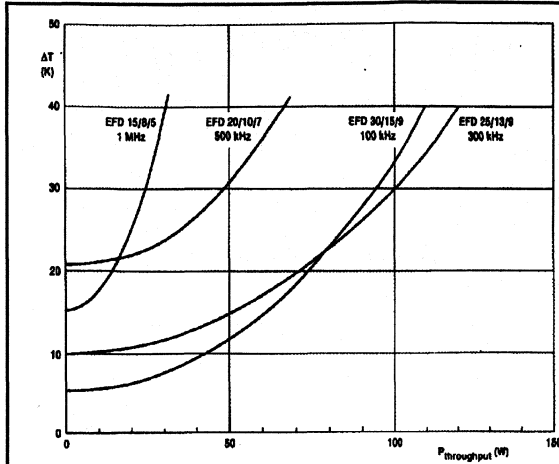


Fig. 11 Temp rise versus P_{th} for ETD based transformers with 3F3 material.

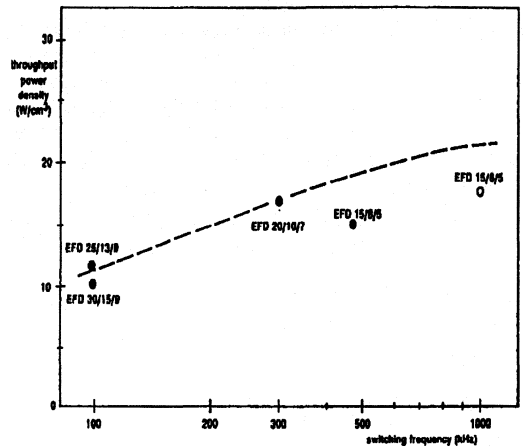


Fig. 12 P_{th} for forward mode transformers based on EFD core with 3F3 material.

As described earlier, high frequency transformer design (above 100kHz) is mainly limited by the temperature rise, caused by heat dissipation from the high frequency core losses as well as the power dissipation in the windings themselves. So the extent of transformer miniaturisation at high frequencies is limited by this rise in temperature (The curie temperature of a typical power ferrite material is around 200°C). As a general rule, maximum transformer efficiency is reached when about 40% of the loss is in the ferrite core, and 60% in the windings. The temperature rise for a range of throughput powers for transformers based on the EFD range in 3F3 material is shown in Fig. 11.

In order to optimise the core dimensions and winding area, a sophisticated computer aided design (CAD) model of a d.c. - d.c. forward mode converter was used. This predicted the temperature rise of the transformer as a function of throughput power. The following parameters were assumed:-

Ferrite core - 3F3.

$V_{in} = 44V$ to $80V$; $V_{out} = 5V, +12V$ and $-12V$.

$T_{amb} = 60^{\circ}C$; $T_{rise} = 40^{\circ}C$.

Primary - Cu wire; Secondary - Cu foil.

(Split sandwiched winding with 2 screens).

The CAD program was used to find an optimised design for the EFD transformer at well chosen frequency bands. The dotted line in Fig. 12 indicates the theoretical result derived from the CAD model. This shows in practice how well the EFD range approximates to the ideal model. The open circle for EFD 15/8/5 in Fig. 12 indicates the maximum optimal switching frequency.

From these results the range was grouped, depending upon core size into their optimal frequency bands.

- 100 to 300kHz - EFD 30/15/9 and EFD 25/13/9.
- 300 to 500kHz - EFD 20/10/7.
- 500kHz to 1MHz - EFD 15/8/5.

These are the recommended frequency ranges for each EFD type. The transformers can operate outside these ranges, but at a reduced efficiency, since the ratio of their core to winding areas would be less than ideal. Table 2 lists the power throughput at certain frequencies for each EFD core.

Core type	100 kHz	300kHz	500kHz	1MHz
EFD 30/15/9	90 - 100 W	110-140W	--	--
EFD 25/13/9	70 - 85 W	90 - 120 W	--	--
EFD 20/10/7	--	50 - 65 W	55 - 70 W	--
EFD 15/8/5	--	--	20 - 30 W	25 - 35 W

Table 2. Power handling capacity for EFD range.

Valid for single-ended forward d.c. - d.c. converter ($V_{in} = 60V$; $V_{out} = 5V$)

Typical EFD throughput power curves given in Fig. 13 show the performance of the low loss 3F3 material as well as 3C85. These results were confirmed from measurements taken during tests on EFD cores in a transformer testing set up. As expected these show that, especially above 300kHz, the 3F3 (compared to 3C85) significantly improves throughput power.

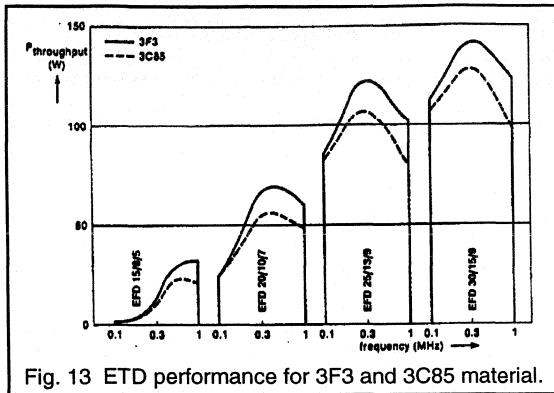


Fig. 13 ETD performance for 3F3 and 3C85 material.

PART 3: Applications

Circuit (transformer) configurations

Forward, flyback and push-pull circuit configurations have been used successfully for many different SMPS applications. This includes mains-isolated square-wave switching over the frequency range 20-100kHz, and with output powers up to 200W. Recent transformer designs have been developed to minimise the effects of leakage inductance and stray capacitance upon these circuits. The influences of the transformer characteristics on the choice of circuit configuration for higher switching frequency applications are now discussed.

The flyback converter

The flyback converter shown in Fig. 14 has leakage inductance between the primary and secondary windings which delays the transfer of power when the primary power transistor turns off. For the example waveforms shown in Fig. 14, the delay lasts for 600ns. During this time, power is returned to the d.c. supply. The circulating power increases with the switching frequency, and in this case would produce 50W at 1MHz. This tends to limit the maximum operating frequency for flyback converters.

The forward converter

The power transistor in the forward converter shown in Fig. 15 normally has a snubber network (and stray circuit capacitance) which protects the transistor at turn-off. This is necessary because the energy stored in the leakage inductance between the primary and secondary windings would produce a large voltage spike at transistor turn-off.

At transistor turn-on the energy stored in the capacitance is discharged and dissipated. For the example waveforms given in Fig. 15, this would be 7.5W at a switching frequency of 1MHz. Furthermore, as in the flyback converter, the circulating magnetising power can also be as high as 50W

at 1MHz, hence reducing the efficiency of the transformer. These characteristics limit the maximum frequency at which forward converters can be usefully applied.

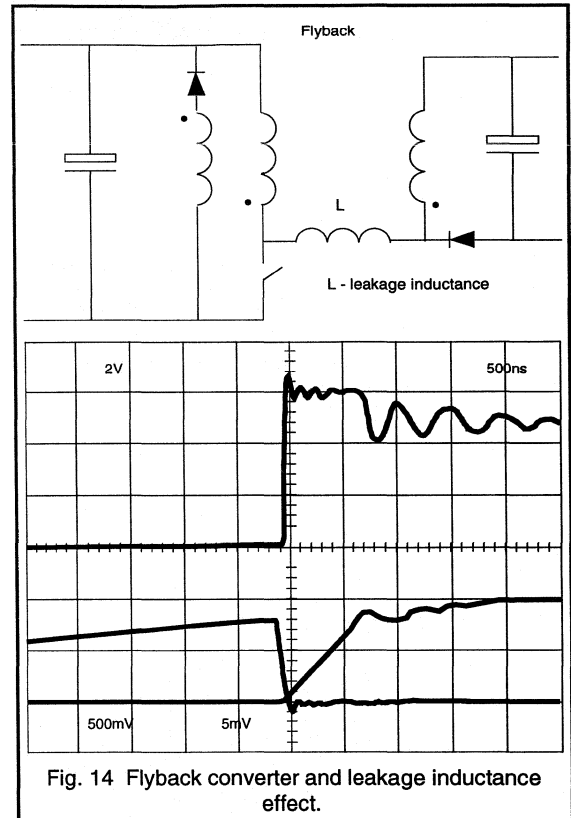


Fig. 14 Flyback converter and leakage inductance effect.

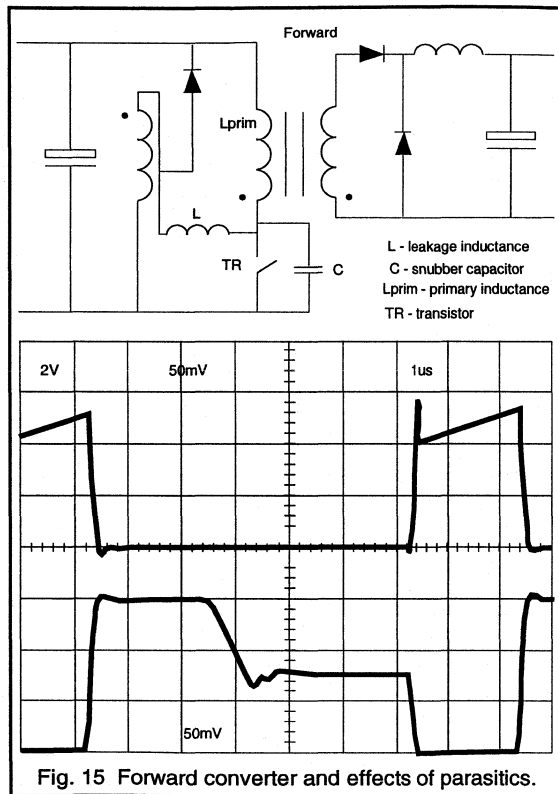
Centre-tapped push-pull converter

The centre-tapped push-pull circuit configuration given in Fig. 16 uses magnetic B/H loop symmetry when driving the transformer. Therefore, when either transistor is turned off, the magnetising current is circulated around the secondary diodes, thereby reducing energy recovery problems or the need for voltage clamping.

However, the transformer must be correctly "flux balanced" by monitoring the current in the transistors to prevent transformer saturation and subsequent transistor failure.

The drain current and voltage waveforms resulting from two examples of push-pull transformer winding construction are also shown in Fig. 16. In Fig. 16(a) (most serious case) the leakage inductance has distorted the waveforms. In Fig. 16(b) it is the circuit capacitance which produces the distortion. These distortions mean that the transistor current

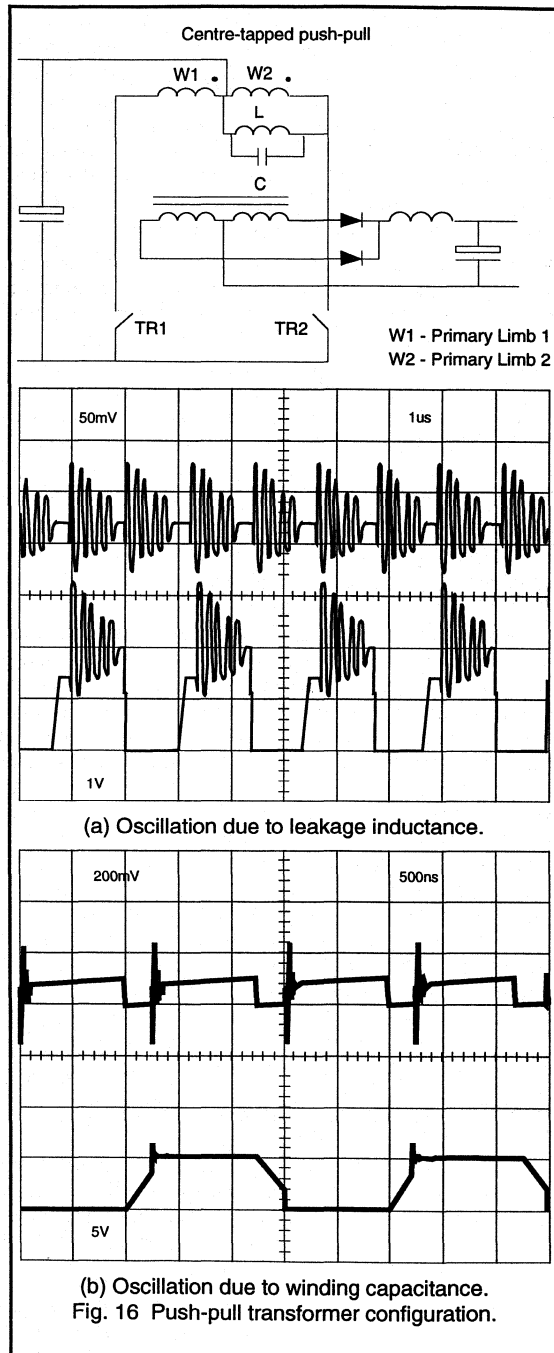
sense waveforms must be adequately filtered, so that the control circuit can vary mark/space correctly and prevent transformer saturation.



As the switching frequency is increased, the accuracy of the current balancing information is reduced by the action of the filtering and there might be a point at which this becomes unacceptable. The filter itself is also dissipative and will also produce a high frequency loss.

The half-bridge converter

The half-bridge push-pull transformer shown in Fig. 17 is inherently self-balancing. Standard winding methods for transformer construction using this configuration are possible at frequencies up to around 1MHz. Fig. 17 also gives waveform examples for the half-bridge transformer. This design allows the most flexibility when choosing a particular switching frequency.



Switching frequency

When designing a transformer and calculating the core loss, the exponent for frequency in the hysteresis loss equation is assumed to be constant at all frequencies. Only the fundamental is considered significant compared to all other harmonics of the square wave. This is a reasonable approximation to make from 20kHz to 100kHz because the contribution of eddy losses and resonant losses to the overall core loss is negligible (see Fig. 4).

As the frequency increases to 1MHz and beyond, the resonant and eddy current losses contribute proportionally more to the overall core loss. This means that the harmonics of a 1MHz square wave have more significance in determining the core loss than those at 100kHz. When the mark/space is reduced, the harmonics increase, and the loss will increase proportionally. This effectively limits the upper frequency of a fixed frequency square-wave, mark/space controlled power supply. However, as outlined, new materials such as 3F3 have been specially developed to keep these high frequency transformer losses as low as possible.

Transformer construction

In the half-bridge push-pull configuration of Fig. 17, during the period that the two primary transistors are off, there is zero volts across the secondary winding. Therefore, the secondary diodes are both conducting and share the choke current. The primary side should also have zero volts across it, but it rings because of the stray capacitance and leakage inductance between the primary and the secondary windings (see waveform of Fig. 17). At 500kHz, using an ETD29 or an EFD20 core, for example, a 1+1 copper strip secondary winding is suitable for providing an output of 5V. This is preferable to using more turns for the secondary winding because the leakage inductance and the amplitude of the ringing during the period that the MOSFETs are off is minimised. Reducing the ringing is of vital importance for the following reasons:-

1. It prevents the anti-parallel diode inherent in the upper MOSFET switch from conducting when the lower transistor is turned on. This will increase the MOSFET dV/dt rating typically by a factor 10, allowing the switching speed to be maximised and the switching losses to be reduced.
2. For low voltage outputs, the ringing will only be slightly reduced by the 1+1 construction. However, the core losses increase significantly at the actual frequency of the ringing (5-10MHz). Hence, any reduction in the ringing amplitude will be beneficial to core loss.

To further optimise the operation of the transformer, and reduce the ringing, the output clamping diodes should be operated with the minimum of secondary leakage inductance and mounted physically close to the transformer.

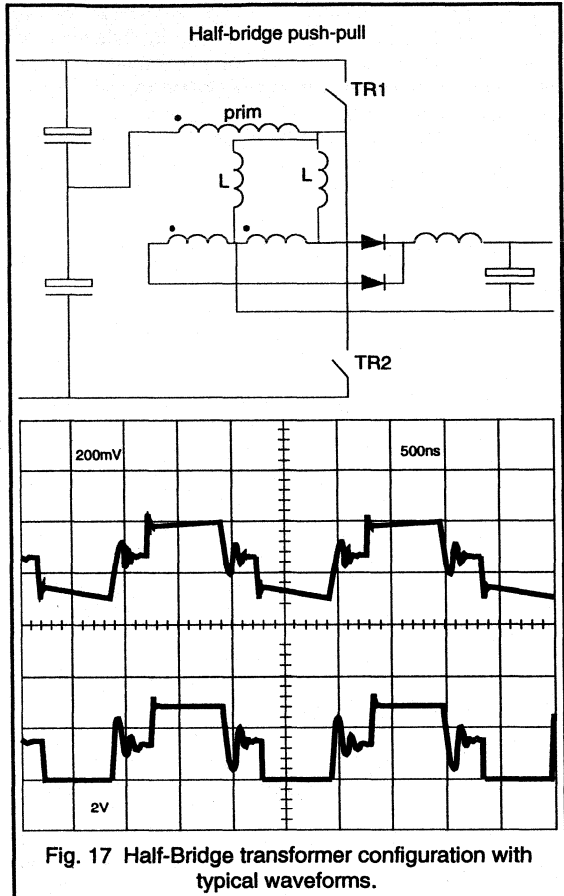


Fig. 17 Half-Bridge transformer configuration with typical waveforms.

Conclusions

To advance the trend towards SMPS miniaturisation, low-loss ferrites for high frequency have been specially developed. A new ferrite material has been presented, the 3F3, which offers excellent high-frequency, low loss characteristics.

A wide range of power ferrite materials is now available which offers performance/cost optimisation for each application. The particular SMPS application slots for the three ferrites discussed in this paper are summarised as follows:-

- 3C8 for low-cost 20-100kHz frequency range.
- 3C85 for high performance 20-150kHz.
- 3F3 for miniaturised high performance power supplies in the frequency range above 150kHz.

A new type of power core shape, the EFD was also introduced. The use of the EFD core also allows further SMPS miniaturisation by providing extremely low build heights in conjunction with very high throughput power densities. Optimum use of the EFD design can be made if the 3F3 material grade is selected. The EFD system is intended for applications with very low height restrictions, and is ideal for use in the d.c. - d.c. converter designs found in modern distributed power systems.

Different transformer winding configurations were also

described (particularly for mains isolated SMPS.) It was found that to obtain the greatest size reduction using the new 3F3 material at very high frequencies, the following application ideas are useful:-

- Use the half-bridge push-pull circuit configuration.
- Minimize the transformer leakage inductance by careful winding construction.
- Minimise the lead-lengths from the transformer to rectifier diodes.

Resonant Power Supplies

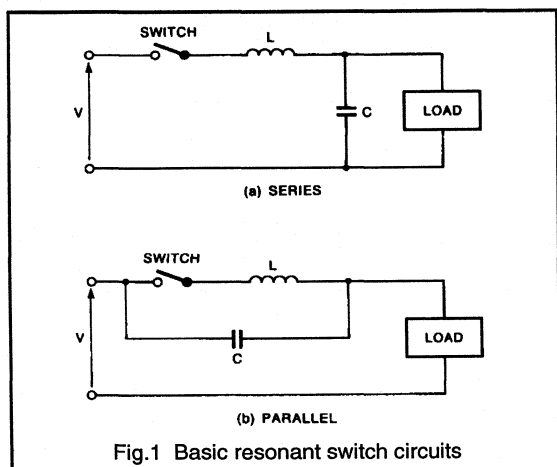
2.5.1. An Introduction To Resonant Power Supplies

Whilst many application requirements can be satisfied by the use of conventional switching topologies, their shortcomings, particularly the switching losses in high power / high frequency circuits, are becoming a serious limitation. Some of the problems can be overcome by the use of resonant, or quasi-resonant, converters.

A resonant converter is a switching converter in which the natural resonance between inductors and capacitors is used to shape the current and voltage waveforms.

There are many ways in which inductors, capacitors and switches can be combined to form resonant circuits. Each of the configurations will have advantages and disadvantages in terms of stress placed on the circuit components.

To reduce switching loss, a resonant converter which allows the switching to be performed at zero current and low di/dt is needed. A range of such circuits can be produced by taking any of the standard converter topologies and replacing the conventional switch with a resonant switch.

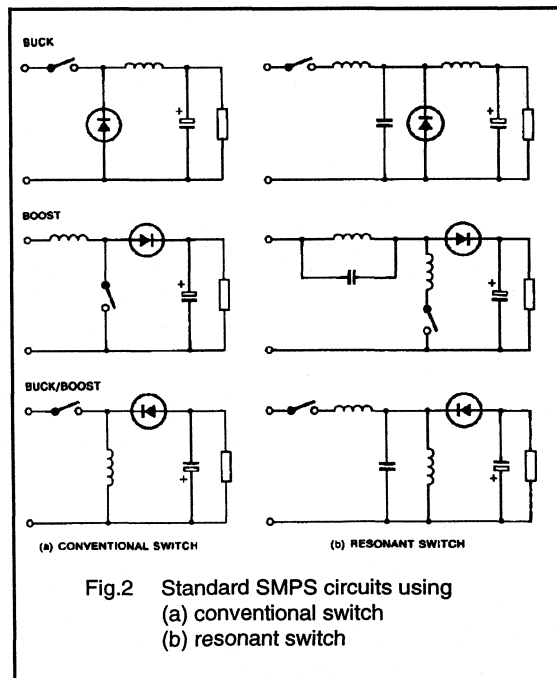


Resonant switch

A resonant switch consists of an active element (the switch) plus an additional inductor, L, and capacitor, C. The values of L and C are chosen so that, during the on time of the switch, the resonant action between them dominates. This ensures that the current through the switch, instead of just increasing linearly and having to be turned off, forms a sinusoid which rises to a peak and falls to zero again.

Two basic resonant switch configurations are shown in Fig.1. Before the switch is closed, C is in a state where it has a small negative charge. With the switch closed, C is discharged into L and then recharged positively. During the recharging extra energy is drawn from the supply to replace that delivered to the load during the previous cycle. With C charged positively, the switch is opened. The energy in C is now transferred to the load, either directly or via the main inductor of the converter. In the process of this transfer, C becomes negatively charged.

Figure 2 shows the three basic SMPS topologies - buck, boost and buck / boost - with both conventional (a) and resonant (b) switches. It should be noted that parasitic inductance and capacitance could form part, or even all, of the components of the resonant network.



Flyback converter

To show how the resonant switch circuit reduces switching loss we will now consider the operation of the flyback converter, firstly with a conventional switch and then with a resonant switch.

Conventional switch

The basic flyback converter circuit is shown in Fig.3(a). If the transformer is assumed to have negligible leakage inductance it can be replaced by a single equivalent inductor L_m and the circuit becomes as shown in Fig.3(b), which is the same as a buck-boost converter shown in Fig.2.

Before the switch S is closed, a current I_o will be flowing in the loop formed by L_m , diode D and the output smoothing capacitor C_o . When S closes, voltage E_s reverse biases the diode, which switches off and blocks the flow of I_o . A current I_s then flows via S and L_m . The only limitations on the initial rate of change of current are the stray inductance in the circuit and the switching speed of S . This means that switching current I_s rises very quickly, leading to large turn-on losses in S and D .

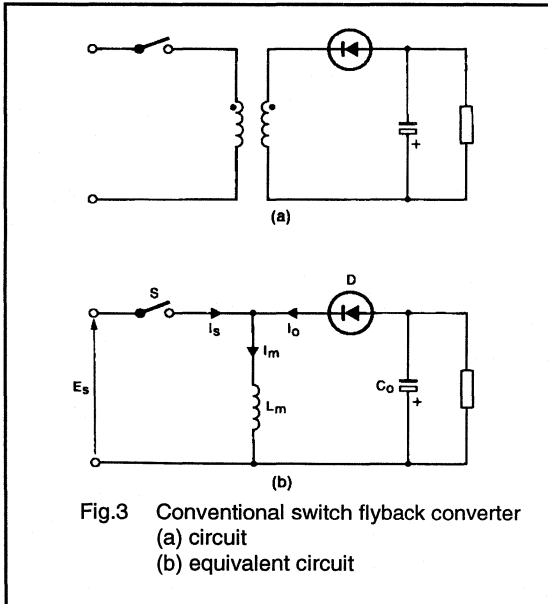


Fig.3 Conventional switch flyback converter
(a) circuit
(b) equivalent circuit

The current I_s rises linearly from I_o until the switch is forced to reopen. The diode is then no longer reverse biased and the current switches back from I_s to I_o via D , with C_o then acting as a voltage source. The losses in this switching will also be very high due to the high level of I_s and the rapid application of the off-state voltage. I_o now falls linearly, delivering a charging current to C_o , until the switch closes again.

Figure 4 shows the current waveforms for I_o and I_s and the current in inductor L_m .

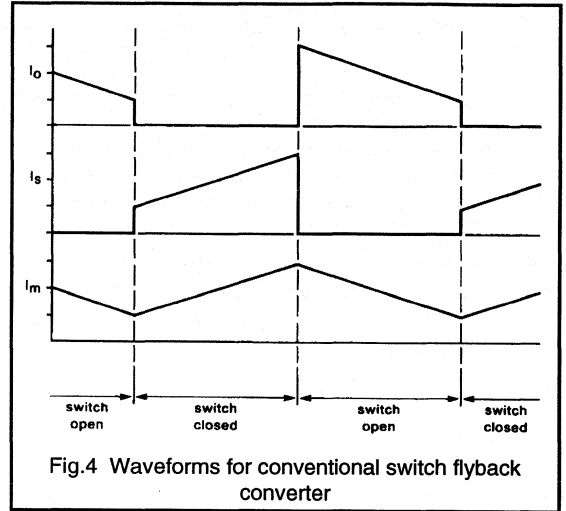


Fig.4 Waveforms for conventional switch flyback converter

Resonant switch

The resonant switch flyback converter circuit is shown in Fig.5(a). The equivalent circuit (Fig.5 (b)) is the same as that for the conventional switch except for the addition of the inductor L_a and capacitor C_a whose values are very much less than those of L_m and C_o respectively.

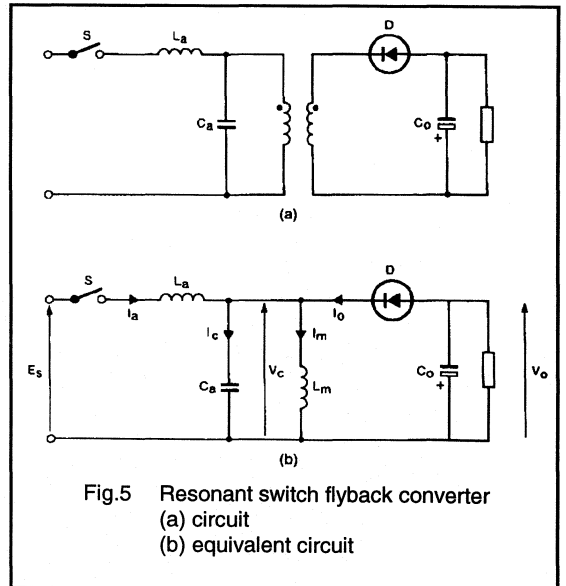


Fig.5 Resonant switch flyback converter
(a) circuit
(b) equivalent circuit

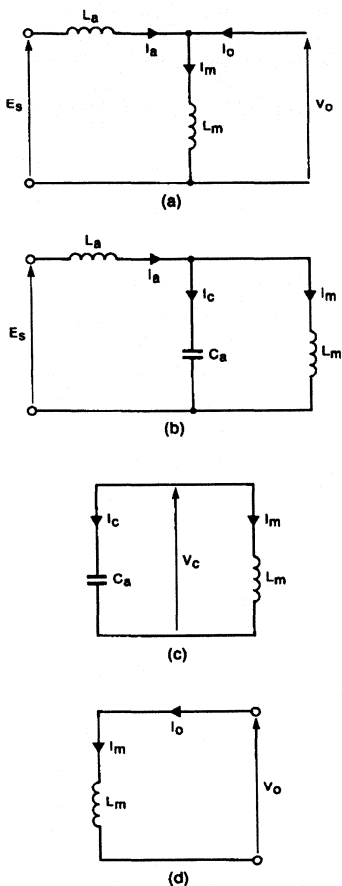


Fig.6 Resonant switch flyback converter operating modes
 (a) Mode 1: S close , D on
 (b) Mode 2: S closed, D off
 (c) Mode 3: S open, D off
 (d) Mode 4: S open, D on

If it is assumed that the switch is closed before the current in L_m has fallen to zero, then the initial equivalent circuit will be as shown in Fig.6(a). The rate of rise of current in S is determined by the value of L_a which, although small, is much larger than the stray inductance that limits current rise in a conventional switch. Turn-on losses are thus significantly reduced. C_o , being much larger than C_a , acts as a voltage source (V_o) preventing current from flowing into C_a and maintaining a constant rate of change of current in L_m . i_a will increase linearly until it equals i_m at which time i_o is zero and diode D turns off.

With D turned off, the equivalent circuit becomes as shown in Fig.6(b). The resonant circuit, L_a , C_a and L_m , causes i_a to increase sinusoidally to a peak and then fall back to zero. S can then be opened again with very low losses.

With the switch open, the circuit is as shown in Fig.6(c). The resonant action between C_a and L_m causes energy to be transferred from the capacitor to the inductor. V_c will fall, passing through zero as i_m reaches a peak, and then will increase in the opposite direction until it exceeds V_o . At which point D becomes forward biased, so it will turn on.

As D turns on (Fig.6(d)) the voltage across C_a becomes clamped and i_m now flows into C_o . i_m falls linearly until the switch is closed again and the cycle repeats.

Voltage and current waveforms for a complete cycle of operation are shown in Fig.7.

From the description of operation it can be seen that the reduced switching losses result from:

- L_a acting as a di/dt limiter at switch on
- The resonant circuit L_a , L_m and C_a ensuring that the current is zero at turn-off

These factors combine to allow the switching devices to be operated at higher frequencies and power levels than was previously possible.

Circuit design

Correct operation of a resonant switch converter depends on the choice of suitable values for the inductors and capacitors. It is not possible to determine these values directly but they can be selected using simple computer models. An example of a model for a resonant switch flyback converter is given below to demonstrate the basic technique that can be used to analyse many different types of resonant circuits. Writing the final computer program will be a simple task for anyone with programming experience and the model will run relatively quickly on even small personnel computers.

Circuit analysis

Here we analyse the operation of a resonant flyback converter circuit in mathematical terms, assuming ideal circuit components.

In the equivalent circuit of the flyback converter, Fig.5(b), there are two switching elements S and D and the circuit has four possible modes of operation:

Mode 1	S closed	D on
Mode 2	S closed	D off
Mode 3	S open	D off
Mode 4	S open	D on

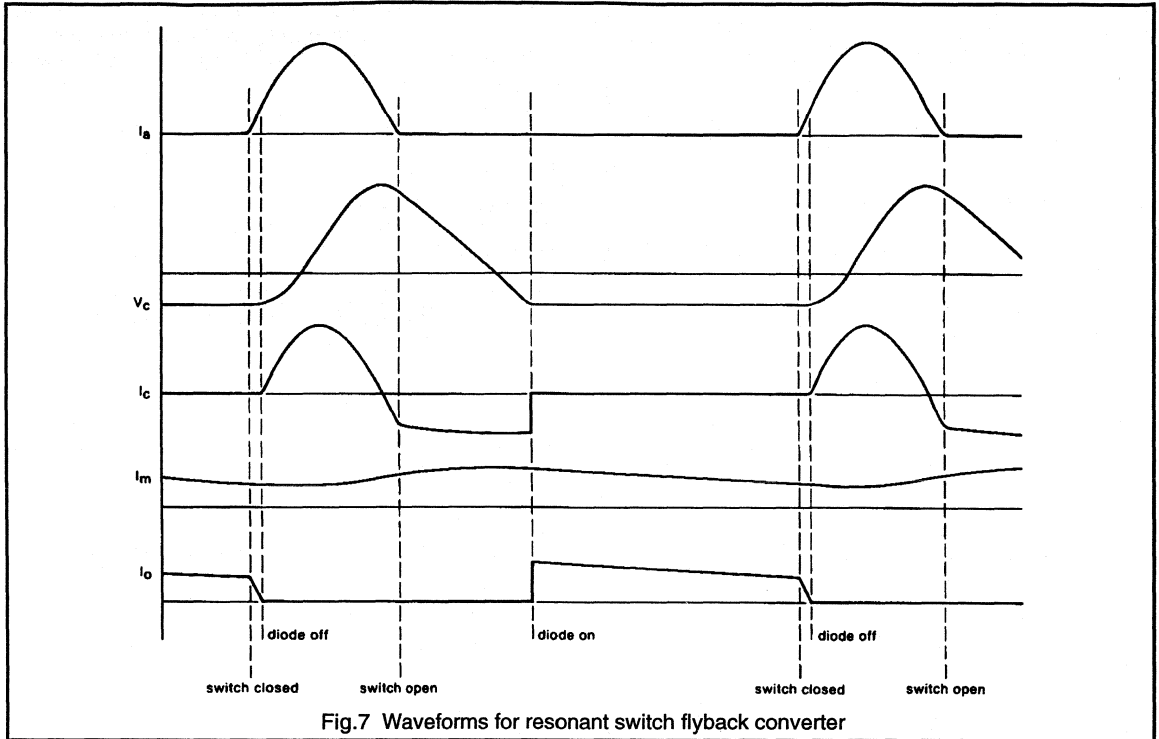


Fig.7 Waveforms for resonant switch flyback converter

Using Laplace analysis of the equivalent circuit for each operating mode, equations can be written for I_a , I_c , I_m , I_o and V_c .

J and U are the values of I_m and V_c respectively at the start of each operating mode i.e. when $t = 0$.

Mode 1

Figure 6(a) shows the equivalent circuit when S is closed and D is on. The large output capacitor C_o as shown acts as voltage source (V_o).

The equations are:

$$I_a = \frac{E_s - U}{L_a} t$$

$$I_m = \frac{U}{L_m} t + J$$

$$I_c = 0$$

$$V_c = U$$

$$I_o = I_m - I_a$$

Mode 2

Figure 6(b) shows the equivalent circuit when S is closed and D is off.

The equations are:

$$I_a = J + A1.t + \frac{A2 - A1}{\omega l} \cdot \sin(\omega l.t)$$

$$I_m = J + A1.t + \frac{A3 - A1}{\omega l} \cdot \sin(\omega l.t)$$

$$I_c = I_a - I_m$$

$$V_c = U + \left(\frac{L_m.(E_s - U) - L_a.U}{L_a + L_m} \right) (1 - \cos(\omega l.t))$$

$$I_o = 0$$

where,

$$A1 = \frac{E_s}{L_a + L_m}$$

$$A2 = \frac{E_s - U}{L_a}$$

$$A3 = \frac{U}{L_m}$$

$$\omega 1 = \sqrt{\left(\frac{La + Lm}{Lm \cdot Ca \cdot La} \right)}$$

Mode 3

Figure 6(c) shows the equivalent circuit when S is open and D is off.

The equations are:

$$Ia = 0$$

$$Im = J \cdot \cos(\omega 2 \cdot t) + \frac{U}{Lm \cdot \omega 2} \cdot \sin(\omega 2 \cdot t)$$

$$Ic = -Im$$

$$Vc = U \cdot \cos(\omega 2 \cdot t) + \frac{J}{Ca \cdot \omega 2} \cdot \sin(\omega 2 \cdot t)$$

$$Io = 0$$

where,

$$\omega 2 = \sqrt{\left(\frac{1}{Lm \cdot Ca} \right)}$$

Mode 4

Figure 6(d) shows the equivalent circuit when S is open and D is on.

The equations are

$$Ia = 0$$

$$Im = J + \frac{U}{Lm} \cdot t$$

$$Ic = 0$$

$$Vc = U$$

$$Io = Im$$

Computer simulation

Using the previous equations, it is possible to write a computer program which will simulate the operation of the circuit.

If S is closed before Im falls to zero, then during a complete cycle each of the operating modes occurs only once, in the sequence mode 1 to mode 4.

The first function of the program is to determine the duration of each mode.

Mode 1

The time between the switch turning on and the current Ia reach Im is given by:

$$T1 = \frac{J1 \cdot Lm \cdot La}{Lm \cdot (Es - Vo) - U1 \cdot La}$$

J1, the initial value of Im chosen by the designer, determines the average output current. U1 is the initial value of Vc. If Im is greater than zero, D will still be on so Vc and therefore U1 will equal Vo.

Mode 2

The duration, T2, of the second mode cannot be found directly and must be determined by numerical methods. T2 ends when Ia falls back to zero, so by successive approximation of t in the mode 2 equation for Ia, it is possible to find T2.

J and U at the start of mode 2, i.e., J2 and U2, are found by solving the mode 1 equations for Im and Vc respectively at t = T1.

For any given set of circuit values there is a value of J1 above which Ia will not reach zero. This condition has to be detected by the program. Decreasing the value of La or increasing the value of Lm or Ca will allow Ia to reach zero.

Mode 3

Mode 3 operation ends when Vc = Vo. The duration, T3, is given by:

$$T3 = \frac{1}{\omega} \cdot 2 \cdot \left\{ \cos^{-1} \left(\frac{Vo}{\sqrt{U3^2 + A4^2}} \right) - \tan^{-1} \left(\frac{A4}{U3} \right) \right\}$$

where,

$$A4 = \frac{J3}{Ca \cdot \omega 2}$$

and J3 and U3 are the values of Im and Vc respectively at the start of mode 3.

Mode 4

If the circuit operation is stable then the value of Im, when S is again closed, will equal J1 and the duration of the mode will be

$$T4 = \frac{Lm \cdot (J4 - J1)}{U4}$$

Where J4 and U4 are the values of Im and Vc at the start of mode 4.

Calculation of Io and Vd

Having found the durations of the four modes, the average output current in D can be calculated, from:

$$Io(av) = \frac{T4 \cdot (J4 + J1) + T1 \cdot J1}{2 \cdot (T1 + T2 + T3 + T4)}$$

Peak, RMS and average values of the current in S (Ia) can be determined by numerical analysis during modes 1 and 2. The voltage across S is given by

$$V_s = E_s - V_c$$

These values will be needed when the components S and D are chosen.

Conclusions

Resonant combinations of inductors and capacitors can be used to shape the current and voltage waveforms in switching converters. This shaping can be used to:

- reduce RFI and EMI,
- eliminate the effects of parasitic inductance and capacitance,

- introduce a degree of self limiting under fault conditions,
- reduce switching losses.

The resonant switch configuration is one way of reducing switching losses in the main active device. It can be adapted for use in all the standard square wave circuit topologies and with all device types.

Although the analysis of resonant circuits is more complex than the analysis of square wave circuits, it is still straightforward if the operation of the circuit is broken down into its different modes. Such an analysis will yield a set of equations which can be combined into a computer program, to produce a model of the system which can be run relatively quickly on even small computers.

2.5.2. Resonant Power Supply Converters - The Solution For Mains Pollution Problems

Many switch mode power supplies which operate directly from the mains supply, use an electrolytic buffer capacitor, after the bridge rectifier, to smooth the 100/120 Hz ripple on the DC supply to the switching circuit. This capacitive input filter causes mains pollution by introducing harmonic currents and therefore cannot be used in supplies with output powers above 165W. (TV, IEC norm 555-2, part 2: Harmonics, sub clause 4.2).

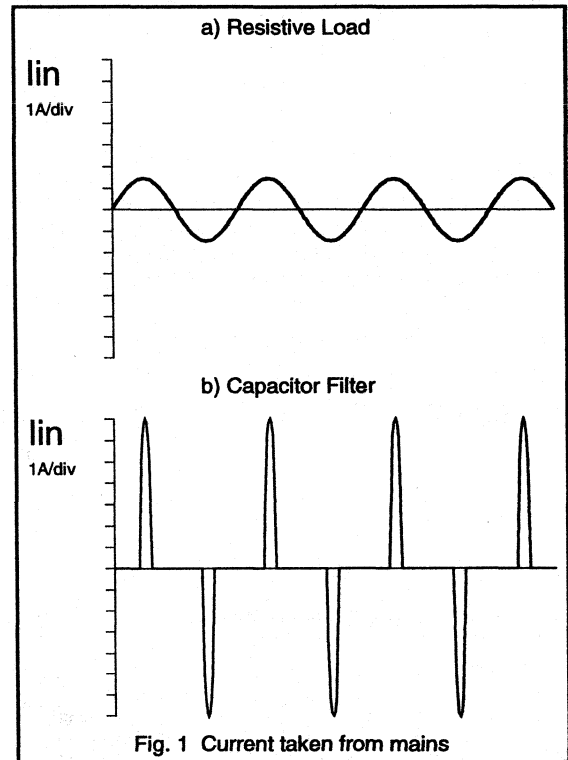
The smoothing capacitor can be charged only when the mains voltage is greater than the DC voltage. Therefore the input current will take the form of high amplitude, short duration pulses. For comparison, the load current for a 220W resistive load (an RMS current of 1A for 220V mains/line) and the load current for a 220W rectifier with capacitive input buffer are shown in Fig. 1.

The peak value of the current with the capacitor load is 5 times higher than for the resistive load, while the RMS current is doubled. It is understandable that the electricity supply authorities do not like this kind of load, because it results in high levels of harmonic current and a power factor below 0.5. It is, therefore, necessary to find alternative methods of generating a smooth DC voltage from the mains.

The PRE-CONVERTER switched mode supply is one possible solution. Such a converter can operate from the unsmoothed rectified mains/line voltage and can produce a DC voltage with only a small 100/120 Hz ripple. By adding a HF transformer it is possible to produce any value of DC voltage and provide isolation if necessary.

By proper frequency modulation of the pre-converter, the input current can be made sinusoidal and in-phase with the voltage. The mains/line now 'sees' a resistive load, the harmonic distortion will be reduced to very low levels and the power factor will be close to 1.

A pre-converter has to be able to operate from input voltages between zero (at the zero crossings) and the peak value of mains/line voltage and still give a constant output voltage. The SMPS converter that can fulfil these conditions is the 'flyback' or 'ringing' choke converter. This SMPS converter has the boost and buck properties needed by a pre-converter. However, the possibility of stability problems under 'no load' operation and its moderate conversion efficiency, means that this converter is not the most attractive solution for this application.



The RESONANT POWER SUPPLY (RPS) has the right properties for pre-converter systems. The boost and buck properties of a resonant L-C circuit around its resonant frequency are well known. In principle any current can be boosted up to any voltage for a PARALLEL RESONANT L-C circuit. Furthermore, the current and voltage wave forms in a resonant converter are more or less sinusoidal, resulting in a good conversion efficiency and there are no stability problems at no load operating conditions.

Resonant pre-converter circuits

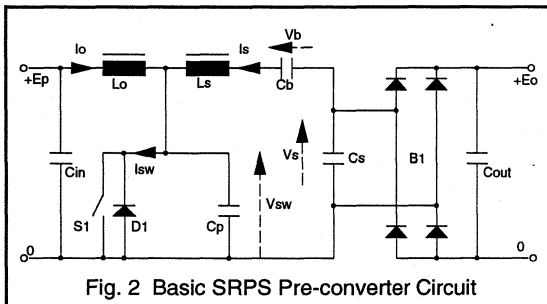
There are two basic resonant power supply (RPS) principles that can be considered, namely:

- The SERIES RESONANT POWER SUPPLY (SRPS), where a series resonant L-C circuit determines the no load operation cycle time. The output power increases with increasing operation cycle time (thus with decreasing operation frequency).

- The PARALLEL RESONANT POWER SUPPLY (PRPS), where a parallel resonant L-C circuit determines the no load operation cycle time. The output power increases with decreasing operation cycle time (thus with increasing operation frequency).

The basic SRPS converter circuit

A basic SRPS converter topology is shown in Fig. 2. For simplicity in the following description, the input voltage E_p is taken to be constant - 310 VDC for the 220VAC mains/line. If the circuit is to appear as a 'resistive' load to the mains, then the output power of the pre-converter has to be proportional to the square of the instantaneous value of E_p . This means that the peak output power of the circuit must be equal to twice the average output power. So a 250W pre-converter has to be delivering 500W when E_p is at its peak.

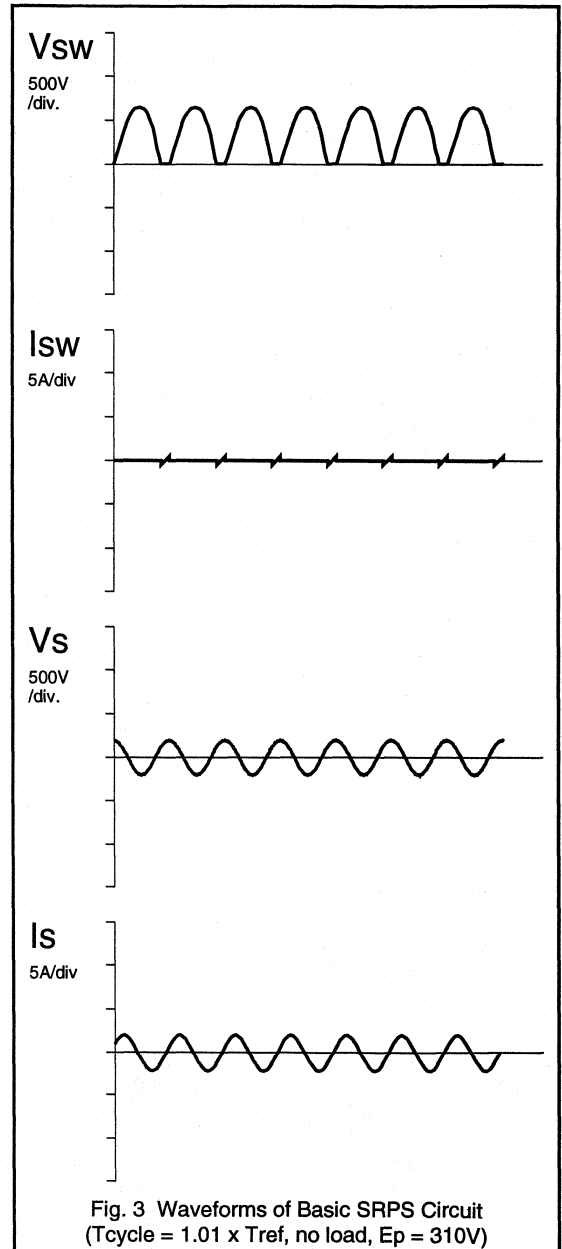


In Fig. 2, the semiconductor switch S1 has an anti-parallel diode D1 to avoid a negative voltages across S1. Principally, a diode in series with S1 also gives a suitable SRPS pre-converter, but it slightly increases the positive peak voltage on S1 without giving an advantage over the circuit with anti-parallel diode. The lower value of the RMS current in S1 and thus the reduction in its on-state losses is completely cancelled by increased turn-on losses in this device.

Furthermore, stability problems can occur under no load conditions for the circuit with series diode (infinitely small current pulses in S1). The circuit with anti-parallel diode has no infinitely short current pulses under no load conditions, because the positive current in S1 will be preceded by the negative current in D1. As a result, no nett DC current is supplied to the circuit at finite pulse widths.

The input inductance L_o forms the connection between the input voltage and the switch voltage V_{sw} . A 'SERIES' resonant L-C circuit, consisting of the capacitor C_p (when both S1 and D1 are OFF), the inductance L_s , the DC voltage blocking capacitor C_b and the capacitor C_s (when B1 is OFF), determines the no load operation frequency. The influence of the input inductance L_o can be neglected if its value is several times that of L_s .

A practical SRPS pre-converter for 250W nett output power (500W peak power conversion) can have component values shown in Table 1.



Capacitor C_p changes the voltage waveform across switch S1/D1 from the rectangular shape associated with SMPS converters, to the sinusoidal shape of an SRPS converter.

L_o	4 mH	8 x L_s
C_p	16 nF	$C_s / 1.5$
L_s	500 μ H	
C_s	24 nF	
C_b	360 nF	15 x C_s
T_{ref}	13.3 μ s	minimum cycle time

Table 1 Component Values for SRPS circuit

The output rectifier bridge B1 has been connected in parallel with the output capacitor C_s . The whole converter also can be viewed as a parametric amplifier, where the switch S1 or the diode D1 modulate the value of C_p between C_p and infinity, while the output bridge B1 has similar influence on the value of the capacitor C_s . Heavier load means longer conduction of S1/D1 and of B1, so that some automatic frequency adaptation of the SRPS circuit takes place at operation frequencies below the no load resonant frequency. The output power of the SRPS increases with decreasing operation frequency.

Fig. 3 shows time plots of some of the voltages and currents of the basic SRPS circuit for the minimum ON time of S1/D1.

Under no load operation, the voltage V_{sw} is a pure sine wave superimposed on the input voltage with an amplitude equal to this voltage. The operation cycle time is approximately equal to the series resonant circuit cycle time, T_{ref} , for no load conditions. The voltage V_{sw} and V_s and the current I_s are sine waves with a low harmonic distortion. The input current I_o is a low amplitude sine wave and it has no DC component for zero load.

In order to give an impression of the boosting properties of the SRPS converter, the no load voltages and currents for an operation cycle time of $1.25 \times T_{ref}$ are plotted in Fig. 4.

Fig. 3 gives the minimum 'ON' time condition for the S1/D1 switch and thus the minimum output voltage amplitude for a given input voltage. The minimum ratio of the amplitude of V_s and the input voltage E_p , with the component values given earlier, has been found to be:

$$\frac{V_s}{E_p} = 0.7$$

It will be obvious, that the value of the output voltage E_o has to be in excess of the minimum amplitude of V_s . Thus:

$$E_o > 0.7 \times E_p$$

A practical value of E_o has to be about 10% in excess of this minimum value in order to deal with tolerances in component values, thus:

$$E_o > 0.8 \times E_p$$

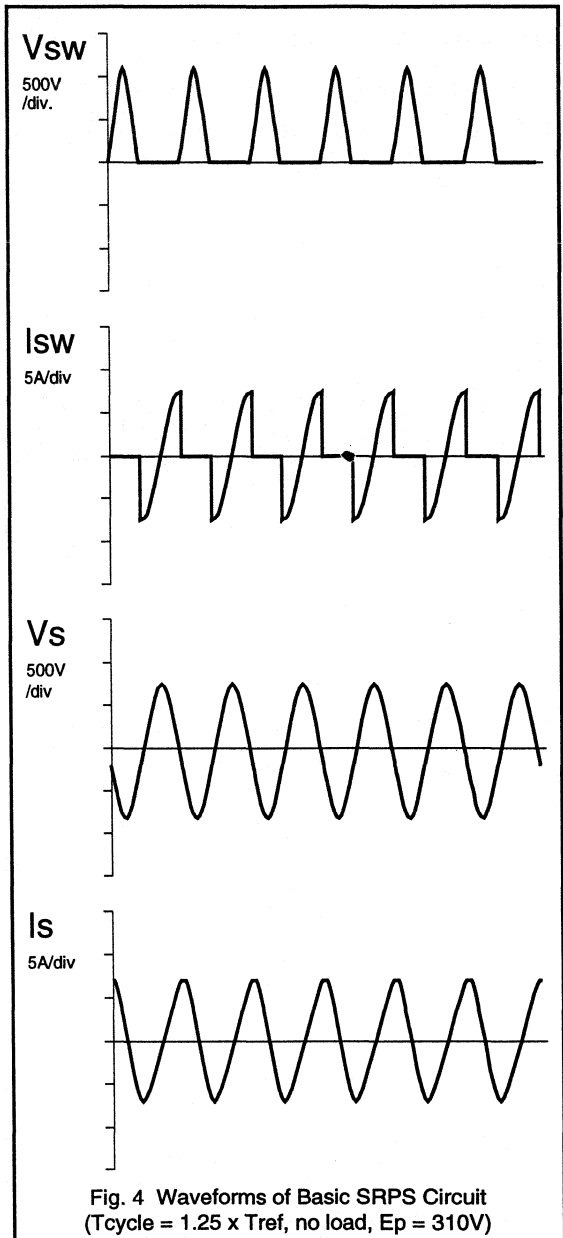


Fig. 4 Waveforms of Basic SRPS Circuit
($T_{cycle} = 1.25 \times T_{ref}$, no load, $E_p = 310V$)

To realise the situation shown in Fig. 4, the output voltage E_o has to be increased considerably for no load operation for the same E_p or E_p can be decreased considerably for the same E_o . In fact, the relation between E_o and E_p in this figure is found to be:

$$E_o > 2.7 \times E_p$$

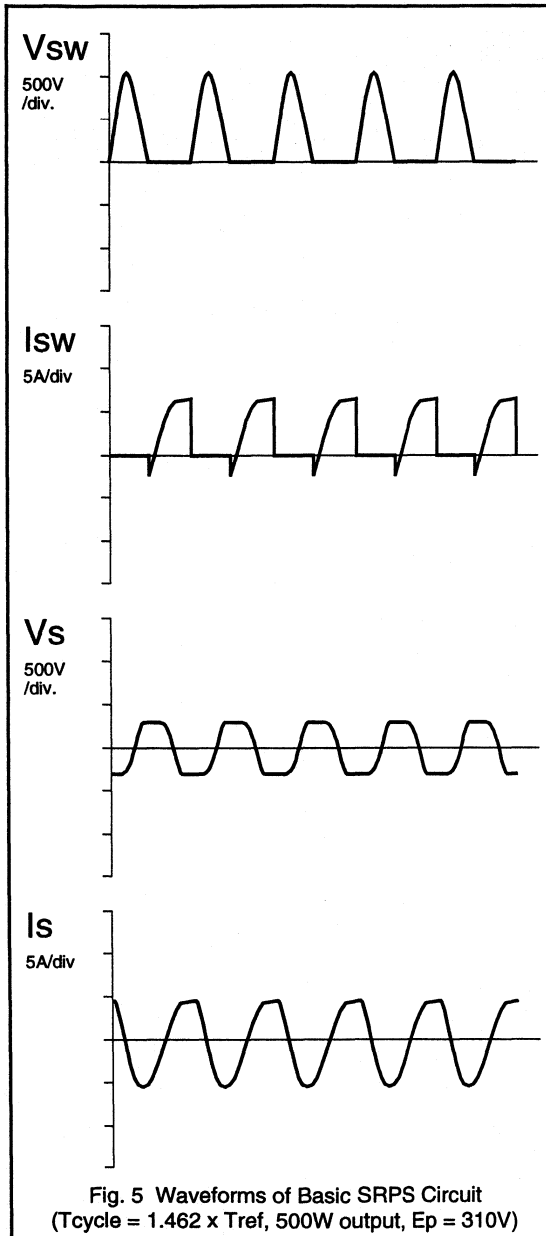


Fig. 5 Waveforms of Basic SRPS Circuit
(Cycle = $1.462 \times T_{ref}$, 500W output, $E_p = 310V$)

Finally, Fig. 5 shows the voltages and currents for full load ($P_{out} = 500W$) at $E_p = 310V$ and $E_o = 300V$. The input current I_o is not shown but is a DC current of 1.6A with a small ripple current. The cycle time has been increased to $1.45 \times T_{ref}$ to get the 500W output power, giving an operating frequency of about 50 kHz.

It should be noted that S1 has to switch 'OFF' a high current at a relatively high dV/dt , resulting in significant turn-off losses. These losses are the main reason to prefer PRPS over SRPS for pre-converter applications.

The basic PRPS converter circuit

A basic PRPS converter topology is shown in Fig. 6. Just as for the basic SRPS pre-converter, we will assume a DC supply voltage E_p of 310 Vdc and a peak output power of 500W, i.e. a nett output power of 250W average.

The topology of Fig. 6 (PRPS) is almost identical to the topology of Fig. 2 (SRPS), except for the following points:

- Diode D1 is now in series with the switch S1 instead of in anti-parallel.
- Capacitor C_p has been omitted.

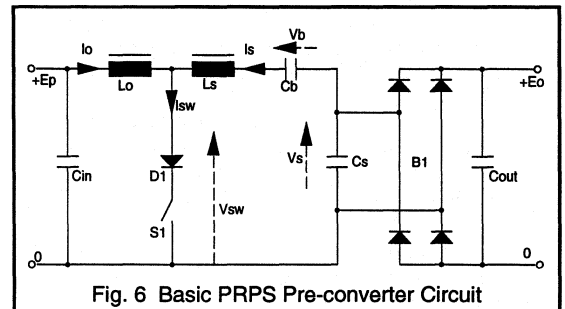


Fig. 6 Basic PRPS Pre-converter Circuit

The value of the two inductors L_o and L_s remain the same as they were in the SRPS, but the values of C_b and C_s are changed to obtain proper PRPS circuit operation. Having D_1 in series with S_1 does not lead to 'no-load' stability problems because, in the PRPS circuit, both the amplitude and the duration of the S_1 current pulse are reduced as the output power decreases.

The input inductance L_o again forms the connection between the input voltage E_p and the switch voltage V_{sw} (across D_1 and S_1 in series). A 'PARALLEL' resonant L-C circuit, consisting of the series connection of L_o and L_s , the DC voltage blocking capacitor C_b and the capacitor C_s (both the switch S_1 and the diode bridge B_1 OFF) now determines the no load operation frequency. The value of the input capacitor C_{in} is chosen to be sufficiently large with respect to C_s to be neglected with respect to the no load operation frequency.

A practical PRPS pre-converter for 250W nett output power (500W peak power) can have component values as shown in Table 2.

Lo	4 mH	8 x Ls
Ls	500 μH	
Cs	24 nF	
Cb	48 nF	2 x Cs

Table 2 Component Values for PRPS circuit

To be able to put a full wave rectifier across capacitor Cs, the DC voltage blocking capacitor Cb cannot have a value of several times Cs. Therefore, a value of only twice Cs has been chosen for Cb. This ratio gives good practical results in combination with an output voltage, Eo, of 450V.

The parallel L-C circuit consists of series combinations of Lo and Ls and Cb and Cs. The output rectifier bridge now modulates the value of the capacitor between 2/3 Cs and 2 Cs (Cb and Cs in series and Cb only). It should be noted that the resonant frequencies of the two states differ by a factor of $\sqrt{3}$.

The switch S1 modulates the inductance value of the parallel L-C circuit between Lo + Ls and Ls. This is combined with a change in input voltage from zero (S1 ON) and Ep (S1 OFF). Again, the PRPS can be seen as a parametric amplifier, but now with both inductance and capacitance modulation.

In contrast with the SRPS circuit, the output power of a PRPS converter will increase with increasing operation frequency, thus with decreasing operation cycle time.

Under no load conditions and maximum operation cycle time, the output voltage and current will be near sinusoidal and will have their minimum no load values. This minimum output voltage can be calculated from

$$V_s > E_p \cdot \frac{(L_o + L_p)}{L_o} \cdot \frac{C_b}{(C_b + C_s)}$$

Substituting the values for Lo, Ls, Cb and Cs in the formula gives

$$V_s > 0.75 \times E_p$$

An output voltage choice of Eo = 450 V for Ep = 375 V will, therefore, be amply sufficient.

The voltage Vsw, the current Isw, the output voltage Vs and the current Is for the maximum operation cycle time, i.e. about equal to Tref, are shown in Fig. 7.

To get an impression of the boosting properties of the PRPS circuit, the no load voltages and currents are shown, for an operation cycle time Tcycle = 0.975 x Tref, in Fig. 8. It can be seen that the output voltage has been increased by a factor 2.5 with only a very small decrease of operation cycle time.

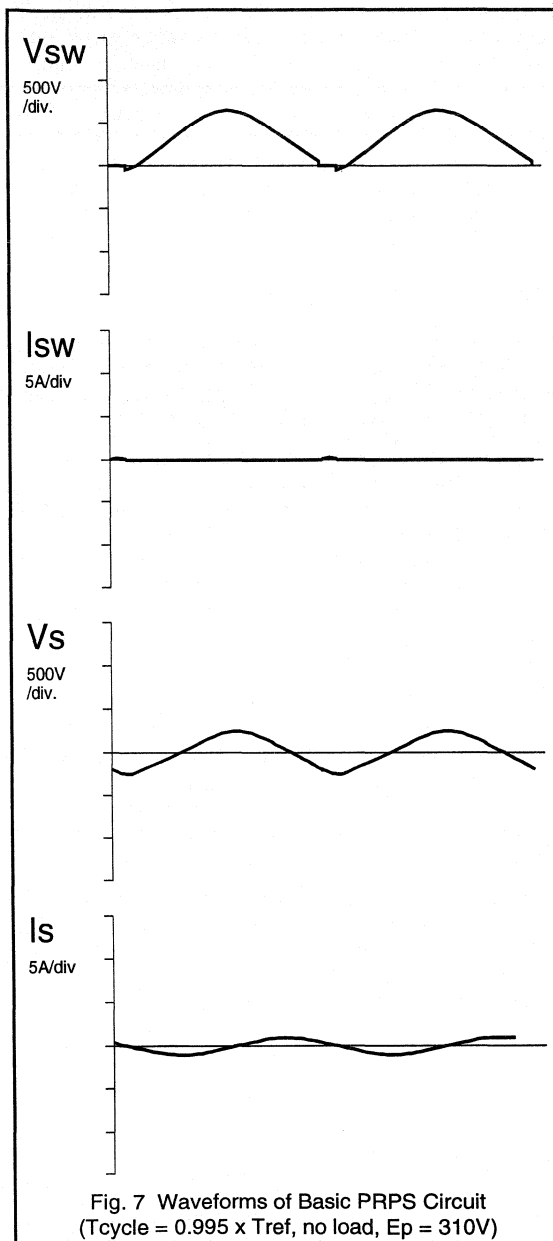


Fig. 7 Waveforms of Basic PRPS Circuit
(Tcycle = 0.995 x Tref, no load, Ep = 310V)

Finally, the full load voltages and currents are shown in Fig. 9 (output power 500W at Eo = 450V and Ep = 310V). It should be noted that the operation cycle time has been decreased to .5694 x Tref.

The significant feature of the PRPS circuit is that the current in the main switching device S1 is brought down to zero by the circuit and not by the device itself. Device S1 can now be turned off without loss. The negative voltage which causes the current to fall, is supported by diode D1, which needs to be a fast recovery type like the BYR79. The reverse recovery loss in D1 is small because the resonant action of the circuit make the rate of fall of current relatively slow - up to two orders of magnitude slower than in a standard SMPS.

SRPS and PRPS compared

A pre-conditioner can be implemented using either an SRPS or PRPS topology. The capacitor and inductor values are roughly the same, as are the peak values of voltage and current. The main difference between the circuits is in the switching requirements of S1 and D1.

In the SRPS, the turn on loss of S1 is very low - the voltage across S1 is zero and the current rises relatively slowly. However the turn off loss is large - S1 has to turn off a large current and, although the dV_{sw}/dt is moderated by C_p it is still relatively fast. On the other hand, the turn off loss in D1 is negligible - no voltage is applied to the diode until S1 is turned off giving plenty of time for reverse recovery - but the turn on loss may be significant because the dI_{sw}/dt is un-restrained.

In the PRPS circuit, however, the turn off loss in S1 is close to zero but the recovery loss in D1 is not negligible - I_{sw} falls through zero and the negative voltage appears across the diode. S1 is turned on from a high voltage so there will be some loss in both S1 and D1 even though the rate of rise of current is moderated by L_s .

It is generally true that reducing turn off loss produces a bigger cost/performance benefit than reducing turn on loss. It is also true that losses in diodes are usually much lower than in their associated switching device. Since the PRPS configuration reduces turn off loss in S1 to zero it appears that PRPS is a better choice than SRPS as a resonant pre-converter.

Therefore, the remainder of this paper will concentrate on PRPS circuits.

PRPS transformer for >1kW

The practical PRPS circuits in this paper all use a transformer with a built-in leakage inductance to give mains isolation and inductance L_s . The inexpensive U-64 core, used in large quantities in the line deflection and EHT circuits in colour TV sets, can be used successfully as the transformer core in PRPS converters with a nett output power in excess of 1000W.

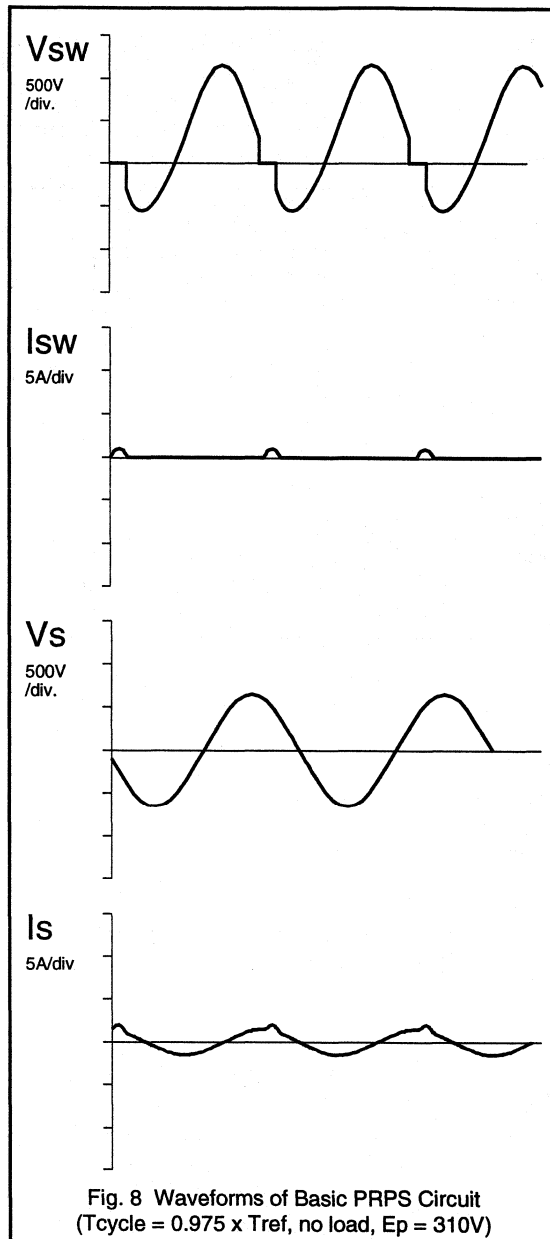


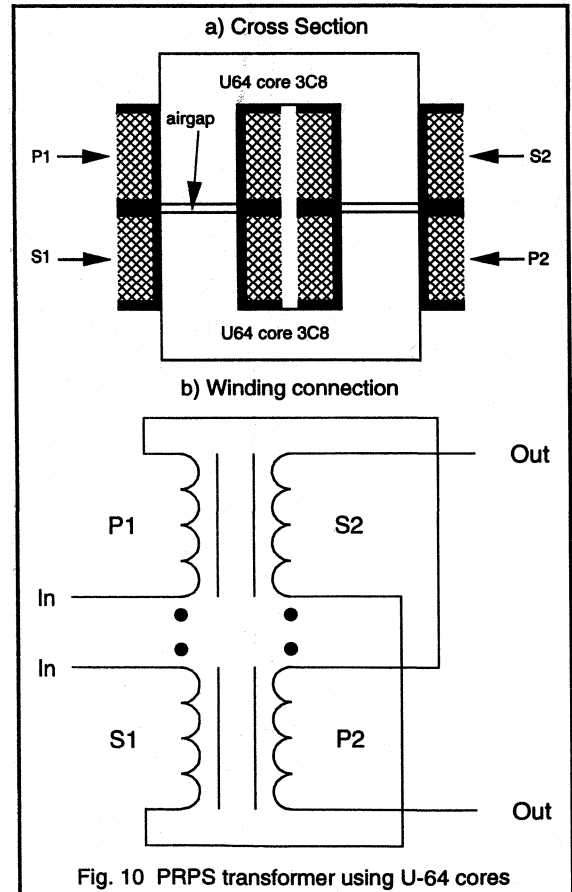
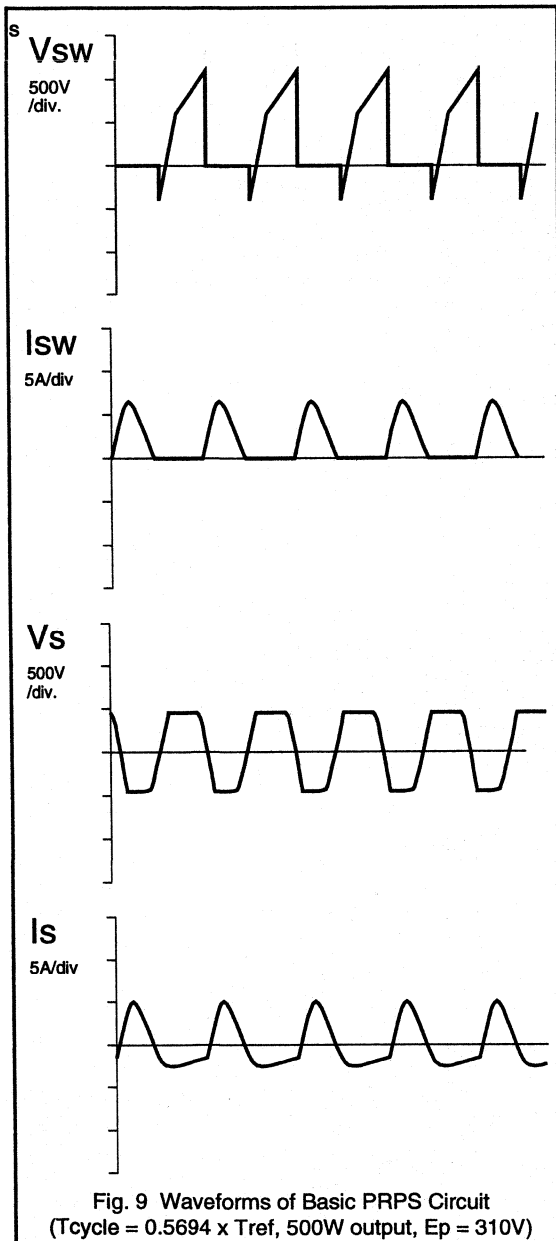
Fig. 10 illustrates a PRPS transformer constructed with a pair of U-64 cores. Both the primary and secondary windings are split into two halves. Each leg of the U-core is fitted with a two-chamber coil former with a primary and a secondary winding. To achieve a reasonable 'leakage

inductance' L_s , the primary and secondary coils are crossed. Thus each U-core has one primary and one secondary coil.

A pre-converter transformer with this arrangement offers several advantages over the 'standard' SMPS transformer using E-cores.

- It will be easier to meet the mains isolation requirements, particularly with respect to creepage distances.
- The thermal properties will be much better because the winding is distributed over both core legs.
- The mean length of a turn is less than with a single core leg, reducing copper loss.
- The two leg arrangement will need only 70% of the turns of the one leg design. This is because of the active (magnetic) fluxing of both legs.
- It is a simpler and hence less expensive transformer to wind.

One disadvantage of this arrangement is that the windings are not layered. This means that 'skin effect' will have to be overcome by using Litz wire for both the primary and secondary windings.



The equivalent electrical circuit diagram of the PRPS transformer is given in Fig. 11. It is the well known 'Tee' circuit with primary winding(s) leakage inductance L_{lp} , a magnetisation inductance L_m and secondary winding(s) leakage inductance L_{ls} , followed by an 'ideal' transformer for the output voltage transformation.

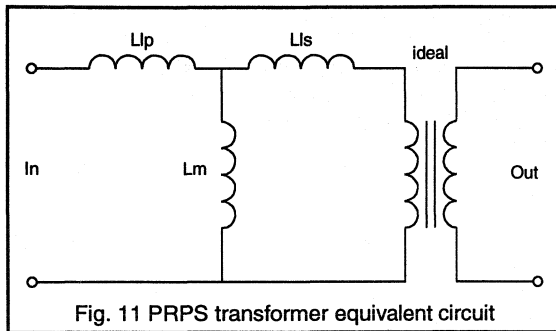


Fig. 11 PRPS transformer equivalent circuit

The primary and secondary leakage inductance is determined by the transformer construction and, in particular, by the positioning of the windings. In the symmetrical arrangement of Fig. 10, the values of L_{lp} and L_{ls} will be equal. L_{lp} and L_{ls} are also proportional to the square of the number of primary turns as is L_m . However, L_m is also strongly dependent on the width of the 'airgap' between the two U-cores. The airgap can be adjusted to give a value of L_m between 2 and 100 times $L_{lp}+L_{ls}$.

The transformer can be characterised by two inductance measurements:

- L_x , the measured primary inductance with the secondary winding(s) shorted.
- L_y , the measured primary inductance with the secondary winding(s) open circuit

It can be seen from the equivalent circuit diagram that,

$$L_x = L_{lp} + \frac{L_m \cdot L_{ls}}{L_m + L_{ls}}$$

$$L_y = L_{lp} + L_m$$

If the transformer is assumed to be symmetrical then,

$$L_{lp} = L_{ls}$$

rearranging gives,

$$L_{lp} = L_y - \sqrt{L_y^2 - L_x \cdot L_y}$$

$$L_m = \sqrt{L_y^2 - L_x \cdot L_y}$$

If the airgap is $<50\mu\text{m}$ then L_m will be at least 100 times the value of L_{lp} or L_{ls} . In this case,

$$L_x \approx L_{lp} + L_{ls}$$

and

$$L_y \approx L_m$$

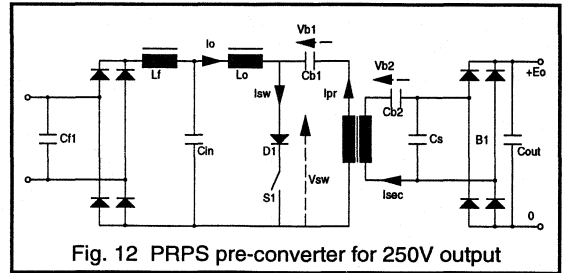


Fig. 12 PRPS pre-converter for 250V output

A PRPS pre-converter transformer for 1250W nett output has been constructed to the arrangement shown in Fig. 10. It had a primary consisting of two 36 turn windings connected in series, wound using 600 x 0.07mm Litz wire. The number of turns on the secondary varied depending on the required output voltage. Measurements of this transformer gave the following values for L_x and L_y .

$$L_x = 200 \mu\text{H}$$

$$L_y = 1600 \mu\text{H} \text{ (Note that this value is strongly influenced by the size of the airgap)}$$

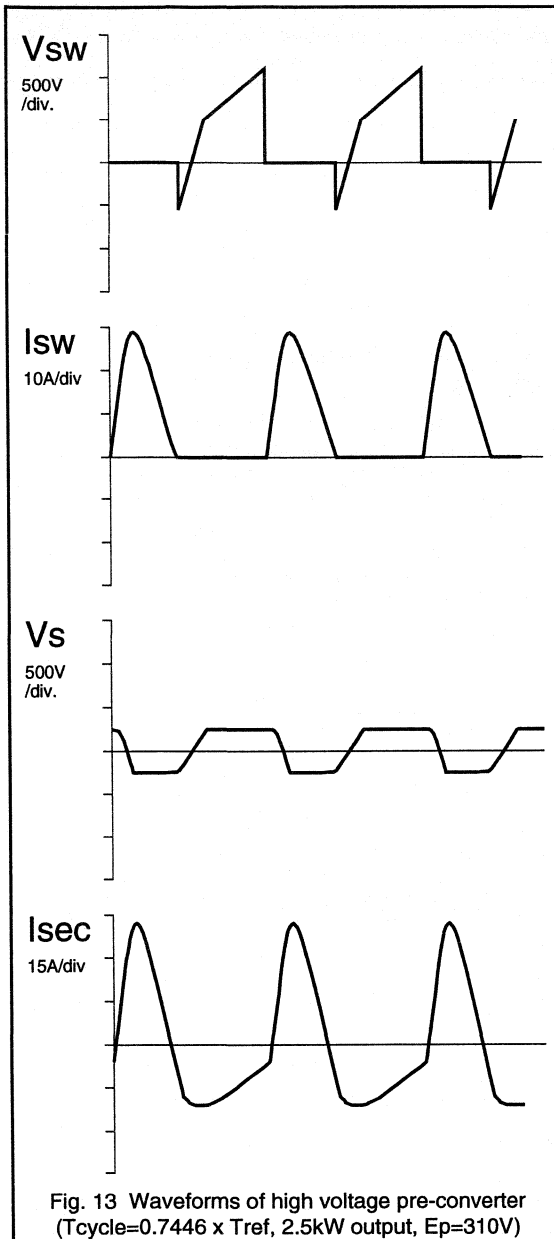
PRPS pre-converter for high output voltages

The circuit shown in Fig. 12 is a PRPS pre-converter using the type of transformer mentioned earlier. This circuit is intended to deliver 1250W at a relatively high voltage - in this case 250V. To achieve an final output voltage of 250V with an effective output voltage, E_o , of 450V means having a transformer with a turns ratio of 8:5.

Cf1	2μF	2 x 1μF
Cin	2μF	2 x 1μF
Cb1	0.2μF	2 x 0.1μF
Cb2	1.36μF	2 x 0.68μF
Cs	0.3μF	2 x 0.15μF
Lf	1600μH	
Lo	1600μH	
Lx	200μH	
Ly	1600μH	

Table 3 Component Values for High Output Voltage PRPS circuit

The transformer has replaced the inductance L_s in the basic circuit diagram of Fig. 6. The DC voltage blocking capacitor C_b has been split up into a primary blocking capacitor C_{b1} and a secondary blocking capacitor C_{b2} . There will, therefore, be no DC current in $Tr1$ so in principle the transformer does not need an airgap. However, experience



has shown that a limited value of magnetisation inductance improves the operation of the circuit, so an airgap has been included which keeps the L_y value, of $Tr1$, equal to L_o .

The pre-converter circuit has been completed by the addition of capacitor $Cf1$, rectifier bridge and filter inductor L_f (an iron cored choke). The combination of $Cf1$, L_f , C_{in} and L_o prevents a significant switching frequency signal appearing at the mains terminals.

The component values shown in table 3 are used in the circuit of Fig. 12. With these values the no load reference cycle time will be $49.7 \mu\text{s}$. Therefore, the no load operating frequency is just over 20 kHz.

Figs. 13 and 14 show the waveforms associated with the circuit when the input voltage is 310 V and the circuit is delivering 2.5 kW

E_p	Pout (PRPS)	Pout (R load)	% Deviation
310.0	2501	2501	0.0%
308.3	2476	2474	0.1%
303.2	2389	2392	-0.1%
294.8	2249	2262	-0.6%
283.2	2068	2087	-0.9%
268.5	1857	1876	-1.0%
250.8	1621	1637	-1.0%
230.4	1375	1382	-0.5%
207.4	1128	1119	0.8%
182.2	890	864	3.0%
155.0	668	625	6.8%
126.1	472	414	14.1%
95.8	305	239	27.7%
64.5	171	108	57.9%
32.4	70	27	156.2%

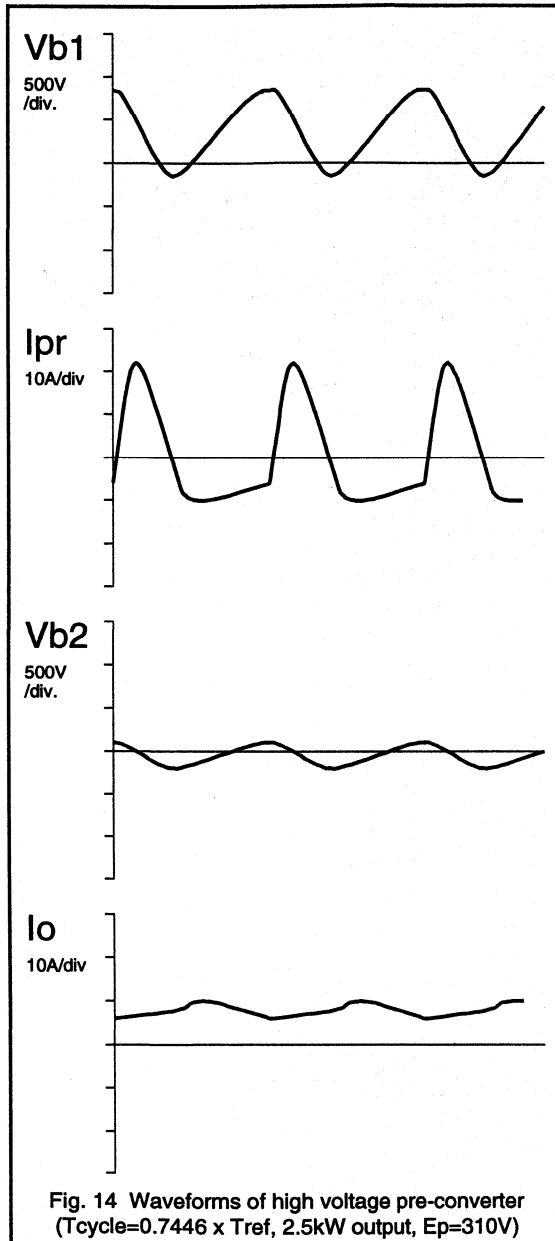
Table 4 Output power of PRPS pre-converter.

Of particular interest is I_o because it can be easily measured with a low value resistor. This current will be used to control power output of the PRPS pre-converter. I_o will be compared with a reference, I_{oref} , which will be proportional to input voltage E_p . The comparison of I_o and I_{oref} should be done at the right time, namely during the period when I_o has a negative slope. The switch $S1$ is turned ON as soon as the value of I_o drops below I_{oref} .

The computed values of Pout for 15 values of E_p which would be achieved using this control strategy are given in Table 4. As a comparison the output power for a resistive load is also shown in Table 4.

It can be seen from Table 4, that the PRPS output power closely matches the power of a purely resistive load except for E_p values near the zero crossings of the mains/line voltage.

Of course, an average output power control loop (with a time constant far in excess of the 10 (8.3) ms cycle time of a half mains/line period) is required to determine the



proportionality constant between the mains/line voltage and I_{loref} for the mains/line voltage variations and for the output power control.

It can also be concluded, from table 4, that the PRPS circuit can indeed fulfil the pre-converter action successfully, i.e. a resistive load for the mains voltage can be easily achieved, thus no mains distortion and a power factor >0.99 is possible.

The circuit shown in Fig. 12 is only suitable for high output voltages. At low output voltages (below 100V for output powers in excess of 1000W), the secondary blocking capacitor C_{b2} has to have a high value and pass a large current and is, therefore, an expensive component. If a low output voltage pre-converter is required, then an alternative arrangement is needed.

PRPS pre-converter for low output voltages

The high cost of C_{b2} , in a low output voltage PRPS pre-converter, could be avoided if it could be eliminated from the circuit. The problem is that removing C_{b2} allows a DC current to flow in the transformer. The resulting flux can be handled by increasing the airgap between the cores of the transformer. This will have the additional effect of reducing L_y from 1600 μH to 800 μH . This change has been incorporated in the circuit shown in Fig. 15, which is intended to deliver 1200W at 60V.

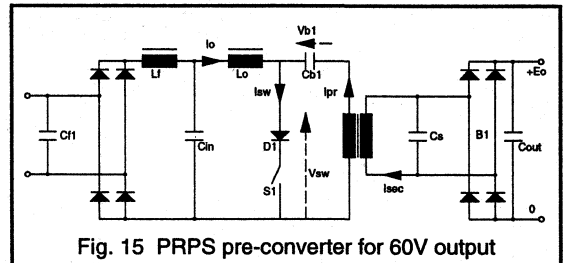


Fig. 15 PRPS pre-converter for 60V output

To get 1200W net from a transformer of the type shown in Fig. 10 it is necessary to change the number of primary turns N_p and thus decrease the value of L_x . Suitable values would be:

- N_p (primary turns) 2 x 28 (600 x .07 mm Litz wire)
- N_s (secondary turns) 2 x 4 (flat Litz wire 7 mm²)

The air gap in the transformer should be adjusted to give an L_x of 125 μH .

Suitable values for the other components are given in table 5. The reference cycle time, T_{ref} , with these values will be 39 μs .

The inductance L_o can be made with either a pair of U-64 cores - with the winding distributed over both legs- or with a pair of E-cores.

Cf1	2 μ F	2 x 1 μ F
Cin	2 μ F	2 x 1 μ F
Cb1	0.15 μ F	
Cs	3.75 μ F	5 x 0.75 μ F
Lf	1600 μ H	
Lo	1600 μ H	

Table 5 Component Values for Low Output Voltage PRPS circuit

In practice, PRPS pre-converters produce about 150W for each Amp(rms) flowing in the primary winding. So for a 1200W converter:

$$I_{pr} = 8A$$

$$I_{sec} = 56A \text{ (at 60V and 20A)}$$

The voltage and current wave forms for the circuit of Fig. 15 are similar to those shown in Figs. 13 and 14, except for the amplitudes in the secondary side.

This configuration of PRPS pre-converter is viable for output voltages as low as 40 V. Below this, however, the value and current rating of Cs becomes excessive and it is likely that alternative configurations would be more cost effective.

Control circuit for PRPS converters

Figure 16 shows a simple control circuit for PRPS converters. It is constructed from MOS ICs and standard comparators. The analogue control section for the output power stabilisation is not shown because it will, in principle, be no different than for an SMPS converter.

The PRPS control circuit comprises of a dual sawtooth oscillator whose frequency can be adjusted by applying a voltage to X1. The output of this oscillator is fed to the clock pulse input of a divide-by-8 counter. The highest oscillator frequency needs to be just over 8x the highest expected operating frequency of the PRPS power section.

The oscillator can be stopped by applying a hold up signal (low) to G1. This hold-up input is used to modulate the cycle time of the control circuit. As soon as this 'hold up' signal is removed (high), a pulse will be sent to the divide-by-8 circuit which then advances one position.

The counter has 8 outputs, Q0-Q7. Output Q0 will go high either synchronously following Q7 or asynchronously with a high on pin 15. Output Q0 sets a flip-flop consisting of a 2 and a 3 input NOR-gate. The output terminal X8 then goes high to indicate that the main switching device S1 should turn on.

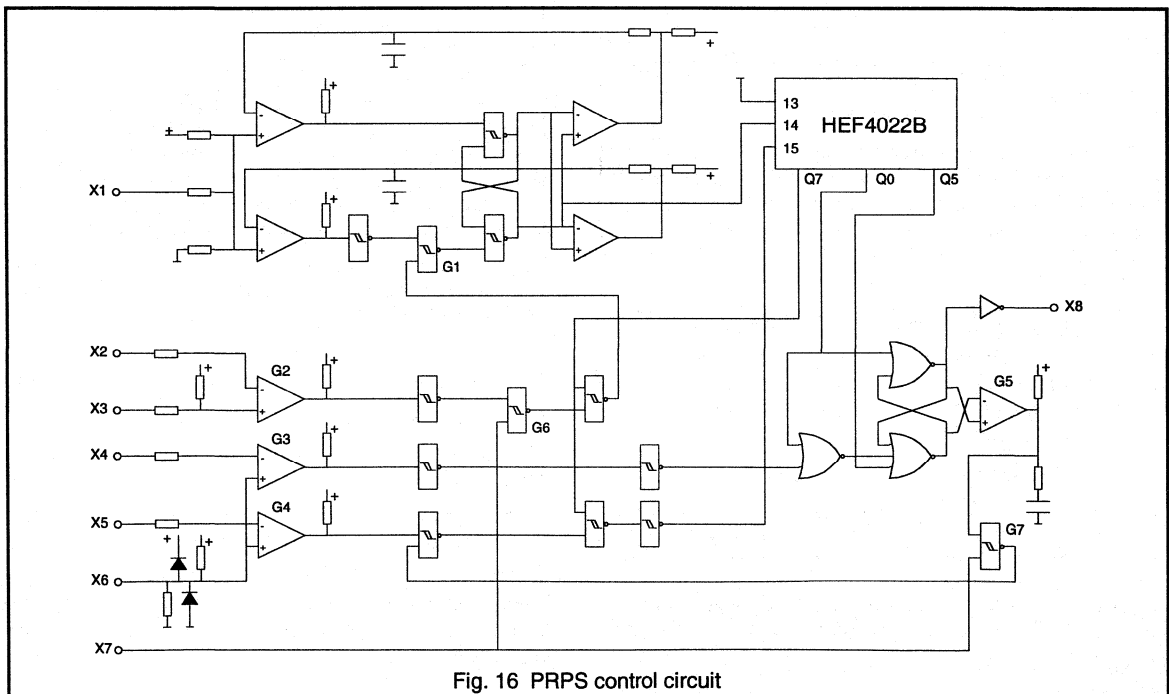


Fig. 16 PRPS control circuit

The Q7 output is used to enable both the 'hold-up' signal for the oscillator and the reset input for the divide-by-8, i.e. both the 'hold-up' and the reset only can be active if there is a '1' at Q7. The output flip-flop is reset either by the negative voltage across S1-D1 - via comparator G3 - or by the sixth position, Q5, of the counter. To prevent the possibility of immediate reset of the flip-flop, the indication of negative voltage across S1-D1 is blanked out while Q0 is high.

The voltage across S1-D1 is connected to terminal X6 via a high value resistor (220 kΩ). X4 is connected to the negative supply line of the power circuit. Comparator G3 then gives logical information about the polarity of the voltage across S1-D1.

Information about the amplitude of this voltage is obtained via comparator G4. A reference voltage, proportional to the mains voltage, is connected to X5. If the attenuated S1-D1 voltage falls below this reference, and Q7 is high, the counter will be reset and S1 will be turned ON. This is an emergency measure in case the normal current control loop via the comparator G2 fails to disable the 'hold up' signal. This could occur if there were a false current reference signal at X2.

The best strategy for the control of a PRPS pre-converter is by comparing the current, I_o , in the input inductor, L_o , with a mains proportional reference current. In Fig. 16 a signal, proportional to I_o , is connected to X3 and the reference signal to X2. As soon as I_o falls below the reference value the 'hold-up' signal is removed, the counter is advanced from Q7 to Q0 and S1 is turned ON.

A '1' at input X7 allows the control circuit to run, whereas a '0' will cause the PRPS to switch OFF in a controlled manner. When X7 goes high, the output of NAND gate G7 goes low. This signal is used to reset the counter which takes Q0 high, turns on S1 and starts the operating cycle. The output of G5, which was pulled high while the circuit was stopped, is now driven low and is kept low by the RC network as long as S1 continues to be switched. This 'low' keeps the output of G7 high and allows the correct signal to be fed from G4 to the counter reset. The high on X7 also enables G6 and lets the information from G2 - the 'current' comparator - through to the 'hold up' circuit.

If X7 is taken low then G6 is disabled and the signal which would start the next switching cycle is not allowed to get through. The counter will continue to run until Q7 goes high at which time the circuit will be 'held up' and the operating cycle will be halted.

The cycle time will be adjusted by changing the reference value at X2. This signal will be a series of half sinewaves whose peak value is proportional to the power that the pre-converter needs to deliver to the keep the output

voltage at the required level. This control strategy has been tested on various PRPS circuits and fulfils all the requirements properly.

Modelling PRPS pre-converters

There are no equations which summarise the overall behaviour of a PRPS pre-converter circuit. Determining factors like the throughput power of the circuit and the peak voltages and currents, means developing a computer model. In this model the operation of the circuit is broken down into its separate modes and the appropriate equations derived for each of them.

The circuit of Fig. 6 has, basically, two switches which determine its mode of operation. The first is the combination of S1 and D1 - this is the controllable switch - and the second is the bridge rectifier B1.

Therefore the circuit has four different modes of operation. For all these modes, the time functions for the currents and voltages can be derived by circuit analysis. The four modes are given below:

Mode	S1-D1	Bridge
I	ON	ON
II	ON	OFF
III	OFF	OFF
IV	OFF	ON

Table 6 PRPS Operating Modes

Using Laplace transformation it is possible to derive the time functions for currents I_o and I_s , for the circuit in each of its 4 modes. This method allows the initial values of the currents and voltages to be easily introduced into the equations. The initial conditions of I_o , I_s , V_{b1} and V_s will be indicated by J_o , J_s , U_{b1} and U_s respectively.

Mode I

We will start with the derivation of the time functions for the operation of the PRPS circuit in mode I (S1-D1 ON and B1 ON). The initial conditions are:

$$I_o = J_o$$

$$I_s = J_s = -J_o$$

$$V_{b1} = U_{b1}$$

$$V_s = U_s = E_o$$

Calculation starts at $t = 0$ with the switching ON of S1-D1, while B1 is already conducting, i.e. $J_o > 0$. The following Laplace equations are then valid:

$$\frac{E_p}{s} + L_o J_o = I_o . s . L_o$$

$$\frac{Ub1 + Us}{s} + Ls.Js = Is \cdot \left(s.Ls + \frac{1}{s.Cb1} \right)$$

Note: B1 is conducting, so $Vs = Us = Eo$, i.e. Cs is infinitely large and has no influence on Is.

If we define the following:

$$\omega = \sqrt{\frac{1}{Ls.Cb1}}$$

$$F1 = Jo$$

$$F2 = \frac{Ep}{Lo}$$

$$G1 = Js$$

$$G2 = \frac{Ub1 + Us}{Ls}$$

The Laplace equations for Io and Is can then be written as:

$$Io = \frac{F1}{s} + \frac{F2}{s^2}$$

$$Is = \frac{G1.s}{s^2 + \omega^2} + \frac{G2}{s^2 + \omega^2}$$

The inverse Laplace transformation of these two equations gives the following time functions:

$$Io = F1 + F2.t$$

$$Is = G1 \cdot \cos(\omega.t) + \frac{G2}{\omega} \cdot \sin(\omega.t)$$

To calculate the input power and the voltage Vb1 and Vs, these time functions can be integrated to give Ioint and Isint, thus:

$$Ioint = F1.t + \frac{F2}{2}.t^2$$

$$Isint = \frac{G1}{\omega} \cdot \sin(\omega.t) + \frac{G2}{\omega^2} \cdot (1 - \cos(\omega.t))$$

The input power during the validity of mode I (i.e. during a time interval of length T1) is equal to:

$$Pin(T1) = \frac{Ep.Ioint}{T1}$$

The voltages Vb1 and Vs are equal to:

$$Vb1 = Ub1 - \frac{Isint}{Cb1}$$

$$Vs = Us = Eo$$

In the computer program, these formulae will be stored in a subroutine called sub1.

Mode II

The initial conditions for mode II operation (S1-D1 ON and B1 OFF) are:

$$Io = Jo$$

$$Is = Js$$

$$Vb1 = Ub1$$

$$Vs = Us \text{ (either +Eo or -Eo)}$$

The Laplace equations for Io and Is are now:

$$\frac{Ep}{s} + Lo.Jo = Io.s.Lo$$

$$(Ub1 + Us).s + Ls.Js = Is \cdot \left(s.Ls + \frac{Cb1 + Cs}{s.Cb1.Cs} \right)$$

Define:

$$\omega = \sqrt{\frac{Cb1 + Cs}{Ls.Cb1.Cs}}$$

$$F1 = Jo$$

$$F2 = \frac{Ep}{Lo}$$

$$G1 = Js$$

$$G2 = \frac{Ub1 + Us}{Ls}$$

The Laplace functions for Io and Is are now identical to those for mode I, so the time functions are:

$$Io = F1 + F2.t$$

$$Is = G1 \cdot \cos(\omega.t) + \frac{G2}{\omega} \cdot \sin(\omega.t)$$

$$Ioint = F1.t + \frac{F2}{2}.t^2$$

$$Isint = \frac{G1}{\omega} \cdot \sin(\omega.t) + \frac{G2}{\omega^2} \cdot (1 - \cos(\omega.t))$$

$$Pin(T2) = \frac{Ep.Ioint}{T2}$$

$$Vb1 = Ub1 - \frac{Isint}{Cb1}$$

$$Vs = Us - \frac{Isint}{Cs}$$

In the computer program, these formulae will be stored in a subroutine called sub2.

Mode III

The initial conditions for mode III operation (S1-D1 OFF and B1 OFF) are:

$$I_o = J_o$$

$$I_s = J_s = -J_o$$

$$V_{b1} = U_{b1}$$

$$V_s = U_s$$

The correct Laplace equation for I_s ($I_o = -I_s$) can be expressed by the relationship:

$$\frac{U_{b1} + U_s - E_p}{s} + (L_o + L_s).J_s = I_s \left(s.(L_o + L_s) + \frac{C_{b1} + C_s}{s.C_{b1}.C_s} \right)$$

Define:

$$\omega = \sqrt{\frac{C_{b1} + C_s}{(L_o + L_s).C_{b1}.C_s}}$$

$$G1 = J_s$$

$$G2 = \frac{U_{b1} + U_s - E_p}{L_o + L_s}$$

The time functions can then be expressed by:

$$I_s = G1 . \cos(\omega.t) + \frac{G2}{\omega} . \sin(\omega.t)$$

$$I_o = -I_s$$

$$I_{sint} = \frac{G1}{\omega} . \sin(\omega.t) + \frac{G2}{\omega^2} (1 - \cos(\omega.t))$$

$$I_{oint} = I_{sint}$$

$$P_{in}(T3) = \frac{E_p . I_{oint}}{T3}$$

$$V_{b1} = U_{b1} - \frac{I_{sint}}{C_{b1}}$$

$$V_s = U_s - \frac{I_{sint}}{C_s}$$

In the computer program, these formulae will be stored in a subroutine called sub3.

Mode IV

The initial conditions for the mode IV operation (S1-D1 OFF and B1 ON) are given below:

$$I_o = J_o$$

$$I_s = J_s = -J_o$$

$$V_{b1} = U_{b1}$$

$$V_s = U_s = E_o$$

The Laplace equation for current I_s is now:

$$\frac{U_{b1} + U_s - E_p}{s} + (L_o + L_s).J_s = I_s \left(s.(L_o + L_s) + \frac{1}{s.C_{b1}} \right)$$

Define:

$$\omega = \sqrt{\frac{1}{(L_o + L_s).C_{b1}}}$$

$$G1 = J_s$$

$$G2 = \frac{U_{b1} + U_s - E_p}{L_o + L_s}$$

The time functions are given by,

$$I_s = G1 . \cos(\omega.t) + \frac{G2}{\omega} . \sin(\omega.t)$$

$$I_o = -I_s$$

$$I_{sint} = \frac{G1}{\omega} . \sin(\omega.t) + \frac{G2}{\omega^2} (1 - \cos(\omega.t))$$

$$I_{oint} = I_{sint}$$

$$P_{in}(T4) = \frac{E_p . I_{oint}}{T4}$$

$$V_{b1} = U_{b1} - \frac{I_{sint}}{C_{b1}}$$

$$V_s = U_s$$

In the computer program, these formulae will be stored in a subroutine called sub4.

Program structure

The modelling program can be written around the four subroutines. The central part of the program will make successive calls to the appropriate subroutine. The calculated values of current and voltage will be used to determine when the circuit moves from one mode to the next. The final values of I_o , I_s , V_{b1} and V_s will be used as the initial values, J_o , J_s , U_{b1} and U_s , for the next mode. The actual sequence of the modes depends upon the operating frequency and load condition. Under full load condition when E_p is not close to zero, the sequence of modes will be as shown in Table 7.

One cycle of operation ends when I_o falls below I_{oref} . This would result in S1 being turned ON, putting the circuit in to mode I and starting the cycle once more. At the end of each cycle, the input power can be compared with a reference value (P_{ref}) and I_{oref} can be adjusted until the powers are equal. It is then possible to read various important values

S1-D1	B1	Mode	End Condition
ON	ON	I	$I_s > 0$
ON	OFF	II	$V_s < -E_o$
ON	ON	I	$I_s < 0$
ON	OFF	II	$I_{sw} = I_o + I_s < 0$
OFF	OFF	III	$V_s > E_o$
OFF	ON	IV	$I_o < I_{oref}$

Table 7 PRPS Operating Sequence

such as the initial conditions for I_o , I_s , V_{b1} , V_s , the cycle time, output power, RMS values of I_o and I_s , DC and AC fluxes in the ferrite cores, etc.

Writing a program like this is well within the capabilities of anyone with some experience of programming. The calculations involved are so simple that there will be little difficulty in using almost any programming language. A model produced in this way will be faster and more accurate than could be produced with any of the standard modelling programs.

Conclusions

The PRPS configuration is well suited to the needs of the pre-converter application. It can boost the low mains voltages, near zero crossing, to high levels so that some power is delivered to the load throughout all of the mains cycle. This helps the PRPS appear as a resistive load to the mains.

A PRPS pre-converter can deliver a DC output voltage with low levels of mains ripple using only moderately sized

output smoothing capacitors. The addition of a high frequency transformer gives mains isolation and the ability to have a wide range of output voltages.

The transformer need not be a major additional cost. The high operating frequency means the transformer uses ferrite core and is relatively small (5% of the size of copper / iron transformer). A side by side arrangement of the windings means the transformer is easy to wind, easy to insulate and can have the right leakage inductance to replace the resonant network inductor.

The resonant action of the PRPS circuit allows the main semiconductor switching device to be turned off at zero current. This reduces, considerably, the switching loss of this device allowing a smaller device to be used in higher power / frequency circuits than it could normally resulting in a significant cost saving.

Unfortunately an overall analysis of the performance of a PRPS pre-converter is difficult. However, by breaking the cycle of operation into its logical modes, it becomes easy to generate the time functions for all the currents and voltages. It is simple to incorporate these equations into a computer program to produce an accurate, detailed and fast running model of the system.

The use of pre-converters is become increasingly necessary and the characteristics of PRPS circuits mean that there are well suited to this function. It is easy to overcome the apparent complexity of resonant systems to produce PRPS pre-converters which are elegant, efficient and cost effective.



CHAPTER 3

Motor Control

3.1 AC Motor Control

3.2 DC Motor Control

3.3 Stepper Motor Control

AC Motor Control

3.1.1 Noiseless A.C. Motor Control: Introduction to a 20 kHz System

Controlling an a.c. induction motor by the technique of sine-wave-weighted pulse-width modulation (PWM) switching gives the benefits of smooth torque at low speeds, and also complete speed control from zero up to the nominal rated speed of the motor, with only small additional motor losses.

Traditional power switches such as thyristors need switching frequencies in the audible range, typically between 400 and 1500Hz. In industrial environments, the small amount of acoustic noise produced by the motor with this type of control can be regarded as insignificant. By contrast, however, the same amount of noise in a domestic or office application, such as speed control of a ventilation fan, might prove to be unacceptable.

Now, however, with the advent of power MOSFETs, three-phase PWM inverters operating at ultrasonic frequencies can be designed. A three-phase motor usually makes even less noise when being driven from such a system than when being run directly from the mains because the PWM synthesis generates a purer sine wave than is normally obtainable from the mains.

The carrier frequency is generally about 20kHz and so it is far removed from the modulation frequency, which is typically less than 50Hz, making it economic to use a low-pass filter between the inverter and the motor. By removing the carrier frequency and its sidebands and harmonics, the waveform delivered via the motor leads can be made almost perfectly sinusoidal. RFI radiated by the motor leads, or conducted by the winding-to-frame capacitance of the motor, is therefore almost entirely eliminated. Furthermore, because of the high carrier frequency, it is possible to drive motors which are designed for frequencies higher than the mains, such as 400Hz aircraft motors.

This section describes a three-phase a.c. motor control system which is powered from the single-phase a.c. mains. It is capable of controlling a motor with up to 1kW of shaft output power. Before details are given, the general principles of PWM motor control are outlined.

Principles of Pulse-Width Modulation

Pulse-width modulation (PWM) is the technique of using switching devices to produce the effect of a continuously varying analogue signal; this PWM conversion generally has very high electrical efficiency. In controlling either a three-phase synchronous motor or a three-phase induction motor it is desirable to create three perfectly sinusoidal current waveforms in the motor windings, with relative phase displacements of 120°. The production of sine wave

power via a linear amplifier system would have low efficiency, at best 64%. If instead of the linear circuitry, fast electronic switching devices are used, then the efficiency can be greater than 95%, depending on the characteristics of the semiconductor power switch.

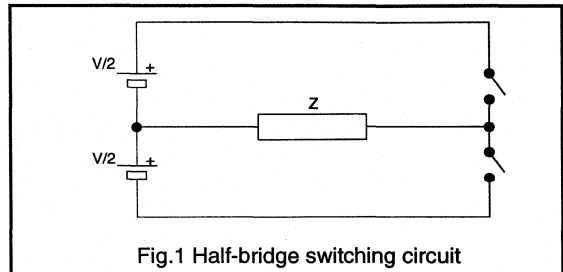


Fig.1 Half-bridge switching circuit

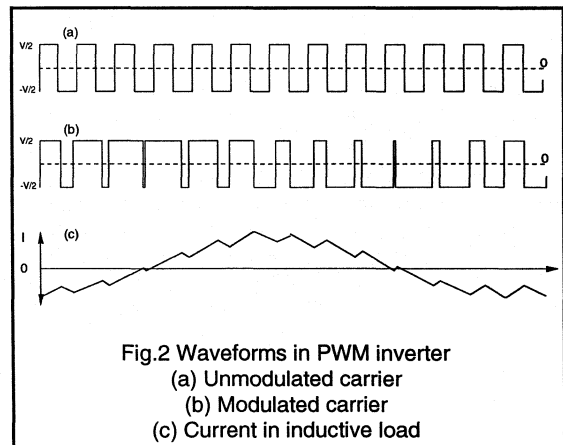


Fig.2 Waveforms in PWM inverter
(a) Unmodulated carrier
(b) Modulated carrier
(c) Current in inductive load

The half-bridge switching circuit in Fig.1 is given as an example: the switches can be any suitable switching semiconductors. If these two switches are turned on alternately for equal times, then the voltage waveform across the load is as shown in Fig.2a. The mean value of this waveform, averaged over one switching cycle is 0. This square wave with a constant 50% duty ratio is known as the 'carrier' frequency. The waveform in Fig.2b shows the effect of a slow variation or 'modulation' of the duty ratio; the mean voltage varies with the duty ratio. The waveform of the resultant load current depends on the impedance of the load Z. If Z is mainly resistive, then the waveform of the current will closely follow that of the modulated square wave. If, however, Z is largely inductive, as with a motor winding or a filter choke, then the switching square wave

will be integrated by the inductor. The result is a load current waveform that depends mainly on the modulation of the duty ratio.

If the duty ratio is varied sinusoidally in time, then the current in an inductive load has the form of a sinewave at the modulation frequency, lagging in phase, and carrying ripple at the switching frequency as shown in Fig.2c. The amplitude of the current can be adjusted by controlling the depth of modulation, that is, the deviation of the duty ratio from 50%. For example, a sinewave PWM signal which varies from 5% to 95%, giving 90% modulation, will produce a current nine times greater than that produced by a signal which varies only from 45% to 55%, giving only 10% modulation.

For three-phase a.c. motor control, three such waveforms are required, necessitating three pairs of switches like those shown in Fig. 1, connected in a three-phase bridge. The inductance required to integrate the waveform can usually be provided by the inductance of the stator windings of the motor, although in some instances it might be provided by the inductance of a separate low-pass filter. The modulations in the three switching waveforms must be maintained at a constant relative phase difference of 120° , so as to maintain motor current sinewaves which are themselves at a constant 120° phase difference. The modulation depth must be varied with the modulation frequency so as to keep the magnetic flux in the motor at approximately the design level.

In practice, the frequency of the modulation is usually between zero and 50Hz. The switching frequency depends on the type of power device that is to be used: until recently, the only devices available were power thyristors or the relatively slow bipolar transistors, and therefore the switching frequency was limited to a maximum of about 1

kHz. With thyristors, this frequency limit was set by the need to provide forced commutation of the thyristor by an external commutation circuit using an additional thyristor, a diode, a capacitor, and an inductor, in a process that takes at least $40\mu\text{s}$. With transistors, the switching frequency was limited by their switching frequency and their long storage times.

In this earlier type of control circuit, therefore, the ratio of carrier frequency to modulation frequency was only about 20:1. Under these conditions the exact duty-ratios and carrier frequencies had to be selected so as to avoid all sub-harmonic torques, that is, torque components at frequencies lower than the modulation frequency. This was done by synchronising the carrier to a selected multiple of the fundamental frequency; the HEF4752V, an excellent IC purpose-designed for a.c. motor control, uses this particular approach. The 1kHz technique is still extremely useful for control of large motors because whenever shaft output powers of more than a few kW are required, three-phase mains input must be used, and there are, as yet, few available switching devices with combined high voltage rating, current rating, and switching speed.

However, using MOSFETs with switching times of much less than $1\mu\text{s}$, the carrier frequency can be raised to the ultrasonic region, that is, to 20kHz or more. There are obvious system benefits with this higher frequency, but there are also several aspects of PWM waveform generation that become easier. It is possible to use a fixed carrier frequency because the sub-harmonics that are produced as a result of the non-synchronisation of the carrier frequency with a multiple of the fundamental are insignificant when the ratio of the carrier frequency to the fundamental frequency is typically about 400:1.

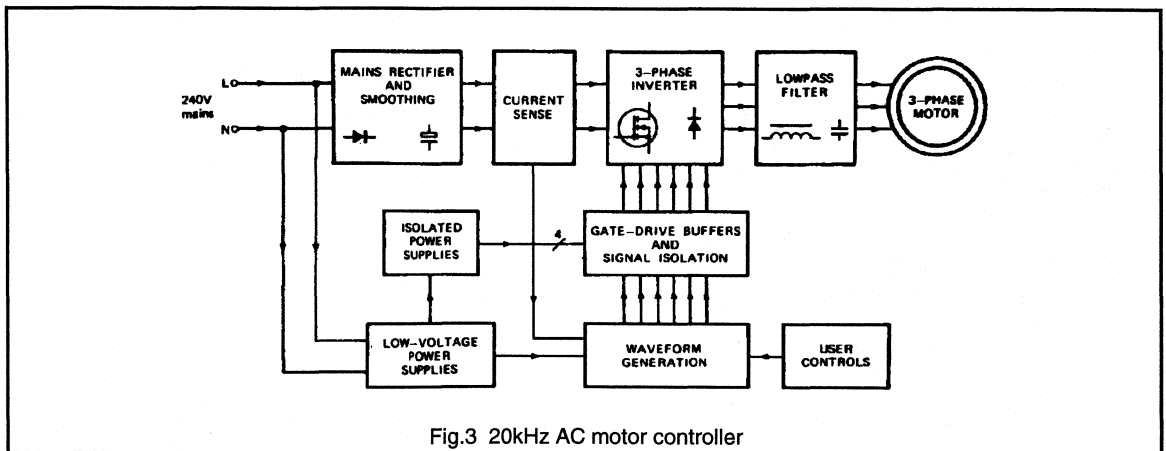


Fig.3 20kHz AC motor controller

To maintain good waveform balance, and thus avoid any d.c. in the motor, and therefore also avoid parasitic torques, a digital waveform generation technique is appropriate. The waveform can be stored as a 'look-up' table of numbers representing the sinewave. To generate the three phases, this table can be read at three points that have the correct 120° phase relationship. The numbers taken from the table represent the duty ratios corresponding to 100% modulation: these numbers can then be scaled down by multiplication or some equivalent technique to give the correct duty-ratio numbers for the modulation depth required.

The speed of the motor is controlled by the rate at which the reading pointers scan the look-up table and this can be as slow as desired. If the pointers are stationary, then the system will be 'frozen' at a particular point on the three-phase sinewave waveform, giving the possibility of obtaining static torque from a synchronous motor at zero speed. The rate at which the numbers are produced by this read-out process from the look-up table is constant and determines the carrier frequency.

To convert these three simultaneous parallel digital numbers into time lengths for pulses, three digital counters are needed. The counters can be designed to give double-edged modulation, such that both the leading edge and the trailing edge of each pulse move with respect to the unmodulated carrier. The line-to-line voltage across the load will have most of its ripple at a frequency of twice the switching frequency, and will have a spectrum with

minimum even harmonics and no significant component below twice the switching frequency. Motor ripple current is therefore low and motor losses are reduced.

There is a further advantage to be obtained from the high ratio of carrier to modulation frequency: by adding a small amount of modulation at the third harmonic frequency of the basic fundamental modulation frequency, the maximum line-to-line output voltage obtainable from the inverter can be increased, for the following reason. The effect of the third harmonic on the output voltage of each phase is to flatten the top of the waveform, thus allowing a higher amplitude of fundamental while still reaching a peak modulation of 100%. When the difference voltage between any two phases is measured, the third harmonic terms cancel, leaving a pure sinewave at the fundamental frequency. This allows the inverter output to deliver the same voltage as the mains input without any significant distortion, and thus to reduce insertion losses to virtually zero.

Overview of a practical system

The principles outlined above are applied to a typical system shown in Fig.3. The incoming a.c. mains is rectified and smoothed to produce about 300V and this is fed to the three-phase inverter via a current-sensing circuit. The inverter chops the d.c. to give 300V peak-to-peak PWM waves at 20kHz, each having low-frequency modulation of its mark-space ratio. The output of the inverter is filtered to remove the 20kHz carrier frequency, and the resultant sinewaves are fed to the a.c. motor.

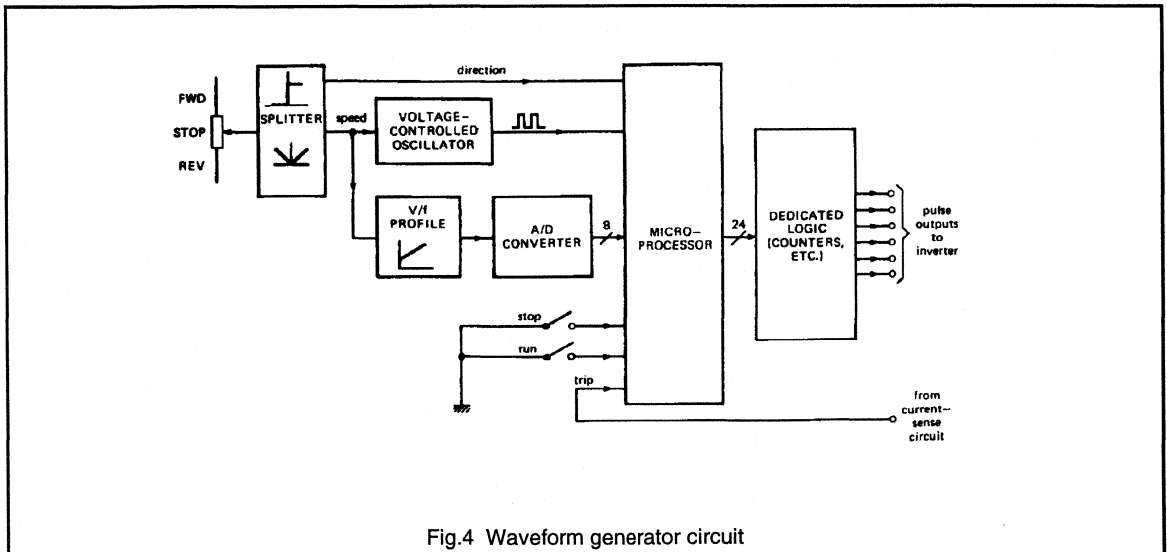


Fig.4 Waveform generator circuit

The six switches in the inverter are under the command of a waveform-generation circuit which determines the conduction time of each switch. Because the control terminals of the six switches are not at the same potential, the outputs of the waveform-generation circuits must be isolated and buffered. A low-voltage power supply feeds the signal processing circuit, and a further low-voltage power supply drives a switch-mode isolating stage to provide floating power supplies to the gate drive circuits.

Signal processing

Fig.4 shows a block diagram of the circuit which generates the PWM control signals for the inverter. The input to the system is a speed-demand voltage and this is also used for setting the required direction of rotation: the analogue speed signal is then separated from the digital direction signal. The speed-demand voltage sets the frequency of the voltage-controlled oscillator (VCO). Information to determine the modulation depth is derived from the speed-control signal by a simple non-linear circuit and is then converted by an analogue-to-digital converter into an 8-bit parallel digital signal.

A dedicated IC, type MAB8051, receives the clock signals from the VCO, the modulation-depth control number from the A/D converter, the direction-control logic signal, and logic inputs from the 'RUN' and 'STOP' switches. By applying digital multiplication processes to internal look-up table values, the microcomputer calculates the 'on-time' for each of the six power switches, and this process is repeated at regular intervals of 50µs, giving a carrier frequency of 20kHz. The pulses from the VCO are used for incrementing the pointers of the look-up table in the microcomputer, and thus control the motor speed.

The output signals of the microcomputer are in the form of three 8-bit parallel numbers: each representing the duty-ratio for the next 50µs switching cycle for one pair of inverter switches, on a scale which represents 0% to 100% on-time for the upper switch and therefore also 100% to 0% on-time for the complementary lower switch. A dedicated logic circuit applies these three numbers from the microcomputer to digital counters and converts each number to a pair of pulse-widths. The two signals produced for each phase are complementary except for a small 'underlap' delay. This delay is necessary to ensure that the switch being turned off recovers its blocking voltage before its partner is turned on, thus preventing 'shoot-through'.

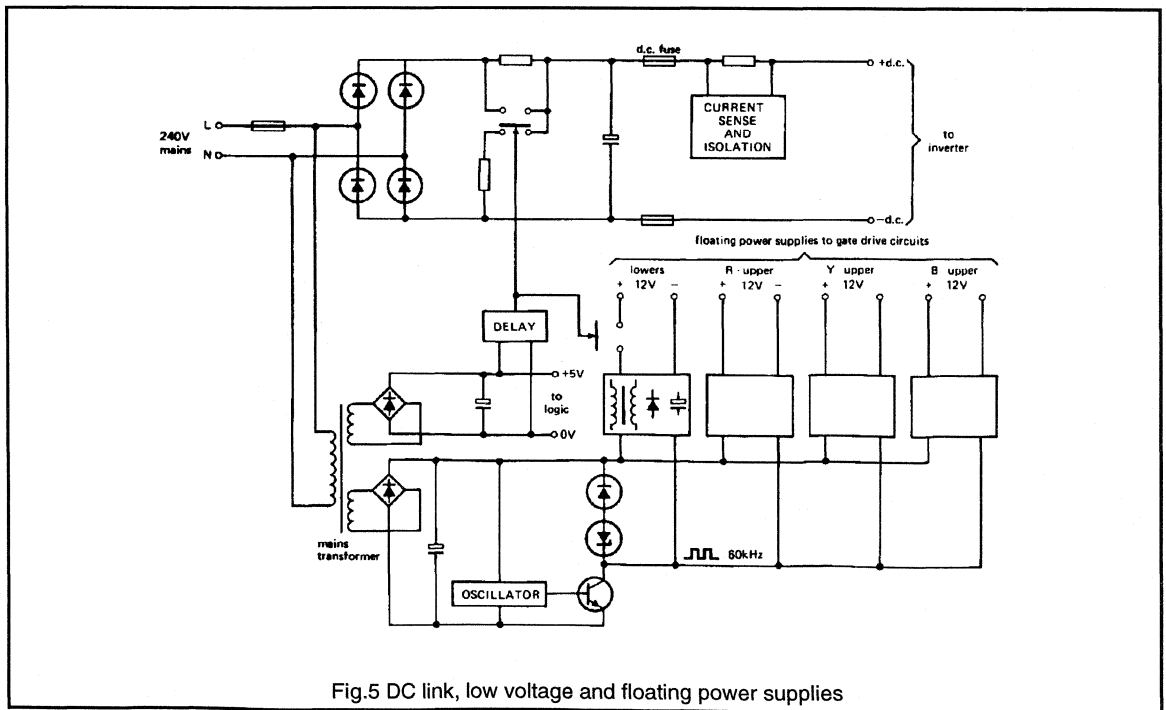


Fig.5 DC link, low voltage and floating power supplies

Other inputs to the microcomputer are the on/off switches, the motor direction logic signal, and the current-sensing signal. Each input triggers a processor interrupt, causing the appropriate action to be taken. The STOP switch and the overcurrent sense signals have the same effect, that of causing the microcomputer to instruct all six power switches in the inverter to turn off. The RUN switch causes the microcomputer to start producing output pulses. Any change in the direction signal first stops the microcomputer which then determines the new direction of rotation and adjusts its output phase rotation accordingly.

D.C. link and power supplies

The d.c. link and the low-voltage power supplies for the system are shown in Fig.5. The high voltage d.c. supply for the inverter is derived from a mains-fed bridge rectifier with a smoothing capacitor; the capacitor conducts both the 100Hz ripple from the rectified single-phase mains, and also the inverter switching ripple. A resistor, or alternatively a thermistor, limits the peak current in the rectifier while the capacitor is being charged initially. This resistor is shorted out by a relay after a time delay, so that the resistor does not dissipate power while the motor is running. As a safety measure, a second resistor discharges the d.c. link capacitor when the mains current is removed.

One of the d.c. link lines carries a low-value resistor to sense the d.c. link current. A simple opto-isolation circuit transmits a d.c. link current overload signal back to the signal processing circuit.

The logic circuitry of the waveform generator is powered conventionally by a 50Hz mains transformer, bridge rectifier, and smoothing capacitor. The transformer has two secondary windings; the second one provides power to a switched-mode power supply (SMPS), in which there is a switching transistor driven at about 60kHz to switch power through isolating transformers. Rectifying the a.c. outputs from the isolating transformers provides floating power supplies for the inverter gate drive circuits. As will be seen below, one supply is needed for the three 'lower' power switches (connected to a common d.c. link negative line), but three separate power supplies are needed for the three 'upper' switches (connected to the three inverter outputs). Thus four isolating transformers are required for the gate supply circuits. For low power systems the gate supplies can be derived directly from the d.c. link without excessive loss.

To prevent spurious turn-on of any inverter switch during the start-up process, the floating power supply to the lower three gate-drive circuits is connected only after a delay. The same delay is used for this as is used for the d.c. link charging-resistor bypass switch.

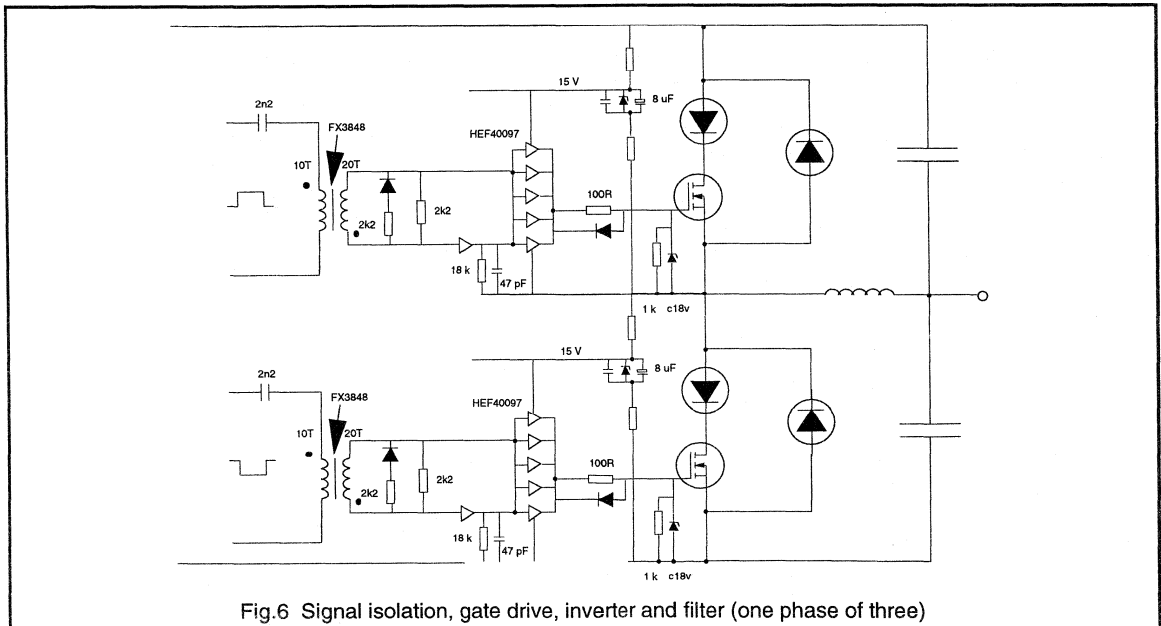


Fig.6 Signal isolation, gate drive, inverter and filter (one phase of three)

Signal isolation, gate drive, and inverter

The most important part of the system is the power inverter and it is the use of MOSFETs, with their short switching times, which makes it possible for the inverter to switch at 20kHz. It is in the area of the drive circuits to the power switches that using MOSFETs gives a saving in the number of components needed. Driving MOSFETs is relatively easy: the total power needed is very small because all that must be provided is the capability to charge and discharge the gate-source capacitance (typically between 1 and 2nF) by a few volts in a short time (less than 100ns). This ensures that the quality of the waveform is not degraded, and that switching losses are minimised.

In this circuit the six pulse outputs from the dedicated logic part of the waveform generator section are coupled to the MOSFET gate driver stages via pulse transformers. (see Fig.6). Each gate drive circuit is powered from one of the four floating power supplies described above. The three 'lower' stages share a common power supply, as the source terminals of the three 'lower' MOSFETs are all at the same potential. Each of the three 'upper' stages has its own floating power supply. The isolated signals are coupled to the gate terminals of the six MOSFETs by small amplifiers capable of delivering a few amperes peak current for a short time. Alternative gate driver circuits may use level shifting devices or opto-couplers. (Refer to "Power MOSFET Gate Drive Circuits" for further details.)

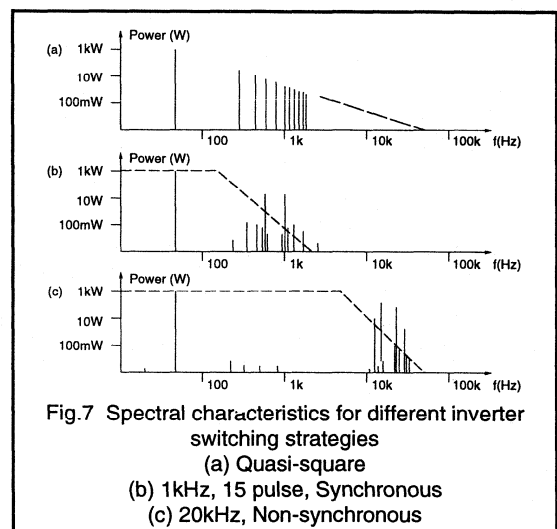
It will be seen from Fig.6 that each MOSFET has two associated diodes. These are necessary because the MOSFETs have built-in anti-parallel diodes with relatively long reverse-recovery times. If these internal diodes were allowed to conduct, then whenever load current commutated from a diode to the opposite MOSFET, a large current would be drawn from the d.c. supply for the duration of the diode reverse-recovery time. This would greatly increase the dissipation in the inverter. To avoid this, an external fast epitaxial diode is connected in anti-parallel with the MOSFET. Because the internal diode of the MOSFET has a very low forward voltage drop, a second low-voltage epitaxial diode must be connected in series with each MOSFET to prevent the internal diode from conducting at all. Thus, whenever the MOSFET is reverse-biased, it is the external anti-parallel diode which conducts, rather than the internal one. FREDFETs have internal diodes which are much faster than those of MOSFETs, opening the way for a further cost-saving by omitting the twelve diodes from the 3-phase inverter.

Output low-pass filter

For conventional, lower frequency inverters the size, weight and cost of output filter stages has held back their proliferation. An advantage of the constant high carrier frequency is that a small, economical low-pass filter can be designed to remove the carrier from the inverter output

waveform. Compared with low frequency systems the filter component has been reduced by an order of magnitude, and can often be eliminated completely. In unfiltered systems cable screening becomes an important issue although on balance the increased cost of screening is less than the cost and weight of filter components.

A typical filter arrangement was shown in Fig.6. As an example, for a 50Hz motor-drive the filter would be designed with a corner-frequency of 100Hz, so that the attenuation at 20kHz would be about 46dB. The carrier frequency component superimposed on the output sinewave would therefore be only a few mV in 200Vrms. Fig.7 shows the relative spectral characteristics of different types of inverter switching strategies.



There are two main advantages in supplying the motor with pure sinewave power. First, the motor losses are small, because there is no rms motor current at the switching frequency, and second, there is less radio-frequency interference (RFI), because the switching frequency current components circulate entirely within the inverter and filter and do not reach the outside world.

Advantages of a 20 kHz system

The principal advantages of the system described here are:

- Controller and motor are acoustically quiet.
- PWM waveform is simple and thus easy to generate.
- Output filter for removal of carrier is economic.
- RFI is low because of output filter.
- No snubbers are required on power devices.
- High efficiency is easily obtainable.
- No insertion loss.

3.1.2 The Effect of a MOSFET's Peak to Average Current Rating on Inverter Efficiency

The control of induction motors using a synthesised sine wave generated using pulse width modulation (PWM) control is becoming increasingly popular. The peak current requirement of switches used for the inverter bridge is based on the maximum current when the output is short circuited. The overcurrent during a short circuit fault is limited by an inductor connected in series with the switches. There is therefore a trade off between the peak current carrying capability of the switch and the size of the inductor. It is demonstrated in this note that the efficiency of the circuit during normal operation of the inverter is affected by the size of this choke. The ratio of peak to average current carrying capability of Philips Powermos is typically about four. This compares favourably with the typical ratio of Insulated Gate Bipolar Transistors (IGBTs) which is about three.

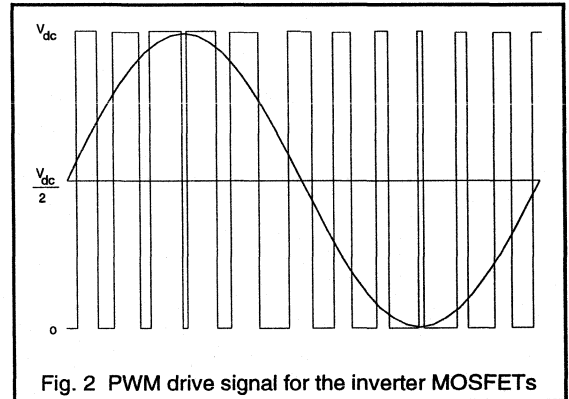


Fig. 2 PWM drive signal for the inverter MOSFETs

If the output of the inverter is short circuited there will be a rapid rise of current in the switches. To limit this peak current an inductor, L_s is often connected in each leg of the inverter as shown in Fig 3. The rate of rise of current under short circuit conditions, is then given in equation 1.

$$\frac{dI_T}{dt} = \frac{V_D}{L_s} \tag{1}$$

A simplified diagram of the inverter and the windings of the induction motor is shown in Fig. 1. The MOSFETs are driven with a PWM signal as shown in Fig. 2. The voltages at the outputs of each leg of the inverter are smoothed using a low pass filter and the inductance of the motor windings. The system has the following advantages; it uses an induction motor which is relatively cheap and maintenance free and it has the facility for 0 to 100% speed control. The near perfect sine waves generated by the PWM technique produce a smooth torque, audible noise is reduced and filtering is made easier since MOSFETs make possible the use of switching frequencies above 20 kHz.

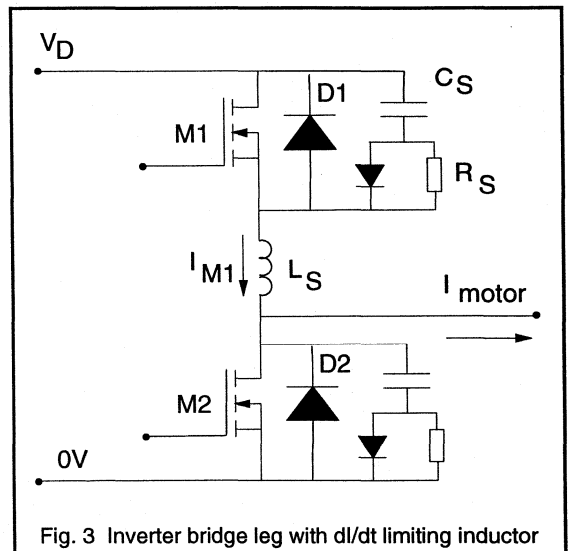


Fig. 3 Inverter bridge leg with di/dt limiting inductor

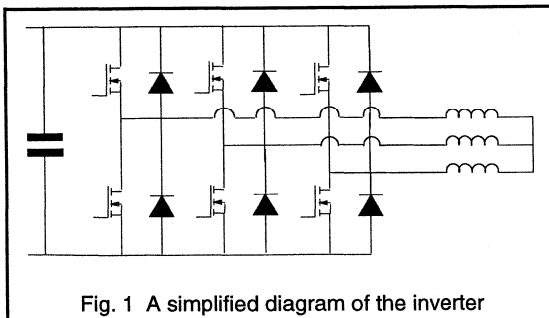


Fig. 1 A simplified diagram of the inverter

When the MOSFETs turn this fault current (I_{sc}) off the energy in the inductor is transferred to a snubber capacitor, C_s . The overvoltage across the MOSFETs is given by equation 2.

$$V = \sqrt{\frac{L_s}{C_s}} \cdot I_{sc} \quad (2)$$

The presence of inductor L_s affects the normal operation of the inverter. When the MOSFET M1 in Fig. 3 turns off the diode D2 does not turn on until the voltage across C_s is equal to the d.c. link voltage, V_D . If the diode did turn on then the rate of rise of current in L_s would be given by equation 3.

$$\frac{dI_{M1}}{dt} = \frac{V_D - V_{CS} - V_{diode}}{L_s} \quad (3)$$

This would be greater than the rate of rise of motor current so $I_{M1} > I_{motor}$ and the diode would have to conduct in the reverse direction, which is clearly not possible.

During the time when the capacitor C_s is charging up to V_D , the voltage across L_s will always be such as to increase the current in the bottom MOSFET, I_{M1} . When $V_{CS} = V_D$ the voltage across L_s will reverse and I_{M1} will fall. Diode D2 will now turn on. The energy stored in L_s will now be transferred to C_s . This energy will subsequently be dissipated in R_s and the MOSFET.

If the ratio of peak to average current carrying capability of the switch is large then it follows from equation 1 that L_s can be made smaller. This reduces the energy that is

transferred to C_s when the MOSFETs switch off during normal operation. Hence the efficiency of the inverter is improved.

The short circuit fault current can be limited by connecting an inductor in the d.c. link as shown in Fig. 4. In this case analysis similar to that outlined above shows that the excellent ratio of peak to average current carrying capability of Philips Powermos again reduces the losses in the inverter. It has been shown that components chosen to ensure safe shutdown of inverters for motor drives can have deleterious effects on the efficiency of the inverter. In particular the addition of an inductor to limit the peak current through the semiconductor switches when the output is short circuited can increase the switching losses. The high peak to average current carrying capability of Philips Powermos reduces the size of this choke and the losses it causes.

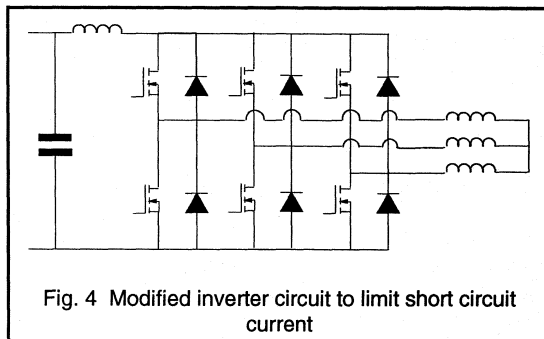


Fig. 4 Modified inverter circuit to limit short circuit current

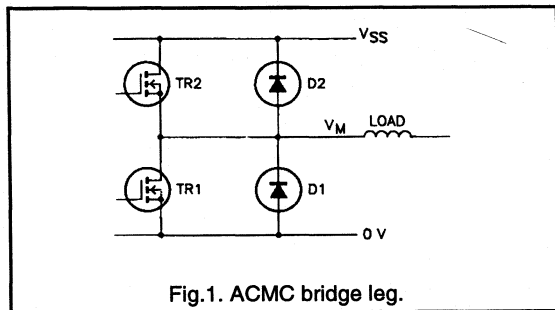
3.1.3 MOSFETs and FREDFETs for Motor Drive Equipment

The paper discusses the properties of the FREDFET, a technology which yields a MOSFET with a very fast built-in reverse diode with properties similar to a discrete fast epitaxial rectifier. It is shown that its characteristics make the device an excellent choice for high frequency bridge leg systems such as 20 kHz AC motor control systems.

Investigations have been carried out in dedicated test circuits as well as in a 20 kHz ACMC system which show that the FREDFET exhibits very low diode losses. It compares favorably with a discrete solution, using two extra diodes to overcome the slow speed of the standard built-in diode, and also with devices from the present standard ranges.

Introduction

The Power MOSFET has inherent in its structure a large built-in diode which is present between the source and drain of the device. Under single switch applications such as forward and flyback converters, this diode isn't forward biased and consequently its presence can be ignored. In the case of bridge legs, however, this diode is forced into forward conduction and the properties of the diode become of prime importance. The reverse recovery of the built-in diode is relatively slow when compared with discrete fast recovery epitaxial diodes (FRED's). As a consequence, the currents flowing through the MOSFET and its diode can be high and the losses considerable.

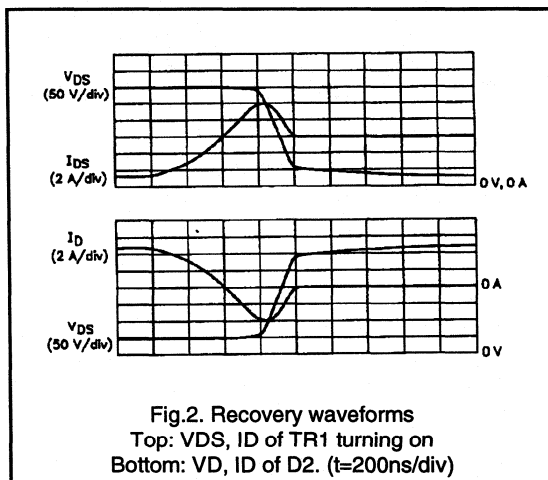


These losses can be reduced through the application of two extra diodes as discussed in section 2. A more elegant solution is a MOSFET with a built-in diode which exhibits properties similar to discrete fast epitaxial rectifiers. The FREDFET has been designed to satisfy this requirement. This paper presents the results of studies, carried out with new FREDFETs, comparing them with both the conventional MOSFET and the discrete solution.

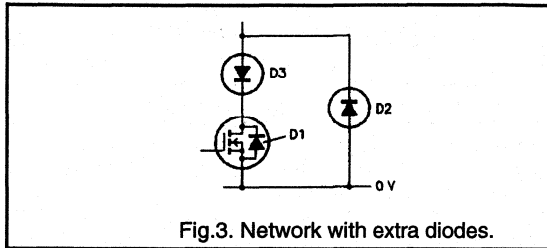
MOSFETs in half bridge circuits

MOSFETs have gained popularity in high frequency AC motor controllers, since they enable frequencies above 20kHz to be used. The short on-times required in ACMC systems make the use of bipolar devices very difficult, due to the storage times. Both the short switching times and the ease of drive of the MOSFET are essential ingredients in the design of an ultrasonic ACMC. Difficulties can arise, however, when trying to use the built-in source to drain diode of the MOSFETs.

One bridge leg of an ACMC is shown in Fig. 1. When current is flowing out of the load, MOSFET T1 and freewheel diode D2 conduct alternately. Conversely, when flowing into the load, the current alternates between TR2 and D1. Consider the case when current is being delivered by the load, such that the pair TR1/D2 carries the current. When the MOSFET conducts current, the voltage at the drain is almost zero and the diode blocks. When the MOSFET is turned off by the drive circuit, the inductive load forces the voltage to increase making diode D2 conductive. Associated with conduction of the diode is a volume of stored charge which must be removed as the MOSFET TR1 returns to its on-state.

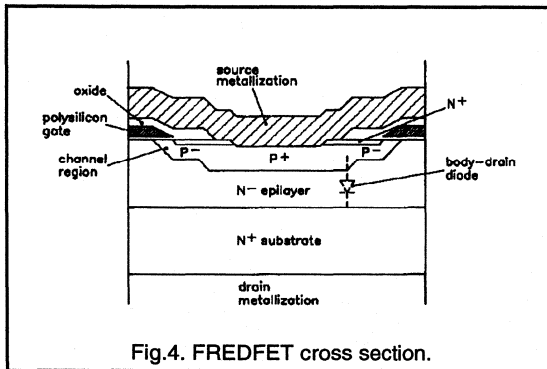


The waveforms appropriate to this situation can be found in Fig.2. One may observe that during the diode recovery time, the voltage across the MOSFET remains high whilst at the same time its current increases rapidly. Temporarily the drain current will increase to a level higher than the load current since the diode recovery current is added to it. Long recovery times and excessive charge storage result in a very high power dissipation in the MOSFET.



Using the inherent source drain diode of a conventional MOSFET as the freewheel diode results in considerable losses, since it is not optimised for fast switching or low stored charge. To avoid such losses the internal diode is usually deactivated by means of a special circuit (see Fig.3). This circuit, using two diodes D2 and D3, ensures that all freewheel current is flowing through the external diode D2 and not through the internal diode D1. When the MOSFET is switched on, the current flows via D3. This circuit is required for each MOSFET in the bridge. The FREDFET, which has a fast built-in diode offers the prospect of a much neater solution for these kind of circuits.

Technology of the FREDFET



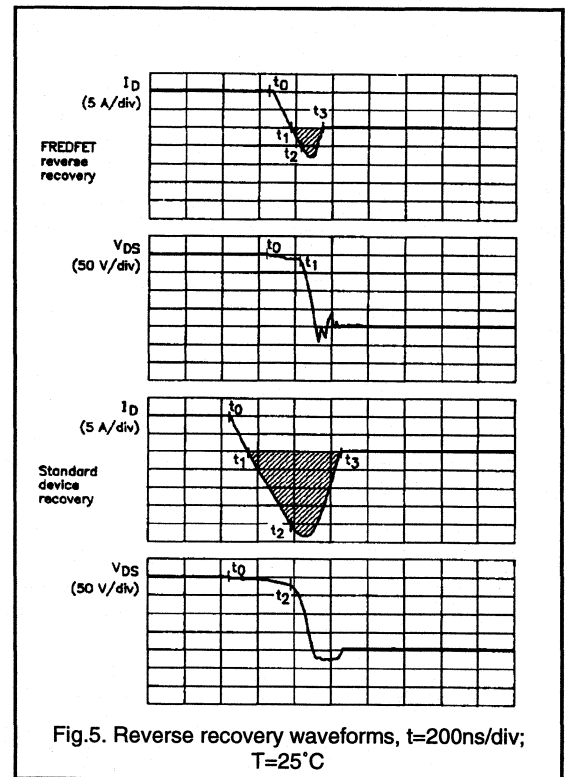
The power MOSFET is a majority carrier device and features fast turn-on and, in particular, fast turn-off. There are no charge storage effects such as in bipolar devices. In bridge leg applications the internal diode can become forward biased and the N- epitaxial region (see Fig.4) is flooded with holes, which must later be removed when the source becomes negatively biased again with respect to the drain.

The stored charge can be removed by holes diffusing from the N- epilayer into the P+ and P-body regions, and also by recombination of holes and electrons in the N- epitaxial region. A significant reduction in the stored charge Q_{rr} can be achieved by doping the devices with heavy metal atoms to introduce recombination centres. A standard MOSFET will normally have a low concentration of recombination

centres. In the FREDFET the heavy metal doping does not have any significant effects on the threshold voltage or the transconductance, however, the efficiency with which the extra recombination centres remove the stored charge is improved substantially. This can be observed when comparing Q_{rr} and t_r results for killed and non-killed devices as described in the next section.

FREDFET measurements

A comparison of the reverse recovery characteristics of the internal diode has been made for a BUK637-500B FREDFET and a similar competitor conventional MOSFET. The devices were tested using an 'LEM 20 A Q_{rr} ' gear.



Oscillograms are presented in fig.5. showing the test waveforms for both the FREDFET and the conventional device. The diode turn-off process commences at $t=t_0$, where upon the forward current (set at 10A) is reduced at a preset 100A/usec. The current falls through zero and the diode passes into reverse conduction signifying the removal of stored charge. At $t=t_2$ sufficient charge has been removed for the formation of a depletion layer across the p-n junction. The dI/dt starts to fall and a voltage builds across an inductance in the source circuit such that the source becomes negatively biased with respect to drain.

Beyond t_2 the di/dt reverses and the diode current begins to fall as the drain-source voltage rises to the clamp setting. The moment t_3 identifies the point at which the diode current has fallen to 10% of its peak value, I_{rrm} .

The reverse recovery time, t_{rr} is defined as t_3-t_1 while the total stored charge Q_{rr} is equal to the area of the shaded region, fig.5. A direct comparison of the diode reverse recovery at 25°C is shown in fig.6. The respective values for t_{rr} , Q_{rr} and I_{rrm} are presented in Table 1.

$T_j = 25^\circ\text{C}$	t_{rr} (ns)	Q_{rr} (uC)	I_{rrm} (A)
BUK637-500B	193	1.2	8
Conventional device	492	7.5	23

Table 1.

It can be seen that Q_{rr} is 84 % lower for the FREDFET while I_{rrm} and t_{rr} approximately 60 % less. Fig.7 shows the same comparison measured at a junction temperature of 150°C. Corresponding values of t_{rr} , Q_{rr} and I_{rrm} are shown in Table 2.

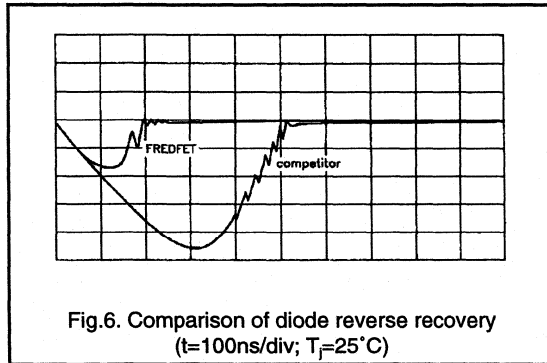


Fig.6. Comparison of diode reverse recovery ($t=100\text{ns/div}$; $T_j=25^\circ\text{C}$)

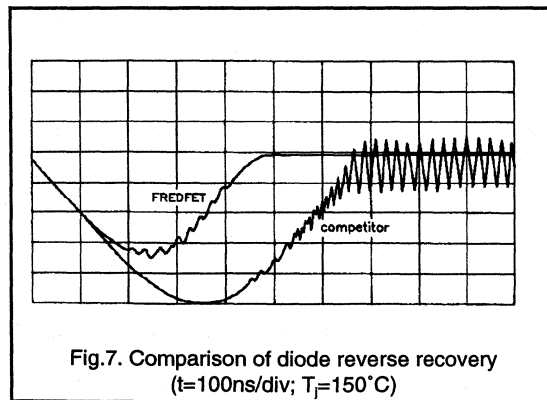


Fig.7. Comparison of diode reverse recovery ($t=100\text{ns/div}$; $T_j=150^\circ\text{C}$)

$T_j = 150^\circ\text{C}$	t_{rr} (ns)	Q_{rr} (uC)	I_{rrm} (A)
BUK637-500B	450	4.5	17
Conventional device	650	10.5	26

Table 2.

While higher temperatures are known to reduce the effectiveness of recombination centres, it is clear that significant improvements still exist even at the peak junction temperature with savings of 55 % in Q_{rr} and over 30 % in I_{rrm} and t_{rr} evident for the FREDFET

Performance in a bridge circuit

The circuit of Fig.8 is a simplified representation of a bridge circuit, and was used to evaluate the performance of the BUK637-500B FREDFET against a conventional MOSFET and a conventional MOSFET configured with both series and parallel diodes.

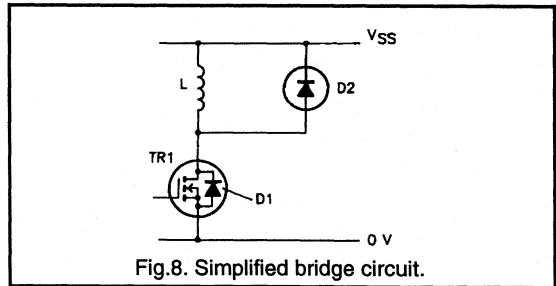
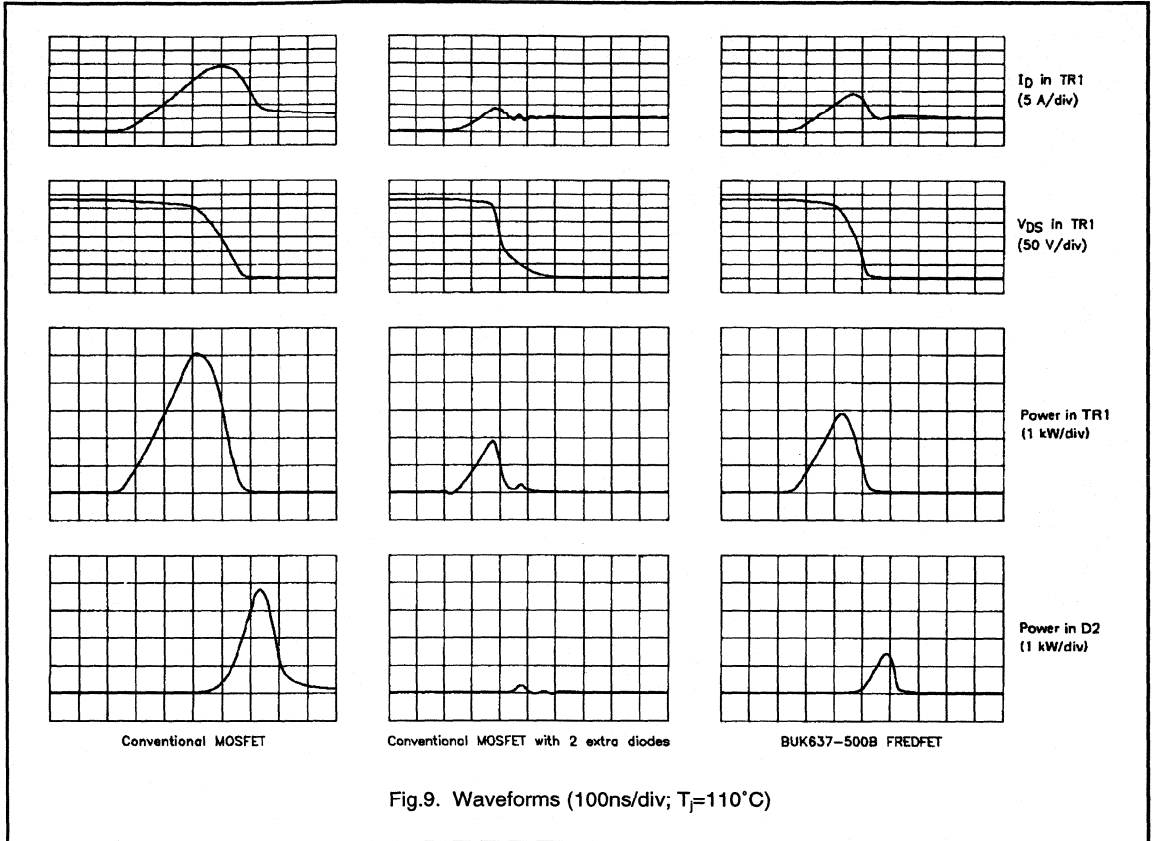


Fig.8. Simplified bridge circuit.

In each case the MOSFET in the bottom leg was switched on until the load current reached the desired value, at which point it was switched off, forcing the load current to flywheel through the inverse diode of the upper leg. The lower device was then switched on again to obtain reverse recovery of the upper diode. The current levels were set to simulate the conditions found in a 20 kHz 1 kVA ACMC. The device in the upper leg was mounted on a temperature controlled heatsink and the test was performed at very low duty cycle such that T_{case} approximated to T_j .

Oscillograms of current and voltage in relation to the lower leg are shown for the conventional device, conventional device plus external diodes and the FREDFET in Fig.9. The freewheel current in the upper diode is related to current in the MOSFET as shown in Fig.2. Also presented are the power waveforms for both the upper and lower legs in each case.



The superior performance of the FREDFET when compared to the conventional device is clear with the current overshoot kept to below 8 A compared to over 18 A using the latter. The lower reverse recovery current and faster trr are reflected in the power waveforms with nearly double the peak power being dissipated in the lower leg using a conventional device compared to that dissipated using the FREDFET. The power dissipated by the internal diode of the FREDFET is also observed to be remarkably reduced in comparison with the conventional MOSFET.

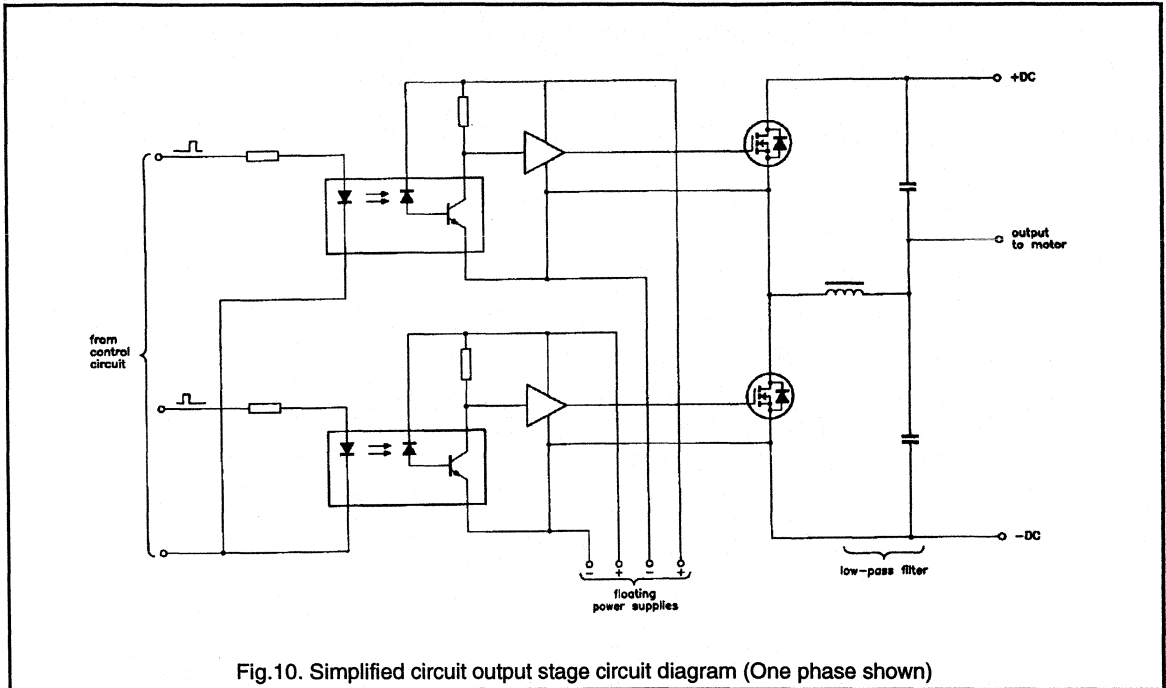
The performance of the three device implementations is summarised in table 3 which shows the total energy dissipated during switching in both legs for each case.

It can be seen that using a conventional MOSFET without the external diode circuitry involves a six fold increase in the energy dissipated in the MOSFET. However if a FREDFET implementation is used the turn-on energy is only a factor of two above the minimum achievable with the extra diodes. Energy loss in the diode itself is relatively small for both the FREDFET and the external diode configuration,

$T_j = 110^\circ\text{C}$	Energy Dissipated	
	Lower Leg (mJ)	Upper Leg (mJ)
Conventional MOSFET	1.2	0.533
MOSFET plus external diodes	0.2	0.035
BUK637-500B FREDFET	0.4	0.095

Table 3.

being less than 25 % that dissipated in the lower leg. For the conventional device the diode loss is more significant, equal to 44 % of the power dissipated during turn-on in the lower leg. The energy value presented above represent only the losses during turn-on, in addition to these are the on-state losses which for the external diode configuration include the extra power dissipated by the series diode.



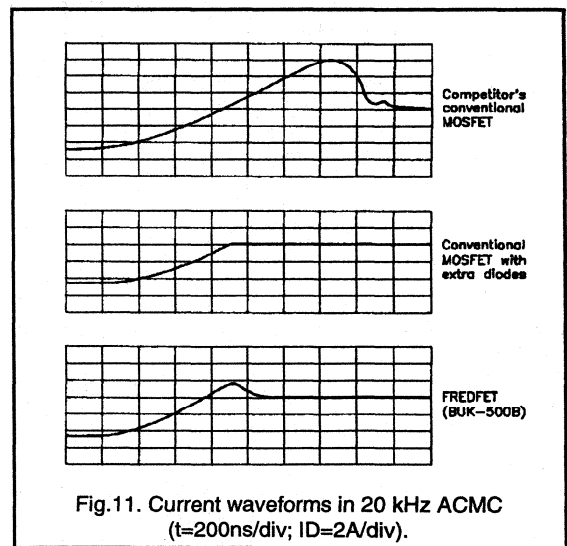
20 kHz ACMC with FREDFETS

The three device options discussed above have each been implemented in a 20 kHz AC Motor Control circuit. The inverter provides a three phase 1 kVA output from a single phase mains input. A simplified diagram of one of the output stages is presented in Fig.10.

Figure 11 shows the current waveforms as the load current commutates from the upper leg (anti-parallel diode in conduction) to the lower leg (turn-on of the MOSFET) for each device option. In each case the load current is 4.5 A. Fig.11a illustrates the large overshoot current obtained with a conventional device while Fig.11b shows what is achieved when the two external diodes are incorporated. Finally Fig.11c shows the current waveform for the FREDFET implementation where the current overshoot is kept below 1.5 A by the built-in fast recovery diode of the device.

Conclusions

It has been shown that the FREDFET compares favorably in ACMC systems compared with the standard MOSFET. The normally employed extra diodes can be omitted thus saving considerable costs in the system. The fast internal diode is seen to be comparable with the normally used fast epitaxial rectifiers and enables a simple ultrasonic ACMC.





3.1.4 A Designers Guide to PowerMOS Devices for Motor Control

This section is intended to be used as a designers guide to the use and selection of power MOSFETS and FREDFETS in a.c. motor control (ACMC) applications. It is particularly concerned with the variable speed operation of induction motors using pulse width modulation (PWM) techniques. One of the most important considerations in the design of ACMC inverters is the optimum choice of power switching device and heatsinking arrangement. Other factors which relate to the losses in the power switch are switching speed and design of suitable gate drive circuits. This section addresses each of these factors and presents a series of design graphs relating system operating temperature to device type and heatsink size for systems rated up to 2.2kW and operated from a single phase supply.

It should be noted that this article refers to some products which may not be available at this time.

Introduction

Variable speed control of induction motors is a widespread requirement in both industrial and domestic applications. The advantages of an induction motor drive over alternative systems such as d.c. motor controllers include:

- high reliability and long life
- low maintenance requirements
- brushless operation
- availability of standard machines.

With the advent of power switching devices able to provide the required ratings for ACMC applications and the availability of fast PWM pattern generation circuits these advantages have lead to an increasing number of applications where the inverter-fed induction motor system produces a cost effective drive. Before considering in detail the use of MOSFETs and FREDFETs in ACMC inverters it is worth briefly considering the principles and operation of the induction motor, the PWM method of voltage control and the characteristics of the switching devices.

The induction motor

Induction motors are three phase machines where the speed of rotation of the stator field (the synchronous speed, N_s) is determined by the number of poles, p , and the frequency of the applied voltage waveforms, f_s .

$$N_s = \frac{120 \cdot f_s}{p} \quad (\text{rpm}) \quad (1)$$

Torque production in an induction motor is due to the interaction of the rotating stator field and currents in the rotor conductors. Torque is developed when the rotor speed 'slips' behind the synchronous speed of the stator travelling field. Fig.1 shows the torque-speed characteristic of an induction motor where ω_s is the speed of the stator field ($\omega_s = 2\pi f_s$) and ω_r is the rotor speed. The difference between the two is usually relatively small and is the slip speed. In this region the rotor speed is approximately proportional to the stator supply frequency, except at very low speeds. The operating point of the motor on its torque-speed characteristic is at the intersection of the load torque line and the motor characteristic. For small amounts of slip and at constant airgap flux the motor torque is proportional to the slip speed.

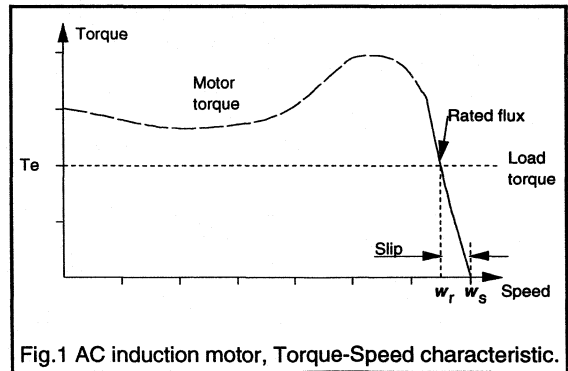


Fig.1 AC induction motor, Torque-Speed characteristic.

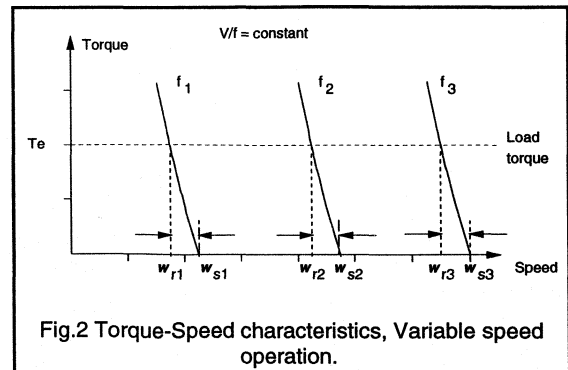


Fig.2 Torque-Speed characteristics, Variable speed operation.

In a variable speed system the motor is operated on a series of torque-speed characteristics as the applied frequency is increased. Fig.2 shows a set of characteristics for three conditions, ω_{s1} , ω_{s2} and ω_{s3} . The corresponding rotor speeds are ω_{r1} , ω_{r2} and ω_{r3} . However in order that the airgap flux in the motor is maintained at its rated value then the applied voltage must be reduced in proportion to the applied frequency of the travelling field. This condition for constant airgap flux gives the constant v/f requirement for variable speed control of a.c. induction motors. At low speeds this requirement may be modified by voltage boosting the supply to the motor in order to overcome the increased proportion of 'IR' voltage drop in the motor windings which occurs at low speeds.

The PWM Inverter

A variable voltage, variable frequency three phase supply for the a.c. induction motor can be generated by the use of a pulse width modulated (PWM) inverter. A schematic diagram of the system is shown in Fig.3. The system consists of a rectified single phase a.c. supply, which is usually smoothed to provide the d.c. supply rails for the main switching devices. Alternate devices in each inverter leg are switched at a high carrier frequency in order to provide the applied voltage waveforms to the motor. During each switching cycle the motor current remains approximately constant due to the inductive nature of the AC motor load.

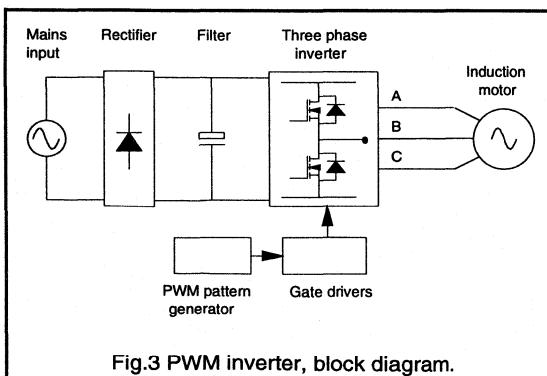


Fig.3 PWM inverter, block diagram.

In the circuit of Fig.3 the main switching devices are MOSFETs and each MOSFET has a freewheeling diode connected in antiparallel. The motor load current is determined by the circuit conditions. When the load current in a particular phase is flowing into the motor then conduction alternates between the top MOSFET and the bottom freewheel diode in that inverter leg. When the load current is flowing from the motor then the bottom MOSFET and top diode conduct alternately. Fig.4 shows a typical

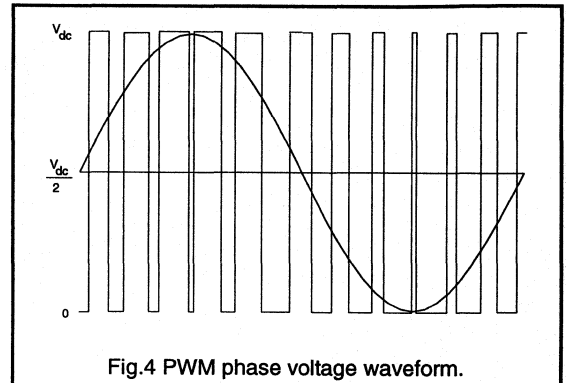


Fig.4 PWM phase voltage waveform.

sinusoidal PWM voltage waveform for one motor phase. The three phases are maintained at 120° relative to each other.

Both the frequency and amplitude of the fundamental component of the output voltage waveform can be varied by controlling the timing of the switching signals to the inverter devices. A dedicated i.c. is usually used to generate the switching signals in order to maintain the required v/f ratio for a particular system.⁽¹⁾ The PWM algorithm introduces a delay between the switching signal applied to the MOSFETs in each inverter leg which allows for the finite switching times of the devices and thus protects the system from shoot-through conditions.

Additional harmonic components of output voltage, such as the third harmonic, can be added to the PWM switching waveform.^(2,3) The effect of adding third harmonic to the output voltage waveform is to increase the amplitude of the fundamental component of output voltage from a fixed d.c. link voltage. This is shown in Fig.5. The third harmonic component of output phase voltage does not appear in the output line voltage due to the voltage cancellation which occurs in a balanced three phase system. Using this technique it is possible to obtain an output line voltage at the motor terminals which is nearly equal to the voltage of the single phase supply to the system.

For many applications the PWM ACDC system is operated at switching speeds in the range 1kHz to 20kHz and above. Operation at ultrasonic frequencies has advantages that the audible noise and RFI interference are considerably reduced. The advantages of PowerMOS devices over bipolar switching devices are most significant at these switching speeds due to the low switching times of PowerMOS devices. Additional advantages include good overload capability and the fact that snubber circuits are not usually required. It is usually straightforward to operate PowerMOS devices in parallel to achieve higher system currents than can be achieved with single devices. This is because the devices have a positive temperature coefficient of resistance and so share the load current

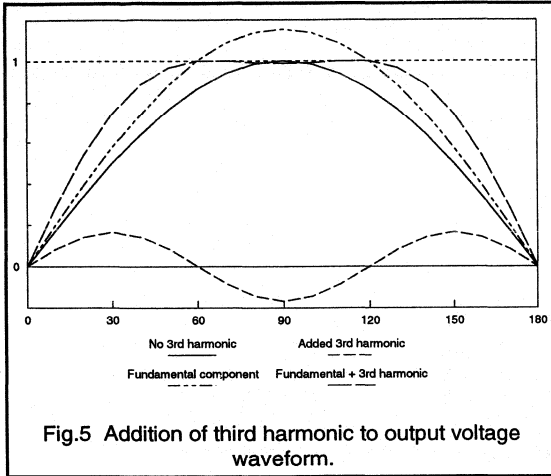


Fig.5 Addition of third harmonic to output voltage waveform.

equally. The simple gate drive requirements of PowerMOS devices means that a single gate circuit can often be used for a range of devices without modification.

MOSFETs and FREDFETs in AC/DC

One of the features associated with the transfer of conduction between the switching devices and the freewheel diodes in an inverter circuit is the reverse recovery of the freewheel diode as each conducting MOSFET returns to its on-state. Reverse recovery current flows due to the removal of stored charge from a diode following conduction. Fig.6 shows the device current paths in an inverter leg when conduction is transferred from the top diode to the bottom MOSFET.

The switching waveforms are shown in Fig.7 where the diode reverse recovery current is I_{rr} and the time taken for the reverse recovery currents to be cleared is t_{rr} . The amount of stored charge removed from the body of the diode is represented by the area Q_{rr} . The reverse recovery current flows through the MOSFET which is being turned on in addition to the load current and thus causes additional turn-on losses. The amount of stored charge increases with increasing temperature for a given diode. Both the magnitude of the reverse recovery current and its duration must be reduced in order to reduce the switching losses of the system.

This effect is important because inherent in the structure of a power MOSFET is a diode between the source and drain of the device which can act as a freewheeling diode in an inverter bridge circuit. The characteristics of this diode are not particularly suited to its use as a freewheel diode due to its excessive charge storage and long recovery time. These would lead to large losses and overcurrents during the MOSFET turn-on cycle.

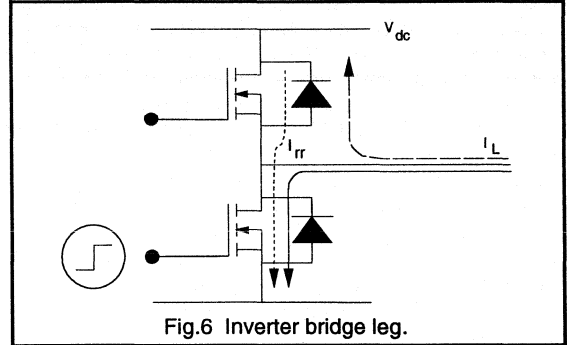


Fig.6 Inverter bridge leg.

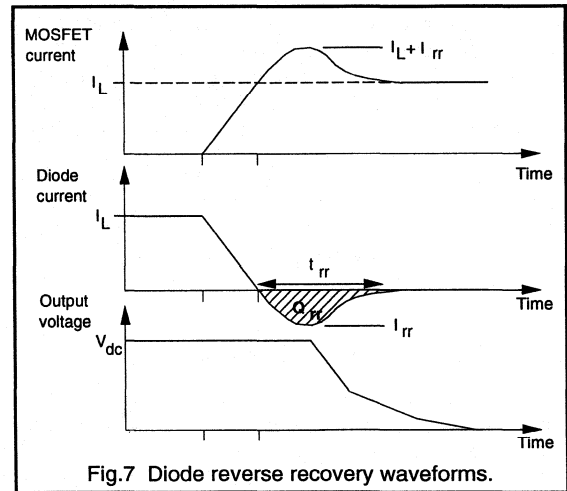


Fig.7 Diode reverse recovery waveforms.

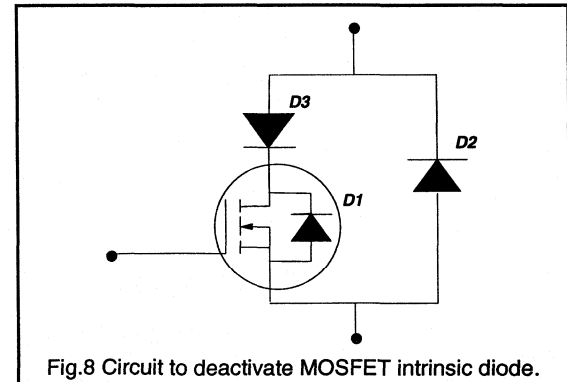


Fig.8 Circuit to deactivate MOSFET intrinsic diode.

In inverter applications the internal diode of a MOSFET is usually deactivated by the circuit of Fig.8. Conduction by the internal MOSFET diode is blocked by the series Schottky diode (D3). This series device must carry all the MOSFET current and so contributes to the total conduction losses. The external diode, usually a fast recovery epitaxial

diode (FRED), carries the freewheel current. This device is chosen such that its low values of I_{rr} and t_{rr} reduce the overall switching losses. The FREDFET is essentially a MOSFET with a very fast built-in diode, and hence can replace the network of Fig.8 with a single device giving a very compact APMC inverter design using only six power switches.⁽⁴⁾ The reverse recovery properties of a FREDFET diode are similar to those of a discrete FRED thus giving a considerably neater circuit without any loss in switching performance.

APMC design considerations

Voltage rating

The first selection criteria for a PowerMOS device in an inverter application is the voltage rating. For a 240V a.c. single phase supply the peak voltage is 340V. Assuming that the rectifier filter removes the voltage ripple components which occur at twice the mains frequency, and dependent on the values of the filter components and rectifier conduction voltage, then the dc link voltage will be around 320V. Devices with a voltage rating of 500V will allow sufficient capability for transient overvoltages to be well within the capability of the device. Thus the dc link voltage is given by:

$$V_{dc} = \sqrt{2} \cdot V_{ac} \quad (2)$$

where V_{ac} is the rms ac input line voltage.

The output phase voltage, shown in Fig.4, switches between the positive and negative inverter rail voltages. The mean value of the output voltage is $V_{dc}/2$. Neglecting the delays which occur due to the finite switching times of the devices then the maximum rms output phase voltage is given by:

$$V_{ph} = \frac{1}{\sqrt{2}} \cdot \frac{V_{dc}}{2} \quad (3)$$

and hence the rms output line voltage is:

$$V_{line} = \sqrt{3} \cdot V_{ph} = \sqrt{3} \cdot \frac{V_{dc}}{2 \cdot \sqrt{2}} \quad (4)$$

Comparing equations (2) and (4) shows that:

$$V_{line} = 0.866 \cdot V_{ac} \quad (5)$$

This shows that the fundamental rms line output voltage is 13% less than the rms ac input voltage. Adding third harmonic to the PWM output waveform can restore this rms output voltage to the ac input voltage. In a practical system the effect of switching delays and device conduction voltages can reduce the output voltage by upto 10-15%.

Current rating

The nameplate rating of an induction motor is usually quoted in terms of its power (W) and power factor (cosφ). The VA requirement of the inverter is found from the simple equation:

$$\text{Power(W)} = \eta \cdot \cos\phi \cdot VA \quad (6)$$

where η is the efficiency. In terms of the rms motor line voltage (V_{line}) and output current (I_L):

$$VA = \sqrt{3} \cdot V_{line} \cdot I_L \quad (7)$$

The efficiency of small ac induction motors can be quite high but they usually run at quite poor power factors, even at rated conditions. For small induction motors (<2.2kW) the efficiency-power factor product is typically in the range 0.55 to 0.65. The exact value will vary from motor to motor and improves with increasing size. Thus from equations (6) and (7) it is possible to calculate the approximate rms current requirement. The peak device current for sinusoidal operation is given by equation (8). (NB. The devices will experience currents in excess of this value at switching instants.)

$$I_{max} = \sqrt{2} \cdot I_L \quad (8)$$

Device package

The device package chosen for a particular application will depend upon device rating, as discussed above, as well as circuit layout and heatsinking considerations. Philips PowerMOS devices are available in a range of package types to suit most applications.

Drive considerations

Unlike bipolar devices the MOSFET is a majority carrier device and so no minority carriers must be moved in and out of the device as it turns on and off. This gives the fast switching performance of MOSFET devices. During switching instants the only current which must be supplied by the gate drive is that required to charge and discharge the device capacitances. In order to switch the device quickly the gate driver must be able to rapidly sink and source currents of upto 1A. For high frequency systems the effect of good gate drive design to control switching times is important as the switching losses can be a significant proportion of the total system losses.

Fig.9 shows an equivalent circuit of the device with the simplest gate drive arrangement. The drain-source capacitance does not significantly affect the switching performance of the device. Temperature only has a small effect on the values of these capacitances and so the device switching times are essentially independent of temperature. The device capacitances, especially C_{GD} , vary with V_{DS} and this variation is plotted in data for all PowerMOS devices.

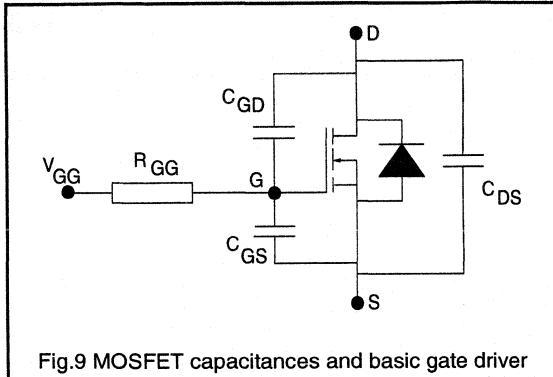


Fig.9 MOSFET capacitances and basic gate driver

Turn-on (Fig. 10)

A turn-on gate voltage pulse commences at t_0 . The gate voltage v_{GS} rises as current flows into the device via R_{GG} . C_{GS} starts to charge up until v_{GS} reaches its threshold value $v_{GS(To)}$ at time t_1 . The device is now operating in its active region with a relatively high power loss. The MOSFET current, rises as a function of $v_{GS} - v_{GS(To)}$ and causes a corresponding fall in the diode current. Thus the rate of fall of diode current, and hence the amount of diode reverse recovery current, is controllable by the rate of rise of v_{GS} . At time t_4 the diode has recovered and the MOSFET current is equal to the load current, I_L . V_{GS} is clamped to $v_{GS(IL)}$ and so the gate current is given by:

$$i_G = \frac{v_{GG} - v_{GS(IL)}}{R_{GG}} \quad (9)$$

This current flows through C_{GD} , discharging it and so the rate of fall of output voltage is given by:

$$\frac{dv_{DS}}{dt} = \frac{i_G}{C_{GD}} = \frac{(v_{GG} - v_{GS(IL)})}{R_{GG} \cdot C_{GD}} \quad (10)$$

The fall in v_{DS} commencing at time t_3 is not linear, principally because C_{GD} increases with reducing v_{DS} . At time t_5 C_{GD} is fully discharged and the device is on. The gate voltage continues to charge up to its final value, v_{GG} . It is usual to have a value of v_{GG} significantly higher than $v_{GS(IL)}$ because $r_{DS(on)}$ falls with increasing v_{GS} . Additionally a high value of v_{GG} speeds up the turn-on time of the device and provides some noise immunity.

Switching losses occur during the period t_1 to t_5 . The minimum turn-on time is usually governed by the dv/dt capability of the system. Reducing the turn-on time increases the amount of diode reverse recovery current and hence increases the peak power dissipation, however the total power dissipated tends to reduce.

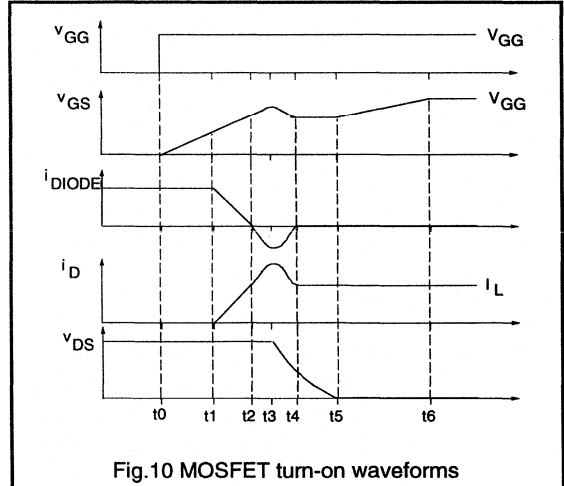


Fig.10 MOSFET turn-on waveforms

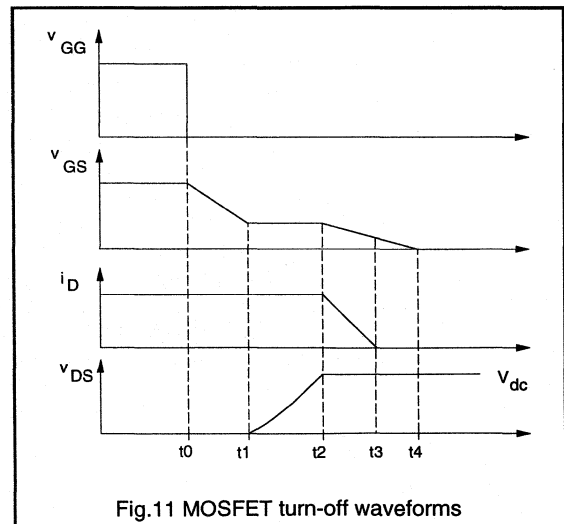


Fig.11 MOSFET turn-off waveforms

Turn-off (Fig. 11)

Unlike the conditions which occur at turn-on there is no interaction between the switching devices at turn-off. The switching waveforms are, therefore, relatively straightforward. The gate voltage is switched to ground or, if very fast turn-off is required, to a negative voltage. During the delay time t_0 to t_1 the gate voltage falls to the value required to maintain the output current, I_O . From time t_1 to t_2 the gate supply is sinking current and C_{GD} charges the drain up to the positive rail voltage. V_{GS} then continues to fall and so the device current falls between times t_2 and t_3 . At t_3 the gate voltage falls below its threshold value and the device turns off. The rate of rise of output voltage is:

$$\frac{dv_{DS}}{dt} = \frac{i_G}{C_{GD}} = \frac{v_{GS(LL)}}{R_{GG} \cdot C_{GD}} \quad (11)$$

Parasitic turn-on

In a high frequency system the device switching times are necessarily short and so the rates of change of inverter output voltage are high. The high values of dv/dt which occur when one device turns on can cause a sufficiently high voltage at the gate of the other device to also turn it on. The coupling occurs via C_{GD} and C_{GS} . If the rate of change of output voltage due to one device turning on is given by dv_{DS}/dt then the voltage that would be seen at the gate of the other device if it were left open circuit is:

$$\frac{dv_{GS}}{dt} = \frac{C_{GD}}{C_{GS} + C_{GD}} \cdot \frac{dv_{DS}}{dt} \quad (12)$$

If C_{GS} is shorted out by a zero impedance, then clearly dv_{GS}/dt can be reduced to zero. In practice achieving a zero impedance in the gate-source circuit is extremely difficult and dv_{GS}/dt will not be zero. In the worst case this rising gate voltage will turn the device fully on and a destructive shoot-through condition occur. If the conditions are less severe then the MOSFET may only turn on for a short period of time giving rise to an additional overcurrent in the turn-on cycle of the device being switched. Parasitic turn-on, as this effect is referred to, must be prevented by either limiting dv_{DS}/dt or by ensuring that v_{GS} is clamped off. In systems where the off-state gate-source voltage is negative then the possibility of parasitic turn-on can be reduced.

Gate drive circuits for ACMC inverters

The previous section discussed device switching waveforms using a resistive gate drive circuit. In this section various alternative gate drive circuits for ACMC applications are presented and compared. The discussion assumes that each MOSFET gate drive circuit is isolated and driven using a CMOS buffer capable of sinking and sourcing the required gate current. In unbuffered gate drive circuits the leakage inductance of an isolating pulse transformer can increase the gate impedance, thus reducing the maximum possible switching rate and making the MOSFET more susceptible to parasitic turn-on. A zener diode clamp protects the gate-source boundary from destructive overvoltages. Identical drivers are used for the top and bottom devices in each inverter leg. The gate drive circuits presented here were tested using BUK638-500A FREDFETS and BUK438-500A MOSFETS in a 20kHz, 2.2kW ACMC system.

Figure 12 shows the simplest arrangement which gives independent control of the turn-on and turn-off of the MOSFET. Increasing the gate impedance to reduce dv_{DS}/dt levels will raise the susceptibility to parasitic turn-on problems. The gate-source voltage can be clamped off

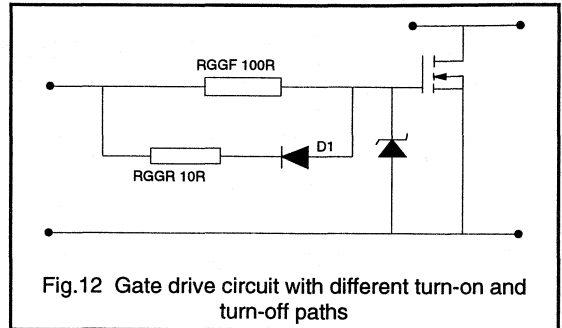


Fig.12 Gate drive circuit with different turn-on and turn-off paths

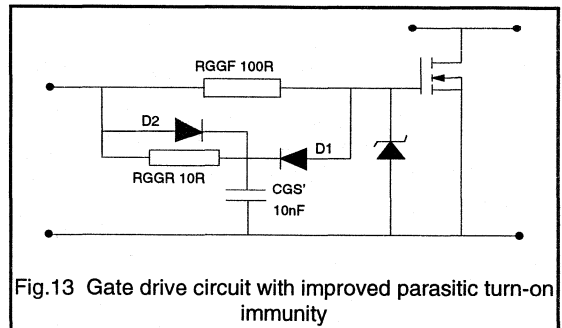


Fig.13 Gate drive circuit with improved parasitic turn-on immunity

more effectively if the dynamic impedance between gate and source is reduced as shown in the circuit of Fig.13. The additional gate-source capacitance ensures that v_{GS} does not rise excessively during conditions when parasitic turn-on could occur (Equation 12). The external capacitor C_{GS}' must be charged up at turn-on. If C_{GS}' is made too large then the current required may be beyond the rating of the drive buffer. The speed-up diode, D2, ensures that the turn-on is not compromised by C_{GS}' and R_{GG} . At turn off the additional capacitance slows down di/dt since the gate-source RC time constant is increased. It must be noted that one effect of the turn-off diode, D1, is to hold the off-state value of v_{GS} above 0V, and hence somewhat closer to the threshold voltage of the device.

An alternative circuit which may be used to hold the MOSFET off-state gate-source voltage below its threshold value is shown in Fig.14. The pnp transistor turns on if the gate-source voltage is pulled up via C_{GD} and C_{GS} and thus the device remains clamped off.

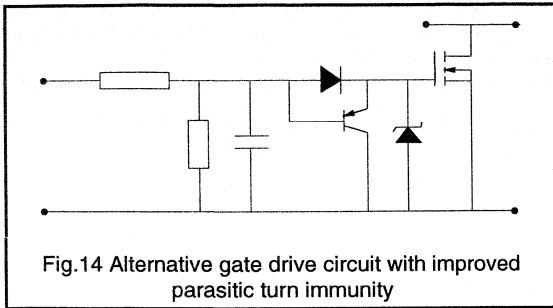


Fig. 14 Alternative gate drive circuit with improved parasitic turn immunity

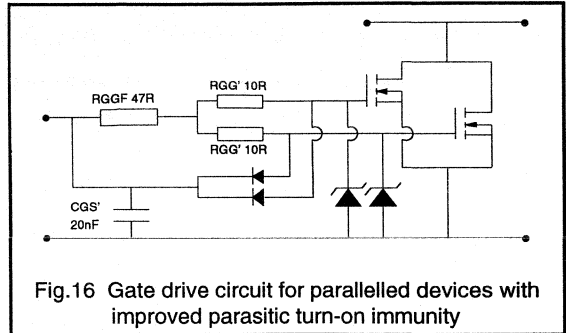


Fig. 16 Gate drive circuit for paralleled devices with improved parasitic turn-on immunity

Paralleling of PowerMOS devices

Moving to a system using paralleled MOSFETs requires only slight modifications to the gate drive circuit. One consideration may be the capability of the drive buffer to provide the currents required at the switching instants. The switching speed of the system can be maintained, using a lower impedance gate drive. It is recommended that small differential resistors, as shown in Fig. 15, are used to damp out any oscillations which may occur between the switching devices and the rest of the circuit. The circuit of Fig. 13 can be modified for operation with paralleled devices to that shown in Fig. 16.

Modelling of parasitic turn-on

Using the simple MOSFET model of Fig.9 it is possible to study the susceptibility to parasitic turn-on of alternative gate drive circuits. Considering the switching instant when the bottom MOSFET is held off and the top MOSFET is switched on, the voltage across the bottom MOSFET swings from the negative inverter rail to the positive one. The switching transient can be modelled by an imposed dv_{DS}/dt across C_{GD} and C_{GS} and hence the effect of gate circuit design and dv_{DS}/dt on v_{GS} can be studied using simple SPICE models.

Typical data sheet values of C_{GD} and C_{GS} for a 500V MOSFET were used. The simulated results assume constant dv_{DS}/dt , that freewheel diode reverse recovery can be neglected and that the off-state gate drive buffer output is at 0V with a sink impedance of around 5Ω. In practice the dv_{DS}/dt causing parasitic turn-on is not constant and is only at its maximum value for a small proportion of the voltage transition. Thus the results shows here represent a 'worst-case' condition for the alternative gate drive circuits used to clamp v_{GS} to below its threshold value, typically 2V to 3V. (The simple circuit model used here ceases to become valid once v_{GS} reaches $v_{GS(TO)}$ (time t_1 in Fig.10) when the MOSFET starts to turn on.)

Fig. 17 shows the relevant waveforms for the circuit of Fig.9 with $R_{GG}=100\Omega$. The top waveform in Fig.17 shows an imposed dv_{DS}/dt of 3.5V/ns and a dc link voltage of 330V. The centre trace of Fig.17 shows that v_{GS} rises quickly (reaching 3V in 25ns); at this point the MOSFET would start to turn on. The bottom trace shows the C_{GD} charging current sinking through the gate drive resistor R_{GG} . For the circuit of Fig. 12 with $R_{GGF}=100\Omega$ and $R_{GGR}=10\Omega$, Fig. 18 shows that the gate source voltage is held down by the reduced drive impedance but still reaches 3V after 35ns.

Circuit layout considerations

The effects of poor circuit design and layout are to increase RFI and noise and to compromise the performance and speed of the system due to stray inductances. The precautions which must be taken to minimise the amount of stray inductance in the circuit include:

- positioning the gate drive circuits, especially zener diodes and dv/dt clamping circuits as close as possible to the power MOSFETs.
- reducing circuit board track lengths to a minimum and using twisted pairs for all interconnections.
- for paralleled devices, keeping the devices close to each other and keeping all connections short and symmetrical.

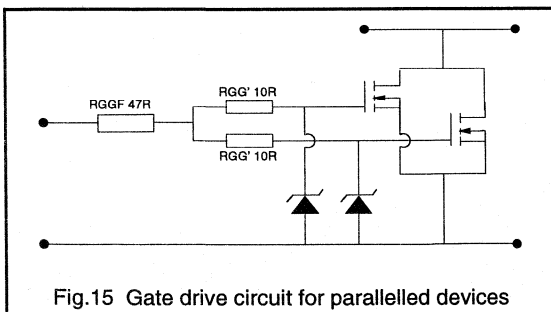


Fig. 15 Gate drive circuit for paralleled devices

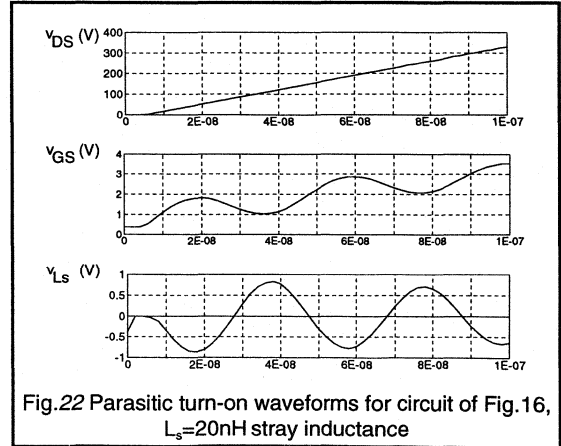
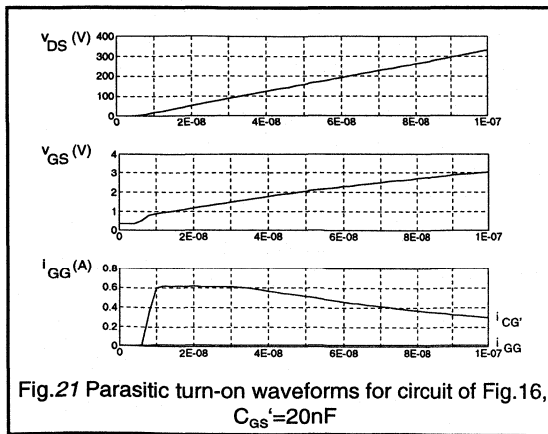
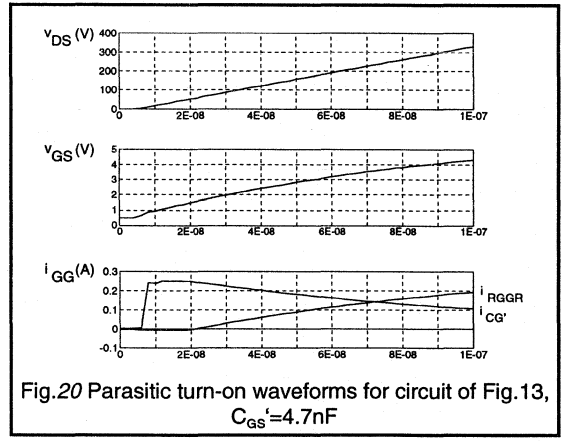
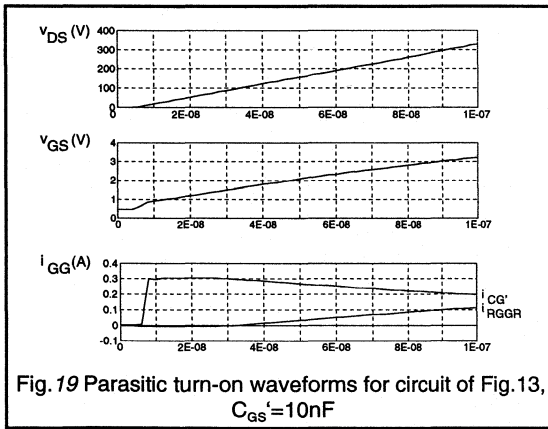
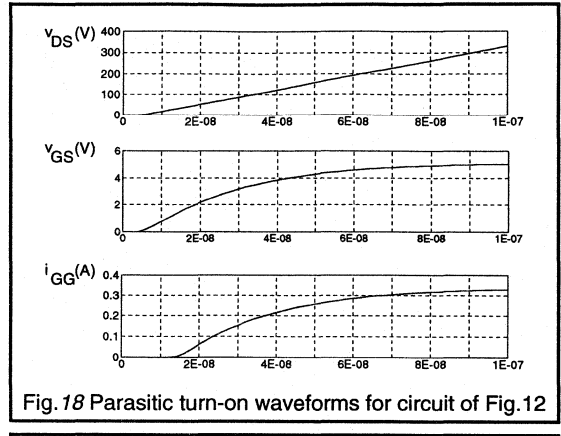
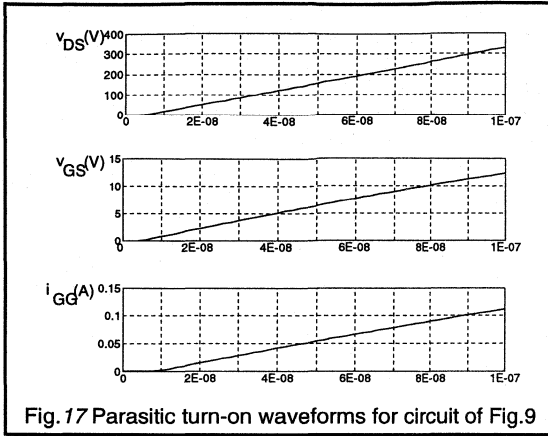


Figure 19 shows the response of the circuit of Figure 13 with $C_{GS}'=10\text{nF}$. Here the gate-source voltage is held down during the parasitic turn-on period and so the MOSFET stays off. If the value of C_{GS}' is reduced to 4.7nF then the results given in Fig.20 show that v_{GS} reaches 3V after 55ns thus reducing immunity to parasitic turn-on.

Figures 21 and 22 show the conditions for parallel connected MOSFETs using the circuit of Fig.16. In Fig.21, for $R_{GG1}=47\Omega$, $R_{GG}'=10\Omega$ and $C_{GS}'=20\text{nF}$, the bottom trace in the figure shows that a potential parasitic turn-on condition is avoided and v_{GS} is held below its threshold value. The bottom trace in Fig.21 shows most of the parasitic turn-on current is taken by C_{GS}' . Figure 22 shows the effect of stray inductance between the gate drive circuit and the PowerMOS device. The circuit of Fig.16 has been modified by the addition of 20nH of stray inductance between the gate node and the dv/dt clamping network. During switching of the top device with $dv/dt=3.5\text{V/ns}$ the stray inductance develops over 0.6V due to coupling via C_{GD} . Clearly this could significantly affect the performance of the drive during normal turn-on, and increase the prospect of the bottom MOSFET being subject to parasitic turn-on problems.

These results show that immunity to parasitic turn-on can be greatly improved by alternative gate circuit design. The SPICE modelled circuits show the worst case conditions of constant dv_{DS}/dt and show that v_{GS} can be held below its threshold voltage using the circuits shown in the previous section. Experimental measurements have confirmed these results in a prototype 20kHz APMC system.

Device losses in APMC inverters

It is important to be able to calculate the losses which occur in the switching devices in order to ensure that device operating temperatures remain within safe limits. Cooling arrangements for the MOSFETs or FREDFETs in an APMC system will depend on maximum allowable operating temperatures, ambient temperature and operating conditions for the system. The components of loss can be examined in more detail:

MOSFET Conduction losses

When a MOSFET or FREDFET is on and carrying load current from drain to source then the conduction ' i^2R ' loss can be calculated. It is important to note that the device current is not the same as the output current, as demonstrated by the waveforms of Fig.23. The figure shows a sinusoidal motor load current waveform and the top and bottom MOSFET currents. The envelopes of the MOSFET

currents are half sinusoids; however the actual device currents are interrupted by the instants when the load current flows through the freewheel diodes. For the purposes of calculating MOSFET conduction losses it is acceptable to neglect the 'gaps' which occur when the freewheel diodes are conducting for the following reasons:

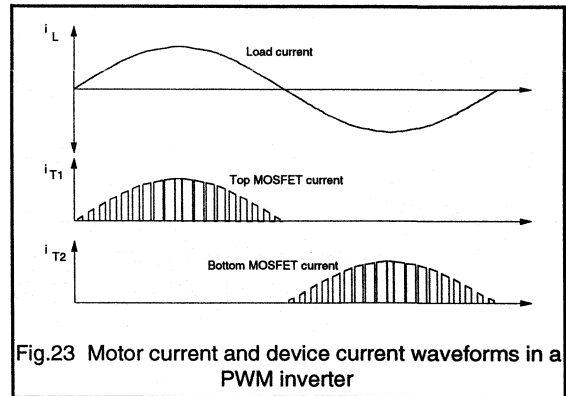


Fig.23 Motor current and device current waveforms in a PWM inverter

-When the motor load current is near its maximum value the switching duty cycle is also near its maximum and so the proportion of time when the diode conducts is quite small and can be neglected.

-When the motor load current is near zero then the switching duty cycle is low but the MOSFET is only conducting small amounts of current. As the MOSFET current is low then the contribution to total conduction loss is small.

Thus if the MOSFET is assumed to be conducting load current for the whole half-period then the conduction losses can be calculated using the current envelope of Fig.23. These losses will be overestimated but the discrepancy will be small. The conduction losses can be given by:

$$P_{M(ON)} = I_T^2 \cdot R_{DS(ON)}(T_J) \quad (13)$$

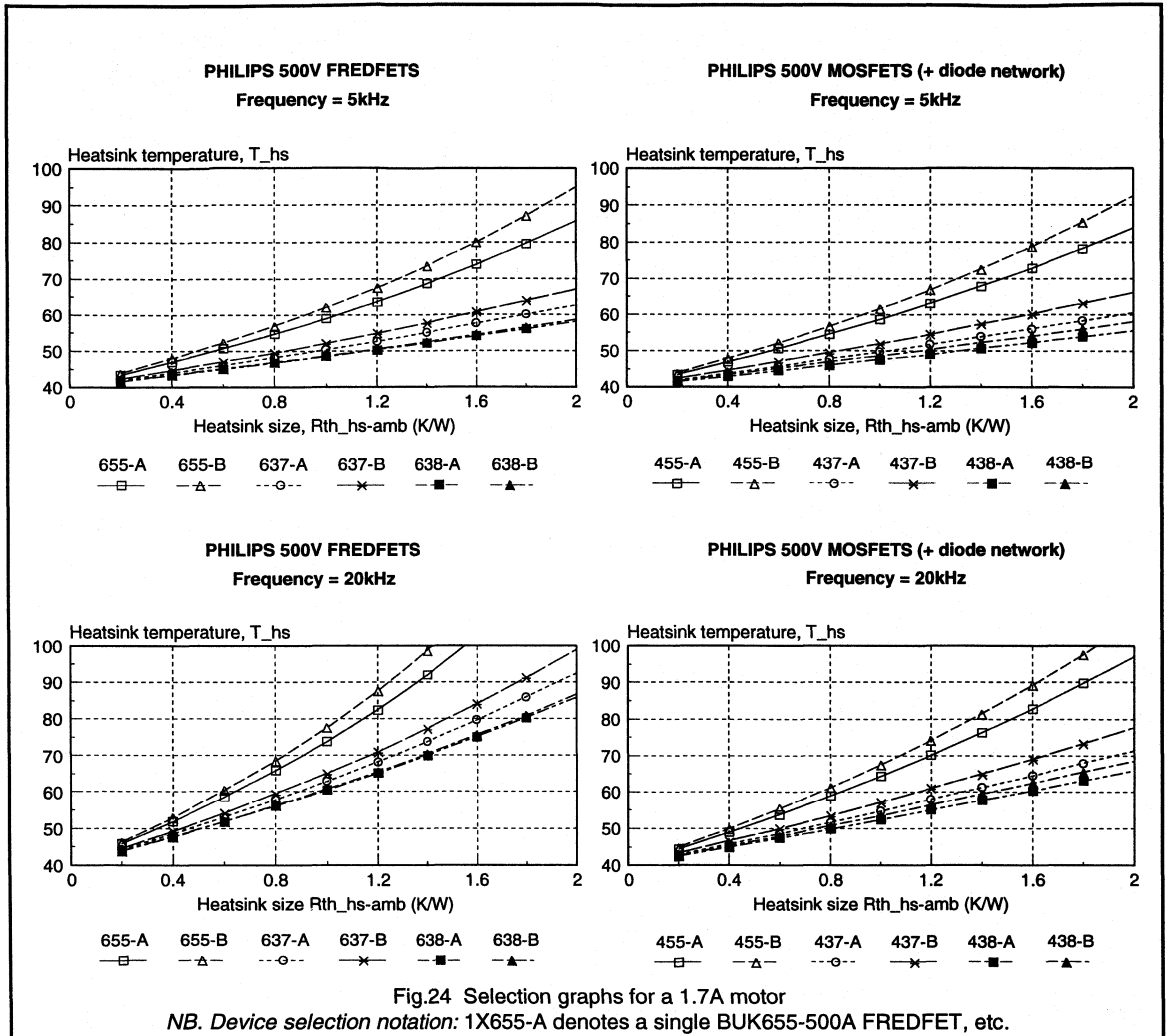
where I_T is the rms value of the half sinusoid MOSFET current envelope.

$$\text{and: } R_{DS(ON)}(T_J) = R_{DS(ON)}(25^\circ\text{C}) \cdot e^{k(T_J-25)} \quad (14)$$

where $k=0.007$ for a 500V MOSFET, and $k=0.006$ for a 500V FREDFET.

I_T is related to the rms motor current, I_L , by:

$$I_T = \frac{I_{\max}}{2} = \frac{I_L}{\sqrt{2}} \quad (15)$$



Additionally in a MOSFET inverter the series blocking Schottky diode (D3 of Fig.8) has conduction losses. The current in this diode is the main MOSFET current and so its loss is approximated by:

$$P_{Sch(ON)} = V_f(T_f) \cdot I_T \quad (16)$$

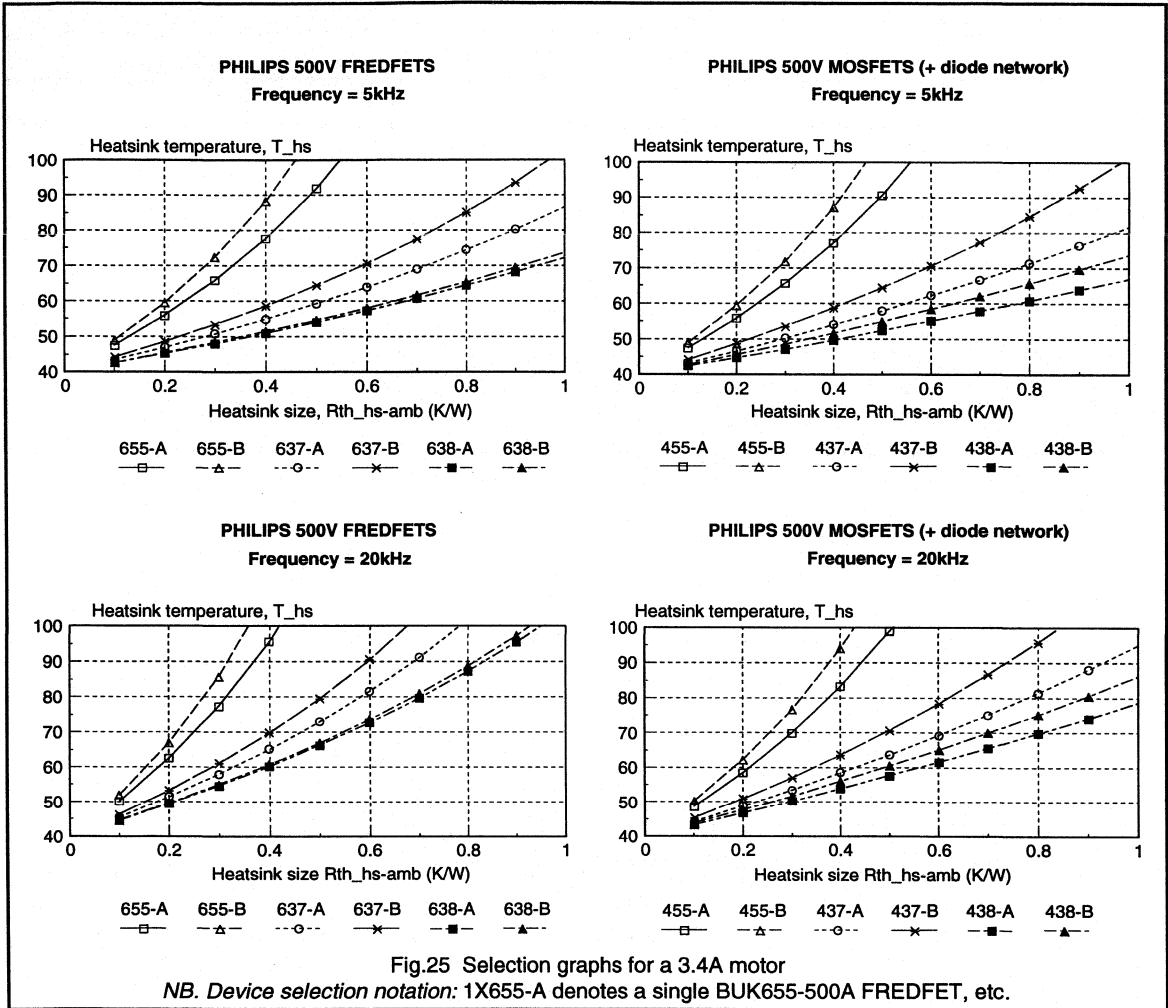
Diode conduction losses

In a MOSFET inverter the freewheel diode losses occur in a discrete device (D2 of Fig.8) although this device is often mounted on the same heatsink as the main switching device. In a FREDFET circuit the diode losses occur in the main device package. The freewheeling diode carries the

'gaps' of current shown in Fig.23 during the periods when its complimentary MOSFET is off. Following the argument used above the diode conduction loss is small and can be neglected. Using this simplification we have effectively transferred the diode conduction loss and included it in the figure for MOSFET conduction loss.

MOSFET switching losses

During the half-cycle of MOSFET conduction the load current switched at each instant is different (Fig.23). The amount of current switched will also depend on the reverse recovery of the bridge leg diodes and hence on the



temperature of the devices. The total turn-on loss ($P_{M(SW)}$) will be a summation of the losses at each switching instant:

$$P_{M(SW)} = \sum_{n=0}^{\infty} f(T_j, I_n) \quad (17)$$

MOSFET turn-off times are usually only limited by dv/dt considerations and hence are as short as possible. The turn-off loss of the MOSFETs or FREDFETs in an inverter is small compared with the turn-on loss and can usually be neglected.

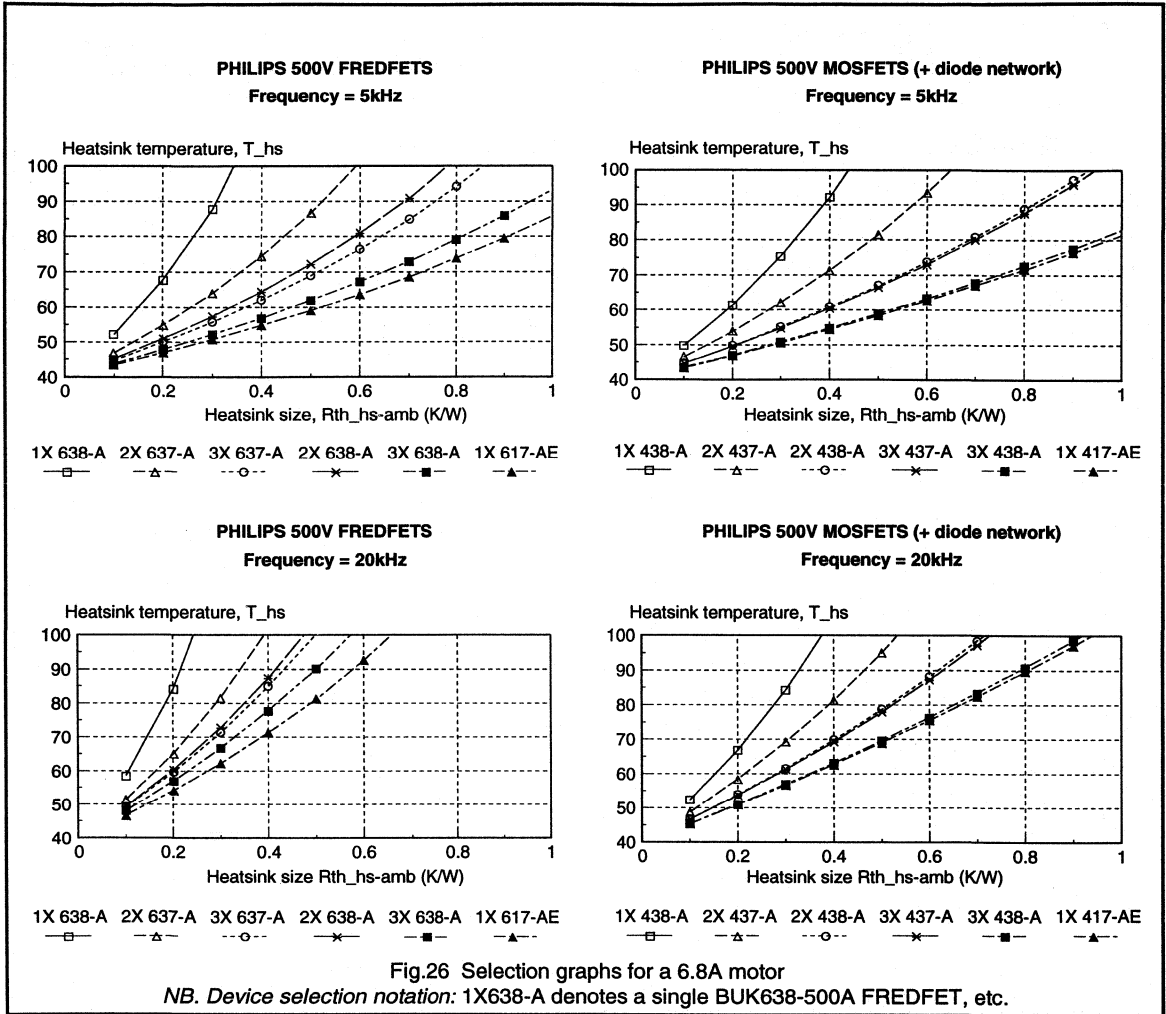
Diode switching losses

Diode turn-off loss ($P_{D(SW)}$) is calculated in a similar manner

to the MOSFET turn-on loss. The factors which affect the diode turn-off waveforms have been discussed earlier. Diode turn-on loss is usually small since the diode will not conduct current unless forward biased. Thus at turn-on the diode is never simultaneously supporting a high voltage and carrying current.

Gate drive losses

Some loss will occur in the gate drive circuit of a PowerMOS device. As the gate drive is only delivering short pulses of current during the switching instants then these losses are negligibly small.



System operating temperatures

In this section the device losses discussed in the previous section are calculated and used to produce a design guide for the correct selection of Philips PowerMOS devices and appropriate heatsink arrangements for ACMC applications. The following factors must be taken into account when calculating the total system loss, P_{LOSS}:

- Device characteristics
- Switching frequency
- Operating temperature
- Load current
- Number of devices used in parallel.
- Additional snubber or di/dt limiting networks.

$$P_{LOSS} = P_{M(ON)} + P_{M(SW)} + P_{D(SW)} + P_{Sch(ON)} \quad (18)$$

For the results presented here the device parameters were taken for the Philips range of 500V MOSFETs and FREDFETs. The on-state losses can be calculated from the equations given above. For this analysis the device switching losses were measured experimentally as functions of device temperature and load current. As there are six sets of devices in an ACMC inverter then the total heatsink requirement can be found from:

$$T_{hs} = T_{ahs} + 6 \cdot P_{LOSS} \cdot R_{th(hs-ahs)} \quad (19)$$

$$T_j = T_{hs} + P_{LOSS} \cdot R_{th(j-hs)} \quad (20)$$

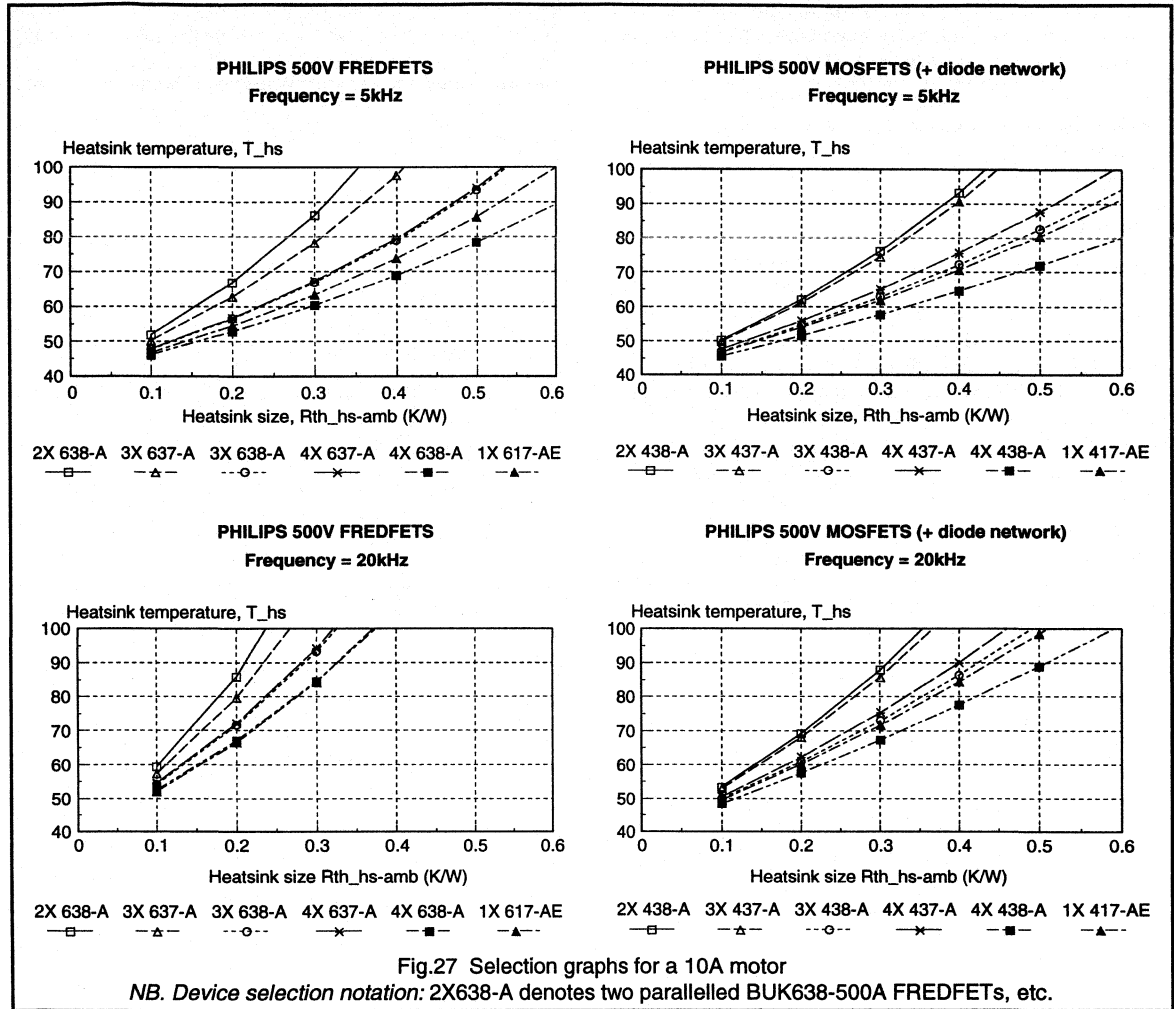


Fig.27 Selection graphs for a 10A motor

NB. Device selection notation: 2X638-A denotes two paralleled BUK638-500A FREDFETs, etc.

Equations 18 to 20 can be used to find the heatsink size ($R_{th(ths-ahs)}$) required for a particular application which will keep the heatsink temperature (T_{hs}) within a required design value. Results are plotted in Figures 24 to 27 for motor currents of $I_L = 1.7A, 3.4A, 6.8A$ and $10.0A$. These currents correspond to the ratings of several standard induction motor sizes. The results assume unsnubbed devices, an ambient temperature of $T_{ahs}=40^{\circ}C$, and are plotted for inverter switching frequencies of 5kHz and 20kHz.

Two examples showing how these results may be used are given below:

- 1) -The first selection graph in Fig.24 shows the possible device selections for 500V FREDFETs in a 5kHz AC/MC

system where the full load RMS motor current is 1.7A. Using a BUK655-500A FREDFET, T_{hs} can be maintained below $70^{\circ}C$ with a total heatsink requirement of 1.2K/W (if each FREDFET was mounted on a separate heatsink then each device would need a 7.2K/W heatsink). The same heatsinking arrangement will give $T_{hs}=50^{\circ}C$ using a BUK638-500A. Alternatively T_{hs} can be maintained below $70^{\circ}C$ using a 2K/W heatsink (12K/W per device) and the BUK637-500B.

- 2) -In Fig.27 the selection graphs for a 10A system are given. The fourth selection graph is for a 20kHz switching frequency using 500V MOSFETs. Here two BUK438-500A devices connected in parallel for each switch will require a total heatsink size of 0.3K/W if the

heatsink temperature is to remain below 90°C. The same temperature can be maintained using a 0.5K/W heatsink and a single BUK417-500AE ISOTOP device.

For different motor currents or alternative PWM switching frequencies the appropriate device and heatsink arrangement for a particular application can be found by interpolating the results presented here.

Conclusions

This section has outlined the basic principles and operation of PWM inverters for ACMC applications using Philips PowerMOS devices. MOSFETs and FREDFETs are the most suitable devices for ACMC systems, especially at high switching speeds. This section has been concerned with systems rated up to 2.2kW operating from a single phase supply and has shown that there is a range of Philips PowerMOS devices ideally suited for these systems.

The characteristics and performance of MOSFETs and FREDFETs in inverter circuits and the effect of gate drive design on their switching performance has been discussed. The possibility of parasitic turn-on of MOSFETs in an inverter bridge leg can be avoided by appropriate gate drive circuit design. Experimental and simulated results have

shown that good switching performance and immunity to parasitic turn-on can be achieved using the Philips range of PowerMOS devices in ACMC applications. Using the device selection graphs presented here the correct MOSFET or FREDFET for a particular application can be chosen. This guide can be used to select the heatsink size and device according to the required motor current, switching frequency and operating temperature.

References

1. Introduction to PWM speed control system for 3-phase AC motors: J.A.Houldsworth, W.B.Rosink: Electronic Components and Applications, Vol 2, No 2, 1980.
2. A new high-quality PWM AC drive: D.A.Grant, J.A.Houldsworth, K.N.Lower: IEEE Transactions, Vol IA-19, No 2, 1983.
3. Variable speed induction motor with integral ultrasonic PWM inverter: J.E.Gilliam, J.A.Houldsworth, L.Hadley: IEEE Conference, APEC, 1988, pp92-96.
4. MOSFETs and FREDFETs in motor drive equipment: Chapter 3.1.3.

3.1.5 A 300V, 40A High Frequency Inverter Pole Using Paralleled FREDFET Modules

Introduction

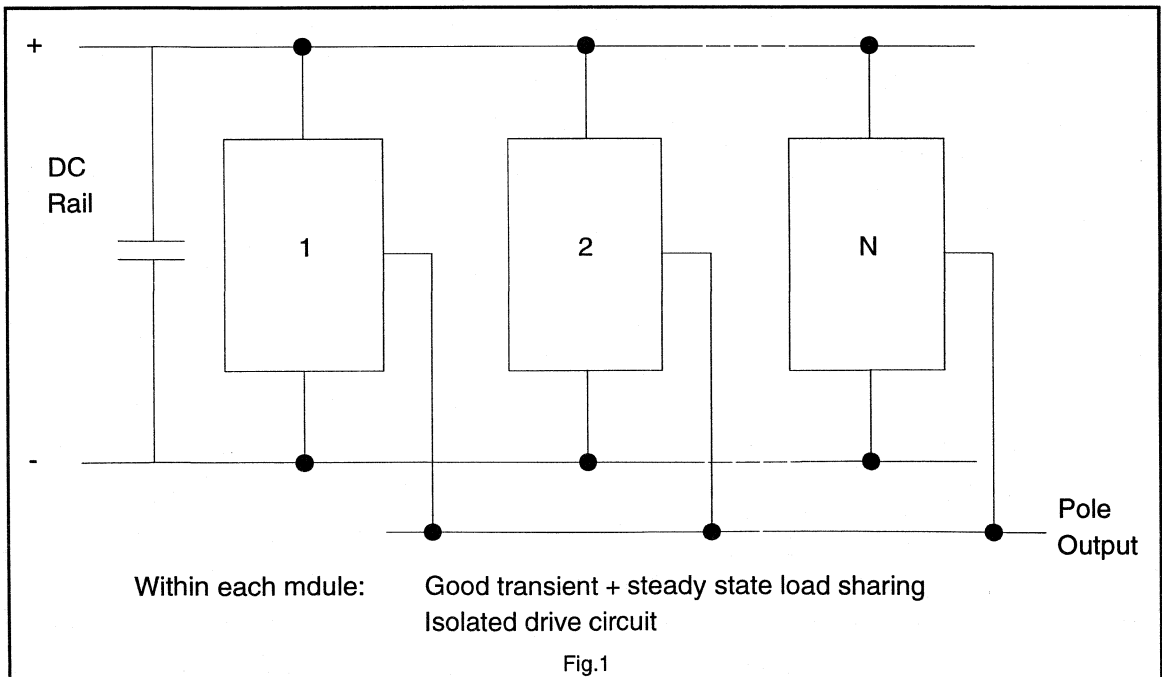
Voltage source inverters which are switched using some form of pulse width modulation are now the standard in low to medium rated AC and brushless DC variable speed drives. At present, because of device limitations the switching (modulation) frequencies used in all but the lowest drive ratings are restricted to a few kHz. There is however a strong technical advantage in using much higher ultrasonic switching frequencies in excess of 20 kHz, the benefits of which include:

- i) The low frequency distortion components in the inverter output waveform are negligible. As a result there is no longer a need to derate the electrical machine in the drive as a consequence of harmonic loss.
- ii) The supply derived acoustic noise is eliminated.
- iii) The DC link filter component values are reduced.

The device best suited for high switching frequencies is the power MOSFET because of its extremely fast switching

time and the absence of secondary breakdown. However, being surface conduction devices, high power rated MOSFETs are difficult and expensive to manufacture and at present single MOSFETs are only suitable for inverter ratings of typically 1-2 kVA per pole. Although higher rated power devices such as bipolar transistors and IGBTs can be switched at medium to high frequencies, the switching losses in these circuits are such that frequencies in excess of 20 kHz are at present difficult to achieve.

Switches with high ratings and fast switching times can be constructed by hard paralleling several lower rated power devices. MOSFETs are particularly suitable because the positive temperature coefficient of the channel resistance tends to enforce good steady-state current sharing between parallel devices. However to achieve good dynamic current sharing during switching, considerable care must be taken in the geometric layout of the paralleled devices on the common heatsink. In addition, the device characteristics may need to be closely matched. As a result modules of paralleled MOSFETs are often expensive.

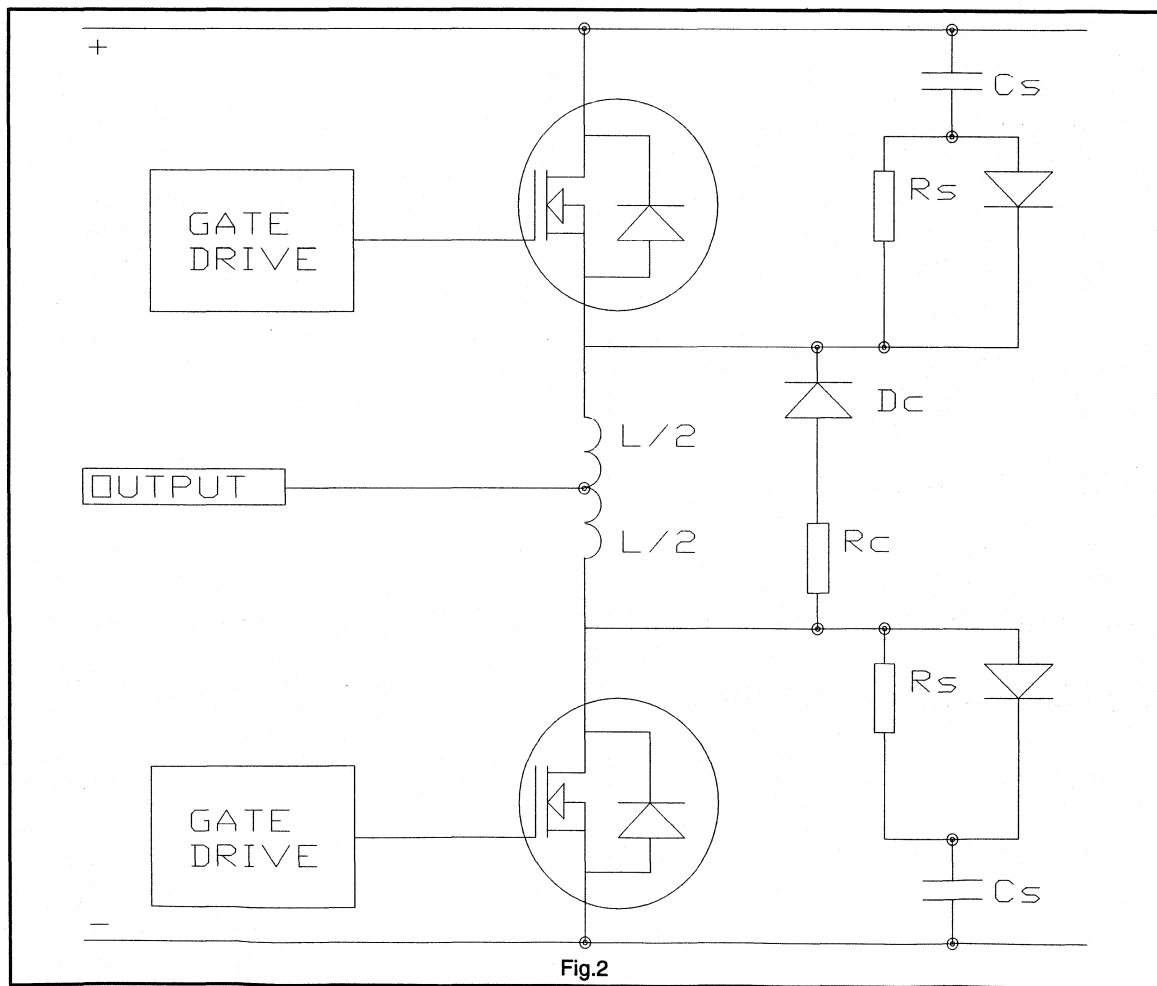


An alternative approach to paralleling is to use small switching aid networks which overcome the constraints of hard paralleling by improving the dynamic load sharing of the individual devices. It is possible to envisage an inverter design where each pole consists of a number of identical pole modules which share a common supply and have outputs connected in parallel, as shown in Fig.1. Each module is designed to operate individually as an inverter pole and contains two power MOSFETs with associated isolated gate drive circuitry. When the modules are connected in parallel their design is such that they will exhibit good transient and steady-state load sharing, the only requirement being that they are mounted on a common

heatsink. In this manner any inverter volt-amp rating can be accommodated by paralleling a sufficient number of pole modules.

Pole module

The power circuit diagram of an individual pole module which is suitable for the second form of paralleling is shown in Fig.2. The design makes use of the integral body diode of the main switching devices and for this purpose the fast recovery characteristics of FREDFETs are particularly suitable. Two snubber circuits and a centre tapped inductance are included in the circuit. These small switching aid networks perform a number of functions in the circuit:



- i) They act to improve the dynamic current sharing between the pole modules when connected in parallel.
- ii) They ensure safe operation of the MOSFET integral body diode. The central inductance controls the peak reverse current of the diode and the snubber network prevents secondary breakdown of the MOSFET parasitic internal transistor as the integral body diode recovers.
- iii) They reduce the switching losses within the main power devices and thus allows maximum use of the available rating.

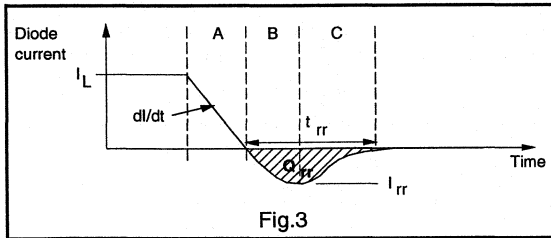


Fig.3

The operation of the circuit is typical of this form of inverter pole. The commutation of the integral body diode will be discussed in detail since it is from this section of the operation that the optimal component values of the switching aid network are determined. The value of the inductor L is chosen to give a minimum energy loss in the circuit and the snubber network is designed to ensure safe recovery of the integral diode at this condition. For example consider the case when there is an inductive load current I_L flowing out of the pole via the integral body diode of the lower MOSFET just prior to the switching of the upper MOSFET. With reference to Fig.3, the subsequent operation is described by the following regions:

Region A: Upper MOSFET is switched on. The current in the lower integral body diode falls at a rate (dl/dt) equal to the DC link voltage V_{DD} divided by the total inductance L of the centre tapped inductance.

Region B: The diode current becomes negative and continues to increase until the junction stored charge has been removed, at which stage the diode recovers corresponding to a peak reverse current I_{RR} .

Region C: The voltage across the lower device increases at a rate (dV/dt) determined by the capacitance C_s of the lower snubber network. The current in the upper MOSFET and the inductor continues to increase and reaches a peak when the voltage across the lower device has risen to the DC link value. At this point the diode D_c becomes forward biased and the stored energy in the inductor begins to discharge through the series resistance R_c .

The energy E_1 gained by the switching aid networks over the above interval is given by:

$$E_1 = \frac{1}{2} I_{RR}^2 L + \frac{1}{2} C_s V_{DD}^2 \quad (1)$$

and is ultimately dissipated in the network resistors R_s , R_c . For a given forward current, the peak reverse current I_{RR} of the diode will increase with increasing dl/dt and can be approximately represented by a constant stored charge, (Q_{RR}) model, where:

$$I_{RR} = \sqrt{2 \left(\frac{dI}{dt} \right) Q_{RR}} \quad (2)$$

Although in practice I_{RR} will tend to increase at a slightly faster rate than that given by equation (2).

Since in the inverter pole circuit

$$\frac{dI}{dt} = \frac{V_{DD}}{L} \quad (3)$$

$$I_{RR} = \sqrt{\frac{2V_{DD}Q_{RR}}{L}} \quad (4)$$

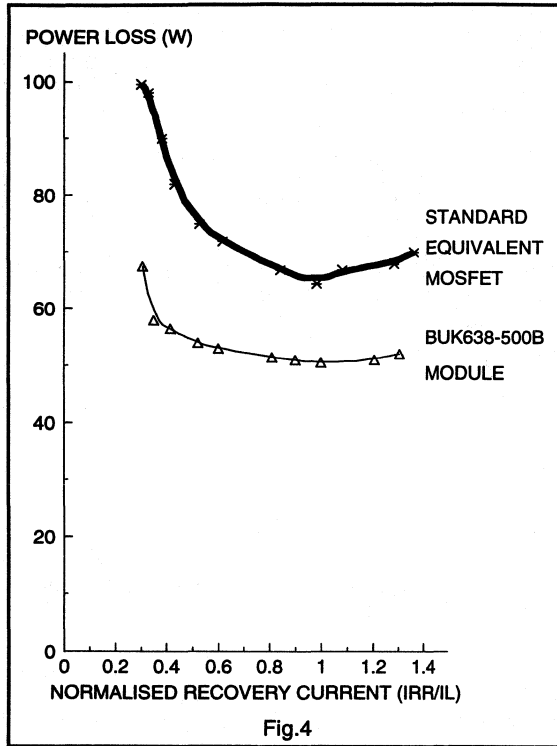
Inspection of equations (1) and (4) shows that the energy loss E_1 remains approximately constant as L is varied.

During the subsequent operation of the inverter pole when the upper MOSFET is turned off and the load current I_L returns to the integral body diode of the lower device, an energy loss E_2 occurs in the inductor and the upper snubber equal to:

$$E_2 = \frac{1}{2} I_L^2 L + \frac{1}{2} C_s V_{DD}^2 \quad (5)$$

This loss can be seen to reduce with L. However as L is reduced both I_{RR} and the peak current in the upper MOSFET will increase and result in higher switching loss in the diode and higher conduction loss in the channel resistance of the upper device.

The value of L which gives minimum energy loss in the pole occurs when there is an optimal balance between the effects described above. Typical measured dependencies of the total energy loss on the peak reverse diode current as L is varied are shown in Fig.4. The characteristics of a similarly rated conventional MOSFET and a fast recovery FREDFET are compared in the figure. In both cases the minimum energy loss occurs at the value of L which gives a reverse recovery current approximately equal to the design load current. However the loss in the FREDFET circuit is considerably lower than with the conventional device. The optimal value of L can be found from the manufacturers specified value of stored charge using equation (4), where



$$L_{opt} = \frac{2V_{DD}Q_{RR}}{I_L^2} \quad (6)$$

The snubber capacitor value C_s is chosen to limit the dV/dt across the integral body diode as it recovers. Experience has shown that a value of $1V/nS$ will ensure safe operation, hence:

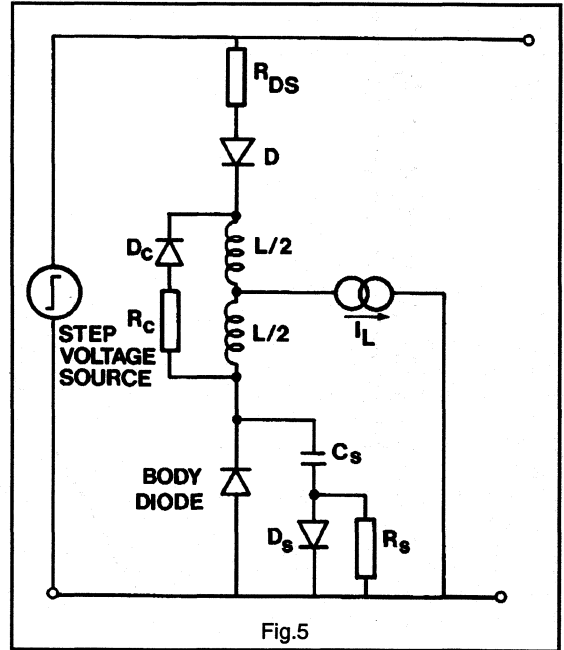
$$C = (I_L) nF \quad (7)$$

The resistive component of the switching aid networks are chosen in the usual manner.

Parallel operation of pole modules

The principle behind the 'soft' paralleling adopted here is to simply connect the outputs of the required number of modules together and feed them with a common DC link and control signals. The transient load sharing between the parallel modules will be influenced by the tolerances in the individual inductor and snubber capacitor values and any variations in the switching instances of the power devices, the latter being as a result of differences in device characteristics and tolerances in the gate drive circuitry. These effects were investigated using the SPICE circuit

simulation package. The SPICE representation of the modules is shown in Fig.5, in which the upper MOSFET channel is modelled by an ideal switch with a series resistance R_{DS} . The full SPICE diode model is used for the lower MOSFET integral body diode, however ideal diode representations are sufficient for the devices in the switching aid networks. The load is assumed to act as a constant current sink over the switching interval.



From the SPICE simulation an estimate of the peak transient current imbalance between the MOSFETs of the two modules was obtained for various differences in the inductors, capacitors and device turn-on times. It was found that the transient current sharing was most sensitive to unequal device switching times. An example of the results obtained from a simulation of two paralleled modules using BUK638-500B FREDFETs are shown in Fig.6. With good gate drive design the difference between device switching times is unlikely to exceed 50nS resulting in a peak transient current mismatch of less than 10%. The load sharing would improve if the value of inductor is increased but this has to be traded off against the increase in switching loss. The effect of the tolerance of the inductor values on the load sharing is given for the same module in Fig.7, where it can be seen that a reasonable tolerance of 10% results in only a 7% imbalance in the currents. The load sharing was found to be relatively insensitive to tolerances in the snubber capacitor values.

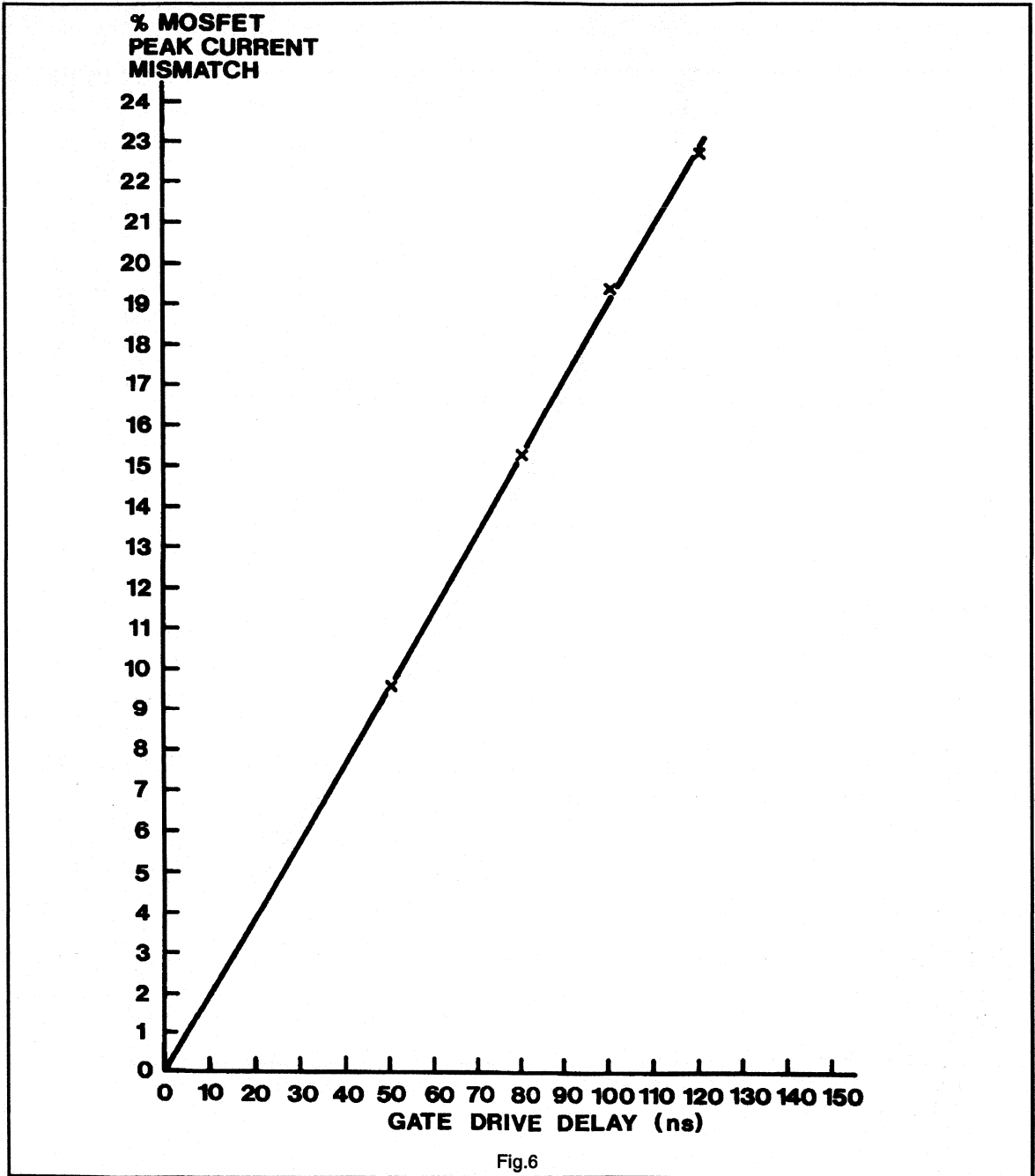
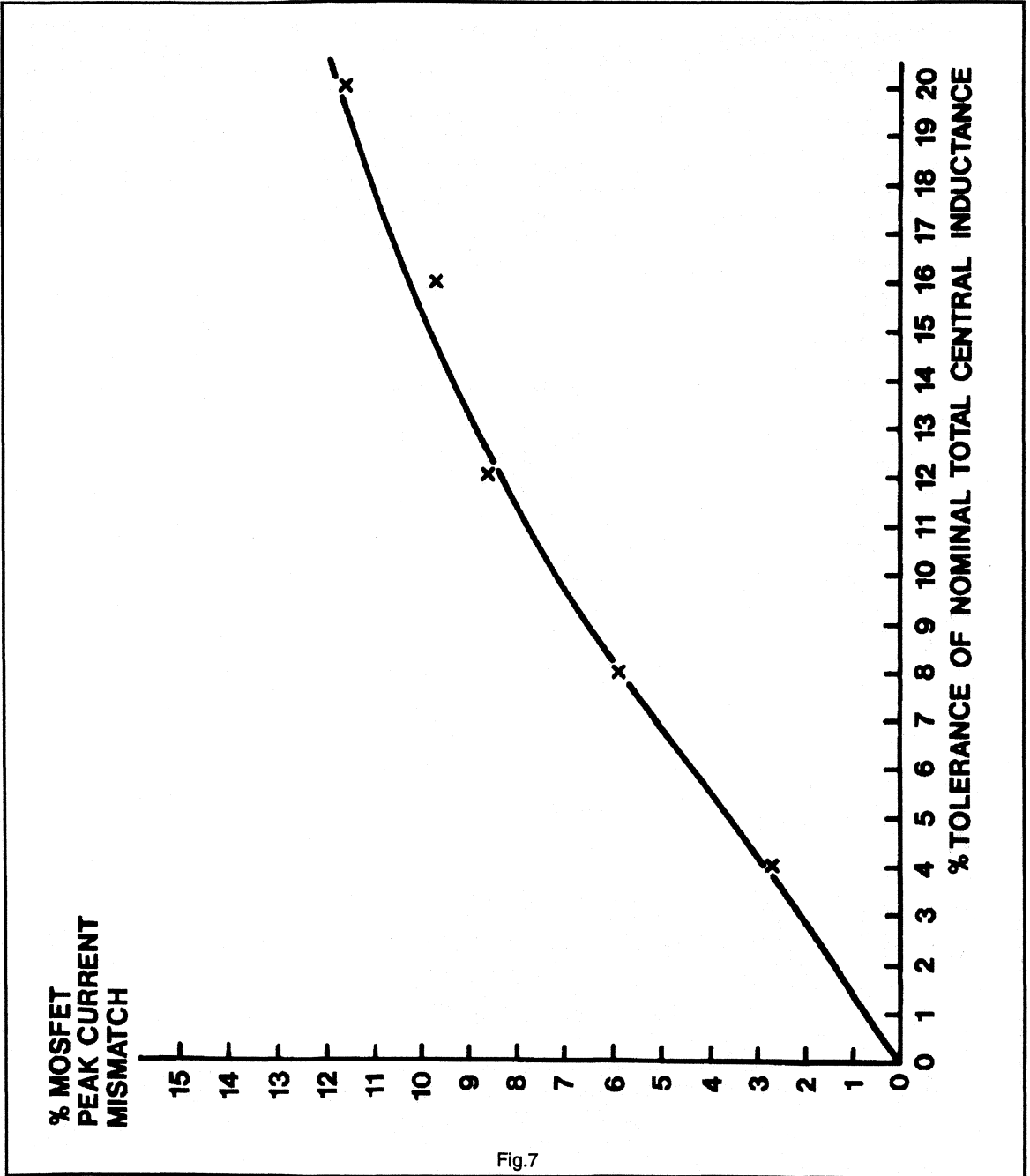


Fig.6



A 300V, 10A pole module design using BUK638-500B FREDFETs

The circuit diagram of a 300V, 10A pole module based on BUK638-500B FREDFETs is given in Fig.8. The inductor value was chosen using the criteria discussed in Section 2.

The conventional R-C snubber network has been replaced by the active circuit shown in Fig.9 and involves the use of a second, low rated BUK455-500B MOSFET which is made to act as a capacitance by invoking the 'Miller' effect. The

active snubber is more efficient at low load currents because it tends to maintain a constant (dV/dt) regardless of the load, and thus the snubber loss is proportional to the current, as opposed to the conventional circuit in which the loss remains constant. In addition the active circuit is compact and lends itself more readily to a hybrid assembly. The major component costs are the secondary MOSFET and a low voltage power diode and compare favourably with those of the conventional high voltage capacitor and high voltage diode.

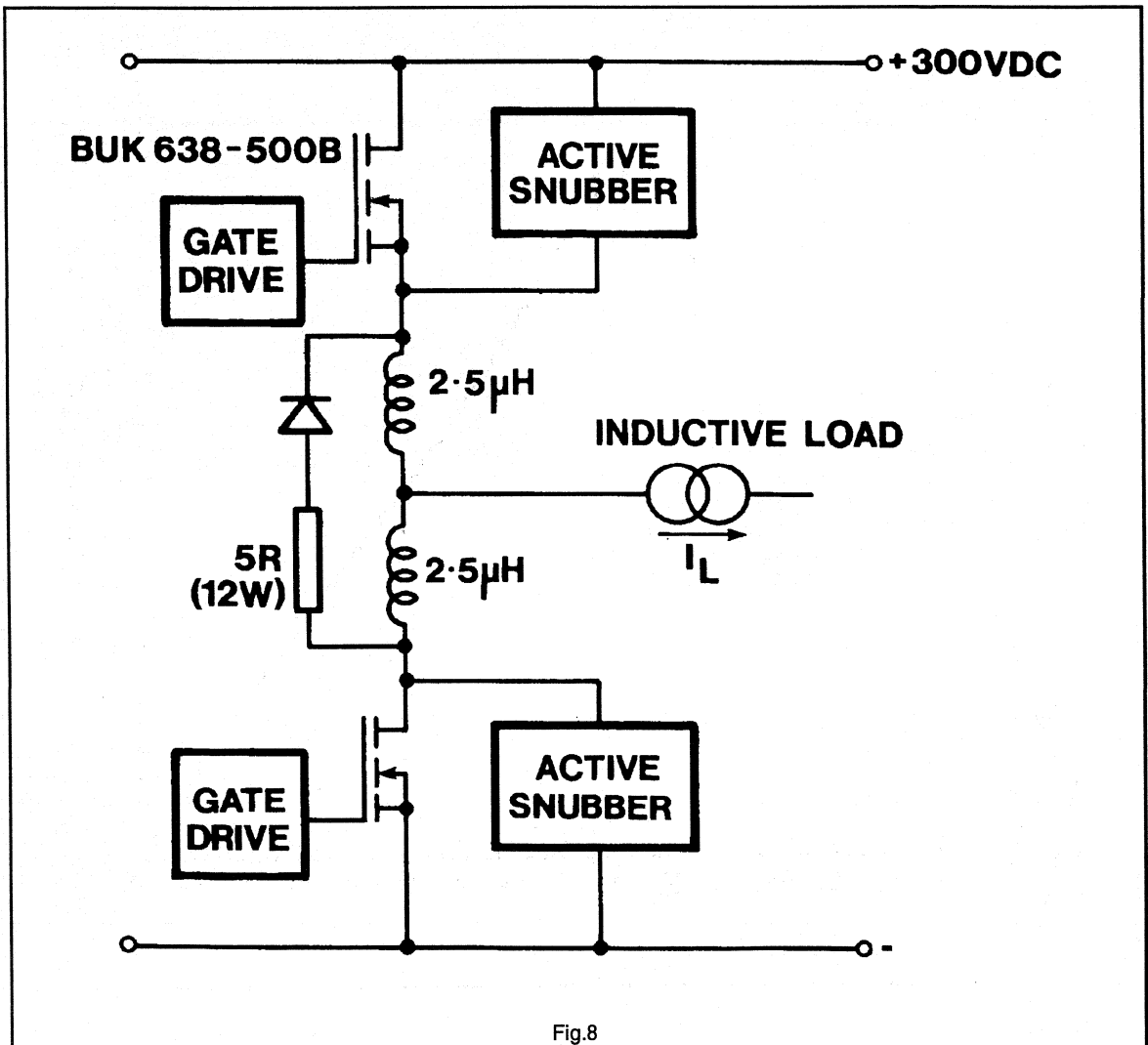


Fig.8

The gate drive circuits are given in Fig.10 and are based upon the pulse transformer configuration described in chapter 1.2.3. A PNP transistor has been added between the gate and source to reduce the drive off-state impedance, to improve the switching and prevent any Miller effect in the main device.

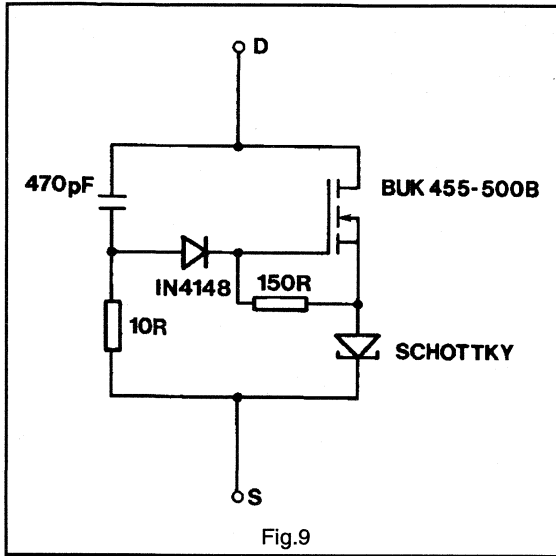


Fig.9

FREDFET module performance

The typical voltage and current waveforms of the upper and lower switching devices are shown in Figures 11 and 12 for the case of a single pole module sourcing the rated current of 10 Amps from a 300V DC link. Fig.12 illustrates how the use of the series inductor and active snubber gives a controlled recovery of the fast integral body diode of the FREDFET.

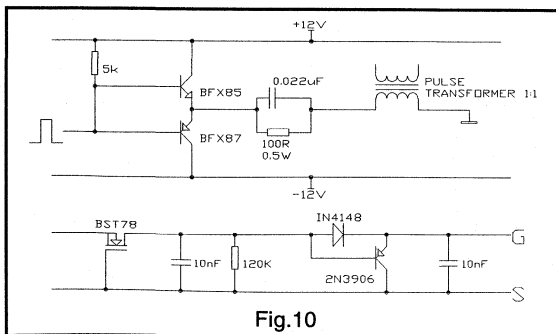


Fig.10

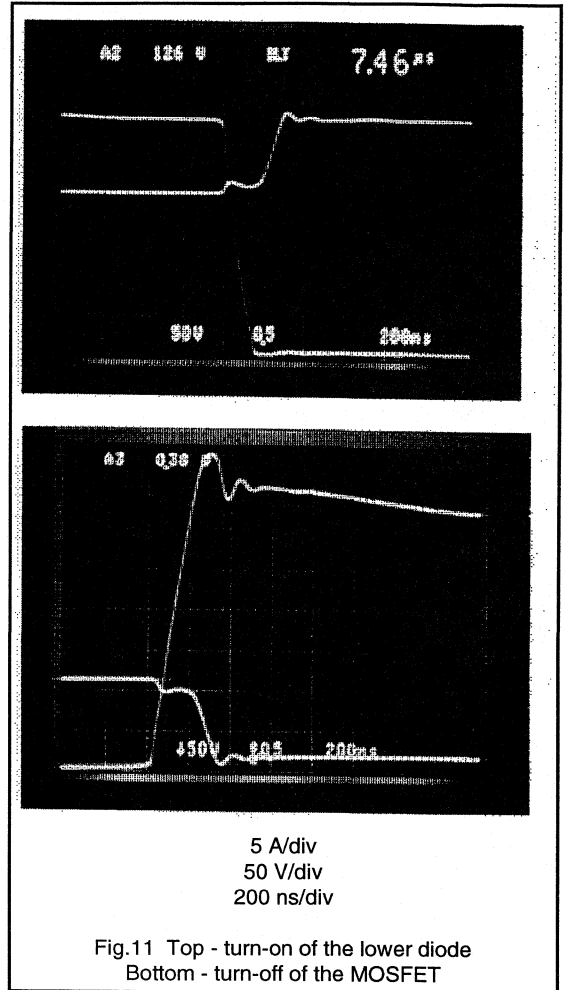
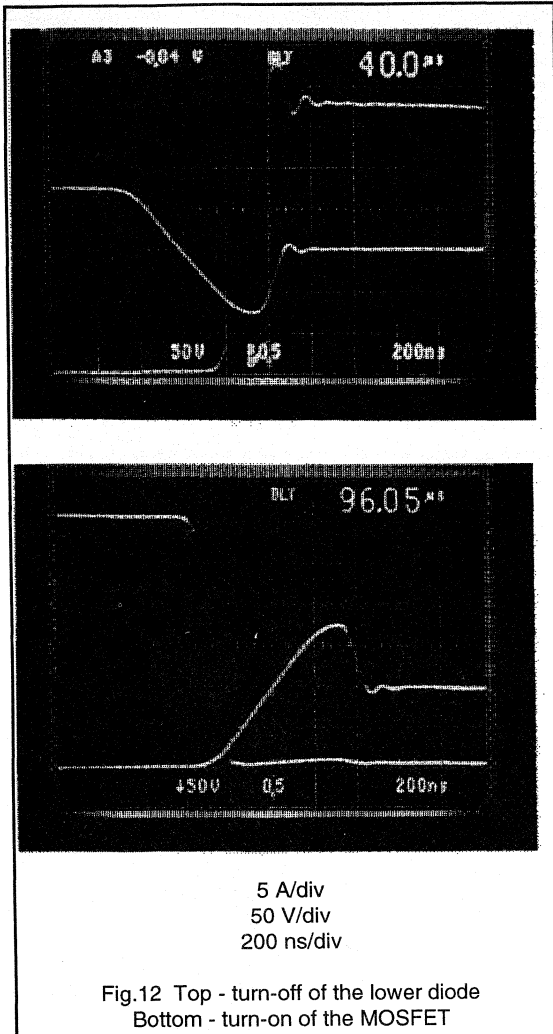
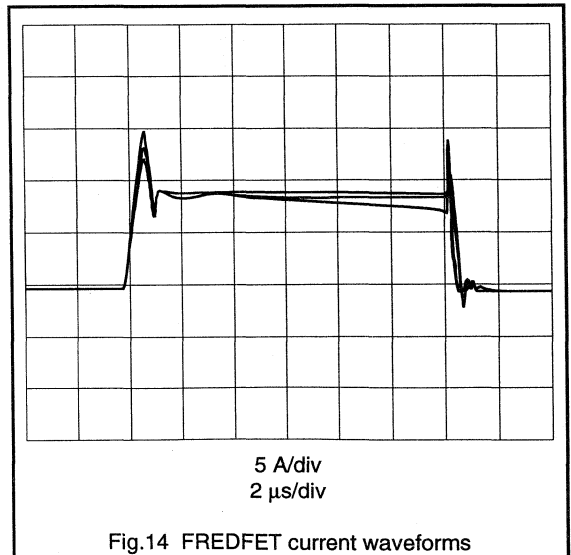
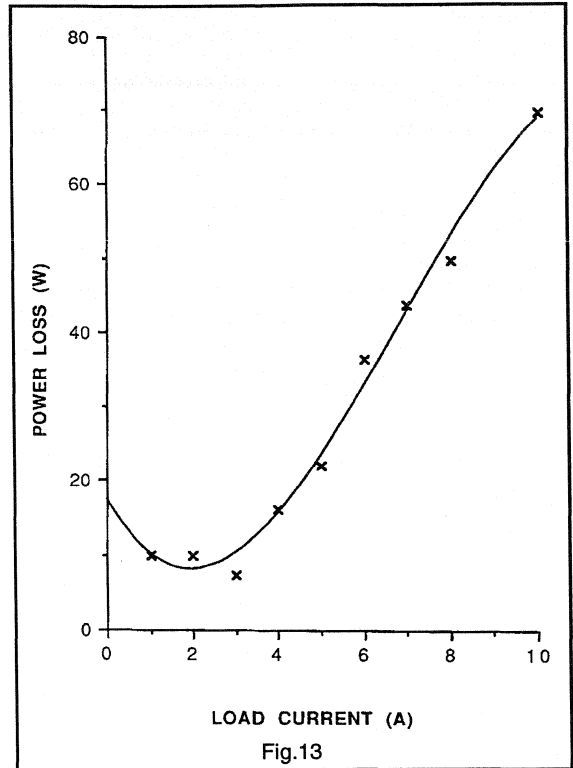


Fig.11 Top - turn-on of the lower diode
Bottom - turn-off of the MOSFET

The losses of an individual module switched at 20 kHz are plotted in Fig.13 as a function of output current. They mainly stem from conduction loss, the switching loss representing only a third of the maximum loss. Because the switching loss occurs mainly in the aid networks the main FREDFETs can be used at close to their full rating. Similarly operation at higher frequencies will not result in a substantial reduction in efficiency, for example at 40 kHz, 10A operation the losses are 95W.



Four modules were connected in parallel and mounted on a common heatsink. The modules operated successfully at 300V with total loads in excess of 40A, four times their individual rating. The common heatsink, which had a thermal resistance to ambient of 0.33°C/W was sufficient to achieve the full 40A, 300V continuous rating of the parallel units at 20 kHz. The current waveforms of the upper FREDFETs in each module are overlaid in Fig.14, where it can be seen that the load sharing is very even, particularly after the initial switching transients.



Conclusion

Parallel, separate MOSFET pole modules provide a method of designing medium rated inverter poles, which can be switched efficiently at frequencies in excess of 20 kHz. The approach is flexible since a single pole module design can be used to achieve a range of inverter volt-amp ratings by paralleling a sufficient number of units.

Through the use of small switching aid networks it is possible to obtain excellent transient and steady-state current sharing between the paralleled modules. The current sharing remains good even if there are substantial variations in component tolerances and the power device

switching times. The switching aid networks also reduce the switching losses in the main devices and allows them to be used to their full rating.

The presented design of a 300V, 10A module based on BUK638-500B, FREDFETs has a full load loss of only 70W. Four of these modules connected in parallel and mounted on a 0.33°C/W heatsink gave an inverter pole with a 300V, 40A continuous rating when switched at 20 kHz. Excellent current sharing between these modules was observed and as a result there would seem to be no technical reasons why further modules could not be paralleled to achieve even higher ratings.

DC Motor Control



3.2.1 Chopper circuits for DC motor control

DC motor drives are used for many speed and position control systems where their excellent performance, ease of control and high efficiency are desirable characteristics. DC motor speed control can be achieved using switch mode DC-DC chopper circuits. For both mains-fed and battery supplied systems, power MOSFETs and FREDFETs are the ideal switching devices for the converter stage. The Philips range of PowerMOS devices includes devices suitable for most DC-DC converters for motor control applications. Additionally, due to the ease with which MOSFETs and FREDFETs can be paralleled, Philips PowerMOS devices can easily be used in chopper circuits for both low power and high power DC motor drives for vehicle, industrial or domestic applications.

Introduction to DC motor drives

In a DC motor, the static field flux is established using either permanent magnets or a stator field winding. The armature winding, on the rotor of a dc machine, carries the main motor current. The armature winding is a series of coils, each connected to segments of a commutator. In order that the motor develops constant torque as the rotor moves, successive armature coils must be connected to the external dc circuit. This is achieved using a pair of stationary brushes held in contact with the commutator.

The motor torque is produced by the interaction of the field flux and the armature current and is given by:

$$T_e \propto I_a \quad (1)$$

The back emf developed across the armature conductors increases with the motor speed:

$$E_a \propto \omega_m \quad (2)$$

Permanent magnet DC motors are limited in terms of power capability and control capability. For field wound DC motors the field current controls the flux and hence the motor torque and speed constants. The field winding can be connected in series with the armature winding, in shunt with it, or can be separately excited. For the separately excited dc motor, shown in Fig.1 the field flux is controlled and the motor can be made to operate in two distinct modes: constant torque operation up to the rated speed of the motor, and then constant power operation above rated speed, as shown in Fig.2. The steady state operation of the motor is described by:

$$V_a = E_a + R_a \cdot I_a \quad (3)$$

For normal motor operation E_a and I_a are positive and the motor is operating in its 'first quadrant'. The motor is said to be operating in its second quadrant, that is braking or regenerating, by reducing V_a below E_a such that I_a is negative. These two quadrants are shown in Fig.3a). If the polarity of the applied voltage is reversed then motoring and regenerating operation can occur with the direction of rotation reversed. Thus by controlling the armature voltage and current polarities, full four-quadrant operation, as shown in Fig.3b), can be achieved.

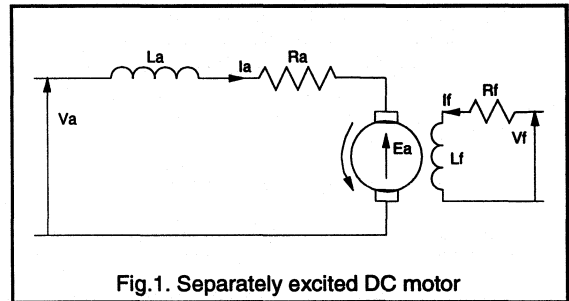


Fig.1. Separately excited DC motor

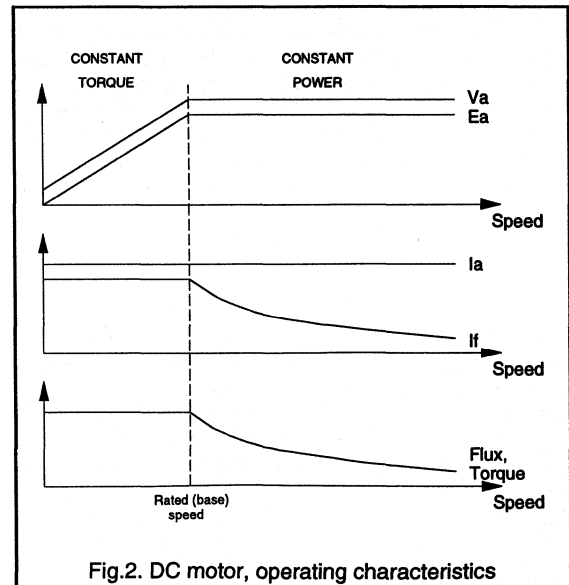
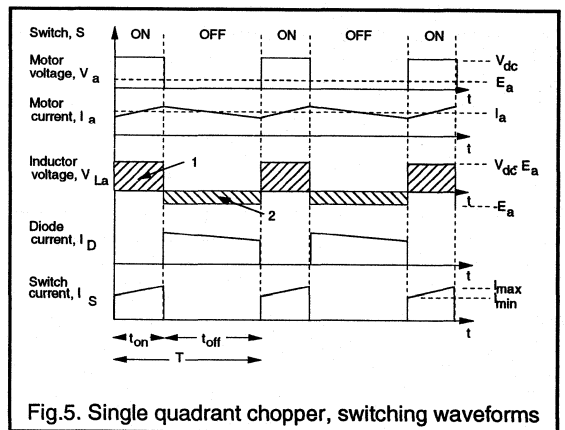
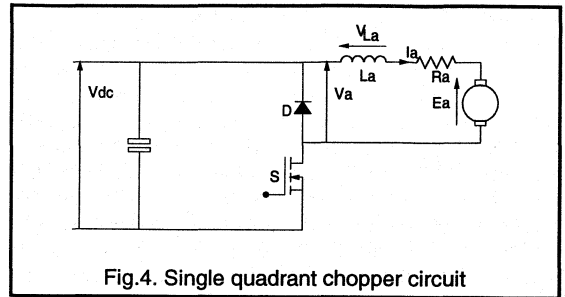
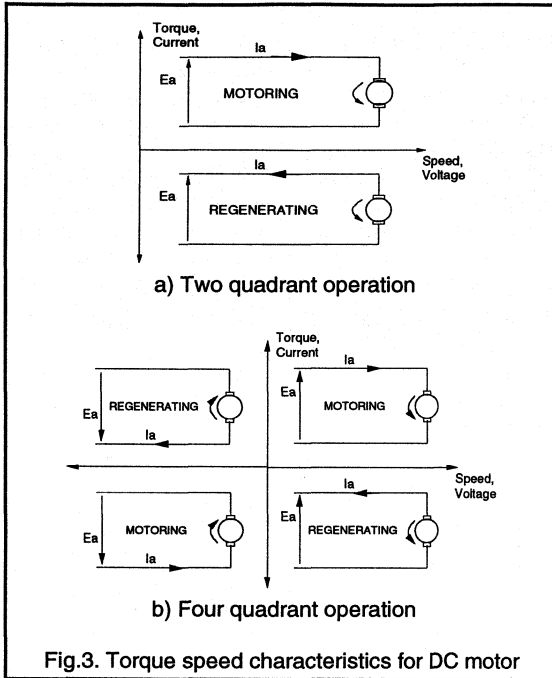


Fig.2. DC motor, operating characteristics



Converter topologies for DC motor drives

Single quadrant (step down) converter

For single quadrant operation the chopper circuit of Fig.4 can be used. The average voltage applied to the motor, and hence its speed, is controlled by varying the duty cycle of the switch, S. Fig.5 shows the switching waveforms for the circuit. During the on time, t_{on} , the supply voltage, V_{dc} , is applied to the motor and the armature current starts to increase. Neglecting the on-state resistance of the switch and the armature winding resistance the voltage across the armature inductance is $V_{dc}-E_a$ and so the rate of rise of armature current is given by:

$$\frac{dI_a}{dt} = \frac{V_{dc} - E_a}{L_a} \tag{4}$$

When the switch turns off the energy stored in the armature inductance must be dissipated. The polarity of the voltage across L_a reverses, the diode D becomes forward biased and the armature current continues to flow. Assuming that the motor speed remains constant and neglecting the forward voltage drop of the freewheeling diode the inductor voltage is equal to $-E_a$. The rate of fall of armature current is given by:

$$\frac{dI_a}{dt} = -\frac{E_a}{L_a} \tag{5}$$

If this switching sequence is repeated at some frequency, then the motor voltage can be controlled by altering the relative duration of the on period and off period. Variation of the duty cycle of the switch (t_{on}/T) to control the motor voltage is referred to as Pulse Width Modulation (PWM) control. As the average voltage across the inductor over a period must be zero then:

$$\int_0^T v_L \cdot dt = \int_0^{t_{on}} v_L \cdot dt + \int_{t_{on}}^T v_L \cdot dt = 0 \tag{6}$$

The integral of inductor voltage for the interval t_{on} corresponds to the shaded area 1 in Fig.5, whilst the integral of inductor voltage for the t_{off} interval corresponds to the shaded area 2 in the Figure. These two areas must be equal and so from equations 4 to 6 or Fig.5 the transfer function of the controller is given by:

$$V_a = \frac{t_{on}}{T} \cdot V_{dc} \tag{7}$$

Two quadrant, half-bridge converter

Figure 6 shows a half bridge circuit for two quadrant dc drive. For motoring operation S1 and D2 operate as described above for the single quadrant controller. The freewheel diode D2 may be the internal diode of a MOSFET or FREDFET, or a discrete device. For regenerative operation the DC motor acts as the active power source and the power flow is from right to left in Fig.6. The regenerating current is controlled by varying the duty cycle of S2. When S2 is on, the negative armature current increases through the switch and the armature inductance. When S2 is turned off D1 becomes forward biased and the current regenerates into the supply. The relevant circuit waveforms are shown in Fig.7, showing the equal areas of the inductor volt-seconds over each period of the switching cycle. During regeneration the transfer function of the converter is given by:

$$V_a = \left(1 - \frac{t_{on}}{T}\right) \cdot V_{dc} \tag{8}$$

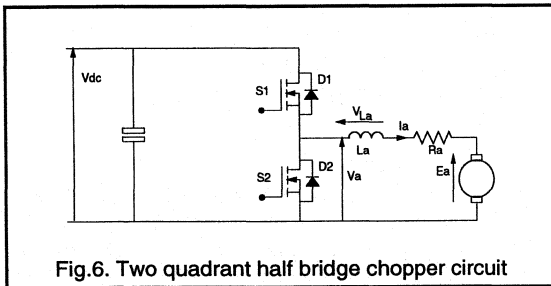


Fig.6. Two quadrant half bridge chopper circuit

Four quadrant, full-bridge converter

If motoring and regenerating operation are required with both directions of rotation then the full bridge converter of Fig.8 is required. Using this configuration allows the polarity of the applied voltage to be reversed, thus reversing the direction of rotation of the motor. Thus in a full bridge converter the motor current and voltage can be controlled independently. The motor voltage Va is given by:

$$V_a = V_{12} - V_{34} \tag{9}$$

where V_{12} is controlled by switching S1 and S2 as described above, and V_{34} by switching S3 and S4. The usual operating mode for a full bridge converter is to group the switching devices so that S1 and S3 are always on simultaneously and that S2 and S4 are on simultaneously. This type of control is then referred to as bipolar control.

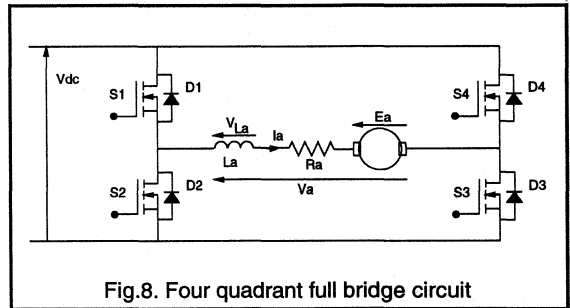


Fig.8. Four quadrant full bridge circuit

MOSFETs and FREDFETs in bridge circuits

In a bridge circuit, conduction transfers between the switching devices and freewheeling diodes as the load current is controlled (eg. switch S2 and diode D1 in Fig.4). Associated with the transfer of conduction between the freewheel diodes and the switching devices is the reverse recovery of the diode as each conducting MOSFET returns to its on-state. Reverse recovery current flows due to the removal of stored charge from a diode PN junction following conduction. Fig.9 shows the device current paths in a half bridge circuit when conduction is transferred from the top diode to the bottom MOSFET.

The switching waveforms are shown in Fig.10 where the diode reverse recovery current is I_r and the time taken for the reverse recovery currents to be cleared is t_{rr} . The amount of stored charge removed from the body of the diode is represented by the area Q_{rr} . The reverse recovery current flows through the MOSFET which is being turned on in addition to the load current and thus causes additional turn-on losses. The amount of stored charge increases with increasing temperature for a given diode. Both the

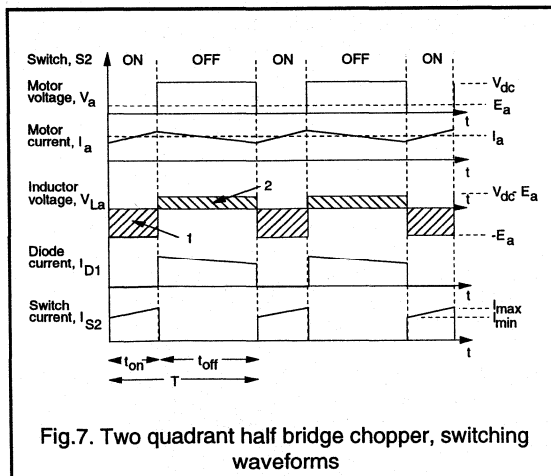


Fig.7. Two quadrant half bridge chopper, switching waveforms

magnitude of the reverse recovery current and its duration must be reduced in order to reduce the switching losses of the system.

This effect is important because inherent in the structure of a power MOSFET there is a diode between the source and drain of the device which can act as a freewheeling diode when forward biased. For most DC motor control applications the reverse recovery characteristics of the MOSFET intrinsic diode are acceptable and do not compromise the switching performance of the half bridge circuit. However, the characteristics of a MOSFET intrinsic diode are not optimised for minimum reverse recovery and so, especially in high frequency systems, the FREDFET is more suitable for use in half bridge circuits.

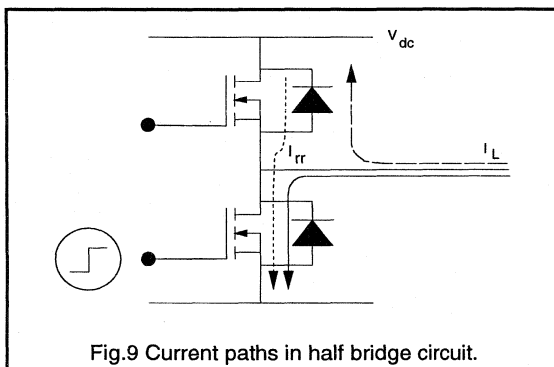


Fig.9 Current paths in half bridge circuit.

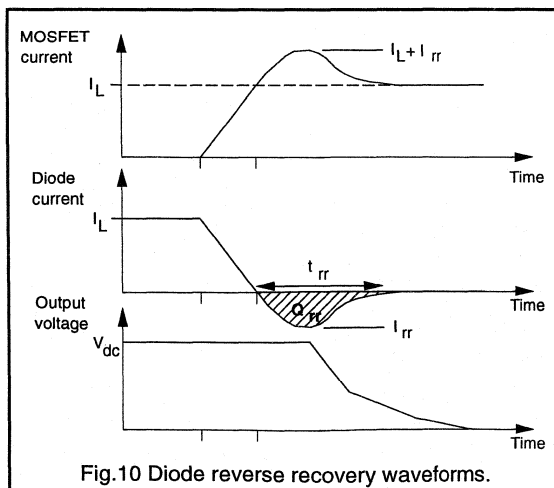


Fig.10 Diode reverse recovery waveforms.

The FREDFET is essentially a MOSFET with a very fast built-in diode where the reverse recovery properties of a FREDFET diode are similar to those of a discrete fast recovery epitaxial diode (FRED). This gives improved switching performance in high frequency applications.

Considerations for converter driven DC motors

Device current rating

The power electronic converter must be matched to the requirements of the motor and the load. DC motor drives can be used to provide torques in excess of the maximum continuous rated torque of the motor for short intervals of time. This is due to the long thermal time constants of the motor. The peak torque requirement of the motor will determine its peak current demand, and hence the peak current requirement for the power switches. The current rating of a PowerMOS device is limited by the maximum junction temperature of the device, which should not be exceeded even for short periods of time due to the short thermal time constant of the devices. The devices must therefore be rated for this peak current condition of the drive. Operation at maximum current usually occurs during acceleration and deceleration periods necessary to meet the performance requirements of DC servo systems.

Device voltage rating

The voltage rating of the power switches will be determined by the power supply DC link voltage and the motor emfs, including those which occur when the motor is operating in its constant power region at above rated speed but below rated torque.

Motor performance

It can be seen from the waveforms of Figures 5 and 7 that the armature current supplied to the motor by the switching converter is not constant. The presence of ripple current in addition to the normal DC current affects the performance of the motor in the following ways:

Torque pulsations. Ripple in the motor current waveform will cause a corresponding ripple in the motor output torque waveform. These torque pulsations may give rise to speed fluctuations unless they are damped out by the inertia of the mechanical system. The torque pulsations occur at high frequencies where they may lead to noise and vibration in the motor laminations and mechanical system.

Losses. Winding losses in a DC motor are proportional to i_{RMS}^2 , whereas the torque developed by the motor is proportional to i_{DC} . Ripple in the motor current will increase the RMS current and thus give rise to additional losses and reduce the system efficiency.

Overcurrents. If the ripple current is large then the peak device current will be significantly higher than the design DC value. The devices must then be rated for this higher current. Current ripple will also increase the current which must be handled by the motor brushes possibly increasing arcing at the brush contacts.

The amount of current ripple depends primarily upon the switching frequency and amount of motor inductance (See equations 4 and 5). Increasing L_a and f_s will both reduce the amount of current ripple. The motor inductance is fixed by the motor selection but can be increased by the addition of a discrete component. Increasing the switching frequency of the system will reduce the amount of current ripple but will increase the switching losses in the power devices.

Using PowerMOS devices in DC drives

For many applications the motor control system is operated at switching speeds in the range 1kHz to 20kHz. PowerMOS devices are ideally suited for this type of converter giving the following advantages:

Switching performance

Unlike bipolar devices the MOSFET is a majority carrier device and so no minority carriers must be moved in and out of the device as it turns on and off. This gives the fast switching performance of MOSFET devices. However, at higher switching speeds the switching losses of the system become important and must be considered in addition to the device on-state losses. The device conduction loss depends on the MOSFET on-state resistance, $R_{DS(ON)}$, which increases with the temperature of the device. Switching times are essentially independent of device temperature. PowerMOS devices have good overload capability and Safe Operating Area (SOAR) which makes them easy to use in a chopper circuit, although the need for snubber circuits will depend on the system operating and performance requirements.

Ease of use

PowerMOS devices are essentially voltage driven switches and so the gate drive circuits required to switch the devices are usually relatively simple low power circuits. It is only during switching instants that the gate drive is that required provide current in order to charge and discharge the device capacitances (shown in Fig.11) and thus switch the device. In order to switch the device quickly the gate driver must be able to rapidly sink and source currents of up to 1A. For the simplest gate drive circuit the MOSFET can be switched using a resistive drive and some gate-source overvoltage protection, as shown in Fig.11. Alternative MOSFET gate drive circuits are discussed more fully elsewhere in this handbook.

Parallelling of PowerMOS devices

It is usually straightforward to operate PowerMOS devices in parallel to achieve higher system currents than can be achieved using single devices. The problems of parallelling PowerMOS are much less than those which occur when using bipolar devices. MOSFETs and FREDFETs have a positive temperature coefficient of $R_{DS(ON)}$ and so tend to share the total load current equally. Any discrepancy in device or circuit resistance which causes one device to be carrying a higher proportion of the total current will cause the losses in that device to increase. The device carrying the increased current will then heat up, its resistance will increase and so the current carried will be reduced. The total load current will therefore be equally shared out between all the parallelled MOSFETs. Current sharing during dynamic (switching) instants is achieved by ensuring good circuit design and layout.

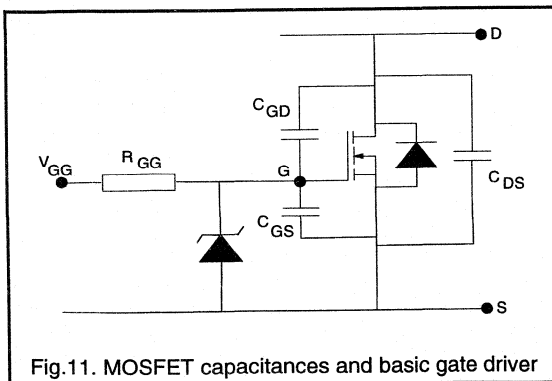


Fig.11. MOSFET capacitances and basic gate driver

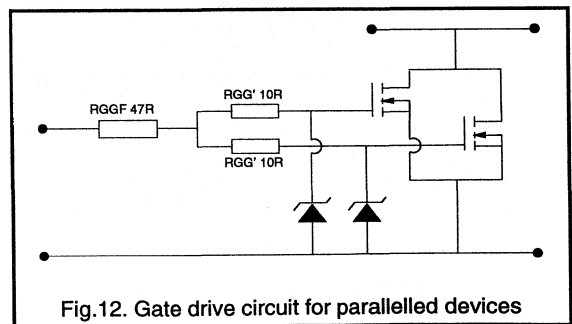


Fig.12. Gate drive circuit for paralleled devices

Moving to a system using paralleled MOSFETs requires only slight modifications to the gate drive circuit. One consideration may be the capability of the drive circuit to provide the currents required at the switching instants. It is recommended that small differential resistors, as shown in Fig.12, are used to damp out any oscillations which may occur between the switching devices and the rest of the circuit.

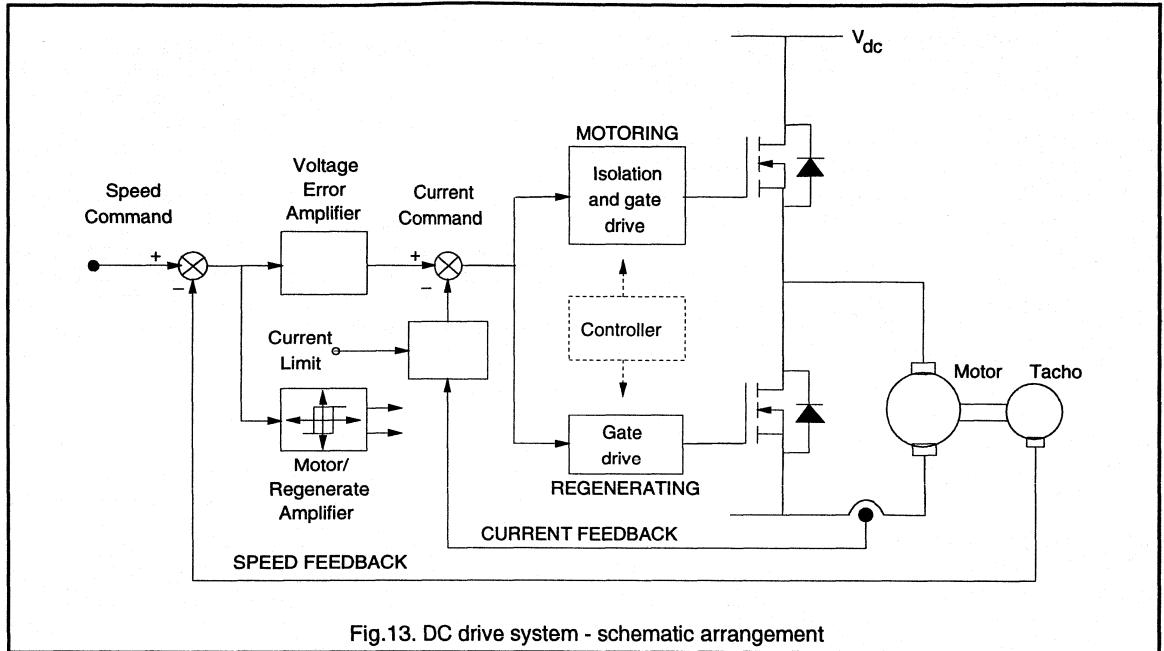


Fig.13. DC drive system - schematic arrangement

Circuit layout considerations

The effects of poor circuit design and layout are to increase RFI and noise and to compromise the performance and speed of the system due to stray inductances. The precautions which must be taken to minimise the amount of stray inductance in the circuit include:

- positioning the gate drive circuits as close as possible to the power MOSFETs.
- reducing circuit board track lengths to a minimum and using twisted pairs for all interconnections.
- for paralleled devices, keeping all connections short and symmetrical.

DC motor control system

Figure 13 shows a schematic arrangement for a two quadrant controller, showing the outer speed control loop and the inner current control loop. The speed feedback signal is derived from a tachogenerator (TGF), although alternatively an approximation to the motor speed can be derived by feeding back a signal proportional to the motor voltage, (AVF). Position feedback can be included for servo applications by using a position encoder on the motor shaft. The speed feedback loop compares the tachogenerator output voltage with a speed reference signal. The voltage error signal gives the current reference command.

The current command signal is compared with the actual motor current in the inner control loop. This control loop includes a current limit setting which protects the motor and the devices from overcurrents. If the controller demands a large speed change then the current demand is maintained below the maximum level by this current limit setting. Motoring or regenerating operation is detected directly from the polarity of the voltage error signal and used to determine whether it is the top or bottom MOSFET which is controlling the current. The motoring/regenerating logic circuit includes some hysteresis to ensure that control does not oscillate between the motoring and regenerating modes at low motor currents.

There are several possible ways of controlling motor current by controlling the switching sequences to the main PowerMOS devices. In tolerance band control the motor current is compared with the reference signal and an allowed current ripple tolerance. During motoring operation if the actual current is greater than the allowed maximum value of the tolerance band then the output comparator turns off the gate drive to the power MOSFET thus allowing the motor current to fall. The current then freewheels until it reaches the lower limit of the tolerance band, when the comparator turns the MOSFET back on. Using this current control strategy the effective switching frequency is variable, depending on the rate at which the armature current changes, but the peak to peak current ripple in the system is constant. Alternatively the devices can be

switched a constant frequency using a PWM method current control. Here the current error signal is compared with a fixed frequency triangular wave and the comparator output is then used to provide the signal for the main switching devices. When the error signal is greater than the triangular wave then the power device is switched on, when the error signal is less than the triangular carrier then the device is switched off.

Conclusions

DC motor controllers using PowerMOS devices can be used in many speed control and servo applications giving excellent drive performance. The advantages of PowerMOS devices include their simple gate drive

requirements, rugged performance and their ease of use in parallel configurations. The intrinsic diode between the drain and source of MOSFETs and FREDFETs can be used as the freewheel diode in half bridge and full bridge circuit configurations giving a cost effective, compact design with the minimum of switching devices. PowerMOS choppers can operate at much higher switching frequencies than thyristor or power transistor controllers, giving reduced current ripple, reduced noise and interference and good dynamic system response. Using higher switching frequencies reduces the need for additional discrete inductances in the motor circuit whilst still achieving low ripple currents in separately excited, permanent magnet and series connected field wound motors.



3.2.2 A switched-mode controller for DC motors

The purpose of this paper is to demonstrate the use of an integrated switched-mode controller generally used for DC power conversion as the primary control and element in a practical Pulse Width Modulated (PWM) DC drive. Basic principles relating to DC motor specifications and drive frequency are presented. The PWM method of switched-mode voltage control is discussed with reference to armature current control, and hence output torque control, of DC motors. A series of circuit configurations are shown to illustrate velocity and position servo applications using a switched mode driver IC. Philips Semiconductors produce a wide range of control ICs for Switched Mode Power Supply (SMPS) applications which can also be used as controllers for PWM driven DC motors. This paper demonstrates how one switched-mode controller, the NE5560, can be used to give a velocity and position servo systems using Philips power MOSFETs as the main power switches. Additional application ideas using the NE5560 controller for constant speed and constant torque operation are also presented.

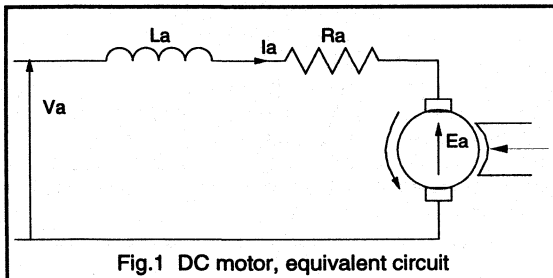


Fig.1 DC motor, equivalent circuit

Principles of the PWM DC motor drive

Pulse width modulated drives may be used with a number of DC motor types: wound field or permanent magnet. The discussion here will be particularly concerned with permanent magnet excited DC motors. This does not impose a restriction on the applicability of switched mode control for DC drives since permanent magnet motors are available in a wide range of sizes, ratings and configurations to suit many applications. The design of a pulse width modulated drive is affected by the characteristics of the DC motor load, and this will now be considered in more detail.

The permanent magnet DC motor may be represented by the simplified equivalent circuit shown in Fig.1. L_a represents the total armature inductance, R_a is the equivalent series resistance, and E_a the armature back emf. This induced emf represents that portion of the total input

energy which is converted to mechanical output. The magnitude of the armature emf is proportional to motor speed.

Motor inductance, which may vary from tens of μH to mH, will have a significant effect on PWM drive designs. This is due to the fact that average motor current is a function of the electrical time constant of the motor, τ_a , where $\tau_a = L_a/R_a$. For a PWM waveform with a period T the ratio of pulse width to switching period is denoted by δ . The average pulse current will depend upon the ratio of the current pulse-width, δT , to the motor electrical time constant, τ_a .

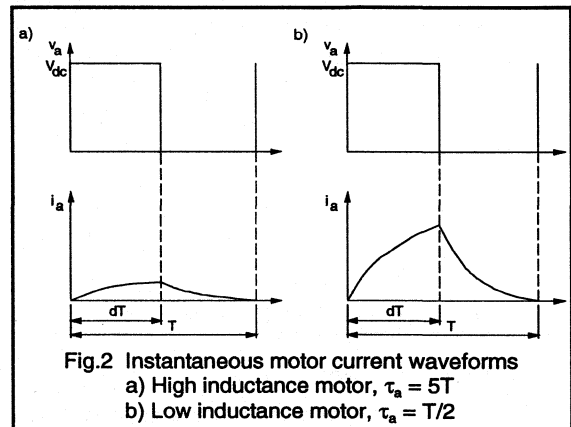


Fig.2 Instantaneous motor current waveforms
a) High inductance motor, $\tau_a = 5T$
b) Low inductance motor, $\tau_a = T/2$

Figure 2 shows the conditions for two different motors and a fixed period PWM waveform. For the case when the motor time constant is much greater than the pulse width, in Fig.2(a) then the current cannot be established in the inductive motor windings during the short duration of the applied pulse. For a low inductance motor and the same pulse width, Fig.2(b), the armature current is easily established. In most instances a motor which has high armature inductance will require a lower PWM drive frequency in order to establish the required current levels, and hence develop the necessary torque. A low inductance motor allows the use of a high switching drive frequency thus resulting in an overall faster system response.

In general, to achieve optimum efficiency in a PWM motor drive at the highest practical frequency, the motor should have an electrical time constant, τ_a , close to the duration of the applied waveform T . ($\tau_a = kT$ where k is small). The printed circuit motor is one of the lowest inductance DC motors available since the armature is etched from a flat disc-like material much like a double-sided printed circuit board. Consequential these low inductance, low inertia

motors also exhibit very fast response with quite high torque. Electrical time constants in the order of 100µs allow these motors to be used with switching rates as high as 100kHz, with typical drive circuits being operated at 10kHz.

Thus an appropriate choice of switching frequency and motor inductance ensures a high average motor current during each switching pulse. Motor current control, and hence torque control, is achieved by varying the width of the applied pulsed waveforms. As the base, or carrier, frequency is held constant then the pulse width relays torque control information to the motor. Torque is dependent on average motor current (equation 1) which, in turn, is controlled by duty cycle.

$$T_e = K_T \bar{I}_a \quad (1)$$

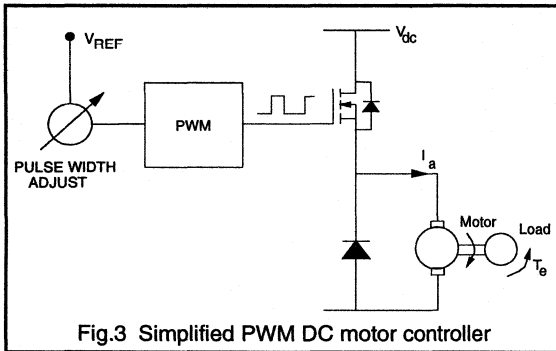


Fig.3 Simplified PWM DC motor controller

PWM motor control

The PWM method of current control will be considered by examining the conditions at motor start-up for a simple arrangement, shown in Fig.3, where the duty cycle is controlled using the DC control voltage, V_{REF} . At start-up the duty cycle is adjusted to be long enough to give sufficient motor starting torque. At zero rotational velocity ($\omega=0$) the back emf, E_a , is zero and so the full DC voltage appears across the series R_a/L_a impedance. The initial motor current is determined according to the equation:

$$L_a \cdot \frac{di_a}{dt} + R_a \cdot i_a = V_{dc} \quad (2)$$

If the duty cycle ratio, controlled using V_{REF} , is given by δ , then the duration of the 'ON' pulse is simply given by δT . During this interval the rise of motor current prior to armature rotation is shown by Equation 3.

$$i_a = \frac{V_{dc}}{R_a} \cdot (1 - e^{-t/\tau_a}) \quad (3)$$

The current in the motor windings rises exponentially at a rate governed mainly by average supply voltage and motor inductance. If the pulse width is close to the time constant of the motor then the current at the end of the first pulse will reach nearly 60% of its maximum value, $I_{max} = V_{dc}/R_a$. This is shown as I_1 in Fig.4. For the remainder of the PWM cycle switch S1 is off and motor current decays through the diode at a rate dependant upon the external circuit constants and internal motor leakage currents, according to the equation:

$$i_a = I_1 \cdot e^{-(t-\delta T)/\tau_a} \quad (4)$$

The motor current at the end of the period, T , remains at a level I_2 , which is then the starting current for the next cycle, as shown in Fig.4. As the switching sequence repeats, sufficient current begins to flow to give an accelerating torque and thus cause armature rotation. As soon as rotation begins, back emf is generated which subtracts from the supply voltage. The motor equation then becomes:

$$L_a \cdot \frac{di_a}{dt} + R_a \cdot i_a = V_{dc} - E_a \quad (5)$$

The current drawn from the supply will consequently be less than that drawn at start-up due to the effect of the motor back emf term, E_a . For a given PWM duty cycle ratio, δ , the motor reaches a quiescent speed governed by the load torque and damping friction. Maximum motor torque is required at start-up in order to accelerate the motor and load inertias to the desired speed. The current required at start-up is therefore also a maximum. At the end of the starting ramp the controller duty cycle is reduced because less current is then needed to maintain the motor speed at its steady state value.

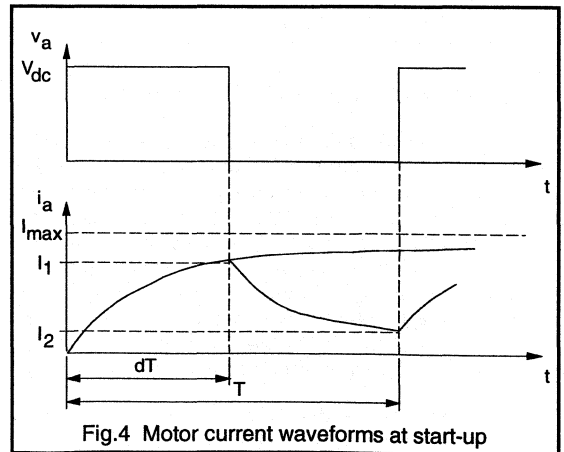
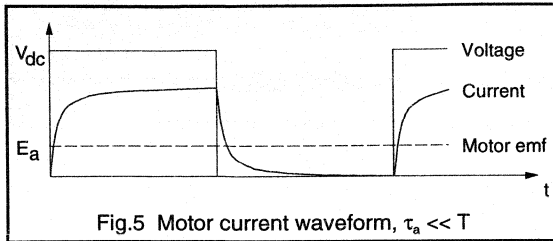


Fig.4 Motor current waveforms at start-up



For a low inductance motor where the electrical time constant is much less than the duty cycle then the motor current waveform will closely follow the applied voltage waveform, as shown in Fig.5. An approximate expression for the average motor current is given by:

$$I_{\text{ave}} = \delta \cdot \frac{(V_{\text{dc}} - E_a)}{R_a} \quad (6)$$

In summary, the principle control variable in the PWM motor control system is 'duty cycle', δ . Motor torque and velocity can be tightly controlled by controlling the PWM duty cycle and motor current.

The switched mode controller

For the remaining portion of the paper integrated switched-mode control will be considered with specific reference to the NE/SE5560 controller IC. This device incorporates control and protection functions for SMPS and DC motor control applications including internal temperature compensation, internal reference voltages, a sawtooth waveform generator, PWM amplifier and output stage. Protection circuitry includes cycle-by-cycle current limiting, soft start capability, overcurrent protection, voltage protection and feedback loop protection circuits. In the following sections some of the features of the controller will be examined and its use in a number of motor drive designs will be presented.

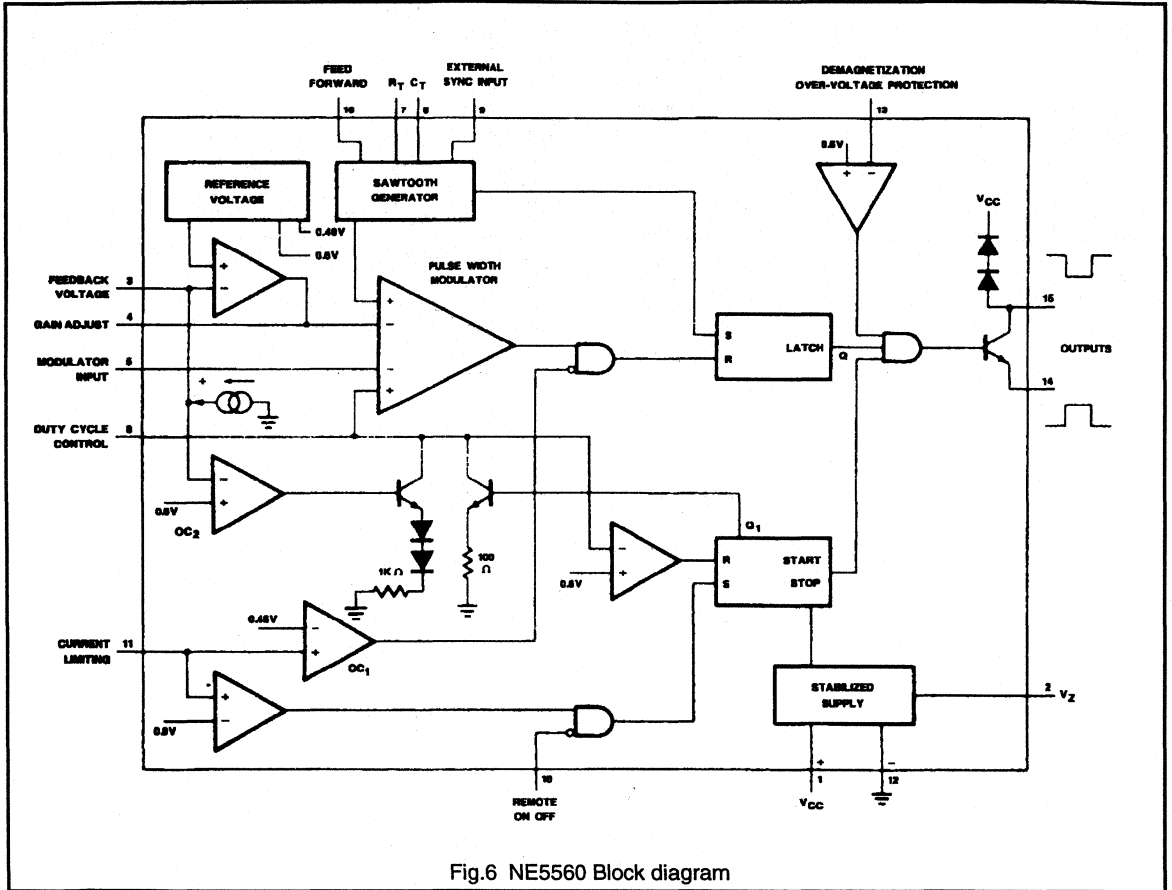


Fig.6 NE5560 Block diagram

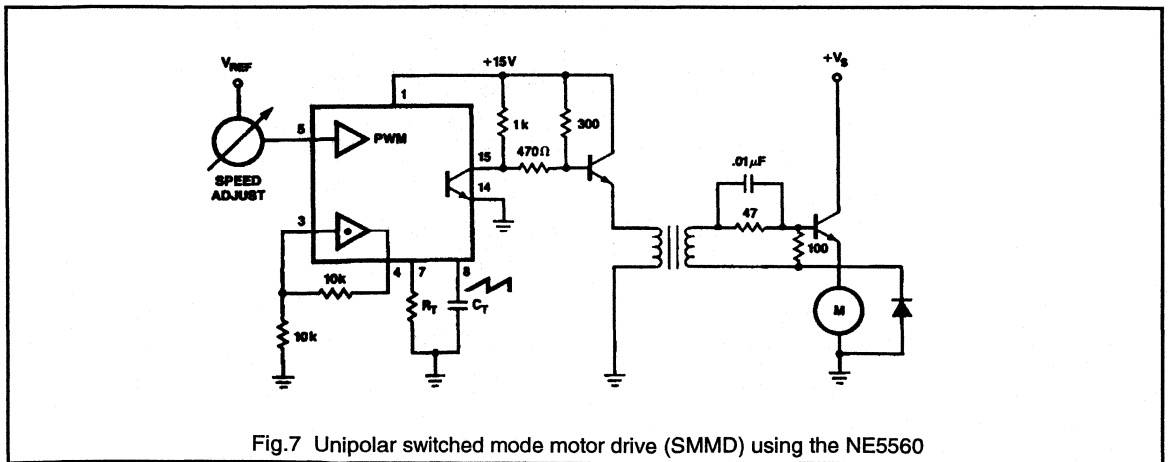
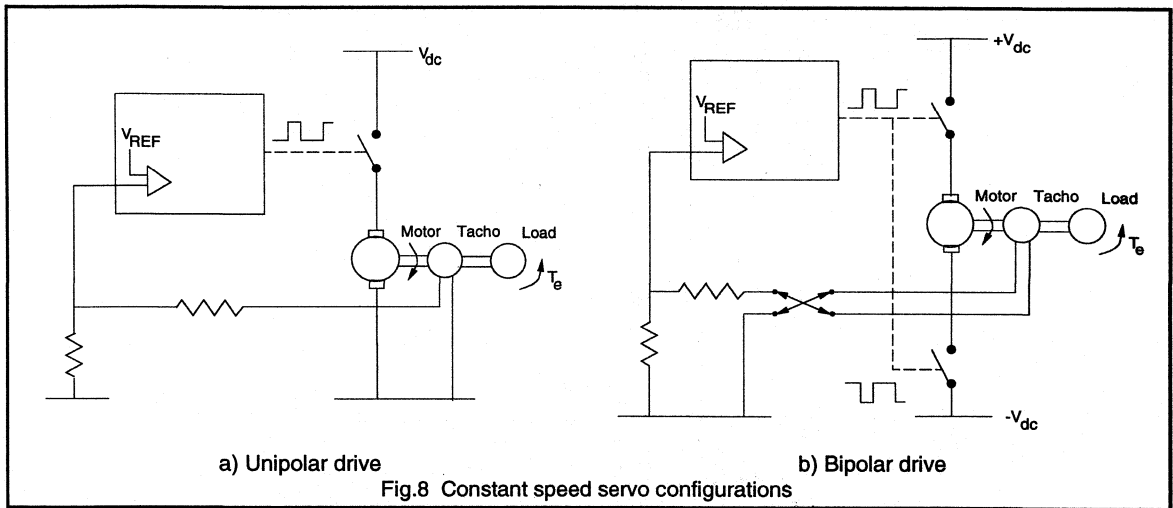
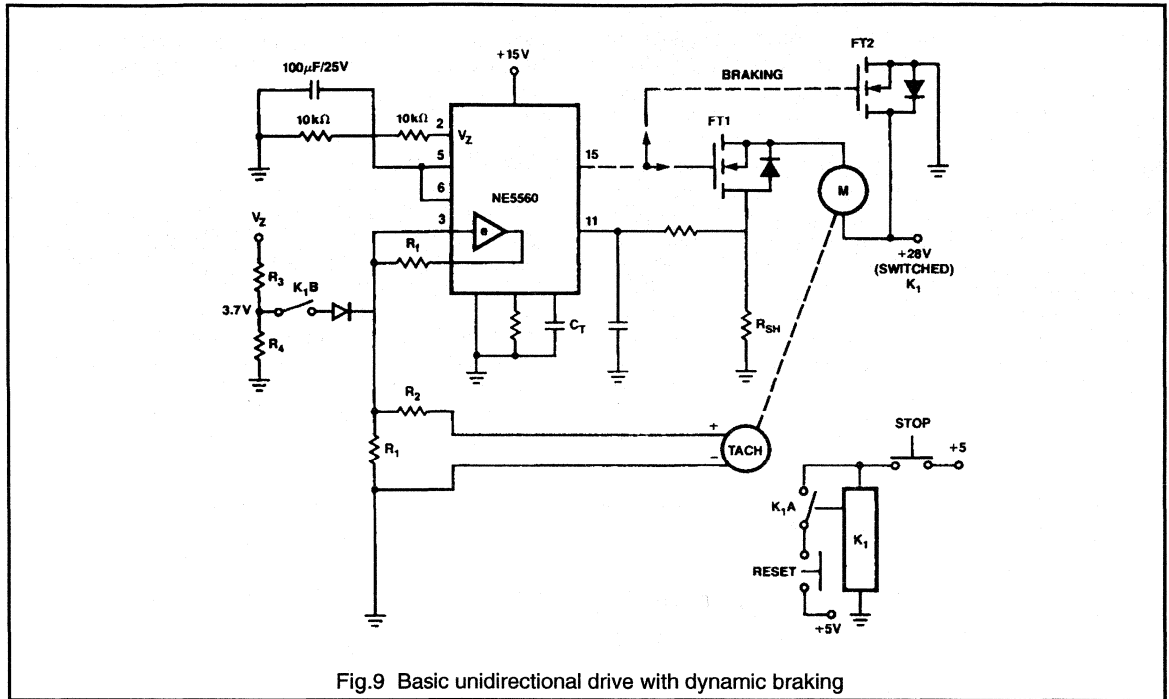


Fig.7 Unipolar switched mode motor drive (SMMD) using the NE5560

The device (see Fig.6) contains an internal voltage reference which is connected to the non-inverting input of the error amplifier. The feedback signal is obtained from either a tachogenerator (TGF - tachogenerator feedback) or from a signal proportional to the armature voltage less the winding iR voltage drop (AVF - armature voltage feedback). This feedback signal must be scaled to centre about the internal voltage reference level. The error amplifier output, in addition to being available for gain adjustment and op amp compensation, is connected internally to the pulse-width modulator. Frequency may be fixed at any value from 50Hz to 100kHz and duty cycle

adjusted at any point from 0 to 98%. Automatic shut-down of the output stage occurs at low supply threshold voltage. The error amplifier has 60dB of open loop gain, is stable for closed loop gains above 40dB and can also be compensated for unity gain. The single ended switching output is from either the emitter or collector of the output stage. The device has protective features such as high speed overcurrent sense which works on a cycle-by-cycle basis to limit duty cycle, plus an additional second level of slow start shutdown. It is this input which can be adapted to act as a motor torque limit detector.





Open loop PWM control using the NE5560

For a given application the switched-mode controller frequency should be set to allow the best dynamic response considering the starting current requirement and motor electrical time constant, as discussed previously. The main drive transistors or MOSFETs must be capable of carrying the peak motor current requirement which occurs at start-up. Device protection using snubber networks and transient suppression networks will depend on the choice of switching device, system ratings and the application requirements. Power MOSFETs provide an excellent solution to many DC drive designs since very low drive power is required and they are self-protected from reverse transients by an internal intrinsic diode. PowerMOS devices may be paralleled for added power handling capability.

Figure 7 shows a simple unipolar drive capable of driving a low voltage motor supplied from an external DC voltage and PWM controlled using the NE5560.

Constant velocity servo

Figure 8 shows in block form the general circuit used to obtain a constant speed switched mode motor drive (SMMD) servo. Figure 8(a) shows a unipolar drive using DC tachometer feedback to the PWM error amplifier. Figure 8(b) shows a bidirectional drive in a half-bridge

configuration. In this case the duty cycle controls the direction of motor rotation in addition to the motor speed. A 50% duty cycle corresponds to the standstill condition. If the average duty cycle is greater than 50% (CW command) then the motor accelerates clockwise, and vice-versa for CCW rotation when the duty cycle is less than 50%. This circuit configuration can be used for both velocity and position servo-designs. The reversing switch allows the tachogenerator output to match the polarity of the PWM reference, which is always positive.

The unipolar drive circuit in Fig.9 uses the NE5560 to develop a SMMD with constant speed control suitable for a small DC motor. The switching device is a single Philips BUK456-100A Power MOSFET capable of over 30 A, with a voltage rating of 100V V_{DS} and $R_{DS(ON)}=0.057\Omega$. The PWM drive from the NE5560 is applied to the gate at a nominal 10kHz, although much higher frequencies are possible. The peak gate to source voltage, V_{GS} , is 15V to ensure minimum $R_{DS(ON)}$ and hence minimum loss in the PowerMOS switch.

A sense resistor is placed in the source lead to monitor motor drive current on a cycle-by-cycle basis. The value of this resistor is set to develop the error amplifier threshold voltage at the desired maximum current. The NE5560 then automatically limits the duty cycle, should this threshold be exceeded. This is therefore used as an auto torque limit feature in addition to simply protecting the switching device.

A slow start network (Pins 2,5,6) gradually ramps up the duty cycle at power on. Fixed braking duty cycle control is achieved by forcing the input error amplifier during braking conditions. The over-current circuit is still active during braking.

SMMD Position servo with μ P control

By coupling the switched mode motor drive in a bidirectional configuration as shown in Fig.10, and then sensing linear position with a potentiometer or LVDT connected to a lead screw, for instance, the position feedback loop can be closed to give a position servo. The input to control position of the mechanical stage may be fed as a DC offset to a summing amplifier whose output is fed to Pin 5 of the NE5560, as shown. Forward lead-lag compensation may be combined with the summing amplifier function to achieve a stable response. A velocity loop may be closed through

the error amplifier at Pin 3. The controller may easily be interfaced to a microprocessor by means of a unipolar D/A converter working in the 1 to 6V output range as an input to Pin 5.

Conclusions

The switched-mode motor drive, SMMD, using small, easily available, monolithic integrated control devices designed for switched-mode power applications may easily be adapted to perform a number of useful and efficient torque, velocity and position control operations. The ready availability of good controller ICs, easily compatible with the Philips range of switching power devices in both bipolar and PowerMOS technologies makes such designs even more effective and easily attainable by the control systems designer.

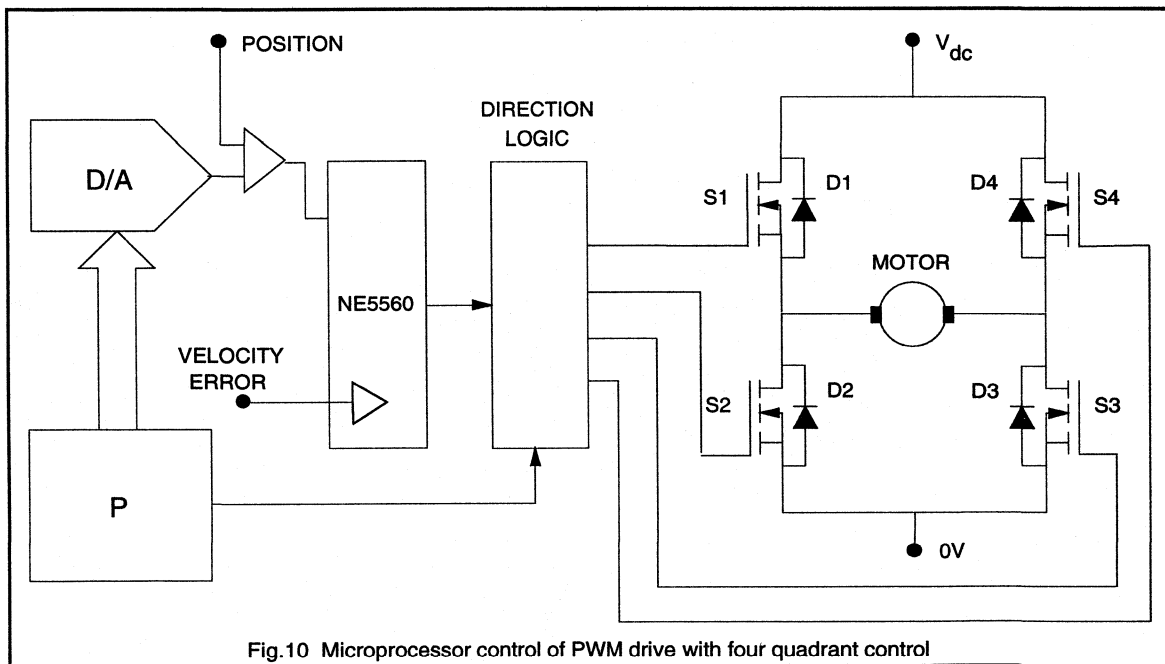


Fig.10 Microprocessor control of PWM drive with four quadrant control



3.2.3 Brushless DC Motor Systems

In recent years the number of drive systems available to designers has increased considerably. The advent and increasing use of stepper motors, inverter-fed ac machines, switched reluctance motors and brushless machines have all addressed particular applications and in some cases these application areas overlap. The correct choice of a drive system for a particular application depends not only upon the speed and torque requirements but also on performance, response, complexity and cost constraints. The brushless DC motor (BDCM) system is emerging as one of the most useful drive options for a wide range of applications ranging from small, low power fans and disc drives, through medium size domestic appliance motors and up to larger industrial and aviaional robotic and servo drives.

This section will review the theory and operation of brushless DC motors and describe some of the considerations to be made when designing BDCM drive systems using PowerMOS devices as the main inverter switches.

Background

The principal advantage of a conventional DC machine compared to an AC machine is the ease with which a DC motor can be controlled to give variable speed operation, including direction reversal and regenerative braking capability. The main disadvantage of a DC machine is that the carbon brushes of a DC motor generate dust and also require maintenance and eventual replacement. The RFI generated by the brushgear of a DC motor can be quite large and, in certain environments, the sparks themselves can be unwelcome or hazardous. The brushless DC motor was developed to achieve the performance of a conventional DC machine without the problems associated with its brushes.

The principal advantages of the BDCM system are:

- Long life and high reliability
- High efficiency
- Operation at high speeds and over a wide speed range
- Peak torque capability from standstill up to high speeds
- Simple rugged rotor construction
- Operation in vacuum or in explosive or hazardous environments
- Elimination of RFI due to brush commutation

DC motor configurations

In a conventional DC motor the field energy is provided by either a permanent magnet or a field winding. Both of these arrangements involve quite large, bulky arrangements for the field. In the case of wound field DC motors this is due

to large number of turns needed to generate the required electromagnetic field in the airgap of the machine. In the case of permanent magnet DC machines the low energy density of traditional permanent magnet materials means that large magnets are required in order to give reasonable airgap fluxes and avoid demagnetisation. If either of these two options are used with the field excitation on the rotor of the machine then the inertia and weight of the rotor make the machine impractical in terms of its size and dynamic response.

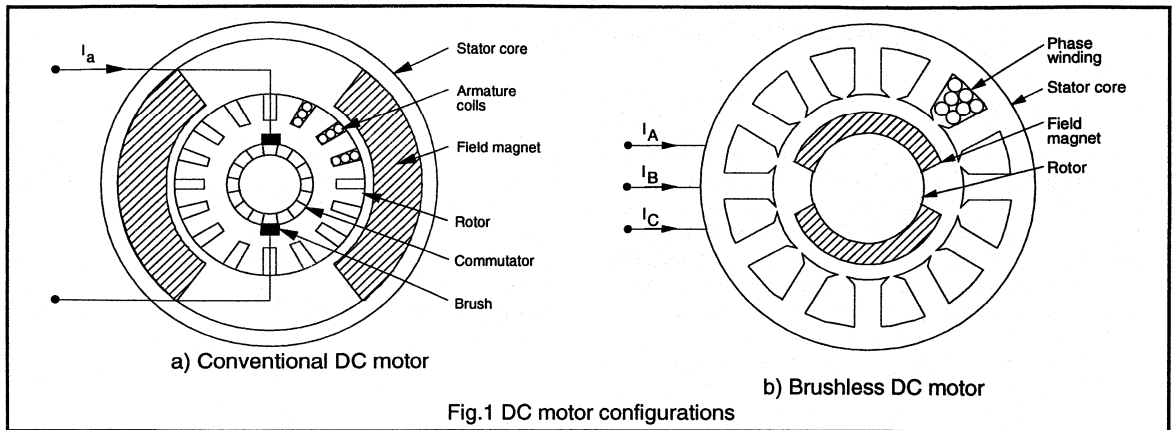
A conventional DC machine has a large number of armature coils on the rotor. Each coil is connected to one segment of a commutator ring. The brushes, mounted on the stator, connect successive commutator segments, and hence armature coils, to the external DC circuit as the motor moves forward. This is necessary to maintain maximum motor torque at all times. The brush/commutator assembly is, in effect, a rotating mechanical changeover switch which controls the direction and flow of current into the armature windings.

In a BDCM the switching of current to the armature coils is carried out statically and electronically rather than mechanically. The power switches are arranged in an inverter bridge configuration in order to achieve bidirectional current flow in the armature coils, i.e. two power switches per coil. It is not possible to have a large number of armature coils, as is the case for a conventional DC motor because this would require a large number of switching devices and hence be difficult to control and expensive. An acceptable compromise is to have only three armature coils and hence six power switches. Reducing the number of armature coils means that the motor is more prone to developing ripple torque in addition to the required DC torque. This problem can be eliminated by good design of the motor. The armature of a three coil brushless DC machine in fact looks similar to the stator of a three phase AC machine and the term 'phase' is more commonly used to describe these three separate coils.

The development of brushless DC machines has made possible by developments in two other technologies: namely those of permanent magnet materials and power semiconductor switches.

Permanent magnet materials

Traditional permanent magnet materials, such as AlNiCo magnets and ferrite magnets, are limited either by their low remanence giving rise to a low airgap flux density in electrical machines, or by their susceptibility to demagnetisation in the presence of high electric fields. However in recent years several new permanent magnet materials have been developed which have much higher



remanent flux densities, and hence airgap flux densities, and high coercivities, making them resistant to demagnetisation under normal operating conditions. Amongst these materials, called 'rare earth' magnets, Samarium Cobalt (SmCo_5 and $\text{Sm}_2\text{Co}_{17}$) and Neodymium-Iron-Boron (Nd-Fe-B) are the most common. These materials, although still quite expensive, give vastly superior performance as the field excitation for a brushless machine.

Due to the increased energy density of rare earth magnets the amount of magnet material required by the application is greatly reduced. The magnet volume using rare earths is small enough that it is feasible to have the permanent magnet field on the rotor of the machine instead of on the stator. This gives a low inertia, high torque motor capable of high performance operation. This resulting motor design, with the armature on the stator and the field on the rotor and shown in Fig.1, can be considered as a conventional DC motor turned 'inside out.'

Power electronic switches

For the 'inside out' BDCM it is still necessary to switch the armature current into successive armature coils as the rotor advances. As the coils are now on the stator of the machine the need for a commutator and brushgear assembly has disappeared. The development of high voltage and high current power switches, initially thyristors, bipolar power transistors and Darlingtons, but more recently MOSFETs, FREDFETs, SensorFETs and IGBTs, has meant that motors of quite large powers can be controlled electronically, giving a feasible BDCM system. The question of appropriate device selection for brushless DC drives will be considered later.

System description (Fig.2)

DC power supply

The fixed DC voltage is derived from either a battery supply, low voltage power supply or from a rectified mains input. The input voltage may be 12V or 24V as used in many automotive applications, 12V-48V for applications such as disc drives or tape drives, or 150V-550V for single-phase or three-phase mains-fed applications such as domestic appliances or industrial servo drives or machine tools.

Inverter

The inverter bridge is the main power conversion stage and it is the switching sequence of the power devices which controls the direction, speed and torque delivered by the motor. The power switches can be either bipolar devices or, more commonly, PowerMOS devices. Mixed device inverters, for example systems using pnp Darlingtons as the high side power switches and MOSFETs as the low side switches, are also possible. The freewheel diodes in each inverter leg may be internal to the main power switches as in the case of FREDFETs or may be separate discrete devices in the case of standard MOSFETs or IGBTs. Detailed considerations of inverter design, gate drive design and layout have been considered in separate articles.

The inverter switching speed may be in the range 3kHz to 20kHz and above. For many applications operation at ultrasonic switching speeds (>15-20kHz) is required in order to reduce system noise and vibration, reduce the amplitude of the switching frequency currents and to eliminate switching harmonic pulsations in the motor. Because of the high switching speed capability of PowerMOS devices they are often the most suitable device for BDCM inverters.

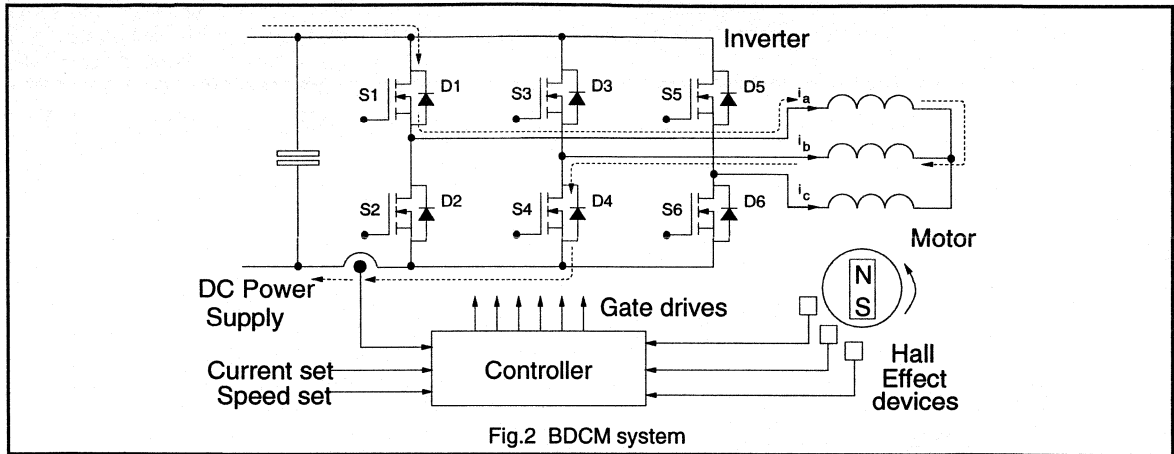


Fig.2 BDCM system

The first choice for the inverter devices might appear to be one with an N-channel MOSFET for the bottom device in each inverter leg and a P-channel device in the top half of each leg. The disadvantage of P-channel devices is that they require around three times more silicon area than equivalent N-channel MOSFETs to achieve the same value of $R_{DS(ON)}$. This makes P-channel devices uncompetitively expensive for many applications. However, using N-channel devices for both the top and bottom switches in an inverter leg means that some sort of floating drive is required for the upper device. Transformer coupled or optically coupled gate driver stages are required, or alternatively, circuits such as the bootstrap circuit shown in Fig.3 can be used to provide the drive for the top device.

In the circuit of Fig.3 the bootstrap capacitor is charged up via the diode D every time the bottom MOSFET is on. When this device turns off the capacitor remains charged up to the gate supply voltage as D is now reverse biased. When a turn-on pulse is applied for the upper MOSFET the bootstrap capacitor provides the necessary gate source voltage to turn the device on.

Motor

A two pole BDCM with the field magnets mounted on the surface of the rotor and with a conventional stator assembly was shown in Fig.1. Machines having higher numbers of poles are often used depending upon the application requirements for motor size, rotor speed and inverter frequency. Alternative motor designs, such as disc motors or interior magnet rotor machines, are also used for some applications. The motor phases are usually connected in a star configuration as shown in Fig.2. Rotor position sensors are required in order to control the switching sequence of the inverter devices. The usual arrangement has three Hall effect sensors, separated by either 60° or 120° , mounted on the stator surface close to the airgap of the machine. As

the rotor advances the switching signals from these Hall Effect latches are decoded into rotor position information in order to determine the inverter firing pattern.

In order to minimise torque ripple the emf induced in each motor phase winding must be constant during all instants in time when that phase is conducting current. Any variation in a motor phase emf whilst it is energised results in a corresponding variation in the torque developed by that phase. The so-called 'trapezoidal emf' motor, shown in Fig.4, has a constant induced emf for 120° and so is a practical motor design which gives optimum performance in a BDCM system.

Controller

The inverter is controlled in order to limit the device currents, and hence control the motor torque, and to set the direction and speed of rotation of the motor. The average output torque is determined by the average current in each phase when energised. As the motor current is equal to the DC link current (Fig.2) then the output torque is proportional to the DC input current, as in a conventional DC motor. The motor speed is synchronous with the applied voltage waveforms and so is controlled by setting the frequency of the inverter switching sequence.

Rotor position feedback signals are derived from the Hall effect devices as discussed earlier or from opto-transducers with a slotted disc arrangement mounted on the rotor shaft. It is also possible to sense rotor position by monitoring the emfs in the motor phase windings but this is somewhat more complex. In some applications the Hall effect sensor outputs can be used to provide a signal which is proportional to the motor speed. This signal can be used in a closed loop controller if required.

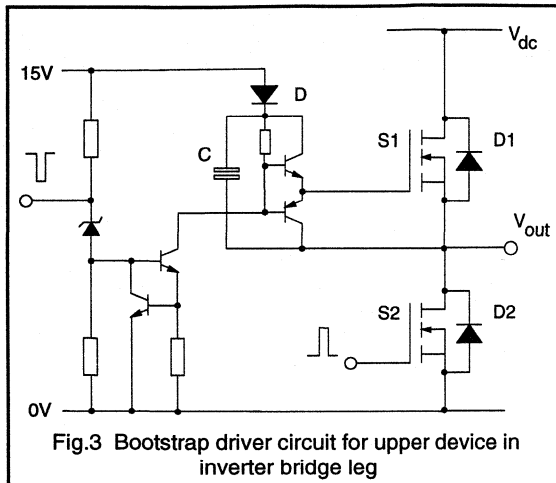


Fig.3 Bootstrap driver circuit for upper device in inverter bridge leg

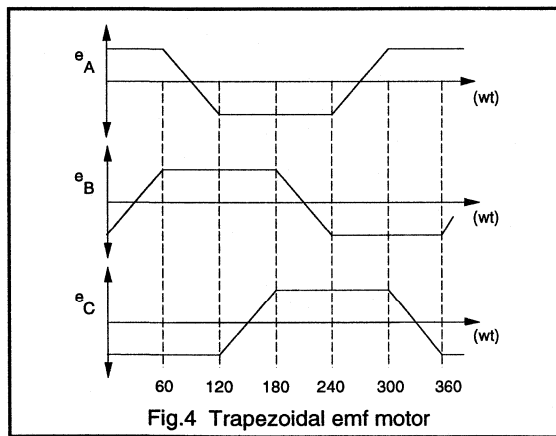


Fig.4 Trapezoidal emf motor

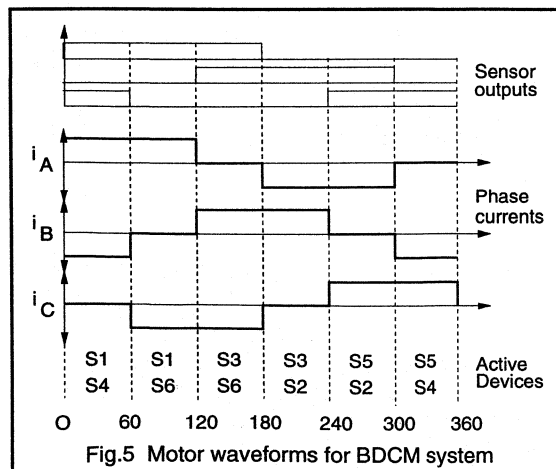


Fig.5 Motor waveforms for BDCM system

The controller also requires a current feedback signal. Usually this is taken from the DC link of the inverter as shown in the Fig.2. The current is controlled using either PWM techniques or hysteresis type of control. A current reference command is compared with the current feedback signal and then used to determine the switching signal to the main power devices. Additional controller functions include undervoltage protection, thermal protection and current ripple limit controls, error amplifier inputs for incorporation in closed loop servos and microprocessor compatible inputs.

Several IC manufacturers offer dedicated ICs providing all the functions for PWM control of brushless DC motors. The Philips version of the NE5570 CMOS controller is one such device which can be used for three phase BDCM systems using a serial data input command from a microprocessor controller. This device contains the PWM comparator and oscillator, dynamic current loop controller and output pre-drivers suitable for a MOSFET power stage. Its operation is described more fully in Philips Application Note AN1281.

Brushless DC motor operation

The operation of a BDCM system can be explained with reference to Fig.5. At any instant in time the rotor position is known by the output states of the three airgap mounted Hall effect devices. The output state of one Hall effect device switches for every 60° of rotation, thus defining six conduction zones as shown in the figure. The switching of the inverter devices is arranged to give symmetrical 120° intervals of positive and negative constant current in each motor phase winding. The position of the sensors and controller logic ensures that the applied currents are in phase with the motor emfs in order to give maximum motor torque at all times.

Referring to Figures 2 and 5, during the first 60° conduction zone switches S1 and S4 are on and the current flows through the 'A' and 'B' phase windings. The 'C' phase is inactive during this interval. At the end of this 60° conduction zone one of the Hall effect devices changes state and so switch S4 turns off and S6 turns on. The switching sequence continues as the motor advances. At any instant in time two motor phases are energised and one motor phase is off. The motor phase current waveforms are described as being 'quasi-square' in shape. The motor windings are energised for two thirds of the total time and the maximum switch duty cycle ratio is one third.

The other function of the controller is to maintain the motor phase currents at their desired constant value for each 120° interval that a particular phase is energised. The precise method of current limiting depends upon the controller algorithm. In order to limit the current to its desired value either one or both of the conducting devices are switched off thus allowing the motor current to freewheel through the

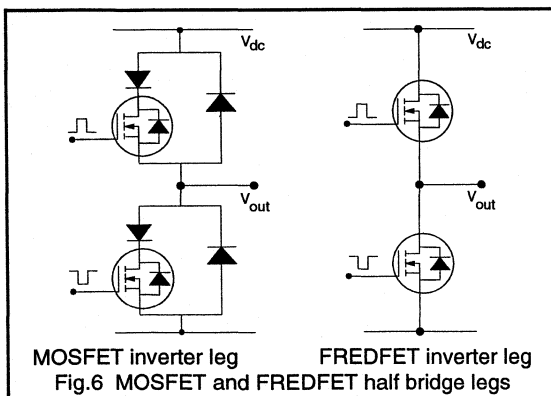
bridge leg diodes. The current is limited by controlling the switch duty cycle to ensure that device current ratings and the motor current rating are not exceeded, especially during start-up conditions or low speed operation. The amount of current ripple is controlled by the switching frequency of a PWM waveform or by the width of a hysteresis band.

Power Semiconductor switches for Brushless DC motors

Philips Semiconductors produce a range of power semiconductor devices suitable for use in BDCM systems. They include transistors, MOSFETs, FREDFETs, Logic Level MOSFETs (L^2 FETs) and IGBTs. These devices are available in a variety of current and voltage ratings and a range of packages, to suit individual applications.

FREDFETs

For higher voltage applications the FREDFET is an appropriate device for the inverter switches in a brushless DC drive. The FREDFET is a PowerMOS device where the characteristics of the MOSFET intrinsic diode have been upgraded to those of a discrete fast recovery diode. Thus the FREDFET is ideally suited to bridge circuits such as that shown in Fig.2 where the recovery properties of the bridge diodes significantly affect the switching performance of the circuit. Fig.6 shows a conventional MOSFET inverter bridge circuit, where the MOSFETs intrinsic diode is disabled by a series Schottky diode. A discrete antiparallel FRED carries the motor freewheeling current. Using the FREDFET reduces the component count and circuit layout complexity considerably.



L^2 FETs

For many lower voltage applications logic level FETs (L^2 FETs) can be used to interface the power circuit with standard TTL or CMOS drive circuits without the need for level shifting stages. L^2 FETs require gate source voltage of only 5V to be fully turned on and typically have $V_{GS(th)} = 1-2V$. Using Philips L^2 FETs in BDCM applications such as

tape or disc drives where the MOSFETs are driven directly by a controller IC produces an efficient overall design with the minimum of gate drive components.

IGBTs

IGBTs are especially suited to higher power applications where the conduction losses of a MOSFET begin to become prohibitive. The IGBT is a power transistor which uses a combination of both bipolar and MOS technologies to give a device which has low on-state losses and is easy to drive. The IGBT is finding applications in mains-fed domestic and industrial drive markets. By careful design of the device characteristics the switching losses of an IGBT can be minimised without adversely affecting the conduction losses of the device too severely. Operation of BDCM inverters is possible at switching speeds of up to 20kHz using IGBTs.

Device selection

The first selection criterion for an inverter device is the voltage rating. Philips PowerMOS devices have excellent avalanche ruggedness capability and so are able to survive transient overvoltages which may occur in the inverter circuit. This gives the circuit designer the freedom to choose appropriately rated devices for the application without suffering from the extra device conduction losses which occur when using higher voltage grade devices. In noisy environments or where sustained overvoltages occur then some external protection circuitry will usually be required.

For low voltage and automotive applications 60V devices may be adequate. For mains-fed applications then the DC link voltage is fixed by the external mains supply. A 240V supply will, depending on the DC link filtering arrangement, give a link voltage of around 330V. Using 450V or 500V MOSFETs will allow sufficient margin for transient overvoltages to be well within the device capability.

The current rating of a device is determined by the worst case conditions that the device will experience. These will occur during start-up, overload or stall conditions and should be limited by the BDCM controller. Short circuit protection must be provided by using appropriate fusing or overcurrent trip circuitry.

In addition to the normal motor currents the inverter devices will experience additional currents due to diode reverse recovery effects. The magnitude of these overcurrents will depend on the properties of the freewheel diodes and on the switching rates used in the circuit. Turn-on overcurrents can often be greater than twice the normal load current. The peak to average current capability of MOSFETs is very good (typically 3 to 4) and so they are able to carry overcurrents for short periods of time without damage. For high power applications PowerMOS devices can easily be

paralleled to give the required current ratings providing the circuit is suitably arranged in order to ensure good current sharing under both dynamic and static conditions.

Conclusions

The brushless DC motor has already become an important drive configuration for many applications across a wide range of powers and speeds. The ease of control and

excellent performance of the brushless DC motors will ensure that the number of applications using them will continue to grow for the foreseeable future. The Philips range of PowerMOS devices which includes MOSFETs, FREDFETs, L²FETs and IGBTs are particularly suited for use in inverter circuits for motor controllers due to their low loss characteristics, excellent switching performance and ruggedness.

Stepper Motor Control

3.3.1 Stepper Motor Control

A stepper motor converts digital information into proportional mechanical movement; it is an electro-mechanical device whose spindle rotates in discrete steps when operated from a source that provides programmed current reversals. After the appearance of the stepper motor in applications traditionally employing digital control, the advantages of precise and rapid positioning of objects using stepper motor drive systems became more obvious and this, in turn, led to a greater variety of applications. These now include:

- paper and magnetic tape drives,
- camera iris control and film transport,
- co-ordinate plotters, printers, chart recorders and variable speed chart drives,
- medical equipment,
- fuel control, valve control and variable speed pumps,
- meters, card readers, production line pulse counters
- automatic weighing and labelling systems,
- digital to analogue converters and remote position indicating equipment.

All of these applications have one thing in common - controlled motion. Wherever controlled movement and/or positioning is necessary, the stepper motor can be used to give a fast, flexible and accurate system.

From a mechanical viewpoint, the stepper motor has simple positional control, reliability and precision. Previously, simple, mechanically operated switches often provided adequate control for many positioning systems but increased performance requirements have forced the need for a better drive systems. The advantages of stepper motor systems have been gained at the expense of controller simplicity. The combination of fast controller ICs, low cost, high power, high efficiency switches, particularly MOSFETs, and the ease of use of stepper motors has led to their current widespread use.

The full benefit of a stepper motor can only be realised if it is correctly driven. It requires a dc supply, an electronic switch and a source of control pulses (digital information). The appropriate dc supply is directed into the motor via a power electronic switching network. In effect, the motor moves through one step for each control pulse applied to the power stage electronic switches. The angle of the step depends upon the type of motor and can be from as little as 1.8° to as much as 15° . Consequently, if 24 pulses are fed to the switching network, the shaft of a motor with a 15° step-angle will complete one revolution. The time taken for this action is entirely a function of the rate at which control pulses are applied. These may be generated by an oscillator with adjustable frequency or from a dedicated controller IC.

Principles of operation

Stepper motors can be divided into three principle types:

- permanent magnet stepper motors
- variable reluctance stepper motors
- hybrid stepper motors.

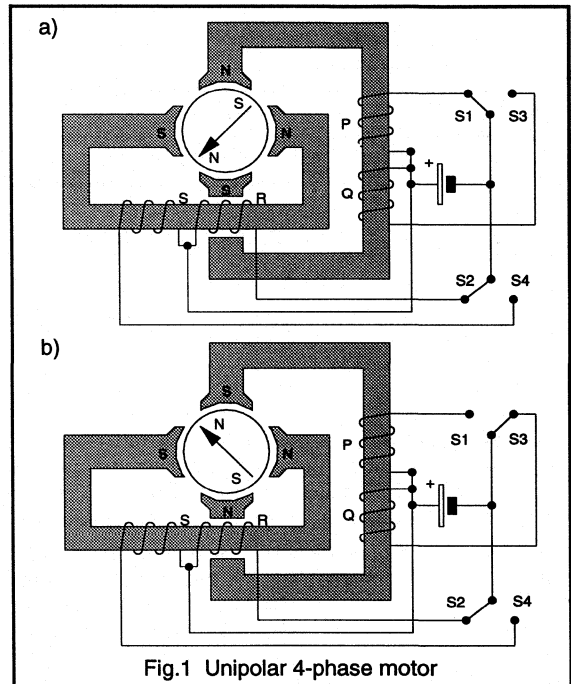


Fig.1 Unipolar 4-phase motor

Permanent magnet stepper motors

The step angle of a permanent magnet stepper motor depends upon the relationship between the number of magnetic poles on its stator assembly and the number of magnetic poles on its rotor. Since the latter is a cylindrical permanent magnet, the poles are fixed, and their number is limited, due to the characteristics of the magnetic material. Enlarging the magnet diameter to provide for a larger number of rotor poles results in a drastic increase in the rotor inertia. This reduces the starting capabilities of such a motor beyond practical use. With a permanent magnet rotor, only relatively large step angles can be obtained. However, the operating step angle can be reduced by using more than one stator stack along the length of the machine and then by offsetting the separate stacks.

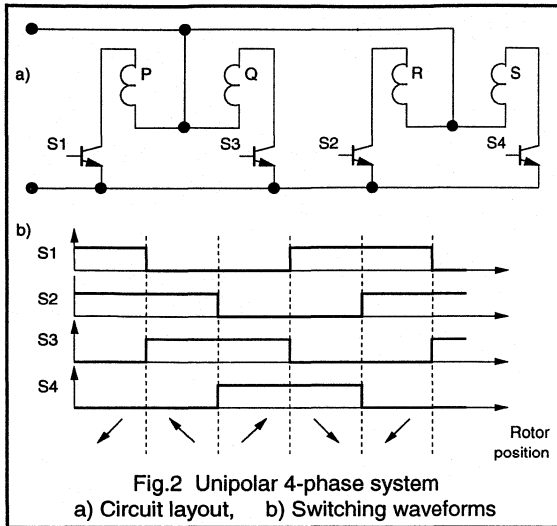


Fig.2 Unipolar 4-phase system
a) Circuit layout, b) Switching waveforms

The stator assembly comprises two or more stators, each having a coil through which current is passed to form a magnetic field. By reversing the direction of current flowing in a coil the north and south poles developed by the coils can be transposed. Reversing the current flow through successive stator coils creates a rotating magnetic field which the permanent-magnet rotor follows. Speed of rotation is thus governed by the rate at which the stator coils (and hence the electromagnetic poles) are switched and the direction of rotation by the actual switching sequence.

There are two methods by which the current flow through stator coils can be reversed and this has led to two classes of stepper motor: those designed for unipolar drive and those for bipolar drive. For ease of description, illustrations in this section which give a diagrammatic representation of a permanent magnet stepper motor show only a 2-pole rotor although it could have as many as 24: the operating principles, however, are the same.

Motors for Unipolar drive

Each stator coil of a motor designed for unipolar drive is provided with a centre-tap which is connected to one side of the supply. The direction of current flowing through a coil is then determined by the end to which the other supply line is connected via a switching device. Switching between the coil halves results in the magnetic poles of the relevant stator being reversed.

Figure 1(a) shows a 4-phase stepper motor in which phases P and R are energised. The north poles at P and R cause the rotor to align in the position indicated. If switch S1 is turned off and S3 turned on, so that phases Q and R are now energised, then the stator field is repositioned and so the conditions illustrated in Fig.1(b) are obtained, i.e. the rotor has moved through 90° to align with the stator field.

From this it can be seen that by altering the switching sequence for switches S1, S2, S3 and S4 the rotor can be made to advance in either direction.

Figure 2(a) shows the drive configuration for a unipolar 4-phase motor. The switching sequence of the power switches is shown in Fig.2(b). Two motor phases are energised at any one time thus giving the rotation of the stator field and required stepping motion.

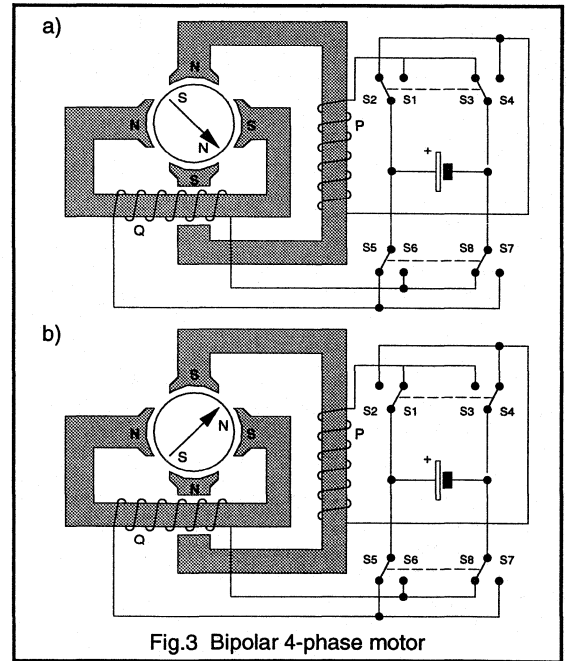
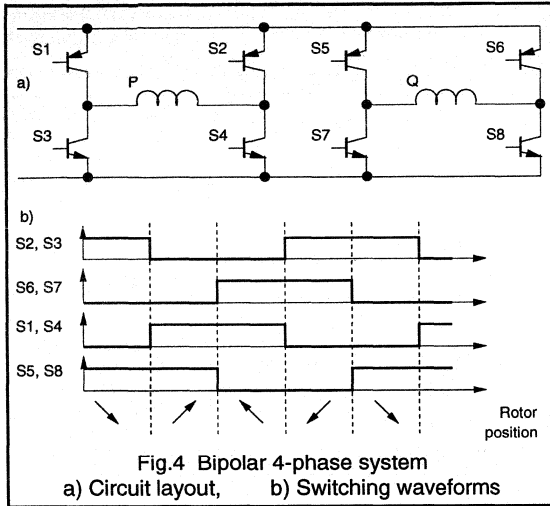


Fig.3 Bipolar 4-phase motor

Motors for Bipolar drive

The stator coils of a motor designed for bipolar drive have no centre-tap. Instead of using alternate coil-halves to produce a reversal of current-flow through the stator windings, the current is now reversed through the entire coil by switching both supply lines. Operation of a motor with bipolar drive is identical to that of one with unipolar drive, and is shown in Fig.3. Here, when the polarity of current in phase P is reversed using switches S1 to S4 the stator field realigns and the rotor moves accordingly. Figure 4(a) shows the drive configuration for a bipolar 4-phase motor. The devices are always switched as pairs, i.e. S1 and S4, S2 and S3. The switching waveforms for this configuration are shown in Fig.4(b).

The advantages of using motors with bipolar drive are shown in Fig.5. This compares the performance of a unipolar motor with its bipolar equivalent. Unipolar motors



develop less torque at low stepping rates than their bipolar counter-parts, although at higher stepping rates the torque developed by both types of motor is nearly the same.

The 4-phase unipolar motor shown in Fig.1 has two coils per phase which must be wound on one bobbin for each stator (bifilar winding), ie. four coils in total. Because the two coils occupy the same space as a single coil in equivalent bipolar types, the wire is thinner and coil resistance higher. Bipolar motors have only one coil per

bobbin so that 2-stator motors have two coils and 4-stator motors four coils. Unipolar motors require only a simple drive circuit - only four power transistors instead of eight. Moreover, the switching time requirements are less severe for unipolar drives. For a bipolar drive, care must be taken with switching times to ensure that two opposing transistors are not switched on at the same time, thus shorting out the supply. Properly operated, bipolar windings give optimum motor performance at low to medium stepping rates.

Variable reluctance stepper motors

In a variable reluctance stepper motor the motion is achieved by using the force of attraction between a magnetised component (the stator pole excited by a controlled current) and a passive steel component (the rotor pole). As successive stator poles are energised different rotor poles are attracted towards the nearest active pole, thus giving the required stepping motion. Figure 6 shows the simplest variable reluctance motor configuration having six stator poles and four rotor poles. The rotor is simply a shaped steel shaft. The stator winding is arranged so that one stator phase winding is on each stator pole.

Figure 6(a) shows the condition when the 'A' phase of the motor is energised and rotor pole 1 is aligned with the energised winding. If stator phase 'A' is switched off and phase 'B' is switched on then rotor pole 2 (which is the nearest rotor pole to any 'B' phase pole) experiences an attractive force due to the energised 'B' phase. The rotor advances to the position shown in Fig.6(b).

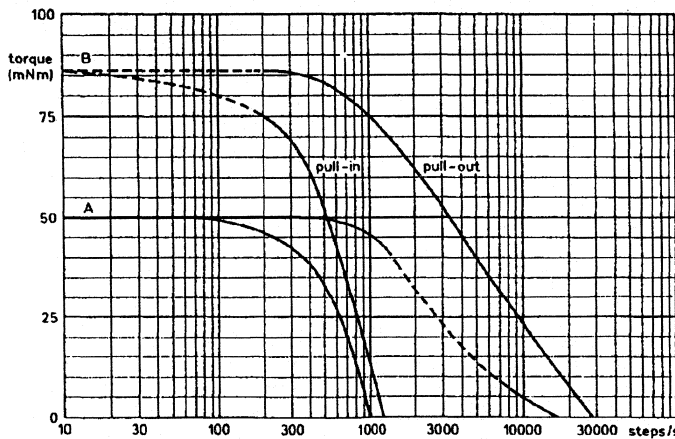
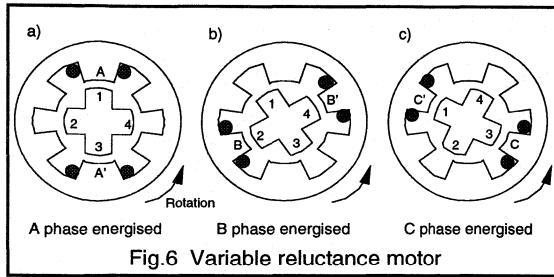


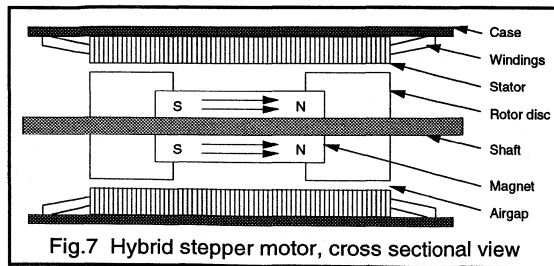
Fig.5 Torque vs. stepping rate characteristic
A) Unipolar motor B) Bipolar motor

If, subsequently, phase 'C' is energised then rotor pole 1 will align with the 'C' phase, as shown in Fig.6(c). The step angle of a variable reluctance motor can be reduced by having more than one set of offset rotor poles which are built up along the stack length of the machine. Different offset rotor poles align with the stator poles at each step position.



Hybrid stepper motors

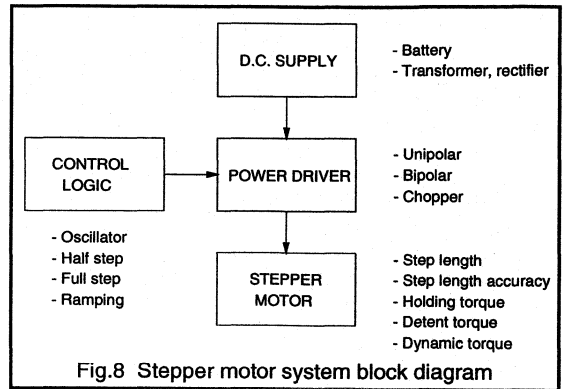
The usual configuration for a hybrid stepper motor operates using the torque production methods found in both permanent magnet and variable reluctance motors. This gives a higher performance system with a low volume, and hence a low rotor inertia, and small step angles. The rotor of a hybrid stepper motor consists of an axially aligned magnet and a pair of toothed discs, one at each end of the rotor stack. The general layout is shown in Fig.7. The teeth of the discs are misaligned with respect to each other with the result that as the stator phase windings are energised different teeth align with the stator poles, in a similar way to those in a variable reluctance motor. The addition of the permanent magnet on the rotor introduces a polarity in the way that the rotor teeth align with the stator poles. Again multi-stack motors are used to reduce the step length further. Alternative hybrid stepper motor configurations have the magnets on the stator, but operate in a broadly similar manner.



Stepper motor systems

Proper selection of the right stepper motor for a specific application calls for a thorough understanding of the characteristics of the motor and its drive circuitry. Figure 8

shows schematically the four constituent parts of a stepper motor system together with the most important aspects of each. These will be briefly considered below.



The stepper motor

Typical standard step motor angles are shown below:

Step angle	Steps per revolution
0.9°	400
1.8°	200
3.6°	100
3.75°	96
7.5°	48
15.0°	24

The no load step angle accuracy is specified for each type of motor. For example, a motor having a step angle of 7.5° and will typically position to within 20' (i.e. 5%) whether the motor is made to move for 1 step or 1000 steps. The step angle error is non-cumulative and averages to zero every four steps, i.e. 360°. Every four steps the rotor returns to the same position with respect to magnetic polarity and flux paths. For this reason, when very accurate positioning is required, it is advisable to divide the required movement into multiples of four steps. This is known as the 4-step mode of operation.

Torque

Three torques are used to define stepper motor operation:

Holding torque

At standstill, when energised, a certain amount of torque is required to deflect a motor by one step. This is known as the holding torque. When a torque is applied that exceeds the holding torque the motor will rotate continuously. The holding torque is normally higher than the working torque and acts as a strong brake in holding a load in position.

Detent torque

Due to their permanent magnets, hybrid stepper motors and permanent magnet stepper motors have a braking torque even when the stator windings are unenergised. This is referred to as the detent torque.

Working (dynamic) torque

The dynamic characteristics of a stepper motor are described by the curves of torque versus stepping rate. Typical curves were shown in Fig.5. The pull-in curve shows the load a motor can start and stop without losing steps when operated at a constant stepping rate. The pull-out curve shows the torque available when the motor is gradually accelerated to and decelerated from its required working speed. The area between the two curves is known as the slew range. The characteristic curves are used to define the correct motor selection for any particular application.

Overshoot

After executing each single step the rotor tends to overshoot and oscillate about its final position as shown in Fig.9(a). This is normal behaviour for any pulsed dynamic system. The actual response depends on the load and on the power input provided by the drive. The response can be modified by increasing the frictional load or by adding mechanical damping. However, mechanical dampers such as friction discs or fluid flywheels add to system cost and complexity and so it is usually better to damp electronically.

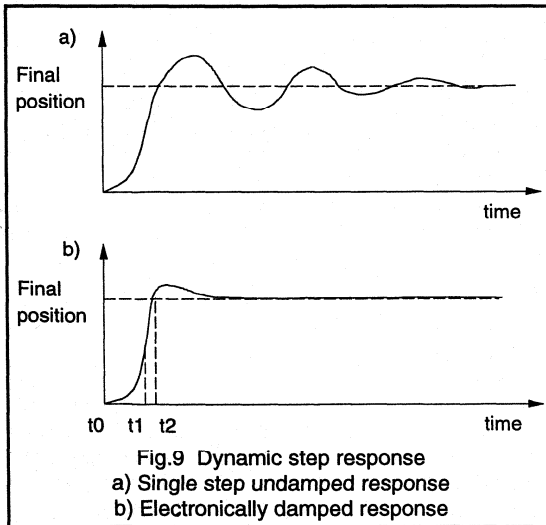


Fig.9 Dynamic step response
a) Single step undamped response
b) Electronically damped response

Two methods of electronic damping are commonly used - the simplest being to delay the final pulse in an incremental pulse train such that the effective length of the final step is reduced. Alternatively, every pulse, or just the final pulse in a train, can be modified into three stages, as shown in Fig.9(b). Using this method of damping a forward pulse is applied at time t_0 , a reverse pulse is applied at t_1 in order

to slow the rotor down and then finally a second forward pulse is applied at t_2 which ensures the rotor comes to rest at the desired position. The accelerating torque which is developed from this final pulse is less than that for a full step and so the shaft overshoot is significantly reduced.

Multiple stepping

There are often several alternatives available in order to make a desired incremental movement. For example, a rotation of 90° can be reached in 6 steps of a 15° motor, 12 steps of 7.5° motor or in 50 steps of a 1.8° motor. Generally, a movement executed in a large number of small steps will result in less overshoot, be stiffer and more accurate than one executed in smaller number of large steps. Also there is more opportunity to control the velocity by starting slowly, accelerating to full speed and then decelerating to a standstill with minimum oscillation about the final position if small step lengths are used.

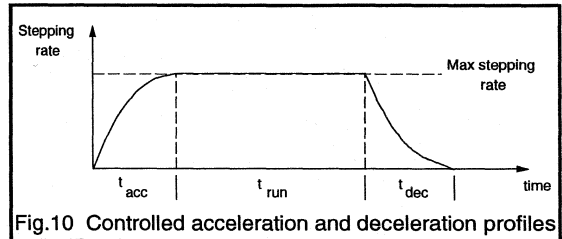


Fig.10 Controlled acceleration and deceleration profiles

A voltage controlled oscillator and charging capacitor are usually used for acceleration (or ramp) control of the motor. The RC time constant of the ramp controller is used to give different ramp rates. Figure 10 shows a typical curve of step rate against time for an incremental movement with equal acceleration and deceleration times.

Resonance

A stepper motor operated at no-load over its entire operating frequency range will exhibit resonance points that are either audible or can be detected by vibration sensors. If any are objectionable then these drive frequencies should be avoided, a softer drive used, or alternatively extra inertia or external damping added.

Drive methods

The normal drive method is the 4-step sequence mentioned above. However, other methods can be used depending on the coil configuration and the logic pattern in which the coils are switched:

Wave drive

Energising only one winding at a time is called wave excitation and produces the same position increment as the 4-step sequence. Figure 11 shows the stepping sequence for the bipolar 4-phase motor, which was discussed earlier and shown in Fig.4. Since only one winding is energised,

holding torque and working torque are reduced by 30%. This can, within limits, be compensated by increasing supply voltage. The advantage of this form of drive is higher efficiency, but at the cost of reduced step accuracy.

Half-step mode

It is also possible to step a motor in a half-step sequence, thus producing half steps, for example 3.75° steps from a 7.5° motor. A possible drawback for some applications is that the holding torque is alternately strong and weak on successive motor steps. This is because on 'full' steps only one phase winding is energised whilst on the 'half' steps two stator windings are energised. Also, because current and flux paths differ on alternate steps, accuracy will be worse than when full stepping. The switching sequence for a 4-phase bipolar drive is shown in Fig.12.

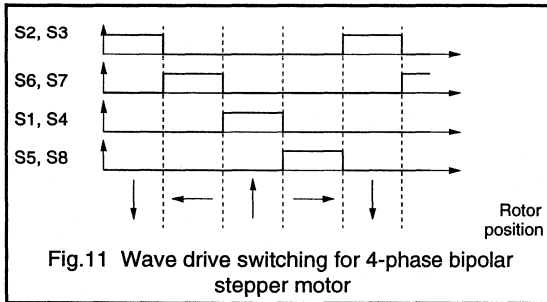


Fig.11 Wave drive switching for 4-phase bipolar stepper motor

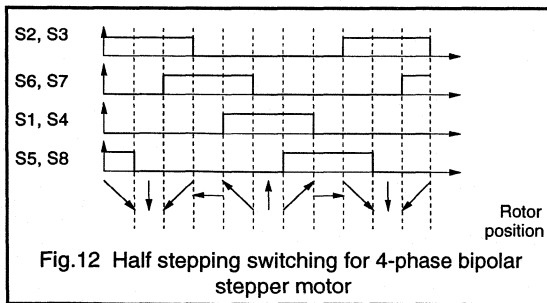


Fig.12 Half stepping switching for 4-phase bipolar stepper motor

Supply considerations

When a motor is operated at a fixed rated voltage its torque output decreases as step rate rises. This is because the increasing back EMF and the rise time of the coil current limits the power actually delivered to the motor. The effect is governed by the motor time constant (L/R). Because of their higher winding resistance unipolar motors have a better L/R ratio than their bipolar equivalents. The effect can be compensated by either increasing the power supply voltage to maintain constant current as stepping rate increases, or by increasing supply voltage by a fixed amount and adding series resistors to the circuit.

Adding series resistors to the drive circuit can improve the motor performance at high stepping rates by reducing the L/R ratio. Adding a series resistor three times the winding resistance would give a modified ratio of L/4R. Supply voltage would then have to be increased to four times the motor rated voltage to maintain rated current. The addition of the extra resistance greatly reduces the drive efficiency. If the increased power consumption is objectionable some other drive method such as a bi-level voltage supply or a chopper supply should be used.

Bi-level drive

With a bi-level drive the motor is operated below rated voltage at zero step rate (holding) and above rated voltage when stepping. It is most efficient for fixed stepping rates. The high voltage may be turned on by current sensing resistors or, as in the circuit of Fig.13, by means of the inductively generated turn-off current spikes. At zero step rate the windings are energised from the low voltage. As the windings are switched in the 4-step sequence, diodes D1, D2, D3 and D4 turn on the high voltage supply transistors S1 and S2.

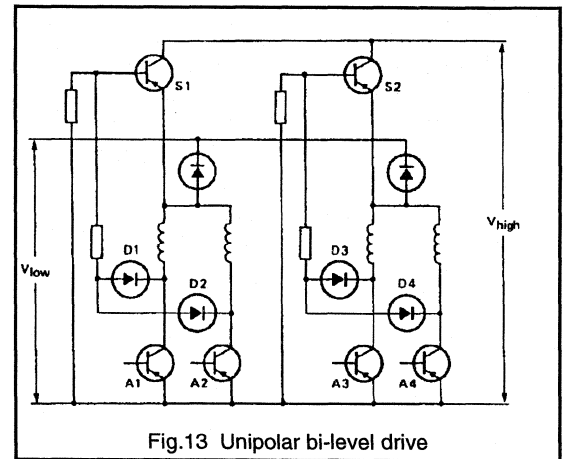


Fig.13 Unipolar bi-level drive

Chopper drive

A chopper drive maintains current at an average level by switching the supply on until an upper current level is reached and then switching it off until a lower level is reached. A chopper drive is best suited to fast acceleration and variable frequency applications. It is more efficient than an analogue constant current regulated supply. In the chopper circuit shown in Fig.14, V+ would be typically 5 to 10 times the motor rated voltage.

Spike suppression

When windings are turned-off, high voltage spikes are induced which could damage the drive circuit if not suppressed. They are usually suppressed by a diode across each winding. A disadvantage is that torque output

is reduced unless the voltage across the transistors is allowed to build up to about twice the supply voltage. The higher this voltage the faster the induced fields and currents collapse and performance is, therefore, better. For this reason a zener diode or series resistor is usually added as in Fig. 15.

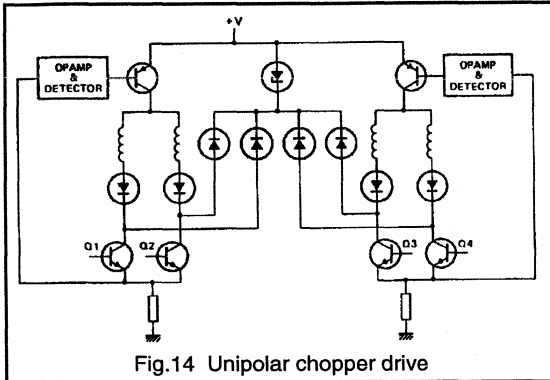


Fig. 14 Unipolar chopper drive

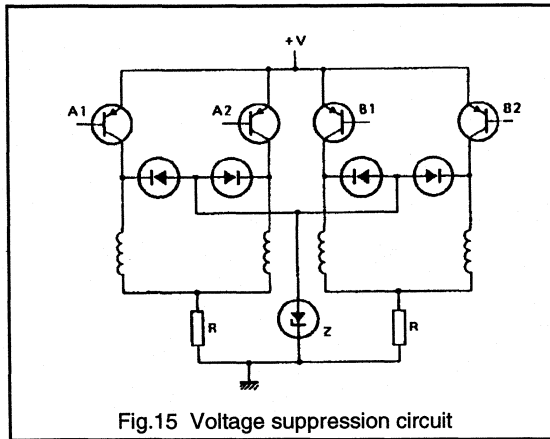


Fig. 15 Voltage suppression circuit

Performance limitations

At standstill or low step rates, increasing the supply voltage produces proportionally higher torque until the motor magnetically saturates. Near saturation the motor becomes less efficient so that increased power in unjustifiable. The maximum speed of a stepper motor is limited by inductance and eddy current losses. At a certain step rate the heating effect of these losses limits any further attempt to get more speed or torque out of a motor by driving it harder.

Terminology

Detent Torque: The maximum torque that can be applied to the spindle of an unexcited motor without causing continuous rotation.
Unit: Nm.

Deviation: The change in spindle position from the unloaded holding position when a certain torque is applied to the spindle of an excited motor.
Unit: degrees.

Holding Torque: The maximum steady torque that can be externally applied to the spindle of an excited motor without causing continuous rotation.
Unit: Nm.

Maximum Pull-In Rate (Speed): The maximum switching rate (speed) at which an unloaded motor can start without losing steps.
Unit: steps/s (revs/min).

Maximum Pull Out Rate (Speed): The maximum switching rate (speed) which the unloaded motor can follow without losing steps.
Unit: steps/s (revs/min).

Maximum Working Torque: The maximum torque that can be obtained from the motor:
Unit: Nm.

Overshoot: The maximum amplitude of the oscillation around the final holding position of the rotor after cessation of the switching pulses
Unit: degrees.

Permanent Overshoot: The number of steps the rotor moves after cessation of the applied switching pulses.
Unit: steps.

Phase: Each winding connected across the supply voltage.

Pull In Rate (Speed): The maximum switching rate (speed) at which a frictionally loaded motor can start without losing steps.
Unit: steps/s (revs/min).

Pull In Torque: The maximum switching rate (speed) which a frictionally loaded motor can follow without losing steps.
Unit: steps/s (revs/min).

Pull Out Torque: The maximum torque that can be applied to a motor spindle when running at the pull out rate.
Unit: Nm.

Start Range: The range of switching rates within which a motor can start without losing steps.

Step Angle: The nominal angle that the motor spindle must turn through between adjacent steps.
Unit: degrees.

Stepping Rate: The number of step positions passed by a fixed point on the rotor per second.
Unit: steps/s.

Slew Range: The range of switching rates within which a motor can run unidirectionally and follow the switching rate (within a certain maximum acceleration) without losing steps, but cannot start, stop or reverse.

CHAPTER 4

Televisions and Monitors

- 4.1 Power Devices in TV Applications
(including selection guides)*
- 4.2 Deflection Circuit Examples*
- 4.3 SMPS Circuit Examples*
- 4.4 Monitor Deflection and SMPS Example*



*Power Devices in TV & Monitor Applications
(including selection guides)*



4.1.1 An Introduction to Horizontal Deflection

Introduction

This section starts with the operation of the power semiconductors in a simple deflection test circuit leading to a functional explanation of a typical TV horizontal deflection circuit. The operation of the common correction circuits are discussed and the secondary function of the horizontal deflection circuit described.

Deflection Test Circuit

The horizontal deflection test circuit used to assess Philips deflection transistors is shown in Fig. 1 below. L_c represents the horizontal deflection coils.

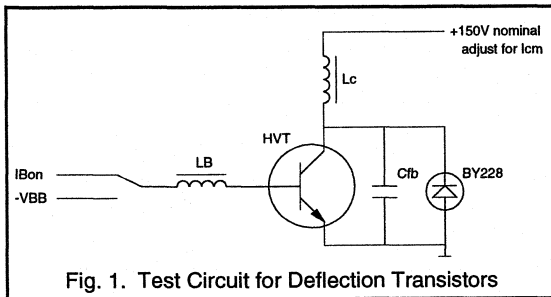


Fig. 1. Test Circuit for Deflection Transistors

This circuit is a simplification of a practical horizontal deflection circuit. It can be used to produce the voltage and current waveforms seen by both the transistor and the diode in a real horizontal deflection circuit. It is, therefore, very useful as a test circuit for switching times and power dissipation. The waveforms produced by the test circuit are shown in Fig. 2.

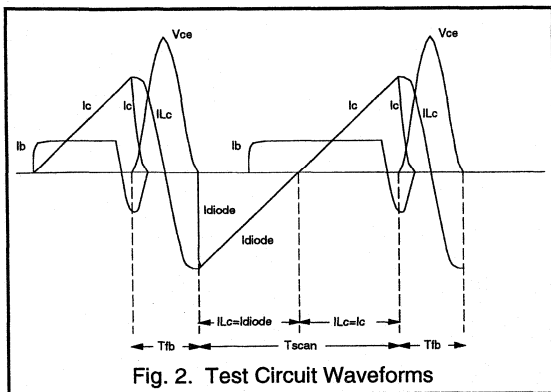


Fig. 2. Test Circuit Waveforms

Cycle of Operation

Briefly going through one cycle of operation, the sequence of events is as follows. (This can be followed through on the waveforms shown in detail in Fig. 3, by starting on the left and following the stages numbered 1 to 8).

1. Turn on the deflection transistor by applying a positive current drive to the base. The voltage on the collector is now approximately 0.5V because the device is fully on. This means that the voltage across the coil, L_c , is the full line voltage; in this case 150V.
2. According to the law, $V = L \cdot di/dt$, the current in the coil L_c will now start to rise with a gradient given by $150V/L_c$. This portion of the coil current (I_{Lc}), is the sawtooth portion of the collector current in the transistor (I_c).
3. Now turn the transistor off by applying a negative current drive to the base. Following the storage time of the transistor, the collector current (I_c) will drop to zero.
4. The current in L_c (I_{Lc}) is still flowing! This current, typically 4.5A for testing the BU2508A, cannot flow through the transistor any more, nor can it flow through the reverse biased diode, BY228. It, therefore, flows into the flyback capacitor, C_{fb} , and so the capacitor voltage rises as I_{Lc} falls. Because C_{fb} is connected across the transistor, the rise in capacitor voltage is seen as a rise in V_{ce} across the transistor.

L_c will transfer all its energy to C_{fb} . The capacitor voltage reaches its peak value, typically 1200V, at the point where I_{Lc} crosses zero.

5. Now we have a situation where there is zero energy in L_c but there is a very large voltage across it. So I_{Lc} will rise, and since this current is supplied by C_{fb} , the voltage across C_{fb} falls. This is, of course, a resonant LC circuit and essentially it is energy which is flowing, first from the inductor, L_c , to the capacitor, C_{fb} , and then from the capacitor, C_{fb} , to the inductor, L_c . Note that the current in L_c is now flowing in the opposite direction to what it was previously. It is, therefore, a negative current.

6. This resonance would continue, with the coil current and the capacitor voltage following sinusoidal paths, were it not for the diode, BY228. When the capacitor voltage starts to go negative the diode becomes forward biased and effectively clamps the capacitor voltage to approximately -1.5V, the diode VF drop. This also clamps the voltage across L_c to approximately the same value as it was when the transistor was conducting, ie the line voltage (150V). Note that the coil current is now being conducted by the diode, and hence $I_{Lc} = I_{diode}$.

7. So we have again a current ramp in I_{Lc} with a di/dt equal to $150/I_{Lc}$. This current starts with a value equal to the value it had at the end of the transistor on time (neglecting circuit losses). It is, however, flowing in the opposite (negative) direction and so the positive di/dt will bring it back towards zero.

8. Before I_{Lc} actually reaches zero, the base drive is re-applied to the transistor. This means that when I_{Lc} does reach zero, we arrive back at the same conditions we had at the beginning of stage 1; i.e. the transistor is on, the current in I_{Lc} is zero and the voltage across L_c is the line voltage (150V).

TV Operating Principle

In a television set, or a computer monitor, the picture information is written onto the screen one line at a time. Each of these horizontal lines of picture information is written onto the screen by scanning the screen from left to right with an electron beam. This electron beam is produced by a gun situated at the back of the tube, and it is accelerated towards the screen by a high potential (typically 25kV). The beam is deflected from left to right magnetically, by varying the current in a set of horizontal deflection coils positioned between the gun and the screen.

The screen is phosphor coated, and when the high energy electron beam strikes the phosphor coating the phosphor gives off visible light. The density of electrons in the electron beam can be varied: phosphor brightness depends on beam density, and so the instantaneous brightness of the scanning spot can be varied at a fast rate as each line of picture information is written onto the screen. A set of vertical deflection coils deflects the beam vertically at the end of each horizontal scan and so lines of picture information can be built up, one after the other. The vertical deflection frequency (or *field rate*) for European sets is 50 Hz (alternate line scanning, giving 25 complete screens of information per second).

With no current in the horizontal deflection coils, the magnetic field between them is zero and so the electron beam hits the centre of the screen. With a negative current in the coils, the resultant magnetic field deflects the electron beam to the left side of the screen. With a positive coil current the deflection is to the right.

Now consider the characteristic deflection waveforms, Fig. 3. The current I_{Lc} represents the current in the horizontal deflection coils. During the period where the current in the deflection coils is ramping linearly from its peak negative value to its peak positive value, the electron beam is scanning the screen from left to right. This is the scan time, T_{scan} .

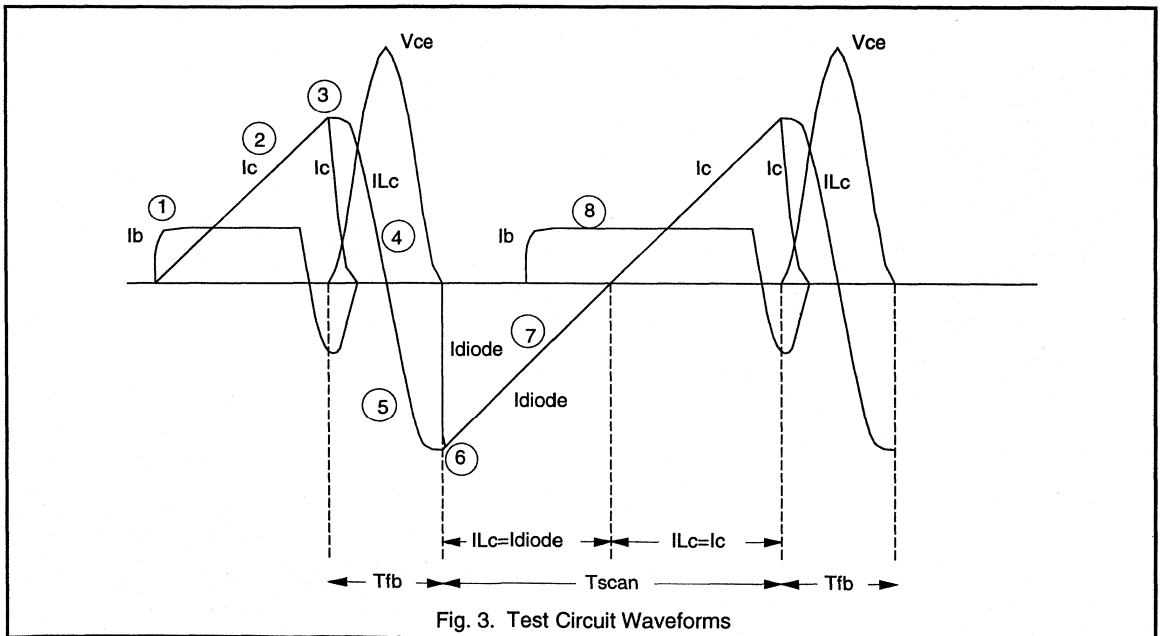


Fig. 3. Test Circuit Waveforms

During the period where the horizontal deflection coil current flows into the flyback capacitor, and then back into the coil (the half cosine curve at the end of the scan period), the electron beam is rapidly moving from the right side of the screen to the left. This is called the flyback period, T_{fb} , and no information is written onto the screen during this part of the cycle.

S-Correction

The actual TV horizontal deflection circuit differs from the test circuit in a number of ways that improve the picture quality. The simplified deflection circuit shown in Fig. 1 can be redrawn as shown in Fig. 4 where L_c is the horizontal deflection yoke and C_s is charged to the line voltage (150V).

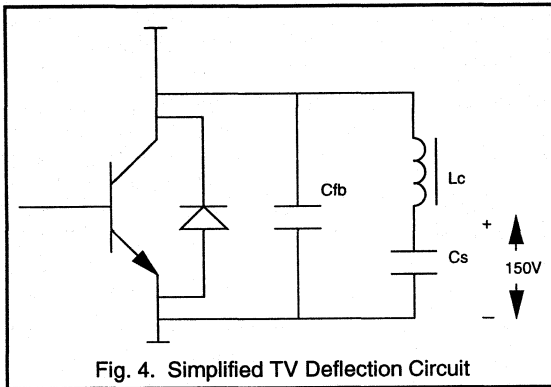


Fig. 4. Simplified TV Deflection Circuit

The advantage of this arrangement is that, by carefully selecting the value of C_s , one form of picture distortion is corrected for as follows.

The front of the TV tube is flat, rather than curved, and so during each horizontal scan the electron beam travels a greater distance to the edges of the screen than it does to the middle. A linear deflection coil current would tend to over deflect the beam as it travelled towards the edges of the screen. This would result in a set of 'equidistant' lines appearing on the screen as shown in Fig. 5 below.

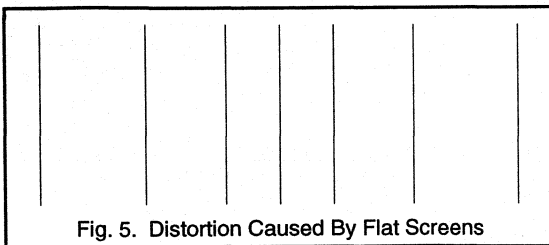


Fig. 5. Distortion Caused By Flat Screens

The voltage on the capacitor, C_s , will be modulated by the deflection coil current, I_{Lc} . When the diode is in forward conduction and the current in L_c is 'negative', the voltage on C_s will rise as C_s becomes more charged. When the transistor is conducting and the current in L_c is 'positive', the voltage on C_s will drop as C_s discharges. This is shown in Fig. 6 below.

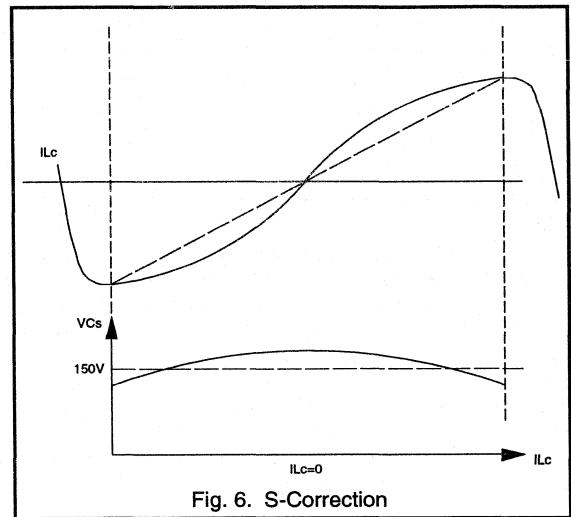


Fig. 6. S-Correction

This will give an 'S' shape to the current ramp in the deflection coils which corrects for the path difference between the centre and the edge of a flat screen tube. Hence the value of the capacitor, C_s , is quite critical. C_s is known as the S-correction capacitor.

Linearity Correction

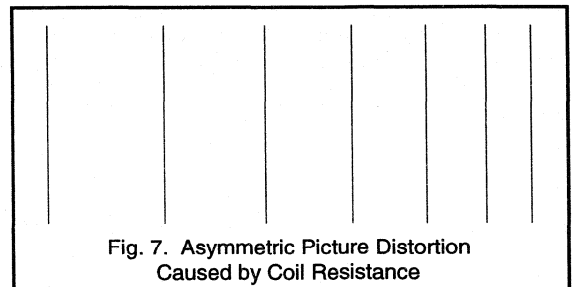


Fig. 7. Asymmetric Picture Distortion Caused by Coil Resistance

The voltage across the deflection coil is also modulated by the voltage drop across the series resistance of the coil. This parasitic resistance (R_{Lc}) causes an asymmetric picture distortion. A set of 'equidistant' vertical lines would appear on the screen as shown in Fig. 7. The voltage across the coils is falling as the beam scans the screen

from left to right. The beam, therefore, travels more slowly towards the right side of the screen and the lines are drawn closer together, see Fig. 8.

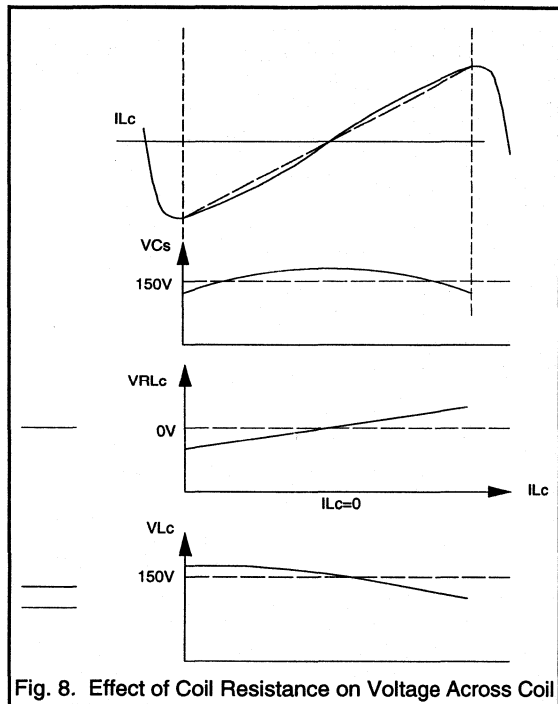


Fig. 8. Effect of Coil Resistance on Voltage Across Coil

V_{RLc} is the voltage drop across the resistive component of L_c . Subtracting this from the voltage across C_s (V_{Cs}) gives the voltage across the inductive component on the deflection coils (V_{Lc}). To compensate for the voltage drop across the parasitic coil resistance we need a component with a negative resistance to place in series with the coil. This negative resistance effect is mimicked by using a saturable inductance, L_{sat} , in series with the deflection coils as shown in Fig. 9 below.

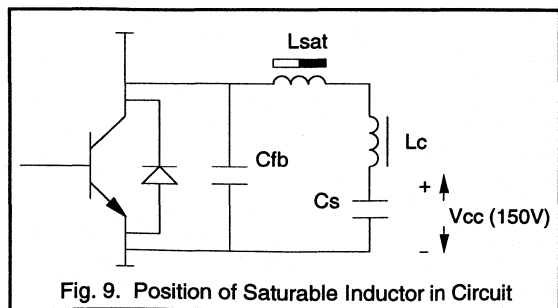


Fig. 9. Position of Saturable Inductor in Circuit

For an inductor with a low saturation current, the relationship between inductance and current is as shown in Fig. 10. As the current is increased much above zero, the core saturates and so the inductance drops. This happens if the current is conducted in either direction.

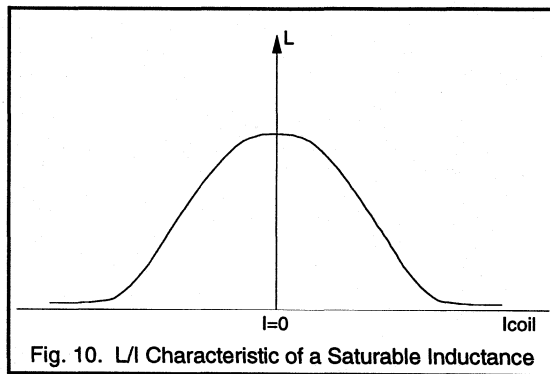


Fig. 10. L/I Characteristic of a Saturable Inductance

By taking a saturable inductance and premagnetising the core, we add a dc bias to this characteristic as shown in Fig. 11 below.

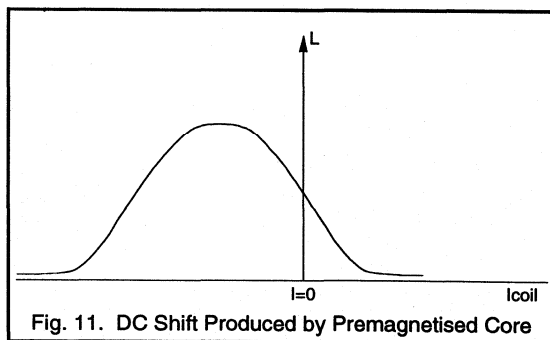
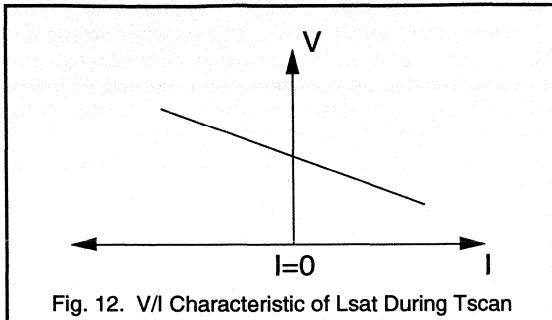


Fig. 11. DC Shift Produced by Premagnetised Core

Since L_{sat} has a much lower inductance than L_c , the dI/dt through L_{sat} is governed by the deflection coils, and is therefore dI_{Lc}/dt . The voltage drop across L_{sat} is therefore given by $V = L_{sat} \cdot dI_{Lc}/dt$. During the scan time, T_{scan} , dI_{Lc}/dt is approximately constant in value, and so the voltage/current characteristics of L_{sat} during the scan time are as shown in Fig. 12 below.

This is the characteristic required and so the voltage developed across L_{sat} , the linearity correction coil, compensates for the series resistance of the deflection coils.

Fig. 12. V/I Characteristic of L_{sat} During T_{scan}

Cs Losses

So the circuit shown in Fig. 9 now gives the desired deflection waveforms. The electron beam scans the screen at a uniform rate on each horizontal scan. However, the circuit is not lossless and unless C_s is kept topped up the dc voltage on C_s , V_{cc} , will gradually decay. To prevent this from happening a voltage supply can be added across C_s but this introduces other problems.

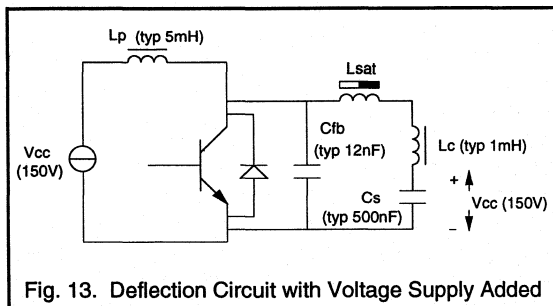


Fig. 13. Deflection Circuit with Voltage Supply Added

The average voltage across L_c *must* be zero. A dc voltage across L_c would generate a dc current which would produce a picture shift to the right. Applying V_{cc} directly to C_s would result in a dc current component through the deflection coils, so C_s must be charged to V_{cc} by some other way. Applying V_{cc} to C_s via the deflection coils overcomes this problem.

A large choke inductance, L_p , in series with the V_{cc} supply is necessary to prevent an enormous increase in the current through the power switch. Without it the V_{cc} supply would be shorted out every time the transistor was turned on. Typically the arrangement shown in Fig. 13 will result in a 20% increase in the current through the power switch and the power diode.

East-West Correction

So to recap on the circuit so far: the series resistance of the deflection coils is compensated for by the linearity correction coil, L_{sat} , and the varying length of the electron beam path, as the beam scans the screen from left to right,

is compensated for by the S-correction capacitor, C_s . This capacitor modulates the voltage across the deflection coils during each horizontal scan, modulating the magnetic field ramp between them, and thus keeping the speed at which the electron beam scans the screen constant.

However, as the picture information is written onto the screen, by writing one line of information after another, a further variation in the length of the beam path is introduced as the beam scans the screen from top to bottom. The length of the beam path to the edge of the screen is shorter when the central lines of picture information are being written than it is when the lines at the top or the bottom of the screen are being written.

This means that a higher peak magnetic field is required to deflect the beam to the screen edges when the beam is writing the central lines of picture information, than that required to deflect the beam to the screen edges when the lines of picture information at the top and bottom of the screen are being written.

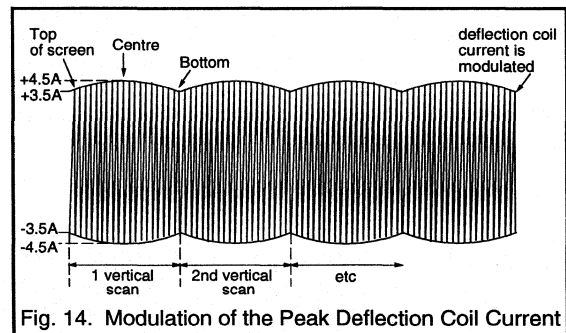


Fig. 14. Modulation of the Peak Deflection Coil Current

This requires increasing the peak deflection coil current gradually over the first half of each vertical scan, and then reducing it gradually over the later half of each vertical scan (see Fig. 14). This is done by modulating the voltage across the deflection coils. This process is known as east-west correction.

The line voltage, V_{cc} , is supplied by a winding on the SMPS transformer. This voltage is regulated by the SMPS and during the operation of the TV set it is constant.

In order to achieve the required modulation of the voltage across the deflection coils, a simple linear regulator could be added in series with L_p . One disadvantage of this solution is that it increases the circuit losses.

The Line Output Transformer (LOT)

The horizontal deflection transistor serves another purpose as well as deflecting the beam: driving the line output transformer (LOT). The LOT has a number of low voltage outputs but its primary function is to generate the EHT voltages to accelerate and focus the electron beam.

Fortunately, this function can be combined with a feature previously described as a cure for C_s losses; the inductive choke, L_p . The LOT has a large primary inductance that serves the purpose of L_p so a separate choke is not required, see Fig. 15 below.

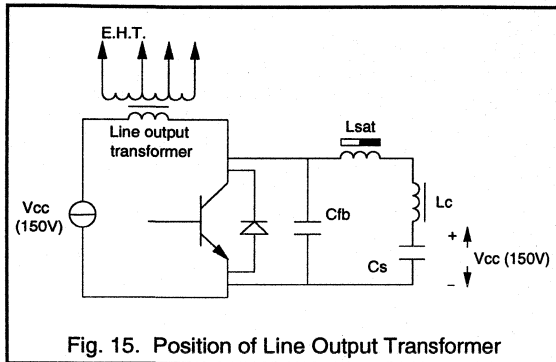


Fig. 15. Position of Line Output Transformer

A lot of power may be drawn from the LOT but the deflection must not be affected. In order to keep the secondary windings of the LOT at fixed voltages, we need to keep the voltage across the primary winding fixed. Therefore, the requirements for the LOT and a regulated supply to L_p are in conflict.

'Real' and 'Dummy' Deflection Circuits

As a way around this problem, consider a 'dummy' deflection circuit in series with the 'real' deflection circuit. This enables one circuit to meet the requirements for deflection, including east-west correction, and the dummy circuit meets the requirements for the LOT, see Fig. 16.

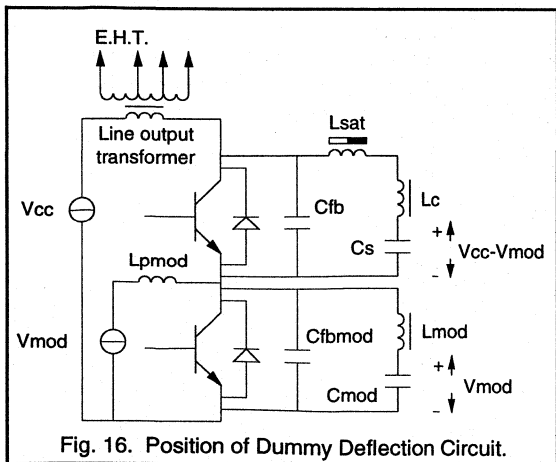


Fig. 16. Position of Dummy Deflection Circuit.

The two deflection circuits operate in direct synchronisation. V_{mod} is a voltage between zero and 30V that controls the east-west correction. Thus we can vary the voltage across the deflection coils in the 'real' deflection circuit without varying the voltage across the primary of the LOT in the 'dummy' circuit.

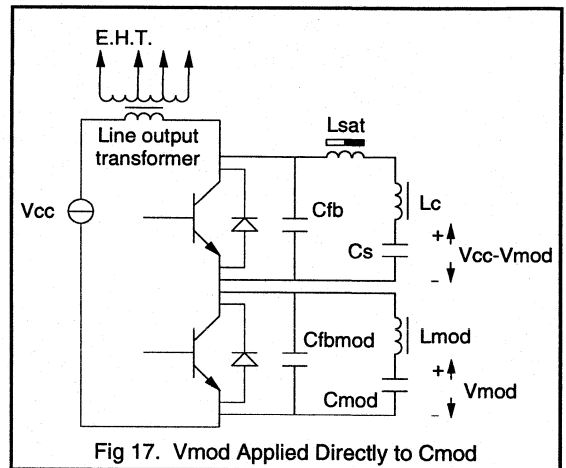


Fig 17. V_{mod} Applied Directly to C_{mod}

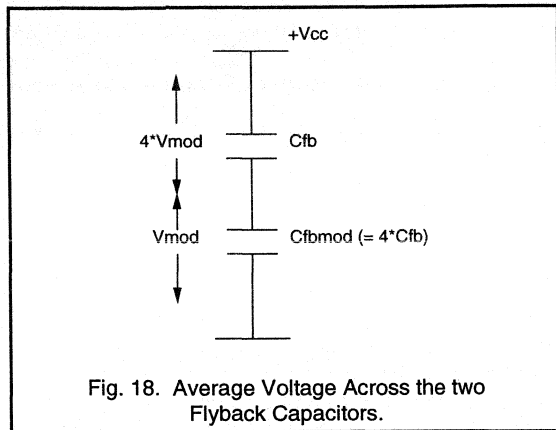
For proper flyback tuning, the 'real' and 'dummy' deflection circuits and the LOT must be tuned to the same flyback frequency. The two deflection circuits are tuned through careful selection of the flyback capacitors. In the case of the LOT the capacitance of the windings provides the necessary capacitance (typically 2nF) for correct tuning.

Since L_{mod} is only an inductor and not a real deflection component, a net dc current through it is not a problem. Therefore, we can apply V_{mod} directly to C_{mod} and this way reduce the component count by removing L_{pmod} , see Fig. 17.

L_{mod} is a quarter of the value of L_c . C_{fbmod} is four times as big as C_{fb} . C_{mod} is not critical as long as it is large enough to supply the required energy.

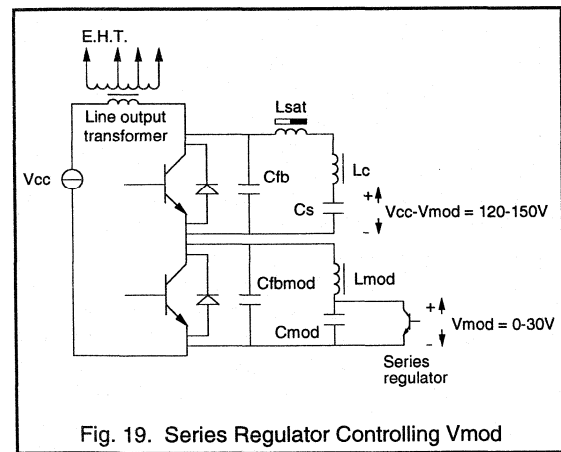
Suppose there is no voltage supplied externally to C_{mod} . The supply voltage, V_{cc} , will split according to the ratio of the impedances of the two circuits. In fact, the V_{cc} will split according to the ratio of the two flyback capacitors, C_{fb} and C_{fbmod} , as shown in Fig. 18.

The average voltage across C_{fbmod} will automatically be 30V (for $V_{cc} = 150V$), if no external voltages are applied to the 'dummy' circuit. Consequently, C_{mod} will become charged to 30V. The two deflection circuits are always operating in direct synchronisation. Under the condition where V_{mod} is 30V the currents in the two circuits would also be equal.



The range of V_{mod} required is 0 to 30V. V_{mod} is reduced below 30V as current is drawn from C_{mod} . An external supply to C_{mod} is never needed. This is the arrangement used in practice.

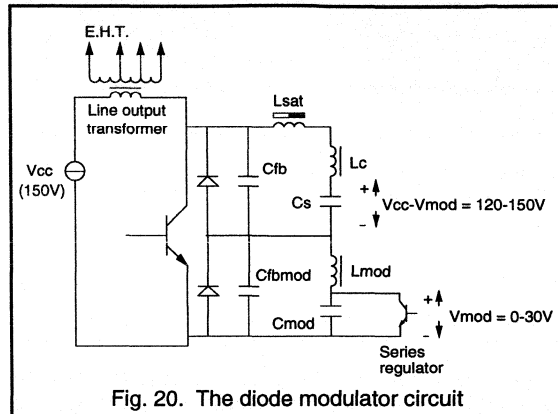
To draw current from C_{mod} a series linear regulator is added across C_{mod} as shown in Fig. 19.



Diode Modulator Circuit

The circuit is now quite close to an actual TV horizontal deflection circuit. As the two transistors are switching in perfect synchronisation this circuit can be simplified further by removing one transistor, as shown in Fig. 20. This arrangement makes no difference to the operation of the circuit.

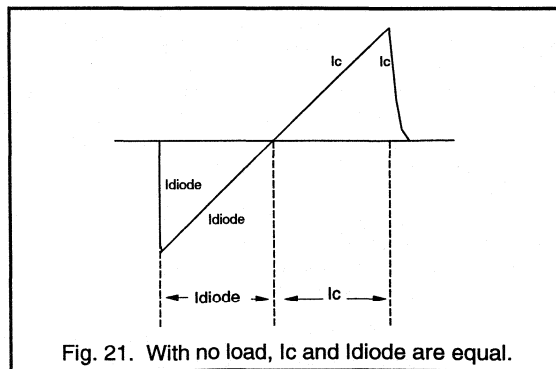
The circuit in Fig. 20 now shows all the features of the horizontal deflection diode modulator circuit. These features should be distinguishable when studying actual circuit diagrams.



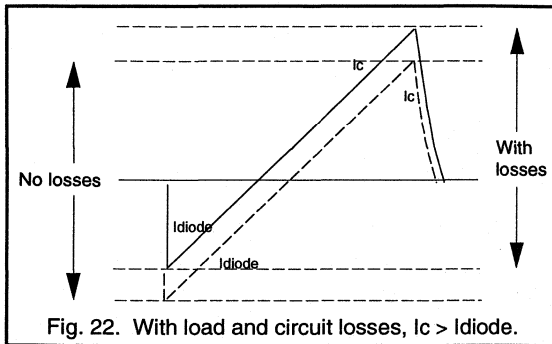
Diode Modulator: Upper Diode

First consider the voltage requirements. In this respect, the worst case conditions for the upper diode are when $V_{mod} = 0V$. Under these conditions the upper diode must support the full flyback voltage. Therefore, the peak voltage limiting value on the upper diode must match the V_{CES} limit of the transistor.

Now consider the current requirements. With no circuit losses, the currents in the diode and the transistor are as shown in Fig. 21 where I_c is the transistor current and I_{diode} is the diode current. Of this current, 80% flows in the deflection coils and 20% flows in the LOT primary.



With circuit losses included, the transistor current will exceed the diode current. Circuit losses add a dc component to the waveform shown in Fig. 21. The loading on the LOT contributes a further dc component, increasing the transistor current and reducing the diode current still further, Fig. 22.



For example, for a current which is 12A peak to peak, 10A of this will be deflection current and 2A will be LOT current. With no load, the peak diode current would be equal to the peak transistor current, i.e. both would equal 6A. However, the LOT requires 1A dc in order to power the secondary windings. This makes the peak diode current 5A and the peak transistor current 7A. These are practical values for a 32 kHz black line S (i.e. EHT = 30kV) TV set.

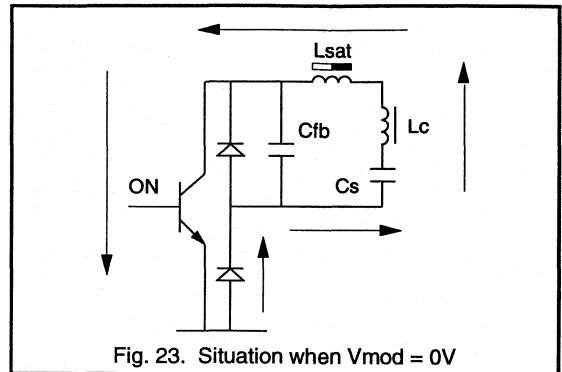
The diode must conduct the full current immediately after the flyback period. Until the forward recovery voltage of the diode has been reached the diode cannot conduct. A high forward recovery voltage device would impede the start of the scan. If once the forward recovery voltage has been reached the device takes a long time before falling to its V_F level then the voltage across the deflection coils would be non-linear and, therefore, cause picture distortion. For a 32 kHz set the diode must recover to less than 5V in under 0.5µs.

Diode Modulator: Lower Diode

First consider the voltage requirements. At one extreme, all the flyback voltage is across the top diode and at the other extreme, the worst case condition for the lower diode is when the flyback voltage is split between the two diodes in the ratio 4:1 (i.e. when V_{mod} is at its maximum value of 30V). The voltage limiting value on the lower diode is, therefore, usually given as one quarter of the rating of the top diode. So, if the transistor is 1500V, the top diode is also 1500V and the bottom diode is 400V.

However, it is not uncommon for fault conditions to occur in TV circuits that cause large voltage spikes on the lower diode. To accommodate such occurrences, a 600V device is often used as the lower diode.

Now consider the current requirements. The lower diode must take the same current as the horizontal deflection coil, Fig. 23, and so its current requirement is the same as that of the top diode.



As shown in Fig. 23, the lower diode is conducting its peak current immediately before the flyback period and switches off as the transistor. Therefore, the reverse recovery of the lower diode must be very fast to minimise circuit losses.

Diode Modulator Circuit Example

Putting the above diode requirements into the circuit of Fig. 20 enable a typical 16 kHz TV horizontal deflection circuit to be constructed, see Fig. 24. This circuit is representative of a modern 25" TV design. The deflection transistor, BU2508A, will run with a peak I_c of 4.5A at 16 kHz. The combined inductance and capacitance will produce a flyback pulse of typically 1200V peak and 13µs width. The upper diode, BY228, has the same current and voltage capability as the deflection transistor. The lower diode, BYW95C, has the same current capability but a reduced voltage rating. More often than not, 600V devices are used as the lower diode with 1500V upper diodes.

The dc supply comes from the TV SMPS circuit. The SMPS will use a power switch also, typically BUT11AF in 16 kHz TV. A transformer will provide all the high power dc supplies required for the TV. For a 150V supply a high voltage diode will be used in the output stage, typically BY229-600. The LOT generates the EHT to accelerate the electron beam, typically a voltage of 25kV is produced.

In smaller TV's (14-21") this circuit could be much simplified. For smaller screen sizes EW correction is not essential and the diode modulator is not usually present. The circuit now uses a single diode and capacitor. The diode can be incorporated in the deflection transistor, for example, the BU2508D. Also for the smaller screen sizes it is common that the tube technology allows for lower flyback voltages. In these applications the 1000V BUT11A and BUT12A are often used.

In larger 16 kHz TV's (28" and above) and all 32 kHz TV's the axial diodes will not normally be capable in terms of current handling. These diodes are replaced by devices in TO220 type power outlines: BY359 for the upper diode and

BY229-600 or BYV29-500 for the lower diode. Also larger deflection transistors are available: BU2520A and BU2525A.

The same sort of scaling is also applicable to monitor deflection circuits. All monitors tend to use 1500V deflection transistors and upper diodes. The BU2508D (ie with diode) is often used so that the BY228 can be used as the upper

diode. Using a D-type deflection transistor takes some current from the diode modulator but does not affect the operating principle. For the high frequency (up to 82 kHz), multi-sync monitors BU2522A and BU2527A deflection transistors are used. Above 64 kHz the BY459 is used as an upper diode.

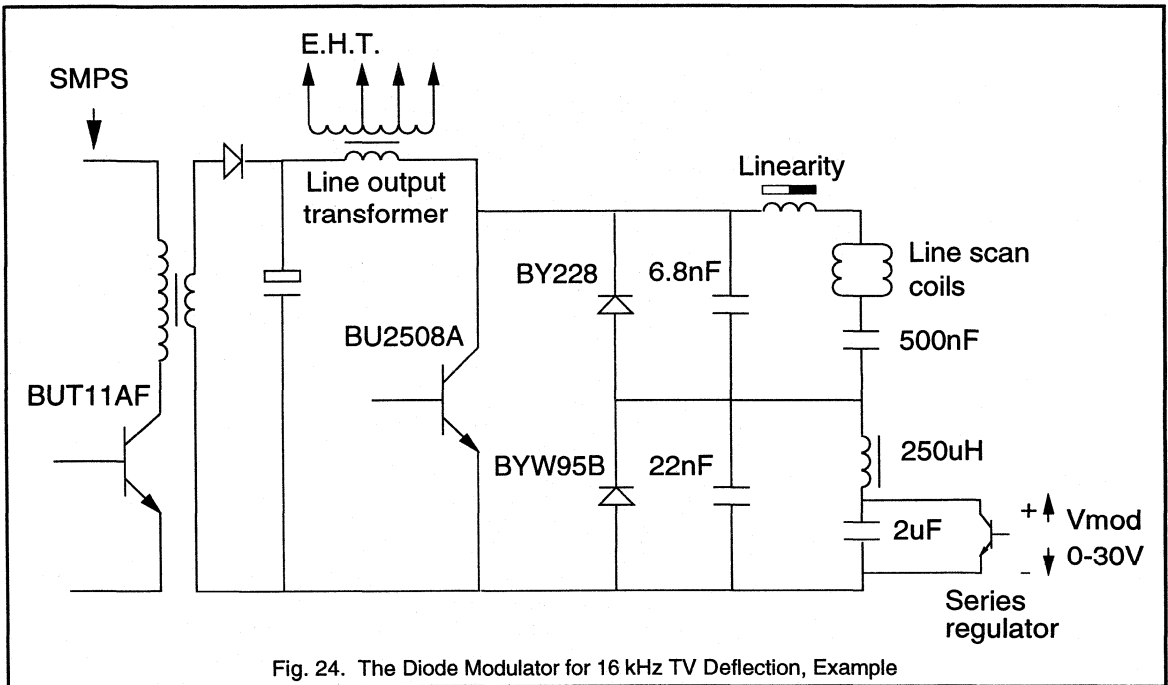


Fig. 24. The Diode Modulator for 16 kHz TV Deflection, Example



4.1.2 The BU25XXA/D Range of Deflection Transistors

Introduction

The BU25XXA range forms the heart of Philips Semiconductors 1500V power bipolar transistors. This technology offers world class dissipation in its target application of 16 kHz TV horizontal deflection circuits. The range has been extended for state-of-the-art large screen TV (8 A, 32 kHz) and all the volume monitor applications (up to 6 A, 64 kHz). The successful application of the BU25XXA range in all sectors of TV & monitor horizontal deflection has proved it to be a global technology.

As a further improvement, the BU25XXD range of devices have been introduced. Using BU25XXA technology, horizontal deflection transistors incorporating base-emitter resistive damping and a collector-emitter damper diode have been produced. The devices in this range are specifically aimed at the small-screen 16 kHz TV and 48 kHz monitor applications where the use of a D-type device can offer a significant cost-saving. The D-types offer the same performance as the A-type equivalent with only slightly increased dissipation, at a similar cost.

Specification Notes

The I_{CSAT} value defines the peak current reached in a horizontal deflection circuit during normal operation for which optimum performance is obtained. Unlike other specification points, it is not necessary to inset this value in a real application. Operation either much above or below the specified I_{CSAT} value will result in less than optimum performance. For higher frequencies the I_{CSAT} should be lowered to keep the dissipation down.

The V_{CESM} value defines the peak voltage applied under any condition. The BU25XXA/D range could operate under continuous switching to 1500V in a deflection circuit without any degradation to performance but exceeding 1500V is neither recommended nor guaranteed. In normal running the peak flyback voltage is typically 1150V but a 1500V device is required for fault conditions.

The storage time, t_s , and fall time, t_f , limits are given for operation at the I_{CSAT} value and the frequency of operation given by the application limit.

The BU25XXA Range Selection Guide

Device	Specification				Application	
	I_{CSAT}	V_{CESM}	t_s	t_f	TV	Monitor
BU2508A/AF/AX	4.5 A	1500 V	6.0 μ s	600 ns	$\leq 25"$, 16 kHz	-
	4.0 A	1500 V	5.5 μ s	400 ns	-	14", SVGA, 38 kHz
BU2520A/AF/AX	6.0 A	1500 V	5.5 μ s	500 ns	$\leq 29"$, 16 kHz	15", SVGA, 48 kHz
			4.0 μ s	350 ns	$\leq 28"$, 32 kHz	
BU2525A/AF/AX	8.0 A	1500 V	4.0 μ s	350 ns	$\leq 32"$, 32 kHz	(17", 64 kHz)
BU2522A/AF/AX	6.0 A	1500 V	2.0 μ s	250 ns	-	15", 64 kHz
BU2527A/AF/AX	6.0 A	1500 V	2.0 μ s	200 ns	-	17", 64 kHz

The BU25XXD Range Selection Guide

Device	Specification				Application	
	I_{CSAT}	V_{CESM}	t_s	t_f	TV	Monitor
BU2506DF/DX	3.0 A	1500 V	6.0 μ s	500 ns	$\leq 23"$, 16 kHz	-
BU2508D/DF/DX	4.5 A	1500 V	6.0 μ s	600 ns	$\leq 25"$, 16 kHz	14", SVGA, 38 kHz
BU2520D/DF/DX	6.0 A	1500 V	5.5 μ s	500 ns	$\leq 29"$, 16 kHz	15", SVGA, 48 kHz

Application Notes

The applications given in the selection guide should be seen as an indication of the limits that successful designs have been achieved for that device type. This should help in the selection of a device for a given application at the design concept stage. For example, a 15" monitor requiring operation up to 6 A at 64 kHz could use either a BU2522A or BU2527A. If the design has specific constraints on switching and dissipation then the BU2527A is the best option, but if cost is also a prime consideration then the smaller chip BU2522A could be used with only slightly degraded performance. For an optimised design the BU2525A can be used in 17", 64 kHz applications but the BU2527A is the recommended choice.

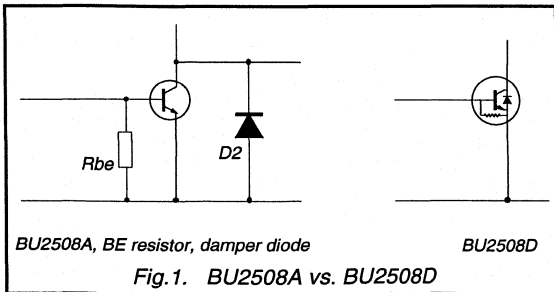
Outlines

Philips Semiconductors recognise both the varying design criteria and the market availability of device outlines and this is reflected in the range of outlines offered for the BU25XXA/D range. Three different outlines are offered for the devices available, one non-isolated (SOT93) and two isolated/full-pack designs (SOT199, TOP3D). The outline is defined by the last letter in the type number, for example:

BU2508A	SOT93	non-isolated
BU2508AF	SOT199	isolated
BU2508AX	TOP3D	isolated

All three outlines are high quality packages manufactured to Philips Total Quality Management standards.

The Benefits of the D-type



The BU2508D technology incorporates the damper diode and a base-emitter damping resistor, see Fig.1. In the target 16 kHz applications the damper diode is usually an axial type (eg. BY228), the D-type deflection transistor incorporates this device in a monolithic structure. This presents a significant cost-saving in the application. The base-emitter resistor eliminates the need for external damping at the transistor base-emitter. The only

consideration for replacing an A-type with a D-type is that the base current required for optimised switching is slightly higher for the D-type.

For higher currents and frequencies where diode modulator circuits are used it appears at first that use of the D-types is not possible. However, this is not so; D-type transistors can be used WITH diode modulators in a beneficial way. For example, a 15", 48 kHz SVGA monitor utilising a diode modulator is at the borderline between an axial upper damper diode and a TO220 type. The dissipation is such that if an axial diode is used some sort of thermal management may be necessary. By using a D-type transistor some of the current is taken by the diode in the D-type relieving the discrete upper damper device. Use of a D-type in this way has allowed an axial diode to be used in place of a TO220 type making a significant cost saving.

Causes of Dissipation

In the cycle of operation there are four distinct phases: turn-on, on, turn-off, off. Each phase is a potential cause of dissipation. Of course, for enhanced circuit performance dissipation in the deflection transistor must be minimised.

a) Turn-on. The primary function of a deflection transistor is to assist in the sweep of the beam across the screen of the display, ie to horizontally deflect the beam. As the deflection transistor turns-on the beam is scanning from just less than half way across. At mid-screen the beam is un-deflected, ie the deflection current is zero. So, the deflection transistor turns on with a small negative collector current, I_C ramping up through zero. At turn-on there are no sudden severe load requirements that cause significant dissipation. In horizontal deflection turn-on dissipation is negligible.

b) On-state. As the beam is deflected from the centre of the screen to the right - hand side the I_C increases as determined by the voltage across the deflection coil. The resulting voltage drop across the deflection transistor, V_{CE} depends not only on this I_C but also on the base drive: for high I_B the V_{CE} will be low; for low I_B the V_{CE} will be high. For high I_B the transistor is said to be overdriven giving low on-state dissipation. For low I_B the transistor is said to be underdriven giving higher on-state dissipation.

c) Turn-off. Turn-off starts when the forward I_B is stopped. This is followed 2 - 6 μs later (depending on the device and application) by the I_C peaking. This delay is called the storage time, t_s of the device. During this time the V_{CE} rises as the current rises causing increased dissipation: the longer t_s the higher the dissipation. As the I_C peaks so scanning ends and the process of flyback begins. Now, as the I_C falls (in time t_f , the fall-time) the V_{CE} rises to the peak flyback voltage; this a phase of high dissipation.

Turn-off is the dominant loss phase for all deflection transistors. The device characteristics in this phase are of much interest to the TV & monitor design engineers.

d) Off-state. In an optimised drive circuit the device will be off for V_{CE} above 250V in flyback. For the rest of the flyback the collector-emitter is reverse biased while the base-emitter will also be reverse biased: between -1 to -4V. Any leakage through the device will be the cause of dissipation. For the BU25XXA/D range, low-contaminant processing ensures that the bulk leakage is very low. Also, the long-established Philips glass passivation has very low leakage. The device characteristics coupled with the low pulse width and duty cycle of the flyback mean that the losses in the off-state are negligible.

In a D-type deflection transistor there is an additional cause of dissipation:

e) Diode Conduction. At the end of flyback the next scan will start. As the flyback voltage goes negative so the diode conducts, this clamps the voltage on the flyback capacitor. The fixed voltage provides a fixed ramp in current through the deflection coil and through the diode; the beam sweeps from the left towards the centre of the screen. At, or near, the centre this current approaches zero ending the diode conduction phase. The dissipation here is dominated by two characteristics of the diode: the forward recovery and the on-state voltage drop. This can be a significant cause of dissipation in a D-type transistor.

The effect of both underdrive and overdrive on the device is increased device dissipation and hence increased junction temperature. In general, the higher the junction temperature the shorter the lifetime of the device in the application. Optimised drive circuit design and good thermal management can bring the device junction temperature down to well below the limit T_{jmax} . Such considerations enhance the reliability of the deflection transistor in the application. It is essential that care is taken at the design stage to optimise the base drive for the device product spread.

Dynamic Testing

The BU25XXA/D range is assessed in a deflection switching test circuit designed to simulate the most demanding running conditions of the application. The horizontal deflection coils, which form the major part of the collector load, are represented by a variable inductance L_c and the flyback and diode modulator circuits by a single diode, BY228 and variable capacitance, C_{fb} . For BU2508A/AF/AX TV applications the test circuit is shown in Fig.2 below.

This circuit generates the characteristic deflection waveforms, Fig.3, from which the storage time, fall time and energy loss at turn-off can be measured. These parameters define the device performance in the application.

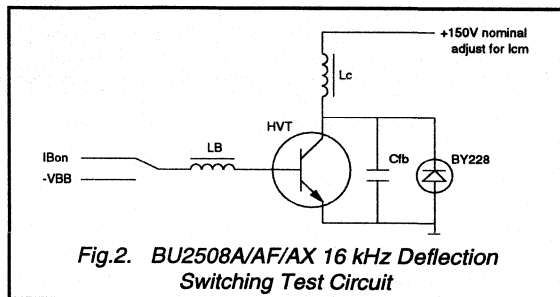


Fig.2. BU2508A/AF/AX 16 kHz Deflection Switching Test Circuit

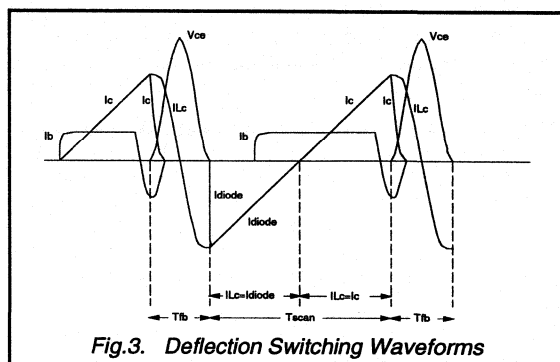


Fig.3. Deflection Switching Waveforms

It is not valid to do a single-shot test for the switching parameters as the characteristics of the n th pulse depend on the previous $(n-1)$ th pulse. To achieve this the tester works in a double pulse mode.

'Bathtub' Curves

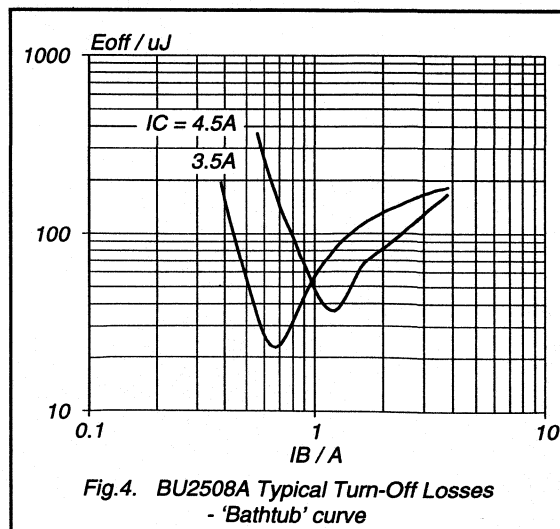


Fig.4. BU2508A Typical Turn-Off Losses - 'Bathtub' curve

A plot of base current, I_B , against turn off dissipation, E_{off} , for one BU2508A measured in the switching test circuit at a peak collector current of 4.5A gives the characteristic 'bathtub' shape shown in Fig.4 above. From this curve the tolerance to base drive variations can be assessed and the optimum I_B determined for a given I_C .

The switching performance is also determined by the peak reverse base current at switch off. For a typical h_{FE} device, of all types in the BU25XXA/D range, a peak reverse base current, I_{Boff} , equal to one half the typical peak I_C is recommended for optimum dissipation. This is largely determined by the drive transformer and is usually difficult to be fine-tuned. In the typical non-simultaneous base drive circuit the level of forward base current, I_B , is easily controlled, hence, the presentation of the turn-off losses versus I_B .

The 'bathtub' curves are plotted for a reverse base voltage at turn-off of -4V. This level of reverse base drive is recommended for the BU25XXA/D range as it reduces the risk of any noise, or ring, forward biasing the base-emitter during flyback. However, in well-engineered designs the BU25XXA/D can operate just as well with a reverse base voltage at turn-off of only -1V. This tolerance to base drive is very useful to design engineers.

On the far left of the curve, at low I_B values, the device is severely underdriven resulting in a high turn off dissipation. As the base drive is increased the degree of underdrive is reduced and the device remains in saturation for a larger proportion of its on time. This is the reason for the initial decrease in E_{off} with increasing I_B seen in the 'bathtub' curve. Eventually, the optimum drive is reached and the turn off dissipation, E_{off} , is at its minimum value. Increasing the base drive still further results in overdrive and the appearance of an I_C tail at turn off. The result of this, as can be seen in the 'bathtub' curve, is increasing turn off losses with increasing I_B .

Typically, this curve has steep sides and a flatter central portion; this gives it the shape of the cross-section through a bathtub, hence the name 'bathtub' curve !

The BU25XXA/D technology gives a sharper looking curve but a much lower level of E_{off}/P_{off} than competitor types. For optimised drive the BU25XXA/D technology offers world class dissipation in 16 kHz TV deflection circuits.

Process Control

The success of the BU25XXA/D range has enabled significant enhancements to be made to the benefit of both our customers and ourselves. By utilising a continuous cycle of quality improvement coupled with high volume production, Philips Semiconductors can demonstrate their excellent process control in specified h_{FE} and dissipation

limits. This control is achieved by manufacturing capability rather than test selections. This process control improves manufacturing throughput and yield and, hence, customer deliveries. The improvements in manufacturing result in higher process capability indices enabling the introduction of tightened internal test specifications.

Critical Parameter Distribution Fact Sheets

Industry standard data sheets for all power semiconductor devices offer an introduction to the device fundamentals and can usually be used for a quick comparison between competitor types. Detailed use of a specific device requires much more information than is contained in any data sheet. This is particularly relevant to high voltage bipolar transistors, and especially horizontal deflection transistors. A horizontal deflection transistor is only as good as the base circuit that drives it. The growth of power MOSFET's is mainly due to the difficulties in driving bipolar transistors. However, MOSFET technology is not suitable for horizontal deflection applications, Philips Semiconductors are actively involved in supplying the support tools necessary for the successful design-in of their BU25XXA/D range.

Recognising the designers requirements Philips Semiconductors now provide critical parameter distribution fact sheets for the BU25XXA/D range. This additional data should be used in conjunction with the data sheets to give a full picture of the device capabilities and characteristics over the production spread.

The fact sheets give limit curves for the power dissipation in the device caused by turn-off, P_{off} , at a given operating frequency and range of load current, I_C all at 85°C (a typical operating temperature for TV and monitor applications). These curves provide limits to the typical 'bathtub' curves given in data. It is important to recognise that these fact sheet curves represent the LIMIT of production when comparing the BU25XXA/D range with competitor types which offer this information as TYPICAL only, if at all. This information displays the technical performance of the device and the measurement capability available.

Contained in the fact sheets is evidence of the world class dissipation limits obtained by the BU25XXA/D range. As an example, the BU2508A/AF/AX 'bathtub' limit curves are shown in Figs.5-7.

These fact sheets also contain limit h_{FE} curves for $V_{CE} = 1$ V and 5 V at three different temperatures: -40°C, 25°C, and 85°C. The range of temperatures chosen reflects the range of customer requirements. These limit curves define the device characteristics for all the important extremes of operation. As an example the BU2508A/AF/AX limit h_{FE} curves for $V_{CE} = 1$ V and 5 V at 25°C are shown in Figs.8-9 below. The 100% test points are indicated by arrows.

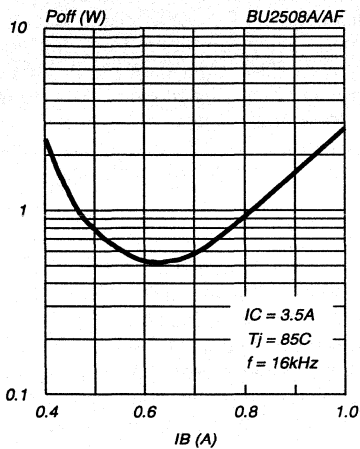


Fig.5. BU2508A/AF/AX
Max. P_{off} vs. I_B
for $I_C = 3.5A$ @ $85^\circ C$

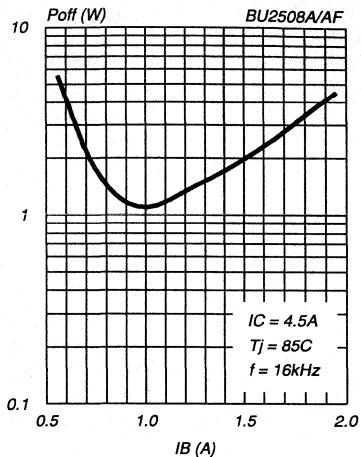


Fig.6. BU2508A/AF/AX
Max. P_{off} vs. I_B
for $I_C = 4.5A$ @ $85^\circ C$

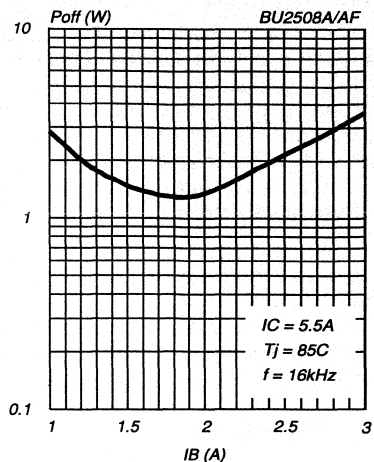


Fig.7. BU2508A/AF/AX
Max. P_{off} vs. I_B
for $I_C = 5.5A$ @ $85^\circ C$

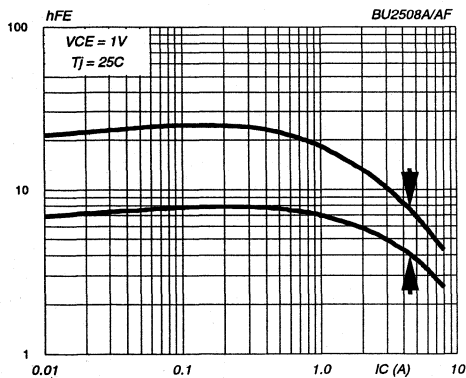


Fig.8. BU2508A/AF/AX h_{FE} vs I_C @ 1 V, $25^\circ C$

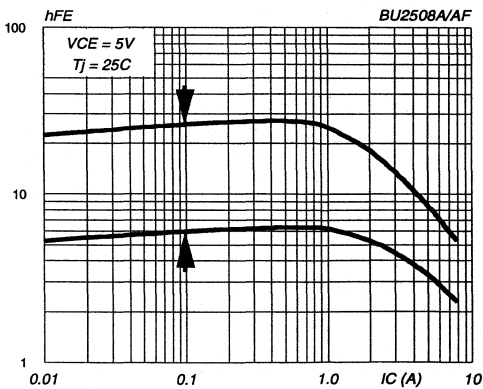


Fig.9. BU2508A/AF/AX h_{FE} vs I_C @ 5 V, $25^\circ C$

Drive Circuits

It was stated previously that a horizontal deflection transistor is only as good as the base circuit that drives it. Philips Semiconductors address this problem by providing fact sheets with an example of a drive circuit for the target applications. The drive circuits presented are of the industry standard non-simultaneous base drive type utilising commercially available Philips components. An example of these drive circuits is shown for the BU2508A in Fig.10 below.

This drive circuit is not an end in itself but a means to an end: it produces the waveforms at the base that enable the load set by V_{cc} , L_c and C_{fb} to be switched most efficiently. For this reason the waveforms produced by this circuit are also presented in the fact sheet. Again, for the BU2508A example given above the waveforms are shown in Figs.11-15 below.

The drive circuit employed in the application could be quite different to the one given above in Fig.10 but the base drive waveforms in Figs.11 & 13 must be replicated for optimised switching.

The fundamental concept of the non-simultaneous base drive is well established in the TV and monitor industry for driving the horizontal deflection transistor. Individual designs, however, can differ significantly. A different transformer design may enable the required base current to be generated without the addition of L_b and D_1 , R_b . Driving R_p from a low voltage supply could reduce the cost by allowing a low voltage transistor, Q_1 and capacitor, C_d to be used.

The resistor R_{be} is necessary to eliminate any overshoot in the V_{be} at the end of the base-emitter avalanche that could turn the transistor on during flyback. Such an event would lead to an early failure of the transistor by exceeding the forward biased safe-operating area (FBSOA). In circuits operating at higher frequencies resistive damping alone is usually not sufficient and RC damping is required.

In this application, the BU2508A could be replaced by the BU2508D in the circuit of Fig.10. This would allow the BY228 and R_{be} resistor to be removed from the circuit.

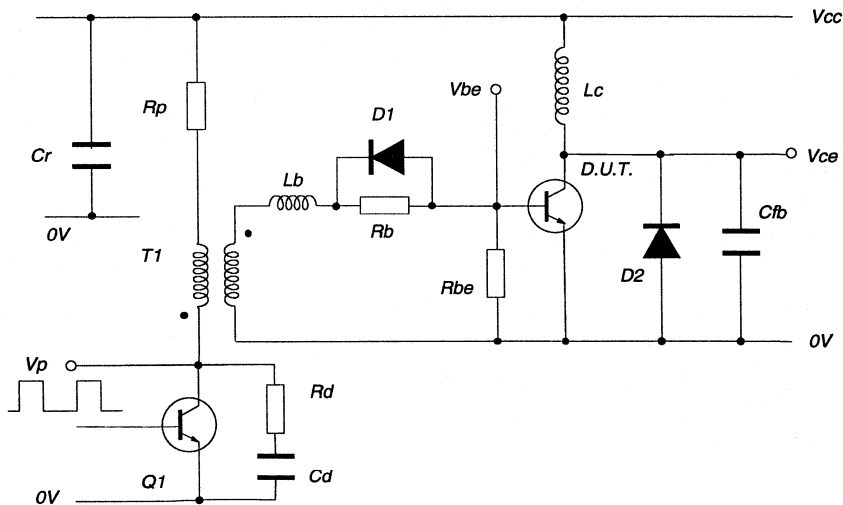


Fig.10. BU2508A 4.5 A, 16 kHz Drive Circuit

Components and values: $R_p = 1 \text{ k}\Omega$, 2 W; $C_r = 100 \text{ nF}$; $R_d = 560 \Omega$; $C_d = 470 \text{ pF}$, 500 V; Q_1 Philips BF819; T_1 Philips AT4043/87 Transformer; $L_b = 0.5 \mu\text{H}$; $R_b = 0.5 \Omega$, 0.5 W; D_1 Philips BYV28-50; $R_{be} = 50 \Omega$; $L_c = 1 \text{ mH}$; $C_{fb} = 12 \text{ nF}$, 2 kV; D_2 Philips BY228; $V_{cc} = 115 \text{ V}$.

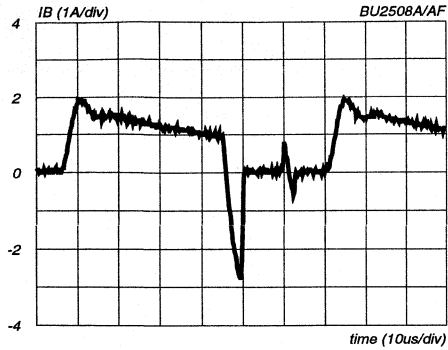


Fig.11. BU2508A/AF I_B vs. time

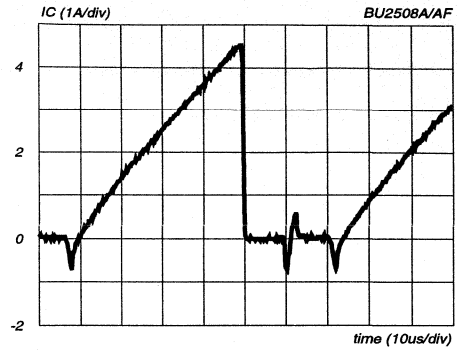


Fig.12. BU2508A/AF I_C vs. time

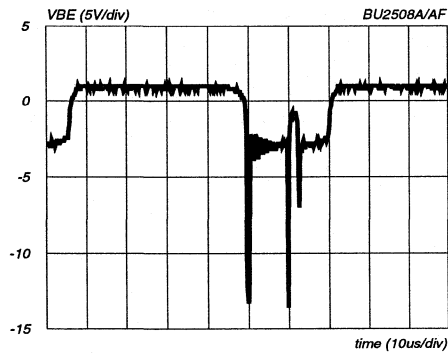


Fig.13. BU2508A/AF V_{BE} vs. time

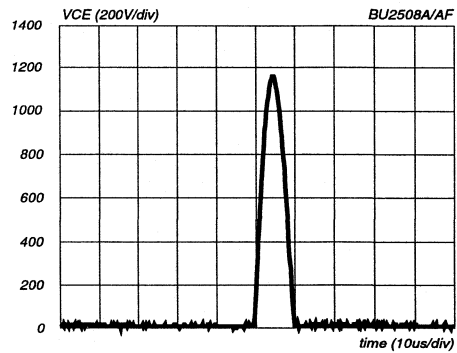


Fig.14. BU2508A/AF V_{CE} vs. time

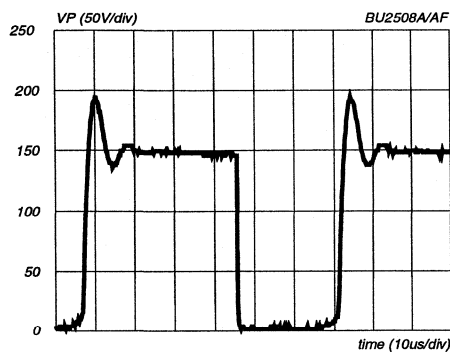


Fig.15. V_p vs. time

$$I_{B(end)} = 0.9 - 1.1 \text{ A}; I_{Cmax} = 4.5 \pm 0.25 \text{ A};$$

$$|I_{B(off)}| \geq 2.0 \text{ A};$$

$$V_{CEmax} = 1100 - 1200 \text{ V}$$



4.1.3 Philips HVT's for TV & Monitor Applications

This section simplifies the selection of the power switches required for the SMPS and horizontal deflection in TV and monitor applications. Both high voltage bipolar transistors and power MOSFET devices are included in this review. As well as information specific to the Philips Semiconductors range of devices, general selection criteria are established.

HVT's for TV & Monitor SMPS

The vast majority of television and monitors have switch mode power supplies that are required to generate an 90 - 170V supply for the line deflection stage, plus a number of lower voltage outputs for audio, small signal etc. By far the easiest and most cost effective way of fulfilling these requirements is to use a flyback topology. Discontinuous mode operation is generally preferred because it offers easier control and smaller transformer sizes than continuous mode.

For the smaller screen size TV's, where cost is a dominant factor, bipolar HVT's dominate. For large screen TV and monitors power MOSFET's are usually chosen.

The peak voltage across the switching transistor in a flyback converter is twice the peak dc link voltage *plus* an overshoot voltage which is dependent on the transformer leakage inductance and the snubber capacitance. Thus, for a given mains input voltage there is a minimum voltage requirement on the transistor. Increasing the transformer leakage and/or reducing the snubber capacitance will increase the minimum voltage requirement on the transistor.

a) Power MOSFET's

For TV's operating just with 110/120V mains applications a device which can be used with peak voltages below 400V is required. For these applications the power MOSFET is used almost exclusively. A wide variety of 400V power MOSFET's are available, leading to lower device costs, which coupled with the easier drive requirements of the MOSFET make this an attractive alternative to a bipolar switch.

For 220/240V and, more recently, for universal input mains applications where an 800V device is generally required the cost of power MOSFET is prohibitive. However, improvements both in circuit design and device quality has meant that a 600V device can be used in these applications.

Philips Semiconductors have a comprehensive range of powerMOS devices for these applications. The main parameters of these devices most applicable to TV and monitor SMPS applications are summarised in Table 1.

Part Number	V _{DSS}	R _{DS(ON)}	@ I _D
BUK454-400B	400 V	1.8 Ω	1.5 A
BUK455-400B	400 V	1.0 Ω	2.5 A
BUK457-400B	400 V	0.5 Ω	6.5 A
BUK454-600B	600 V	4.5 Ω	1.2 A
BUK455-600B	600 V	2.5 Ω	2.5 A
BUK457-600B	600 V	1.2 Ω	6.5 A
BUK454-800A	800 V	6.0 Ω	1.0 A
BUK456-800A	800 V	3.0 Ω	1.5 A
BUK438-800A	800 V	1.5 Ω	4.0 A

Table 1. Philips PowerMOS HVT's for TV & Monitor SMPS Applications

The V_{DSS} value is the maximum permissible drain-source voltage of the powerMOS in accordance with the Absolute Maximum System (IEC 134). The R_{DS(ON)} value is the maximum on-state resistance of the powerMOS at the specified drain current, I_D.

b) Bipolar HVT's

Bipolar HVT's still have an important role in TV SMPS applications. Many new TV designs are slight improvements on existing designs incorporating a new control or signal feature (eg Fasttext, SCART sockets) which do not demand the re-design of the SMPS. If there has been a good experience with an existing SMPS it is not surprising that these designs should continue in new TV models.

For 220/240V mains driven flyback converters, generally, a 1000V bipolar HVT is used. The full voltage capability of the transistor can be used as the limit under worst case conditions but it must never be exceeded. In circuits where the transformer leakage inductance is high, and voltages in excess of 1000V can occur, a device with a higher voltage handling capability is required.

Philips Semiconductors have a comprehensive range of bipolar HVT devices for these applications. The main parameters of these devices most applicable to TV SMPS applications are summarised in Table 1.

Part Number	V _{CESM}	V _{CEO}	I _{Csat}	V _{CEsat}
BUX85	1000 V	450 V	1 A	1.0 V
BUT11A	1000 V	450 V	2.5 A	1.5 V
BUT18A	1000 V	450 V	4 A	1.5 V
BUT12A	1000 V	450 V	5 A	1.5 V
BUW13A	1000 V	450 V	8 A	1.5 V
BU506	1500 V	700 V	3 A	1.0 V
BU508A	1500 V	700 V	4.5 A	1.0 V

Table 2. Philips Bipolar HVT's for TV SMPS Applications

The V_{CESM} value is the maximum permissible collector-emitter voltage of the transistor when the base is shorted to the emitter or is at a potential lower than the emitter contact. The V_{CEO} value is the maximum permissible collector-emitter voltage of the transistor when the base is open circuit. Both voltage limits are in accordance with the Absolute Maximum System (IEC 134). The V_{CEsat} value is the maximum collector emitter saturation voltage of the transistor, measured at a collector current of I_{Csat} and the recommended base current.

c) Selection procedures

Some simple calculations can be made to establish the device requirements. The first requirement to be met is that the peak voltage and current values are within the capabilities of the device. For a flyback converter the peak voltage and current values experienced by the power switch are given by the equations in Table 3.

Peak voltage across the device	$(2 \times V_{s(max)}) + \sigma$
Peak device current	$2 \times \frac{P_{th}}{\delta_m \times V_{s(min)}}$

Table 3. Peak Voltage and Current in a Flyback Converter.

where:

- V_{s(max)} = maximum dc link voltage
- σ = voltage overshoot due to transformer leakage
- V_{s(min)} = minimum dc link voltage
- P_{th} = throughput power of SMPS
- δ_m = maximum duty cycle of SMPS

Note: in this example, the throughput power is equal to the input power less the circuit losses up to the power switch.

MOSFET or bipolar?

The main factors influencing this decision are ease of drive and cost, given the limitation on percentage of throughput power which can be dissipated in the power switch. MOSFETs require lower drive energy and less complicated drive circuitry. They also have negligible switching losses below 50 kHz. However, large chip sizes are required in order to keep on state losses low (especially as breakdown voltage is increased). Thus the larger chip size of the MOSFET is traded off against its capacity for cheaper and easier drive circuitry and higher switching frequencies.

For 110/120V mains driven TV power supplies the 400V MOSFET dominates. At 220/240V there is a split between bipolar and power MOSFET

Which MOSFET?

The optimum MOSFET for a given circuit can be chosen on the basis that the device dissipation must not exceed a certain percentage of throughput power. Using this as a selection criterion, and assuming negligible switching losses, the maximum throughput power which a given MOSFET is capable of switching is calculated using the equation;

$$P_{th(max)} = \frac{3 \times \tau \times V_{s(min)}^2 \times \delta_{max}}{4 \times R_{ds(125C)}}$$

where:

- P_{th(max)} = maximum throughput power
- δ_{max} = maximum duty cycle
- τ = required transistor loss (expressed as a fraction of the output power)
- R_{ds(125C)} = R_{DS(ON)} at 125°C
- V_{s(min)} = minimum dc link voltage

A transistor loss of 5% of output power gives a good compromise between device cost, circuit efficiency and heatsink size (ie τ = 0.05)

Note that the R_{DS(ON)} value to be used in the calculation is at 125°C (a practical value for junction temperature during normal running). The R_{DS(ON)} specified in the device data is measured at 25°C. As junction temperature is increased the R_{DS(ON)} increases, increasing the on state losses of the MOSFET. The extent of the increase depends on the device voltage, see Fig. 1.

For 400V MOSFET's R_{ds(125C)} = 1.98 x R_{DS(ON)} @ 25°C, where R_{DS(ON)} @ 25°C is the value given in device data.

For 800V MOSFET's R_{ds(125C)} = 2.11 x R_{DS(ON)} @ 25°C.

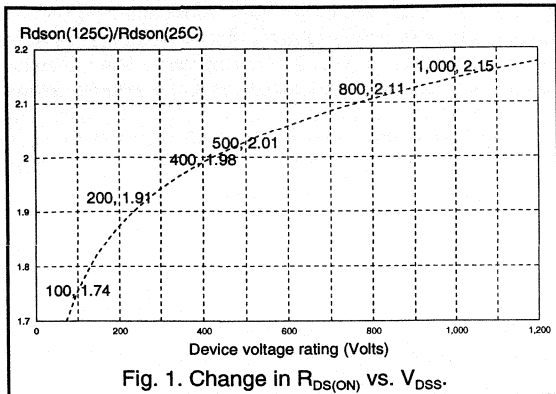


Fig. 1. Change in $R_{DS(ON)}$ vs. V_{DSS} .

Which bipolar?

For maximum utilisation of a bipolar transistor it should be run at its data I_{Csat} . This gives a good compromise between cost, drive requirements and switching losses. Using this as a selection criterion the maximum output power which a given bipolar transistor is capable of switching is calculated using the equation;

$$P_{th(max)} = \delta_{max} \times V_{s(min)} \times \frac{I_{Csat}}{2}$$

- where: $P_{th(max)}$ = maximum throughput power
- δ_{max} = maximum duty cycle
- $V_{s(min)}$ = minimum dc link voltage
- I_{Csat} = I_{Csat} in transistor data

d) Selection table

Using the selection procedures just discussed, and the device data given previously, the following selection table of suitable devices for flyback converters of various output powers has been constructed.

Output Power	110/120V (ac) mains	220/240V (ac) mains
50 W	BUK454-400B	BUK454-600B BUK454-800A BUX85
100 W	BUK455-400B	BUK455-600B BUK456-800A BUT11A/BU506
150 W	BUK457-400B	BUK457-600B BUK438-800B BUT12A/BU506
200 W	BUK457-400B	BUK438-800A BUW13A/BU508A

Table 4. Power Switch Selection Table

HVT's for TV & Monitor Horizontal Deflection

This application is one of the few remaining applications which is entirely serviced by bipolar devices. The technology is not yet commercially available to provide MOSFET or IGBT devices for this application. A horizontal deflection transistor is required for each TV and monitor employing a standard cathode ray tube display.

The deflection transistor is required to conduct a current ramp as the electron beam sweeps across the screen and then withstand a high voltage peak as the beam flies back before the next scan starts. The peak current and voltage in the application define the device required. In addition to this, the deflection transistor is required to switch between the peak current and peak voltage states as quickly and efficiently as possible. In this application the switching and dissipation requirements are equally as important as the voltage and current requirements.

Standard TV switches at a frequency of 16 kHz, rising to 32 kHz for improved definition TV (IDTV). In the future, high definition TV (HDTV) will switch between 48 and 64 kHz.

Standard VGA monitors switch at 31 kHz, rising to 48 kHz for SVGA. However, many other (as yet unnamed) modes exist for PC monitors and work stations, extending up to 100 kHz switching frequencies.

Vertical deflection is much lower in frequency (50 to 70 Hz) and will not be discussed as this uses lower power devices (typically 150V / 0.5A).

a) Voltage and Current Requirements

For a given scan frequency the voltage and current requirements of the horizontal deflection transistor are not fixed. However, the suitable transistors are all linked by the relationship;

$$I_{Csat} \times V_{CESM} = constant$$

The derivation of this law is as follows:

The horizontal deflection angle (typically 110°) covered in a given time is proportional to the magnetic field sweep between the horizontal deflection coils. This is in turn proportional to the product of the number of turns on the deflection coils and the peak to peak current. The average current in the deflection coils is zero and hence the peak positive current in the coils is half the peak to peak current. These relationships yield the following equation;

$$B \propto n \times I$$

where:

B = magnetic field sweep between the horizontal deflection coils

n = number of turns on the horizontal deflection coils

I = peak positive current in the horizontal deflection coils

The inductance of the horizontal deflection coils, L, is proportional to the square of the number of turns, ie

$$L \propto n^2$$

Combining these two equations gives

$$B^2 \propto L \times I^2$$

and so for a given deflection angle and horizontal scan frequency, and therefore a given B, L x I² is a constant.

For a given deflection frequency the flyback time is also fixed. Flyback time is related to the deflection coil inductance, L, and the flyback capacitance, C, by the equation

$$t_{fb} \propto \sqrt{L \times C}$$

During the flyback period the energy in the deflection coils (1/2.LI²) is transferred to the flyback capacitor and so the voltage across the flyback capacitor rises. Assuming all the energy is conserved during this transfer, the increase in voltage across the flyback capacitor, δV, is given by

$$\frac{1}{2} \times L \times I^2 = \frac{1}{2} \times C \times \delta V^2$$

So, if LI² is a constant then CδV² is a constant also. Therefore, as LC is a constant so is (δV)². So we have:

$$\delta V \times I = constant$$

δV is the voltage rise across the flyback capacitor due to the energy transferred from the deflection coils during the flyback period. The peak voltage across the flyback capacitor, V_{peak}, is given by

$$V_{peak} = \delta V + V_{CC}$$

where: V_{CC} = line voltage (typically +150 V)

The flyback capacitor is positioned across the collector emitter of the horizontal deflection transistor. Therefore, the peak voltage across the flyback capacitor is also the peak voltage across the collector - emitter of the deflection transistor.

In order to protect the transistor against overload conditions (eg picture tube flash) a good design practice is to allow V_{CEpeak} to be 80% of the V_{CESM} rating. V_{CC} is generally around 10% of the V_{CEpeak} (in order to obtain the correct ratio of scan time to flyback time). This gives

$$V_{CESM} \geq 1.25 \times \delta V + 190$$

All the positive current in the horizontal deflection coils is conducted by the horizontal deflection transistor. However, this is not the peak current in the transistor. The transistor is normally also required to conduct the current in the primary of the line output transformer (LOT). Typically, this will increase the peak current in the deflection transistor by 40%. For optimum deflection circuit design the peak current in the transistor will be its I_{Csat} rating, ie

$$I_{Csat} = 1.4 \times I$$

Therefore, for a given deflection angle and a given horizontal scan frequency the horizontal deflection circuit can be designed around any one of a number of devices. However, the suitable devices are all linked by the equation

$$I_{Csat} \times V_{CESM} = constant$$

Summary

For a given horizontal deflection angle and horizontal scan frequency

$$V_{CESM} \geq 1.25 \times \delta V + 190$$

$$I_{Csat} = 1.4 \times I$$

$$I_{Csat} \times V_{CESM} = constant$$

$$L \times I^2 = C \times \delta V^2 = constant$$

where:

V_{CESM} = maximum voltage rating of the horizontal deflection transistor

I_{Csat} = I_{Csat} rating of the horizontal deflection transistor

δV = voltage rise on the flyback capacitor due to the energy transfer from the horizontal deflection coils

I = peak positive current in the horizontal deflection coils

L = inductance of the horizontal deflection coils

C = value of flyback capacitance

These relationships apply only for the assumptions declared previously.

b) Switching and Dissipation Requirements

In TV, for a given scan frequency the minimum on time of the transistor is well defined. For 16 kHz systems the transistor on time is not less than 26 μs and for 32 kHz systems it is not less than 13 μs. This enables the required storage time of the transistor to be well defined. For 16 kHz systems a maximum storage time of 6.5 μs is the typical requirement. For 32 kHz systems the required maximum storage time is typically 4.0 μs. For higher frequencies the required maximum storage time is reduced still further.

In monitor applications, especially multi frequency models, the on time is not well defined. There are many different frequency modes and several control ic's giving different duty cycles. However, it can be said that the higher the frequency, the shorter the storage time required.

Storage time in the circuit can always be reduced by turning the transistor off harder. However, this eventually leads to a collector current tail at turn off and as a consequence the turn off dissipation increases. Turn off dissipation accounts for the bulk of the losses in a deflection transistor and it is crucial that this is kept to a minimum. The deflection transistor must be tolerant to drive and load variations if it is to achieve a low turn off dissipation because the east-west correction on larger screen television sets means that circuit conditions are not constant. Turn off can be optimised during the design phase by ensuring that the peak reverse base current is roughly half of the peak collector current and the negative base drive voltage is between 2 and 5V.

Turn on performance is not a critical issue in deflection circuits. At turn on of the deflection transistor the I_C is low, the V_{CE} is low and, therefore, the dissipation is low. The actual turn on performance of the transistor has a negligible effect.

c) HVT's for Horizontal Deflection

The deflection circuit must satisfy any specified cost, efficiency and EMC requirements before it can be called acceptable. A very high voltage deflection transistor would allow a lower deflection coil current to be used, reducing the level of EM radiation from the deflection coils, but it would require a higher line voltage and it would also result in higher switching losses in the transistor. A very high deflection coil current would allow a lower voltage deflection transistor to be used and a lower line voltage. This would also yield lower switching losses in the deflection transistor. However, high currents in the deflection coils could lead to EMC problems, and the need to keep the resistive coil losses low would mean that thicker wire would have to be used for the windings. Above a certain point the skin depth effect makes it necessary to use litz wire.

For 16 kHz and 32 kHz applications the 1500V bipolar transistor has become the designers first choice, although many 16 kHz systems could work well using 1000V devices. However, concern over fault conditions that can cause odd high voltage pulses has seen 1500V adopted as the 'standard'. The collector currents involved range from 2.5A peak to 8A peak for TV and 3.5A peak to 7A peak for monitors. The transistors for these applications are now considered.

16 kHz applications

Table 5 lists the 1500V transistors for 16 kHz TV deflection systems and a summary of their main characteristics.

Part Number	V_{CESM}	I_{Csat}	Application
BU505/D	1500V	2A	Monochrome sets
BU506/D BU2506DF	1500V	3A	90° Colour; ≤ 23"
BU508A/D BU2508A/D	1500V	4.5A	110° Colour; 21-25"
BU2520A/D	1500V	6A	110° Colour; 25-29"

Table 5. Transistors for 16 kHz TV deflection

All of the above types are available in both non-isolated and isolated outlines (F-pack), except the BU2506DF - F-pack only. Isolated outlines remove the need for an insulating spacer to be used between device and heatsink. Devices are available both with and without a damper diode (eg without: BU505, BU2520A and with: BU505D, BU2520D). The BU2506DF is only available with a damper diode.

The BU25XX family is a recent addition to the range of Philips deflection transistors. Far from being just another 1500V transistor, the BU25XX has been specifically designed for horizontal deflection. By targeting the device for this very specialised application it has been possible to achieve a dissipation performance in deflection circuits which is exceptional.

The BU2520A uses the superior technology of the BU25XX family applied to a large chip area. The BU2508A has an h_{FE} of 5 at 5V V_{CE} and 4A I_C . The BU2520A has an h_{FE} of 5 at 5V V_{CE} and 6A I_C . This gives designers working on large colour television sets a high h_{FE} deflection transistor with a high current capability. The high h_{FE} reduces the forward base drive energy requirements. The high current capability enables the energy drawn from the line output transformer to be increased. Using a BU2520A device allows the EHT energy to be increased for brighter pictures (a feature of new 'black line' tubes) without having to increase the forward base drive energy to the deflection transistor.

32 kHz applications

Table 6 gives the 1500V transistors for 32 kHz deflection systems and a summary of their main characteristics.

Part Number	V_{CESM}	I_{Csat}	Application
BU2520A	1500V	6A	110° Colour; ≤ 28"
BU2525A	1500V	8A	110° Colour; ≤ 32"

Table 6. Transistors for 32 kHz deflection

For the foreseeable future 32 kHz TV will be concentrated at the large screen sector ($\geq 25''$). These TV's will employ diode modulator circuits lessening the need for D-type transistors. With a switching frequency twice that of conventional TV the dissipation in these devices will be higher. For this reason the non-isolated versions, with lower thermal resistance, will be prevalent in these applications.

Monitor applications

The applications given in Table 7 should be seen as an indication of the limits that successful designs have been achieved for that device type. This should help in the selection of a device for a given application at the design concept stage. For example, a 15" monitor requiring operation up to 6A at 64 kHz could use either a BU2522A, a BU2525A or a BU2527A. If the design has specific constraints on switching and dissipation then the BU2525A and BU2527A would be better. If, as well, a guaranteed RBSOA is required then the BU2527A is the best choice.

Table 7 gives the 1500V transistors for monitor deflection systems, concentrating on the common pc and industry standard work station modes.

Part Number	V_{CESM}	I_{Csat}	Application
BU2508A/D	1500V	4.5A	14", SVGA, 38 kHz
BU2520A	1500V	6A	15", SVGA, 48 kHz
BU2522A	1500V	6A	15", 64 kHz
BU2525A	1500V	8A	(17", 64 kHz)
BU2527A	1500V	6A	17", 64 kHz

Table 7. Transistors for Monitor deflection

All devices are available in non-isolated and isolated outlines. The excellent dissipation of this range of devices means that, even at monitor switching frequencies, devices in an isolated package can be used

4.1.4 TV and Monitor Damper Diodes

Introduction

Philips Semiconductors supply a complete range of diodes for the horizontal deflection stage of all volume TV and monitor applications. This note describes the range of Philips parts for the damper (also called efficiency) diode in horizontal deflection. The damper diode has some unusual application specific requirements that are explained in this section.

Damper diodes form an essential part of the horizontal deflection circuit. The choice of diode has an effect on the total circuit dissipation and the display integrity. A poor selection can lead to unnecessary power loss and a visible picture distortion.

As well as a full range of discrete devices for the damper diode application Philips offer a range of horizontal deflection transistors with integrated damper diodes. These devices offer a cost and space saving, especially beneficial for high volume TV production.

Discrete Damper Diode Selection Guide

I_{FWM} , $I_{F(AV)}$. The quoted $I_{F(AV)}$ values do not correspond to any particular current in the application. The values are standard data format for selection purposes and comparison with competitor types. In general, the larger the $I_{F(AV)}$ the higher the deflection coil current and/or frequency in the application. A more meaningful specification is I_{FWM} , this refers to the peak operating current in a 16 kHz TV application given a standard current characteristic. The application columns in table 1 define the limit fitness for use of each diode.

V_{RSM} . The damper diode should have a voltage capability equal to the deflection transistor. In most applications this will be 1500V. The V_{RSM} value equates to the peak flyback voltage. The diode data should not be viewed as that for other diodes where it is quite common to use devices with V_{RSM} 5 or 10 times greater than the peak circuit voltage. Damper diodes will operate in horizontal deflection circuits with peak flyback voltages up to the specified limit. However, the limit V_{RSM} should not be exceeded in any circumstance. In practice, a device with V_{RSM} of 1500V will be found in applications with peak flyback voltages of 1300V in normal running; fault conditions do not usually see more than a 200V rise in flyback voltage.

Outline. The Philips range spans the available outlines for this application from axial to TO220 type. The SOD57 and SOD64 are hermetically sealed axial - leaded glass envelopes. These outlines combine the ability to house large chips with proven reliability and low cost. For high ambient temperatures with severe switching requirements the addition of cooling fins may be necessary to achieve successful operation at the application limit.

For higher currents and frequencies there are devices in TO220 type outlines. TO220AC is a two-legged non-isolated outline. The pin-out is such that the tab is always the cathode. For an isolated equivalent outline there are SOD100 and the newer SOD113. The SOD100 is the traditional isolated TO220 outline allowing the device to be attached to a common heatsink without any separate isolation. The SOD113 is an enhanced version of SOD100 offering an improved isolation specification. Philips offer a complete range of mounting accessories for all these outlines.

Device Type	Specification			Application	
	I_{FWM} , $I_{F(AV)}$	V_{RSM}	Outline	TV	Monitor
BY448	4 A	1650 V	SOD57	≤ 21", 16 kHz	-
BY228	5 A	1650 V	SOD64	25", 16 kHz	-
BY328	6 A	1500 V	SOD64	28", 16 kHz	14", SVGA, 38 kHz
BY428	4 A	1500 V	SOD64	21", 32 kHz	14", 64 kHz
BY359 BY359F(X)	10 A	1500 V	TO220AC SOD100 (SOD113)	36", 32 kHz	17", 64 kHz
BY459 BY459F	10 A	1500 V	TO220AC SOD100	HDTV	19", 1280x1024, 82 kHz

Table.1 Philips Semiconductors Damper Diode Selection Guide

Horizontal Deflection Transistors with Integrated Damper Diode

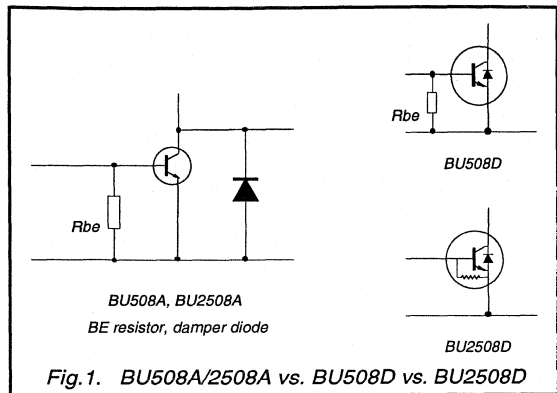


Fig. 1. BU508A/2508A vs. BU508D vs. BU2508D

The range of devices available covers most high volume TV & Monitor applications where designers require a choice of devices to meet their requirements. The differences are shown in Fig. 1 above. These devices are all monolithic structures. The process of integrating the diode does not reduce the performance of the deflection transistor.

For traditional horizontal deflection circuits with a single damper diode it is easy to see the benefits of integrating the deflection transistor and damper diode. The additional dissipation in the integrated damper diode should be taken into account in the thermal management considerations. The use of the deflection transistor with integrated diode allows a simpler layout with lower component count and cost.

For circuit designs that employ a diode modulator circuit it is still quite common to employ a deflection transistor with an integrated damper diode. In these circuits the current

is shared between the integrated diode and the discrete modulator damper diode. This technique allows smaller discrete diodes to be used or reduced thermal management for the discrete device. For example, this could allow the circuit designer to remove any cooling fins on an axial diode; or replace a TO220 type with a cheaper axial type of discrete diode in the modulator.

Table 2 below shows a selection of Philips Semiconductors' horizontal deflection transistors with an integrated damper diode.

I_{CSat} This value is an indication of the peak collector current in a 16 kHz TV horizontal deflection circuit for which optimum dissipation and switching can be obtained. For the diode the I_{CSat} value should also be taken as the peak current (ignoring any instantaneous spikes at the start of scan). For higher frequency applications in monitors the I_{CSat} value reduces slightly.

V_{CESM} The voltage capability of the deflection transistor and damper diode are the same. As for discrete devices, there is no need for excessive insets. The V_{CESM} value equates to the peak flyback voltage and, as for the V_{RSM} of a discrete damper diode, should not be exceeded under any circumstance.

Outlines. Devices are available in three different outlines, one non-isolated (SOT93) and two isolated/full-pack designs (SOT199, TOP3D). The outline is defined by the last letter in the type number, for example:

BU2508D	SOT93	non-isolated
BU2508DF	SOT199	isolated
BU2508DX	TOP3D	isolated

All three outlines are high quality packages manufactured to Philips Total Quality Management standards.

Device Type	Specification			Application	
	I_{CSat}	V_{CESM}	Outline	TV	Monitor
BU2506DF BU2506DX	3.5 A	1500 V	SOT199 TOP3D (SOT399)	21", 16 kHz	-
BU508D BU508DF	4.5 A	1500 V	SOT93 SOT199	21-25", 16 kHz	-
BU2508D BU2508DF BU2508DX	4.5 A	1500 V	SOT93 SOT199 TOP3D (SOT399)	21-25", 16 kHz	14", 38 kHz, VGA
BU2520D BU2520DF BU2520DX	6 A	1500 V	SOT93 SOT199 TOP3D (SOT399)	25-29" 16 kHz	14", 48 kHz, SVGA

Table 2 Philips Semiconductors Deflection Transistors with Integrated Damper Diode Selection Guide

Operating Cycle

The waveforms in Fig. 2 below show the deflection coil current and flyback voltage in a simplified horizontal deflection circuit. In Fig. 2 the damper diode current is highlighted. All the flyback voltage is applied across the damper diode. These waveforms are valid for both the traditional type of deflection circuit (Fig. 3) and the diode modulator deflection circuit (Fig. 4).

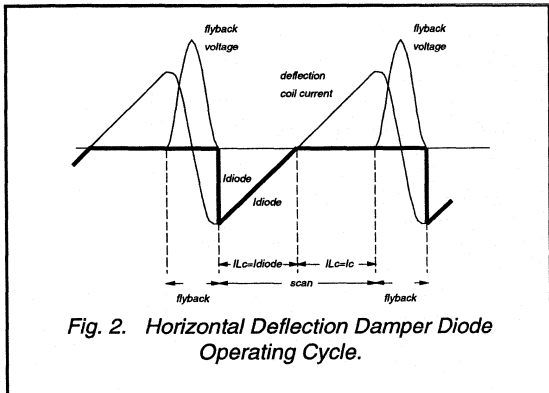


Fig. 2. Horizontal Deflection Damper Diode Operating Cycle.

During flyback the energy in the deflection coil, L_c is transferred to the flyback capacitor, C_{fb} . With the transfer of energy the voltage on C_{fb} , hence the voltage across the diode, rises sinusoidally until all the energy is transferred. Now the current in L_c is zero and the diode and C_{fb} are at the peak flyback voltage. The energy now transfers back to L_c . As the energy is transferred the voltage decreases

until all the energy is back in L_c when there is no voltage across C_{fb} , and maximum current through L_c . If there was no diode present, this operation would continue with the energy transferring back to C_{fb} with the voltage continuing to decrease until all the energy in L_c had been transferred; the peak voltage now reversed. But with the damper diode in place across C_{fb} (see Figs. 3 & 4), as the voltage falls negative the diode will be forward biased and tend to conduct.

Consider now the application requirement which is to establish a peak negative current in L_c before the start of the next scan. As the decreasing voltage on C_{fb} tends to zero so the current in L_c reaches a peak negative value and the next scan can start. The transfer of energy into the capacitor has to be stopped during the scan, hence the addition of the damper diode.

Most TV & monitor display circuits will employ an element of over-scanning; this means at the start of diode conduction the beam will be off-screen. Over-scanning is introduced to reduce the effect of any spurious switching characteristics as the diode switches.

Power Dissipation

There are two significant factors contributing to power dissipation in a damper diode: forward recovery and on-state forward bias. Reverse recovery and reverse bias losses are negligible in this application. As a general rule, the total dissipation is half forward recovery and half forward bias. To explain this further we have to consider the operating cycle of the diode in detail.

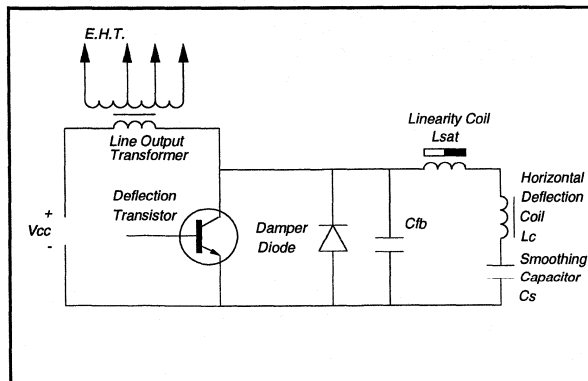


Fig. 3. Traditional Deflection Circuit.

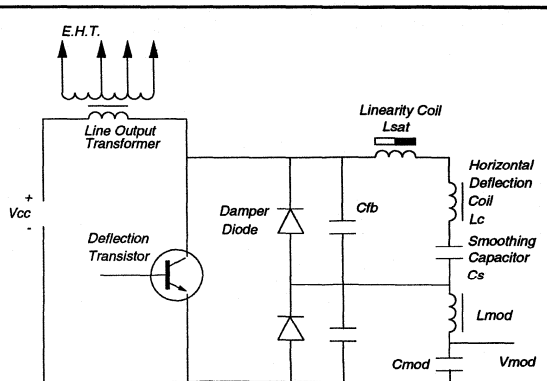


Fig. 4. Diode Modulator Circuit Example.

Forward Recovery. As the voltage goes negative the electric field builds up across the diode. The device design and process technology determine the point at which conduction starts. At the start of conduction the voltage is a maximum: the forward recovery voltage, V_{fr} . A detailed view of the damper diode voltage and current at the start of diode conduction is given in Fig. 5 below. As the current flows the voltage across the diode drops to its steady-state V_F value; the time this takes is called the forward recovery time, t_{fr} .

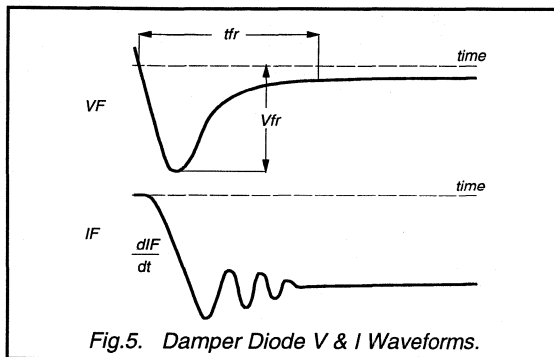


Fig.5. Damper Diode V & I Waveforms.

The values for V_{fr} and t_{fr} are application dependent. In general, V_{fr} is $\leq 20V$; t_{fr} is $\leq 50ns$ for V_F to fall to $2V$; and the rate of rise in diode current, dI_F/dt , will be between $25 - 90 A/\mu s$. A 'good' damper diode will not only have low V_{fr} and low t_{fr} but as a result, it will also allow the current to switch to the diode faster, giving a higher dI_F/dt .

Forward Bias. As the beam scans from the left towards the centre the voltage drop across the diode is determined by the device V_F characteristic for a given L_c current. As the beam scans from left to right the diode current decreases.

Measurement of the V_F is not possible in the application. The best indication of the losses comes from the maximum hot V_F information contained in the datasheets.

Reverse Recovery & Reverse Bias. To the right of centre screen L_c current becomes positive and, hence, current no longer flows through the damper diode. In reverse recovery the damper diode does not experience any high current - high voltage characteristic that would be a cause of significant dissipation.

During flyback the diode is reverse biased, another possible cause of dissipation. The combined effects of reverse recovery and reverse bias are negligible in comparison to forward recovery and forward bias.

Picture Distortion

The diode does not start to conduct until the forward recovery voltage is approached: a device with a high forward recovery voltage, V_{fr} , will take longer to start conduction than a device with a low V_{fr} . A delay in the start of diode conduction means that the deflection coil current is dominated by the flyback capacitor, C_{fb} at the start of the scan. This can cause a visible distortion to the left-hand side of the display.

The voltage across the diode modulates the voltage across the coil. For a device with a long forward recovery time, t_{fr} , the diode forward recovery characteristics will affect the voltage across the deflection coil at the start of the scan. This can also cause a visible distortion to the left-hand side of the display.

For display circuit optimisation it is essential that the requirements for the damper diode are understood and taken into account in device selection.

TV Deflection Circuit Examples



4.2.1 Application Information for the 16 kHz Black Line Picture Tubes

With the introduction of the black line picture tubes new drive circuits are required. To have full benefits, the EHT voltage and beam current must be increased. This section describes the horizontal deflection and EHT generation. Some hints for vertical deflection and video amplifiers are given as well.

Summary

This section describes the horizontal deflection circuitry of the black line picture tube A66EAK022X11 and A59EAK022X11. To take full advantage of this new tube it must be driven at 27.5kV @ 1.3mA. This implies that in an ordinary combined EHT and deflection stage in the no load condition, zero beam current, the high voltage increases to about 29.5kV. The main change to this circuit, compared with existing circuits, is the line output transformer (AT2077/34) uses four layer DSB technology.

For the vertical deflection a minor modification on PCALE report ETV8831 is given. The video output stage suited to this tube is described in PCALE report ETV8811.

1. Introduction

One step in improving picture quality is the introduction of the black line picture tube. With this tube day-time TV viewing with a bright high contrast picture becomes possible. To achieve this the picture tube is provided with a dark screen and increased EHT power capability by means of an invar shadow mask.

When the 45AX black line picture tube is compared with the existing 45AX tubes the following modifications in the application must be made.

- Increase of the EHT power to 27.5kV @ 1.8mA beam current.
- Increase of the cut off voltage to 160V.

To cope with this high EHT power demand, a new line output transformer has been developed (AT2077/34). The main

part of this section is dedicated to the horizontal deflection. For supply, vertical deflection and video amplifier details reference will be made to separate reports.

Special care is taken to suppress certain geometrical picture distortions which otherwise would become noticeable at the increased levels of dynamic EHT load variations. These distortions are the result of oscillations in the line output stage.

All measurements and circuits are based and tested on the 66FS picture tube. Since the 59FS tube is electrically identical to the 66FS tube this circuit is also suited for the 59FS picture tube. With some minor circuit modifications (component values) this circuit is also suited for 33" picture tubes.

2. Circuit Description

The horizontal deflection board is built up of four major parts, see Fig. 1.

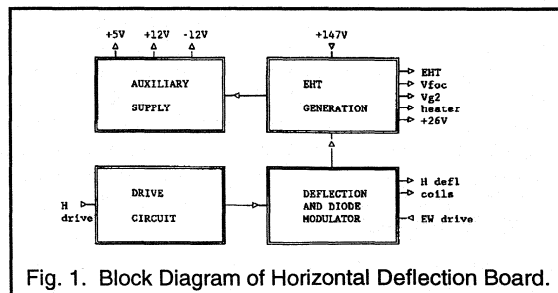


Fig. 1. Block Diagram of Horizontal Deflection Board.

In high end TV sets a lot of low voltage supply current is required. In this design a separate transformer in parallel to the line output transformer is foreseen for the generation of these auxiliary supplies. In applications where this auxiliary power is not required this part can be omitted by simply leaving out the additional transformer. The other parts of this horizontal deflection are more or less classic.

2.1 Drive Circuit

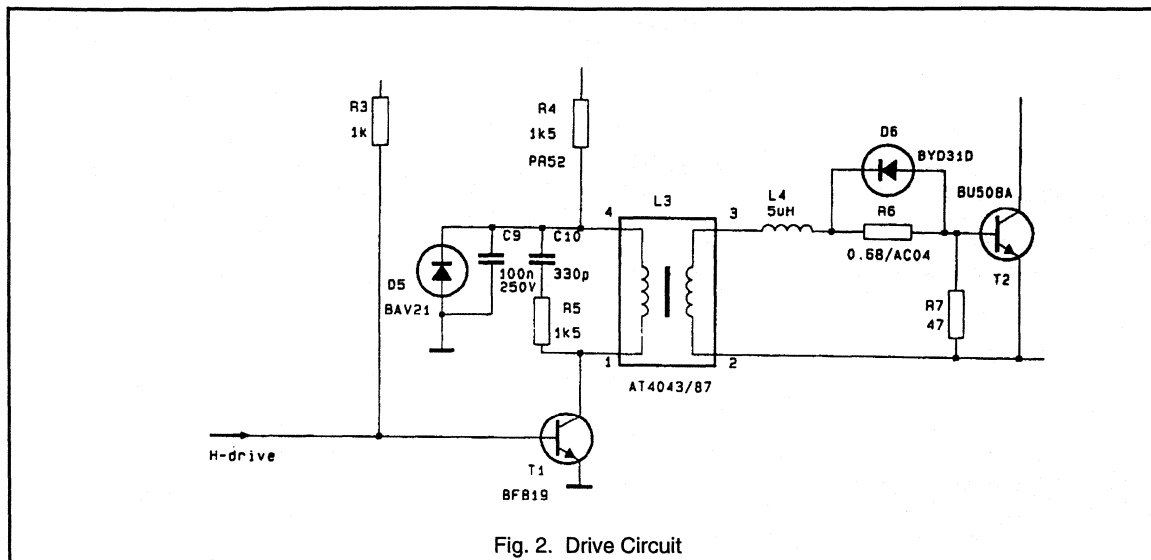


Fig. 2. Drive Circuit

The horizontal drive circuit is a classical transformer coupled inverting driver stage. When driver transistor T1 is conducting energy is stored in the transformer. When T1 is turned off the magnetising current continues to flow in the secondary side of the transformer thus turning on the deflection transistor. At this time the voltage on the secondary side of the driver transformer is positive ($V_{BE} + I_B \times R6$). When the driver transistor turns on again this secondary voltage reverses and will start to turn off the deflection transistor. At the same time energy is stored in the transformer again.

During this turn off action the forward base drive current decreases with a controlled di/dt , thereby removing the stored charge from the deflection transistor. The di/dt depends on the negative secondary voltage and the leakage inductance. As a rule of thumb, the deflection transistor stops conducting when its negative base current is about half the collector peak current.

To prevent the deflection transistor from turning on during flyback due to parasitic ringing on the secondary side of the driver transformer a damper resistor is connected in parallel with the base emitter junction of the deflection transistor.

Also at the primary side of the driver transformer a damper network is added (R5 & C10) to limit the peak voltage on the driver transistor.

D5 is added for those applications where in the standby mode the deflection stage is turned off by means of continuous conduction of the driver transistor. The explanation is as follows:

When T1 is suddenly made to conduct continuously, a low frequency oscillation will occur in C9 and the primary of L3. As soon as the voltage at pin 4 of L3 becomes negative T2 starts conducting until the driver transformer is demagnetised. This will cause an extremely high collector current surge. D5 prevents pin 4 of L3 going negative and so this fault condition is avoided. For those applications where this condition cannot occur, D5 can be omitted.

2.2 Deflection Circuit

The horizontal deflection stage contains the diode modulator which not only provides east-west raster correction but also inner pincushion correction, picture width adjustment and EHT compensation. It is not easy to achieve optimum scan linearity over the whole screen. Either the linearity inside the PAL test circle is good and outside the circle the performance is poor, or the average performance over the whole screen is good but inside the test circle deviation is visible. In this application the S-correction capacitors C15 and C16 are balanced in such a way that a good compromise for the scan linearity is achieved.

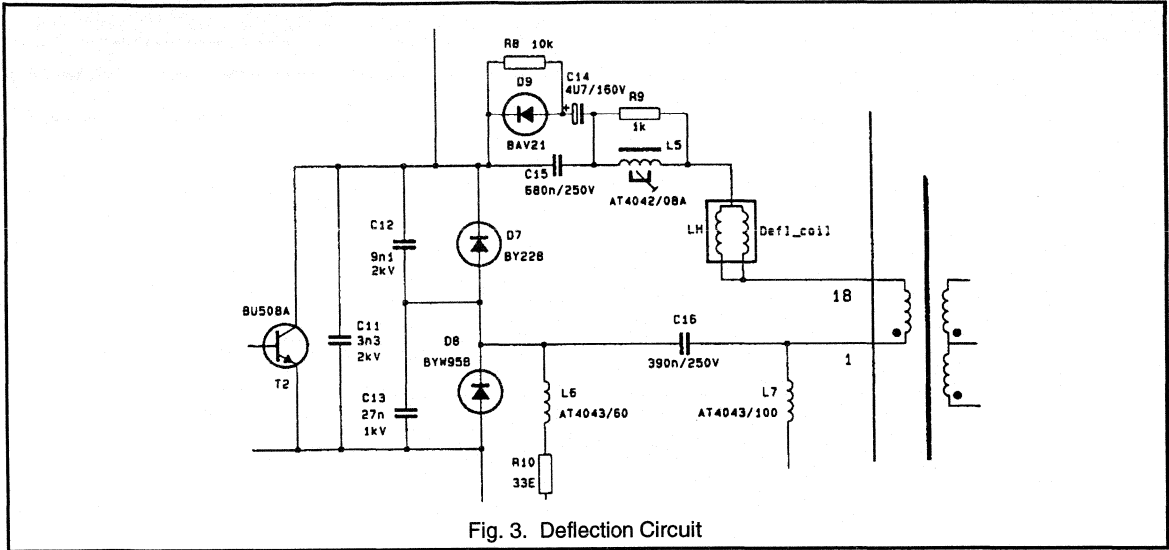


Fig. 3. Deflection Circuit

As already stated in the introduction, due to high beam current in combined EHT and deflection stages picture distortions will occur.

One of these effects is the so called cross-hatch "noses", visible as horizontal phase ringing just below each horizontal white line. During a bright horizontal line the EHT at the picture tube decreases. In the next flyback the picture tube capacitor is recharged by the line output transformer. This energy is taken from the S-correction capacitor, which must be recharged via the primary winding of the line output transformer. This action has a resonance of a few kHz and thus oscillation is visible at the screen.

To avoid this a diode rectifier is connected in parallel with the S-correction capacitor (D9, C14, R8). The energy taken from the S-correction capacitor can now be recharged by C14.

Another geometry distortion is the "Krückstockeffekt". Due to trapezium correction the EW-drive signal applied to L6 can be discontinuous. This will cause amplitude ringing at the top of the screen. An effective way to damp this ringing is a resistor in series with the EW-injection coil.

The consequence of the above mentioned measures is that the drive reserve of the diode modulator has decreased. To compensate for this a separate winding of the line output transformer is connected in series with the deflection coils.

2.3 EHT Generation

For an optimum performance the black line picture tube must be driven at an increased EHT of 27.5kV @ 1.3mA_{av}. This implies that the EHT in the no load condition, zero beam current, will be about 29.5kV. To generate this increased EHT a newly designed line output transformer is used with a 4-layer diode split EHT section. From an integrated potentiometer the adjustable focus and grid 2 voltages are taken.

Also the frame supply voltage (26V) and video supply voltage (180V) are taken from the line output transformer. The auxiliary windings of this transformer can be connected rather freely so that a diverse range of auxiliary supplies can be obtained. The only restriction is that the RMS value of the current in a given winding may not exceed 2A. Furthermore the supply current for the heater is obtained from this transformer just like the Φ2 feedback pulse (positive) and a (negative) pulse to synchronise the SMPS.

2.4 Auxiliary Supply

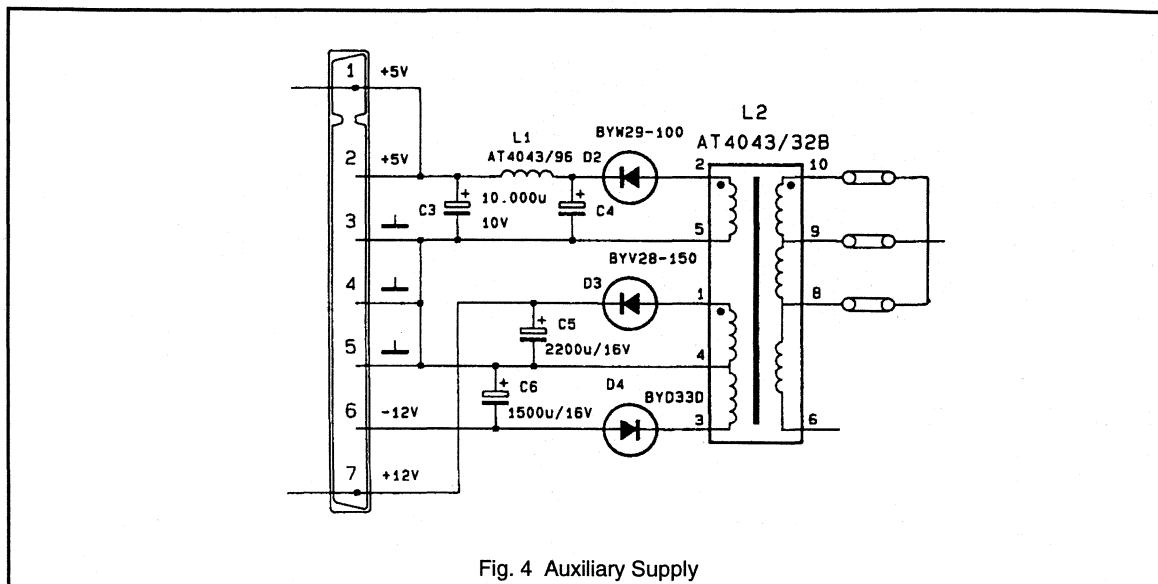


Fig. 4 Auxiliary Supply

When more auxiliary power than can be handled by the line output transformer is required, an auxiliary supply transformer, as shown in Fig. 4, is a good alternative. Such an extra transformer in parallel with the primary winding of the line output transformer is an efficient way to generate low voltage high current supplies. As the transformer is optimised for this purpose no additional stabilisation is required.

Due to the high inductance of the primary winding no influence on the collector current is noticeable. Output voltages are very close to the target values (fine adjustment with primary taps) and have low R_i (HT line is stabilised).

2.5 Additional Circuit Information

12V supply:

The SMPS used in this concept delivers 16V unregulated. This needs to be regulated to supply the sync processing IC which operates at 12V. This regulation can be done on the sync processing board or the horizontal deflection board since this also acts as a power distribution board.

Tuning voltage:

The tuning voltage is created simply by means of a series resistor R1 and a 30V reference diode located at the tuning board.

EHT compensation:

For proper picture performance it is essential that EHT information is available to compensate picture width and height for EHT variations. For this reason the aquadag is connected to the foot point of the line output transformer. This point is connected to ground by C18 and to the 26V by a non linear resistor network (R12, D11, R13, R14). This network is designed in such a way that it matches with the non linear impedance of the line output transformer and C18 matches with the picture tube capacitance. Thus the voltage available at the foot point of the line output transformer is a good representation of the EHT variation. This EHT information is sent to the geometry processor TDA8433. This information can also be used for beam current limiting. It must then be fed to the video processor for contrast/brightness reduction.

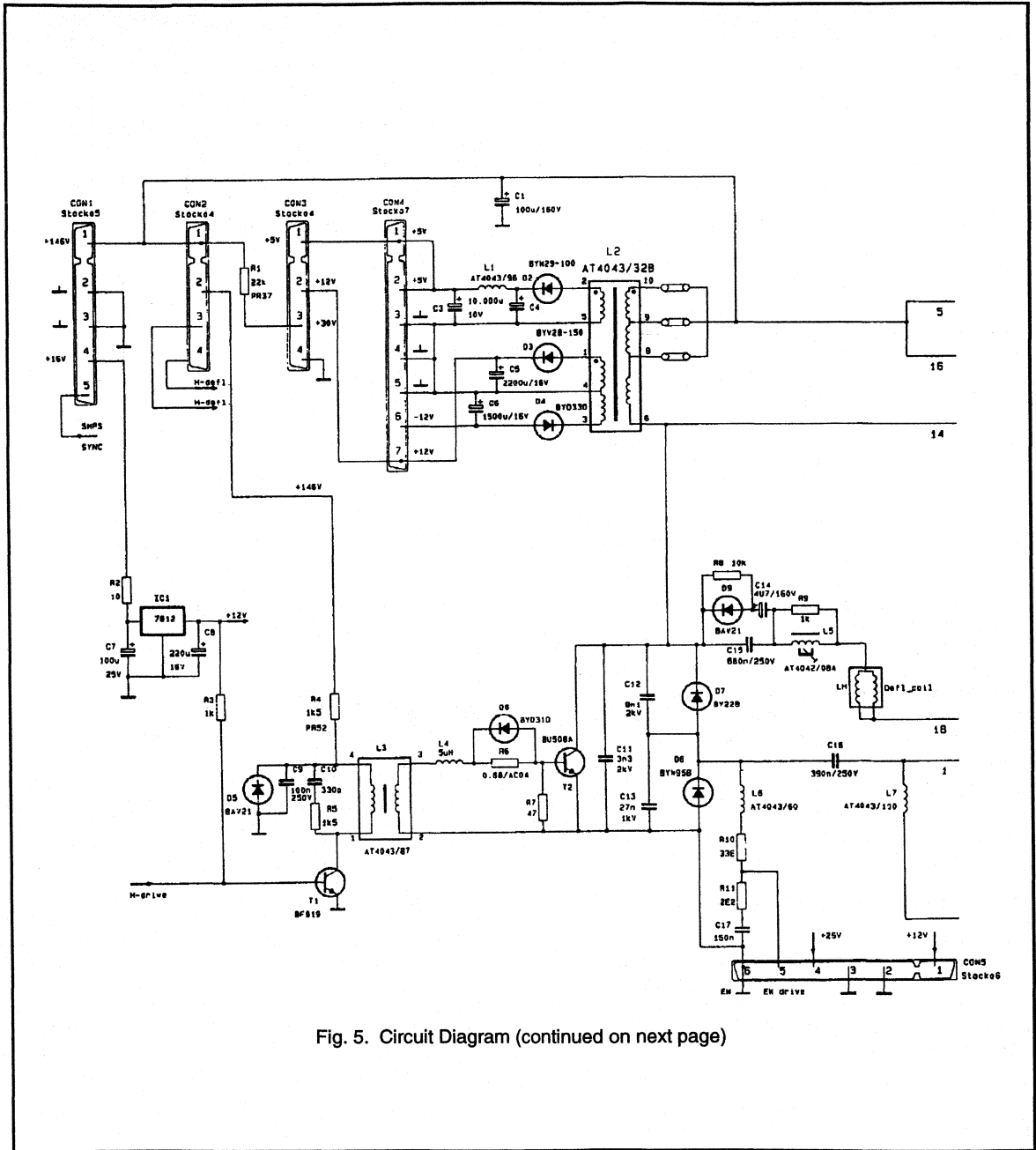


Fig. 5. Circuit Diagram (continued on next page)

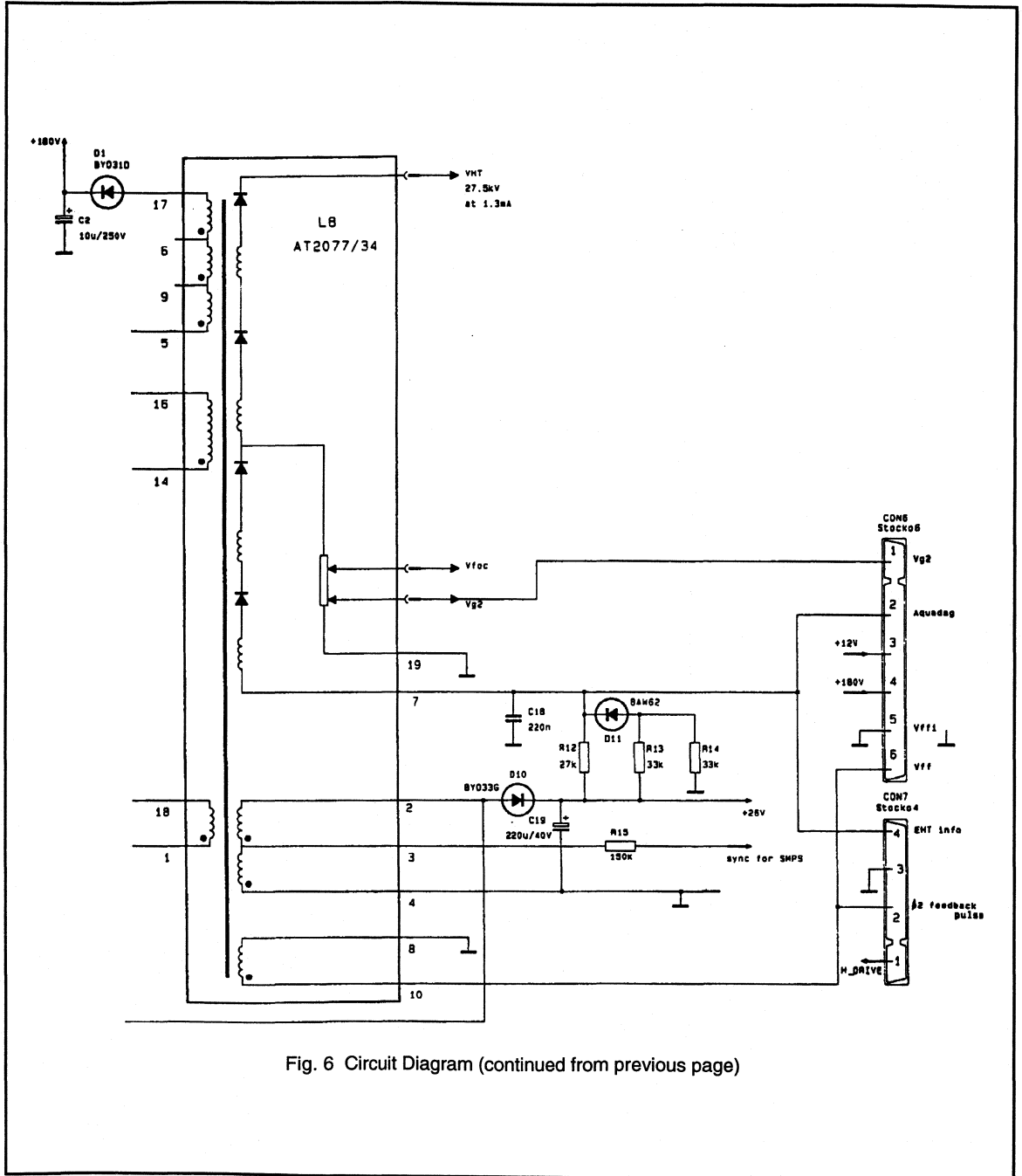
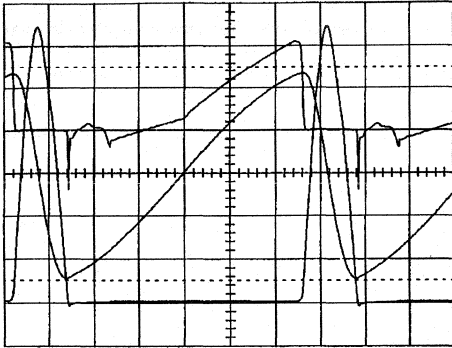


Fig. 6 Circuit Diagram (continued from previous page)

3. Oscillograms

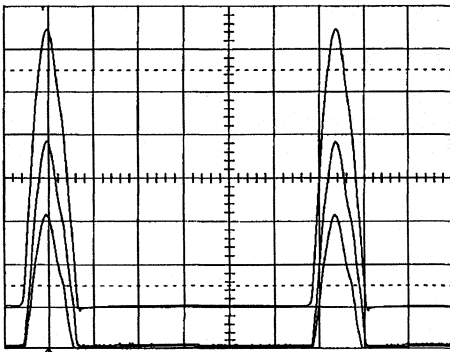


Oscillogram 1:

In this oscillogram the lower trace is the voltage across the deflection transistor (200V/div). The middle trace is the current in the horizontal deflection coil (1A/div). The upper trace is the collector current in the deflection transistor (2A/div). The time base is 10 μ s/div.

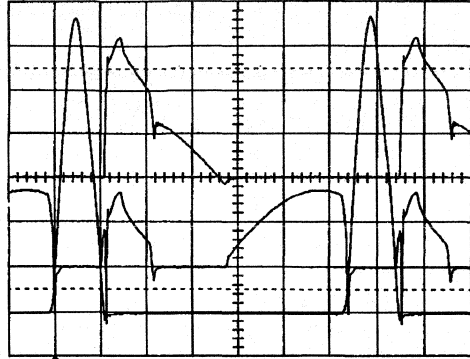
Remarks:

At the end of flyback there is a negative overshoot at the collector voltage. This is caused by the relative slow forward recovery of the damper diode. A part of this current is reverse conducted by the deflection transistor. About 12 μ s after the start of the scan the deflection transistor is turned on and starts reverse conducting and takes over a part of the current in the damper diodes. See also oscillogram 3.



Oscillogram 2:

The upper trace is the voltage across the deflection transistor (200V/div). The lower two traces are the minimum and maximum voltage in the diode modulator (cathode D8) with nominal EW and amplitude settings (50V/div). The time base is 10 μ s/div.

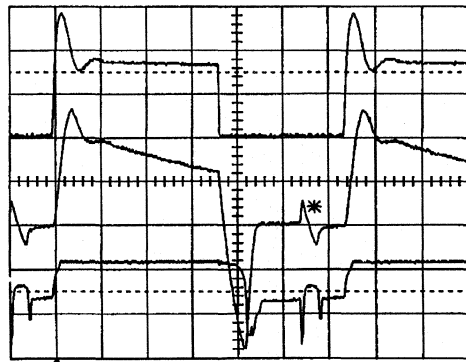


Oscillogram 3:

In the upper trace the current in the upper diode is shown (1A/div). The middle trace is the current in the lower diode (1A/div). The time base is 10 μ s/div.

Remarks:

12 μ s after the start of the scan the deflection transistor is turned on. Current in the diode modulator is then taken over by the deflection transistor. See also oscillogram 1.



Oscillogram 4:

In the upper trace the collector voltage of the driver transistor is shown (100V/div). The middle trace is the base drive current of the deflection transistor (1A/div). The lower trace is the base emitter voltage of the deflection transistor (5V/div). The time base is 10 μ s/div.

Remarks:

The overshoot at the collector voltage of the driver transistor is damped by R5 and C10. The current spike in the base drive current (marked with *) is the reverse conduction of the deflection transistor during the forward recovery of the damper diode. See also oscillogram 1.

4. Vertical Deflection, Synchronisation and Geometry Control

The vertical deflection, synchronisation and geometry control circuits are based on an existing PCALE report (ref 3). Because for this application another tube and line output transformer are used some minor modifications are required (component values), see Fig. 7.

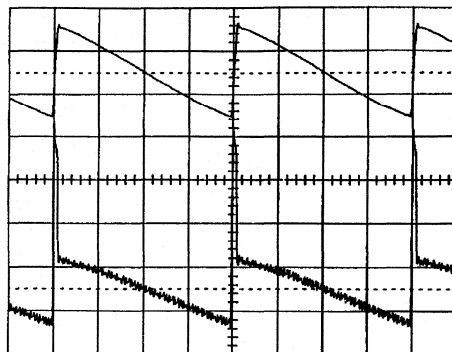
- Due to the increased deflection current, the vertical feedback resistor must be decreased: one of the 2.2Ω resistors becomes 1Ω.

- Due to the increased beam current, the EHT compensation network at pin 24 of the TDA8433 needs to be modified: 120kΩ → 100kΩ, 82kΩ → 150kΩ, 27kΩ → 33kΩ, 68 nF → 10 nF.

- For additional phase shift pin 14 of the TDA2579 is biased with a current from a negative voltage source (rectified from the Φ₂ feedback pulse). While this feedback pulse is smaller than in the original circuit, the 240kΩ resistor must be increased to 1.2MΩ.

Orientation values for the TDA8433 register settings are:

reg	hex
00	25
01	5A
02	07
03	2C
04	2B
05	16
06	16
07	15
08	22
09	21
0A	21
0B	0F
0F	04



Oscillogram 5:
Vertical deflection current (1A/div) and the output voltage (pin 5) of TDA3654 (10V/div). The time base is 5ms/div.

Remarks:
The noise on the output voltage is cross talk from the line deflection coils.

5. Video Amplifiers

The gun of this picture tube is a new design and has its optimum performance at a cut off voltage, $V_{CO} = 160V$. This implies that the video supply voltage should be at least 20V higher, so $V_{video} \geq 180V$. A video amplifier very well suited for this purpose is the TDA6100.

The RMS voltage of the heater winding of the line output transformer is $V_{10} = 7.35V_{RMS}$, so a series resistor must be used (3.9Ω; 400mW).

6. References

Information from this section was extracted from "Application information for the 16 kHz black line picture tube A66EAK022X11 and A59EAK022X11"; ETV89010 by Han Misdom.

1. "Some aspects of the diode modulator"; EDS7805 by C.H.J. Bergmans.
2. "A synchronous 200W Switched Mode Power Supply intended for 32kHz TV"; ETV89009 by Henk Simons.
3. "Deflection processor TDA8433 with I²C-bus control"; ETV8831 by D.J.A. Teuling
4. "Application of the TDA6100 video output stage"; ETV8811 by D.J.A. Teuling



4.2.2 32 kHz / 100 Hz Deflection Circuits for the 66FS Black Line Picture Tube

This report contains a description of deflection circuitry (horizontal 32 kHz, vertical 50-120 Hz) for the 66FS picture tube A66EAK22X42. This design is intended for flicker free TV applications. Provision is made to supply the power for the frequency conversion box.

Summary

The 66FS picture tube is compatible but not identical with the types of the 45AX range. To obtain the typical Black line high contrast and high brightness, the beam current and EHT must be increased at nominal operating conditions. This higher EHT also improves the spot quality. The deflection current is increased because of the higher EHT and reduced sensitivity of the deflection unit.

In comparison with laboratory report ETV8713, describing deflection circuits for 45AX, most modifications are found in the horizontal deflection stage. To generate the increased EHT power a new line output transformer (LOT) with a four layer EHT coil is used. To handle the higher deflection currents two transistors are used in parallel and also two flyback capacitors are used. We have also taken the opportunity to introduce the TDA8433. This deflection processor -in BiMOS technology- is the successor of the TDA8432.

The vertical deflection stage is redesigned in such a way that vertical shift signals can be inserted without bouncing effects. The insertion of vertical shift signals is necessary in 100 Hz operation for a proper interlace.

1. Introduction

In this report a description is given of double line and frame frequency (32 kHz; 100 Hz) deflection circuits for the 66FS

picture tube A66EAK22X42. The report is based on report ETV8906, describing these circuits for the 78FS picture tube¹. By changing some component values the pcb for the 78FS can also be applied to drive the picture tube A66EAK22X42. In the line output stage the output transistor BU2508 is used.

2. General description

2.1 Block diagram

The block diagram is given in Fig. 1. The main interconnections are given as well. The separate blocks can be recognised in the circuit diagram.

The separate H and V sync and V shift are available from the frequency conversion box.

2.2 Circuit architecture

A key component in this set up is the deflection processor TDA8433. The horizontal and vertical picture geometry can be controlled by means of I²C bus commands. Because this deflection processor has no vertical oscillator, there will be no vertical deflection when there are no vertical sync pulses applied to the set. For laboratory purpose a separate vertical oscillator is added to make the monitor part a self contained unit. When incorporated in a receiver this vertical oscillator can be omitted. When there are no vertical sync pulses, the guard circuit of the vertical output stage will blank the video information. This prevents spot burn-in of the tube.

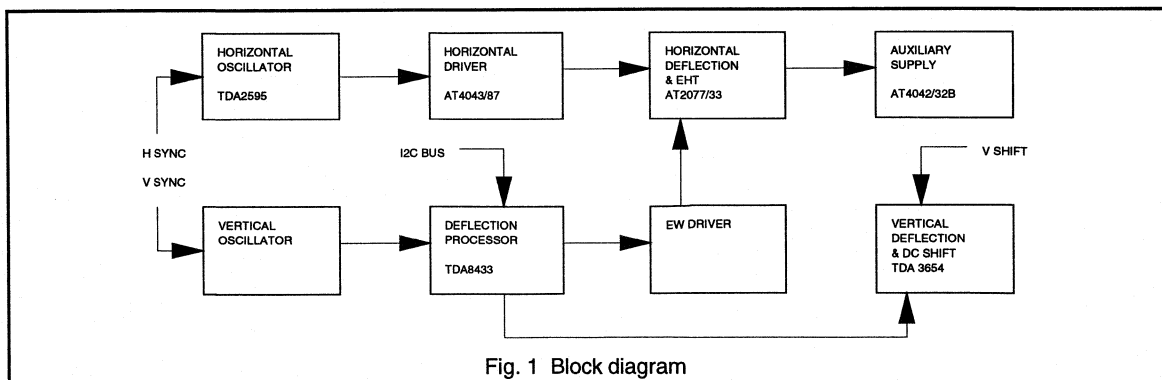


Fig. 1 Block diagram

The vertical deflection stage consists of the well known TDA3654 vertical output IC. To make vertical shift insertion possible, the output stage is slightly redesigned. This ac coupled output stage now has a quasi dc coupled behaviour.

The EW driver is a voltage amplifier, acting as a buffer between the deflection processor and the diode modulator.

The block "horizontal oscillator" consists of the TDA2595 with its $\Phi 1$ and $\Phi 2$ loop, the horizontal oscillator itself and sandcastle generation. The other features of this ic are not used.

Coupling between the TDA2595 and the deflection stage is made by the horizontal driver stage. This stage is a transformer coupled inverting driver stage.

The horizontal deflection stage is a classic concept. It consists of a combined deflection and EHT generation. It also comprises linearity correction, S-correction, inner pin cushion correction and a dc shift circuit. The LOT (AT2077/33) belongs to the transformer family DSB (diode split box) and has four EHT layers. It delivers the following voltages:

- * EHT = 27.5 kV @ 1.3mA
- * Focus = 0.22 - 0.30 x EHT
- * V_{g2} = 0.011 - 0.033 x EHT
- * Heater $\approx 10.4V_{RMS}$
- * Video supply = 192V
- * Frame supply = 28V
- * $\Phi 2$ ref. pulse = +40V_{pp}

Furthermore the LOT has some taps which can be useful when the application is modified.

In parallel to the primary winding of the LOT the auxiliary supply transformer (AT4043/32B) is located. This auxiliary supply delivers the following voltages:

- * +5V @ 5A
- * +15V @ 1A
- * -12V @ 1A

These supply voltages are intended for the digital and analog signal processing circuits.

The philosophy behind this circuit needs some further explanation.

It is very difficult to generate exactly 5V at the output of an SMPS or LOT. Due to an optimum winding design of this kind of transformer, the voltage ratio per turn is high (2 - 5V per turn). This implies that a stabilizer is required. A switching post regulator adds to the circuit complexity and cost. A dissipative series stabiliser needs at least 2V, so for a 5A supply the losses are already 10W.

The auxiliary transformer used in this concept is optimised for generating these low voltages at high currents. The winding design is such that no stabilizer is required after the rectifier. Due to the high primary inductance of this transformer the collector current increase of the deflection transistor is negligible.

If the auxiliary loads are low, this auxiliary supply transformer can be omitted and the unused taps of the LOT can be used to generate these voltages.

3. Circuit description

Using circuit diagram blocks the total concept will be explained. This will be done with reference to the function blocks of Fig. 1. The complete circuit diagram is given in Figs. 11-13.

3.1 Vertical oscillator

As already stated in section 2.2 this vertical oscillator can be omitted in a final design. The circuit is shown in Fig. 2.

This oscillator is the well known astable multivibrator built up around T8 and T9. This oscillator is free running at 45 Hz and can be synchronised up to at least 120 Hz. T7 is an additional sync transistor and is ac coupled to the vertical sync signal (TTL level).

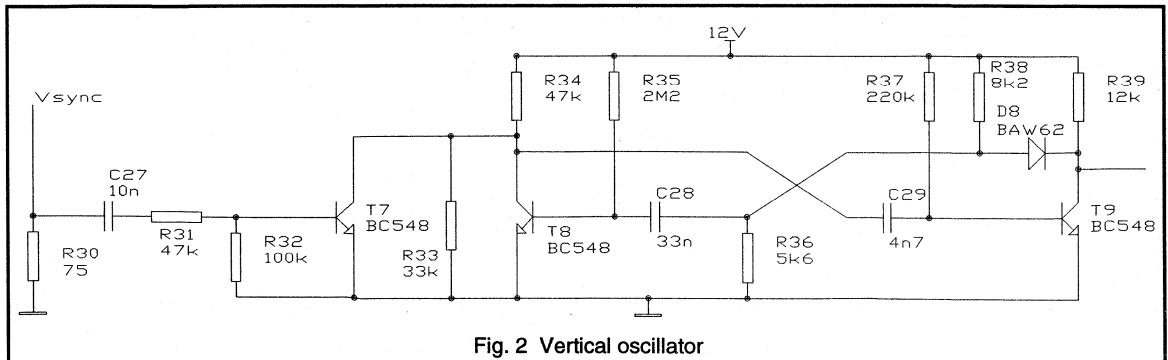


Fig. 2 Vertical oscillator

3.2 Deflection processor TDA8433

The TDA8433 is an analog, I²C bus controlled, deflection processor. It generates the vertical deflection current waveform and the EW (East-West) waveform. The necessary corrections on these waveforms are I²C bus controlled. This ic also includes some DACs and ADCs. They can be used for control functions of other circuitry².

The resistor at pin 4 determines the reference current for this ic. Pin 2 is the vertical sync input. At the capacitor at pin 5 (C-flyback) a triangle waveform is generated which is used for internal timing. This signal is used to generate the vertical sawtooth at pin 22 (C-saw). At pin 23 (C-amp1) a storage capacitor of the amplitude stabilisation loop is found whose voltage determines the amplitude of the sawtooth. The V-sync input can only handle unequal spacings of the pulses if there is a 2-sequence (e.g. Teletext 312-313 lines). A 4-sequence from the 100 Hz box cannot be handled by the amplitude loop.

The vertical sawtooth is internally connected to the "geometry control" section. In this section S-correction, vertical shift and linearity correction are added to the sawtooth by I²C commands. The amplitude is controlled by pin 24 (EHT-comp) to compensate for EHT variations.

From here the signal goes to one input of the internal error amplifier. The other input is connected to pin 21 and the output to pin 20. By means of an I²C command the external input pin can be selected as an inverting or non-inverting input. This provision is made to handle both non-inverting and inverting vertical output stages.

The block "geometry control" also generates the EW parabola. The I²C bus controllable functions are: parabola, corner, trapezium and picture width. By means of the signal at pin 24 this signal is corrected for EHT variations. The EW drive output is available on pin 19.

On the digital side of this IC we find the following functions:

Pin 15 (SCL) is the Serial CLock and pin 14 (SDA) is the Serial DATA. Pin 1 is the address pin and can either be connected to ground or +12V. The three external DA converters can be controlled by the bus: DACA, DACB & DACC. With DACA the horizontal free running frequency of the TDA2595 can be adjusted. The other two DACs (pin 7 & 6) are not used. They can be used for H-shift and H-phase control. See appendix A.

Pins 9 and 10 are output switch functions: not used in this application. When pin 10 is programmed high, it can be used as an input pin. Together with pin 17 it forms a comparator. Pin 10 is connected to the $\Phi 1$ voltage of the TDA2595 and pin 17 to the reference voltage. In this way an I²C bus signal is available whether the horizontal oscillator is in centre, locked and mute or coincidence so information can be sent to the IN-input. This also makes automatic f_o adjustment possible.

The supply part of this IC contains 4 pins. Pin 18 is ground for the geometry and sawtooth part: pin 13 is ground for the output stages and I²C bus. Pin 12 is the +12V input and at pin 16 an external capacitor is required for filtering the +5V (internally generated).

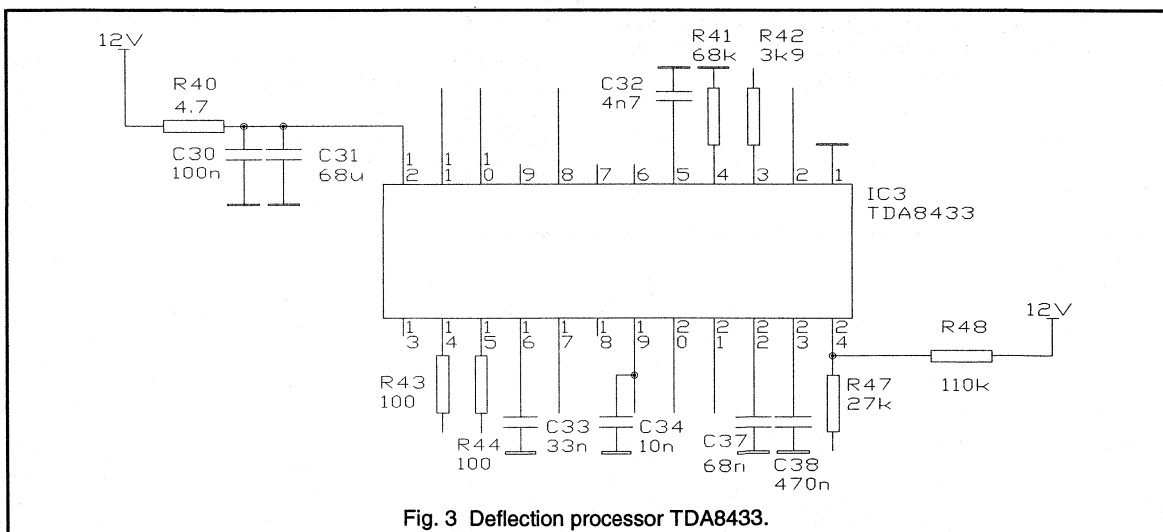


Fig. 3 Deflection processor TDA8433.

3.3 Vertical output stage

The vertical output stage is controlled by the well known TDA3654. To make this stage suited for 100 Hz TV some modifications of the ordinary solution are required. The circuit is shown in Fig. 4.

A damper network is located in parallel to the vertical deflection coil. The values depend on the characteristics of the deflection unit. The line ripple that is injected from the horizontal deflection coil is damped by the series connection of R55 and C48. R55 reduces the line ripple to an acceptable value. C48 is added to block the relatively low vertical deflection voltage in order to limit the dissipation in R55. A resonant circuit is created by C48 and the inductance of the deflection coil. R54 is a critical damper for this circuit to minimise excessive oscillations after the vertical flyback.

The deflection current is sensed by two 1.5 Ω resistors in parallel and fed back to the deflection processor. The network C36, R45 and C35 is added for a stable loop transfer because of the non resistive load at the output of the TDA3654.

The output stage is ac coupled. The dc bias point is fixed by the resistors R60 and R61. By the V-shift setting of the TDA8433 vertical shift of the picture is possible.

An additional shift circuit is connected in parallel to the dc shift circuit to make an alternating frame shift possible. It consists of T11 and its series elements. When T11 is conducting a small dc current will flow through the deflection coil. Due to the S-correction of the vertical deflection current a smaller current is required at the top and bottom than in the middle of the tube to guarantee proper interlacing across the whole screen. Therefore, the waveform of the shift current is derived from the parabola voltage of C49. A potentiometer is provided because this interface setting is critical.

The drive signal required for this alternating frame shift is generated by the 100 Hz conversion box.

If two independent shift signals are needed, the whole circuit must be duplicated.

3.4 Horizontal oscillator

The horizontal oscillator used is the TDA2595. The horizontal sync signal (TTL level) is divided and ac coupled to the input pin 11. At pin 14 the reference current is set by a 13 kΩ resistor. The sawtooth capacitor is connected to pin 16. The free running frequency is 31.25 kHz and determined by the value of its capacitor and the reference current. By varying the reference current the free running frequency can be adjusted. This is done using the DAC-A output (pin 8) of the TDA8433 via resistor R25, see section 3.2.

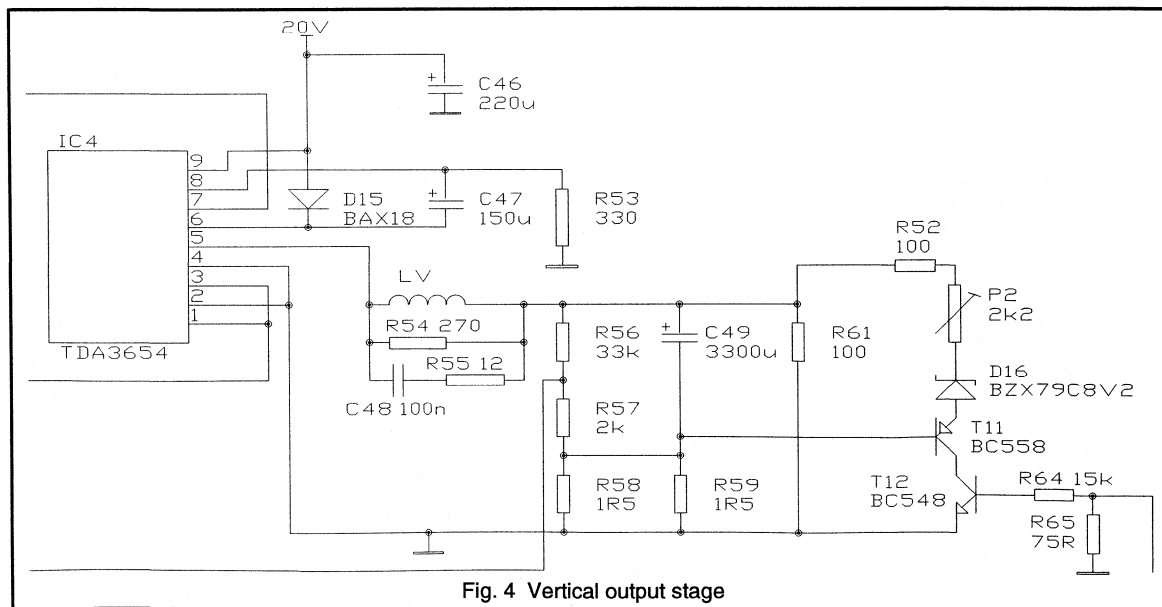


Fig. 4 Vertical output stage

This oscillator is locked to the incoming sync signal by a PLL (Phase Locked Loop). The starting point of the horizontal sawtooth is compared with the horizontal sync. If this starting point is not in the middle of the horizontal sync pulse, an error signal will appear at pin 17. Via R27 the current of pin 14 is affected and thus the horizontal phase can be locked. The loop filter consists of C25, R28 and C26.

The output of the oscillator is internally connected to a second PLL $\Phi 2$ and to a phase shifter. The phase shifted signal is available via an output stage at pin 4 (horizontal output). This signal drives the deflection stage. A feedback signal of the deflection stage is applied to the other input of the $\Phi 2$ phase detector (pin 2). In this way the horizontal flyback of the deflection stage is locked to the oscillator and thus to the sync as well. The loop filter of $\Phi 2$ consists of one capacitor at pin 3. This second PLL has a much larger bandwidth to compensate for the storage time variations in the deflection transistors.

At pin 6 a two level sandcastle pulse is available. It is mixed with the vertical blanking signal of the TDA8433 or the flyback of the TDA3654 to generate a three level sandcastle. See also the description of TDA8433 section 3.2 and TDA3654 section 3.3.

Pin 7 is the mute output. This signal is sent to the TDA8433 so that "oscillator locked" information is available at the I²C bus.

As these kinds of ic are sensitive to supply pollution provision is made for a local supply filter R21, C18 and C19.

For layout recommendations see section 4.

3.5 Horizontal drive circuit

The horizontal drive circuit is a classical transformer coupled inverting driver stage. When driver transistor T1 is conducting, energy is stored in the transformer. When T1 is turned off the magnetising current continues to flow in the secondary side of the transformer thus turning on the deflection transistor. At this time the voltage on the secondary side of the driver transformer is positive ($V_{BE} + I_B \cdot R_6$). When the driver transistor turns on again this secondary voltage reverses. At the same time energy is stored in the transformer again.

During this turn off action the forward base drive current decreases with a controlled di_b/dt , thereby removing the stored charge from the deflection transistor. The di_b/dt depends on the negative secondary voltage and the leakage inductance. When the drive circuit is designed properly, the deflection transistor stops conducting when its negative base current is about half the collector peak current.

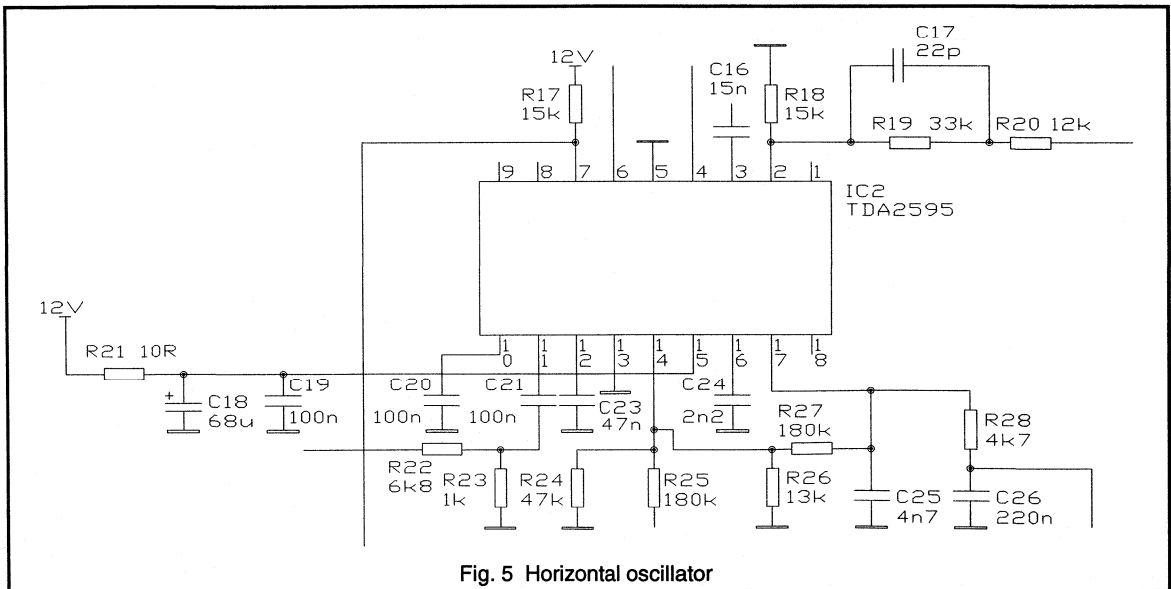


Fig. 5 Horizontal oscillator

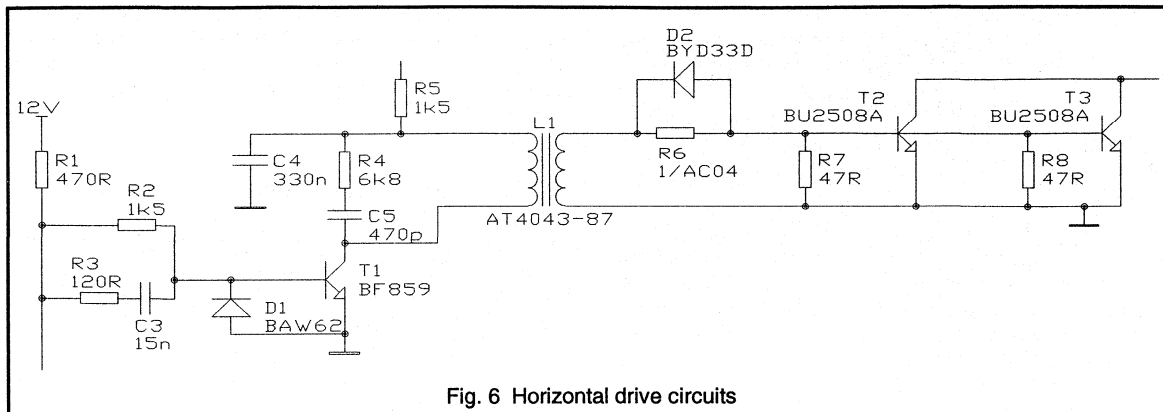


Fig. 6 Horizontal drive circuits

To prevent the deflection transistor from turning on during flyback due to parasitic ringing on the secondary side of the driver transformer a damp resistor is connected in parallel with the base emitter junction of the deflection transistor.

Also at the primary side of the driver transformer a damp network is added (R4 & C5) to limit the peak voltage on the driver transistor.

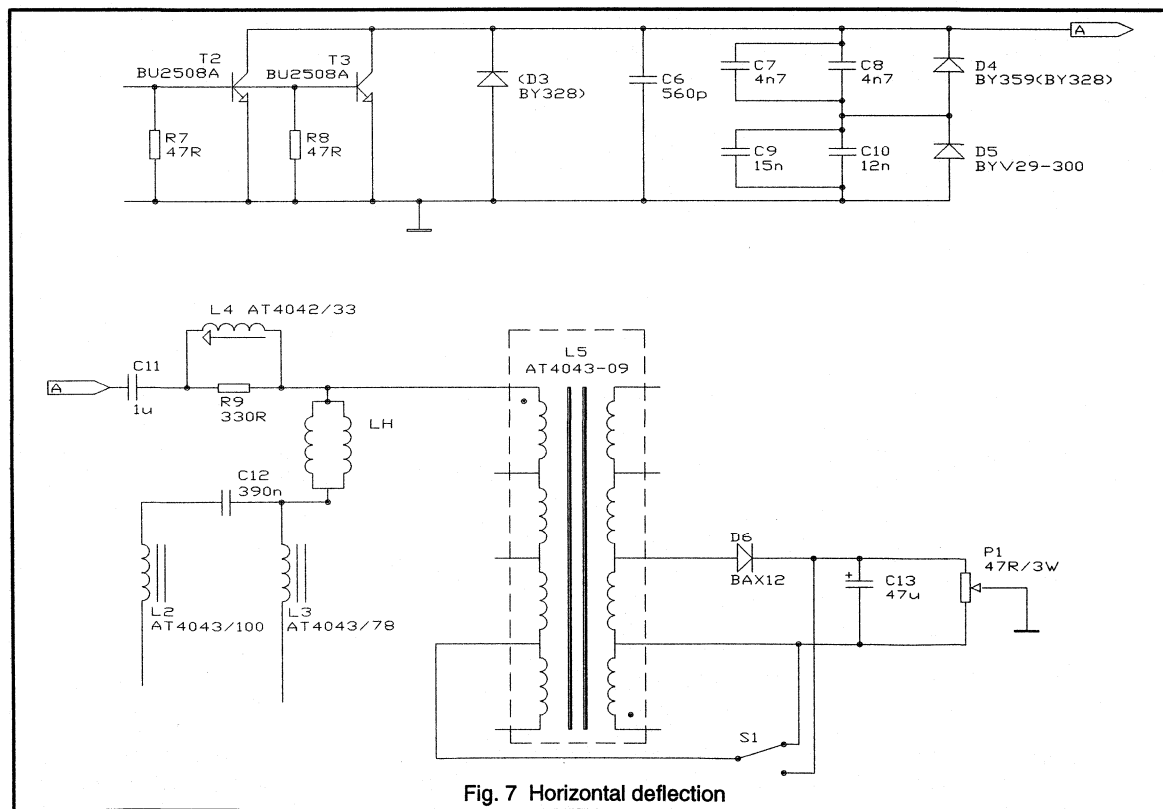


Fig. 7 Horizontal deflection

3.6 Horizontal deflection

The horizontal deflection is the classical deflection stage with the diode modulator which not only provides the EW raster correction but also inner pincushion correction. Due to the high frequency in combination with large currents some problems do appear here. The horizontal deflection coil needs 10.4A peak-to-peak. This results in a collector peak current of 6-7A, too much to handle with one BU2508A. So, two transistors are used in parallel. If the print layout is made in a proper way no special precautions are required to use this type of transistor in a parallel configuration. (NB the circuit was constructed before the BU2525A became available.)

For the flyback capacitor the current is too high as well. So, here, also, two devices are used in parallel. The S-correction capacitors do not have problems in handling the current.

There are two possible solutions for the damper diodes. The BY359 is a high current damper diode available in isolated and non-isolated TO220 packages. This device has been re-designed for operation as a damper diode specifically for 32 kHz deflection systems. An alternative solution is to place a third diode in direct parallel with the collector-emitter's of the deflection transistors. This option allows two cheaper axial diodes to be used in the modulator, eg BY328. This option is shown in Fig. 7.

For full performance of scan linearity a horizontal dc shift circuit is incorporated. In an ordinary TV set the horizontal off centre of the picture tube is compensated by the phase shift of the horizontal oscillator. This, however, introduces a linearity error in the deflection. In many cases this error is acceptable; if not, it can be compensated by means of an adjustable linearity corrector.

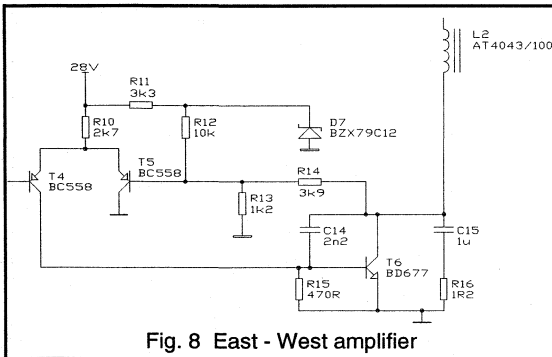


Fig. 8 East - West amplifier

The most proper way of picture alignment is the following: the linearity corrector is only used for compensating the linearity error caused by the resistive part of the impedance of the horizontal deflection yoke. The off centre of the tube is compensated by a shift circuit. Therefore, a dc shift circuit is incorporated. This circuit has been built up around L5.

With P1 the amount of shift current can be adjusted and with S1 the polarity can be selected. The horizontal shift can be made bus controlled by using DAC-B or DAC-C of the TDA8433. A suggestion for a suitable interface is given in Appendix 2.

3.7 East - West correction

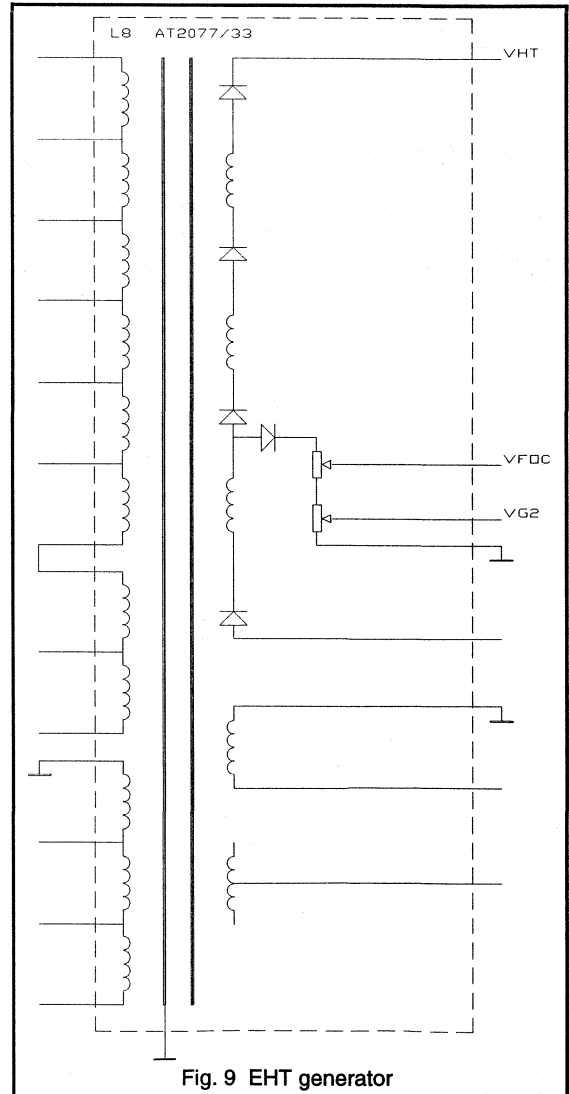


Fig. 9 EHT generator

The EW waveform is generated by the deflection processor TDA8433. An external amplifier feeds this correction to the horizontal deflection stage. It is injected in deflection via

L2. The possible corrections are: picture width, EW parabola, corner correction, trapezium and EHT compensation.

The EW amplifier is shown in Fig. 8. It consists of a Darlington power transistor, T6, a differential amplifier, T4 & T5, and a feedback network R13 R14. R12 is added for proper dc bias. Because this amplifier has a non real load, special attention is paid to loop stability. Across T6 there is a miller capacitor, C14. The line ripple current of L2 flows mainly through C15 and R16.

3.8 EHT generation

The darker glass requires a higher EHT power for an equal light output. An increase of only the beam current has two disadvantages: a larger spot size and a higher drive from the video amplifiers. An increase of only the high voltage would come in conflict with the legislation on X-ray radiation.

As a compromise an EHT of 27.5kV @ 1.3mA is chosen. A new design of LOT is used, see Fig. 9. This LOT is a four layer diode split box (DSB) design with extra high voltage capability. From an integrated potentiometer the adjustable focus and grid 2 voltages are taken.

3.9 Auxiliary supply

Some of the auxiliary supplies are taken from the LOT such as heater, video and frame supply. The other auxiliary supplies are taken from a separate transformer. The philosophy behind this concept is explained in section 2.2.

The auxiliary transformer is connected in parallel to the LOT. On the secondary side of this transformer the auxiliary voltages are taken. These outputs supply the signal processing circuitry (5V @ 5A, 12V @ 1A, -12V @ 1A).

The primary inductance of this transformer is relatively high, so the increase of collector current in the deflection transistor is low. To adjust the output voltage the primary winding has some taps. Due to the relative high ESR of the 5V smoothing capacitors a π -filter is required.

With moderate current levels all the auxiliary supplies can be taken from the LOT.

4. PCB design considerations

For general information see reference 3.

4.1 TDA2595

The following tracks and pins of the TDA2595 are critical and need special attention:

- * The track length at pin 14 - reference pin - to its peripherals should be kept as short as possible.

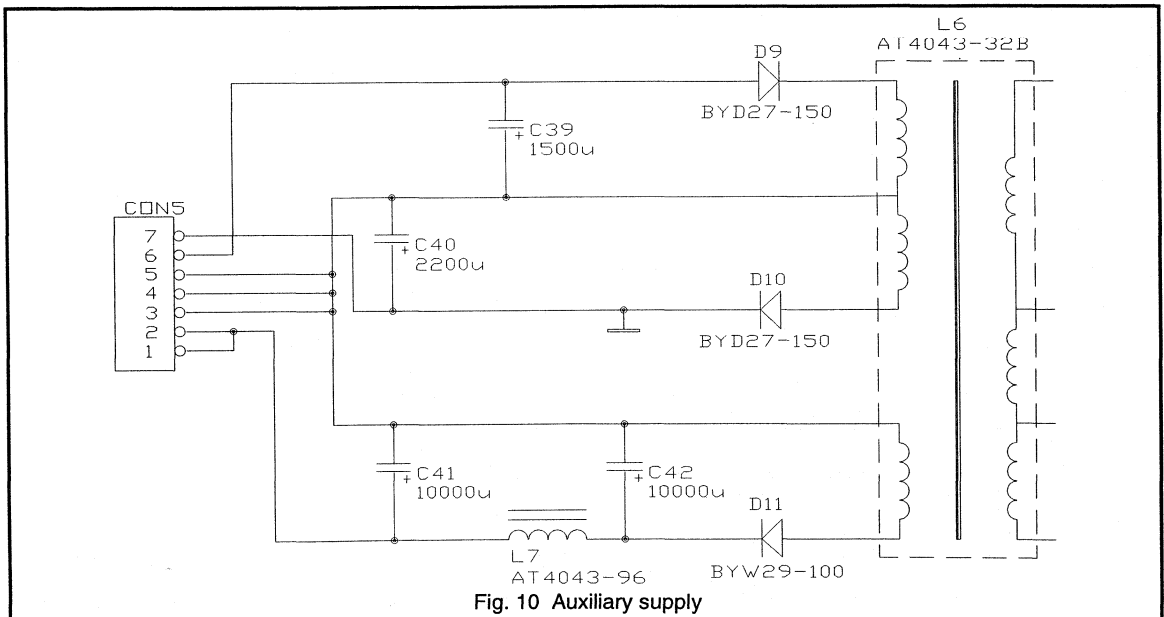


Fig. 10 Auxiliary supply

- * The peripheral components connected to pins 14, 16, 3, 17 and 15 should be connected directly to the ground of this ic.
- * The ground track of this ic may not carry current from other parts of the set.
- * As this ic is sensitive to high frequency ripple on the supply rail, local decoupling is essential.

4.2 TDA8433

The following tracks and pins of the TDA8433 are critical and need special attention:

- * The components connected to pins 4, 5, 12, 16, 19, 22 and 23 should be connected to the analog ground (pin 18) and as close as possible.
- * The track length of the pins 4, 5, 22 and 23 should be as short as possible.
- * The ground track of this ic may not carry current from other parts of the set.
- * Local decoupling is essential because this ic is sensitive to high frequency ripple on the supply rail.

4.3 Horizontal deflection and supplies

This kind of circuit carries currents with high di/dt . The loops that contain these currents should have an area as small as possible to limit magnetic radiation. Examples are the loop of deflection coil with the deflection transistors, diodes and flyback capacitors. Also the loop formed by smoothing capacitor C43, primary of LOT and deflection transistor should be kept small.

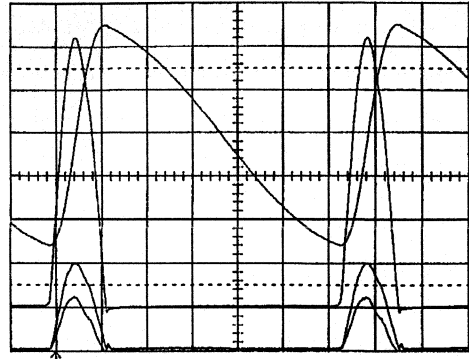
In case of rectifiers the ground track between transformer winding and smoothing capacitor may not be a part of any other ground track.

4.4 Drive circuit

To ensure current balance in the deflection transistors, the base and emitter tracks of the two transistors should be as similar as possible to create the same impedances for both transistors.

5. Oscillograms

All oscillograms were taken under nominal load conditions of the auxiliary supply and 1mA beam current.



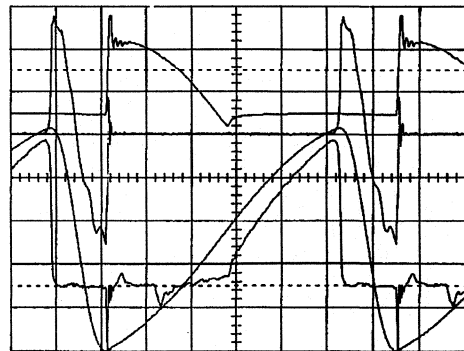
Oscillogram 1:

In this oscillogram the upper two traces show the average deflection current (2A/div) and the voltage across the deflection transistors (200V/div). The peak V_{CE} is 1244V.

The lower two traces are the minimum and maximum values at the mid-point of the diode modulator (100V/div) due to EW modulation.

Remarks:

At the end of flyback there is a negative over shoot at the collector voltage. This is caused by the forward recovery of the damper diode.



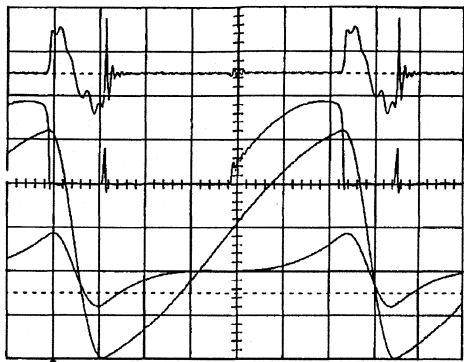
Oscillogram 2:

The lower trace is the current in the deflection transistors. The upper trace is the current in damper diode D4 and the middle trace is the current in the upper flyback capacitors (C7 + C8). All current settings 2A/div.

Remarks:

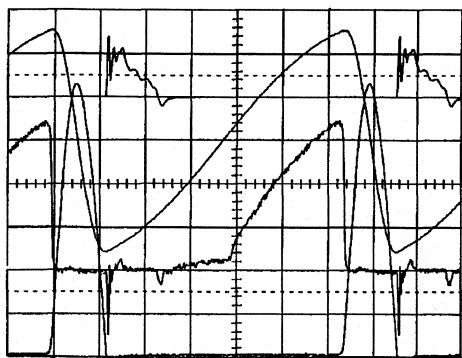
At the end of flyback the current in the flyback capacitor is taken over by the damper diodes. Due to parasitic capacitance and inductance ringing occurs. $5\mu s$ later there

is a negative current in the deflection transistor. This is reverse conducting of the base-collector of the transistor caused by the fact that the base drive is already turned on.



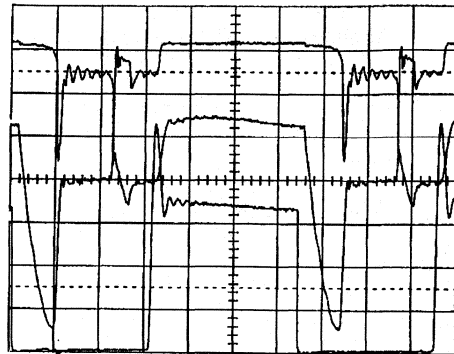
Oscilloscope 3:

In this oscilloscope the upper trace is the current in the lower flyback capacitors C9 + C10. The second trace is the current in the diode D5. In the bottom part the current in the bridge coil is given and the deflection current is shown once more as a reference. All settings 2A/div.



Oscilloscope 4:

In this oscilloscope the deflection transistor I_c and V_{CE} are given as a reference. The upper trace is the current in the third diode D3. As soon as the deflection transistor is turned on the current of D3 is taken over by the transistors. All current settings 2A/div.



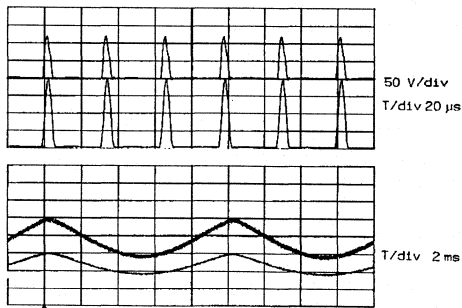
Oscilloscope 5:

The upper trace is the V_{BE} of the deflection transistors (5V/div). The middle trace is the I_B of the deflection transistors (1A/div). The lower trace is the V_{CE} of the driver transistor T1 (50V/div).

Remarks:

The overshoot at the rising edge of the driver transistor is caused by the leakage inductance of the driver transformer. By means of the damping network R4, C5 this overshoot is limited. This network is chosen in such a way that the ringing is critically damped.

The base drive circuit is designed in such a way that the peak of the negative base drive current, I_{Boff} , is approximately half the collector current, I_C . During turn off the V_{BE} of the deflection transistor should remain negative. To achieve this the ringing is damped by R7 and R8.

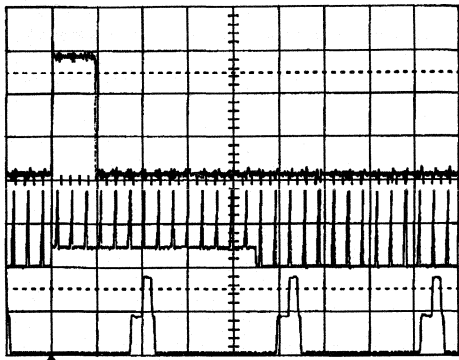


Oscilloscope 6:

This split screen oscilloscope was made with two different time base settings. In the upper grid the minimum and maximum values of the flyback pulses across C9 + C10 of the diode modulator are given under nominal conditions. The lower grid shows the amplified EW drive signal (collector T6 5V/div) and the output of the TDA8433 (pin 19 2V/div).

Remarks:

At the collector of T6 some line ripple is visible.

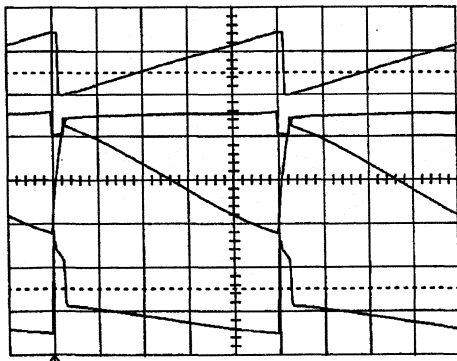


Oscillogram 7:

The upper trace gives the vertical sync signal (1V/div, 100 μ s/div). The middle trace is the sandcastle (5V/div, 100 μ s/div). The lower trace is the sandcastle during vertical scan (5V/div, 10 μ s/div).

Remark:

This three level sandcastle pulse is the sum of the two level sandcastle of the TDA2595 and the vertical blanking of the TDA8433.

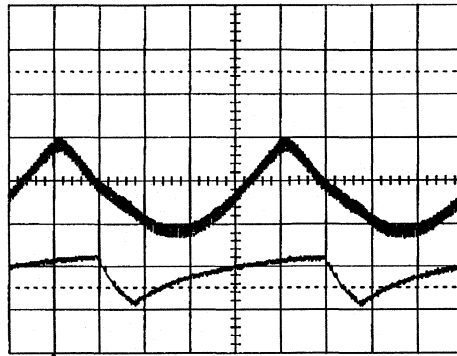


Oscillogram 8:

The upper trace is the generated sawtooth at pin 22 of the TDA8433 (5V/div). The second trace is the output signal of the error amplifier of the TDA8433 pin 20 (5V/div). The third trace is the sawtooth current in the vertical deflection coil (1A/div). The lower trace is the output signal of the vertical output amplifier TDA3654 pin 5 (20V/div).

Remark:

Due to the L/R of the vertical deflection coil the current in the coil can not follow the fast retrace time of the sawtooth generator. The output amplifier clamps after the flyback to $2xV_b$. When the control loop locks after the flyback, a slight voltage overshoot can be found at the output of the TDA3654. This is damped by C48, R55 and R54.



Oscillogram 9:

The lower trace is the voltage at the foot point of the line output transformer (10V/div). This signal is a representation of the EHT variations needed by the anti breathing.

The upper trace is the EW waveform at T6 (5V/div). On the EW waveform a correction signal is added to prevent the picture from breathing.

6. References

Information for this section was extracted from "32kHz/100Hz deflection circuits for the 66FS Black Line picture tube A66EAK22X42"; ETV89012 by J.v.d.Hooff.

1. P.C.A.L.E. report ETV8906. "32 kHz / 100 Hz deflection circuits for the 78FS picture tube" by Mr. J.A.C. Misdorn.
2. C.A.B. report ETV8612. "Computer controlled TV; the deflection processor TDA8432" by Messrs. E.M. Ponte and S.J. van Raalte.
3. C.A.B. report ETV8702: "EMC in TV receivers and monitors" by Mr. D.J.A. Teuling.

7. Circuit diagrams

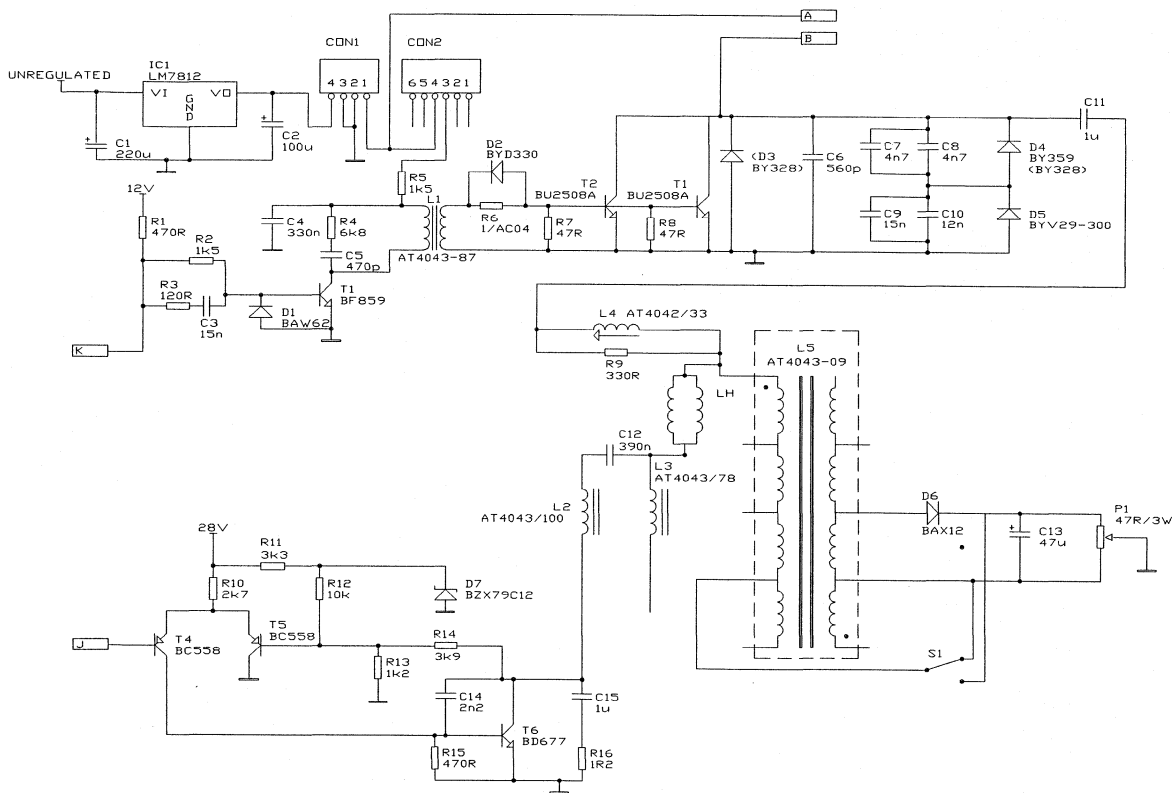


Fig. 11 Horizontal Deflection and EW Amplifier

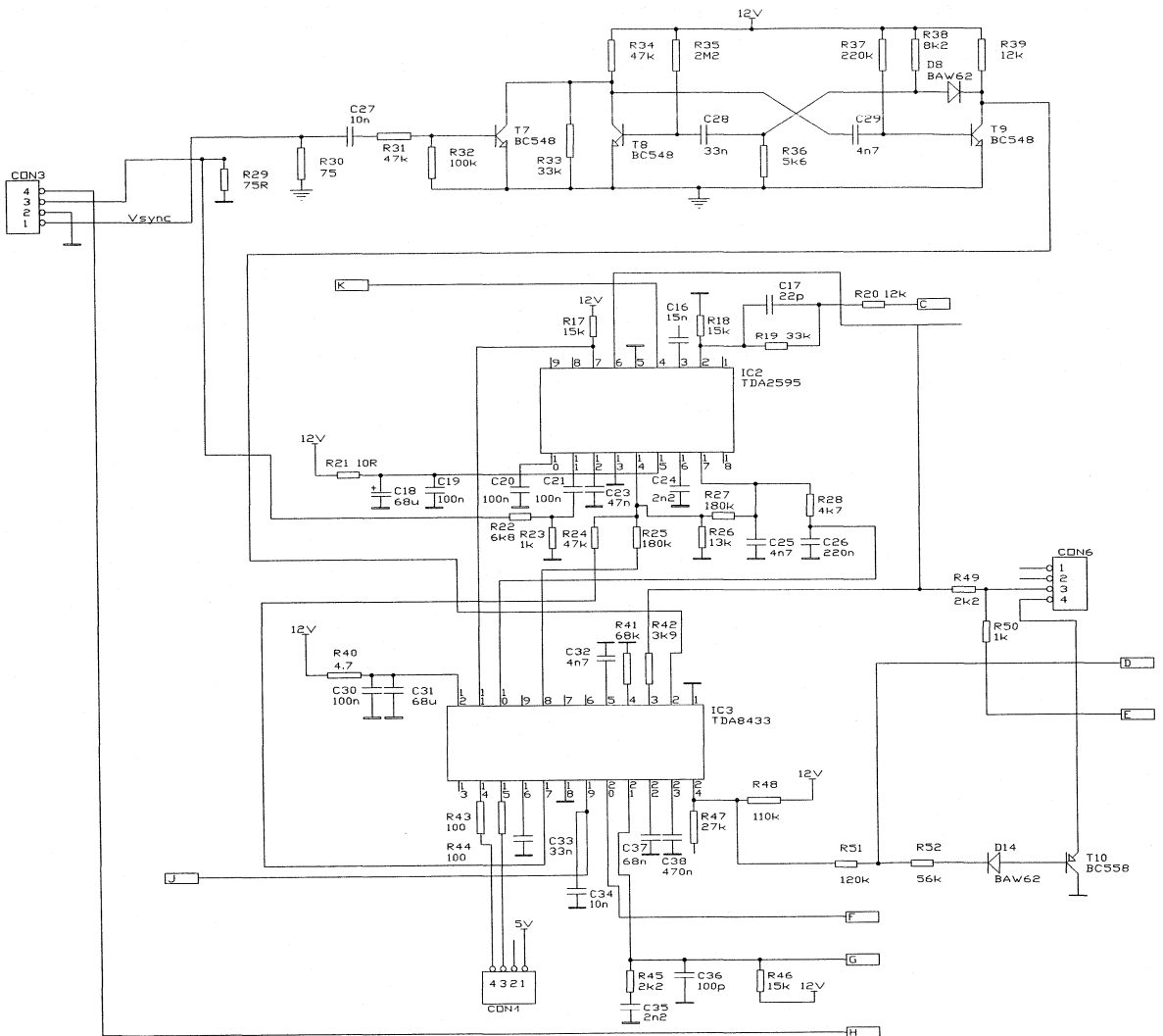


Fig. 12 Deflection Processor and Horizontal & Vertical Oscillators

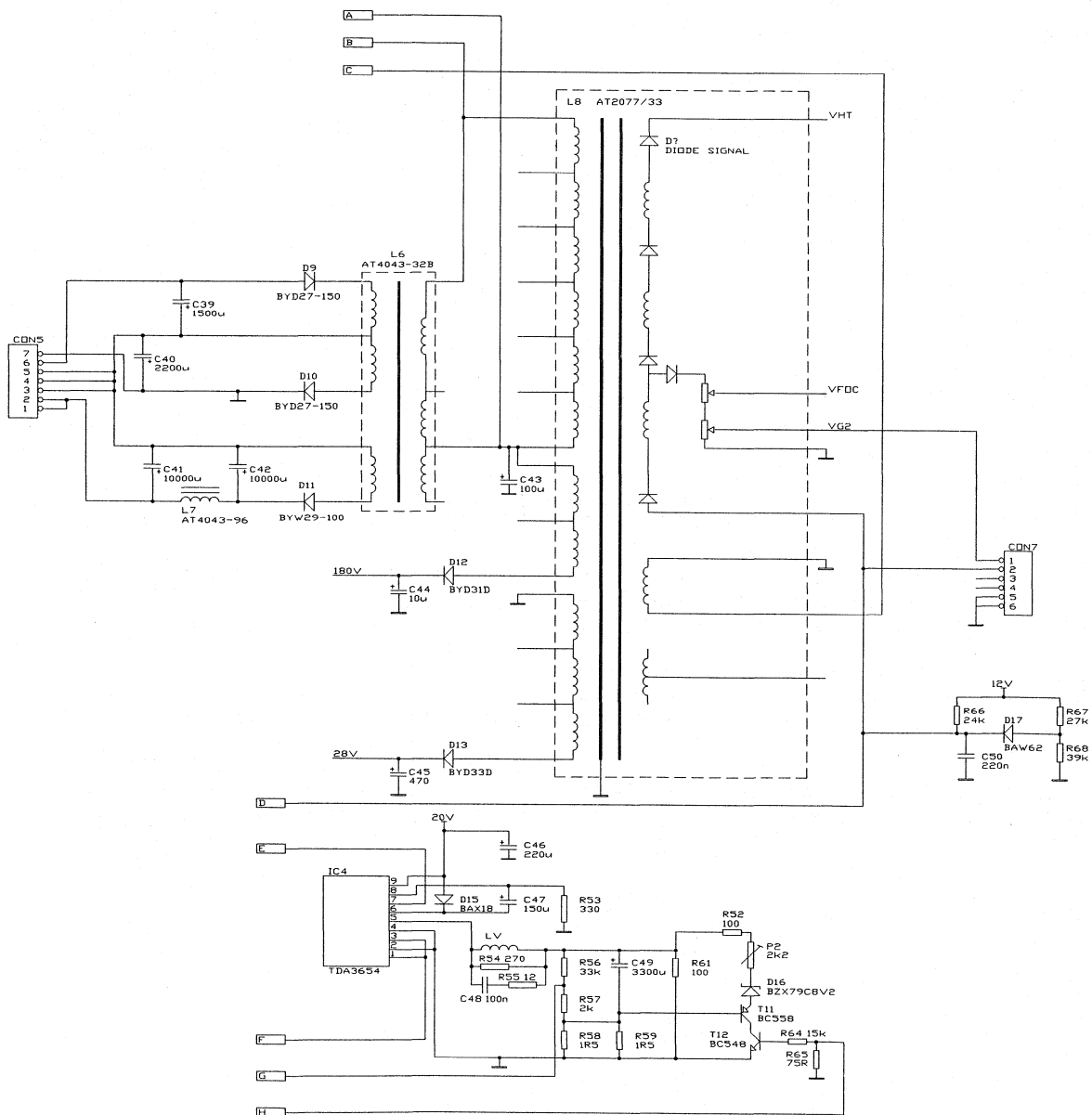


Fig. 13 Auxiliary supply, EHT Generator and Vertical Output Stage

Appendix A

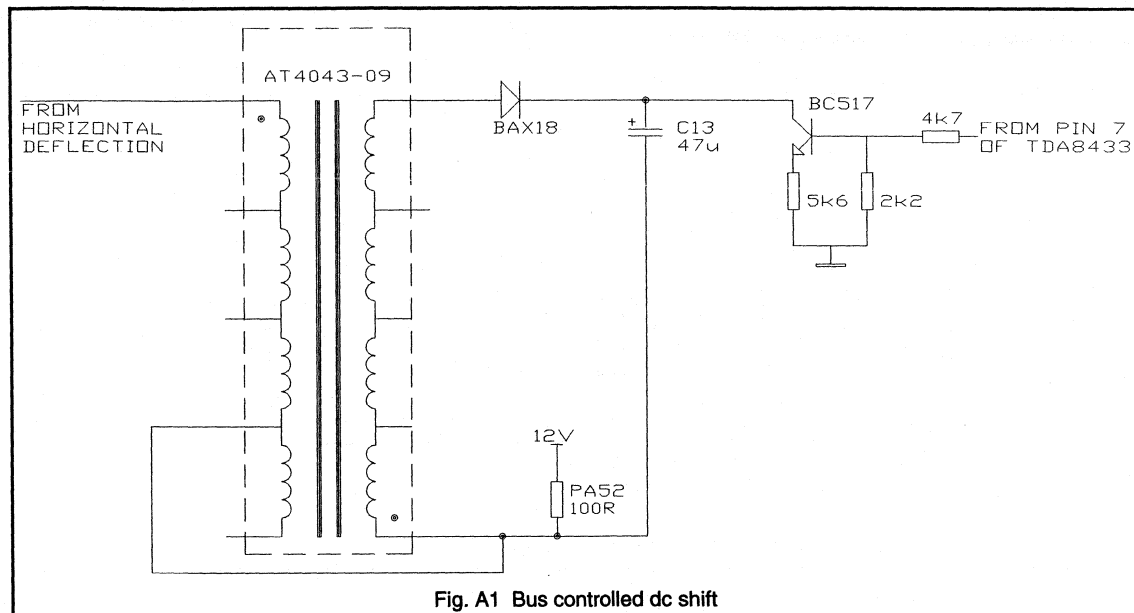


Fig. A1 Bus controlled dc shift

The deflection processor TDA8433 has three DAC's. In this application only one DAC (DAC-A) is used. In this section some ideas are given to use the other two DAC's.

DAC-B is a 6-bit DAC, like DAC-A, and is controlled by the H-PHASE register. Its output voltages can be controlled from 0.5V to 10.5V typically. The output resistance is less than 1kΩ.

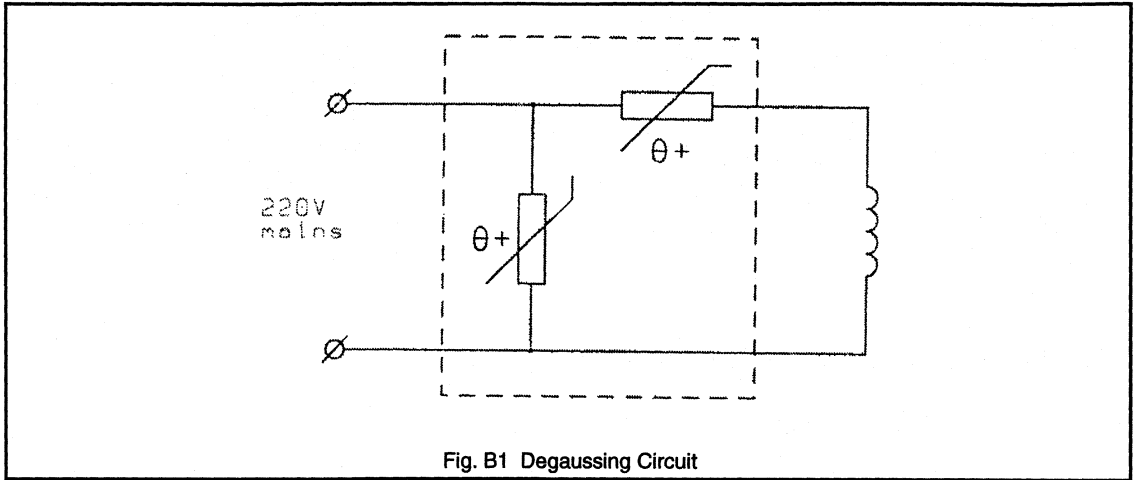
DAC-C is a 2-bit DAC and is controlled by the VTRA and VTRC bits. Its typical output characteristic is:

VTRA	VTRC	Output voltage	Output resistance
0	0	12V	7.5kΩ
0	1	5.3V	3.3kΩ
1	0	1.7V	1.0kΩ
1	1	0.3V	<1kΩ

All settings in the set that are now manual controls can be made I²C bus controlled by using one of these DAC's. The only restriction is that the alignment is controlled with a dc voltage. Otherwise an interface circuit is needed.

Appendix B

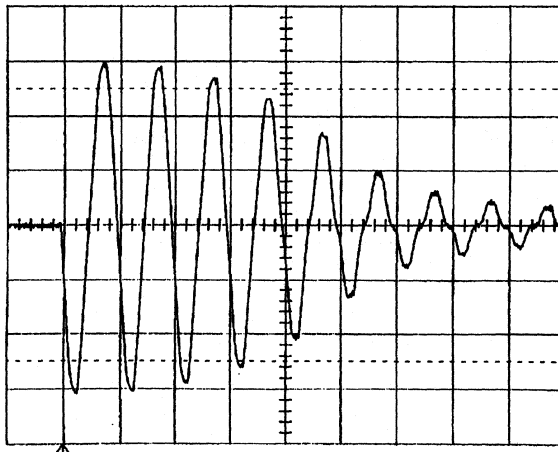
As a degaussing circuit the following suggestion is given.



Parts list:

Dual degaussing PTC : 2322 662 96116

Degaussing coil : 3111 268 20301



Oscillogram 10:

Current in degaussing coil 2A/div.

SMPS Circuit Examples



4.3.1 A 70W Full Performance TV SMPS Using The TDA8380

The following report describes the operation of a 70W full performance switched mode power supply for use in television.

The TDA8380 SMPS control ic is used in a mains isolated, asynchronous flyback converter configuration.

The power supply incorporates the following features:

- Full mains range (110 - 265Vrms)
- AT3010/110LL SMPS transformer
- BUT11A switching transistor
- Standby (suppression of output voltages by 50%)
- Standby supply (5V, 100mA)
- Facility for synchronisation (using a pulse transformer)
- Short start-up time (less than 0.3 sec at 220Vrms)
- Provision for anti-breathing circuit
- Output voltages 147V/57W, 25V/5W, 16V/7.5W

A full description of circuit operation, a circuit diagram and circuit performance figures are given.

A further additional circuit diagram is included in which the above power supply incorporates a power MOS switching transistor for a mains range of 90 - 135Vrms. Also details are given on an extension to the power capability of the supply, up to 120W output, for European mains using the bipolar switching transistor.

1. Introduction

The TDA8380 control ic has been designed to enable safe, reliable and efficient SMPS to be realised at minimum cost for TV and monitor applications. For further information on the ic, reference should be made to 'Integrated SMPS Control Circuit TDA8380' (ref. 1).

The 70W design employs a currently available AT3010/110LL foil wound transformer and the BUT11A bipolar switching transistor.

Feedback is taken from the secondary side to give less than 1% line and load regulation over the whole range. The output voltage is suitably divided down and compared in an error amplifier with a fixed reference voltage. The error amplifier then drives an optocoupler, which passes the error signal to the primary side directly into the TDA8380. A secondary side error amplifier is used to reduce the importance of the optocoupler characteristics.

Standby is achieved by injecting a signal into the feedback loop on the secondary side, suppressing all output voltages by 50%. A 5V standby supply is available relieving the need for a separate standby supply. During standby conditions the line output oscillator is halted to disconnect the main B+ load.

Synchronisation of the power supply to external control circuits is possible through a loosely coupled pulse transformer.

Appendix A gives a circuit diagram and a short description of the use of the power MOS switching transistor in the 70W supply. The mains range is 90 - 135Vrms.

Appendix B gives notes on how to extend the power capability of the 70W power supply to 105W, 32 kHz and 120W, 30 kHz. Both these power supplies have a mains range of 180 - 265Vrms.

2. TV SMPS design

Flyback versus Forward Converter.

Although this ic can be applied in any type of SMPS, for example in FORWARD (or Buck) or FLYBACK (or Buck-boost) converters, the preferred SMPS type for TV applications is the Flyback converter. This is mainly because it allows for mains isolation of the TV chassis. Other advantages it affords in comparison with a forward converter are:

- (a) It does not need 'crow-bar' protection against the input voltage appearing across the chassis in the event of short-circuit failure of the power switching transistor.
- (b) The load permissible on auxiliary output supplies is not related (and, therefore, not limited) by the main line timebase supply (B+ voltage) load. Thus the auxiliary supply is available when there is no B+ voltage load, and this is important for servicing and fault finding on a TV chassis.

With the Flyback converter, however, mains pollution and visible interference require to be minimised by careful PCB layout and customarily a mains input filter is used.

Discontinuous versus Continuous Current Mode Operation:

Operation can be in the 'continuous' or in the 'discontinuous' current mode.

In the discontinuous mode the power switching transistor is not allowed to switch on until the SMPS transformer core is demagnetised. This has the advantages:

- (a) It is inherently a safer mode of operation, since for all operating conditions, other than a dead-short of the output or a very severe overload transient occurring when the power transistor is conducting near peak current, it is not possible for the core to saturate. To protect for these two exceptions, the very fast (second level) current protection is included.
- (b) Steep current pulse edges at switch-on are eliminated (important from point of view of Radio Frequency Interference problems).

Satisfactory performance, in terms of voltage regulation and input mains voltage range, can be obtained using the discontinuous mode which is, therefore, preferred for TV applications.

For this type of converter, the voltage transfer function can be deduced from the Volt-second equilibrium condition for a unity turns ratio transformer:

$$V_i \times d \times T = V_o \times \bar{d} \times T \quad (1)$$

$$\frac{V_o}{V_i} = \frac{d}{\bar{d}}$$

where: $\bar{d} = (1 - d)$

Taking into consideration the transformer turns ration $n = N_p/N_s$, then:

$$\frac{n \times V_o}{V_i} = \frac{d}{\bar{d}} \quad (2)$$

- where: T = oscillator period
- N_p = transformer primary turns
- N_s = transformer secondary turns
- d = on time of output transistor
- \bar{d} = conduction time of output rectifier
- V_o = output B+ voltage
- V_i = input DC voltage

The limit condition for 'discontinuous' current mode operation occurs at minimum input voltage and maximum load.

Thus, for this condition $\bar{d} = (1 - d)$
so that

$$\frac{n \times V_o}{V_{imin}} = \frac{d_{max}}{(1 - d_{max})} \quad (3)$$

The power output (including losses supplied via the transformer) is:

$$P = \frac{V_i^2 \times d^2}{2 \times L_p \times f} \quad (4)$$

- where: L_p = primary inductance of transformer
- f = frequency of operation

from which general expressions for d , L_p and f can be obtained in terms of the power.

Thus, for a given transformer (n, L_p) the value of d_{max} can be calculated from (3) and the required frequency of operation from:

$$f = \frac{d_{max}^2 \times V_{imin}^2}{2 \times P \times L_p} \quad (5)$$

The peak current in the power switching transistor is given by:

$$I_p = \frac{V_i \times d}{L_p \times f} \quad (6)$$

The peak voltage across the power switching transistor (excluding ringing) is:

$$V_i + (n \times V_o)$$

Since most transformers produce ringing, a clamp circuit may be necessary and in order to slow the rising edge of the voltage a snubber circuit is usually required.

3. General circuit description

This section gives an overall general description of the power supply.

Fig. 1 shows a block diagram of the circuit functions. Descriptions of specific circuits will be carried out in the next section.

3.1 Mains filter

This is positioned at the ac mains input. Its function is to minimise mains pollution resulting from RFI generated within the SMPS due to fast transients of voltage and current. It is designed to meet the required mains pollution regulations (C.I.S.P.R. Special Committee on Radio Frequency Perturbation).

3.2 Rectification and Smoothing

The mains voltage is rectified and smoothed to provide a dc supply which is switched through the SMPS transformer.

3.3 SMPS Controller

This drives the power switching transistor regulating the frequency and the amount of current pulsed through the transformer primary. Thus, the controller regulates the energy transferred to the secondary windings. A voltage feedback signal which is representative of the output voltage is fed back to the controller in order to regulate the output voltage. At start up the supply voltage for the controller ic is derived from the rectified mains. A 'take-over' winding on the transformer supplies the ic once normal operation is established.

3.4 Transformer secondary circuits

The dc output voltage is obtained by simple rectification and smoothing of the transformer secondary voltage.

3.5 Feedback Attenuator

The output voltage to be regulated is fed back via an attenuator to the error amplifier.

3.6 Error Amplifier

The error amplifier compares the feedback signal with a fixed reference voltage to give an error signal which is passed to the primary side via an optocoupler.

Mains isolation is provided within the optocoupler and the power transformer, between the input primary and take-over, and the output secondary windings.

4. Detailed circuit description

This section gives a detailed description of each of the functions of the power supply circuit (Fig. 2).

4.1 Mains Input and Rectification

Diodes V1 to V4 rectify the ac mains voltage and, together with a smoothing capacitor C13, provide a dc input HT voltage for the SMPS. R1 is placed in series with the input to limit the initial peak inrush current whenever the power supply is switched on when C13 is fully discharged.

C1 and C3 together with L1 form a mains filter to minimise the feedback of RFI into the mains supply.

C6 to C9 suppress RFI signals generated by the rectifier diodes.

Asymmetrical mains pollution is reduced by the insertion of R26 and C18 between primary ground ('hot side') and secondary earth ('cold side') of the power supply. These components are required to satisfy the mains isolation requirements.

4.2 Control ic TDA8380

This section describes the function of each pin of the TDA8380 and its associated components.

Pin 1 - Emitter of Forward Drive Transistor:

The TDA8380 incorporates a direct drive output stage consisting of two NPN transistors. The collector and emitter of each are connected to separate pins of the ic (pins 1,2,15,16). The forward base drive current for the switching transistor is limited by R15. C16 acts as a voltage source equal to the zener voltage of V7 and is used for the negative base drive.

When the reverse drive transistor is turned on the zener voltage appears across L2, causing stored charge to be removed from the switching transistor, thereby ensuring correct storage time and minimum transistor dissipation during turn-off.

Pin 2 - Collector of the Forward Drive Transistor:

Connected through a resistor to the ic reservoir capacitor.

Pin 3 - Demagnetisation Sensing

Demagnetisation protects the core of the transformer against saturation by sensing the voltage across a transformer winding. In this application operation is in the discontinuous current mode. Sensing is achieved by resistor R10 from the take-over winding of the transformer to pin 3 of the ic. Fig. 3 illustrates demagnetisation operation at low mains where the turn-on pulse is delayed until demagnetisation of the transformer is complete.

Pin 4 - Low Supply Trip:

Connected to the ic ground (pin 14), the low supply protection level is 8.4V.

Pin 5 - IC supply:

On power-up the ic supply is first drawn from C15. This capacitor is charged up directly from the rectified mains through bleed resistors R21 and R24.

Once the SMPS is running, the supply for the ic is taken over by the SMPS transformer. R12 prevents peak rectification of spikes. V8 rectifies the flyback signal which is smoothed by C15 to give a dc level. R16 limits the current drawn by the forward drive transistor. R9 and C5 provide a filtered dc supply to pin 5.

Pin 6 - Reference Current:

This pin allows the external setting of the IC current source. This is set by R11.

Pin 7 - Voltage Feedback:

This is the input to the internal error amplifier for primary side feedback. Feedback in this case is taken from the secondary side and passed through a separate secondary side error amplifier where it is compared with a reference voltage. The error signal is then passed directly into the duty pin (pin 9) via an optocoupler.

To ensure that the Transfer Characteristic Generator (TCG) in the ic remains optional a 'pseudo' feedback voltage from the 'take-over' winding of the SMPS transformer is applied to pin 7. R3 and R4 provide a nominal 2.5V level at pin 7 during normal operation of the power supply.

Pin 8 - Stability:

This is the output of the error amplifier which is left open circuit.

Pin 9 - Duty:

This is the input to the pulse width modulator and is directly driven by the optocoupler transistor. R2, C2 and C27 form a frequency compensation network.

Pin 10- Oscillator:

The frequency of the internal oscillator is set here by C4 and R11 on pin 6 (nominally 25 kHz).

Pin 11 - Synchronisation:

This is achieved by a loosely coupled pulse transformer passing sync pulses from the secondary to the primary side of the power supply (see later section).

Pin 12- Slow Start:

The slow start option is selected here by the use of capacitor C11. Fig. 4 shows a typical slow-start.

Pin 13- Over-Current Protection:

To keep the collector current of V10 within safe operating limits over-current protection is incorporated into the power supply. R27 is the collector current monitoring resistor providing a negative going signal. This voltage is then shifted to a positive level with respect to ground potential by a reference current from the ic flowing through R14. An extra voltage shift is provided by R34 which varies with the ic supply voltage. This is particularly useful in output short circuit conditions. If the main regulated output is progressively short circuited, then all SMPS transformer flyback voltages will decrease, respectively, and hence the shift level of the current protection function leading to lower short circuit output currents (current foldback). The signal at pin 13 is then compared with two internal voltage levels to provide the two forms of current protection.

(The addition of R34 may not work in other power supplies using the TDA8380 because careful attention has to be given to the ratio of current through R34 to current output at pin 13 and to the start-up sequence of the power supply at different mains and loads. Conventional current protection can be achieved by omitting R34 and changing R14 to 13 k Ω and V13 to BYW95C).

Fig. 5 illustrates the current protection waveform.

Pin 14- Ground**Pin 15- Emitter of Reverse Drive Transistor:**

Grounded to the emitter of the switching transistor.

Pin 16- Collector of reverse drive transistor.**4.3 Error Amplifier**

The external error amplifier consists of two PNP transistors, V15 and V16, connected to form a high gain comparator. The stabilized reference voltage for the comparator is derived from a series-connected resistor R28 and zener diodes V5 and V6 at the SMPS output. The voltage to be compared with the reference voltage is a sample of the 147V output derived from a potential divider (R29, R31 and R5). The optocoupler is directly driven with the error signal from the comparator. The level of the 147V output can be adjusted by R5.

4.4 Standby

In standby mode the power supply output voltages are suppressed to 50% of their normal level. Standby is achieved by reducing the reference voltage used in the comparator circuit and thus the power supply regulates at a lower output voltage level. A +5V dc level is applied to the standby input, which turns transistor V14 on. The voltage reference level is halved from 12.4V to 6.2V and the main 147V output is reduced to 75V. In this condition the power supply still maintains a 5V standby supply. In the television receiver during standby the line output oscillator should be halted to disconnect the main 147V load.

To return the power supply to its normal operating levels, the standby input is removed.

The speed of transition to and from standby is controlled by the time constant of R13, R32 and C23.

4.5 Synchronisation

Synchronisation of the power supply is achieved by a loosely coupled mains isolated pulse transformer. Sync pulses of +5V are applied to the sync input at a frequency slightly lower than the free running frequency of the power supply. R6 limits the current in the primary winding of the pulse transformer and R8 loads the secondary winding. The pulse transformer differentiates the sync pulse input to create negative and positive going transitions of the sync input. The ac coupling (C14) shifts the entire signal positive and the internal circuitry of the ic clamps the negative going excursions to 0.85V. The positive going spikes are removed by a transistor in the ic and the negative going spikes are used to synchronise the oscillator. Fig. 6 shows plots of how the power supply is synchronised to a lower frequency.

A series RC network (C28, R35) is connected from pin 11 to ground to filter out high frequency noise which may interfere with synchronisation.

If the synchronisation option is not to be used, the sync input may be left open circuit. Another alternative is to short-circuit C14 and remove T2.

4.6 Beam Current Limiting (BCL)

Anti-breathing technique, whereby the 147V voltage is reduced for increasing beam current in such a manner as to compensate for the increase in picture size due to the fall in EHT. The components concerned are R30, C24, R7.

4.7 Power Switching Transistor

Pulsing of the transformer is carried out by the BUT11A bipolar power transistor under the control of the TDA8380.

Fig. 7 shows plots of the current through and voltage across the BUT11A. The base drive waveforms are shown in Figs. 8(a)-(b) during standby conditions.

Fig. 9 is a plot of the instantaneous power dissipated in the transistor during turn-off.

4.8 Snubber Network

A snubber network has been added across the switching transistor to protect it from excessive switching dissipation and to suppress ringing on the SMPS transformer.

The dV/dt limiter consists of V9, C17, R22 and R23. When V10 is switched off, part of the energy stored in the leakage inductance of the SMPS transformer will charge C17. When V10 is switched on again this energy is dissipated in R22 and R23. When such a network is omitted, this energy must be dissipated in the switching transistor itself.

R22 and R23 are calculated in such a way that they also act as a network, damping the residual energy in the winding capacitance of the transformer when the secondary rectifiers have stopped conducting.

4.9 Outputs

There are three secondary rectifiers; the 147V (scan voltage for deflection stage), 25V (audio supply) and 16V (small signal supply). The 5V standby supply is derived from a regulator connected to the 16V output.

R25 and C25 form a damping network to dissipate the energy in the high frequency ringing on the B+ secondary winding. Fig. 10 shows the current through and voltage across the B+ winding.

A short circuit or overload of these outputs will cause the power supply to repeatedly go through the slow start procedure.

5. Performance specification

Mains input:	110 - 265V ac	50 - 60 Hz	
Outputs:	B+	147 V	57 W
	Audio	25 V	5 W
	L.T.	16 V	7.5 W
	Standby	5 V	0.5 W

Switching frequency: 25 kHz

Efficiency (normal operation): 72 %

Line and load regulation: 0.1 %

Start-up time (220V rms, full load): 300 msec (B+)
225 msec (+5 V standby)

Max. collector current: 2.3 A

Max collector voltage: 870 V

Forward base current: Normal operation 0.30 A min.
0.39 A max.
Standby (*) 0.20 A min.
0.24 A max.

ic supply voltage: Normal operation 18.5 V min.
21.0 V max.
Standby (*) 8.8 V min.
9.7 V max.

Ripple output voltage (110V rms, 50 Hz, full load):

Frequency	B+ (mV)	L.T. (mV)	Audio (mV)	Standby (mV)
25 kHz	600	230	145	20
199 Hz	230	50	60	-

* The only load in this condition is the standby load.

6. Output short-circuit foldback

The SMPS incorporates duty factor foldback protection for short circuits on the 147V (B+) output. Fig. 11 shows the plot of the foldback characteristic for increasing load on the 147V output using conventional protection and current foldback techniques.

8. References

- Ref. 1. "Integrated SMPS Control Circuit TDA8380". Philips Components Publication Number 9398 358 40011 December 1988.

Appendix A

70W FULL PERFORMANCE USING POWER MOS (BUK456-800A)

A power MOS switching transistor was incorporated into the 70W power supply design. This new power supply has a mains range of 90 - 135V rms. A circuit diagram is given in Fig. 12. Oscillograms of the power MOS gate and drain switching waveforms are given in Figs. 13 and 14.

Alterations to Existing 70W Bipolar Transistor Design

(i) The value of C17 in the snubber is smaller, hence less dissipation in the snubber resistors. The dV/dt at the drain is now higher, but the power MOS transistor has much lower switching losses than the bipolar transistor.

The smaller value of C17 causes the 100 kHz ringing on the primary winding of the SMPS transformer after flyback to be more prevalent. This ringing has an effect on the demagnetisation function causing premature operation. To overcome this a resistive divider network has been used on pin 3 to minimise the effect of ringing.

(ii) The value of R14, the current protection shift register, is increased. This is to compensate for the fact that the power MOS transistor does not suffer from storage effects at turn-off.

(iii) The filtering on the take-over winding for the ic supply is increased. This is because the average current demanded by the gate drive of the power MOS is much less than in the case of the bipolar transistor. Energy in switching

spikes on the flyback voltage cannot be channelled into the gate of the power MOS and so has to be dissipated in increased filtering.

A smaller value for the gate-source resistor is used to provide extra loading on the transformer winding.

(iv) C13 is increased to filter the higher current ripple at low mains voltages.

(v) A larger heatsink for the switching transistor is necessary due to the higher on-resistance of the power MOS transistor facilitating the need for higher heat dissipation.

Performance Specification

Mains supply:	90 - 135V rms		
Switching frequency:	20.8 kHz		
Outputs:	B+	147 V	57 W
	Audio	25 V	5 W
	L.T.	16 V	7.5 W
	Standby	5 V	0.5 W
Regulation:	0.1 %		
Peak drain voltage:	650 V		
Peak drain current:	2.3 A		
Start-up time	300 msec		

Addendum

Alternative Cheap BUT11A Base Drive Design Eliminating 5 W Zener Diode

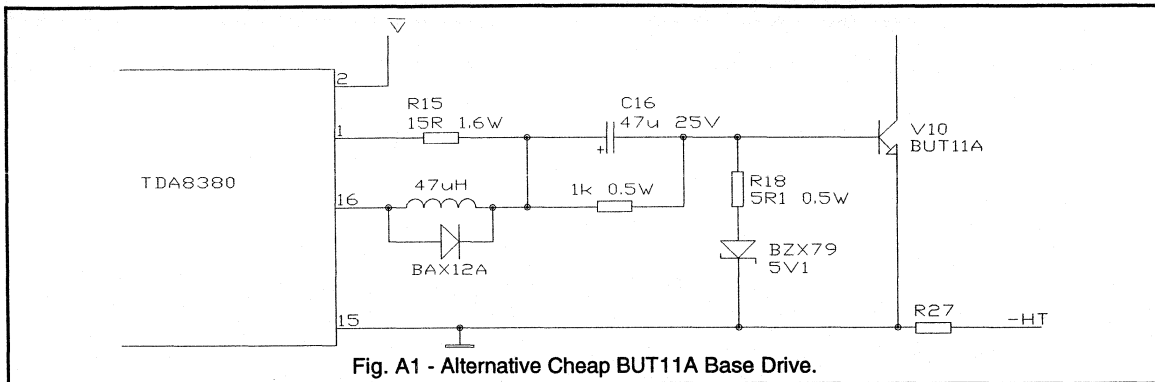


Fig. A1 - Alternative Cheap BUT11A Base Drive.

An alternative base drive for the power switching transistor (BUT11A) has been designed to eliminate the 5W zener diode 1N5339B (V7) to reduce cost.

Alternative Low Cost Base Drive

This design has not been implemented into a PCB design yet, but the existing PCB design requires little alteration to accommodate the changes.

When the forward drive resistor is turned on at the start of the duty cycle, a current defined by R15 passes through C16 and into the base of the BUT11A. The 1 kΩ resistor in parallel with C16 discharges the capacitor when the SMPS is off to help starting at low mains. When the reverse drive transistor is turned on, the 5.1V zener diode appears across C16 clamping the voltage across it, thus a reverse

current flows from the base of the BUT11A through C16 and L2 turning off the power switching transistor. Some forward current does flow through the 5.1V zener diode, but not enough to warrant a power zener. The BAX12A diode across the inductor is to prevent large negative going spikes appearing at pin 1 of the ic; this can also be used in the previous base drive.

Base Measurements

Forward base current:	250mA min 400mA max
Standby mode (standby load only)	190mA min 250mA max
BUT11A storage time:	1.4μsec

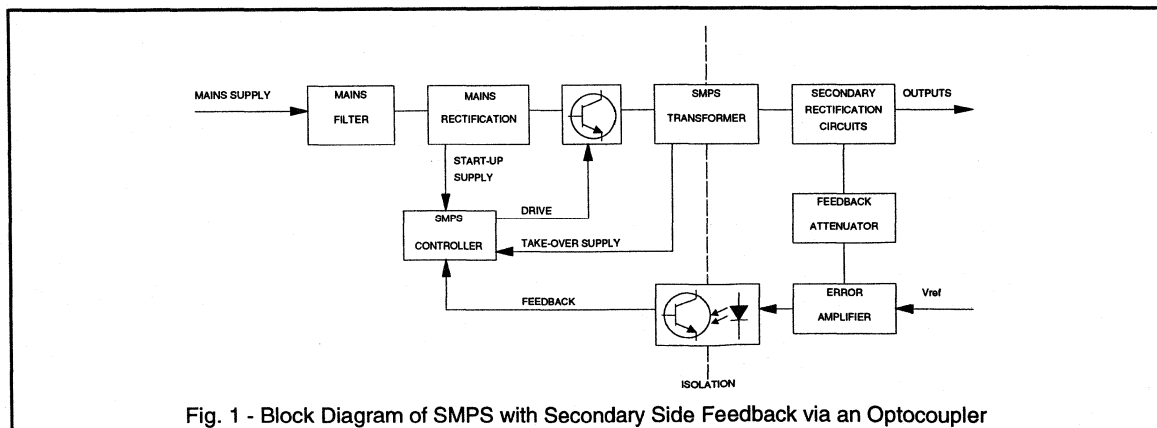
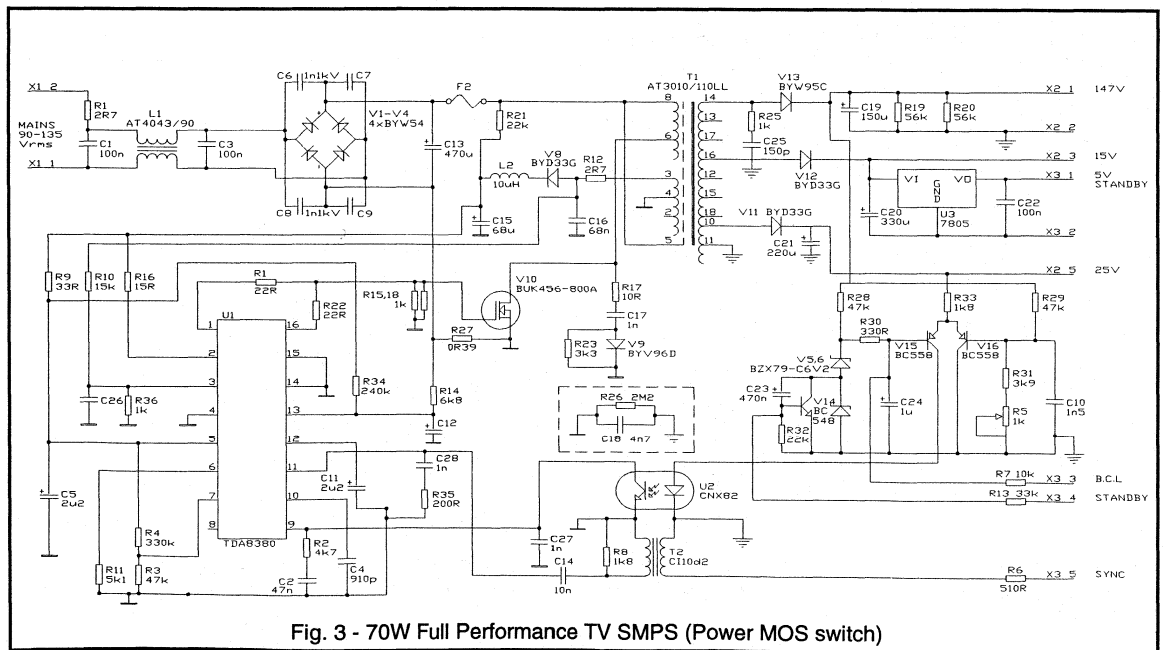
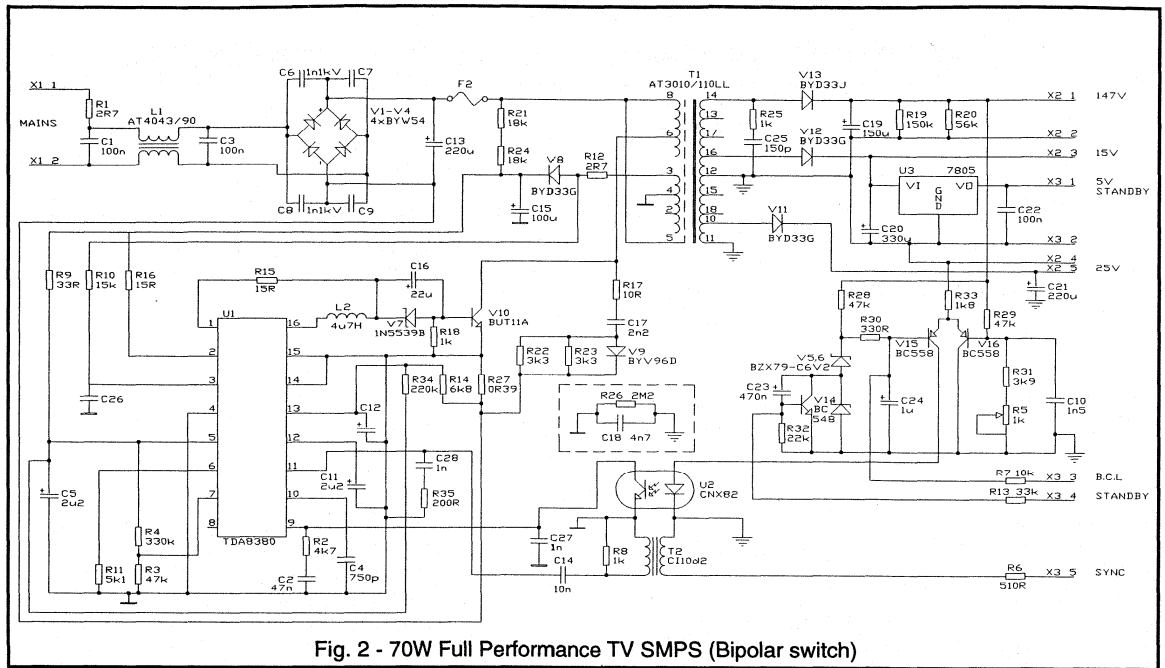


Fig. 1 - Block Diagram of SMPS with Secondary Side Feedback via an Optocoupler



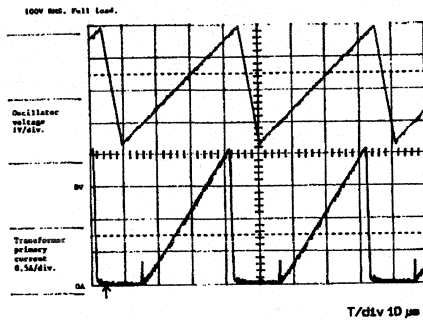


Fig. 4 - Demagnetisation operation. Oscilloscope of the Oscillator Waveform and Transformer Primary Current

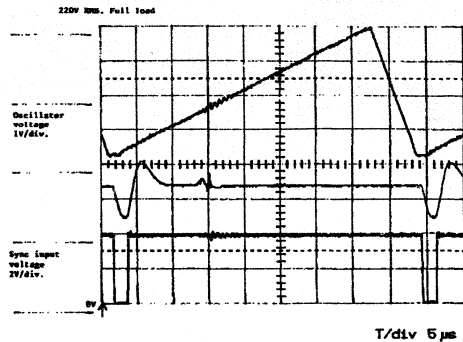


Fig. 7 - Synchronisation. Oscilloscope of Oscillator Voltage, Voltage at Pin 11 (TDA8380) and Sync Input Voltage

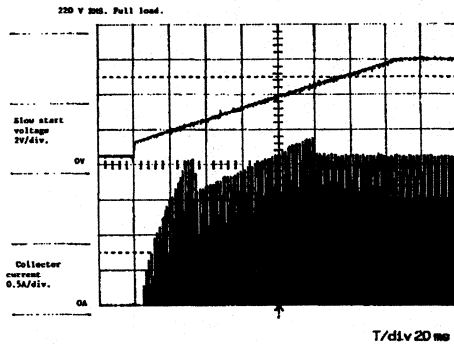


Fig. 5 - Slow Start. Oscilloscope of the Voltage at the Slow Start Pin (TDA8380) and Current through the Switching Transistor.

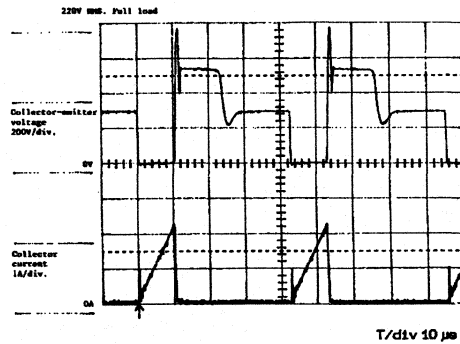


Fig. 8 - Switching waveforms. Oscilloscope of the current through and voltage across BUT11A.

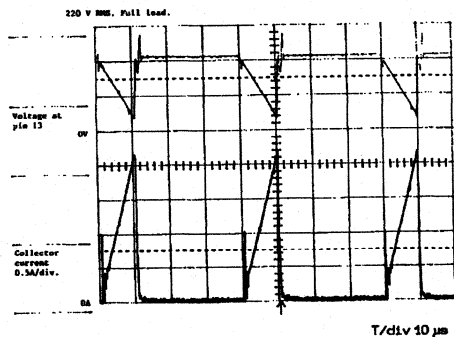


Fig. 6 - Current protection. Oscilloscope of voltage at Pin 13 (TDA8380) and the Current through the Switching Transistor

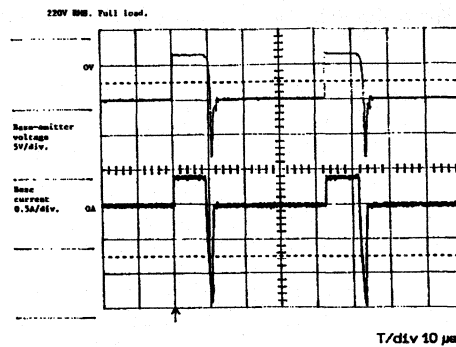


Fig. 9 - BUT11A Base Waveforms. Oscilloscope of Base-Emitter Voltage and Base Current Waveforms for BUT11A

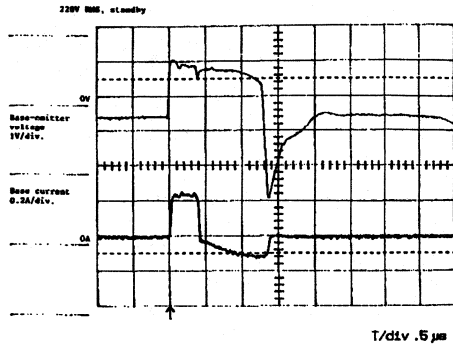


Fig. 10 - BUT11A Base Waveforms During Standby. Oscillograms of Base-Emitter and Base Current Waveforms for BUT11A in Standby Conditions

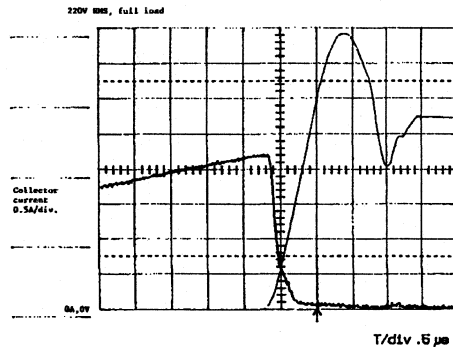


Fig. 11 - Turn off dissipation in BUT11A. Oscillogram of Collector-Emitter Voltage and Collector Current for BUT11A

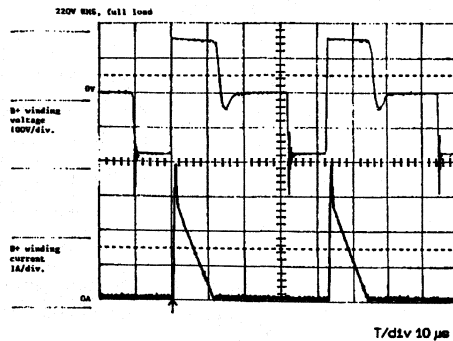


Fig. 12 - B+ Winding. Oscillogram of Voltage Across and Current Through the B+ Winding

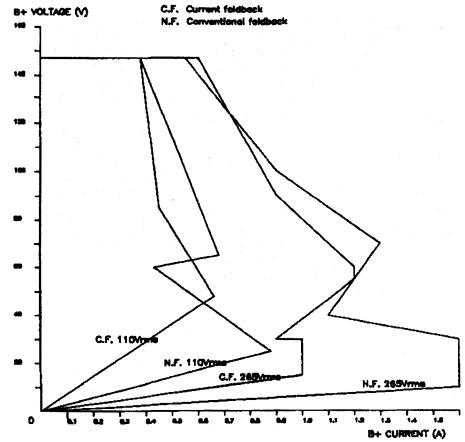


Fig. 13 - Plot of Duty Factor Foldback using Current Feedback and Conventional Foldback Techniques

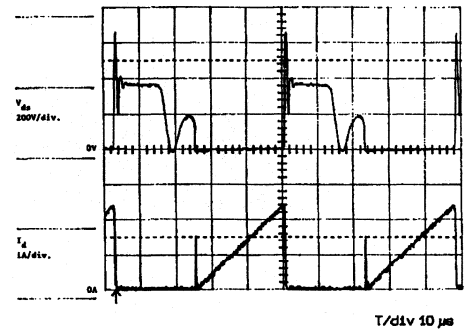


Fig. 14 - Oscillogram of Drain-Source Voltage and Drain Current for Power MOS Transistor (BUK456-800A) at Full Load, 110V rms

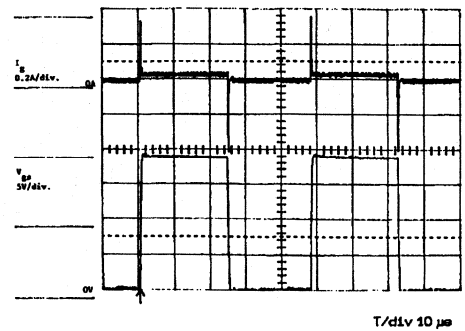


Fig. 15 - Oscillogram of Gate Current and Gate Source Voltage for Power MOS Transistor (BUK456-800A) at Full Load, 110V rms

4.3.2 A Synchronous 200W SMPS for 16 and 32 kHz TV

Description of 200W Switched Mode Power supply incorporating the AT3020/01A transformer, the TDA8380 control IC, one opto-coupler for feedback, synchronisation and remote on/off. The SMPS is intended for TV and can be synchronised to 32 kHz by flyback pulses of either 32 or 16 kHz. A 5V standby supply is also provided.

1. Introduction

In this report a description is given of a 200W SMPS circuit and evaluation board, incorporating the TDA8380 control IC, the new SMPS transformer AT3020/01A and the BUW13 power switching transistor. The SMPS is a flyback converter that has been designed to handle a maximum average output power of 200W and a peak power of 250W. The free running frequency of the SMPS is 34 kHz, while it can also be synchronised down to 32 kHz by either 16 or 32 kHz line flyback pulses. For testing purposes no pre-loading is required. The circuit operates at a mains input voltage of 185-265V_{RMS}, 50-60Hz. The output voltages are 150V, 32V and 16V. The 150V output is short circuit proof, while the 32V and 16V can be made short-circuit proof.

A new wire wound SMPS transformer has been designed. This transformer, the AT3020/01A with an EE46/46/30 core (grade 3C85), has a new winding technique which makes the RFI screens superfluous. Thanks to its low leakage inductance, the efficiency of the system is high (88%).

The control IC TDA8380 receives its start-up supply from the rectified mains voltage. The takeover supply is derived from a flyback and forward auxiliary winding on the transformer. This IC offers many attractive operating features: it directly drives the power switching transistor and incorporates several overload protections.

Due to its high current h_{FE} , the BUW13 was chosen as the power switching transistor. For an output power of up to 150W, the BUT12 can be used. A CNG82 opto-coupler is used for feedback. If synchronisation is not required, the cheaper CNX82A can be used.

For the supply of some digital IC's in the standby mode, a small self-oscillating supply is used: the so called μ SOPS (5V, 300mA). In the standby mode the output voltages will be fully suppressed.

A printed circuit board (no 3634) is available incorporating the 200W SMPS and μ SOPS but without mains filter.

2. Circuit description

2.1 Block Diagram

Fig.1 shows the block diagram of the 200W mains isolated flyback converter.

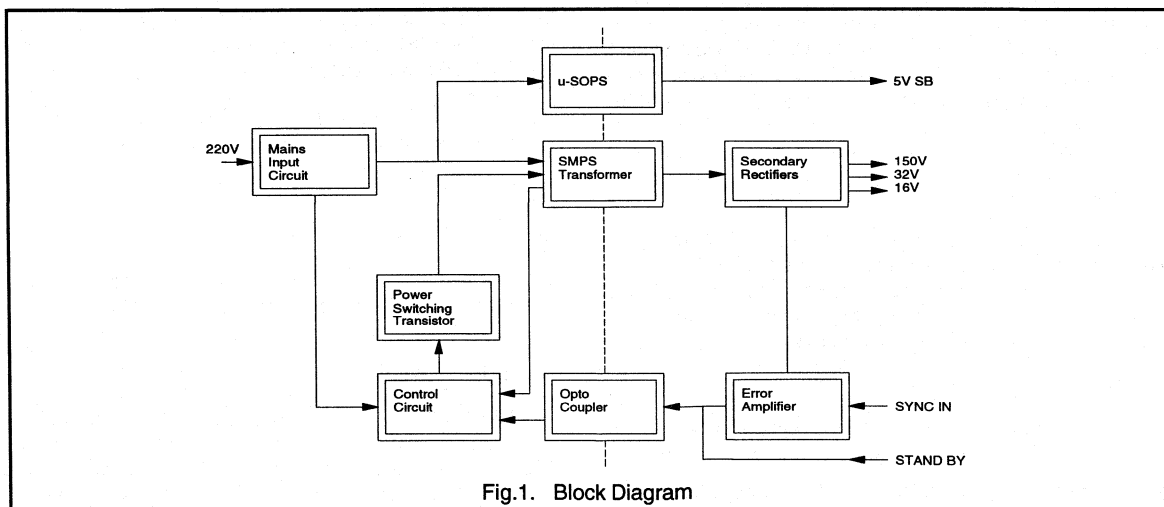
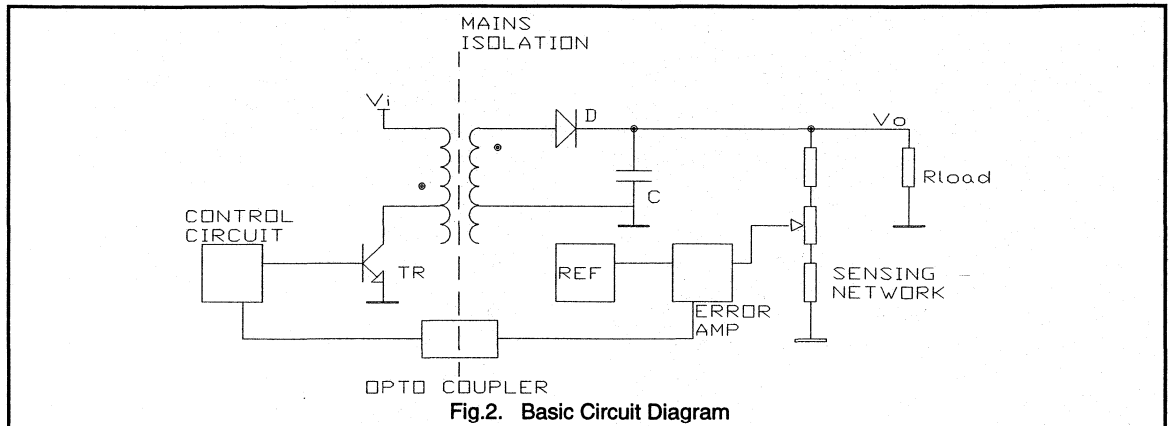


Fig.1. Block Diagram



The 200W SMPS evaluation board does not contain an RFI filter, fuses or a degaussing circuit. These components should be located on the inlet of the mains cord into the TV set. The mains input voltage is rectified by bridge rectifying diodes and the dc supply to the SMPS transformer (AT3020/01A) is smoothed by a 220 μ F buffer capacitor. The control IC TDA8380 derives its start-up supply from this dc voltage and as soon as the IC supply voltage exceeds a certain limit, the IC is initialised. Hereafter, the duty factor of the SMPS power switching transistor (BUW13) increases slowly from zero upwards and its rate of increase is controlled until the SMPS output voltage reaches its nominal level. The take over supply is derived from a flyback and forward rectifier connected to an auxiliary winding of the SMPS transformer. The SMPS is a flyback converter that operates in the discontinuous mode. At the secondary side the flyback voltage is rectified. One of the output voltages is fed back via an attenuator circuit to the error amplifier. The error signal is sent back via the opto-coupler circuit to the duty cycle control input of the IC TDA8380.

For standby purposes the μ SOPS delivers a 5V supply. In the standby mode the output voltages will be fully suppressed. The SMPS runs at a fixed frequency of 34 kHz, however, it can also be synchronised down to 32 kHz by either 16 or 32 kHz line flyback pulses.

2.2 Basic Operation

Fig.2 shows the basic circuit of the mains isolated flyback converter.

The control IC TDA8380 directly drives the power output transistor. When the transistor conducts, a linear increasing current flows through the primary winding of the transformer. As a consequence energy is stored in the

transformer. After switching off the transistor, the stored energy is transferred into the load via diode D. The attenuated output voltage V_o is compared with the reference voltage, REF, in the error amplifier. The error signal is fed back via the opto-coupler to the control IC. By controlling the duty cycle of the drive pulses the output voltage V_o is kept constant.

The flyback converter under discussion has been designed for the discontinuous current mode. The principle of this circuit has already been described in chapter 2 "Switch Mode Power Supplies". For a nominal output voltage of 150V, 185V_{RMS} mains, a maximum load of 250W and a fixed free running frequency of 34 kHz, the primary inductance of the transformer can be calculated. The required primary inductance is $L_p = 420\mu\text{H} \pm 10\%$.

An attractive feature of this SMPS is that it can be synchronised down to 32 kHz by either 16 or 32 kHz line flyback pulses.

3. Circuit diagram

The circuit diagram is given in section 8, Fig.3; detailed information about several parts of the supply follows.

3.1 Mains input

The diode bridge D1 to D4 rectifies the mains input voltage and the dc supply to the SMPS is smoothed by C5. Capacitors C1 to C4 suppress the RFI generated by the diodes in the mains bridge rectifier. If C5 is fully discharged, the inrush current has to be limited by R1 to protect the bridge rectifier diodes. During continuous operation of the SMPS this resistor is for efficiency reasons short circuited

by a thyristor, THY1. After the soft start of the SMPS, thyristor THY1 is fired continuously by the peak voltage clamp of the SMPS via R3 and C6.

3.2 Start-up supply

The control IC TDA8380 receives its start-up supply from the mains rectified voltage by the low wattage resistor R4. The IC is initialised as soon as the voltage on the supply pin 5 reaches 17V. This takes approximately 1.5s (Oscillogram 6). Shorter times are possible by lowering the value of R4. During the time leading up to the initialisation of the IC, the base coupling capacitor C10/C11 is pre-charged. So, the power switching transistor T1 is switched off correctly during the start up period. With a duty cycle from zero onwards, the SMPS starts up. The take over supply is derived from a forward and flyback auxiliary winding on the transformer (AT3020/01A). The forward rectifying diode D7 ensures that a temporary decrease of the supply voltage of the IC is restricted. After a while the flyback rectifying diode D6 directly provides all the current needed by the IC. During continuous operation of the SMPS the supply voltage for the IC is about 17V.

3.3 Control IC

The integrated SMPS control circuit TDA8380 offers many attractive operating features. It controls the SMPS power throughput and regulation by pulse-width modulation. It can directly drive the power switching transistor and it can operate at a fixed frequency or a line locked frequency. A detailed description is given in Reference [1]. The function of each pin is described below.

- Pin 1 Emitter of the forward drive transistor. It directly drives the power transistor with a source current of about 0.7A.
- Pin 2 Collector of the forward transistor. This pin is connected via R14 to the supply. Resistor R14 and R15 mainly determine the source current of the power switching transistor.
- Pin 3 Demagnetisation sensing. For this flyback converter, operating in discontinuous mode, the voltage across the SMPS transformer is sensed via R12 and R13.
- Pin 4 Low supply-voltage protection level. This pin is connected to ground, so the min. V_{cc} of the IC is set at 8.4V.
- Pin 5 IC supply. When the mains input is applied to the SMPS, the IC supply reservoir capacitor C9 is charged by a current determined by resistor R4. When the voltage at pin 5 reaches 17V, the IC initialises and diode D6 rectifies the flyback signal from winding 10/11 of the SMPS transformer to supply the IC with 17V.

- Pin 6 Master reference current setting. Resistor R11 sets the master reference current for the TDA8380 to 600 μ A.
- Pin 7 Voltage feedback and overvoltage protection. The flyback signal from winding 10/11 of the SMPS transformer is smoothed by D6/R7/C9, to give a dc level that varies in proportion to variations in the 150V output. This level is reduced by the divider R9/R10 and fed to pin 7.
- Pin 8 In this application the feedback amplifier of the TDA8380 is not used. However, an overvoltage on pin 7 will still activate a protection and slow start sequence.
- Pin 9 Output of the error amplifier. Not used.
- Pin 10 Oscillator. A 680pF capacitor C15 is connected to this pin; together with resistor R11 (4k3) the oscillator frequency is set to 34 kHz.
- Pin 11 Synchronisation. The trailing edge of the positive sync-pulses, which are superimposed on the linear feedback signal, synchronise the oscillator.
- Pin 12 Slow-start (capacitor C17) and maximum duty cycle (R20).
- Pin 13 Over current protection. The over current protection safeguards the power switching transistor for being overloaded with a too high collector peak current. For that reason resistors R22 to R26 in the emitter circuit of the power switching transistor sense the collector current. This negative going signal is dc shifted into a positive signal with respect to ground by a dc current from pin 13 flowing through R21, while C18 removes the spikes.
- Pin 14 Ground
- Pin 15 Emitter of the reverse drive transistor, connected to ground.
- Pin 16 Collector of the reverse drive transistor. See drive of the BUW13 SMPS power transistor.

3.4 SMPS Transformer

As already mentioned before, the transformer (AT3020/01A) has been designed to handle a maximum output power of 200W and a peak power of 250W. The nominal primary inductance is 420 μ H. To keep the leakage inductance (~2%) as small as possible, a turns ratio of 1:1 was chosen. The magnetic circuit of the transformer comprises two Ferroxcube E46/23/30 cores, grade 3C85. The coil is built-up in layers of copper wire, separated from each other by insulation foil. Thanks to a clever winding design no screens had to be applied, and as a result, the size of this transformer could be reduced significantly with respect to the transformer described in Reference [2].

The energy stored in the leakage inductance will be dissipated in the dV/dT limiter (D8/C13/R19) and peak voltage clamp (D5/C7/R5); the energy stored in the parasitic winding capacitance in the power switching transistor T1 and damping networks (R6/C8 and R37/C28).

3.5 Power switching transistor

By fixing the primary inductance of the transformer and its operating frequency, the collector peak current of the power switching transistor is fixed. At a peak output power of 250W the I_c peak is approximately 6.5A. On the other hand, the maximum base drive is determined by the control IC TDA8380: $I_{source\ max} = 0.75A$. The BUW13 has a sufficient high current gain and, moreover, the I_{boff} could be kept within the limit of the control IC: $I_{sink\ max} = 2.5A$. For slightly lower maximum power (150W) the BUT12 can be used as the power switching transistor. Note that, in that case, current sensing resistor R21 has to be reduced.

The correct forward drive of the transistor is provided by the supply voltage of the IC and R14/R15, resulting in an I_{bon} of 0.7A. To obtain a correct negative base drive, the bias voltage across C10/C11 is kept constant by three BAW62 diodes (D9 to D11). During turn off, inductor L1 (1.7 μ H) in combination with the bias voltage, determines the negative base current ($-dI/dt$) of the power switching transistor. R17 and C12 damp the ringing of the base-emitter and prevents parasitic switch on of T1 during the flyback.

3.6 Secondary rectifiers

The three secondary flyback rectifiers deliver the 150V (line deflection supply), 32V (audio supply) and 16V (small signal supply). A 12V stabiliser is not provided on the PC board. The load determines the dissipation in the rectifying diodes and hence the size of the heatsink (D15) and copper area. The number of electrolytic capacitors is determined by the load (ripple current) and the ESR of the capacitors.

To prevent interference between the SMPS switching frequency and the line frequency an L-C filter has been added. The inductor is L2 while the capacitor is located on the line deflection board. If the SMPS is running in the synchronous mode, the filter action is not required and L2 can be replaced by a 1 Ω resistor. The feedback voltage for the control circuit is taken in front of this L-C filter.

To prevent cross-talk, the audio supply is brought out floating. The negative of the 32V supply is connected to ground via R38 to prevent static charge of this transformer winding if kept unused. If there is an overload on the 32V or 16V supply, the currents in the secondary transformer windings can be excessive before the over-current protection of the IC is activated. The use of a fuse or fusible resistor (1 Ω / 4W) at position J3 and a fusible resistor (1 Ω / 1W) at J4 will make the SMPS short circuit proof also on these two outputs.

3.7 Error amplifier

The error-amplifier consists of a single transistor T5. The base of this transistor receives the filtered and divided output signal while the emitter is connected to the reference voltage (ZD3). The output current of this error-amplifier is fed to the opto-coupler. As the current through T5 and hence its gain will settle at a value inversely proportional to the current gain of the opto-coupler, the SMPS loop gain will be independent of tolerance or ageing of the opto-coupler. The current through ZD3 is fixed by R42 at 2mA. By keeping it constant, the temperature dependence of the V_{be} of T5 is compensated by that of ZD3 [3].

3.8 Opto-coupler

For feedback and mains isolation an opto-coupler (CNG82) is used. As already mentioned before, the opto-coupler is driven in such a way, that the large variation of IC/IF of the opto-coupler is filtered by means of R27 and C19. The emitter of the transistor drives the output-amplifier T2. This transistor is used for keeping the operating voltage of the phototransistor constant; this keeps the bandwidth high.

Except for feedback, the opto-coupler is also used for synchronisation. For this purpose, the sync pulses are superimposed on the linear feedback signal. The slower CNX82A can also be used at the expense of the wave-shape and delay of the sync pulse. Then at 16 kHz the maximum power will be restricted somewhat due to unequal duty factors of the odd and even SMPS pulses.

For standby operation, the opto-coupler diode is driven in forward ($I_F = 2mA$) either by switch-on transistor T6 or by externally driving resistor R43. In this mode the output voltages will be switched off.

3.9 Standby supply

For the supply of some digital IC's in the standby mode, a small self-oscillating, current-mode controlled flyback converter delivers 5V/300mA. It uses the same mains input filter, bridge rectifier and RFI/safety capacitor C22 as the main SMPS. For mains isolation and power conversion a small transformer (AT3006/300) is used. The power switching transistor BUX87 requires a small heatsink [4].

4. Synchronisation

The SMPS can be synchronised down to 32 kHz by either 16 or 32 kHz ($\pm 4\%$) negative-going pulses on pin 5 of J17, with a pulse width of 18% of the line time (Eg. line flyback pulses). The amplitude of the sync-pulse measured at the sync-input, should lie between 2 and 6V. The sync-pulses are superimposed on the linear feedback signal. This can only be done, if they do not affect the voltage stabilisation. To obtain short rise and fall times of the sync-pulse at the sync-input of the TDA8380, the CNG82(A) should be used. Capacitor C16 ac couples the sync-pulses to pin 11 of the

TDA8380. The oscillator sawtooth is triggered by the trailing edge of the positive sync-pulse at pin 11 and all subsequent sync-pulses are ignored until the oscillator sawtooth is completed. The oscillator is then inhibited until the end of the next positive sync-pulse. The free-running oscillator frequency is determined by R11 (4k3) and C15 (680pF). Both components should be 1% tolerance types.

If synchronisation of the SMPS is not needed, the following components can be deleted: C19, C35; R29, R27, R49, R50, R51; D18, R19; T2. The opto-coupler CNG82 can be replaced by the CNX82A. Jumpers J1 and J2 should be in place.

5. Mains interference

RFI measurements are made of the SMPS (200W) together with the μ SOPS and a mains input filter, consisting of the AT4043/93 and two X-capacitors (220nF). The results must stay below the limits of EN55013, which are drawn in the graph shown later. The measurements just meet the limits. If the SMPS is used with more than 165W input power, measures must be included to meet the IEC552-2 standard on mains pollution by higher harmonics.

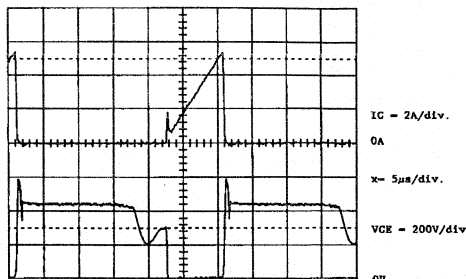
6. Performance

INPUT	185-265V RMS	50/60Hz	
OUTPUTS	150V 1.0A STABILISED	LINE SCAN	
	32V 1.5A UNSTABILISED	AUDIO	
	16V 0.2A UNSTABILISED	SMALL SIGNAL	
RIPPLE peak to peak	150V	$\leq 10\text{mV}$	SWITCHING FREQUENCY
		$\leq 20\text{mV}$	100Hz
	32V	$\leq 150\text{mV}$	SWITCHING FREQUENCY
		$\leq 10\text{mV}$	100Hz
	16V	$\leq 50\text{mV}$	SWITCHING FREQUENCY
		$\leq 10\text{mV}$	100Hz
EFFICIENCY	88%	200W LOAD	
SWITCHING FREQ.	34kHz		

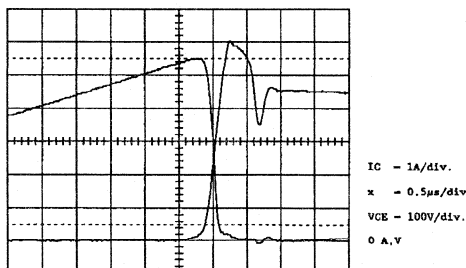
7. Oscillograms

The oscillograms have been made at the following conditions, unless otherwise indicated.

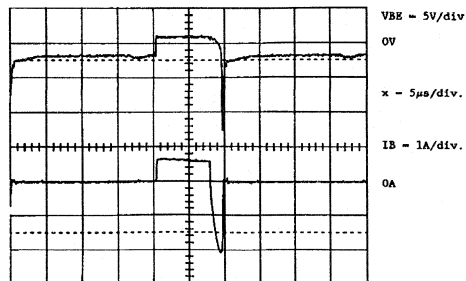
$V_{\text{input}} = 220\text{V RMS}$ Load = 200W not synchronised.



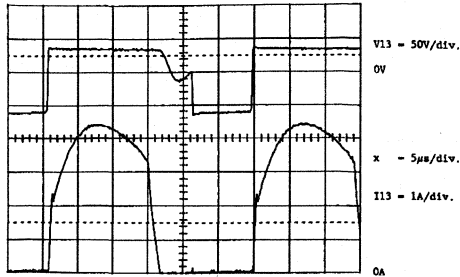
Oscillogram 1. Collector Current and Collector Voltage of the BUW13.



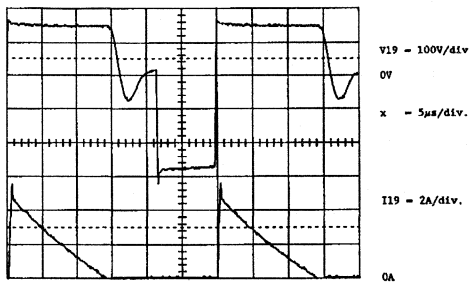
Oscillogram 2. Collector Current and Collector Voltage of the BUW13.



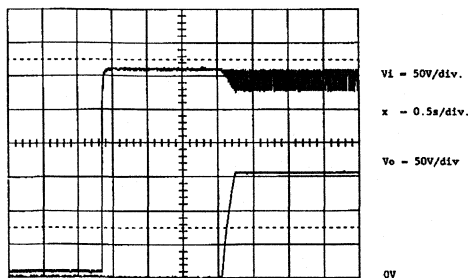
Oscillogram 3. Base Emitter Voltage and Base Current of the BUW13.



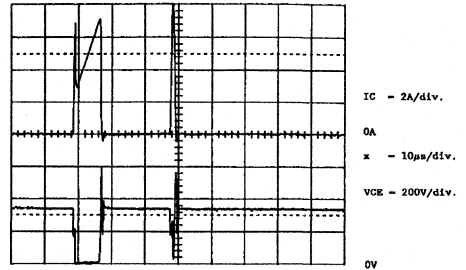
Oscillogram 4. Voltage and Current at pin 13 of the transformer.



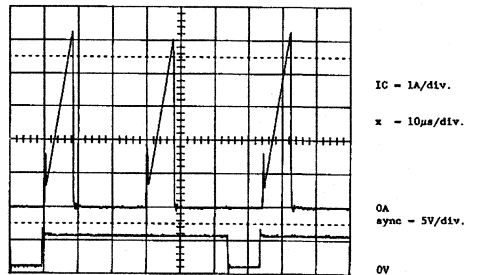
Oscillogram 5. Voltage and Current at pin 19 of the transformer.



Oscillogram 6. SMPS switch on behaviour.



Oscillogram 7. BUW13 Collector Current and Voltage at short circuit 150V output.



Oscillogram 8. BUW13 Collector Current and 15.625kHz sync pulses.

References

Information for this section was extracted from "Synchronous 200W Switched Mode Power Supply for 16 and 32 kHz TV"; ETV89009 by H.Simons.

- [1] Integrated SMPS control circuit TDA8380. Philips Semiconductors Publication Number 9398 358 40011 Date: 12/88.
- [2] ETV8711 A 200W switched mode power supply for 32kHz TV. Author: H.Misdorn. Date: 01/09/87.
- [3] ETV89003 Novel optocoupler circuit for the TDA8380. Author: H.Verhees. Date: 2/89.
- [4] ETV8834 A dual output miniature stand by power supply. Author: H.Buthker.

8. Circuit diagram.

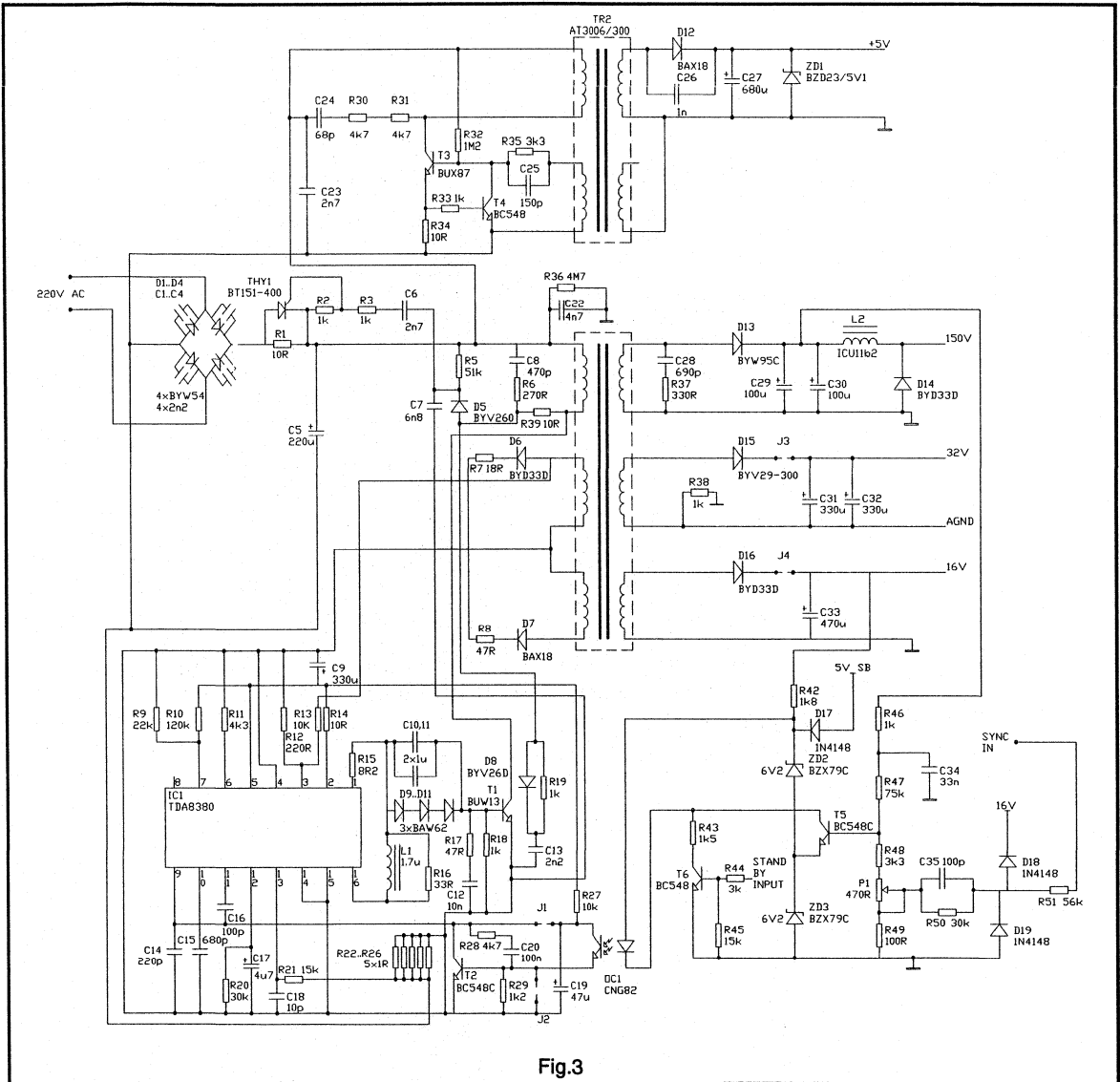
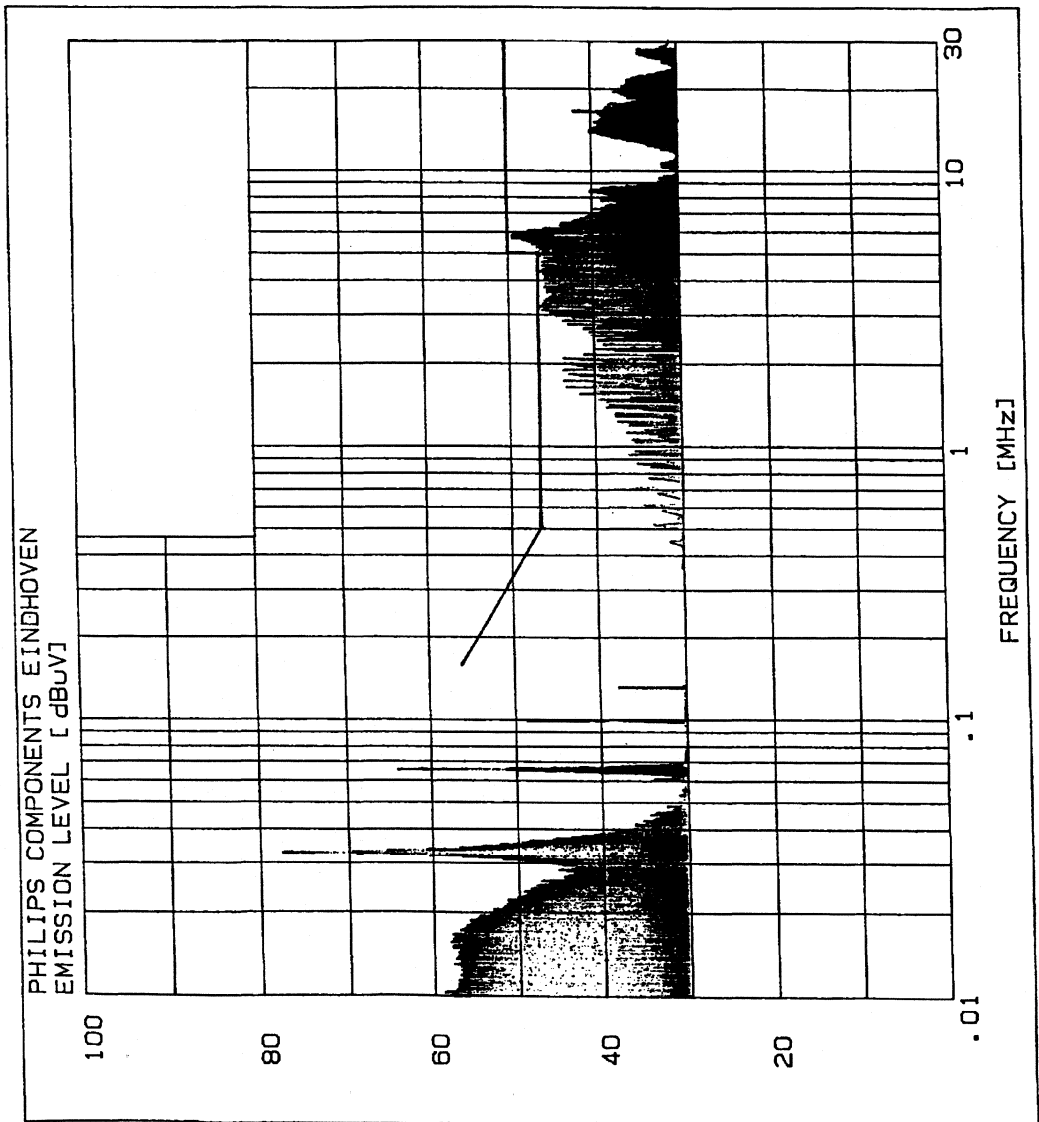


Fig.3

9. RFI measurement



Monitor Deflection Circuit Example



4.4.1 A Versatile 30 - 64 kHz Autosync Monitor

This section describes the supply and deflection circuits for driving the 15" FS M36EDR colour monitor tube. Key features of this monitor design are auto synchronisation, full mains range, dc control, good picture stability and high contrast. The circuit uses a low number of components without making compromises to the performance.

1. Introduction

The increasing number of suppliers of video interface cards, creates a variety of video standards. The most widely used standard at this moment is the VGA mode. Already this standard gives a choice of three different modes, giving resolutions between 720x350 to 640x480 pixels. The horizontal frequency is fixed at 31.5 kHz, while the vertical frequency varies between 60 and 70 Hz.

New standards, with resolutions up to 800x600 and even 1024x768 pixels, are becoming popular very rapidly, although the old standards are still present on these new interface boards.

This increase in resolution calls for larger screens, compared to the nowadays widely spread standard 14" tube, due to the minimum discernible detail at a convenient viewing distance. Furthermore, the electronic drive circuits of the picture tube have to be able to adapt to the various standards.

As a successor of the standard 14" high resolution colour picture tube, the 15" Flat Square M36EDR series tubes offer a noticeable increase in useful screen area (14": 190x262 mm²; 15": 210x280 mm²), while the total cabinet size hardly increases, and offering a resolution up to 1024x768 pixels (pitch is .28mm.). The M36EDR series offers a wide range of deflection impedances and an excellent performance with respect to convergence and geometry distortion, resulting in simple deflection electronics. For the end user, the tube offers a very pleasant flat and square screen, with hardly any disturbing visible effects.

To display the new, as well as the old video standards, on this new tube, the electronic circuits are becoming more complex. For example, to display 768 lines, without disturbing screen flicker, the line frequency must be increased to 57 kHz. The horizontal deflection circuit described in this report is able to synchronise over a continuous frequency range from 30 to 64 kHz, while the vertical frequency may vary between 50 and 110 Hz. The circuit is built around the advanced monitor deflection controller TDA4851, significantly reducing the component count of the total circuit, while providing a high standard of performance. The vertical deflection output stage is the

TDA4861. This power operational amplifier offers the designer great flexibility with respect to input signals and supply voltages.

The increase in resolution also demands that the video channels are able to drive the picture tube with ever higher frequencies, due to the increasing amount of pixels on one video line in a decreasing period of time (increase of line frequency). For example, to display 1024 pixels on one line at 57 kHz line rate, the video amplifiers must be capable of handling dot frequencies up to 65 MHz.

This report covers the electronic circuits for driving the horizontal and vertical deflection coils of a 15"FS tube, for generating all the grid voltages necessary for this tube (the cathodes are driven by the video amplifiers), and a full mains range supply, generating the supply voltages.

2. Supply

This autosync monitor is equipped with a full mains range switched mode power supply (90 - 265Vac) with a maximum output power of about 90W¹. This mains isolated power supply is running asynchronous, because of the large frequency range of the horizontal deflection stage.

To handle the required output power a new wire wound SMPS transformer, the CE422v, was designed. The controller IC is the TDA8380² directly driving the power switch BUT11A. Feedback is obtained through an opto-coupler circuit that senses the +155V output, the line supply voltage. The output voltages of the SMPS are:

- + 155 V @ 350 mA Horizontal deflection and EHT generation
- + 10.5 V @ 450 mA Vertical deflection
- 10.5 V @ 650 mA Vertical deflection and CRT heater
- + 30 V @ 30 mA Vertical deflection (flyback)
- + 12 V @ 400 mA Video, IC and small signal supply

The +12V supply is derived from the +17V supply rail by means of a separate voltage stabiliser.

An extra winding on the transformer, not used in this circuit, delivers a -17V supply. The rectifier and smoothing capacitor are not implemented in this design.

As this switched mode power supply is running asynchronous, additional measures are taken to prevent interference. All output lines are equipped with LC or RC filters.

The +155V rail is protected against short circuit by means of the TDA8380, while the +12V output is protected by the IC voltage stabiliser. To make the low voltage outputs protected against short circuit, fuses or non flammable resistors are used in the output lines.

2.1 Degaussing

The demo monitor is equipped with a conventional automatic degaussing circuit, making use of one duo PTC. For full mains range application the inrush and steady state current are just on the limit. If support is needed please contact the local or regional sales/application office.

2.2 Provisions for full-mains range

To make the SMPS full mains range the following provisions are made:

The slow start capacitor C15 is reduced to 0.47 μ F to shorten the start up time.

The overcurrent protection is extended in order to ensure proper working of the IC with respect to the first trip level.

The IC supply capacitor C13 is increased to 220 μ F to prevent excessive voltage drop during start up.

3. Deflection

The deflection circuit is greatly simplified by making use of the advanced monitor deflection controller TDA4851. This is an upgraded version of the TDA4850 mainly with respect to horizontal line jitter. To accommodate a horizontal frequency range from 30 to 64 kHz, the input frequency is continuously monitored by an F/V converter, in order to adapt the central frequency of the TDA4851. The minimum and maximum frequencies of this circuit are limited by an upper and lower clamp.

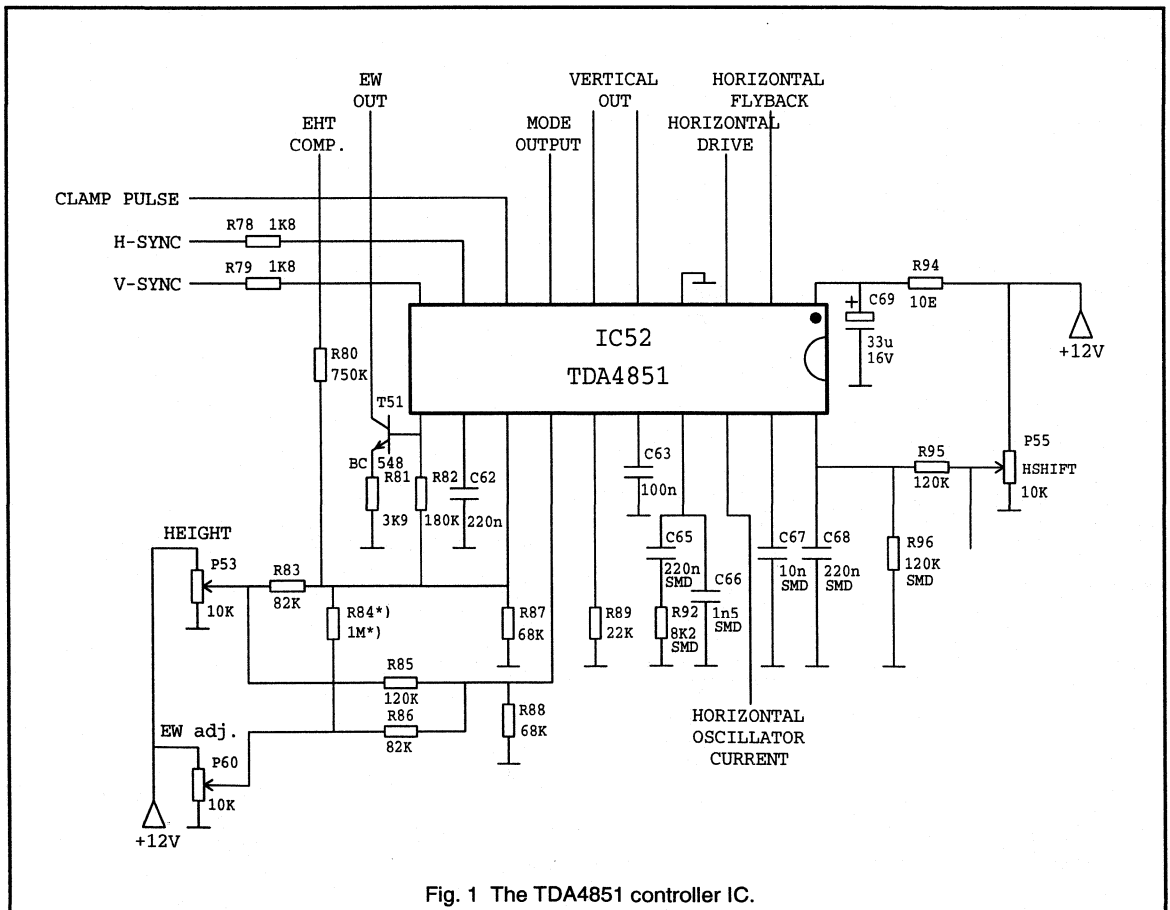


Fig. 1 The TDA4851 controller IC.

The TDA4851 drives a line driver stage and a, so-called, T-on driver stage. The line driver is of the well known transformer coupled non-simultaneous type, giving the designer a free choice where to put the line output transistor with respect to the supply voltage. The T-on driver stage drives a switching transistor, synchronised with the horizontal frequency to control the horizontal scan voltage. The conducting period of this switch is kept constant over the whole frequency range, resulting in a constant picture width, independent of the scan frequency.

The TDA4851 also drives the vertical output stage TDA4861. DC coupling of the deflection coil to this amplifier, together with the high linearity of the drive signals from the TDA4851, offer an excellent linear vertical deflection, without bouncing effects after a mode change.

East-west correction of the horizontal deflection and picture width control is performed by the width control stage.

Horizontal S-correction is performed by one fixed capacitor, plus a selection of three additional capacitors. This minimum set-up is chosen to keep the circuit simple, while giving the minimum amount of distortion at four selected frequencies. The S-correction capacitor selection circuit drives floating FET switches.

Vertical S-correction is achieved by modulation of the vertical amplitude control current with a parabola voltage.

The line output transformer AT2090/01 generates the anode, focus and grid 2 voltages for the picture tube. The built-in bleeder with smoothing capacitor provides an excellent source for retrieving EHT information. This information is used to stabilise the picture width and height.

The primary winding of the line output transformer is also used as the choke of the switch mode scan control stage. This architecture has the advantage of using only four wire wound components: LOT, bridge coil, base drive transformer and horizontal linearity coil.

The auxiliary windings on the line output transformer deliver supply voltages for the grid-1 circuit and video output stages and provide information for the protection circuit.

The various circuits will now be discussed in detail in the next sections.

3.1 Advanced monitor deflection controller TDA4851

The heart of the deflection circuit is the advanced monitor deflection controller, the TDA4851, see Fig. 1. This deflection controller is driven by separate horizontal and vertical synchronisation pulses. Although the TDA4851 can process a sync-on-green signal, this is not implemented in this monitor. The polarity of these pulses can be chosen freely, except for VGA modes, their amplitude must be TTL level. With these pulses, the horizontal and vertical oscillators are synchronized. The horizontal output drives

the line driver, the vertical drive signals are connected to the vertical output stage IC51. A parabola voltage for driving the east-west correction stage and a clamping signal for the video stages are also generated by the TDA4851.

3.1.2 Horizontal part

The horizontal oscillator is synchronized with the pulse on pin 9: TTL amplitude, positive or negative polarity and accepting composite sync (sync-on-green is not implemented in this design). The catching range is limited to $\pm 6.5\%$. The oscillator frequency is set by C67 and the dc current in pin 18, which in this application is set by a dc current source, driven by the frequency to voltage converter. Compared to the TDA4850, the current in pin 18 of the TDA4851 is approximately 10 times higher to achieve a lower phase jitter.

The low-pass filter in the first phase locked loop is connected to pin 17. In a single frequency application, the values of the filter components are fixed. For a frequency range from 30 to 64 kHz, the values of the filter components are set by the lowest frequency, resulting in a less than optimum response for the higher frequencies. For reasons of simplicity, the filter is fixed here, but should be adapted to the actual frequency for best response.

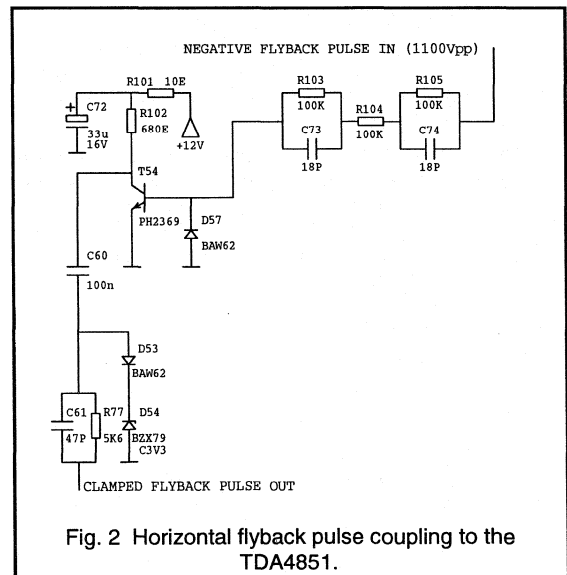


Fig. 2 Horizontal flyback pulse coupling to the TDA4851.

The synchronised horizontal oscillator drives the second phase locked loop, in which the horizontal flyback pulse is used as feedback to position the horizontal drive pulse in relation to the horizontal sync pulse. Low-pass filtering is performed by capacitor C68 connected to pin 20. Phase shift can be accomplished with a dc current in pin 20.

Nominal phase shift is set with resistor R96. User adjustable phase control is available through P55, controlling the dc current in pin 20.

The horizontal flyback pulse is connected to pin 2. The TDA4851 expects a positive flyback pulse, see Fig. 2. The negative flyback pulse from the line output stage is inverted and ac coupled to pin 2 of the TDA4851.

3.1.3 Vertical part

The vertical oscillator can be synchronized with a pulse on pin 10 (or combined sync to pin 9) over a range of 50 to 110 Hz without adjustment and with constant amplitude output signal. Frequency determining elements R89/C63 and the amplitude stabilisation loop capacitor C62, should not be changed.

The output signals of the vertical part are two balanced currents, available on pins 5 and 6. Both currents consist of an equal dc part and an adjustable sawtooth part. The adjustment is achieved by means of controlling the dc current in pin 13. There are five signals which determine the current in pin 13:

1. R87 sets the nominal dc current;
2. P53 allows user control of the picture height via R83;
3. By means of R82, the amplitude control current is modulated with a parabola current. In this way, vertical S-correction is achieved. The disadvantage of this method, is that the amount of S-correction is dependent on the setting of the east-west control potmeter P60.
4. R84 compensates for a change of the east-west correction voltage (explanation: when the east-west voltage on pin 11 is changed by means of the 'EW par.' potmeter P60, the mean dc voltage on pin 11 changes, influencing the vertical amplitude via R82).

The influence of the east-west setting on the vertical amplitude is small, therefore, R84 is marked optional, it's not absolutely necessary.

5. Changes in the EHT voltage compensate the vertical amplitude via R80.

3.1.4 East-west parabola

A parabola voltage is available on pin 11, for driving the pincushion correction stage. The bottom of this parabola voltage, equal to the middle of the screen, is set internally on 1.2V, independent of the amplitude setting. In this way, adjusting the parabola amplitude changes the horizontal width in the corners only, while the amplitude in the middle of the screen remains constant.

Amplitude adjustment of the parabola voltage is achieved by a dc current in pin 14. No user control is available, adjustment is only possible with P60 on the main deflection/supply printed circuit board. The amplitude of the parabola voltage is corrected for changes in the vertical amplitude setting by means of R85. The amplitude of the parabola voltage is independent of the vertical scan frequency.

The parabola voltage from pin 11 is connected to the base of T51. The collector current is then transferred to the picture width driver. In that stage the amplitude is multiplied with the horizontal frequency, to achieve a correction independent of the horizontal frequency.

3.5 Miscellaneous I

A clamping signal for the video pre-amplifier, ic TDA4881, is generated in the TDA4851. This clamping signal is available on pin 8, and is only present when horizontal sync pulses are present on pin 9.

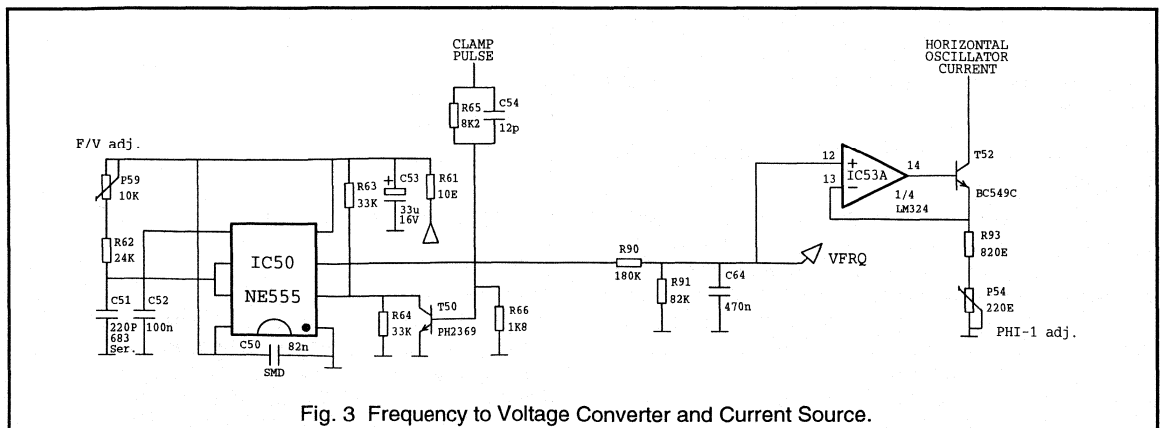


Fig. 3 Frequency to Voltage Converter and Current Source.

The mode input/output pin 7 is connected to a switching transistor T76. This transistor is driven by comparator IC56B. This comparator detects whether or not the incoming horizontal frequency is below 33 kHz. In this case, the TDA4851 assumes a VGA signal is present, resulting in an automatic adjustment of the vertical amplitude, depending on the sync. polarity. Above 33 kHz, the internal mode detector of the TDA4851 is switched off with T76, to prevent automatic vertical amplitude adjustment.

3.2 Additions to the TDA4851 for auto-synch operation

Since the catching range of the horizontal section of the TDA4851 is only $\pm 6.5\%$, the frequency range from 30 to 64 kHz cannot be covered without extra circuits. To accommodate the specified range, the horizontal oscillator current (pin 18) is constantly adapted to the incoming horizontal sync pulse frequency. This is achieved by means of a frequency to voltage converter driving a current source. To protect the power output stages from too low and too high frequencies, voltage clamps on the drive voltage of the current source keep the frequency of the horizontal oscillator of the TDA4851 within the specified limits of 30 to 64 kHz.

3.2.1 F/V Converter

The frequency to voltage converter is built around one-shot IC50, see Fig. 3. R65/66 attenuate the signal from pin 8 of the TDA4851 in such a way that only the horizontal clamp pulses (5.5Vpeak) and the vertical blanking pulses (1.9Vpeak) do not drive T50. This has the advantage that the incoming horizontal sync pulse is not disturbed in any way, and the sync pulse polarity and amplitude variations of the incoming sync pulse are of no influence to the circuit.

The output pulses of IC50 pin 3 are attenuated and filtered with R90/91 and C64. The dc voltage VFRQ is used to drive the current source and the S- correction capacitor selection circuit. The width of the output pulse of the one-shot can be adjusted with P59 (F/V adj.). This potmeter should be adjusted in such a way, that the switching of the S-correction capacitors is performed at the desired frequencies.

The conversion factor S of this F/V converter is:

$$S = \{t_c + 1.1 \times (R_{62} + P_{59}) \times C_{51}\} \times \{R_{91} / (R_{90} + R_{91})\} \times U_o$$

where:

t_c width of the TDA4851 clamp pulse: $1\mu s$

$1.1 \times (R_{62} + P_{59}) \times C_{51}$ width of the output pulse of the one-shot IC50: $5.81 - 8.23\mu s$

$R_{91} / (R_{90} + R_{91})$ attenuation of the output pulse: 0.313

U_o amplitude of the output pulse: 10.8V

The duration of the output pulse of the one-shot is affected by the trigger pulse. During time t_c the output voltage is already high, while the charging of C51 is halted. This results in:

$$S = 23.0 \text{ to } 31.2 \text{ mV / kHz}$$

The voltage VFRQ can be found with the following formula:

$$V_{FRQ} = F_H \times S$$

where F_H is the horizontal scan frequency. With $S = 27.1\text{mV/kHz}$, this results in:

$$V_{FRQ}(31.47 \text{ kHz}) = 31470 \times 27.1 \times 10^{-3}$$

$$V_{FRQ}(31.47 \text{ kHz}) = 853 \text{ mV}$$

and:

$$V_{FRQ}(63.69 \text{ kHz}) = 63690 \times 27.1 \times 10^{-3}$$

$$V_{FRQ}(63.69 \text{ kHz}) = 1726 \text{ mV}$$

Because the resistor divider for the s-correction capacitors is fixed, the conversion factor S is adjusted to the voltage VREF, feeding the divider.

3.2.2 Current source

The current source for driving pin 18 of the TDA4851 is build around op. amp. IC53A and T52.

The collector current of T52 can be adjusted with P54 to adapt to the actual conversion factor S and for the tolerance on the oscillator capacitor C67 on pin 19 of IC52. This must be done after the conversion factor S is adjusted with P59 to the correct s-correction switching frequency.

3.2.3 Voltage clamps

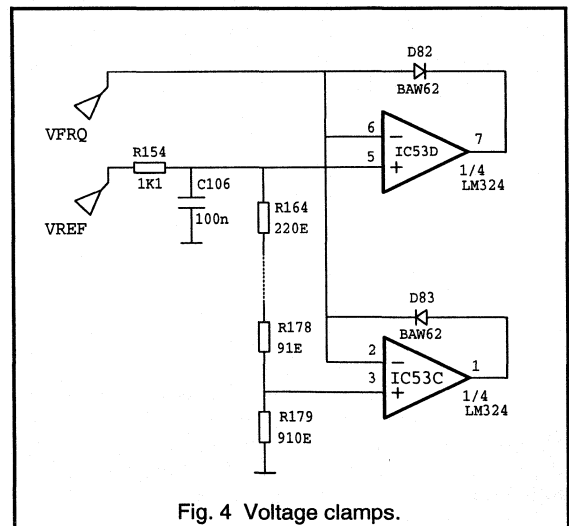


Fig. 4 Voltage clamps.

To prevent the horizontal power output stage from running at either too low, or too high, a frequency, the drive voltage for the current source is limited. IC53C limits the lower voltage and IC53D the upper voltage, see Fig.4. The frequency range of the TDA4851 is now limited to 30 kHz minimum and 66 kHz maximum.

Reference for the comparators IC53C/D is a voltage divider network, driven by IC53B. The input voltage for IC53B is the temperature compensated reference voltage at pin 15 of the TDA4851.

3.3 Horizontal scan control driver

In order to keep the picture width constant, independent of the horizontal scan frequency, the scan voltage is continuously adapted. The relation:

$$V_{\text{scan}} = L \times I \times f_H$$

is valid. From this equation, it can be seen that with increasing scan frequency, the supply voltage must also increase proportionally.

Realisation of this demand is in fact quite simple. The horizontal drive pulse from the TDA4851 triggers one-shot IC54. The output pulse width of this one-shot is constant, independent of the trigger frequency. Therefore, the duty-cycle increases with increasing frequency. Via buffer stage T62/T63, FET switch T64 is controlled. In this way, the scan voltage for the horizontal deflection output stage is controlled, according to the previously stated relation.

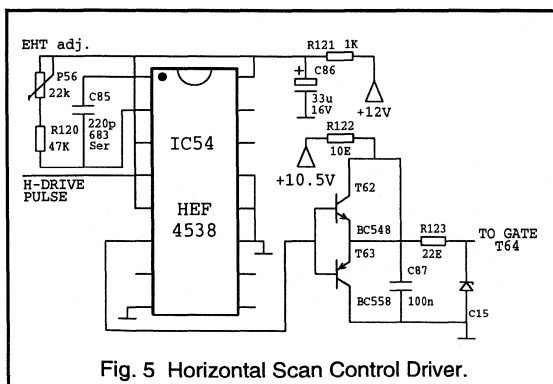


Fig. 5 Horizontal Scan Control Driver.

IC54 is a retriggerable one-shot, see Fig. 5, which is important at higher scan frequencies (above 66 kHz), where the duty-cycle becomes 1.0. In case of a non-retriggerable one-shot, the duty-cycle would suddenly drop to 0.5. This would not only result in half the deflection amplitude, but also in a drop of the EHT.

One other important item is the phase relation between the drive pulses of T53 and T64. When the horizontal output stage is in the flyback part, T64 must always conduct (in order to keep the EHT constant). This is realised by choosing the appropriate trigger edge (positive edge of the horizontal drive pulse) and by a lower limit of the adjustment range of the pulse width, to ensure T64 is conducting all through the flyback period of the horizontal deflection stage.

3.4 S-correction capacitor selection

The necessary value of the S-correction capacitor varies with the horizontal frequency, given a certain deflection coil impedance and screen radius. The correct capacitor value is chosen from eight different values through a combination of one fixed and a choice of three capacitors.

The voltage VFRQ, representing the horizontal scan frequency, is connected to the inverting inputs of seven comparators IC56/57. Each non-inverting input of these comparators is connected to a different output of a resistor ladder R154/164-170/178/179. This resistor ladder is fed by a voltage VREF.

At pin 15 of IC52 a temperature compensated voltage of, typically, 3.0V is available for setting the vertical oscillator current (R89). To avoid extra loading of this pin, a voltage follower with high input impedance IC53b is used. The output of op. amp. IC53b is a stable dc voltage with very low output impedance: VREF.

Resistors R171 to R177 provide each comparator with some hysteresis to prevent parasitic oscillations on the switch-over points.

The comparator outputs are connected to an 8-3 multiplexer IC58. The outputs of IC58 drive transistors T73/74/75. These transistors can withstand the possible high voltages (max. 150V) that drive the S-correction capacitor switches.

D79/80/81 are added to prevent T73/74/75 from break down during line flyback. In this way, the selection of the resistors sets the frequencies when the circuit switches to another S-correction capacitor value.

3.5 Picture width driver

Since pin-cushion distortion is a fixed percentage of the scan voltage, the peak to peak parabola voltage, correcting the pin-cushion distortion, must be adapted to the actual scan frequency. This multiplication is achieved in the same manner as the scan voltage for horizontal deflection is adapted.

One-shot IC55, see Fig. 7, is triggered with pulses having the same frequency as the horizontal scan frequency. But now, also the parabola voltage modulates the width of the output pulse. This output pulse is integrated through R138/C98; the voltage drives a common base stage T69.

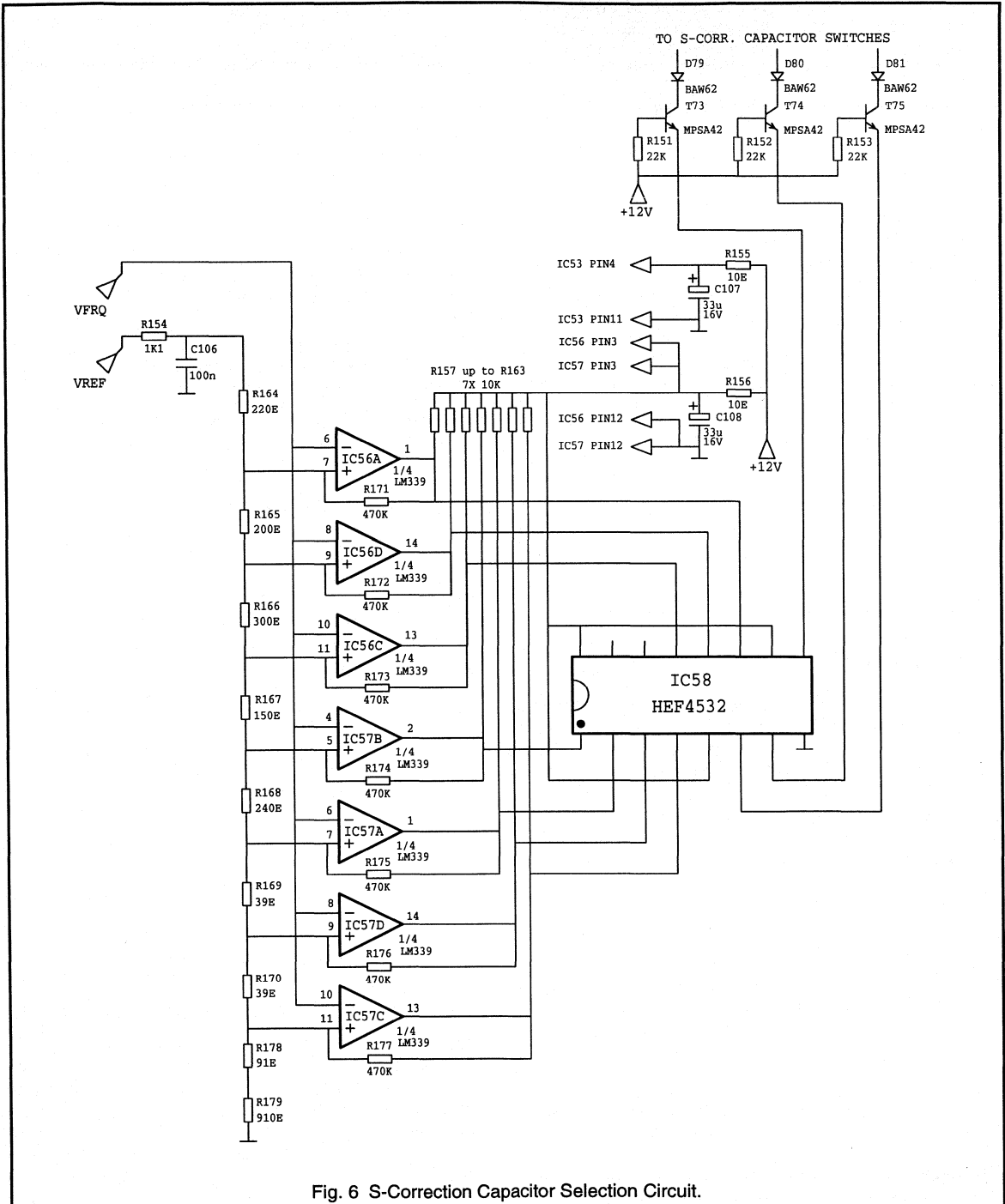


Fig. 6 S-Correction Capacitor Selection Circuit.

In this way, the modulation is converted to the collector current of T69 (IEW), simplifying the interface to the east-west power stage, which is connected to the +155V supply.

Two other functions are also incorporated in this part of the circuit:

- User control of the picture width via P58; and
- Compensation for variation of the EHT; achieved through R136 - the information is supplied by the EHT compensation circuit.

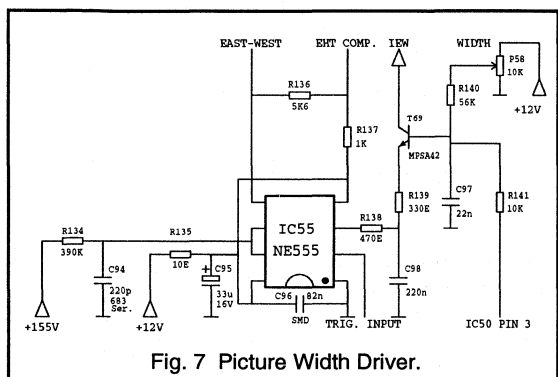


Fig. 7 Picture Width Driver.

3.6 Horizontal deflection output stage

To allow a frequency range of 30 to 64 kHz, additional measures have to be taken to keep the deflection current and the EHT constant. This is realised by continuously adapting the scan voltage to the horizontal frequency by means of the horizontal scan control. The scan control switch T64 is connected to ground, resulting in simple gate drive. The horizontal deflection output transistor T55 is connected to the supply rail because the driver transformer L50 already provides isolation. The primary winding of the Line Output Transformer L54 is used as a choke.

This set-up of horizontal deflection has two disadvantages:

1. The pincushion correction stage is either floating or connected to the same supply rail as the line output transistor, T55. In this concept, connection to the supply rail is chosen, and driving it with a current IEW from the small-signal circuit.
2. The S-correction capacitor switches are floating, which makes it less simple to drive them.

The biggest advantage of this deflection stage is that a minimum of wire wound components has been used.

3.6.1 Line driver stage

The circuit is shown in Fig. 8. As driver device T53 a small MOSFET (BSN274) is chosen. Its advantages over a bipolar device on this particular application are: less power dissipation (enabling smaller encapsulation), less drive power required, better switching behaviour and no storage time (so no additional stress on the Φ_2 loop). To protect the gate the standard precautions (zener diode and series resistor) are taken.

The driver transformer is equipped with a damper network at the primary side (C71/R98) to damp excessive ringing. On the secondary side a damper (C76/R107) is present between the base and emitter of the deflection transistor T55.

In order to achieve sufficient negative drive voltage during flyback, resistor R106 and diode D58 are added. Proper $-di_v/dt$ is achieved by the leakage inductance of L50.

When the X-ray protection is activated, the inverting driver stage will be turned on continuously. This will switch off T55, but also cause a low frequency swing in the driver transformer. To prevent voltage inversion across the primary winding of driver transformer L50, which would turn on the deflection transistor T55 for a relatively long time, D55 is added. A second measure, that must be implemented when X-ray protection is installed, is increasing the power rating of the current source resistor R97 to 16W (!) or using an electronic resistor with a current fold back characteristic.

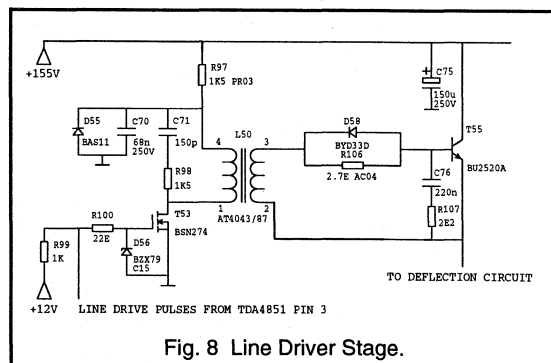


Fig. 8 Line Driver Stage.

3.6.2 Horizontal scan control output stage

At double the line frequency, the scan voltage must be doubled as well to have the same picture width on the screen. Furthermore, the supply voltage to the line output transformer must be proportional to the horizontal line frequency to have constant EHT over the whole frequency range. To achieve this, a synchronous switching series regulator is added. This series regulator operates with a constant T-on time.

3.6.3 Power output stage

The power output stage, see Fig. 11, is a conventional one with a diode modulator.

Because this stage is connected to the supply rail, the flyback pulse has negative polarity. This makes the use of T54, see Fig. 2, necessary because the deflection controller IC52 expects a positive flyback pulse.

As lower damper diodes two low voltage diodes BYW96D in series are chosen because they switch faster than one single high voltage device.

As deflection transistor, the BU2520A is chosen. This device performs remarkably well over the frequency range of 30 to 64 kHz.

The value of flyback capacitor C78 depends on the impedance of the line deflection coils and the desired flyback time. With 180µH deflection coil impedance, C78 should be 5n6/2kV, with 220µH impedance, C78 should be 4n7/2kV.

3.6.4 East-west power stage

To drive the diode modulator, the drive current "IEW" must be converted to a voltage by means of R109. A power buffer T56/57, see Fig. 12, drives the diode modulator. To prevent high ac currents from flowing through T56, an additional filter R108/C80 is added.

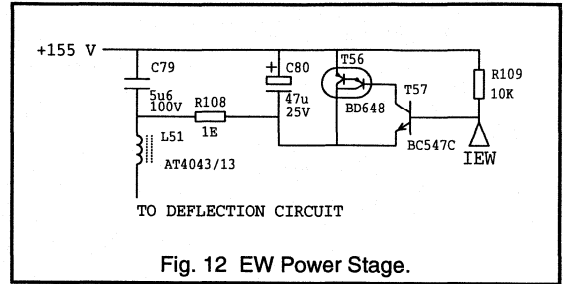


Fig. 12 EW Power Stage.

3.6.5 S-correction capacitor switches

The curvature of the screen determines the percentage S-correction. This percentage is constant and independent of frequency. Since the scan voltage is adapted according to the horizontal frequency, the S-correction voltage also has to be adapted, according to the frequency. The value of the S-correction capacitor is determined with the following equation:

$$C_s = T_p^2 / (8 \times \sigma \times L_n)$$

where:

- T_p = the visible line period time;
- σ = the percentage of S-correction;
- L_n = the impedance of the deflection coil.

With a constant flyback time of 3µs, this gives the results as shown in Fig. 14. These values are realised in the circuit shown in Fig. 13.

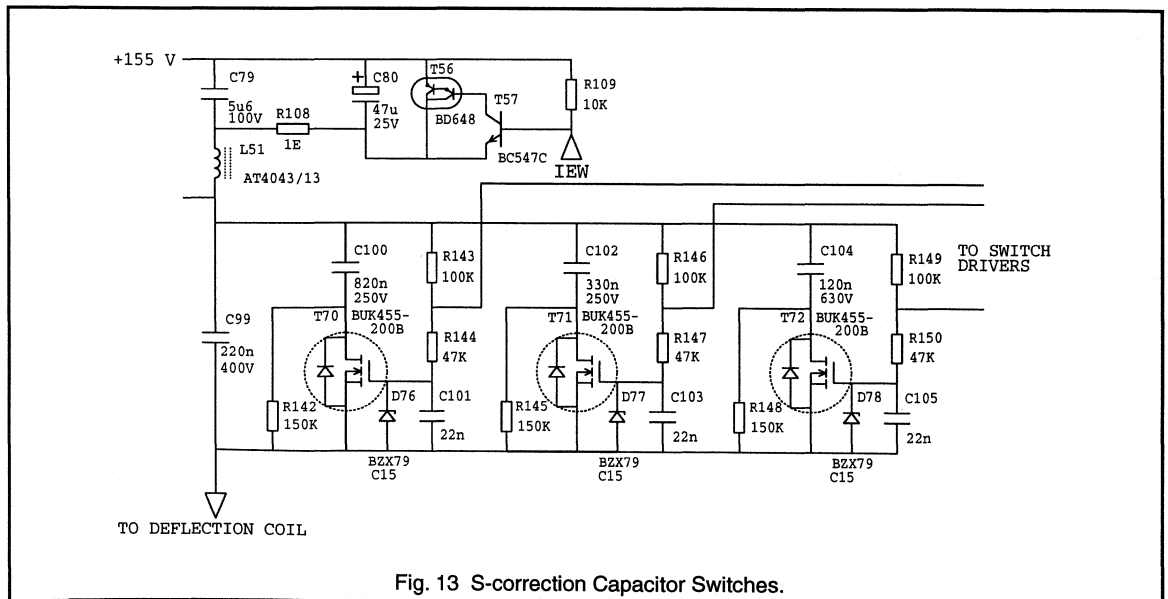
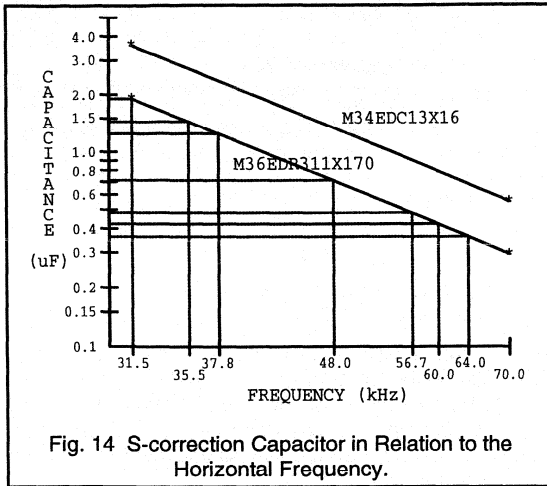


Fig. 13 S-correction Capacitor Switches.

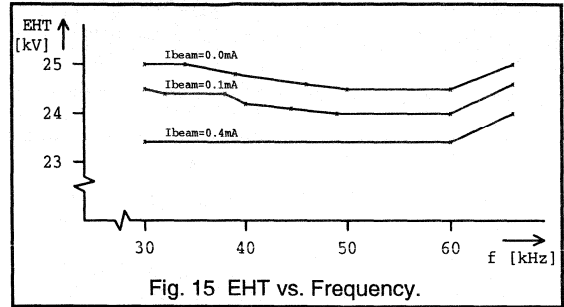


Each switch contains a MOSFET with built-in anti parallel diode, see Fig. 14. When, for instance, T75, see Fig. 5, is not conducting, C101 will be charged via R143/144 and T70 will conduct. D76 prevents the gate from too high voltages. When T75 conducts, the voltage at C101 will be zero and T70 will block. Such a switch can also be build with a bipolar device, however that would require a higher drive current, resulting in high losses because of the ac and dc voltage difference between drive and switch.

The switch itself functions as follows. During the first part of scan the current is conducted by the MOSFET; the S-correction capacitor will be charged. During the second part of scan the current will be conducted by the anti parallel diode. In case the MOSFET is not conducting, the S-correction capacitor will not be charged during first part of scan, except from a very small current through the resistors parallel to the MOSFET switches. So, during the second part of the scan the V_{DS} will remain positive and the anti-parallel diode will not conduct.

3.6.6 EHT, Focus and Vg2

The EHT, focus and Vg2 are generated by the Line Output Transformer (LOT) AT2090/01. This transformer can be used up to 85 kHz and has a built-in bleeder (with focus and Vg2 potentiometers) and an EHT smoothing capacitor of 3nF. Not only the flyback but also the scan voltages are frequency independent. So, auxiliary voltages can be extracted from the LOT in the ordinary way. There is one exception: often the heater voltage for the CRT is taken from an unrectified winding of the line output transformer. Since due to T-on the RMS value is not frequency independent, the CRT heater must be supplied from a rectified winding. For practical reasons in this design an SMPS voltage was more suited (-10.5V).



3.7 Vertical deflection

The vertical deflection output stage used in this design is the TDA4861 (IC51), see Fig.16. This vertical output stage can be considered as a power operational amplifier with an extra flyback generator and guard circuit.

The inputs are driven by the balanced outputs of the TDA4851. The TDA4851 supplies complementary drive currents, which can be directly connected to the input pins of the output stage.

To determine the values of resistors R71/75, conventional operational amplifier theory is applicable. This theory says that, in practical cases, the differential input voltage of an operational amplifier always equals zero:

$$V_2 = V_3$$

$$I_{out} \times R_{72} - I_{drive} \times R_{71} = I_{drive} \times R_{75}$$

For simplicity of design, R71 and R75 have the same value R_i :

$$R_i = I_{out} \times R_{72} / (2 \times I_{drive})$$

The peak output current is the peak current for the deflection coil used in the design (here peak $I_{out} = 0.75A$), I_{drive} is the drive current from the TDA4851: $250\mu A$. The value of resistor R72 can be chosen freely within certain limits:

1. The power dissipation in the resistor may not exceed the power rating of the resistor used;
2. The voltage drop across R72 is subtracted from the total available peak to peak coil drive voltage;
3. The minimum resistance is limited by the ground plane, which introduces a tolerance that has to be minimised with respect to the resistor value.

A good choice for R72 is 1Ω , the lowest available resistor value in the normal range. This leads to the following result:

$$R_i = 0.75 \times 1 / (2 \times 250 \times 10^{-6})$$

$$R_i = 1500 \Omega$$

Amplitude control is realised by adjustment of the output of the TDA4851.

Vertical shift, a user control, is possible by P52. Injecting a dc current in one of the summation points, results in a dc current through the deflection coil. The 0 to +12V from the potmeter P52 is translated into a dc current in R71 by means of resistors R73/74. Design considerations for these two resistors are: a potmeter in middle position (the dc current in the coil should be zero) and the maximum shift range.

The resistors values in the circuit diagram allow a shift range of ± 15 mm.

The output of the TDA4861 is DC coupled with the deflection coil, resulting in a bounce-free behaviour. Together with the fast response of the TDA4851 after a frequency change, this combination offers a stable picture within two frames.

For stability reasons, the combination R70/C56 is added between the output and the most negative supply voltage. If no damping resistor is present on the deflection coil, R69 should be added. Its value has to be determined experimentally.

The supply voltages for the TDA4861 are ± 10.5 V, allowing simple dc coupling of the deflection coil. For flyback, an extra supply voltage of +30V is connected to pin 8. This results in a fast flyback of 300 μ s.

The vertical guard pulse, available on pin 9, is connected to the Vg1 circuit to provide vertical blanking and protection in case no deflection coil is connected.

Diode D52 protects the TDA4861 in case the flyback voltage is missing or drops faster than the +10.5V at switching off of the circuit.

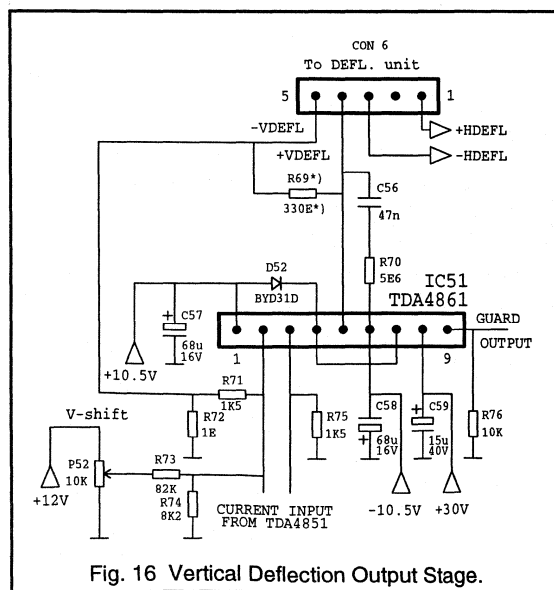


Fig. 16 Vertical Deflection Output Stage.

3.8 Miscellaneous II

3.8.1 EHT compensation

With the aid of the built-in EHT capacitor and focus / Vg2 divider in the LOT, the EHT voltage can be monitored in a very easy way. When the time constant of these built-in components is equal to the time constant of (R128+P57)/C92, then at LOT pin 12 an exact (divided) copy of the EHT can be found. This signal is buffered by T66 and inverted by T67, see Fig. 17.

Due to the tolerance on the Focus / Vg2 bleeder an adjustment is required (P57).

The EHT information signal goes to T68, the inverted signal modulates the picture width driver, in order to compensate the horizontal deflection for EHT variations. The non-inverted output of T68 is fed to the vertical amplitude control pin of the TDA4851 to compensate the vertical deflection for EHT variations.

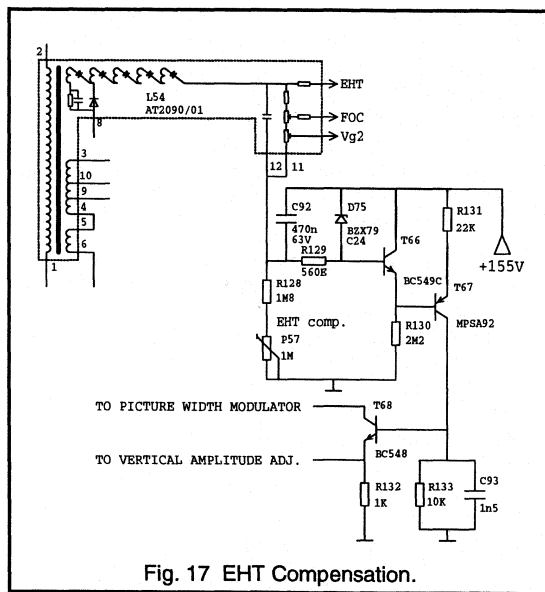


Fig. 17 EHT Compensation.

3.8.2 Beam current limiting

The long-term average anode current for the given tube is 700 μ A. This current is measured at the lower side of the EHT winding of the LOT, L54. The anode current flows through resistor R126, connected to the +12V rail. When the voltage across this resistor increases (with increasing anode current), the base voltage of T65 drops. With a high contrast setting, 6V dc on pin 9 of connector 2, the beam current limiter (BCL) will be activated at an average anode current of:

$$I_a = \{ +U_v - U_{contrast} + U_{be}(T65) + U(D74) \} / R126 - I_{bleeder}$$

$$I_a = \{ (12 - 6 + 0.65 + 0.5) / 15,000 \} - \{ 25,000 / (300 \times 10^6) \}$$

$$I_a = 394 \mu A$$

3.8.3 Vg1 supply

This monitor is equipped with an ac coupled video output stage, using a supply voltage of 65V. After dc restoration, the highest black level is approximately 45V, with respect to ground. This implies that, with a tube requiring a cut-off of 125V, Vg1 must be -80V.

At C84 a negative flyback pulse is rectified (-130V). During normal operation T58 is saturated and Vg1 will be -80V. If T58 is not conducting, Vg1 will be -130V which will cut-off the tube completely. This will be the case in the following conditions:

- vertical guard (failure in the vertical output stage;
- absence of vertical supply (+10.5V); and
- absence of horizontal deflection (e.g. power switch off).

Vertical guard. When the vertical output stage generates a vertical guard pulse, via D64 the base of T58 will become high, which will turn off this transistor. Vg1 will be -130V.

Absence of vertical supply. When there is no vertical supply, the vertical output stage can not generate a guard pulse either. Therefore, the Vg1 circuit is connected to the vertical supply rail. When the +10.5V supply is missing, T58 cannot conduct, resulting in Vg1 = -130V.

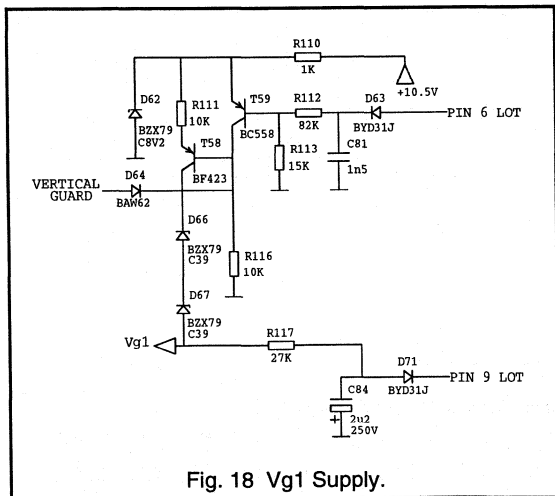


Fig. 18 Vg1 Supply.

Absence of horizontal deflection. When there is no horizontal deflection the line flyback pulse will be small or not present at all. This line flyback pulse is peak-peak rectified at C81 and thus keeping T59 blocked. When flyback pulses disappear, caused by a failure in the Line

Output Stage or at switch-off, T59 will conduct, causing T58 to be blocked, and Vg1 will be -130V (C84 is large enough to hold Vg1 on -130 Volts until the EHT is discharged).

3.8.4 Blanking for TDA4881

Horizontal blanking pulses are derived from the line flyback pulses as delivered by the circuit around T54, see Fig. 2. The cathode of D51 is connected to the collector of T54. To limit the amplitude of the blanking pulses, D50 is added, see Fig. 19.

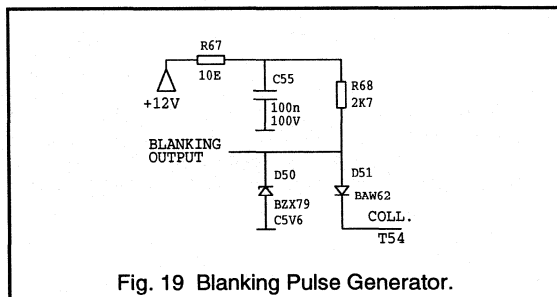


Fig. 19 Blanking Pulse Generator.

3.8.5 Video supply

The ac coupled video output amplifiers require a supply voltage of:

$$V_s = V_{swing} + V_{min} + (V_s - V_{max})$$

$$V_s = 50 + 10 + 5 V$$

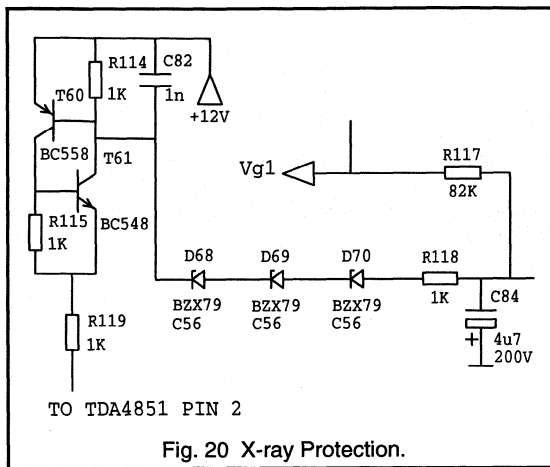
$$V_s = 65 V$$

The secondary windings 3-4 and 5-6 of the LOT, L54, are connected in series and stacked on the +10.5V supply. The output voltage of rectifier diode D65 and capacitor C83 is 66V.

3.8.6 X-ray protection

A failure in the horizontal scan control section, could cause a dangerous situation: the EHT might rise to an unacceptable high level. The thyristor, consisting of T60/61, see Fig. 20, is fired when the flyback voltage rises to an unacceptable level. The flyback input pin 2 of the TDA4851 is forced high. This causes the horizontal drive output pin 3 of the TDA4851 to be turned off (output voltage is high). The line driver will be turned on, turning off the line output transistor. The T-on driver will not be triggered any more. The result is that the complete line output stage stops working, so that the EHT will drop automatically.

Blanking is achieved, through the normal blanking circuit. Furthermore, the Vg1 voltage will also drop, in order to cut-off the tube.



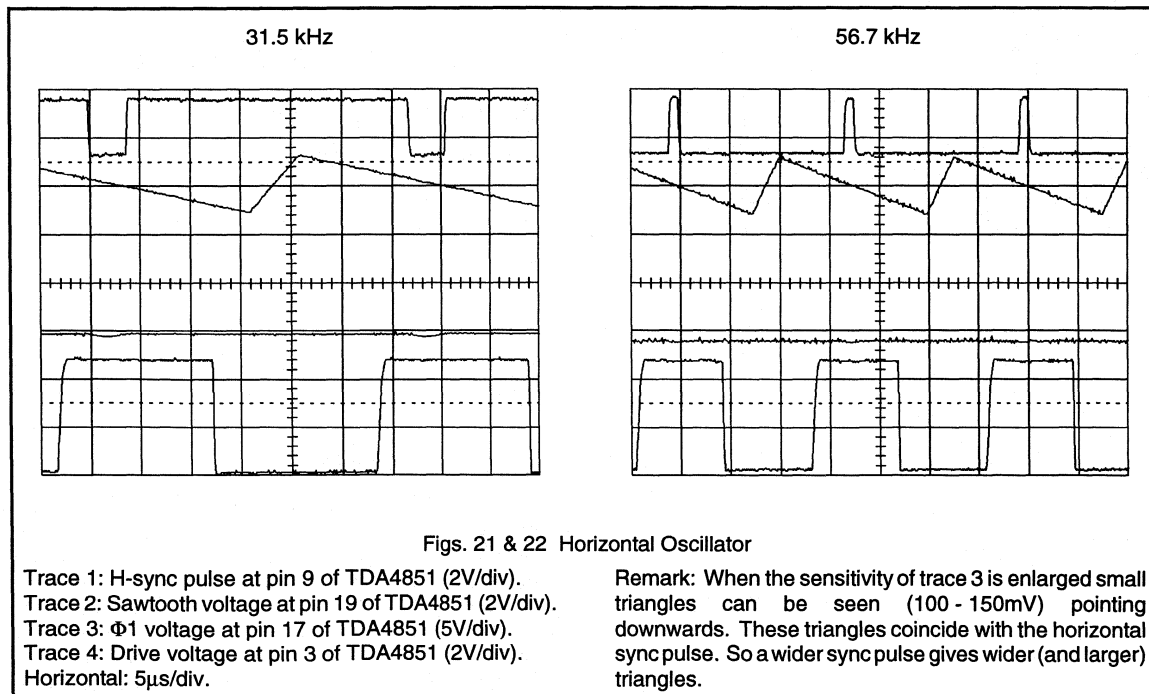
4. Oscilloscopes

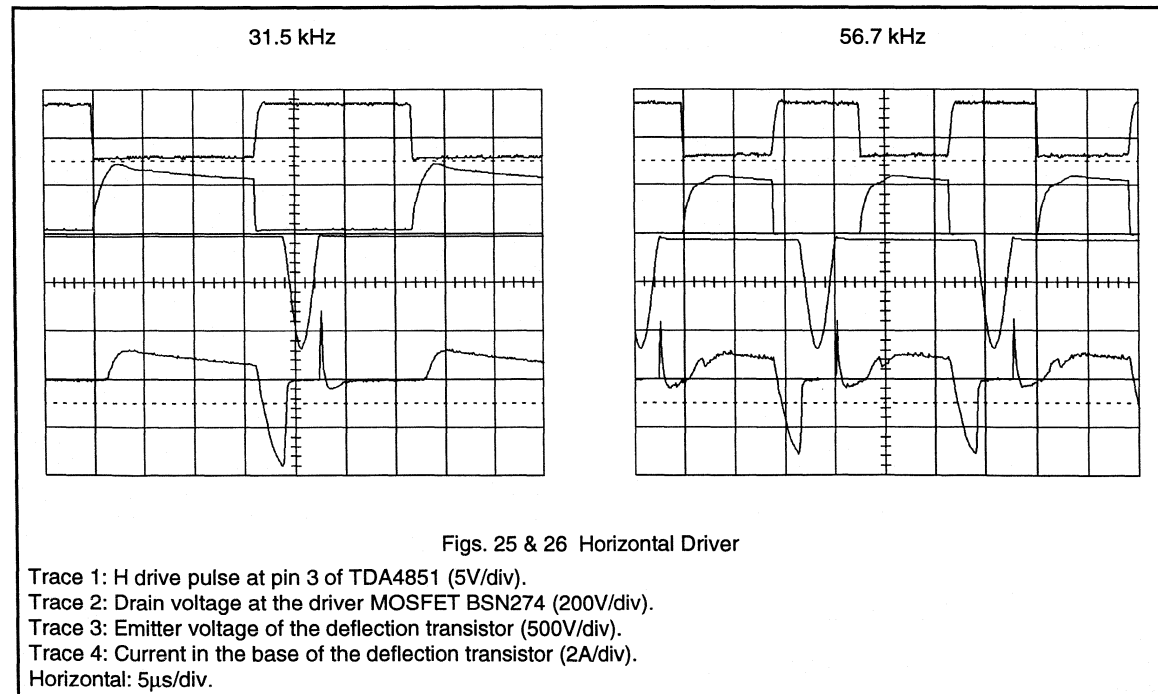
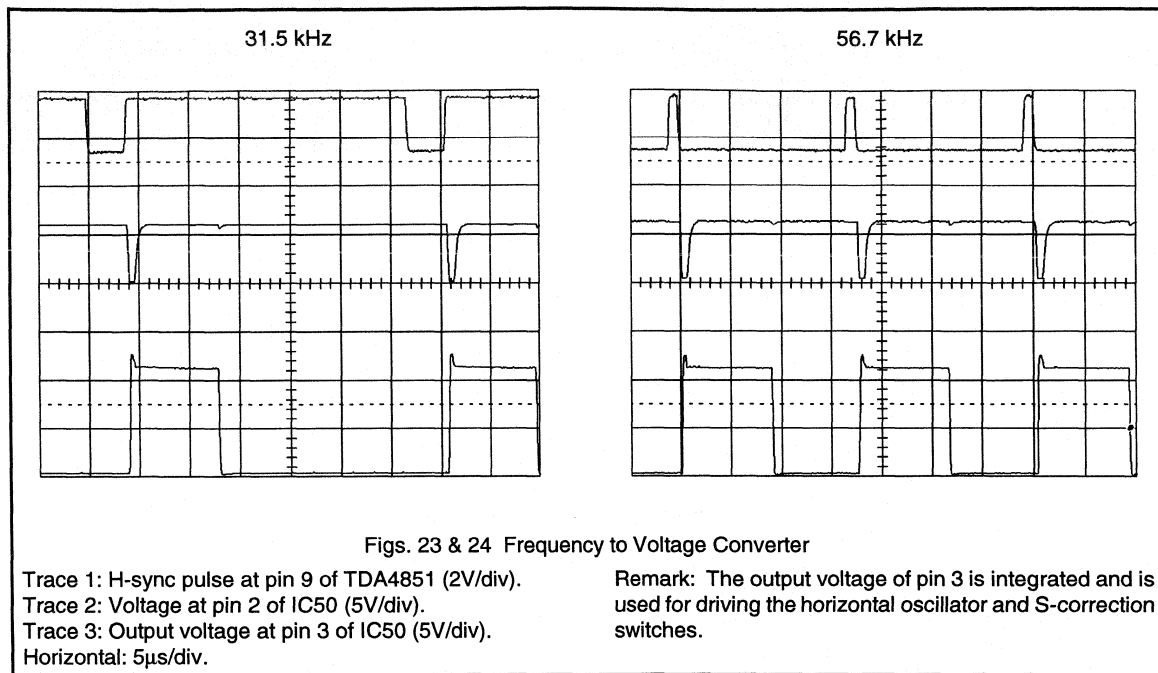
The oscillograms given are meant as a guide-line in debugging and aligning the circuit and together with the above text it can also be of help in understanding the circuit.

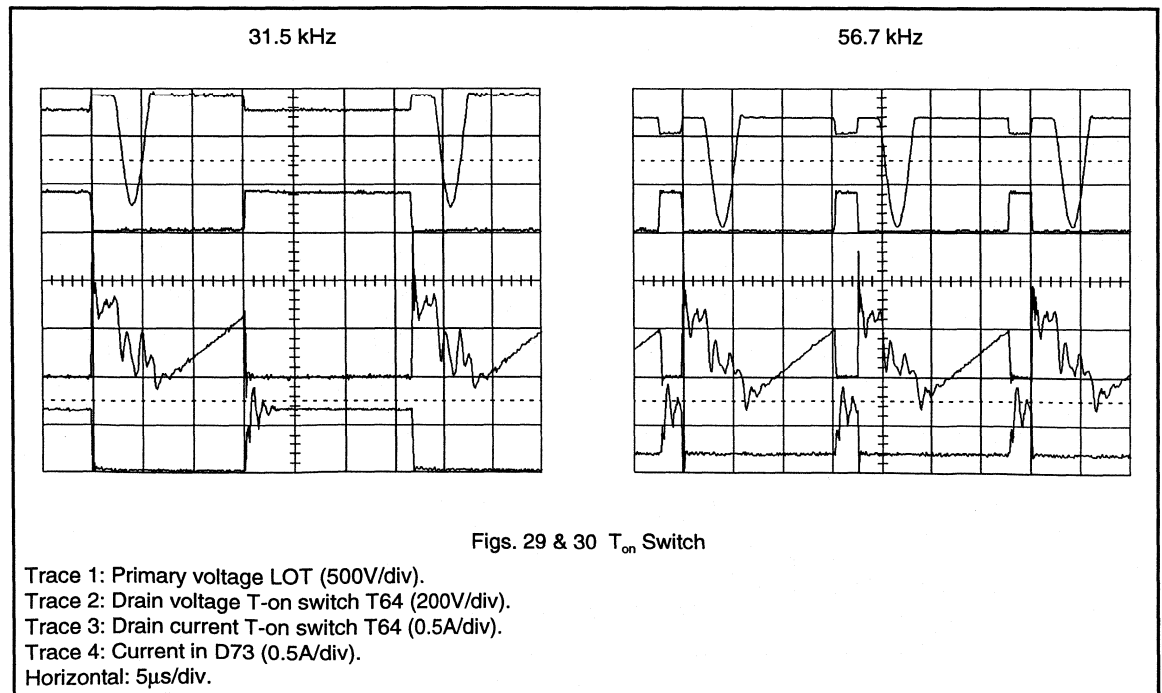
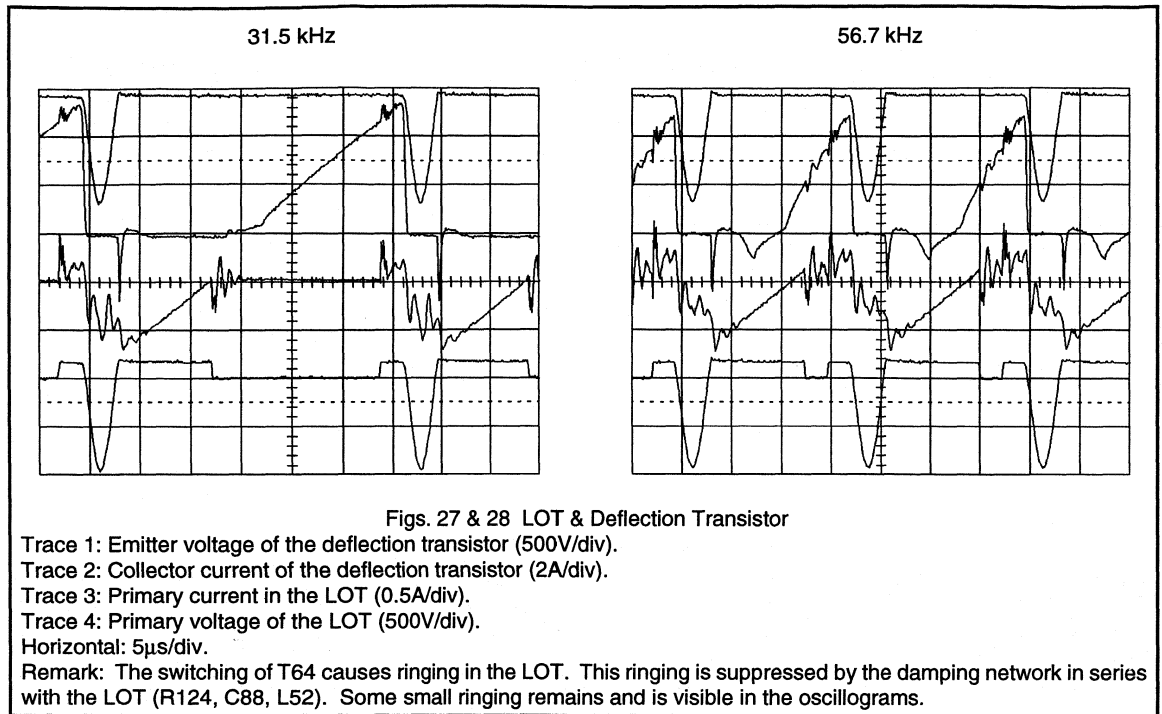
All oscillograms concerning the horizontal sync processing and deflection are given at two frequencies (31.5 & 56.7 kHz).

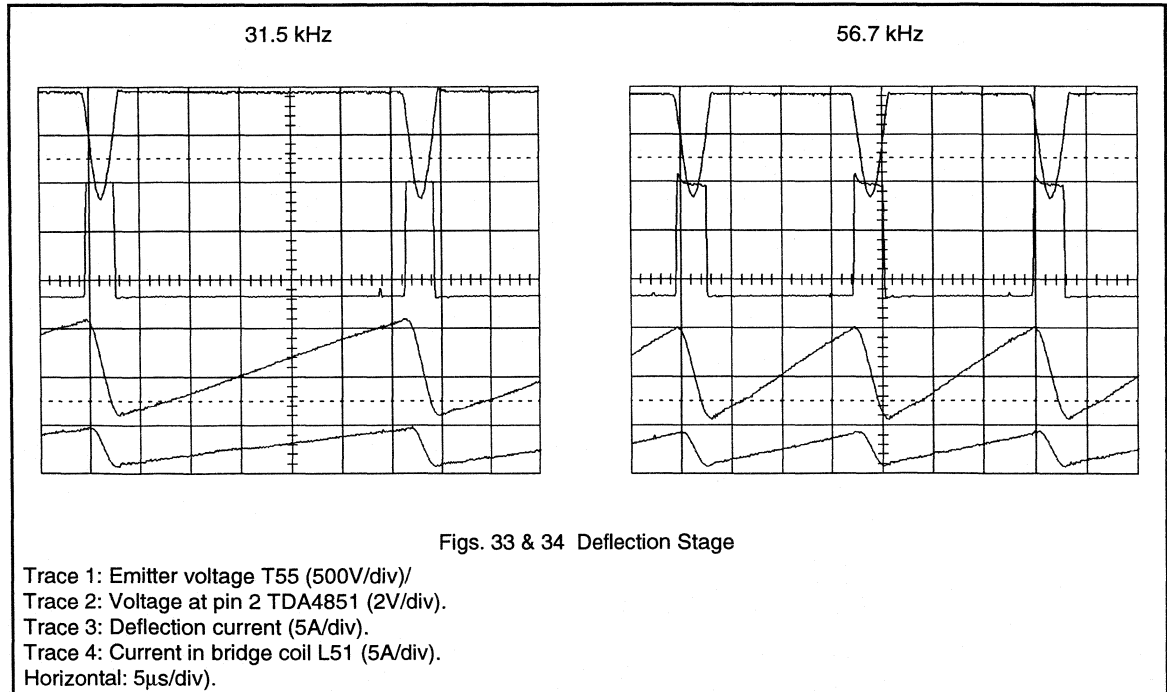
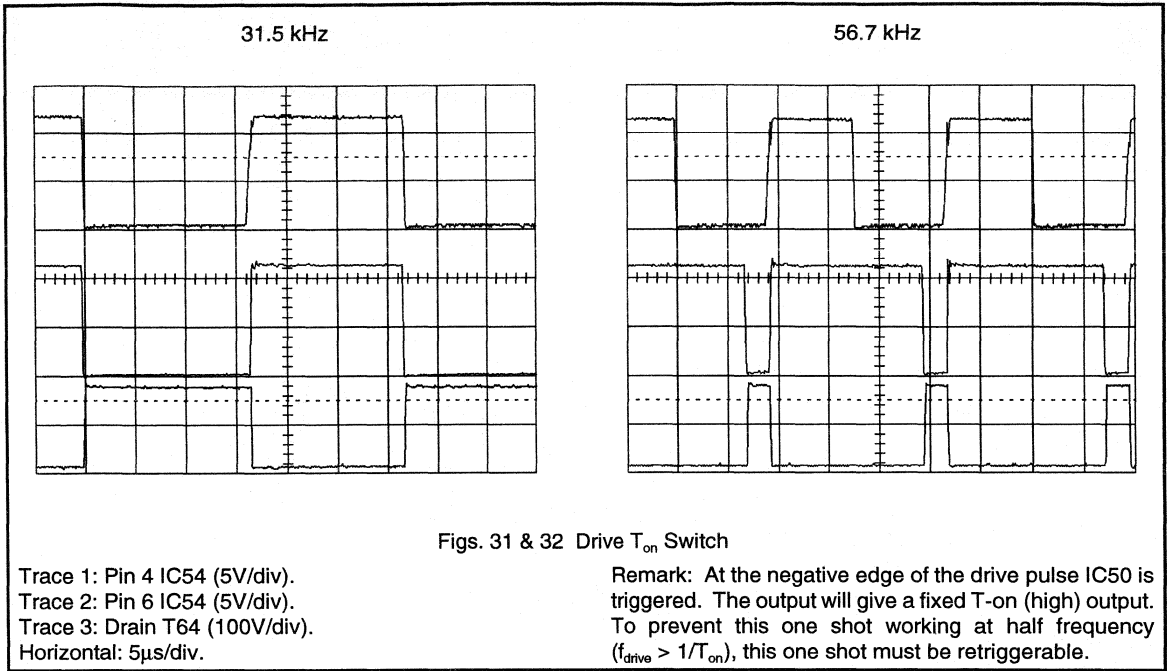
The relative position of the traces in the oscillograms with respect to ground is not given. It is assumed that the reader has enough knowledge of the circuits to understand them without this indication.

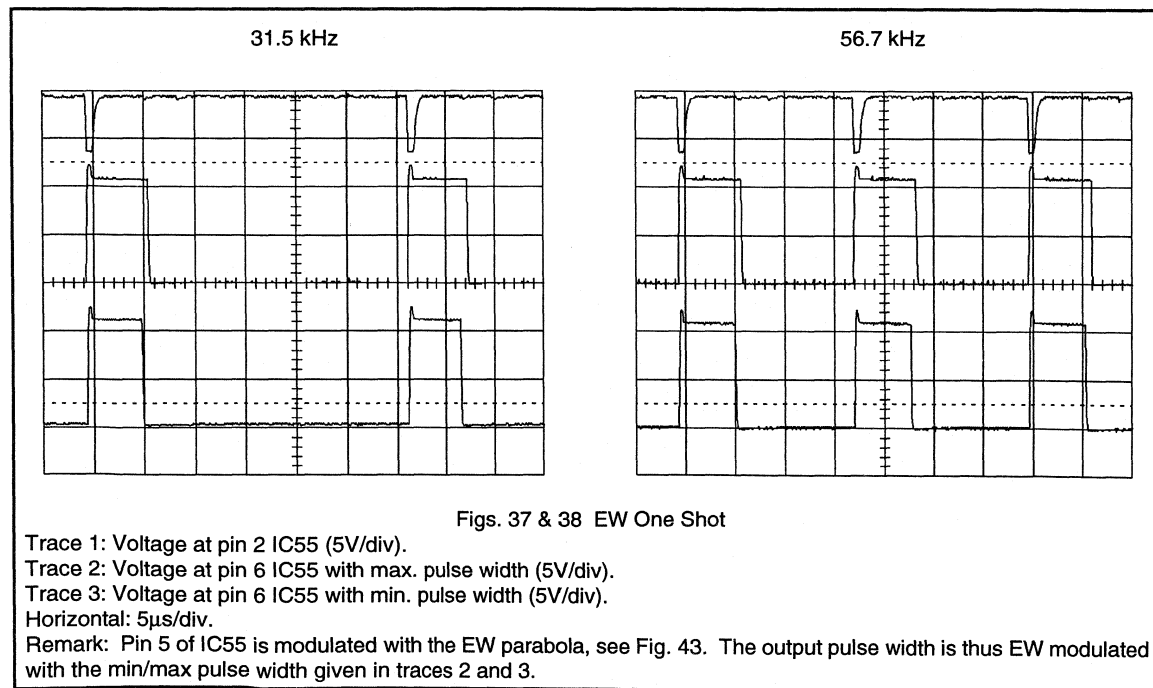
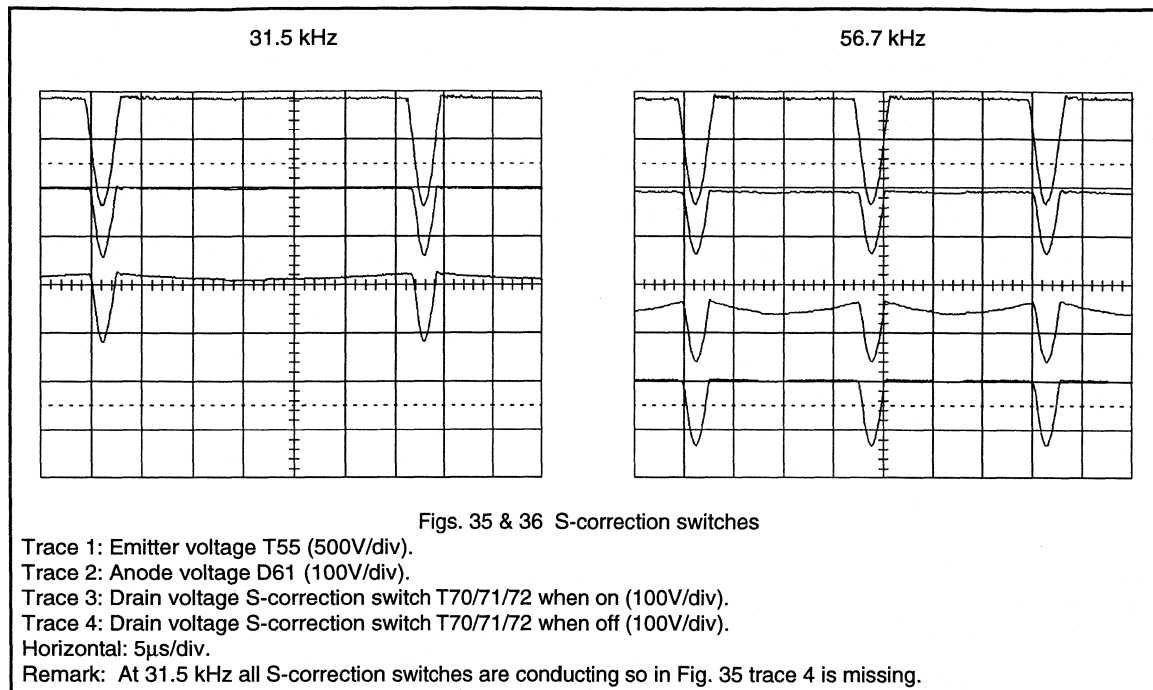
In all the following figures trace 1 is at the top leading to trace 4 at the bottom of each oscillogram.

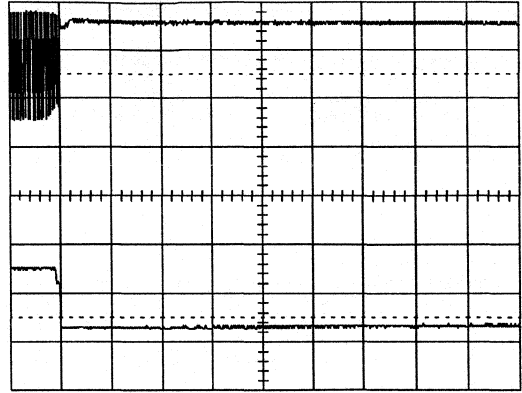
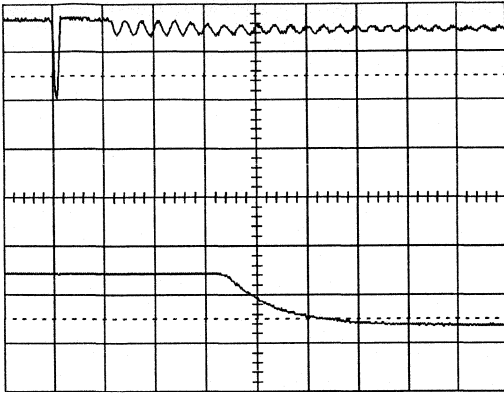












Figs. 39 & 40 Vg1 Switch Off

Trace 1: Emitter voltage T55 (500V/div).
Trace 2: Vg1 (50V/div).
Horizontal left: 20 μ s/div.
Horizontal right: 1s/div.

Remark: The time constant of the picture tube and EHT capacitor/bleeder is about 1.6s, so Vg1 is still -130V as the picture tube is fully discharged. Vg1 will also blank the screen in case of vertical guard and failure of the +10.5V supply.

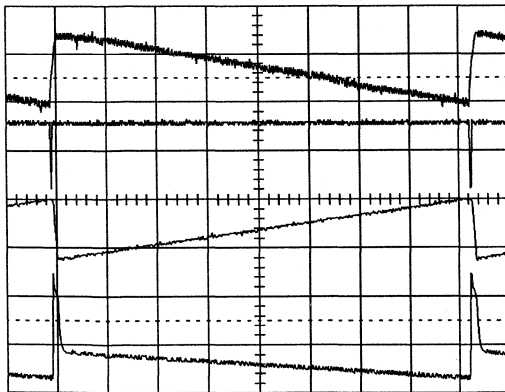
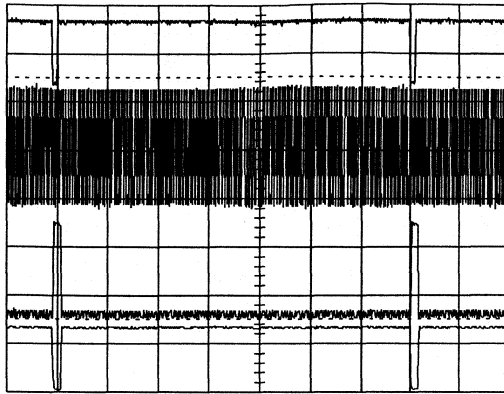


Fig. 41 Vertical Deflection

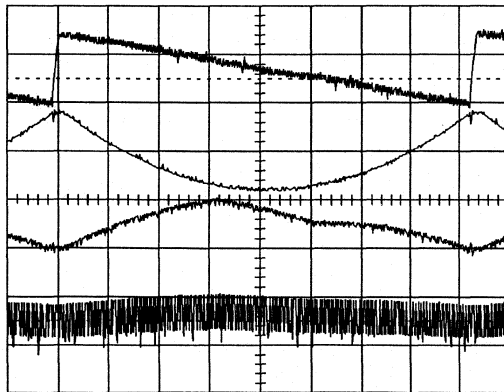
Trace 1: Vertical deflection current (1A/div).
Trace 2: Sync pulse at pin 10 TDA4851 (2V/div).
Trace 3: Vertical oscillator voltage pin 16 TDA4851 (2V/div).
Trace 4: Output voltage at pin 5 TDA4861 (20V/div).
Horizontal: 2ms/div.

Remark: During vertical sync pin 8 will be 2V (not visible in this oscillogram due to sampling effect of the DSO used).



Trace 1: Vertical sync pulse at pin 10 TDA4851 (2V/div).
Trace 2: Voltage at pin 8 TDA4851 (2V/div).
Trace 3: Guard voltage at pin 9 TDA4861 (5V/div).
Trace 4: Vg1 (50V/div).
Horizontal: 2ms/div.

Fig. 42 Blanking and Guard



Trace 1: Vertical deflection current (1A/div).
Trace 2: EW output (pin 11) of TDA4851 (1V/div).
Trace 3: Pin 5 IC55 (1V/div).
Trace 4: Filtered voltage of pin 3 IC55 (0.5V/div).
Horizontal: 2ms/div.

Remark: In the middle of the picture tube a white bar with high intensity was displayed. At trace 3 the superimposed EHT compensation signal for picture width correction can be seen. At trace 4 some line ripple is visible, see Figs. 37&38.

Fig. 43 EW waveforms

8. IC50 and IC55, both NE555 timers, should be fitted with an SMD supply bypass capacitor connected directly across the supply pins. The reason for this is, to keep the current transient at switch-over of the output as small as possible.
9. The pulses from the F/V converter, IC50 in Fig. 3, and the picture width driver, IC55 in Fig. 7, must not interfere with the sawtooth voltage of the horizontal oscillator, IC52 in Fig. 1.

Examples of good layout solutions with SMD components are shown in Fig. 45.

6. References

The information in this section has been extracted from the following report:

A Versatile 30 - 64 kHz Autosync Monitor

Author: H.Misdorn / H.Verhees
Report no.: ETV92003
12NC:

For a complete understanding of this application leading to actual implementation of this design the above report should be consulted. Other essential reference sources are as follows:

Improvements on the 30 - 64 kHz Autosync Monitor

Author: H.Verhees
Report no.: ETV92008
12NC:

Full Mains Range 150W SMPS for TV and Monitors

Author: H.Simons
Report no.: ETV/AN92011
12NC.:

Advanced Monitor Deflection Controllers TDA4851 and TDA4852

Author: H.Verhees
Report no.: ETV93003
12NC:

Integrated SMPS Control Circuit TDA8380

Author:
Report no.:
12NC: 9398 358 40011

Specification of Bus Controlled Monitor

Author: J.Shy, T.H.Wu and J.Chiou
Report no.: Taiwan/AN9101
12NC:

Improvements on the 30 to 64 kHz Autosync Monitor

Author: H.Verhees
Report no.: ETV92008
12NC:

Electromagnetic Compatibility and PCB Constraints

Author: M.J.Coenen
Report no.: ESG89001
12NC: 9398 067 20011

CHAPTER 5

Automotive Power Electronics

*5.1 Automotive Motor Control
(including selection guides)*

*5.2 Automotive Lamp Control
(including selection guides)*

5.3 The TOPFET

5.4 Automotive Ignition



*Automotive Motor Control
(including selection guides)*

5.1.1 Automotive Motor Control with Philips MOSFETS

The trend for comfort and convenience features in today's cars means that more electric motors are required than ever - a glance at Table 1 will show that up to 30 motors may be used in top of the range models, and the next generation of cars will require most of these features as standard in middle of the range models.

All these motors need to be activated and deactivated, usually from the dashboard; that requires a lot of copper cable in the wiring harnesses - up to 4km in overall length, weighing about 20 kg. Such a harness might contain over 1000 wires, each requiring connectors at either end and taking up to six hours to build. Not only does this represent a cost and weight penalty, it can also create major 'bottlenecks' at locations such as door hinges, where it becomes almost impossible to physically accommodate the 70-80 wires required. Now, if the motor switching, reversing or speed control were to be done at the load by semiconductor switches, these in turn can be driven via much thinner, lighter wiring thus alleviating the bottlenecks. Even greater savings - approaching the weight of a passenger - can be achieved by incorporating multiplex wiring controlled by a serial bus.

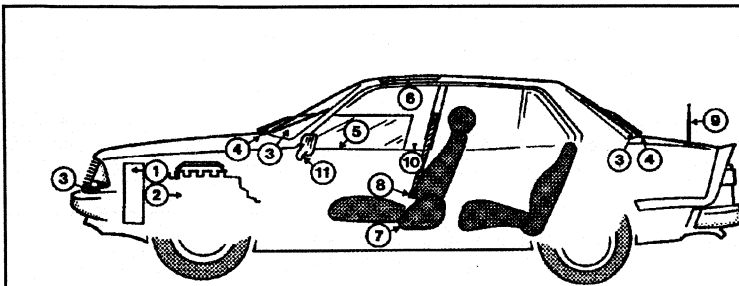
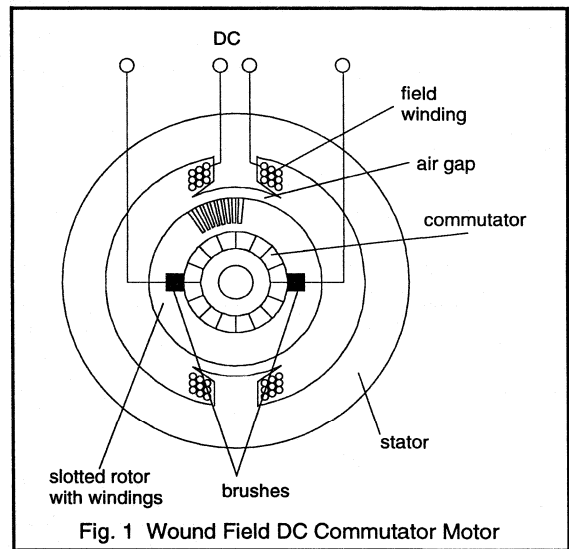
Types of motors used in automobiles

Motor design for automotive applications represents an attempt at achieving the optimum compromise between conflicting requirements. The torque/speed characteristic demanded by the application must be satisfied while taking account of the constraints of the materials, of space and of cost.

There are four main families of DC motors which are, or which have the potential to be used in automobiles.

Wound field DC Commutator Motors

Traditionally motors with wound stator fields, a rotor supply fed via brushes and a multi-segment commutator - see Fig. 1 - have been widely used. Recently, however, they have been largely replaced by permanent magnet motors. Characteristically they are found with square frames. They may be Series wound (with high torque at start up but tend to 'run away' on no-load), Shunt wound (with relatively flat speed/torque characteristics) or (rarely) Compound wound.



MOSFETs control motors for:

1. radiator fans
2. fuel pumps
3. front, rear and headlamp wipers
4. front and rear washer units
5. window lifters
6. sun-roofs
7. seat adjustments
8. seat belts
9. radio aerials
10. door locks
11. mirror adjustment

motor application	typical power (W)	nominal current (A)	typical number of such motors	type of drive	typical number of switches per motor	proposed standard BUK-	MOSFET [*] L ² FET BUK-	comments
air-conditioning	300	25	1	unidirectional, variable speed	1	456	556	Active suspension may also require such high power motors
radiator fan	120-240	10-20	1	unidirectional, variable speed	1	455	555	These motors may go brushless, requiring 3 to 6 lower rated switches
fuel pump	100	8	1	unidirectional	1	453	553	
wipers: front			1-2	unidirectional, variable speed				Reversing action is at present mechanical. This could be done electronically using 2 or 4 switches
rear	60-100	5-8	1		1	452/453	552/553	
headlamp			2					
washers: front			1-2					
rear	30-60	2.5-5	1-2	unidirectional	1	452	552	
window lifter	25-120	2-10	2-4	reversible	4	452/455	552/555	
sun-roof	40-100	3.5-8	1	reversible	4	452/453	552/553	
seat adjustment (slide, recline, lift, lumbar)	50	4	4-16	reversible	4	453	553	
seat belt	50	4	2-4	reversible	4	453	553	
pop-up headlamp	50	4	2	reversible	4	453	553	
radio aerial	25	2	1	reversible	4	452	552	
door lock	12-36	1-3	6-9	reversible	4	451/452	551/552	
mirror adjustment	12	1	2	reversible	4	451	551	
[*] These are meant for guidance only. Specific applications should be checked against individual users requirements. In addition to standard and L ² FETs, FredFETs and low and high side TOPFETs might be considered. Also a variety of isolated, non-isolated and surface mount package options are available								

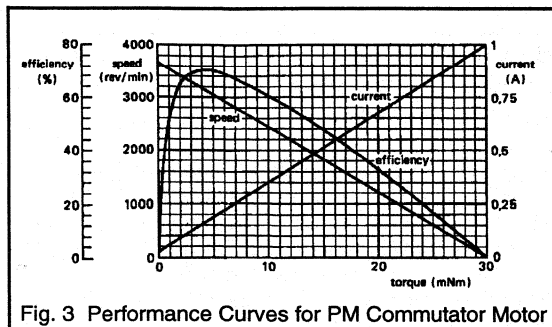
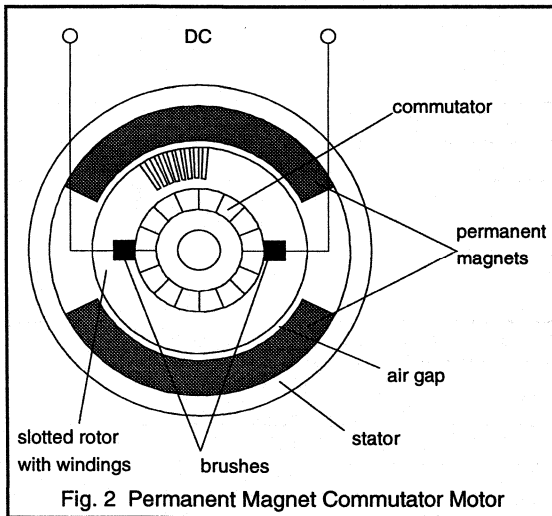
Table 1 Typical motor and switch requirements in top of range car.

Permanent Magnet (PM) DC Commutator Motors

These are now the most commonly used motors in modern cars. The permanent magnet forms the stator, the rotor consists of slotted iron containing the copper windings - see Fig. 2. They have a lighter rotor and a smaller frame size than wound field machines. Typical weight ratios between a PM and a wound field motor are:

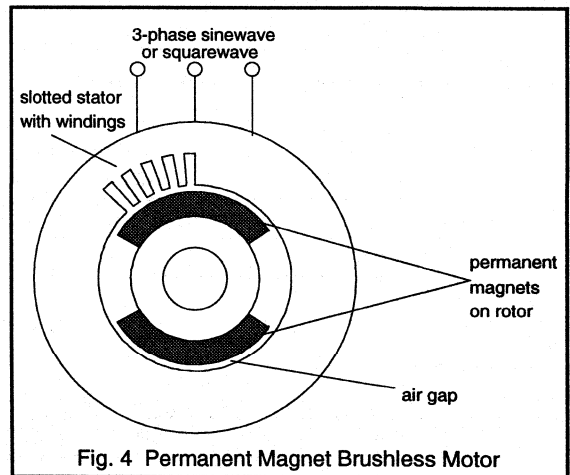
Copper	1:10
Magnets	1:7
Rotor	1:2.5
Case	1:1

PM motors have a linear torque/speed characteristic - see Fig. 3 for typical curves relating torque, speed, current and efficiency. (Philips 4322 010 76130). They are generally used below 5000 rpm. Their inductance (typically 100 - 500 μH) is much lower than wound field machines. New materials (e.g. neodymium iron boron compounds) offer even more powerful fields in smaller volumes.



PM Brushless DC Motors

Although common in EDP systems, brushless DC motors are not yet used extensively in cars. They are under consideration for certain specialised functions, e.g. fuel pump where their 'arc free' operation makes them attractive. They have a wound stator field and a permanent magnet rotor - Fig. 4. As their name suggests they have neither mechanical commutator nor brushes, thus eliminating brush noise/wear and associated maintenance. Instead they depend on electronic commutation and they require a rotor position monitor, which may incorporate Hall effect sensors, magneto resistors or induced signals in the non energised winding. Thanks to their lightweight, low inertia rotor they offer high efficiency, high power density, high speed operation and high acceleration. They can be used as servos.



Switched Reluctance Motors

These motors - see Fig. 5 - are the wound field equivalent to the PM brushless DC machine, with similar advantages and limitations. Again, not yet widely used, they have been proposed for some of the larger motor applications such as radiator and air conditioning fans, where their high power/weight ratio makes them attractive. They can also be used as stepper motors in such applications as ABS and throttle control.

Motor drive configurations

The type of motor has a considerable influence on the configuration of the drive circuit. The two families of DC motors, commutator and brushless need different drive circuits. However suitably chosen MOSFETs can be used to advantage with both.

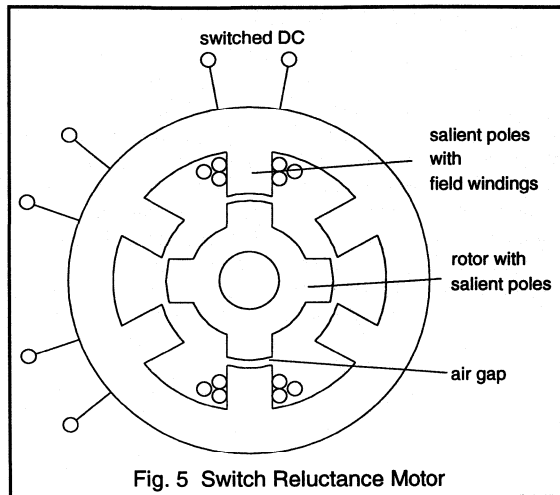


Fig. 5 Switch Reluctance Motor

Commutator Motors

Both permanent magnet and wound field commutator motors can be controlled by a switch in series with the DC supply - Fig. 6. Traditionally relays have been used, but they are not considered to be very reliable, particularly in high vibration environments. Semiconductors offer an attractive alternative, providing:

- low on-state voltage drop.
- low drive power requirements.
- immunity from vibration.

The Power MOSFET scores on all counts, offering ON resistances measured in mΩ and requiring only a few volts (at almost zero current) at the gate, to achieve this.

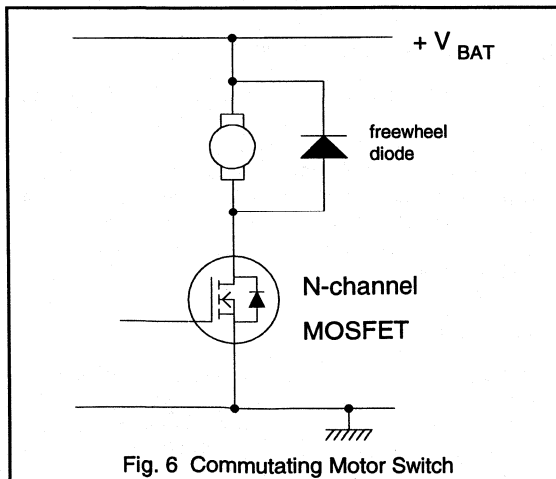


Fig. 6 Commutating Motor Switch

When a motor is switched off, it may or may not be running. If it is, then the motor acts as a voltage source and the rotating mechanical energy must be dissipated either by friction or by being transformed into electrical energy and returned to the supply via the inherent anti-parallel diode of the MOSFET. If it is not turning, then the motor appears as purely an inductance and for a low side switch the voltage transient developed will take the MOSFET into avalanche. Now, depending on the magnitude of the energy stored in the field and the avalanche capability of the MOSFETs, a diode in parallel with the motor may or may not be required.

As a first approximation, if

$$\frac{1}{2} \cdot L_m I_m^2 < W_{DSS}$$

then a diode may not be needed.

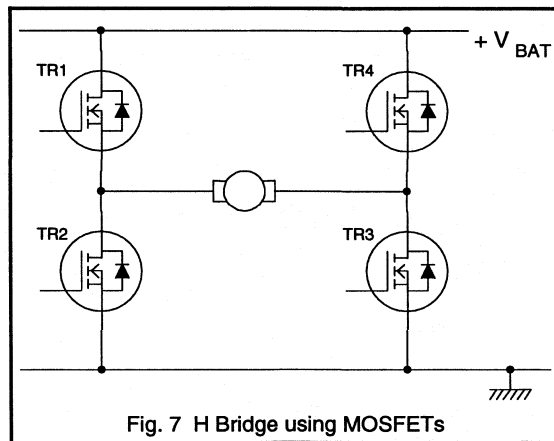


Fig. 7 H Bridge using MOSFETs

Reversing the polarity of the supply, to a commutator motor, reverses the direction of rotation. This usually requires an H bridge of semiconductors, see Fig. 7. In this case the built in diodes, inherent in MOSFETs, mean that no extra diodes are necessary. It should be noted that there are now two devices in series with the motor. So, to maintain the same low level of on-state voltage drop, each MOSFET must be doubled in area. With four devices in all, this means a reversing H bridge requires 8 x the crystal area needed by a unidirectional drive.

Chopping the supply, controls the mean voltage applied to the motor, and hence its speed. In the case of the H bridge TR1 and TR4 might be used to control direction, while a chopping signal (typically 20kHz) is applied to TR3 or TR2. When reversing the direction of rotation, it is preferable to arrange the gating logic so that the system goes through a condition where TR1, TR2, TR3 and TR4 are all off.

Switched Field Motors

PM brushless motors typically require 6 switches to generate the rotating field, see Fig. 8. Although there are motors, which operate at lower power density, which can be driven from 3 switches. The circuit in Fig. 9 shows a low side switch version of such a drive. A similar arrangement with high side switches would be possible.

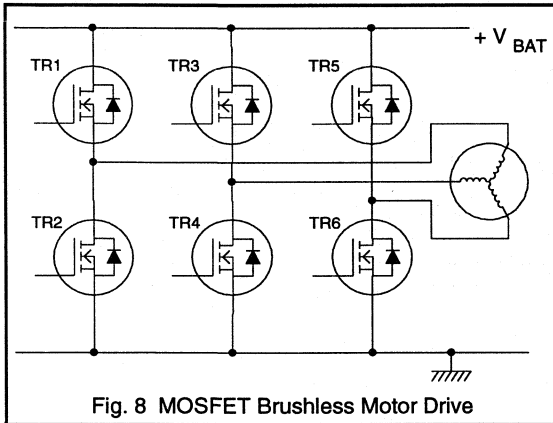


Fig. 8 MOSFET Brushless Motor Drive

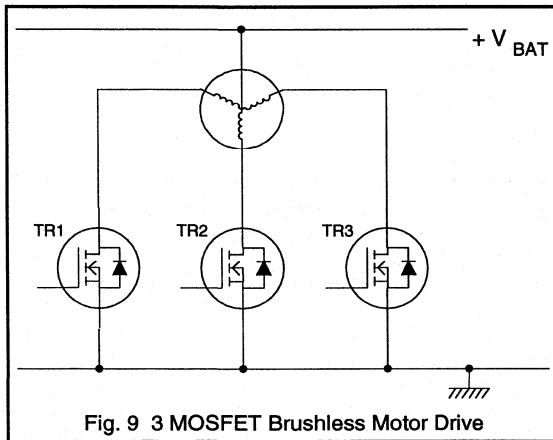


Fig. 9 3 MOSFET Brushless Motor Drive

Switched reluctance motors may use as few as 4 or as many as 12 switches to generate the rotating field, a 4 switch version is shown in Fig. 10.

The speed and direction of all switched field motors is controlled by the timing of the field pulses. In the case of brushless DC machines these timing pulses can be derived from a dedicated IC such as the Philips NE5570. Rotor position sensing is required - using, for example, magnetoresistive sensors - to determine which windings should be energised. Compared with a DC commutator motor, the power switches for a brushless motor have to be fast, because they must switch at every commutation.

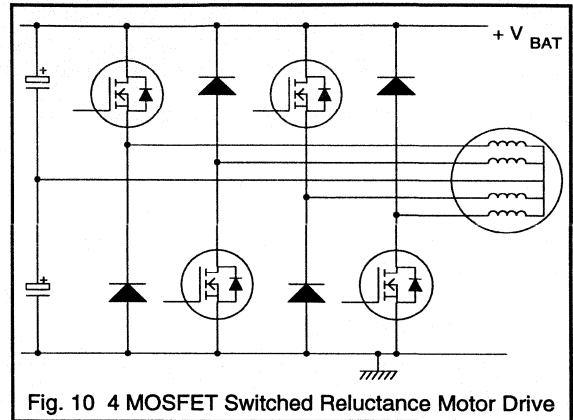


Fig. 10 4 MOSFET Switched Reluctance Motor Drive

PWM speed control pushes up the required switching speed even further. Philips MOSFETs are designed so that both switch and inbuilt diode are capable of efficient switching at the highest frequencies and voltages encountered in automotive applications.

High side drivers

Often, in automobiles, there is a requirement for the switch to be connected to the positive battery terminal with the load connected via the common chassis to negative. Negative earth reduces corrosion and low side load is safer when loads are being worked on or replaced. Also, when H bridges are considered the upper arms are of course high side switches.

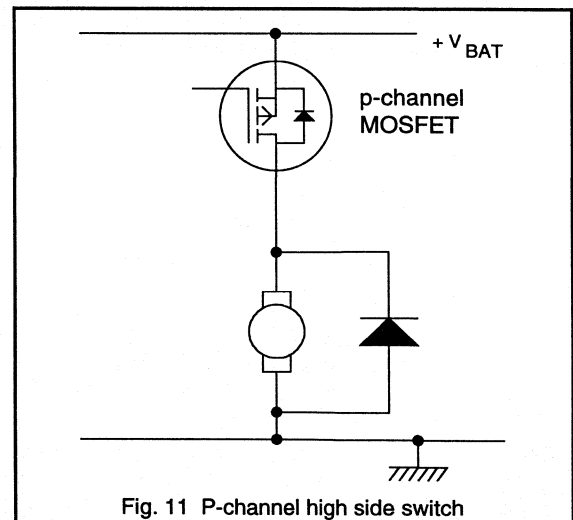


Fig. 11 P-channel high side switch

There are two MOSFET possibilities for high side switches:

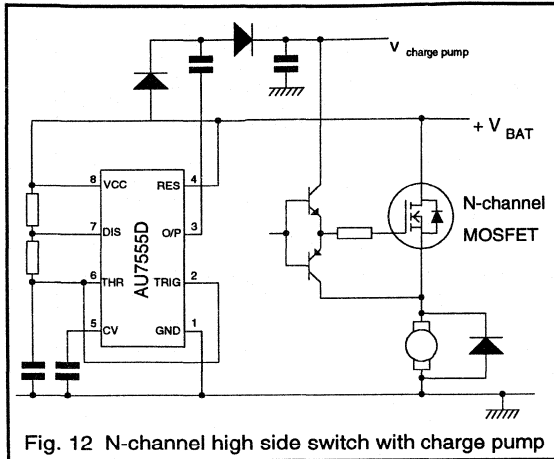


Fig. 12 N-channel high side switch with charge pump

- P-channel switches.** These simplify the drive circuit which only needs referencing to the positive supply, see Fig. 11. Unfortunately p-channel devices require almost three times the silicon area to achieve the same on resistance as n-channel MOSFETs, which increases cost. Also P-channel devices that can be operated from logic level signals are not readily available.

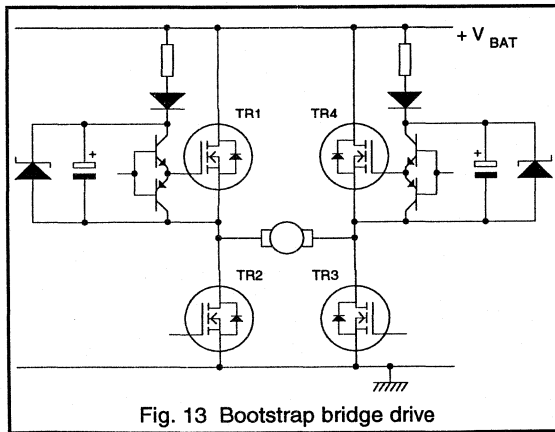


Fig. 13 Bootstrap bridge drive

- N-channel switches.** To ensure that these are fully turned on, the gate must be driven 10 V higher than the positive supply for conventional MOSFETs or 5 V higher for Logic Level types. This higher voltage might be derived from an auxiliary supply, but the cost of 'bussing' this around the vehicle is considerable.

The additional drive can be obtained locally from a charge pump, an example in shown in Fig. 12. An oscillator (e.g Philips AU7555D) free runs to generate a rectangular 12 V waveform, typically at around 100kHz. A voltage doubler then raises this to around twice the battery voltage. This arrangement is equally suitable for 'DC' or chopper drives.

An alternative approach for H bridge choppers is to use the MOSFETs themselves to generate the drive voltage with a bootstrap circuit as shown in Fig. 13. This circuit works well over a range of mark-space ratios from 5% to 95%. Zener diodes should be used in this circuit to limit the transients that may be introduced onto the auxiliary line.

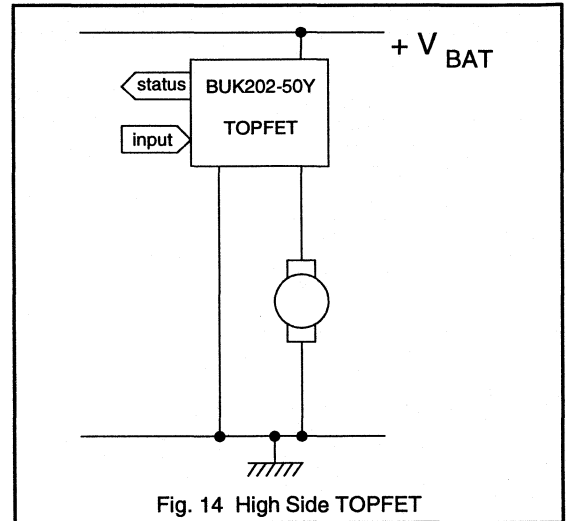


Fig. 14 High Side TOPFET

High Side TOPFET

The ideal high side switch to drive motor loads would be one which could be switched on and off by a ground referenced logic signal, is fully self-protected against short circuit motors and over temperatures and is capable of reporting on the load status to a central controller.

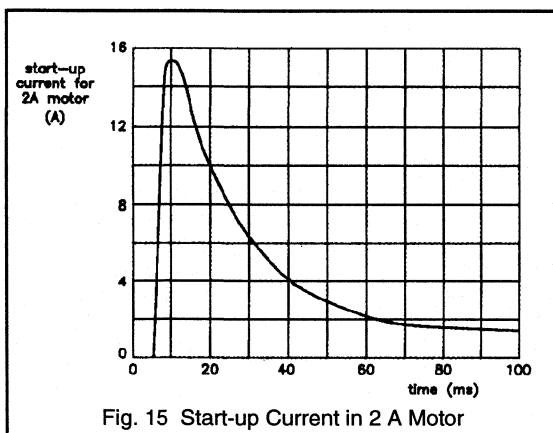
The Philips response to these requirements is a range of high side TOPFETs. The range contains devices with $R_{DS(ON)}$ from 38 to 220 mΩ, with and without internal ground resistors. All the devices feature on board charge pump and level shifting, short circuit and thermal protection and status reporting of such conditions as open or short circuit load. As can be seen in Fig. 14, the use of a TOPFET makes the circuit for a protected high side drive for a motor very simple.

Currents in motor circuits

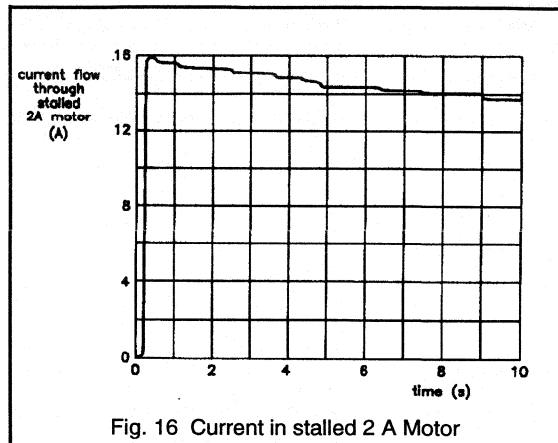
There are 5 classes of current that can flow in a motor circuit:-

- nominal** - this is the maximum steady state current that will flow when the motor is performing its function under normal conditions. It is characterised by its relatively low level and its long duration.

- **overload** - this is the current which flows when the motor is driving a load greater than it is capable of driving continuously, but is still performing its function i.e not stalled. This is not necessarily a fault condition - some applications where the motor is used infrequently and for only a short time, use a smaller motor, than would be needed for continuous operation, and over-run it. In these cases the nominal current is often the overload current. Overload currents tend to be about twice the nominal current and have a duration between 5 and 60 seconds.
- **inrush** - or starting currents are typical 5 to 8 times the nominal current and have a duration of around 100 ms, see Fig. 15. The starting torque of a motor is governed by this current so if high torque is required then the control circuit must not restrict the current. Conversely if starting torque is not critical, then current limiting techniques can be employed which will allow smaller devices to be used and permit sensitive fault thresholds to be used.



- **stall** - if the motor cannot turn then the current is limited only by the series resistance of the motor windings and the switch. In this case, a current of 5-8 times the running current can flow through the combination. Fig. 16 shows the current that flows through a stalled 2 A motor - the current gradually falls as the temperature, and consequently the resistance, of the motor and the MOSFET rises.
- **short circuit** - if the motor is shorted out then the current is limited only by the resistance of the switch and the wiring. The normal protection method, in this case, is a fuse. Unless other current control methods are used then it is the I²t rating of the fuse which determines how long the current will flow.



It is important that the devices, selected for the control circuit, can operate reliably with all of these currents. With some types of switching device, it is necessary to select on the basis of the absolute maximum current alone. Often this results in a large and expensive device being used. The characteristics of MOSFETs, in particular their thermally limited SOAR (no second breakdown), allows the designer to specify a much smaller device whose performance more closely matches the needs of the circuit.

Device requirements

Voltage

The highest voltage encountered under normal operation is 16 V, under jump start this can rise to 22 V. In the case where the battery becomes disconnected with the alternator running the voltage can rise to 50 V (assuming external protection is present) or 60 V in the case of 24 V vehicles see Table 2. Thus the normal voltage requirement is 50/60v, however the power supply rail in a vehicle is particularly noisy. The switching of the numerous inductive loads generates local voltage spikes and surges of both polarities. These can occur singly or in bursts, have magnitudes of 100 V or more and durations of the order of 1ms.

It is important to choose MOSFETs capable of withstanding these stresses, either by ensuring V_{DS} exceeds the value of the transients or by selecting 50/60 V devices with sufficient avalanche energy capability to absorb the pulse. For transients in excess of these values it is necessary to provide external protection.

However, the TOPFET range of devices, both low and high side, have overvoltage protection on chip. As a consequence they are rated to withstand very much higher transient energies.

Voltage Range	Cause
>50 (60) [*]	coupling of spurious spikes
30 to 50	clamped load dump
22 to 30	voltage surge on cut-off of inductive loads
16 to 22 (32 to 40) [*]	jump start or regulator degraded
10.5 to 16 (20 to 32) [*]	normal operating condition
8 to 10.5	alternator degraded
6 to 8	starting a petrol engine
(9 to 12) [*]	
0 to 6 (0 to 6) [*]	starting a diesel engine
negative	negative peaks or reverse connected battery
[*] 24 V supply	

Table 2 Conditions Affecting Abnormal Supply Voltages

Temperature

The ambient temperature requirement in the passenger compartment is -40 to +85°C, and -40 to +125°C under the bonnet. All Philips MOSFETs shown in Table 1 have $T_{jmax} = 175^{\circ}\text{C}$.

The TOPFETs have a maximum operating T_j of 150°C because above this temperature the on chip protection circuits may react and turn the device off. This prevents the device from damage that could result from over dissipation. This protection eases the problems of the thermal design by reducing the need for large safety margins.

L²FETs

The supply voltage in an automobile derived from the battery is only 12 V (nominal). This can vary from 10.5 V to 16 V under normal operation. It is important that the MOSFET switches be fully turned on under these conditions, not forgetting that for high side switches it may be necessary to derive the gate drive from a charge pump or bootstrap.

Whilst a gate source voltage of 6 V is usually sufficient to turn a conventional MOSFET on, to achieve the lowest on resistance, 10 V is required. Thus the margin between available and required gate drive voltage may be quite tight in automotive drive applications.

One way to ease the problem is to use Logic Level MOSFETs (L²FET), such as the BUK553-60A or BUK555-60A, which achieve a very low on resistance state with only 5 V gate-source.

Conclusions

There is an increasing demand for low cost, reliable electronic switching of motors in automobiles. Despite the wide variety of motor types and drive configurations there is a Philips Power MOSFET solution to all of these demands. The broad range of types includes standard and logic level FETs, FredFETs, high and low side TOPFETs. The combination of low on-state resistance, ease of drive and ruggedness makes them an attractive choice in the arduous automotive environment.

*Automotive Lamp Control
(including selection guides)*

5.2.1 Automotive Lamp Control with Philips MOSFETS

The modern motor vehicle, with its many features, is a complex electrical system. The safe and efficient operation of this system calls for sophisticated electronic control. A significant part of any control system is the device which switches the power to the load. It is important that the right type of device is chosen for this job because it can have a major influence on the overall system cost and effectiveness. This choice should be influenced by the nature of the load. This article will discuss the features of the various types of switching device - both mechanical and solid state. These factors will be put into the context of the needs of a device for the control of resistive loads like lamps and heaters. It will be shown that solid state devices allow the designer a greater degree of control than mechanical switches and that the features of Power MOSFETs make them well suited to use in automotive applications.

Choice of switch type

Mechanical or solid-state

Designers of automotive systems now have the choice of either mechanical or solid-state switches. Although mechanical switches can prove to be a cheap solution they do have their limitations. Solid-state switches overcome these limitations and provide the designer with several useful additional features.

Areas where the limitations of relays become apparent include:-

- **Reliability** - to achieve the required levels of sensitivity and efficiency means that relay coils have to be wound with many turns of very fine wire. This wire is susceptible to damage under conditions of high mechanical stress - vibration and shock.
- **Mounting** - special assembly techniques are needed when dealing with automotive relays. Their outlines are not compatible with the common methods of automated assembly like auto insertion and surface mounting.
- **Dissipation** - the power loss in the coil of a relay is not negligible - the resulting temperature rise makes it unwise to mount other components in close proximity. In some multiple relay applications it is necessary to provide cooling by ventilation.
- **Temperature** - the maximum operating temperature of relays is typically in the range 70°C - 85°C.
- **Corrosion** - the unsealed mechanism of relays are vulnerable in contaminating and corrosive environments.

- **Overloads** - relays can also prove to be unreliable under high transient load conditions. The arcing which occurs when switching high currents and voltages causes contact wear leading eventually to high resistance or even the contacts welding together.
- **Hazardous Materials** - to achieve the preferred switching performance, relays need to use materials like cadmium. The use of such materials is becoming restricted by legislation on health and safety grounds.
- **Noise** - the operation of a relay is not silent. This is proving to be unacceptably intrusive when relays are sited in the passenger compartment.

Solid-state switches can overcome these limitations but can also give the designer the option of introducing the following useful features:-

- **Current limiting** - a relay has two states - on or off so the current which flows depends only on the load. There is no mechanism which allows a relay to regulate the current which flows through it. The best that a relay can do is to try and turn off, when a high current is detected, but because they are so slow, very large currents may be flowing before the relay can react and damage may have already been caused. However the characteristics of solid state devices like MOSFETs and bipolar transistors allow them to control the current. This allows designers the chance to introduce systems which can handle faults in a safe and controlled manner.
- **Control of switching rate** - the lack of control that a relay has over the current proves to be a limitation not only during fault conditions but also during normal switching. Without control, the rate at which current changes, di/dt , depends only on the external circuit and extremely high rates can result. The combination of high di/dt and the contact bounce that relays are prone to, creates an 'electrically' noisy environment for surrounding systems. The control available with solid-state switches permits the designer to restrain the current and produce 'soft' switching eliminating any possible EMC problems.

Power MOSFET or Bipolar Transistor

All solid-state switches have significant advantages over relays but there are different types of solid-state switch and their particular characteristics need to be taken into account if an optimum choice is to be made. There are two major types of solid-state switches which are suitable for use in automotive applications - power MOSFETs and bipolar transistors - and several factors need to be considered if the optimum choice is to be made.

- **Overload** - The choice of device type can be influenced by the magnitude and duration of overload currents associated with the application - for example the inrush current of lamps. This factor is particularly important because the maximum current that can be safely conducted by a bipolar transistor is independent of its duration. Whereas the safe operating area of a MOSFET allows it to handle short duration currents very much greater than its DC rating.
- **Drive power** - There can be a significant difference between the total power needed to drive bipolar and MOS transistors. A MOSFET's oxide insulation makes it a voltage controlled device whereas a bipolar needs current drive. However, most control circuits are voltage rather than current orientated and the conversion to current operation often involves the used of loss inducing resistors.
- **Reverse protection** - If the switching device is required to survive reverse conduction conditions then it is necessary to have a diode, connected in anti parallel, around it. If the device is a bipolar transistor then an extra component will be needed. However the device is a MOSFET then it has an inherent body / drain diode which will perform this function without the additional expenditure in components or board space.

Logic level and standard mosfets

The battery voltage in a car is a nominal 12 V. This can vary from 10.5 V to 16 V under normal operation and can fall as low as 6 V during starting. It is important that MOSFET switches be fully turned on at these voltages, bearing in mind that for a high-side switches it may be necessary to derive the gate voltage from a charge pump circuit. While a V_{GS} of 6 V is usually sufficient to turn a standard MOSFET on, 10 V is required to achieve the lowest on-state resistance, $R_{DS(ON)}$. Thus the margin between available and required gate drive voltage may be quite tight in automotive drive applications. One way to overcome this problem is to use L²FETs such as the BUK553-60A or BUK555-60A, which achieve a very low $R_{DS(ON)}$ with a V_{GS} of only 5 V.

Switch configuration

A load's control circuit can be sited in either its positive or negative feeds. These are referred to as high side and low side switching respectively. Which configuration is chosen often depends on the location of the load/switch and the wiring scheme of the vehicle but other factors like safety can be overriding. The use of semiconductor switches introduces another element into the decision process because of the need to ensure that they are being driven correctly.

Low Side Switch

In this arrangement the load is permanently connected (perhaps via a fuse and the ignition switch) to the positive supply. The switching device is connected between the negative terminal of the load and the vehicle ground. This, together with the almost universal practice of referencing control signals to the vehicle ground, makes the implementation of a low side switch with MOSFETs extremely simple. The circuit shown in Fig. 1 shows a MOSFET connected as a low side switch to a lamp load. The Source terminal of the MOSFET is connected to ground so the control signal, which is also referenced to ground, can be connected to the Gate.

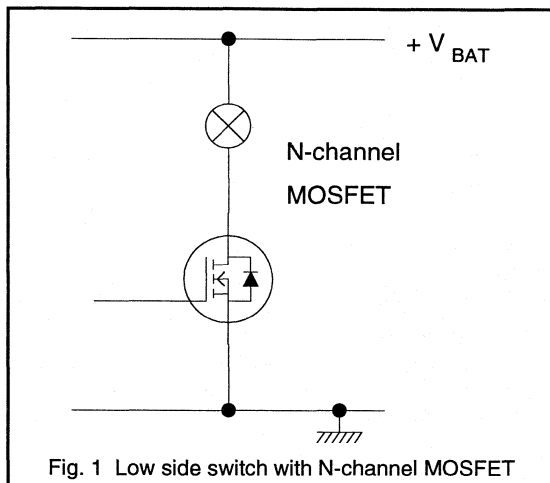
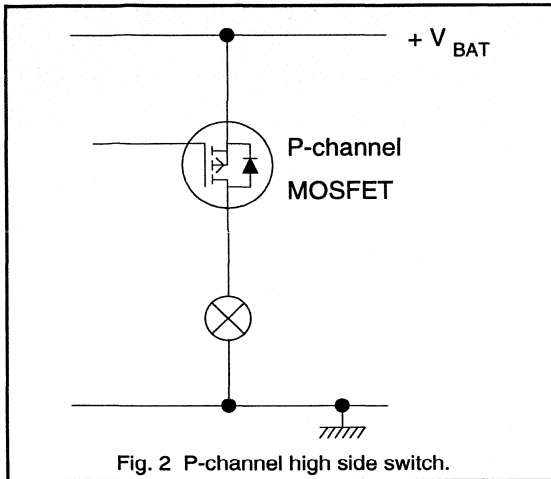


Fig. 1 Low side switch with N-channel MOSFET

High Side Drivers

Often, however, there is a requirement for the switch to be connected to the positive battery terminal with the load connected via the common chassis to the negative. This arrangement reduces electrochemical corrosion and the risk of accidentally activating the device during maintenance.

One method of creating such a high side switch is to use P-channel rather than N-channel MOSFETs. A typical arrangement is shown in Fig. 2. In this the source is connected to the +ve feed and the drain to the load. The MOSFET can be turned ON by taking the control line to zero and it will be OFF when the gate is at +ve supply voltage. Unfortunately P-channel MOSFETs require almost three times the silicon area to achieve the same low on-state resistance as N-channel types and so are much more expensive. An additional problem is the difficulty of obtaining P-channel devices with low enough gate threshold voltage to operate reliably at low battery voltages.

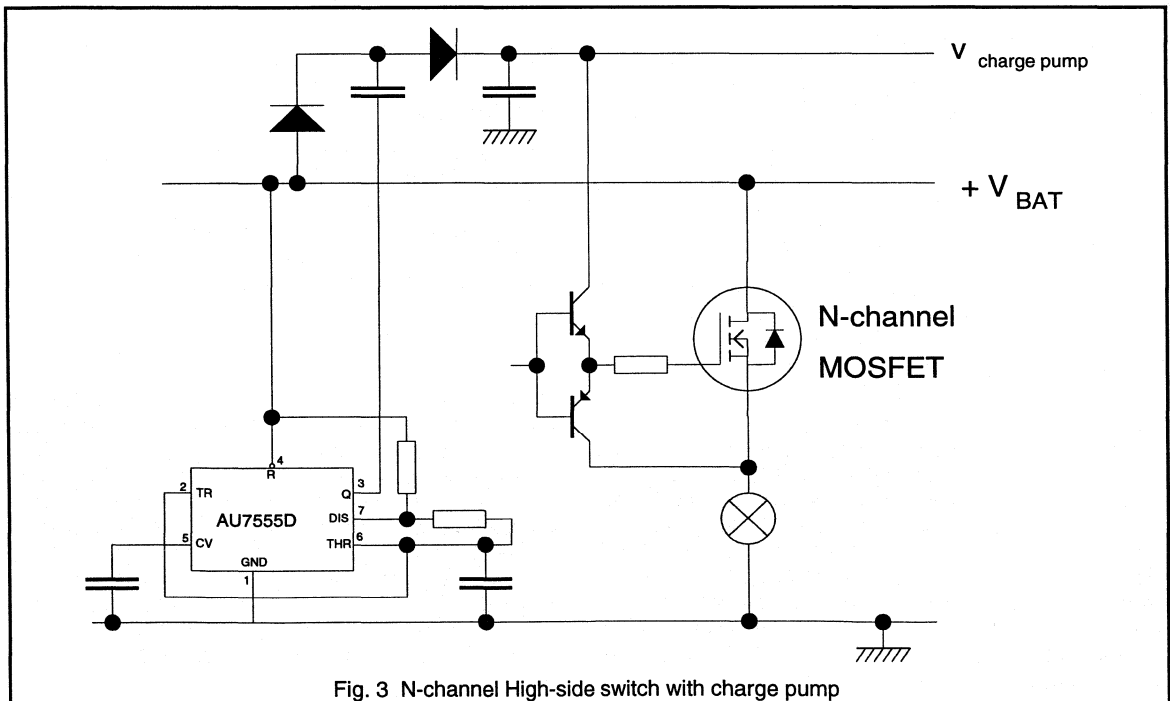


Using N-channel devices overcomes these problems but involves a more complicated drive circuit.

To ensure that a n-channel MOSFET is fully turned on, the gate must be driven 10 V higher than its source, for conventional MOSFETs, or 5 V higher for Logic Level (L²) FETs. With the source connected to the load and with most

of the supply being dropped across the it, the gate has to taken to a voltage higher than the supply voltage. This higher voltage might be derived from an auxiliary supply, but the cost of 'bussing' this around the vehicle would be high. Figure 3 shows how this auxiliary supply could be produced locally. It consists of an oscillator - based around the Philips AU7555D - running at approximately 100 kHz which is driving a charge pump which nearly doubles the supply voltage.

An alternative approach, which can be used when the device doesn't have to be continuously ON, for example PWM lamp dimming or lamp flashing, is shown in Fig. 4. In this bootstrap arrangement capacitor C is charged to the supply voltage when the MOSFET is OFF. When the MOSFET is turned ON, its source terminal, and the negative end of C, rises to the supply voltage. The potential of the positive end of C is now higher than the +ve supply and diode D is reverse biased preventing C from being discharged. C can now act as the high voltage supply for the gate. The inevitable leakages will tend to discharge C and hence reduce the gate/source voltage, but with good components it is easy to ensure that a voltage high enough to keep the MOSFET fully ON is available for several seconds.



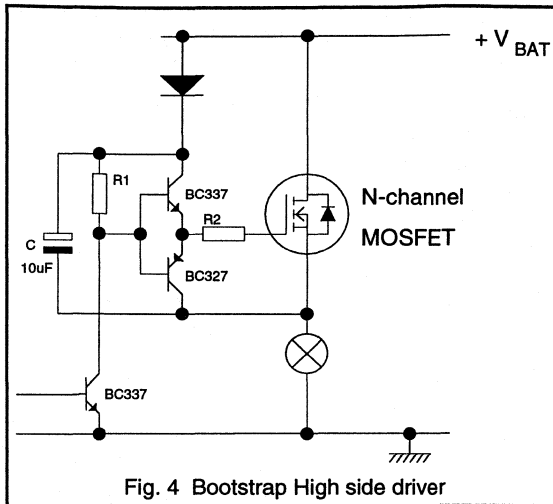


Fig. 4 Bootstrap High side driver

Inrush current

Any circuit or device which is intended to drive either a lamp or a heater must be able to handle not only the normal running current but also the inrush current at start up. All lamps and many heaters are essentially resistors made from metal conductors whose resistivity will increase with temperature.

In the case of lamps, the extremely high operating temperature (3000 K) means that the hot to cold resistance ratio is large. Typical values for a 60 W headlamp bulb are:-

	filament resistance	current
cold (-40°C)	0.17 Ω	70 A
hot	2.4 Ω	5 A

The figures given for the currents assume that there is 12 V across the lamp, in practice wiring and switch resistance will reduce the cold current somewhat, but the ratio will still be large. The actual ratio depends upon the size and construction of the lamp but figures between 10 and 14 are common. For safety, the higher figure should be used.

The low thermal mass and the high power dissipation (850 W peak in 60W lamp) means that the lamp heats up very quickly. This means that the current falls from its peak value equally quickly. The time it takes for the current to fall back to its normal value depends on the size and construction of the lamp - the larger the lamp the longer it will take to heat up. Typically the current will have an exponentially decay with a time constant of 1 - 10 ms. The waveforms in Fig. 5 show the typical inrush current for a 60 W lamp being switched on by a MOSFET. The initial temperature of the lamp filament was 25°C.

The normal operating temperature of a heater is not as high as that of a lamp, so the inrush current is rarely greater than twice the nominal current and often less. The duration of the 'inrush' can, however, last for many minutes and it may be this current which is used to define the 'normal' operating condition.

Being essentially resistive, lamps and heaters have very low inductance. This means that the current in the load will rise as quickly as the rest of the wiring will let it. This can lead to serious interference problems.

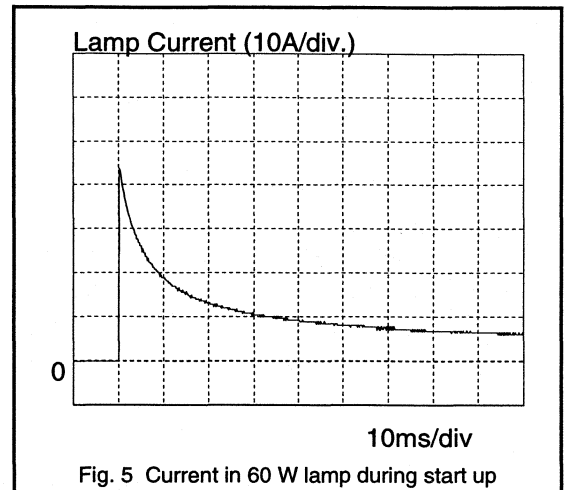


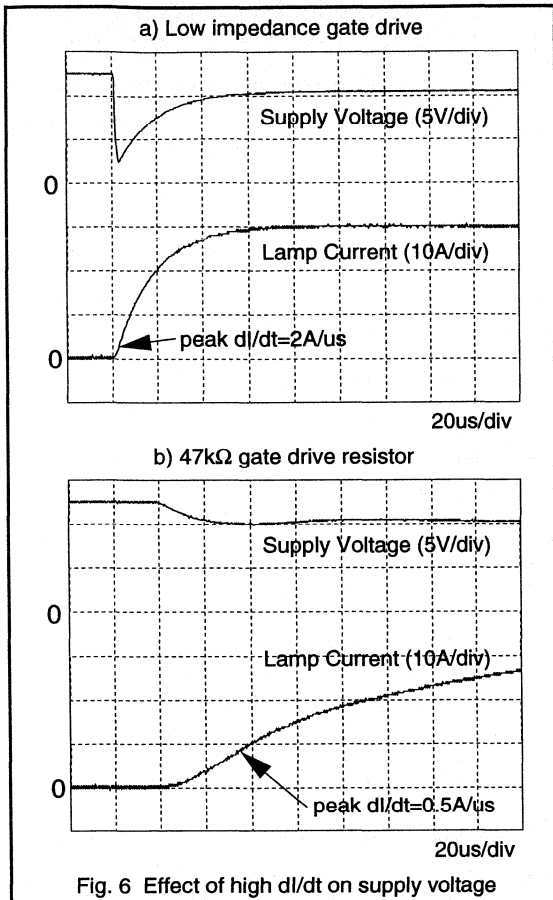
Fig. 5 Current in 60 W lamp during start up

Switch rate

The inductance associated with the supply wires in a car, is not negligible - a figure of 5µH is often quoted. This inductance, combined with the high rates of change of current associated with the switching of resistive loads and lamps, results in transient voltage appearing on the supply leads. The magnitude of the transient is given by:-

$$V_{\text{transient}} = -L \cdot \frac{dI}{dt}$$

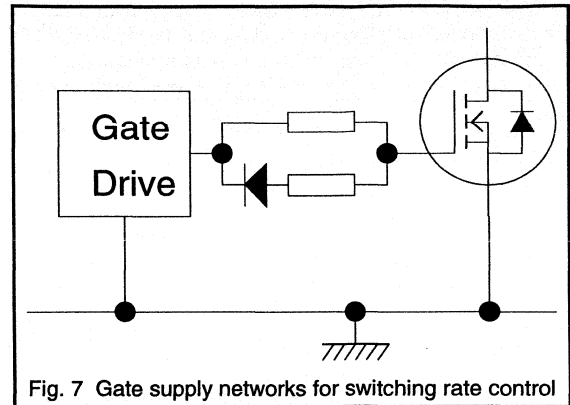
For example a current which rises as slowly as 2 A/µs will cause a 10 V dip in the supply to the switching circuit. This effect can be clearly seen in the waveforms of Fig. 6a. Such a perturbation can have an effect in two ways. In the first case the control circuit may be upset by having its supply reduced to only 2 V and may, if not specifically designed to cope with it, fail to function correctly. In the second case, it is easy for a transient as large as this, with its significant high frequency content, to be transmitted into adjacent conductors in the wiring loom. If some of the conductors are signal wires then false triggering of other functions could result.



The dip will be reduced to manageable proportions if the di/dt can be held to $0.5 A/\mu s$. Since the loads are resistive, achieving this means reducing the rate that the voltage is applied to the load. This type of 'soft' starting is relatively easy to implement when the controlling device is a Power MOSFET. All that is needed is to put resistance in series with the gate drive.

The plots shown in Fig. 6b illustrate the effect inserting $47 k\Omega$ in series with the gate supply of a BUK455-60A. The load for these tests was a 60W lamp being supplied from a battery via a $5 \mu H$ inductor. The dip in voltage due to di/dt is now lost in the voltage drop from the wiring resistance.

The rate at which current falls at turn off is also important. High negative di/dt will result in a large positive spike on the supply rails. As with the negative dip, this spike could cause interference in adjacent wires but it could also cause overvoltage damage. Unlike the turn on dip which can never be greater than 12 V, the magnitude of the turn off spike is potentially unlimited. In practice, however, it is extremely



unlikely that the voltage would exceed 30 V. Transient voltages of this magnitude are relatively common in the automotive environment and all circuits should be able to withstand them. It is still worthwhile keeping the turn off transient under control by ensuring that the di/dt is low enough - a figure of $<1 A/\mu s$ is standard.

Soft turn off, like soft turn on, is easy to implement if the controlling device is a Power MOSFET. In fact the same series resistor can be used to limit both the turn on and turn off rates. With a lamp load, however, this method will give a much slower turn off than is really necessary because of the large difference between the current at turn on and turn off. If this is a problem then an additional resistor and diode put in parallel with the first resistor - see Fig. 7 - will speed up the turn off.

MOSFET selection

The type of device chosen for a particular application depends upon the features that the control circuit needs to have. Table 3 lists the available MOSFET types and some of their features that would be useful in automotive applications.

Having chosen the type of MOSFET it becomes necessary to decide on the size of device. With MOSFETs this decision is made easier because, in its on-state, a MOSFET can be treated as a resistance and because its safe operating area (SOAR) is set by thermal considerations only (no second breakdown effects). The first stage of the selection process is to choose a device on the basis of the nominal current requirement. The next stage is to check that the inrush current, of the particular application and the drive method used, does not result in the MOSFET exceeding the transient thermal ratings. Having selected a device that is capable of switching the load the designer can then use the quoted values for the on-state resistance ($R_{DS(ON)}$) to check that any on-state voltage drop

requirements are being met. Tables 3 and 4 lists many of the different of lamps and resistive loads found in cars and suggests MOSFET types that can be used to control them.

MOSFET Type	Features
Standard	Wide range of current ratings from 5 to >100 A. Wide range of package styles Fast recovery anti-parallel diode (60 / 100 V types) Extremely fast switching.
L ² FET	as standard + Fully operational with low voltage supply
Low side TOPFET	as L ² FET + overvoltage protection overload protection over temperature protection 3 and 5 pin versions linear and switching control
High side TOPFET	Single component providing:- high side switch (on chip charge pump and level shifting) device protection load protection status reporting CMOS compatible input

TABLE 1 MOSFET Types and Features

The automotive environment

The environment that circuits and devices can be subjected to in automotive applications can prove to be extremely severe. Knowledge of the conditions that can exist is necessary to ensure that suitable devices and circuits are chosen. The two most stressful aspects of the environment are the temperature and voltage.

Temperature

The lowest temperature that is likely to be reached is -40°C. This is related to the minimum outside temperature and may be lower under some special circumstances. The maximum temperature depends to a great extent upon the siting of circuits. The general ambient temperature in the engine compartment can be quite high and it is reasonable to assume that devices will see temperatures of 125°C. Within the passenger area, conditions are somewhat more benign, but in areas where heat is generated and air flow is restricted, the temperature will be higher than might be

expected. For this reason it is necessary to assume that the circuits and devices will have to work in an ambient temperature of 85°C.

Voltage

It is possible to split the voltage conditions that can occur into two groups - Normal and Abnormal. 'Normal' conditions are essentially those which can be present for very long periods of time. Under such conditions it is reasonable to expect devices and circuits to be completely operational and to suffer no ill effects. 'Abnormal' conditions are characterised by their temporary nature. They are not expected to persist for long periods and during them, some loss in device / circuit performance can be expected and, in some cases, is allowable.

Normal voltages

When considering the 'Normal' environment it is important to included both the typical and extreme cases. The crucial condition for most devices and circuits is when the engine is running. At this time the supply voltage can be anywhere between 10.5 and 16 V in '12 V' systems or between 20 and 32 V in '24 V' systems.

The other significant 'normal' operating mode is when engine not running. In this state the supply voltage could be very low but voltages below some level must be considered as a fault condition. However some circuits will have to operate with voltages as low as 6 V.

Voltage Level		Cause
12 V systems	24 V systems	
40 V - 50 V	60 V - 75 V	external spikes
30 V - 40 V	50 V - 60 V	clamped load dump
22 V - 30 V	22 V - 30 V	inductive load switch off
16 V - 22 V	32 V - 40 V	jump start
16 V - 22 V	32 V - 40 V	faulty regulator
8 V - 10.5 V	12 V - 20 V	faulty alternator
6 V - 8 V	9 V - 12 V	starting a petrol engine
0 V - 6 V	0 V - 6 V	starting a diesel engine

Table 2 Abnormal Supply Voltages

Abnormal voltages

It is possible to envisage a situation in which nearly any voltage could appear on the supply wires of a vehicle. How extreme the voltages get depends to a great extent upon the protection, both deliberate and incidental, built into the system. The actual voltage that appears at the terminals of a circuit is also influenced strongly by its location and the location of the protection. Analysis of the automotive environment has produced a list of expected abnormal conditions. The values of voltage that these conditions can be expected to produce are shown in Table 2.

Load	Typical Power	Nominal Current	Peak Inrush Current	Number of lamps /car	Recommended MOSFET ¹			
					Standard FET SOT186	TO220	Logic Level FET SOT186	TO220
headlamp	60 W	5 A	70 A	2	BUK445-60A	BUK455-60A	BUK545-60A	BUK555-60A
	55 W	4.6 A	64 A					
	45 W	3.8 A	53 A					
	40 W	3.3 A	47 A					
spotlight	55 W	4.6 A	64 A	2	BUK445-60A	BUK455-60A	BUK545-60A	BUK555-60A
front fog light	55 W	4.6 A	64 A	2	BUK445-60A	BUK455-60A	BUK545-60A	BUK555-60A
rear fog light	21 W	1.8 A	25 A	2	BUK442-60A BUK443-60A ²	BUK452-60A BUK453-60A ²	BUK542-60A BUK543-60A ²	BUK552-60A BUK553-60A ²
front sidelight	5 W	0.4 A	6 A	2	BUK441-60A	BUK451-60A	BUK541-60A	BUK551-60A
rear sidelight	5 W	0.42 A	5.8 A	2	BUK441-60A	BUK451-60A	BUK541-60A	BUK551-60A
	10 W	0.83 A	12 A	2				
brake light	21 W	1.8 A	25 A	2	BUK442-60A BUK443-60A ²	BUK452-60A BUK453-60A ²	BUK542-60A BUK543-60A ²	BUK552-60A BUK553-60A ²
direction indicator light	21 W	1.8 A	25 A	4	BUK442-60A BUK443-60A ²	BUK452-60A BUK453-60A ²	BUK542-60A BUK543-60A ²	BUK552-60A BUK553-60A ²
side marker light	3 W	0.25 A	3.5 A	4	BUK441-60A	BUK451-60A	BUK541-60A	BUK551-60A
	4 W	0.33 A	4.7 A	4				
	5 W	0.42 A	5.8 A	4				
license plate light	3 W	0.25 A	3.5 A	2	BUK441-60A	BUK451-60A	BUK541-60A	BUK551-60A
	5 W	0.42 A	5.8 A	1				
reversing / backup light	21 W	1.8 A	25 A	2	BUK442-60A BUK443-60A ²	BUK452-60A BUK453-60A ²	BUK542-60A BUK543-60A ²	BUK552-60A BUK553-60A ²
instrument panel light	2.2 W	0.18 A	2.5 A	5	BUK441-60A	BUK451-60A	BUK541-60A	BUK551-60A
courtesy light	2.2 W	0.18 A	2.5 A	4	BUK441-60A	BUK451-60A	BUK541-60A	BUK551-60A
door light	2.2 W	0.18 A	2.5 A	4	BUK441-60A	BUK451-60A	BUK541-60A	BUK551-60A
boot / bonnet light	2.2 W	0.18 A	2.5 A	4	BUK441-60A	BUK451-60A	BUK541-60A	BUK551-60A
Notes								
¹ These are meant for general guidance only. Specific applications should be checked against individual users' requirements. In addition to standard and logic level MOSFETs, high and low side TOPFETs might also be considered.								
² This device can be used to control two bulbs simultaneously.								

TABLE 3 Automotive lamps - characteristics and recommended MOSFET drivers

Load	Typical Power	Nominal Current	Number /car	TO220	Recommended MOSFET ¹ SOT186(A) F-pack	Comments
screen heater	300-600 W	25-50 A	1	2 x BUK556-60H		Devices connected in parallel
seat heater	100-120 W	8-10 A	2	BUK452-60A ²	BUK442-60A ²	
Notes						
¹ These are meant for general guidance only. Specific applications should be checked against individual users' requirements. In addition to standard MOSFETs, L ² FETs, low and high side TOPFETs might also be considered.						
² To achieve an on-state voltage drop of <1 V the BUKxx3-60A device should be used.						

TABLE 4 Automotive Resistive Loads - characteristics and recommended MOSFET drivers

The TOPFET



5.3.1 An Introduction to the 3 pin TOPFET

The TOPFET (Temperature and Overload Protected MOSFET) concept has been developed by Philips Semiconductors and is achieved by the addition of a series of dedicated on-chip protection circuits to a low voltage power MOSFET. The resulting device has all the advantages of a conventional power MOSFET (low $R_{DS(on)}$, logic level or standard gate voltage drive) with the additional benefit of integrated protection from hazardous overstress conditions.

TOPFETs are designed for operation in low voltage power applications, particularly automotive electronic systems. The operation and protection features of the TOPFET range of devices also make them suitable for other low voltage power systems. TOPFETs can be used for all common load types currently controlled by conventional power MOSFETs.

The first generation of TOPFET devices are summarised in Table 1.

Protection strategy

A functional block diagram and the circuit symbol of the first generation 3-pin TOPFETs are shown in Fig. 1. The functional block diagram indicates that the logic and protection circuits are supplied directly from the input pin. This places a requirement on the user that the input voltage must be sufficiently high to ensure that the protection circuits are being correctly driven.

The TOPFET includes an internal resistance between the input pin and the power MOSFET gate. This is required to ensure that the protection circuits are supplied even under conditions when the circuits have been activated to turn off the power MOSFET stage. The value of this resistance has been chosen to be a suitable compromise between the requirements of switching speed and drive capability.

Variants of this configuration with differing input resistor values (higher or lower) will be produced to suit different application requirements.

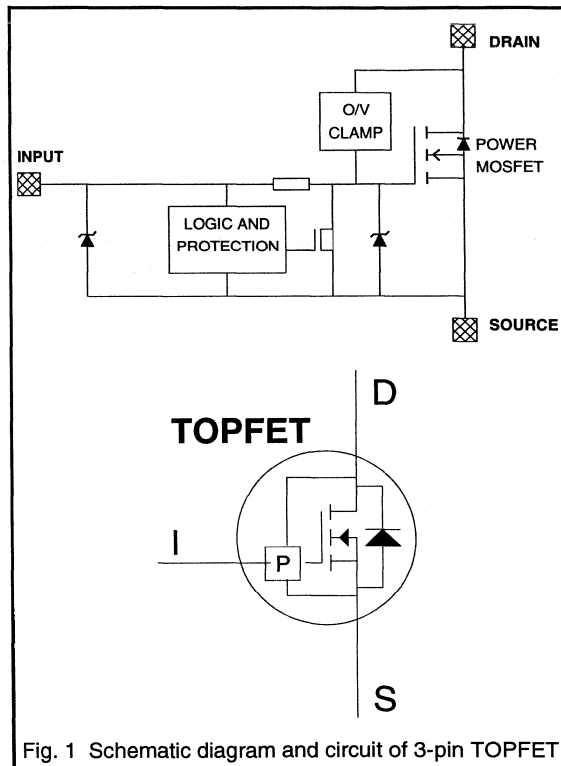


Fig. 1 Schematic diagram and circuit of 3-pin TOPFET

TOPFET	Package	V_{DS} (V)	$R_{DS(on)}$ (m Ω)	at $V_{IS} =$ (V)
BUK100-50GL	TO220	50	125	5
BUK100-50GS	TO220	50	100	10
BUK101-50GL	TO220	50	60	5
BUK101-50GS	TO220	50	50	10
BUK102-50GL	TO220	50	35	5
BUK102-50GS	TO220	50	28	10

Table 1. 3-pin TOPFET type range

Overtemperature protection

TOPFETs include an on-chip protection circuit which measures the absolute temperature of the device. If the chip temperature rises to a dangerous level then the overtemperature protection circuit operates to turn off the power MOSFET stage. Once tripped, the device remains protected until it is reset via the input pin. In the tripped condition the gate of the power MOSFET stage is pulled down by the control logic and so some current is drawn by the input pin of the TOPFET. If the overtemperature condition persists after the gate has been reset then the protection circuit is reactivated.

Short circuit protection

In the case of short circuit faults the rate of rise of temperature in a MOSFET switch can be very rapid. Guaranteed protection under this type of condition is best achieved using the on-chip protection strategy which is implemented in the TOPFET range of devices. The short circuit protection circuit acts rapidly to protect the device if the temperature of the TOPFET rises excessively.

The TOPFET does not limit the current in the power circuit under normal operation. This ensures that the TOPFET does not affect the operation of circuits where large inrush currents are required. As with the overtemperature protection circuit, the short circuit protection circuit turns off the power MOSFET gate via the control logic and is reset by taking the input pin low.

Overvoltage protection

Transient overvoltage protection is an additional feature of the TOPFET range. This is achieved by a combination of a rugged avalanche breakdown characteristic in the PowerMOS stage and an internal dynamic clamp circuit. Operation is guaranteed by an overvoltage clamping energy rating for the TOPFET. Overvoltage protection gives guarantees against fault conditions in the system as well as the ability for unclamped inductive load turn-off.

ESD protection

The input pin of the TOPFET is protected with an ESD protection zener. This device protects the PowerMOS gate and the TOPFET circuit from ESD transients. The energy in the ESD pulse is dissipated in the ESD source rather than in the TOPFET itself. This input zener diode cannot be used in the continuous breakdown mode and so is the determining factor in setting the maximum allowable TOPFET input voltage.

One feature of the implementation of the protection circuits used in the first generation TOPFET devices is that the input cannot be reverse biased with respect to the source. This must be adhered to at all times. When the TOPFET is in reverse conduction the protection circuits are not active.

5.3.2 An Introduction to the 5 pin TOPFET

The TOPFET (Temperature and Overload Protected MOSFET) concept has been developed by Philips Semiconductors and is achieved by the addition of a series of dedicated on-chip protection circuits to a low voltage power MOSFET. The resulting device has the advantages of a conventional power MOSFET (low $R_{DS(on)}$, logic level gate voltage drive) with the additional benefit of integrated protection from hazardous overstress conditions.

TOPFETs are designed for operation in low voltage power applications, particularly automotive electronic systems. The operation and protection features of the TOPFET range of devices also make them suitable for other low voltage power systems. TOPFETs can be used for all common load types currently controlled by conventional power MOSFETs.

The second generation of TOPFET devices offers enhanced protection and drive capabilities making them suitable for a wide variety of applications, including those requiring fast switching (eg PWM control) or linear control. The circuit diagram for the 5-pin TOPFET types is shown in Fig. 1. The key features of these devices are:

- Overtemperature protection
- Short circuit load protection
- Overvoltage protection
- Full ESD protection
- Direct access to the gate of the Power MOSFET.
- Flag signal reporting of certain fault conditions
- Separate protection circuit supply

The 5-pin TOPFET range is summarised in Table 1.

Overtemperature protection

TOPFETs include an on-chip protection circuit which measures the absolute temperature of the device. If the

chip temperature rises to a dangerous level then the overtemperature protection circuit operates to turn off the power MOSFET stage. Once tripped the device remains protected until it is reset via the protection supply pin.

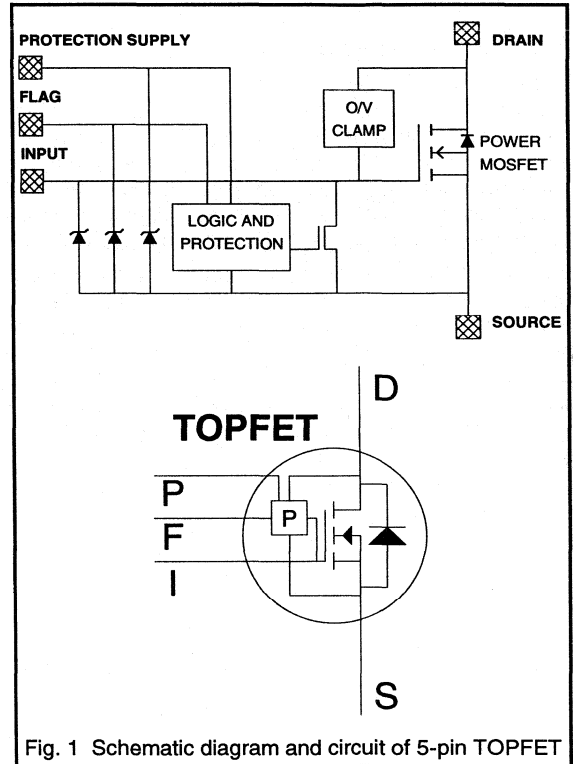


Fig. 1 Schematic diagram and circuit of 5-pin TOPFET

TOPFET	Package	V_{DS} (V)	$R_{DS(ON)}$ (m Ω)	at V_{IS} (V)	for $V_{PSP} >$ (V)
BUK105-50L	SOT263	50	60	5	4
			50	7	4.4
BUK105-50S	SOT263	50	60	5	5
			50	7	5.4

Table 1. 5-pin TOPFET type range

In the tripped condition the gate of the power MOSFET stage is pulled down by the control logic and so current is drawn by the input pin of the TOPFET. A minimum value of external gate drive resistor is specified in order that the protection circuit can turn off the PowerMOS stage and thus protect the device. The flag pin gives a logic high output to indicate that a fault has occurred. If the overtemperature condition persists after the protection supply has been reset then the protection circuit is reactivated.

Short circuit protection

In the case of short circuit faults the rate of rise of temperature in a MOSFET switch can be very rapid. Guaranteed protection under this type of condition is best achieved using the on-chip protection strategy which is implemented in the TOPFET range of devices. The short circuit protection circuit acts rapidly to protect the device if the temperature of the TOPFET rises excessively.

The TOPFET does not limit the current in the power circuit under normal operation. This ensures that the TOPFET does not affect the operation of circuits where large inrush currents are required. As with the overtemperature protection circuit the short circuit protection circuit turns off the power MOSFET gate via the control logic and provides a flag signal. The TOPFET is reset by taking the protection supply pin low.

Overvoltage protection

Transient overvoltage protection is an additional feature of the TOPFET range. This is achieved by a combination of a rugged avalanche breakdown characteristic in the PowerMOS stage and an internal dynamic clamp circuit.

ESD protection

The input pin, flag pin and protection supply pins of the TOPFET are all protected with ESD protection zeners. These devices protect the PowerMOS gate and the TOPFET circuits from ESD transients. The protection devices cannot be used in continuous breakdown.

Protection supply

An error condition is recorded and the flag signal is activated if the protection supply is absent. Valid protection is only guaranteed once the protection supply is in excess of V_{PSP} (See Table 1).

One feature of the implementation of the protection circuits used in this generation of TOPFET devices is that the input, flag or protection supply pins cannot be reverse biased with respect to the source. This must be adhered to at all times. When the TOPFET is in reverse conduction the protection circuits are not active.

5.3.3 BUK101-50DL - a Microcontroller compatible TOPFET

The TOPFET version BUK101-50DL can be directly controlled by the port outputs of standard microcontrollers and other high impedance driver stages. This member of the TOPFET family has the same functional features as its predecessors BUK101-50GS and BUK101-50GL. All these versions are 3-pin devices for the replacement of Power MOSFETs or partially protected Power MOSFETs. They are internally protected against over temperature, short circuit load, overvoltage and electrostatic discharge. For more information concerning the basic technical concept of TOPFET see Philips Technical Publication 'TOPFET - A NEW CONCEPT IN PROTECTED MOSFET'. This section covers the special features of the BUK101-50DL version, criteria for driver stage design and application.

Overview on BUK101-50 versions

The GS, GL and DL versions of the BUK101-50 TOPFET each have the same functionality but differ in their input characteristics. Table 1 gives an overview on these characteristics.

Type	Nominal Input Voltage (V)	Normal Input Current (mA)	Latched Input Current (mA)	Max. Input Voltage (V)
GS	10	1.0	4.0	11
GL	5	0.35	2.0	6
DL	5	0.35	0.65	6

Table 1. Comparison of GS, GL and DL versions

Table 1 shows that the GS version (S for Standard type) is specified for 10V driver outputs while the GL and DL versions (L for Logic Level type) are specified for 5V logic level driver outputs. The two logic level types differ in the input current, I_{ISL} , which flows when the device is in its 'latched' state i.e. shutdown has occurred due to over temperature or short circuit load. The GL version is suitable for pulsed applications up to 1kHz and needs a push-pull driver stage while the DL version is optimised for high impedance drive circuits and can handle pulsed applications up to 100Hz.

Criteria for choice/design of driver stage

Figure 1 shows a simplified circuit diagram for the input of a 3-pin TOPFET. Also indicated is the high level output impedance of the driver stage R_{out} .

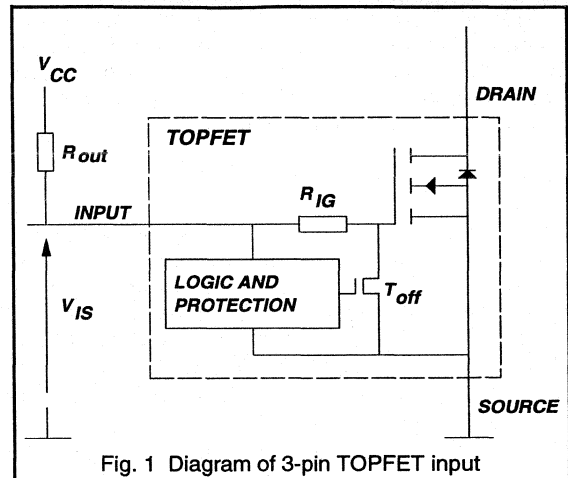


Fig. 1 Diagram of 3-pin TOPFET input

For all versions the internal circuits for over temperature and short circuit load protection are supplied from the input pin. This determines the input current I_{IS} under normal conditions, i.e. the Power MOS transistor is on and T_{off} in Fig. 1 is off. To ensure proper function of the protection circuits, a minimum input voltage $V_{IS} = 4V$ has to be applied. If, however, the device has turned off due to over temperature or short circuit load (i.e. transistor T_{off} in Fig. 1 is on), a minimum of $V_{IS} = 3.5V$ is required to keep the device in its 'latched' state. Latched means that the device will stay off even if the error condition has disappeared. Figure 1 indicates that under this condition the input current I_{ISL} will be increased due to the additional current that has to be sourced into resistor R_{IG} . R_{IG} allows the Power MOS gate to be pulled down internally while the input pin is at high level. The typical value of R_{IG} in the GL version is $4k\Omega$, while for the DL version this value has been increased to $30k\Omega$. Thus the maximum input current has been reduced to allow for high impedance driver stages such as microcontroller port outputs.

The criteria stated above result in the following requirements on the driver stage output resistance R_{out} :

$$\text{Normal: } R_{out} \leq \frac{V_{cc} - 4V}{I_{IS}(V_{IS} = 4V)} \quad (1)$$

$$\text{Latched: } R_{out} \leq \frac{V_{cc} - 3.5V}{I_{IS}(V_{IS} = 3.5V)} \quad (2)$$

The maximum input currents of the BUK101-50DL are specified as follows:

$$I_{IS,max} = 270\mu A \text{ at } V_{IS} = 4V$$

$$I_{ISL,max} = 430\mu A \text{ at } V_{IS} = 3.5V$$

Considering a 5V supply, equation (2) leads to a maximum output resistance $R_{out,max} = 3.5k\Omega$.

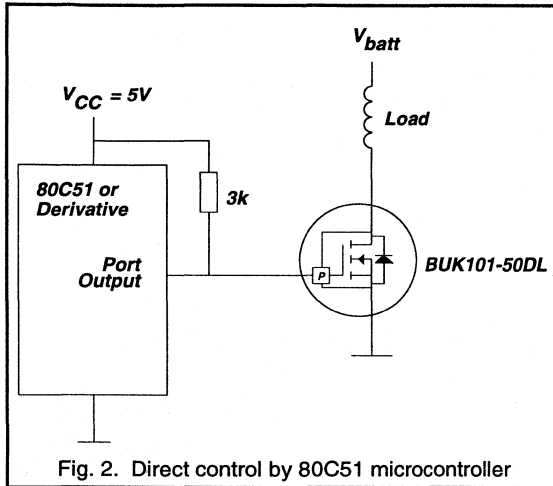


Fig. 2. Direct control by 80C51 microcontroller

Application example - 80C51 microcontroller as TOPFET driver

Figure 2 shows an application that takes advantage of the low input current of the BUK101-50DL. As has been shown above, the external pull-up resistor $R_{pull-up}$ in this circuit should have a maximum value of $3.5k\Omega$ at $V_{CC} = 5V$ for safe operation of the TOPFET protection circuits. An additional requirement is that the TOPFET must be off when the port output is at low level. Thus the limited sinking capability of

the port output demands a minimum value for $R_{pull-up}$. For the 80C51 microcontroller family a maximum output voltage of $V_{out,low} = 0.45V$ is specified at a sink current of 1.6mA for ports 1 to 3 and 3.2mA for port 0. This voltage level is safely below the minimum turn-on threshold $V_{IS(TO)} = 1V$ of the TOPFET. Considering $V_{CC} = 5V$ and the above specification of the port output, the minimum value for $R_{pull-up}$ is:

$$R_{pull-up} \geq \frac{5V - 0.45V}{1.6mA} = 2.8k\Omega$$

Thus a value of $3k\Omega$ meets the requirements.

Other applications for the BUK101-50DL

Logic IC as driver

Besides microcontroller port outputs the BUK101-50DL can also be driven by standard 5V logic IC families. Table 2 gives an overview on these families and states - if necessary - the minimum value for a pull-up resistor.

Family	$R_{pull-up min}$
TTL	300 Ω
LSTTL	620 Ω
STTL	240 Ω
HE4000B	no $R_{pull-up}$ required
HCMOS	no $R_{pull-up}$ required
ACL	no $R_{pull-up}$ required

Table 2. 5 V logic IC families driving the BUK101-50DL

High Side driver

The low input current of the BUK101-50DL is also advantageous, when using the device as a high side switch. In this configuration the low drive requirements mean that smaller capacitors are needed in charge pump or bootstrap circuits. This subject is described more fully in section 5.3.6.

5.3.4 Protection with 5 pin TOPFETs

TOPFETs in the 5-pin SOT263 outline extend the range of application of TOPFET to circuits requiring faster switching or protected linear operation. 3-pin TOPFETs are ideal for use in DC and low frequency switching applications but the need to generate the protection supply from the input is a limitation. Providing a separate pin for the protection supply gives the designer freedom to control the input / MOSFET gate in the way he chooses.

This note will look at the organisation of the 5-pin devices and then discuss some of the more important operational considerations. Application examples will be presented in the later sections in this chapter.

Functional description

The logic and protection circuits within this device are similar to those in the 3-pin TOPFETs but the configuration has been modified (see Fig. 1) to give greater operational versatility.

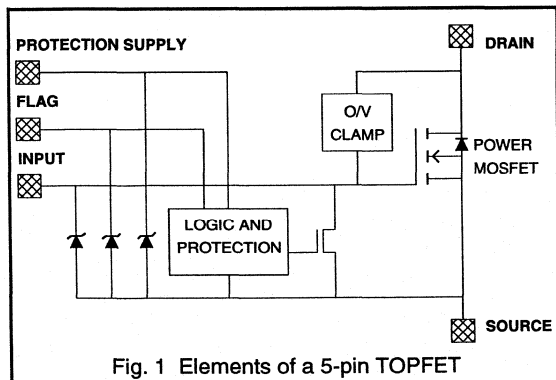


Fig. 1 Elements of a 5-pin TOPFET

These devices use pin 2 of the SOT263 as a flag and pin 4 as the supply / reset to the logic and protection circuits. Separating the protection supply from the input has allowed the internal input gate resistor to be removed. (In a 3-pin TOPFET, this resistor is needed to maintain the protection supply during latched fault conditions).

The operation of the protection circuits has not been changed. If there is an overvoltage between drain and source, the overvoltage protection circuit will still try to turn

the MOSFET partially ON. In an overtemperature or overload situation the TOPFET will turn on the gate pull-down transistor and attempt to turn itself OFF.

The flag indicates when the TOPFET has been tripped by an overtemperature, overload or short circuit condition. It will also indicate if the protection supply is absent, for example during a reset. It should be pointed out that the flag low state does not mean that the protection supply is high enough, just that it is present.

The flag is the open drain of a MOS transistor which is OFF to indicate a fault. It is intended that the flag pin is connected to a 10 k Ω pull-up resistor. This arrangement gives the flag a failsafe characteristic.

Operational considerations

Supplying the protection circuits from their own pin, rather than sharing a pin with the MOSFET gate drive, has several beneficial effects. One is that it allows the MOSFET gate to be independently controlled without adversely affecting the protection features. This is particularly useful when TOPFET is being used as a linear controller.

The removal of the input gate resistor gives the designer the opportunity of selecting the most appropriate value. It is important to understand that if TOPFET is to protect itself, it needs to control its gate by overriding the external drive circuit. It can only do this if the impedance of the driver is high enough. The conditions for satisfactory operation are given in Table 1.

Protection level	Minimum driver impedance		
	ON drive		OFF drive
	5 V	10 V	input / source
Full self protection	1 k Ω	2 k Ω	100 Ω
Overvoltage protection only	0 Ω	0 Ω	100 Ω
Overtemperature, overload and short circuit protection only	1 k Ω	2 k Ω	0 Ω

Table 1. Driver impedance and protection level

The simplest way of satisfying the self protection requirements is to fit a 2 k Ω resistor between the driver and the input pin. This is simple in a linear controller but may not be feasible in a switching controller where this resistance will result in a significant turn OFF delay. An alternative may be to have an ON drive via 2 k Ω and an OFF drive via 100 Ω .

If lower turn ON drive impedance is needed then the approach would be to use the flag output to control the signal being fed to the driver circuit. It should be noted that to have overvoltage protection the turn OFF impedance must still be > 100 Ω .

The S and L versions differ only in the protection supply voltage range. The L types are designed to be supplied from the output of 5 V logic ICs, like the 74HC/HCT families. The S types are intended to be supplied with a nominal 10 V from either HEF4000 type logic, linear ICs (e.g operational amplifiers) or discrete circuits.

One additional benefit of the independent protection supply is that, unlike 3-pin L types, the input of a 5-pin L type can be as high as 11 V, allowing a significantly lower $R_{DS(ON)}$ to be achieved.

It is important to realise that, at high levels of input voltage, the MOSFET transfer characteristic of both L and S types will allow a very high current to flow during shorted load situations. This current, flowing through the resistance in the connections between the chip's source metalisation and the source pad on the pcb, will give a significant volt drop. Since the return for the protection supply will be to the pcb source bond pad, the volt drop will subtract from the effective protection supply voltage. To compensate for this effect, the minimum protection supply voltage, V_{PSP} , is increased at high levels of input voltage, V_{IS} . For example the minimum V_{PSP} of the BUK105-50L is 4 V if $V_{IS} \leq 5$ V. If, however, the input is taken to 7 V, to achieve an $R_{DS(ON)}$ of 50 m Ω , V_{PSP} must be ≥ 4.4 V. A curve in data (reproduced as Fig. 2) gives minimum V_{PSP} values for V_{IS} from 0 to 11 V.

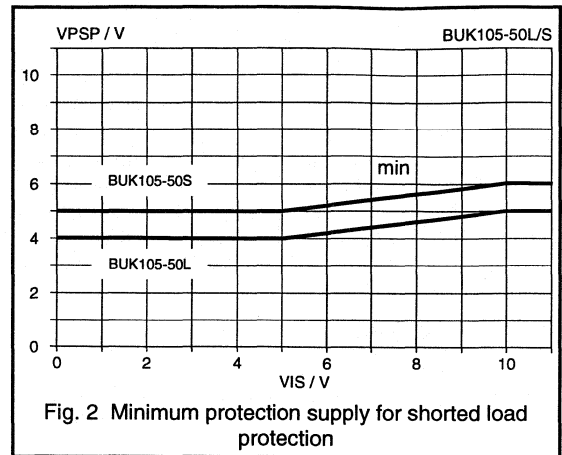


Fig. 2 Minimum protection supply for shorted load protection

The input, flag and protection supply pins are all protected against the effects of ESD by special diodes between the pin and source. It is important to realise that these devices are not designed to run in continuous forward or reverse conduction. This means that the continuous voltage between these pins and source should be > 0 and < 11 V.

Reverse Battery

There is always a risk that the car's battery could be reversed. If this happened to a system where a TOPFET is fitted then the TOPFET will survive provided:

- the current flowing through the body drain diode is restricted by the load to a level which does not cause the TOPFET to over dissipate,
- the current flowing out of the input, flag and protection supply pins is < 10 mA.

5.3.5 Driving TOPFETs

The output of a TOPFET is similar to that of a Power MOSFET. However, the TOPFET's protection features make the input characteristics significantly different. As a consequence, TOPFETs have different drive requirements. This fact sheet describes these requirements and suggests suitable drivers for the different TOPFET versions.

3-Pin TOPFET

Input requirements

3-pin TOPFETs can replace ordinary MOSFETs in many circuits if the driver can meet certain conditions. The first of these conditions is the need to keep within the TOPFET's V_{IS} ratings and in particular to keep the input positive with respect to the source. The second is the need to provide an adequate supply to the protection circuits even when the TOPFET has tripped and the input current is significantly higher.

Table 1 summarises these requirements. It gives the limiting values of V_{IS} , the minimum input voltage for valid protection in normal and latched mode and the normal and latched input currents for each 3-pin TOPFET.

Drivers

The complementary drive arrangement shown in Fig. 1 is well suited to the input requirements of 3-pin TOPFETs. The transistors shown are the output of a CMOS IC gate, which for some TOPFETs may have sufficient drive. If not, a push pull drive with discrete devices should be used. Suitable CMOS families are given in Table 1.

The BUK101-50DL has a very low input current requirement, achieved by increasing the value of the internal input resistor - at the expense of a significant increase in switching times. This means that this device can be driven from the output port of an 80C51 micro controller as shown in Fig. 2. Designers should be aware that other high resistance / low current TOPFETs could be produced if they are requested.

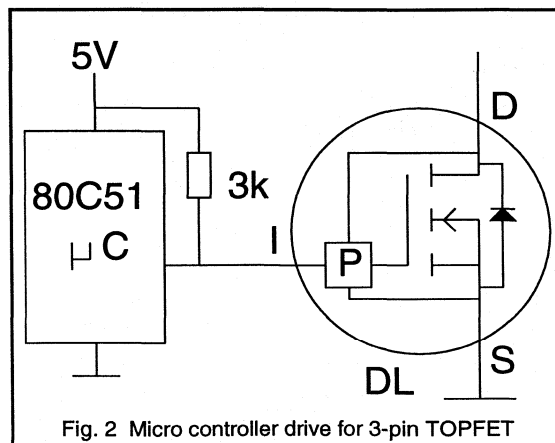
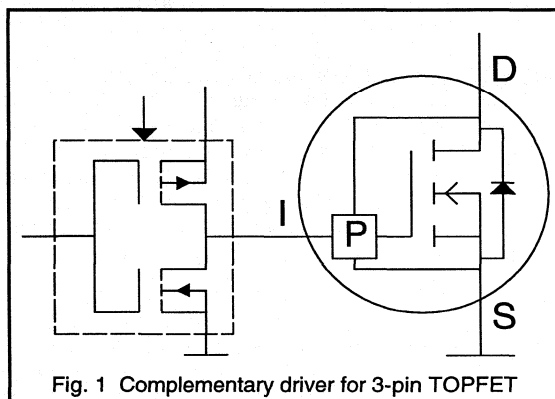
5-Pin TOPFET

Input Requirements

The requirements of a 5-pin TOPFET are somewhat different to that of a 3-pin device. The first major difference

is that both the input and the protection pins need to be supplied. The second difference is that the input resistance is external and is selected by the designer. One requirement which remains is the need to keep both the input-source and protection-source voltages within the range 0 to 11 V.

The protection pin driver must be able to keep the voltage above V_{PSP} when supplying the protection current, I_{PS} . With the 5-pin device the protection supply is independent, so the current drawn when TOPFET trips does not change.



Type	Input voltage (V)				Input Current (mA)		Driver
	limiting value		for valid protection		normal	latched	
	min.	max.	normal	latched			
BUK100-50GS	0	11	5	3.5	1.0	5.0	HEF / Discrete HEF / Discrete Discrete
BUK101-50GS	0	11	5	3.5	1.0	4.0	
BUK102-50GS	0	11	5	3.5	1.0	20	
BUK100-50GL	0	6	4	3.5	0.35	2.0	HC/HCT HC/HCT
BUK101-50GL	0	6	4	3.5	0.35	2.0	
BUK102-50GL	0	6	4	3.5	0.35	10	Discrete
BUK101-50DL	0	6	4	3.5	0.35	0.65	Micro

Table 1 Input parameters of 3-pin TOPFETs

The input pin requirements depend on the mode of operation chosen by the designer. If the TOPFET is expected to turn itself off, in overtemperature or shorted load situations, then the output impedance of the drive needs to be $> 2 \text{ k}\Omega$. This will allow the TOPFET's internal turn-off transistor to pull the input pin low. If, however, the circuit uses the TOPFET flag to signal to the driver to turn off, then driver resistance can be very much lower.

Independent of which method is used for overload turn-off, there is a separate requirement to ensure adequate overvoltage clamping. If this feature is needed then the input to source resistance of the driver - when it is pulling the input low - needs to be $> 100 \Omega$. If it is lower, then the TOPFET's internal clamping drive will be unable to raise the gate voltage high enough to turn the MOSFET on.

Drives

The drive for the protection pin can, most conveniently, be supplied by a CMOS IC gate. A 74HC or HCT for L type devices or a HEF4000 series device for the S type. Care is needed however to ensure that the minimum protection voltage, V_{PSP} , requirements are still met when the input voltage, V_{IS} is high and the load is shorted.

A typical high impedance drive arrangement, which lets TOPFET protect itself against shorted load, overtemperature and overvoltage, is shown in Fig. 3.

One method of creating a fast drive is shown in Fig. 4. In this arrangement a NOR gate with a low impedance output stage drives the input via a 100Ω resistor. One input of the NOR gate is connected to the flag pin and will be pulled high by the $10 \text{ k}\Omega$ pull-up resistor if the TOPFET indicates

a fault. With one input high, the output of the gate will be low turning the TOPFET off. The 100Ω resistor ensures that the overvoltage clamp is still operational.

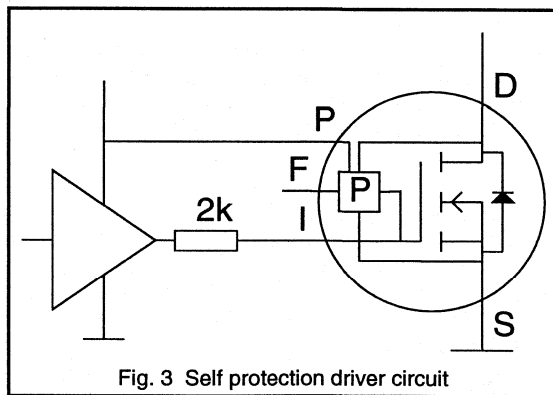


Fig. 3 Self protection driver circuit

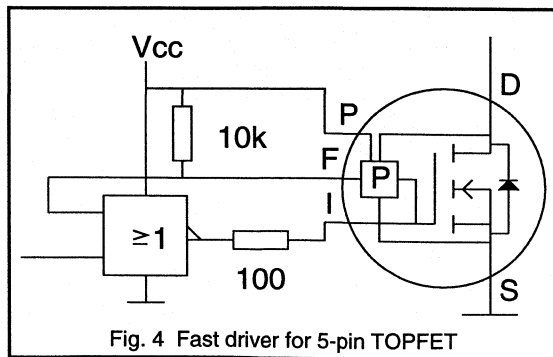


Fig. 4 Fast driver for 5-pin TOPFET

5.3.6 High Side PWM Lamp Dimmer using TOPFET

Although the 3-pin TOPFETs were designed for low side switch applications, they can, by using standard MOSFET bootstrap techniques, be used in applications which need high side control. One such application is the dimming of automotive headlamps and panel lamps. These applications need not only a high side switch but also slow, controlled switching to reduce problems of EMI.

This note will give details of a circuit which fulfils the operational requirements of this application and, because it uses a TOPFET, is well protected against shorted load and overvoltage faults.

Circuit Description

The circuit shown in Fig. 1 shows the high side PWM dimmer circuit. All the main components are shown, the only exception being the source of the PWM control signal. The circuit of Fig. 1 assumes that the signal is a rectangular pulse train of the required frequency and duty cycle, with an amplitude of 10 V.

The input signal is attenuated by R2 and R3 and fed to the base of Q1. The combination of R1 and Q1 will invert and level shift the signal and feed it to the input of the BUK101-50GS TOPFET.

D1, C1 and the TOPFET form the bootstrap circuit. The low end of C1 is connected to the TOPFET source. When TOPFET is OFF its source is close to ground, so C1 charges to Vbat via D1. When TOPFET turns ON, its source rises to nearly Vbat, lifting the high end of C1 well above Vbat. C1 can, therefore, provide more than enough voltage to drive the TOPFET input. In fact, when Vbat is higher than normal, the voltage would exceed the continuous V_{IS} rating of the BUK101-50GS, so D3 is included to restrict the input voltage to below 11 V.

Capacitor C2 adds to the Miller capacitance of Q1 and limits the rate of change of collector voltage. The TOPFET acts like a source follower circuit, so the load voltage rises and falls at the same rate as the collector-emitter voltage of Q1.

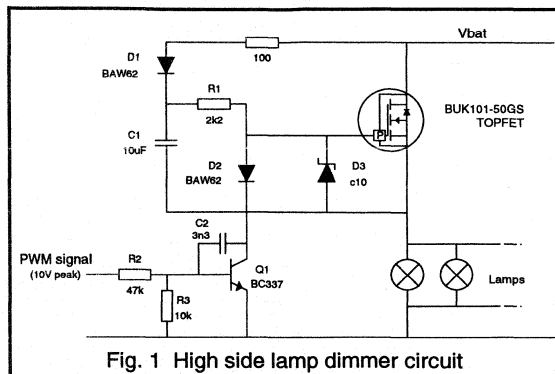


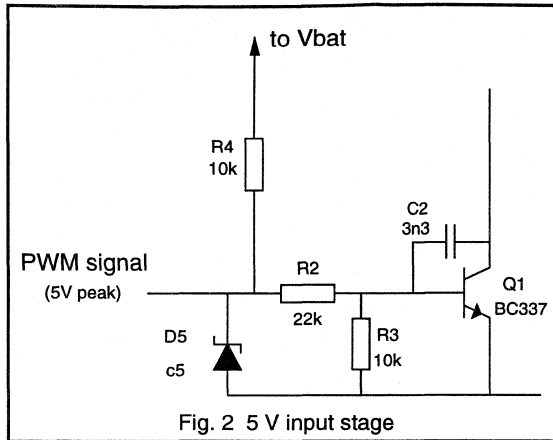
Fig. 1 High side lamp dimmer circuit

Component Values

With the components specified the circuit will operate at a frequency between 50 and 200 Hz and has rise and fall times of about 300 μ s. This slow switching means that the minimum OFF time, for satisfactory bootstrap operation, is about 1 ms. At 50 Hz this gives a maximum duty cycle of 95%.

The value of C1 has been chosen to ensure that TOPFET input current does not cause the C1 voltage to fall significantly during the maximum ON time. This means that the lowest on state dissipation is being achieved. Lower values could be used but the voltage droop would be greater and care would be needed to ensure that the input voltage does not fall below the V_{ISP} of the TOPFET, otherwise the protection features may not function.

The rate of switching can be changed by adjusting the value of C2. Larger values would reduce switching speed. Considerable care is needed when switching times become very long because while the input voltage is below the V_{ISP} the TOPFET is unprotected. Switching times can be reduced to about 50 μ s by reducing the value of C2 to 470 pF. To reduce the switching times further will mean a change to the input drive.

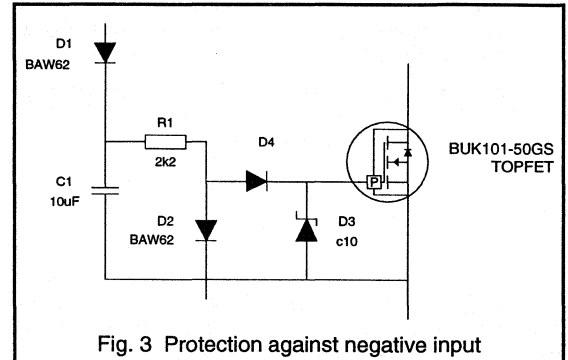


Switching rate, in particular the turn-off rate, is also influenced by the amplitude of the input signal. R2 and R3 have been chosen to give similar rise and fall times with an input of 10 V. If the input amplitude is lower the fall time would increase. This can be compensated for by lower attenuation. An input modified for 5 V input is shown in Fig. 2. This arrangement also includes D5 to clamp the input voltage to 5 V and R4 to allow the use of an open collector or drain drivers.

Operation in fault conditions

TOPFET will protect itself against high voltage supply line transients by partially turning on and restricting the applied voltage to about 60 V. In high side applications the remainder of high voltage may appear across the load. In many systems the grounding and smoothing arrangements will ensure that this will not be a problem. In some configurations the TOPFET source will rise above ground while the input is held at ground. This means that the

TOPFET input will be negative while its drain-source voltage is high. This may damage the TOPFET. This difficulty can be eliminated by the input circuit shown in Fig. 3. In this circuit diode D4 will turn off if the source voltage rises. The input is, therefore, no longer clamped by the drive and can rise with the source, eliminating the risk of damage.



If the load becomes short circuit, TOPFET will trip as soon as the temperature of the power part of the chip becomes too high. Since this circuit is a PWM controller the TOPFET will be reset at the end of the ON period. During the period between tripping and the start of the next cycle the TOPFET will cool. It will, therefore, turn on when the input goes high again and the short circuit current will flow until TOPFET is tripped once more.

TOPFET is able to withstand this type of operation for a considerable period of time but not necessarily indefinitely. The dissipation is considerable, the temperatures could be high and operating life may be affected. It is advisable, therefore, that short circuit operation is evaluated.

5.3.7 Linear Control with TOPFET

Although the pulse width modulation, PWM, method of motor speed control is often preferred over the linear method it is not without problems. Some of these are totally eliminated in linear controllers. However, linear control techniques have their own limitations. By using a Philips TOPFET as the power device some of the disadvantages are removed giving a fully protected, linear control system.

This note will compare linear and PWM controllers. It will then give details of a circuit based around a BUK105-50S which shows that, with a TOPFET, it is simple to produce a fully protected, linear controller for adjusting the speed of a car heater fan.

Linear and PWM Control

PWM is often selected as the method of controlling the speed of a brush motor because it is more efficient than linear control. The reduction in energy loss results from a reduction in the loss in the controlling power device. The loss is lower because the device is only transiently in the high dissipation state of being partially ON. To keep the loss as low as possible, the transition time needs to be kept short, implying fast switching and high values of dV/dt and dI/dt . It is these fast switching rates which create the electrical noise that can be such a problem in automotive applications.

Linear control does not create this noise because it holds the output at a steady value. The power device is continuously in the partially ON state and its dissipation is high. If, however, this heat can be handled and the inefficiency is acceptable then linear control may be the better choice.

Device Selection Factors

In PWM control, on-state dissipation is the major energy loss, so $R_{DS(ON)}$ is the main selection criterion. In linear control, maximum dissipation occurs when half the supply voltage is being dropped across the device. In this state $R_{DS(ON)}$ is not relevant as dissipation is being controlled by the load and the supply. The limiting factor in this case is the need to dissipate the energy and keep the junction temperature to a safe value. The selection, therefore, is based on junction to mounting base and mounting base to heatsink thermal resistance. $R_{DS(ON)}$ cannot be ignored, however, because it sets the residual voltage loss at maximum speed which can be important.

TOPFET in Linear Control

The circuit shown in Fig. 10. is a linear controller for a car heater fan based around a BUK105-50S. TOPFET is well suited to this application because it is a real power device in a real power package giving it good thermal characteristics and low $R_{DS(ON)}$. The 5-pin TOPFET is used because the protection circuits need to be supplied independently from the input. The on-chip overtemperature protection feature of TOPFET is precisely the protection strategy needed in this type of high dissipation application.

Input Pin

In this circuit the input of the TOPFET is connected, via R1 and D1, to the output of an operational amplifier. The TOPFET drain voltage is attenuated by R2/R3 and fed to the positive input of the amplifier. The negative input is connected to the wiper of the speed setting potentiometer. This TOPFET/op-amp arrangement creates a non-inverting amplifier with a gain of

$$gain = \frac{(R2 + R3)}{R3}$$

In such a low frequency system the presence of R1 at 2.2 k Ω will not have a significant effect on normal operation. However, if TOPFET is tripped, its internal gate source transistor will be turned on and, because R1 is greater than the 2 k Ω needed for self protection (see R₁ in the data sheet), the MOSFET gate will be pulled down and the TOPFET will be OFF.

Diode D1 prevents the input of the TOPFET being pulled negative with respect to the source.

Protection Supply

To ensure that the overtemperature and shorted load protection circuits work, the protection supply pin needs to be connected to an adequate supply. To allow TOPFET to be reset, provision has to be made to switch this so it can fall below the minimum reset voltage, V_{PSR} . Possibly the easiest way to achieve this is by feeding the protection supply from a CMOS gate.

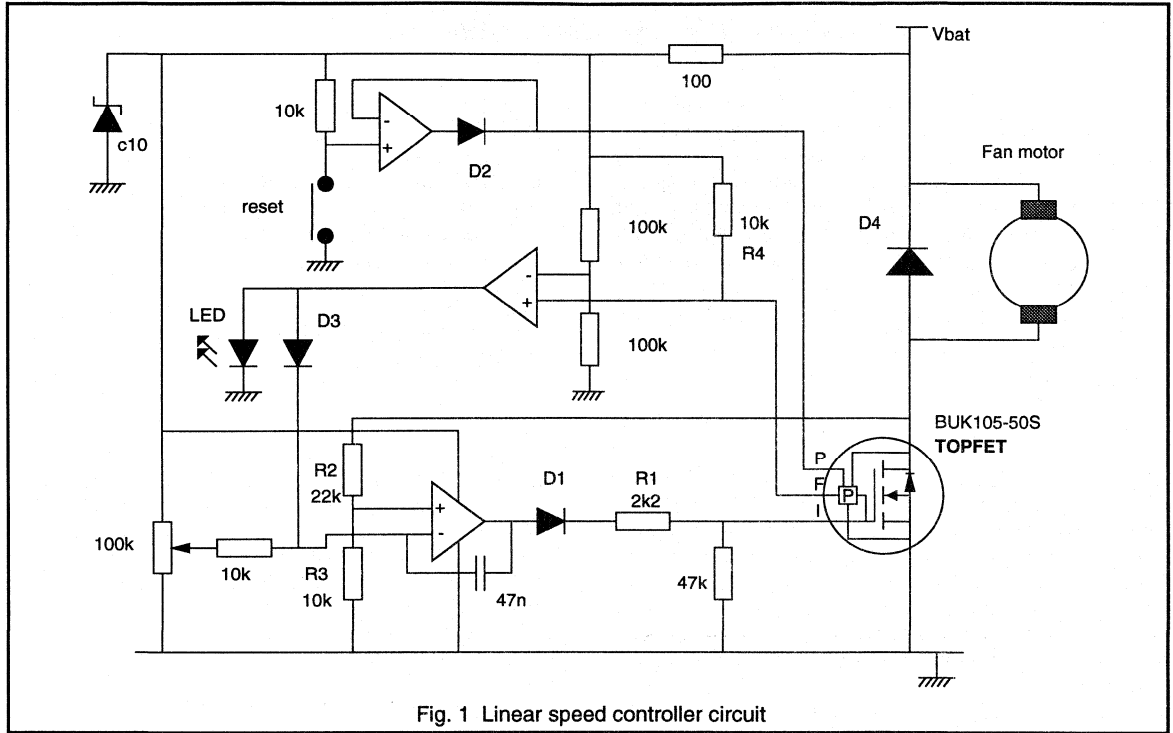


Fig. 1 Linear speed controller circuit

Two versions of BUK105-50 are available, 'S' and 'L'. They differ in their protection supply requirements. L devices are designed to operate from a nominal 5 V. This makes them compatible with 5 V logic families like the 74HC and HCT series. L types can be driven at 10 V but as curves in the data show the protection characteristics are affected. On the other hand, S devices are designed to work with a nominal 10 V such as is available from HEF4000 logic gates.

If this circuit were part of a larger system then it is likely that such a gate would be available. In the circuit given here the protection pin is connected to the output of an op-amp wired as a non-inverting buffer. The buffer input is pulled up to the +ve rail with 10 k Ω . The protection supply can be taken low - to reset the TOPFET - by a pushbutton which grounds the input of the buffer.

Flag pin

In this circuit the flag pin is connected to a 10 k Ω pull-up resistor, R4. In a more sophisticated system this signal could then be fed to the input of a logic gate and used to inform the system controller of a fault condition. The

controller could use this information to initiate a reset sequence or perhaps shut down the circuit and record the fact in a maintenance record store.

In this simpler system the flag output feeds the input of an op-amp wired as a comparator which in turn indicates a fault by lighting a LED. The output is also fed via D3 to the input of the speed controller op-amp. This overrides the signal from the speed adjusting potentiometer and takes the TOPFET input low. This arrangement has been used - even though the circuit has been designed to allow the TOPFET to self protect - to prevent the TOPFET from turning back on when there is no protection supply, for example during reset.

Drain pin

Freewheel diode D4 is needed if the energy stored in the motor inductance exceeds the TOPFET's non-repetitive inductive turn-off energy rating at the designed operating junction temperature. The overvoltage clamping of the TOPFET is still needed, however, to protect against supply line transients.

5.3.8 PWM Control with TOPFET

Speed control of permanent magnet dc motors is required in many automotive and industrial applications, such as blower fan drives. The need for protected load outputs in such systems can be met by using a TOPFET with its inherent protection against short circuit, overtemperature, overvoltage and ESD. In section 5.3.7 the two basic methods for speed control, linear and PWM, are compared and discussed and a circuit example for linear control is given. This section gives an example of a PWM drive circuit using a 5-pin TOPFET.

Circuit Description

The circuit shown in Fig. 1 contains all the elements needed to produce a PWM circuit which can control the speed of a heater fan motor. The power device, because it is a TOPFET, can survive if the load is partially or completely shorted, if overvoltage transients appear on the supply lines or if the cooling is, or becomes, insufficient.

In a PWM control system the supply to the motor has to be switched periodically at a frequency significantly above its mechanical time constant. The net armature voltage and thus the motor speed is controlled by the duty cycle, i.e. on-time/period, of the control signal. With the component values shown, the circuit operates at a frequency of 20kHz. This means that any mechanical noise created by the switching is ultrasonic. The main building blocks of the circuit are the PWM generator, the power driver and the interface between the two.

PWM Generator

In Fig. 1, OP1 together with T1 and T2 form a saw-tooth generator, whose frequency is determined by R1 and C1. OP2 compares the saw-tooth voltage waveform at its inverting input with the voltage determined by the potentiometer P1. The output of OP2 is high as long as the saw-tooth voltage is less than the P1 voltage. As a result, the higher the voltage at P1, the longer the positive pulse width and thus the higher the duty cycle of the signal at the output of OP2.

Interface PWM Generator - TOPFET

The output signal of OP2 is fed to emitter-followers T4 and T5. These act as a low impedance driver for the input of the TOPFET. The drive is needed to achieve the short switching times which keep the dynamic switching losses of the TOPFET below the on-state losses.

Resistor R15 is included between the driver T4/T5 and the TOPFET input to ensure proper function of the TOPFET's internal overvoltage protection. This overvoltage protection is an active clamp circuit that will try to pull up the gate of the TOPFET's power MOSFET (i.e. the input pin) if the drain-source voltage exceeds 50V. A minimum resistance of 100Ω between input and ground is needed for the active clamp to succeed.

If the load is shorted or the TOPFET's junction temperature is too high, the internal sensors of the TOPFET will detect it and inform the protection logic which will turn off the internal flag transistor. The flag pin, which is connected to the drain of this transistor, will be pulled high by resistor R16. This will turn on transistor T3 pulling the input to the driver stage, T4/T5, low and hence turning the TOPFET off.

The TOPFET will remain in this state - even if the error condition disappears - until a reset is applied. The 5-pin TOPFETs are reset by taking the protection SUPPLY pin below V_{PSR} . In this circuit this is done by closing the reset switch, pulling the protection pin to ground. In this state there is no protection supply so the TOPFET is unprotected. However, the TOPFET indicates the absence of a protection supply by the flag transistor remaining off. In this circuit this causes the drive to the TOPFET to be low hence the TOPFET will stay off. The TOPFET will resume normal operation when the reset switch is opened and the protection supply is re-established.

Power Stage

In this circuit, the main power switch is a BUK105-50L which has an $R_{DS(ON)}$ of 60 mΩ @ $V_{IS} = 5$ V. The L version of the BUK105 has been chosen so that the protection supply can be fed from the available 5 V supply. The maximum protection supply current, I_{PS} , is 350 μA, the voltage drop across R17 could be 0.42 V. Even if the voltage is regulated as low as 4.5 V, the protection supply will still be > 4 V, the minimum V_{PSP} for valid protection with a V_{IS} of 5 V.

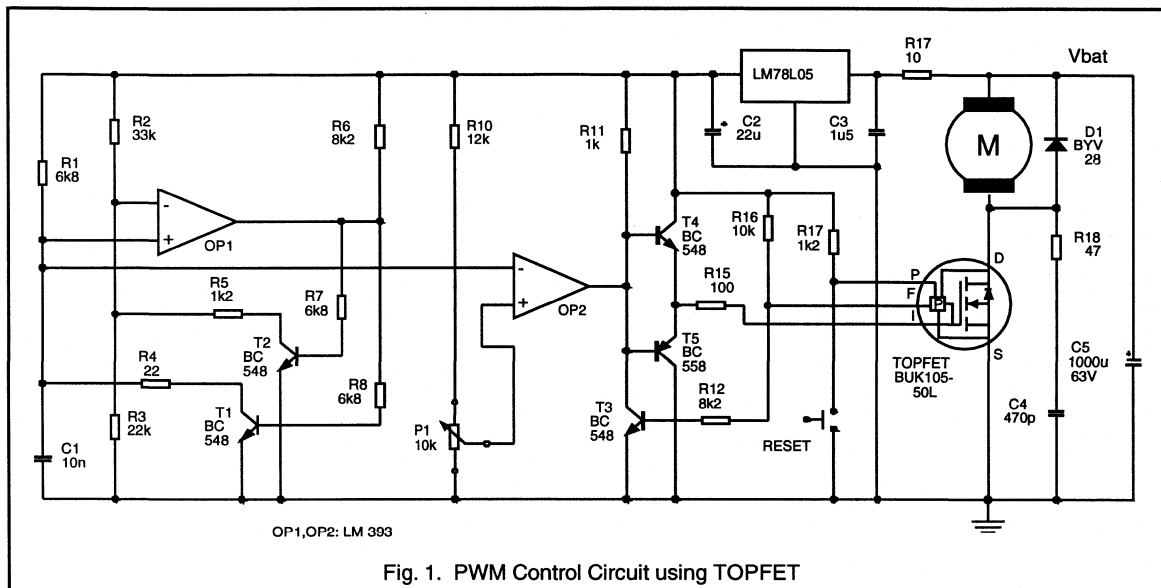
If a lower $R_{DS(ON)}$ were needed this could be achieved by modifying the circuit to give a higher V_{IS} on the TOPFET. A $V_{IS} = 7$ V would give an $R_{DS(ON)} = 50$ mΩ. An input voltage as high as 10 V could be used but any increase must be accompanied by an increase in the protection supply voltage. A curve showing the required V_{PSP} for the full range of input voltage is given in the data sheet.

The given circuit can be used in both 12V and 24V systems because, with an input voltage of 5V, the TOPFET is short circuit protected up to a supply voltage of 35V. However, if a supply this high is expected then the dissipation and voltage rating of the regulator would need to be studied.

D1 is a freewheel diode across the motor load which must be present even though the TOPFET has an internal clamp circuit. This is because the dissipation resulting from

repetitively clamping at 20 kHz is very high, much higher than any power switch of this size would be able to handle. R18/C4 are optional devices that slow down switching, reducing dV/dt and hence RF noise emission.

Capacitor C5 helps to decouple the circuit from the supply and prevents excessive di/dt on the power lines and the excessive voltage spikes it would produce.



5.3.9 Isolated Drive for TOPFET

An isolated drive for a power transistor is required if an electronic replacement of an electromechanical relay is to be realised. By using a TOPFET, with its integrated protection functions, in combination with an isolated input drive, the following advantages over an electromechanical relay can be achieved:

- o Permanent short circuit protection
- o Over temperature protection
- o Active clamping at inductive turn-off
- o Logic level control
- o Higher switching frequency

This section presents a complete circuit example of a transformer isolated drive. It also discusses other isolation techniques particularly in relation to meeting TOPFET's specific requirements.

Basic Methods for Isolated INPUT Drives

Opto-Isolated Drives

For this method a light emitter (e.g. LED or lamp) and a photo-device is needed. The latter can be subdivided into two groups:

Photo Resistors/Transistors

With these devices a 'switch' can be built to control the input voltage of a TOPFET. They cannot provide the power needed to drive the input so a separate supply is needed. In low side configurations this can be the main supply directly. In high side configurations an input voltage above main supply level is needed which could be generated by a charge pump. However, the supply connection needed for this type of opto-isolated drive is not needed with an electromechanical relay. So an opto-isolated drive with photo resistors/transistors cannot serve as a universal relay replacement.

Photo Cells

The drive energy from a control pin can be transferred to the input pin of a power device by means of photo cells. This would eliminate the need for the additional supply connection. Integrated devices exist that combine an LED and a chain of photo-cells. They are designed to drive ordinary power MOSFETs so their output current, due to the low efficiency of the photo-cells, is only a few μA . This is not enough to supply the protection circuits of a TOPFET so this method cannot be used to provide isolated drive for a TOPFET.

Transformer Isolated Drives

As with photo-cells, pulse transformers provide a means of transferring energy from the control pin to the input of the power device. However, the transfer efficiency of a pulse transformer is much higher, so the protection circuits of a TOPFET can be supplied satisfactorily.

Extremely small pulse transformers are now available, and some outlines are suitable for surface mount. It is, therefore, realistic and practical to use this method to create a relay replacement for high and low side configurations.

Circuit Description

Figure 1 shows a transformer-isolated drive circuit for TOPFET. As discussed above, a TOPFET in combination with this drive circuit can be employed either in high side or low side configuration without modifications on the driver side. The drive signal on the transformer's primary side is a pulse train that is rectified on the secondary side to provide a continuous input voltage V_{IS} for the TOPFET. For the given dimensioning, a pulse rate in the range of 100kHz is well suited. A high pulse rate is advantageous as it allows the dimensions of the transformer and smoothing capacitor, C2, to be minimised.

On the primary side, a voltage is applied to the transformer when T1 is on. The positive pulse amplitude is limited by D7 on the secondary side. The drain current of T1 and the transformer current are limited by R1.

During the off period of T1, the transformer's primary current freewheels through D1 and D2. Thus the absolute maximum value for the negative pulse amplitude on the primary winding is equal to the sum of breakdown voltage of zener diode D2 and forward diode drop across D1. At a duty cycle of 50%, this value should be at least as high as the positive pulse amplitude. This allows the primary current to reach zero and thus the magnetic flux in the core to be reset while T1 is off. The maximum off-state drain-source voltage of T1 occurs if the secondary winding of the transformer is left open. It is the sum of supply voltage V_P , zener voltage of D2 and forward voltage drop across D1.

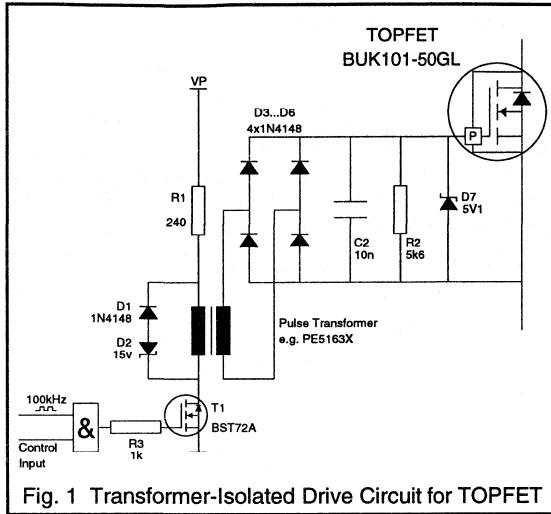


Fig. 1 Transformer-Isolated Drive Circuit for TOPFET

Using a bridge rectifier on the secondary side makes use of both positive and negative pulses to generate the input-to-source voltage V_{IS} for driving the TOPFET. This increases the efficiency. It also reduces the ripple on V_{IS} , therefore the ripple on the load current and hence the electromagnetic noise emission.

The minimum value for V_{IS} is set by the need to have enough voltage for correct operation of the TOPFET's overload protection circuits. The maximum is determined by the breakdown voltage of the ESD protection diode at the input pin. Taking this into account, V_{IS} should be within the range of 4V-6V in the case of the TOPFET type BUK101-50GL. In the given circuit the lower limit of V_{IS} is determined by

the minimum supply voltage V_P on the primary side, the transformer ratio, and the diode voltage drops at the bridge rectifier. Zener diode D7 ensures that V_{IS} cannot exceed the upper voltage limit.

The time constant of R2 and smoothing capacitor C2 determine the fall time of V_{IS} after the control input at the primary side goes low. A fall time significantly longer than that chosen here should be avoided for the following reason.

After a TOPFET has turned off to protect itself, it is latched off so it stays in the off-state as long as V_{IS} is high. To reset the TOPFET, V_{IS} must go low. In this circuit this happens when the control input at the primary side goes low, disconnecting the drive pulses from the gate of T1. On the secondary side, this allows C2 to be discharged by R2 and hence V_{IS} to decrease. When V_{IS} has fallen below the protection reset voltage level V_{ISR} , the fault latch will reset and an internal transistor, which holds the gate low, will turn off. The gate voltage will now rise to the C2 voltage and the TOPFET's output MOSFET will conduct again. The MOSFET will be fully off when V_{IS} falls below the TOPFET threshold voltage $V_{IS(TH)}$. In the range between V_{ISR} and $V_{IS(TH)}$ (max. 3.5V-1V for the BUK101-50GL) the output MOSFET may conduct while the protection circuits are non-active. For safe reset of a latched TOPFET with a shorted load, this V_{IS} -range must be passed through within a limited time interval. With the dimensioning of R2 and C2 shown in Fig. 1, this time interval is approximately 130 μ s. The BUK101-50GL is guaranteed to withstand a hard short circuit for > 300 μ s at a battery voltage of 35V and $V_{IS}=5$ V. So the chosen values of R2 and C2 ensure safe turn-off of the TOPFET.

5.3.10 3 pin and 5 pin TOPFET Leadforms

The TOPFET (Temperature and Overload Protected MOSFET) range of devices from Philips Semiconductors is based on conventional vertical power MOSFET technology with the advantages of on-chip protection circuitry. Using this approach the devices are able to achieve the very low values of $R_{DS(on)}$ which are required in applications for automotive and other power circuits. TOPFET devices are currently available in two topologies for maximum compatibility with the requirements of circuit designers.

3-pin TOPFETs TO220	R_{thj-mb} (K/W)	5-pin TOPFETs SOT263	R_{thj-mb} (K/W)
BUK100-50GL	3.1	BUK104-50L	3.1
BUK100-50GS	3.1	BUK104-50S	3.1
BUK101-50GL	1.67	BUK105-50L	1.67
BUK101-50GS	1.67	BUK105-50S	1.67
BUK102-50GL	1.0	BUK106-50L	1.0
BUK102-50GS	1.0	BUK106-50S	1.0

Table 1. 3-pin and 5-pin TOPFET type ranges

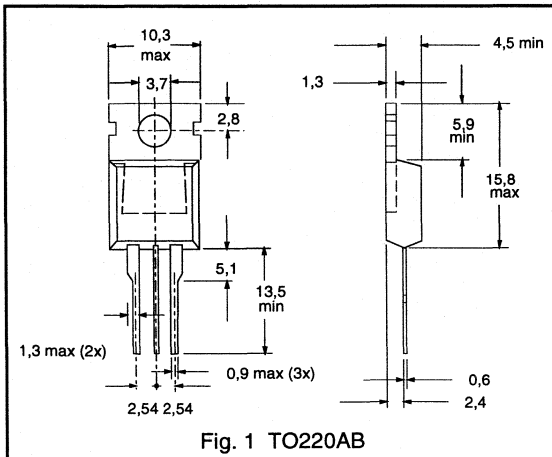


Fig. 1 TO220AB

The 3-pin TOPFETs are assembled in the standard TO220-AB package (Fig. 1), which is also sometimes known as SOT78. The 5-pin versions are assembled in the SOT263 PENTAWATT package (Fig. 2). Depending upon the load and the application the devices can be operated in free air or attached to a heatsink. When using a heatsink the advantage of these outlines lies in the very low thermal impedance which can be achieved. Table 1 shows the thermal resistances for the range of TOPFET devices.

Although these outlines are industry standards, on occasions users have the need to form the leads of the devices to accommodate a variety of assembly requirements. Philips Semiconductors can offer a number of standard pre-formed leadbend options to make the purchase and specification of leadformed devices easier.

These pre-forms satisfy the basic rules concerning the bending and forming of copper leads and ensure that, for example, the bend radius is not less than the thickness of the lead and that there is sufficient material at the base of the plastic moulding to enable the act of pre-forming to take place without damage to the crystal or its die attach and wire-bonding.

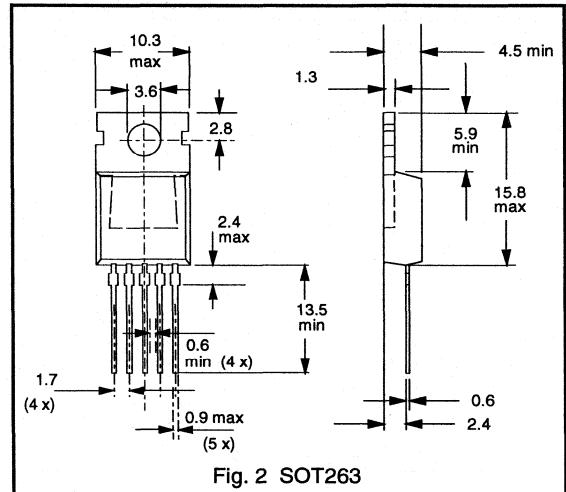


Fig. 2 SOT263

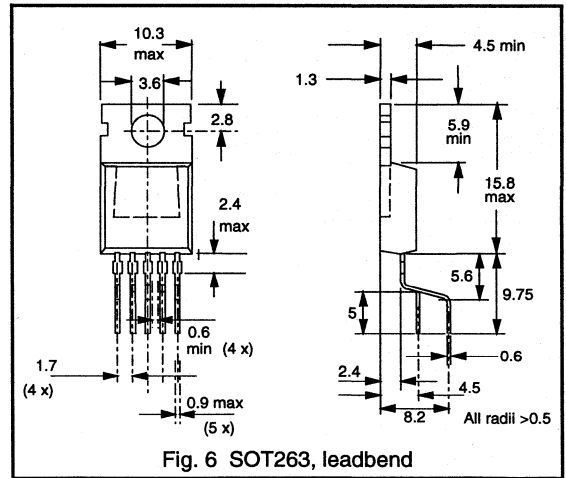
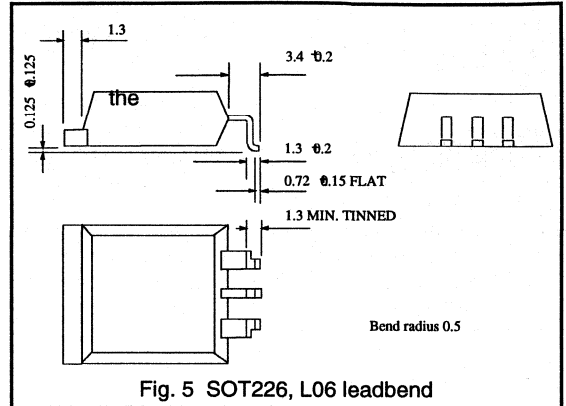
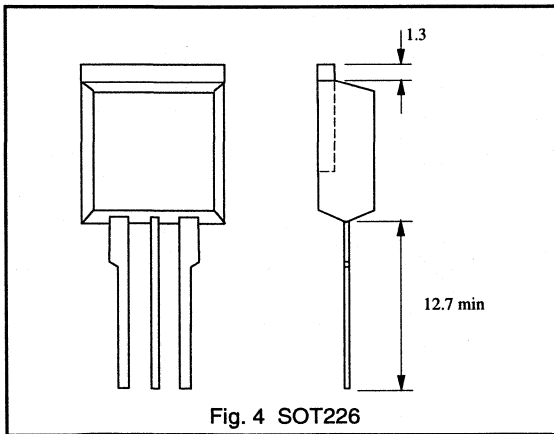
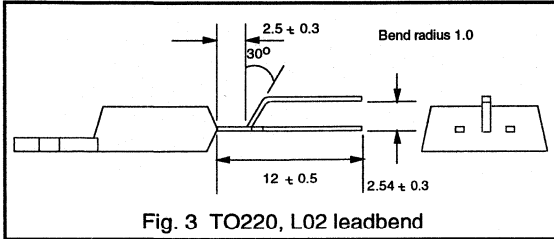
Figure 3 shows leadform option L02 for a TO220 type. A device with this standard leadbend can be ordered by specifying /L02 as the suffix for the device type. For example, a BUK101-50GL with this leadbend is specified by ordering type BUK101-50GL/L02.

In addition to this, there is often the necessity to crop the tab off the device to make a low profile version, when height above the pcb is restricted. Again, without control, there is a risk of fracturing the crystal during this process but Philips Semiconductors can offer this option (SOT226), shown in Fig. 4, which can be ordered by specifying the suffix /CR to the device type number, eg. BUK102-50GS/CR.

For surface mountable TOPFETs, the leadbend option L06 means that the device can be used in applications where a low profile is required. With this option an electrical contact

from the pcb to the tab of the device is possible. The device is shown in Fig. 5 and, for the BUK100-50GS would be specified as the BUK-100-50GS/CRL06.

For 5-pin TOPFET the device is available in the leadbent SOT263 outline as standard (Fig. 6). For the leadform option the device type number is modified by the addition of the suffix P to the SOT263 type name, eg BUK104-50L (SOT263) becomes BUK104-50LP (leadbent SOT263).



5.3.11 TOPFET Input Voltage

Low side TOPFET data sheets specify that the voltage between the input and source pins should not be less than 0 V, in other words should not go negative. In many circumstances, sound layout using normal logic gates will ensure that this condition is always satisfied. However, in some situations it is difficult to design a circuit in which this condition is met under all conditions. This section explains the reason for the quoted rating and shows that it is a limit in only a few circumstances. The paper will also illustrate how negative inputs can be generated. Section 5.1.12 shows how negative inputs can be prevented and recommends a simple method of stopping a TOPFET being damaged if negative inputs do occur.

Reason for specification limit

All the pins of a low side TOPFET are protected against ESD. The input pin - the most sensitive pin of a normal MOSFET - is protected by a special diode connected between the input and the source. In the presence of an ESD pulse, this diode conducts and clamps the voltage on the input pin to a safe level.

The diode is formed by an area of n++ in a p+ region which is diffused into the n- epi layer, see Fig. 1. The input pin is connected to the n++ region and then to the rest of the circuits. The p+ region is connected by the metalisation to the source area of the power MOSFET part of the TOPFET. However, the p+ region also connects to the n- epi layer and hence to the drain via the n+ substrate. The ESD diode is formed by the n++ / p+ junction. However, the n++ and p+ diffusions in the n- epi also create a parasitic npn transistor. It is the presence of this transistor which makes the negative input rating necessary.

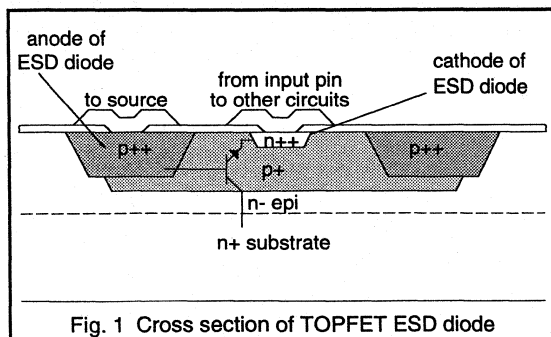


Fig. 1 Cross section of TOPFET ESD diode

With an input potential lower than the source potential, the input acts as an emitter, the drain as a collector and the source as a base, so the potential difference will act as bias for the parasitic transistor. The diffusion concentrations used to create a good ESD protection diode create a transistor with a limited forward SOA. The characteristics of the transistor mean that it can be damaged if its V_{CE} is greater than 30 V when its base is forward biased. For the TOPFET this means that damage could be caused only if the input goes negative while the drain voltage is > 30 V.

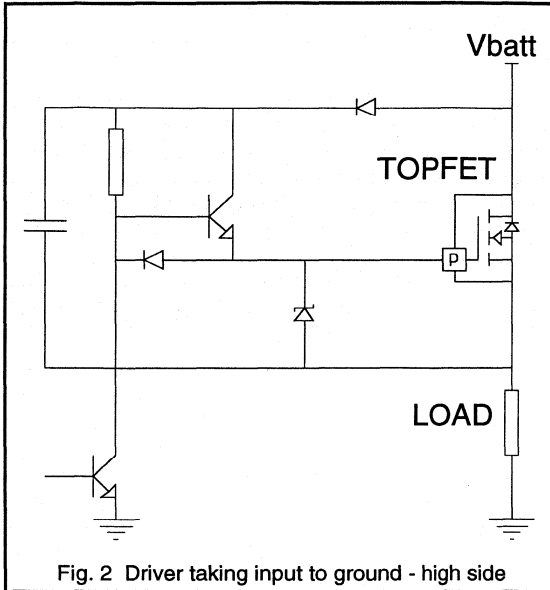
It should be noted that the conditions which may damage the transistor assume the impedance of the bias supply is low. If the bias is restricted the limits of SOA are different so the drain voltage needed for damage will be different. In any event at drain voltages < 30 V, a negative input will cause the parasitic transistor to conduct but will not cause damage.

Conditions creating negative input

The most obvious effect of the minimum V_{IS} is to preclude the use of negative drive to speed up turn off. However, this technique is only justifiable in very high frequency circuits and TOPFET is intended for use in DC or low frequency applications, so it is unlikely that this type of drive will be under consideration. The typical TOPFET driver stage will be unipolar using gates or discrete transistors from positive supply rails only. These drivers will turn the TOPFET off either by removing the drive and allowing TOPFET to turn itself off, via its internal pull down resistor, or by pulling the input to zero volts. It would appear, therefore, that negative inputs should not occur, but in some situations and with some circuit configurations they can.

High side circuits

A negative input can be created if an overvoltage transient is applied to an off-state TOPFET being used as a high side switch. A TOPFET will start to conduct if a supply line voltage transient exceeds its clamping voltage. The current now flowing through the TOPFET will also flow through the low side load, raising the source potential above ground. The driver stage may be designed to turn the TOPFET off by pulling the input to ground as in Fig. 2. If it is, then the conditions for harmful negative input have been created - the drain voltage is > 30 V, the input is at ground and the source potential is higher, so the input is negative.

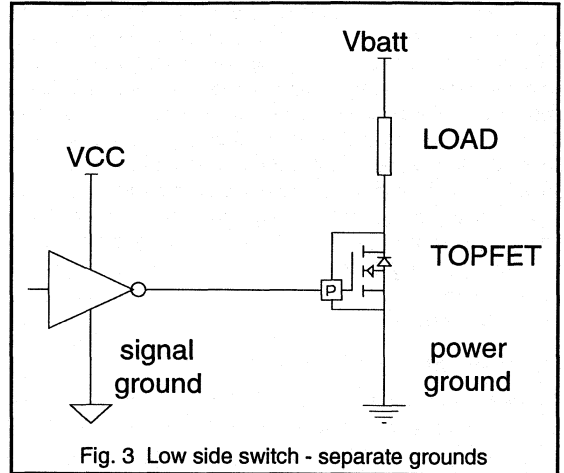


Low side circuits

In some circumstances it is possible to create negative input in a low side configuration. In the previous example it was a small current in relatively large resistance that raised the source above ground. The same effect can be created by a large current in the low, but not negligible, resistance of the wiring between the source pin and ground.

Systems are often configured with separate power and signal grounds and it is possible that the driver will be referenced to signal ground, see Fig. 3. In this case the TOPFET input will be pulled to signal ground potential when it is being turned off. The source will be connected to power ground and the common connection between the grounds

may be a considerable distance from the TOPFET. The resistance of the wiring will be low but even 20 mΩ may be significant if the current is high.



There are two occasions when a large enough current could be flowing. The first is during the turn-on of a load with a high inrush current, for example a cold incandescent lamp. The second is when the load is shorted out. If the TOPFET turns off while this current is flowing, the energy in the inductance of the wiring from the load to the TOPFET drain would raise the drain voltage, possibly to greater than 30 V. The high current, as high as 60 A, in the source to ground wiring, say 20 mΩ, would raise the source 1.2 V above ground. So, the combination of conditions which may damage a TOPFET have been created.

The circuits and circumstances mentioned in this paper are only examples and other hazardous negative input situations will exist. Methods of preventing negative input and of stopping a TOPFET being damaged, if negative inputs do occur, is presented in section 5.1.12.

5.3.12 Negative Input and TOPFET

Low side TOPFET data sheets specify that the voltage between the input and source pins should not be less than 0 V, ie. should not go negative. This limit is needed to prevent the parasitic transistor, formed by the input ESD protection diode in the n-epi, being damaged in some circumstances. The reason for the limit and the causes of potentially damaging conditions are discussed more fully in section 5.3.11. This section will show how damaging negative inputs can be prevented and recommend a simple method of stopping low side TOPFETs being damaged if negative inputs do occur.

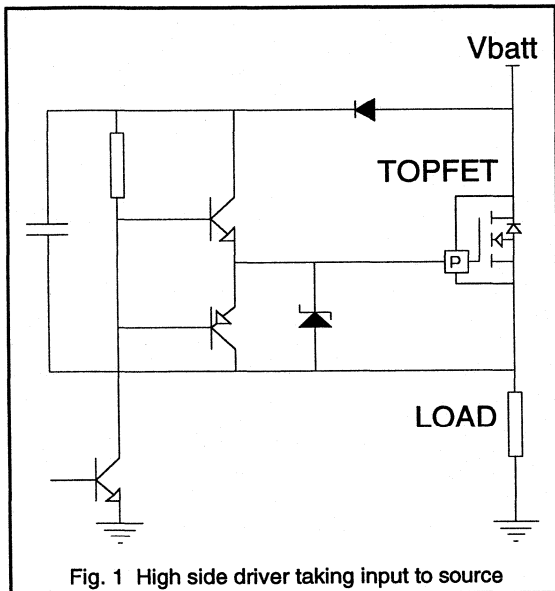


Fig. 1 High side driver taking input to source

Avoiding negative input

Section 5.3.11 gave examples of high and low side drive configurations which could, in some circumstances, generate a potentially damaging negative input. There are two ways to prevent the input from being taken too low. The first is to fit a diode in series with the input pin. The cathode of the diode would be connected to the TOPFET. The diode would conduct while the driver output was high but would turn off and isolate the input pin when the driver tried to pull the input low. The driver would now not be driving the TOPFET off but would be allowing it to turn itself off via its internal input - source resistor.

The second method is to arrange the drive so that it turns the TOPFET off by pulling the input to the source rather than to ground. The circuit shown in Fig. 1 shows a high side drive in which this has been achieved. The TOPFET is turned off by a pnp transistor being turned on and pulling the input to the source.

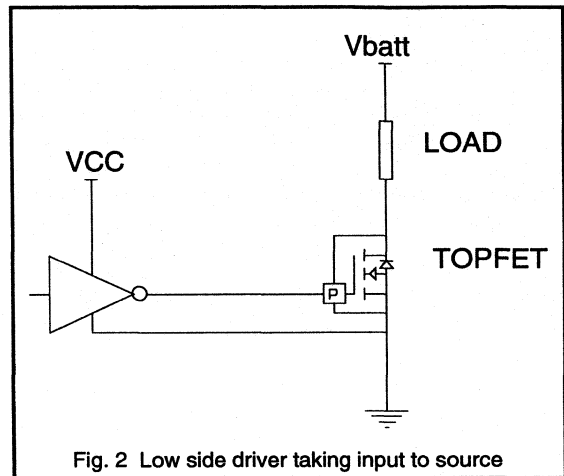


Fig. 2 Low side driver taking input to source

Figure 2 shows a low side drive where the GND pin of the CMOS gate is connected as close as possible to the TOPFET source pin. Once more the effect is to turn off the TOPFET by pulling the input to source.

If negative inputs cannot be avoided

The technique of referencing drivers to the source pin helps prevent negative inputs being generated. It is used in most power MOSFET switching situations and should be used with TOPFET wherever possible. If negative inputs cannot be eliminated there are ways of preventing them from causing damage to a TOPFET.

Although published data gives 0 V as the lower limit of V_{IS} , lower values can be acceptable. The V_{IS} limit of 0 V ensures that the SOA of the parasitic transistor associated with the ESD diode is never exceeded. The arrangement shown in Fig. 3 can be used to ensure this. This shows the parasitic npn transistor of the TOPFET and two additional anti-parallel diodes in series with the input.

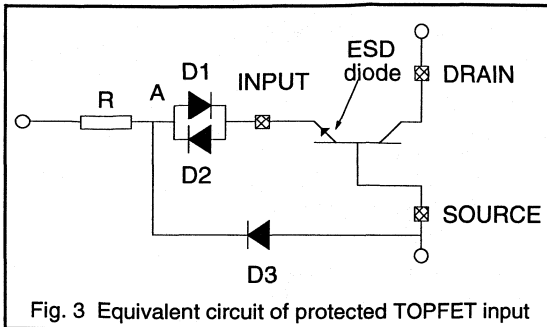


Fig. 3 Equivalent circuit of protected TOPFET input

If the drive voltage goes negative, the diode D1 (see fig. 3) is reverse biased and diodes D2 and D3 are forward biased. The voltage between Source and point A is limited by D3 and the current is limited by R. This voltage is divided between D2 and the base-emitter junction of the ESD diode. The current flowing through the ESD diode's base-emitter junction is therefore negligible and so the SOA of this transistor is not exceeded. This means that all the conditions needed to damage the device can be avoided and the TOPFET is protected against negative input.

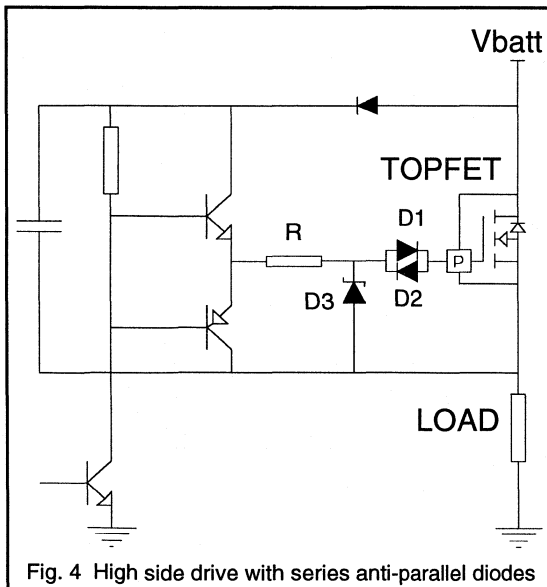


Fig. 4 High side drive with series anti-parallel diodes

In the normal on state, D1 will be forward biased but it will create a voltage drop of about 0.5 V between point A and the TOPFET input. To enable a 3 pin TOPFET to protect itself, its input must be >4.0 V so the designer needs to ensure that the voltage at A is >4.5 V.

During a normal turn-off the gate discharge current will flow through the forward biased D2. No special measures are needed to cope with D2's voltage drop because 0.5 V is well below the TOPFET's threshold voltage so it will be properly turned off if point A is taken to 0 V.

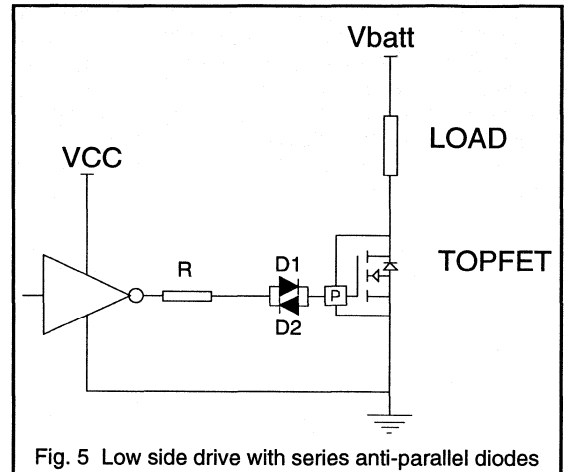


Fig. 5 Low side drive with series anti-parallel diodes

Figure 4 shows the high side drive of Fig. 1 modified to include the series anti-parallel diodes, D1 and D2. D3 is already present in the form of the input voltage limiting zener so the only extra components are the series anti-parallel diodes. A modified low side drive is shown in Fig. 5. Here D1 and D2 are fitted between the output of a cmos gate and the TOPFET input pin. In this circuit, diode limiting is provided by the bipolar parasitic diode inherent in cmos output stages.

Series resistor values

The recommended minimum resistor values are,

Types	Over-voltage transient	Minimum series resistor
3-Pin	< 200 V for 2 ms	50 Ω
3-Pin	< 300 V for 2 ms	300 Ω
5-Pin	< 100 V for 2 ms	200 Ω
5-Pin	< 200 V for 2 ms	1000 Ω
5-Pin	< 300 V for 2 ms	2000 Ω

If the negative voltage between point A and the source is present for a longer period of time than 2 ms then a larger value of series resistor may be required.

5.3.13 Switching Inductive Loads with TOPFET

If there is current flowing in the coil of a solenoid or a relay then there is energy stored in the inductance. At turn-off this energy has to be removed from the coil and dissipated somewhere. During this process, an extremely high voltage will be generated unless measures are taken to limit it. This voltage can lead to breakdown and, beyond a certain energy level, damage to the switching transistor. Common methods of controlling this voltage are a freewheel diode in parallel with the inductor or a suppressor diode in parallel with the switching transistor.

A TOPFET with its overvoltage clamping feature can save these extra elements, provided that its limiting values are not exceeded during the turn-off procedure. This section shows a simplified method of estimating the dissipated energy and the junction temperature rise in a TOPFET at inductive turn-off. The equations given here are first order approximations. They act as an aid in determining the need for an external freewheel or suppressor element.

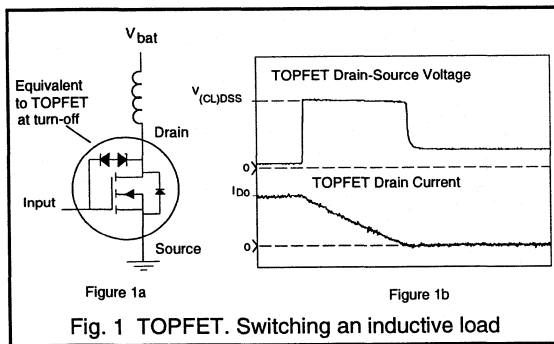


Fig. 1 TOPFET. Switching an inductive load

TOPFET behaviour

Figure 1 shows an equivalent circuit diagram and the shapes of drain current I_D and drain-source voltage V_{DS} versus time for a TOPFET switching an inductor. The overvoltage clamp feature of TOPFET is represented by a zener diode that drives the output power MOSFET into conduction if V_{DS} rises too high. In this state the TOPFET acts as an active clamp element, limiting its own V_{DS} to typically 60V.

Saving of external overvoltage protection

The TOPFET clamp feature is the only voltage limiting required if the energy associated with turn-off, E_{clamp} , does not increase the TOPFET's junction temperature too far. The following section shows how to estimate E_{clamp} . Limiting values for the energies E_{DSM} for non-repetitive clamping and E_{DRM} for repetitive clamping are stated in the data sheet. E_{DSM} relates to a peak junction temperature of 225°C reached during clamping which is acceptable if it occurs only a few times in the lifetime of a device. Thus E_{DSM} should only be used when deciding on the necessity for external protection against overvoltage transients that occur extremely rarely.

However, when switching inductive loads, absorbing E_{clamp} is a normal condition. So to achieve the best longterm reliability, the peak junction temperature should not exceed 150°C. A method for estimating the peak junction temperature is given later.

In this type of repetitive clamping application, the E_{DRM} rating in the data sheet can be compared with E_{clamp} to give an initial indication of need for external voltage limiting. This initial assessment should be followed by a temperature calculation to find the maximum allowable mounting base temperature and thus the heatsink requirements.

Estimation of clamping energy

The energy stored in the coil of a solenoid valve or a relay with the inductance L at a current I is:

$$E_L = \frac{1}{2} L I^2 \quad (1)$$

The clamping energy E_{clamp} in the TOPFET during an inductive turn-off follows from equation (1) and the fact that, during clamping, the battery also delivers energy to the TOPFET:

$$E_{clamp} = \frac{1}{2} L I_{D0}^2 \frac{V_{(CL)DSS}}{V_{(CL)DSS} - V_{bat}} \quad (2)$$

In (2) I_{D0} is the drain current at start of turn-off, $V_{(CL)DSS}$ the TOPFET's typical drain-source clamping voltage, V_{bat} the battery voltage and L the load inductance. Equation (2) assumes an inductor with no resistance. In practice, there will be some resistance, which will dissipate a fraction of E_{clamp} . Therefore, (2) represents a worst case situation.

Estimation of junction temperature

The peak junction temperature during clamping can be estimated by adding the maximum temperature rise ΔT_j to the average junction temperature, T_{j0} .

$$T_{j, pk} = T_{j0} + \Delta T_j \quad (3)$$

Measurements have shown that ΔT_j can be approximated by

$$\Delta T_j = \frac{5}{6} V_{(CL)DSS} \cdot I_{D0} \cdot Z_{th} \quad (4)$$

Where Z_{th} is the transient thermal impedance for a pulse width of $\frac{1}{3}$ of the time in clamping, which, for a coil resistance of zero Ohms, is:

$$t_{clamp} = \frac{L \cdot I_{D0}}{V_{(CL)DSS} - V_{bat}} \quad (5)$$

Average dissipation will make T_{j0} higher than the mounting base temperature T_{mb} , which can be assumed as constant, if the TOPFET is mounted on a heatsink. In repetitive switching applications, both on-state losses and turn-off losses contribute to the average dissipation. So T_{j0} will be:

$$T_{j0} = T_{mb} + \left(E_{clamp} \cdot f + I_{RMS}^2 \cdot R_{DS(ON)} \right) \cdot R_{th, j-mb} \quad (6)$$

In (6) I_{RMS} is the root mean square value of the load current and $R_{DS(ON)}$ is the on-state resistance of the TOPFET. In non repetitive applications, the average dissipation is the on state dissipation so T_{j0} is:

$$T_{j0} = T_{mb} + I_{D0}^2 \cdot R_{DS(ON)} \cdot R_{th, j-mb} \quad (7)$$

If these calculations indicate that the peak junction temperature is less than T_{jmax} , then external voltage limiting is not needed.

Calculation examples

Both examples are carried out for $V_{bat}=13V$ and a BUK101-50GS with a clamping voltage of 60 V. For calculation of on-state losses, the maximum $R_{DS(ON)}$ at $T_j=150^\circ C$ of 87.5 m Ω is taken.

Example 1: An inductor with $L=10$ mH is switched off non-repetitively at a dc current $I_{D0}=7$ A.

(5) gives $t_{clamp} = 1.5$ ms. The BUK101 data curve indicates a Z_{th} of about 0.28 K/W at $t_{clamp}/3 = 500$ μs . (4) then gives a ΔT_j of about 100 K. It is a non repetitive application so use (7) to find T_{j0} , which indicates that T_j is about 7°C above T_{mb} due to on-state losses. From the ΔT_j and T_{j0} figures it can be inferred:

$$T_{j, pk} < 150^\circ C \text{ for } T_{mb} < (150-100-7)^\circ C = 43^\circ C.$$

Example 2: An inductor with $L=3$ mH is switched at $I_{D0}=4$ A and a frequency of 100Hz and a duty cycle of 0.5.

(2) yields a clamp energy of 31 mJ, which is less than the E_{DRM} rating of the BUK101 of 40 mJ so repetitive clamping is allowed. (6) yields that T_{j0} will be about 8 K above T_{mb} . From (4) and (5), ΔT_j can be estimated to be < 30 K. These figures imply that this load can be safely driven if the T_{mb} of the BUK101-50GS is < 112°C.

5.3.14 Driving DC Motors with TOPFET

Examples for motor drive circuits using low side TOPFET have already been given in section 5.3.7: "Linear Control with TOPFET", and section 5.3.8: "PWM Control with TOPFET". This section discusses the characteristics of DC motors that have to be considered when designing a drive circuit with low side TOPFET and gives examples of some basic drive circuits.

Important motor characteristics

The permanent magnet motor is the most common type of motor for driving a wide range of applications including small industrial drives, cooling fans and model cars. Therefore, the following discussions are based on this type. The equivalent circuit of these motors is shown in Fig. 1, where R_A and L_A represent the resistance and inductance of the armature.

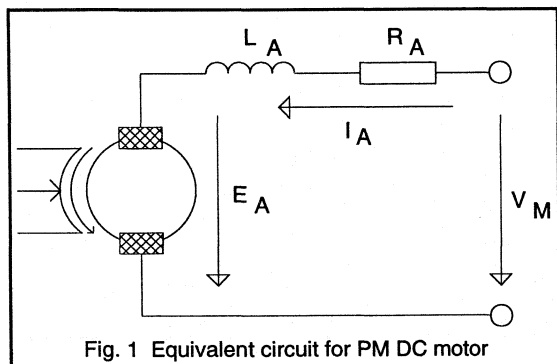


Fig. 1 Equivalent circuit for PM DC motor

Inrush current

Correct operation of some mechanical loads creates a special starting torque requirement for the motor. Since motor torque is proportional to motor current, high starting torque can only be achieved if the inrush current is allowed to be high. The TOPFETs BUK100...BUK106 do not use current limiting techniques to provide overload protection, so the inrush current they can deliver to a motor is limited only by the forward transconductance g_{fs} . To meet extreme starting torque requirements, an 'S' type with 10 V control is to be preferred over an 'L' type with 5 V control because 'S' types can deliver approximately twice the current of 'L' types. Typical currents can be judged from the data sheet $I_{D(SC)}$ in the section TRANSFER CHARACTERISTICS.

Stall current

The stall current of a dc motor is limited by the armature resistance, R_A in Fig. 1, and can reach values of 5-8 times

the nominal current. This current will cause overheating in the motor which may damage the winding insulation or demagnetize the stator magnets.

The current would also cause extra dissipation in the driver but a TOPFET, with its over temperature protection, would survive a permanent stall condition. In addition, with careful thermal design, the TOPFET can also be used to prevent damage to the motor.

Inductive kick back at turn-off

The energy stored in the armature inductance, L_A , has to be removed when the motor is turning off. As in the case of inductive loads such as solenoid valves and relay coils, this is usually done by a freewheel diode. Provided that the energy is within its E_{DRM} rating, a TOPFET's overvoltage protection feature can be used instead of a freewheel diode. Section 5.3.13: "Switching Inductive Loads with TOPFET", covers this topic in more detail and gives a simple calculation method to assess the need for a freewheel diode. If overtemperature shutdown due to a stalled motor can occur, a freewheel diode is generally recommended. Without freewheel diode the TOPFET would have to absorb a very high energy at a junction temperature of at least 150 °C.

In the case of pulsed operation of the motor (e.g. pulse width modulation for speed control), the use of a freewheel diode is advisable. Without it, motor current ripple would be higher and the loss in the switching device could be as high as it would be in a linear control circuit.

Special effects of back EMF

Effects at running out

The back EMF, E_A , of a motor is proportional to the rotational speed. When the TOPFET is turned off, the motor acts as a generator and E_A can serve as the feedback signal in a PWM control system.

Although the back EMF voltage of many motors is, during normal running, below its terminal voltage, in some situations and with some motors the peak back EMF can exceed the terminal voltage. Shortly after turn-off these EMF peaks may even exceed the battery voltage plus one diode drop. In this case the EMF can supply current into the battery circuit by forward biasing the TOPFET's Source-Drain diode (see Fig. 2a). As a result of the internal structure of a low side TOPFET, the Source-Drain diode current will create a conduction path from the Input to the Drain. The current through this path can be limited to a safe

value by including a series resistance R_i as shown in Fig. 2a. Recommended values for R_i are 100Ω for 5V drivers and 220Ω for drivers above 6V.

For 5 pin TOPFETs a path is also created from the Protection Supply and Flag pins. In this case, sufficient current limiting is often provided by the resistors that are fitted to connect the Flag and Protection Supply pins to V_{cc} (see Fig. 2c). The actual resistor values must be determined from consideration of the TOPFET and control circuit data sheets.

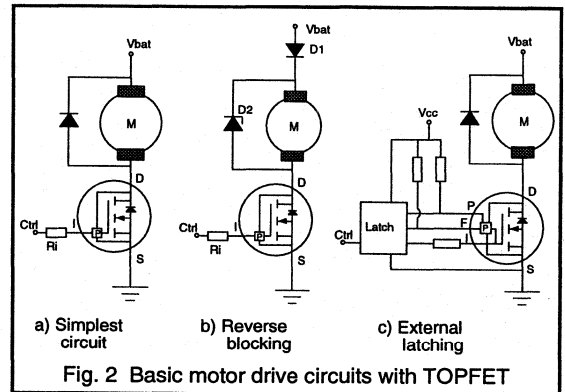
Effects of intermittent short circuit

When a TOPFET's short circuit protection has tripped due to a short circuited motor, the motor will continue to turn. In this situation the motor acts as a generator and its current is reversed. The motor will lose rotational energy and, if the short circuit remains long enough, will stop. In practice however, contact sparking can cause intermittent short circuits. In this case the short circuit may be interrupted before the motor has stopped. After the interruption the generator current will continue to flow, forced by the armature inductance L_A . A path for this negative current into the battery is provided via TOPFET's Source-Drain diode. As described in the above section, currents into Input, Protection Supply and Flag terminals should then be limited by means of series resistances.

Besides this, TOPFET's internal circuits are non-active while its Source-Drain diode is forward biased and a previous overload shutdown will not stay latched. As a consequence, a TOPFET that has turned off due to a short circuit across its motor load may turn on again if the short

circuit opens before the motor has stopped. This behaviour will not damage the TOPFET. However, Figs 2b and 2c show ways of avoiding it if it is not acceptable.

The first method (Fig. 2b) is to avoid forward biasing of TOPFET's Source-Drain diode by means of a series diode D1. An alternative path for the generator current is provided by zener diode D2. (It is worth noting that interruption of the current path with D1 will be required in applications where reverse battery must not activate the motor.) If the inclusion of a power diode into the motor circuit is not acceptable the alternative shown in Fig. 2c can be used. In this approach the flag signal sets an external latch when the TOPFET is tripped by the short circuit. In this way the TOPFET status is stored even when its Source-Drain diode is forward biased. If the TOPFET is being driven from a microcontroller, the 'latch' function could be implemented in software.



5.3.15 An Introduction to the High Side TOPFET

The introduction of high side TOPFETs enhances the range of protected power MOSFETs available from Philips. These devices combine the real power handling ability of low $R_{DS(ON)}$ MOSFETs with protection circuits and the interfacing to allow ground referenced logic signals to control a high side switch.

Type range

Table 1 shows the range of high side TOPFETs. Included in the range are devices with on-state resistance in the range 38 to 220 m Ω . For each of the types an 'X' or 'Y' variant can be supplied ('Y' types have an additional internal resistor in the ground line). All the devices are 50 V types designed for use in 12 V automotive systems.

Type	$R_{DS(ON)}$ (m Ω)
BUK200-50X / BUK200-50Y	100
BUK201-50X / BUK201-50Y	60
BUK202-50X / BUK202-50Y	38
BUK203-50X / BUK203-50Y	220

Table 1. High side TOPFET type range

Features

Particular care has been taken during the development of the high side TOPFET to make a device which closely matches the requirements of the automotive designer.

Overload Protection -

High side TOPFETs are protected from the full range of overload conditions. Low level overloads which result in higher than expected dissipation can cause the TOPFET to overheat. In this case the overtemperature sensor will trip and the TOPFET will turn itself off until the chip temperature falls below the reset point. In the event of a medium level overload, which could allow a high current to flow, TOPFET will limit the current, and hence dissipation, to a level which allows the overtemperature sensor time to react and turn the TOPFET off until it cools sufficiently. In high overload situations, like hard short circuits, the voltage

developed across the TOPFET will cause the short circuit detector to react and latch the TOPFET off until it is reset by toggling the input. Both modes of overload turn-off are reported by pulling the status pin low.

Supply undervoltage lockout -

If the battery to ground voltage is too low for its circuits to work correctly a high side TOPFET will turn off.

Open load detection -

TOPFET monitors its own on-state voltage drop. If the drop is too low, indicating that the current is very small probably because the load is open circuit, TOPFET will report this by pulling the status pin low.

Quiescent current -

One factor of great importance, particularly as the number of devices in a car increases, is quiescent current. In TOPFETs, the supply which feeds the circuits is turned off when the input is low. This reduces off state current consumption from typically 25 μ A to less than 1 μ A.

Ground resistor -

For the fullest protection against the harsh automotive electrical environment, it is often necessary to fit a resistor between the ground pin of a high side device and module ground. To help with this the Y types of the TOPFET range have this resistor integrated on the chip. Apart from the obvious saving in component count, this approach has the advantage that the resistor is now in a package where its dissipation can be easily handled. (This feature is particularly useful when long duration reverse battery situations are being considered).

Inductive load turn-off clamping -

TOPFETs have a network between the MOSFET gate and the ground pin. This network sets the maximum negative potential between the load and ground pins. If the potential tries to exceed this figure, for example during inductive load turn-off, TOPFET will partially turn on, clamping the voltage at the load pin.

EMC

Electromagnetic compatibility is an increasingly important factor in all electronic designs. EMC covers the immunity and the emissions, both conducted and radiated, of electronic units and systems. The directives and tests are rarely applicable to individual electronic components although the behaviour of devices can have a significant influence on EMC performance. In recognition of this, TOPFET has been designed to create as few EMC problems as possible.

	Test Voltage	Pulse width
Pulse 1a	-100 V	0.05 ms
Pulse 1b		2 ms
Pulse 2a	+100 V	0.05 ms
Pulse 2b		0.5 ms
Pulse 3a	-200 V	0.1 μ s
Pulse 3b	+200 V	0.1 μ s
Pulse 5	+46.5 V	400 ms

Table 2. TOPFET transient tests

Conducted immunity -

One area where TOPFET helps with EMC is with its inherent immunity to conducted transients. The voltage supply of a vehicle is notorious for its transients and circuits and systems have to be designed to handle them. On the TOPFET chip are separate circuits which allow the output MOSFET and the control circuits to withstand transients between the battery and both the load and ground pins. The range of transients which high side TOPFETs can survive is shown in Table 2.

Low emission -

High side switch devices generate their gate drive voltage with oscillators and charge pumps running at high frequency - often in excess of 1 MHz. Unless care is taken in the basic design of the device, emissions at the oscillator frequency or its harmonics can appear at the ground and load pins.

The TOPFET designers have taken the necessary care. The appropriate choice of oscillator and charge pump circuits and the inclusion of on-chip filtering have reduced emissions considerably. Some indication of the

improvement can be obtained by simply looking at the current in the ground pin with an AC coupled current probe. Waveforms for the ground pin current of a Philips TOPFET and another manufacturer's high side switch are shown in Fig. 1.

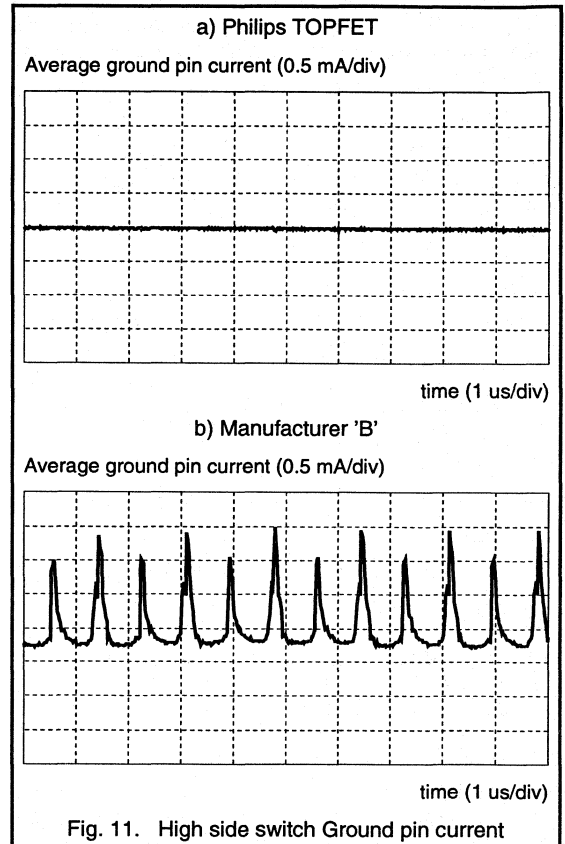


Fig. 11. High side switch Ground pin current

Conclusions

High side TOPFETs are real power devices designed for controlling a wide range of automotive loads. The care taken during their design means that TOPFETs are compatible with circuit designers' protection and EMC requirements.

5.3.16 High Side Linear Drive with TOPFET

This section describes a complete high side linear drive circuit using a TOPFET. A low side linear TOPFET drive circuit is described in section 5.3.7 and the principal pros and cons of linear versus PWM drivers are discussed there. The most important differences between high and low side linear drives are:

- The high side drive needs a charge pump circuit to provide an input voltage higher than the battery voltage.
- In the high side drive the load provides negative feedback for the output transistor. Therefore, the control loop circuit needed to maintain stability in a low side drive can be saved.

The circuit described in this paper was designed for and tested with a 200W fan motor for cars.

Circuit description

The complete high side linear drive circuit can be split up into two blocks:

- The drive circuit
- The charge pump

Drive circuit

Figure 1 shows the drive circuit. Motor speed is controlled by changing the TOPFET's input voltage and therefore its voltage drop. A 5-pin TOPFET is used because this type allows the protection circuit to be supplied independently of the input. This is necessary because in this application the input-source voltage may become too low to supply the protection circuit of a 3-pin TOPFET.

The TOPFET's input voltage and therefore the speed of the fan motor is determined by potentiometer R5. The TOPFET is operating as a source follower. The inherent negative feedback of this configuration will automatically ensure that the source potential will equal the input potential (minus the gate-source voltage) no matter what current is flowing in the motor.

An increase in motor load will tend to slow the motor reducing its back EMF and creating a demand for extra current. The extra current would increase the voltage drop across the TOPFET, lowering the source potential. Since the input potential has been set, the lower source potential

increases the gate-source voltage turning the TOPFET on harder. The voltage drop will now reduce, returning the source - hence motor voltage - to its original value but at a higher current level. All of this means that even without an external feedback network, motor speed is inherently stable, although not absolutely constant, under the full range of motor loads.

Transistor T2 works as a current generator and supplies the protection circuit of the TOPFET. T2 is switchable via transistor T1 and Schottky diode D3. If the potentiometer is in position A, transistors T1 and T2 are switched off allowing R11 to pull the protection supply voltage to 0 V. This feature means the TOPFET, if it has tripped due to over temperature or overload, can be reset by turning the potentiometer to position A.

Position A is also the standby mode. With both transistors switched off, the drive circuit has a very small current consumption. This means that in standby the current consumption of the whole circuit (drive and charge pump) is about 0.3mA.

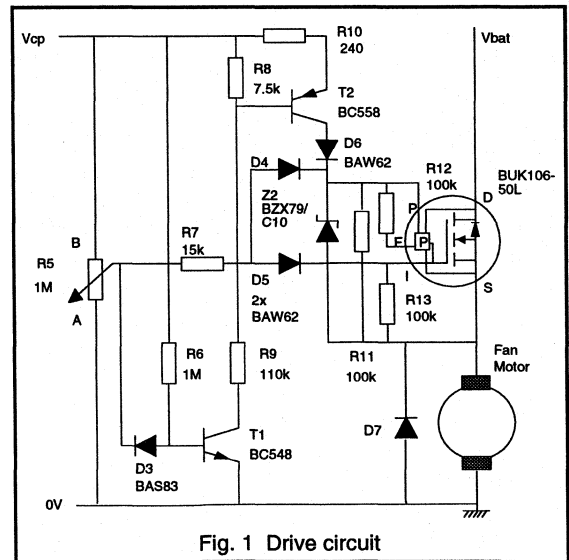


Fig. 1 Drive circuit

TOPFET interface

Negative potentials are not permitted between a TOPFET's protection supply (P), input (I) or flag (F) and its source. This must be considered, especially when designing high side drivers, where the source potential is determined by the load voltage.

If an overvoltage pulse occurs at the supply terminal while the TOPFET is off, the source potential will rise with the overvoltage as soon as the TOPFET's clamp voltage is exceeded. At this time the P,F and I pins should not be clamped with reference to ground, but should be allowed to rise with the source potential. In this circuit this is achieved by diodes D5 and D6 in the feeds to the I,P and F pins.

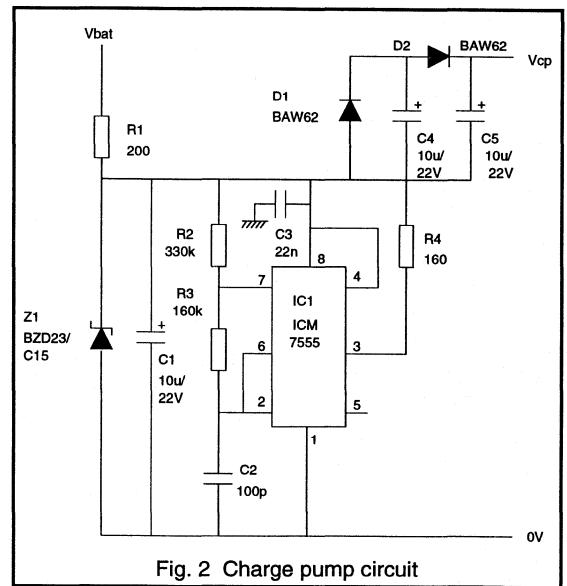
Zener diode Z2 limits the maximum protection supply and flag voltages to about 10 V and, via D4, the input-source voltage to about 10.6 V. Resistor R7 has a value high enough to allow the TOPFET's internal protection circuits to turn off the device in the event of an over temperature or short circuit load.

Charge pump

Figure 2 shows the charge pump circuit. IC1 works as an astable pulse generator at a frequency of 20 kHz which, together with D1, D2, C4, C5 produces a voltage doubler. The ICM7555 is a type with low current consumption. This is an important feature because the circuit consumes current, even when the driver circuit is in standby mode.

In its normal operating mode, the drive circuit has a typical current consumption of 1.5mA which determines the values of C4 and C5. R4 is included to limit the output current of IC1. The charge pump generates an output voltage of about 22V at a battery voltage of 12.6V. Z1, R1 and C1 will smooth and limit the supply to the circuit and provide protection from voltage spikes.

For correct operation of TOPFET's active protection circuits, sufficient voltage has to be applied to its protection pin. The minimum protection supply voltage for the BUK106-50L is 4V for input voltages V_{is} up to 6.5V (see data sheet Fig. 17). For the circuit presented and the component values given, this requirement is met with a battery voltage as low as 8 V. If operation at a lower battery voltage is needed then a voltage tripler charge pump could be used in place of the voltage doubler proposed in this paper.



Automotive Ignition

5.4.1 An Introduction to Electronic Automotive Ignition

The function of an automotive ignition circuit is to provide a spark of sufficient energy to ignite the compressed air-fuel mixture at the appropriate time. Increasingly, electronics is being used to optimise the ignition event. This is now necessary to ensure conformance with emission regulations and to achieve maximum engine performance, fuel economy and engine efficiency. This section will look at some important aspects of the power stage of an electronic ignition system. Other sections in this chapter will look more closely at the power devices for this application.

Electronic ignition circuit

There are several different configurations for electronic ignition. Some are still being studied and there are several already in use. But by far the most common configuration for the power stage is that shown in Fig. 1. With this arrangement there is no distributor. The circuit shown is for a four cylinder engine and has two separate power circuits each feeding two cylinders. Extra power stages can be added for 6 and 8 cylinder engines. When one power stage fires, both plugs will spark but, by choosing pairs of cylinders which are 360° out of phase in the 4-stroke cycle, only one will have a mixture that can be ignited - the other will be approaching tdc at the end of the exhaust stroke.

Operation

During normal operation the transistor will be turned on some time before the spark is needed (t_1 in Fig. 2). Current will now rise at a rate given by the equation

$$\text{rate of rise} = \frac{di}{dt} = \frac{V}{L} \quad (1)$$

where V is the voltage across the primary of the coil. When the spark is needed (t_3), the transistor is turned off. The current in the inductance will try to stop flowing but it can only change at the rate given by (1). This means that voltage on the primary is forced to become large and negative. Transformer action increases the secondary voltage until it reaches the voltage needed to create a spark at the plugs - minimum 5 kV but may be 10 to 30 kV. Current now flows through the spark and the secondary winding, the voltage now falls back to that necessary to maintain the current in the spark, t_5 . When all the coil energy has been delivered, t_6 , the voltage at the collector falls to the battery voltage.

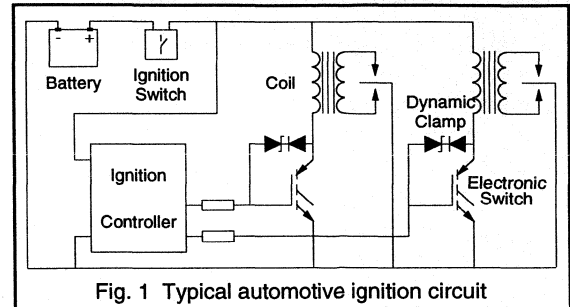


Fig. 1 Typical automotive ignition circuit

Spark energy

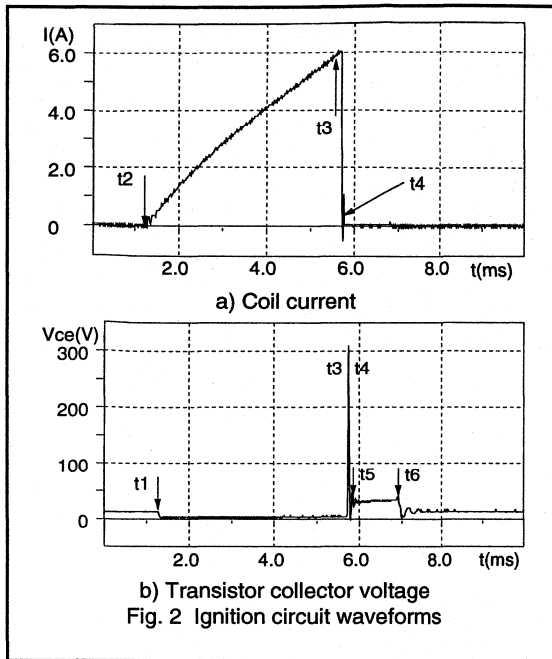
Under ideal conditions the mixture can be ignited with a spark energy of 0.3 mJ but, for reliable ignition under all possible engine conditions, spark energies in the range 60mJ to 150mJ are needed. The energy comes from the coil and is the energy stored as flux generated by the current that was allowed to build up in the primary. The energy stored in the magnetic field of the coil is:

$$E_{\text{prim}} = \frac{1}{2} L_{\text{prim}} i^2 \quad (2)$$

Timing

The timing of the spark is one of the most critical factors in achieving optimum engine performance. The controller uses information about engine speed, temperature, fuel etc. to decide how far before tdc the spark is needed. It then uses data from crankshaft position sensors to decide when to signal for a spark.

One factor which the controller cannot control is the delay between it issuing the command to spark and the spark being generated. Part of this delay is the time it takes the transistor to start turning off together with the rate at which the transistor voltage rises. The controller can make allowance for this delay but in many systems this is no more than a fixed offset. In practice the delay will vary with variations in the drive circuit, temperature and between devices - with some transistor types being more susceptible to variation than others.



Dwell

As mentioned earlier, proper ignition means there must be enough energy stored in the coil when the spark is needed, so the transistor must be turned on soon enough to allow time for the current to reach the required level. However, turning on too soon will mean that the current is higher than it needs to be. Although proper spark timing and energy is more important, optimum coil current is also significant. Higher currents create higher loss which reduces efficiency and increases the problems of thermal management. They can also reduce the life and reliability of the coil and create major difficulties when designing for survival under fault conditions like open circuit secondary.

The time to turn on the transistor is governed by (1). Coil inductance is an attribute of the coil but the primary voltage depends on battery voltage and the voltage drop across the transistor. Battery voltage can vary widely and can be very

low particularly during engine cranking. Ensuring that the circuit operates reasonably well at these low voltages means keeping the transistor voltage drop as low as possible.

Fault conditions

Automotive systems must be reliable. Achieving high reliability means designing systems that can survive all the operating environments that the automobile can produce. Some of the harshest conditions are the fault conditions.

Open circuit secondary

Disconnection of a spark plug lead means that the stored coil energy cannot be dissipated in the spark. Unless steps are taken to prevent it, the voltage will be forced higher until it reaches the breakdown voltage of the transistor. The combination of high current and voltage would probably destroy the device. The solution to this problem is to operate the transistor in dynamic clamping. This can be achieved either by connecting a network between collector and the gate/base or by using a device with the network already integrated into it. With this arrangement the voltage rises to the clamping voltage, the transistor then turns on partially, with enough drive to allow the coil current to flow at a collector emitter voltage equal to the clamping voltage. The clamping voltage is set higher than the voltage normally needed to generate the spark.

Reverse Battery

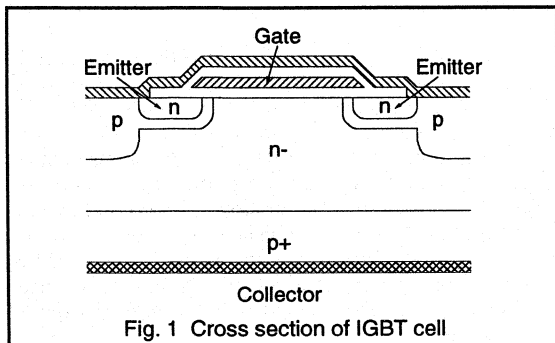
Another condition which must be survived is when the battery connections are reversed. Ideally no current should flow and this can be achieved with some transistors which have a reverse blocking voltage greater than the battery voltage. With many transistors, however, reverse blocking is not guaranteed and to block the current means adding a diode in series. This is rarely acceptable because the diode forward voltage drop adds too much to the effective voltage drop. The alternatives are to allow the current to flow either by using a transistor which is rated to operate with reverse current or by fitting a diode in anti-parallel with the transistor.

5.4.2 IGBTs for Automotive Ignition

This publication describes a range of power transistors for automotive ignition applications from Philips Semiconductors. This range of IGBTs has been specifically optimised for the demanding conditions of ignition circuits. The IGBT is a voltage controlled, low loss, high power transistor which gives the ease of drive and low conduction losses that are required in automotive ignition circuits. The Philips range of ignition IGBTs includes conventional IGBT devices with standard gate drive input. It also includes a range of standard and logic level input protected IGBTs with integral gate drain and gate source clamping diodes.

Introduction to the IGBT

The structure of an IGBT is similar to that of a Power MOSFET, both being created by the parallel connection of many thousands of identical cells. Figure 1 shows the cross section of one IGBT cell. The only difference between this drawing and one for a MOSFET would be the polarity of the substrate - the MOSFET would be n+ rather than the p+ of the IGBT. Since the gate structures are identical the IGBT like the MOSFET is a voltage driven device with an extremely high input impedance.



Bipolar operation

Where the IGBT differs is in the characteristics of the output device. Conduction in a MOSFET is by majority carriers only but the p substrate silicon used for IGBTs promotes injection and gives bipolar conduction with both majority and minority carriers. The effect of this is to make the on state voltage drop of a high voltage IGBT much lower than that of the same size and voltage MOSFET. This feature is particularly useful in automotive ignition where high voltage devices are needed which can operate from low voltage supplies. In recognition of its combination of MOSFET input and bipolar output, the terminals of an IGBT are called Collector, Emitter and Gate.

Input Voltage

IGBTs, like MOSFETs, can have standard or logic level gate sensitivity. A standard device has a threshold voltage of typically 3.5 V - the threshold voltage is the gate voltage needed to allow the IGBT to conduct 1 mA, i.e. just started to turn on. To be fully on, with an acceptable low V_{CE} , the gate voltage needs to be 8.5 V. In some situations, such as engine cranking, the battery voltage falls to less than 6 V and achieving adequate drive may be a problem.

An alternative would be to use a logic level IGBT which has a threshold of typically 1.5 V and is fully on with 5 V.

Another factor in the choice between standard or logic level, is that of noise immunity. In this application it can be very important that the IGBT is fully off, in a very low leakage state, when the driver stage output is LOW. Unfortunately, the LOW that a driver produces may not create a gate to emitter voltage of 0 V.

The threshold voltage of an IGBT falls as temperature rises. So the gate emitter voltage of a logic level IGBT (at $T_j = 120^\circ\text{C}$) needs to be $< 0.7\text{V}$ to ensure that it is off. A standard level part, with its higher threshold, has more immunity and it would still be off if the voltage was $< 1.4\text{V}$.

Turn off control

The time between the gate signal arriving at the IGBT and the collector voltage rising is known as the delay time, t_d . An ignition system produces a spark when the collector voltage rises. Since the timing of the spark is critical, it is advantageous to have good control of t_d . With the IGBT, unlike some other ignition switches, t_d is dominated by gate charge and so can be very low and is easily controlled by the resistance of the driver circuit.

Safe Operating Area

One of the worst situations for creating IGBT latch up is inductive turn off. Such a turn off takes place in electronic ignition. IGBTs, for ignition applications, are specified with a safe operating area (SOA) and limiting value of collector current that can be safely switched under clamped inductive load conditions (I_{CLM}). Providing that the device is operated within its safe operating area (SOA) dynamic latch-up (or SOA failure) cannot occur. Philips ignition IGBTs have a large turn-off SOA and a large energy handling capability making them easy to use in ignition circuits.

Feature	Advantage
IGBTs	
•Voltage driven	-Low gate drive power -Simple gate circuit
•Logic level capability	-Low battery operation
•Bipolar operation	-Low conduction loss -Small device size
•PowerMOS/bipolar structure	-Negligible Storage time -Reverse blocking -Energy handling
•Large SOA	-No snubber required -Design flexibility
Clamped IGBTs	
•Integral clamp diodes	-Design simplicity -Overvoltage protection -Clamp voltage control -Improved reliability -ESD protection

Table 1. Advantages of IGBTs

Reverse Battery

The n- p+ junction, see Fig. 1, which is inherent in the structure of the IGBT, creates a reverse blocking junction. This junction, although unable to support very high reverse voltages, is able to block voltages in excess of a battery voltage. This gives the IGBT a reverse battery blocking capability which ensures that reverse battery fault conditions will not give rise to high currents which could damage the IGBT or any other components in the ignition circuit.

Clamped IGBT

A refinement of the conventional IGBT is the clamped or protected IGBT. This is produced by adding extra

processing stages which allows polysilicon diodes, of known breakdown voltage, to be integrated with the IGBT structure. A short chain of diodes is connected between the gate and the emitter. This gives ESD protection by clamping the voltage, which can be applied across the gate emitter oxide, to a safe value.

A much longer chain, with a combined breakdown voltage of several hundreds of volts, is connected between the collector and the gate. This chain makes the IGBT into a dynamic clamp - possibly the best way of ensuring survival during ignition faults like open circuit secondary. The position of the diode chains is shown in the circuit symbol, see Fig. 2.

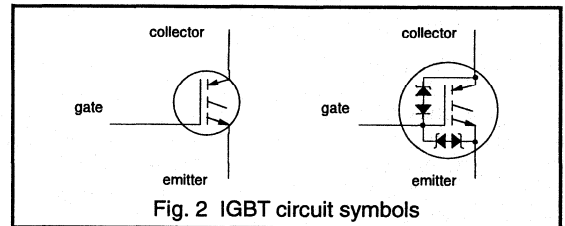


Fig. 2 IGBT circuit symbols

Conclusions

The Philips Semiconductors BUK854-500IS ignition IGBTs and clamped IGBTs BUK856-400IZ and BUK856-450IX are specifically designed to give a low loss, easy to drive and rugged solution to the demanding applications of automotive ignition circuits. IGBTs require the minimum of external components in the gate drive circuit and give negligible drive losses. The energy handling and reverse blocking capabilities of the device make it suitable for use in automotive environments - even under fault conditions. Voltage clamping and ESD protection give ease of design and use, improved reliability and performance in the ignition controller circuit.

5.4.3 Electronic Switches for Automotive Ignition

Earlier sections in this chapter have discussed the nature of automotive electronic ignition and looked at a range of IGBTs which have been optimised for use in this type of application. This section will compare ignition IGBTs with ignition darlington transistors and come to the conclusions that IGBTs have several advantages which would be useful to the automotive designer.

Darlington transistors

In the past, the darlington transistor has been the favoured power transistor for ignition applications. The darlington connection is, in fact, a cascade of two separate bipolar transistors. The combination increases the gain allowing the high voltage device to be controlled by a relatively low power driver stage.

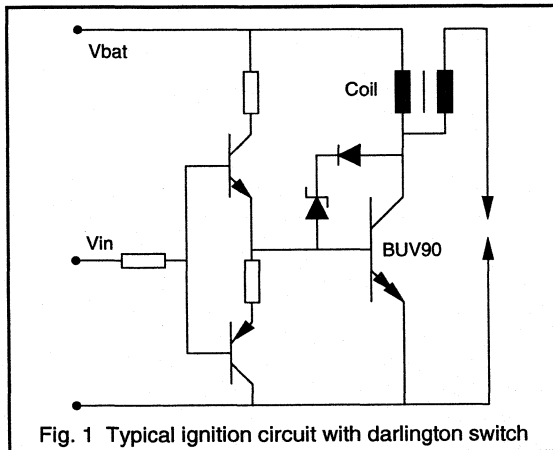


Fig. 1 Typical ignition circuit with darlington switch

As the darlington is a bipolar device it has a relatively low on-state voltage drop even though it can block a high voltage. The low voltage drop keeps conduction losses low and allows the ignition circuit to function at low battery voltages.

The disadvantage of a darlington is the complexity and cost of the base drive. Even though the gain is improved, by the darlington connection, a large gate current is still needed (approx. 100 mA) a circuit similar to that shown in Fig. 1 will be needed. It would be inefficient and costly to supply a current this large from the stabilised 5 V rail, so the supply could be the battery. This means that the drive dissipation when the transistor is on, is about 1.2 W and the average dissipation about 0.5 W. This level of dissipation requires a special driver IC or a circuit using discretes. All of this adds to the cost complexity and thermal problems of the ignition system.

The low on-state voltage drop of a bipolar device is the result of minority carrier injection. However, the minority carrier injection also introduces 'stored charge' into the device which must be removed at turn-off. The charge is extracted, at least partially, as negative base current during the period known as the storage time, t_s . How long this takes, depends on the amount of stored charge and the rate it is extracted. The amount of charge varies from device to device, with the level of the current and with temperature. The rate of extraction depends on the drive circuit and whether a 'simple' circuit like that of Fig. 1 is used or one which uses negative drive to remove the charge more quickly.

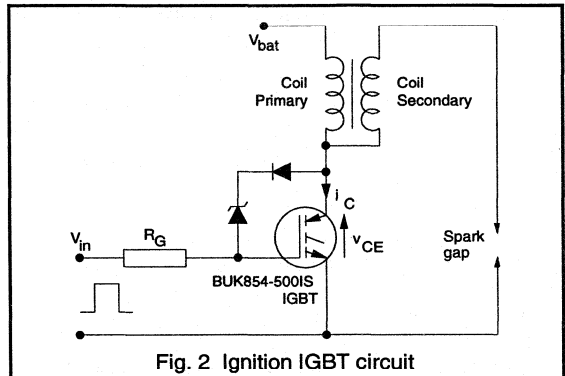


Fig. 2 Ignition IGBT circuit

Storage time adds to the delay between the input changing state and the spark being produced and the uncertainty in storage time, which results from the large number of variables, adds to the inaccuracy of the ignition timing.

Typical ignition darlington transistors often include an internal antiparallel diode connected across the main emitter-collector terminals as shown in Fig. 1. This diode is not necessary for the normal operation of the ignition circuit and its function is simply to protect the darlington from reverse battery faults. However, during this condition, the diode does allow large reverse currents to flow through the ignition circuit.

IGBTs

The IGBT is a combination of bipolar transistor and Power MOSFET technologies. It has the advantage of the low on-state voltage drop of a bipolar darlington and can also be voltage driven in the same way as a Power MOSFET. This gives a highly efficient, easy to drive, minimum loss solution for the switching transistor in an ignition circuit.

A typical ignition circuit using the Philips BUK854-500IS IGBT is shown in Fig. 2; the saving in gate drive components is self evident. The need for a special driver stage is eliminated because drive dissipation for an IGBT will be approximately 10 μ W which can be easily supplied by standard ICs. The BUK854-500IS has a voltage rating of 500V and standard gate threshold voltage, and is assembled in the TO220 package.

Clamped IGBTs

One of the most exciting features of IGBT technology is the ability to integrate protection functions into the IGBT to give significant advantages to the designer of power circuits. The BUK856-400IZ and BUK856-450IX are two such devices which have been specifically designed for automotive ignition circuits. The BUK856-400IZ is a logic level device, the BUK856-450IX has a standard gate threshold. The nominal clamp voltages are 400V and 450V respectively.

In these devices the dynamic clamp network shown in Fig. 2 is fabricated directly onto the IGBT. This gives guaranteed clamping of the IGBT at a fixed clamp voltage without the need for an external circuit. The clamp voltage is held to very tight tolerances over the full temperature range (-40°C to +150°C) required in automotive applications.

In both these devices gate-source protection diodes have also been incorporated into the structure of the devices to give full protection against ESD damage during handling and assembly of the device into engine management units.

IGBTs and darlingtons - A performance comparison

The performance of the BUK856-400IZ ignition IGBT has been compared with that of a typical ignition darlington in the ignition circuit of Fig. 1.

At turn-off the darlington switched considerably slower than the IGBT. The time between the input going low and the spark was 32 μ s for the darlington and only 19 μ s for the IGBT.

Table 1 shows a breakdown of the ignition system losses and demonstrates that whilst the device losses are slightly higher in the IGBT, the overall losses are higher in the darlington circuit due to extra loss in the base drive.

Power loss (W)	$V_{\text{clamp}}=400\text{V}$, $I_{\text{Cmax}}=6.0\text{A}$	
100Hz, (3000rpm)	IGBT	darlington
Conduction	1.37	1.16
Switching	0.71	0.79
Drive	0.00001	0.5
Total	2.08	2.45

Table 1. IGBT and darlington ignition circuit losses

Conclusion

Table 2 summarises the comparison between the IGBT and the darlington as the power switch in automotive ignition. The comparison shows that the darlington is good in the application but that the IGBT has some clear advantages making it significantly better.

	IGBT	darlington
Driver component count	Low	High
Speed of response, 'time to spark'	Fast	Slow
Total loss	Better	Good
Drive power	Low	High
Logic level operation	Yes	Yes
Open circuit load	Yes	Yes
Reverse blocking	Yes	No
Package size	Small	Large
Inbuilt voltage clamp	Possible	Possible
Inbuilt protection	Yes	No

Table 2. Performance comparison

CHAPTER 6

Power Control with Thyristors and Triacs

6.1 Using Thyristors and Triacs

6.2 Thyristor and Triac Applications

6.3 Hi-Com Triacs

Using Thyristors and Triacs

6.1.1 Introduction to Thyristors and Triacs

Brief summary of the thyristor family

The term thyristor is a generic name for a semiconductor switch having four or more layers and is, in essence, a p-n-p-n sandwich. Thyristors form a large family and it is helpful to consider the constituents which determine the type of any given thyristor. If an ohmic connection is made to the first p region and the last n region, and no other connection is made, the device is a diode thyristor. If an additional ohmic connection is made to the intermediate n region (n gate type) or the intermediate p region (p gate type), the device is a triode thyristor. If an ohmic connection is made to both intermediate regions, the device is a tetrode thyristor. All such devices have a forward characteristic of the general form shown in Fig. 1.

There are three types of thyristor reverse characteristic: blocking (as in normal diodes), conducting (large currents at low reverse voltages) and approximate mirror image of the forward characteristic (bidirectional thyristors). Reverse blocking devices usually have four layers or less whereas reverse conducting and mirror image devices usually have five layers.

The simplest thyristor structure, and the most common, is the reverse blocking triode thyristor (usually simply referred to as the 'thyristor' or SCR 'silicon controlled rectifier'). Its circuit symbol and basic structure are shown in Fig. 2.

The most complex common thyristor structure is the bidirectional triode thyristor, or triac. The triac (shown in Fig. 3) is able to pass current bidirectionally and is therefore an a.c. power control device. Its performance is that of a pair of thyristors in anti-parallel with a single gate terminal. The triac needs only one heatsink, but this must be large enough to remove the heat caused by bidirectional current flow. Triac gate triggering circuits must be designed with care to ensure that unwanted conduction, i.e. loss of control, does not occur when triggering lasts too long.

Thyristors and triacs are both bipolar devices. They have very low on-state voltages but, because the minority charge carriers in the devices must be removed before they can block an applied voltage, the switching times are comparatively long. This limits thyristor switching circuits to low frequency applications. Triacs are used almost exclusively at mains supply frequencies of 50 or 60Hz, while in some applications this extends up to the 400Hz supply frequency as used in aircraft.

The voltage blocking capabilities of thyristors and triacs are quite high: the highest voltage rating for the Philips range is 800V, while the currents ($I_{T(RMS)}$) range from 0.8A to 25A.

The devices are available as surface mount components, or as non-isolated or isolated discrete devices, depending on the device rating.

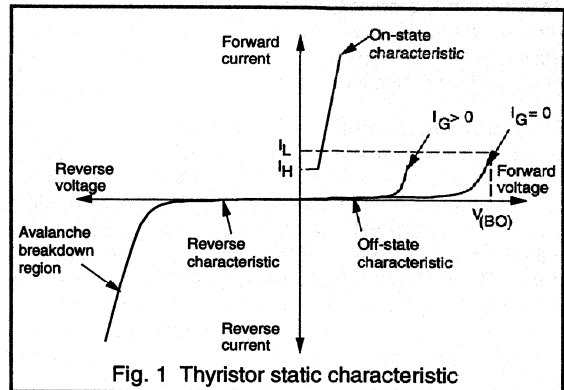


Fig. 1 Thyristor static characteristic

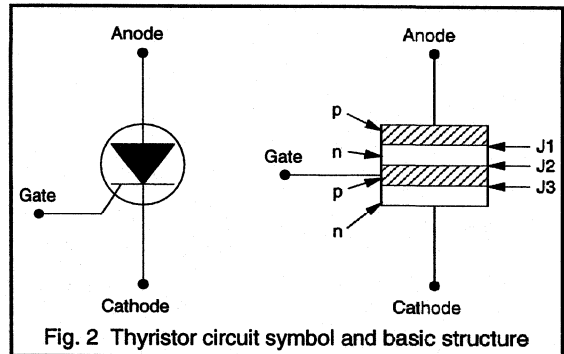


Fig. 2 Thyristor circuit symbol and basic structure

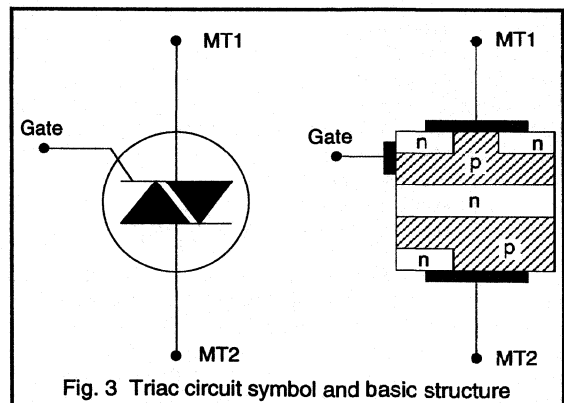
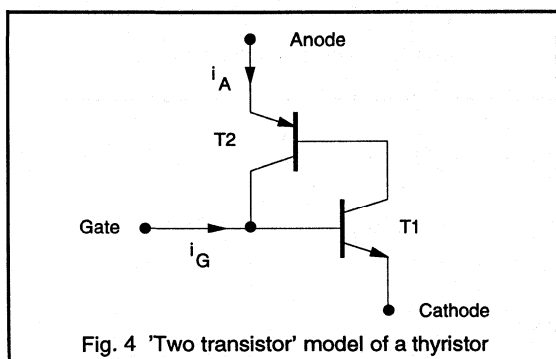


Fig. 3 Triac circuit symbol and basic structure

Thyristor operation

The operation of the thyristor can be understood from Fig. 2. When the thyristor cathode is more positive than the anode then junctions J1 and J3 are reverse biased and the device blocks. When the anode is more positive than the cathode, junctions J1 and J3 are forward biased. As J2 is reverse biased, then the device still blocks forward voltage. If the reverse voltage across J2 is made to reach its avalanche breakdown level then the device conducts like a single forward-biased junction.

The 'two transistor' model of Fig. 4 can be used to consider the p-n-p-n structure of a thyristor as the interconnection of an npn transistor T_1 and a pnp transistor T_2 . The collector of T_1 provides the base current for T_2 . Base current for T_1 is provided by the external gate current in addition to the collector current from T_2 . If the gain in the base-collector loop of T_1 and T_2 exceeds unity then the loop current can be maintained regeneratively. When this condition occurs then both T_1 and T_2 are driven into saturation and the thyristor is said to be 'latched'. The anode to cathode current is then only limited by the external circuit.



There are several mechanisms by which a thyristor can be latched. The usual method is by a current applied to the gate. This gate current starts the regenerative action in the thyristor and causes the anode current to increase. The gains of transistors T_1 and T_2 are current dependent and increase as the current through T_1 and T_2 increases. With increasing anode current the loop gain increases sufficiently such that the gate current can be removed without T_1 and T_2 coming out of saturation.

Thus a thyristor can be switched on by a signal at the gate terminal but, because of the way that the current then latches, the thyristor cannot be turned off by the gate. The thyristor must be turned off by using the external circuit to break the regenerative current loop between transistors T_1 and T_2 . Reverse biasing the device will initiate turn-off once the anode current drops below a minimum specified value, called the holding current value, I_H .

Thyristor turn-on methods

Turn-on by exceeding the breakover voltage

When the breakover voltage, V_{BO} , across a thyristor is exceeded, the thyristor turns on. The breakover voltage of a thyristor will be greater than the rated maximum voltage of the device. At the breakover voltage the value of the thyristor anode current is called the latching current, I_L .

Breakover voltage triggering is not normally used as a triggering method, and most circuit designs attempt to avoid its occurrence. When a thyristor is triggered by exceeding V_{BO} the fall time of the forward voltage is quite low (about 1/20th of the time taken when the thyristor is gate-triggered). As a general rule, however, although a thyristor switches faster with V_{BO} turn-on than with gate turn-on, the permitted di/dt for breakover voltage turn-on is lower.

Turn-on by leakage current

As the junction temperature of a thyristor rises, the leakage current also increases. Eventually, if the junction temperature is allowed to rise sufficiently, leakage current would become large enough to initiate latching of the regenerative loop of the thyristor and allow forward conduction. At a certain critical temperature (above $T_{j(max)}$) the thyristor will not support any blocking voltage at all.

Turn-on by dV/dt

Any p-n junction has capacitance - the larger the junction area the larger the capacitance. If a voltage ramp is applied across the anode-to-cathode of a p-n-p-n device, a current will flow in the device to charge the device capacitance according to the relation:

$$i_c = C \cdot \frac{dv}{dt} \quad (1)$$

If the charging current becomes large enough, the density of moving current carriers in the device induces switch-on.

Turn-on by gate triggering

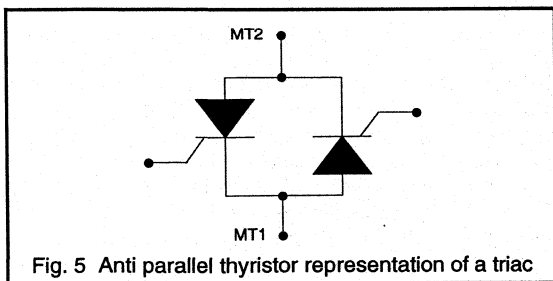
Gate triggering is the usual method of turning a thyristor on. Application of current to the thyristor gate initiates the latching mechanism discussed in the previous section. The characteristic of Fig. 1 showed that the thyristor will switch to its on-state condition with forward bias voltages less than V_{BO} when the gate current is greater than zero. The gate current and voltage requirements which ensure triggering of a particular device are always quoted in the device data. As thyristor triggering characteristics are temperature dependant, the amplitude and duration of the gate pulse must be sufficient to ensure that the thyristor latches under all possible conditions.

During gate turn-on, the rate of rise of thyristor anode current di_F/dt is determined by the external circuit conditions. However, the whole active area of the thyristor (or triac) cannot be turned on simultaneously: the area nearest to the gate turns on first, followed by the remainder of the device. At turn-on it is important that the rate of rise of current does not exceed the specified rating. If di_F/dt is excessive then only a limited area of the device will have been turned on as the anode current increases. The resulting localised heating of the device will cause degradation and could lead to eventual device failure.

A suitably high gate current and large rate of rise of gate current (di_G/dt) ensures that the thyristor turns on quickly (providing that the gate power ratings are not exceeded) thus increasing the thyristor turn-on di/dt capability. Once the thyristor has latched then the gate drive can be reduced or removed completely. Gate power dissipation can also be reduced by triggering the thyristor using a pulsed signal.

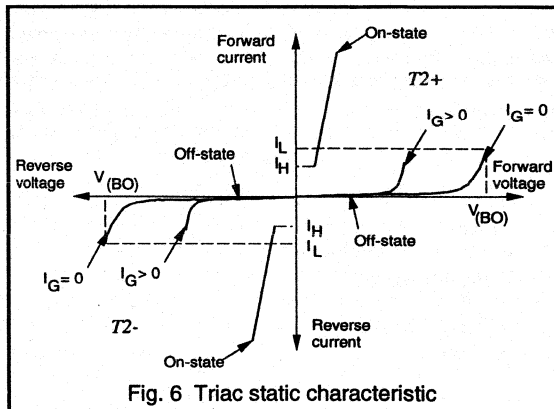
Triac operation

The triac can be considered as two thyristors connected in antiparallel as shown in Fig. 5. The single gate terminal is common to both thyristors. The main terminals MT1 and MT2 are connected to both p and n regions of the device and the current path through the layers of the device depends upon the polarity of the applied voltage between the main terminals. The device polarity is usually described with reference to MT1, where the term MT2+ denotes that terminal MT2 is positive with respect to terminal MT1.



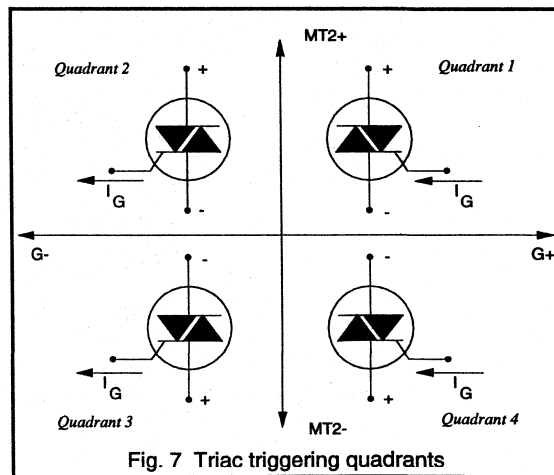
The on-state characteristic of the triac is similar to that of a thyristor and is shown in Fig. 6. Table 1 and Fig. 7 summarise the different gate triggering configurations for triacs.

Due to the physical layout of the semiconductor layers in a triac, the values of latching current (I_L), holding current (I_H) and gate trigger current (I_{GT}) vary slightly between the different operating quadrants. In general, for any triac, the latching current is slightly higher in the second (MT2+, G-) quadrant than the other quadrants, whilst the gate trigger current is slightly higher in fourth (MT2-, G+) quadrant.



Quadrant	Polarity of MT2 wrt MT1	Gate polarity
1 (1+)	MT2+	G+
2 (1-)	MT2+	G-
3 (3-)	MT2-	G-
4 (3+)	MT2-	G+

Table 1. Operating quadrants for triacs



For applications where the gate sensitivity is critical and where the device must trigger reliably and evenly for applied voltages in both directions it may be preferable to use a negative current triggering circuit. If the gate drive circuit is arranged so that only quadrants 2 and 3 are used (i.e. G- operation) then the triac is never used in the fourth quadrant where I_{GT} is highest.

For some applications it is advantageous to trigger triacs with a pulsating signal and thus reduce the gate power dissipation. To ensure bidirectional conduction, especially with a very inductive load, the trigger pulses must continue until the end of each mains half-cycle. If single trigger pulses are used, one-way conduction (rectification) results when the trigger angle is smaller than the load phase angle.

Philips produce ranges of triacs having the same current and voltage ratings but with different gate sensitivities. A device with a relatively insensitive gate will be more immune to false triggering due to noise on the gate signal and also will be more immune to commutating dv/dt turn-on. Sensitive gate triacs are used in applications where the device is driven from a controller IC or low power gate circuit.

The diac

It is also worthwhile to consider the operation and characteristics of the diac in the context of multilayer bipolar devices. The diac is more strictly a transistor than a thyristor, but has an important role in many thyristor and triac triggering circuits. It is manufactured by diffusing an n-type impurity into both sides of a p-type slice to give a two terminal device with symmetrical electrical characteristics. As shown in the characteristic of Fig. 8, the diac blocks applied voltages in either direction until the breakover voltage, V_{BO} is reached. The diac voltage then breaks back to a lower output voltage V_0 . Important diac parameters are breakover voltage, breakover current and breakback voltage as shown in the figure.

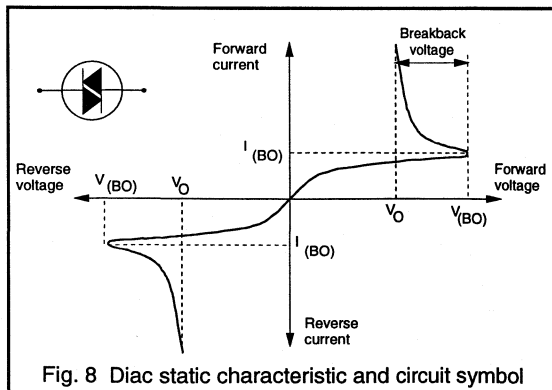


Fig. 8 Diac static characteristic and circuit symbol

Gate requirements for triggering

To a first approximation, the gate-to-cathode junction of a thyristor or triac acts as a p-n diode. The forward characteristic is as shown in Fig. 9. For a given thyristor type there will be a spread in forward characteristics of gate junctions and a spread with temperature.

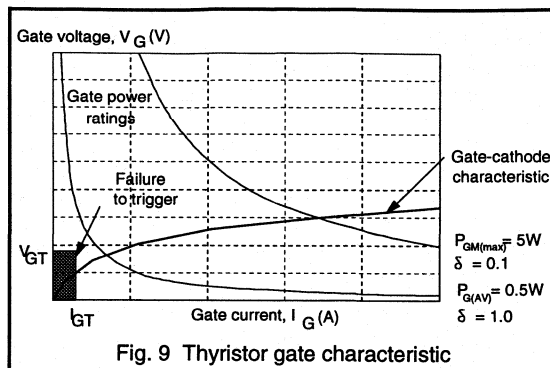


Fig. 9 Thyristor gate characteristic

The gate triggering characteristic is limited by the gate power dissipation. Figure 9 also shows the continuous power rating curve ($P_{G(AV)}=0.5W$) for a typical device and the peak gate power curve ($P_{GM(max)}=5W$). When designing a gate circuit to reliably trigger a triac or thyristor the gate signal must lie on a locus within the area of certain device triggering. Continuous steady operation would demand that the 0.5W curve be used to limit the load line of the gate drive circuit. For pulsed operation the triggering locus can be increased. If the 5W peak gate power curve is used, the duty cycle must not exceed

$$\delta_{max} = \frac{P_{G(AV)}}{P_{GM}} = \frac{0.5}{5} = 0.1 \quad (2)$$

At the other end of the scale, the level below which triggering becomes uncertain is determined by the minimum number of carriers needed in the gate-cathode junction to bring the thyristor into conduction by regenerative action. The trigger circuit load line must not encroach into the failure to trigger region shown in Fig. 9 if triggering is to be guaranteed. The minimum voltage and minimum current to trigger all devices (V_{GT} and I_{GT}) decreases with increasing temperature. Data sheets for Philips thyristors and triacs show the variation of V_{GT} and I_{GT} with temperature.

Thyristor commutation

A thyristor turns off by a mechanism known as 'natural turn-off', that is, when the main anode-cathode current drops below the holding value. It is important to remember, however, that the thyristor will turn on again if the reapplied forward voltage occurs before a minimum time period has elapsed; this is because the charge carriers in the thyristor at the time of turn-off take a finite time to recombine. Thyristor turn-off is achieved by two main methods - self commutation or external commutation.

Self Commutation

In self-commutation circuits the thyristor will automatically turn off at a predetermined time after triggering. The thyristor conduction period is determined by a property of the commutation circuit, such as the resonant cycle of an LC-circuit or the Volt-Second capability of a saturable inductor. The energy needed for commutation is delivered by a capacitor included in the commutation circuit.

LC circuit in series with the thyristor

When the thyristor is triggered, the resulting main current excites the resonant circuit. After half a resonant cycle, the LC circuit starts to reverse the anode current and turns the thyristor off. The thyristor conduction interval is half a resonant cycle. It is essential for proper commutation that the resonant circuit be less than critically damped. Fig. 10 shows the circuit diagram and the relevant waveforms for this arrangement.

LC Circuit in parallel with the thyristor

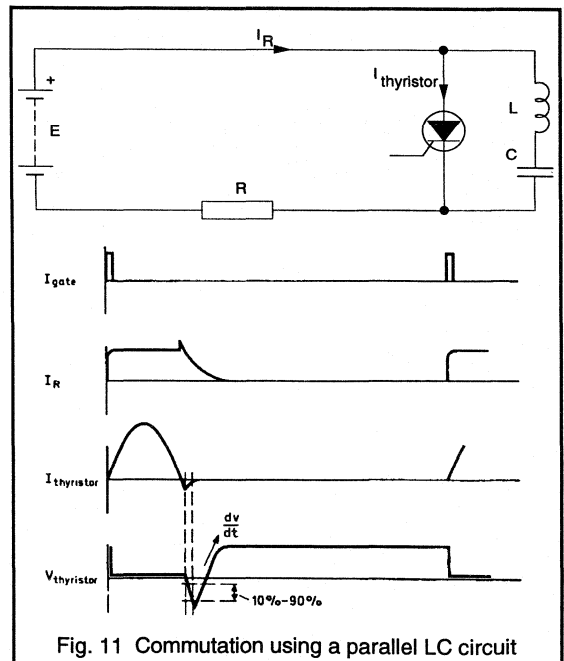
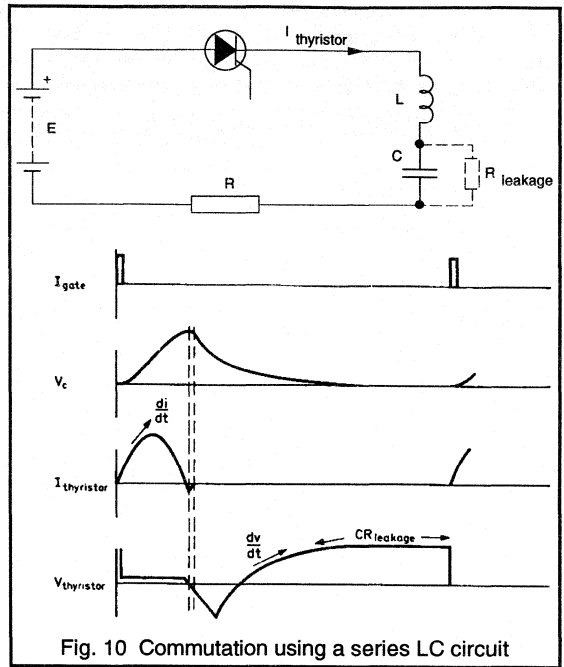
Initially the capacitor charges to the supply voltage. When the thyristor is triggered the load current flows but at the same time the capacitor discharges through the thyristor in the forward direction. When the capacitor has discharged (i.e. after one resonant half-cycle of the LC circuit), it begins to charge in the opposite direction and, when this charging current is greater than the thyristor forward current, the thyristor turns off. The circuit diagram and commutation waveforms are shown in Fig. 11.

External commutation

If the supply is an alternating voltage, the thyristor can conduct only during the positive half cycle. The thyristor naturally switches off at the end of each positive half cycle. The circuit and device waveforms for this method of commutation are shown in Fig. 12. It is important to ensure that the duration of a half cycle is greater than the thyristor turn-off time.

Reverse recovery

In typical thyristors the reverse recovery time is of the order of a few micro-seconds. This time increases with increase of forward current and also increases as the forward current decay rate, di_T/dt , decreases. Reverse recovery time is the period during which reverse recovery current flows (t_1 to t_3 in Fig. 13) and it is the period between the point at which forward current ceases and the earliest point at which the reverse recovery current has dropped to 10% of its peak value.



Reverse recovery current can cause high values of turn-on current in full-wave rectifier circuits (where thyristors are used as rectifying elements) and in certain inverter circuits. It should also be remembered that, if thyristors are connected in series, the reverse voltage distribution can be seriously affected by mismatch of reverse recovery times.

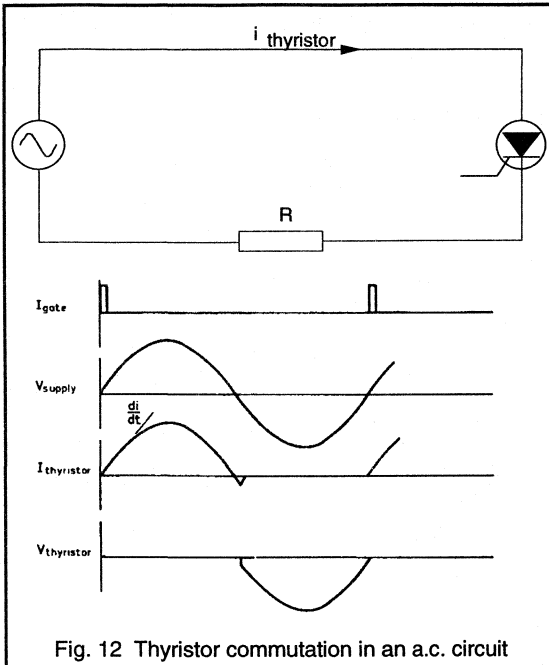


Fig. 12 Thyristor commutation in an a.c. circuit

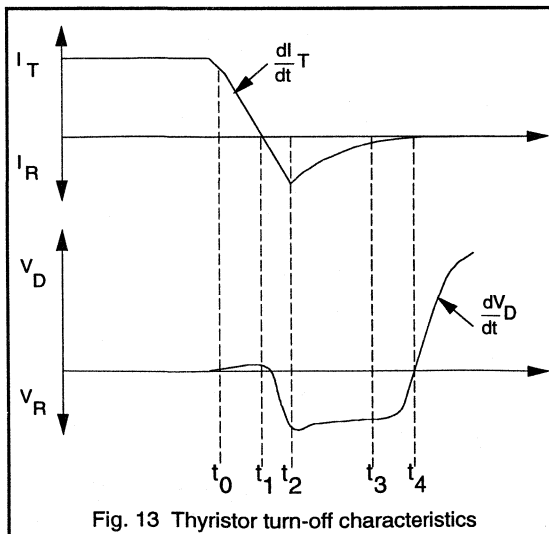


Fig. 13 Thyristor turn-off characteristics

Turn-off time

Turn-off time is the interval between the instant when thyristor current reverses and the point at which the thyristor can block reapplied forward voltage (t_1 to t_4 in Fig. 13). If forward voltage is applied to a thyristor too soon after the main current has ceased to flow, the thyristor will turn on. The circuit commutated turn-off time increases with:

- junction temperature
- forward current amplitude
- rate of fall of forward current
- rate of rise of forward blocking voltage
- forward blocking voltage.

Thus the turn-off time is specified for defined operating conditions. Circuit turn-off time is the turn-off time that the circuit presents to the thyristor; it must, of course, be greater than the thyristor turn-off time.

Triac commutation

Unlike the thyristor, the triac can conduct irrespective of the polarity of the applied voltage. Thus the triac does not experience a circuit-imposed turn-off time which allows each anti-parallel thyristor to fully recover from its conducting state as it is reverse biased. As the voltage across the triac passes through zero and starts to increase, then the alternate thyristor of the triac can fail to block the applied voltage and immediately conduct in the opposite direction. Triac-controlled circuits therefore require careful design in order to ensure that the triac does not fail to commutate (switch off) at the end of each half-cycle as expected.

It is important to consider the commutation performance of devices in circuits where either di/dt or dV/dt can be large. In resistive load applications (e.g. lamp loads) current surges at turn-on or during temporary over-current conditions may introduce abnormally high rates of change of current which may cause the triac to fail to commutate. In inductive circuits, such as motor control applications or circuits where a dc load is controlled by a triac via a bridge rectifier, it is usually necessary to protect the triac against unwanted commutation due to $dv_{(com)}/dt$.

The commutating $dv_{(com)}/dt$ limit for a triac is less than the static dv/dt limit because at commutation the recently conducting portion of the triac which is being switched off has introduced stored charge to the triac. The amount of stored charge depends upon the reverse recovery characteristics of the triac. It is significantly affected by junction temperature and the rate of fall of anode current prior to commutation ($di_{(com)}/dt$). Following high rates of change of current the capacity of the triac to withstand high reapplied rates of change of voltage is reduced. Data sheet specifications for triacs give characteristics showing the

maximum allowable rate of rise of commutating voltage against device temperature and rate of fall of anode current which will not cause a device to trigger.

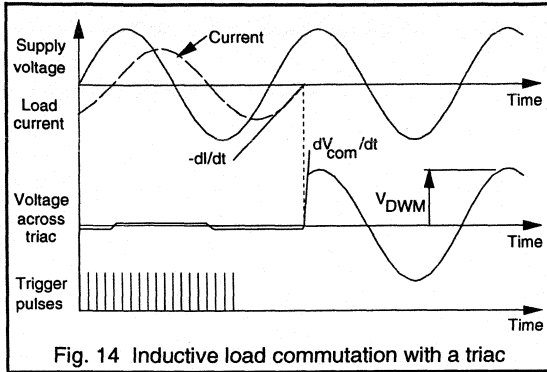


Fig. 14 Inductive load commutation with a triac

Consider the situation when a triac is conducting in one direction and the applied ac voltage changes polarity. For the case of an inductive load the current in the triac does not fall to its holding current level until some time later. This is shown in Fig. 14. At the time that the triac current has reached the holding current the mains voltage has risen to some value and so the triac must immediately block that voltage. The rate of rise of blocking voltage following commutation (dv_{com}/dt) can be quite high.

The usual method is to place a dv/dt -limiting R-C snubber in parallel with the triac. Additionally, because commutating dv/dt turn-on is dependent upon the rate of fall of triac current, then in circuits with large rates of change of anode current, the ability of a triac to withstand high rates of rise of reapplied voltage is improved by limiting the di/dt using a series inductor. This topic is discussed more fully in the section entitled 'Using thyristors and triacs'.

Conclusions

This article has presented the basic parameters and characteristics of triacs and thyristors and shown how the structure of the devices determines their operation. Important turn-on and turn-off conditions and limitations of the devices have been presented in order to demonstrate the capabilities of the devices and show the designer those areas which require careful consideration. The device characteristics which determine gate triggering requirements of thyristors and triacs have been presented.

Subsequent articles in this chapter will deal with the use, operation and limitations of thyristors and triacs in practical applications, and will present some detailed design and operational considerations for thyristors and triacs in phase control and integral cycle control applications.

6.1.2 Using Thyristors and Triacs

This chapter is concerned with the uses, operation and protection of thyristors and triacs. Two types of circuit cover the vast majority of applications for thyristors and triacs: static switching circuits and phase control circuits. The characteristics and uses of these two types of circuit will be discussed. Various gate drive circuits and protection circuits for thyristor and triacs are also presented. The use of these circuits will enable designers to operate the devices reliably and within their specified limits.

Thyristor and triac control techniques

There are two main techniques of controlling thyristors and triacs - on-off triggering (or static switching) and phase control. In on-off triggering, the power switch is allowed to conduct for a certain number of half-cycles and then it is kept off for a number of half-cycles. Thus, by varying the ratio of "on-time" to "off-time", the average power supplied to the load can be controlled. The switching device either completely activates or deactivates the load circuit. In phase control circuits, the thyristor or triac is triggered into conduction at some point after the start of each half-cycle. Control is achieved on a cycle-by-cycle basis by variation of the point in the cycle at which the thyristor is triggered.

Static switching applications

Thyristors and triacs are the ideal power switching devices for many high power circuits such as heaters, enabling the load to be controlled by a low power signal, in place of a relay or other electro-mechanical switch.

In a high power circuit where the power switch may connect or disconnect the load at any point of the mains cycle then large amounts of RFI (radio frequency interference) are likely to occur at the instants of switching. The large variations in load may also cause disruptions to the supply voltage. The RFI and voltage variation produced by high power switching in a.c. mains circuits is unacceptable in many environments and is controlled by statutory limits. The limits depend upon the type of environment (industrial or domestic) and the rating of the load being switched.

RFI occurs at any time when there is a step change in current caused by the closing of a switch (mechanical or semiconductor). The energy levels of this interference can be quite high in circuits such as heating elements. However, if the switch is closed at the moment the supply voltage passes through zero there is no step rise in current and thus no radio frequency interference. Similarly, at turn-off, a large amount of high frequency interference can be caused by di/dt imposed voltage transients in inductive circuits.

Circuit-generated RFI can be almost completely eliminated by ensuring that the turn-on switching instants correspond to the zero-crossing points of the a.c. mains supply. This technique is known as synchronous (or zero voltage) switching control as opposed to the technique of allowing the switching points to occur at any time during the a.c. cycle, which is referred to as asynchronous control.

In a.c. circuits using thyristors and triacs the devices naturally switch off when the current falls below the device holding current. Thus turn-off RFI does not occur.

Asynchronous control

In asynchronous control the thyristor or triac may be triggered at a point in the mains voltage other than the zero voltage crossover point. Asynchronous control circuits are usually relatively cheap but liable to produce RFI.

Synchronous control

In synchronous control systems the switching instants are synchronised with zero crossings of the supply voltage. They also have the advantage that, as the thyristors conduct over complete half cycles, the power factor is very good. This method of power control is mostly used to control temperature. The repetition period, T , is adjusted to suit the controlled process (within statutory limits). Temperature ripple is eliminated when the repetition period is made much smaller than the thermal time constant of the system.

Figure 1 shows the principle of time-proportional control. RFI and turn-on di/dt are reduced, and the best power factor (sinusoidal load current) is obtained by triggering synchronously. The average power delivered to a resistive load, R_L , is proportional to t_{on}/T (i.e. linear control) and is given by equation 1.

$$P_{out} = \frac{V_{(RMS)}^2}{R_L} \cdot \frac{t_{on}}{T} \quad (1)$$

where: T is the controller repetition period
 t_{on} is controller 'on' time
 $V_{(RMS)}$ is the rms a.c. input voltage.

Elsewhere in this handbook the operation of a controller i.c. (the TDA1023) is described. This device is specifically designed to implement time-proportional control of heaters using Philips triacs.

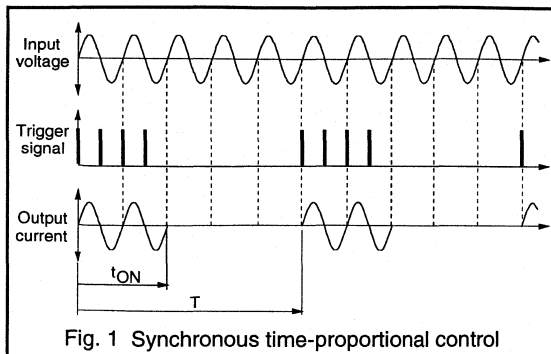


Fig. 1 Synchronous time-proportional control

Phase control

Phase control circuits are used for low power applications such as lamp control or universal motor speed control, where RFI emissions can be filtered relatively easily. The power delivered to the load is controlled by the timing of the thyristor (or triac) turn-on point.

The two most common phase controller configurations are 'half wave control', where the controlling device is a single thyristor and 'full wave control', where the controlling device is a triac or a pair of anti-parallel thyristors. These two control strategies are considered in more detail below:

Resistive loads

The operation of a phase controller with a resistive load is the simplest situation to analyse. Waveforms for a full wave controlled resistive load are shown in Fig. 2. The triac is triggered at angle δ , and applies the supply voltage to the load. The triac then conducts for the remainder of the positive half-cycle, turning off when the anode current drops below the holding current, as the voltage becomes zero at $\theta=180^\circ$. The triac is then re-triggered at angle $(180+\delta)^\circ$, and conducts for the remainder of the negative half-cycle, turning off when its anode voltage becomes zero at 360° .

The sequence is repeated giving current pulses of alternating polarity which are fed to the load. The duration of each pulse is the conduction angle α , that is $(180-\delta)^\circ$. The output power is therefore controlled by variation of the trigger angle δ .

For all values of α other than $\alpha=180^\circ$ the load current is non-sinusoidal. Thus, because of the generation of harmonics, the power factor presented to the a.c. supply will be less than unity except when $\delta=0$.

For a sinusoidal current the rectified mean current, $I_{T(AV)}$, and the rms current, $I_{T(RMS)}$, are related to the peak current, $I_{T(MAX)}$, by equation 2.

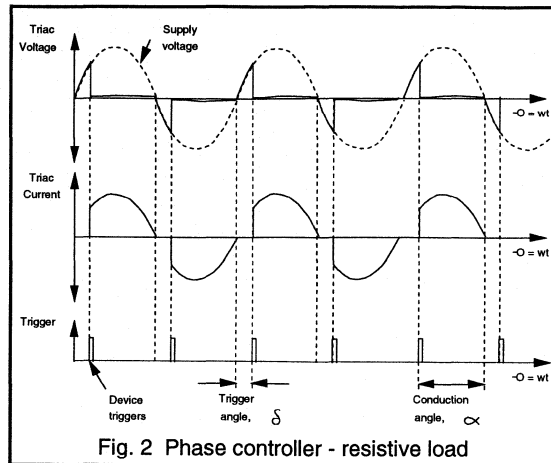


Fig. 2 Phase controller - resistive load

$$I_{T(AV)} = \frac{2 \cdot I_{T(MAX)}}{\pi} = 0.637 I_{T(MAX)}$$

$$I_{T(RMS)} = \frac{I_{T(MAX)}}{\sqrt{2}} = 0.707 I_{T(MAX)} \quad (2)$$

where

$$I_{T(MAX)} = \frac{V_{T(MAX)}}{R_L} = \frac{\sqrt{2} V_{(RMS)}}{R_L} \quad (3)$$

From equation 2 the 'crest factor', c , (also known as the 'peak factor') of the current waveform is defined as:

$$\text{Crest factor, } c = \frac{I_{T(MAX)}}{I_{T(RMS)}} \quad (4)$$

The current 'form factor,' a , is defined by:

$$\text{Form factor, } a = \frac{I_{T(RMS)}}{I_{T(AV)}} \quad (5)$$

Thus, for sinusoidal currents:

$$a = \frac{I_{T(RMS)}}{I_{T(AV)}} = 1.111; \quad c = \frac{I_{T(MAX)}}{I_{T(RMS)}} = 1.414 \quad (6)$$

For the non-sinusoidal waveforms which occur in a phase controlled circuit, the device currents are modified due to the delay which occurs before the power device is triggered. The crest factor of equation 4 and the form factor of equation 5 can be used to describe variation of the current waveshape from the sinusoidal case.

Half wave controller

Figure 3a) shows the simplest type of thyristor half-wave phase controller for a resistive load. The load current waveform is given in Fig. 3b). The variation of average load current, $I_{T(AV)}$, rms load current, $I_{T(RMS)}$ and load power over the full period of the a.c mains, with trigger angle are given in equation 7.

$$I_{T(AV)} = I_{T(AV)\max} \cdot \frac{(1 - \cos \alpha)}{2} \qquad I_{T(AV)\max} = \frac{I_{T(MAX)}}{\pi}$$

$$I_{T(RMS)} = I_{T(RMS)\max} \left(\frac{\alpha - \frac{1}{2} \sin 2\alpha}{\pi} \right)^{\frac{1}{2}} \qquad I_{T(RMS)\max} = \frac{I_{T(MAX)}}{2}$$

$$P_{(out)} = P_{(out)\max} \cdot \left(\frac{\alpha - \frac{1}{2} \sin 2\alpha}{\pi} \right) \qquad P_{(out)\max} = \frac{I_{T(MAX)}^2 R_L}{4} \quad (7)$$

N.B. When using equation 7 all values of α must be in radians. For each case the maximum value occurs when $\alpha=180^\circ$ ($\alpha=\pi$ radians).

At $\alpha=180^\circ$ the crest factor and form factor for a half wave controller are given by:

$$a = \frac{I_{T(RMS)}}{I_{T(AV)}} = 1.571; \qquad c = \frac{I_{T(MAX)}}{I_{T(RMS)}} = 2.0 \quad (8)$$

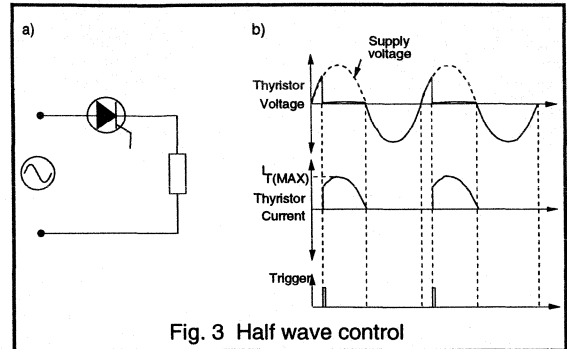


Fig. 3 Half wave control

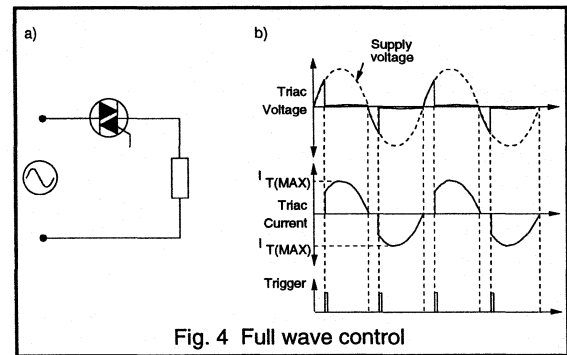


Fig. 4 Full wave control

The variation of normalised average current, $I_{T(AV)}/I_{T(AV)\max}$, rms current $I_{T(RMS)}/I_{T(RMS)\max}$, and power, $P_{(out)}/P_{(out)\max}$, for equations 7 and 9 are plotted in Fig. 5.

Figure 6 shows the variation of current form factor with conduction angle for the half wave controller and the full wave controller of Figs. 3 and 4.

Full wave controller

Figure 4 shows the circuit and load current waveforms for a full-wave controller using two antiparallel thyristors, or a triac, as the controlling device. The variation of rectified mean current, $I_{T(AV)}$, rms current, $I_{T(RMS)}$, and load power with trigger angle are given by equation 9.

$$I_{T(AV)} = I_{T(AV)\max} \cdot \frac{(1 - \cos \alpha)}{2} \qquad I_{T(AV)\max} = \frac{2I_{T(MAX)}}{\pi}$$

$$I_{T(RMS)} = I_{T(RMS)\max} \left(\frac{\alpha - \frac{1}{2} \sin 2\alpha}{\pi} \right)^{\frac{1}{2}} \qquad I_{T(RMS)\max} = \frac{I_{T(MAX)}}{\sqrt{2}}$$

$$P_{(out)} = P_{(out)\max} \cdot \left(\frac{\alpha - \frac{1}{2} \sin 2\alpha}{\pi} \right) \qquad P_{(out)\max} = \frac{I_{T(MAX)}^2 R_L}{2} \quad (9)$$

N.B. When using equation 9 all value of α must be in radians. For each case the maximum value occurs when $\alpha=180^\circ$ ($\alpha=\pi$ radians).

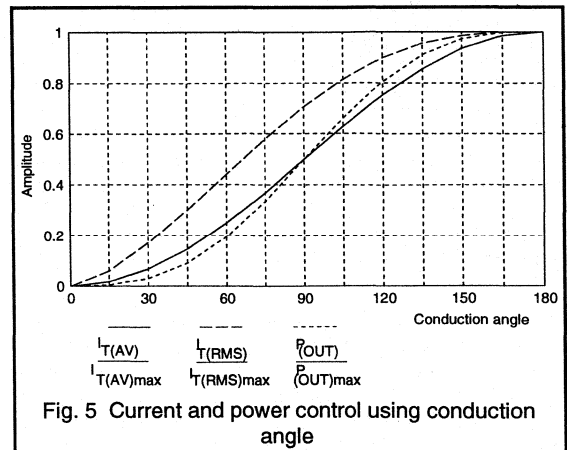


Fig. 5 Current and power control using conduction angle

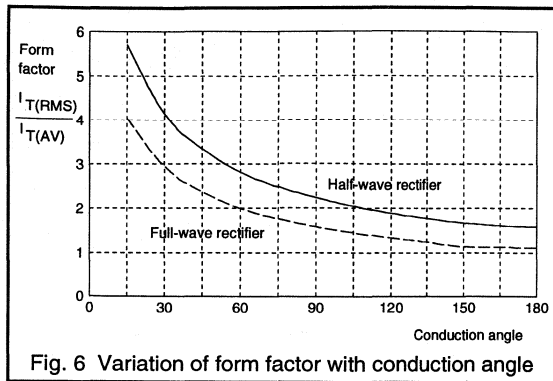


Fig. 6 Variation of form factor with conduction angle

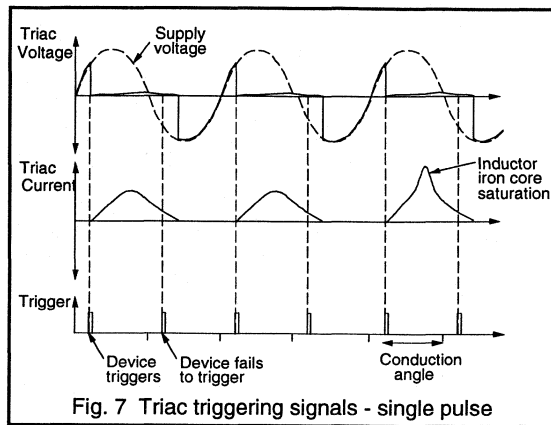


Fig. 7 Triac triggering signals - single pulse

Inductive loads

The circuit waveforms for a phase controller with an inductive load or an active load (for example, a motor) are more complex than those for a purely resistive load. The circuit waveforms depend on the load power factor (which may be variable) as well as the triggering angle.

For a bidirectional controller (i.e. triac or pair of anti-parallel thyristors), maximum output, that is, sinusoidal load current, occurs when the trigger angle equals the phase angle. When the trigger angle, δ , is greater than the load phase angle, ϕ , then the load current will become discontinuous and the triac (or thyristor) will block some portion of the input voltage until it is retriggered.

If the trigger angle is less than the phase angle then the load current in one direction will not have fallen back to zero at the time that the device is retriggered in the opposite direction. This is shown in Fig. 7. The triac fails to be triggered as the gate pulse has finished and so the triac then acts as a rectifier. In Fig. 7 the triac is only triggered by the gate pulses when the applied supply voltage is positive (+ quadrant). However, the gate pulses which occur one half period later have no effect because the triac is still conducting in the opposite direction. Thus unidirectional current flows in the main circuit, eventually saturating the load inductance.

This problem can be avoided by using a trigger pulse train as shown in Fig. 8. The triac triggers on the first gate pulse after the load current has reached the latching current I_L in the 3+ quadrant. The trigger pulse train must cease before the mains voltage passes through zero otherwise the triac will continue to conduct in the reverse direction.

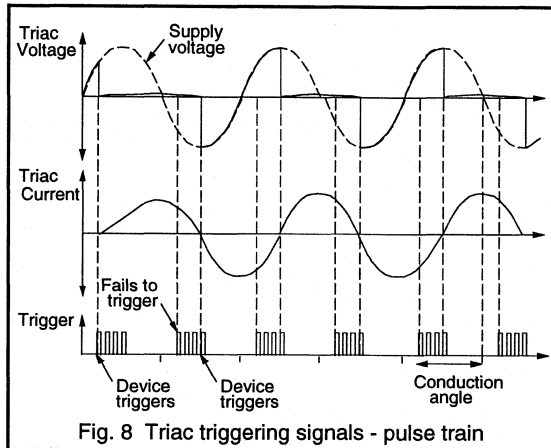


Fig. 8 Triac triggering signals - pulse train

Gate circuits for thyristors and triacs

As discussed in the introductory article of this chapter, a thyristor or triac can be triggered into conduction when a voltage of the appropriate polarity is applied across the main terminals and a suitable current is applied to the gate. This can be achieved using a delay network of the type shown in Fig. 9a). Greater triggering stability and noise immunity can be achieved if a diac is used (see Fig. 9b). This gives a trigger circuit which is suitable for both thyristors and triacs.

Figure 10 shows several alternative gate drive circuits suitable for typical triac and thyristor applications. In each circuit the gate-cathode resistor protects the device from false triggering due to noise - this is especially important for sensitive gate devices. In addition opto-isolated thyristor and triac drivers are available which are compatible with the Philips range of devices.

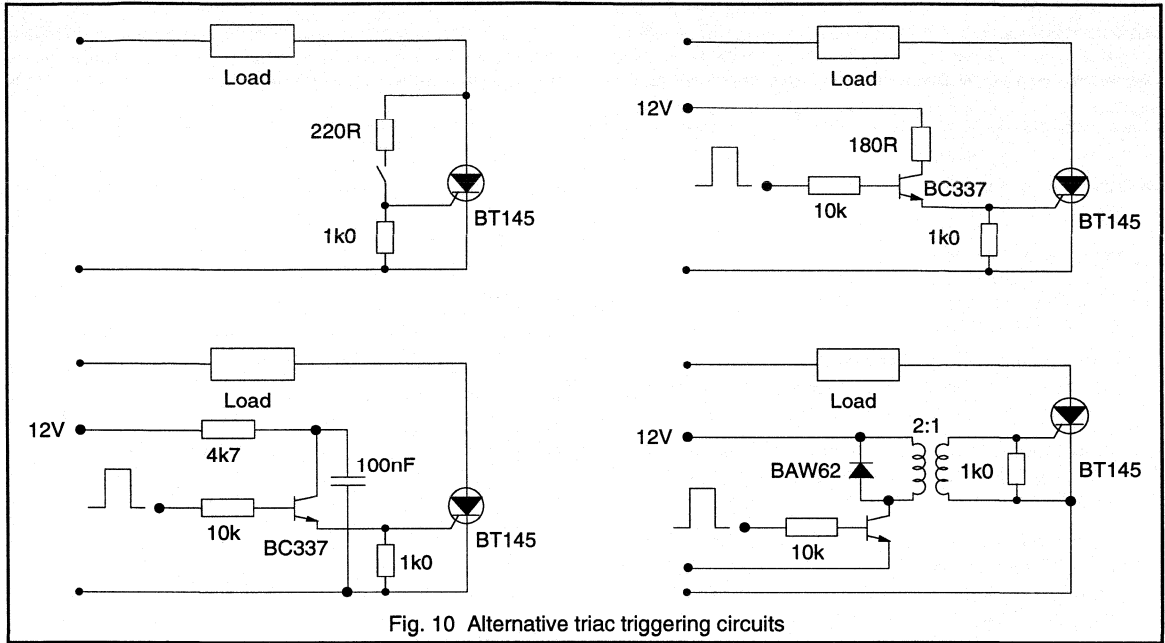


Fig. 10 Alternative triac triggering circuits

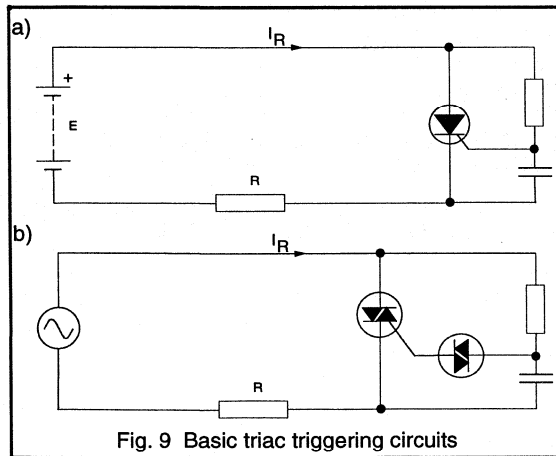


Fig. 9 Basic triac triggering circuits

In some applications it may be necessary to cascade a sensitive gate device with a larger power device to give a sensitive gate circuit with a high power handling capability. A typical solution which involves triggering the smaller device (BT169) from a logic-level controller to turn on the larger device (BT151) is shown in Fig. 11.

Figure 12 shows an isolated triac triggering circuit suitable for zero voltage switching applications. This type of circuit is also known as a solid state relay (SSR). The function of

the Q1/R2/R3 stage is that the BC547 is on at all instants in time when the applied voltage waveform is high and thus holds the BT169 off. If the BT169 is off then no gate signal is applied to the triac and the load is switched off.

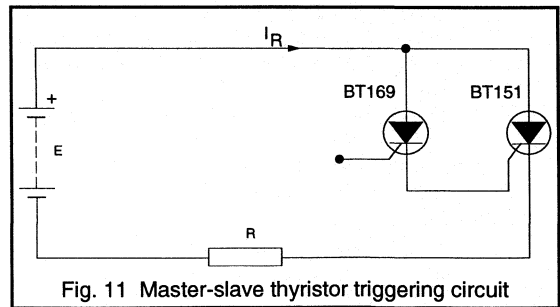


Fig. 11 Master-slave thyristor triggering circuit

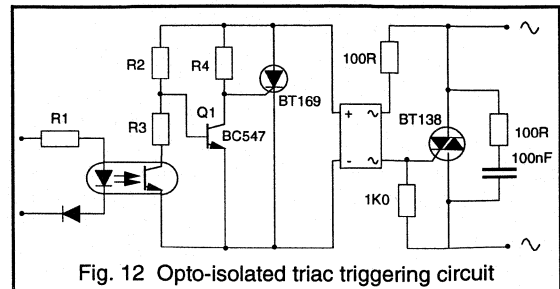


Fig. 12 Opto-isolated triac triggering circuit

If the input signal is switched high then the photo-transistor turns on. If this occurs when the mains voltage is high then Q1 remains on. When the line voltage passes through its next zero crossing in either direction the photo transistor ensures that Q1 stays off long enough for the BT169 to trigger. This then turns the triac on. Once the thyristor turns on, the drive circuit is deprived of its power due to the lower voltage drop of the BT169. The triac is retriggered every half cycle.

Voltage transient protection

There are three major sources of transient which may affect thyristor and triac circuits:

- the mains supply (e.g. lightning)
- other mains and load switches (opening and closing)
- the rectifying and load circuit (commutation)

In order to ensure reliable circuit operation these transients must be suppressed by additional components, removed at source or allowed for in component ratings.

Three types of circuit are commonly employed to suppress voltage transients - a snubber network across the device, a choke between the power device and external circuit or an overvoltage protection such as a varistor.

Series line chokes

A series choke may be used to limit peak fault currents to assist in the fuse protection of thyristors and triacs. If the choke is used in conjunction with fuse protection, it must retain its inductance to very large values of current, and so for this reason it is usually an air-cored component. Alternatively, if the choke is only required to reduce the dv/dt across non-conducting devices then the inductance needs only to be maintained up to quite low currents. Ferrite-cored chokes may be adequate provided that the windings are capable of carrying the full-load current. Usually only a few microhenries of inductance are required to limit the circuit di/dt to an acceptable level. This protects the devices from turning on too quickly and avoids potential device degradation.

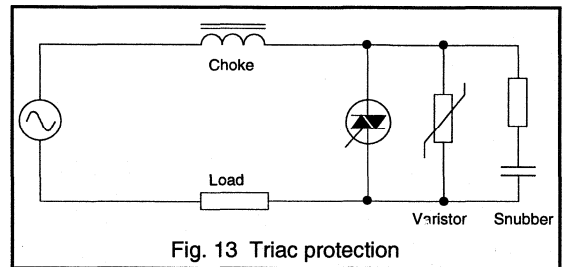
For instance, a 220V a.c. supply with $20\mu\text{H}$ source inductance gives a maximum di/dt of $(220\sqrt{2})/20=16\text{A}/\mu\text{s}$. Chokes used to soften commutation should preferably be saturable so as to maintain regulation and avoid deterioration of the power factor. As their impedance reduces at high current, they have very little effect on the inrush current.

The addition of di/dt limiting chokes is especially important in triac circuits where the load is controlled via a bridge rectifier. At the voltage zero-crossing points the conduction transfers between diodes in the bridge network, and the rate of fall of triac current is limited only by the stray inductance in the a.c. circuit. The large value of commutating di/dt may cause the triac to retrigger due to

commutating $dv_{(com)}/dt$. A small choke in the a.c. circuit will limit the $di_{(com)}/dt$ to an acceptable level. An alternative topology which avoids triac commutation problems is to control the load on the d.c. side.

Snubber networks

Snubber networks ensure that the device is not exposed to excessive rates of change of voltage during transient conditions. This is particularly important when considering the commutation behaviour of triacs, which has been discussed elsewhere.



The following equations can be used to calculate the values of the snubber components required to keep the reapplied dv/dt for a triac within the $dv_{(com)}/dt$ rating for that device. The parameters which affect the choice of snubber components are the value of load inductance, frequency of the a.c. supply and rms load current. The value of the snubber resistor needs to be large enough to damp the circuit and avoid voltage overshoots. The snubber capacitor should be rated for the full a.c. voltage of the system. The snubber resistor needs to be rated at 0.5W.

For circuits where the load power factor, $\cos\phi$, ≥ 0.7 the snubber values are given approximately by:

$$C \geq 25L \left(\frac{f I_{T(RMS)}}{dv_{(com)}/dt} \right)^2$$

$$R = \sqrt{\frac{3L}{C}} \quad (9)$$

where: L is the load inductance
f is the supply frequency
 $I_{T(RMS)}$ is the rms device current
 $dv_{(com)}/dt$ is the device commutating dv/dt rating.

The presence of a snubber across the device can improve the turn-on performance of the triac by using the snubber capacitor discharge current in addition to the load current to ensure that the triac latches at turn-on. The value of the snubber resistor must be large enough to limit the peak capacitor discharge current through the triac to within the turn-on di/dt limit of the device.

Varistor

The use of a metal oxide varistor (MOV), as shown in Fig. 13, protects the device from transient overvoltages which may occur due to mains disturbances.

Overcurrent protection

Like all other semiconductor devices, triacs have an infinite life if they are used within their ratings. However, they rapidly overheat when passing excessive current because the thermal capacitance of their junction is small. Overcurrent protective devices (circuit breakers, fuses) must, therefore, be fast-acting.

Inrush condition

Motors, incandescent lamp or transformer loads give rise to an inrush condition. Lamp and motor inrush currents are avoided by starting the control at a large trigger angle. Transformer inrush currents are avoided by adjusting the initial trigger angle to a value roughly equal to the load phase angle. No damage occurs when the amount of inrush current is below the inrush current rating curve quoted in the device data sheet (see the chapter 'Understanding thyristor and triac data').

Short-circuit condition

Fuses for protecting triacs should be fast acting, and the amount of fuse I^2t to clear the circuit must be less than the I^2t rating of the triac. Because the fuses open the circuit rapidly, they have a current limiting action in the event of a short-circuit. High voltage fuses exhibit low clearing I^2t but the fuse arc voltage may be dangerous unless triacs with a sufficiently high voltage rating are used.

Conclusions

This paper has outlined the most common uses and applications of thyristor and triac circuits. The type of circuit used depends upon the degree of control required and the nature of the load. Several types of gate circuit and device protection circuit have been presented. The amount of device protection required will depend upon the conditions imposed on the device by the application circuit. The protection circuits presented here will be suitable for the majority of applications giving a cheap, efficient overall design which uses the device to its full capability with complete protection and confidence.

6.1.3 The Peak Current Handling Capability of Thyristors

The ability of a thyristor to withstand peak currents many times the size of its average rating is well known. However, there is little information about the factors affecting the peak current capability. This section will investigate the effect of pulse duration on the peak current capability of thyristors.

Data sheets for thyristors always quote a figure for the maximum surge current that the device can survive. This figure assumes a half sine pulse with a width of either 10 ms or 8.3 ms, which are the conditions applicable for 50/60 Hz mains operation. This limit is not absolute; narrow pulses with much higher peaks can be handled without damage but little information is available to enable the designer to determine how high this current is. This section will discuss some of the factors affecting a thyristor's peak current capability and review the existing prediction methods. It will go on to present the results of an evaluation of the peak current handling capabilities for pulses as narrow as 10 μ s for the BT151, BT152 and BT145 thyristors. It will also propose a method for estimating a thyristor's peak current capability for a half sine pulse with a duration between 10 μ s and 10 ms from its quoted surge rating.

Energy Handling

In addition to the maximum surge current, data sheets often quote a figure called "I²t for fusing". This number is used to select appropriate fuses for device protection. I²t represents the energy that can be passed by the device without damage. In fact it is not the passage of the energy which causes damage, but the heating of the crystal by the energy absorbed by the device which causes damage.

If the period over which the energy is delivered is long, the absorbed energy has time to spread to all areas of the device capable of storing it - like the edges of the crystal, the plastic encapsulation, the mounting tab and for very long times the heatsink - therefore the temperature rise in the crystal is moderated. If, however, the delivery period is short - say a single half sine pulse of current with a duration of <10 ms - the areas to which the energy can spread for the actual duration of the pulse are limited. This means that the crystal keeps all the energy giving a much bigger temperature rise. For very short pulses (<0.1 ms) and large crystal, the problem is even worse because not all of the active area of a thyristor crystal is turned on simultaneously - conduction tends to spread out from the gate area - so the current pulse passes through only part of the crystal resulting in a higher level of dissipation and an even more restricted area for absorbing it.

Expected Results

I²t is normally quoted at 10 ms, assuming that the surge is a half sine pulse, and is derived from the surge current from:

$$I^2t = \left(\frac{I_{TSM}}{\sqrt{2}} \right)^2 \cdot 0.01$$

This calculates the RMS current by dividing I_{TSM} by $\sqrt{2}$

Under the simplest of analyses I²t would be assumed to be constant so a device's peak current capability could be calculated from:

$$I_{pk} = I_{TSM} \cdot \left(\frac{0.01}{t_p} \right)^{\frac{1}{2}}$$

where I_{pk} is the peak of a half sine current pulse with a duration of t_p . However, experience and experiments have shown that such an approach is inaccurate. To overcome this, other 'rules' have been derived.

One of these 'rules' suggests that it is not I²t which is constant but I³t or I⁴t. Another suggestion is that the 'constancy' continuously changes from I²t to I⁴t as the pulses become shorter. All these rules are expressed in the general equation:

$$I_{pk} = I_{TSM} \cdot \left(\frac{0.01}{t_p} \right)^{\frac{1}{N}}$$

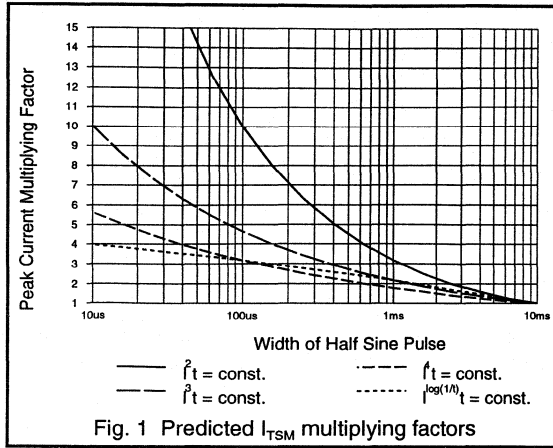
where N is either constant or a function of the pulse width, for example:

$$N = \log \left(\frac{1}{t_p} \right)$$

The graph shown in Fig. 1 shows what several of these 'rules' predict would happen to the peak current capability if they were true. Unfortunately little or no real information currently exists to indicate the validity of these rules. Tests have been performed on three groups of devices - BT151, BT152 and BT145 - to gather the data which would, hopefully, decide which was correct.

Test Circuit

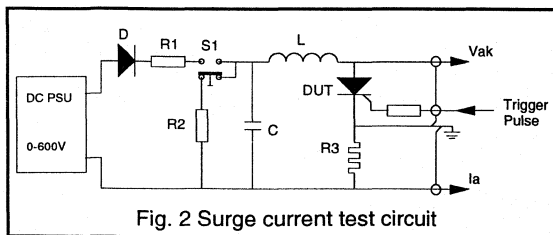
The technique chosen to measure the peak current capability of the devices was the stepped surge method. In this test, the device is subjected to a series of current pulses of increasing magnitude until it receives a surge which causes measurable degradation.



Circuit Description

The circuits used to perform the required measurements were of the form shown in Fig. 2. They produce half sine pulses of current from the resonant discharge of C via L. Triggering of the device under test (DUT) itself is used to initiate the discharge. The gate signal used for all the tests was a 100 mA / 1 µs pulse fed from a pulse generator in single-shot mode.

The magnitude of the current pulse is adjusted by changing the voltage to which C is initially charged by varying the output of the PSU. The pulse is monitored by viewing the voltage across R3 on an digital storage oscilloscope. R1 and D protect the power supply. R1 limits the current from the supply when DUT fails and during the recharging of C. D attempts to prevent any high voltage spikes being fed back into the PSU.



Pushbutton S1 and resistor R2 are a safety feature. R2 keeps C discharged until S1 is pressed. The trigger pulse needs a button on the pulse generator to be pressed which means both hands are occupied and kept away from the test circuit high voltages.

Choice of L & C

The width of the half sine pulse from an LC circuit is:

$$t_{pulse} = \pi \cdot \sqrt{L \cdot C}$$

and the theoretical peak value of the current is:

$$I_{peak} = V \cdot \sqrt{\frac{C}{L}}$$

These equations assume that the circuit has no series resistance to damp the resonant action which would result in a longer but lower pulse. Minimising these effects was considered to be important so care was taken during the building of the circuits to keep the resistance to a minimum. To this end capacitors with low ESR were chosen, the inductors were wound using heavy gauge wire and the loop C / L / DUT / R3 was kept as short as possible.

It was decided to test the devices at three different pulse widths - 10 µs, 100 µs and 1 ms - so three sets of L and C were needed. The values were selected with the help of a 'spreadsheet' program running on an PC compatible computer. The values which were finally chosen are shown in Table 1. Also given in Table 1 are the theoretical peak currents that the L / C combination would produce for a initial voltage on C of 600 V.

Test Procedure

As mentioned earlier, the test method called for each device to be subjected to a series of current pulses of increasing amplitude. The resolution with which the current capability is assessed is defined by the size of each increase in current. It was decided that steps of approximately 5% would give reasonable resolution.

Experimentation indicated that the clearest indication of device damage was obtained by looking for changes in the off-state breakdown voltage. So after each current pulse the DUT was removed from the test circuit and checked on a curve tracer. This procedure did slow the testing but it was felt that it would result in greater accuracy.

Pulse Width	C (µF)	L (µH)	I _{peak} (A)
10 µs	13.6	0.75	2564
100 µs	100	10	1885
1 ms	660	154	1244

Table 1. Inductor and Capacitor Values

It was also decided that, since this work was attempting to determine the current that a device could survive - not which killed it, the figure actually quoted in the results for a device's current capability would be the value of the pulse prior to the one which caused damage.

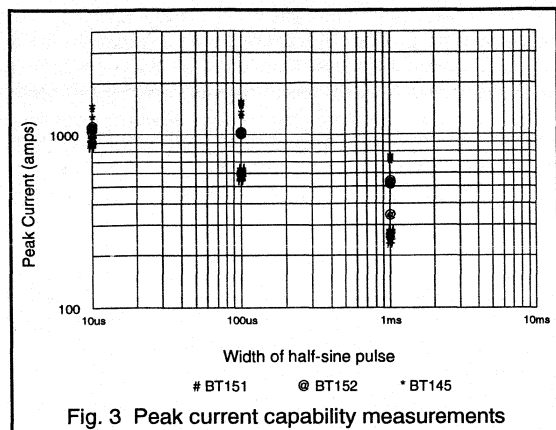


Fig. 3 Peak current capability measurements

Test Results

Figure 3 is a graph showing the measured current capabilities of all of the tested devices. Table 2 summarises the measurements by giving the mean of the results for the three device types at each of the pulse widths. Table 3 expresses the mean values as factors of the device I_{TSM} rating. This table also gives the factors that the various 'rules' would have predicted for the various pulse widths.

Pulse Width	Mean Peak Current Capability (Amps)		
	BT151	BT152	BT145
10 µs	912	1092	1333
100 µs	595	1021	1328
1 ms	264	490	697

Table 2. Measured Current Capability

Pulse Width	Measured Factor			Predicted Factor (by I^2t rule)			
	BT 151	BT 152	BT 145	n=2	n=3	n=4	n=log(1/t)
10 µs	9.1	5.5	4.4	31.6	10.0	5.6	4.0
100 µs	6.0	5.1	4.4	10.0	4.6	3.2	3.2
1 ms	2.6	2.4	2.3	3.2	2.2	1.8	2.2

Table 3. Measured and Predicted I_{TSM} Multiplication Factors

Interpretation of Results

It had been hoped that the measurements would give clear indication of which of the 'rules' would give the most accurate prediction of performance. However, an inspection of Table 3 clearly shows that there is no

correlation between any of the predicted factors and the measured factors. In fact the variation in the factors between the various device types would indicate that no rule based on an I^2t function alone can give an accurate prediction. This implies that something else will have to be taken into account.

Further study of Fig. 3 reveals that the difference in the peak current capability of the three device types is becoming less as the pulses become shorter. This could be explained by a reduction in the active area of the larger crystals, making them appear to be smaller than they actually are. This is consistent with the known fact that not all areas of a thyristor turn on simultaneously - the conduction region tends to spread out from the gate. If the pulse duration is less than the time it takes for all areas of the device to turn on, then the current flows through only part of the crystal, reducing the effective size of the device. If the rate at which the conduction area turns on is constant then the time taken for a small device to be completely ON is shorter than for a large device. This would explain why the performance increase of the BT145 starts falling off before that of the BT151.

Proposed Prediction Method

The above interpretation leads one to believe that the original energy handling rule, which says that I^2t is a constant, may still be correct but that the performance it predicts will 'roll off' if the pulse duration is less than some critical value. The equation which was developed to have the necessary characteristics is:

$$I_{pk} = I_{TSM} \cdot \left(\frac{0.01}{t_p} \right)^{\frac{1}{2}} \cdot \left(\frac{t_p}{t_p + t_{crit}} \right)^{\frac{1}{2}}$$

which simplifies to:-

$$I_{pk} = I_{TSM} \cdot \sqrt{\left(\frac{0.01}{t_p + t_{crit}} \right)}$$

where t_{crit} is proportional to - but not necessarily equal to - the time taken to turn on all the active area of the crystal and is calculated from:-

$$t_{crit} = \frac{A}{R}$$

where: A = crystal area
R = constant expressing the rate at which the area is turned on.

Preferably, A should be the area of the cathode but this information is not always available. As an alternative the total crystal area can be used if the value of R is adjusted accordingly. This will inevitably introduce an error because cathode and crystal areas are not directly proportional, but it should be relatively small.

R was determined empirically to be approximately 0.02 m²/s. Using this value of R gives the values of t_{crit} shown in Table 3. Using these values in the above equation predicts that the peak current handling capability of the BT151, BT152 and BT145 would be as shown in Fig. 4.

Device	t _{crit}
BT151	148 μs
BT152	410 μs
BT145	563 μs

Table 3. Calculated Values of t_{crit}

Conclusions

The first conclusion that can be drawn from this work is that a thyristor, with average rating of only 7.5A, is capable of conducting, without damage, a peak current greater than 100 times this value in a short pulse. Furthermore the power required to trigger the device into conducting this current can be <1 μW. This capability has always been known and indeed the surge rating given in the data sheet gives a value for it at pulse widths of around 10 ms. What has been missing is a reliable method of predicting what the peak current capability of a device is for much shorter pulses.

The results obtained using the test methods indicate that the previously suggested 'rules' fail to take into account the effect that crystal size has on the increase in performance.

In this section, an equation has been proposed which takes crystal size into account by using it to calculate a factor called t_{crit}. This time is then used to 'roll off' the performance increase predicted by the original energy handling equation - I²t = constant. This results in what is believed to be a more accurate means of estimating the capability of a device for a half sine pulse with a duration between 10 μs and 10 ms.

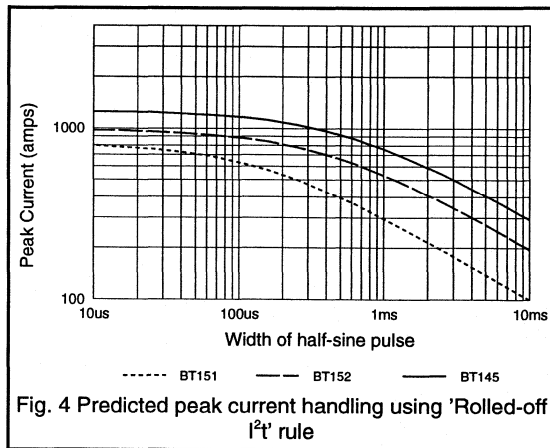


Fig. 4 Predicted peak current handling using 'Rolled-off I²t' rule

6.1.4 Understanding Thyristor and Triac Data

The importance of reliable and comprehensive data for power semiconductor devices, together with the advantages of the absolute maximum rating system, is clear. This present article describes the data sheet descriptions of Philips thyristors and triacs, and aims to enable the circuit designer to use our published data to the full and to be confident that it truly describes the performance of the devices.

A brief survey of short-form catalogues is an insufficient method of comparing different devices. Published ratings and characteristics require supporting information to truly describe the capabilities of devices; thus comparisons between devices whose performance appears to be similar should not be made on economic grounds alone. Manufacturers have been known to quote ratings in such a way as to give a false impression of the capabilities of their devices.

Ratings and characteristics given in published data should always be quoted with the conditions to which they apply, and these conditions should be those likely to occur in operation. Furthermore, it is important to define the rating or characteristic being quoted. Only if data is both complete and unambiguous can a true comparison be made between the capabilities of different types.

Thyristors

Thyristor is a generic term for a semiconductor device which has four semiconductor layers and operates as a switch, having stable on and off states. A thyristor can have two, three, or four terminals but common usage has confined the term thyristor to three terminal devices. Two-terminal devices are known as switching diodes, and four-terminal devices are known as silicon controlled switches. The common, or three-terminal, thyristor is also known as the reverse blocking triode thyristor or the silicon controlled rectifier (SCR). Fig. 1 shows the circuit symbol and a schematic diagram of the thyristor. All Philips thyristors are p-gate types; that is, the anode is connected to the metal tab.

The thyristor will conduct a load current in one direction only, as will a rectifier diode. However, the thyristor will only conduct this load current when it has been 'triggered'; this is the essential property of the thyristor.

Fig. 2 shows the static characteristic of the thyristor. When a small negative voltage is applied to the device, only a small reverse leakage current flows. As the reverse voltage is increased, the leakage current increases until avalanche breakdown occurs. If a positive voltage is applied, then again a small forward leakage current flows which increases as the forward voltage increases. When the

forward voltage reaches the breakover voltage $V_{(BO)}$, turn-on is initiated by avalanche breakdown and the voltage across the thyristor falls to the on state voltage V_T .

However, turn-on can occur when the forward (anode-to-cathode) voltage is less than $V_{(BO)}$ if the thyristor is triggered by injecting a pulse of current into the gate. If the device is to remain in the on state, this trigger pulse must remain until the current through the thyristor exceeds the latching current I_L . Once the on state is established, the holding current I_H is the minimum current that can flow through the thyristor and still maintain conduction. The load current must be reduced to below I_H to turn the thyristor off; for instance, by reducing the voltage across the thyristor and load to zero.

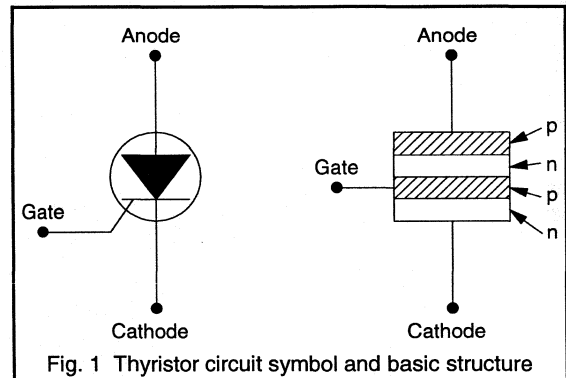


Fig. 1 Thyristor circuit symbol and basic structure

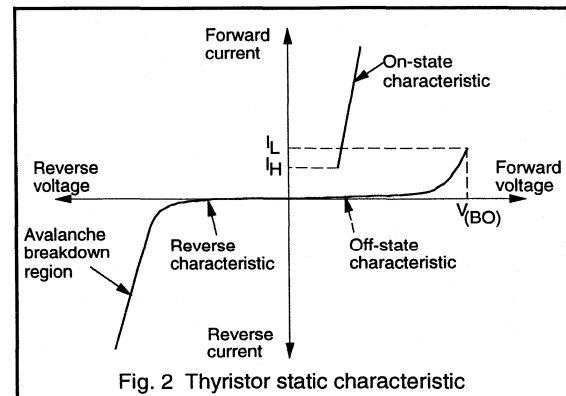


Fig. 2 Thyristor static characteristic

Thyristors are normally turned on by triggering with a gate signal but they can also be turned on by exceeding either the forward breakover voltage or the permitted rate of rise

of anode voltage dV/dt . However, these alternative methods of switching to the conducting state should be avoided by suitable circuit design.

Triacs

The triac, or bidirectional triode thyristor, is a device that can be used to pass or block current in either direction. It is therefore an a.c. power control device. It is equivalent to two thyristors in anti-parallel with a common gate electrode. However, it only requires one heatsink compared to the two heatsinks required for the anti-parallel thyristor configuration. Thus the triac saves both cost and space in a.c. applications.

Figure 3 shows the triac circuit symbol and a simplified cross-section of the device. The triac has two main terminals MT1 and MT2 (the load connections) and a single gate. The main terminals are connected to both p and n regions since current can be conducted in both directions. The gate is similarly connected, since a triac can be triggered by both negative and positive pulses.

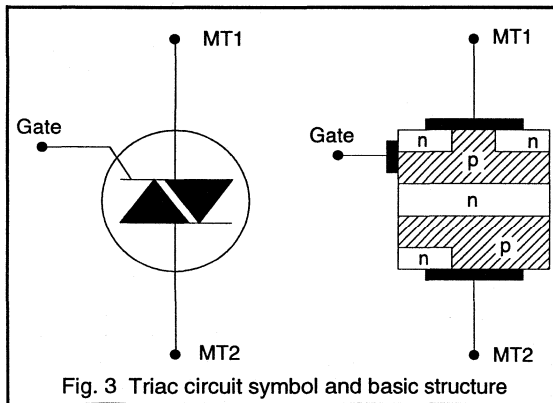


Fig. 3 Triac circuit symbol and basic structure

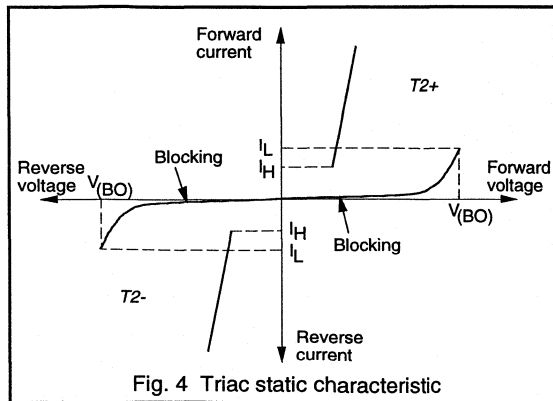


Fig. 4 Triac static characteristic

The on state voltage/current characteristic of a triac resembles that of a thyristor. The triac static characteristic of Fig. 4 shows that the triac is a bidirectional switch. The condition when terminal 2 of the triac is positive with respect to terminal 1 is denoted in data by the term 'T2+'. If the triac is not triggered, the small leakage current increases as the voltage increases until the breakover voltage $V_{(BO)}$ is reached and the triac then turns on. As with the thyristor, however, the triac can be triggered below $V_{(BO)}$ by a gate pulse, provided that the current through the device exceeds the latching current I_L before the trigger pulse is removed. The triac, like the thyristor, has holding current values below which conduction cannot be maintained.

When terminal 2 is negative with respect to terminal 1 (T2-) the blocking and conducting characteristics are similar to those in the T2+ condition, but the polarities are reversed. The triac can be triggered in both directions by either negative (G-) or positive (G+) pulses on the gate, as shown in Table 1. The actual values of gate trigger current, holding current and latching current may be slightly different in the different operating quadrants of the triac due to the internal structure of the device.

Quadrant	Polarity of T2 wrt T1	Gate polarity
1 (1+)	T2+	G+
2 (1-)	T2+	G-
3 (3-)	T2-	G-
4 (3+)	T2-	G+

Table 1. Operating quadrants for triacs

Device data

Anode to cathode voltage ratings

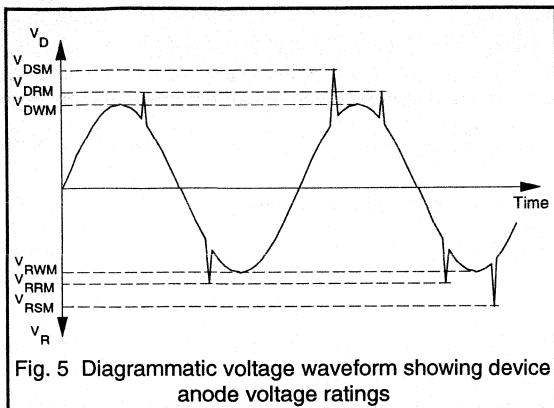
The voltage of the a.c. mains is usually regarded as a smooth sinewave. In practice, however, there is a variety of transients, some occurring regularly and others only occasionally (Fig. 5). Although some transients may be removed by filters, thyristors must still handle anode to cathode voltages in excess of the nominal mains value.

The following reverse off-state $V_{(BO)}$ ratings are given in our published data:

V_{RSM} : the non-repetitive peak reverse voltage. This is the allowable peak value of non-repetitive voltage transients, and is quoted with the maximum duration of transient that can be handled (usually $t < 10ms$).

V_{RRM} : the repetitive peak reverse voltage. This is the allowable peak value of transients occurring every cycle.

V_{RWM} : the peak working reverse voltage. This is the maximum continuous peak voltage rating in the reverse direction, neglecting transients. It corresponds to the peak negative value (often with a safety factor) of the sinusoidal supply voltage.



The forward off-state voltages corresponding to V_{RSM} , V_{RRM} and V_{RWM} are listed below.

V_{DSM} : the non-repetitive peak off-state voltage applied in the forward direction.

V_{DRM} : the repetitive peak off-state voltage applied in the forward direction.

V_{DWM} : the peak working off-state voltage applied in the forward direction.

Both the repetitive and non-repetitive voltage ratings are determined partly by the voltage limit that prevents the thyristor being driven into forward or reverse breakdown, and partly by the instantaneous energy (resulting from an increase in leakage current) that can be dissipated in the device without exceeding the rated junction temperature.

When a thyristor is to operate directly from the mains supply, it is advisable to choose a device whose repetitive peak voltage ratings V_{RRM} and V_{DRM} are at least 1.5 times the peak value of the sinusoidal supply voltage. This figure forms part of the device type number; for example BT151-650R, where 650 corresponds to V_{DRM} , $V_{RRM}=650V$ and the final R (for Reverse) indicates that the anode of the device is connected to the metal tab.

Anode-to-cathode current ratings

The following current ratings, described by the waveforms shown in Fig. 6, are given in our published data. Note that the suffix $_T$ implies that the thyristor is in the on state.

$I_{T(AV)}$: the average value of the idealised mains current waveform taken over one cycle, assuming conduction over 180° . For devices mounted on heatsinks, the $I_{T(AV)}$ rating should be quoted for a particular mounting-base temperature T_{mb} ; our devices are generally characterised at a mounting-base temperature of at least $85^\circ C$. A device can have an artificially high current rating if the

mounting-base temperature is unrealistically low; ratings with no associated mounting-base temperature should be regarded with suspicion.

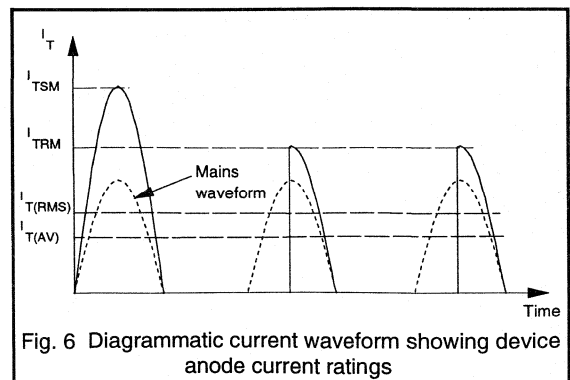
$I_{T(RMS)}$: the rms on-state current. This rating gives the maximum rms current that the thyristor can handle. It is important for applications when the device current waveform is described by a high value form factor. For such conditions the rms current rather than the average current may be the limiting rating.

$I_{T(RM)}$: the repetitive peak forward current. This rating is the peak current that can be drawn each cycle providing that the average and rms current ratings are not exceeded.

I_{TSM} : the non-repetitive (surge) peak forward current. This rating is the peak permitted value of non-repetitive transients, and depends on the duration of the surge. Our published data quotes the I_{TSM} rating for $t=10ms$, the duration of a half-cycle of 50Hz mains. However, some manufacturers quote I_{TSM} for $t=8.3ms$ (half-cycle of 60Hz mains), and thus surge ratings for devices quoted at $t=8.3ms$ should be approximately downrated (multiplied by 0.83) before comparing them with $t=10ms$ surge ratings.

The surge rating also depends on the conditions under which it occurs. Our data sheets quote I_{TSM} rating under the worst probable conditions, that is, $T_J=T_{J(max)}$ immediately prior to the surge, followed by reapplied $V_{RWM(max)}$ immediately after the surge. An unrealistically high I_{TSM} rating could be quoted if, for example, $T_J < T_{J(max)}$ prior to the surge and then the full rated voltage is not reapplied.

Published data also includes curves for I_{TSM} against time which show the maximum allowable rms current which can occur during inrush or start-up conditions. The duration of the inrush transient and the mounting base temperature prior to operation determine the maximum allowable rms inrush current.



di/dt : the rate of rise of on-state current permissible after triggering. An excessive rate of rise of current causes local heating and thus damage to the device. The rate of rise of current is determined by both the supply and load impedances, and can be limited by additional series inductance in the circuit.

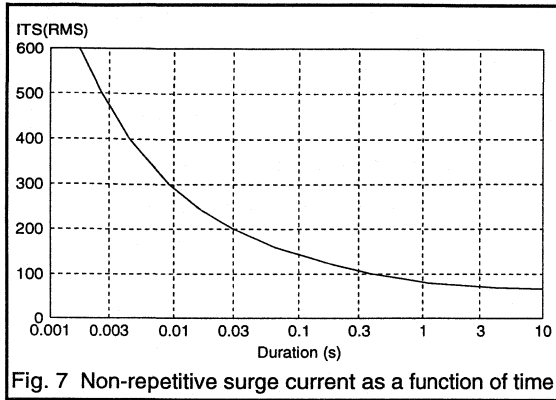


Fig. 7 Non-repetitive surge current as a function of time

I^2t : a dimensional convenience specifying the capability of a thyristor to absorb energy. This rating is required for the selection of fuses to protect the thyristor against excessive currents caused by fault conditions. It is normally only valid over the range 3 to 10ms. In our published data, a value is quoted for 10ms, in which case:

$$I^2t = \int i^2 \cdot dt \quad (1)$$

$$= \left(\frac{I_{TSM}}{\sqrt{2}} \right)^2 \times 10 \cdot 10^{-3} \quad (A^2s)$$

The user should match the minimum I^2t capability of the thyristor to the worst case I^2t let-through of a range of nominally rated fuses in order to select a fuse that will protect the device under worst probable conditions.

Values of I^2t other than those quoted for 10ms can be estimated by referring to the appropriate published curves of non-repetitive surge current against time. For example, Fig. 7 is the non repetitive surge current curve for a thyristor whose I^2t at 10ms is $800A^2s$. From Fig. 7, $I_{TS(RMS)}$ at 3ms is 470A and therefore I^2t at 3ms is given by:

$$I^2t(3ms) = I_{TS(RMS)}^2 \times t$$

$$= 470^2 \times 3 \cdot 10^{-3}$$

$$= 662.7A^2s$$

To summarise, when selecting an appropriate fuse the following conditions must be taken into account.

1. The fuse must have an rms current rating equal to, or less than, that of the thyristor it is to protect.
2. The I^2t at the rms working voltage must be less than that of the thyristor taken over the fuse operating time.
3. The arc voltage of the fuse must be less than the V_{RSM} rating of the thyristor.

Gate-to-cathode ratings

The following gate-to-cathode ratings are given in the published data.

V_{RGM} : the gate peak reverse voltage.

$P_{G(AV)}$: the mean gate power, averaged over a 20ms period.

P_{GM} : the peak gate power dissipation.

The gate-to-cathode power ratings should not be exceeded if over-heating of the gate-cathode junction is to be avoided.

Temperature ratings

Two temperature ratings are given in the published data.

T_{stg} : the storage temperature. Both maximum and minimum values of the temperature at which a device can be stored are given.

T_j : the junction temperature. This is one of the principal semiconductor ratings since it limits the maximum power that a device can handle. The junction temperature rating quoted in our published data is the highest value of junction temperature at which the device may be continuously operated to ensure a long life.

Thermal characteristics

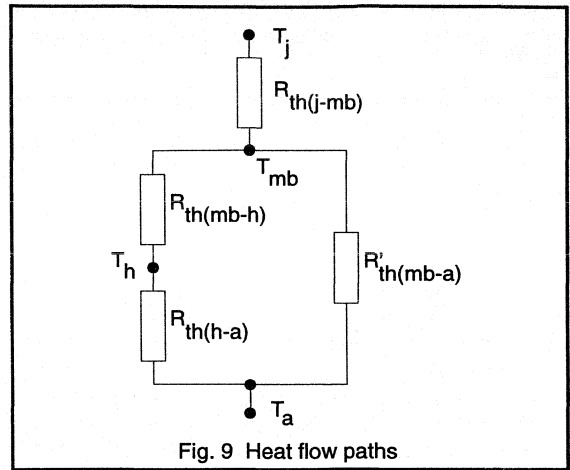
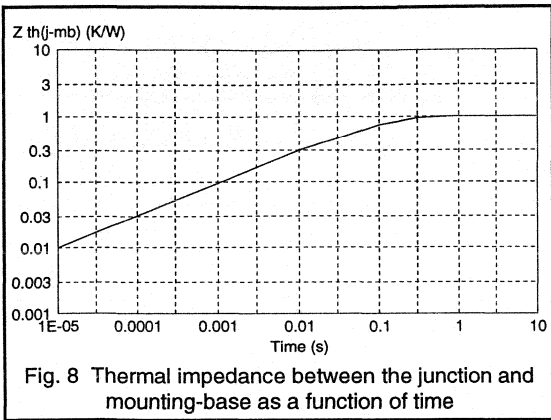
The following thermal resistances and impedances are given in our data.

$R_{th(j-a)}$: the thermal resistance between the junction of the device and ambient (assumed to be the surrounding air).

$R_{th(j-mb)}$: the thermal resistance between the junction and mounting base of the device.

$R_{th(mb-h)}$: the thermal resistance between the mounting base of the device and the heatsink (contact thermal resistance).

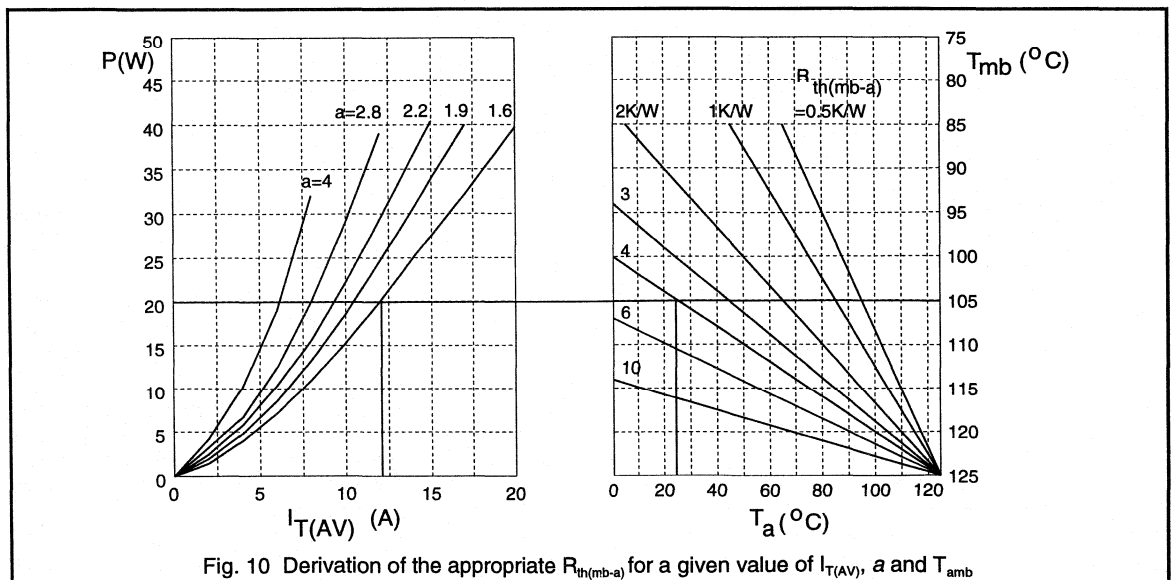
$Z_{th(j-mb)}$: the transient thermal impedance between the junction and mounting-base of the device. The value given in the published data is for non-repetitive conditions and a particular pulse duration. Under pulse conditions, thermal impedances rather than thermal resistances should be considered. Higher peak power dissipation is permitted under pulse conditions since the materials in a thyristor have a definite thermal capacity, and thus the critical junction temperature will not be reached instantaneously, even when excessive power is being dissipated in the device. The published data also contains graphs of $Z_{th(j-mb)}$ against time (for non-repetitive conditions) such as those shown in Fig. 8.



$$R_{th(mb-a)} = R_{th(mb-h)} + R_{th(h-a)} \quad (2)$$

The values of the various thermal resistances between the thyristor junction and the surroundings must be considered to ensure that the junction temperature rating is not exceeded. The heat generated in a semiconductor chip flows by various paths to the surroundings. Fig. 9 shows the various thermal resistances to be taken into account in this process. With no heatsink, the thermal resistance from the mounting-base to the surroundings is given by $R_{th(mb-a)}$. When a heatsink is used, the heat loss direct to the surroundings from the mounting-base is negligible owing to the relatively high value of $R_{th(mb-h)}$ and thus:

Where appropriate, our published data contains power graphs such as that in Fig. 10. These characteristics relate the total power P dissipated in the thyristor, the average forward current $I_{T(AV)}$, the ambient temperature T_a , and the thermal resistance $R_{th(mb-a)}$, with the form factor, a , as a parameter. They enable the designer to work out the required mounting arrangement from the conditions under which the thyristor is to be operated.



Usually, the characteristics are designed for use in 50Hz sinusoidal applications, when the procedure below should be followed.

1. Determine the values of $I_{T(AV)}$ and $I_{T(RMS)}$ for the relevant application.
2. Determine the form factor, which is given by:

$$a = \frac{I_{T(RMS)}}{I_{T(AV)}} \quad (3)$$

3. Starting from the appropriate value of $I_{T(AV)}$ on a curve such as Fig. 10, move vertically upwards to intersect the appropriate form factor curve (interpolating if necessary).
4. This intersection gives the power dissipated in the thyristor on the left-hand axis of the combined graph and the mounting base temperature on the right hand axis.
5. Moving horizontally across from this intersection to the appropriate value of ambient temperature gives the required mounting base to ambient thermal resistance $R_{th(mb-a)}$.
6. The required heatsink thermal resistance $R_{th(h-a)}$ can now be calculated from Equation 2 since the mounting base to heatsink thermal resistance $R_{th(mb-h)}$ is given in the published data.

Example

The thyristor to which Fig. 10 applies is operated at an average forward current $I_{T(AV)}$ of 12A and an rms forward current $I_{T(RMS)}$ of 19.2A. The maximum anticipated ambient temperature is 25°C. Now, Equation 3 gives,

$$a = \frac{19.2}{12} = 1.6$$

Figure 10 gives the power as $P=20W$ and the mounting-base temperature as $T_{mb}=105^{\circ}C$. Also, at this power and ambient temperature of 25°C, Fig. 10 gives the value of $R_{th(mb-a)}$ to be 4°C/W. The published data gives the value of $R_{th(mb-h)}$ (using a heatsink compound) to be 0.2°C/W and then Equation 2 gives

$$R_{th(h-a)} = 4 - 0.2 = 3.8^{\circ}C/W$$

Mounting torque

Two values of mounting torque are given in the published data. A minimum value is quoted below which the contact thermal resistance rises owing to poor contact, and a maximum value is given above which the contact thermal resistance again rises owing to deformation of the tab or cracking of the crystal.

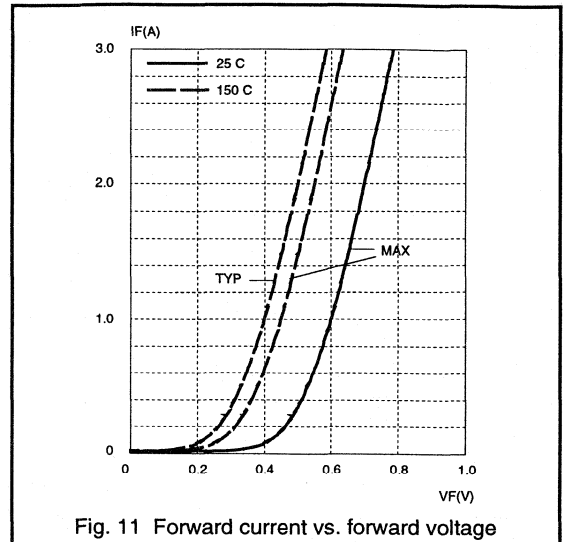


Fig. 11 Forward current vs. forward voltage

The surface of a device case and heatsink cannot be perfectly flat, and thus contact will take place on several points only, with a small air-gap over the rest of the contact area. The use of a soft substance to fill this gap will lower the contact thermal resistance. We recommend the use of proprietary heatsinking compounds which consist of a silicone grease loaded with an electrically insulating and good thermal conducting powder such as alumina.

Anode-to-cathode characteristics

The following anode-to-cathode characteristics are included in the published data.

I_R : the reverse current. This parameter is given for the worst probable conditions; that is, the reverse voltage $V_R=V_{RWM(max)}$ and a high T_J .

I_D : the off-state current. This parameter is again given for the worst probable conditions; that is, the forward voltage $V_D=V_{DWM(max)}$ and a high T_J .

I_L : the latching current (Fig. 2). This parameter is quoted at a particular value of junction temperature.

I_H : the holding current (Fig. 2). This parameter is quoted at a particular value of junction temperature.

V_T : the forward voltage when the thyristor is conducting. This parameter is measured at particular values of forward current and junction temperature. The junction temperature is usually low ($T_J=25^{\circ}C$, for example) since this is the worst case. The measurement must be performed under pulse conditions to maintain the low junction temperature. The published data also contains curves of forward current against forward voltage, usually for two values of the junction temperature: 25°C and $T_{J(max)}$ (Fig. 11).

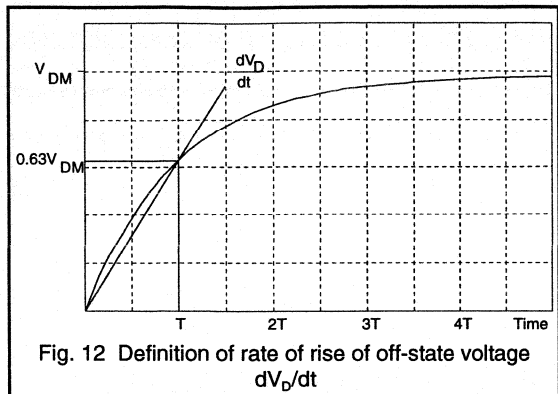


Fig. 12 Definition of rate of rise of off-state dV_D/dt

dV_D/dt : the rate of rise of off-state voltage that will not trigger any device. This parameter is given at maximum values of junction temperature $T_{j(max)}$ and forward voltage $V_D = V_{DRM(max)}$.

The values of dV_D/dt quoted in our published data are normally specified assuming an exponential waveform. This facilitates the design of RC snubber circuits for device protection when required. Fig. 12 illustrates the definition of dV_D/dt . The final voltage applied to the device V_{DM} is chosen as $V_{DRM(max)}$ and the junction temperature is $T_j = T_{j(max)}$.

Fig. 12 shows that dV_D/dt is given by the expression:

$$\begin{aligned} \frac{dV_D}{dt} &= \frac{0.63V_{DM}}{T} \\ &= \frac{0.63 \times 2/3 V_{DRM(max)}}{T} \\ &= \frac{0.42V_{DRM(max)}}{T} \quad (V/\mu s) \end{aligned}$$

where T is the exponential time constant.

The dV_D/dt capability of a thyristor increases as the junction temperature decreases. Thus curves such as those shown in Fig. 13a) are provided in the published data so that designers can uprate devices operated at lower junction temperatures.

The dV_D/dt characteristic can also be increased by operating the device at a low supply voltage. Thus the published data also contains curves such as Fig. 13b) which shows how dV_D/dt increases as the ratio $V_{DM}/V_{DRM(max)}$ max decreases. Note that V_{DM} is unlikely to be greater than $2/3 V_{DRM(max)}$ (usually owing to the restriction of $V_{DWM(max)}$) and therefore the fact that dV_D/dt approaches zero as V_{DM} increases above the value of $2/3 V_{DRM(max)}$ does not cause problems.

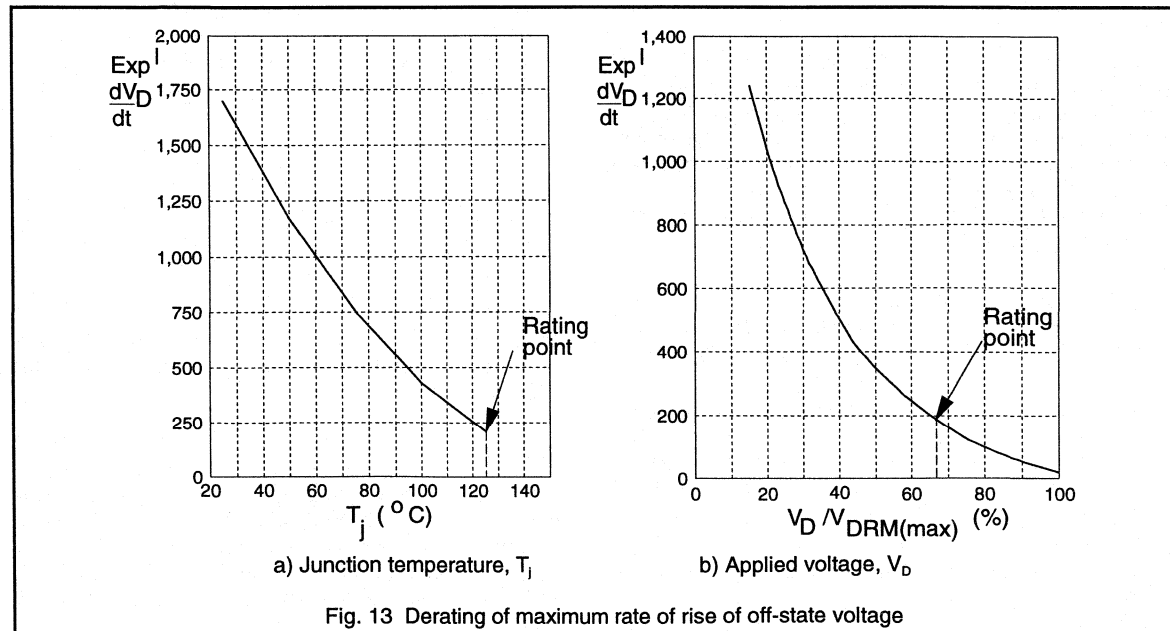
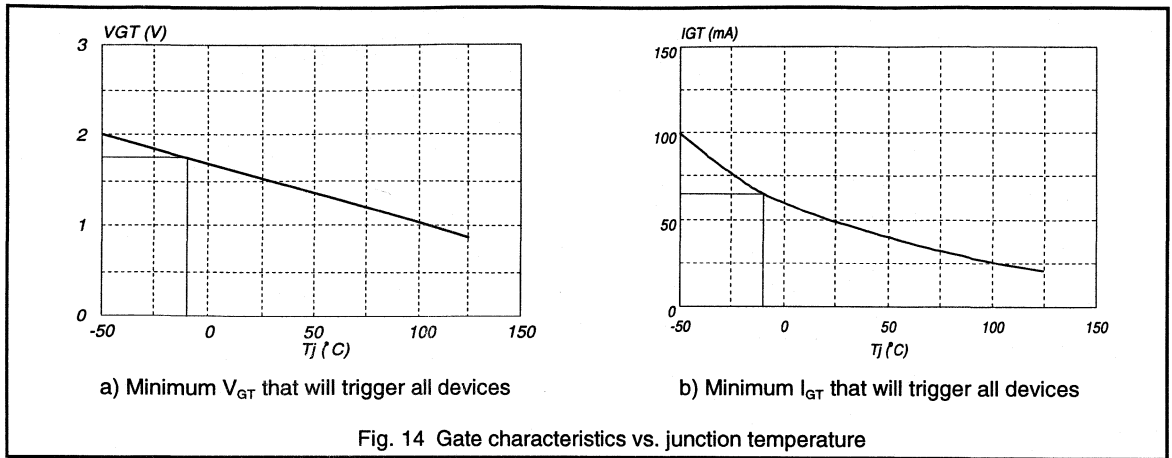


Fig. 13 Derating of maximum rate of rise of off-state voltage



Gate-to-cathode characteristics

The following gate-to-cathode characteristics are given in the published data.

V_{GT} : the gate-to-cathode voltage that will trigger all devices. This characteristic should be quoted for particular values of applied voltage V_D and low junction temperature.

I_{GT} : the gate-to-cathode current that will trigger all devices. This characteristic should be quoted for the same conditions given above.

A gate drive circuit must be designed which is capable of supplying at least the required minimum voltage and current without exceeding the maximum power rating of the gate junction. Curves such as those shown in Fig. 14 (which relate the minimum values of V_{GT} and I_{GT} for safe triggering to the junction temperature) are provided in data. The following design procedure is recommended to construct a gate drive circuit load-line on the power curves shown in Fig. 15.

1. Determine the maximum average gate power dissipation $P_{G(AV)}$ from the published data (normally 0.5W, 1.0W, or 2.0W) and then use the appropriate choice of x-axis scaling in Fig. 15.
2. Estimate the minimum ambient temperature at which the device will operate, and then determine the minimum values of V_{GT} and I_{GT} from curves such as Figs. 14a) and 14b) in the published data. Note that it is assumed that at switch-on $T_J = T_a$.
3. Determine the minimum open-circuit voltage of the trigger pulse drive circuit: this is the first co-ordinate on the load line at $I_G = 0$.

4. Using the appropriate horizontal scaling for the device ($P_{G(AV)} = 0.5W, 1.0W$ or $2.0W$), plot a second point on the power curve whose co-ordinates are given by $V_{GT(min)}$ and $5 \times I_{GT(min)}$. Construct a load line between these two points. The slope of this load gives the maximum allowable source resistance for the drive circuit.
5. Check the power dissipation by ensuring that the load line must not intersect the curve for the maximum peak gate power $P_{GM(max)}$ which is the outermost ($\delta = 0.1$) curve of Fig. 15. The load line must also not intersect the curve which represents the maximum average gate power $P_{G(AV)}$ modified by the pulse mark-space ratio, where:

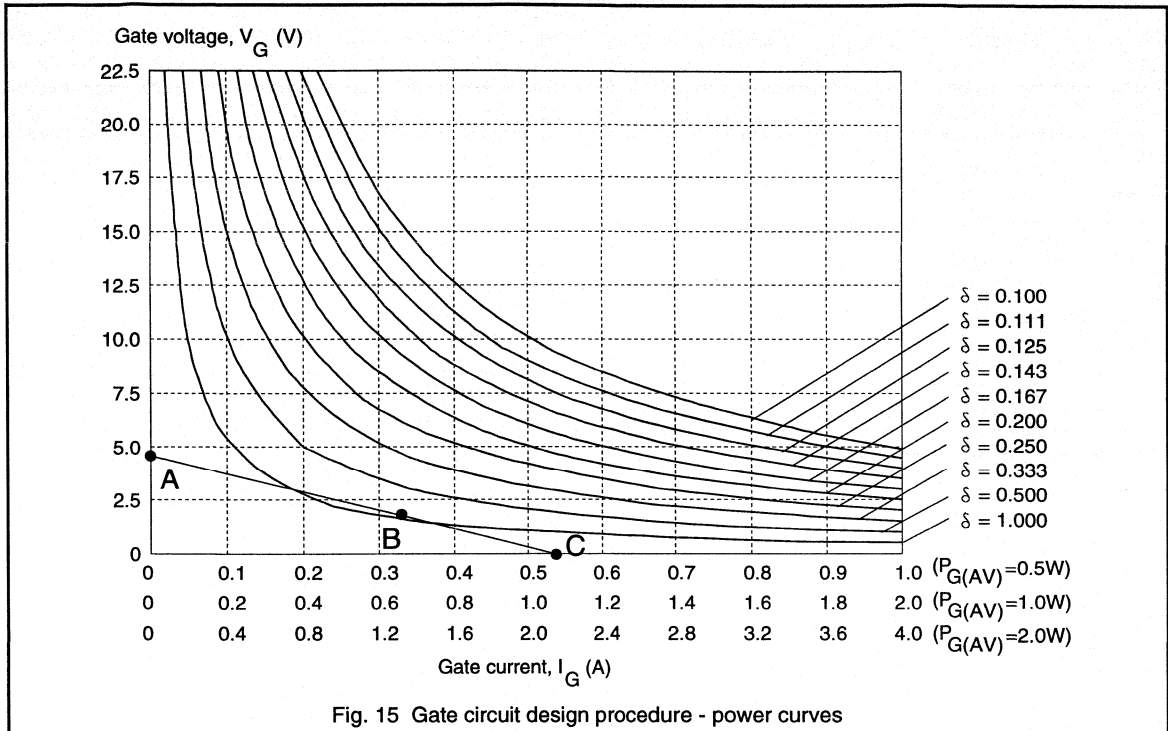
$$P_{GM(max)} = \frac{P_{AV}}{\delta} \quad (5)$$

For instance, in Fig. 15, for a thyristor with $P_{G(AV)} = 1W$, the $\delta = 0.25$ curve can be used for a gate drive with a 1:3 mark-space ratio giving an allowable maximum gate power dissipation of $P_{GM(max)} = 4W$.

An illustration of how the above design procedure operates to give an acceptable gate drive circuit is presented in the following example.

Example

A thyristor has the V_{GT}/T_J and I_{GT}/T_J characteristics shown in Fig. 14 and is rated with $P_{G(AV)} = 0.5W$ and $P_{GM(max)} = 5W$. A suitable trigger circuit operating with $\delta_{max} = 0.25$, $V_{GT(min)} = 4.5V$, $I_{GT(max)} = 620mA$ and $T_{a(min)} = -10^\circ C$ is to be designed. Determine its suitability for this device.



1. Select the top x-axis scale of Fig. 15 ($P_{G(AV)}=0.5W$).
2. From Fig. 14, $V_{GT(min)}=1.75V$, and $I_{GT(min)}=66mA$.
3. At minimum supply voltage, the open-circuit gate voltage is 4.5V, giving point 'A' in Fig. 15. Point B is plotted at the co-ordinates $V_{GT(min)}$ and $5xI_{GT(min)}$, that is at 1.75V and 330mA, and load line ABC is constructed as shown. Note that point C is the maximum current required at $I_G=570mA$ and is within the capability of the drive circuit.
4. As required the load line does not intersect the $P_{G(max)}$ ($\delta=0.1$). The gate drive duty cycle, δ , is 0.25. Therefore $P_{G(max)} = P_{G(AV)}/\delta = 0.5/0.25 = 2W$. As required, the load line ABC does not intersect the $\delta=0.25$ curve.

pulse and the onset of the anode current which is known as the delay time t_d (Fig. 16). The time taken for the anode voltage to fall from 90% to 10% of its initial value is known as the rise time t_r . The sum of the delay time and the rise time is known as the gate-controlled turn-on time t_{gt} .

The gate controlled turn-on time depends on the conditions under which it is measured, and thus the following conditions should be specified in the published data.

- Off-state voltage; usually $V_D=V_{DWM(max)}$.
- On-state current.
- Gate trigger current; high gate currents reduce t_{gt} .
- Rate of rise of gate current; high values reduce t_{gt} .
- Junction temperature; high temperatures reduce t_{gt} .

Switching characteristics

Two important switching characteristics are usually included in our published data. They are the gate-controlled turn-on time t_{gt} (divided into a turn-on delay time, t_d , and a rise time, t_r) and the circuit-commutated turn-off time, t_q .

Gate-controlled turn-on time, t_{gt}

Anode current does not commence flowing in the thyristor at the instant that the gate current is applied. There is a period which elapses between the application of the trigger

Circuit-commutated turn-off time

When a thyristor has been conducting and is reverse-biased, it does not immediately go into the forward blocking state: minority charge carriers have to be cleared away by recombination and diffusion processes before the device can block reapplied off-state voltage. The time from the instant that the anode current passes through zero to the instant that the thyristor is capable of blocking reapplied off-state voltage is the circuit-commutated turn-off time t_q (Fig. 17).

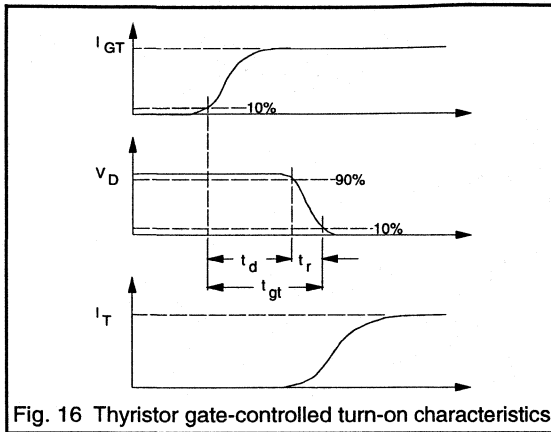


Fig. 16 Thyristor gate-controlled turn-on characteristics

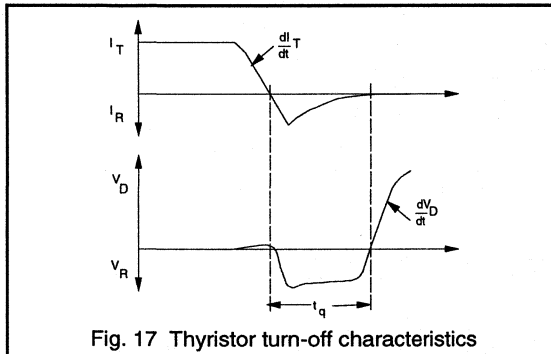


Fig. 17 Thyristor turn-off characteristics

The following conditions should be given when t_q is quoted.

- On-state current; high currents increase t_q .
- Reverse voltage; low voltages increase t_q .
- Rate of fall of anode current; high rates increase t_q .
- Rate of rise of re-applied off-state voltage; high rates increase t_q .
- Junction temperature; high temperatures increase t_q .
- Gate bias; negative voltages decrease t_q .

Triac ratings

The ratings and characteristics of the triac are similar to those of the thyristor, except that the triac does not have any reverse voltage ratings (a reverse voltage in one quadrant is the forward voltage in the opposite quadrant). However, one characteristic requires special attention when choosing triacs; the rate of re-applied voltage that the triac will withstand without uncontrolled turn-on.

If a triac is turned off by simply rapidly reversing the supply voltage, the recovery current in the device would simply switch it on in the opposite direction. To guarantee reduction of the current below its holding value, the supply voltage must be reduced to zero and held there for a sufficient time

to allow the recombination of any stored charge in the device. To ensure turn-off, the rate of fall of current during the commutation interval (turn-off period) and the rate of rise of re-applied voltage after commutation must both be restricted. An excessive rate of fall of current creates a large number of residual charge carriers which are then available to initiate turn-on when the voltage across the triac rises.

With supply frequencies up to around 400Hz and a sinusoidal waveform, commutation does not present any problems when the load is purely resistive, since the current and voltage are in phase. As shown in Fig. 18 the rate of fall of on-state current $-di/dt$, given by Equation 6, and the rate of rise of commutating voltage dV_{com}/dt , given by equation 7, are sufficiently low to allow the stored charge in the device to fully recombine. The triac is thus easily able to block the rising re-applied voltage dV_{com}/dt .

$$di/dt = 2\pi f \cdot \sqrt{2} I_{T(RMS)} \quad (6)$$

$$dV_{com}/dt = 2\pi f \cdot \sqrt{2} V_{(RMS)} \quad (7)$$

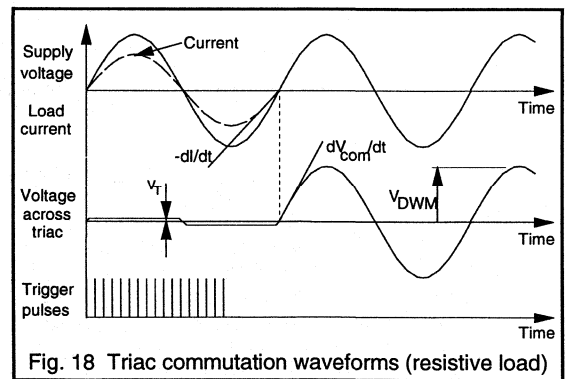


Fig. 18 Triac commutation waveforms (resistive load)

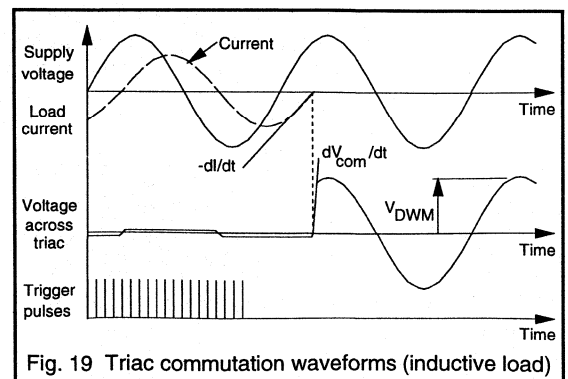


Fig. 19 Triac commutation waveforms (inductive load)

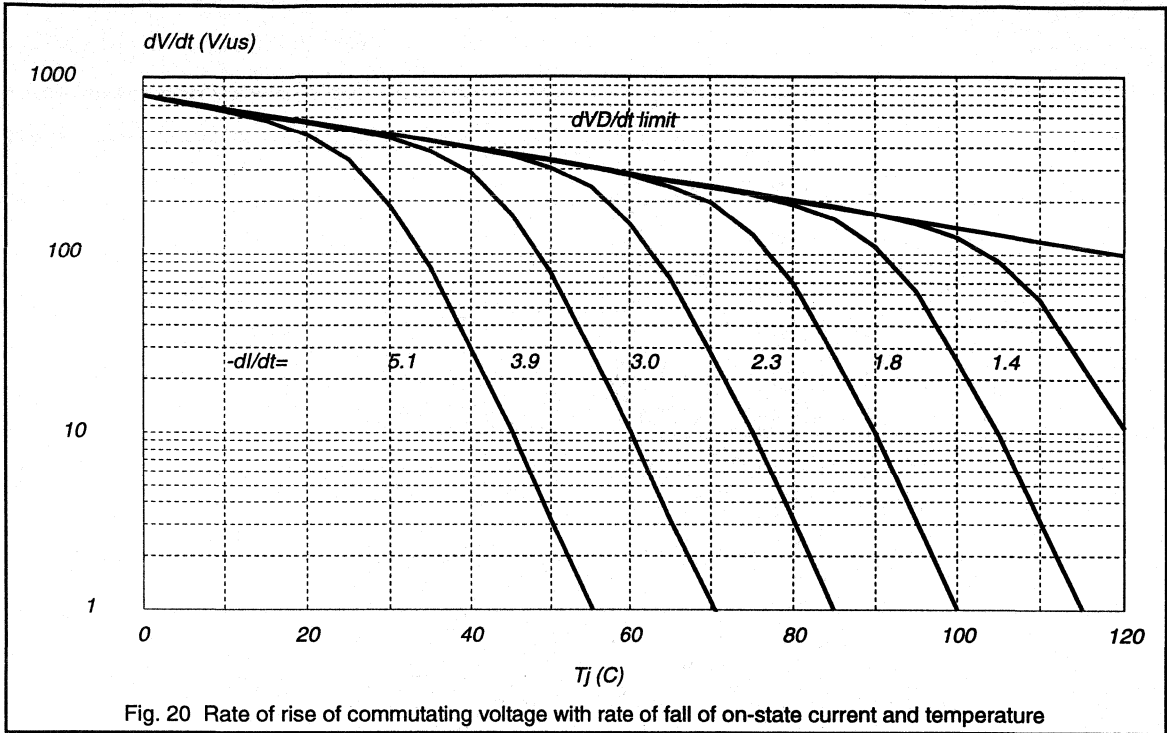


Fig. 20 Rate of rise of commutating voltage with rate of fall of on-state current and temperature

However, with an inductive load (Fig. 19) the current lags behind the voltage and consequently commutation can present special difficulties. When the on-state current has fallen to zero after a triac has been conducting in one direction the supply voltage in the opposite direction will have already reached a significant value. The rate of fall of triac current will still be given by Equation 6 but the rate of rise of reapplied voltage, dV_{com}/dt will be very large. The triac may switch on immediately unless dV/dt is held less than that quoted in the published data by suitable circuit design. Alternatively, the circuit design can remain simple if Hi-Com triacs are employed instead. Sections 6.3.1 and 6.3.2 explain the advantages of using Hi-Com triacs in such inductive circuits.

The maximum rate of rise of commutating voltage which will not cause the device to trigger spuriously is an essential part of the triac published data. However, dV_{com}/dt is meaningless unless the conditions which are applicable are provided, particularly the rate of fall of on-state current $-di_T/dt$. Our published data also contains graphs such as

Fig. 20 which relate dV_{com}/dt to junction temperature with $-di_T/dt$ as a parameter. The characteristic dV_{com}/dt is specified under the worst probable conditions, namely:

- mounting base temperature, $T_{mb} = T_{mb(max)}$
- reapplied off-state voltage, $V_D = V_{DWM(max)}$
- rms current, $I_{T(RMS)} = I_{T(RMS)(max)}$

In order that designers may economise their circuits as far as possible, we offer device selections with the same current ratings but with different values of dV_{com}/dt (at the same value of $-di_T/dt$) for some of our triac families. The dV/dt capability can be traded off against the gate sensitivity ($I_{GT(max)}$) of the device. Sensitive gate triacs (i.e. those which require only a small amount of gate current to trigger the device) have less ability to withstand high values of dV_{com}/dt before sufficient current flows within the device to initiate turn-on. These different device selections are differentiated by suffixes which are added to the device type number eg. BT137-600E.

Detailed design considerations for dV_{com}/dt limiting in inductive circuits when using triacs are considered in separate articles in this handbook.



Thyristor and Triac Applications

6.2.1 Triac Control of DC Inductive Loads

The problem of inductive loads

This publication investigates the commutation problem encountered when triacs are used in phase control circuits with inductive loads. Commutation failure is likely to occur owing to circuit inductance imposing a sudden rise of voltage on the triac after conduction. Control of transformers supplying an inductively loaded bridge rectifier is particularly troublesome because of the added effect of rapid current decay during commutation. For a better understanding of the nature of the problem, the commutation behaviour is summarised here.

Triacs are bipolar power control elements that may turn on with either polarity of voltage applied between their main terminals. Unlike thyristors there is no circuit-imposed turn-off time. To ensure commutation the decay rate of current before turn-off and the rate of rise of reapplied voltage must both be held below specified limits. An excessive current decay rate has a profound effect on the maximum rate of rise of voltage that can be sustained, as then a large amount of stored charge is available to initiate the turn-on in the next half cycle.

Figure 1 shows the condition for a triac controlled transformer followed by a rectifier with inductive load. The load inductance forces the rectifier diodes into conduction whenever the instantaneous dc output voltage drops to zero. The transformer secondary is thus shorted for some time after the zero transitions of the mains voltage and a reverse voltage is applied to the triac, turning it off. Because of transformer leakage inductance the triac does not turn off immediately but continues to conduct over what is called the commutation interval (see Fig. 1).

During the commutation interval a high rate of decay of current (di_{com}/dt) results for two reasons. Firstly the rate of fall of current is high because the leakage inductance of most transformers is low. This is necessary to achieve a small dc output voltage loss (represented by the shaded areas in the voltage waveform of Fig. 1) in the transformer. Secondly, with an inductive rectifier load a substantial current flows when commutation starts to occur.

The large value of di_{com}/dt results in a high rate of rise of voltage, dv/dt . Since the current decays rapidly the peak reverse recovery current I_{RRM} is fairly large. Upon turn-off, I_{RRM} is abruptly transferred to the snubber elements R and C so the voltage abruptly rises to the level $R \cdot I_{RRM}$ (C is initially discharged). Owing to the high value of both di_{com}/dt and dv/dt , loss of control follows unless measures are taken to prevent it.

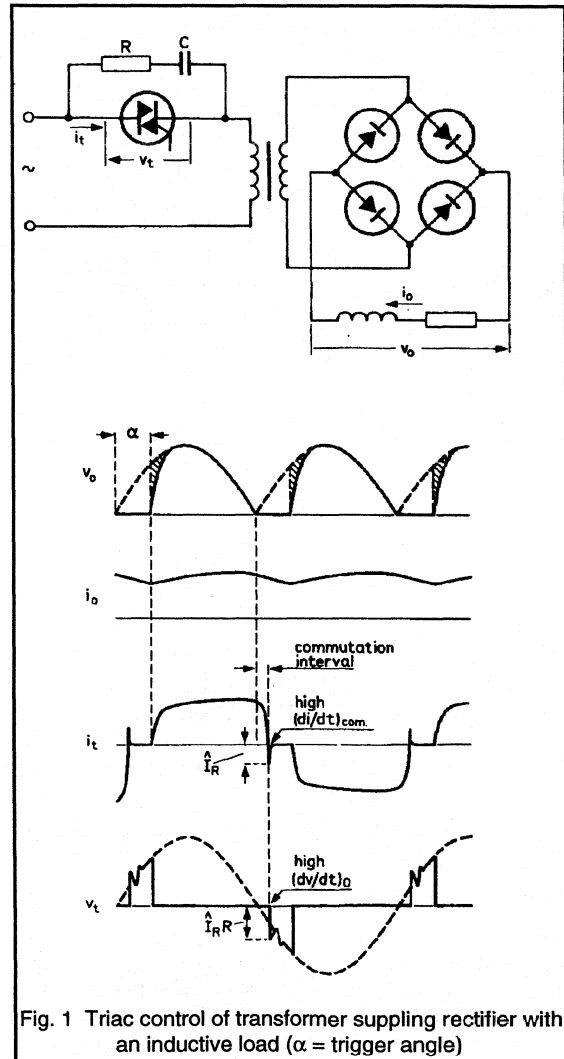


Fig. 1 Triac control of transformer supplying rectifier with an inductive load ($\alpha =$ trigger angle)

Obtaining reliable commutation

A saturable choke in series with the transformer primary proves effective in achieving reliable commutation (Fig. 2). Saturation should occur at a fraction of the rated load current so that the loss in the rectifier output voltage is minimised. At low currents the total inductance is large, thus softening the commutation and eliminating transients. The choke delays the rise in voltage so a quiescent period of a few tens of microseconds is introduced, during which time

the triac can recover. There is usually no difficulty in designing a choke such that the decay rate of current (di_{com}/dt) and the rate of rise of voltage (dv/dt) are sufficiently reduced to ensure reliable control.

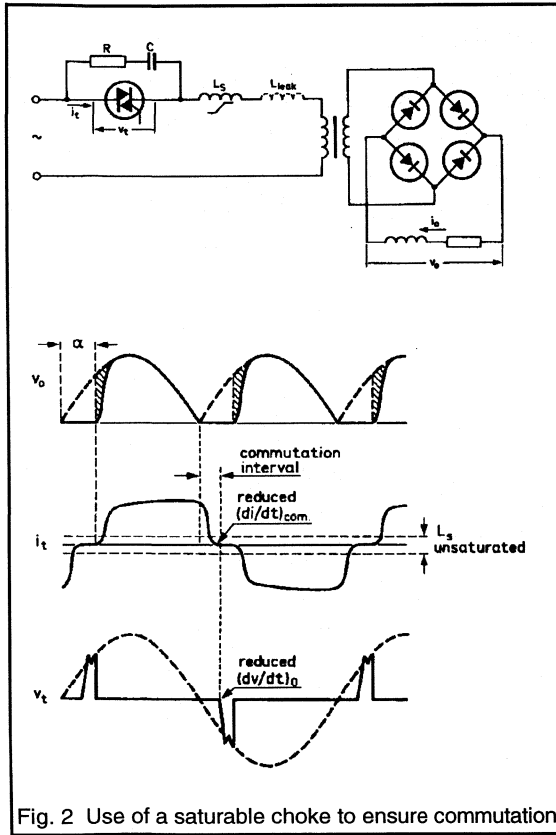


Fig. 2 Use of a saturable choke to ensure commutation

Circuit analysis

Over the commutation interval the transformer secondary is shorted as the load inductance keeps the rectifier diodes in conduction, so the simplified diagram of Fig. 3 applies. If the load time constant is much larger than the mains period then the load current can be assumed to be purely dc. The waveforms of triac voltage and current are given in Fig. 4. The mains voltage is given by $v_i = V_s \sin \omega t$. As the commutation interval is a fraction of the ac period then the rate of change of voltage during the commutation interval can be assumed to be linear, giving:

$$v_i = -\hat{V} \omega t \quad (1)$$

Over the period 0 to t_2 the voltage across the saturable choke L_s and leakage inductance L_{leak} is equal to v_i (assuming the triac on-state voltage to be negligible). Assuming for this analysis that L_s remains in saturation (dashed portion in i_t waveform) then if L_{sat} is the saturated inductance, the following expression can be derived:

$$(L_{leak} + L_{sat}) \cdot di/dt = -\hat{V} \omega t \quad (2)$$

where di/dt is the rate of change of triac current.

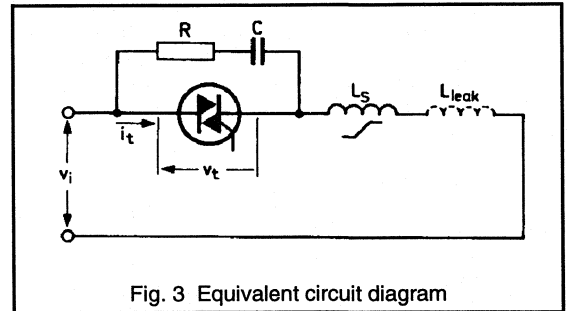


Fig. 3 Equivalent circuit diagram

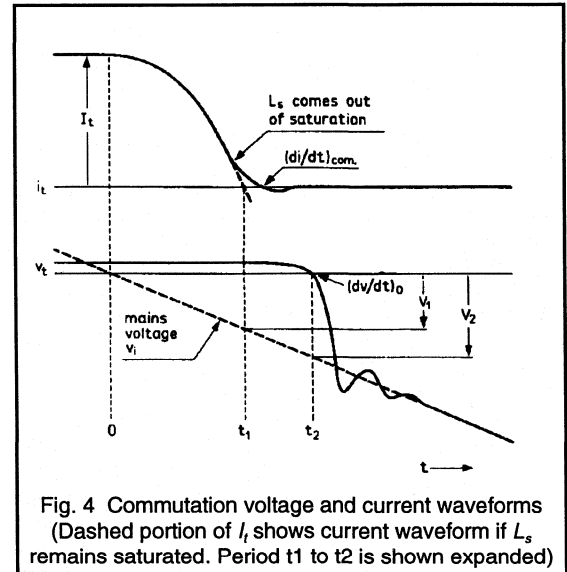


Fig. 4 Commutation voltage and current waveforms (Dashed portion of i_t shows current waveform if L_s remains saturated. Period t_1 to t_2 is shown expanded)

Integrating equation (2) gives:

$$i_t = I_t - \frac{\hat{V} \omega t^2}{2(L_{leak} + L_{sat})} \quad (3)$$

where I_t is the current prior to commutation.

At time t_1 , current i_1 passes through zero, so, from (3):

$$t_1 = \sqrt{\frac{2I_1(L_{leak} + L_{sat})}{\hat{V}\omega}} \quad (4)$$

At t_1 , the mains voltage has attained the value V_1 which is found by combining equations (1) and (4) to give:

$$V_1 = -\sqrt{2\omega\hat{V}I_1(L_{leak} + L_{sat})} \quad (5)$$

Choke L_s comes out of saturation at low current levels so the triac turn-off point is delayed to time t_2 . Since in a practical circuit the delay is only of the order of 50 μ s, the mains voltage V_2 at the instant of turn-off is very nearly equal to V_1 . Thus from equation 5:

$$V_2 \approx -\sqrt{2\omega\hat{V}I_1(L_{leak} + L_{sat})} \quad (6)$$

The triac conducts until time t_2 . Denoting the value of unsaturated inductance as L_{unsat} , the current decay rate at zero current is given by:

$$\begin{aligned} \frac{di_c}{dt} &= \frac{V_2}{(L_{leak} + L_{unsat})} \\ &= -\frac{\sqrt{2\omega\hat{V}I_1(L_{leak} + L_{sat})}}{L_{leak} + L_{unsat}} \end{aligned} \quad (7)$$

The initial rate of rise of off-state voltage, dv_{com}/dt , can now be derived. This parameter is decisive for the behaviour of the triac, since a much greater dv/dt can be sustained after carrier recombination, that is, when the off-state voltage has reached a substantial value.

At time t_2 the triac turns off but the voltage across it is still zero. The voltage drop across L_s and L_{leak} is equal to V_2 and the rate of rise of current carried by these inductances, di_L/dt , is given in equation (7). The rate of rise of triac voltage dv/dt is determined by di_L/dt and the values of the snubber components R and C.

$$\frac{dv}{dt} = R \cdot \frac{di_L}{dt} + \frac{i}{C} \quad (8)$$

When the interval t_1 to t_2 is long enough, the triac has fully recovered at time t_2 , and so the current i to be taken over by the parallel RC snubber network is zero. At time t_2 , dv/dt is equal to the initial rate of rise of voltage dv_0/dt . From equations (7) and (8):

$$\frac{dv_0}{dt} = \frac{R}{L_{leak} + L_{unsat}} \sqrt{2\omega\hat{V}I_1(L_{leak} + L_{sat})} \quad (9)$$

In circuits where no transformer is interposed between the triac and rectifier, some series inductance is still needed to restrict turn-on di/dt . In that case Equations (7) and (9) are still valid by omitting L_{leak} .

Example - DC motor load

The motor control circuit of Fig. 5 illustrates the use of the design method proposed in the previous section. Since the motor has a fairly high inductance it may be considered as a constant current source, giving a severe test condition for triac commutation.

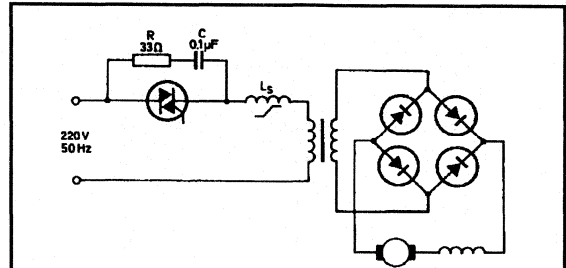


Fig. 5 DC Motor test circuit.

Choke	$L_{unsat}=2.25\text{mH}$, 30 turns on 36x23x10mm ³ toroid core
Transformer	220V/150V, 6kVA, 0.9mH leakage inductance
Motor	Series wound DC motor, Leakage inductance = 30mH

With $L_{leak} = 0.9\text{mH}$, $L_{unsat} = 2.25\text{mH}$ and $L_{sat} \ll L_{leak}$ the circuit conditions can be calculated for a triac current of $I_1 = 20\text{A}$ and a 220V, 50Hz supply. Using equations (7) and (9) gives $di_L/dt = -18.3\text{A/ms}$ and $dv_0/dt = 0.6\text{V}/\mu\text{s}$. These values can be compared with the commutation limits of the device to ensure that reliable commutation can be expected.

The inductance in the ac circuit also restricts turn-on di/dt which, for a continuous dc load current is:

$$\frac{di_{on}}{dt} \approx \frac{v_i}{t_{on}R} + \frac{v_i}{L_{leak} + L_{unsat}} \quad (10)$$

where v_i is the instantaneous ac input voltage, t_{on} is the turn-on time of the triac and R is the snubber resistance. Maximum turn-on di/dt occurs at the peak value of input voltage, v_i . The initial rise of on-state current depends on the snubber discharge current through R as well as the limiting effect of the circuit inductance.

The oscillograms of Figs. 6 to 10 illustrate circuit performance. With no choke added a large dv/dt was observed (Figs. 6 and 7) and so consequently commutation failed when motor current was increased to around 9A. As seen from Figs. 8 to 10 the choke softens commutation so that dependable control results even at 23A motor current. At this current (Fig. 10) the quiescent interval is about $30\mu s$, which is adequate time for the triac to recover.

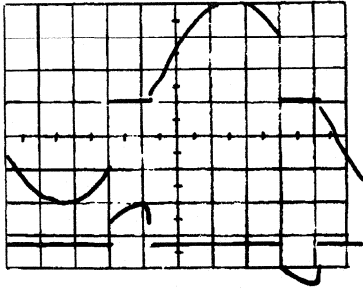


Fig. 6 Triac voltage and current. No series choke.
7A motor current. Timebase: 2ms/div
Upper trace: Triac voltage, v_t (100V/div)
Lower trace: Triac current, i_t (5A/div)

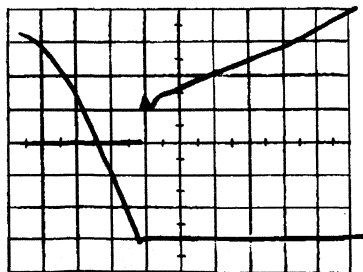


Fig. 7 Triac voltage and current. No series choke.
7A motor current. N.B. Snap-off current
Timebase: $100\mu s$ /div
Upper trace: Triac voltage, v_t (20V/div)
Lower trace: Triac current, i_t (1A/div)

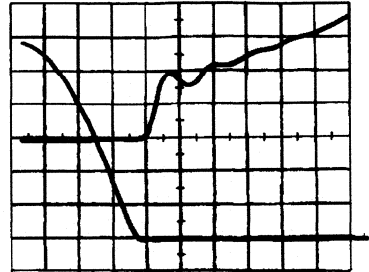


Fig. 8 Triac voltage and current. Series choke added.
7A motor current. Timebase: $100\mu s$ /div
Upper trace: Triac voltage, v_t (20V/div)
Lower trace: Triac current, i_t (1A/div)

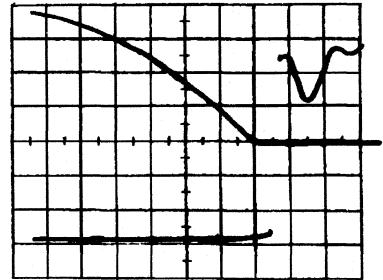


Fig. 9 Triac voltage and current. Series choke added.
23A motor current. Timebase: $100\mu s$ /div
Upper trace: Triac voltage, v_t (10V/div)
Lower trace: Triac current, i_t (5A/div)

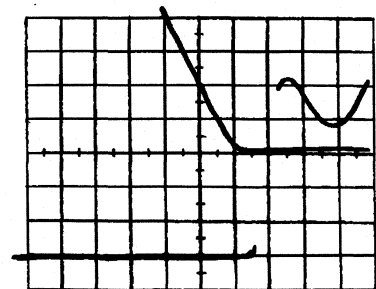


Fig. 10 Triac voltage and current. Series choke added
23A motor current. N.B. slight reverse recovery current
Timebase: $50\mu s$ /div
Upper trace: Triac voltage, v_t (10V/div)
Lower trace: Triac current, i_t (1A/div)

6.2.2 Domestic Power Control with Triacs and Thyristors

The increasing demand for more sophisticated domestic products can, in part, be met by providing the user with some form of electronic power control. This control can be used, for example, to adjust the suction of a vacuum cleaner, the brightness of room lighting or the speed of food mixers and electric drills.

It might be assumed that the cost of the electronics would be high, but this is not necessarily the case. With triacs and thyristors it is possible to produce high performance mains controllers which use only a few simple components. The following notes give details of some typical control circuits and highlight areas for special attention when adapting the designs for specific applications.

Vacuum cleaner suction control

The competitive nature of the vacuum cleaner market has led to the development of a wide variety of machine types and accessories. In many cases, the speed of the motor remains constant and, if suction control is attempted, it consists merely of an adjustable vent in the air flow path. Electronic suction control sounds somewhat expensive and unnecessarily complicated for such an elementary application. In fact, by using a BT138 triac, a simple but nevertheless effective and reliable suction control circuit (Fig. 1) can be constructed very economically, and is suitable for all types of cleaner with a power consumption of up to 900W.

The heart of the circuit is the BT138. This is a glass passivated triac which can withstand high voltage bidirectional transients and has a very high thermal cycling performance. Furthermore its very low thermal impedance minimizes heatsink requirements.

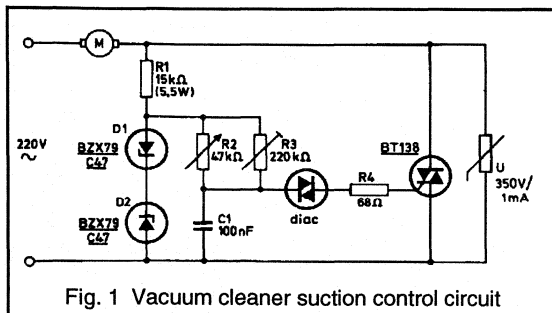


Fig. 1 Vacuum cleaner suction control circuit

Circuit Description

In Fig. 1 the BT138 is the power control element. Its action is controlled by a diac which is switched on by a charge on C_1 , under the control of potentiometer R_2 . The resistance of the diac is virtually infinite as long as the voltage across it

remains within the breakover voltage limits, $-V_{BO}$ to $+V_{BO}$. During each half cycle of the mains sinewave, C_1 charges until the voltage across it exceeds the diac breakover voltage. The diac then switches on and C_1 discharges itself into the gate of the triac and switches it on. Diodes D_1 and D_2 stabilise the supply voltage to the charging circuit so that its operation is independent of mains voltage fluctuations. If $-V_{BO}$ and $+V_{BO}$ are equal and opposite, the triac will be triggered at the same time after the start of either a positive or negative half cycle. The conduction angle, and therefore the speed of the motor and the cleaner suction, is determined by the adjustment of R_2 . Preset potentiometer R_3 is used to set the minimum suction level. The width and amplitude of the trigger pulses are kept constant by gate resistor R_4 . The zinc oxide voltage dependent resistor (U) minimises the possibility of damage to the triac due to very high voltage transients that may be superimposed on the mains supply voltage. Figure 2 shows the current and voltage waveforms for the triac when the conduction angle is 30° .

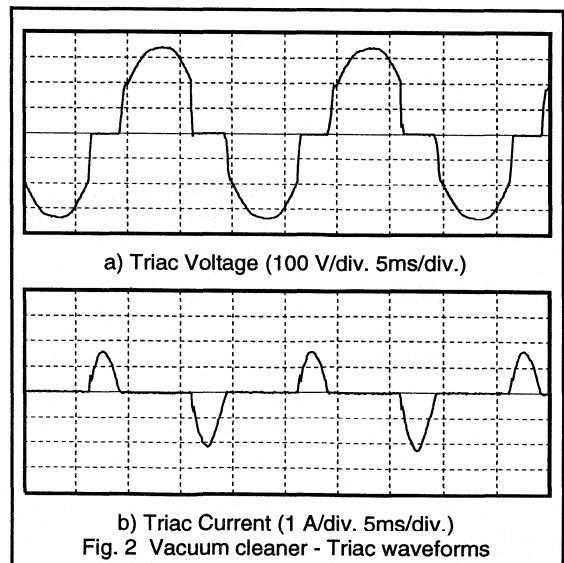


Fig. 2 Vacuum cleaner - Triac waveforms

Circuit Performance

A laboratory model of the circuit has been tested to determine the range of control that it has over the suction power of a typical vacuum cleaner. For the test, the cleaner was loaded with a water column. The result of the test is shown graphically in Fig. 3. The measured range of water column height (100 to 1100 mm) translates into a wide air flow range - from little more than a whisper to full suction.

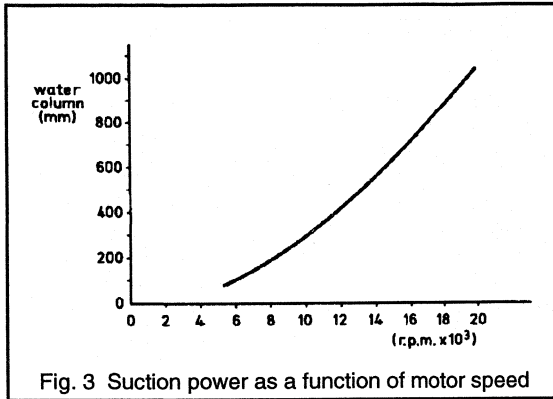


Fig. 3 Suction power as a function of motor speed

As suction power is a function of the speed of the vacuum cleaner motor, a second test was carried out to determine the range of motor speed control under conditions of minimum and maximum air flow (i.e. with the suction blocked and unrestricted). This test also checked the motor speed variation due to $\pm 10\%$ variation of a nominal 220 V AC mains supply. The initial test conditions were: unrestricted flow; mains supply 198 V (220 V - 10%); R_2 at maximum resistance, and R_3 set so that the motor just ran. Table 1 shows the results of the test. N_{min} is the speed at which the motor just runs and N_{max} is the speed of the motor with R_2 set at minimum resistance.

mains voltage (V)	blocked air flow		unrestricted air flow	
	N_{min} (rpm)	N_{max} (rpm)	N_{min} (rpm)	N_{max} (rpm)
198	5300	17100	4300	15400
220	6250	19000	5000	17100
242	7400	20000	6000	18200

Table 1. Motor speed figures for circuit of Fig. 1

The table shows that the speed setting range is wide. The ratio of N_{max} to N_{min} is 3.42:1, for 220 V mains and unrestricted airflow. The variation of motor speed due to variation of the mains input is quite small and represents a negligible change of suction. If D_1 and D_2 are omitted from the circuit, the speed setting ratio is reduced to 1.82:1 under the same conditions. The table also shows that the difference between the N_{min} for minimum and maximum air flow is quite small. This implies that speed stabilisation is unnecessary.

Special Design Considerations

The circuit shown in Fig. 1 has been shown to work well in a typical vacuum cleaner application. But motors and environments do vary, so some aspects of the design should be looked at carefully before it is finalised.

Circuit positioning

The siting of the circuit, within the case of the cleaner, is particularly important. In some areas within the cleaner the temperature can be quite high. The circuit, and in particular the triac and its heatsink, should not be placed in one of these areas if the designer is to avoid problems keeping the temperature of the triac below T_{jmax} .

Starting current

Another factor that may lead to thermal problems is that of inrush current. The starting current of a vacuum cleaner motor is typically as shown in Fig. 4. The rms current during the first 20 ms could be 20 A or more. The current decays to its steady state value in about 1 s. To ensure that the triac does not overheat, reference should be made to the inrush current curves in the triac data sheet, the curve for the BT138 is reproduced in Fig. 5.

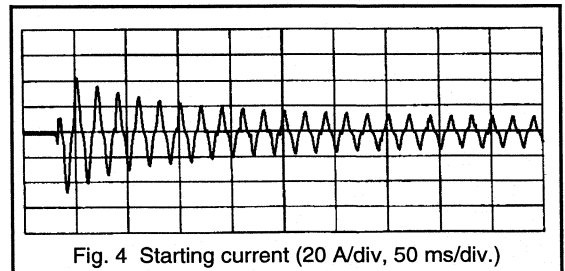


Fig. 4 Starting current (20 A/div, 50 ms/div.)

cycle number.	time (ms)	peak current (A)	rms current (A)	'limit' current (A)
1	20	49	22	24
2	40	41	18	21
3	60	35	13	19.5
4	80	32	14	18.5
5	100	29	13	18
10	200	20	9	15.5
20	400	14	6.3	14

Table 2. Currents during starting

The first step in checking for a problem is to estimate the mounting base temperature, T_{mb} , prior to starting. A reasonable figure would be the worst case steady state value of T_{mb} during normal running.

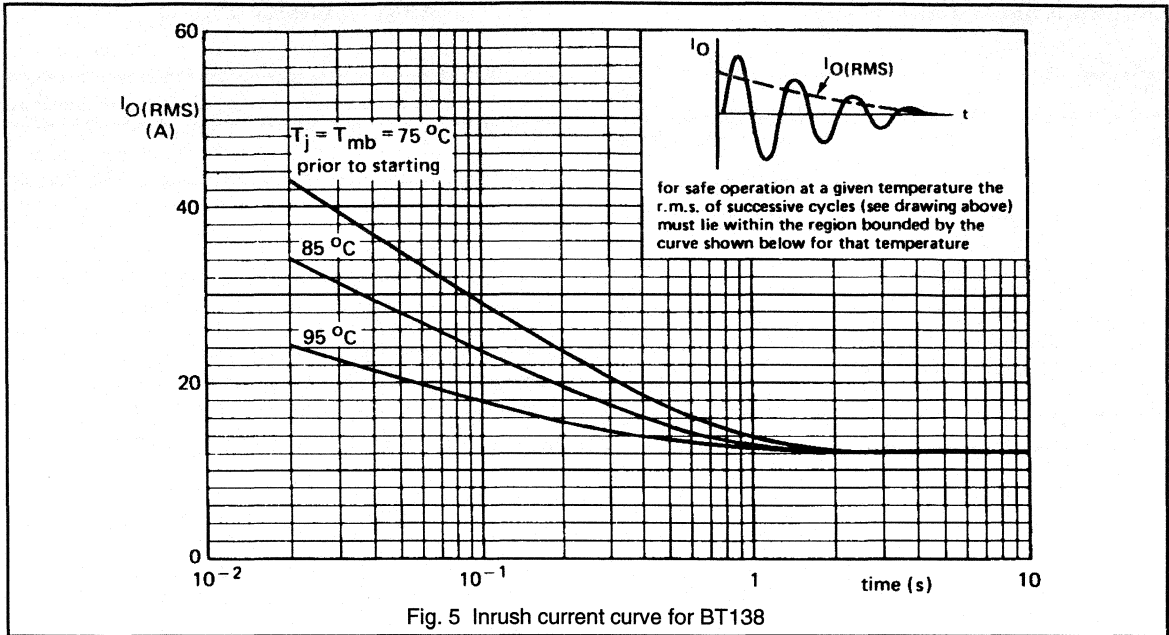


Fig. 5 Inrush current curve for BT138

Step 2 is to calculate the rms value of one cycle of the starting current at several times during start up and step 3 is to compare these figures with the values taken from the appropriate line of the inrush current curve.

As an example consider the performance of the BT138 driving a motor whose starting current is shown in Fig. 4. Direct measurement indicated that during normal running the T_{mb} of a BT138 mounted on a particular heatsink, would be no more than 22°C above ambient. From other measurements it was estimated that the ambient temperature would not exceed 73°C . These figures give a worst case steady state T_{mb} of 95°C . It can be assumed that this is the highest temperature that the mounting base could be, prior to starting - a reasonable assumption which covers the case where the motor has been running for a long time, is turned off and then started again before there has been any cooling.

The rms values of cycles 1 to 5, 10 and 20 of the starting current are given in Table 2. Since the current is not an ideal sine wave these have been calculated from the peak current by assuming a crest factor (peak to rms) of 2.23. Also shown are the relevant $I_{O(RMS)}$ figures from the 95°C line of Fig. 5. Since 'actual' inrush current is always less than the 'allowed' current it is safe to use the BT138 under the proposed conditions to control the motor. It should be noted that because the crest factor is $>\sqrt{2}$ the dissipation of the BT138 will be less than assumed by the inrush current curves of Fig. 5.

Commutation

The circuit shown in Fig. 1 has no RC snubber. This was because the values of di/dt and dV/dt generated by the circuit were well within the capability of the BT138. This will often be the case with vacuum cleaner motors for two reasons:

- these motors introduce only a small phase shift in the current, so the voltage step is small and the dV/dt is low,
- the steady state value of the current is much less than the maximum rating of the BT138, this amounts to a di/dt well within the capability of the BT138.

However care must be taken to ensure that this is true in all applications. In particular, care should be taken to ensure that the triac switches correctly even during starting. If a snubber is found to be necessary then a $100\ \Omega$ $0.5\ \text{W}$ resistor in series with a $0.1\ \mu\text{F}$ capacitor will be more than adequate in most circumstances.

Interference

It is, of course, necessary to check that the overall equipment complies with local regulations for conducted and radiated interference. However, the measures taken to suppress the electrical 'noise' of the motor combined with the motor itself will often be more than sufficient to overcome the interference generated by the switching of the triac but this must be checked in all applications.

Domestic lamp dimmer

The use of light dimmers, once the prerogative of entertainment centres, has now become widespread in the home. It is necessary to ensure that the component parts of these units are simple and reliable so that they are compatible with the domestic environment.

The glass passivated BT138 triac meets these requirements. Firstly, it has a peak non-repetitive on-state current handling capability of up to 90 A which means it can easily withstand the inrush current that occurs when a cold lamp is switched on. It can also withstand high voltage bidirectional transients and its low thermal impedance minimizes heatsink requirements.

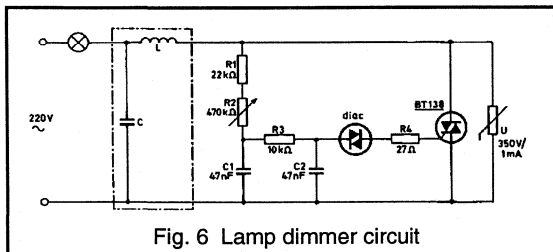


Fig. 6 Lamp dimmer circuit

Circuit Description

A simple circuit of a light dimmer using the BT138 is given in Fig. 6. The BT138 is the power control element, triggered via the diac. The setting of potentiometer R_2 determines the phase difference between the mains sine wave and the voltage across C_2 . This in turn sets the triac triggering angle and the lamp intensity.

The resistance of the diac is very high as long as the voltage across it remains within its breakover voltage limits, $-V_{BO}$ to $+V_{BO}$. Each half cycle of the mains charges C_2 via R_1 , R_2 and R_3 until the voltage being applied to the diac reaches one of its breakover levels. The diac then conducts and C_2 discharges into the gate of the triac, switching it on. If $-V_{BO}$ and $+V_{BO}$ are equal and opposite, the triac will be triggered at the same time after the start of either a positive or negative half cycle. If C_1 were not included in the circuit, the voltage across C_2 would change abruptly after triggering and cause the phase relationship between the mains voltage and voltage across C_2 to progressively alter. This would cause an undesirable hysteresis effect. The voltage across C_1 partially restores the voltage across C_2 after triggering and thereby minimizes the hysteresis effect. The width and amplitude of the trigger pulses are kept constant by gate resistor R_4 . The VDR minimizes the possibility of the triac being damaged by high voltage transients that may be superimposed on the mains supply voltage.

Special Design Considerations

Circuit rating

The BT138 has an rms current rating of 12 A. It is, therefore, capable of controlling loads with a rating of 2 kW or more. However, the load of this circuit must be restricted to a much lower level. There are two reasons for this. The first is to keep mains distortion within the allowed limits, without the necessity of expensive filter networks. The second reason is to limit dissipation. If, as is likely, the circuit is to be mounted in the wall in place of a conventional switch, then air circulation is going to be very restricted and the ambient temperature around the circuit will be quite high. It is important for reliability reasons to ensure that the temperature of the BT138 never exceeds T_{jmax} , so the dissipation of the triac must be kept to a low level.

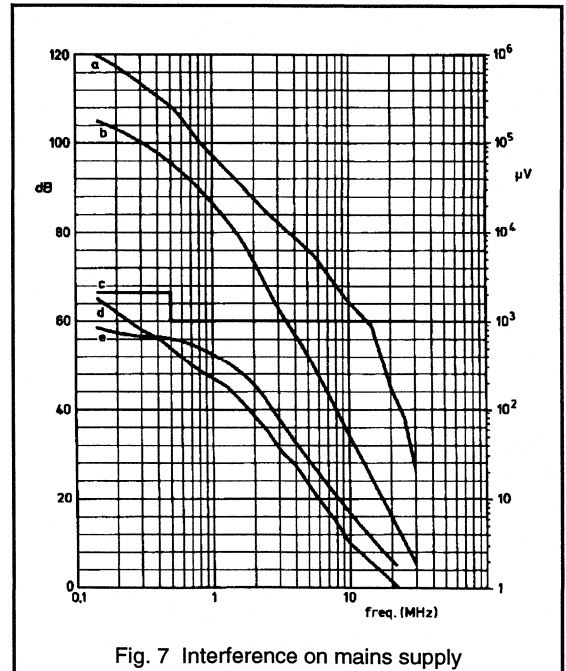


Fig. 7 Interference on mains supply

Interference

Regulations concerning conducted and radiated interference vary considerably from country to country but it is likely that some form of filter will be needed. The simple LC filter shown within the dashed-lined box in Fig. 6 is often all that is needed. The values of the filter components will vary, but a combination of 0.15 μ F capacitor and a low Q inductor of 2.5 μ H was found to be sufficient for the circuit to meet the C.I.S.P.R. limits. This is illustrated by the plots shown in Fig. 7. Curves (a) and (b) show the level of noise on the mains supply for the circuit, without filter, when

controlling 550 W and 25 W loads respectively. Curves (d) and (e) are for the circuit with filter connected showing that the C.I.S.P.R. limit, which is curve (c), has been met.

Filter inductor

Having selected the value of filter inductor, the designer has then to decide how to make it. Construction will not be too critical - it is not necessary to achieve a high Q - and there will be considerable room for reducing its size. However, care must be taken to ensure that the inductor does not saturate when the inrush current of a cold lamp flows through it. If the inductor does saturate then the filter capacitor will, effectively, be shorted out by the triac. In this case the triac current could rise faster than the di/dt rating allows. This could cause progressive damage to the triac resulting in premature failure.

Speed control for food mixers and electric drills

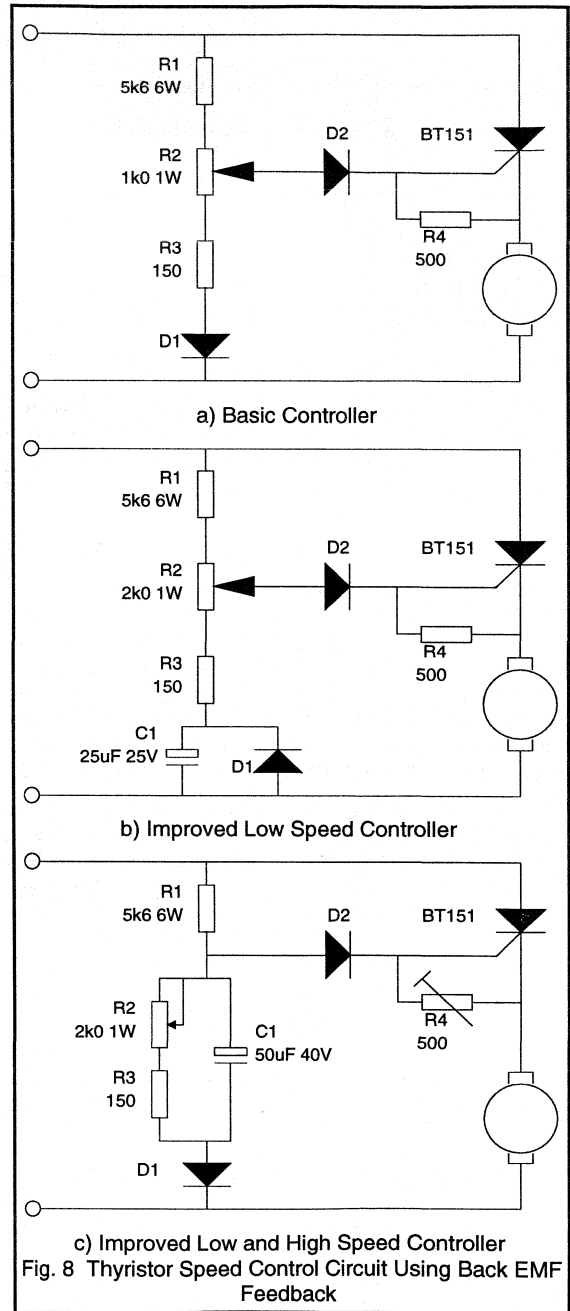
Food mixers and electric hand drills are products whose useability is improved by the addition of electronic speed control. But they are products where costs have to be tightly controlled so the choice of circuit is very important. This decision is made harder by the need to have a good speed regulation under the widely varying loads that these products are subjected to.

The circuits to be described provide continuous control of motor speed over a wide speed range by adjusting the conduction angle of a BT151 thyristor. They compensate for load variation by adjusting the firing angle when there is a change in the motor speed - as indicated by a change in its back EMF.

Back EMF Feedback Circuits

A simple motor speed control circuit that employs back EMF to compensate for changes in motor load and mains voltage is shown in Fig. 8(a). The resistor chain R_1, R_2, R_3 and diode D_1 provide a positive going reference potential to the thyristor gate via diode D_2 . Diode D_1 is used to reduce the dissipation in the resistor chain by some 50% and diode D_2 isolates the trigger circuit with the thyristor in the on-state. When the thyristor is not conducting the motor produces a back EMF voltage across the armature proportional to residual flux and motor speed. This appears as a positive potential at the thyristor cathode.

A thyristor fires when its gate potential is greater than cathode potential by some fixed amount. Depending on the waveform shape and amplitude at the gate, the circuit may function in several modes.



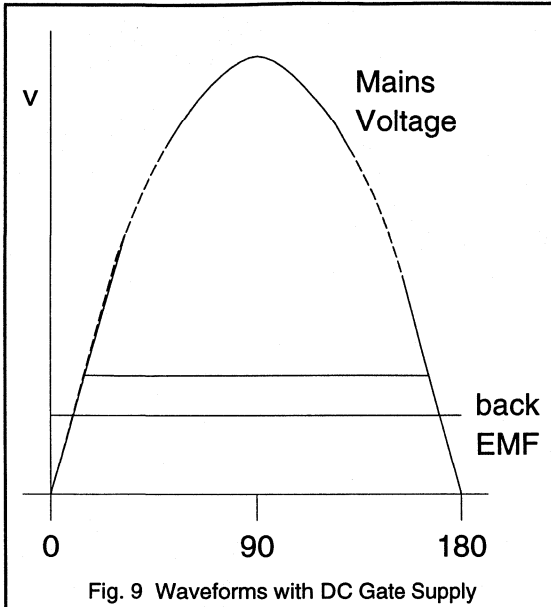


Fig. 9 Waveforms with DC Gate Supply

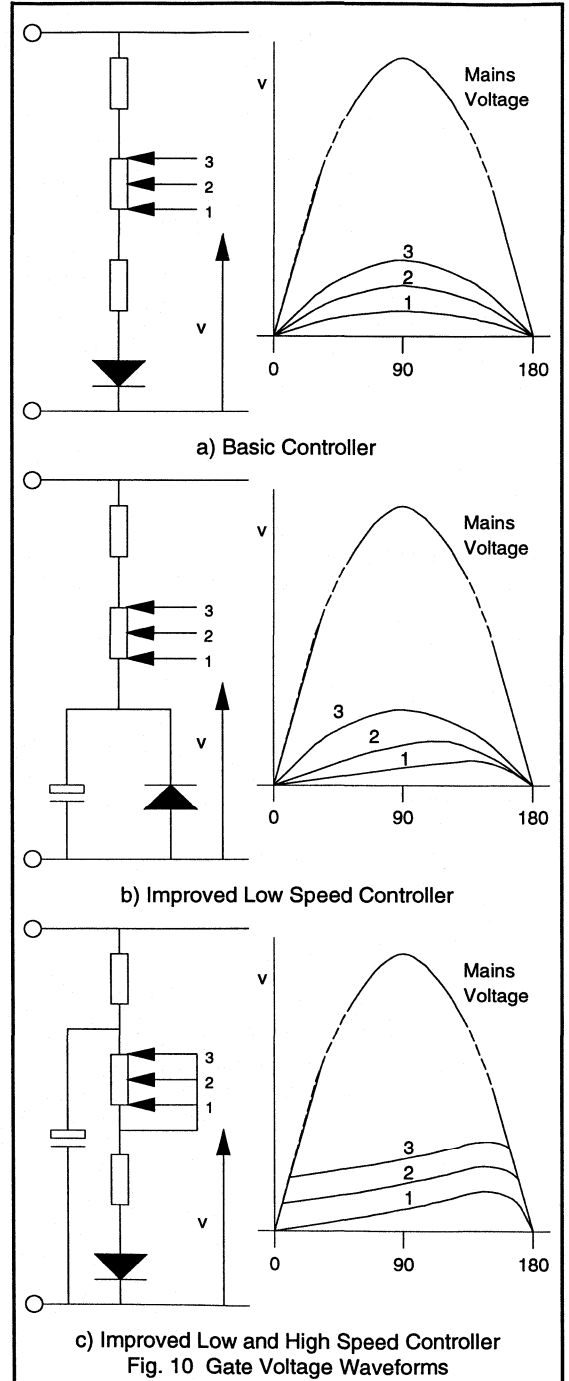
If, for example, during positive half cycles a constant DC potential was applied at the gate (see Fig. 9), the thyristor would continue to fire at the beginning of each cycle until the back EMF was large enough to prevent firing. Thyristor firing would then continue intermittently at the beginning of the positive cycles to maintain some average motor speed.

Referring to Fig. 8(a) the waveform appearing at the thyristor gate will approximate to a half sine wave, Fig. 10(a). As a result it is impossible for the firing angle to be later than 90° - the most positive value of the trigger potential. At lower motor speeds the firing angle might need to be 130° for smooth operation. If the maximum firing angle is limited to 90° then intermittent firing and roughness of motor operation will result.

If, however, the waveform at the gate has a positive slope value to an angle of at least 130° then it will be possible to have a stable firing point at low speeds. Such a waveform can be produced if there is some phase shift in the trigger network.

Stable Firing at Small Conduction Angles

The trigger network of the circuit shown in Fig. 8(b) has been modified by the addition of a capacitor C_1 and diode D_1 . The diode clamps the capacitor potential at zero during the negative going half cycles of the mains input. The waveform developed across the capacitor has a positive slope to some 140° , allowing thyristor triggering to be delayed to this point.



c) Improved Low and High Speed Controller
Fig. 10 Gate Voltage Waveforms

As the slider of R_2 is moved towards R_1 , the peak of the waveform at the gate will move towards 90° as shown in Fig. 10(b). As the speed increases, the no load firing angle will also advance by a similar amount so stability will be maintained. This circuit will give smoother and more stable performance than the circuit of Fig. 8(a). It will, however, give a marginally greater speed drop for a given motor loading at low speed settings. At the maximum speed settings the circuit of Fig. 8(a) approximates to that of Fig. 8(b).

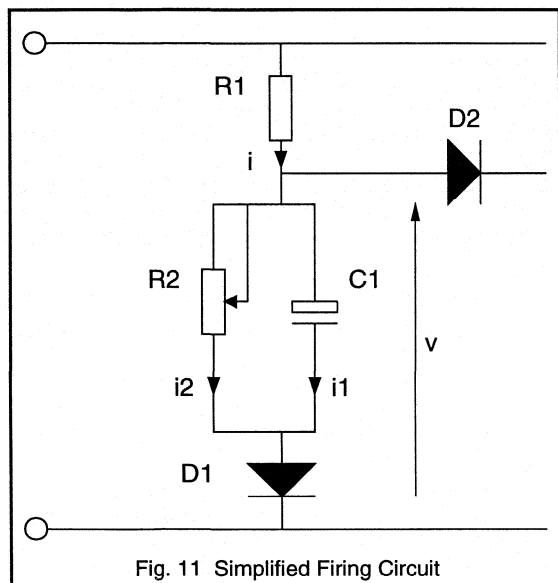


Fig. 11 Simplified Firing Circuit

Improved Motor Performance With Stable Firing

Both the circuits so far discussed have gate voltage waveforms that are of near linear slope from the zero point of each positive half cycle, see Figs. 10(a) and (b). This means that the only time that the thyristor can be fired early in the mains cycle, say at 20° , is when the back EMF and hence motor speed is very low. This effect tends to prevent smooth running at high speeds and high loads.

Stable triggering, at low angles, can be achieved if the gate voltage ramp starts each cycle at a small positive level. This means that the time to reach the minimum trigger voltage is reduced. The circuit of Fig. 8(c) is one way of achieving this. In this circuit capacitor C_1 is charged during positive half cycles via resistor R_1 and diode D_1 . During negative half cycles the only discharge path for capacitor C_1 is via resistors R_2 and R_3 .

Diode D_1 also prevents C_1 from being discharged as the thyristor switches off by the inductively generated pulse from the motor. As the value of resistor R_2 is increased, capacitor C_1 is discharged less during negative half cycles but its charging waveform remains substantially unchanged. Hence the result of varying R_2 is to shift the DC level of the ramp waveform produced across C_1 .

Diode D_2 isolates the triggering circuit when the thyristor is ON. Resistor R_4 adjusts minimum speed, and by effectively bleeding a constant current, in conjunction with the gate current from the triggering circuit, it enables resistor R_2 to give consistent speed settings.

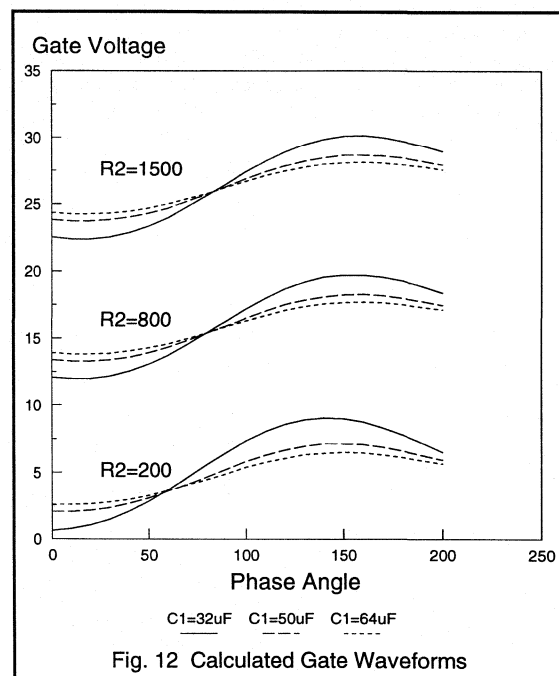


Fig. 12 Calculated Gate Waveforms

Circuit Design

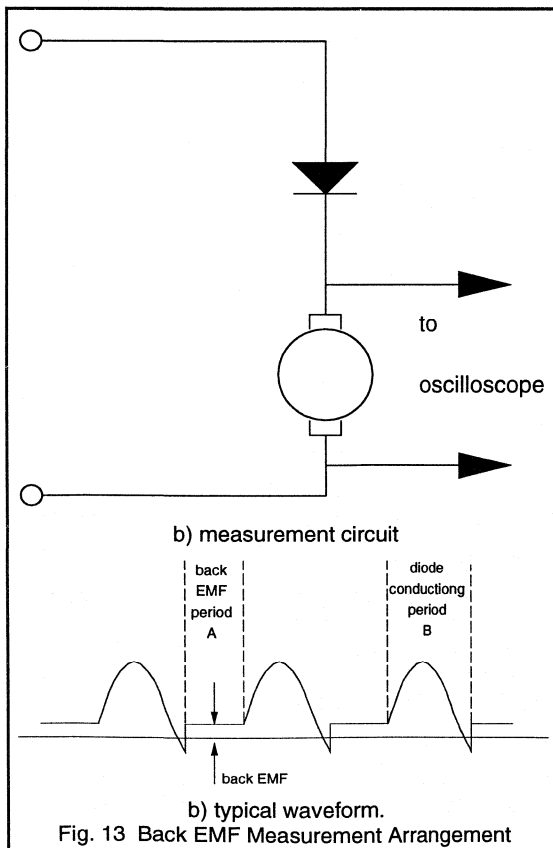
If the speed controller is to be effective it must have stable thyristor firing angles at all speeds and give the best possible speed regulation with variations of motor load. The circuit of Fig. 8(c) gives a motor performance that satisfies both of the above requirements.

There are two factors that are important in the circuit operation in order to obtain the above requirements.

- The value of positive slope of the waveform appearing at the thyristor gate.
- The phase angle at which the positive peak gate voltage is reached during a positive half cycle of mains input.

As previously described the charging of capacitor C_1 by resistor R_1 determines the rate of rise of voltage at the thyristor gate during the positive half cycle. However, resistor R_1 must also have a value such that several times the maximum thyristor gate current passes through the RC network to D_1 . This current will then give consistent speed settings with the spread of thyristor gate currents when the minimum speed is set by resistor R_4 .

The positive slope value of the thyristor gate voltage will have to be fixed according to the motor used. A motor that gives a smooth back EMF voltage will allow a low slope value to be used, giving good torque speed characteristics. Some motors have coarser back EMF waveforms, with voltage undulations and spikes, and a steeper slope of thyristor gate voltage must be used in order to obtain stable motor operation. The value of capacitor C_1 is chosen to provide the required positive slope of the thyristor gate voltage.



Some calculations have been made on the circuit of Fig. 8(c) simplified to the form of Fig. 11, where it is assumed that current flowing to the thyristor gate is small compared with the current flowing through resistor R_1 . An expression has been derived for the voltage that would appear at the anode of D_2 in terms of R_1 , R_2 and C_1 and is given later. Component values have been substituted into the expression to give the thyristor gate waveforms shown in Fig. 12.

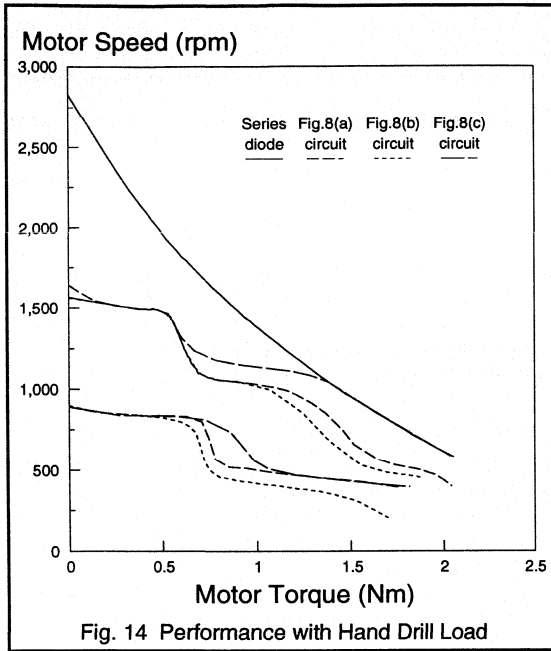
In order to adjust the circuit to suit a given motor, the back EMF of the motor must be known. This may be measured using the arrangement shown in Fig. 13. The voltage appearing across the motor is measured during the period when the series diode is not conducting (period A). The voltage so obtained will be the motor back EMF at its top speed on half wave operation, and corresponds to the back EMF that would be obtained from the unloaded motor at its highest speed when thyristor controlled. In practice, since the mains input is a sine wave, there is little increase in the 'no load' speed when the firing angle is reduced to less than about 70° .

The value of resistor R_2 in Fig. 8(c) determines the motor 'no load' speed setting. The waveforms of Fig. 12 may be used as a guide to obtaining the value of this resistor. It must be chosen so that at 70° and at its highest value, the gate voltage is higher than the measured back EMF by about 2 V - the forward gate/cathode voltage of the thyristor.

The thyristor is turned ON when a trigger waveform, shown in Fig. 12, exceeds the back EMF by the gate/cathode voltage. So, if the back EMF varies within a cycle then there will be a cycle to cycle variation in the firing angle. Normally, random variations of the firing angle by 20° are tolerable. If, for example, there were variations in the back EMF of 1 V, then with a firing angle of 70° and a capacitor of $32 \mu\text{F}$, the variation of firing angle would be about 12° . With capacitor values of $50 \mu\text{F}$ and $64 \mu\text{F}$ the firing angles variations would be 19° and 25° respectively. Therefore, a capacitor value of $50 \mu\text{F}$ would be suitable.

Performance

The torque speed characteristics of the three circuits, when used to drive an electric drill, are compared in Fig. 14. It may be seen that the circuit of Fig. 8(b) has a poorer performance than the two other circuits. That of Fig. 8(c) may be seen to give a similar performance to the circuit of Fig. 8(a) at low speeds but, at high speeds and torques, it is better. It should be noted that the circuits of Figs. 8(b) and (c) provide low speed operation free from the intermittent firing and noise of the Fig. 8(a) circuit. Figure 15 compares the circuits of Fig. 8(a) and 8(c) when the load is a food mixer motor.



the gate voltage waveforms shown in Fig. 12. The analysis assumes that the current drawn by the thyristor gate is negligible in comparison with the current flowing in R_1 .

The charging current i_1 for capacitor C_1 in Fig. 11, is given by:

$$i_1 = \frac{dq}{dt} = C_1 \frac{dv}{dt}$$

and

$$i_2 = \frac{v}{R_2}$$

Representing a mains half sine wave by $f(E)$ where E is the peak mains voltage.

$$i = \frac{f(E) - v}{R_1} = i_1 + i_2$$

therefore,

$$\frac{f(E) - v}{R_1} = C_1 \frac{dv}{dt} + \frac{v}{R_2}$$

where i, i_1, i_2 are instantaneous currents.

Simplifying:-

$$C_1 \frac{dv}{dt} + v \left(\frac{1}{R_1} + \frac{1}{R_2} \right) = \frac{f(E)}{R_1}$$

Fourier analysis of a half sinewave gives:-

$$f(E) = E \left\{ \frac{1}{\pi} + \frac{1}{2} \sin(\theta) - \frac{2}{\pi} \sum_{n=2,4,6,\dots}^{\infty} \frac{\cos(n\theta)}{n^2 - 1} \right\}$$

neglecting terms of the Fourier series with $n > 2$, then

$$C_1 \frac{dv}{dt} + v \left(\frac{1}{R_1} + \frac{1}{R_2} \right) = \frac{E}{R_1} \left\{ \frac{1}{\pi} + \frac{1}{2} \sin(\omega t) - \frac{2}{3\pi} \cos(2\omega t) \right\}$$

then

$$C_1 \frac{dv}{dt} + v \left(\frac{1}{R_1} + \frac{1}{R_2} \right) - \frac{E}{R_1 \pi} = \frac{E}{R_1} \left\{ \frac{1}{2} \sin(\omega t) - \frac{2}{3\pi} \cos(2\omega t) \right\} \quad (1)$$

simplifies to

$$A \frac{dv}{dt} + Bv - D = X \sin(\omega t) - Y \cos(2\omega t) \quad (2)$$

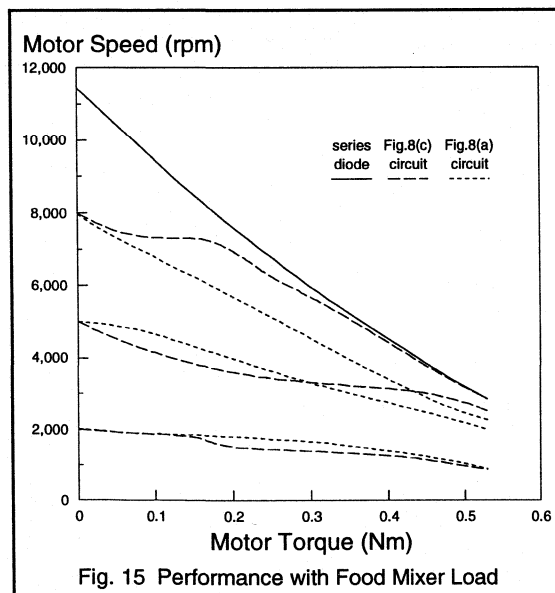
where A, B, D, X, Y are constants.

Put

$$v = a \sin(\omega t) + b \cos(\omega t)$$

$$+ c \sin(2\omega t) + d \cos(2\omega t) + \frac{D}{B} \quad (3)$$

where a, b, c, d are constants.



Circuit Calculations

The following analysis derives an expression for voltage 'v' at the anode of D_2 . This expression can be used to produce

$$\frac{dv}{dt} = a\omega \cos(\omega t) - b\omega \sin(\omega t) + 2c\omega \cos(2\omega t) - 2d\omega \sin(2\omega t) \quad (4)$$

substituting (3) and (4) in equation (2) and equating terms in $\cos(\omega t)$, $\cos(2\omega t)$, $\sin(\omega t)$, $\sin(2\omega t)$, then

$$v = \frac{BX}{A^2\omega^2 + B^2} \cdot \sin(\omega t) - \frac{A\omega X}{A^2\omega^2 + B^2} \cdot \cos(\omega t) - \frac{2A\omega Y}{4A^2\omega^2 + B^2} \cdot \sin(2\omega t) - \frac{BY}{4A^2\omega^2 + B^2} \cdot \cos(2\omega t) + \frac{D}{B}$$

substituting for the constants in equation (2) gives:

$$v = R_2 E \cdot \frac{(R_1 + R_2) \sin(\omega t) - \omega C_1 R_1 R_2 \cos(\omega t)}{2\omega^2 C_1^2 R_1^2 R_2^2 + (R_1 + R_2)^2} + R_2 E \cdot \frac{1}{\pi(R_1 + R_2)} - R_2 E \cdot \frac{4\omega C_1 R_1 R_2 \sin(2\omega t) + 4(R_1 + R_2) \cos(2\omega t)}{3\pi[4\omega^2 C_1^2 R_1^2 R_2^2 + (R_1 + R_2)^2]}$$

This may be simplified since

$$(R_1 + R_2)^2 \ll 2\omega^2 C_1^2 R_1^2 R_2^2$$

So the voltage that the trigger circuit would apply to the gate (assuming the gate draws no current) is given by:

$$v = \frac{R_2 E}{\pi(R_1 + R_2)} + \frac{R_2 E}{2\omega^2 C_1^2 R_1^2 R_2^2} \{ (R_1 + R_2) \sin(\omega t) - \omega C_1 R_1 R_2 \cos(\omega t) - \frac{2}{3\pi} \omega C_1 R_1 R_2 \sin(2\omega t) - \frac{1}{3\pi} (R_1 + R_2) \cos(2\omega t) \}$$

Solving this equation for a different values of C_1 and positions of R_2 gives the curves shown in Fig. 12.

Conclusions

The addition of electronic control can enhance the overall useability of many domestic products. Cost and performance requirements are major factors when determining the type of control circuit to be used in these applications. It is possible, using thyristors and triacs, to construct a range of phase control circuits which can meet many of these cost and operational requirements.

Although these circuits are not complex and use only simple components, it is still important to design with care to ensure that the best performance is achieved. This report has given examples of some of these circuits and has highlighted the areas of their design requiring particular care.

6.2.3 Design of a Time Proportional Temperature Controller

Electronic temperature control is no longer new: phase and on/off controls for heaters have been widely used to replace mechanical switches. However, both phase control and on/off control have disadvantages. Conventional phase control allows fully-proportional control of the power dissipated in the load, but the high rates of change of current and voltage cause RFI and transients on the mains supply. Because of this effect, phase control is not allowed to be used for domestic heaters. Simple on/off control with zero-voltage switching avoids generation of RFI but the amount of hysteresis required to prevent temperature oscillations does not give the required control accuracy.

The principle of time-proportional control

Time proportional control combines the zero-voltage switching of on/off control with the accuracy of proportional control and so eliminates the disadvantages of these two alternative systems. Time-proportional control regulates the load power such that there will be no overshoot or undershoot of the desired temperature as is the case with normal on/off systems. The TDA1023 has been designed to provide time-proportional control for room heaters and electric heating elements using a minimum number of external components. It incorporates additional features to provide fail-safe operation and fine control of the temperature.

There are three states of operation when using time-proportional control:

- load switched fully off,
- load power proportional to the difference between actual and desired temperatures,
- load switched fully on.

Figure 1 illustrates the principle; the load is switched on once and off once in a fixed repetition period, the ratio of the on and off periods providing the proportional control. This method of control can cause mains flicker; the mains voltage changes slightly each time the load is switched on or off.

CENELEC, the European Committee for Electro-technical Standardisation, has published rules which limit the rate at which domestic heating apparatus may be switched on and off. Table 1 gives the minimum repetition period for a range of load powers and common mains voltages from CENELEC publication EN50.006.

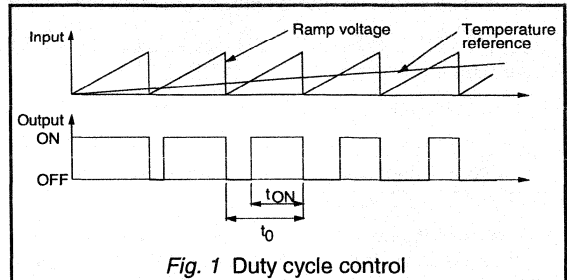


Fig. 1 Duty cycle control

Appliance Power (W)	Repetition period, t_0 (s)		
	220V	240V	380V
600	0.2	0.2	
800	0.8	0.3	0.1
1000	2.0	1.0	0.2
1200	4.6	2.0	0.2
1400	7.0	4.3	0.2
1600	10.0	6.3	0.3
1800	16.0	8.9	0.5
2000	24.0	13.0	0.9
2200	32.0	17.0	1.3
2400	40.0	24.0	1.9
2600		31.0	2.6
2800			3.6

Table 1. CENELEC minimum repetition periods for Domestic Heater Applications

Description of the TDA1023

The TDA1023 is a 16-pin dual in-line integrated circuit designed to provide time-proportional power control of electrical heating elements. The TDA1023 is ideally suited for the control of:

- Panel heaters
- Cooker elements
- Electric irons
- Water heaters
- Industrial applications, e.g. temperature controlled oil baths, air conditioners.

The TDA1023 Incorporates the following functions:

- A stabilised power supply. The TDA1023 may be connected directly to the AC mains using either a dropping resistor or capacitor. It provides a stabilised reference voltage for the temperature-sensing network.

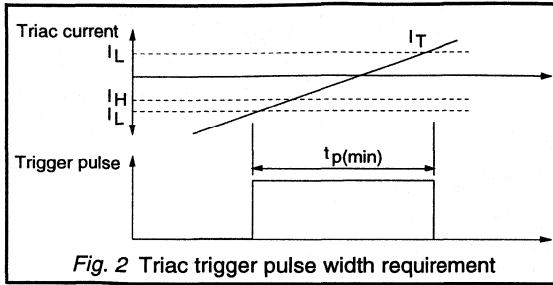


Fig. 2 Triac trigger pulse width requirement

- A zero-crossing detector to synchronise the output trigger pulses to the zero-crossings of the mains supply. The detector produces a pulse, the duration of which is determined by an external resistor, centred on the zero-crossing of the mains voltage.
- A comparator with adjustable hysteresis, preventing spurious triggering of the output. This compares a thermistor voltage, a function of the room temperature, with the voltage from the temperature selection dial.
- A voltage translation circuit for the potentiometer input. Normally, the relatively small temperature variation in a room (5°C to 30°C) corresponds to a narrow angle of rotation of a potentiometer shaft. Use of this circuit doubles the angle of rotation of the potentiometer shaft for the same temperature range.
- A sensor fail-safe circuit to prevent triggering if the thermistor input becomes open or short-circuited.

- A timing generator with an adjustable proportional band. This allows a full 100% control of the load current over a temperature range of only 1°C or 5°C. The repetition period of the timing generator may be set by an external capacitor to conform to the CENELEC specifications for mains load switching.
- An output amplifier with a current-limited output. The amplifier has an output current capability of at least 200mA and is stabilised to 10V while the current limit is not exceeded.
- Input buffers, to isolate the voltage translation circuit and comparator from external influences.
- A control gate circuit to activate the output if there is a mains zero-crossing, the comparator is ON and the fail-safe comparator is OFF.

Although designed specifically for time proportional control, the TDA1023 is also suitable for applications requiring on/off control if the timing generator is not used.

Required Duration of Triac Trigger Pulse

The main advantage of triggering at the instant when the applied voltage passes through zero is that this mode of operation renders the use of RF suppression components unnecessary. For time-proportional control, continuous conduction of the triac may be required for many cycles of the mains supply. To maintain conduction while the load current is approaching the zero-crossing, the trigger pulse must last from the time when the load current falls to the value of the triac holding current (I_H), until the time when the load current reaches the triac latching current (I_L).

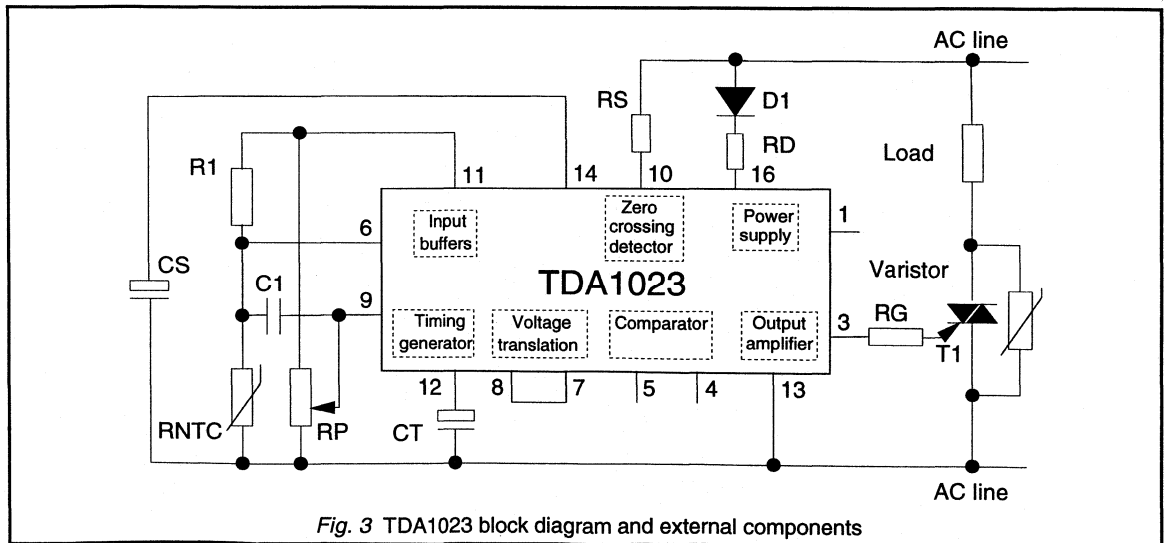


Fig. 3 TDA1023 block diagram and external components

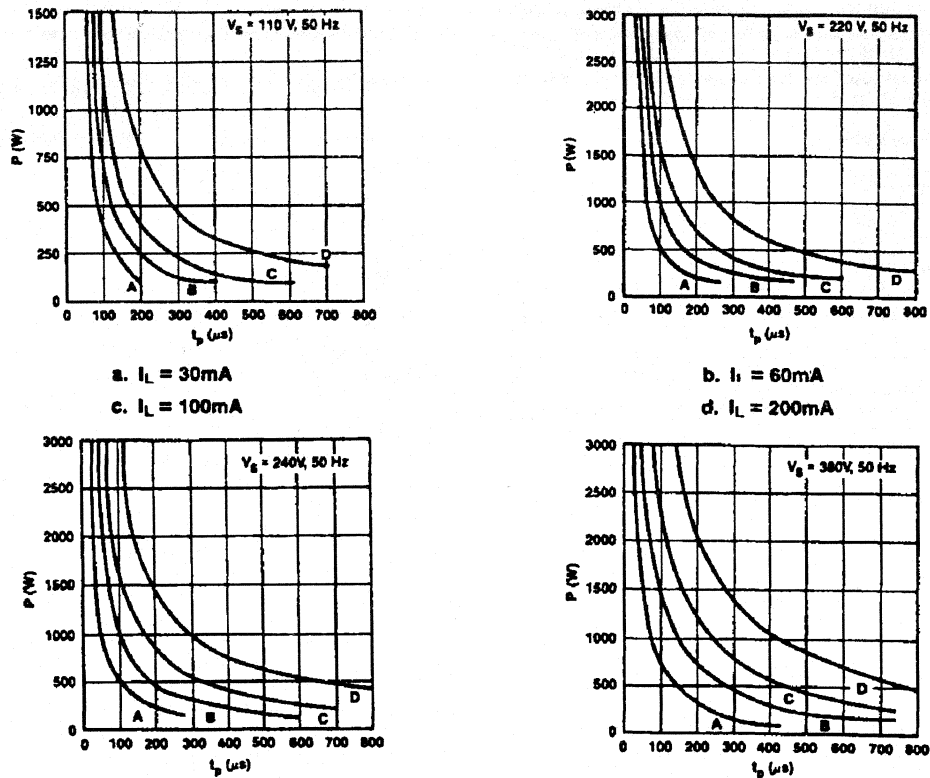


Fig. 4 Minimum pulse width as a function of supply voltage and latching current

In general, the latching current of a triac is higher than the holding current, so the minimum trigger pulse duration may be taken as twice the time for the load current in the triac (I_L) to rise from zero to the triac's latching current. See Fig. 2. The current passed by the triac is a function of its on-state voltage, the load resistance, and the applied voltage. The trigger pulse width is therefore a function of:

- triac latching current (I_L)
- applied AC voltage ($v = V_s \sin \omega t$)
- load resistance (R)
- on-state voltage of the triac (V_T) at I_L .

The load resistance is related to the nominal load power, P and nominal supply voltage, V_s by $R = V_s^2 / P$. Assuming that the load resistance has a tolerance of 5% and the AC voltage variation is 10%, the minimum required width of the

trigger pulse in the worst case can be calculated. The graphs of Fig. 4 show $t_{p(\text{MIN})}$ as a function of P for four common mains voltages with values of 30mA, 60mA, 100mA, and 200mA for the triac latching current I_L and a maximum on-state voltage of $V_T = 1.2V$ at I_L .

Selection of external components

The external components required by the TDA1023 determine the operation of the device. The following paragraphs describe the selection of these components to ensure reliable operation under worst-case conditions.

Synchronisation Resistor, R_s

A current comparator is used as a zero-crossing detector to provide trigger pulse synchronisation. It compares the current through the synchronisation resistor (R_s) with a reference current. As the supply voltage passes through

zero, the current in the synchronisation resistor becomes less than the reference current and a trigger pulse is given until the current in R_s increases above the reference level.

Thus, the duration of the trigger pulse depends upon the rate of change of current in R_s at the supply voltage zero-crossing point. This rate of change is affected by:

- the AC supply voltage
- the supply frequency
- the value of the synchronisation resistor.

Fig. 5 shows the value of R_s as a function of trigger pulse width, with the AC supply voltage as a parameter.

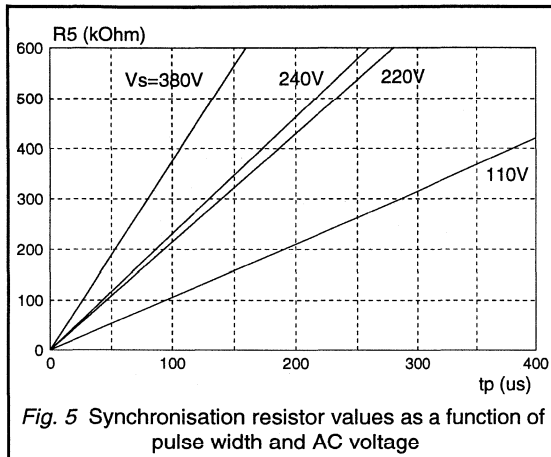


Fig. 5 Synchronisation resistor values as a function of pulse width and AC voltage

Gate Resistor R_g

The guaranteed minimum amplitude of the output trigger pulse of the TDA1023 is specified as 10V at an output current less than 200mA. The output stage is protected against damage due to short-circuits by current-limiting action when the current rises above 200mA.

Although the output is current-limited, it is still advantageous to include a gate series resistor in the circuit. Inclusion of a gate resistor to limit the gate current to the minimum value required reduces the overall current consumption and the power dissipation in the mains dropping resistor. Furthermore, the point at which current limiting occurs is subject to considerable variation between samples of the TDA1023: a gate resistor will reduce the effect of this in production circuits.

The rectangular output V/I characteristic of the TDA1023 is shown in Fig. 6. Load lines for various values of gate resistor have been plotted on this diagram so that the maximum value of gate resistor can be selected by plotting horizontal and vertical lines to represent the required minimum gate current and voltage. The following example illustrates the use of Fig. 6.

The triac to be triggered is a Philips BT139. At 0°C the trigger pulse requirements for a standard BT139 are:

$$I_{GT} = 98 \text{ mA}$$

$$V_{GT} = 1.6 \text{ V}$$

These figures are for triggering with a positive gate pulse when MT_2 is negative with respect to MT_1 . The lines representing $V_{GT} = 1.6V$ and $I_{GT} = 98 \text{ mA}$ cross the load line for a gate resistor value of 82 Ω . The maximum value of gate resistor is therefore 82 Ω .

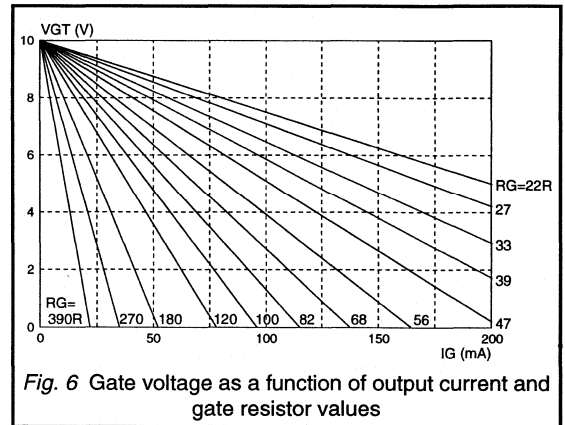


Fig. 6 Gate voltage as a function of output current and gate resistor values

Gate Termination Resistor R_{pd}

The TDA1023 has a resistor approximately 1.5k Ω between Pin 1 and Pin 13. This is intended for use as a pull-down resistor when sensitive triacs are being used.

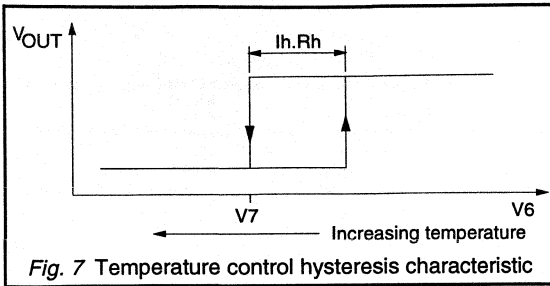
The Proportional Band Resistor R_s

The proportional band is the input voltage range that provides control of 0% to 100% of the load power. The TDA1023 has a built-in proportional band of $V_{pb} = 80mV$ (corresponding to about 1°C) which can be increased by the addition of resistor R_s between Pin 5 and ground. The maximum proportional band of 400mV is obtained by shorting Pin 5 to ground.

Hysteresis Resistor R_4

The comparator of the TDA1023 is designed with built-in hysteresis to eliminate instability and oscillation of the output which would cause spurious triggering of the triac. Apart from providing a stable two-state output, the hysteresis gives the comparator increased noise immunity and prevents half-waving.

Figure 7 shows the application of hysteresis to the comparator and the transfer characteristic obtained. The built-in hysteresis is 20mV; this may be increased by adding a resistor (R_4) from Pin 4 to ground which increases the current I_H . Pin 4 shorted to ground gives a maximum of 320mV. Table 2 gives the value of R_4 for a range of hysteresis settings.



When the proportional band (V_{pb}) is increased, it may be necessary to increase the hysteresis voltage (V_h). Table 2 also shows a range of proportional band settings, the values of R_5 required for these, the corresponding minimum hysteresis voltage and the maximum value of hysteresis resistor R_4 .

Proportional Band (mV)	R_5 (k Ω)	R_4 (k Ω)	Hysteresis band (mV)
80	-	-	20
160	3.3	9.1	40
240	1.1	4.3	60
320	0.43	2.7	80
400	0.0	1.8	100

Table 2. Choice of components R_4 and R_5

Voltage (V)	AC rating (μ F)	DC value (μ F)	Catalogue Number
25	47	68	2222 016 90129
40	33	47	2222 016 90131
25	22	33	2222 015 90102
40	15	22	2222 015 90101
25	10	15	2222 015 90099
40	6.8	10	2222 015 90098

Table 3. Preferred capacitors for use with TDA1023

Power (W)	CENELEC t_0 (s)	C_T (DC) (μ F)	$t_{0(nom)}$ (s)	$t_{0(min)}$ (s)	$t_{0(max)}$ (s)
2000	24.0	68	41	22	65
1800	16.0	47	28	15	45
1600	10.0	33	20	11	32
1400	7.0	22	13	7	21
1200	4.6	15	9	4.8	14
1000	2.0	10	6	3.2	9.6
800	0.8	10	6	3.2	9.6
600	0.3	10	6	3.2	9.6

Table 4. Timing capacitor values for 220V operation

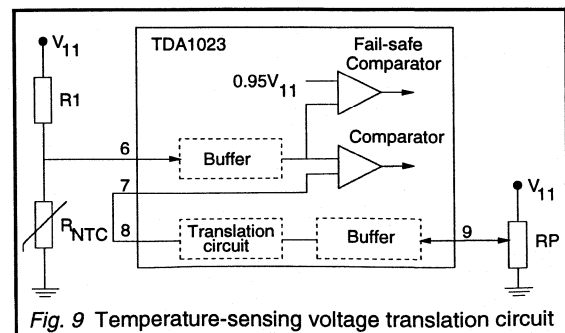
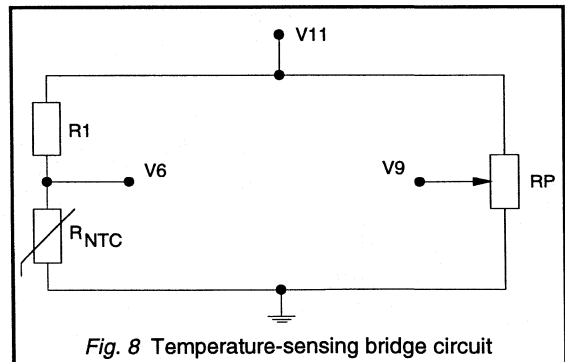
Smoothing Capacitor, C_s

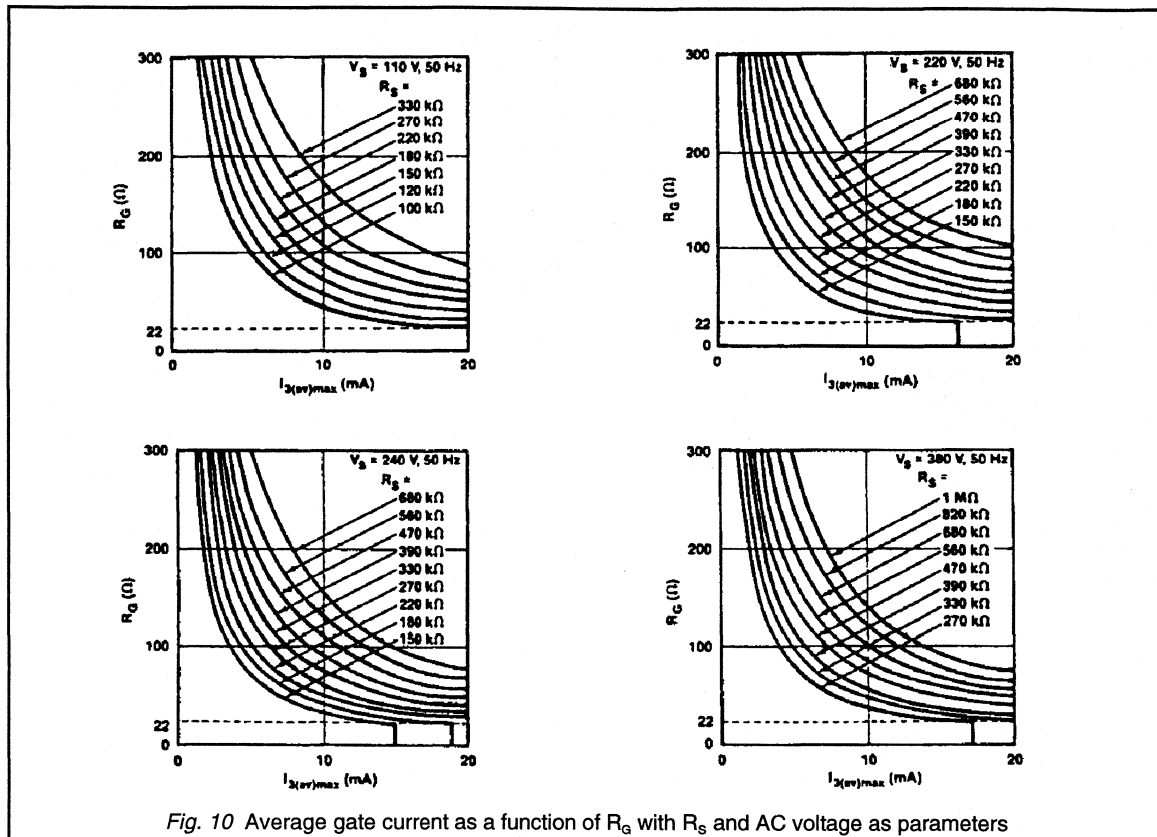
The smoothing capacitor is required to provide the supply current to the TDA1023 during the negative half cycles of the mains voltage waveform. As the TDA1023 possesses an internal voltage stabilization circuit, a high input ripple voltage can be tolerated. A practical preferred value of C_s is 220 μ F, 16V.

Timing Capacitor, C_T

The minimum repetition period required for a particular application was given in Table 1. This timing is selected using the external capacitor C_T . Typical electrolytic capacitors have wide tolerances: up to -10% to +50%. Moreover, the effective DC capacitance is different from the marked (AC) value, usually greater. Thus, the use of standard capacitors may lead to repetition periods far in excess of those required. A range of electrolytic capacitors has been developed for use with the TDA1023 (Table 3). All further references to C_T assume the use of the preferred capacitors which have the following advantages:

- DC capacitance is known for each marked AC value.
- Tolerance for the DC capacitance is $\pm 20\%$.
- Very low leakage current ($< 1\mu$ A).
- Long lifetime ($> 100,000$ hours at 40°C).





The timing circuit

The TDA1023 employs a triangular waveform for timing purposes. The advantages of using a triangular waveform are that for a given capacitor value the triangular waveform provides twice the repetition period that the sawtooth gives. This allows the use of smaller capacitors and minimises the effects of the capacitor leakage current thus reducing the spread in repetition periods.

The published data for the TDA1023 specifies the repetition period as $0.6 \text{ s} \pm 0.2 \text{ s}/\mu\text{F}$. Table 4 shows the minimum preferred value of C_T (DC value) to provide the required minimum repetition time for a range of appliance powers operating at 220V AC. The resulting nominal, minimum, and maximum repetition times are also given.

Input voltage translation circuit

Figure 8 shows a temperature sensing network which requires a minimum of components and eliminates performance spreads due to potentiometer tolerances. For applications where the input voltage variation is very much

less than the available voltage then the required temperature will be controlled by a small angle of rotation of the potentiometer shaft. The TDA1023 voltage translation circuit allows the use of 80% of the potentiometer rotation giving accurate control of the temperature. If the voltage translation circuit is not used then pins 9 and 11 must be shorted together to disable the circuit. A block diagram of the translation circuit is shown in Fig. 9.

Fail-safe circuits

The TDA1023 is fail-safe for both short-circuit and open-circuit conditions. Either of these conditions will prevent production of trigger pulses for the triac.

Short-circuit sensing is automatically obtained from the normal temperature sensing circuit. When the thermistor input voltage is zero, the triac will never be triggered because the potentiometer slider voltage will be higher. To sense the open-circuit thermistor condition, an extra comparator is used. This fail-safe comparator will inhibit output pulses if the thermistor input voltage rises above a

reference value (see Fig. 9).

Determination of required supply current

Before any calculations concerning the required supply current can be made, the maximum average output current of the TDA1023 must be determined. The minimum supply current required is the sum of the following currents:

- the maximum average output current
- the current drawn by the temperature-sense circuit
- the current required by the integrated circuit.

For worst-case conditions, a 5% tolerance for R_s and R_a and a 10% variation of the mains is assumed. Figure 10 shows graphs of $I_{G(AV)max}$ as a function of R_a and R_s for four 50Hz supply voltages. Below $R_a=22\Omega$ there is no further increase in I_a as the output current is limited. The current drawn by the temperature-sensing circuit must not be greater than 1mA. The current consumption of the

TDA1023 depends upon the hysteresis and proportional band settings. Figure 11 shows the minimum supply current as a function of the average output current for limit settings.

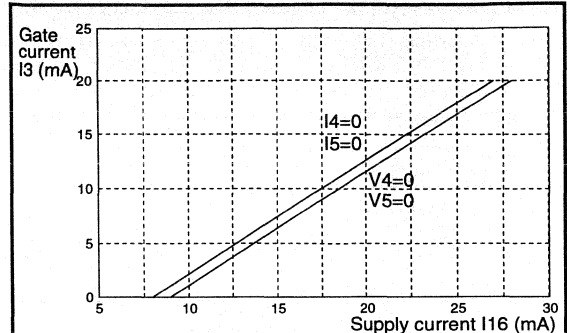


Fig. 11 Maximum required input current as function of gate current for limits of hysteresis band settings

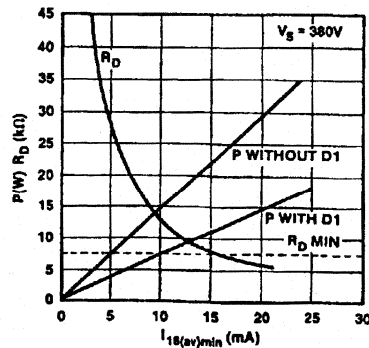
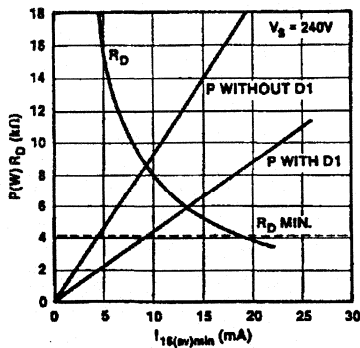
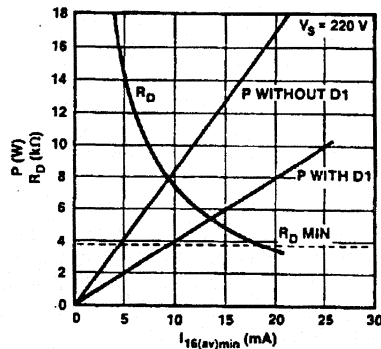
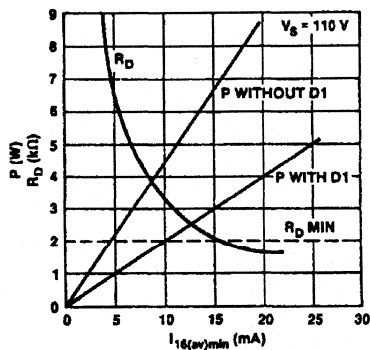


Fig. 12 Input current as a function of R_D and power dissipation (with and without series diode)

The mains dropping resistor, R_D

The value of the mains dropping resistor must be chosen such that the average supply current to the input of the TDA1023 is at least equal to the required minimum. The value of the resistor R_D is defined by the maximum current that can flow into Pin 16, the maximum peak mains voltage, and the minimum voltage at Pin 16. Table 5 shows practical values for $R_{D(\min)}$ for four common mains supply voltages

Supply voltage V_s (V)	$R_{D(\min)}$ (k Ω)
110	2.0
220	3.9
240	4.3
380	7.5

Table 5. Mains dropping resistor values

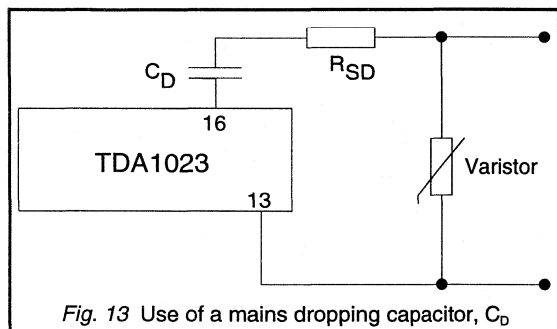


Fig. 13 Use of a mains dropping capacitor, C_D

The power dissipated by the dropping resistor has been computed for four mains voltages as a function of R_D and the results plotted on the graphs of Fig. 12. The power dissipated in R_D may be considerably reduced by the addition of a series diode as in Fig. 14. In this case there is no conduction through R_D during the negative half-cycle of the supply voltage, giving a reduction of more than 50% of the power dissipated in R_D .

Use of a mains dropping capacitor

It is possible to replace the mains dropping resistor and series diode with a capacitor, Fig. 13, and thereby reduce the power dissipation in the voltage reduction components still further. However, for mains voltages below 200V, the power dissipated by the dropping resistor is comparatively small and the use of a capacitor is not considered to be necessary. For mains voltages above 240V, the additional cost of the required high-voltage capacitor is not justified. For these reasons, it is recommended that capacitive voltage reduction is only used with mains supplies of 200V(RMS) or 240V(RMS).

When selecting a capacitor for mains voltage reduction, the following points must be considered:

- **AC voltage rating**

- **Suppression of mains-borne transients** - A voltage-dependent resistor must be connected across the mains input to limit mains borne transients. For $R_{SD}=390\Omega$ this yields a maximum transient voltage of about 740V. For 220V operation, a VDR (catalogue number 2322 594 13512) will limit the supply voltage to the required level during current transients of up to about 200A. For 240V operation, a VDR (catalogue number 2322 594 13912) will limit the supply voltage to the required level during current transients of up to about 80A.

- **Limit of Inrush current** - The capacitor C_D must not be chosen so large that the input current to the TDA1023 violates the absolute maximum specified in the published data. A practical value for C_D is 680nF. Resistor R_{SD} must also limit the peak value of the inrush current to less than 2A under worst case operating conditions. With a 240V (+10%) supply, the value of 390Ω (-5%) will limit the worst case peak value of the inrush current to:

$$\frac{240 \times 1.1}{0.95 \times 390} \sqrt{2} = 1.01A$$

Triac protection

If the mains dropping circuit consists of capacitor C_D and resistor R_{SD} , a VDR must be included in the circuit as described above. This VDR will also protect the triac against current surges in the mains supply. If the mains dropping circuit consists of resistor R_D and diode D1, the VDR may be connected directly across the triac, giving improved protection due to the series resistance of the heater. Current surges in the supply will not harm the TDA1023 as the dropping resistor will limit the current to a safe level.

Application examples

The TDA1023 is intended primarily for room temperature control using electric panel heaters. The controllable heater power range is from 400W to 2000W, although the upper limit may be increased by suitable choice of triacs and/or heatsinks. The TDA1023 may also be used as a time proportional switch for cooker elements and similar devices, giving 100% control of the power dissipation.

1. Domestic panel heater controller

Figure 3 showed the design for a time proportional heater control using the TDA1023. Economies may be gained by the use of smaller or lower power components and so two versions are described in Table 6. Version A, for heaters from 400W to 1200W, uses a BT138 triac and a 15 μ F timing capacitor, version B, for heaters from 1200W to 2000W, uses a BT139 triac and a 68 μ F timing capacitor. Table 6 gives the necessary component values under worst case conditions for each of these versions for use with mains supplies of 220V, 50Hz.

The capacitor C1 has been included in the circuit of Fig. 3 to minimise sensor line interference pick-up. This is only necessary when the sensor is remote from the control circuit. The built-in hysteresis and proportional band provides optimum performance for panel heaters so pins 4 and 5 are not connected.

Component	Version A 400W - 1200W	Version B 1200W - 2000W
T ₁	BT138-500	BT139-500
VDR ¹	350V, 1mA	350V, 1mA
D ₁	BYX10G	BYX10G
R ₁ ²	18.7kΩ	18.7kΩ
R _{NTC} ³	R25=22kΩ, B=4200k	R25=22kΩ, B=4200k
R _p	22kΩ	22kΩ
R _D	4.3kΩ	6.2kΩ
R _G	82Ω	82Ω
R _S	430kΩ	180kΩ
C ₁	47nF	47nF
C _S	220μF, 16V	220μF, 16V
C _T	15μF (DC)	68μF (DC)
C _D ⁴	680nF	470nF
R _{SD} ⁴	390Ω	390Ω

- Notes:** 1. Cat. No. 2322 594 13512
2. 1% tolerance
3. Cat. No. 2322 642 12223
4. Only required if used in place of D₁ and R_D

Table 6. 220V, 50Hz temperature controller components

2. Temperature control of 2kW load.

For a load power of 2kW the BT139 triac must be used. The circuit is also that shown in Fig. 3. Table 7 gives a summary of the required component values.

Component	Value	Remarks
T ₁	BT139-500	
VDR	350V, 1mA	No. 2322 594 13912
D ₁	BYX10G	
R ₁	18.7kΩ	1% tolerance
R _{NTC}	R25=22kΩ, B=4200k	No. 2322 642 12223
R _p	22kΩ	
R _D	6.8kΩ	
R _G	82Ω	
R _S	150kΩ	
C ₁	47nF	
C _S	220μF, 16V	
C _T	47μF (DC)	No. 2222 016 90129

Table 7. 2000W, 220V, 50Hz temperature controller

Value of R_S

The required trigger pulse width can be found from Fig. 4 as a function of the load power, latch current and supply voltage (2000W, 60mA, and 220V, 50Hz, respectively): $t_{p(\min)}=64\mu\text{s}$. A value of R_S=135kΩ provides a trigger pulse of the required duration. The next preferred value above this is 150kΩ, providing a $t_{p(\min)}$ of approximately 70μs.

Value of R_G

The maximum value of R_G that may be used is determined by the minimum conditions to reliably trigger all samples of the triac. In Fig. 6 it can be seen that the operation point of 1.6V and 98 mA lies on the load line for 82Ω and this is the value chosen.

Value of C_T

For a load of 2kW, the repetition period must be at least 24s (from Table 1). From Table 4 the minimum preferred value of C_T to provide this period is 68μF. However, due to the different performance under AC and DC conditions, then from Table 3, the actual capacitor used should be 47μF, 25V.

Value of R₁ and R_p

For control over the range 5°C to 35°C and a thermistor characteristics with R₂₅=22kΩ, a suitable value of R₁ is 18.7kΩ ±1%. A suitable value for R_p is 22kΩ.

Value of R_D

First, the maximum average output current must be found. From Fig. 10 the maximum gate current I_G is given as a function of the values of resistors R_S and R_G. For this circuit I_{G(AV)max}=5 mA. Once the maximum average output current is known, the minimum required supply current can be found from Fig. 11. With minimum hysteresis and proportional band, the average value of the supply current is 12.5 mA. Using this value of input current the required value of R_D can be found from Fig. 12 giving R_D = 5.6 kΩ. The power dissipation in the resistor when diode D₁ is present in the circuit is then 5 W.

3. Time proportional power control

The TDA1023 may be used to provide proportional control of devices such as electric cooker elements. The temperature-sensing bridge is replaced by a potentiometer, the power in the load being proportional to the potentiometer setting. Proportional power control is thus obtained while the potentiometer voltage lies between the upper and lower limits of the triangular waveform comparator input.

As the timing capacitor is charged and discharged by current sources, the voltage across it will never reach zero, so that load power will be zero before the potentiometer reaches its minimum setting. Similarly, maximum load power is reached before the maximum setting of the potentiometer. This effect can be reduced by the addition of resistors R₁ and R₂. To ensure that 0% and 100% load

Hi-Com Triacs

6.3.1 Understanding Hi-Com Triacs

Hi-Com triacs from Philips Semiconductors are specifically designed to give superior triac commutation performance in the control of motors for domestic equipment and tools. These devices are suitable for use with a wide variety of motor and inductive loads without the need for a protective snubber. The use of a Hi-Com triac greatly simplifies circuit design and gives significant cost savings to the designer.

This product information sheet explains how the superior characteristics and performance of Hi-Com triacs removes design limitations of standard devices.

Triac commutation explained

A triac is an AC conduction device, and may be thought of as two antiparallel thyristors monolithically integrated onto the same silicon chip.

In phase control circuits the triac often has to be triggered into conduction part way into each half cycle. This means that at the end of each half cycle the on-state current in one direction must drop to zero and not resume in the other direction until the device is triggered again. This "commutation" turn-off capability is at the heart of triac power control applications.

If the triac were truly two separate thyristors this requirement would not present any problems. However, as the two are on the same piece of silicon there is the possibility that the "reverse recovery current" (due to unrecombined charge carriers) of one thyristor as it turns off, may act as gate current to trigger the other thyristor as the voltage rises in the opposite direction. This is described as a "commutation failure" and results in the triac continuing to conduct in the opposite direction instead of blocking.

The probability of any device failing commutation is dependent on the rate of rise of reverse voltage (dV/dt) and the rate of decrease of conduction current (dI/dt). The higher the dI/dt the more unrecombined charge carriers are left at the instant of turn-off. The higher the dV/dt the more probable it is that some of these carriers will act as gate current. Thus the commutation capability of any device is usually specified in terms of the turn-off dI/dt and the re-applied dV/dt it can withstand, at any particular junction temperature.

If a triac has to be operated in an inductive load circuit with a combination of dI/dt and dV/dt that exceeds its specification, it is necessary to use an RC-snubber network in parallel with the device to limit the dV/dt . This is at a penalty of extra circuit complexity and dissipation in the snubber. The "High Commutation" triacs (Hi-Com triacs) are designed to have superior commutation capability, so that even at a high rate of turn-off (dI/dt) and a high rate of re-applied dV/dt they can be used without the aid of a

snubber network, thus greatly simplifying the circuit. The design features of Hi-Com devices that have made this possible are:

Geometric separation of the two antiparallel thyristors

Commutation failure can be avoided by physically separating the two 'thyristor halves' of a triac. However, separating them into two discrete chips would remove the advantage of a triac being triggerable in both directions by the same gate connection. Within the integrated structure of a Hi-Com triac the two halves of the device are kept further apart by modifying the layout of the chip in order to lessen the chance of conduction in one half affecting the other half.

Emitter shorting

"Emitter shorts" refer to the on-chip resistive paths between emitter and base of a transistor. A higher degree of emitter shorting means the presence of more such paths and lower resistance values in them. The use of emitter shorts in a triac has two effects on commutation.

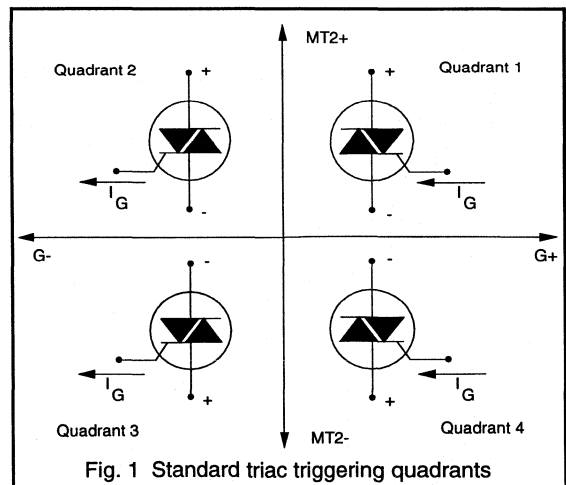


Fig. 1 Standard triac triggering quadrants

Firstly it reduces the gain of the internal transistors that make up the triac. This means there will be fewer carriers left to recombine when the conduction current falls to zero, and therefore a smaller probability that a sufficient number will be available to re-trigger the triac. The second way in which emitter shorts help commutation is that any unrecombined carriers in the conducting thyristor at turn-off

will have more chance of flowing out through the emitter shorts (of the opposite thyristor) rather than acting as gate current to trigger that thyristor on.

The Hi-Com triacs have a higher degree of emitter shorting both around the periphery of the device and in the central part of the active area. This both reduces the number of carriers available, and lessens the danger of any available carriers acting as gate current for undesirable triggering.

Modified gate structure

The gate of a triac allows conduction in both directions to be initiated by either a positive or a negative current pulse between gate (G) and main terminal (MT1). The four different modes of triggering are often called 1+, 1-, 3- and 3+ (or sometimes quadrants 1, 2, 3 and 4) and are shown in Fig. 1.

This triggering versatility arises from the fact that the gate consists of some elements which conduct temporarily during the turn-on phase. In particular, one of the triggering modes, 3+ (or quadrant 4), relies on the main terminal 1 supplying electrons to trigger a thyristor element in the gate-MT1 boundary. Conduction then spreads to the main thyristor element from this boundary.

Unfortunately the carrier distribution in this triggering mode of operation is very similar to that existing when the triac is commutating in the 1-to-3 direction (i.e changing from

conduction with MT2 positive to blocking with MT1 positive). The presence of the element in the gate to allow 3+ triggering will therefore always also undermine commutation capability in the 1-to-3 direction. For this reason the Hi-Com triacs have a modified gate design to remove this structure. This incurs the penalty that the 3+ trigger mode cannot be used, but it greatly improves the commutation performance of the device.

Conclusions

By modifications to the internal design and layout of the triac it is possible to achieve a high commutation capability triac for use in inductive and motor load applications. These modifications have been implemented in the Hi-Com range of devices from Philips Semiconductors. The devices can be used in all typical motor control applications without the need for a snubber circuit. The commutation capability of the devices is well in excess of the operating conditions in typical applications.

As the loss of the fourth trigger quadrant can usually be tolerated in most designs, Hi-Com triacs can be used in existing motor control applications without the snubber network required for a standard device. This gives the designer significant savings in design simplicity, board space and system cost.

6.3.2 Using Hi-Com Triacs

Hi-Com triacs from Philips Semiconductors are specifically designed to give superior triac commutation performance in the control of motors for domestic equipment and tools. These devices are suitable for use with a wide variety of motor and inductive loads without the need for a snubber. The use of a Hi-Com triac greatly simplifies circuit design and gives significant cost savings to the designer.

This product information sheet explains how the need for a triac snubber arises and how the superior performance of Hi-Com triacs removes design limitations of standard devices. The Hi-Com range is summarised in Table 1.

Triac commutation

For resistive loads the device current is in phase with the line voltage. Under such conditions triac turn-off (commutation) occurs at the voltage "zero-crossover" point. This is not a very severe condition for triac commutation: the slow rising dV/dt gives time for the triac to turn off (commutate) easily.

The situation is quite different with inductive or motor loads. For these circuits conduction current lags behind the line voltage as shown in Fig. 1. When triac commutation occurs the rate of rise of voltage in the opposite direction can be very rapid and is governed by the circuit and device

characteristics. This high dV/dt means there is a much higher probability of charge carriers in the device re-triggering the triac and causing a commutation failure.

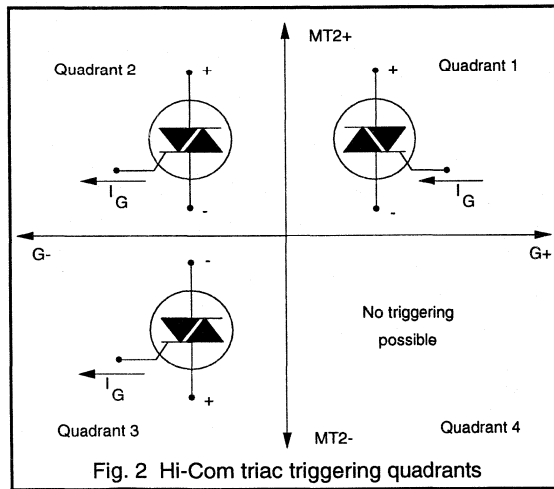
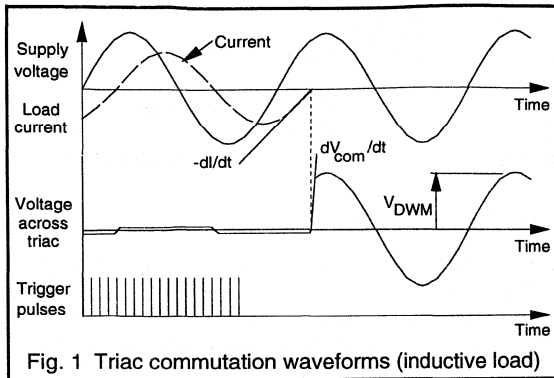
Hi-Com triacs

Hi-Com triacs are specifically designed for use with ac inductive loads such as motors. As commutation capability is not an issue for resistive load applications then standard triacs are still the most appropriate devices for these applications. The significant advantage of a Hi-Com triac is that it has no limitation on the rate of rise of reapplied voltage at commutation. This removes the requirement for a snubber circuit in inductive load circuits. An additional advantage of the Hi-Com design is that the off-state (static) dV/dt capability of the device is also significantly improved.

When using Hi-Com triacs in inductive load applications the trigger circuit cannot trigger the device in the fourth (3+) quadrant (Fig. 2). Fortunately the vast majority of circuit designs do not require this mode of operation and so are suitable for use with Hi-Com triacs without modification. The circuit of Fig. 3 is a typical example of the simplest type of trigger circuit. Hi-Com triacs are equally suitable for use with microcontroller trigger circuits.

Parameter		BTA212-600B	BTA212-800B	BTA216-600B	BTA216-800B
Repetitive peak voltage	V_{DRM} (V)	600	800	600	800
RMS on-state current	$I_{T(RMS)}$ (A)	12	12	16	16
Gate trigger current	I_{GT} (mA)	2 - 50	2 - 50	2 - 50	2 - 50
Off state dV/dt	dV_D/dt (V/ μ s)	1000	1000	1000	1000
Commutating di/dt	di_{com}/dt (A/ms)	24	24	28	28
Turn-on di/dt	di_T/dt (A/ μ s)	50	50	50	50
Package		TO220	TO220	TO220	TO220

Table 1. Philips Semiconductors Hi-Com Triac range

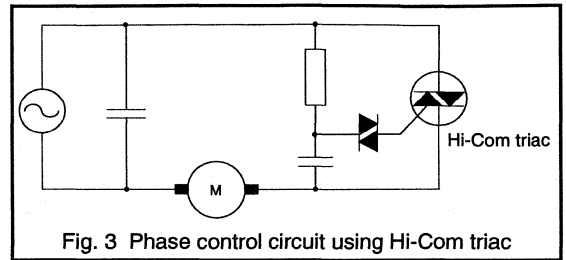


Device limiting values

i) Trigger current, I_{GT}

Trigger current for the Hi-Com triacs is in the range 2mA to 50mA. This means that gate currents due to noise that are below 2mA in amplitude can be guaranteed not to trigger the devices. This gives the devices a noise immunity feature that is important in many applications. The trigger current delivered by the trigger circuit must be greater than 50mA under all conditions in order to guarantee triggering of the device when required. As discussed above, triggering is

only possible in the 1+, 1- and 3- quadrants.



ii) Rate of change of current, di_{com}/dt

Hi-Com triacs do not require a snubber network providing that the rate of change of current prior to commutation is less than the rating specified in the device data sheet. This di_{com}/dt limit is well in excess of the currents that occur in the device under normal operating conditions, during transients such as start-up and faults such as the stalled motor condition.

For the 12A Hi-Com triacs the limit commutating current is typically 24A/ms at 125°C. This corresponds to an RMS current of 54A at 50Hz. For the 16A Hi-Com triacs the limit commutating current is typically 28A/ms at 125°C. This corresponds to an RMS current of 63A at 50Hz. Typical stall currents for an 800W domestic appliance motor are in the range 15A to 20A and so the commutation capability of the Hi-Com triacs is well above the requirement for this type of application.

Conclusions

The Hi-Com range of devices from Philips Semiconductors can be used in all typical motor control applications without the need for a snubber circuit. The commutation capability of the devices is well in excess of the operating conditions in typical applications.

As the loss of the fourth trigger quadrant can usually be tolerated in most designs, Hi-Com triacs can be used in existing motor control applications. By removing the snubber the use of a Hi-Com triac gives the designer significant savings in design simplicity, board space and system cost.

CHAPTER 7

Thermal Management

7.1 Thermal Considerations

Thermal Considerations



7.1.1 Thermal Considerations for Power Semiconductors

The perfect power switch is not yet available. All power semiconductors dissipate power internally both during the on-state and during the transition between the on and off states. The amount of power dissipated internally generally speaking increases in line with the power being switched by the semiconductor. The capability of a switch to operate in a particular circuit will therefore depend upon the amount of power dissipated internally and the rise in the operating temperature of the silicon junction that this power dissipation causes. It is therefore important that circuit designers are familiar with the thermal characteristics of power semiconductors and are able to calculate power dissipation limits and junction operating temperatures.

This chapter is divided into two parts. Part One describes the essential thermal properties of semiconductors and explains the concept of a limit in terms of continuous mode and pulse mode operation. Part Two gives worked examples showing junction temperature calculations for a variety of applied power pulse waveforms.

PART ONE

The power dissipation limit

The maximum allowable power dissipation forms a limit to the safe operating area of power transistors. Power dissipation causes a rise in junction temperature which will, in turn, start chemical and metallurgical changes. The rate at which these changes proceed is exponentially related to temperature, and thus prolonged operation of a power transistor above its junction temperature rating is liable to result in reduced life. Operation of a device at, or below, its power dissipation rating (together with careful consideration of thermal resistances associated with the device) ensures that the junction temperature rating is not exceeded.

All power semiconductors have a power dissipation limitation. For rectifier products such as diodes, thyristors and triacs, the power dissipation rating can be easily translated in terms of current ratings; in the on-state the voltage drop is well defined. Transistors are, however, somewhat more complicated. A transistor, be it a power MOSFET or a bipolar, can operate in its on-state at any voltage up to its maximum rating depending on the circuit conditions. It is therefore necessary to specify a Safe Operating Area (SOA) for transistors which specifies the power dissipation limit in terms of a series of boundaries in the current and voltage plane. These operating areas are usually presented for mounting base temperatures of 25 °C. At higher temperatures, operating conditions must be checked to ensure that junction temperatures are not exceeding the desired operating level.

Continuous power dissipation

The total power dissipation in a semiconductor may be calculated from the product of the on-state voltage and the forward conduction current. The heat dissipated in the junction of the device flows through the thermal resistance between the junction and the mounting base, R_{thj-mb} . The thermal equivalent circuit of Fig. 1 illustrates this heat flow; P_{tot} can be regarded as a thermal current, and the temperature difference between the junction and mounting base ΔT_{j-mb} as a thermal voltage. By analogy with Ohm's law, it follows that:

$$P_{tot} = \frac{T_j - T_{mb}}{R_{thj-mb}} \quad 1$$

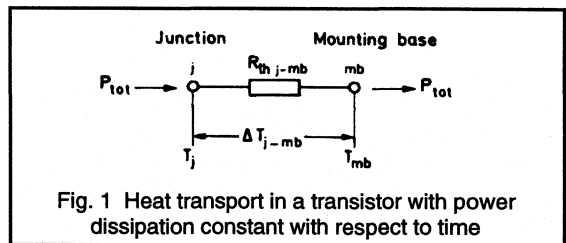


Fig. 1 Heat transport in a transistor with power dissipation constant with respect to time

Fig. 2 shows the dependence of the maximum power dissipation on the temperature of the mounting base. $P_{tot\ max K}$ is limited either by a maximum temperature difference:

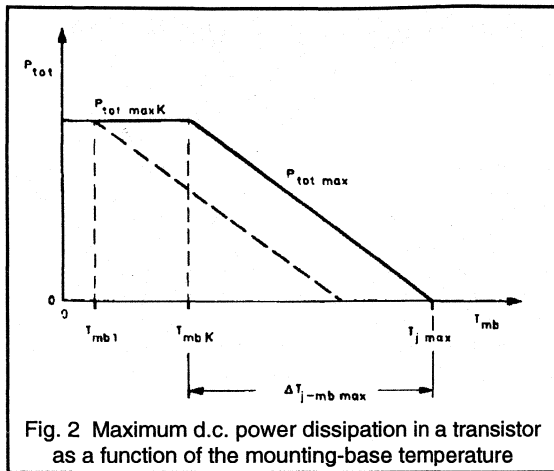
$$\Delta T_{j-mb\ max} = T_{j\ max} - T_{mb\ K} \quad 2$$

or by the maximum junction temperature $T_{j\ max}$ ($T_{mb\ K}$ is usually 25°C and is the value of T_{mb} above which the maximum power dissipation must be reduced to maintain the operating point within the safe operating area).

In the first case, $T_{mb} \leq T_{mb\ K}$:

$$P_{tot\ max K} = \frac{\Delta T_{j-mb\ max}}{R_{thj-mb}}; \quad 3$$

that is, the power dissipation has a fixed limit value ($P_{tot\ max K}$ is the maximum d.c. power dissipation below $T_{mb\ K}$). If the transistor is subjected to a mounting-base temperature $T_{mb 1}$, its junction temperature will be less than $T_{j\ max}$ by an amount ($T_{mb K} - T_{mb 1}$), as shown by the broken line in Fig. 2.



In the second case, $T_{mb} > T_{mb K}$:

$$P_{tot\ max} = \frac{T_{j\ max} - T_{mb}}{R_{thj-mb}} \quad 4$$

that is, the power dissipation must be reduced as the mounting base temperature increases along the sloping straight line in Fig. 2. Equation 4 shows that the lower the thermal resistance R_{thj-mb} , the steeper is the slope of the line. In this case, T_{mb} is the maximum mounting-base temperature that can occur in operation.

Example

The following data is provided for a particular transistor.

$$P_{tot\ max K} = 75\ W$$

$$T_{j\ max} = 175\ ^\circ C$$

$$R_{thj-mb} \leq 2\ K/W$$

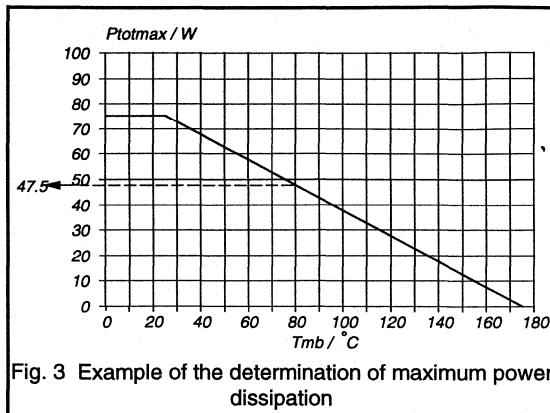
The maximum permissible power dissipation for continuous operation at a maximum mounting-base temperature of $T_{mb} = 80\ ^\circ C$ is required.

Note that the maximum value of T_{mb} is chosen to be significantly higher than the maximum ambient temperature to prevent an excessively large heatsink being required.

From Eq. 4 we obtain:

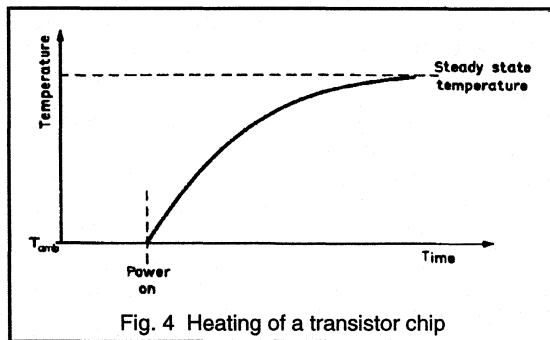
$$P_{tot\ max} = \frac{175 - 80}{2}\ W, = 47.5\ W$$

Provided that the transistor is operated within SOA limits, this value is permissible since it is below $P_{tot\ max K}$. The same result can be obtained graphically from the $P_{tot\ max}$ diagram (Fig. 3) for the relevant transistor.



Pulse power operation

When a power transistor is subjected to a pulsed load, higher peak power dissipation is permitted. The materials in a power transistor have a definite thermal capacity, and thus the critical junction temperature will not be reached instantaneously, even when excessive power is being dissipated in the device. The power dissipation limit may be extended for intermittent operation. The size of the extension will depend on the duration of the operation period (that is, pulse duration) and the frequency with which operation occurs (that is, duty factor).



If power is applied to a transistor, the device will immediately start to warm up (Fig. 4). If the power dissipation continues, a balance will be struck between heat generation and removal resulting in the stabilisation of T_j and ΔT_{j-mb} . Some heat energy will be stored by the thermal capacity of the device, and the stable conditions will be determined by the thermal resistances associated with the transistor and its thermal environment. When the power dissipation ceases, the device will cool (the heating and cooling laws will be identical, see Fig. 5). However, if the power dissipation ceases before the temperature of the transistor stabilises, the peak values of T_j and ΔT_{j-mb} will be less than the values

reached for the same level of continuous power dissipation (Fig. 6). If the second pulse is identical to the first, the peak temperature attained by the device at the end of the second pulse will be greater than that at the end of the first pulse. Further pulses will build up the temperature until some new stable situation is attained (Fig. 7). The temperature of the device in this stable condition will fluctuate above and below the mean. If the upward excursions extend into the region of excessive T_j , then the life expectancy of the device may be reduced. This can happen with high-power low-duty-factor pulses, even though the average power is below the d.c. rating of the device.

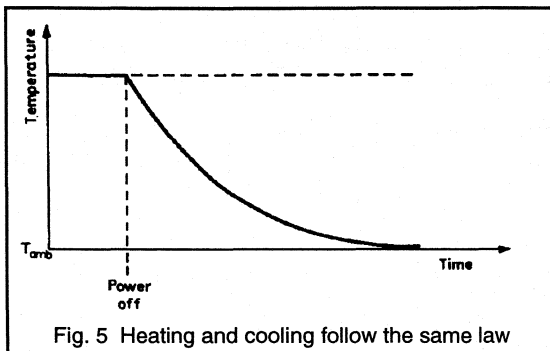


Fig. 5 Heating and cooling follow the same law

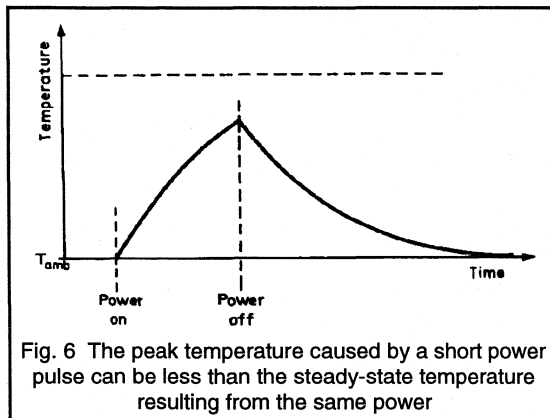


Fig. 6 The peak temperature caused by a short power pulse can be less than the steady-state temperature resulting from the same power

Fig. 8 shows a typical safe operating area for d.c. operation of a power MOSFET. The corresponding rectangular-pulse operating areas with a fixed duty factor, $\delta = 0$, and the pulse time t_p as a parameter, are also shown. These boundaries represent the largest possible extension of the operating area for particular pulse times. When the pulse time becomes very short, the power dissipation does not have a limiting action and the pulse current and maximum voltage form the only limits. This rectangle represents the largest possible pulse operating area.

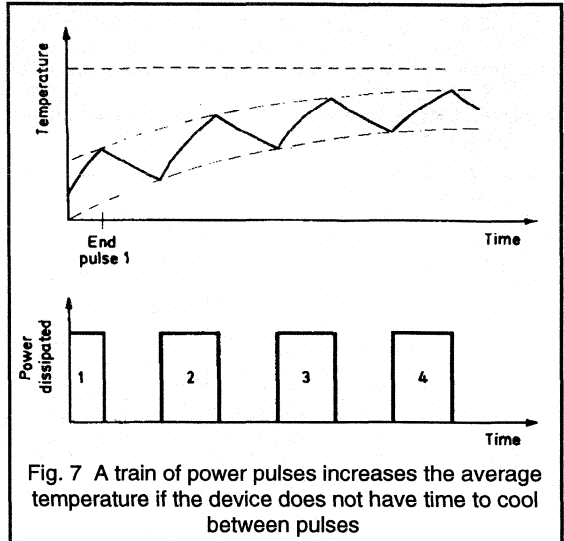


Fig. 7 A train of power pulses increases the average temperature if the device does not have time to cool between pulses

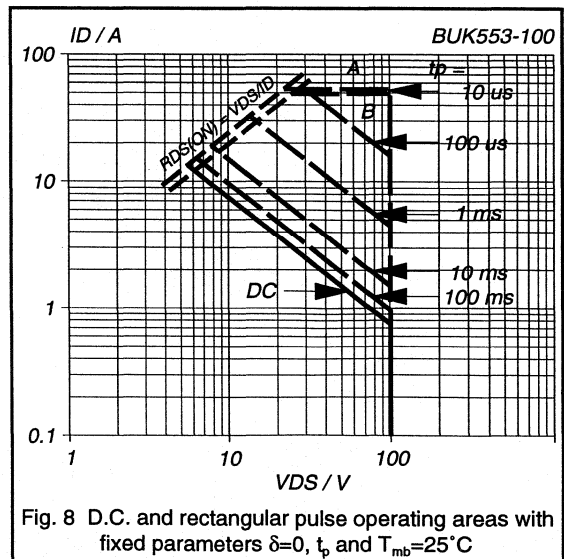


Fig. 8 D.C. and rectangular pulse operating areas with fixed parameters $\delta=0$, t_p and $T_{mb}=25^\circ C$

In general, the shorter the pulse and the lower the frequency, the lower the temperature that the junction reaches. By analogy with Eq. 3, it follows that:

$$P_{tot M} = \frac{T_j - T_{mb}}{Z_{thj-mb}}, \quad 5$$

where Z_{thj-mb} is the transient thermal impedance between the junction and mounting base of the device. It depends on the pulse duration t_p , and the duty factor δ , where:

$$\delta = \frac{t_p}{T}$$

6

and T is the pulse period. Fig. 9 shows a typical family of curves for thermal impedance against pulse duration, with duty factor as a parameter.

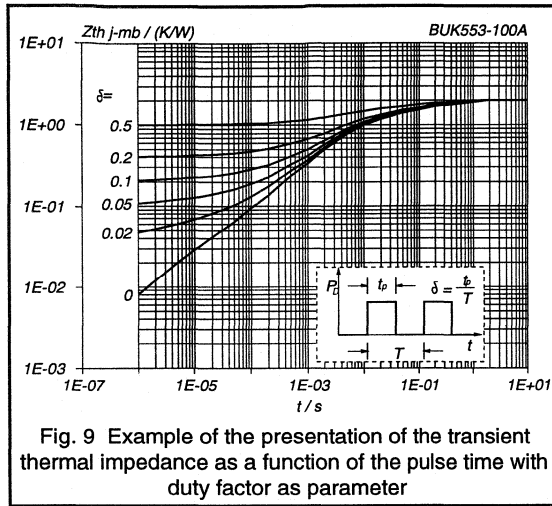


Fig. 9 Example of the presentation of the transient thermal impedance as a function of the pulse time with duty factor as parameter

Again, the maximum pulse power dissipation is limited either by the maximum temperature difference $\Delta T_{j-mb \max}$ (Eq. 2), or by the maximum junction temperature $T_{j \max}$, and so by analogy with Eqs. 3 and 4:

$$P_{tot \max K} = \frac{\Delta T_{j-mb \max}}{Z_{thj-mb}}, \quad 7$$

when $T_{mb} \leq T_{mb K}$, and:

$$P_{tot M \max} = \frac{T_{j \max} - T_{mb}}{Z_{thj-mb}}, \quad 8$$

when $T_{mb} > T_{mb K}$. That is, below a mounting-base temperature of $T_{mb K}$, the maximum power dissipation has a fixed limit value; and above $T_{mb K}$, the power dissipation must be reduced linearly with increasing mounting-base temperature.

Short pulse duration (Fig. 10a)

As the pulse duration becomes very short, the fluctuations of junction temperature become negligible, owing to the internal thermal capacity of the transistor. Consequently, the only factor to be considered is the heating of the junction by the average power dissipation; that is:

$$P_{tot(av)} = \delta P_{tot M} \quad 9$$

The transient thermal impedance becomes:

$$\lim_{t_p \rightarrow 0} Z_{thj-mb} = \delta R_{thj-mb}$$

10

The Z_{thj-mb} curves approach this value asymptotically as t_p decreases. Fig. 9 shows that, for duty factors in the range 0.1 to 0.5, the limit values given by Eq. 10 have virtually been reached at $t_p = 10^{-6}$ s.

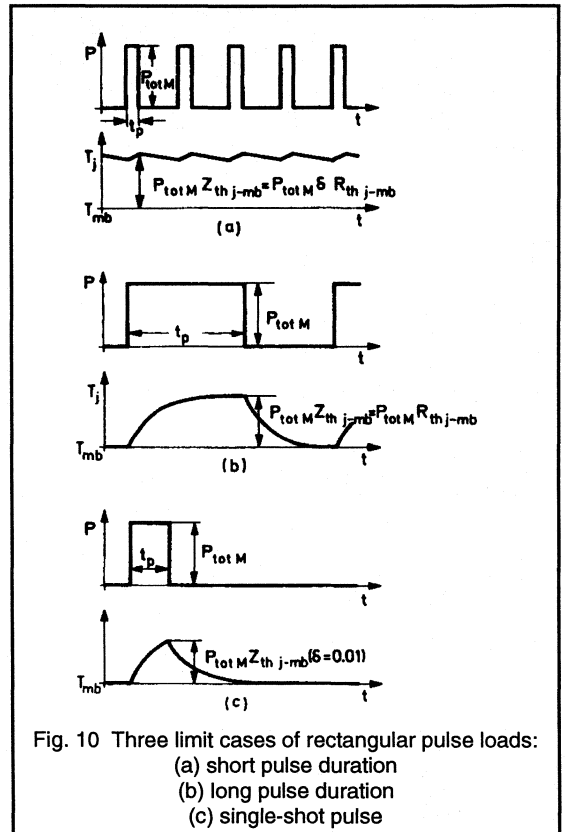


Fig. 10 Three limit cases of rectangular pulse loads:
(a) short pulse duration
(b) long pulse duration
(c) single-shot pulse

Long pulse duration (Fig. 10b)

As the pulse duration increases, the junction temperature approaches a stationary value towards the end of a pulse. The transient thermal impedance tends to the thermal resistance for continuous power dissipation; that is:

$$\lim_{t_p \rightarrow \infty} Z_{thj-mb} = R_{thj-mb} \quad 11$$

Fig. 9 shows that Z_{thj-mb} approaches this value as t_p becomes large. In general, transient thermal effects die out in most power transistors within 0.1 to 1.0 seconds. This time depends on the material and construction of the case, the size of the chip, the way it is mounted, and other factors. Power pulses with a duration in excess of this time have approximately the same effect as a continuous load.

Single-shot pulses (Fig. 10c)

As the duty factor becomes very small, the junction tends to cool down completely between pulses so that each pulse can be treated individually. When considering single pulses, the Z_{thj-mb} values for $\delta = 0$ (Fig. 9) give sufficiently accurate results.

PART TWO

Calculating junction temperatures

Most applications which include power semiconductors usually involve some form of pulse mode operation. This section gives several worked examples showing how junction temperatures can be simply calculated. Examples are given for a variety of waveforms:

- (1) Periodic Waveforms
- (2) Single Shot Waveforms
- (3) Composite Waveforms
- (4) A Pulse Burst
- (5) Non Rectangular Pulses

From the point of view of reliability it is most important to know what the peak junction temperature will be when the power waveform is applied and also what the average junction temperature is going to be.

Peak junction temperature will usually occur at the end of an applied pulse and its calculation will involve transient thermal impedance. The average junction temperature (where applicable) is calculated by working out the average power dissipation using the d.c. thermal resistance.

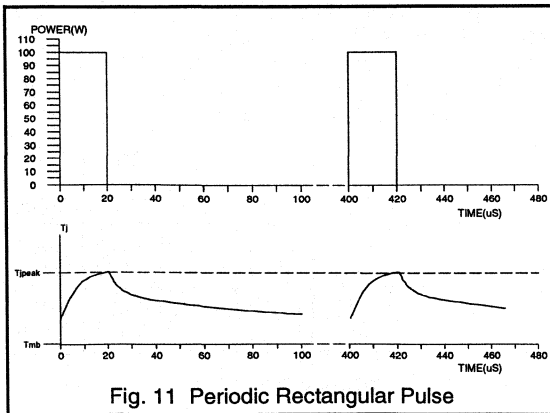


Fig. 11 Periodic Rectangular Pulse

When considering the junction temperature in a device, the following formula is used:

$$T_j = T_{mb} + \Delta T_{j-mb} \quad 14$$

where ΔT_{j-mb} is found from a rearrangement of equation 7. In all the following examples the mounting base temperature (T_{mb}) is assumed to be 75°C.

Periodic rectangular pulse

Fig. 11 shows an example of a periodic rectangular pulse. This type of pulse is commonly found in switching applications. 100W is dissipated every 400µs for a period of 20µs, representing a duty cycle (δ) of 0.05. The peak junction temperature is calculated as follows:

$$\text{Peak } T_j: \quad t = 2 \times 10^{-5} \text{ s}$$

$$P = 100 \text{ W}$$

$$\delta = \frac{20}{400} = 0.05$$

$$Z_{thj-mb} = 0.12 \text{ K/W}$$

$$\Delta T_{j-mb} = P \times Z_{thj-mb} = 100 \times 0.12 = 12^\circ \text{C}$$

$$T_j = T_{mb} + \Delta T_{j-mb} = 75 + 12 = 87^\circ \text{C}$$

$$\text{Average } T_j: \quad P_{av} = P \times \delta = 100 \times 0.05 = 5 \text{ W}$$

$$\Delta T_{j-mb(av)} = P_{av} \times Z_{thj-mb(\delta=1)} = 5 \times 2 = 10^\circ \text{C}$$

$$T_{j(av)} = T_{mb} + \Delta T_{j-mb(av)} = 75 + 10 = 85^\circ \text{C}$$

The value for Z_{thj-mb} is taken from the $\delta=0.05$ curve shown in Fig. 12 (This diagram repeats Fig. 9 but has been simplified for clarity). The above calculation shows that the peak junction temperature will be 85°C.

Single shot rectangular pulse

Fig. 13 shows an example of a single shot rectangular pulse. The pulse used is the same as in the previous example, which should highlight the differences between periodic and single shot thermal calculations. For a single shot pulse, the time period between pulses is infinity, ie the duty cycle $\delta=0$. In this example 100W is dissipated for a period of 20µs. To work out the peak junction temperature the following steps are used:

$$t = 2 \times 10^{-5} \text{ s}$$

$$P = 100 \text{ W}$$

$$\delta = 0$$

$$Z_{thj-mb} = 0.04 \text{ K/W}$$

$$\Delta T_{j-mb} = P \times Z_{thj-mb} = 100 \times 0.04 = 4^\circ \text{C}$$

The value for Z_{thj-mb} is taken from the $\delta=0$ curve shown in Fig. 12. The above calculation shows that the peak junction temperature will be 4°C above the mounting base temperature.

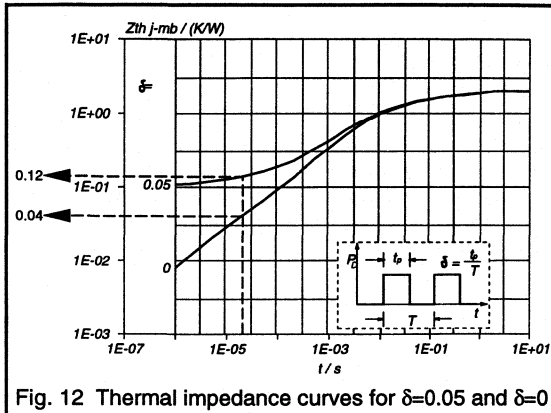


Fig. 12 Thermal impedance curves for $\delta=0.05$ and $\delta=0$

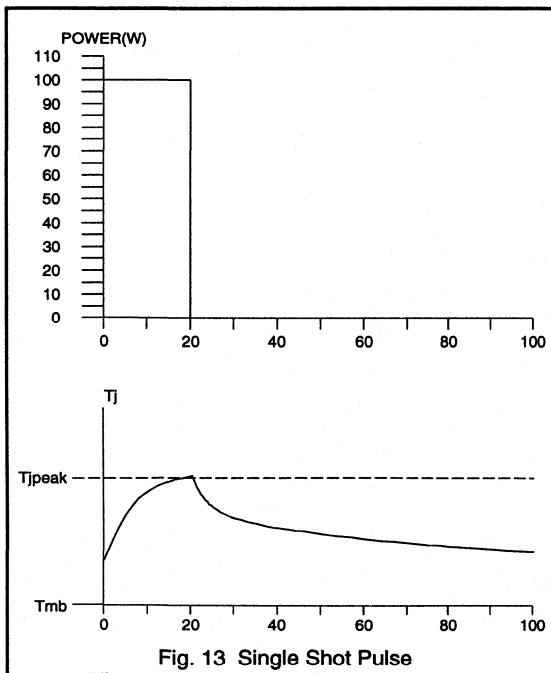


Fig. 13 Single Shot Pulse

For a single shot pulse, the average power dissipated and average junction temperature are not relevant.

Composite rectangular pulse

In practice, a power device frequently has to handle composite waveforms, rather than the simple rectangular pulses shown so far. This type of signal can be simulated by superimposing several rectangular pulses which have a common period, but both positive and negative amplitudes, in addition to suitable values of t_p and δ .

By way of an example, consider the composite waveform shown in Fig. 14. To show the way in which the method used for periodic rectangular pulses is extended to cover composite waveforms, the waveform shown has been chosen to be an extension of the periodic rectangular pulse example. The period is $400\mu s$, and the waveform consists of three rectangular pulses, namely $40W$ for $10\mu s$, $20W$ for $150\mu s$ and $100W$ for $20\mu s$. The peak junction temperature may be calculated at any point in the cycle. To be able to add the various effects of the pulses at this time, all the pulses, both positive and negative, must end at time t_x in the first calculation and t_y in the second calculation. Positive pulses increase the junction temperature, while negative pulses decrease it.

Calculation for time t_x

$$\begin{aligned} \Delta T_{j-mb@x} = & P_1 Z_{thj-mb}(t_1) + P_2 Z_{thj-mb}(t_2) \\ & + P_3 Z_{thj-mb}(t_4) - P_1 Z_{thj-mb}(t_2) \\ & - P_2 Z_{thj-mb}(t_4) \end{aligned} \quad 15$$

In equation 15, the values for P_1 , P_2 and P_3 are known: $P_1=40W$, $P_2=20W$ and $P_3=100W$. The Z_{th} values are taken from Fig. 9. For each term in the equation, the equivalent duty cycle must be worked out. For instance the first superimposed pulse in Fig. 14 lasts for a time $t_1 = 180\mu s$, representing a duty cycle of $180/400 = 0.45 = \delta$. These values can then be used in conjunction with Fig. 9 to find a value for Z_{th} , which in this case is $0.9K/W$. Table 1a gives the values calculated for this example.

		t1	t2	t3	t4
		180μs	170μs	150μs	20μs
Repetitive T=400μs	δ	0.450	0.425	0.375	0.050
	Z _{th}	0.900	0.850	0.800	0.130
Single Shot T=∞	δ	0.000	0.000	0.000	0.000
	Z _{th}	0.130	0.125	0.120	0.040

Table 1a. Composite pulse parameters for time t_x

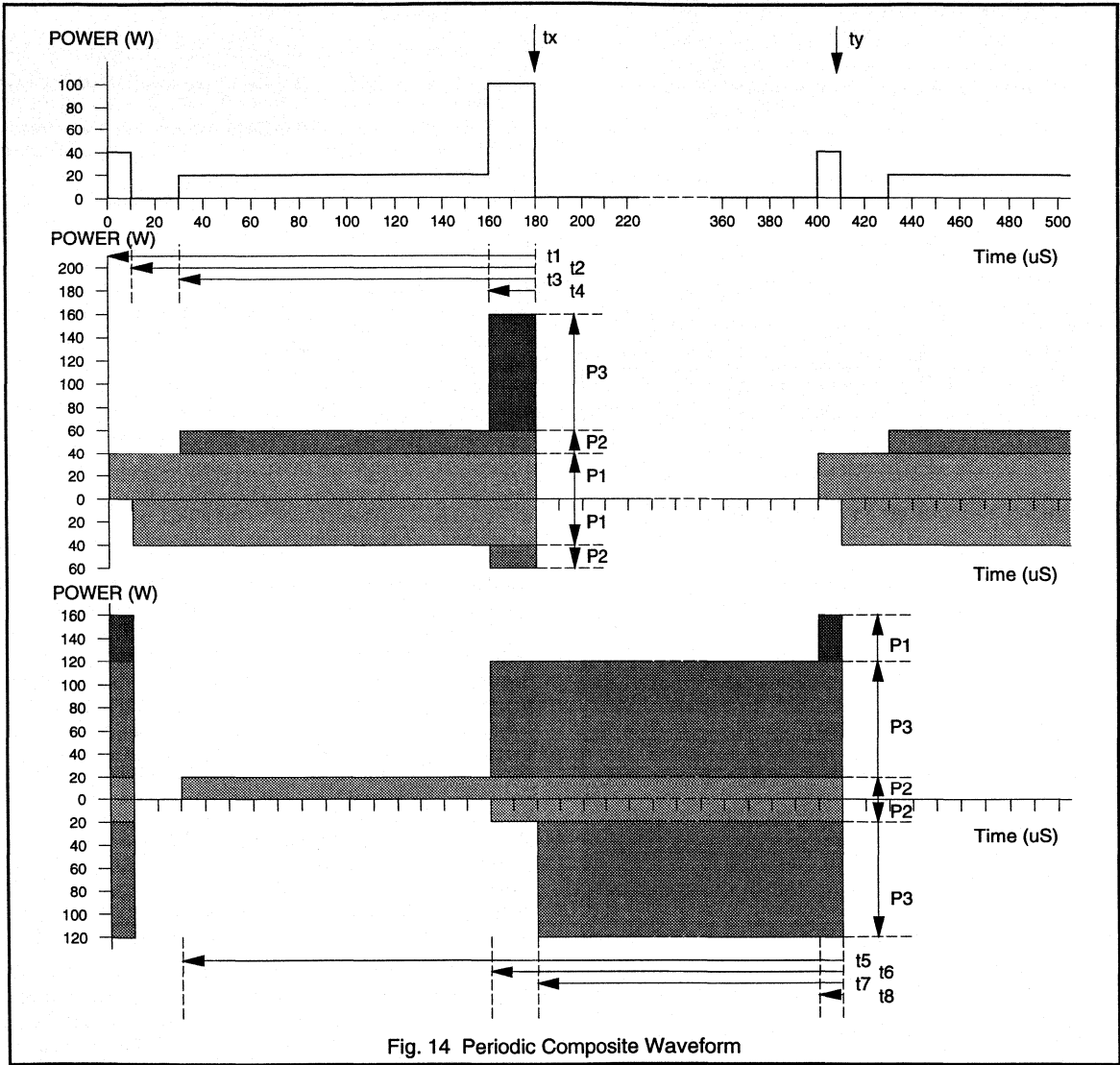


Fig. 14 Periodic Composite Waveform

Substituting these values into equation 15 for $T_{j-mb@x}$ gives

Repetitive:

$$\Delta T_{j-mb@x} = 40 \times 0.9 + 20 \times 0.85 + 100 \times 0.13 - 40 \times 0.85 - 20 \times 0.13 = 29.4^{\circ}\text{C}$$

$$T_j = T_{mb} + \Delta T_{j-mb} = 75 + 29.4 = 104.4^{\circ}\text{C}$$

Single Shot:

$$\Delta T_{j-mb@x} = 40 \times 0.13 + 20 \times 0.125 + 100 \times 0.04 - 40 \times 0.125 - 20 \times 0.04 = 5.9^{\circ}\text{C}$$

$$T_j = T_{mb} + \Delta T_{j-mb} = 75 + 5.9 = 80.9^{\circ}\text{C}$$

Hence the peak values of T_j are 104.4°C for the repetitive case, and 80.9°C for the single shot case.

Calculation for time t_y

$$\begin{aligned} \Delta T_{j-mb@y} = & P_2 \cdot Z_{thj-mb}(t5) + P_3 \cdot Z_{thj-mb}(t6) \\ & + P_1 \cdot Z_{thj-mb}(t8) - P_2 \cdot Z_{thj-mb}(t6) \\ & - P_3 \cdot Z_{thj-mb}(t7) \end{aligned} \quad 16$$

where $Z_{thj-mb}(t)$ is the transient thermal impedance for a pulse time t .

		t5 380µs	t6 250µs	t7 230µs	t8 10µs
Repetitive T=400µs	δ Z_{th}	0.950 1.950	0.625 1.300	0.575 1.250	0.025 0.080
Single Shot T=∞	δ Z_{th}	0.000 0.200	0.000 0.160	0.000 0.150	0.000 0.030

Table 1b. Composite pulse parameters for time t_y

Substituting these values into equation 16 for $T_{j-mb@y}$ gives

Repetitive: $\Delta T_{j-mb@y} = 20 \times 1.95 + 100 \times 1.3$
 $+ 40 \times 0.08 - 20 \times 1.3$
 $- 100 \times 1.25$
 $= 21.2^\circ\text{C}$
 $T_j = T_{mb} + \Delta T_{j-mb} = 75 + 21.2 = 96.2^\circ\text{C}$

Single Shot: $\Delta T_{j-mb@y} = 20 \times 0.2 + 100 \times 0.16$
 $+ 40 \times 0.03 - 20 \times 0.16$
 $- 100 \times 0.15$
 $= 3^\circ\text{C}$
 $T_j = T_{mb} + \Delta T_{j-mb} = 75 + 3 = 78^\circ\text{C}$

Hence the peak values of T_j are 96.2°C for the repetitive case, and 78°C for the single shot case.

The average power dissipation and the average junction temperature can be calculated as follows:

$$\begin{aligned} P_{av} &= \frac{25 \times 10 + 5 \times 130 + 20 \times 100}{400} \\ &= 7.25\text{W} \\ \Delta T_{j-mb(av)} &= P_{av} \times Z_{thj-mb}(\delta=1) = 7.25 \times 2 = 14.5^\circ\text{C} \\ T_{j(av)} &= T_{mb} + \Delta T_{j-mb(av)} = 75 + 14.5 = 89.5^\circ\text{C} \end{aligned}$$

Clearly, the junction temperature at time t_x should be higher than that at time t_y , and this is proven in the above calculations.

Burst pulses

Power devices are frequently subjected to a burst of pulses. This type of signal can be treated as a composite waveform and as in the previous example simulated by superimposing several rectangular pulses which have a common period, but both positive and negative amplitudes, in addition to suitable values of t_p and δ .

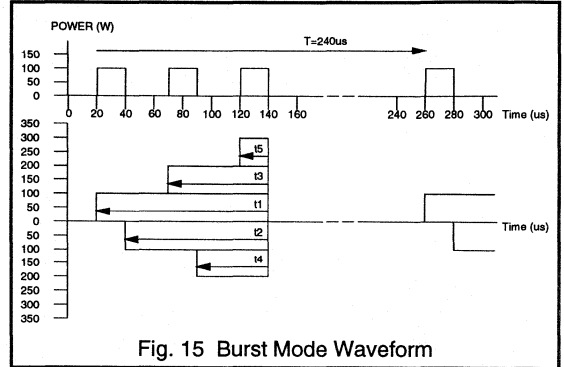


Fig. 15 Burst Mode Waveform

Consider the waveform shown in Fig. 15. The period is $240\mu\text{s}$, and the burst consists of three rectangular pulses of 100W power and $20\mu\text{s}$ duration, separated by $30\mu\text{s}$. The peak junction temperature will occur at the end of each burst at time $t_x = 140\mu\text{s}$. To be able to add the various effects of the pulses at this time, all the pulses, both positive and negative, must end at time t_x . Positive pulses increase the junction temperature, while negative pulses decrease it.

$$\begin{aligned} \Delta T_{j-mb@x} = & P \cdot Z_{thj-mb}(t1) + P \cdot Z_{thj-mb}(t3) \\ & + P \cdot Z_{thj-mb}(t5) - P \cdot Z_{thj-mb}(t2) \\ & - P \cdot Z_{thj-mb}(t4) \end{aligned} \quad 17$$

where $Z_{thj-mb}(t)$ is the transient thermal impedance for a pulse time t .

The Z_{th} values are taken from Fig. 9. For each term in the equation, the equivalent duty cycle must be worked out. These values can then be used in conjunction with Fig. 9 to find a value for Z_{th} . Table 2 gives the values calculated for this example.

		t1 120µs	t2 100µs	t3 70µs	t4 50µs	t5 20µs
Repetitive T=240µs	δ Z_{th}	0.500 1.100	0.420 0.800	0.290 0.600	0.210 0.430	0.083 0.210
Single Shot T=∞	δ Z_{th}	0.000 0.100	0.000 0.090	0.000 0.075	0.000 0.060	0.000 0.040

Table 2. Burst Mode pulse parameters

Substituting these values into equation 17 gives

Repetitive:

$$\begin{aligned} \Delta T_{j-mb@x} &= 100 \times 1.10 + 100 \times 0.60 \\ &+ 100 \times 0.21 - 100 \times 0.80 \\ &- 100 \times 0.43 \\ &= 68^\circ\text{C} \\ T_j &= 75 + 68 = 143^\circ\text{C} \end{aligned}$$

Single Shot:

$$\begin{aligned} \Delta T_{j-mb@x} &= 100 \times 0.10 + 100 \times 0.075 \\ &+ 100 \times 0.04 - 100 \times 0.09 \\ &- 100 \times 0.06 \\ &= 6.5^\circ\text{C} \\ T_j &= 75 + 6.5 = 81.5^\circ\text{C} \end{aligned}$$

Hence the peak value of T_j is 143°C for the repetitive case and 81.5°C for the single shot case. To calculate the average junction temperature $T_{j(av)}$:

$$\begin{aligned} P_{av} &= \frac{3 \times 100 \times 20}{240} \\ &= 25\text{W} \\ \Delta T_{j-mb(av)} &= P_{av} \times Z_{thj-mb(\delta=1)} = 25 \times 2 = 50^\circ\text{C} \\ T_{j(av)} &= 75 + 50 = 125^\circ\text{C} \end{aligned}$$

The above example for the repetitive waveform highlights a case where the average junction temperature (125°C) is well within limits but the composite pulse calculation shows the peak junction temperature to be significantly higher. For reasons of improved long term reliability it is usual to operate devices with a peak junction temperature below 125°C .

Non-rectangular pulses

So far, the worked examples have only covered rectangular waveforms. However, triangular, trapezoidal and sinusoidal waveforms are also common. In order to apply the above thermal calculations to non rectangular waveforms, the waveform is approximated by a series of rectangles. Each rectangle represents part of the waveform. The equivalent rectangle must be equal in area to the section of the waveform it represents (ie the same energy) and also be of the same peak power. With reference to Fig. 16, a triangular waveform has been approximated to one rectangle in the first example, and two rectangles in the second. Obviously, increasing the number of sections the waveform is split into will improve the accuracy of the thermal calculations.

In the first example, there is only one rectangular pulse, of duration $50\mu\text{s}$, dissipating 50W . So again using equation 14 and a rearrangement of equation 7:

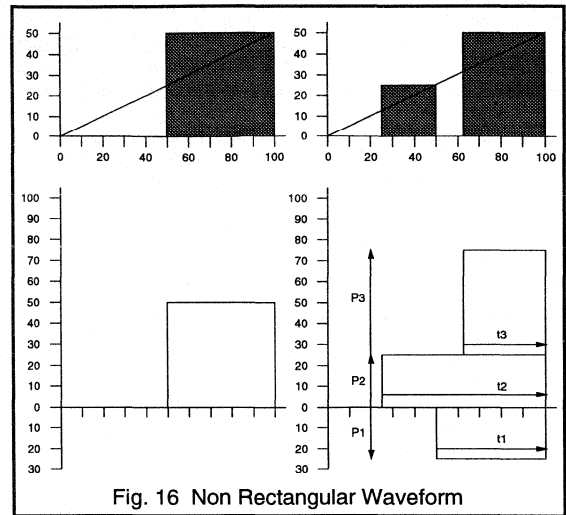


Fig. 16 Non Rectangular Waveform

$$\Delta T_{j-mb} = P_{totM} \times Z_{thj-mb}$$

Single Shot $\Delta T_{j-mb} = 50 \times 0.065 = 3.25^\circ\text{C}$
 $T_{jpeak} = 75 + 3.25 = 78.5^\circ\text{C}$

10% Duty cycle $\Delta T_{j-mb} = 50 \times 0.230 = 11.5^\circ\text{C}$
 $T_{jpeak} = 75 + 11.5 = 86.5^\circ\text{C}$

50% Duty cycle $\Delta T_{j-mb} = 50 \times 1.000 = 50^\circ\text{C}$
 $T_{jpeak} = 75 + 50 = 125^\circ\text{C}$

When the waveform is split into two rectangular pulses:

$$\Delta T_{j-mb} = P_3 \cdot Z_{thj-mb(t3)} + P_1 \cdot Z_{thj-mb(t1)} - P_2 \cdot Z_{thj-mb(t2)} \quad 18$$

For this example $P_1 = 25\text{W}$, $P_2 = 25\text{W}$, $P_3 = 50\text{W}$. Table 3 below shows the rest of the parameters:

		t1	t2	t3
		75μs	50μs	37.5μs
Single Shot $T=\infty$	D	0.000	0.000	0.000
	Z_{th}	0.085	0.065	0.055
10% Duty Cycle $T=1000\mu\text{s}$	D	0.075	0.050	0.037
	Z_{th}	0.210	0.140	0.120
50% Duty Cycle $T=200\mu\text{s}$	D	0.375	0.250	0.188
	Z_{th}	0.700	0.500	0.420

Table 3. Non Rectangular Pulse Calculations

Sustituting these values into equation 18 gives:

$$\begin{aligned} \text{Single shot} \quad \Delta T_{j-mb} &= 50 \times 0.055 + 25 \times 0.085 - 25 \times 0.065 \\ &= 3.25^\circ\text{C} \end{aligned}$$

$$T_{jpeak} = 75 + 3.25 = 78.5^\circ\text{C}$$

$$\begin{aligned} \text{10% Duty cycle} \quad \Delta T_{j-mb} &= 50 \times 0.12 + 25 \times 0.21 - 25 \times 0.14 \\ &= 7.75^\circ\text{C} \end{aligned}$$

$$T_{jpeak} = 75 + 7.75 = 82.5^\circ\text{C}$$

$$\begin{aligned} \text{50% Duty cycle} \quad \Delta T_{j-mb} &= 50 \times 0.42 + 25 \times 0.7 - 25 \times 0.5 \\ &= 26^\circ\text{C} \end{aligned}$$

$$T_{jpeak} = 75 + 26 = 101^\circ\text{C}$$

To calculate the average junction temperature:

$$\begin{aligned} \text{10% Duty Cycle} \quad P_{av} &= \frac{50 \times 50}{1000} \\ &= 2.5\text{W} \end{aligned}$$

$$\Delta T_{j-mb(av)} = P_{av} \times Z_{thj-mb(\delta=1)} = 2.5 \times 2 = 5^\circ\text{C}$$

$$T_{j(av)} = 75 + 5 = 80^\circ\text{C}$$

50% Duty Cycle

$$P_{av} = \frac{50 \times 50}{200}$$

$$= 12.5\text{W}$$

$$\Delta T_{j-mb(av)} = P_{av} \times Z_{thj-mb(\delta=1)} = 12.5 \times 2 = 25^\circ\text{C}$$

$$T_{j(av)} = 75 + 25 = 100^\circ\text{C}$$

Conclusion

A method has been presented to allow the calculation of average and peak junction temperatures for a variety of pulse types. Several worked examples have shown calculations for various common waveforms. The method for non rectangular pulses can be applied to any wave shape, allowing temperature calculations for waveforms such as exponential and sinusoidal power pulses. For pulses such as these, care must be taken to ensure that the calculation gives the peak junction temperature, as it may not occur at the end of the pulse. In this instance several calculations must be performed with different endpoints to find the maximum junction temperature.

7.1.2 Heat Dissipation

All semiconductor failure mechanisms are temperature dependent and so the lower the junction temperature, the higher the reliability of the circuit. Thus our data specifies a maximum junction temperature which should not be exceeded under the worst probable conditions. However, derating the operating temperature from T_{jmax} is always desirable to improve the reliability still further. The junction temperature depends on both the power dissipated in the device and the thermal resistances (or impedances) associated with the device. Thus careful consideration of these thermal resistances (or impedances) allows the user to calculate the maximum power dissipation that will keep the junction temperature below a chosen value.

The formulae and diagrams given in this section can only be considered as a guide for determining the nature of a heatsink. This is because the thermal resistance of a heatsink depends on numerous parameters which cannot be predetermined. They include the position of the transistor on the heatsink, the extent to which air can flow unhindered, the ratio of the lengths of the sides of the heatsink, the screening effect of nearby components, and heating from these components. It is always advisable to check important temperatures in the finished equipment under the worst probable operating conditions. The more complex the heat dissipation conditions, the more important it becomes to carry out such checks.

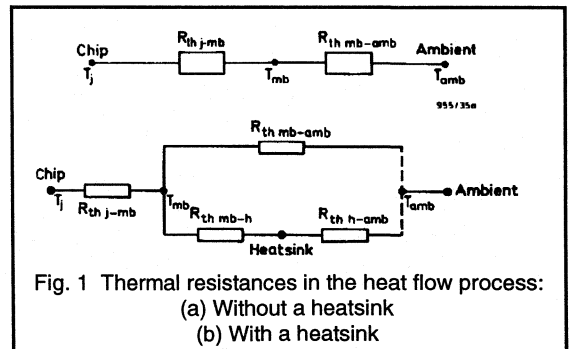
Heat flow path

The heat generated in a semiconductor chip flows by various paths to the surroundings. Small signal devices do not usually require heatsinking; the heat flows from the junction to the mounting base which is in close contact with the case. Heat is then lost by the case to the surroundings by convection and radiation (Fig. 1a). Power transistors, however, are usually mounted on heatsinks because of the higher power dissipation they experience. Heat flows from the transistor case to the heatsink by way of contact pressure, and the heatsink loses heat to the surroundings by convection and radiation, or by conduction to cooling water (Fig. 1b). Generally air cooling is used so that the ambient referred to in Fig.1 is usually the surrounding air. Note that if this is the air inside an equipment case, the additional thermal resistance between the inside and outside of the equipment case should be taken into account.

Contact thermal resistance $R_{th\ mb-h}$

The thermal resistance between the transistor mounting base and the heatsink depends on the quality and size of the contact areas, the type of any intermediate plates used, and the contact pressure. Care should be taken when drilling holes in heatsinks to avoid burring and distorting the

metal, and both mating surfaces should be clean. Paint finishes of normal thickness, up to 50 μm (as a protection against electrolytic voltage corrosion), barely affect the thermal resistance. Transistor case and heatsink surfaces can never be perfectly flat, and so contact will take place on several points only, with a small air-gap over the rest of the area. The use of a soft substance to fill this gap lowers the contact thermal resistance. Normally, the gap is filled with a heatsinking compound which remains fairly viscous at normal transistor operating temperatures and has a high thermal conductivity. The use of such a compound also prevents moisture from penetrating between the contact surfaces. Proprietary heatsinking compounds are available which consist of a silicone grease loaded with some electrically insulating good thermally conducting powder such as alumina. The contact thermal resistance $R_{th\ mb-h}$ is usually small with respect to $(R_{th\ j-mb} + R_{th\ h-amb})$ when cooling is by natural convection. However, the heatsink thermal resistance $R_{th\ h-amb}$ can be very small when either forced ventilation or water cooling are used, and thus a close thermal contact between the transistor case and heatsink becomes particularly important.



Thermal resistance calculations

Fig. 1a shows that, when a heatsink is not used, the total thermal resistance between junction and ambient is given by:

$$R_{thj-amb} = R_{thj-mb} + R_{thmb-amb} \quad 1$$

However, power transistors are generally mounted on a heatsink since $R_{thj-amb}$ is not usually small enough to maintain temperatures within the chip below desired levels.

Fig. 1b shows that, when a heatsink is used, the total thermal resistance is given by:

$$R_{thj-amb} = R_{thj-mb} + R_{thmb-h} + R_{thh-amb} \quad 2$$

Note that the direct heat loss from the transistor case to the surroundings through $R_{th\,mb-amb}$ is negligibly small.

The first stage in determining the size and nature of the required heatsink is to calculate the maximum heatsink thermal resistance $R_{th\,h-amb}$ that will maintain the junction temperature below the desired value

Continuous operation

Under dc conditions, the maximum heatsink thermal resistance can be calculated directly from the maximum desired junction temperature.

$$R_{th\,j-amb} = \frac{T_j - T_{amb}}{P_{tot(av)}} \quad 3$$

and

$$R_{th\,j-mb} = \frac{T_j - T_{mb}}{P_{tot(av)}} \quad 4$$

Combining equations 2 and 3 gives:

$$R_{th\,h-amb} = \frac{T_j - T_{amb}}{P_{tot(av)}} - R_{th\,j-mb} - R_{th\,mb-h} \quad 5$$

and substituting Eq 4 into Eq 5 gives:

$$R_{th\,h-amb} = \frac{T_{mb} - T_{amb}}{P_{tot(av)}} - R_{th\,mb-h} \quad 6$$

The values of $R_{th\,j-mb}$ and $R_{th\,mb-h}$ are given in the published data. Thus, either Eq. 5 or Eq.6 can be used to find the maximum heatsink thermal resistance.

Intermittent operation

The thermal equivalent circuits of Fig. 1 are inappropriate for intermittent operation, and the thermal impedance $Z_{th\,j-mb}$ should be considered.

$$P_{totM} = \frac{T_j - T_{mb}}{Z_{th\,j-mb}}$$

thus:

$$T_{mb} = T_j - P_{totM} \cdot Z_{th\,j-mb} \quad 7$$

The mounting-base temperature has always been assumed to remain constant under intermittent operation. This assumption is known to be valid in practice provided that the pulse time is less than about one second. The mounting-base temperature does not change significantly under these conditions as indicated in Fig. 2. This is because heatsinks have a high thermal capacity and thus a high thermal time-constant.

Thus Eq.6 is valid for intermittent operation, provided that the pulse time is less than one second. The value of T_{mb} can be calculated from Eq. 7, and the heatsink thermal resistance can be obtained from Eq.6.

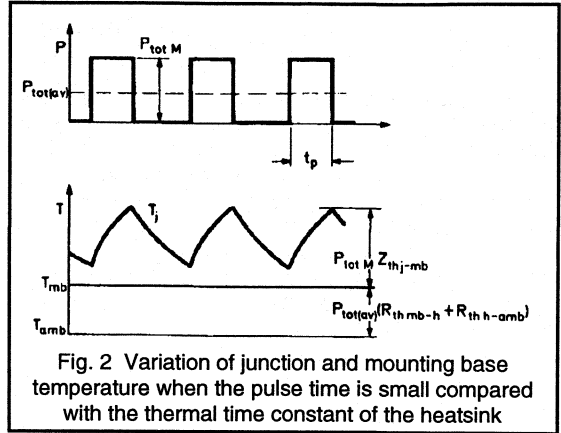


Fig. 2 Variation of junction and mounting base temperature when the pulse time is small compared with the thermal time constant of the heatsink

The thermal time constant of a transistor is defined as that time at which the junction temperature has reached 70% of its final value after being subjected to a constant power dissipation at a constant mounting base temperature.

Now, if the pulse duration t_p exceeds one second, the transistor is temporarily in thermal equilibrium since such a pulse duration is significantly greater than the thermal time-constant of most transistors. Consequently, for pulse times of more than one second, the temperature difference $T_j - T_{mb}$ reaches a stationary final value (Fig. 3) and Eq.7 should be replaced by:

$$T_{mb} = T_j - P_{totM} \cdot R_{th\,j-mb} \quad 8$$

In addition, it is no longer valid to assume that the mounting base temperature is constant since the pulse time is also no longer small with respect to the thermal time constant of the heatsink.

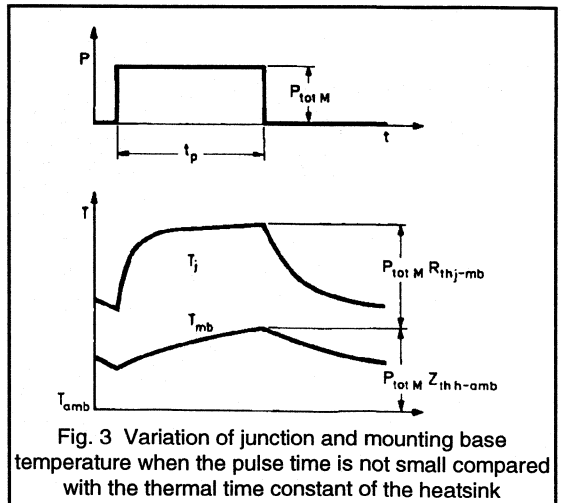


Fig. 3 Variation of junction and mounting base temperature when the pulse time is not small compared with the thermal time constant of the heatsink

Smaller heatsinks for intermittent operation

In many instances, the thermal capacity of a heatsink can be utilised to design a smaller heatsink for intermittent operation than would be necessary for the same level of continuous power dissipation. The average power dissipation in Eq.6 is replaced by the peak power dissipation to obtain the value of the thermal impedance between the heatsink and the surroundings

$$Z_{thh-amb} = \frac{T_{mb} - T_{amb}}{P_{totM}} - R_{thmb-h} \quad 9$$

The value of $Z_{thh-amb}$ will be less than the comparable thermal resistance and thus a smaller heatsink can be designed than that obtained using the too large value calculated from Eq.6.

Heatsinks

Three varieties of heatsink are in common use: flat plates (including chassis), diecast finned heatsinks, and extruded finned heatsinks. The material normally used for heatsink construction is aluminium although copper may be used with advantage for flat-sheet heatsinks. Small finned clips are sometimes used to improve the dissipation of low-power transistors.

Heatsink finish

Heatsink thermal resistance is a function of surface finish. A painted surface will have a greater emissivity than a bright unpainted one. The effect is most marked with flat plate heatsinks, where about one third of the heat is dissipated by radiation. The colour of the paint used is relatively unimportant, and the thermal resistance of a flat plate heatsink painted gloss white will be only about 3% higher than that of the same heatsink painted matt black. With finned heatsinks, painting is less effective since heat radiated from most fins will fall on adjacent fins but it is still worthwhile. Both anodising and etching will decrease the thermal resistivity. Metallic type paints, such as aluminium paint, have the lowest emissivities, although they are approximately ten times better than a bright aluminium metal finish.

Flat-plate heatsinks

The simplest type of heatsink is a flat metal plate to which the transistor is attached. Such heatsinks are used both in the form of separate plates and as the equipment chassis itself. The thermal resistance obtained depends on the thickness, area and orientation of the plate, as well as on the finish and power dissipated. A plate mounted horizontally will have about twice the thermal resistance of a vertically mounted plate. This is particularly important where the equipment chassis itself is used as the heatsink.

In Fig. 4, the thermal resistance of a blackened heatsink is plotted against surface area (one side) with power dissipation as a parameter. The graph is accurate to within 25% for nearly square plates, where the ratio of the lengths of the sides is less than 1.25:1.

Finned heatsinks

Finned heatsinks may be made by stacking flat plates, although it is usually more economical to use ready made diecast or extruded heatsinks. Since most commercially available finned heatsinks are of reasonably optimum design, it is possible to compare them on the basis of the overall volume which they occupy. This comparison is made in Fig. 5 for heatsinks with their fins mounted vertically; again, the graph is accurate to 25%.

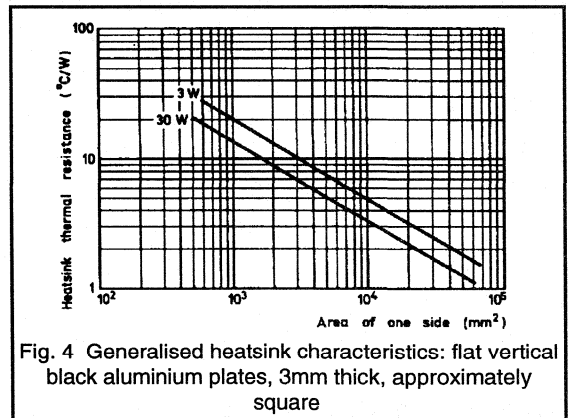


Fig. 4 Generalised heatsink characteristics: flat vertical black aluminium plates, 3mm thick, approximately square

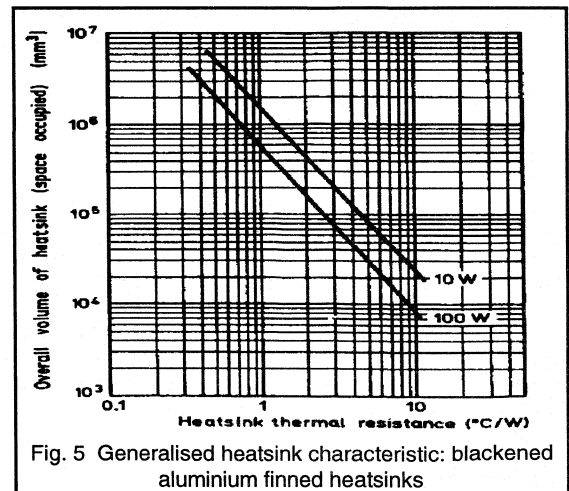


Fig. 5 Generalised heatsink characteristic: blackened aluminium finned heatsinks

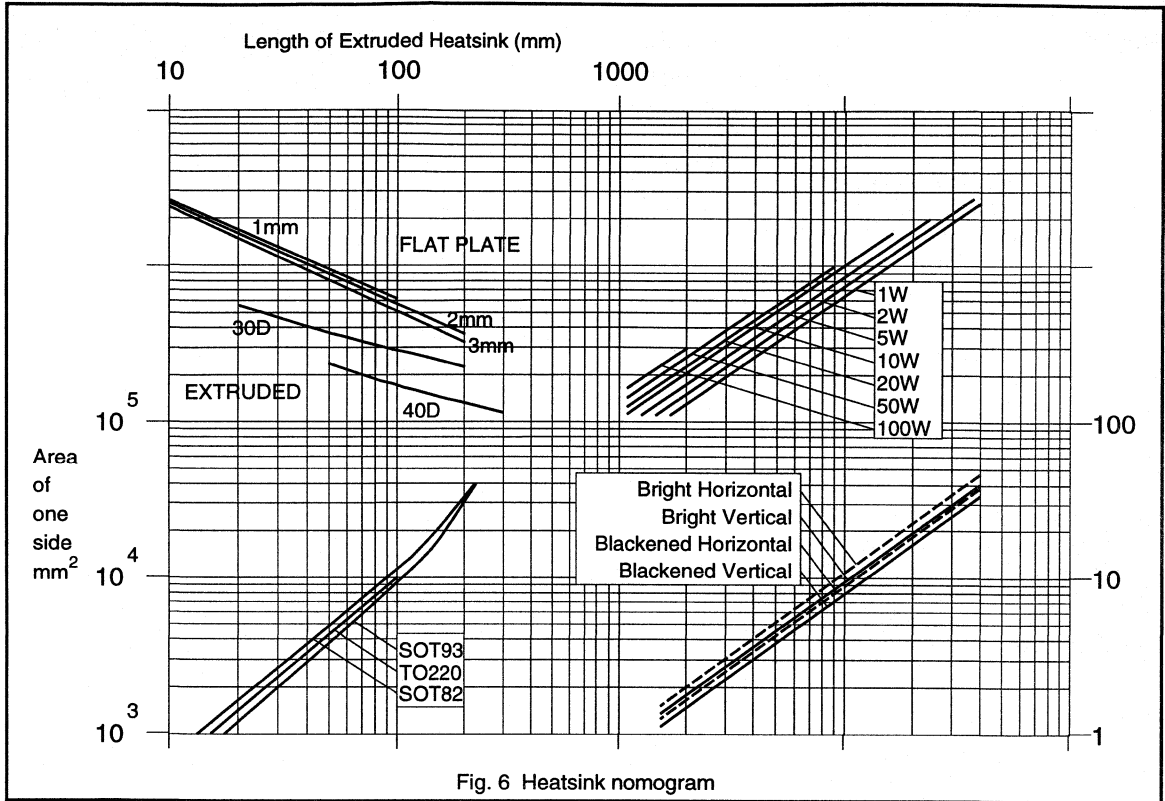


Fig. 6 Heatsink nomogram

Heatsink dimensions

The maximum thermal resistance through which sufficient power can be dissipated without damaging the transistor can be calculated as discussed previously. This section explains how to arrive at a type and size of heatsink that gives a sufficiently low thermal resistance.

Natural air cooling

The required size of aluminium heatsinks - whether flat or extruded (finned) can be derived from the nomogram in Fig. 6. Like all heatsink diagrams, the nomogram does not give exact values for $R_{th\ h-amb}$ as a function of the dimensions since the practical conditions always deviate to some extent from those under which the nomogram was drawn up. The actual values for the heatsink thermal resistance may differ by up to 10% from the nomogram values. Consequently, it is advisable to take temperature measurements in the finished equipment, particularly where the thermal conditions are critical.

The conditions to which the nomogram applies are as follows:

- natural air cooling (unimpeded natural convection with no build up of heat);
- ambient temperature about 25°C, measured about 50mm below the lower edge of the heatsink (see Fig. 7);
- atmospheric pressure about 10 N/m²;
- single mounting (that is, not affected by nearby heatsinks);
- distance between the bottom of the heatsink and the base of a draught-free space about 100mm (see Fig. 7);
- transistor mounted roughly in the centre of the heatsink (this is not so important for finned heatsinks because of the good thermal conduction).

The appropriately-sized heatsink is found as follows.

1. Enter the nomogram from the right hand side of section 1 at the appropriate $R_{th\ h-amb}$ value (see Fig. 8). Move horizontally to the left, until the appropriate curve for orientation and surface finish is reached.
2. Move vertically upwards to intersect the appropriate power dissipation curve in section 2.

3. Move horizontally to the left into section 3 for the desired thickness of a flat-plate heatsink, or the type of extrusion.
4. If an extruded heatsink is required, move vertically upwards to obtain its length (Figs. 9a and 9b give the outlines of the extrusions).
5. If a flat-plate heatsink is to be used, move vertically downwards to intersect the appropriate curve for envelope type in section 4.
6. Move horizontally to the left to obtain heatsink area.
7. The heatsink dimensions should not exceed the ratio of 1.25:1.

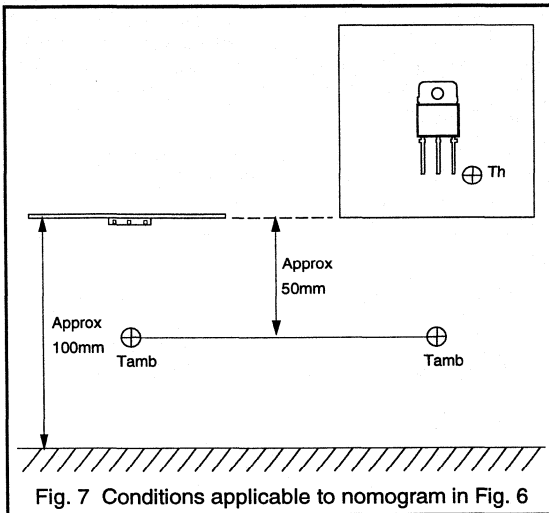


Fig. 7 Conditions applicable to nomogram in Fig. 6

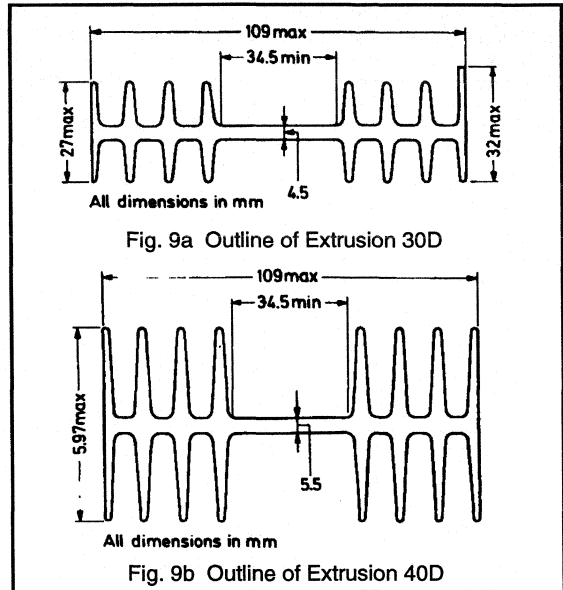


Fig. 9a Outline of Extrusion 30D

Fig. 9b Outline of Extrusion 40D

The curves in section 2 take account of the non linear nature of the relationship between the temperature drop across the heatsink and the power dissipation loss. Thus, at a constant value of the heatsink thermal resistance, the greater the power dissipation, the smaller is the required size of heatsink. This is illustrated by the following example.

Example

An extruded heatsink mounted vertically and with a painted surface is required to have a maximum thermal resistance of $R_{th\ h-amb} = 2.6\ ^\circ\text{C}/\text{W}$ at the following powers:

$$(a) P_{tot(av)} = 5W \quad (b) P_{tot(av)} = 50W$$

Enter the nomogram at the appropriate value of the thermal resistance in section 1, and via either the 50W or 5W line in section 2, the appropriate lengths of the extruded heatsink 30D are found to be:

$$(a) \text{ length} = 110\text{mm} \text{ and } (b) \text{ length} = 44\text{mm}.$$

Case (b) requires a shorter length since the temperature difference is ten times greater than in case (a).

As the ambient temperature increases beyond 25°C , so does the temperature of the heatsink and thus the thermal resistance (at constant power) decreases owing to the increasing role of radiation in the heat removal process. Consequently, a heatsink with dimensions derived from Fig. 6 at $T_{amb} > 25^\circ\text{C}$ will be more than adequate. If the maximum ambient temperature is less than 25°C , then the thermal resistance will increase slightly. However, any

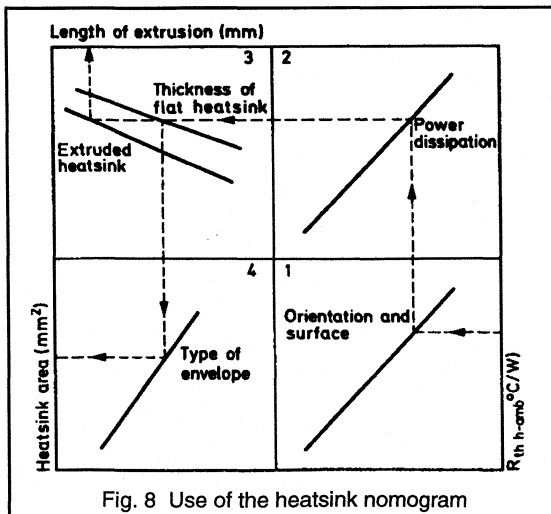


Fig. 8 Use of the heatsink nomogram

increase will lie within the limits of accuracy of the nomogram and within the limits set by other uncertainties associated with heatsink calculations.

For heatsinks with relatively small areas, a considerable part of the heat is dissipated from the transistor case. This is why the curves in section 4 tend to flatten out with decreasing heatsink area. The area of extruded heatsinks is always large with respect to the surface of the transistor case, even when the length is small.

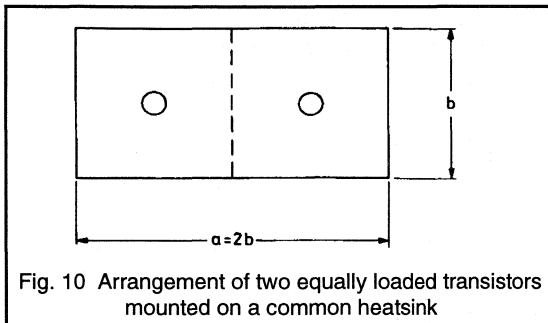


Fig. 10 Arrangement of two equally loaded transistors mounted on a common heatsink

If several transistors are mounted on a common heatsink, each transistor should be associated with a particular section of the heatsink (either an area or length according to type) whose maximum thermal resistance is calculated from equations 5 or 6; that is, without taking the heat produced by nearby transistors into account. From the sum

of these areas or lengths, the size of the common heatsink can then be obtained. If a flat heatsink is used, the transistors are best arranged as shown in Fig. 10. The maximum mounting base temperatures of transistors in such a grouping should always be checked once the equipment has been constructed.

Forced air cooling

If the thermal resistance needs to be much less than 1°C/W , or the heatsink not too large, forced air cooling by means of fans can be provided. Apart from the size of the heatsink, the thermal resistance now only depends on the speed of the cooling air. Provided that the cooling air flows parallel to the fins and with sufficient speed ($>0.5\text{m/s}$), the thermal resistance hardly depends on the power dissipation and the orientation of the heatsink. Note that turbulence in the air current can result in practical values deviating from theoretical values.

Fig. 11 shows the form in which the thermal resistances for forced air cooling are given in the case of extruded heatsinks. It also shows the reduction in thermal resistance or length of heatsink which may be obtained with forced air cooling.

The effect of forced air cooling in the case of flat heatsinks is seen from Fig. 12. Here, too, the dissipated power and the orientation of the heatsink have only a slight effect on the thermal resistance, provided that the air flow is sufficiently fast.

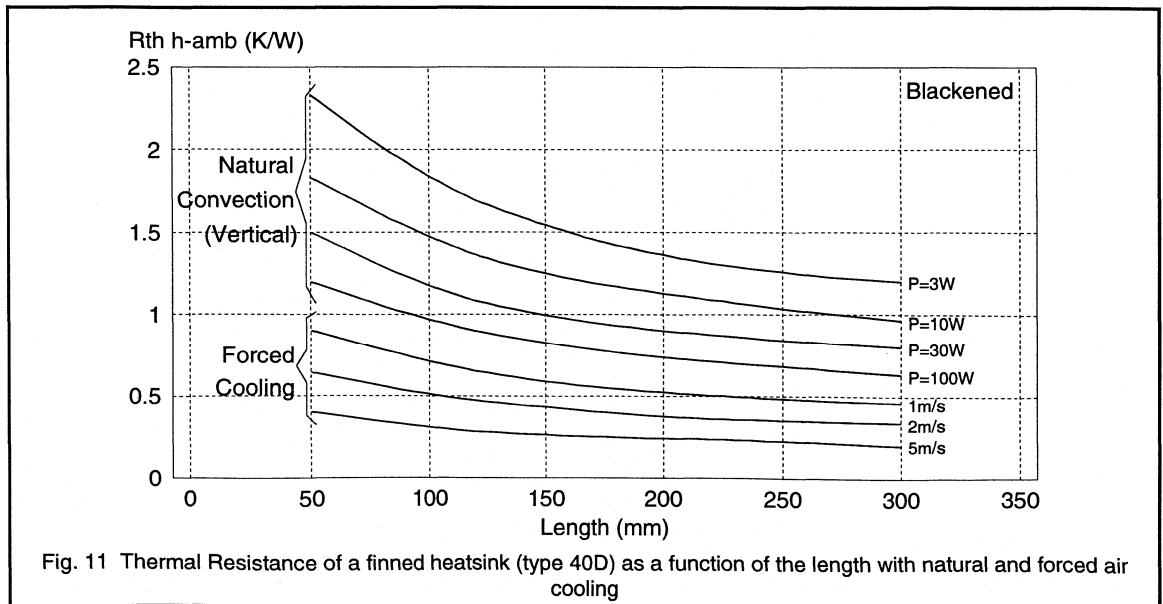


Fig. 11 Thermal Resistance of a finned heatsink (type 40D) as a function of the length with natural and forced air cooling

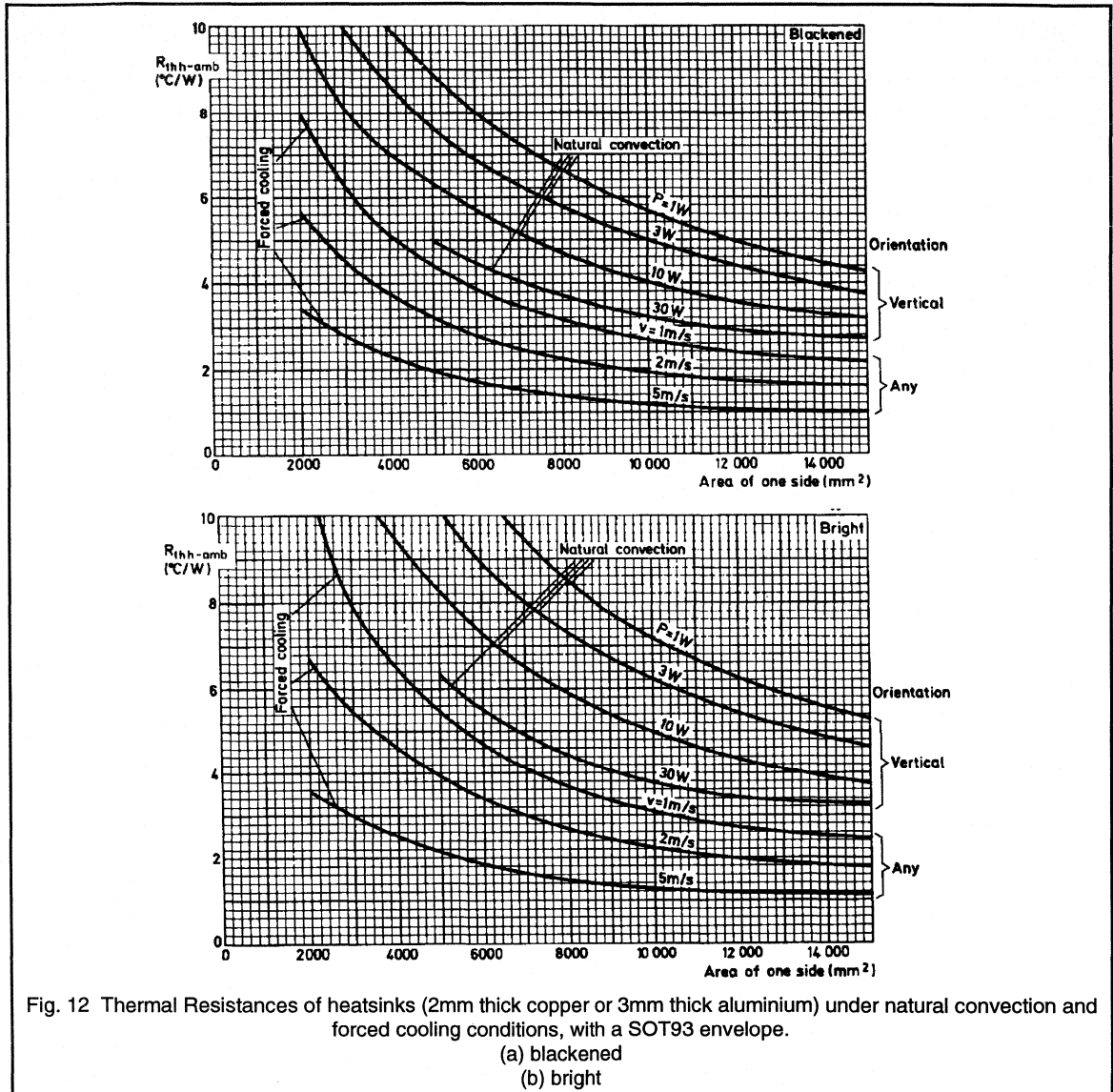


Fig. 12 Thermal Resistances of heatsinks (2mm thick copper or 3mm thick aluminium) under natural convection and forced cooling conditions, with a SOT93 envelope.

(a) blackened
(b) bright

Summary

The majority of power transistors require heatsinking, and once the maximum thermal resistance that will maintain the device's junction temperature below its rating has been calculated, a heatsink of appropriate type and size can be chosen. The practical conditions under which a transistor will be operated are likely to differ from the theoretical

considerations used to determine the required heatsink, and thus temperatures should always be checked in the finished equipment. Finally, some applications require a small heatsink, or one with a very low thermal resistance, in which case forced air cooling by means of fans should be provided.

CHAPTER 8

Lighting

8.1 Fluorescent Lamp Control

Fluorescent Lamp Control

8.1.1 Efficient Fluorescent Lighting using Electronic Ballasts

This section provides a general background to fluorescent lamps and their control requirements, with emphasis placed on high frequency electronic ballasts and their advantages over conventional 50/60Hz "magnetic" ballasts. Simplified examples of popular electronic ballast topologies suitable for low cost / economy applications are introduced.

The fluorescent lamp.

A fluorescent tube is a low pressure mercury vapour discharge lamp containing an inert gas consisting of argon or krypton at low pressure (below 1 atmosphere) plus a small measured dose of mercury. There is a filament at each end which, when hot, emit electrons to sustain the discharge when the lamp is operating. The mercury vapour discharge produces ultraviolet light which is converted to visible light by the phosphors coating the inside of the glass tube. The glass blocks the exit of the ultraviolet radiation but allows the visible radiation through. See Fig. 1.

Fluorescent tubes exist in many shapes and sizes. Apart from the many compact types that have appeared on the market in recent years as energy efficient replacements for incandescent lamps, the traditional linear tubes range from 150mm 4W up to the very high output 2400mm 215W.

Modern fluorescent tubes incorporating the latest triphosphor technology (i.e. red, green and blue phosphors similar to those used in modern high brightness television picture tubes) possess efficacies of around 80 lumens per lamp Watt compared with 68 lumens per lamp Watt for the older most efficient "white" fluorescent tubes and around 12 lumens per Watt for an incandescent bulb. Moreover, the triphosphor lamps reveal colour and skin tones more accurately than the standard "white" lamps, which suffer from a deficiency in output at the red end of the spectrum. This results in a greenish hue and a suppression of red colours from anything illuminated by them.

The elimination of the traditional causes of criticism for fluorescent lighting means that this form of lighting is becoming more acceptable in wider applications than ever before. Adjustment of the ratios of the three phosphors can create colour appearances from a very warm, intimate, incandescent equivalent colour temperature of 2700K through the cool, clean, businesslike 4000K to the very cool daylight colour temperature of 6500K, all with high efficacies and good colour rendering properties. Before the availability of triphosphors, these qualities have always been mutually exclusive. You could either have high efficacy and poor colour rendering or poor efficacy and good colour rendering, but not both.

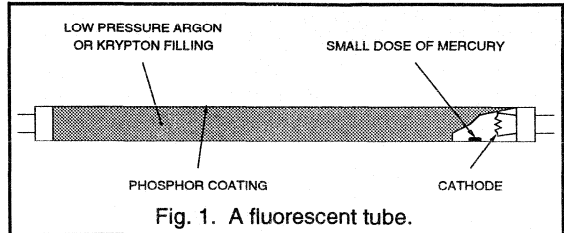


Fig. 1. A fluorescent tube.

A non-operating fluorescent tube will appear as an open circuit, since there is no electrical connection from one end to the other. In order to "strike the arc", a high voltage must be applied across the lamp in order to ionise the gas within. This will instantly "cold start" the lamp and shorten its life by sputtering electron-emitting material from its cathodes.

However, if the cathodes (heaters) are first preheated to generate a space charge of electrons at each end of the lamp, the strike voltage is considerably reduced and lamp life will not be unduly compromised by the start-up.

As soon as arc current flows, the lamp's electrical impedance will drop. It now exhibits a negative impedance characteristic, where an increase in current is accompanied by a reduction in lamp voltage. There must therefore be a current limiting device in circuit to prevent the rapid onset of runaway and destruction of the lamp.

The lamp running current should ideally be sinusoidal to minimise the radiation of electromagnetic interference from the lamp and its supply wires. Sinusoidal lamp current also maximises lamp life. A peak current approaching twice the RMS current will prematurely deplete the electron emitting material from the lamp cathodes. (For a sinewave the peak value is only 1.414 times the RMS value.)

There should also be no D.C. component to the lamp current; that is, the positive and negative half cycles should be of equal duration. If this is not the case, the resulting partial rectification will result in premature depletion of the electron emitter from one of the lamp cathodes.

The ballast.

The requirements of a fluorescent lamp ballast are to:

- Preheat the cathodes to induce electron emission.
- Provide the starting voltage to initiate the discharge.
- Limit the running current to the correct value.

There are several types of mains frequency "magnetic" ballast available. By far the most common circuit for 230V mains supplies has traditionally been the switchstart ballast (see Fig. 2), where lamp ballasting is provided by the choke. Other circuits include, in order of popularity, the semi-resonant circuit and the quickstart circuit.

The switchstart circuit has been widely adopted because of its simplicity, low cost and improved efficiency when compared with the alternative options mentioned above. Another reason is that the 230V mains voltage is sufficiently higher than the tube running voltage to allow the use of the simple series impedance ballast in almost all cases. Where this is not possible, for example in most 120V supplied circuits, the lamp is controlled by a quickstart circuit incorporating voltage step-up.

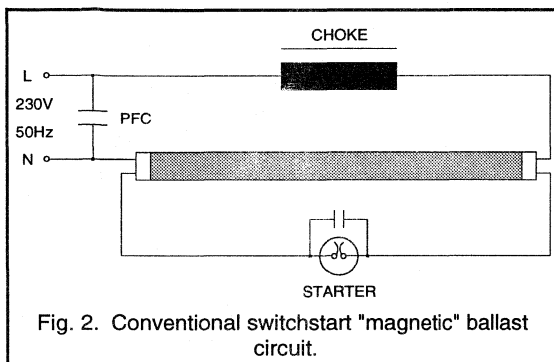


Fig. 2. Conventional switchstart "magnetic" ballast circuit.

Switchstart ballast operation.

When the voltage is applied to the circuit, the lamp does not operate at first, so the full mains voltage appears across the starter via the choke and lamp cathodes.

The starter consists of bi metallic contacts sealed within a small discharge bulb with an inert gas filling such as argon or neon. The mains voltage causes a glow discharge within the starter which heats up the bi metallic contacts, causing them to close. This completes the circuit and allows preheat current to flow through the choke and both cathodes.

Since the glow discharge within the starter has now ceased, the bi metallic contacts cool down and open. Because the inductance of the choke tries to maintain current flow, the voltage across the lamp rises rapidly and strikes the lamp. If it does not, the starter's contacts close again and the cycle repeats.

Once the lamp has started, the choke controls its current and voltage to the correct levels. The lamp running current is enough to keep the cathodes (heaters) hot and emitting electrons without the need for separate heater supplies, which would otherwise be wasteful of energy. Since the lamp's running voltage is much lower than the mains voltage, there is now not enough voltage to cause a glow discharge in the starter, so it remains open circuit.

The power factor correction (PFC) capacitor draws leading current from the mains to compensate for the lagging current drawn by the lamp circuit.

Why electronic ballasts?

Electronic ballasts have been available for well over a decade. Recent leaps in performance, coupled with ever increasing energy costs, the increased awareness of the advantages they offer, the increasing environmental awareness of the consumer, and the increased acceptability of the new fluorescent light sources in existing and new applications, have seen an upsurge in electronic ballast use since the beginning of the 1990's.

Replacing the most efficient low loss mains frequency switchstart ballast with an electronic ballast leads to reduced energy consumption and improved performance. The reasons for this are detailed below.

Increased light output.

If the operating frequency is increased from 50Hz to above the audible limit of 20kHz, fluorescent lamps can produce around 10% more light for the same input power (see Fig. 3). Alternatively, the input power can be reduced for the same light output.

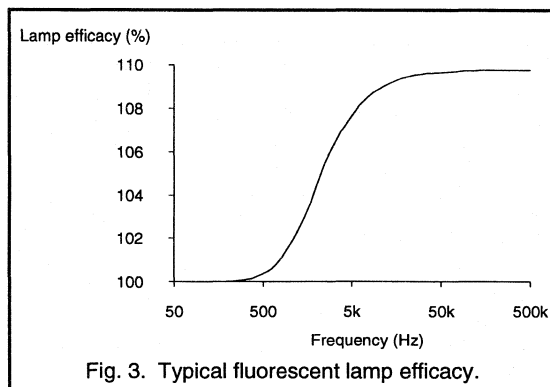


Fig. 3. Typical fluorescent lamp efficacy.

Flicker eliminated.

A fluorescent lamp operating at 50/60Hz will extinguish twice every cycle as the mains sinewave passes through zero. This produces 100/120Hz flicker which is noticeable or irritating to some people. It will also produce the well-known and potentially dangerous stroboscopic effects on rotating machinery.

If the lamp is operated at high frequency, however, it produces continuous light. This is because the time constant and hence the response time of the discharge is too slow for the lamp to have a chance to extinguish during each cycle.

The output waveform of an electronic ballast will usually be slightly modulated by 100/120Hz "ripple". Provided this is kept to a reasonable level by filtering within the ballast, the drawbacks associated with 100/120Hz flicker are eliminated.

Audible noise eliminated.

Since electronic ballasts operate above the audible range, they do not suffer from the audible noise problems that can occur with mains frequency magnetic ballasts. The familiar buzzing noise is caused by vibrations in the laminations and coil of the choke. This can then excite vibrations in the steel body of the fitting which effectively amplifies the original noise.

Lower ballast power.

An electronic ballast will consume less power and therefore dissipate less heat than a mains frequency magnetic ballast. For example, for two 1500mm 58W energy-saving lamps, the typical ballast power dissipation might be 13W per ballast for two 50Hz magnetic ballasts compared with 9W for a single electronic ballast driving two lamps.

The energy-saving benefits of electronic ballasts have made it possible to obtain the same light output from fluorescent lamps as would be obtained using a conventional 50/60Hz magnetic ballast, for a total circuit power (i.e. lamp and ballast) that is actually less than the rated lamp power alone. This is due to two reasons.

Firstly, the lamp can be underrun at high frequency for the same light output. Secondly, the power consumed by the ballast can be so low that the total circuit power is still less than the rated power printed on the lamp. Because of this, energy cost reductions of 20 - 25% are achievable.

Extended lamp life.

An electronic ballast which "soft starts" the lamp (i.e. provides preheat to the cathodes before applying a controlled starting pulse) will dislodge a minimum quantity of material from the cathodes during starting. This will give longer lamp life when compared to the uncontrolled impulses to which the lamp is subjected in a switchstart circuit.

Versatile lamp control.

Electronic ballasts are available which permit lamp dimming. This gives substantial energy savings in situations where the lights are linked to an automatic control system which detects ambient light levels and adjusts lamp

output to maintain a constant level of illumination. Lights may also be programmed to dim during intervals when areas are not in use, for example during lunch breaks.

Electronic ballasts can incorporate feedback to detect the operating conditions of the lamp(s) so that failed lamps can be switched off to avoid annoying flicker and possible ballast damage. They can also incorporate regulation, whereby a constant light output is maintained over a range of input voltages. Operation can be either from AC or DC supplies for emergency lighting applications.

Compact and light weight.

Owing to the high frequency of operation, the magnetic components in an electronic ballast are compact and lightweight with cores of ferrite material, whereas at mains frequency the ballast choke must be larger and heavier with bulkier copper windings and a core of laminated steel.

The shape and geometry of a mains frequency choke is determined by magnetic efficiency requirements, whereas the circuitry within an electronic ballast can be arranged to produce a very slim final package. This permits new levels of slimness and compactness for the final ballast.

Electronic ballast topologies.

The typical building blocks of an electronic ballast are shown in Fig. 4.

An increasing number of electronic ballasts are employing active power factor correction in the form of a boost converter between the rectifier and DC filter stages. (Figure 5 shows a simplified boost converter arrangement.) This obliges the ballast to draw current over most of each mains half cycle instead of the usual current spike that a rectifier / DC filter would demand at each peak of the voltage waveform. This reduces the harmonic content of the current and improves the power factor. It will also reduce the size of the electromagnetic interference (EMI) filter required, since filtering is now required at the higher harmonic frequencies of the boost converter switching frequency instead of at the mains frequency and harmonics of it.

Electronic ballasts take many forms. The simplest and most economical form might consist of a free-running self-oscillating circuit using bipolar transistors. This would be an open loop circuit (i.e. no feedback to detect lamp operating conditions).

More expensive options might contain a controlled oscillator in a closed loop circuit using MOSFETs. Here, features could include regulation for varying AC and DC supply voltages, adjustable lamp brightness, soft starting and a mechanism to detect and shut down failed lamps.

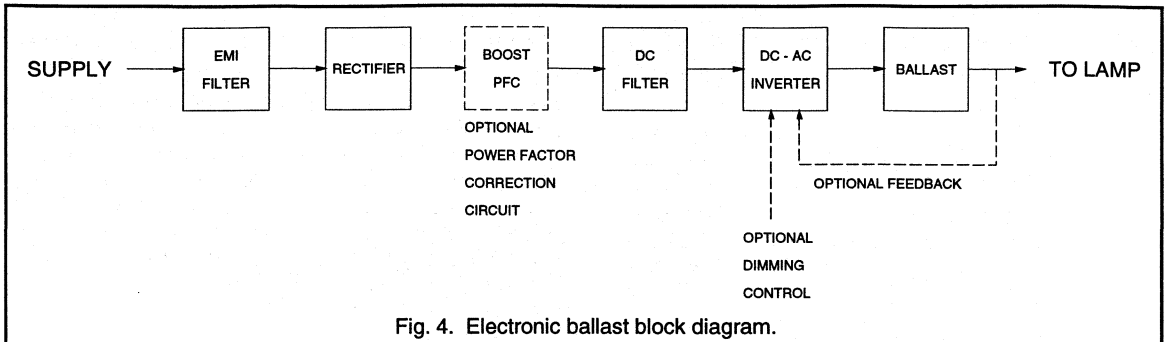


Fig. 4. Electronic ballast block diagram.

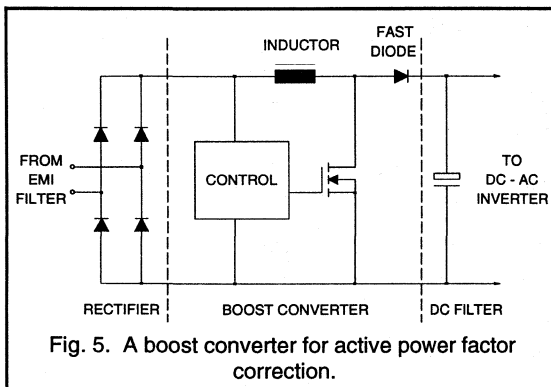


Fig. 5. A boost converter for active power factor correction.

The flyback inverter.

The most basic form of electronic ballast uses the flyback inverter as shown in Fig. 6. Its use is restricted mainly to low voltage DC, low power ballasts as used in handlamps, leisure lighting and emergency lighting. The arrangement might typically be used to operate tubes of 4W to 13W ratings only because of the excessive voltage and current stresses and switching losses that would be experienced by the transistor in higher power mains voltage versions.

Voltage step-up to drive the lamp from the low voltage supply is achieved by the turns ratio of the transformer primary and secondary, while oscillation is maintained by the positive feedback supplied by the auxiliary winding connected to the transistor's base. The values of R and C, in combination with the transformer's primary inductance, set the oscillation frequency and the mark / space ratio of the switching (which should be 1:1 for the reason given in the first section).

Lamp current limiting (or ballasting) is provided by the partial magnetic coupling of the transformer's primary winding to its secondary winding, giving rise to a leakage inductance. This circuit is only suitable for the applications

mentioned because, since it is a non-resonant circuit and no output waveform shaping is provided, the lamp current is spiky and rich in harmonics.

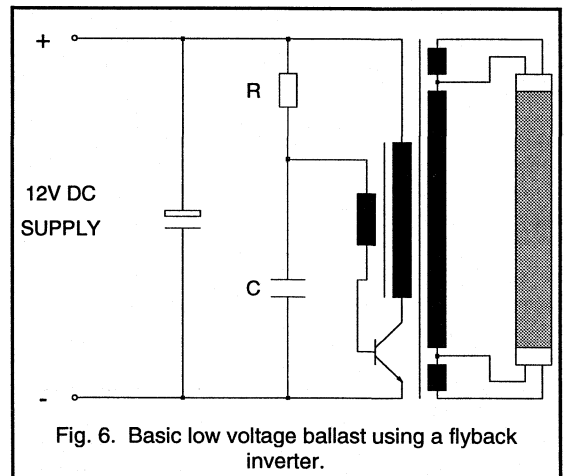


Fig. 6. Basic low voltage ballast using a flyback inverter.

Mains powered electronic ballasts, on the other hand, almost always use two switching power transistors in a push pull or half bridge configuration. This can either be a self oscillating or a driven oscillator circuit. The driven oscillator option permits easier lamp control and dimming. The self oscillating option has cost advantages where the benefits of high frequency lighting are required without the necessity for lamp dimming.

The push pull inverter.

A push pull circuit can appear as a voltage fed inverter with series resonant load or a current fed inverter with parallel resonant load. In both cases a centre tapped transformer is required.

Voltage fed push pull inverter.

Figure 7 shows a simplified circuit. This example provides isolation of the output from the mains supply with a separate secondary winding.

In the voltage fed arrangement, the D.C. rail voltage is fed straight to the centre tap. Both ends of the winding are connected to zero volts via transistors, which are alternately switched on during operation. The alternate passage of current in opposite directions through each half of the primary winding induces a square wave voltage across the secondary.

Since the full D.C. rail voltage appears across half the primary winding at a time, twice this voltage will appear across the whole primary winding. This means that during each transistor's "off" period, it will experience a maximum theoretical V_{CE} of $2 \times$ D.C. rail voltage.

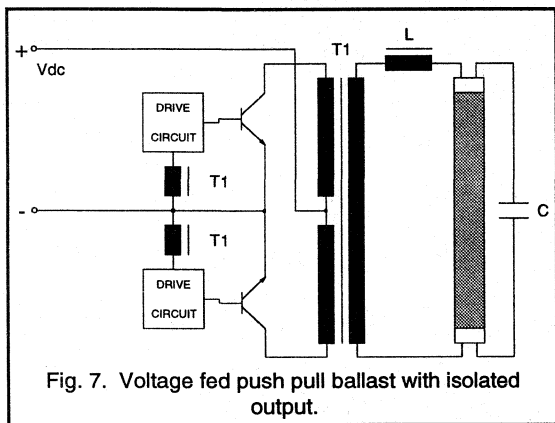


Fig. 7. Voltage fed push pull ballast with isolated output.

When power is first applied, the secondary voltage should not be high enough to cold start the lamp, which should remain in the high impedance state. The only current flowing will be through the series resonant combination of L & C , and both lamp cathodes. This preheat current will be enough to initiate electron emission from the cathodes which will in turn lower the lamp striking voltage to a point where the voltage across the capacitor can then start the lamp (usually within a second).

After starting, the lamp voltage will drop and the current will be limited and filtered by L . C will help to filter out residual harmonic frequencies and its current will fall to negligible proportions at the fundamental operating frequency. The resulting lamp current will closely resemble a sinewave.

The transistor base drives are derived from auxiliary windings on the transformer which provide the necessary positive feedback. An advantage with this transformer-based arrangement is the isolation it provides between the lamp and the mains supply.

Current fed parallel resonant push pull inverter.

The main difference with this circuit over the previous one is that the D.C. rail voltage is fed to the transformer centre tap via an inductor which acts as a current source. A capacitor C across the transformer primary forms a parallel resonant load in combination with the primary winding inductance (see Fig. 8). Instead of a square wave as in the voltage fed circuit, a full wave rectified sinewave appears at the centre tap whose theoretical peak amplitude is $\pi/2 \times V_{DC}$. Twice this amplitude appears across the whole winding for the same reason as in the voltage fed push pull circuit. Therefore the maximum theoretical $V_{CE} = \pi \times V_{DC}$.

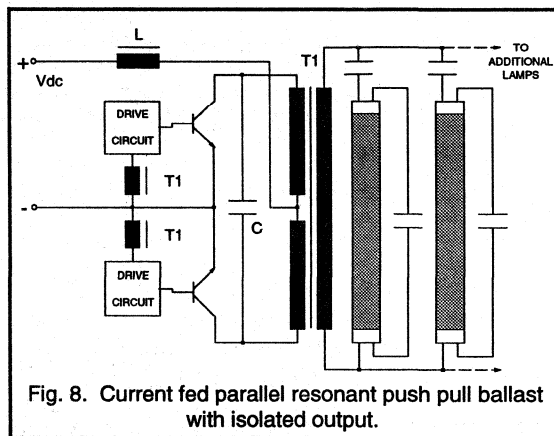


Fig. 8. Current fed parallel resonant push pull ballast with isolated output.

Since each successive half sine produces current flow in opposite directions through the two half windings, a sinewave is produced across the whole winding whose peak to peak amplitude is $2\pi \times V_{DC}$.

The additional cost of the inductor might be regarded as a disadvantage. However, the beauty of current fed parallel resonant circuits, of which this is one example, is that they naturally produce a sinusoidal output, so selection of the ballast components for their harmonic filtering properties is no longer so important. This allows the use of a series ballast capacitor instead of the series L normally required.

Another benefit with this type of circuit is its ability to continue normal operation with varying or open circuit loads. This permits independent operation of parallel-connected lamps across the secondary, each with its own ballast capacitor, where failure of one or more lamps will not affect the operation of the remaining lamps. This is unlike series-connected lamps, where the failure of one tube will disable all the tubes on that ballast.

Sinusoidal output topologies are very popular in the self oscillating low cost ballast market because of these advantages and the circuit simplicity.

The half bridge inverter.

The half bridge topology contains two npn transistors connected in series across the D.C. rail with the load connected to their mid point. The half bridge is so called because the return path for the load current is provided by two series-connected capacitors across the D.C. rail. (A full bridge circuit would have transistors in these positions also, but this arrangement is rarely used in electronic ballasts for fluorescent lamps. Although the required voltage rating of the transistors would be halved, this would not compensate for the increased cost of four power transistors instead of two, and the extra complication of controlling the timing of the switching of all four transistors.)

The two capacitors, which have a very low reactance and are essentially a short circuit at the ballast operating frequency, create a mid-point A.C. reference between the D.C. rails. This blocks the D.C. offset equal to half the rail voltage that would be applied to the lamp if the return path were merely taken to one of the rails.

Current fed parallel resonant half bridge inverter.

Figure 9 shows the simplified circuit. Transformer isolation is provided, and the sinusoidal output permits the use of ballast capacitors as for the current fed push pull topology. The series inductance L in each power supply line acts as the current source.

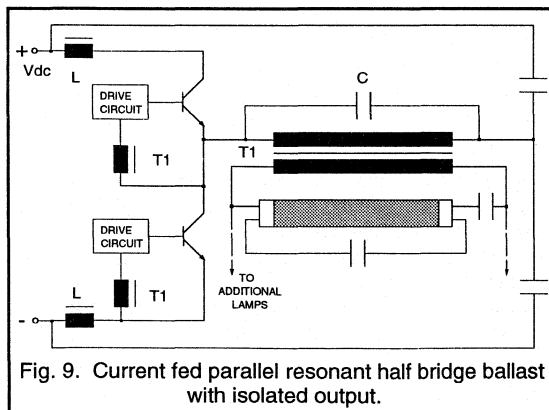


Fig. 9. Current fed parallel resonant half bridge ballast with isolated output.

As each transistor conducts in turn, the current fed resonant load causes alternate polarity half sinewaves with peak voltages of $\pi/2 \times V_{DC}$ to appear at one end of the transformer primary. Each half sine appears across the non-conducting transistor. Therefore the maximum theoretical $V_{CE} = \pi/2 \times V_{DC}$.

The sum of these half sines produces a full sinewave with a peak to peak amplitude of $\pi \times V_{DC}$. However, as the return current flows to the A.C. half rail created by the half bridge capacitors, only half this voltage appears across the primary, resulting in a peak to peak primary voltage of $\pi/2 \times V_{DC}$.

Voltage fed half bridge inverter.

See Fig. 10. This circuit does not employ a transformer so output isolation is not provided. Feedback to drive the transistors is now supplied from two auxiliary windings on the current transformer CT1 in the lamp current path.

As this is a voltage fed circuit whose output is not naturally sinusoidal, lamp starting, ballasting and waveform shaping are provided by the series L and parallel C as for the voltage fed push pull circuit.

In the voltage fed half bridge circuit, since the transistors are "firmly anchored" to the supply rails without any current source series inductance, they will experience a maximum theoretical V_{CE} equal to the D.C. rail voltage.

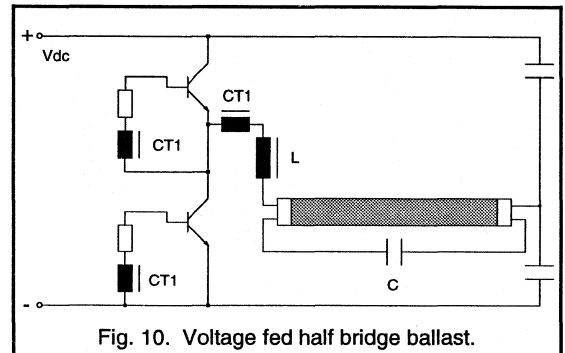


Fig. 10. Voltage fed half bridge ballast.

Variation on the voltage fed half bridge circuit.

A variation on this circuit is shown in Fig. 11, where the two half bridge capacitors are replaced by the single D.C. blocking capacitor C2. This enables the load to be returned to the positive D.C. rail.

The circuit operates as follows:

On initial power-up, before the lamp has struck, C1, L and C2 form a series resonant circuit. C2 is larger than C1 so it looks like a short circuit compared to C1. C1 therefore dominates and dictates the resonant frequency in combination with L. A high voltage is developed across C1 at resonance which starts the tube. At this point the tube voltage across C1 collapses and C2 then takes over in dictating a lower running frequency in combination with L.

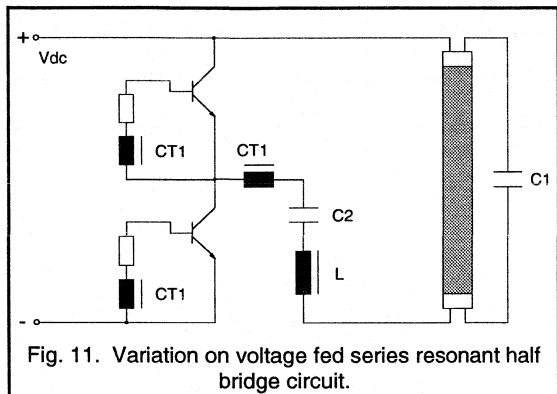


Fig. 11. Variation on voltage fed series resonant half bridge circuit.

This circuit is the one most commonly used in the electronically ballasted compact fluorescent lamps and it lends itself to driven as well as self oscillating circuits.

Summary.

The circuit examples presented in this Publication all use bipolar transistors, mainly for cost advantage reasons, especially where high voltage devices up to 1000V rating

and above are required. Ballast manufacturers have perfected many good, reliable designs using such devices in circuits based on the simplified topologies shown.

Popular topologies for low cost electronic ballasts have proved to be the current fed parallel resonant circuits. To summarise the reasons for this, they naturally produce the ideal sinewave output. This permits the use of simple ballast capacitors instead of inductors. The circuits also maintain safe operation with abnormal load conditions. Lamps can be operated in parallel, where the failure of one or more lamp will not disable the remaining lamps.

The current fed topologies require higher voltage transistors than the voltage fed topologies. For example, for the current fed half bridge topology, allowing for safety margins of around 400V for voltage spikes at start-up and 110% mains voltage, a 120V ballast would require transistors with typical voltage ratings of at least 700V. The ratings for 230V mains would typically be at least 950V, and for 277V mains typical voltage ratings of at least 1100V would be required.

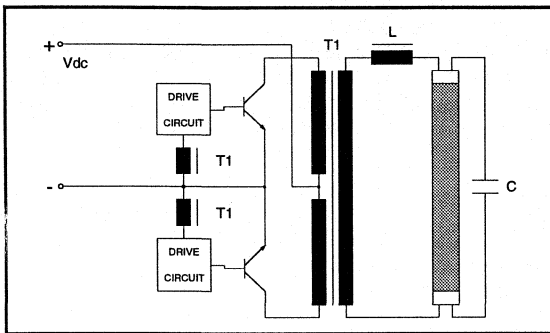
The ratings for a current fed push pull topology would be 1000V, 1500V and 1750V respectively.

8.1.2 Electronic Ballasts - Philips Transistor Selection Guide

Section 8.1.1 provides an introduction to fluorescent lamps and the circuits required to operate them for maximum life and efficiency. Several simplified electronic ballast topologies are introduced.

This section lists those topologies with the theoretical voltage demands they place on the transistors, together with a selection table of suitable Philips transistors.

a) Voltage fed push pull inverter.



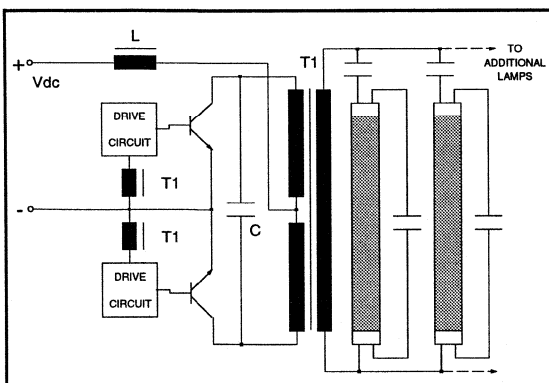
The D.C. rail voltage appears at the transformer centre tap.

Therefore $V_{c.t.} = V_{DC}$.

Half of the transformer's primary winding is energised with the full D.C. rail voltage at any one time. Therefore twice this voltage will appear across the whole winding (autotransformer effect). This voltage appears across each transistor in turn when it is non-conducting. So, during stable circuit operation and neglecting unforeseen voltage spikes:

$$V_{CE(max)} = 2 \times V_{DC}$$

b) Current fed push pull inverter.



The transformer centre tap is no longer connected directly to the D.C. rail. The voltage developed across the series inductor L as each transistor conducts results in a positive half sinewave at the centre tap whose average voltage is equal to the D.C. rail voltage. A half sine instead of a rectangular pulse is produced because of the resonant nature of the load.

Therefore $V_{c.t.(ave)} = V_{DC}$.

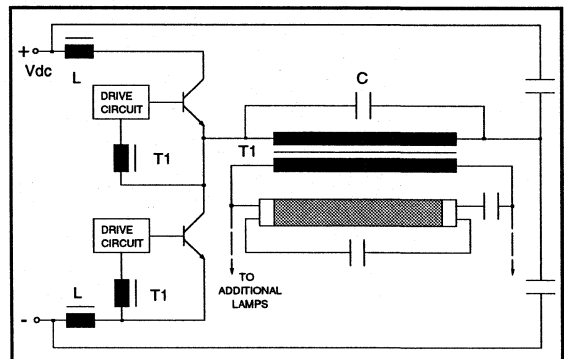
The peak value of this waveform can be shown by integration to be $\pi/2$ x its average value.

Therefore $V_{c.t.(pk)} = \pi/2 \times V_{c.t.(ave)} = \pi/2 \times V_{DC}$.

Each successive half sine is conducted through alternate halves of the primary, so twice this amplitude appears across the full primary. This gives a peak voltage of twice the peak centre tap voltage appearing across the non-conducting transistor (as for the voltage fed push pull circuit), so:

$$V_{CE(pk)} = \pi \times V_{DC}$$

c) Current fed half bridge inverter.



The transformer primary is driven from one end by the collector-emitter junction point of the two transistors. If this were a voltage fed circuit without any series L, the primary would be alternately connected to the positive and negative rails by the alternate transistor switching to produce a square wave with a peak to peak amplitude of V_{DC} . However, because this is a current fed resonant circuit, the conduction of each transistor will produce a half sine whose average voltage is equal to the D.C. rail voltage.

Therefore $V_{(ave)} = V_{DC}$.

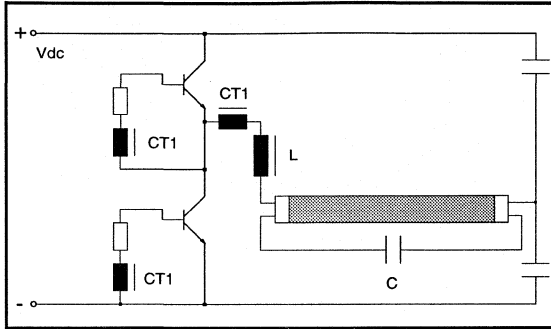
By integrating it can be shown that the half sine will have a peak amplitude of $\pi/2$ x its average value.

Therefore $V_{(pk)} = \pi/2 \times V_{(ave)} = \pi/2 \times V_{DC}$.

This voltage appears across the non-conducting transistor, so:

$$V_{CE(pk)} = \pi/2 \times V_{DC}$$

d) Voltage fed half bridge inverter.



As the transistors are now connected directly to the D.C. rails, their alternate switching will switch the transformer primary between the D.C. rails only.

Therefore $V_{(max)} = V_{DC}$.

As this voltage appears across the non-conducting transistor:

$$V_{CE(max)} = V_{DC}$$

Transistor selection guide.

This guide lists suitable transistors with maximum recommended output powers for the different topologies. It assumes that the ballast's D.C. rail is obtained from rectified and smoothed A.C. mains. If boost power factor correction is included which boosts the D.C. rail voltage to around 400V irrespective of mains voltage, the suggested transistors for 277V mains should be selected.

TOPOLOGY:		a) V. fed P.P.		b) C. fed P.P.		c) C. fed H.B.		d) V. fed H.B.	
A.C. SUPPLY:	120V	BUX84 BUT211 BUT18A BUT12A BUW12A	35W 90W 110W 140W 140W	BUX87 BUX85 BUT11A BUT18A BUT12A BUW12A	13W 55W 140W 170W 230W 230W	BUX84 BUT211 BUT18A BUT12A BUW12A	25W 70W 80W 110W 110W	BUX100 BUT211 BUT18A BUT12A BUW12A	15W 40W 55W 70W 70W
	230V	BUX87 BUX85 BUT11A BUT18A BUT12A BUW12A	15W 70W 170W 210W 280W 280W	BU1508AX BU508A	360W 360W	BUX87 BUX85 BUT11A BUT18A BUT12A BUW12A	13W 55W 140W 160W 220W 220W	BUX84 BUT211 BUT18A BUT12A BUW12A	30W 80W 100W 140W 140W
	277V & most boosted designs	BU1508AX BU508A	280W 280W	BU1706A BU1706AX BU1708AX	215W 215W 340W	BU1508AX BU508A	220W 220W	BUX84 BUT211 BUT18A BUT12A BUW12A	40W 100W 125W 170W 170W

8.1.3 An Electronic Ballast - Base Drive Optimisation

This section investigates the transistor base drive circuit in a current fed half bridge ballast. (Fig. 1 shows the simplified circuit.) The effect on switching waveforms of progressing from a simple base drive circuit to the optimised solution will be shown.

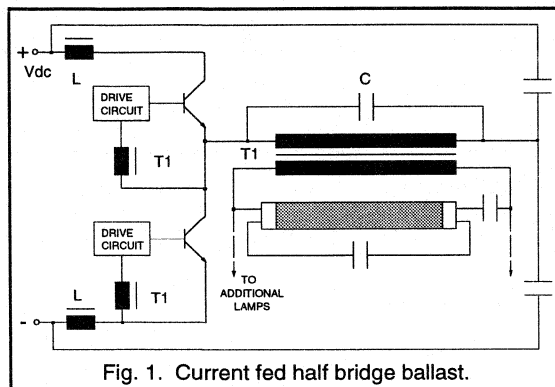


Fig. 1. Current fed half bridge ballast.

Base drive requirements.

1. Each transistor must not be overdriven and oversaturated when conducting otherwise excessive base power dissipation will result. The time will also be increased in bringing the transistor out of saturation during turn-off, leading to increased switching losses.
2. The transistor must not be underdriven because this will result in excessive collector-to-emitter voltage (V_{CE}) during conduction, leading to excessive ON-state losses or inability to sustain oscillation. However, because the transistor is unsaturated, there will be less charge to extract from the base, resulting in a shorter storage time and faster turn-off.
3. Reliable and correct circuit operation should be maintained for all expected transistor gains, maximum and minimum load, maximum and minimum supply voltage and all component tolerances.

Base drive optimisation.

The transformer's auxiliary windings which provide base drive might contain just one or two turns each. In order to provide rapid transistor turn-off, their peak loaded output

voltage would need to be such that the transistor 'sees' a turn-off voltage of around minus 5V. An approximation to this drive voltage could be arrived at empirically by increasing the number of auxiliary turns one by one. Any final voltage adjustment, if necessary, can be achieved by varying the base drive components.

Simple base drive.

In order to meet the requirements of non-saturation and rapid turn-off, the simplest base drive might consist of a resistor to limit the positive base current and a Schottky diode in parallel with it to discharge the base as quickly as possible. See Fig. 2.

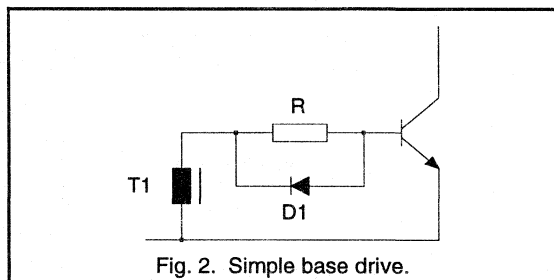
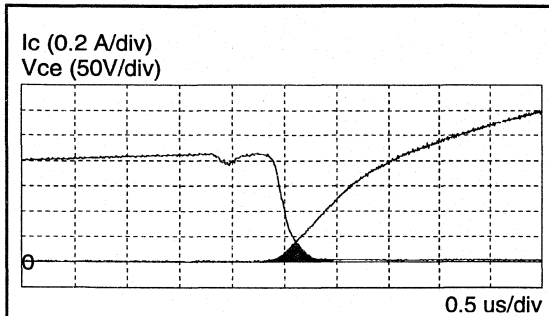


Fig. 2. Simple base drive.

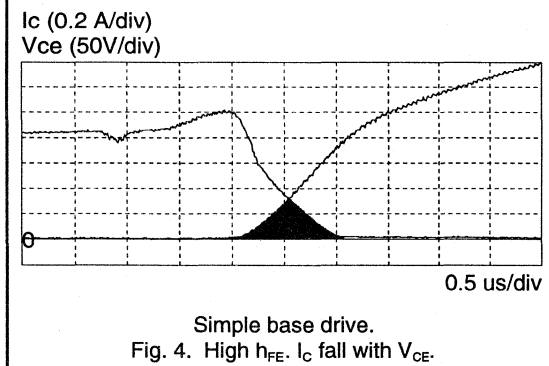
A Schottky diode is specified for its fast switching and low forward voltage drop to best meet the rapid turn-off requirements. A 1A 40V device such as the BYV10-40 is ideally suited.

If the resistor is selected empirically so that the transistor is barely saturating, this simple circuit will work, but only for a given load current, supply voltage, transistor gain and base drive voltage from the transformer auxiliary winding. Altering any of these conditions will either cause underdriving of the transistor and, ultimately, cessation of oscillation, or else the transistor will be overdriven, causing increased collector current fall time and excessive switching losses.

For example, the resistor value was optimised for transistors with low gain limits. Fig. 3 shows the resulting I_C fall at transistor turn-off, while Fig. 4 shows the effect of replacing the transistor with a high gain limit sample. The shaded areas bounded by the I_C and V_{CE} curves represent transistor power dissipation during switching.



Simple base drive.
Fig. 3. Low h_{FE} . I_C fall with V_{CE} .



Simple base drive.
Fig. 4. High h_{FE} . I_C fall with V_{CE} .

Improved circuit.

What is required is a means of providing enough base drive under worst case conditions of maximum load current, minimum supply voltage, minimum transistor gain and minimum base drive voltage, while avoiding excessive saturation in the opposite condition. This can be achieved by diverting excess positive base drive current into the collector path when the transistor is fully turned on. This requirement is partly met by a Baker Clamp arrangement as shown in Fig. 5.

When the transistor is fully conducting, V_{CE} will be at a minimum. This will bring V_C close to V_B so that any excess base drive will then flow through anti saturation diode D2 to the collector. As a first approximation, the single resistor R is divided equally into two and D2 taps its voltage from the mid point. Figs. 6 and 7 show the resulting I_C fall waveforms. Considerably reduced transistor saturation is evident.

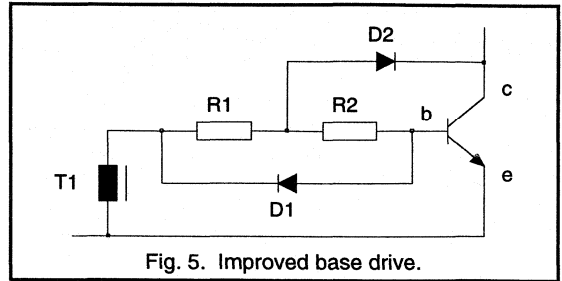
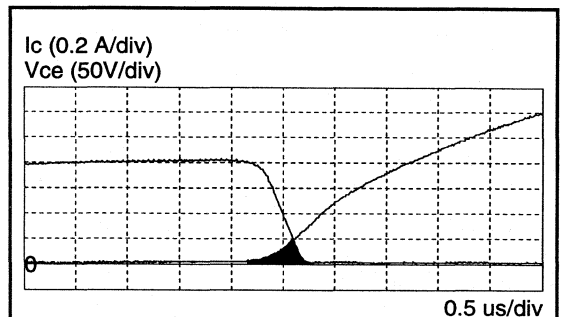
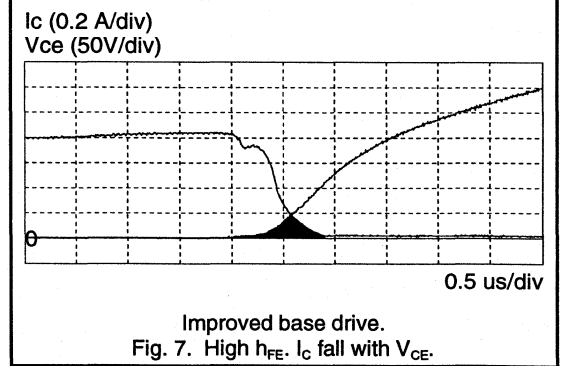


Fig. 5. Improved base drive.



Improved base drive.
Fig. 6. Low h_{FE} . I_C fall with V_{CE} .



Improved base drive.
Fig. 7. High h_{FE} . I_C fall with V_{CE} .

With regard to the base waveforms, where the simple circuit produces more base drive current than is necessary, as shown in Fig. 8, the improved circuit reduces this to that shown in Fig. 9.

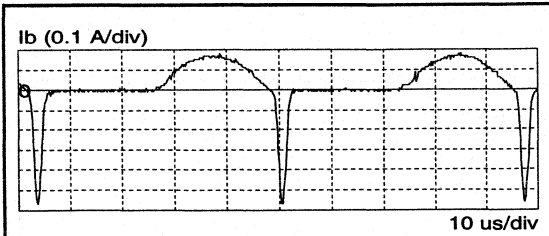


Fig. 8. Simple base drive.
High h_{FE} , I_B .

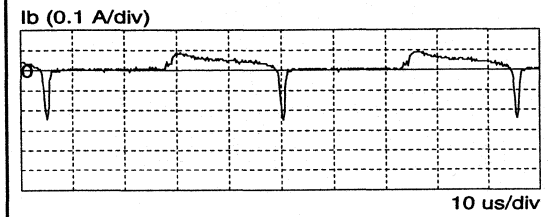
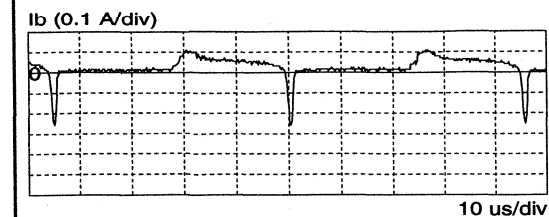
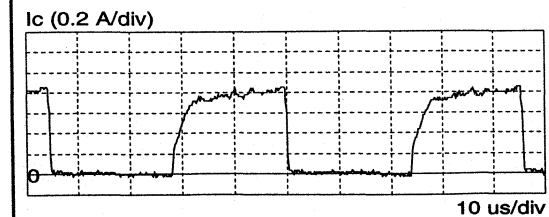
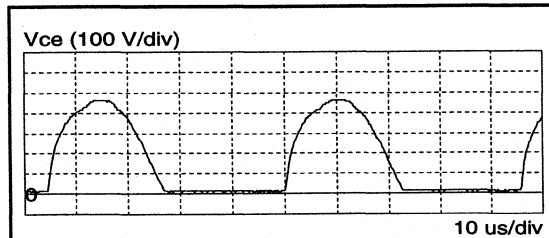


Fig. 9. Improved base drive.
High h_{FE} , I_B .

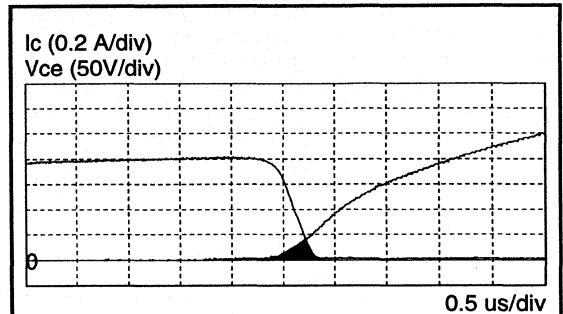
Optimised base drive.



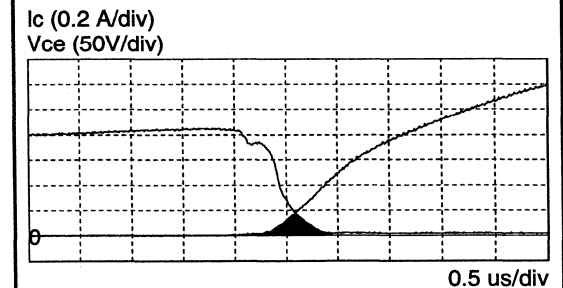
Optimised base drive.
Fig. 10. High h_{FE} , V_{CE} , I_C and I_B .

To ensure correct operation under all conditions, base drive can be optimised by adjusting the ratio of the two resistors to vary the amount of tap-off voltage. With the base resistor divided equally into two, this particular circuit suffered from a lack of base drive at low supply voltage. Too much drive had been diverted away from the base. This was corrected by moving the tap-off point to the right to split the resistor two thirds to one third to reduce the amount of diverted base drive. Referring to Fig. 5, R1 becomes $2/3 \times R$ and R2 becomes $1/3 \times R$.

Figs. 11 and 12 show the optimised IC fall waveforms. A few cycles of the switching waveforms with optimised base drive are shown in Fig. 10.



Optimised base drive.
Fig. 11. Low h_{FE} , I_C fall with V_{CE} .



Optimised base drive.
Fig. 12. High h_{FE} , I_C fall with V_{CE} .

Startup circuit.

The half bridge circuit as described so far cannot start of its own accord. Both transistors are off and will remain off when power is applied until one of them is artificially turned on to draw current through the transformer primary. This will then induce a voltage in the auxiliary windings which will provide the necessary base drive to maintain self oscillation. Startup is usually achieved using a diac such as the BR100/03. The circuit is shown in Fig. 13.

When power is first applied, oscillator start-up is achieved as follows:

Transistors Q1 and Q2 are initially non conducting. Resistor R4, whose value will be several hundred kilohms, provides a high impedance path between Q2's collector and the positive rail to ensure that Q2 has the full D.C. rail voltage across it prior to start-up.

Capacitor C charges up via R1 until the breakover voltage of the diac D8 is reached. The diac breaks over and dumps the capacitor's charge into the base of Q2 to turn it on. Q2 draws current through the transformer primary. From now on, oscillation is maintained by the voltages induced on the auxiliary base drive windings.

Diode D1 discharges C every time Q2 turns on, thereby preventing the diac's breakover voltage being reached during normal circuit oscillation. This avoids repeated triggering of the diac when it is not required, so preventing oversaturation of Q2. (The length of time for C to charge to the diac's breakover voltage is much longer than the time between ON periods of Q2.)

D4 and D5 provide reverse current protection for Q1 and Q2.

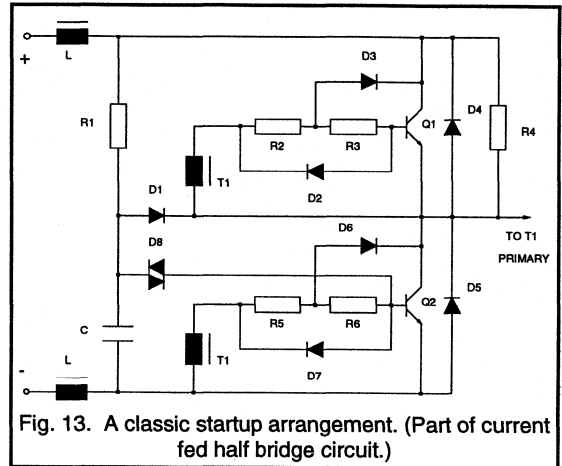


Fig. 13. A classic startup arrangement. (Part of current fed half bridge circuit.)

Philips Semiconductors – a worldwide company

Argentina: IEROD, Av. Juramento 1992 - 14.b, (1428)
BUENOS AIRES, Tel. (541)786 7633, Fax. (541)786 9367

Australia: 34 Waterloo Road, NORTH RYDE, NSW 2113,
Tel. (02)805 4455, Fax. (02)805 4466

Austria: Triester Str. 64, A-1101 WIEN, P.O. Box 213,
Tel. (01)60 101-1236, Fax. (01)60 101-1211

Belgium: Postbus 90050, 5600 PB EINDHOVEN, The Netherlands,
Tel. (31)40 783 749, Fax. (31)40 788 399

Brazil: Rua do Rocio 220 - 5th floor, Suite 51,
CEP: 04552-903-SÃO PAULO-SP, Brazil.
P.O. Box 7383 (01064-970).

Tel. (011)821-2333, Fax. (011)829-1849

Canada: PHILIPS SEMICONDUCTORS/COMPONENTS:
Tel. (800) 234-7381, Fax. (708) 296-8556

Chile: Av. Santa Maria 0760, SANTIAGO,
Tel. (02)773 816, Fax. (02)777 6730

Colombia: IPRELENTO LTDA, Carrera 21 No. 56-17,
77621 BOGOTÁ, Tel. (571)249 7624/(571)217 4609,
Fax. (571)217 4549

Denmark: Prags Boulevard 80, PB 1919, DK-2300 COPENHAGEN S,
Tel. (032)88 2636, Fax. (031)57 1949

Finland: Sinikalliontie 3, FIN-02630 ESPOO,
Tel. (9)0-50261, Fax. (9)0-520971

France: 4 Rue du Port-aux-Vins, BP317,
92156 SURESNES Cedex,
Tel. (01)4099 6161, Fax. (01)4099 6427

Germany: P.O. Box 10 63 23, 20043 HAMBURG,
Tel. (040)3296-0, Fax. (040)3296 213.

Greece: No. 15, 25th March Street, GR 17778 TAVROS,
Tel. (01)4894 339/4894 911, Fax. (01)4814 240

Hong Kong: PHILIPS HONG KONG Ltd., 6/F Philips Ind. Bldg.,
24-28 Kung Yip St., KWAI CHUNG, N.T.,
Tel. (852)424 5121, Fax. (852)428 6729

India: Philips INDIA Ltd, Shivsagar Estate, A Block,
Dr. Annie Besant Rd. Worli, Bombay 400 018
Tel. (022)4938 541, Fax. (022)4938 722

Indonesia: Philips House, Jalan H.R. Rasuna Said Kav. 3-4,
P.O. Box 4252, JAKARTA 12950,
Tel. (021)5201 122, Fax. (021)5205 189

Ireland: Newstead, Clonskeagh, DUBLIN 14,
Tel. (01)640 000, Fax. (01)640 200

Italy: PHILIPS SEMICONDUCTORS S.r.l.,
Piazza IV Novembre 3, 20124 MILANO,
Tel. (0039)2 6752 2531, Fax. (0039)2 6752 2557

Japan: Philips Bldg 13-37, Kohnan 2-chome, Minato-ku, TOKYO 108,
Tel. (03)3740 5028, Fax. (03)3740 0580

Korea: (Republic of) Philips House, 260-199 Itaewon-dong,
Yongsan-ku, SEOUL, Tel. (02)794-5011, Fax. (02)798-8022

Malaysia: No. 76 Jalan Universiti, 46200 PETALING JAYA,
SELANGOR, Tel. (03)750 5214, Fax. (03)757 4880

Mexico: 5900 Gateway East, Suite 200, EL PASO, TX 79905,
Tel. 9-5(800)234-7381, Fax. (708)296-8556

Netherlands: Postbus 90050, 5600 PB EINDHOVEN, Bldg. VB
Tel. (040)783749, Fax. (040)788399

New Zealand: 2 Wagener Place, C.P.O. Box 1041, AUCKLAND,
Tel. (09)849-4160, Fax. (09)849-7811

Norway: Box 1, Manglerud 0612, OSLO,
Tel. (022)74 8000, Fax. (022)74 8341

Pakistan: Philips Electrical Industries of Pakistan Ltd.,
Exchange Bldg. ST-2/A, Block 9, KDA Scheme 5, Clifton,
KARACHI 75600, Tel. (021)587 4641-49,
Fax. (021)577035/5874546.

Philippines: PHILIPS SEMICONDUCTORS PHILIPPINES Inc.,
106 Valero St. Salcedo Village, P.O. Box 2108 MCC, MAKATI,
Metro MANILA, Tel. (02)810 0161, Fax. (02)817 3474

Portugal: PHILIPS PORTUGUESA, S.A.,
Rua dr. António Loureiro Borges 5, Arquiparque - Miraflores,
Apartado 300, 2795 LINDA-A-VELHA,
Tel. (01)4163160/4163333, Fax. (01)4163174/4163366.

Singapore: Lorong 1, Toa Payoh, SINGAPORE 1231,
Tel. (65)350 2000, Fax. (65)251 6500

South Africa: S.A. PHILIPS Pty Ltd.,
195-215 Main Road Martindale, 2092 JOHANNESBURG,
P.O. Box 7430 Johannesburg 2000,
Tel. (011)470-5911, Fax. (011)470-5494.

Spain: Balmes 22, 08007 BARCELONA,
Tel. (03)301 6312, Fax. (03)301 42 43

Sweden: Kottbygatan 7, Akalla. S-164 85 STOCKHOLM,
Tel. (0)8-632 2000, Fax. (0)8-632 2745

Switzerland: Allmendstrasse 140, CH-8027 ZÜRICH,
Tel. (01)488 2211, Fax. (01)481 77 30

Taiwan: PHILIPS TAIWAN Ltd., 23-30F, 66, Chung Hsiao West
Road, Sec. 1. Taipei, Taiwan ROC, P.O. Box 22978,
TAIPEI 100, Tel. (02)388 7666, Fax. (02)382 4382.

Thailand: PHILIPS ELECTRONICS (THAILAND) Ltd.,
209/2 Sanpavuth-Bangna Road Prakanong,
Bangkok 10260, THAILAND,
Tel. (662)398-0141, Fax. (662)398-3319.

Turkey: Talatpasa Cad. No. 5, 80640 GÜLTEPE/ISTANBUL,
Tel. (0212)279 2770, Fax. (0212)269 3094

United Kingdom: Philips Semiconductors LTD.,
276 Bath Road, Hayes, MIDDLESEX UB3 5BX,
Tel. (081)730-5000, Fax. (081)754-8421

United States: 811 East Arques Avenue, SUNNYVALE,
CA 94088-3409, Tel. (800)234-7381, Fax. (708)296-8556

Uruguay: Coronel Mora 433, MONTEVIDEO,
Tel. (02)70-4044, Fax. (02)92 0601

For all other countries apply to: Philips Semiconductors,
International Marketing and Sales, Building BE-p,
P.O. Box 218, 5600 MD, EINDHOVEN, The Netherlands,
Telex 35000 phtnl, Fax. +31-40-724825

SCD36

© Philips Electronics N.V. 1994

All rights are reserved. Reproduction in whole or in part is prohibited without the prior written consent of the copyright owner.

The information presented in this document does not form part of any quotation or contract, is believed to be accurate and reliable and may be changed without notice. No liability will be accepted by the publisher for any consequence of its use. Publication thereof does not convey nor imply any license under patent- or other industrial or intellectual property rights.

Printed in The Netherlands

1133011/12000/02

Document order number:

Date of release: December 1994

9398 652 85011